HOST GENETICS IN VIRAL PATHOGENESIS AND CONTROLS

EDITED BY: Ping An, Ju-Tao Guo and Cheryl Ann Winkler
PUBLISHED IN: Frontiers in Genetics, Frontiers in Immunology and Frontiers in Microbiology

frontiers Research Topics

Frontiers eBook Copyright Statement

The copyright in the text of individual articles in this eBook is the property of their respective authors or their respective institutions or funders. The copyright in graphics and images within each article may be subject to copyright of other parties. In both cases this is subject to a license granted to Frontiers.

The compilation of articles constituting this eBook is the property of Frontiers.

Each article within this eBook, and the eBook itself, are published under the most recent version of the Creative Commons CC-BY licence. The version current at the date of publication of this eBook is CC-BY 4.0. If the CC-BY licence is updated, the licence granted by Frontiers is automatically updated to the new version.

When exercising any right under the CC-BY licence, Frontiers must be attributed as the original publisher of the article or eBook, as applicable.

Authors have the responsibility of ensuring that any graphics or other materials which are the property of others may be included in the CC-BY licence, but this should be checked before relying on the CC-BY licence to reproduce those materials. Any copyright notices relating to those materials must be complied with.

Copyright and source acknowledgement notices may not be removed and must be displayed in any copy, derivative work or partial copy which includes the elements in question.

All copyright, and all rights therein, are protected by national and international copyright laws. The above represents a summary only. For further information please read Frontiers' Conditions for Website Use and Copyright Statement, and the applicable CC-BY licence.

ISSN 1664-8714
ISBN 978-2-88963-263-3
DOI 10.3389/978-2-88963-263-3

About Frontiers

Frontiers is more than just an open-access publisher of scholarly articles: it is a pioneering approach to the world of academia, radically improving the way scholarly research is managed. The grand vision of Frontiers is a world where all people have an equal opportunity to seek, share and generate knowledge. Frontiers provides immediate and permanent online open access to all its publications, but this alone is not enough to realize our grand goals.

Frontiers Journal Series

The Frontiers Journal Series is a multi-tier and interdisciplinary set of open-access, online journals, promising a paradigm shift from the current review, selection and dissemination processes in academic publishing. All Frontiers journals are driven by researchers for researchers; therefore, they constitute a service to the scholarly community. At the same time, the Frontiers Journal Series operates on a revolutionary invention, the tiered publishing system, initially addressing specific communities of scholars, and gradually climbing up to broader public understanding, thus serving the interests of the lay society, too.

Dedication to Quality

Each Frontiers article is a landmark of the highest quality, thanks to genuinely collaborative interactions between authors and review editors, who include some of the world's best academicians. Research must be certified by peers before entering a stream of knowledge that may eventually reach the public - and shape society; therefore, Frontiers only applies the most rigorous and unbiased reviews.
Frontiers revolutionizes research publishing by freely delivering the most outstanding research, evaluated with no bias from both the academic and social point of view. By applying the most advanced information technologies, Frontiers is catapulting scholarly publishing into a new generation.

What are Frontiers Research Topics?

Frontiers Research Topics are very popular trademarks of the Frontiers Journals Series: they are collections of at least ten articles, all centered on a particular subject. With their unique mix of varied contributions from Original Research to Review Articles, Frontiers Research Topics unify the most influential researchers, the latest key findings and historical advances in a hot research area! Find out more on how to host your own Frontiers Research Topic or contribute to one as an author by contacting the Frontiers Editorial Office: researchtopics@frontiersin.org

HOST GENETICS IN VIRAL PATHOGENESIS AND CONTROLS

Topic Editors:
Ping An, Frederick National Laboratory for Cancer Research (NIH), United States
Ju-Tao Guo, Baruch S. Blumberg Institute, United States
Cheryl Ann Winkler, Frederick National Laboratory for Cancer Research (NIH), United States

Citation: An, P., Guo, J.-T., Winkler, C. A., eds. (2019). Host Genetics in Viral Pathogenesis and Controls. Lausanne: Frontiers Media SA.
doi: 10.3389/978-2-88963-263-3

Table of Contents

05 ***Editorial: Host Genetics in Viral Pathogenesis and Control***
Ping An, Ju-Tao Guo and Cheryl A. Winkler

09 ***Initial Influenza Virus Replication can be Limited in Allergic Asthma Through Rapid Induction of Type III Interferons in Respiratory Epithelium***
Sujin An, Yung Jin Jeon, Ara Jo, Hyun Jung Lim, Young Eun Han, Sung Woo Cho, Hye Young Kim and Hyun Jik Kim

23 ***The cGas–Sting Signaling Pathway is Required for the Innate Immune Response Against Ectromelia Virus***
Wen-Yu Cheng, Xiao-Bing He, Huai-Jie Jia, Guo-Hua Chen, Qi-Wang Jin, Zhao-Lin Long and Zhi-Zhong Jing

37 ***Molecular Mechanisms for the Adaptive Switching Between the OAS/RNase L and OASL/RIG-I Pathways in Birds and Mammals***
Enguang Rong, Xiaoxue Wang, Hualan Chen, Chenghuai Yang, Jiaxiang Hu, Wenjie Liu, Zeng Wang, Xiaoyun Chen, Haixue Zheng, Juan Pu, Honglei Sun, Jacqueline Smith, David W. Burt, Jinhua Liu, Ning Li and Yinhua Huang

51 ***Host and Viral Genetic Variation in HBV-Related Hepatocellular Carcinoma***
Ping An, Jinghang Xu, Yanyan Yu and Cheryl A. Winkler

66 ***KIR3DL1-Negative CD8 T Cells and KIR3DL1-Negative Natural Killer Cells Contribute to the Advantageous Control of Early Human Immunodeficiency Virus Type 1 Infection in HLA-B Bw4 Homozygous Individuals***
Xin Zhang, Xiaofan Lu, Christiane Moog, Lin Yuan, Zhiying Liu, Zhen Li, Wei Xia, Yuefang Zhou, Hao Wu, Tong Zhang and Bin Su

83 ***Chickens Expressing IFIT5 Ameliorate Clinical Outcome and Pathology of Highly Pathogenic Avian Influenza and Velogenic Newcastle Disease Viruses***
Mohammed A. Rohaim, Diwakar Santhakumar, Rania F. El Naggar, Munir Iqbal, Hussein A. Hussein and Muhammad Munir

97 ***Chaperones, Membrane Trafficking and Signal Transduction Proteins Regulate Zaire Ebola Virus trVLPs and Interact With trVLP Elements***
Dong-Shan Yu, Tian-Hao Weng, Chen-Yu Hu, Zhi-Gang Wu, Yan-Hua Li, Lin-Fang Cheng, Nan-Ping Wu, Lan-Juan Li and Hang-Ping Yao

108 ***EGFR as a Negative Regulatory Protein Adjusts the Activity and Mobility of NHE3 in the Cell Membrane of IPEC-J2 Cells With TGEV Infection***
Zhou Yang, Ling Ran, Peng Yuan, Yang Yang, Kai Wang, Luyi Xie, Shilei Huang, Jia Liu and Zhenhui Song

119 ***Comparative Transcriptomic and Metagenomic Analyses of Influenza Virus-Infected Nasal Epithelial Cells From Multiple Individuals Reveal Specific Nasal-Initiated Signatures***
Kai Sen Tan, Yan Yan, Wai Ling Hiromi Koh, Liang Li, Hyungwon Choi, Thai Tran, Richard Sugrue, De Yun Wang and Vincent T. Chow

131 ***Dysregulated miRNAome and Proteome of PPRV Infected Goat PBMCs Reveal a Coordinated Immune Response***
Alok Khanduri, Amit Ranjan Sahu, Sajad Ahmad Wani, Raja Ishaq Nabi Khan, Aruna Pandey, Shikha Saxena, Waseem Akram Malla, Piyali Mondal, Kaushal Kishor Rajak, D. Muthuchelvan, Bina Mishra, Aditya P. Sahoo, Yash Pal Singh, Raj Kumar Singh, Ravi Kumar Gandham and Bishnu Prasad Mishra

144 ***IFITM Genes, Variants, and Their Roles in the Control and Pathogenesis of Viral Infections***
Xuesen Zhao, Jiarui Li, Cheryl A. Winkler, Ping An and Ju-Tao Guo

156 ***Interaction of the Host and Viral Genome and Their Influence on HIV Disease***
Riley H. Tough and Paul J. McLaren

165 ***Impact of APOL1 Genetic Variants on HIV-1 Infection and Disease Progression***
Ping An, Gregory D. Kirk, Sophie Limou, Elizabeth Binns-Roemer, Jeffrey B. Kopp and Cheryl A. Winkler

171 ***Inhibitor of Sarco/Endoplasmic Reticulum Calcium-ATPase Impairs Multiple Steps of Paramyxovirus Replication***
Naveen Kumar, Nitin Khandelwal, Ram Kumar, Yogesh Chander, Krishan Dutt Rawat, Kundan Kumar Chaubey, Shalini Sharma, Shoor Vir Singh, Thachamvally Riyesh, Bhupendra N. Tripathi and Sanjay Barua

183 ***Immune Activations and Viral Tissue Compartmentalization During Progressive HIV-1 Infection of Humanized Mice***
Hang Su, Yan Cheng, Sruthi Sravanam, Saumi Mathews, Santhi Gorantla, Larisa Y. Poluektova, Prasanta K. Dash and Howard E. Gendelman

200 ***Non-muscle Myosin II: Role in Microbial Infection and its Potential as a Therapeutic Target***
Lei Tan, Xiaomin Yuan, Yisong Liu, Xiong Cai, Shiyin Guo and Aibing Wang

211 ***Clinical Significance of Polymorphisms in Immune Response Genes in Hepatitis C-Related Hepatocellular Carcinoma***
Valli De Re, Maria Lina Tornesello, Mariangela De Zorzi, Laura Caggiari, Francesca Pezzuto, Patrizia Leone, Vito Racanelli, Gianfranco Lauletta, Laura Gragnani, Angela Buonadonna, Emanuela Vaccher, Anna Linda Zignego, Agostino Steffan and Franco M. Buonaguro

221 ***Elucidating the Host Interactome of EV-A71 2C Reveals Viral Dependency Factors***
Ye Li, Xia Jian, Peiqi Yin, Guofeng Zhu and Leiliang Zhang

234 ***Host Genetics of Cytomegalovirus Pathogenesis***
Efe Sezgin, Ping An and Cheryl A. Winkler

249 ***Host Genetic Determinants of Hepatitis B Virus Infection***
Zhenhua Zhang, Changtai Wang, Zhongping Liu, Guizhou Zou, Jun Li and Mengji Lu

273 ***Large-Scale "OMICS" Studies to Explore the Physiopatholgy of HIV-1 Infection***
Sigrid Le Clerc, Sophie Limou and Jean-François Zagury

frontiers in Genetics

EDITORIAL
published: 08 November 2019
doi: 10.3389/fgene.2019.01038

Editorial: Host Genetics in Viral Pathogenesis and Control

Ping An[1], Ju-Tao Guo[2] and Cheryl A. Winkler[1]*

[1] Basic Research Laboratory, Molecular Genetic Epidemiology Section, Basic Science Program, Frederick National Laboratory for Cancer Research, Frederick, MD, United States, [2] Baruch S. Blumberg Institute, Hepatitis B Foundation, Doylestown, PA, United States

Keywords: Genetic epidemiology, GWAS, HBV, HIV-1, host susceptibility, innate immunity, variant, viral infection

Editorial on the Research Topic

Host Genetics in Viral Pathogenesis and Control

HOST GENETIC SUSCEPTIBILTY/RESISTANCE TO VIRAL INFECTIONS

Viral diseases contribute to substantial morbidity and mortality and remain a major threat to global health. Although vaccines are notably successful in the prevention of many infections, effective vaccines are not available for most viruses including the pandemic human immunodeficiency virus (HIV) and hepatitis C virus (HCV). Direct antiviral agents can efficiently inhibit the replication of certain viruses but generally do not provide sterilizing cures, with the notable exception of HCV infection. Emerging and re-emerging viruses have caused an increasing number of disease outbreaks in humans and animals. There is unmet medical need to further our understanding of viral pathogenesis to enable more effective control and prevention of viral infections. Elucidating virus–host interaction is an essential step toward this goal.

Viruses generally show variation in both acquisition susceptibility and clinical presentations, suggesting that viral pathogenesis is due to complex interactions between host and viruses. This variability following viral infection has been attributed to a variety of factors, including viral strain and sequence variation as well as age, immune status and genetic background of host. This Research Topic included 21 review or original articles focused on multiple aspects of virus–host interactions, utilizing myriad cellular, genomic, and omics-based approaches to identify key genes and pathways in host defensive and virus offensive strategies.

HOST PROVIRAL FACTORS

Viruses are obligate intracellular parasites that depend on host cellular functions for almost every step of their replication cycle. Host cellular factors required for viral replication, *i.e.*, host proviral factors (HPF), are usually identified through loss-of-function genetic screening approaches. By utilizing RNAi knockdown of host cellular gene expression in an Ebola virus infection cell model, Yu et al. validated 11 host proteins that support viral replication by testing for their interaction with viral proteins or RNA. Using a combination of pharmacological and genetic approaches, Yang et al. revealed that swine transmissible gastroenteritis virus induced diarrhea by interacting with its cellular receptor, epidermal growth factor receptor (EGFR), to weaken the Na+/water absorption ability of the Na+/H+ exchanger protein in small intestine epithelial cells. An EGFR inhibitor reduced viral proliferation and restored Na+ absorption. Li et al. identified novel host proviral factors required for the replication of enterovirus A71

OPEN ACCESS

Edited and Reviewed by:
Dana C. Crawford, Case Western Reserve University, United States

****Correspondence:***
Ping An
anp@mail.nih.gov

Specialty section:
This article was submitted to Applied Genetic Epidemiology, a section of the journal Frontiers in Genetics

Received: *21 August 2019*
Accepted: *27 September 2019*
Published: *08 November 2019*

Citation:
An P, Guo J-T and Winkler CA (2019) Editorial: Host Genetics in Viral Pathogenesis and Control. Front. Genet. 10:1038. doi: 10.3389/fgene.2019.01038

that causes hand, foot and mouth disease by immunoprecipitation and mass spectrometry methods.

Due to the limited success of direct antiviral agents in curing viral infections and lack of antiviral therapeutics for emerging viral infections, considerable efforts have been expended to identify HPF vulnerabilities for antiviral drug development. Thus far, an antagonist of HIV-1 cellular coreceptor C–C chemokine receptor type 5 (CCR5) has been approved by the US Food and Drug Administration for treating HIV-1 infection. Myrcludex B, a lipopeptide that specifically inhibits Hepatitis B virus (HBV) and hepatitis D virus (HDV) entry into hepatocytes *via* their cell surface receptor, is currently in clinical trials for treatment of HBV and HDV infection (Blank et al., 2016). In this Topic, Tan et al. reviewed the evidence that actin-binding protein non-muscle myosin II (NM II) is upregulated in diverse viral and bacterial infections and its involvement in multiple steps of viral replication, revealing the potential of NM II inhibitors for treating the microbial infection. Generally, targeting HPFs for essential steps of the viral lifecycle could provide broad spectrum inhibition against different families of viruses which share the same cellular factor, although overcoming potential toxicity may prove challenging (Chang et al., 2015). Unlike direct antiviral agents that are subject to the emergence of drug resistant viruses, particularly under the condition of monotherapies, host-targeting antivirals antagonizing HPFs are less likely to induce drug resistance due to the higher genetic barrier (Zeisel et al., 2013). Kumar et al. reported that a small molecule inhibitor of a cellular $Ca2^{+}$ ATPase gene can inhibit the replication of two paramyxoviruses by blocking viral entry as well as biosynthesis, suggesting it as a novel target of host-targeting antivirals.

GENETICS OF INNATE IMMUNE CONTROL OF VIRAL INFECTION

Innate antiviral immunity provides the first line of defense against invading pathogens by sensing pathogen-associated molecular patterns through pattern-recognition receptors. For instance, activation of cytoplasmic DNA sensor cyclic GMP-AMP synthase (cGAS) triggers interferon (IFN) production to defend against DNA viruses and retroviruses (Gao et al., 2013), which is also essential for IFN induction in mousepox infection (Chang et al.). IFNs restrict viral replication through induction of hundreds of IFN-stimulated genes (ISGs) that mediate antiviral effector functions (Chan and Gack, 2016). Genetic variation in the multiple innate immune pathway genes that elicit antiviral effector functions affect the fate of viral infection.

Among ISGs, interferon-induced transmembrane proteins (IFITMs), expressed at the plasma membrane and membrane of endocytic vesicles, restrict the infection of many different enveloped viruses by inhibiting the fusion of viral envelop with cellular membranes. Zhao et al. systematically reviewed the structural function relationship of IFITM proteins and natural genetic variations associated with acquisition and pathogenesis of viral infections. For instance, *IFITM3* variants that reduce gene expression or encode truncated protein are associated with higher risk to influenza infection and more severe clinical course. Host cells use 2′-5′-oligoadenylate synthetase (OAS)/Ribonuclease L (RNase L) to degrade viral RNA and/or induce IFN production *via* retinoic acid-inducible gene I (RIG-I) to defend RNA viruses. Ron et al. investigated how avian and mammalian OASL (OAS like) differentially inhibited the replication of a broad range of RNA viruses *via* these two pathways. Moreover, Rohaim et al. showed that transgenic chickens expressed IFN-induced protein IFIT5 have reduced pathology and virus shedding, providing proof of principle for developing genetically modified chickens with enhanced innate immunity for viral prevention.

MicroRNAs (miRNAs), regulating the expression of genes post-transcriptionally, are also effective in regulating the expression of immune response genes (Rodriguez et al., 2007). By integrative miRNA and proteome profiling, Khanduri et al. identified the top 10 miRNAs that regulate the major immune response pathways to the goat plaque-causing virus. Future integrative miRNA–mRNA–protein network analyses may identify key regulators of viral–host interactions.

Interestingly, An et al. showed a protective role of intranasal administration of IFN-λ to influenza A virus infection. By comparative transcriptomic and metagenomic profiling, Tan et al. demonstrated that an *in vitro* nasal system to influenza virus reflects the *in vivo* immune and metabolic microenvironment, thus suitable for translational development. Gendelman's group compared the temporal and spatial host immune activation status in tissue compartments of HIV-1 infection in chimeric humanized mouse models transplanted with hematopoietic stem cells or mature human peripheral lymphocytes (Su et al.). Based on this line of work, Gendelman and collaborators reported that a combination of long-acting antiretroviral therapy (ART) and CRISPR-Cas9 for excision of integrated proviral DNA in the host genome successfully lead to permanent HIV-1 eradication in humanized mice (Dash et al., 2019). This work has important implications for curing HIV-1 infection in humans.

IDENTIFYING VIRAL RESTRICTION GENES BY GENETIC AND OMIC EPIDEMIOLOGICAL APPROACHES

HBV and HIV, which affect millions of people worldwide, contribute to substantial morbidity and mortality, and have no cure. To identify host genes that modify viral infection, several genome-wide association studies (GWAS) have been performed identifying genes associated with viral acquisition, disease progression, and clinical outcomes. A recognized limitation of GWAS studies is the high propensity for false-positive associations, and many associations have not been replicated or validated in subsequent studies. In addition, small studies are underpowered to identify small effect size variants or those with low population frequencies. Several articles provided critical reviews of HBV, HIV and cytomegalovirus (CMV) human genetic association studies and summarized the evidence supporting implicated genetic variants; the consensus message is that omics-based approaches are needed to identify critical host genes and pathways involved in the infectious process and pathophysiological mechanisms. Zhang

et al. summarized association studies of host genetic variation with HBV infection, clinical outcomes, therapeutic efficacy, and responses to vaccines. They provided an evidence-based categorization of SNP associations based on study power, replication, and functional validation, with the HLA-DP and DQ genes showing replication among different studies. A review by An et al. concluded that individual variance in development of HBV-related hepatocellular carcinoma (HCC) is multifactorial and attributable to HBV genotype and mutations, host predisposing germline genetic variations, the acquisition of tumor-specific somatic mutations, as well as environmental factors. Before precision medicine can be fully utilized in early diagnosis and prognosis of HCC, a deeper understanding of the interplay of viral, environmental, and host factors is required. A major knowledge gap identified by An et al. is the paucity of established germline variants and somatic mutations that drive tumorigenesis and their pathophysiology. De Re et al. studied multiple clinical outcomes in Italian patients infected with HCV and found that variants in *IFNL3* and *TLR2* are risk factors for HCV-related HCC; by comparison, in Asian patients the combination of *IFNL3* and *PD-1.6* markers better define the HCV-related outcomes, likely due to divergent variant distributions in the two populations and highlighting the need for genetic studies in diverse populations.

Despite multiple GWAS and meta-analyses, only *HLA* class I and *CCR5* variant alleles have been securely identified with HIV acquisition or progression to AIDS, suggesting that many more rare variants, with the potential for large effect sizes, or common variants with small effect sizes remain undiscovered. Tough and McLaren assessed the interaction of the host and viral genome and their influence on HIV disease. They estimated that 30% of variance is attributable to common heritable effects of host genetic variation. Viral sequence variability, shaped by both random mutations and the selective pressure of the human immune response (i.e. HLA protective epitopes), also influences disease progression, emphasizing the need to study HIV infection in the context of both host and viral genetic variation. Le Clerc et al. provide an overview of the results of large-scale "omics" technologies to identify host genes that contribute to HIV pathogenesis, including genotype association and functional genomic, transcriptomic, proteomic and epigenomic screens. The authors consider that the lack of signals by GWAS, beyond *HLA* and *CCR5*, are partially attributable to false negatives due to the statistical constraints (stringent multiple testing corrections) and the overall small sample size of most HIV GWAS studies. Moving forward, integrative analysis of big multi-omics datasets in a collaborative setting is key to capture the multidimensional complexity of HIV-1 pathogenesis and to reveal actionable targets for drug development.

CD8 T cells and natural killer (NK) cells are key players in the host immune response to viral infection, but the functions of these cells can be repressed by cell surface inhibitory molecules particularly, the killer cell immunoglobulin-like receptor KIR3DL1. HLA-Bw4 homozygosity has been associated with control of HIV-1 replication and protection from AIDS (Flores-Villanueva et al., 2001) and is carried in the two major HIV protective alleles *HLA-B**27 and *HLA-B**57. By quantifying multiple immune activation and response markers in acute HIV-1 patients carrying Bw4 homozygousity, Zhang et al. demonstrated that KIR3DL1$^-$ CD8 T/NK cells, conferring stronger T cell activation and response, contribute to the control of early HIV-1 replication.

An et al. studied African-specific alleles in *APOL1*, encoding the trypanolytic Apolipoprotein L1 protein. The two coding alleles restore the ability of APOL1 to lyse African trypanosomes causing human trypanosomiasis in carriers at the cost of increased risk of kidney disease in homozgyotes (Genovese et al., 2010). Although *in vitro* evidence suggests that APOL1 restricts HIV by multiple mechanisms (Taylor et al., 2014), An et al. found no evidence that *APOL1* renal risk variants affected HIV-1 susceptibility, viral load and disease progression to AIDS. Sezgin et al. reviewed human genes involved in human CMV infection and related diseases including HIV-1 opportunistic infection. They highlighted the relationship of immunoglobulin (Ig) allotype variation and CMV antibody response and immune-modulating genes that effect susceptibility to CMV diseases.

CONCLUSION

The articles in this Topic provide a comprehensive overview of the state of genetic and omic-based tools to elucidate the genetic architecture underpinning susceptibility to viral infections and the pathogenesis of viral diseases. Although omics-driven viral-host interaction studies are in their infancy, integrated omics-based investigations should reveal host factors that can be exploited for the prevention and effective treatment of viral infections.

AUTHOR CONTRIBUTIONS

All authors co-edited the Research Topic. All authors wrote, edited, and approved the final version of the Editorial.

FUNDING

The project was supported by grants from the U.S. National Institutes of Health (AI113267), the Commonwealth of Pennsylvania through the Hepatitis B Foundation. This project has been funded in part with Federal funds from the Frederick National Laboratory for Cancer Research, National Institutes of Health, under contract HHSN261200800001E and by the Intramural Research Program of the NIH, National Cancer Institute, Center for Cancer Research.

ACKNOWLEDGMENTS

The Editors would like to thank all Research Topic Authors and additional editors for their contributions.

REFERENCES

Blank, A., Markert, C., Hohmann, N., Carls, A., Mikus, G., Lehr, T., et al. (2016). First-in-human application of the novel hepatitis B and hepatitis D virus entry inhibitor myrcludex B. *J. Hepatol.* 65, 483–489. doi: 10.1016/j.jhep.2016.04.013

Chan, Y. K., and Gack, M. U. (2016). Viral evasion of intracellular DNA and RNA sensing. *Nat. Rev. Microbiol.* 14, 360–373. doi: 10.1038/nrmicro.2016.45

Chang, J., Block, T. M., and Guo, J. T. (2015). Viral resistance of MOGS-CDG patients implies a broad-spectrum strategy against acute virus infections. *Antivir. Ther.* 20, 257–259. doi: 10.3851/IMP2907

Dash, P. K., Kaminski, R., Bella, R., Su, H., Mathews, S., Ahooyi, T. M., et al. (2019). Sequential LASER ART and CRISPR treatments eliminate HIV-1 in a subset of infected humanized mice. *Nat. Commun.* 10, 2753. doi: 10.1038/s41467-019-10366-y

Flores-Villanueva, P. O., Yunis, E. J., Delgado, J. C., Vittinghoff, E., Buchbinder, S., Leung, J. Y., et al. (2001). Control of HIV-1 viremia and protection from AIDS are associated with HLA-Bw4 homozygosity. *Proc. Natl. Acad. Sci. U S A* 98, 5140–5145. doi: 10.1073/pnas.071548198

Gao, D., Wu, J., Wu, Y. T., Du, F., Aroh, C., Yan, N., et al. (2013). Cyclic GMP-AMP synthase is an innate immune sensor of HIV and other retroviruses. *Science* 341, 903–906. doi: 10.1126/science.1240933

Genovese, G., Friedman, D. J., Ross, M. D., Lecordier, L., Uzureau, P., Freedman, B. I., et al. (2010). Association of trypanolytic ApoL1 variants with kidney disease in African Americans. *Science* 329, 841–845. doi: 10.1126/science.1193032

Kellam, P., and Weiss, R. A. (2019). Protecting fetal development. *Science* 365, 118–119.

Rodriguez, A., Vigorito, E., Clare, S., Warren, M. V., Couttet, P., Soond, D. R., et al. (2007). Requirement of bic/microRNA-155 for normal immune function. *Science* 316, 608–11. doi: 10.1126/science.1139253

Taylor, H. E., Khatua, A. K., and Popik, W. (2014). The innate immune factor apolipoprotein L1 restricts HIV-1 infection. *J. Virol.* 88, 592–603. doi: 10.1128/JVI.02828-13

Zeisel, M. B., Lupberger, J., Fofana, I., and Baumert, T. F. (2013). Host-targeting agents for prevention and treatment of chronic hepatitis C - perspectives and challenges. *J. Hepatol.* 58, 375–384. doi: 10.1016/j.jhep.2012.09.022

Disclaimer: The content of this publication does not necessarily reflect the views or policies of the Department of Health and Human Services, nor does mention of trade names, commercial products, or organizations imply endorsement by the U.S. Government.

Conflict of Interest: The authors declare that the research was conducted in the absence of any commercial or financial relationships that could be construed as a potential conflict of interest.

Copyright © 2019 An, Guo and Winkler. This is an open-access article distributed under the terms of the Creative Commons Attribution License (CC BY). The use, distribution or reproduction in other forums is permitted, provided the original author(s) and the copyright owner(s) are credited and that the original publication in this journal is cited, in accordance with accepted academic practice. No use, distribution or reproduction is permitted which does not comply with these terms.

frontiers in Immunology

ORIGINAL RESEARCH
published: 17 May 2018
doi: 10.3389/fimmu.2018.00986

Initial Influenza Virus Replication Can Be Limited in Allergic Asthma Through Rapid Induction of Type III Interferons in Respiratory Epithelium

*Sujin An[1], Yung Jin Jeon[1,2], Ara Jo[1], Hyun Jung Lim[2], Young Eun Han[2], Sung Woo Cho[2], Hye Young Kim[3] and Hyun Jik Kim[1,2]**

[1] Department of Otorhinolaryngology, Seoul National University College of Medicine, Seoul, South Korea, [2] Seoul National University Hospital, Seoul, South Korea, [3] The Laboratory of Mucosal Immunology, Department of Biomedical Sciences, Seoul National University College of Medicine, Institute of Allergy and Clinical Immunology, Seoul National University Medical Research Center, Seoul, South Korea

OPEN ACCESS

Edited by:
Ping An,
Frederick National Laboratory for Cancer Research (NIH), United States

Reviewed by:
Ju-Tao Guo,
Baruch S. Blumberg Institute, United States
Yuhuan LI,
Institute of Medicinal Biotechnology (CAMS), China
Alan Chen-Yu Hsu,
University of Newcastle, Australia

***Correspondence:**
Hyun Jik Kim
hyunjerry@snu.ac.kr

Specialty section:
This article was submitted to Viral Immunology, a section of the journal Frontiers in Immunology

Received: 29 January 2018
Accepted: 20 April 2018
Published: 17 May 2018

Citation:
An S, Jeon YJ, Jo A, Lim HJ, Han YE, Cho SW, Kim HY and Kim HJ (2018) Initial Influenza Virus Replication Can Be Limited in Allergic Asthma Through Rapid Induction of Type III Interferons in Respiratory Epithelium. Front. Immunol. 9:986. doi: 10.3389/fimmu.2018.00986

Although asthmatics has been considered to be highly susceptible to respiratory viral infection and most studies have focused on exacerbation of asthma by influenza A virus (IAV) infection, few experimental evidences exist to directly demonstrate that asthmatic mice are actually resistant to IAV infection. Here, we show that asthmatic mice are not highly susceptible to IAV in the early stage of infection and type III interferon (IFN) maintains antiviral immune response in the lung of IAV-infected asthmatic mouse resulting in inhibition of initial viral spread. C57BL/6 mice with allergic asthma were infected with IAV (WS/33: H1N1) and survival rate, body weight, viral titer, histopathological findings of lung and cytokine profiles including IFNs and Th2 cytokines were measured. Notably, asthmatic mice were significantly resistant to IAV and showed lower viral load until 7 days after infection. Furthermore, IAV-infected asthmatic mice exhibited decreased Th2-related inflammation in lung tissue until 7 days. These increased antiviral resistant mechanism and reduced Th2 inflammation were attributable to rapid induction of type III IFNs and blockade of type III IFNs in asthmatic lung led to aggravated IAV infection and to enhance the production of Th2 cytokines. Asthmatic mice showed bi-phasic responses against IAV-caused lung infection such as rapid production of type III IFNs and subsequent induction of type II IFNs. Actually, IAV-infected asthmatic mice become vulnerable to IAV infection after 7 days with noticeable morbidity and severe weight loss. However, intranasal administration of type III IFNs protects completely asthmatic mice from IAV-mediated immunopathology and lung infection until 14 days after infection. Taken together, our study indicates that the rapid induction of type III IFN might be distinctive immunological findings in the respiratory tract of IAV-infected asthmatic mice at the early stage of infection and crucial for suppression of initial viral spread *in vivo* asthma accompanying with restriction of Th2 cytokine productions.

Keywords: influenza A virus, type III interferon, Th2 cytokines, asthma, acute viral lung infection

INTRODUCTION

Allergic asthma is caused by sensitization to innocuous allergens *via* airway exposure. This type of asthma is thought to arise from an imbalance in T helper type I (Th1)-Th2 immune regulation, resulting in increased levels of the Th2 cytokines interleukin (IL)-4, IL-5, and IL-13, which have been proven to be important drivers of allergic airway inflammation in asthma (1, 2). Asthma exacerbations are acute attacks of asthma, accompanied by sudden decrease of lung function, most often precipitated by a respiratory viral infection and are responsible for the vast majority of the mortality associated with asthma. Although adequate control of asthma has been achieved, more appropriate controls for respiratory viral infection are needed to reduce acute exacerbation of respiratory symptoms in asthmatics (3, 4).

The innate immune system of the respiratory epithelium serves as the first line of antiviral defense against invading respiratory viruses including influenza A virus (IAV) (5). Traditionally, the antiviral innate immune response has been thought to be exclusively mediated by type I interferons (IFNs) followed by the adaptive immune response (5, 6). However, emerging evidence indicates that type III IFN is likely to be mainly required for immune responses in respiratory tract. In particular, type III IFN has been shown to be dominant IFN which is produced in respiratory tract against respiratory viral infection and provide front-line protection against respiratory virus to suppress initial viral spread in respiratory epithelium (7, 8). Moreover, type III IFN-mediated innate immune response is necessary to protect the lungs from IAV infection beyond antiviral properties of type I IFNs (9).

Impaired innate immune responses have been reported to be potentially responsible for the increased susceptibility to infections in asthmatics. Moreover, dysregulation of antiviral immune responses related to Th2 cytokines has been suggested to explain the higher susceptibility of the asthmatic respiratory epithelium to viral infection (10–12). Strong links between low expression of type III IFNs, severity of allergic asthma, and asthma exacerbations have been described (13). In the absence of detectable viral infection, asthmatic patients with active disease still exhibit an inverse correlation between type III IFN level and the severity of allergic response in the airways (12). However, some studies have also investigated whether asthmatic mice are more resistant to respiratory viral infection and which bystander immune mechanisms are activated during the induction of asthma and contribute to protecting the asthmatics against respiratory viral infection (14, 15).

To address the antiviral resistance of IAV-infected asthmatic mice, we sought to determine first if the asthmatic mice are more susceptible or resistant to IAV infection. We found that the asthmatic mice were not highly susceptible to IAV infection and type III IFNs were preferentially induced in the lung of IAV-infected asthmatic mouse at early stage of infection. Rapid induction of type III IFNs led to accelerated clearance of IAV, accompanied by increased type II IFN secretion. In addition, intranasal administration of type III IFNs provided more potent antiviral resistance to IAV-infected asthmatic mice. This study suggest that a better understanding about the role of type III IFNs in this asthmatic airway need to be achieved to prevent higher viral loads in the asthmatic airway and it can provide new insights into strategies for reducing asthmatic exacerbation from respiratory viral infection.

MATERIALS AND METHODS

Allergen Sensitization and Challenge Protocol

C57BL/6J (B6) mice (Orientalbio, Seoul, Korea) aged 7 weeks (19–23 g) were used for the development of non-asthmatic and asthmatic mice. Asthma was induced by first sensitizing male B6 mice intraperitoneally (i.p.) with OVA in aluminum hydroxide and then challenging intranasally (i.n.) with soluble OVA (OVA/OVA). Phosphate-buffered saline (PBS)-challenged mice (OVA/PBS) (hereafter referred to as non-asthmatic mice) were used as a negative control. B6 mice were sensitized with two intraperitoneal injections on days 0 and 14 of 7.5 μg OVA (Grade V; Sigma, MO, USA) complexed with aluminum hydroxide as adjuvant (Sigma, MO, USA). On days 21, 22, 23, and 24, mice were challenged intranasally with 7.5 g OVA mixed with PBS (OVA/OVA). Control mice received an intraperitoneal injection of OVA at the same concentration and were challenged with PBS alone by intranasal inoculation (OVA/PBS). Airway hyper-responsiveness (AHR) was measured in anesthetized mechanically ventilated B6 mice (Flexivent ventilator, SciReq, Montreal, QC, Canada) at 24 h after the last intranasal OVA exposure. AHR was measured invasively using a body plethysmograph (Buxco Electronics, Inc., Wilmington, NC, USA).

Mice and Virus Inoculation

Influenza A virus (WS/33: H1N1, ATCC, Manassas, VA, USA) was used to induce acute viral lung infection. Virus stocks were grown in Madin–Darby canine kidney cells in virus growth medium according to a standard procedure (16). Briefly, after 48 h of incubation at 37°C, the supernatants were harvested and centrifuged at 5,000 rpm for 30 min to remove cellular debris. Virus stocks were titrated on MDCK cells using a tissue culture infectious dose assay and stored at −80°C. The B6 mice used in the study, like other commercially available strains of inbred mice, carry a dysfunctional Mx1 gene and are not congenic B6 mice with a functional Mx1 gene, which are derived from influenza-resistant mice.

For viral infections, IAV (WS/33, H1N1; 213 pfu in 30 μl PBS) were inoculated into WT mice by intranasal delivery and asthmatic mice (OVA/OVA) were also infected with IAV at 25 days after first sensitization. Mice were euthanized at the end of each experiment with overdose of tiletamine/zolazepam (5 mg) and xylazine (0.23 mg) and after euthanizing, bronchoalveolar lavage (BAL) fluid was obtained from the lungs by lavaging with 1,000 μl 0.5 mM ethylene diamine tetraacetic acid in PBS after cannulation of the trachea. The BAL fluid was used for enzyme-linked immunosorbent assay (ELISA) for measuring secreted protein levels and plaque assay to determine the viral titer. Mouse lung tissue was also harvested for real-time polymerase chain reaction (PCR), microarray, and immunohistochemistry analyses.

Real-Time PCR

Lung tissue was obtained from mice infected with WS/33 (H1N1) on 1, 3, 5, 7, 10, and 14 days postinfection, after which total RNA was isolated using TRIzol (Invitrogen). cDNA was synthesized from 3 μg of RNA with random hexamer primers and Moloney murine leukemia virus reverse transcriptase (Perkin Elmer Life Sciences, Waltham, MA, USA and Roche Applied Science, Indianapolis, IN, USA). Amplification was performed using the TaqMan Universal PCR Master Mix (PE Biosystems, Foster City, CA, USA) according to the manufacturer's protocol. Briefly, amplification reactions had a total volume of 12 μl and contained 2 μl of cDNA (reverse transcription mixture), oligonucleotide primers (final concentration of 800 nM), and TaqMan hybridization probe (200 nM). Real-time PCR probes were labeled at the 5′ end with carboxyfluorescein (FAM) and at the 3′ end with the quencher carboxytetramethylrhodamine (TAMRA).

To quantify the intracellular levels of viral RNA and host gene expression levels, cellular RNA was used to generate cDNA. IAV level was monitored using quantitative PCR to amplify the *PA* gene (segment 3) with forward and reverse primers and probe 5′-ggccgactacactctcgatga-3′, 5′-tgtcttatggtgaatagcctggttt-3′, and 5′-agcagggctaggatc-3′, respectively. Primers for mouse IFN-α, IFN-β, IFN-$\lambda_{2/3}$, and IFN-γ were purchased from Applied Biosystems (Foster City, CA, USA). Real-time PCR was performed using the PE Biosystems ABI PRISM® 7700 Sequence Detection System. Thermocyling parameters were as follows: 50°C for 2 min, 95°C for 10 min, and then 40 cycles of 95°C for 15 s and 60°C for 1 min. Target mRNA levels were quantified using target-specific primer and probe sets for IAV WS/33 (H1N1), IFN-α, IFN-β, IFN-$\lambda_{2/3}$, and IFN-γ. All PCR assays were quantitative and utilized plasmids containing the target gene sequences as standards. All reactions were performed in triplicate, and all real-time PCR data were normalized to the level of the housekeeping gene glyceraldehyde phosphate dehydrogenase (1×10^6 copies) to correct for variation between samples.

Quantification of Secreted Cytokines

The levels of secreted IFN-α (42120-1), IFN-β (42400-1), IFN-λ2/3 (DY1789B), and IFN-γ (DY485) were quantified using a Duoset ELISA kit (R&D Systems; Minneapolis, MN, USA) according to the manufacturer's instructions for BAL fluid. This kit detects IFN-β, IL-28A, IL-28B, and IFN-γ. The working range of the assay was 62.5–4,000 pg/ml. The levels of secreted IL-4, IL-5, IL-6, and IL-13 were measured using a Luminex multiplex assay (R&D Systems) according to the manufacturer's instructions.

Inoculation With IFN-$\lambda_{2/3}$-Neutralizing and IFN-γ-Neutralizing Antibodies

Specific neutralizing antibodies against IFN-$\lambda_{2/3}$ and IFN-γ were used to functionally inhibit IFN-λ and IFN-γ in the mouse respiratory tract. Anti-IFN-$\lambda_{2/3}$ (cat number: MAB1789) and anti-IFN-γ (cat number: MAB4851) neutralizing antibodies and isotype-control antibodies (rat IgG) were purchased from R&D Systems.

These antibodies were found to inhibit the secretion of IFN-$\lambda_{2/3}$ and IFN-γ by more than 70% in BAL fluid. Neutralizing antibodies (10 μg/30 μl) were mixed with PBS and inoculated by intranasal delivery according to the manufacturer's instructions (R&D Systems Inc.), concurrent with IAV infection. This procedure did not affect mouse viability. ELISA analysis confirmed that the neutralizing antibodies partially inhibited IFN-$\lambda_{2/3}$ and IFN-γ secretion.

Intranasal Delivery of Recombinant IFN-$\lambda_{2/3}$

To determine whether IFN-$\lambda_{2/3}$ controls acute IAV lung infection in our *in vivo* model, WT mice ($N = 5$) were administered recombinant IFN-$\lambda_{2/3}$ *via* the intranasal route in a total volume of 30 μl PBS. The recombinant IFN-$\lambda_{2/3}$ was purchased from Invitrogen (Carlsbad, CA, USA). IFN-λ_2 and IFN-λ_3 were mixed (IFN-λ_2: 1 μg, IFN-λ_3: 1 μg), and recombinant IFN-$\lambda_{2/3}$ was inoculated into mice by intranasal delivery at the same time as IAV infection. IAV-infected mice were treated with mixed recombinant IFN-λ through the nasal cavity.

Immunohistochemistry and Histological Analysis

Lung tissue was fixed in 10% (vol/vol) neutral buffered formalin and embedded in paraffin. Paraffin-embedded tissue slices were stained with hematoxylin/eosin (H&E) or periodic acid Schiff (PAS) solution (Sigma, Deisenhofen, Germany). Histopathological analysis of inflammatory cells in H&E-stained lung sections was performed in a blinded fashion using a semi-quantitative scoring system as previously described (13). Lung sections from at least five mice were examined. Briefly, peribronchiolar inflammation was scored as follows: 0, normal; 1, a few cells; 2, a ring of inflammatory cells one layer deep; 3, a ring of inflammatory cells two to four cells deep; and 4, a ring of inflammatory cells more than four cells deep (maximum score = 8). The histological score for PBS/PBS control mouse lung tissue was 0. At least six separate areas from similar sections within a single mouse were assessed, and at least five mice were assessed. The five best sections were used for evaluation. PMNs were counted by an examiner who was blinded to the experimental group; results are expressed as the number of cells per high power field.

Plaque Assay

Virus samples were serially diluted with PBS. Confluent monolayers of MDCK cells in six-well plates were washed twice with PBS and then infected in duplicate with 250 μl/well of each virus dilution. The plates were incubated at 37°C for 45 min to facilitate virus adsorption. Following adsorption, a 1% agarose overlay in complete MEM supplemented with TPCK trypsin (1 μg/ml) and 1% fetal bovine serum was applied. The plates were incubated at 37°C, after which cells were fixed with 10% formalin at 2 days postinfection.

Flow Cytometry

Single-cell suspensions were stained with the following monoclonal antibodies: Texas Red-anti-CD45 (Invitrogen), fluorescein isothiocyanate-anti-lineage cocktail (anti-CD3, anti-CD11c, anti-

CD11b, anti-CD19, anti-CD49b, anti-F4/80, and anti-FcεRIα), Brilliant Violet 421-anti-Siglec-F (BD Biosciences), allophycocyanin (APC)-anti-CD11b, PE/Cy7-anit-CD90.2, and PE-anti-NK1.1 (BioLegend). All samples were blocked with 1 μg Fc block (from 2.4G2 ATCC HB-197) for 15 min before antibody staining at 4°C for 30 min in PBS containing 2% FCS (2% FCS-PBS). Cells were washed twice in 2% FCS-PBS, after which data were collected on a BD LSRFortessa X-20 cytometer (BD Biosciences). Data analysis was performed using FlowJo v10 10.1r1 (FlowJo, LLC, Ashland, OR, USA).

Intracellular Cytokine Staining

For intracellular cytokine staining, single-cell suspensions were incubated in RPMI medium containing 10% FBS with PMA (100 ng/ml), ionomycin (1 μg/ml), and GolgiStop (BD) at 37°C for 4 h. After surface staining, the cells were fixed and permeabilized with a Fixation/Permeabilization Kit (eBioscience). Finally, the cells were stained with PE-anti-T-bet and APC-anti-IFN-γ antibodies (Biolegend). The respective isotype-control antibody was also used for each experiment.

Statistical Analyses

Real-time PCR, plaque assay, and ELISA results are presented as median values (interquartile ranges for 25 and 75%). The statistical significance of differences between two groups was determined by the Mann–Whitney test. Histological scores were also evaluated by a non-parametric test (Wilcoxon rank sum test). All statistical analysis was performed with GraphPad Prism software (version 5; GraphPad Software, La Jolla, CA, USA). p Values <0.05 were considered to be statistically significant.

RESULTS

OVA-Sensitized/Challenged C57BL/6 (B6) Mice Exhibit a Typical Asthmatic Phenotype

To assess the influence of allergic airway inflammation on susceptibility to respiratory viral infection, we developed an OVA-sensitized/challenged allergic asthma mouse model on a B6 genetic background (**Figure 1A**). Initially, AHR was measured in mice after inoculation of methacholine. Asthmatic mice (OVA/OVA) were observed to have a methacholine-induced increase in total lung resistance ($N = 3$, **Figure 1B**). As a complementary approach, H&E- and PAS-stained micrographs of lung sections were obtained from non-asthmatic (OVA/PBS) and asthmatic mice. Histological analysis revealed that the lungs of asthmatic mice were severely inflamed, with extensive inflammatory cell infiltration at the peribronchial areas of the lung. This infiltration was accompanied by significantly increased goblet cell metaplasia (**Figure 1C**). We found that the number of eosinophils was also increased in total lung tissue of asthmatic mice, and that the numbers of lymphocytes, neutrophils, and eosinophils were significantly increased in the BAL fluid of asthmatic mice (**Figures 1D,E**). Collectively, these findings demonstrate that an allergic asthma mouse model could be established with B6 mice, and that this model could be used to investigate the susceptibility of asthmatic mice to influenza virus infection.

Asthmatic Mice Are Not Highly Susceptible to IAV Infection

Previously, we found that IAV-infected non-asthmatic mice exhibited a significant decrease in mean body weight and a decrease in body temperature, with the lowest drop at 7 dpi. They also showed 80% survival until 14 dpi (17). In this study, non-asthmatic mice ($N = 5$) and asthmatic mice ($N = 5$) were inoculated with WS/33 (H1N1) to determine the susceptibility of asthmatic mice to IAV lung infection. Then, the body weights and survival rates of non-asthmatic and asthmatic mice were compared until 7 dpi. Non-asthmatic mice showed significant weight loss from 5 dpi, and 20% of the mice died in the first 7 days after IAV infection. However, asthmatic mice did not exhibit significant weight loss or noticeable morbidity until 7 dpi, and all asthmatic mice survived the IAV infection (**Figures 2A,B**). The levels of IAV mRNA in non-asthmatic and asthmatic mice lung were next analyzed by real-time PCR, and the viral titers in the BAL fluid were measured by plaque assay at 7 dpi. The mean level of IAV mRNA and the mean viral titer were both significantly elevated at 7 dpi (mRNA level: 2.1×10^4, viral titer: 3.3×10^5 pfu/ml) in non-asthmatic mice. By contrast, the levels of IAV mRNA and viral titer were much lower in IAV-infected asthmatic mice (mRNA level: 1.4×10^3, viral titer: 8.1×10^4 pfu/ml, **Figures 2C,D**). As a complementary approach, lung sections were obtained from non-asthmatic and asthmatic mice at 7 dpi, and H&E-stained micrographs were generated. Histological analysis revealed severe subepithelial consolidation, peribronchial edema, and increased epithelium detachment in non-asthmatic mouse lung sections harvested at 7 dpi. The lungs of asthmatic mice were severely inflamed, with extensive inflammatory cell infiltration at the peribronchial areas without IAV infection. Notably, these histopathological findings were not detectable in the lung sections harvested from IAV-infected asthmatic mice at 7 dpi and the mean histological score was significantly lower in IAV-infected asthmatic mice (8.6 for the non-asthmatic mice vs. 1.8 for the asthmatic mice) (**Figure 2E**). This finding was accompanied by significantly increased goblet cell metaplasia in asthmatic mice, whereas remarkable reduction of goblet cells was observed in the respiratory epithelium of IAV-infected asthmatic mice at 7 dpi (13.2 in asthmatic mice vs. 4.6 in IAV-infected asthmatic mice, **Figure 2F**). In addition, AHR was measured after inoculation of methacholine in IAV-infected asthmatic mice at 7 dpi and a methacholine-induced increase in total lung resistance was not observed in IAV-infected asthmatic mice (Figure S1 in Supplementary Material).

A multiplex assay was next performed to quantify the levels of secreted Th2 cytokines, such as IL-4, IL-5, and IL-13, in the BAL fluid of asthmatic mice. While higher secretion of Th2 cytokines was observed at 7 dpi in asthmatic mice without IAV infection (IL-4: 532.3 ± 85.1 pg/ml, IL-5: 964.7 ± 98.5 ng/ml, IL-13: 2,487.5 ± 765.5 ng/ml), cytokine secretion was significantly attenuated in IAV-infected asthmatic mice (IL-4: 64.2 ± 11.5 pg/ml, IL-5: 121.7 ± 32.6 ng/ml, IL-13: 498.5 ± 104.8 ng/ml, **Figure 2G**). These results indicate that asthmatic mice were not highly susceptible to IAV infection. Moreover, IAV-infected asthmatic mice

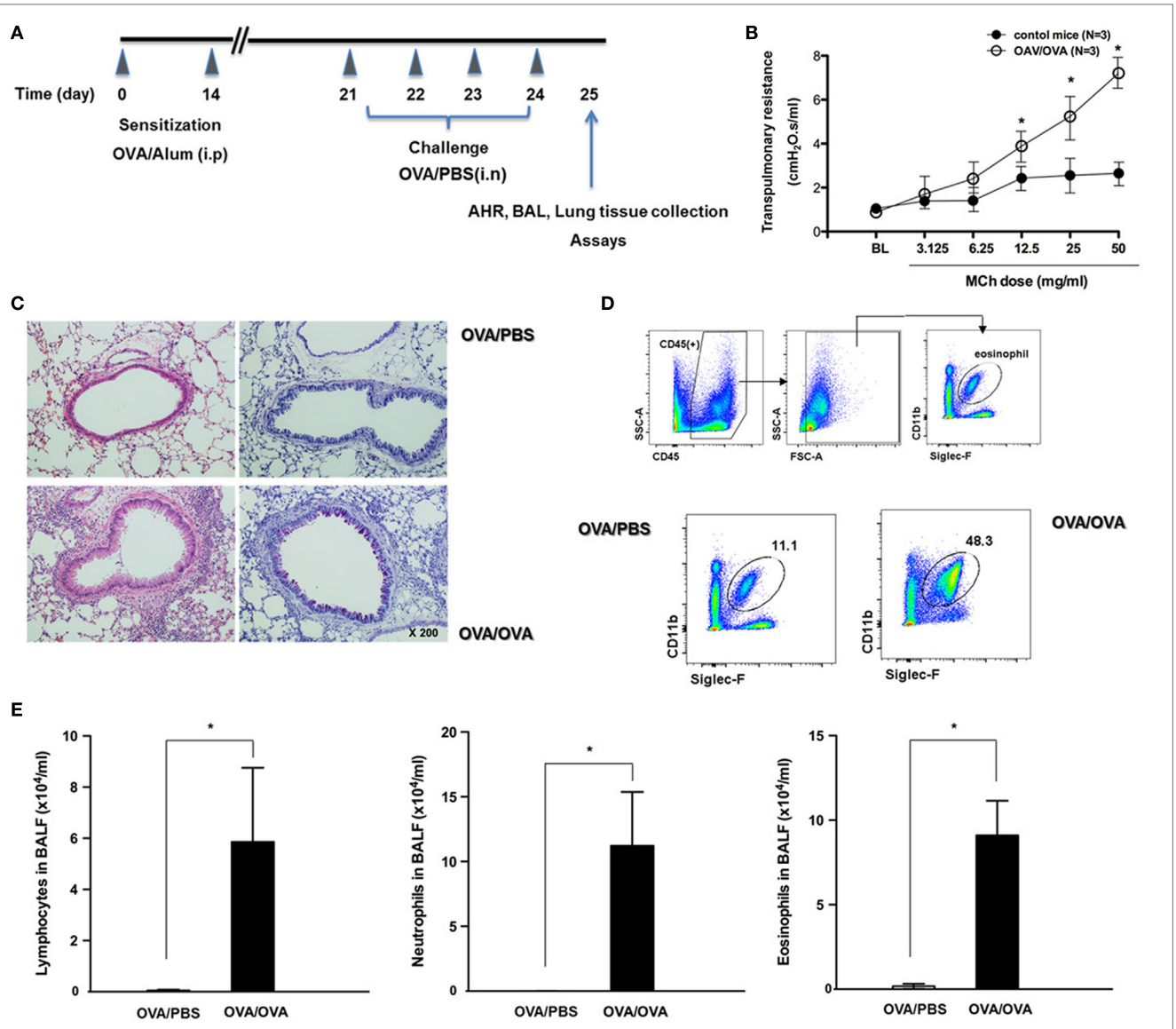

FIGURE 1 | The development of allergic asthmatic mouse model. **(A)** The experimental protocol for development of allergic asthmatic mouse using C57BL/6. Non-asthmatic mice [OVA/phosphate-buffered saline (PBS), $N = 5$]. **(B)** Airway hyper-responsiveness was measured as methacholine-induced increases in transpulmonary resistance in mechanically ventilated mice. Data are expressed as mean value of percentage increased from base line of the transpulmonary resistance ± SD values of three mice (white dot: OVA/OVA, black dot: OVA/PBS). **(C)** Histological assessment of mucus secretion in asthmatic mice. Periodic acid Schiff-stained sections were assessed from five mice. **(D)** Flow cytometric analysis was done for isolation of eosinophils using anti-CD11c and anti-Siglec-F antibodies. **(E)** Bronchoalveolar lavage (BAL) fluid differential counts for lymphocytes, neutrophils, and eosinophils expressed as mean ± SD.

exhibited minimal induction of Th2 cytokine secretion accompanying decreased asthma-related histopathological findings, including goblet cell hyperplasia.

Asthmatic Mice Maintain Intact IFN-Related Innate Immunity After IAV Infection

To assess whether the increased antiviral resistance of asthmatic mice was due to an increased IFN-related immune response, we investigated the influence of asthma status on induction of IFN from the respiratory tract after IAV infection. Real-time PCR analysis revealed that the mRNA levels of IFN-α_4, IFN-β, and IFN-$\lambda_{2/3}$ were higher at day 7 after IAV infection in lung tissue from non-asthmatic mice (IFN-α4: $1.2 \times 10^4 \pm 3.4 \times 10^3$, IFN-β: $2.8 \times 10^4 \pm 4.3 \times 10^3$, IFN-$\lambda_{2/3}$:$1.4 \times 10^5 \pm 5.2 \times 10^4$, **Figure 3A**) but minimal induction of IFN mRNA, especially IFN-$\lambda_{2/3}$, was observed in lung tissue from IAV-infected asthmatic mice (IFN-$\lambda_{2/3}$:$4.8 \times 10^4 \pm 1.4 \times 10^4$). Next, ELISA was performed to quantify the levels of secreted IFNs in the BAL fluid after IAV infection. The levels of secreted IFN-β and IFN-$\lambda_{2/3}$ were all increased

at day 7 after IAV infection in the BAL fluid of non-asthmatic mice (IFN-β: 1,514.5 ± 387.7 pg/ml, IFN-$\lambda_{2/3}$: 3,298.6 ± 869.4 pg/ml), but IAV-infected asthmatic mice exhibited impaired secretion of IFN-β and IFN-$\lambda_{2/3}$ at 7 dpi (IFN-β: 219.5 ± 47.6 ng/ml, IFN-$\lambda_{2/3}$: 683.4 ± 97.7 ng/ml) (**Figure 3B**). However, significantly higher induction of IFN-γ mRNA ($6.4 \times 10^4 \pm 1.4 \times 10^4$) and protein

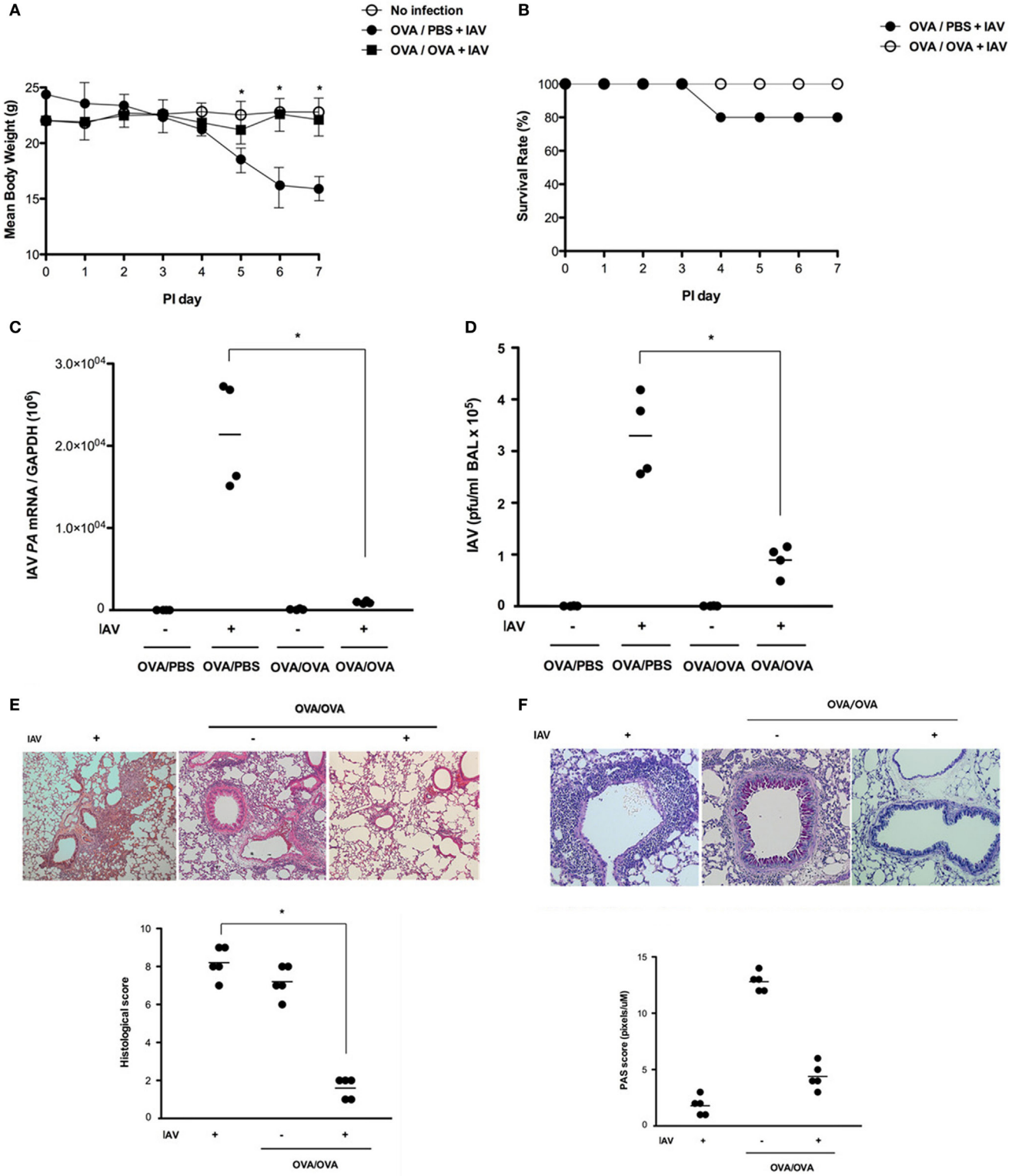

FIGURE 2 | Continued

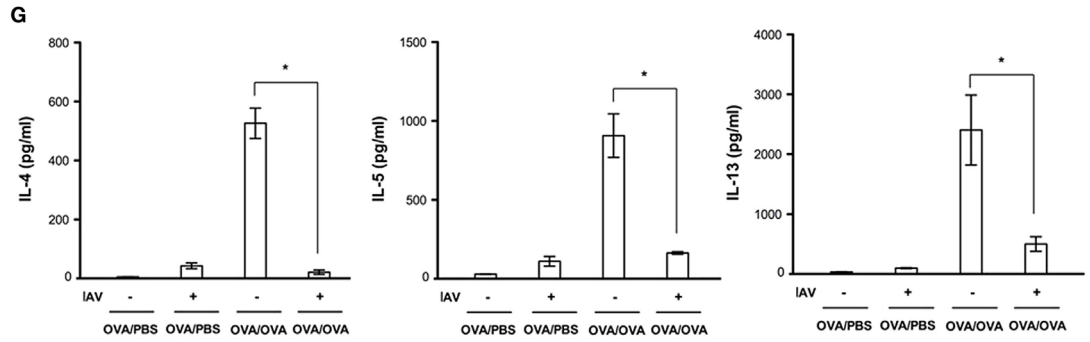

FIGURE 2 | Kinetics of influenza A virus (IAV) infection in non-asthmatic and asthmatic mice. Non-asthmatic ($N = 5$) and asthmatic mice ($N = 5$) were infected with 213 pfu IAV WS/33 (H1N1), and body weight **(A)** and survival rate [**(B)**, $N = 20$] were assessed until 7 dpi. The IAV mRNA **(C)** and viral titer **(D)** in lung tissue and bronchoalveolar lavage (BAL) fluid, respectively, were determined at 7 dpi. Hematoxylin/eosin (H&E)-stained micrographs were also generated from lung sections obtained at 7 dpi **(E)**. Histological assessment for mucus secretion was performed on periodic acid Schiff (PAS)-stained lung sections of asthmatic mice **(F)**. A multiplex assay was performed to quantify the levels of secreted Th2 cytokines (i.e., IL-4, IL-5, and IL-13) in the BAL fluid of non-asthmatic and asthmatic mice **(G)**. Micrographs shown are representative of lung sections from five mice. Polymerase chain reaction, plaque assay, and multiplex assay results are presented as mean ± SD from five independent experiments (*$p < 0.05$ compared with the levels of non-asthmatic and asthmatic mice at 7 dpi).

secretion (1,865.7 ± 731.4 pg/ml) were observed at 7 dpi in the lung tissue and BAL fluid of IAV-infected asthmatic mice compared with non-asthmatic mice (mRNA: $2.4 \times 10^3 \pm 5.4 \times 10^2$, protein: 286.3 ± 48.7 pg/ml). This finding suggests that the IFN-γ production in IAV-infected asthmatic mice observed at 7 dpi might be critically involved in resistance to IAV infection and decreased secretion of Th2 cytokines in the asthmatic respiratory tract.

While neither IFN-β nor IFN-$\lambda_{2/3}$ was induced in the respiratory tract of IAV-infected asthmatic mice at 7 days after infection, we next analyzed the levels of these IFNs in asthmatic mice until 7 days after infection to determine if rapid and transient alterations occurred. To this end, asthmatic mice were infected with IAV WS/33 (H1N1) *via* the intranasal route (213 pfu/30 μl), and the production of IFNs and Th2 cytokines was measured at 0, 1, 3, 5, and 7 dpi.

Real-time PCR and ELISA analyses revealed that induction of IFN-γ mRNA and secretion of IFN-γ did not occur until 5 dpi ($3.6 \times 10^4 \pm 6.5 \times 10^3$ and 2,482.5 ± 587.3 pg/ml, respectively) in IAV-infected asthmatic mice, with the highest levels exhibited at 7 dpi. By contrast, transcription ($2.8 \times 10^4 \pm 4.6 \times 10^3$) and secretion of IFN-$\lambda_{2/3}$ (3,002.4 ± 1,284.9 pg/ml) were elevated most significantly at 1 dpi compared with the mRNA levels of IFN-α and -β; these levels gradually decreased until 7 dpi (**Figures 3C,D**). This rapid production of IFN-$\lambda_{2/3}$ was accompanied by significant reduction of IL-4, IL-5, and IL-13 in the BAL fluid of IAV-infected asthmatic mice until 7 dpi (**Figure 3E**). Goblet cell metaplasia and hyper-secretion of airway mucus appeared to be significantly reduced from 3 dpi; moreover, PAS score of asthmatic mice were lowest at 7 days after IAV infection (PI 0d: 12.7, PI 1d: 7.8, PI 3d: 2.6, PI 5d: 1.4, PI 7d: 1.3, **Figure 3F**).

These findings show that IFN-$\lambda_{2/3}$ and IFN-γ were both markedly induced, and that IFN-$\lambda_{2/3}$ induction was driven rapidly after IAV infection in the lungs of IAV-infected asthmatic mice than IFN-γ. This induction appears to reduce Th2 cytokine secretion in asthmatic mice after infection, which might be required for the enhanced resistance of asthmatic mice to IAV replication.

Rapid Induction of IFN-λ Limits IAV Replication in the Lungs of Asthmatic Mice and Controls IFN-γ Secretion From Respiratory Epithelial Cells

We next analyzed whether IFN-$\lambda_{2/3}$ and IFN-γ were required to control IAV replication and whether their levels influenced host susceptibility to infection in asthmatic mice. Asthmatic mice ($N = 5$) were infected with IAV WS/33 (H1N1) *via* the intranasal route (213 pfu/30 μl) and simultaneously administered neutralizing antibodies (10 μg/30 μl) that functionally inhibit either IFN-$\lambda_{2/3}$ or IFN-γ. Histological analysis of IAV-infected asthmatic mouse lung tissue showed that severe inflammation with PMN infiltration at the peribronchial areas was not observed at 7 dpi, and that the histological scores returned to normal levels. However, greater lung damage and greater mean histological scores were observed after administration of IFN-$\lambda_{2/3}$- and γ-neutralizing antibodies (IAV infection: 2.6 vs. IAV + IFN-$\lambda_{2/3}$-neutralizing antibodies: 12.4, IAV + IFN-γ-neutralizing antibodies: 12.5; **Figure 4A**). Furthermore, the viral titer in the BAL fluid was significantly higher in IAV-infected asthmatic mice that received IFN-$\lambda_{2/3}$-($1.3 \times 10^6 \pm 3.8 \times 10^5$) and γ-neutralizing antibodies ($1.4 \times 10^6 \pm 2.6 \times 10^5$) compared with IAV-infected asthmatic mice ($2.4 \times 10^4 \pm 1.6 \times 10^3$) (**Figure 4B**).

Influenza A virus infection has been shown to incite a robust IFN-γ response in the lung, promoting the development of adaptive immunity (18). IFN-γ has been proposed to be predominantly produced by activated innate lymphoid cell type I (ILC1) and natural killer (NK) cells (19). Our current findings also showed production of IFN-γ peaked at 7 dpi in the lung tissue and BAL fluid of IAV-infected asthmatic mice and we investigated the target cells that produce IFN-γ in asthmatic mice at 7 dpi. Non-asthmatic and asthmatic mice were infected with IAV

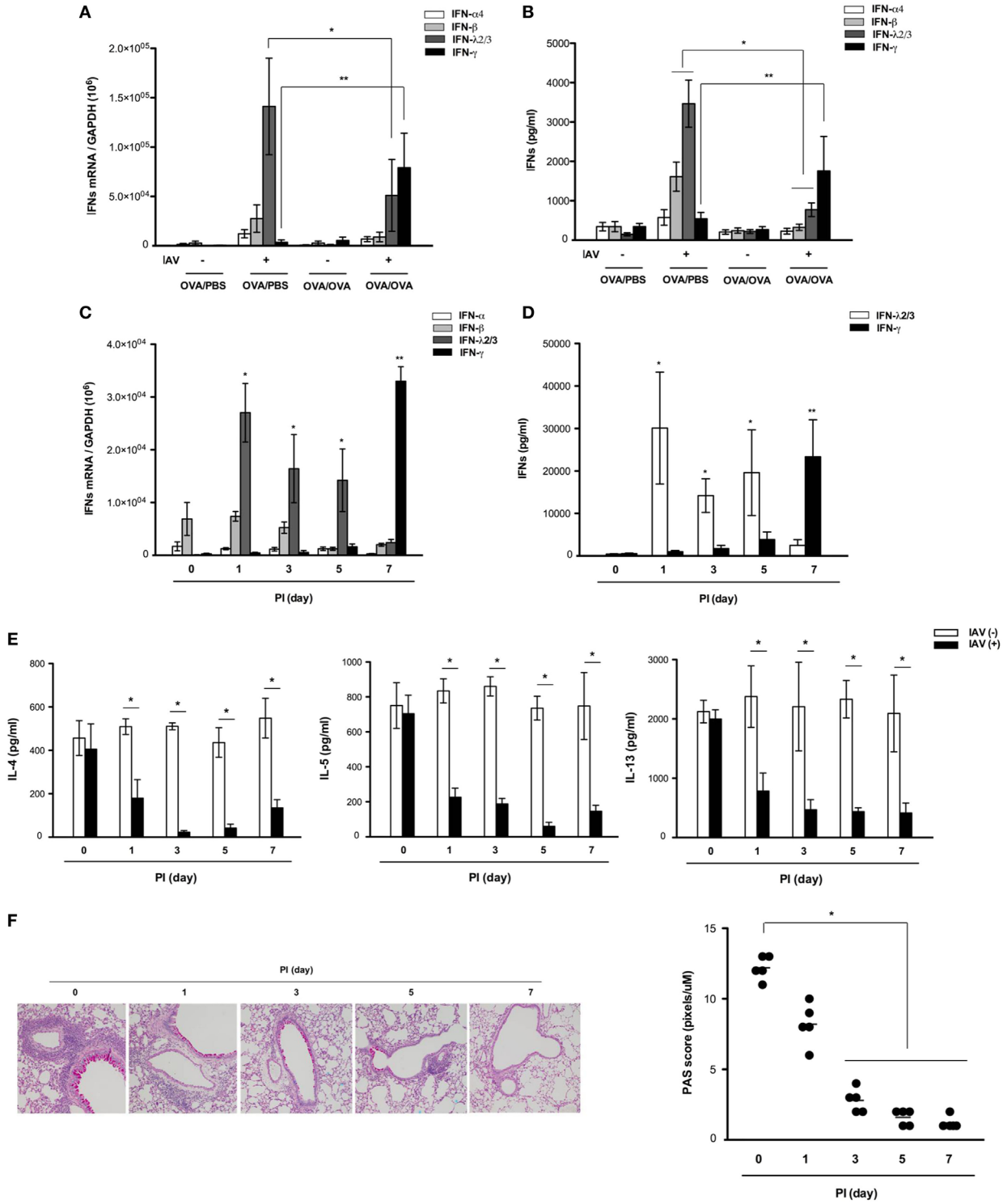

FIGURE 3 | Expression and secretion of various interferons (IFNs) after influenza A virus (IAV) infection of non-asthmatic and asthmatic mice. Non-asthmatic ($N = 5$) and asthmatic mice ($N = 5$) were infected with 213 pfu IAV WS/33 (H1N1). The mRNA levels in the lung **(A)** and levels of secreted IFN-α, IFN-β, IFN-$\lambda_{2/3}$, and IFN-γ in bronchoalveolar lavage (BAL) fluid **(B)** were determined by real-time polymerase chain reaction (PCR) and enzyme-linked immunosorbent assay, respectively, at 7 days after infection. The mRNA levels and levels of secreted IFN-α, IFN-β, IFN-$\lambda_{2/3}$, and IFN-γ in the lung **(C)** and BAL fluid **(D)** were determined in IAV-infected asthmatic mice until 7 dpi. A multiplex assay was performed to quantify the levels of secreted Th2 cytokines in the BAL fluid of IAV-infected asthmatic mice until 7 dpi **(E)**. Histological assessment was performed using periodic acid Schiff (PAS)-stained lung sections of asthmatic mice ($N = 5$) **(F)** harvested at 0 ($N = 5$), 1 ($N = 5$), 3 ($N = 5$), 5 ($N = 5$), and 7 ($N = 5$) dpi. Micrographs shown are representative of five mice. PCR, plaque assay, and multiplex assay results are presented as mean ± SD from five independent experiments (*,**$p < 0.05$ compared with the levels in non-asthmatic and asthmatic mice at 7 dpi, **Figures 2B–D** *IFN-$\lambda_{2/3}$, **IFN-γ).

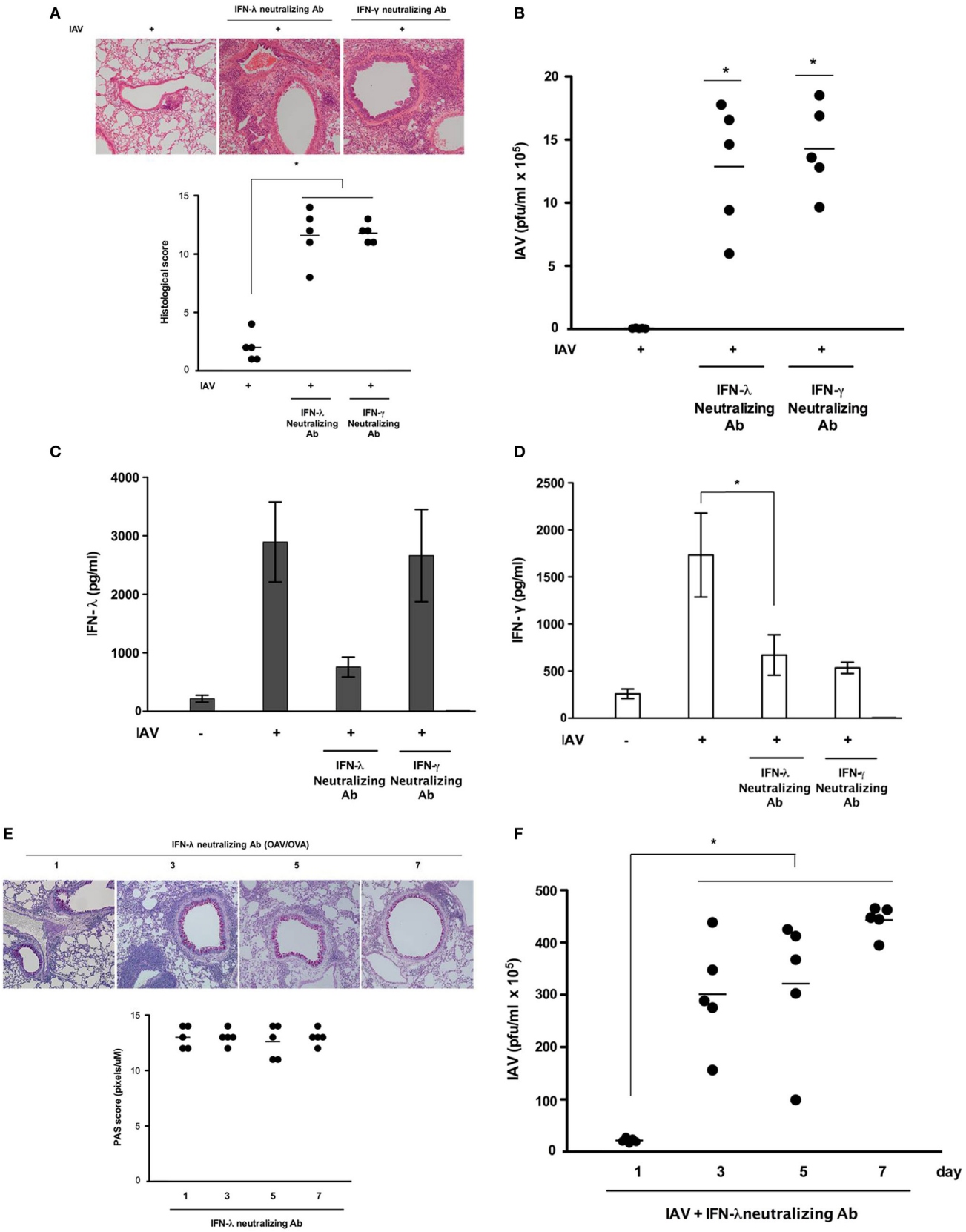

FIGURE 4 | Continued

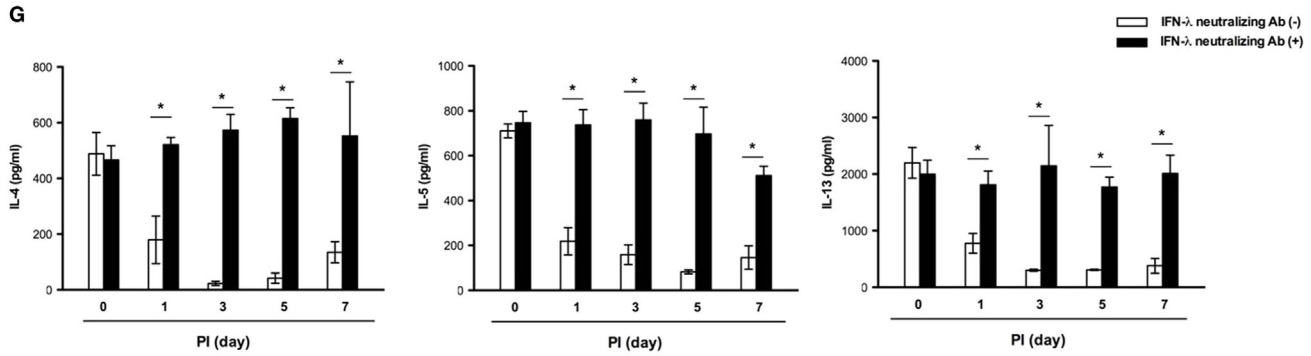

FIGURE 4 | Acute influenza A virus (IAV) infection is aggravated in asthmatic mice administered neutralizing antibodies against interferon (IFN)-$\lambda_{2/3}$ and IFN-γ. Asthmatic mice with isotype-control (rat IgG) antibodies were infected with 213 pfu IAV WS/33 (H1N1) ($N = 5$) and treated with neutralizing antibodies against IFN-$\lambda_{2/3}$ ($N = 5$) or IFN-γ ($N = 5$). Hematoxylin/eosin (H&E)-stained micrographs were generated from lung sections obtained from IAV-infected asthmatic mice on day 7 **(A)**. Viral titer **(B)** and secreted IFN level **(C,D)** were determined by plaque assay and enzyme-linked immunosorbent assay. Histological assessment was performed using periodic acid Schiff (PAS)-stained lung sections of asthmatic mice ($N = 5$) **(E)**. Viral titer **(F)** and Th2 cytokine levels **(G)** were assessed using a plaque assay and a multiplex assay at 0 ($N = 5$), 1 ($N = 5$), 3 ($N = 5$), 5 ($N = 5$), and 7 ($N = 5$) dpi. Micrographs shown are representative of lung sections from five mice. Polymerase chain reaction, plaque assay, and multiplex assay results are presented as mean ± SD from five independent experiments (*$p < 0.05$ compared with the values of mice treated with IgG and neutralizing antibodies).

WS/33 (H1N1) (213 pfu/30 μl), and lung tissue was harvested for flow cytometry to assess the immune cells producing IFN-γ. The cytometry results showed that the percentages of IFN-γ-producing ILC1 ($CD90.2^+Lin^-Tbet^+IFN\text{-}\gamma^+$) cells (Figure S2A in Supplementary Material) and NK cells ($NK1.1^+CD3e^-IFN\text{-}\gamma^+$) (Figure S2B in Supplementary Material) were not increased in the lungs of IAV-infected asthmatic mice at 7 dpi (ILC1: 24.7%, NK cell: 50.4%) compared with those of non-asthmatic mice after infection (ILC1: 54.2%, NK cell: 52.6%). However, IFN-γ-positive cells were notably observed at the bronchial epithelium in IAV-infected asthmatic mice (Figure S3 in Supplementary Material). Then, we also investigate the correlation between IFN-λ and -γ in IAV-infected asthmatic mice with administration of IFN-$\lambda_{2/3}$- and γ-neutralizing antibodies. The ELISA results showed that IAV-induced IFN-λ secretion was not altered in the BAL fluid of asthmatic mice with IFN-γ-neutralizing Ab, whereas IAV-induced IFN-γ secretion (1,724.5 ± 378.5 pg/ml) was significantly reduced in asthmatic mice that were administered IFN-$\lambda_{2/3}$-neutralizing antibodies before IAV infection (669.5 ± 214.6 pg/ml) (**Figures 4C,D**). In addition, the decreased goblet cell metaplasia and airway mucus secretion observed after IAV infection were not seen until 7 dpi in the lung tissue of IAV-infected asthmatic mice inoculated with IFN-$\lambda_{2/3}$-neutralizing antibodies (**Figure 4E**). This finding was accompanied by higher viral titer until 7 dpi (PI 3d: $3.0 \times 10^6 + 1.3 \times 10^6$, PI 5d: $3.1 \times 10^6 + 1.8 \times 10^6$, PI 7d: $4.3 \times 10^6 + 1.6 \times 10^5$, **Figure 4F**). A multiplex assay was also performed to quantify the levels of the secreted Th2 cytokines IL-4, IL-5, IL-6, and IL-13, in the BAL fluid of IAV-infected asthmatic mice with functional blocking of IFN-$\lambda_{2/3}$. As noted above, secretion of Th2 cytokines was significantly attenuated in IAV-infected asthmatic mice, whereas it was not attenuated in IAV-infected mice that were inoculated with IFN-$\lambda_{2/3}$-neutralizing antibodies (**Figure 4G**).

Overall, these results indicate that neither ILC1 nor NK cells contributed to the increased production of IFN-γ in IAV-infected asthmatic mice. They also indicate that IFN-γ is produced predominantly at the respiratory epithelium in the lungs of IAV-infected asthmatic mice. The rapid induction of IFN-$\lambda_{2/3}$ could be related to the robust induction of IFN-γ at 7 days after IAV infection in respiratory epithelium of asthmatic mice; this induction seems to be central for expedite antiviral immune response and for limiting Th2 cytokine secretion after IAV infection.

Asthmatic Mice Become Vulnerable to IAV Infection After 7 Days, but Intranasal Administration of IFN-$\lambda_{2/3}$ Effectively Protects Them From IAV

Asthmatic mice ($N = 5$) were infected with IAV WS/33 (H1N1) *via* the intranasal route (213 pfu/30 μl), and two gross determinants of virus-induced morbidity, mean body weight and survival rate, were measured until 14 dpi. Different results were observed after 7 dpi and IAV-infected asthmatic mice showed significant weight loss from 9 dpi (**Figure 5A**). Specifically, noticeable morbidity was also observed in IAV-infected asthmatic mice and all of the mice were dead by 14 days after IAV infection, with a mean body weight about 15 g at the time of death (**Figures 5A,B**). We found that the expression levels of TNF-α, IL-1β, and Ccl7 were significantly elevated in IAV-infected asthmatic mice at 14 dpi compared with their levels at 7 dpi (**Figure 5C**). Moreover, IAV-infected asthmatic mice produced significantly less IFN-$\lambda_{2/3}$ (PI 7d: 3,892.5 ± 643.8 pg/ml, PI 14d: 273.5 ± 81.7 pg/ml) and IFN-γ (PI 7d: 31,322.6 ± 7,318.4 pg/ml, PI 14d: 2,284.2 ± 378.5 pg/ml) (**Figure 5D**). Although IFN-$\lambda_{2/3}$ production was driven rapidly after IAV infection in the respiratory tract of IAV-infected asthmatic mice, asthmatic mice became vulnerable to IAV infection by 7 days after infection, at which they exhibited severe lung damage.

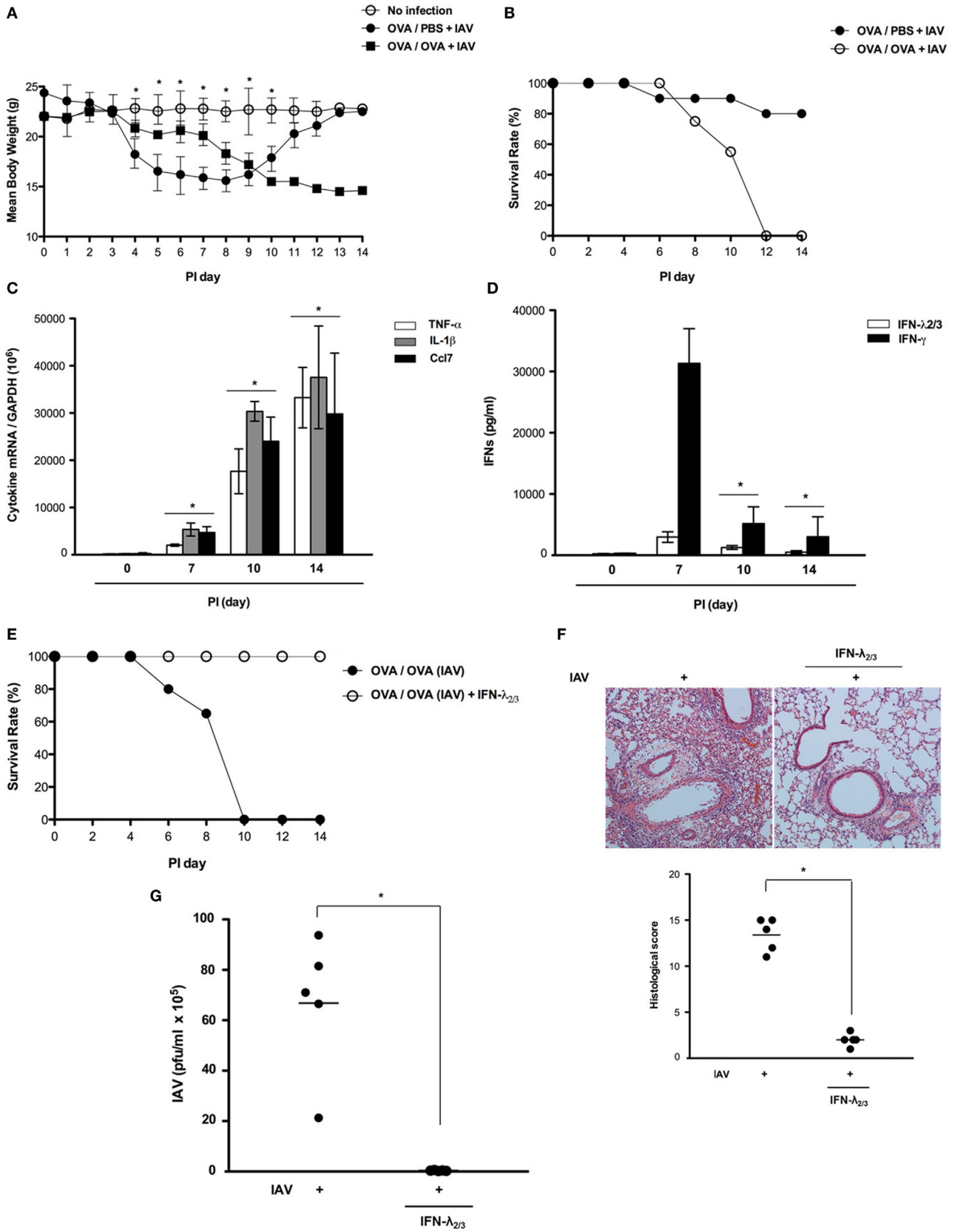

FIGURE 5 | Continued

FIGURE 5 | Interferon (IFN)-$\lambda_{2/3}$ exerts a potent antiviral effect against influenza A virus (IAV) infection in the mouse lung. Non-asthmatic mice ($N = 5$) and asthmatic mice ($N = 5$) were infected with 213 pfu IAV WS/33 (H1N1), and body weight **(A)** and survival rate [**(B)**, $N = 20$] were assessed until 14 dpi. The mRNA levels of TNF-α, IL-1β, and Ccl7 **(C)** and the levels of secreted IFN-$\lambda_{2/3}$ and IFN-γ **(D)** in the lung and bronchoalveolar lavage fluid were determined. Asthmatic mice were infected with 213 pfu IAV WS/33 (H1N1) and treated with recombinant IFN-$\lambda_{2/3}$ (IFN-λ_2: 1 μg and IFN-λ_3: 1 μg/30 μl) ($N = 5$). As a control, the diluent phosphate-buffered saline was used ($N = 5$). Survival rate [**(E)**, $N = 20$], hematoxylin/eosin-stained lung histologic findings **(F)**, and viral titer **(G)** were determined at 14 dpi. Micrographs are representative of lung sections from five mice. Polymerase chain reaction, plaque assay, and enzyme-linked immunosorbent assay results are presented as mean ± SD from five independent experiments ($^*p < 0.05$ compared with the values of mice with recombinant IFN-$\lambda_{2/3}$).

To determine whether exogenous compensation of IFN-$\lambda_{2/3}$ protects asthmatic mice from IAV infection at 14 dpi, asthmatic mice ($N = 5$) were administered recombinant IFN-$\lambda_{2/3}$ (IFN-λ_2: 1 μg, IFN-λ_3: 1 μg) *via* the intranasal route and simultaneously inoculated with IAV WS/33 (H1N1). Interestingly, all IAV-infected asthmatic mice that received intranasal IFN-$\lambda_{2/3}$ survived. Moreover, IAV-mediated histopathological lung inflammation was not observed in IFN-$\lambda_{2/3}$-treated asthmatic mice, and viral titer was significantly lower in IFN-$\lambda_{2/3}$-treated asthmatic mice (IAV: 6.2×10^6, IAV + IFN-$\lambda_{2/3}$: 1.7×10^3) (**Figures 5E–G**). These findings suggest that the enhanced vulnerability to IAV infection of asthmatic mice could be controlled by intranasal administration of IFN-$\lambda_{2/3}$ until 14 dpi.

DISCUSSION

This study provides a different view of the antiviral innate immune system in the asthmatic respiratory tract. Specifically, it has been generally accepted that the asthmatic airway is highly vulnerable to respiratory viral infection due to its reduced production of IFNs, which are required for clearance of viral infection and lower induction of IFNs can be involved in robust production of Th2 cytokines (10–12). Here, we showed that IFN-$\lambda_{2/3}$ is induced rapidly in asthmatic mice after IAV infection, and that this cytokine is important for maintaining the antiviral immune response against IAV lung infection and for restricting Th2 cytokine secretion in asthmatic mice. These effects were observed within 7 days. Our findings also imply that intranasal administration of IFN-$\lambda_{2/3}$ is a potential strategy for controlling the enhanced susceptibility of asthmatic mice to IAV infection from 7 days postchallenge onward.

Asthmatics have been reported to have increased susceptibility to respiratory viral infection including increased severity, longer duration of respiratory symptoms, and acute exacerbation of asthma (20, 21). This increased susceptibility to respiratory viral infection has been shown to be mediated by novel mechanisms including virus-induced secretion of epithelial-derived Th2 cytokines, deficient apoptosis of viral-infected cells, and lower production of IFNs after viral infection at the asthmatic airway epithelium (22, 23). In particular, IFNs are the most important component of the innate immune response and have been shown to be involved in defective innate immune responses to respiratory viral infection. The asthmatic airway epithelium appears to be profoundly deficient in viral-induced production of IFNs; reduced induction of IFNs has been shown to dampen the adaptive immune response (24–26). Although *in vivo* asthma model does not show exactly same characteristics or phenotypes as human asthma, we thought B6-oriented asthmatic model exhibit the biomedical relevance with human asthma considering histological findings, increased AHR after methacholine inhalation and peribronchial infiltration of inflammatory cells. This model could be used to investigate the susceptibility of asthmatic mice to influenza virus infection. The experiments performed here showed that asthmatic mice exhibited a significantly lower survival rate and greater loss of body weight, accompanied by higher viral titer, from 7 days after IAV lung infection onward. In addition, induction of IFN-$\lambda_{2/3}$ and -γ was significantly impaired in asthmatic mouse lung tissue at 14 days after IAV infection. To the best of our knowledge, deficient innate immune responses (including reduced induction of IFNs) are expected in the asthmatic respiratory tract. Additional research aiming to understand the mechanisms driving these deficient innate immune responses is urgently required to reduce the susceptibility to viral infection of asthmatics.

While most studies have focused on exacerbation of asthma by influenza viral lung infection and the higher susceptibility to influenza virus of asthmatics, studies using a novel mouse model of asthma and influenza infection have shown that asthmatic mice are highly susceptible to influenza viral infection compared with non-asthmatic mice. Such studies are necessary for identifying novel targets for the development of effective therapies against viral infection in asthmatics (11–13).

The different hypothesis has been introduced that asthmatic mice are more resistant to influenza virus as a result of a lower viral burden in the lungs than control mice, leading to improvement of their clinical condition (14). This prompt viral clearance in asthmatic mice has been shown to be mediated by increased production of antiviral cytokines, activation of NK cells, and enhanced antigen-specific CD8+ T cell activity after infection. Other immunological mechanisms explaining the viral resistance of asthmatic mice have also been suggested that the increased survival of asthmatic mice was due to increased TGF-β-mediated tolerance to influenza infection-mediated tissue damage, rather than enhanced antiviral immunity (15). We think that it will be of interest to determine whether asthmatic mice might be also resistant to lung infection by IAV, which causes an exacerbation of asthmatic symptoms and higher mortality.

In this study, we found that asthmatic mice were also resistant to IAV infection until 7 days. Specifically, all mice survived, the mean viral titer was significantly lower, and the IAV-induced lung pathologies were reduced. Interestingly, IAV infection led to reduced Th2-related immune responses, including decreased IL-4, IL-5, and IL-13 secretion. Moreover, resolution of extensive asthma-related lung pathologies such as goblet cell hyperplasia was observed consistently in the lungs of IAV-infected asthmatic mice at 7 dpi. Based on these results, we estimate that asthmatic mice were not completely vulnerable to influenza virus infection and particularly asthmatic mice exhibited distinct immune

mechanisms for resisting respiratory viral infection and restricting Th2 immunopathology in the respiratory tract.

We focused on the phase at which IFN-$\lambda_{2/3}$ is rapidly induced in the lungs of IAV-infected asthmatic mice and IFN-$\lambda_{2/3}$ contributes to resistance to IAV infection in asthmatic mice. In allergic airway diseases, IFN-λ cytokines are critical for driving Th1 differentiation *in vivo* and limiting Th2 and Th17 responses in the airway (7, 10). Our data also show that IFN-$\lambda_{2/3}$ in particular was preferentially secreted in the lungs of IAV-infected asthmatic mice from 1 dpi and its level was maintained until 7 days. In addition, secretion of IFN-$\lambda_{2/3}$ drives the transcription of IFN-γ, which was accompanied by increased viral clearance in respiratory epithelium and attenuation of Th2 cytokine secretion in IAV-infected asthmatic mice from 1 dpi onward. Interestingly, functional inhibition of IFN-$\lambda_{2/3}$ in IAV-infected asthmatic mice aggravated IAV infection. Moreover, the level of Th2 cytokine and the degree of asthma-related lung histopathological findings *in vivo* were improved after IAV infection. Given these findings, the impairment of IFN-$\lambda_{2/3}$ induction in response to viral infection in asthmatics has profound implications relating to the pathogenesis of virus-induced asthma exacerbation. Thus, rapid production of IFN-$\lambda_{2/3}$ in the lungs of asthmatic mice in response to IAV infection could constitute the primary antiviral defense and could also restrict the secretion of Th2 cytokines. Previously, we found that the highest mRNA IFN-$\lambda_{2/3}$ level and the highest level of secreted IFN-$\lambda_{2/3}$ were observed at 10 dpi in the lungs of IAV-infected B6 mice (17, 27). By contrast, IFN-$\lambda_{2/3}$ was released in the lungs of asthmatic mice from 1 day after IAV infection and this rapid production and maintenance of IFN-λs until 5 days after infection was accompanied by increase of IFN-γ secretion at 7 dpi. The levels of secreted IFN-β was increased by 3 dpi and the highest level of IFN-β secretion was also observed at 7 dpi in the lung of IAV-infected non-asthmatic mice (17) but IFN-β was minimally induced in the lung of IAV-infected asthmatic mice until 7 dpi. We hypothesize that the pattern of IFN secretion in response to IAV infection was altered in asthmatic mice. Specifically, asthmatic mice exhibited more rapid release of IFN-$\lambda_{2/3}$, which is a central mediator of the antiviral immune response. This mechanism could explain the high resistance of asthmatic mice to respiratory viral infection at the early stage of IAV infection.

Although IFN-$\lambda_{2/3}$ production was rapidly driven after IAV infection in the respiratory tract of IAV-infected asthmatic mice, asthmatic mice became vulnerable to the effect of IAV infection after 7 dpi and the levels of secreted IFN-β, IFN-$\lambda_{2/3}$, and IFN-γ were completely reduced at 14 dpi in the lung of IAV-infected asthmatic mice. However, intranasal delivery of IFN-$\lambda_{2/3}$ was shown to almost completely inhibit viral replication in IAV-infected asthmatic mice, as demonstrated by the significantly decreased viral titer in the lungs of mice that received intranasal IFN-$\lambda_{2/3}$ compared with that of non-infected mice. In addition, the lungs of mice that received intranasal IFN-$\lambda_{2/3}$ exhibited similar histological results to those of non-infected mice. Therefore, strategies involving the compensation or maintenance of IFN-λ are new opportunities for invoking an effective antiviral defense against IAV infection. IFN-λ is thus a promising new target for reducing susceptibility to respiratory viral infection in asthmatics.

In summary, rapid induction of IFN-λ is a distinctive immunologic finding in IAV-infected asthmatic mice and this effect is accompanied by reduced initial viral spread in asthmatic lung. This rapid induction of IFN-λ is crucial for controlling viral load and for maintaining effective antiviral immune mechanisms in asthmatics at early stage of infection. Our study provides compelling evidence that IFN-λ could have therapeutic potential for treating IAV-related respiratory infection in asthmatics.

ETHICS STATEMENT

All experiments were approved by the Institutional Review Board of Seoul National University College of Medicine (IRB number 2015-2642) and were carried out in accordance to LABORATORY ANIMAL ACT of Korean Ministry of Food and Drug Safety for enhancing the ethics and reliability on animal testing through appropriate administration of laboratory animals and animal testing.

AUTHOR CONTRIBUTIONS

Conception and design: SA, YJ, and HJK. Designed research: YJ, AJ, YH, HL, and HYK. Analyzed experimental data and performed the data interpretation including flow cytometry: SC and HJK. Drafted the manuscript for important intellectual content: SC and HJK.

FUNDING

This work was supported by a grant from the Korea Healthcare Technology R&D Project of the Ministry for Health, Welfare, and Family Affairs (HI15C0694 to HJK). It was also supported by a grant from the Korea Health Technology R&D Project through the Korea Health Industry Development Institute (KHIDI), funded by the Ministry of Health & Welfare, Republic of Korea (HI15C2923 to HJK).

SUPPLEMENTARY MATERIAL

The Supplementary Material for this article can be found online at https://www.frontiersin.org/articles/10.3389/fimmu.2018.00986/full#supplementary-material.

FIGURE S1 | Transpulmonary resistance in IAV-infected asthmatic mice. Airway hyper-responsiveness was measured as methacholine-induced increases in transpulmonary resistance in mechanically ventilated mice. Data are expressed as mean value of percentage increased from base line of the transpulmonary resistance ± SD values of three mice (White dot: OVA/OVA, Black dot:OVA/PBS, Black square:IAV-infected OVA/OVA).

FIGURE S2 | Flow cytometric analysis for ILC1 and NK cells. The percentage of IFN-γ produced ILC1 (Tbet+Lineage-IFN-γ+) **(A)** and NK cells **(B)** (NK1.1+CD3e-IFN-γ+) were evaluated in the lung tissue of non-asthmatic (OVA/PBS) and asthmatic mice (OVA/OVA) before and after IAV infection.

FIGURE S3 | Immunohistochemistry for IFN-γ in non-asthmatic and asthmatic mice. Immunohistochemical analysis of IFN-γ using DAB chromogen was performed in lung sections from non-asthmatic (OVA/PBS) and asthmatic mice (OVA/OVA) before and after IAV infection. The number of IFN-γ-positive cells was significantly increased in the lung tissue of IAV-infected asthmatic mice and bronchial epithelial cells showed strong expression of IFN-γ (Original magnification x200).

REFERENCES

1. Umetsu DT, DeKruyff RH. The regulation of allergy and asthma. *Immunol Rev* (2006) 212:238–55. doi:10.1111/j.0105-2896.2006.00413.x
2. Kubo M. Innate and adaptive type 2 immunity in lung allergic inflammation. *Immunol Rev* (2017) 278:162–72. doi:10.1111/imr.12557
3. Castillo JR, Peters SP, Busse WW. Asthma exacerbations: pathogenesis, prevention, and treatment. *J Allergy Clin Immunol Pract* (2017) 5:918–27. doi:10.1016/j.jaip.2017.05.001
4. Holt PG, Strickland DH. Interactions between innate and adaptive immunity in asthma pathogenesis: new perspectives from studies on acute exacerbations. *J Allergy Clin Immunol* (2010) 125:963–72. doi:10.1016/j.jaci.2010.02.011
5. Garcia-Sastre A, Biron CA. Type 1 interferons and the virus-host relationship: a lesson in detente. *Science* (2006) 312:879–82. doi:10.1126/science.1125676
6. Cheon H, Holvey-Bates EG, Schoggins JW, Forster S, Hertzog P, Imanaka N, et al. IFNbeta-dependent increases in STAT1, STAT2, and IRF9 mediate resistance to viruses and DNA damage. *EMBO J* (2013) 32:2751–63. doi:10.1038/emboj.2013.203
7. Galani IE, Triantafyllia V, Eleminiadou EE, Koltsida O, Stavropoulos A, Manioudaki M, et al. Interferon-lambda mediates non-redundant front-line antiviral protection against influenza virus infection without compromising host fitness. *Immunity* (2017) 46:875–90. doi:10.1016/j.immuni.2017.04.025
8. Jewell NA, Cline T, Mertz SE, Smirnov SV, Flaño E, Schindler C, et al. Lambda interferon is the predominant interferon induced by influenza A virus infection in vivo. *J Virol* (2010) 84:11515–22. doi:10.1128/JVI.01703-09
9. Kim BJ, Cho SW, Jeon YJ, An S, Jo A, Lim JH, et al. Intranasal delivery of Duox2 DNA using cationic polymer can prevent acute influenza A viral infection in vivo lung. *Appl Microbiol Biotechnol* (2018) 102:105–15. doi:10.1007/s00253-017-8512-1
10. Contoli M, Ito K, Padovani A, Poletti D, Marku B, Edwards MR, et al. Th2 cytokines impair innate immune responses to rhinovirus in respiratory epithelial cells. *Allergy* (2015) 70:910–20. doi:10.1111/all.12627
11. Message SD, Laza-Stanca V, Mallia P, Parker HL, Zhu J, Kebadze T, et al. Rhinovirus-induced lower respiratory illness is increased in asthma and related to virus load and Th1/2 cytokine and IL-10 production. *Proc Natl Acad Sci U S A* (2008) 105:13562–7. doi:10.1073/pnas.0804181105
12. Contoli M, Message SD, Laza-Stanca V, Edwards MR, Wark PA, Bartlett NW, et al. Role of deficient type III interferon-lambda production in asthma exacerbations. *Nat Med* (2006) 12:1023–6. doi:10.1038/nm1462
13. Koltsida O, Hausding M, Stavropoulos A, Koch S, Tzelepis G, Ubel C, et al. IL-28A (IFN-lambda2) modulates lung DC function to promote Th1 immune skewing and suppress allergic airway disease. *EMBO Mol Med* (2011) 3:348–61. doi:10.1002/emmm.201100142
14. Ishikawa H, Sasaki H, Fukui T, Fujita K, Kutsukake E, Matsumoto T. Mice with asthma are more resistant to influenza virus infection and NK cells activated by the induction of asthma have potentially protective effects. *J Clin Immunol* (2012) 32:256–67. doi:10.1007/s10875-011-9619-2
15. Furuya Y, Furuya AK, Roberts S, Sanfilippo AM, Salmon SL, Metzger DW. Prevention of influenza virus-induced immunopathology by TGF-beta produced during allergic asthma. *PLoS Pathog* (2015) 11:e1005180. doi:10.1371/journal.ppat.1005180
16. Patel DA, You Y, Huang G, Byers DE, Kim HJ, Agapov E, et al. Interferon response and respiratory virus control are preserved in bronchial epithelial cells in asthma. *J Allergy Clin Immunol* (2014) 134:1402–12. doi:10.1016/j.jaci.2014.07.013
17. Kim S, Kim MJ, Kim CH, Kang JW, Shin HK, Kim DY, et al. The superiority of IFN-lambda as a therapeutic candidate to control acute influenza viral lung infection. *Am J Respir Cell Mol Biol* (2017) 56:202–12. doi:10.1165/rcmb.2016-0174OC
18. Verhoeven D, Perry S, Pryharski K. Control of influenza infection is impaired by diminished interferon-γ secretion by CD4 T cells in the lungs of toddler mice. *J Leukoc Biol* (2016) 100:203–12. doi:10.1189/jlb.4A1014-497RR
19. Dahl ME, Dabbagh K, Liggitt D, Kim S, Lewis DB. Viral-induced T helper type 1 responses enhance allergic disease by effects on lung dendritic cells. *Nat Immunol* (2004) 5:337–43. doi:10.1038/ni1041
20. Steinke JW, Borish L. Immune responses in rhinovirus-induced asthma exacerbations. *Curr Allergy Asthma Rep* (2016) 16:78. doi:10.1007/s11882-016-0661-2
21. Toussaint M, Jackson DJ, Swieboda D, Guedán A, Tsourouktsoglou TD, Ching YM, et al. Host DNA released by NETosis promotes rhinovirus-induced type-2 allergic asthma exacerbation. *Nat Med* (2017) 23:681–91. doi:10.1038/nm.4332
22. Jarjour NN, Esnault S. Interleukin-33: a potential link between rhinovirus infections and asthma exacerbation. *Am J Respir Crit Care Med* (2014) 190:1336–7. doi:10.1164/rccm.201411-1949ED
23. Johnston SL. Innate immunity in the pathogenesis of virus-induced asthma exacerbations. *Proc Am Thorac Soc* (2007) 4:267–70. doi:10.1513/pats.200701-030AW
24. Tworek D, Heroux D, O'Byrne SN, Mitchell P, O'Byrne PM, Denburg JA. Toll-like receptor-induced expression of epithelial cytokine receptors on haemopoietic progenitors is altered in allergic asthma. *Clin Exp Allergy* (2017) 47:900–8. doi:10.1111/cea.12913
25. Riese RJ, Finn PW, Shapiro SD. Influenza and asthma: adding to the respiratory burden. *Nat Immunol* (2004) 5:243–4. doi:10.1038/ni0304-243
26. Sykes A, Edwards MR, Macintyre J, del Rosario A, Bakhsoliani E, Trujillo-Torralbo MB, et al. Rhinovirus 16-induced IFN-alpha and IFN-beta are deficient in bronchoalveolar lavage cells in asthmatic patients. *J Allergy Clin Immunol* (2012) 29:1506–14. doi:10.1016/j.jaci.2012.03.044
27. Hong SN, Kim JY, Kim H, Kim DY, Won TB, Han DH, et al. Duox2 is required for the transcription of pattern recognition receptors in acute viral lung infection: an interferon-independent regulatory mechanism. *Antiviral Res* (2016) 134:1–5. doi:10.1016/j.antiviral.2016.08.017

Conflict of Interest Statement: The authors declare that the research was conducted in the absence of any commercial or financial relationships that could be construed as a potential conflict of interests.

Copyright © 2018 An, Jeon, Jo, Lim, Han, Cho, Kim and Kim. This is an open-access article distributed under the terms of the Creative Commons Attribution License (CC BY). The use, distribution or reproduction in other forums is permitted, provided the original author(s) and the copyright owner are credited and that the original publication in this journal is cited, in accordance with accepted academic practice. No use, distribution or reproduction is permitted which does not comply with these terms.

frontiers in Immunology

ORIGINAL RESEARCH
published: 14 June 2018
doi: 10.3389/fimmu.2018.01297

The cGas–Sting Signaling Pathway Is Required for the Innate Immune Response Against Ectromelia Virus

*Wen-Yu Cheng†, Xiao-Bing He†, Huai-Jie Jia, Guo-Hua Chen, Qi-Wang Jin, Zhao-Lin Long and Zhi-Zhong Jing**

State Key Laboratory of Veterinary Etiological Biology, Key Laboratory of Veterinary Public Health of Agriculture Ministry, Lanzhou Veterinary Research Institute, Chinese Academy of Agricultural Sciences, Lanzhou, China

Activation of the DNA-dependent innate immune pathway plays a pivotal role in the host defense against poxvirus. Cyclic GMP-AMP synthase (cGAS) is a key cytosolic DNA sensor that produces the cyclic dinucleotide cGMP-AMP (cGAMP) upon activation, which triggers stimulator of interferon genes (STING), leading to type I Interferons (IFNs) production and an antiviral response. Ectromelia virus (ECTV) has emerged as a valuable model for investigating the host–Orthopoxvirus relationship. However, the role of cGas–Sting pathway in response to ECTV is not clearly understood. Here, we showed that murine cells (L929 and RAW264.7) mount type I IFN responses to ECTV that are dependent upon cGas, Sting, TANK binding kinase 1 (Tbk1), and interferon regulatory factor 3 (Irf3) signaling. Disruption of cGas or Sting expression in mouse macrophages blocked the type I IFN production and facilitated ECTV replication. Consistently, mice deficient in cGas or Sting exhibited lower type I IFN levels and higher viral loads, and are more susceptible to mousepox. Collectively, our study indicates that the cGas–Sting pathway is critical for sensing of ECTV infection, inducing the type I IFN production, and controlling ECTV replication.

Keywords: innate immunity, cGas, Sting, type I interferon, ectromelia virus

OPEN ACCESS

Edited by:
Ping An,
Frederick National Laboratory for Cancer Research (NIH), United States

Reviewed by:
Hiroyuki Oshiumi,
Kumamoto University, Japan
Ju-Tao Guo,
Baruch S. Blumberg Institute, United States
Michael Paul Gantier,
Hudson Institute of Medical Research, Australia

****Correspondence:***
Zhi-Zhong Jing
zhizhongj@163.com

†Co-first authors.

Specialty section:
This article was submitted to Viral Immunology, a section of the journal Frontiers in Immunology

Received: *30 January 2018*
Accepted: *24 May 2018*
Published: *14 June 2018*

Citation:
Cheng W-Y, He X-B, Jia H-J, Chen G-H, Jin Q-W, Long Z-L and Jing Z-Z (2018) The cGas–Sting Signaling Pathway Is Required for the Innate Immune Response Against Ectromelia Virus. Front. Immunol. 9:1297. doi: 10.3389/fimmu.2018.01297

INTRODUCTION

Innate immune responses to pathogen infection are initiated with the recognition of microbial pathogen-associated molecular patterns (PAMPs) through a limited number of germline-encoded receptors called pattern-recognition receptors (PRRs) (1–3). PAMPs represent conserved molecule motifs within a class of microbes that are recognized by cells of the innate immune system, which include lipopolysaccharides, peptidoglycans, or nucleic acids (RNA and DNA) (2–4). PRRs exist in the plasma or endosomal membranes, cytoplasm, and nucleus of some cell types to sense both extracellular and intracellular infections (5–7). Nucleic acid-sensing PRRs are one of the major subsets of PRRs that sense DNA and RNA (7–9). Some members of these membrane-bound PRRs, such as Toll-like receptors (TLR3, 7, 8, and 9), are located in the endosomes that detect environmental RNA or DNA, while others, such as the DNA sensors AIM2-like receptors (AIM2, IFI16, and IFIX) and cyclic GMP-AMP synthase (cGAS), and the RNA sensors RIG-I-like receptors (RIG-I, MDA5, and LPG2), recognize microbial nucleic acid in the cytosol and/or nucleus (10–13). Following the recognition of microbial RNA or DNA, the PRRs are activated through conformational changes or specific modifications that drive the induction of type I interferon (IFN) and pro-inflammatory cytokines to protect the host from the invading pathogens (14–16).

Currently, an increasing number of studies have suggested that the cGAS–stimulator of interferon genes (STING) pathway of cytosolic DNA sensing plays a major role in the immune defense against microbial pathogens (17). Upon recognition of DNA viruses, retroviruses, and

intracellular bacteria, cGAS catalyzes the formation of the second messenger molecule cGMP-AMP (cGAMP), which in turn associates with and activates the STING (17–19). The activation of STING leads to its dimerization, relocalization, and prion-like aggregation, which then associates with TANK binding kinase 1 (TBK1) and causes the recruitment of interferon regulatory factor 3 (IRF3) (5). IRF3 phosphorylates and translocates to the nucleus where the production of type I IFNs is induced (19–21). Furthermore, it has been reported that STING acts as a direct sensor of cyclic dinucleotides such as mammalian 2′3′-cGAMP and prokaryotic 3′3′-cGAMP, c-di-GMP, c-di-AMP, which can also induce the production of type I IFNs (21, 22).

Poxviruses are large, enveloped, double-stranded DNA viruses that replicate entirely in the cytoplasm and cause human and veterinary diseases. The orthopoxvirus (OPV) genus of Poxviridae, including variola virus (VARV), vaccinia virus (VACV), monkeypox virus (MPXV), cowpox virus, and ectromelia virus (ECTV), cause acute infections in their target hosts. Despite the eradication of smallpox through a global vaccination campaign spearheaded by the World Health Organization in the late 1970s, other OPVs have been reported to persist in various animal species following natural or experimental infections (23). Currently, with the emergence of zoonotic MPXV, the outbreaks of VACV infections in dairy cattle and their transmission to humans, and cases of cowpox in humans, there is still great and essential significance as well as interest in the molecular mechanisms of poxvirus infections and/or protection from OPV infections (24, 25). ECTV, a mouse specific pathogen that causes mousepox, is closely related to VARV and has been used as a model for the study of the pathogenesis and immunobiology of OPV infection (26, 27).

Following ECTV infection, type I IFNs were shown to be induced *in vitro* and *in vivo* (28, 29). C57BL/6 mice deficient in *Ifnar1*, which encodes subunit 1 of IFNAR, an IFN α/β receptor, are highly susceptible to ECTV infections (28, 30, 31). Studies performed on murine cells and C57BL/6 mice have demonstrated that the induction of type I IFNs in draining lymph nodes (dLNs) during ECTV infections is because of the recognition of the virus indirectly by the TLR9–MyD88–interferon response factor 7 (IRF7) pathway and directly by the STING–IRF7/nuclear factor kappa B (NF-κB) pathway (32). Mice deficient in TLR9 and its adaptor protein MyD88 show higher viral loads, more serious pathology in the liver and spleen, and increased susceptible to ECTV infection than wild-type (WT) mice (31–34). Moreover, C57BL/6 mice deficient in the transcription factors IRF7 and NF-κB, which are downstream targets of both TLR9–MyD88 and STING, are also highly susceptible to mousepox (32). Notably, STING, as a critical adapter of the cytosolic DNA sensor, is also essential for the resistance to lethal ECTV infections as well as the expression of type I IFNs in the dLNs *in vivo* (32, 35). However, Dai (DNA-dependent activator of IFN-regulatory factors), a cytosolic DNA sensor upstream of STING, was demonstrated to be less important for resistance to mousepox (32). Therefore, the PRRs upstream of STING that contribute to the recognition of ECTV and resistance to mousepox remain unclear. In addition, cGAS has been recently discovered to be a general cytosolic DNA sensor upstream of STING that recognizes cytoplasmic DNA derived from a large spectrum of DNA viruses, retroviruses, bacteria, fungi, and parasites (4–7). Not surprisingly, VACV as DNA virus has the ability to trigger type I IFN production responses *via* cGas–Sting pathway (36). However, it is currently not known whether the cGAS is an important innate immune DNA sensor also for ECTV infection.

Here, we examine the contribution of the cGas–Sting pathway to the antiviral response to ECTV *in vitro* and *in vivo*. We showed that murine L929 and RAW264.7 cells, but not NIH3T3 cells, mount type I IFN responses against ECTV infection *via* the cGas–Sting pathway. Disruption of cGas and Sting expression by RNA interference or gene knockout impaired the expression of type I IFNs at the mRNA or protein levels induced by the virus. The induction of type I IFNs were abolished in *Tlr9*$^{-/-}$, *cGas*$^{-/-}$, *Sting*$^{-/-}$, *Tbk1*$^{-/-}$, and *Irf3*$^{-/-}$ macrophages (RAW264.7 and peritoneal macrophages) and had significantly increased viral titers in *cGas*$^{-/-}$ and *Sting*$^{-/-}$ RAW264.7 cells, respectively, compared with WT cells. We also demonstrate that ECTV infection triggered the phosphorylation of Tbk1 and Irf3. *In vivo*, mice deficient in *Tlr9*, *cGas*, or *Sting* blocked the production of type I IFNs and showed higher viral loads and serious pathology in the liver and spleen, and were more susceptible to lethality caused by infections with ECTV as compared with WT mice. Our results confirm that the cGas–Sting pathway is required for resistance to ECTV infections.

MATERIALS AND METHODS

Cells and Virus

Vero (African green monkey kidney cell line), L929 (murine fibroblast cell line), NIH3T3 (murine embryo fibroblast cell line), and HEK293T cells were obtained from the China Center for Type Culture Collection, and were maintained in Dulbecco's Modified Eagle's Medium (DMEM, Hyclone) supplemented with 10% sterile fetal bovine serum (Gibco), 100 IU of penicillin/mL, and 100 μg/mL of streptomycin, and incubated at 37°C in the presence of 5% CO_2. RAW-Lucia ISG (rawl-isg), RAW-Lucia ISG-KO-cGas (rawl-kocgas), RAW-Lucia ISG-KO-Sting (rawl-kostg), RAW-Lucia ISG-KO-Irf3 (rawl-koirf3), and RAW-Lucia ISG-KO-Tbk1 (rawl-kotbk) cells were purchased from the InvivoGen company and were grown in DMEM (Gibco) supplemented with 10% sterile fetal bovine serum (Gibco), 100 μg/mL of Normocin, and 200 μg/mL of Zeocin (InvivoGen).

The WT strain of ECTV was originally isolated from a naturally infected laboratory mouse and then propagated in Vero cells (37). Plaque-purified ECTV was serially passaged, and the virus titer was measured by plaque assays on Vero cells. UV-inactivated ECTV was irradiated under short-wave (254 nm) ultraviolet light for 2 h. The infectivity of UV-inactivated ECTV was confirmed by the inability of the UV light-exposed viruses to produce a cytopathic effect on the monolayers of Vero cells.

Plasmids

The murine cGas gene was amplified and cloned into the pCMV-Tag2b vector with a FLAG tag on the N terminus. Expression plasmids for HA-tagged Sting-wt (S-wt) (puno1ha-mstingwt) and

Sting-gt (puno1-msting-gt) were purchased from the InvivoGen company, and their expressions were confirmed with immunoblotting. The IFN-β reporter and pRL-TK control plasmids for the reporter luciferase assays used in the study were described elsewhere (38). All constructs were confirmed using DNA sequencing.

Transfection and Luciferase Reporter Assay

Transient transfection was carried out using the FuGENE® HD transfection reagent (E2311, Promega) following the manufacturer's instructions. HEK293T cells were seeded in 96-well plates at a density of 1×10^5 cells/well and cultured until the cells reached approximately 70–80% confluency. Next, 10 ng of pRL-TK renilla luciferase reporter plasmid and 100 ng of IFN-β firefly luciferase reporter plasmid were transfected together with 100 ng of the indicated expression plasmids. After a 24-h transfection, cells were stimulated with poly(dA:dT)/LyoVec (2 μg/mL), ISD/LyoVec (1 μg/mL), 2′3′-cGAMP (20 μg/mL), and ECTV (MOI of 1) for 15 h, respectively. Luciferase activity was determined using the Dual-Glo® Luciferase Assay System (E2920, Promega).

RNA Isolation and qRT-PCR

Total RNA was extracted from cellular or tissue (spleen) samples using TRIzol reagent (Invitrogen), and first-strand cDNA was synthesized using the PrimeScript RT reagent kit (RR047A, TaKaRa) following the manufacturer's instructions. SYBR Green premix (RR820A, TaKaRa) was used for qRT-PCR with a Two Step Real-Time PCR Detection System (Bio-Rad). The primer sequences used for the qPCR were as follows: *Ifn*-α*4*, 5′-CCTGTGTGATGCAGGAACC-3′ and 5′-TCACCTCCCAGGCACAGA-3′; *Ifn*-β, 5′-CAGCTCCAAGAAAGGACGAAC-3′ and 5′-GGCAGTGTAACTCTTCTGCAT-3′; *Ifit1*, 5′-ACAGCAACCATGGGAGAGAATGCTG-3′ and 5′-ACGTAGGCCAGGAGGTTGTGCAT-3′; β-*actin*, 5′-GGCTGTATTCCCCTCCATCG-3′ and 5′-CCAGTTGGTAACAATGCCATGT-3′. Data were normalized to the mRNA levels of the housekeeping gene β-actin. Relative gene expression data were analyzed using the $2^{-\Delta\Delta Ct}$ method.

RNA Interference

Chemically synthesized siRNA duplexes were obtained from Gene-Pharma and transfected using the FuGENE® HD transfection reagent (E2311, Promega) according to the manufacturer's instructions. Briefly, a total of 1.0×10^5 L929 or NIH3T3 cells were seeded onto 12-well plates and transfected at a density of 80% with a final concentration of 100 nM of the indicated siRNAs or si-NC. The siRNA oligonucleotides were as follows: si-Sting, 5′-CGAAAUAACUGCCGCCUCATT-3′; si-cGas1, 5′-GAUUGAGCUACAAGAAUAUTT-3′;si-cGas2,5′-GAGGAAAUCCGCUGAGUCATT-3′; and si-NC (negative control), 5′-UUCUUCGAACGUGUCACGUTT-3′.

Enzyme-Linked Immunosorbent Assay (ELISA)

RAW264.7 cells and peritoneal macrophages were stimulated with virus or other reagents for the indicated times. Cell culture supernatants and mouse serum were collected, and levels of mouse IFN-β (439407, BioLegend) were measured according to manufacturer's instructions.

Western Blot Analysis

For the preparation of soluble cell extracts, harvested cells were washed two times with cold phosphate-buffered saline (PBS) and then were lysed in RIPA buffer containing protease and phosphatase inhibitors (P0013, Beyotime Biotechnology, China). The protein concentration of cell lysates was determined by bicinchoninic acid (BCA) assay (QuantiPro BCA Assay Kit, Sigma-Aldrich) according to the manufacturer's instructions. Equal amount of total protein (25 μg) was resolved by electrophoresis on 12% Bis–Tris polyacrylamide gels (Shanghai Sangon Biotech, China) and transferred to polyvinylidene fluoride membranes (Immobilon-P Transfer membranes, Millipore). Membranes were blocked for 2 h at room temperature in 5% (wt/vol) Tris-buffered saline supplemented with 0.1% Tween 20 (TBST)-diluted bovine serum albumin (BSA, Amresco) buffer. Membranes were incubated with primary antibody diluted in 5% (wt/vol) BSA and 1× TSBT at 4°C overnight. The primary antibodies used include anti-HA (66006-1, Proteintech), anti-FLAG (F3165, Sigma-Aldrich), anti-β-actin (60008-1, Proteintech), anti-cGas (#31659, Cell Signaling Technology), anti-Irf3 (#4302, Cell Signaling Technology), anti-Sting (#13647, Cell Signaling Technology), anti-Tbk1 (#3504, Cell Signaling Technology), anti-phospho-Irf3 (#4947, Cell Signaling Technology), and anti-phospho-Tbk1 (#5483, Cell Signaling Technology). Antibody signals were detected by the enhanced chemiluminescence detection kit (#1705062, Bio-Rad) after incubation with an appropriate secondary antibody conjugated to horseradish peroxidase. All the membranes were imaged using the ChemiDoc XRS$^+$ system (Bio-Rad).

Mice and Animal Experiments

Specific pathogen-free C57BL/6 mice (B6 strain) between 6 and 10 weeks of age were purchased from the Laboratory Animal Center of Lanzhou Veterinary Research Institute (LVRI), Chinese Academy of Agriculture Science (CAAS). The *cGas*$^{-/-}$ [B6(C)-*Mb21d1*$^{tm1d(EUCOMM)Hmgu}$/J], *Sting*$^{gt/gt}$ (C57BL/6J-*Tmem173*^{gt}/J), *Irf3*$^{-/-}$ (B6; 129S6-*Irf3*^{tm1Ttg}/TtgRbrc), and *Tlr9*$^{-/-}$ (C57BL/6J-*Tlr9*^{M7Btlr}/Mmjax) mice were originally purchased from the Jackson Laboratory and were bred at the Laboratory Animal Centre of LVRI, CAAS. Mice aged between 6 and 10 weeks were challenged with 3×10^3 or 1.0×10^6 plaque-forming units (PFU) of virus per mouse by subcutaneous injection into the left footpad. Serum of infected mice was collected at 6, 12, 24, and 48 h post-infection (hpi) and 3, 5, and 7 days post-infection (dpi) for ELISA assay. For the determination of survival, the mice were checked daily. For viral titer, a portion of the spleen or liver was removed aseptically from the mice and frozen at −70°C. The tissues from each mouse were weighted and homogenized in PBS to a 10% (wt/vol) lysate. The lysate was frozen and thawed three times and titrated by the plaque-forming assay.

Generation of Murine Peritoneal Macrophages

Murine peritoneal macrophages were generated as described (39). Briefly, C57BL/6 mice (WT), *Tlr9*$^{-/-}$, *cGas*$^{-/-}$, *Sting*$^{gt/gt}$, and

Irf3$^{-/-}$ mice were injected with 1 mL of 3.8% Brewer thioglycollate medium (T9032, Sigma-Aldrich) into the peritoneal cavity for 5 days. Then mice were euthanized by cervical dislocation and pull back the abdominal skin to expose the transparent peritoneal skin. Macrophages were collected by using syringes to inject cold DPBS into the peritoneal cavity of each mouse. The peritoneal fluid was centrifuged for 10 min to remove the supernatant. Cells were resuspended and cultured in 12-well plates at a density of 1×10^6 cells/well. After an 18-h incubation, cells were infected with ECTV (MOI, 5) for 15 or 18 h. Subsequently, the culture media were collected for ELISA, and cells were harvested for western blot analysis.

ECTV Genomic DNA Copy Number and Viral Titer Measurements

Genomic DNA was extracted from the mouse spleen or liver tissues using a viral RNA/DNA extraction kit (9766, TaKaRa) according to manufacturer's protocol. ECTV genomic DNA copy numbers were determined by qPCR using ECTV P4b gene specific primers: 5′-GTAGAACGACGCCAGAATAAGATA-3′ and 5′-AGAAGATATCAGACGATCCACAATC-3′. A standard curve was established from a cloned DNA fragment of the ECTV P4b gene (40). Cycle threshold (Ct) values obtained by the real-time PCR were plotted on the standard curve to calculate the viral DNA copy number. The titer of ECTV in the cellular and tissue samples was measured by the plaque assay using Vero cells in 12-well plates. Several 10-fold serial dilutions of the samples were added to individual wells of Vero cell monolayers for 2 h. After adsorption, the supernatants were removed, washed three times in PBS, and then the cells were incubated with 1.0% (wt/vol) high-viscosity carboxy-methyl cellulose (Sigma-Aldrich). At 6 dpi, cells were fixed with 4% formalin for 4 h and then stained with 0.5% crystal violet solution for 20 min to visualize plaques.

Histological Analysis

Livers were harvested and fixed with 10% neutral buffered formalin solution and then were embedded in paraffin. The paraffin-embedded specimens were cut into 5-μm sections and then stained with hematoxylin and eosin. Each slide with the samples was photographed with a digital optical microscope (Olympus, Tokyo, Japan).

Statistical Analysis

Data are expressed as means ± SD. Statistical analyses were performed by one-way analysis of variance followed by the Duncan's multiple range test using the SPSS software (SPSS 18.0 for Windows; SPSS, Chicago, IL, USA). For survival experiments, we used the log-rank (Mantel–Cox). In all figures, ND, not detected; ns, not significant; $^*P \leq 0.05$; $^{**}P \leq 0.01$; and $^{***}P \leq 0.001$.

RESULTS

ECTV-Induced Type I IFN Production in L929 and RAW 264.7 Cells, but Not in NIH3T3 Cells

To verify that an ECTV infection can induce type I IFNs production, three cell lines including NIH3T3, L929, and RAW 264.7 were chosen for determining the expression of type I IFNs during the ECTV infection. We found that ISD or ECTV-induced IFN-β production in L929 and RAW264.7 cells, but not in NIH3T3 cells (Figure S1A in Supplementary Material). To assess the time course of the induction of type I IFNs expression by the ECTV infection, RAW264.7 cells were infected with ECTV at an MOI of 5 and harvested for measuring the levels of IFN-α4 and IFN-β transcript using qRT-PCR at the indicated time points. The expression dynamics of *IFN-α4* and *IFN-β* showed that the mRNA levels of the two cytokines were upregulated and peaked at 18 hpi (Figures S1D,E in Supplementary Material), which was consistent with the protein levels of IFN-β as determined by ELISA (Figure S1F in Supplementary Material). In addition, a dose dependency of type I IFNs induced by ECTV in RAW264.7 cells was also confirmed using increasing doses of virus from an MOI of 0.1–5. As shown in Figures S1B,C in Supplementary Material, the expression levels of IFN-α4 and IFN-β were increased with higher doses of ECTV, which reached the highest level at an MOI of 5. We then used an MOI of 5 for the ECTV infection in the rest of the *in vitro* infection experiments reported in this paper.

Sting and cGas Are Required for the Induction of IFN-β During the ECTV Infection

In view of the importance of the cGAS–STING pathway in the production of type I IFNs upon infections by DNA virus, we hypothesize that the type I IFN gene expression induced by ECTV might be through cGas and Sting. To investigate the roles of murine cGas and Sting in response to the ECTV infection, we first compared the ability of ECTV to stimulate cGas-induced pathways in human cells. HEK293T cells were transfected with murine cGas or in combination with Sting, and then infected/stimulated with ECTV, poly(dA:dT), ISD, or 2′3′-cGAMP. The protein levels of cGas and Sting overexpressed in HEK293T cells were confirmed by immunoblotting (**Figure 1A**). As previously mentioned, cGAS and STING are poorly expressed in HEK293T cells (7, 41). As predicted, the increased IFN-β promoter activity was only observed in cGas and Sting co-transfected cells (**Figure 1B**). Moreover, the induction of the IFN-β promoter showed that all of the three reagents and ECTV have stimulatory potency, and the triggered IFN-β response was entirely Sting-dependent. Consistent with previous studies (42, 43), the magnitude of the IFN-β induction by ISD was higher than others in cGas and Sting co-transfected cells. HEK293T cells were then used to examine the role of Sting in IFN-β expression during the infection. As compared with the co-transfected treatment, HEK293T cells transfected with Sting alone induced at lower levels of IFN-β expression (**Figure 1C**), suggesting the Sting expression alone cannot entirely drive IFN-β expression.

To validate the function of the cGas–Sting pathway in the activation of IFN-β with ECTV, the induction of IFN-β expression by cGas and Sting in a dose-dependent manner was observed during the ECTV infection (**Figures 1D,E**). In addition, we tested the induction of the IFN-β promoter activated by ECTV or UV-inactivated ECTV in the presence of cGas (50 ng) and/or Sting (50 or 100 ng) (**Figures 1F,G**). As shown in **Figures 1F,G**, UV-inactivated ECTV can also induce the expression of IFN-β.

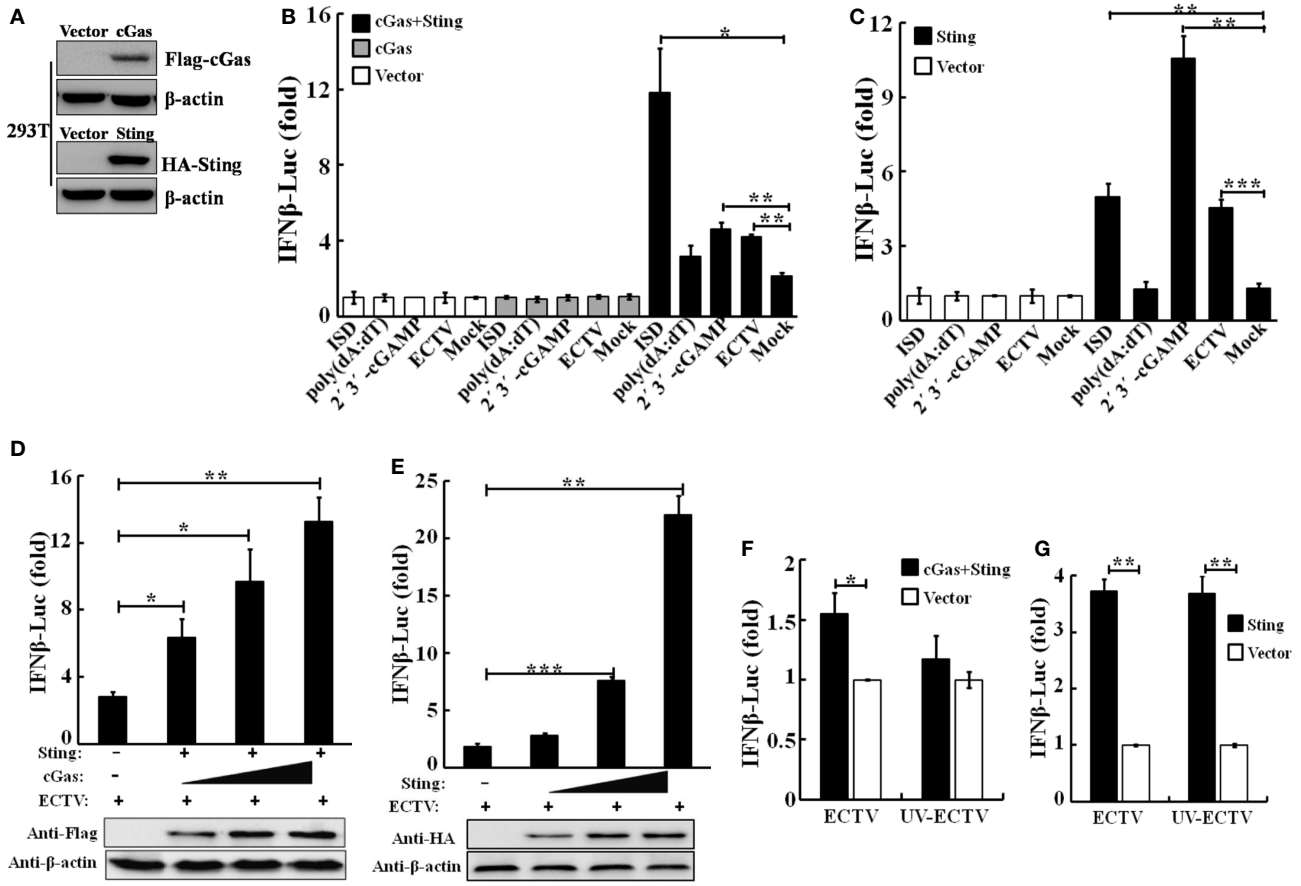

FIGURE 1 | Sting and cGas are required for the induction of IFN-β during ectromelia virus (ECTV) infection. **(A)** Overexpressed cGas, Sting, and β-actin protein levels in HEK293T cells were evaluated by Western blot. HEK293T cells (1×10^5) were seeded in a 96-well plate and then were transfected with pRL-TK *Renilla* luciferase reporter plasmid (10 ng/well), IFN-β firefly luciferase reporter plasmids (100 ng/well), and together with cGas (100 ng/well), Sting (100 ng/well), cGas + Sting (50 ng per plasmid per well), or vector only (100 ng/well) **(B,C)**. After a 24-h transfection, cells were either stimulated with poly(dA:dT)/LyoVec (2 μg/mL), ISD/LyoVec (1 μg/mL), 2′3′-cGMP-AMP (cGAMP) (20 μg/mL), or infected with ECTV (MOI of 1) for 15 h, respectively. Luciferase activity was determined using the Dual-Glo® Luciferase Assay System. **(D)** HEK293T cells were transfected with Sting expressing plasmid (50 ng/well), and increasing doses of plasmids expressing cGas (25, 50, and 100 ng/well) combined with decreasing doses of vector (75, 50, and 0 ng/well). **(E)** HEK293T cells were transfected with increasing doses of plasmids expressing Sting (25, 50, and 100 ng/well) combined with decreasing doses of vector (75, 50, and 0 ng/well). After a 24-h transfection, cells were infected with ECTV at an MOI of 1 for 15 h. Expression of transfected cells with increasing doses cGas or Sting was examined by immunoblot analysis. HEK293T cells were transfected with cyclic GMP-AMP synthase (cGAS) (50 ng) combined with Sting (50 ng) expressing plasmids **(F)** or Sting (100 ng) expressing plasmids **(G)**, and 24 h later, cells were infected with ECTV and UV-inactivated ECTV at an MOI of 1 for 15 h. Luciferase activity was determined using the Dual-Glo Luciferase Assay System. All the data were averaged from three independent experiments in biological triplicate and represents mean ± SD. Statistical analyses were performed by a *t*-test **(F,G)** or one-way analysis of variance followed by the Duncan's multiple range test (*$P \leq 0.05$; **$P \leq 0.01$; and ***$P \leq 0.001$).

As the host range of ECTV is restricted, we next investigated the roles of cGas and Sting in response to ECTV infection in murine cells. NIH3T3 and L929 cells were transfected with expression plasmids or siRNAs for cGas or Sting, and then were infected with ECTV. Overexpression or knockdown of cGas and Sting in these two cell lines were confirmed by immunoblotting as shown in **Figure 2** and Figure S2 in Supplementary Material. Overexpression of cGas or S-wt resulted in the increased induction of IFN-α, IFN-β, and Ifit1 mRNA levels in ECTV-infected L929 cells, but which were non-existent in cells transfected with Sting-gt (a point mutation that results in the loss of Sting expression) (**Figure 2B**). Expectedly, knockdown of either cGas or Sting decreased the induction of IFN-α, IFN-β, and Ifit1 mRNA levels in L929 cells with the ECTV infection (**Figure 2D**). However, the mRNA levels of the three molecules (IFN-α, IFN-β, and Ifit1) showed no significant changes in NIH3T3 cells, and thus may not have a function in the cGas–Sting pathway in this cell line (Figures S2B,D in Supplementary Material). Therefore, this suggests that the cGAS and STING may be responsible for sensing ECTV infections and inducing type I IFN expression.

ECTV Infection Induces the Phosphorylation of Tbk1 and Irf3

It is well known that TBK1 and IRF3 are two important factors of multiple antiviral signaling pathways, including cytosolic DNA

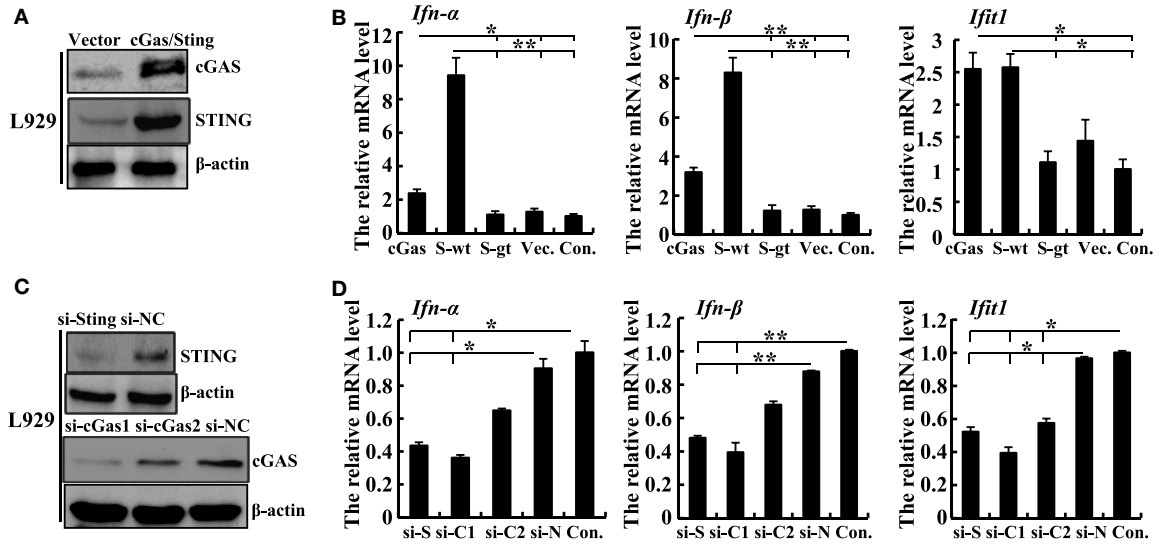

FIGURE 2 | Sting and cGas are required for the induction of IFN-β during ectromelia virus (ECTV) infection in L929 cells. **(A)** Western blot analysis of overexpressed cGas, Sting, and β-actin protein levels in L929 cells. **(B)** L929 (2×10^5) cells were seeded in a 12-well plate and then were transfected with cGas, Sting-wt (S-wt), Sting-gt (S-gt), or empty (Vec.) plasmids. Thirty hours after transfection, cells were infected with ECTV (MOI of 5) for 18 h, and then the mRNA levels of IFN-α, IFN-β, and Ifit1 were analyzed by qPCR. **(C)** Western blot analysis of siRNA knockdown of cGas, Sting, and β-actin protein levels in L929 cells. **(D)** L929 (2×10^5) cells were seeded in a 12-well plate and then were transfected with siRNAs for cGas (si-C1 and si-C2), Sting (si-S), or si-NC (si-N). Thirty-six hours after transfection, cells were infected with ECTV (MOI of 5) for 18 h, and then the mRNA levels of IFN-α, IFN-β, and Ifit1 were analyzed by qPCR. All the data represent mean ± SD of biological triplicates from at least three independent experiments. Statistical analyses were performed by one-way analysis of variance followed by the Duncan's multiple range test. Con. means control group, which cells were only infected with ECTV (MOI of 5). In this figure, $^*P \leq 0.05$ and $^{**}P \leq 0.01$.

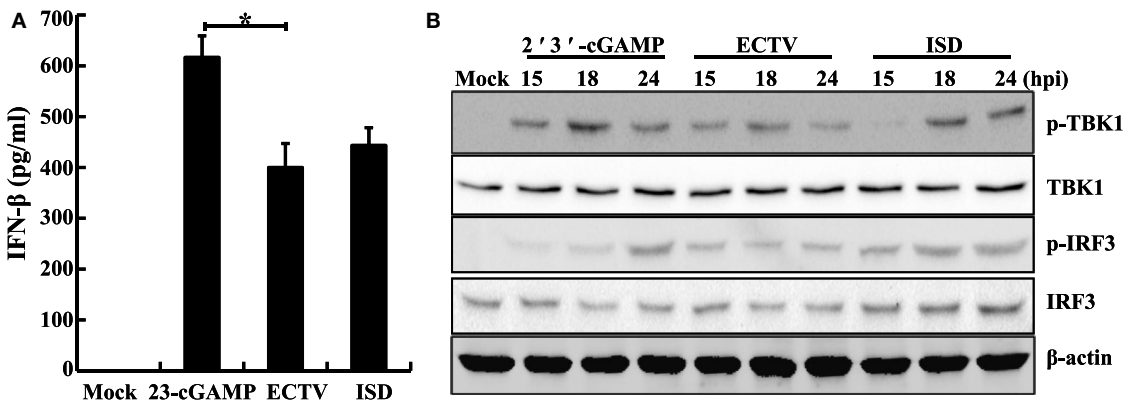

FIGURE 3 | Ectromelia virus (ECTV) infection induces the phosphorylation of Tbk1 and Irf3. RAW264.7 cells (1×10^6) were either stimulated with poly(dA:dT)/LyoVec (2 μg/mL), ISD/LyoVec (1 μg/mL), 2′3′-cGMP-AMP (cGAMP) (20 μg/mL), or infected with ECTV (MOI of 5). The supernatants were collected at 18 h post-infection (hpi) for determining the concentrations of IFN-β by using enzyme-linked immunosorbent assay (ELISA) **(A)**, and cells were collected at 15, 18, and 24 hpi. All the collected cells were used for western blot analysis using anti-phospho-Tbk1, anti-Tbk1, anti-phospho-Irf3, and anti-Irf3 **(B)**. β-Actin was used as a loading control. The ELISA data were averaged from three independent experiments in biological triplicate. The data were analyzed using a one-way analysis of variance followed by the Duncan's multiple range test. Results of western blot analysis shown are representative of three independent experiments ($^*P \leq 0.05$).

sensor signaling such as through the cGAS–STING signaling pathway (44). We performed western blot analysis of ECTV-infected L929, NIH3T3, and RAW264.7 cells, and found that the ECTV infection triggered Tbk1 and Irf3 phosphorylation in RAW264.7 and L929 cells, which reached peaks at 18 hpi (Figures S3A,B in Supplementary Material), whereas it failed to do so in NIH3T3 cells (Figure S3C in Supplementary Material), indicating that ECTV induced the levels of phosphorylation of Tbk1 and Irf3 in L929 and RAW264.7 cells in a cell type-dependent manner (15, 45). In addition, upon stimulation with ISD and 2′3′-cGAMP, the Irf3 and Tbk1 were phosphorylated, and IFN-β was secreted in RAW264.7 cells (**Figures 3A,B**). Notably, much higher levels of phosphorylation of Tbk1 and Irf3 were stimulated by ISD and 2′3′-cGAMP than by the ECTV infection, indicating that

ECTV might express some potent immunomodulators that are involved in the modulation of TBK1 and IRF3 phosphorylation. Alternatively, this may be due to a stronger stimulation with the concentrations of cGAMP or ISD.

The cGas–Sting–Tbk1–Irf3 Pathway Drives the Early IFN Response to ECTV

The critical role of Tlr9 for type I IFNs induction in ECTV-infected mice has been recently emphasized (32). Other PRRs, such as DAI, a receptor upstream of Sting, has been ruled out for driving the expression of type I IFNs during ECTV infections (32). As previously described, cGAS acts as a general cytosolic DNA sensor upstream of STING that is responsible for the recognition of several DNA viruses, including VACV, modified vaccinia virus Ankara (MVA), herpes simplex virus 1 (HSV-1), murine gammaherpesvirus 68 (MHV68), Kaposi's sarcoma-associated herpesvirus, adenovirus, human papilloma viruses, hepatitis B virus, and human cytomegalovirus (36, 41, 46–50). However, whether the cGas also recognizes ECTV and induces the production of type I IFNs are largely unknown so far. Subsequently, to investigate the contributions of the cGas–Sting–Tbk1–Irf3 pathway for driving the production of type I IFNs during the ECTV infection, *cGas*$^{-/-}$, *Sting*$^{-/-}$, *Tbk1*$^{-/-}$, and *Irf3*$^{-/-}$ RAW264.7 cells were challenged with ECTV, and the secretion of IFN-β and levels of phosphorylation of IRF3 and TBK1 were detected by ELISA and immunoblotting, respectively. As shown in **Figures 4A,B**, we found that ECTV-induced IFN-β secretion was reduced by nearly 82% in *cGas*$^{-/-}$ cells, while the *Sting*$^{-/-}$ cells nearly abolished the secretion of IFN-β, which suggests the *cGas* deficiency might be partially complemented by other receptors upstream of STING, such as IFI16 (mouse: Ifi204) and DDX41. Similar to *Sting*$^{-/-}$ cells, ECTV-induced IFN-β secretion was barely detectable in *Tbk1*$^{-/-}$ and *Irf3*$^{-/-}$ cells (**Figures 4C,D**, respectively). In addition, the phosphorylation levels of IRF3 and TBK1 were not detected in these knockout cells by western blot analysis. As compared with WT cells, Tbk1 and Irf3 phosphorylation were severely impaired in cGas-deficient cells (**Figure 4A**). Consistently, the phosphorylation of Irf3 and Tbk1 in *Sting*$^{-/-}$ cells appeared weaker than in the WT cells (**Figure 4B**). As expected, cells deficient in Tbk1 or Irf3 appeared to have weaker levels of Tbk1 or Irf3 phosphorylation, respectively (**Figures 4C,D**), indicating other pathways involved in Tbk1 or Irf3 were activated during the ECTV infection.

Furthermore, to confirm these results in primary cells, peritoneal macrophages were generated from WT, *Tlr9*$^{-/-}$, *cGas*$^{-/-}$, *Sting*$^{gt/gt}$, and *Irf3*$^{-/-}$ mice and the type I IFN induction and phosphorylation of TBK1 or IRF3 upon ECTV infection were evaluated. As shown in **Figures 5A,B**, the IFN-β secretion was only detected in WT, *cGas*$^{-/-}$, and *Sting*$^{gt/gt}$ cells. As compared

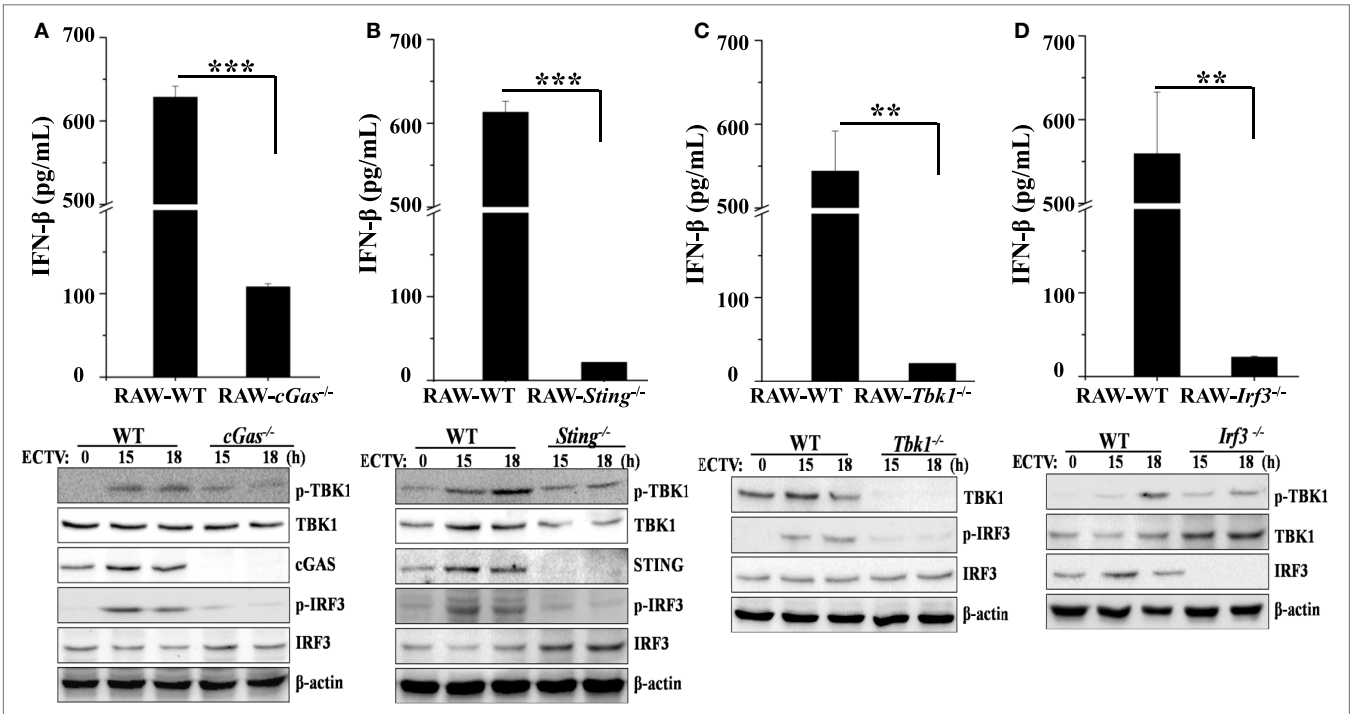

FIGURE 4 | The cGas–Sting–Tbk1–Irf3 pathway contributes to the induction of IFN-β in RAW264.7 cells by ectromelia virus (ECTV). *cGas*$^{-/-}$ **(A)**, *Sting*$^{-/-}$ **(B)**, *Irf3*$^{-/-}$ **(C)**, and *Tbk1*$^{-/-}$ **(D)** RAW264.7 and wild-type (WT) cells were infected with ECTV at an MOI of 5. Supernatants were collected 18 h post-infection (hpi) for determining the concentrations of IFN-β by using enzyme-linked immunosorbent assay (ELISA), and cells were collected at 15 and 18 hpi for western blot analysis using anti-phospho-Tbk1, anti-Tbk1, anti-phospho-Irf3, and anti-Irf3. β-Actin was used as a loading control. The ELISA data are averaged from three independent experiments in biological triplicate. Results of western blot analysis shown are representative of three independent experiments. The data were analyzed using a *t*-test on SPSS software (**$P \leq 0.01$ and ***$P \leq 0.001$).

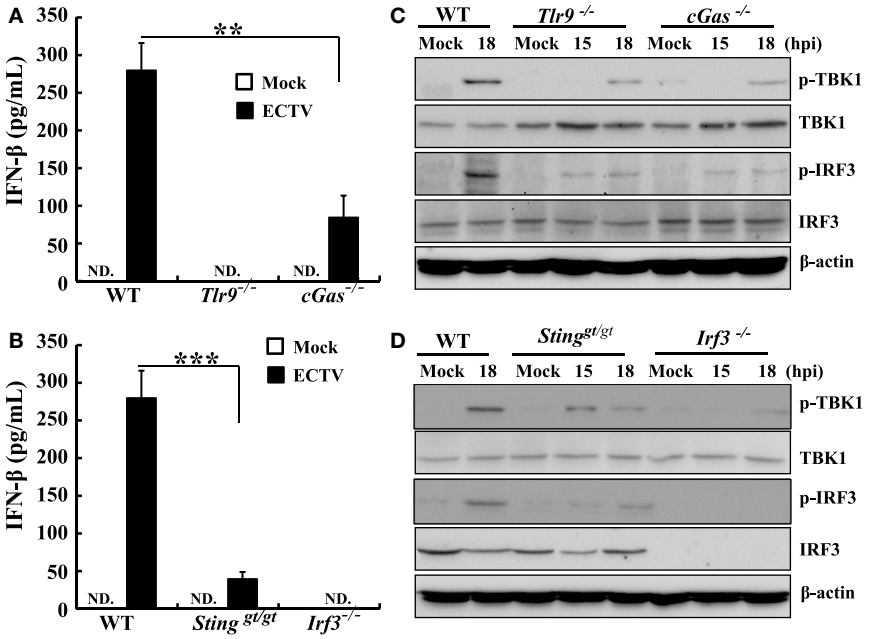

FIGURE 5 | Murine peritoneal macrophages response ectromelia virus (ECTV) infection was dependent on Tlr9 and cGas–Sting–Irf3 pathway. Peritoneal macrophages generated from wild-type (WT), *cGas*$^{-/-}$, *Sting*$^{gt/gt}$, *Tlr9*$^{-/-}$, and *Irf3*$^{-/-}$ mice were non-infected or infected with ECTV at an MOI of 5. Supernatants were collected 18 h post-infection (hpi) for determining the concentrations of IFN-β by using enzyme-linked immunosorbent assay (ELISA) **(A,B)**, and cells were collected at 15 and 18 hpi for western blot analysis using anti-phospho-Tbk1, anti-Tbk1, anti-phospho-Irf3, and anti-Irf3 **(C,D)**. β-Actin was used as a loading control. The ELISA data were averaged from two independent experiments in biological triplicate. Results of western blot analysis shown are representative of two independent experiments. The data were analyzed using a *t*-test on SPSS software. In this figure, ND, not detected; $^{**}P \leq 0.01$ and $^{***}P \leq 0.001$.

with WT cells, ECTV-induced IFN-β secretion was reduced by 70 and 86% in *cGas*$^{-/-}$, and *Sting*$^{gt/gt}$ cells, respectively, while the *Tlr9*$^{-/-}$ and *Irf3*$^{-/-}$ cells abolished the secretion of IFN-β. Similarly, the phosphorylation of TBK1 or IRF3 induced by ECTV were severely impaired in all these gene knockout peritoneal macrophages (**Figures 5C,D**). Taken together, these results definitively show that ECTV infection is capable of activating the cGas–Sting–Tbk1–Irf3 axis and Tlr9, leading to the transcription of type I IFNs.

Sting and cGas Restrict ECTV Replication in RAW264.7 Cells

It has been previously reported that STING has the ability to control viral replication (15, 51, 52). To address whether the cGas–Sting pathway has the ability to restrict ECTV replication, *cGas*$^{-/-}$, *Sting*$^{-/-}$, and WT RAW264.7 cells were infected with two doses (MOI of 0.1 and 5) of virus, and viral titers were assessed after 24 and 48 hpi. Significant increases in the amount of viral progeny released were observed in *cGas*$^{-/-}$ and *Sting*$^{-/-}$ cells compared with WT cells at all time points. At a low MOI of 0.1, cells deficient in Sting showed more increased viral replication than those lacking cGas, which showed a fourfold and twofold increase in *Sting*$^{-/-}$ and *cGas*$^{-/-}$ cells, respectively, as compared with WT cells at 24 hpi (**Figure 6A**). At 48 hpi, similar results were observed but a higher enhanced replication was observed in knockout cells (20-fold and 5.7-fold in *Sting*$^{-/-}$ and *cGas*$^{-/-}$ cells, respectively) (**Figure 6A**). Moreover, ECTV growth curves were generated at an infection dose of MOI of 5. As compared with a low infection dose, we observed reduced progeny release (3.2-fold and 2.5-fold in *Sting*$^{-/-}$ and *cGas*$^{-/-}$ cells, respectively) at 48 hpi (**Figure 6B**). Collectively, these results demonstrate that cGas and Sting have abilities to restrict ECTV replication *in vitro*.

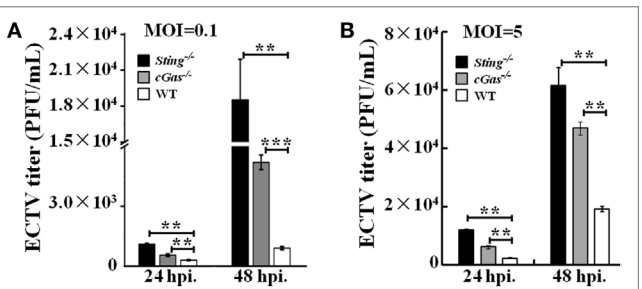

FIGURE 6 | Sting and cGas restrict ectromelia virus (ECTV) replication in RAW264.7 cells. *Sting*$^{-/-}$, *cGas*$^{-/-}$, and wild-type (WT) cells were infected with ECTV at an MOI of 0.1 **(A)** or 5 **(B)**. After a 2-h incubation, the supernatants were replaced with fresh medium supplemented with 1% fetal bovine serum, and then the supernatants were collected at the indicated time points for viral titer measurements by using the plaque assay. All the data represent mean ± SD of biological triplicates from at least three independent experiments. The data were analyzed using a one-way analysis of variance followed by the Duncan's multiple range test ($^{**}P \leq 0.01$ and $^{***}P \leq 0.001$).

Sting and cGas Are Critical for Mousepox Resistance *In Vivo*

Our *in vitro* studies reveal the cGas-Sting pathway plays an essential role in controlling ECTV infection *via* inducing the production of type I IFNs. To further investigate whether the cGAS–STING axis was required for resistance to mousepox *in vivo*, $Tlr9^{-/-}$, $cGas^{-/-}$, $Sting^{gt/gt}$, and WT C57BL/6 mice were infected with a low (3×10^3 PFU per mouse) and high dose (1.0×10^6 PFU per mouse) of ECTV in the footpad, respectively. We found that after infection with a low dose (3×10^3 PFU per mouse) of ECTV, mice deficient in Tlr9 ($Tlr9^{-/-}$) or Sting ($Sting^{gt/gt}$) were highly susceptible to mousepox. In agreement with previous studies, death occurred in 100% of $Tlr9^{-/-}$ but only in 72.4% of $Sting^{gt/gt}$ mice (**Figure 7A**). However, mice lacking *cGas* ($cGas^{-/-}$) showed no lethality, similar to WT mice. Consistently, viral genome copy number and viral loads in the livers and spleens of $Tlr9^{-/-}$ and $Sting^{gt/gt}$ mice but not of $cGas^{-/-}$ mice were significantly higher than in WT mice (**Figures 7D–G**). Moreover, the livers of $Tlr9^{-/-}$ and $Sting^{gt/gt}$ mice showed severe pathology as determined by histology, which were mild in both $cGas^{-/-}$ and WT mice (**Figure 7C**). More infiltration of inflammatory cells and massive necrosis were observed in the livers of $Tlr9^{-/-}$ and $Sting^{gt/gt}$ mice. We next assayed the mRNA levels of IFN-β in the spleen at 3 dpi as well as the secretion of IFN-β in the serum of infected mice at 6, 12, 24, and 48 hpi and 3, 5, and 7 dpi. Unfortunately, none of the serum samples from all the infected mice were detectable. The expression of IFN-β in the spleens was significantly lower in $Tlr9^{-/-}$ and $Sting^{gt/gt}$ but not in $cGas^{-/-}$ and WT mice (**Figure 7B**). Nevertheless, $Tlr9^{-/-}$ mice expressed significantly lower levels of IFN-β than $Sting^{gt/gt}$ mice (**Figure 7B**). Thus, $Tlr9^{-/-}$ and $Sting^{gt/gt}$ mice are both critical for resistance to ECTV infection at a relatively low dose.

Considering the results obtained from a low dose of infection, we found slightly reduced expression of IFN-β, mild pathology, and higher viral loads in $cGas^{-/-}$ mice than in WT mice; therefore, a lethal dose of virus (1.0×10^6 PFU per mouse) was used for further animal infections. Similar to the low infection dose, $Tlr9^{-/-}$ and $Sting^{gt/gt}$ mice were more susceptible to ECTV infection, but both resulted in 100% mortality. The $cGas^{-/-}$ mice had a lower survival rate (14%) and succumbed to disease more rapidly than WT mice. All $Tlr9^{-/-}$ mice died between 5 and 6 dpi, and viral loads, viral genome copy number, and pathology were therefore only performed in the remaining three groups (**Figure 8A**). Accordingly, vial genome copy number and viral loads in the livers and spleens of $Sting^{gt/gt}$ and $cGas^{-/-}$ mice were higher than in WT mice (**Figures 8D–G**). Meanwhile, the $Sting^{gt/gt}$ and $cGas^{-/-}$ mice showed more infiltration of inflammatory cells and more severe bridging necrosis than WT mice as determined by histology (**Figure 8C**). Furthermore, the expressions of IFN-β in the spleens of $Tlr9^{-/-}$, $Sting^{gt/gt}$, and $cGas^{-/-}$ mice were significantly

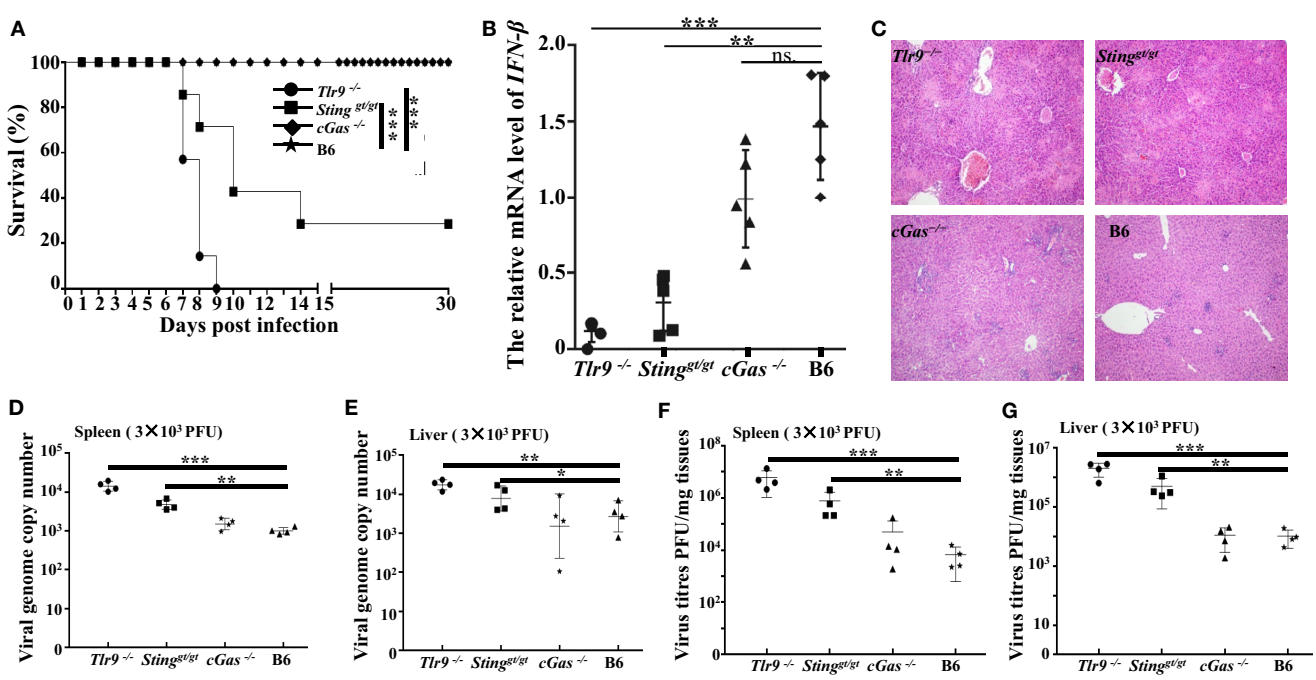

FIGURE 7 | Tlr9 and Sting are critical for resistance to ectromelia virus (ECTV) at a low infection dose. $Sting^{gt/gt}$, $cGas^{-/-}$, $Tlr9^{-/-}$, and wild-type (WT) mice (B6) were infected with 3×10^3 plaque-forming units (PFUs) of ECTV in the left footpad. **(A)** Mice were monitored twice daily over 30 days for survival. **(B)** The expression of IFN-β in the spleens of the indicated mice at 3 days post-infection (dpi) was examined by qPCR. **(C)** Liver sections of the indicated mice at 7 dpi were stained with hematoxylin and eosin. **(D–G)** The spleen and liver from infected mice were harvested at 7 dpi, and then the viral genome copy numbers **(D,E)** and viral loads **(F,G)** were determined by qPCR and plaque assay, respectively. Statistical analyses were performed by one-way analysis of variance followed by the Duncan's multiple range test. For survival experiments, we used the log-rank (Mantel–Cox). In this figure, ns, not significant; $^*P \leq 0.05$; $^{**}P \leq 0.01$; and $^{***}P \leq 0.001$.

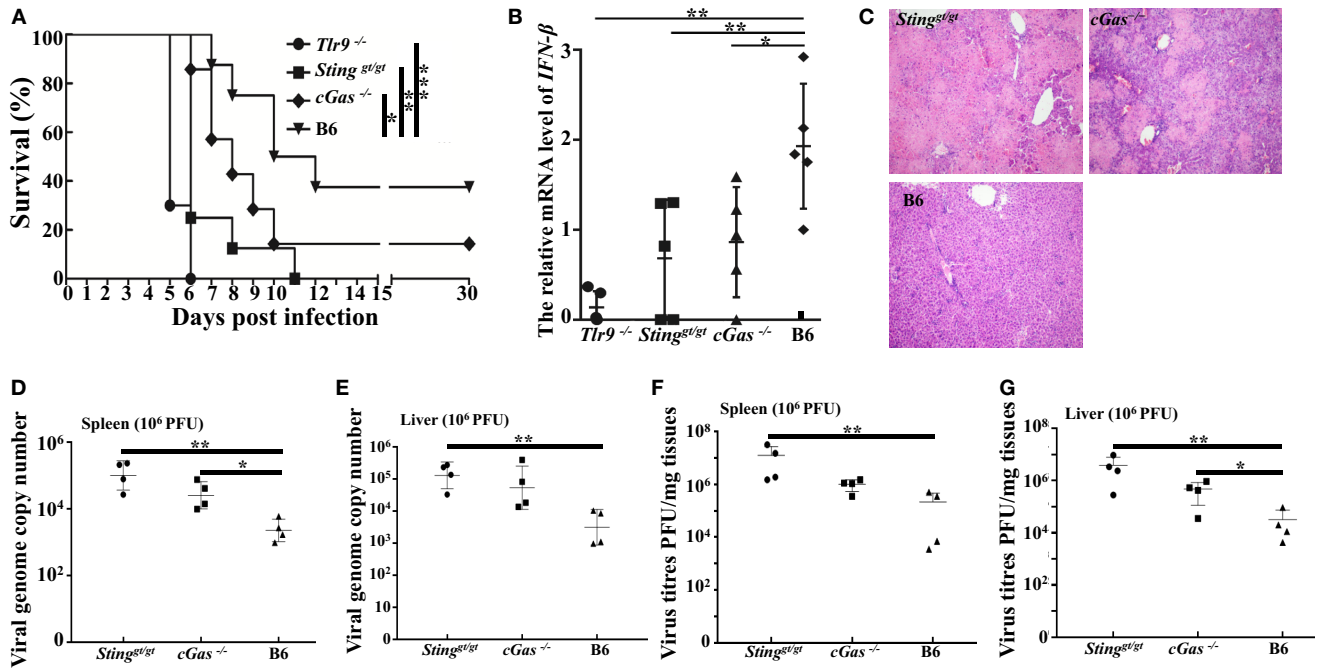

FIGURE 8 | Tlr9, Sting, and cGas are critical for resistance to ectromelia virus (ECTV) at a high infection dose. *Sting*$^{gt/gt}$, *cGas*$^{-/-}$, *Tlr9*$^{-/-}$, and wild-type (WT) mice (B6) were infected with 1 × 10^6 plaque-forming units (PFUs) of ECTV in the left footpad. **(A)** Mice were monitored twice daily over 30 d for survival. **(B)** Expression of IFN-β in the spleens of the indicated mice at 3 days post-infection (dpi) was examined by qPCR. **(C)** Liver sections of the indicated mice at 7 dpi were stained with hematoxylin and eosin. **(D–G)** The spleen and liver from infected mice were harvested at 7 dpi, and then viral genome copy numbers **(D**,**E)** and viral loads **(F**,**G)** were determined by qPCR and plaque assay, respectively. Statistical analyses were performed by one-way analysis of variance followed by the Duncan's multiple range test. For survival experiments, we used the log-rank (Mantel–Cox). In this figure, ns, not significant; *$P \leq 0.05$; **$P \leq 0.01$; and ***$P \leq 0.001$.

lower than that in WT mice (**Figure 8B**). Thus, in addition to Tlr9, the cGas–Sting pathway is also essential for survival against ECTV infections.

DISCUSSION

Recognition of pathogen-derived DNA is a vital strategy by which the innate immune system responds to microbial invasions. Atypical or mislocalized DNA can engage multiple innate immune pathways to trigger the production of type I IFNs and the establishment of the cellular antiviral state (53). TLR9 is a receptor for unmethylated CpG DNA motifs presents in the endosomal membranes of phagocytic cells. Signaling through Tlr9 is induced by ECTV to produce type I IFNs responses in plasmacytoid dendritic cells (pDCs) but not in classical dendritic cells (cDCs) (33). The recognition of ECTV in a Tlr9-dependent manner to produce type I IFNs has been well established *in vitro* and *in vivo* (32–34). Experimentally, Tlr9 has been concluded to be the only TLR required for mousepox resistance by ruling out other TLR members (32). Recently, Sting, a critical mediator of the cytosolic DNA-sensing pathway, has been confirmed to have essential roles in the resistance to ECTV infections (32). In addition, the cGAS–STING pathway is emerging as the dominant cytosolic DNA-sensing pathway in infections by DNA viruses (5, 8, 19). Furthermore, it has recently been demonstrated that Dai was not the critical DNA sensor upstream of Sting for the recognition of ECTV infection and the induction of type I IFNs (32). However, the receptor upstream of Sting that senses ECTV to drive the expression of type I IFNs has not yet been identified. Therefore, we hypothesized that the cGas–Sting pathway contributes to the production of type I IFNs in ECTV-infected cells.

Using the *in vitro* ECTV-infection model, we have demonstrated that ECTV induces type I IFN production in L929 and RAW264.7 cells, but not in NIH3T3 cells. Similarly, ECTV can stimulate the production of IFN-α in pDCs but not in cDCs (33). Consistent with the determination of the phosphorylation of TBK1 and IRF3, ECTV infections triggered the phosphorylation of Tbk1 and Irf3 in L929 and RAW264.7 cells, whereas it fails to do so in NIH3T3 cells. Moreover, overexpression or knockdown levels of cGas and Sting have no significant effect on type I IFN expression levels in ECTV-infected NIH3T3 cells. As described in previous studies, not all cell lines are able to respond to DNA viruses or cytosolic DNA, and the deficiency or poor expression of some key factors involved in the innate immune response results in the failure of type I IFN production (45). Thus, the NIH3T3 cell line is not suitable for the study of innate immune pathways. In addition, the IFN-β luciferase promoter assay revealed that overexpression of cGas and Sting can induce IFN-β promoter activation following an ECTV infection. Accordingly, the cGas or Sting-activating ligands ISD and 2′3′-cGAMP displayed higher

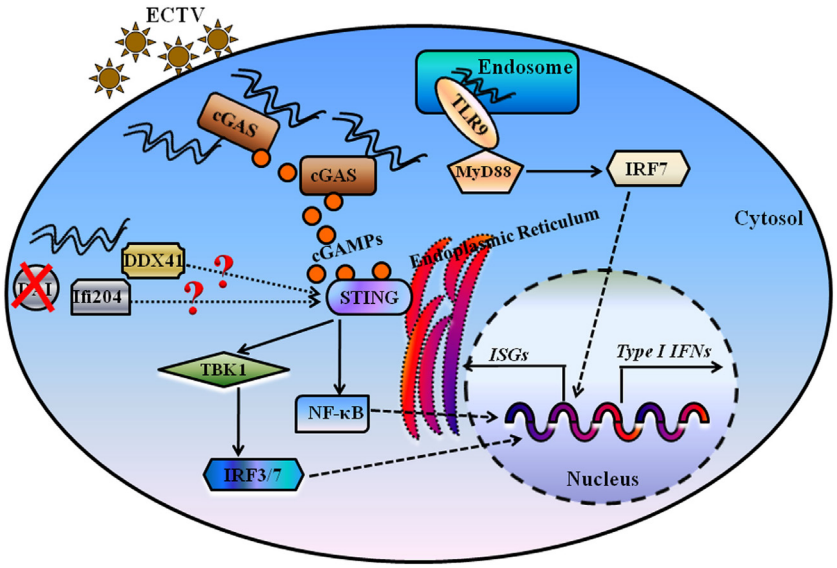

FIGURE 9 | Proposed model for illustrating the essential roles of DNA sensors in recognition and innate interferons (IFNs) production during ectromelia virus (ECTV) infection. Upon viral entry, some of ECTV virions are processed in the endosome, and viral DNA is firstly detected by Tlr9, which signals through the Myd88–Irf7 axis to promote expression of type I IFNs. Moreover, some of viral DNA is detected by the cytosolic DNA sensor cGas, and cGas catalyzes the formation of cGMP-AMP (cGAMP), which through the Sting–Tbk1–Irf3/7 axis leads to the activation of IFN responses. Other cytosolic DNA sensors, including Ifi204 and Ddx41, potentially recognize viral DNA present in the cytoplasm for the activation of IFN responses. DAI, one of the receptors upstream of Sting, has been ruled out as the critical DNA sensor for the activation of IFN responses during an ECTV infection.

stimulatory potency but not poly(dA:dT). As for poly(dA:dT), this ligand has no effect on the induction of type I IFN in the absence or presence of cGas or Sting, and it is possible that the RNA polyIII–RIG-I pathway is involved in a poly(dA:dT) mediated-IFN response (42, 54). ECTV encodes host–response modifiers (HRMs) of both NF-κB and type I IFN pathways (55–58). The mechanism of action of HRMs to inhibit the host immune response is by disrupting receptor–ligand interactions but also acts through impeding cytokine secretion or modulating post-ligation signaling (55, 56). Thus, the lower levels of IFN-β expression induced by ECTV may result from the modification of the type I IFN pathways by ECTV-encoded HRMs. Alternatively, a higher stimulatory potency of ISD and 2′3′-cGAMP is observed because they are "pure" ligands. Moreover, compared with ISD and 2′3′-cGAMP, the lower levels of phosphorylation of Irf3 and Tbk1 induced by ECTV needs to be more fully confirmed in future studies.

The STING has been identified as a pivotal signaling adaptor for the cytosolic DNA sensors and the induction of type I IFN. Besides cGAS, a series of studies have established several other cytosolic DNA sensors utilizing STING as an adaptor, including IFI16 (mouse: Ifi204), DAI, and DDX41 (54, 59, 60). We found nearly 97 and 86% reduced IFN-β induction in ECTV-infected *Sting*$^{-/-}$ RAW264.7 cells and *Sting*$^{gt/gt}$ peritoneal macrophages, respectively, whereas IFN-β induction was reduced by 82% in cGas-deficient RAW264.7 cells and 70% in *cGas*$^{-/-}$ peritoneal macrophages, suggesting other Sting-dependent DNA sensors might also be involved in the IFN-β production. However, Dai has been ruled out as the DNA receptor upstream of Sting for the recognition of ECTV *in vivo* because no differences were observed in the survival rate and type I IFNs expression between *Dai*$^{-/-}$ and WT mice (32). We have not yet determined the contributions of Ifi204 and Ddx41 to the induction of type I IFN production in ECTV infections. However, data from modified vaccinia virus Ankara (MVA), an attenuated VACV also belonging to OPV, showed that DDX41 is required for the MVA-induced phosphorylation of TBK1 and IRF3 in macrophages, and no significant differences were observed for MVA-induced type I IFN production in IFI16-deficient cDCs, as compared with WT cells (36). Thus, the exact functions of Ifi204 and Ddx41 or other specific candidate receptors in the resistance to ECTV need to be investigated in the future. Alternatively, an STING-dependent but cGAS-independent pathway was reported in the production of type I IFN and ISGs, which was stimulated by membrane perturbation, including virus–cell fusion, liposome–cell fusion or cell–cell fusion that act as a danger signal (61, 62). Here, the different reduction of IFN-β in Sting-deficient and cGas-deficient macrophages could originate from the capacity of STING to sense the viral particles directly. Therefore, it should be pointed out that an indirect activity of cGas cannot be ruled out for the production of type I IFN through STING-dependent but cGAS-independent pathway in this study.

ECTV causes a lethal infection to mice but displays different pathogenicity among different mouse genotypes (63). It was established that C57BL/6 mice were classified as resistant, with a 50% lethal dose (LD_{50}) > 10^5 PFU, whereas BALB/c mice are susceptible (LD_{50} < 10 PFU) to ECTV infection (64). Using two infection doses, 3×10^3 PFU and 10^6 PFU, data from the

survival rates, pathology, and IFN-β induction of infected mice revealed the importance of Tlr9 in the resistance to mousepox, which is consistent with the recent finding that Tlr9 is the only TLR required for resistance to mousepox. By contrast, the role of cGas in the resistance to mousepox is not outstanding at the low dose of infection, but its importance was highlighted at the high dose of infection, which suggests that a weak or no role of cGas–Sting pathway is involved at a low dose of infection. However, mice deficient in Sting are more susceptible to mousepox than cGas-deficient mice, suggesting other Sting-dependent pathways might sense ECTV to drive type I IFN expression. As mentioned earlier, Dai has been ruled out, and Ifi204 and Ddx41 need to be further evaluated. Fortunately, it has been established that the production of IFN-α is mostly through Sting-Irf3 and the production of IFN-β is through Sting–NF-κB (31, 32). We therefore postulate that when the viral particle fuses to the cell membrane, the ECTV genomic DNA are endocytosed and are sensed by TLR9 in the endosomal/lysosomal compartment. On the other hand, the ECTV capsid is broken down in the cytoplasm, triggering leakage of the viral DNA into the cytoplasm and leading to the detection of viral DNA by cGas and other cytosolic DNA sensors, and the expression of type I IFNs through the Sting adapter (**Figure 9**). In addition, it has been shown that TLR9 contributes to the production of type I IFNs to systemic viral infections, while cytosolic nucleic acid sensors including cGAS, IFI16 (mouse: Ifi204), RIG-I, and MDA5 mediate local immune responses to viral infections (36). Notably, the secretion of IFN-β in the serum of all mice through a subcutaneous infection was undetectable in our study, suggesting the cGas–Sting pathway might be responsible for local type I IFNs production at the early stage of ECTV infections. Furthermore, at the late stage of viral infections, Tlr9 may contribute to the production of type I IFNs in a systemic ECTV infection. Moreover, AIM2 is another cytosolic DNA sensor but activates ASC-caspase-1-dependent inflammasome in response to cytosolic dsDNA, leading to the generation of IL-1β and IL-18 (65, 66). However, AIM2 inflammasome can attenuate cGAS–STING-mediated type I IFNs production in resistance to VACV, HSV-1, VSV, and SeV infections (8). Also, we found that *Aim2*$^{-/-}$ and *caspase-1*$^{-/-}$ mice were resistant to ECTV infection compared with the WT mice, which was associated with lower viral loads and milder pathology in the spleens and livers of *Aim2*$^{-/-}$ and *caspase-1*$^{-/-}$ mice (unpublished data). Interestingly, a recent published study has reported that Irf7 is necessary for Tlr9–Myd88 and Sting–Irf7/NF-κB pathway the expression of pro-inflammatory cytokines and type I IFNs, respectively, but not Irf3, with ECTV infection *in vivo* (31, 32). However, we found that Irf3 is required for the ECTV-induced type I IFN production *in vitro*, but the roles of Irf3/7 in the induction of pro-inflammatory cytokines and type I IFNs are not investigated *in vitro* and/or *in vivo*, and would need to be confirmed in future studies. In addition, cGAS triggers innate immune responses through the production of the second messenger cGAMP, which binds and activates the STING, and ultimately leads to induction of type I IFNs by the activation of the TBK1 and IRF3. Then, further studies are needed to elucidate whether the cGAMP is produced upon ECTV infection.

In summary, we present data demonstrating the critical role of the cGas–Sting pathway in ECTV-induced type I IFN production *in vitro* and *in vivo*. ECTV was sensed by cGas and induced the production of type I IFN through the Sting–Tbk1–Irf3 axis to restrict the replication of virus. Although the importance of the Tlr9–Myd88 pathway in mousepox resistance has been well established, the cytosolic DNA-sensing pathways, especially the cGas–Sting pathway, also act sequentially to orchestrate resistance to ECTV infection.

ETHICS STATEMENT

All mice were handled in accordance with the Good Animal Practice Requirements of the Animal Ethics Procedures and Guidelines of the People's Republic of China, and the protocol was reviewed and approved by the Animal Ethics Committee of Lanzhou Veterinary Research Institute, Chinese Academy of Agricultural Science (Permit No. LVRIAEC2016-005).

AUTHOR CONTRIBUTIONS

W-YC, Z-ZJ, and X-BH conceived and designed the study and critically revised the manuscript. W-YC, H-JJ, G-HC, Z-LL, and Q-WJ performed the experiments, analyzed the data, and drafted the manuscript. W-YC wrote the paper. All the authors read and approved the final manuscript.

ACKNOWLEDGMENTS

We gratefully acknowledge Laboratory Animal Center of Lanzhou Veterinary Research Institute for raising animals. We thank Friedemann Weber (Justus-Liebig University Giessen) for critically reading the manuscript. All the authors would like to acknowledge Editage for English language editing.

FUNDING

This work was supported by grants from the Natural Science Funds for the Natural Science Foundation of Gansu (17JR5RA325), the Fundamental Research Funds for the Lanzhou Veterinary Research Institute (1610312016019), the Fundamental Research Funds for the Chinese Academy of Agricultural Sciences (1610312017005), and National Natural Science Funds for the National Natural Science Foundation of China (31302072). The funder had no role in study design, data collection and analysis, decision to publish, or preparation of the manuscript.

SUPPLEMENTARY MATERIAL

The Supplementary Material for this article can be found online at https://www.frontiersin.org/articles/10.3389/fimmu.2018.01297/full#supplementary-material.

FIGURE S1 | Ectromelia virus (ECTV) induces type I IFN production in L929 and RAW264.7 cells. **(A)** NIH3T3, L929, and RAW264.7 cells were either stimulated with ISD (at a final concentration of 1 μg/mL) or infected with ECTV at an MOI of 5. Supernatants were collected at 18 h post-infection (hpi). The concentrations of IFN-β in supernatants were determined by enzyme-linked immunosorbent assay

(ELISA). RAW264.7 cells (1×10^6) were infected with ECTV at an MOI of 0.1, 0.5, 1, 2, or 5. Subsequently, cells were washed twice with cold phosphate-buffered saline and were collected at 18 hpi. Total RNA was extracted using TRIzol reagent and reverse transcribed into cDNA, which was used to determine the relative mRNA levels of IFN-α **(B)** and IFN-β **(C)**. RAW264.7 cells (1×10^6) were infected with ECTV at an MOI of 5. Cells and supernatants were separately collected at 0, 4, 8, 12, 15, 18, and 24 hpi. Total RNA was extracted using TRIzol Reagent and reverse transcribed into cDNA, which was determined the relative mRNA levels of IFN-α **(D)** and IFN-β **(E)**. The concentrations of IFN-β in supernatants were determined by ELISA **(F)**. All results are shown as mean ± SD from four independent experiments. Statistical analyses were performed by one-way analysis of variance followed by the Duncan's multiple range test. In this figure, ND, not detected.

FIGURE S2 | Sting and cGas are not required for the induction of IFN-β during ectromelia virus (ECTV) infection in NIH3T3 cells. **(A)** Western blot analysis of overexpressed cGas, Sting, and β-actin protein levels in NIH3T3 cells. **(B)** NIH3T3 (1×10^5) cells were seeded in a 12-well plate and then were transfected with cGas, Sting-wt (S-wt), Sting-gt (S-gt), or empty (Vec.) plasmids. Thirty hours after transfection, cells were infected with ECTV (MOI of 5) for 18 h, and then the mRNA levels of IFN-α, IFN-β, and Ifit1 were analyzed by qPCR. **(C)** Western blot analysis of siRNA knockdown of cGas, Sting, and β-actin protein levels in NIH3T3 cells. **(D)** NIH3T3 (1×10^5) cells were seeded in a 12-well plate and then were transfected with siRNAs for cGas (si-C1 and si-C2), Sting (si-S), or si-NC (si-N). Thirty-six hours after transfection, cells were infected with ECTV (MOI of 5) for 18 h, and then the mRNA levels of IFN-α, IFN-β, and Ifit1 were analyzed by qPCR. All the data represent mean ± SD of biological triplicates from at least three independent experiments. Statistical analyses were performed by one-way analysis of variance followed by the Duncan's multiple range test. Con. means control group, which cells were only infected with ECTV (MOI of 5).

FIGURE S3 | Ectromelia virus (ECTV) infection induces the phosphorylation of Tbk1 and Irf3 in L929 cells and RAW264.7 cells, but not in NIH3T3 cells. L929 cells **(A)** and NIH3T3 cells **(C)** (1×10^6) were uninfected or infected with ECTV at an MOI of 5 and were collected at 4, 8, 12, 15, 18, and 24 h post-infection (hpi). **(B)** RAW264.7 cells (1×10^6) were uninfected or infected with ECTV at an MOI of 5 and were collected at 3, 6, 12, 18, and 24 hpi. Results shown are representative of three independent experiments.

REFERENCES

1. Wu J, Chen ZJ. Innate immune sensing and signaling of cytosolic nucleic acids. *Annu Rev Immunol* (2014) 32:461–88. doi:10.1146/annurev-immunol-032713-120156
2. Cao X. Self-regulation and cross-regulation of pattern-recognition receptor signaling in health and disease. *Nat Rev Immunol* (2016) 16:35–50. doi:10.1038/nri.2015.8
3. Broz P, Monack DM. Newly described pattern recognition receptors team up against intracellular pathogens. *Nat Rev Immunol* (2013) 13:551–65. doi:10.1038/nri3479
4. Kieser KJ, Kagan JC. Multi-receptor detection of individual bacterial products by the innate immune system. *Nat Rev Immunol* (2017) 17:376–90. doi:10.1038/nri.2017.25
5. Tao J, Zhou X, Jiang Z. cGAS-cGAMP-STING: the three musketeers of cytosolic DNA sensing and signaling. *IUBMB Life* (2016) 68:858–70. doi:10.1002/iub.1566
6. Gao J, Tao J, Liang W, Jiang Z. Cyclic (di)nucleotides: the common language shared by microbe and host. *Curr Opin Microbiol* (2016) 30:79–87. doi:10.1016/j.mib.2015.12.005
7. Sun W, Li Y, Chen L, Chen H, You F, Zhou X, et al. ERIS, an endoplasmic reticulum IFN stimulator, activates innate immune signaling through dimerization. *Proc Natl Acad Sci U S A* (2009) 106:8653–8. doi:10.1073/pnas.0900850106
8. Wang Y, Ning X, Gao P, Wu S, Sha M, Lv M, et al. Inflammasome activation triggers caspase-1-mediated cleavage of cGAS to regulate responses to DNA virus infection. *Immunity* (2017) 46:393–404. doi:10.1016/j.immuni.2017.02.011
9. Jose SS, Bendickova K, Kepak T, Krenova Z, Fric J. Chronic inflammation in immune aging: role of pattern recognition receptor crosstalk with the telomere complex? *Front Immunol* (2017) 8:1078. doi:10.3389/fimmu.2017.01078
10. Liu CH, Liu H, Ge B. Innate immunity in tuberculosis: host defense vs pathogen evasion. *Cell Mol Immunol* (2017) 14(12):963–75. doi:10.1038/cmi.2017.88
11. Rosadini CV, Kagan JC. Microbial strategies for antagonizing toll-like-receptor signal transduction. *Curr Opin Immunol* (2015) 32:61–70. doi:10.1016/j.coi.2014.12.011
12. Majer O, Liu B, Barton GM. Nucleic acid-sensing TLRs: trafficking and regulation. *Curr Opin Immunol* (2017) 44:26–33. doi:10.1016/j.coi.2016.10.003
13. Hu MM, Liao CY, Yang Q, Xie XQ, Shu HB. Innate immunity to RNA virus is regulated by temporal and reversible sumoylation of RIG-I and MDA5. *J Exp Med* (2017) 214:973–89. doi:10.1084/jem.20161015
14. Hu MM, Xie XQ, Yang Q, Liao CY, Ye W, Lin H, et al. TRIM38 negatively regulates TLR3/4-mediated innate immune and inflammatory responses by two sequential and distinct mechanisms. *J Immunol* (2015) 195:4415–25. doi:10.4049/jimmunol.1500859
15. Ran Y, Shu HB, Wang YY. MITA/STING: a central and multifaceted mediator in innate immune response. *Cytokine Growth Factor Rev* (2014) 25:631–9. doi:10.1016/j.cytogfr.2014.05.003
16. Li Q, Yan J, Mao AP, Li C, Ran Y, Shu HB, et al. Tripartite motif 8 (TRIM8) modulates TNFα- and IL-1β-triggered NF-κB activation by targeting TAK1 for K63-linked polyubiquitination. *Proc Natl Acad Sci U S A* (2011) 108:19341–6. doi:10.1073/pnas.1110946108
17. Gao D, Wu J, Wu YT, Du F, Aroh C, Yan N, et al. Cyclic GMP-AMP synthase is an innate immune sensor of HIV and other retroviruses. *Science* (2013) 341:903–6. doi:10.1126/science.1240933
18. Herzner AM, Hagmann CA, Goldeck M, Wolter S, Kübler K, Wittmann S, et al. Sequence-specific activation of the DNA sensor cGAS by Y-form DNA structures as found in primary HIV-1 cDNA. *Nat Immunol* (2015) 16:1025–33. doi:10.1038/ni.3267
19. Xia P, Wang S, Gao P, Gao G, Fan Z. DNA sensor cGAS-mediated immune recognition. *Protein Cell* (2016) 7:777–91. doi:10.1007/s13238-016-0320-3
20. Santhakumar D, Rubbenstroth D, Martinez-Sobrido L, Munir M. Avian Interferons and their antiviral effectors. *Front Immunol* (2017) 8:49. doi:10.3389/fimmu.2017.00049
21. Shu C, Li X, Li P. The mechanism of double-stranded DNA sensing through the cGAS-STING pathway. *Cytokine Growth Factor Rev* (2014) 25:641–8. doi:10.1016/j.cytogfr.2014.06.006
22. Ablasser A, Schmid-Burgk JL, Hemmerling I, Horvath GL, Schmidt T, Latz E, et al. Cell intrinsic immunity spreads to bystander cells via the intercellular transfer of cGAMP. *Nature* (2013) 503:530–4. doi:10.1038/nature12640
23. Damon IK, Damaso CR, McFadden G. Are we there yet? The smallpox research agenda using variola virus. *PLoS Pathog* (2014) 10:e1004108. doi:10.1371/journal.ppat.1004108
24. Arita I, Francis D. Is it time to destroy the smallpox virus? *Science* (2014) 345:1010. doi:10.1126/science.345.6200.1010-a
25. Reardon S. 'Forgotten' NIH smallpox virus languishes on death row. *Nature* (2014) 514:544. doi:10.1038/514544a
26. Garver J, Weber L, Vela EM, Anderson M, Warren R, Merchlinsky M, et al. Ectromelia virus disease characterization in the BALB/c mouse: a surrogate model for assessment of smallpox medical countermeasures. *Viruses* (2016) 8:7. doi:10.3390/v8070203
27. Usme-Ciro JA, Paredes A, Walteros DM, Tolosa-Pérez EN, Laiton-Donato K, Pinzón MD, et al. Detection and molecular characterization of zoonotic poxviruses circulating in the Amazon Region of Colombia, 2014. *Emerg Infect Dis* (2017) 23:649–53. doi:10.3201/eid2304.161041
28. Sigal LJ. The pathogenesis and immunobiology of mousepox. *Adv Immunol* (2016) 129:251–76. doi:10.1016/bs.ai.2015.10.001
29. Dolega P, Szulc-Dabrowska L, Bossowska M, Mielcarska M, Nowak Z, Toka FN. Innate immune gene transcript level associated with the infection of macrophages with ectromelia virus in two different mouse strains. *Viral Immunol* (2017) 30:315–29. doi:10.1089/vim.2016.0173
30. Xu RH, Cohen M, Tang Y, Lazear E, Whitbeck JC, Eisenberg RJ, et al. The orthopoxvirus type I IFN binding protein is essential for virulence and an

effective target for vaccination. *J Exp Med* (2008) 205:981–92. doi:10.1084/jem.20071854
31. Rubio D, Xu RH, Remakus S, Krouse TE, Truckenmiller ME, Thapa RJ, et al. Crosstalk between the type 1 interferon and nuclear factor kappa B pathways confers resistance to a lethal virus infection. *Cell Host Microbe* (2013) 13:701–10. doi:10.1016/j.chom.2013.04.015
32. Xu RH, Wong EB, Rubio D, Roscoe F, Ma X, Nair S, et al. Sequential activation of two pathogen-sensing pathways required for type I interferon expression and resistance to an acute DNA virus infection. *Immunity* (2015) 43:1148–59. doi:10.1016/j.immuni.2015.11.015
33. Samuelsson C, Hausmann J, Lauterbach H, Schmidt M, Akira S, Wagner H, et al. Survival of lethal poxvirus infection in mice depends on TLR9, and therapeutic vaccination provides protection. *J Clin Invest* (2008) 118:1776–84. doi:10.1172/JCI33940
34. Sutherland DB, Ranasinghe C, Regner M, Phipps S, Matthaei KI, Day SL, et al. Evaluating vaccinia virus cytokine co-expression in TLR GKO mice. *Immunol Cell Biol* (2011) 89:706–15. doi:10.1038/icb.2010.157
35. Ishii KJ, Kawagoe T, Koyama S, Matsui K, Kumar H, Kawai T, et al. TANK-binding kinase-1 delineates innate and adaptive immune responses to DNA vaccines. *Nature* (2008) 451:725–9. doi:10.1038/nature06537
36. Dai P, Wang W, Cao H, Avogadri F, Dai L, Drexler I, et al. Modified vaccinia virus Ankara triggers type I IFN production in murine conventional dendritic cells via a cGAS/STING-mediated cytosolic DNA-sensing pathway. *PLoS Pathog* (2014) 10:e1003989. doi:10.1371/journal.ppat.1003989
37. Cheng WY, Jia HJ, He XB, Chen GH, Feng Y, Wang CY, et al. Comparison of host gene expression profiles in spleen tissues of genetically susceptible and resistant mice during ECTV infection. *Biomed Res Int* (2017) 2017:6456180. doi:10.1155/2017/6456180
38. Li T, He X, Jia H, Chen G, Zeng S, Fang Y, et al. Molecular cloning and functional characterization of murine toll-like receptor 8. *Mol Med Rep* (2016) 13:1119–26. doi:10.3892/mmr.2015.4668
39. Layoun A, Samba M, Santos MM. Isolation of murine peritoneal macrophages to carry out gene expression analysis upon toll-like receptors stimulation. *J Vis Exp* (2015) 98:e52749. doi:10.3791/52749
40. Cheng W, He X, Jia H, Chen G, Wang C, Zhang J, et al. Development of a SYBR Green I real-time PCR for detection and quantitation of orthopoxvirus by using Ectromelia virus. *Mol Cell Probes* (2017) 38:45–50. doi:10.1016/j.mcp.2017.12.001
41. Sun L, Wu J, Du F, Chen X, Chen ZJ. Cyclic GMP-AMP synthase is a cytosolic DNA sensor that activates the type I interferon pathway. *Science* (2013) 339:786–91. doi:10.1126/science.1232458
42. Brunette RL, Young JM, Whitley DG, Brodsky IE, Malik HS, Stetson DB. Extensive evolutionary and functional diversity among mammalian AIM2-like receptors. *J Exp Med* (2012) 209:1969–83. doi:10.1084/jem.20121960
43. Zhang Y, Yeruva L, Marinov A, Prantner D, Wyrick PB, Lupashin V, et al. The DNA sensor, cyclic GMP-AMP synthase, is essential for induction of IFN-β during *Chlamydia trachomatis* infection. *J Immunol* (2014) 193:2394–404. doi:10.4049/jimmunol.1302718
44. Chen Q, Sun L, Chen ZJ. Regulation and function of the cGAS-STING pathway of cytosolic DNA sensing. *Nat Immunol* (2016) 17:1142–9. doi:10.1038/ni.3558
45. Fang R, Wang C, Jiang Q, Lv M, Gao P, Yu X, et al. NEMO-IKKβ are essential for IRF3 and NF-κB activation in the cGAS-STING pathway. *J Immunol* (2017) 199:3222–33. doi:10.4049/jimmunol.1700699
46. Schoggins JW, MacDuff DA, Imanaka N, Gainey MD, Shrestha B, Eitson JL, et al. Pan-viral specificity of IFN-induced genes reveals new roles for cGAS in innate immunity. *Nature* (2014) 505:691–5. doi:10.1038/nature12862
47. Lam E, Stein S, Falck-Pedersen E. Adenovirus detection by the cGAS/STING/TBK1 DNA sensing cascade. *J Virol* (2014) 88:974–81. doi:10.1128/JVI.02702-13
48. Lau L, Gray EE, Brunette RL, Stetson DB. DNA tumor virus oncogenes antagonize the cGAS-STING DNA-sensing pathway. *Science* (2015) 350:568–71. doi:10.1126/science.aab3291
49. Dansako H, Ueda Y, Okumura N, Satoh S, Sugiyama M, Mizokami M, et al. The cyclic GMP-AMP synthetase-STING signaling pathway is required for both the innate immune response against HBV and the suppression of HBV assembly. *FEBS J* (2016) 283:144–56. doi:10.1111/febs.13563
50. Paijo J, Döring M, Spanier J, Grabski E, Nooruzzaman M, Schmidt T, et al. cGAS senses human cytomegalovirus and induces type I interferon responses in human monocyte-derived cells. *PLoS Pathog* (2016) 12:e1005546. doi:10.1371/journal.ppat.1005546
51. Aguirre S, Maestre AM, Pagni S, Patel JR, Savage T, Gutman D, et al. DENV inhibits type I IFN production in infected cells by cleaving human STING. *PLoS Pathog* (2012) 8:e1002934. doi:10.1371/journal.ppat.1002934
52. Lio CW, McDonald B, Takahashi M, Dhanwani R, Sharma N, Huang J, et al. cGAS-STING signaling regulates initial innate control of cytomegalovirus infection. *J Virol* (2016) 90:7789–97. doi:10.1128/JVI.01040-16
53. Konno H, Barber GN. The STING controlled cytosolic-DNA activated innate immune pathway and microbial disease. *Microbes Infect* (2014) 16:998–1001. doi:10.1016/j.micinf.2014.10.002
54. Zhang Z, Yuan B, Bao M, Lu N, Kim T, Liu YJ. The helicase DDX41 senses intracellular DNA mediated by the adaptor STING in dendritic cells. *Nat Immunol* (2011) 12:959–65. doi:10.1038/ni.2091
55. Seet BT, Johnston JB, Brunetti CR, Barrett JW, Everett H, Cameron C, et al. Poxviruses and immune evasion. *Annu Rev Immunol* (2003) 21:377–423. doi:10.1146/annurev.immunol.21.120601.141049
56. Esteban DJ, Buller RM. Ectromelia virus: the causative agent of mousepox. *J Gen Virol* (2005) 86:2645–59. doi:10.1099/vir.0.81090-0
57. van Buuren N, Burles K, Schriewer J, Mehta N, Parker S, Buller RM, et al. EVM005: an ectromelia-encoded protein with dual roles in NF-κB inhibition and virulence. *PLoS Pathog* (2014) 10:e1004326. doi:10.1371/journal.ppat.1004326
58. Burles K, van Buuren N, Barry M. Ectromelia virus encodes a family of Ankyrin/F-box proteins that regulate NF-κB. *Virology* (2014) 46(8–470): 351–62. doi:10.1016/j.virol.2014.08.030
59. Storek KM, Gertsvolf NA, Ohlson MB, Monack DM. cGAS and Ifi204 cooperate to produce type I IFNs in response to *Francisella* infection. *J Immunol* (2015) 194:3236–45. doi:10.4049/jimmunol.1402764
60. Parvatiyar K, Zhang Z, Teles RM, Ouyang S, Jiang Y, Iyer SS, et al. The helicase DDX41 recognizes the bacterial secondary messengers cyclic di-GMP and cyclic di-AMP to activate a type I interferon immune response. *Nat Immunol* (2012) 13:1155–61. doi:10.1038/ni.2460
61. Holm CK, Jensen SB, Jakobsen MR, Cheshenko N, Horan KA, Moeller HB, et al. Virus-cell fusion as a trigger of innate immunity dependent on the adaptor STING. *Nat Immunol* (2012) 13(8):737–43. doi:10.1038/ni.2350
62. Holm CK, Rahbek SH, Gad HH, Bak RO, Jakobsen MR, Jiang Z, et al. Influenza A virus targets a cGAS-independent STING pathway that controls enveloped RNA viruses. *Nat Commun* (2016) 7:10680. doi:10.1038/ncomms10680
63. Szulc-Dabrowska L, Gieryńska M, Boratyńska-Jasińska A, Martyniszyn L, Winnicka A, Niemiałtowski MG. Quantitative immunophenotypic analysis of antigen-presenting cells involved in ectromelia virus antigen presentation in BALB/c and C57BL/6 mice. *Pathog Dis* (2013) 68:105–15. doi:10.1111/2049-632X.12054
64. Melo-Silva CR, Tscharke DC, Lobigs M, Koskinen A, Wong YC, Buller RM, et al. The ectromelia virus SPI-2 protein causes lethal mousepox by preventing NK cell responses. *J Virol* (2011) 85:11170–82. doi:10.1128/JVI.00256-11
65. Fernandes-Alnemri T, Yu JW, Datta P, Wu J, Alnemri ES. AIM2 activates the inflammasome and cell death in response to cytoplasmic DNA. *Nature* (2009) 458:509–13. doi:10.1038/nature07710
66. Rathinam VA, Jiang Z, Waggoner SN, Sharma S, Cole LE, Waggoner L, et al. The AIM2 inflammasome is essential for host defense against cytosolic bacteria and DNA viruses. *Nat Immunol* (2010) 11:395–402. doi:10.1038/ni.1864

Conflict of Interest Statement: The authors declare that the research was conducted in the absence of any commercial or financial relationships that could be construed as a potential conflict of interest.

Copyright © 2018 Cheng, He, Jia, Chen, Jin, Long and Jing. This is an open-access article distributed under the terms of the Creative Commons Attribution License (CC BY). The use, distribution or reproduction in other forums is permitted, provided the original author(s) and the copyright owner are credited and that the original publication in this journal is cited, in accordance with accepted academic practice. No use, distribution or reproduction is permitted which does not comply with these terms.

frontiers in Immunology

ORIGINAL RESEARCH
published: 20 June 2018
doi: 10.3389/fimmu.2018.01398

Molecular Mechanisms for the Adaptive Switching Between the OAS/RNase L and OASL/RIG-I Pathways in Birds and Mammals

Enguang Rong[1†], Xiaoxue Wang[1†], Hualan Chen[2], Chenghuai Yang[3], Jiaxiang Hu[1], Wenjie Liu[1], Zeng Wang[2], Xiaoyun Chen[3], Haixue Zheng[4], Juan Pu[5], Honglei Sun[5], Jacqueline Smith[6], David W. Burt[6], Jinhua Liu[5], Ning Li[1] and Yinhua Huang[1]**

[1] State Key Laboratory for Agrobiotechnology, China Agricultural University, Beijing, China, [2] Animal Influenza Laboratory of the Ministry of Agriculture and National Key Laboratory of Veterinary Biotechnology, Harbin Veterinary Research Institute, Chinese Academy of Agricultural Sciences, Harbin, China, [3] China Institute of Veterinary Drugs Control, Beijing, China, [4] State Key Laboratory of Veterinary Etiological Biology and National Foot and Mouth Diseases Reference Laboratory, Lanzhou Veterinary Research Institute, Chinese Academy of Agricultural Sciences, Lanzhou, China, [5] Key Laboratory of Animal Epidemiology and Zoonosis, Ministry of Agriculture, College of Veterinary Medicine, China Agricultural University, Beijing, China, [6] The Roslin Institute and Royal (Dick) School of Veterinary Studies, University of Edinburgh, Edinburgh, United Kingdom

Host cells develop the OAS/RNase L [2′–5′–oligoadenylate synthetase (OAS)/ribonuclease L] system to degrade cellular and viral RNA, and/or the OASL/RIG-I (2′–5′–OAS like/retinoic acid inducible protein I) system to enhance RIG-I-mediated IFN induction, thus providing the first line of defense against viral infection. The 2′–5′–OAS-like (OASL) protein may activate the OAS/RNase L system using its typical OAS-like domain (OLD) or mimic the K63-linked pUb to enhance antiviral activity of the OASL/RIG-I system using its two tandem ubiquitin-like domains (UBLs). We first describe that divergent avian (duck and ostrich) OASL inhibit the replication of a broad range of RNA viruses by activating and magnifying the OAS/RNase L pathway in a UBL-dependent manner. This is in sharp contrast to mammalian enzymatic OASL, which activates and magnifies the OAS/RNase L pathway in a UBL-independent manner, similar to 2′–5′–oligoadenylate synthetase 1 (OAS1). We further show that both avian and mammalian OASL can reversibly exchange to activate and magnify the OAS/RNase L and OASL/RIG-I system by introducing only three key residues, suggesting that ancient OASL possess 2–5A [$p_x5'A(2'p5'A)_n$; x = 1-3; n ≥ 2] activity and has functionally switched to the OASL/RIG-I pathway recently. Our findings indicate the molecular mechanisms involved in the switching of avian and mammalian OASL molecules to activate and enhance the OAS/RNase L and OASL/RIG-I pathways in response to infection by RNA viruses.

Keywords: birds, mammals, OASL, OAS/RNase L pathway, OASL/RIG-I pathway

OPEN ACCESS

Edited by:
Cheryl Ann Winkler, Frederick National Laboratory for Cancer Research (NIH), United States

Reviewed by:
Jianzhong Zhu, Yangzhou University, China
François J. M. A. Meurens, INRA UMR703 Ecole Nationale Vétérinaire, Agroalimentaire et de l'alimentation de Nantes-Atlantique, France

***Correspondence:**
Jinhua Liu
ljh@cau.edu.cn;
Yinhua Huang
cauhyh@cau.edu.cn

†These authors have contributed equally to this work.

Specialty section:
This article was submitted to Viral Immunology, a section of the journal Frontiers in Immunology

Received: *30 March 2018*
Accepted: *05 June 2018*
Published: *20 June 2018*

Citation:
Rong E, Wang X, Chen H, Yang C, Hu J, Liu W, Wang Z, Chen X, Zheng H, Pu J, Sun H, Smith J, Burt DW, Liu J, Li N and Huang Y (2018) Molecular Mechanisms for the Adaptive Switching Between the OAS/RNase L and OASL/RIG-I Pathways in Birds and Mammals. Front. Immunol. 9:1398. doi: 10.3389/fimmu.2018.01398

INTRODUCTION

RNA viruses pose large challenges to human health and animal production with high mutation rates, rapid replication kinetics, and complex evolutionary dynamics (1, 2). To defend against virus infections, the host cellular innate immune system recognizes pathogen-associated molecular patterns with various pattern recognition receptors and activates a rapid antiviral response. After which,

host cells secrete interferons (IFNs) to activate and stimulate a cascade of pathways for antiviral factors, including hundreds of IFN-stimulated genes (ISGs) (3, 4). Among ISGs, 2′–5′-oligoadenylate synthetase (OAS) plays a critical role in antiviral immunity by synthesizing 2–5As, which induces RNA degradation by activating a latent RNase (RNase L) pathway (5, 6).

The OAS repertoire is classed into four subfamilies that encode proteins of different isoforms in Metazoa. The small isoform [2′–5′-oligoadenylate synthetase 1 (OAS1)] consists of one copy of the enzymatic OAS domain, whereas the medium (OAS2) and large (OAS3) isoforms have one or two additional non-enzymatic OAS-like domains (OLDs) in the N-terminus. OASL presents an enzymatic (e.g., mouse Oasl2, mOasl2) or non-enzymatic OLD domain (e.g., human OASL, hOASL; mouse Oasl1, mOasl1) in the N-terminus and two tandem ubiquitin-like domains (UBLs) in the C-terminus (7–9). Recent evolutionary analyses suggested that adaptive selections to circumvent viral-encoded inhibitors in the OAS gene family have driven their functional diversity (10, 11). For example, all OAS subfamilies (OAS1-3) synthesize 2–5As to activate RNase L upon binding dsRNA (12, 13). However, *OAS1* prefers to bind cytosolic dsRNA with fewer than 20 bp and a 3′-single-stranded pyrimidine motif (5), whereas *OAS3* has a strong ability to bind long dsRNA (>50 bp) (12). Such adaptive change is even significant in the OASL subfamily, where the non-enzymatic hOASL mediates RIG-I activation to inhibit virus replication by mimicking polyubiquitin and upregulating the expression of IFNβ, TNFα, and IL-8, whereas the ortholog of hOASL in mouse (the non-enzymatic mOasl1) negatively regulates antiviral immunity by inhibiting the translation of IFN-regulatory factor 7 (IRF7) (14, 15). Moreover, the paralog of hOASL in mouse (mOasl2) synthesizes 2–5As activates RNase L and induces rRNA degradation after detecting dsRNA, similar to OAS1-3 (9).

Compared to mammals, birds have a contractive OAS family, which contains one member (OASL) in most birds belonging to the *Carinatae* group (e.g., ducks) and two members (OAS1 and OASL) in a few birds belonging to the *Ratitae* group (e.g., ostriches). Sequence alignment of 22 avian OASL molecules showed that they hold three conserved aspartic acid (D, homologous to D75-D77-D148 in human OAS1) residues, which serve as metal ion ligands and are required to activate the enzymatic activity to synthesize 2–5As (16). However, whether and how birds (especially *Carinataes*) can recognize divergent RNA viruses to activate the OAS/RNase L system and/or enhance the OASL/RIG-I system using one OAS member (OASL) (where mammals do it with a functionally diverse OAS family), is largely unknown.

Here, we find that avian OASLs activate and enhance the OAS/RNase L pathway to inhibit replication of a positive single-stranded RNA virus, two strains of double-stranded RNA viruses, and four strains of negative single-stranded RNA viruses, which requires both their OLD and UBL domains. This differs from the situation in mammals, where one mammalian OASL (mOasl2) and one mammalian OASL mutant (hOASL-3D) activate and magnify the OAS/RNase L pathway to inhibit viral replication with their OLD domains like *OAS1* (**Figure 1**). Upon introduction of mutations at three D residues homologous to D75-D77-D148 of hOAS1, avian OASL-3D*, and mOasl2-3D* lose the ability to synthesize 2–5As, enhance the RIG-I antiviral activation, and upregulate the expression of many genes downstream of RIG-I in a virus- and UBL-dependent manner, similarly to hOASL (**Figure 1**). These results indicated that avian and mammalian OASLs could be an effective target for alternative regulation of the OAS/RNase L and OASL/RIG-I pathways during viral infection.

RESULTS

Duck and Ostrich OASL Proteins Lead to Resistance to Infection by a Broad Range of RNA Viruses

Duck *RIG-I* can detect influenza A virus and induces an antiviral response in chicken embryonic fibroblasts (DF1) cells, where the RIG-I is absent (17). To determine the role of avian OASL in the immune response, we compared viral replication of a highly pathogenic (A/duck/Hubei/49/05, DK/49) and a weakly pathogenic (A/goose/Hubei/65/05, GS/65) H5N1 virus in DF1 cells expressing duck *OASL* ($DF1^{dOASL+/+}$) to the corresponding in duck *RIG-I* recovery-expression DF1 cells ($DF1^{dRIG\text{-}I+/+}$). Interestingly, $DF1^{dOASL+/+}$ and $DF1^{dRIG\text{-}I+/+}$ cells showed comparatively lower levels of DK/49 and GS/65 virus titers compared to DF1 cells expressing empty vectors, supporting that duck *OASL* can efficiently prevent viral infection, similarly to duck *RIG-I* (**Figures 2A,B**). We further found that $DF1^{dOASL+/+}$ cells have a reduced expression of the matrix gene vRNA and mRNA of the DK/49 virus using a strand-specific real-time RT-PCR methods (18), implying that the dOASL may affect virus transport and transcription (Figure S1 in Supplementary Material). We then generated OASL-deficient DF1 cells ($DF1^{OASL-/-}$) using the CRISPR/Cas9-mediated genome editing method (Figure S2 in Supplementary Material) (19). As expected, $DF1^{dOASL+/+}$ cells had a significantly lower level of the CK/0513 (A chicken/huabei/0513/2007) H5N1 virus, whereas $DF1^{OASL-/-}$ cells showed a significantly higher level of the CK/0513 virus compared to DF1 cells expressing an empty vector (**Figure 2C**). Similarly, we found that ostrich OASL (oOASL), representing ancient avian OASLs (20), significantly inhibited the replication of CK/0513 virus in DF1 cells (**Figure 2D**; Figure S1 in Supplementary Material), supporting that avian OASLs play a critical role in the immune response to influenza A viruses, similarly to some mammalian OASLs.

We next investigated the antiviral activity of avian OASLs against diverse viruses. Interestingly, the expression of either dOASL or oOASL in DF1 cells significantly reduced the replication of another negative single-stranded RNA virus (Newcastle disease virus, NDV/La Sota) and two double-stranded RNA viruses (infectious bursal disease virus, IBDV/B87 and respiratory enteric orphan virus, REOV/Z97/C10). In contrast, the absence of OASL in DF1 cells significantly enhanced the viral replication of the above three viruses (**Figures 2E–J**). Further analysis indicated that dOASL inhibited the replication of a positive single-stranded RNA virus (Foot-and-mouth disease virus, FMDV/O/Mya) in porcine kidney cells (IBRS2) (**Figure 2K**). However, neither dOASL nor oOASL reduced replication of two strains of double-stranded DNA virus in DF1 cells (fowlpox virus, FPV/CVCC/AV1003) or in porcine kidney epithelial (PK15) cells (pseudorabies virus, PRV/Henan/2014) (Figure S3 in Supplementary Material).

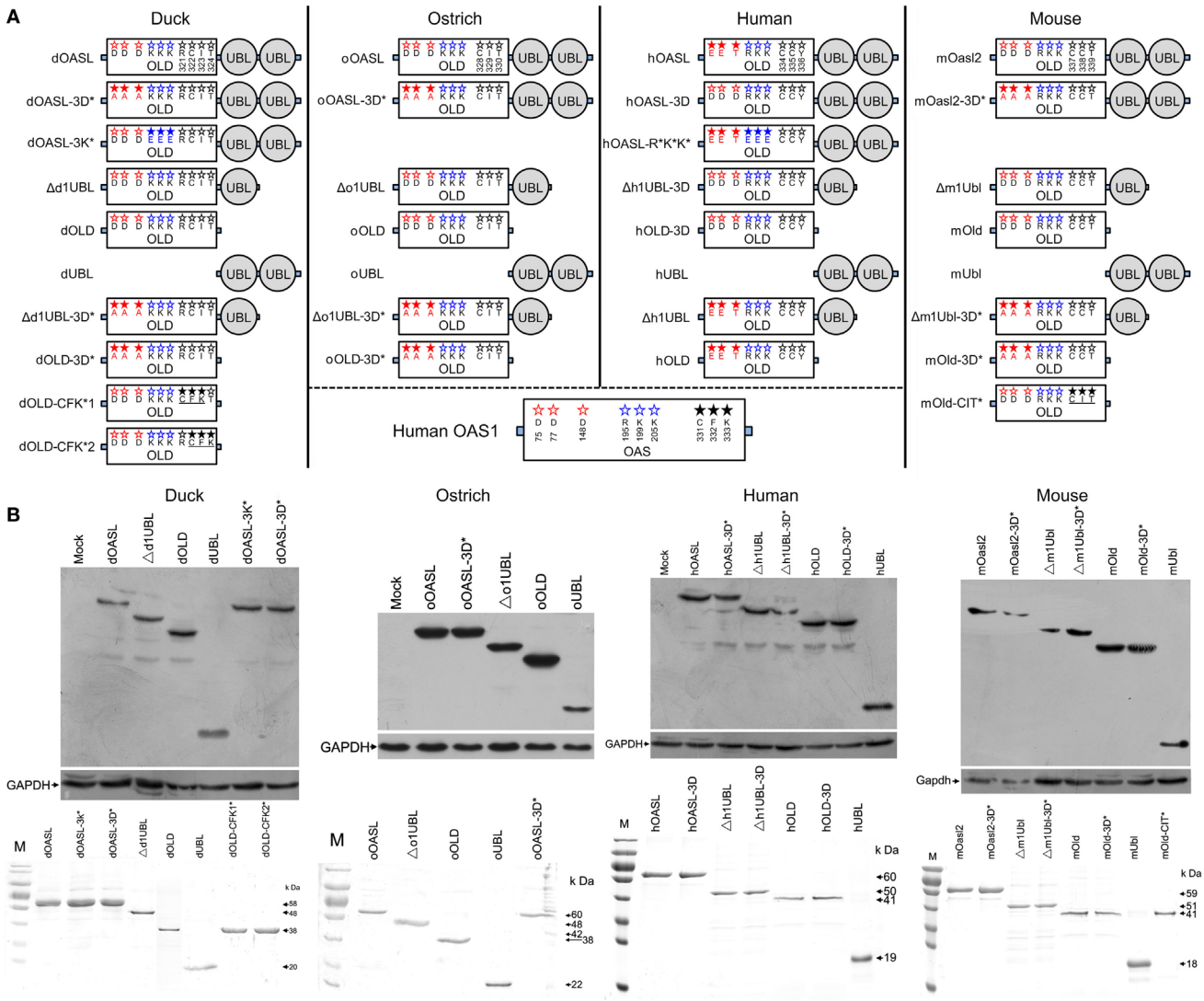

FIGURE 1 | Domain organizations, purification, and expression in cells of duck, ostrich, human, and mouse OASL proteins and their mutants. **(A)** Schematic diagram of OASLs, their mutants and truncations. Red, green, and black letter in OLD domain mean amino acids being homologous to D75-D77-D148, R195-K199-K205, and C331-F332-K333 (CFK motif) of human 2′–5′-oligoadenylate synthetase 1, respectively. **(B)** Western blot analyses of OASLs, their mutants and truncations in DF1 (duck and ostrich) or A549 (human and mouse) cells (up), and His-tagged recombinant proteins (down). Western blot analysis was detected using Flag or c-Myc antibody. GAPDH (1:5,000) was used as a protein loading control. The purified proteins were analyzed by SDS-PAGE.

Taken together, avian OASL shows antiviral activity against a wide range of RNA viruses but not against DNA viruses.

Duck and Ostrich OASL Proteins Activate and Magnify the OAS/RNase L Pathway to Induce Viral RNA Degradation Similarly to Mouse Oasl2

To investigate whether avian OASL activates the OAS/RNase L pathway to decay viral RNA, we first examined the 2–5A synthesis activities of duck (58 kDa) and ostrich (60 kDa) recombinant OASL proteins through a heat-inactivated 2–5A synthetase reaction. As expected, both dOASL and oOASL produced superimposed elution profiles with more than three peaks using poly(I:C) (pIC) as an activator, supporting that avian OASL synthesizes dimeric (pppApA), trimeric (pppApApA), and longer oligomers like human OAS1 (hOAS1) and mOasl2 (**Figure 3A**). Among four types of tested divalent cations, Mg^{2+} and Mn^{2+} stimulated the 2–5A activity of dOASL at a high level, whereas Zn^{2+} and Ca^{2+} stimulated this activity only at a low level (**Figure 3B**). Furthermore, both low (an average size of 0.2–1 kb) and high (an average size of 1.5–8 kb) weight pIC stimulated the 2–5A activity of dOASL and oOASL at a high level (**Figure 3C**), while poly(dA:dT) (pAT, a surrogate for dsDNA viruses) stimulated the 2–5A activity of dOASL and oOASL at a low level (**Figures 3D,E**).

To test whether avian OASL activates RNase L to degrade RNA with their 2–5A products, we examined the rRNA integrity in different DF1 cells using a rRNA cleavage assay after induction with

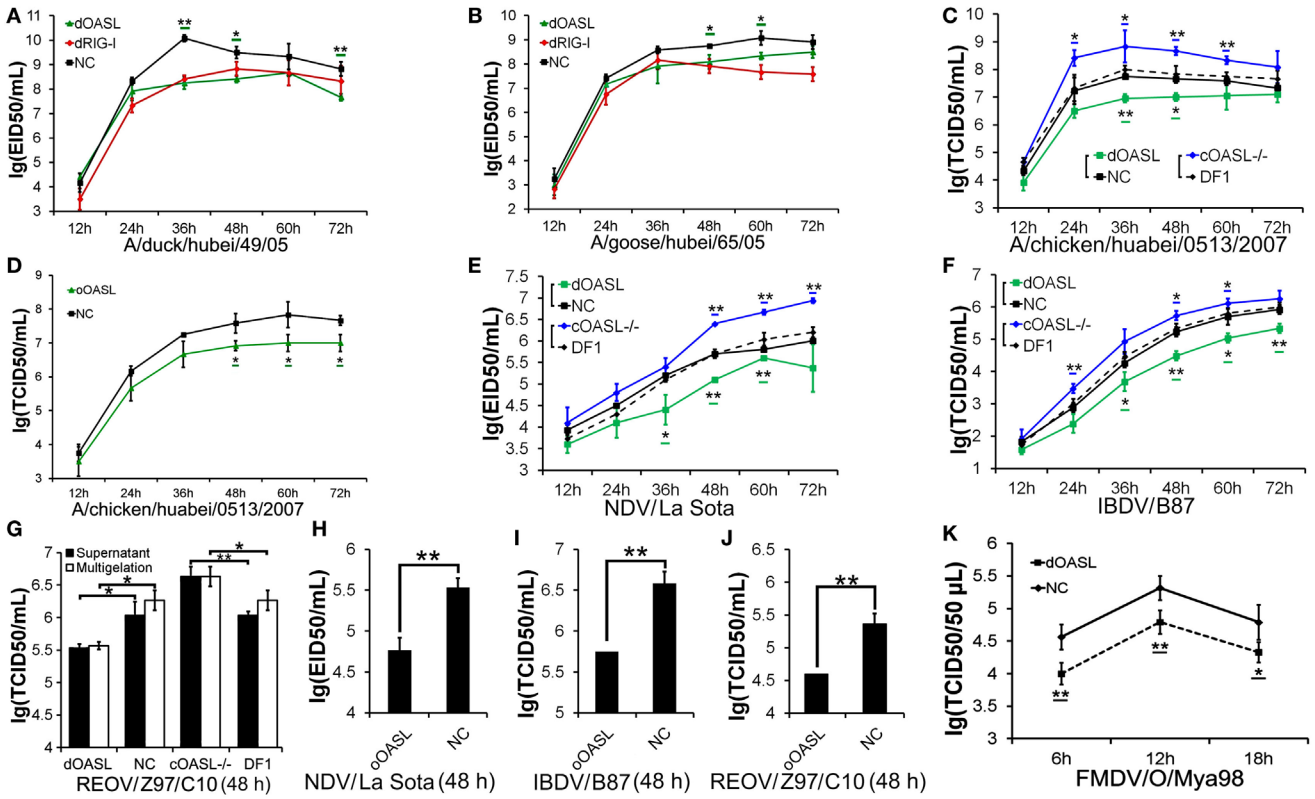

FIGURE 2 | Duck and ostrich OASL proteins inhibit a broad range of RNA virus replications and the loss of chicken OASL enhances these RNA virus replications. Cells infected with virus were harvested at the indicated time points and subjected to EID50 assays or TCID50 assays on MDCK, DF1, Vero, or BHK21 cells (two–tailed Student's *t*-test, $n = 3$). The data are expressed as the mean ± SD. $^{*}P < 0.05$; $^{**}P < 0.01$. **(A,B)** DF1$^{dOASL+/+}$ cells have fewer DK/49 **(A)** and GS/65 **(B)** virus. DF1$^{dRIG-I+/+}$ cells were a positive control for antiviral activity. **(C)** DF1$^{dOASL+/+}$ cells exhibited lower level than NC cells, while DF1$^{OASL-/-}$ (chicken OASL-deficient DF1) cells had higher level than wild-type DF1 cells, of CK/0513 virus. NC is chicken DF1 cell expressing empty vector. **(D)** DF1 cells expressing oOASL exhibited lower level of CK/0513 virus titers. **(E–G)** DF1$^{dOASL+/+}$ cells produced fewer, while DF1$^{OASL-/-}$ cells had more replication of NDV **(E)**, IBDV **(F)**, and REOV **(G)** virus. **(H–J)** DF1 cells expressing oOASL showed a severe reduction in virus titers of NDV **(H)**, IBDV **(I)**, and REOV **(J)** virus. **(K)** IBRS2 cells expressing dOASL had significantly lower FMDV virus titer.

pIC. Expectedly, parental DF1 cells and both dOASL or oOASL recovery-expression DF1$^{OASL-/-}$cells (transfected with dOASL or oOASL) had a low rRNA integrity number (RIN 6.9–7.4), whereas DF1$^{OASL-/-}$ cells had a high RIN (10.0) (**Figure 3F**). This was similar to the case in mammals, in which A549 cells (human alveolar basal epithelial cells) expressing mOasl2 had a low RIN (6.0), and parental A549 cells (containing OAS1-3) had a relatively high RIN (7.6) (**Figure 4H**). Similarly, parental DF1 cells, dOASL and oOASL recovery-expression DF1$^{OASL-/-}$ and A549 cells expressing mOasl2 had a low RIN (8.0, 8.2, 8.0, and 7.3, respectively) after being infected by CK/0513 or PR8 viruses. DF1$^{OASL-/-}$ cells did not induce rRNA degradation and had a high RIN (10.0) (**Figures 3F** and **4I**). In summary, these data support that avian OASLs possess 2–5A synthetase activity and activate the OAS/RNase L pathway to inhibit the replication of a range of RNA viruses.

Similar to OASL, RNase L was also known as an ISG (21). Previous studies indicated that exposure of human prostate cancer cells DU145 to physiologic levels of 2–5A (0.1 M) produces a remarkable transcription of ISG (i.e., ISG15) (22). We, therefore, asked whether OASL enhances the activation of OAS/RNase L signaling to prevent viral infection. Interestingly, we found that both dOASL and oOASL significantly increased the expression of *RNase L* and 10 of 16 genes (*IRF1*, *IRF7*, *IFN*α, *IFN*β, *IFNAR1*, *JAK1*, *STAT1*, *MX1*, *PKR*, and *TNF*α) related to IFN signaling in DF1 $^{OASL-/-}$ cells induced by the CK/0513 virus (**Figures 3G–I**). Similarly, mOasl2 significantly enhanced the expression of *RNase L* and six (*IRF3*, *IFN*α, *IFN*β, *IFIT1*, *IL8*, and *TNF*α) of 10 tested genes related to IFN signaling in A549 cells after infection by the PR8 virus (**Figures 4J–L**). These observations supported that enzymatic OASLs enhance OAS/RNase L signaling to degrade viral RNA and magnify IFN signaling to defend against viral infection.

Duck and Ostrich OASL Reversibly Switch off Their 2–5A Activity Similarly to Human OASL and Mouse Oasl2 When Mutations Were Introduced at Three Conserved D Residues

Previous studies have indicated that three D sites (homologous to D75-D77-D148 in hOAS1) that serve as metal ion ligands are required to synthesize 2–5As (23, 24). To test the effects of these

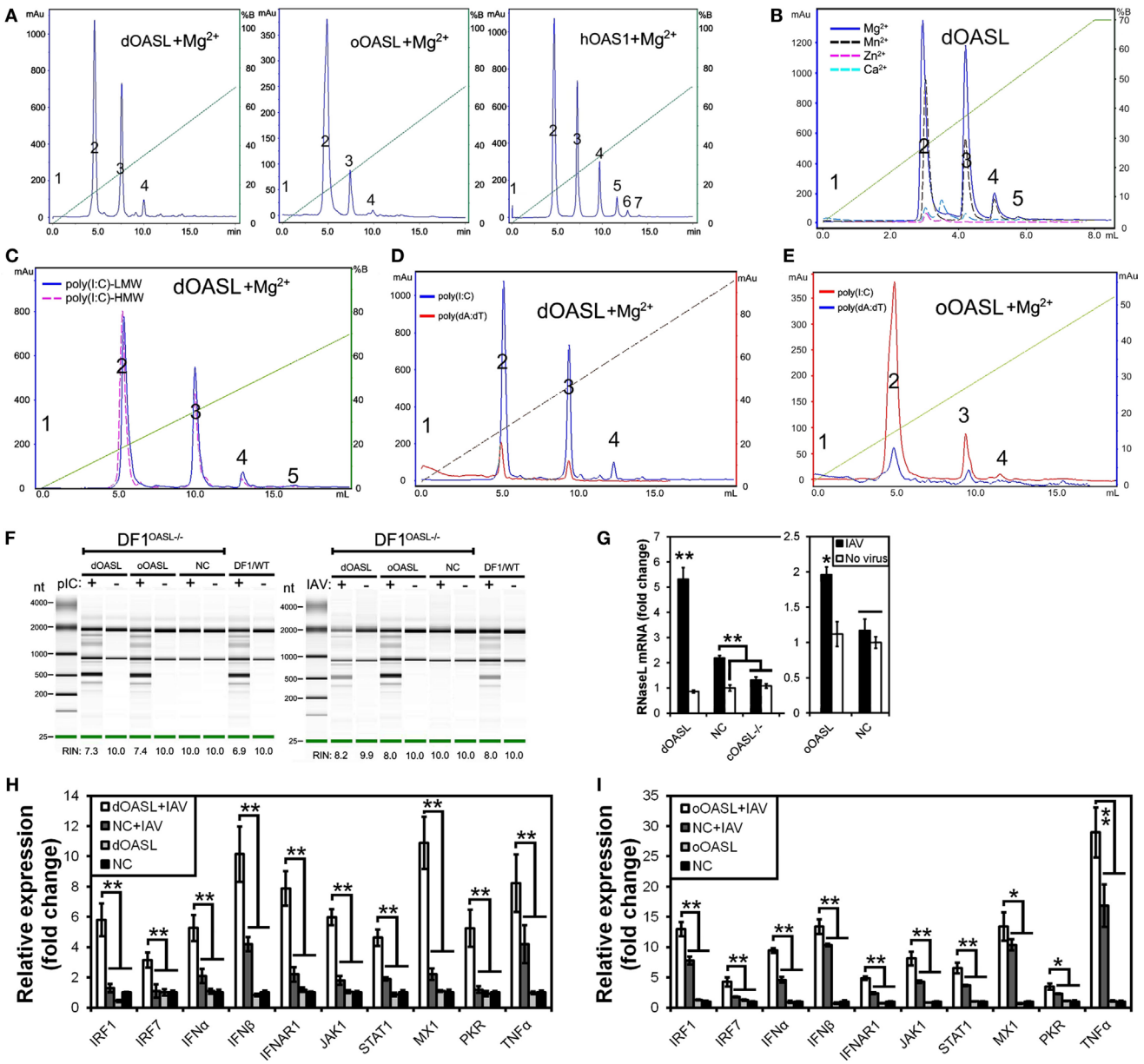

FIGURE 3 | Duck and ostrich OASL proteins synthesize 2–5A to activate and enhance the OAS/RNase L pathway degrading cellular and viral RNA. The 2–5A synthetase reaction was treated with alkaline phosphatase and separated using a Mono Q column. hOAS1 was a positive control for 2–5A activity. Numbers in the elution profiles of A–E represent adenylate, pppApA, pppA(pA)$_2$, pppA(pA)$_3$, pppA(pA)$_4$, pppA(pA)$_5$, pppA(pA)$_6$, respectively. NC is chicken OASL-deficient DF1 cell expressing empty vector. WT is parent DF1 cell. "RIN" is the RNA integrity number. Gene expressions were calculated relative mRNA level to that of *GAPDH* and presented as fold change against the corresponding of NC without CK/0513 infection (two-tailed Student's *t*-test, n = 3). The data are expressed as the mean ± SD. $^*P < 0.05$; $^{**}P < 0.01$. **(A–E)** 2–5As produced by dOASL or oOASL with pIC **(A)**, dOASL with different divalent cations **(B)**, dOASL with HMW or LMW **(C)**, dOASL with pAT **(D)**, oOASL with pAT **(E)**. **(F)** rRNA cleavage induced by dOASL or oOASL in DF1$^{OASL-/-}$ cells transfected with pIC (5 μg/mL) for 4 h or infected with CK/0513 (multiplicity of infection = 1) for 18 h. **(G–I)** dOASL and oOASL significantly increased the expression of *RNase L* **(G)** and 10 genes **(H,I)** related to IFN signaling after infection with CK/0513 virus in DF1$^{OASL-/-}$ cells, respectively.

three D residues on the binding affinity for the dsRNA and 2–5A activity of OASLs, we introduced mutations at the homologous sites of the above three D residues to generate dOASL, oOASL, mOasl2, and hOASL mutants. Interestingly, the mutations of the three D residues switched off the 2–5A activity of the OASLs, but seem not to affect their binding affinity for pIC (Figure S4 in Supplementary Material). For example, dOASL-3D*, oOASL-3D*, and mOasl2-3D* lost their 2–5A activity, whereas hOASL-3D recovered 2–5A activity (**Figures 4A–C**). Detailed analysis indicated that after losing the 2–5A activity, neither dOASL-3D* nor oOASL-3D* induced rRNA degradation or upregulated the expression of *RNase L* or the 16 other genes related to IFN

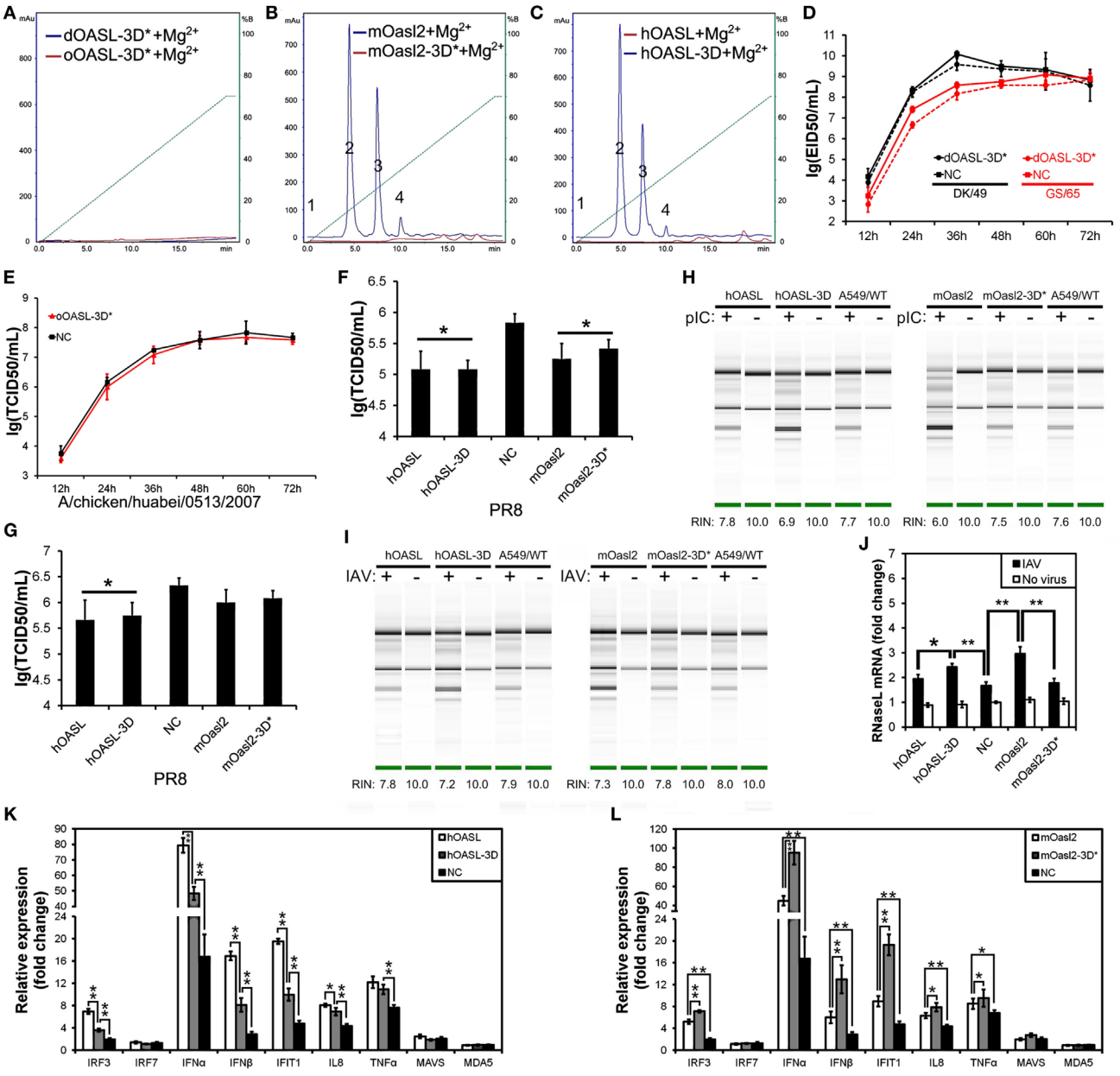

FIGURE 4 | Three conserved sites of duck, ostrich, human, and mouse OASL being homologous to D75-D77-D148 of human 2′–5′-oligoadenylate synthetase 1 are a button for switching on/off the OAS/RNase L pathway. The 2–5A synthetase reaction was treated with alkaline phosphatase and separated using a Mono Q column. Gene expression in cells were calculated relative mRNA level to that of *GAPDH* and presented as fold change against the corresponding of A549 cells expressing empty vector (NC) without PR8 virus infection (two-tailed Student's *t* test, $n = 3$). The data are expressed as the mean ± SD. $^*P < 0.05$; $^{**}P < 0.01$. **(A–C)** The elution profiles produced by dOASL-3D* or oOASL-3D* **(A)**, mOasl2 or mOasl2-3D* **(B)**, and hOASL-3D or hOASL proteins **(C)**. **(D,E)** dOASL-3D* and oOASL-3D* did not inhibit the DK/59 and GS/65 in DF1 cells **(D)** or CK/0513 **(E)** virus replication in DF1$^{OASL-/-}$ cells, whose *RIG-I* is naturally absent. **(F,G)** hOASL-3D and mOasl2 slightly or significantly inhibited the replication of PR8 [multiplicity of infection (MOI) = 0.001] virus in A549 **(F)** or HeLa **(G)** cells. **(H,I)** rRNA cleavage induced by hOASL-3D and mOasl2 in A549 cells stimulated with pIC **(H)** (500 ng/mL) or infected with PR8 virus **(I)** MOI = 1. **(J–L)** hOASL-3D and mOasl2 significantly increased the expression of *RNase L* **(J)** and six genes **(K,L)** related to IFN signaling upon infection with PR8 virus (MOI = 0.001).

signaling, thus failing to prevent virus infection in DF1 cells and DF1$^{OASL-/-}$ (**Figures 4D,E**; Figures S5 and S6 in Supplementary Material). However, nonenzymic mOasl2-3D* failed to induce rRNA degradation and upregulate expression of *RNase L*, but significantly inhibited PR8 virus replication in A549 and HeLa (human cervical carcinoma) cells (**Figures 4F–L**). Moreover, similarly to mOasl2, the expression of hOASL-3D inhibited the PR8 virus replication in both A549 and HeLa cells, induced rRNA degradation when inoculated with either pIC (500 ng/mL) or the PR8 virus (MOI = 1), and increased the expression of *RNase L*, *IRF3*,

*IFN*α, *IFN*β, *IFIT1*, *IL8,* and *TNF*α in A549 cells (**Figures 4F–K**). In summary, these observations suggest that avian and mammalian enzymatic and non-enzymatic OASLs can reversibly change the role in the immune response to viral infection through editing three metal ion ligand sites homologous to D75-D77-D148 in hOAS1.

Unlike the OLDs of Mouse Oasl2 and Human OASL Mutant (OASL-3D), Those of Duck and Ostrich Cannot Efficiently Activate the OAS/RNase L Pathway

To identify domains that are critical for antiviral activity of OASL proteins, we created Flag-tagged truncations of dOASL, oOASL, hOALS-3D, and mOasl2 that lacked one (Δ1UBL) or two UBLs (OLD) (**Figure 1**). Interestingly, like the above four enzymatic full length OASLs, two avian and two mammalian truncations lacking one UBLs (Δd1UBL, Δo1UBL, Δh1UBL-3D, and Δm1Ubl) could significantly inhibit one or two H5N1 virus replications through binding dsRNA to synthesize 2–5As and induce rRNA degradation, upregulate expression of *RNase L* and nine (*IRF1*, *IRF7*, *IFN*α, *IFN*β, *IFNAR1*, *JAK1*, *STAT1*, *MX1,* and *PKR*) or five (*IRF3*, *IFN*α, *IFN*β, *IFIT1* and *TNF*α) other genes related to IFN signaling in DF1$^{OASL-/-}$ or A549 cells (**Figure 5**; Figures S7 and S8 in Supplementary Material). Similarly, two mammalian truncations (hOLD-3D and mOld) lacking both UBLs could bind dsRNA to synthesize 2–5As and induce rRNA degradation, upregulate expression of *RNase L* and four other genes related to IFN signaling (*IRF3*, *IFN*α, *IFN*β, and *IFIT1*), efficiently activate and enhance the OAS/RNase L to inhibit PR8 virus replication in A549 cells (**Figure 6**; Figure S8 in Supplementary Material). In sharp contrast, two avian truncations (dOLD and oOLD) lacking both UBLs neither induce rRNA degradation (**Figures 5D,E**) nor upregulate expression of *RNase L* and genes related to IFN signaling (**Figure 5F**; Figure S7 in Supplementary Material), thus failing to block one or two H5N1 virus replications in the DF1$^{OASL-/-}$ and DF1 cells (**Figures 5A–C**). Detailed analysis indicated that dOLD and oOLD bound dsRNA, but failed to synthesize longer oligomers of 2–5Aswith pIC as an activator (**Figure 5D**; Figure S4 in Supplementary Material). Previous studies demonstrated that a tripeptide motif (CFK) within human *OAS1* and *OAS2* mediates polymerization and affects the synthesis of effective 2–5As (25). We then asked whether mutations in the CFK motif of avian OLD affect their polymerization and further influence their processivity for 2–5A synthesis. We introduced a CFK motif of hOAS1 at a homologous site of dOLD to generate dOLD-CFK*1 and dOLD-CFK*2 substitutions (**Figure 1**). Unexpectedly, upon Mn^{2+} stimulation and pIC, neither dOLD-CFK*1 nor dOLD-CFK*2 synthesized trimeric or longer oligomers. In contrast, the mOld-CIT* substitution containing the CFK motif of dOASL, also synthesized trimeric or longer oligomers, like mOld did (Figure S8C in Supplementary Material). These results suggest that avian OLDs diverged substantially from both mammalian OAS1 and mammalian OLDs, thus it cannot restore the 2–5A activity of avian OLDs efficiently through the compensation of a conserved CFK motif.

Duck and Ostrich UBLs in OASLs, but Not Human OASL Mutant (OASL-3D) and Mouse Oasl2 Ones, Bind dsRNA and Are Required to Activate the OAS/RNase L Pathway

Upon discovering that the UBLs of avian OASLs are essential to exert their antiviral activity, we generated Flag-tagged two-tandem UBL truncations of two avian and mammalian OASLs to investigate their functions in the OAS/RNase L pathway (**Figure 1**). As expected, the two avian (dUBL and oUBL) and two mammalian (hUBL and mUbl) truncations failed to synthesize 2–5As (data not shown), induce rRNA degradation, and change the expression of *RNase L* and genes related to IFN signaling when treated with pIC or infection with H5N1 virus (DK/49, GS/65, CK/0513, or PR8), thus failing to inhibit H5N1 virus replication in DF1 and DF1$^{OASL-/-}$ or A549 cells (Figure S9 in Supplementary Material). These results suggest that the tandem UBLs of avian and mammalian OASLs have no antiviral activity and cannot activate the OAS/RNase L pathway.

Previous studies showed that upon binding dsRNA, OAS synthesizes 2–5As, which in turn activates RNase L to trigger antiviral activity (23, 26, 27). As avian OASLs synthesized short oligomers of 2–5A and failed to activate the OAS/RNase L pathway when their two tandem UBL domains were deleted, we asked whether UBLs improve the 2–5A activity of avian OASLs by enhancing their binding affinity to dsRNA. As expected, dOLD had a lower binding affinity for pIC compared to that of the full protein. However, both mOLD and hOLD-3D showed a comparative level of binding affinity for pIC to their full proteins (Figure S4 in Supplementary Material). Further binding affinity analysis demonstrated that the UBLs of dOASL and oOASLs, but not that of hOASL and mOASL2, bound pIC (Figures S4 and S9 in Supplementary Material). Thus, our data show that the UBL of avian OASLs, but not mammalian OASLs, enhance the binding affinity of OASL to dsRNA and are essential to activate the OAS/RNase L pathway.

Duck and Ostrich OASL Mutants (OASL-3D*) Enhance RIG-I Signaling in a Similar Manner to Human OASL and Mouse Oasl2 Mutant (Oasl2-3D*)

Recent studies have shown that hOASL reduced a broad range of virus replications through enhancing the RIG-I activation (14, 28, 29). Similarly, hOASL and mOasl2-3D* failed to activate and magnify the OAS/RNase L system, but significantly inhibited PR8 virus replication in A549 cells (**Figure 6A**). We, therefore, asked whether both avian and mammalian non-enzymatic OASLs or enzymatic OASL mutants utilize the RIG-I pathway to inhibit viral replication. We generated an additional dOASL mutant (dOASL-3K*) through introducing mutations at three conserved positively charged amino acids (K) in the dsRNA-binding groove (**Figure 1**) (23). As expected, although binding dsRNA, dOASL-3K* together with the other two avian OASL mutants (dOASL-3D* and oOASL-3D*) lacked 2–5A activities and did not activate

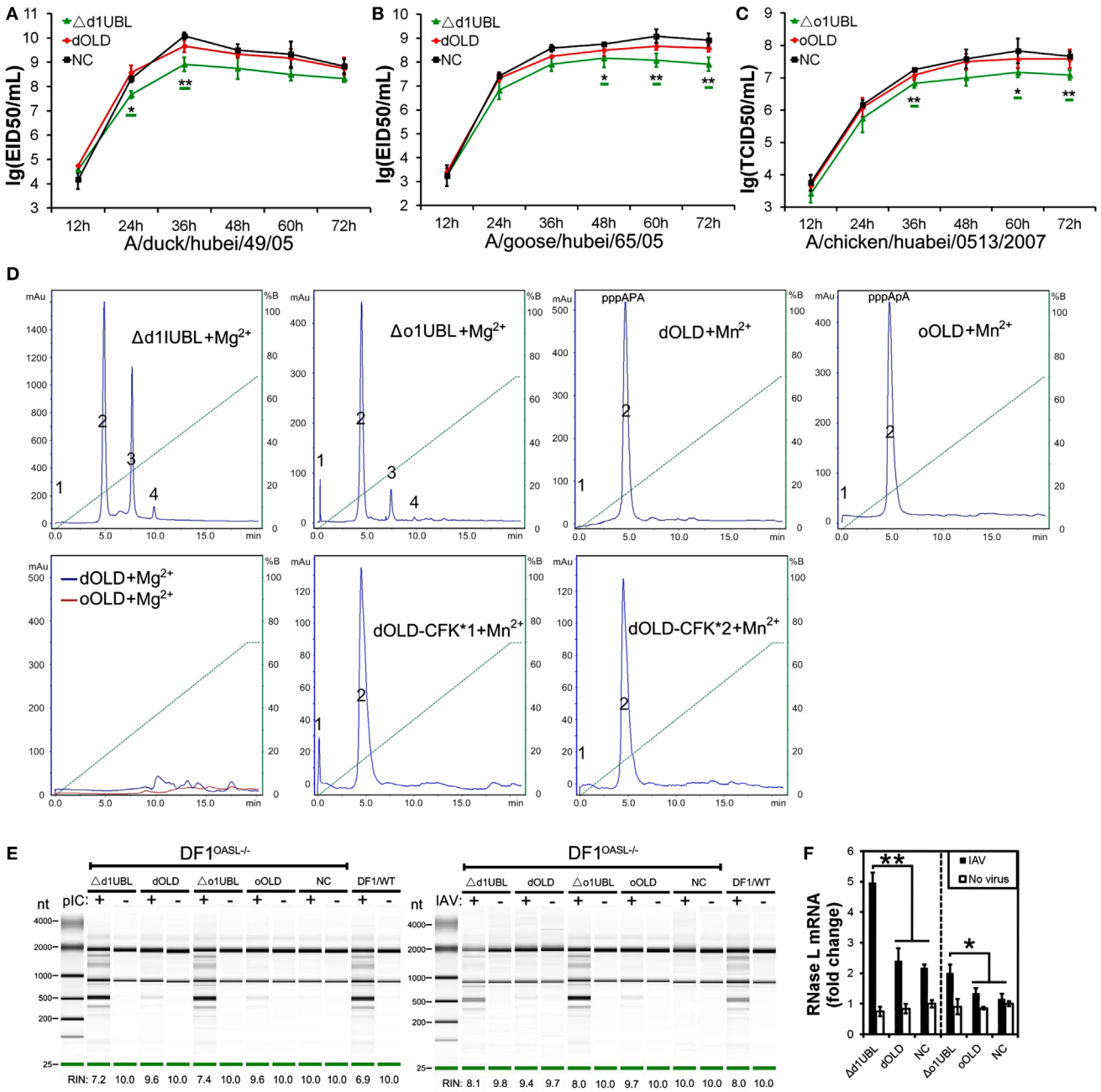

FIGURE 5 | Duck and ostrich OASL activate and magnify the OAS/RNase L pathway in a ubiquitin-like domains (UBL)-dependent manner, while human OASL-3D and mouse Oasl2 do it in a UBL-independent manner. Cells infected with virus were collected at indicated time points to perform EID50 assays or TCID50 assays on MDCK cells. NC is DF1, DF1$^{OASL-/-}$, or A549 cells expressing empty vector. The 2–5A synthetase reaction was treated with alkaline phosphatase and separated using a Mono Q column. "RIN" is the RNA integrity number ($n = 3$). The data are expressed as the mean ± SD. $^{*}P < 0.05$; $^{**}P < 0.01$. **(A–C)** Truncations of dOASL and oOASL lacking one UBL, but not lacking both UBLs, significantly inhibited DK/49 **(A)** and GS/65 **(B)** virus replications in DF1 cells or CK/0513 **(C)** virus replications in DF1$^{OASL-/-}$ cells. **(D)** The elution profiles produced by truncations and truncated mutants of four enzymatic OASL lacking one UBL and two UBLs in reaction. **(E)** rRNA cleavage induced by truncations of dOASL and oOASL in DF1$^{OASL-/-}$ cells transfected with pIC for 4 h or CK/0513 virus (multiplicity of infection = 1) for 18 h. **(F)** Truncations of dOASL and oOASL lacking one UBL, but not lacking two UBLs, significantly increased the expression of *RNase L* upon infection with CK/0513 virus in DF1$^{OASL-/-}$ cells.

RNase L to degrade rRNA, failing to prevent virus infection in DF1 and DF1$^{OASL-/-}$ cells (**Figures 4D,E**; Figures S5 and S6 in Supplementary Material). Because *RIG-I* is absent in chickens, this observation is similar to hOASL, which showed no antiviral activity in the absence of *RIG-I* (17, 29). Interestingly, dOASL-3D* and oOASL-3D*, but not dOASL, oOASL, and dOASL-3K*, significantly enhanced the dRIG-I activation to reduce the CK/0513 virus replication in duck *RIG-I* recovery-expression DF1$^{OASL-/-}$ cells.

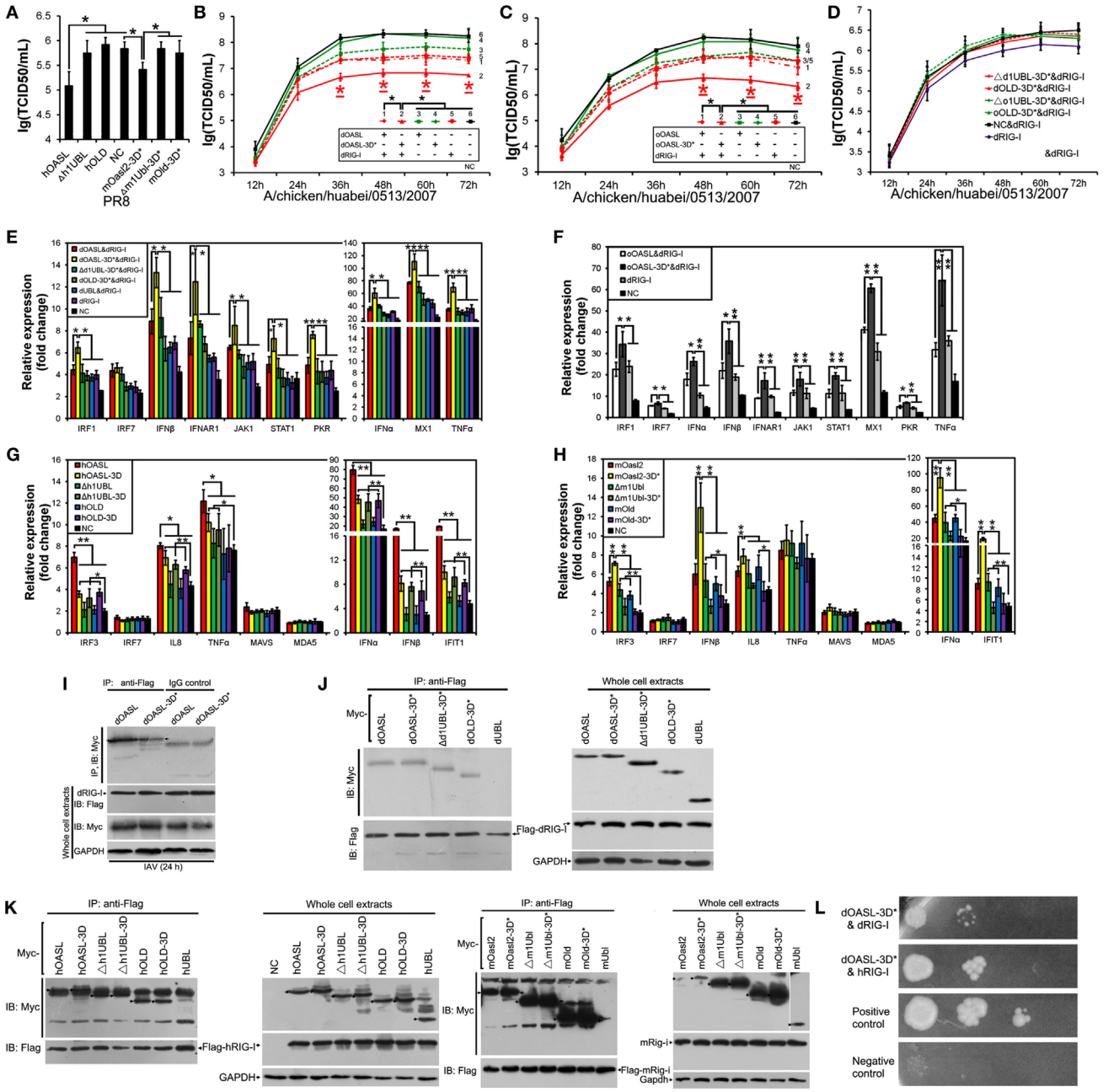

FIGURE 6 | Duck and ostrich OASL-3D* interact with RIG-I and enhance the RIG-I signaling in a ubiquitin-like domains (UBL)-dependent manner, similarly to human OASL and mouse Oasl2-3D*. Cells infected with virus were harvested at the indicated time points and subjected to EID50 or TCID50 assays on MDCK cells. NC is $DF1^{OASL-/-}$ or A549 cells expressing empty vector. Gene expressions in cells were calculated relative mRNA level to that of *GAPDH* and presented as fold change against the corresponding of NC without virus infection (two-tailed Student's *t*-test, $n = 3$). The data are expressed as the mean ± SD. $^{*}P < 0.05$; $^{**}P < 0.01$. **(A,G,H)** hOASL and mOasl2-3D*, but not their truncations, significantly increase expression of six genes downstream of *MAVS* and inhibit PR8 virus replication in A549 cells after infection at 48 h. **(B–F)** Like hOASL and mOasl2-3D*, dOASL-3D* and oOASL-3D*, but not their truncations enhance the antiviral effect of dRIG-I and increased expression of nine genes downstream of *MAVS* in the dRIG-I recovery $DF1^{OASL-/-}$ cells upon CK/0513 infection. **(I–K)** Full length, mutants, and truncations (except UBL) of dOASL, hOASL, and mOasl2 co-precipitate with dRIG-I before and after infected by CK/0513 or PR8 virus. **(L)** Yeast two-hybrid analysis shows that dOASL-3D*, but not dOASL and hOASL, directly interacted with dRIG-I and hRIG-I proteins.

This observation is similar to the case in mammals, where one non-enzymatic (hOASL) and one enzymatic OASL mutant (mOasl2-3D*) significantly enhanced the RIG-I activation, while their enzymatic OASL proteins (hOASL-3D and mOasl2) and another non-enzymatic mutant (hOASL-R*K*K*) did not (**Figures 6A–C**; Figures S10 and S11 in Supplementary Material). Further analysis indicated that all truncations of dOASL-3D*, oOASL-3D*, hOASL, and mOasl2-3D* lacking one or two UBLs failed to reduce the

CK/0513 and PR8 virus replication in duck *RIG-I* recovery-expression DF1$^{OASL-/-}$ or A549 cells (**Figures 6A,D**).

RIG-I targets MAVS to initiate downstream signaling, thereby inducing the transcription of type I IFNs and ISGs. We next evaluated whether OASL-3D* induced the expression of RIG-I signaling. Expectedly, both dOASL-3D* and oOASL-3D*, but not dOASL, oOASL, and dOASL-3K*, significantly increased the expression of nine genes (*IRF1*, *IFN*α, *IFN*β, *IFNAR1*, *JAK1*, *STAT1*, *MX1*, *PKR,* and *TNF*α) downstream of *MAVS* after infecting by CK/0513 virus (**Figures 6E,F**; Figure S10 in Supplementary Material). Whereas neither avian OASL nor their mutants affected the expression of *MAVS*, *MDA5,* and *LGP2* in duck *RIG-I* recovery-expression DF1$^{OASL-/-}$ cells (data not shown). Similarly, two mammalian non-enzymatic OASL proteins (hOASL and mOasl2-3D*), but not their enzymatic OASL proteins, significantly increased the expression of five genes in the RIG-I signaling pathway (*IRF3*, *IFN*α, *IFN*β, *IFIT1*, and *IL8*) in A549 cells infected with the PR8 virus (**Figures 6G,H**; Figure S11 in Supplementary Material). We further compared the gene expression of the RIG-I pathway in duck *RIG-I* recovery-expression DF1$^{OASL-/-}$ cells and A549 cells that expressed truncations lacking one or two UBLs of dOASL-3D*, hOASL, or mOasl2-3D*. This effort found that none of them changed the expression of the above tested genes of the RIG-I signaling pathway with or without IAV infection (**Figures 6E–H**), further supporting that OLD and the two UBLs of avian and mammalian OASLs are essential for magnifying the RIG-I pathway.

We then investigated the interaction between RIG-I and OASL and found that both dOASL and dOASL-3D* co-precipitated with dRIG-I in DF1 cells before and after infection with the CK/0513 virus (**Figures 6I,J**). Similarly, we observed that hOASL, mOasl2, and their mutants (hOASL-3D and mOasl2-3D*) co-precipitated with human or mouse RIG-I in 293T cells (**Figure 6K**). Thus, the mutation of the three conserved D residues did not affect the interaction between OASL and RIG-I. Detailed analysis indicated that UBL-deleted OASL (Δh1UBL, hOLD, Δm1Ubl, and mOld) and their corresponding mutants (Δd1UBL-3D*, dOLD-3D*, Δh1UBL-3D, hOLD-3D, Δm1Ubl-3D*, and mOld-3D*) also interacted with RIG-I, whereas the UBL of OASL alone (dUBL, hUBL, and mUBL) did not (**Figures 6J,K**). This observation, combined with that truncations of avian and mammalian non-enzymatic OASL proteins, did not prevent against virus infection, indicates that the OLD domain of OASL is sufficient to mediate the interaction between OASL and RIG-I but insufficient to enhance RIG-I signaling. We further investigated the module of this interaction using a yeast two-hybrid system. This effort found that among the above OASLs and their mutants from ducks and humans, only dOASL-3D* directly interacted with intact duck and human RIG-I protein (**Figure 6L**).

DISCUSSION

Here, we first demonstrated that, after stimulation by dsRNA, two divergent avian OASLs (dOASL and oOASL) activated RNase L to induce rRNA degradation using their 2–5A products like mammalian enzymatic OASL (mOasl2) (**Figures 3** and **7**). We find that three conserved D residues were crucial to adaptively reversible switching between enzymatic and non-enzymatic OASL, where mutants of one mammalian (mOasl2) and two avian enzymatic OASL (dOASL and oOASL) lose their 2–5A activity and mutant of one mammalian non-enzymatic OASL (hOASL-3D) recover its 2–5A activity. We also found that two avian (dOASL and oOASL) and two mammalian (hOASL-3D and mOasl2) enzymatic OASLs significantly increased the expression of *RNase L* and 10 (*IRF1*, *IRF7*, *IFN*α, *IFN*β, *IFNAR1*, *JAK1*, *STAT1*, *MX1*, *PKR,* and *TNF*α) or six (*IRF3*, *IFN*α, *IFN*β, *IFIT1*, *IL8,* and *TNF*α) genes related to IFN signaling in DF1$^{OASL-/-}$ cells or in A549 cells after infection with the H5N1 (CK/0513 or PR8) virus (**Figures 3** and **4**). This is consistent with the fact that 2–5A induces the gene expression of several ISGs (*P56*, *P54*, *IL8,* and *ISG15*) in DU145 prostate cancer cells and HeLa cells (22). Therefore, our observations support to the theory that the ancient OASL of birds and mammals possessed 2–5A activity and executed their antiviral activity through activating and magnifying the OAS/RNase L pathway and enhancing IFN signaling. Moreover, our functional analyses strengthen the idea that species-specific adaptations appear to accelerate the functional divergence of the OASL molecules. For example, avian OASLs developed a UBL-dependent manner to activate and magnify the RNase L system and IFN signaling to block virus replication. In this UBL-dependent model, the OLDs of avian OASLs bind dsRNA and synthesize 2–5As, but cannot activate RNase L to degrade rRNA and inhibit virus replication (**Figures 5** and **7**). The UBLs of avian OASLs bind dsRNA like their OLDs, and truncations of avian OASLs lacking both UBLs showed weak binding affinity for dsRNA (Figures S4 and S9 in Supplementary Material). These observations, together with the abnormality in the 2–5A synthesis activity of dOLD and oOLD (**Figure 5**), supported the idea that UBLs of avian OASLs have been optimized to bind dsRNA using their enriched positive amino acids (A, H, and L). This optimization, in return, improved avian OASLs' polymerization and processivity for 2–5A synthesis and contributed to the activation and magnification of RNase L signaling. We then hypothesized that avian OASLs could bind dsRNA with different lengths and showed antiviral activity to a range of viruses. This hypothesis was supported by our data. Such as, both dOASL and oOASL synthesized 2–5As at high level after induction with either low or high weight pIC and significantly inhibited the replication of two strains of double-stranded (IBDV/B87 and REOV/Z97/C10) and four strains of negative single-stranded (DK/49, GS/65, CK/0513, and NDV/La Sota) RNA viruses (**Figures 2** and **3**). Additionally, dOASL protected against a strain of positive single-stranded (FMDV/O/Mya) RNA virus infection in IBRS2 cells (**Figure 2**). For mammalian enzymatic OASLs (hOASL-3D and mOasl2), they activate and magnify the RNase L system and IFN signaling to block virus replication in a UBL-independent manner like hOAS1 (30). In this case, both hOLD-3D and mOld could activate RNase L to decay rRNA with their 2–5A products, magnify the RNase L and IFN signaling, and inhibit the PR8 virus replication (**Figure 5**). Since the UBLs of hOASL-3D and mOasl2 did not bind dsRNA, they appear to be functionally redundant for the activation and magnification of the OAS/RNase L system (Figure S4 in Supplementary Material).

Upon detecting viral dsRNA, mammalian enzymatic OASLs activate RNase L to induce the endonucleolytic cleavage of viral

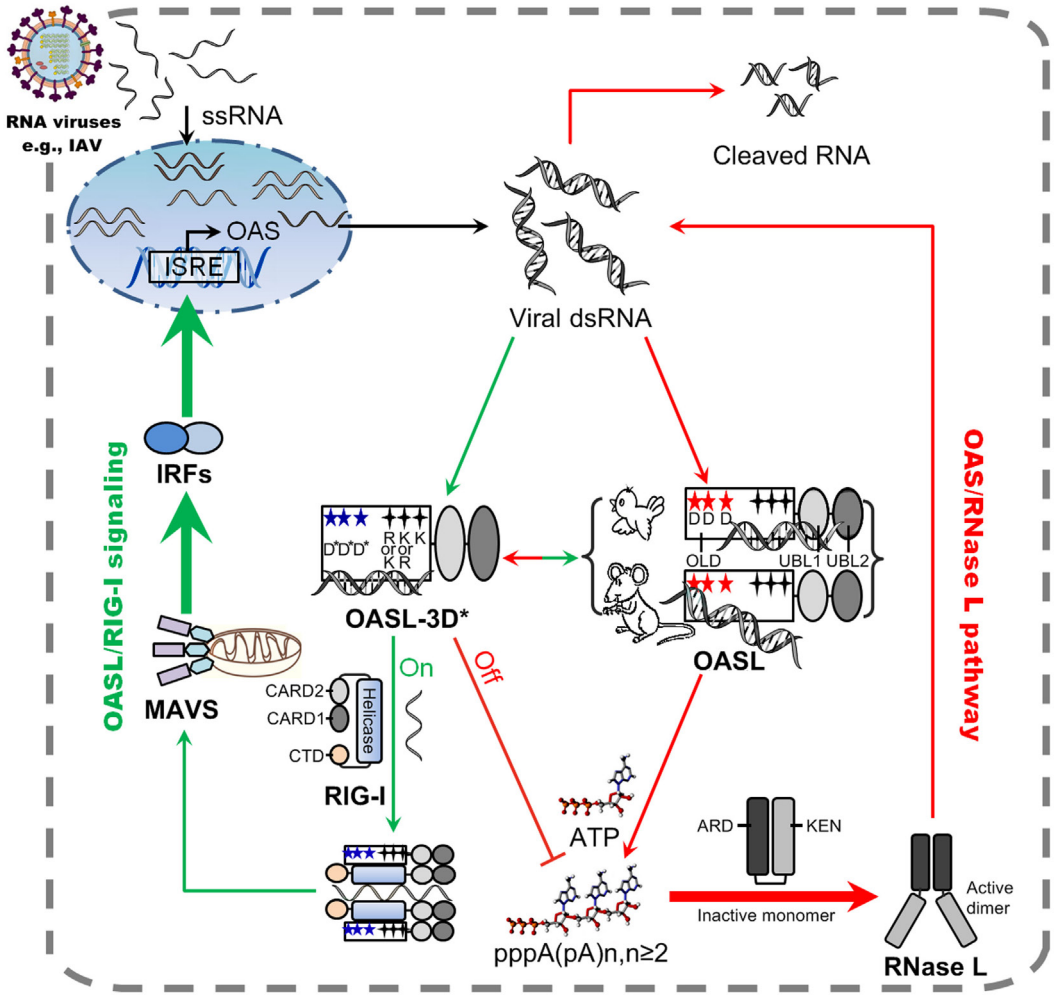

FIGURE 7 | Model of avian and mammalian OASL involvement in RNase L and RIG-I signaling. As a sensor, ancient and enzymatic OASL in birds and mammals contain three aspartic acids (D), which are homologous to D75-D77-D148 in hOAS1 and required to synthesize 2–5As, and three key positively charged amino acids (R/K-K/R-K), which are homologous to R195-K199-K205 in human 2′–5′-oligoadenylate synthetase 1 (OAS1). Both avian and mammalian OASLs develop the potential ability to switch the OAS/RNase L and OASL/RIG-I signaling. In natural, avian OASL activates and magnifies the OAS/RNase L pathway to exert antiviral activity in an UBL-dependent manner, where both its OAS-like domain (OLD) and UBL domains bind dsRNA. While some enzymatic mammalian OASLs activate and magnify the OAS/RNase L pathway to exert antiviral activity in an UBL-independent manner, where only their OLD domains bind dsRNA and synthesizes 2–5A like human OAS1. Some non-enzymatic mammalian OASLs lose 2–5A activity, switch to activate, and enhance RIG-I signaling to inhibit the replications of RNA viruses in a UBL-dependent manner when their three conserved D sites are mutated. Such natural switching between the OAS/RNase L and OASL/RIG-I using OASL molecules were recently, thus, both avian and mammalian OASL may reversibly to activate and magnify one of the above signaling when we introduce mutations at three conserved D sites. Five-pointed star (red): D residue; Five-pointed star (blue): D sites serving as metal ion ligands were mutated to A residue, or E81, E83, and T152 site in hOASL; Four-pointed star (black): three key positively charged amino acids; Four-pointed star (green): three key positively charged amino acids (RKK or KKK) were mutated to E. Abbreviations: OLD, OAS-like domain; UBL, ubiquitin-like domain; ARD, ankyrin repeat domain; KEN, kinase-extension-nuclease domain; CARD, caspase activation and recruitment domain; CTD, carboxy-terminal domain; ISRE, interferon-stimulated response element; MAVS, mitochondrial antiviral signaling protein; IRF, IFN-regulatory factor; ssRNA, single-stranded RNA; dsRNA, double-stranded RNA.

and cellular ssRNAs using their 2–5A products (21, 24, 25), while some mammalian non-enzymatic OASLs (such as human OASL) cannot synthesize 2–5A and activate RNase L to degrade viral and cellular ssRNAs, but can mediate RIG-I activation by mimicking polyubiquitin to inhibit virus replication (14, 29). Interestingly, we found that such natural switching between the OAS/RNase L and OASL/RIG-I signaling are reversible and mediated by three crucial D residues in birds and mammals. When mutations were introduced at three conserved D residues homologous to D75-D77-D148 of hOAS1, two avian (dOASL-3D* and oOASL-3D*) and one mammalian (mOasl2-3D*) OASL mutants lost 2–5A activity and changed to enhance the RIG-I signaling-like hOASL did (**Figures 4** and **7**; Figures S9 and S11 in Supplementary Material). In contrast, one mammalian OASL mutant (hOASL-3D) restored 2–5A activity, activated and magnified the OAS/RNase L pathway like two avian and one mammalian enzymatic OASL did (dOASL, oOASL, and mOsl2) (**Figures 3** and **4**). However, when mutations were introduced at three conserved K (or R)

residues homologous to R195-K199-K205 of hOAS1 in the dsRNA-binding groove (**Figure 1**) (23, 31), dOASL and hOASL mutants (dOASL-3K* and hOASL-R*K*K*) activated and magnified neither the OAS/RNase L nor the RIG-I pathway (Figures S6 and S10 in Supplementary Material). These observations suggested that three conserved D residues in the OLD of OASL acted as a switch for the adaptive exchange between the OAS/RNase L and RIG-I pathways, while three positively charged K (or R) residues in the dsRNA-binding groove of OASLs are essential to both the OAS/RNase L and RIG-I pathways. Moreover, we found that two tandem UBL domains were required for avian and mammalian non-enzymatic OASLs (dOASL-3D*, oOASL-3D*, hOASL, and mOasl2-3D*) to enhance and magnify the RIG-I pathway, even they interacted with RIG-I in a UBL-independent manner (**Figure 6**; Figure S10 in Supplementary Material). The UBL of hOASL was reported to mediate its specific interaction with methyl CpG-binding protein 1 (MBD1), which is an ISG and functions as a transcriptional repressor (32). However, manually querying the MBD1 repertoire against the non-redundant database in NCBI and examining avian genome assemblies in Ensembl (release 87) indicated that MBD1 appears to be absent in birds (data not shown). Thus, avian OASLs may not enhance the RNase L, IFN, and RIG-I signaling by binding the MBD1 protein.

Mouse *Oasl1* specifically suppresses *IRF7* translation by binding to a double stem-loop structure in its 5'UTR, thus negatively regulates IFN during viral infection (15). We found that, unlike mOasl1, dOASL did not suppress *IRF7* translation through binding its 5'UTR (Figure S12 in Supplementary Material). This finding is consistent with our observation that avian OASLs slightly or significantly increase the expression of *IRF7* and then significantly upregulate the expression of *IFN*α and *IFN*β in DF1$^{OASL-/-}$cells infected by the CK/0513 virus (**Figure 3**). Birds, therefore, do not present a negative feedback pathway for the IFN response through OASL like some mammals (i.e., mouse). In the future, our ability to describe the structure of OASL protein using cryo-electron microscopy and to identify target proteins or RNAs through immunoprecipitation combined with high throughput sequencing will extend our knowledge about the role of OASL in the activation and regulation of *RNase L* and IFN signaling as well as RIG-I signaling.

MATERIALS AND METHODS

Facility and Ethics Statement

Studies of one H1N1 (A/Puerto Rico/8/34, PR8) and three H5N1 viruses (A/duck/Hubei/49/05, DK/49; A/goose/Hubei/65/05, GS/65; A chicken/huabei/0513/2007, CK/0513) were conducted in a biosecurity level 3+ laboratory approved by Chinese Ministry of Agriculture or China Agricultural University. The NDV/La Sota, IBDV/B87, REOV/Z97/C10, FPV/CVCC/AV1003, PRV/Henan/2014, and FMDV/O/Mya viruses were maintained in a biosecurity level 2+ laboratory approved by China Institute of Veterinary Drug Control or Lanzhou Veterinary Research Institute. The age of 10 days (10-day-old) chicken embryos were obtained from Hualan Chen's lab, and chicken embryos studies were approved by the Review Board of Harbin Veterinary Research Institute, Chinese Academy of Agricultural Sciences.

Cell Culture and Viral Infections

DF1 (Chicken embryonic fibroblasts cells), 293T (human embryonic kidney 293T cells), A549 (human alveolar basal epithelial cells), HeLa (human cervical carcinoma cells), Vero (African green monkey kidney cells), MDCK (Madin-Darby canine kidney cells), BHK21 (baby hamster kidney fibroblast cells), and C2C12 (murine myoblast cells) were purchased from American Type Culture Collection. PK15 (porcine kidney epithelial cells) and IBRS2 (porcine kidney cells) were obtained from the Cell Resource Center, Peking Union Medical College. All the above cells were maintained in Dulbecco's modified Eagle's medium supplemented with 10% fetal bovine serum (FBS; Gibco, Carlsbad, CA, USA) in an atmosphere of 5% CO_2 at 37°C. Viruses were propagated in 10-day-old chicken embryos. Three samples of cells inoculated with a multiplicity of infection (MOI) of 0.1, 0.01, or 0.001 with one of the above virus after 6, 12, 18, 24, 36, 48, 60, and/or 72 h were collected to monitor virus replication. Titers were calculated by the egg infectious dose (EID50) individuals using the Reed and Muench method (DK/49, GS/65, and NDV), monitored tissue culture infective dose (TCID50) of the cytopathic effect of end-point dilutions (CK/0513, PR8, IBDV, REOV, PRV, and FMDV), or quantified through quantitative PCR with the primer listed in Table S1 in Supplementary Material (FPV).

Construction and Expression of Recombinant Plasmids

The coding sequences of dOASL, dRIG-I, oOASL, and mOasl2 were amplified from whole duck lungs infected with the DK/49 virus, an whole ostrich spleen cDNA library or C2C12 cells according their gene sequences (KC869660.1, XM_009673088, and NM_011854) using the primers in Table S2 in Supplementary Material (33, 34). Truncations and mutants of dOASL, oOASL, hOASL, and mOasl2 were generated using specific PCR and site-directed mutagenesis, respectively (Tables S2–S4 in Supplementary Material). Full-length, truncated and mutant dOASL, dRIG-I, oOASL, hRIG-I, and mRig-i were cloned individually into the piggyBac (containing a Flag-tag) (35), pCMV-Myc, or pCMV-HA vectors (Clontech, Mountain View, CA, USA) (Tables S2–S4 in Supplementary Material) and were transfected to cells using Lipofectamine 3000 (Thermo Fisher, Carlsbad, CA, USA). Gene expression in cells was examined by Western blotting using the anti-Flag, anti-Myc or anti-HA antibody (1:1,000).

Establishment of OASL-Deficient DF1 Cells

DF1 cells were co-transfected with Cas9 nuclease and sgRNA plasmids, subjected to trypsin digestion and limiting dilutions using methods similarly to those applied to human cells (19). Clones with large fragment deletion and biallelic mutations in targeted genes were selected through PCR using gene-specific primers covering the region targeted by sgRNA, and they were subsequently confirmed by sequencing (Tables S5 and S6 in Supplementary Material).

Protein Purification, Detection of 2–5A Activity, and dsRNA-Binding Affinity

Full length, truncated and mutant of OASLs with an affinity His-tag were cloned into the pET-28a(+) vector using the primers

in Tables S3 and S4 in Supplementary Material, and transformed into *Escherichia coli* BL21 Codon Plus RIPL (TransGen, Beijing, China) cells. Bacteria were induced to express OASL protein by the addition of 0.5–1.0 mM isopropyl-β-D-thiogalactoside overnight at 18–25°C and were lysed in 25 mL of buffer A using an AvestinEmulsiFlex C3 (Avestin, Ottawa, ON, Canada). Thereafter, the recombinant proteins were isolated using Ni^{2+}-NTA affinity column chromatography and further purified with a Heparin HiTrap (5 mL) column (GE Healthcare, Uppsala, Sweden). The 2–5A activity of the recombinant proteins was detected using Mono Q purification, similarly to that applied to mOasl1 and mOasl2 (9). Binding affinity of OASL proteins to dsRNA were evaluated using an Octet RED platform (ForteBio, Menlo Park, CA, USA). The affinities were derived by fitting the kinetic data to a 1:1 Langmuir binding model utilizing global fitting algorithms (36). The dissociation constants K_D, K on (association rate), and K off (dissociation rate) were determined by fitting the binding chromatogram data with the Octet User Software (version 3.1).

Co-Immunoprecipitation and Immunoprecipitation

Cells were transfected with equal amounts of Flag- and/or Myc-tagged recombinant plasmids (8 μg) or 3 × Flag-tagged recombinant plasmids (15 μg) using Lipofectamine 3000 reagents (Thermo Fisher, Carlsbad, CA, USA) and lysed in IP lysis buffer (Beyotime, Beijing, China) containing a final concentration of 1 mM PMSF (Beyotime, Beijing, China) after transfection for 24 h. The lysate was cleared using protein A + G agarose (Beyotime, Beijing, China) and specific IgG for 3 h at 4°C and then incubated with anti-Flag immunoglobulin (1:1,000; Abcam, Cambridge, MA, USA) and protein A + G agarose overnight at 4°C. After that, the immunoprecipitated proteins were analyzed using SDS-PAGE following silver staining and a liquid chromatography-mass spectrometry (LC-MS, Q-TOF) assay in BGI-Beijing or Western blotting using a mouse monoclonal c-Myc antibody (1:1,000; Clontech, Mountain View, CA, USA).

Yeast Two-Hybrid Analysis

Full-length RIG-I were cloned into the bait vector pGBKT7 to create fusion proteins with the Gal4 DNA-binding domain and OASL proteins were individually cloned into the prey vector pGADT7. Both recombinant bait and prey vectors were transformed into the *S. cerevisiae* host strain AH109 using the lithium acetate/polyethylene glycol method (Clontech, Mountain View, CA, USA). Positive clones in which the expressed prey protein interacted with the bait protein were selected on minimal double-dropout medium (lacking L and W), assessed on triple selection plates (lacking L, W, and H), and patched onto plates with higher stringency quadruple-dropout medium (without L, W, H, and Adenine). Primers used for the yeast two-hybrid analysis are listed in Table S7 in Supplementary Material.

Quantitative RT-PCR and rRNA Cleavage Assay

Total RNA was isolated from cells using the RNeasy Plus Mini Kit (Qiagen, Hilden, Germany) or TRIzol (Invitrogen, Rockville, MD, USA) reagent. Then, RNA was DNase-treated (Qiagen, Hilden, Germany) and resolved on RNA chips using an Agilent 2100 BioAnalyzer. RNA integrity was assessed by RIN score (37). cDNA was synthesized with Oligo(dT)18 primer or gene-specific primers using the Promega Improm-II reverse transcriptase (Promega, Madison, WI, USA) and used to examine gene expression using primers in Table S1 in Supplementary Material through normalizing the corresponding expression of the *GAPDH* reference gene. Gene differential expression between samples was calculated using $2^{-\Delta\Delta CT}$ method (38).

AUTHOR NOTES

All institutional and national guidelines for the care and use of laboratory animals were followed.

AUTHOR CONTRIBUTIONS

YH, NL, and JL designed the project. ER, XW, and JH constructed recombinant plasmids, generated OASL-positive and OASL-deficient cells, performed rRNA degradation, and carried out quantitative RT-PCR experiments. ER and XW purified recombinant proteins, detected 2-5A activity, carried out RNA binding affinity, and performed other biochemical studies. ER, HC, CY, JL, XW, ZW, WL, XC, HZ, JP, and HS performed virus infection and replication experiments. ER and YH wrote the manuscript. YH, JL, DB, JS, and ER revised the manuscript.

ACKNOWLEDGMENTS

We thank Prof. Zandong Li (China Agricultural University) for providing human and mouse RIG-I recombinant plasmids, Prof. Erguang Li (Nanjing University) for the gift of hOASL recombinant plasmid, Prof. Yaofeng Zhao (China Agricultural University) to provide ostrich spleen cDNA library. We thank Dr. Jianwu Wang (China Agricultural University) for help in the Mono Q and Octet RED platform assays, Prof. Sen Wu (China Agricultural University) and Dr. Yuanwu Ma (Chinese Academy of Medical Sciences) for advice on CRISPR-Cas9 technology. We acknowledge Prof. Youliang Peng, Prof. Huiqiang Lou, and Prof. Jianhui Tian (China Agricultural University) for valuable discussions. This study was funded by the National Natural Science Foundation of China (31772587 and 31471176) and the National Key Research and Development Program (2016YFD0500202).

SUPPLEMENTARY MATERIAL

The Supplementary Material for this article can be found online at https://www.frontiersin.org/articles/10.3389/fimmu.2018.01398/full#supplementary-material.

REFERENCES

1. McDonald SM, Nelson MI, Turner PE, Patton JT. Reassortment in segmented RNA viruses: mechanisms and outcomes. *Nat Rev Microbiol* (2016) 14(7): 448–60. doi:10.1038/nrmicro.2016.46
2. Borderia AV, Stapleford KA, Vignuzzi M. RNA virus population diversity: implications for inter-species transmission. *Curr Opin Virol* (2011) 1(6):643–8. doi:10.1016/j.coviro.2011.09.012
3. Goubau D, Deddouche S, Reis ESC. Cytosolic sensing of viruses. *Immunity* (2013) 38(5):855–69. doi:10.1016/j.immuni.2013.05.007
4. Schoggins JW, Rice CM. Interferon-stimulated genes and their antiviral effector functions. *Curr Opin Virol* (2011) 1(6):519–25. doi:10.1016/j.coviro.2011.10.008
5. Vachon VK, Calderon BM, Conn GL. A novel RNA molecular signature for activation of 2'-5' oligoadenylate synthetase-1. *Nucleic Acids Res* (2015) 43(1): 544–52. doi:10.1093/nar/gku1289
6. Silverman RH. Viral encounters with 2',5'-oligoadenylate synthetase and RNase L during the interferon antiviral response. *J Virol* (2007) 81(6):12720–9. doi:10.1128/JVI.01471-07
7. Choi UY, Kang JS, Hwang YS, Kim YJ. Oligoadenylate synthase-like (OASL) proteins: dual functions and associations with diseases. *Exp Mol Med* (2015) 47:e144. doi:10.1038/emm.2014.110
8. Zhu J, Ghosh A, Sarkar SN. OASL-a new player in controlling antiviral innate immunity. *Curr Opin Virol* (2015) 12:15–9. doi:10.1016/j.coviro.2015.01.010
9. Eskildsen S, Justesen J, Schierup MH, Hartmann R. Characterization of the 2'-5'-oligoadenylate synthetase ubiquitin-like family. *Nucleic Acids Res* (2003) 31(12):3166–73. doi:10.1093/nar/gkg427
10. Sams AJ, Dumaine A, Nedelec Y, Yotova V, Alfieri C, Tanner JE, et al. Adaptively introgressed Neandertal haplotype at the OAS locus functionally impacts innate immune responses in humans. *Genome Biol* (2016) 17(1):246. doi:10.1186/s13059-016-1098-6
11. Hancks DC, Hartley MK, Hagan C, Clark NL, Elde NC. Overlapping patterns of rapid evolution in the nucleic acid sensors cGAS and OAS1 suggest a common mechanism of pathogen antagonism and escape. *PLoS Genet* (2015) 11(5): e1005203. doi:10.1371/journal.pgen.1005203
12. Donovan J, Whitney G, Rath S, Korennykh A. Structural mechanism of sensing long dsRNA via a noncatalytic domain in human oligoadenylate synthetase 3. *Proc Natl Acad Sci U S A* (2015) 112(13):3949–54. doi:10.1073/pnas.1419409112
13. Hovanessian AG, Justesen J. The human 2'-5'oligoadenylate synthetase family: unique interferon-inducible enzymes catalyzing 2'-5' instead of 3'-5' phosphodiester bond formation. *Biochimie* (2007) 89(6):779–88. doi:10.1016/j.biochi.2007.02.003
14. Ibsen MS, Gad HH, Andersen LL, Hornung V, Julkunen I, Sarkar SN, et al. Structural and functional analysis reveals that human OASL binds dsRNA to enhance RIG-I signaling. *Nucleic Acids Res* (2015) 43(6–7):5236–48. doi:10.1093/nar/gkv389
15. Lee MS, Kim B, Oh GT, Kim YJ. OASL1 inhibits translation of the type I interferon-regulating transcription factor IRF7. *Nat Immunol* (2013) 14(4):346–55. doi:10.1038/ni.2535
16. Tatsumi R, Sekiya S, Nakanishi R, Mizutani M, Kojima S, Sokawa Y. Function of ubiquitin-like domain of chicken 2'-5'-oligoadenylate synthetase in conformational stability. *J Interferon Cytokine Res* (2003) 23(11):667–76. doi:10.1089/107999003322558809
17. Barber MR, Aldridge JJ, Webster RG, Magor KE. Association of RIG-I with innate immunity of ducks to influenza. *Proc Natl Acad Sci U S A* (2010) 107(13): 5913–8. doi:10.1073/pnas.1001755107
18. Kawakami E, Watanabe T, Fujii K, Goto H, Watanabe S, Noda T, et al. Strand-specific real-time RT-PCR for distinguishing influenza vRNA, cRNA, and mRNA. *J Virol Methods* (2011) 173(6):1–6. doi:10.1016/j.jviromet.2010.12.014
19. Shalem O, Sanjana NE, Hartenian E, Shi X, Scott DA, Mikkelson T, et al. Genome-scale CRISPR-Cas9 knockout screening in human cells. *Science* (2014) 343(1):84–7. doi:10.1126/science.1247005
20. Hackett SJ, Kimball RT, Reddy S, Bowie RC, Braun EL, Braun MJ, et al. A phylogenomic study of birds reveals their evolutionary history. *Science* (2008) 320(6):1763–8. doi:10.1126/science.1157704
21. De La Cruz-Rivera PC, Kanchwala M, Liang H, Kumar A, Wang LF, Xing C, et al. The IFN response in bats displays distinctive IFN-stimulated gene expression kinetics with atypical RNASEL induction. *J Immunol* (2018) 200(1): 209–17. doi:10.4049/jimmunol.1701214
22. Malathi K, Paranjape JM, Bulanova E, Shim M, Guenther-Johnson JM, Faber PW, et al. A transcriptional signaling pathway in the IFN system mediated by 2'-5'-oligoadenylate activation of RNase L. *Proc Natl Acad Sci U S A* (2005) 102(41):14533–8. doi:10.1073/pnas.0507551102
23. Lohofener J, Steinke N, Kay-Fedorov P, Baruch P, Nikulin A, Tishchenko S, et al. The activation mechanism of 2'-5'-oligoadenylate synthetase gives new insights into OAS/cGAS triggers of innate immunity. *Structure* (2015) 23 (5884):851–62. doi:10.1016/j.str.2015.03.012
24. Sarkar SN, Ghosh A, Wang HW, Sung SS, Sen GC. The nature of the catalytic domain of 2'-5'-oligoadenylate synthetases. *J Biol Chem* (1999) 274(36): 25535–42. doi:10.1074/jbc.274.36.25535
25. Ghosh A, Sarkar SN, Guo W, Bandyopadhyay S, Sen GC. Enzymatic activity of 2'-5'-oligoadenylate synthetase is impaired by specific mutations that affect oligomerization of the protein. *J Biol Chem* (1997) 272(52):33220–6. doi:10.1074/jbc.272.52.33220
26. Li Y, Banerjee S, Wang Y, Goldstein SA, Dong B, Gaughan C, et al. Activation of RNase L is dependent on OAS3 expression during infection with diverse human viruses. *Proc Natl Acad Sci U S A* (2016) 113(8):2241–6. doi:10.1073/pnas.1519657113
27. Malathi K, Dong B, Gale MJ, Silverman RH. Small self-RNA generated by RNase L amplifies antiviral innate immunity. *Nature* (2007) 448(7155):816–9. doi:10.1038/nature06042
28. Dhar J, Cuevas RA, Goswami R, Zhu J, Sarkar SN, Barik S. 2'-5'-Oligoadenylate synthetase-like protein inhibits respiratory syncytial virus replication and is targeted by the viral nonstructural protein 1. *J Virol* (2015) 89(19):10115–9. doi:10.1128/JVI.01076-15
29. Zhu J, Zhang Y, Ghosh A, Cuevas RA, Forero A, Dhar J, et al. Antiviral activity of human OASL protein is mediated by enhancing signaling of the RIG-I RNA sensor. *Immunity* (2014) 40(6):936–48. doi:10.1016/j.immuni.2014.05.007
30. Han Y, Donovan J, Rath S, Whitney G, Chitrakar A, Korennykh A. Structure of human RNase L reveals the basis for regulated RNA decay in the IFN response. *Science* (2014) 343(6176):1244–8. doi:10.1126/science.1249845
31. Donovan J, Dufner M, Korennykh A. Structural basis for cytosolic double-stranded RNA surveillance by human oligoadenylate synthetase 1. *Proc Natl Acad Sci U S A* (2013) 110(5):1652–7. doi:10.1073/pnas.1218528110
32. Andersen JB, Strandbygard DJ, Hartmann R, Justesen J. Interaction between the 2'-5' oligoadenylate synthetase-like protein p59 OASL and the transcriptional repressor methyl CpG-binding protein 1. *Eur J Biochem* (2004) 271(3): 628–36. doi:10.1046/j.1432-1033.2003.03966.x
33. Han B, Yuan H, Wang T, Li B, Ma L, Yu S, et al. Multiple IgH isotypes including IgD, subclasses of IgM, and IgY are expressed in the common ancestors of modern birds. *J Immunol* (2016) 196(12):5138–47. doi:10.4049/jimmunol.1600307
34. Huang Y, Li Y, Burt DW, Chen H, Zhang Y, Qian W, et al. The duck genome and transcriptome provide insight into an avian influenza virus reservoir species. *Nat Genet* (2013) 45(7):776–83. doi:10.1038/ng.2657
35. Wu S, Ying G, Wu Q, Capecchi MR. Toward simpler and faster genome-wide mutagenesis in mice. *Nat Genet* (2007) 39(7):922–30. doi:10.1038/ng2060
36. Heinecke K, Seher A, Schmitz W, Mueller TD, Sebald W, Nickel J. Receptor oligomerization and beyond: a case study in bone morphogenetic proteins. *BMC Biol* (2009) 7(6):59. doi:10.1186/1741-7007-7-59
37. Schroeder A, Mueller O, Stocker S, Salowsky R, Leiber M, Gassmann M, et al. The RIN: an RNA integrity number for assigning integrity values to RNA measurements. *BMC Mol Biol* (2006) 7(6):3. doi:10.1186/1471-2199-7-3
38. Livak KJ, Schmittgen TD. Analysis of relative gene expression data using real-time quantitative PCR and the 2(-Delta Delta C(T)) method. *Methods* (2001) 25(4):402–8. doi:10.1006/meth.2001.1262

Conflict of Interest Statement: The authors declare that the research was conducted in the absence of any commercial or financial relationships that could be construed as a potential conflict of interest.

Copyright © 2018 Rong, Wang, Chen, Yang, Hu, Liu, Wang, Chen, Zheng, Pu, Sun, Smith, Burt, Liu, Li and Huang. This is an open-access article distributed under the terms of the Creative Commons Attribution License (CC BY). The use, distribution or reproduction in other forums is permitted, provided the original author(s) and the copyright owner are credited and that the original publication in this journal is cited, in accordance with accepted academic practice. No use, distribution or reproduction is permitted which does not comply with these terms.

frontiers in Genetics

REVIEW
published: 19 July 2018
doi: 10.3389/fgene.2018.00261

Host and Viral Genetic Variation in HBV-Related Hepatocellular Carcinoma

Ping An[1]*, *Jinghang Xu*[1,2], *Yanyan Yu*[2] and *Cheryl A. Winkler*[1]*

[1] Basic Research Laboratory, National Cancer Institute, Leidos Biomedical Research, Inc., Frederick National Laboratory for Cancer Research, Frederick, MD, United States, [2] Department of Infectious Diseases, Center for Liver Diseases, Peking University First Hospital, Peking University, Beijing, China

Hepatocellular carcinoma (HCC) is the fifth most common cancer in men and the second leading cause of cancer deaths globally. The high prevalence of HCC is due in part to the high prevalence of chronic HBV infection and the high mortality rate is due to the lack of biomarkers for early detection and limited treatment options for late stage HCC. The observed individual variance in development of HCC is attributable to differences in HBV genotype and mutations, host predisposing germline genetic variations, the acquisition of tumor-specific somatic mutations, as well as environmental factors. HBV genotype C and mutations in the *preS, basic core promoter* (*BCP*) or *HBx* regions are associated with an increased risk of HCC. Genome-wide association studies have identified common polymorphisms in *KIF1B*, *HLA-DQ, STAT4,* and *GRIK1* with altered risk of HBV-related HCC. HBV integration into growth control genes (such as *TERT*), pro-oncogenic genes, or tumor suppressor genes and the oncogenic activity of truncated HBx promote hepatocarcinogenesis. Somatic mutations in the *TERT promoter* and classic cancer signaling pathways, including Wnt (*CTNNB1*), cell cycle regulation (*TP53*), and epigenetic modification (*ARID2* and *MLL4*) are frequently detected in hepatic tumor tissues. The identification of HBV and host variation associated with tumor initiation and progression has clinical utility for improving early diagnosis and prognosis; whereas the identification of somatic mutations driving tumorigenesis hold promise to inform precision treatment for HCC patients.

Keywords: genotype, hepatitis B virus, hepatocellular carcinoma, mutation, single nucleotide polymorphisms

OPEN ACCESS

Edited by:
William Scott Bush,
Case Western Reserve University,
United States

Reviewed by:
Michael Scheurer,
Baylor College of Medicine,
United States
Manuel Romero-Gomez,
Universidad de Sevilla, Spain

***Correspondence:**
Ping An
ping.an@nih.gov
Cheryl A. Winkler
winklerc@mail.nih.gov

Specialty section:
This article was submitted to Applied Genetic Epidemiology, a section of the journal Frontiers in Genetics

Received: *13 April 2018*
Accepted: *27 June 2018*
Published: *19 July 2018*

Citation:
An P, Xu J, Yu Y and Winkler CA (2018) Host and Viral Genetic Variation in HBV-Related Hepatocellular Carcinoma. Front. Genet. 9:261. doi: 10.3389/fgene.2018.00261

INTRODUCTION

Hepatocellular carcinoma (HCC) is the fifth most common cancer in men and the second leading cause of cancer deaths worldwide (El-Serag, 2011; Torre et al., 2015). HCC prevalence is highest in East and Southeast Asia and sub-Saharan Africa, but the incidence rates of HCC have increased in the United States and Western Europe over the past few decades (Lee, 2015; Njei et al., 2015). Early diagnosis and surgical resection remain the key to potential curative treatment; however, most HCC patients present with late stage tumors and have poor prognosis. HCC surveillance is mainly based on sonography and alpha-fetoprotein (AFP) measurement, both of which lack sufficient sensitivity and specificity (Yim and Lok, 2006; Bruix et al., 2011).

Hepatitis B virus (HBV) is one of the leading risk factors for HCC, especially in HBV endemic areas. Despite the existence of an effective vaccine, about 257 million people, or 3.5% of the global population, were afflicted with chronic HBV infection in 2015, WHO (2017). The clinical spectrum of chronic HBV infection ranges from asymptomatic carrier status to chronic hepatitis B (CHB), which may evolve to liver cirrhosis and HCC (EASL, 2012). An estimated 8–20% of untreated adults with CHB will develop liver cirrhosis within 5 years (Terrault et al., 2016) and 2–8% of those with cirrhosis develop HCC annually (Yim and Lok, 2006; Bruix et al., 2011; Hung et al., 2017).

Environmental and host risk factors for HCC include childhood acquisition of HBV infection, cirrhosis, aflatoxin B1 exposure, heavy alcohol use, smoking, male sex, advancing age, obesity, type 2 diabetes and an impaired immune response (Bruix et al., 2016). In addition to HBV, hepatitis C virus (HCV) chronic infection is a major cause of HCC, but co-infection by HBV and HCV do not seem to confer greater HCC risk than HBV or HCV monoinfection in a meta-analysis (Cho et al., 2011). Co-infection of HBV and hepatitis delta virus (HDV), occurring in ∼5% of those HBV infected, was associated with 3 to 6-fold higher incidence of HCC in longitudinal cohorts (Fattovich et al., 2000; Romeo et al., 2009; Ji et al., 2012; Kushner et al., 2015).

Family clustering and incidence differences among different ancestry groups suggests that inherited genetic factors may contribute to HCC risk (Shen et al., 1991). Common and rare single nucleotide polymorphisms (SNPs) and structural genomic changes may predispose or restrict HCC development. The identification of moderate to high penetrant genetic variants associated with HBV-related HCC might identify HCC susceptible patients that would lead to earlier intervention and better outcomes (Thomas et al., 2009; Brennan et al., 2011; Michailidou et al., 2015). For example, screening for *BRCA1* and *BRCA2* mutations is routinely used to identify women at risk for breast and ovarian cancer and is routinely used in precision treatment protocols (Brennan et al., 2011; Michailidou et al., 2015).

Somatic mutations occurring in hepatocytes as the consequence of exogenous and endogenous mutagenic factors, are likely involved in HCC initiation and progression, as they are in many other cancers. Identification of cancer diver mutations in HCC are essential for HCC prognostics and for precision therapy targeting perturbed pathways.

Here, we review recent advancements and identify knowledge gaps in HBV-related HCC genetics at three levels: the human host, the virus, and somatic mutations in liver tumors and their associations with clinical outcomes.

HBV

HBV has a partially double-stranded circular DNA genome of ∼3.2 kilobase (kb) pairs, comprising four overlapping open reading frames (ORF): *preS/S*, *P*, *preC/C,* and *X* (Liang, 2009). The *PreS/S* gene region encodes large (preS1+preS2 +S), middle (preS2+S), and small (S) HBsAg envelope proteins (**Figure 1**). The *P* region encodes the polymerase/reverse transcriptase, which is involved in genome replication. The preC/C codes the nucleocapsid hepatitis B core antigen (HBcAg) or the hepatitis B e antigen (HBeAg) translated from initiated codons at the core or precore regions, respectively. HBcAg and HBeAg are biomarkers for HBV active infection or infectivity. The *X* ORF encodes a nonstructural protein (HBx) with multiple functions in viral replication and oncogenic activity (Liang, 2009).

Molecular Mechanisms of HBV-Related HCC

There are at least three prevailing mechanisms proposed for the development of HBV-related HCC (Kremsdorf et al., 2006; Block et al., 2007; Hai et al., 2014; **Figure 1**). First, chronic inflammation and regeneration of hepatocytes during chronic HBV infection may lead to the accumulation of genetic alterations that confer cell growth advantage. Second, the integration of HBV DNA into the host genome may activate the host genes controlling cell proliferation and cause genomic instability. Finally, HBV proteins, mainly HBx, may promote cell proliferation (Kremsdorf et al., 2006; Block et al., 2007; Hai et al., 2014). It is also likely that all three mechanisms contribute to HCC development.

HBV Viral Load

The general consensus is that persistent high-level HBV replication poses greater risk of developing liver cirrhosis and HCC (Sanchez-Tapias et al., 2002; Chen et al., 2006a,b, 2007; Fattovich et al., 2008). A large prospective study, which followed 3653 HBsAg positive participants enrolled in the Taiwanese Reveal-HBV cohort for over a decade, found that HBV DNA levels at study entry were positively correlated with incidence of HCC in a dose-dependent manner. Individuals with HBV levels greater than 1 million copies /mL were 10-fold more likely to develop HCC than those with less than 300 copies/mL (Chen et al., 2006b). Serum HBV DNA viral load is also associated HCC tumor recurrence (Hung et al., 2008; Wu et al., 2009). A viral load of greater than 10,000 copies/mL (2000 IU/mL) was independently associated with HBV-related HCC recurrence in patients who underwent liver resection (Hung et al., 2008). Antiviral therapy in these patients decreased tumor recurrence (Li et al., 2010).

HBV Genotype

Ten HBV genotypes (A to J) that diverge by >8% of their nucleotide sequences have been identified globally. HBV genotypes distribute within distinct geographic regions and ethnic populations(Lin and Kao, 2015). Phylogenetic analysis of HBV genotypes indicate that global distribution of HBV genotypes corresponds with the major prehistoric and modern human migration patterns, after HBV established infection in humans around 33,000 years ago (Paraskevis et al., 2013). Different genotypes prevail in the two regions with the highest HBV and HCC prevalence: genotypes B and C are prevalent in East Asia where vertical transmission is predominant, whereas genotypes A and D are prevalent in sub-Saharan Africa where

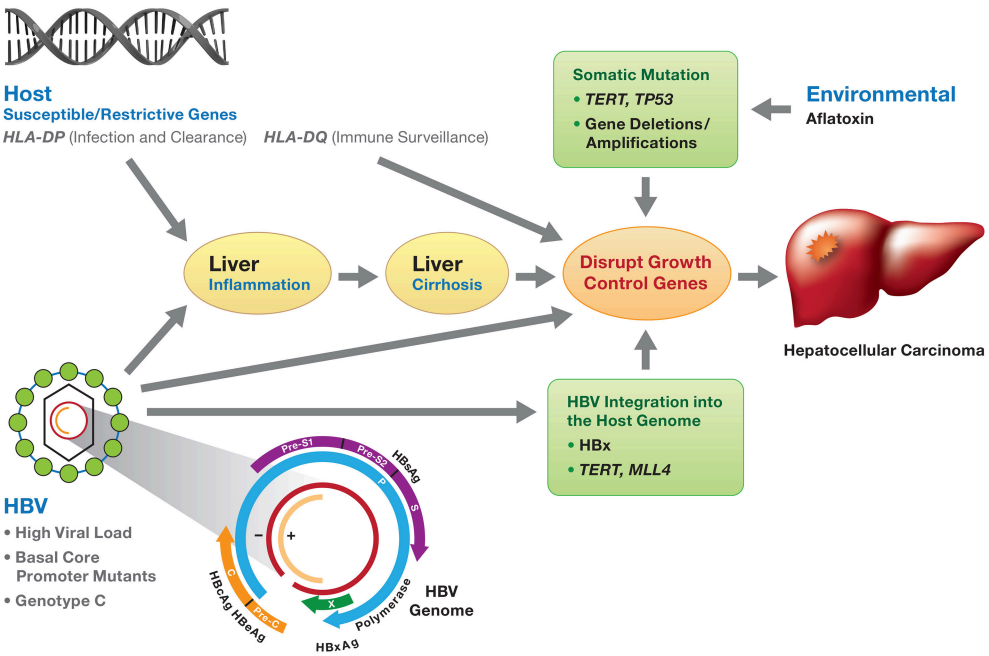

FIGURE 1 | Viral and host genetic factors involved in the development of HBV-induced HCC. HBV infection, if not resolved, may develop to chronic hepatitis and progress to liver cirrhosis and subsequently HCC. Molecular mechanisms of HBV-related HCC involve (1) chronic inflammation and regeneration of hepatocytes; (2) accumulation of genetic alterations that confer cell growth advantage; (3) integration of HBV DNA into the host genome and activation of host genes controlling cell proliferation; (4) genomic instability; and (5) direct promotion of cell proliferation by viral proteins (mainly HBx). The development of HCC is the consequence of the interaction of environmental factors (e.g., aflatoxin), HBV viral factors (genotypes, HBV DNA levels and HBV mutants) and host genetic susceptible variants (e.g., *HLA-DP* variants affecting HBV clearance), along with somatic mutations (*TP53*, *TERT*, gene deletion/amplification) disrupting cell growth control. HBV genotype C and mutations in the *preS, basic core promoter* or *HBx* gene are associated with an increased risk of HCC.

horizontal transmission is more common. HBV genotypes A and D are the main genotypes in low HBV prevalence regions including Europe and North America (Lin and Kao, 2015).

The risk of HCC appears to differ by HBV subtypes. In East Asia, HBV genotype C is associated with higher risk of HCC compared to genotype B (Chan et al., 2004; Yu et al., 2005; Yang et al., 2008; Tseng et al., 2012; Vutien et al., 2013; Lin and Kao, 2015; Raffetti et al., 2016). Serum HBV viral load is significantly higher in patients with HBV genotype C than in those infected with genotype B (Chu et al., 2002; Chan et al., 2004; Yu et al., 2005; Lin and Kao, 2015). The increased risk of HCC might be the consequence of longer exposure to high levels of HBV in patients with genotype C (Kao et al., 2004; Ni et al., 2004). In contrast, HCC risk for genotype D and A appear to be similar, although there are reports that patients with HBV genotype A experience longer sustained remissions (Sanchez-Tapias et al., 2002) and are more responsive to interferon alpha (IFN- α) treatment compared to those infected with HBV genotype D (Erhardt et al., 2005). There are at least 5 co-circulating HBV genotypes in Alaska Native people, which offers rare opportunity for direct comparisons of HCC risk among genotypes. A longitudinal cohort of Alaska Natives followed for over 30 years reported that carriers of genotypes A (OR 4), C (OR 16), and F (OR 14) are at higher risk compared with genotypes B or D (Livingston et al., 2007; Ching et al., 2016). A study of 1,000 Alaska Native children and young adults followed for over 23 years found that HBV genotype F1 was associated with the highest risk for HCC (Gounder et al., 2016). These studies support a strong role for HBV genotypes in predicting HCC risk. In comparison, HCV genotype 3 was also associated with higher risk of HCC compared to other HCV genotypes (van der Meer et al., 2012; Kanwal et al., 2014).

HBV Mutations

HBV DNA replication errors occur at a much higher rate than for other DNA viruses because HBV reverse transcriptase lacks a proofreading function (Chotiyaputta and Lok, 2009). The estimated nucleotide substitution rate was 2.2×10^{-6} substitutions/site/year, which is higher than other DNA viruses but lower than RNA viruses (Paraskevis et al., 2013). Mutations in the HBV genome commonly associated with HCC are summarized in **Table 1**, with the *preC/C* and basic core promoter (*BCP*) regions harboring the most frequent mutations.

Pres/S Region Mutants

PreS mutations, especially the *preS1* deletion, *preS2* deletion, and *preS2* start codon mutations, may induce an unbalanced production of envelope proteins that accumulate in the endoplasmic reticulum (ER) of the hepatocytes, leading to ER stress, oxidative DNA damage and genomic instability (Pollicino et al., 2014). These cytotoxic effects cause liver cell damage and

TABLE 1 | The association of HBV mutants with HCC risk.

Mutation	Frequency[a]		RR or OR (95% CI)	References
	HCC	non-HCC		
***PreS/S* mutants**				
Any *preS* mutation	45.5-72.3%	18.1-26.0%	3.82 (2.59-5.61)[b]	Liu et al., 2009; Yang et al., 2015
PreS deletion	29.2-51.1%	11.3-18.2%	3.98 (2.28-6.95)[b]	Liu et al., 2009; Yang et al., 2015
PreS2 start codon mutation	17.7-21.2%	7.2-8.0%	2.63(1.30-5.34)[b]	Yang et al., 2015
***P* mutants**				
rtA181T/sW172*	Changes over the treatment duration of NAs.		Cumulative incidence of HCC: 1.8% (2/113) in the mutation-absent; 30% (3/10) in the mutation-present	Yeh et al., 2011
***PreC/C* mutants**				
BCP, A1762T/G1764A (xK130M/V131I)	66.5%(2,480/3,729)	39.8% (2,594/6,511)	3.05 (2.35-3.95)	Yang Z. et al., 2016
Enhancer II, C1653T	26.7-46.2%	13.3-28.2%	1.83 (1.21-2.76)[b]	Liu et al., 2009; Yang et al., 2015
BCP, T1753V (xI127T)	25.9-46.2%	15.5-23.5%	2.09 (1.49-2.94)[b]	Liu et al., 2009; Yang et al., 2015
PreC, G1896A	38.8-84.6%	27.9-82.7%	0.77 (0.47-1.26)[b]	Liu et al., 2009; Yang et al., 2015
***X* mutants**				
A10R/S144R double mutation	Not reported.			Shi et al., 2016
xK130M+xV131I+ xV5M (triple) mutations	41.9% (13/31)	11.9%(5/42)	5.34 (1.65-17.309)	Lee et al., 2011

[a] *Frequency ranges were extracted from studies included in the meta-analyses (Liu et al., 2009; Yang et al., 2015).*
[b] *Pooled RR from reference Yang et al. (2015).*
CI, confidence interval; NAs, nucleos(t)ide analogs; OR, odds ratio; RR, relative risk.

regeneration (Pollicino et al., 2014). A meta-analysis of 9 cross-sectional studies including 388 HCC cases demonstrated that any one of the *preS* mutants (C1653T, T1753V, and A1762T/G1764A) was associated with a 3.8-fold increased risk of HCC (Liu et al., 2009), consistent with the result from a recent meta-analysis of prospective studies comprising 360 cases (RR 3.8) (Yang et al., 2015). *PreS/S* deletions and the *Pre S2* start codon mutation had a RR 4.0 and 2.6, respectively (Yang et al., 2015). Specifically, C2964A, C3116T, and C7A were independently associated with an increased risk of HCC (Yin et al., 2010).

Mutations introducing stop codons in the S genomic region have been proposed to enhance tumor development by encoding truncated proteins with transcriptional transactivation activity (Pollicino et al., 2014). The premature stop codon mutations at position 172 or 182 in the S genomic region are associated with higher risk for liver cirrhosis and HCC (Lai et al., 2009; Pollicino et al., 2014).

PreC/C Region Mutants

Mounting evidence supports the importance of the naturally occurring *basal core promoter (BCP)* double mutation, A1762T/G1764A, as a risk factor for HCC (Fang et al., 2008; Yang et al., 2008, 2015; Yang Z. et al., 2016). In a meta-analysis of 15 prospective studies comprising 1336 HCC cases, individuals with the double mutation had a 3-fold higher risk of developing HCC (Yang et al., 2015). In a more recent meta-analysis that included 3729 HCC cases, double mutation carriers had a 5-fold higher HCC risk (Yang Z. et al., 2016). Other prospective long-term follow-up studies found that the incidence of HCC in double mutation carriers was 4 to 5-fold higher (Fang et al., 2008; Yang et al., 2008). The presence of the *BCP* double mutation reduces HBeAg production and viral load before anti-HBe seroconversion (Buckwold et al., 1996; Fang et al., 2009), suggesting that its oncogenic mechanism is not directly attributable to viral replication level. However, the *preC* stop codon G1896A, which prevents the production of HBeAg, does not appear to affect HCC risk as demonstrated in a recent meta-analysis with 600 HCC cases (Yang et al., 2015).

Polymerase/Reverse Transcriptase Region Mutants

Anti-HBV nucleos(t)ide analogs (NAs) are effective in lowering HBV DNA levels through their inhibition of HBV polymerase/reverse transcriptase (Terrault et al., 2016). However, the emergence of and the selection for resistance mutations in the polymerase/reverse transcriptase region confer a virial survival advantage and is a major barrier to the success of NAs treatment. In a longitudinal study of lamivudine (LMV)-resistant CHB patients, emergence of the rtA181T/sW172X mutant in LMV-resistant patients increased the risk of HCC (Lai et al., 2009; Yeh et al., 2011). NIH3T3 cells expressing this mutant showed greater oncogenic potential in nude mice (Lai and Yeh, 2008; Lai et al., 2009). It is an open question whether resistance to other nucelos(t)ide analogs also increases the risk of HCC.

X Region Mutants

HBx protein is a transcriptional activator of various host cellular genes involved in growth control, DNA repair, and epigenetic modification (Xu et al., 2014). It activates the Ras/Raf/mitogen-activated protein (MAP) kinase pathway, which is involved in

hepatocarcinogenesis, and interacts with the tumor protein 53 gene (*TP53*), interfering with its function as a tumor suppressor (Di Bisceglie, 2009).

Certain point mutations in the *HBx* gene, in particular, the K130M and V131I double substitutions, are more frequent in patients with liver cirrhosis and/or HCC than in patients with chronic hepatitis B (Baptista et al., 1999). Due to the partial overlap of BCP with Hbx, the same nucleotide substitutions result in both HBx K130M and V131I and pre-core *BCP* A1762T/G1764A changes. Increasing number of *HBx* mutations is correlated with increased risk of HCC. The double xK130M+xV131I and triple xK130M+xV131I+ xV5M mutations are associated with a 4-5-fold increased the risk of HCC (Lee et al., 2011). Substitutions at position 10, 30, 38, 88, 94, and 144 have also been reported to be associated with HCC (Muroyama et al., 2006; Lee et al., 2011; Wang et al., 2012; Shi et al., 2016; **Table 1**). Even though the precise mechanism remains to be elucidated, *HBx* plays a central role in hepatocarcinogenesis and could be an attractive therapeutic target for HCC suppression.

In summary, major HBV viral factors associated with increased risk of HCC include genotype C and F, higher HBV-DNA levels, mutations in the *preS/S region,* the double mutation A1762T/G1764A in the basic core promoter, and the double or triple mutation K130M, V131I xV5M in the *HBx* gene. Different genotypes of the virus (which are due to the accumulation of viral mutations over time) have differing propensities for the development of HCC. Epidemiological association data and some functional evidence suggest the likely causal role of viral mutations, particularly for genotype differences. However, the temporal and causal relationship of HBV mutations with HCC remains to be firmly established, as most results were obtained from case-control and cross-sectional studies and rarely from prospective longitudinal HBV cohorts. HBV mutations may also increase risk of HCC indirectly by the acquisition of mutations that leads to immune escape and increased viral replication. Higher HBV burden would contribute to chronic inflammation promoting the destruction and regeneration of HBV infected hepatocytes mediated by host cytotoxic T lymphocyte (CTL) immune response and increasing the opportunity for replication errors during cell mitosis (Block et al., 2007). The emergence and accumulation of genetic and epigenetic alterations with cell growth advantage eventually lead to hepatocarcinogenesis (Block et al., 2007). The exact molecular mechanisms by which HBV mutations promote hepatocarcinogenesis warrants further investigation.

HOST GENETIC VARIATION AND HBV-RELATED HCC

Although the incidence of HCC among HBV carriers is much higher (223-fold) than among non-carriers (Beasley et al., 1981), only a fraction of patients with chronic HBV infection develop HCC. Results from twin studies, family clustering studies and incidence differences between continental ancestry groups suggest that host genetic factors contribute to HCC susceptibility (Shen et al., 1991). Genome-wide association studies (GWAS) provide an agnostic (hypothesis-free) method to identify susceptibility and resistance loci for HBV-related HCC. The ability to securely identify genetic susceptibility loci associated with HCC is critically dependent on sample size for sufficient power to detect associations with small to moderate effect sizes in GWAS. This is due to the need to correct for multiple testing that tends to inflate false positive signals; therefore, the human genetics community has determined that a genome-wide significance threshold of $p < 5 \times 10^{-8}$ and independent replication association is required to firmly establish a genotype-phenotype association. The top associations between host genetic variants with HCC are summarized in **Table 2**. Only associations in the HLA class II region have been found to replicate in at least two studies. These studies, performed primarily in East Asians, suggest that no common, moderate to high penetrant alleles contribute to HCC development.

The HCC association of intergenic SNPs near *HLA-DQA1* and *HLA-DQA2*, and *HLA-DQB1*, encoding the alpha and beta chains of the HLA-DQ protein, were identified by GWAS in two large studies (Li et al., 2012; Jiang et al., 2013). HLA class II proteins, comprising HLA-DP, DQ, and DR proteins, play a central role in extracellular antigen presentation to CD4 T cells stimulating B cell that lead to antibody production against foreign pathogens, including HBV and HCV.

Outside of the HLA region, genetic associations with HBV-related HCC have been reported for several genes. A two-stage GWAS composed of five cohorts from East Asian identified the intronic rs17401966 SNP in the *KIF1B* gene (OR = 0.61) with genome-wide significance in a meta-analysis (Zhang et al., 2010). *KIF1B* encodes a kinesin superfamily member involved in the transport of organelles and vesicles. Both germline and somatic loss-of-function mutations in the KIF1B isoform have been detected in multiple cancers (Zhang et al., 2010). However, this association failed to replicate in multiple independent studies, several of which were well-powered (**Table 2**; Hu et al., 2012; Li et al., 2012; Sawai et al., 2012; Jiang et al., 2013; Sopipong et al., 2013). The latest meta-analysis of 12 cohorts found statistical significance only when the original 5 cohorts reporting positive associations were included, but when these 5 cohorts were removed the association was abrogated (Su et al., 2017). Further validation and functional studies are warranted to support or not a role of *KIF1b* variation in HCC.

Other candidate genes implicated by GWAS include *STAT4*, and *GRIK1* (**Table 2**; Li et al., 2012; Jiang et al., 2013). STAT4 is a transcription factor involved in development of Th1 cells and production of IFN-γ, a cytokine with antiviral and antitumor activities. STAT4 rs7574865 is an expression quantitative trait locus (eQTL) with dosage effect in HCC tissues (Jiang et al., 2013). Glutamate receptor GRIK1, is involved in cancer development (Li et al., 2012), though its functional role in HCC has not been experimentally demonstrated. These associations have not yet been replicated or validated by functional assessment. Recently, a functional genomic approach revealed a c-Myc binding SNP that regulates a putative tumor suppressor gene EPB41 and was associated with predisposition to HCC (Yang et al., 2016b).

TABLE 2 | Associations of host genetic variants with HBV-related HCC from GWASs and replication studies.

Chr.	Nearest gene	SNP	Location	Major/ minor allele	Population	Case	Control	No. cases	No. control	MAF cases	MAF controls	Model	OR	95% CI	*P*-value	Study design	References
1p36.22	*KIF1B*	rs17401966	Intron	A/G	Chinese	HBV-HCC	HBV carriers	2,310 (discovery 348)	1,789	0.19	0.28	Add	0.62	0.56–0.69	3.4×10^{-19}	GWAS+ 4 replications	Zhang et al., 2010
					Han Chinese	HBV-HCC	HBV carriers	1,293	1,334	0.27	0.28	Additive	0.99	0.88–1.12	0.92	Replication	Hu et al., 2012
					Japanese, Korean, Hong Kong Chinese	HBV-HCC	HBV carriers ASC+CHB	578	1,351	0.26	0.24	Allelic	1.00	0.85–1.19	0.97	4 replications	Sawai et al., 2012
					Thai	HBV-HCC	HBV carriers	202	196	0.30	0.30	Allelic	0.95	0.70–1.28	0.733	Replication	Sopipong et al., 2013
					Chinese	HBV-HCC	HBV carriers	1,161	1,353	0.27	0.28	Additive	0.98	0.87–1.11	0.79	GWAS	Jiang et al., 2013
					Southern Chinese	HBV-HCC	Non-HCC HBV carriers	357	354	0.29	0.29	Allelic	1.0	NA	0.91	Replication	Chan et al., 2011
					Han Chinese	HBV-HCC	HBV carrier	1,538	1,465	0.27	0.29	Additive	0.90	0.80–1.02	0.091	GWAS	Li et al., 2012
2q32.2-2q32.3	*STAT4*	rs7574865	Intron	G/T	Chinese	HBV-HCC	Non-HCC HBV carriers	5,480 (discovery 1,161)	6,319	0.28	0.32	Additive	0.83	0.78–0.88	2.48×10^{-10}	GWAS+ 6 replications	Jiang et al., 2013
6p21.32	*HLA-DQA2/DQB1*	rs9275319	Intergenic	A/G	Chinese	HBV-HCC	Non-HCC HBV carriers	5,480 (discovery 1,161)	6,319	0.08	0.11	Additive	0.67	0.61–0.74	2.72×10^{-17}	GWAS+ 6 replications	Jiang et al., 2013
6p21.32	*HLA-DQA1/DRB1*	rs9272105	Intergenic	G/A	Han Chinese	HBV-HCC	HBV carrier	5,885 (discovery 1,538)	6,181	0.51	0.45	Additive	1.28	1.22–1.35	5.24×10^{-22}	GWAS+ 2 validations + 1 replication	Li et al., 2012
21q21.3	*GRIK1*	rs455804	Intron	C/A	Han Chinese	HBV-HCC	HBV carrier	5,967 (discovery 1,538)	6,182	0.3	0.34	Additive	0.84	0.80–0.89	5.24×10^{-10}	GWAS+ 2 validations + 1 replication	Li et al., 2012

ASC, asymptomatic carrier; CHB, chronic hepatitis B; Chr., chromosome; CI, confidence interval; GWAS, Genome-Wide Association Study; HBV, hepatitis B virus; HCC, hepatocellular carcinoma; MAF, Minor allele frequency; OR, odds ratio.

A 2011 experts′ commentary highlighted the need for further GWAS studies of HCC with larger subject enrollment, clearly delineated phenotypes, and replication (Budhu and Wang, 2011). The lack of replication for HCC GWAS studies is most likely due to relatively small sample sizes of the study although genetic and phenotypic heterogeneity may have also contributed. True causal variants should have similar effects across all populations while marker SNPs may have different effects in different ancestry or ethnic populations. These differences in effect size or statistical significance in haplotype structure among different populations, the inclusion of trans-ethnic or continental racial populations can be used to refine position of the causal locus by fine-mapping (Franceschini et al., 2012). The newer population specific genotyping arrays, in combination with larger case-control groups representing diverse populations, should reveal additional germline variants that contribute to the observed variance in HBV-HCC susceptibility. Finally, whole genome or exome sequencing might also identify causal rare variants associated with HBV-HCC. These studies should identify critical pathophysiological pathways for HBV-related liver cirrhosis and HCC.

INTERACTION OF HOST GENES AND HBV: HBV DNA INTEGRATION, SOMATIC MUTATIONS AND EPIGENETIC MODIFICATION IN HCC ONCOGENESIS

Environmental factors, HBV genotypes and genetic variation, and host genetic variation are involved in the development and progression of HCC. The interplay between these factors might lead to the initiation of HCC (**Figure 1**).

HBV Integration and HCC

HBV DNA integration into the host genome is one of the proposed molecular mechanisms of hepatocarcinogenesis. HBV-DNA integration occurs during both the acute and chronic stages and integrated HBV-DNA is detectable in 75-90% of HCC tissues (Murakami et al., 2005; Zhao et al., 2016). HBV integration events may cause direct gene disruption, HBV promoter-driven transcription of host genes, viral-host transcript fusion and induce genome instability (Tao et al., 2011; Jiang et al., 2012; Sung et al., 2012), which may lead to activation of proto-oncogenes or inactivation of tumor suppressor genes. Oncogenic activity of the cellular and viral genes resulting from the HBV integration confers a selective growth advantage to cells with accumulation of genetic defects, leading to hepatocarcinogenesis (Tao et al., 2011; Jiang et al., 2012; Sung et al., 2012).

Advanced genome-wide sequencing technology has enabled non-biased genome scans of HBV integration sites in HCCs (**Table 3**; Murakami et al., 2005; Ding et al., 2012; Toh et al., 2013; Lau et al., 2014). HBV integration sites are randomly distributed across the whole genome with a handful of hotspots (Sung et al., 2012). Some investigators found preferential integration in chromosome 10 and 17 (Ding et al., 2012; Toh et al., 2013; Zhao et al., 2016). HBV appears to preferentially integrate near coding genes that are transcriptionally active (Ding et al., 2012; Sung et al., 2012; Toh et al., 2013), as was observed for HIV integration (Maldarelli et al., 2014).

Recurrent HBV integration sites have been detected in many cancer-related genes. The highest frequency of HBV integration is detected in the telomerase reverse transcriptase (*TERT*) gene (Paterlini-Brechot et al., 2003; Murakami et al., 2005; Ding et al., 2012; Fujimoto et al., 2012; Sung et al., 2012; Li et al., 2013; Toh et al., 2013; Lau et al., 2014; Kawai-Kitahata et al., 2016). Integration in the proximity of TERT is correlated with *TERT* gene expression (Sung et al., 2012; Zhao et al., 2016); reactivation of TERT likely confers early clonal advantage during chronic HBV infection. Whole-genome sequencing identified clonal expansion of HBV integration in the *TERT* locus in HCC tumors but not in adjacent non-tumor tissue DNA, suggesting its role in liver carcinogenesis (Fujimoto et al., 2012). Additional commonly identified recurrent target genes for HBV integration in HCC liver tissue are listed in **Table 3**, including *MLL4* and *CCNE1* (Saigo et al., 2008; Ding et al., 2012; Jiang et al., 2012; Sung et al., 2012; Li et al., 2013) among others (Murakami et al., 2005; Tao et al., 2011; Ding et al., 2012; Jiang et al., 2012; Sung et al., 2012; Toh et al., 2013). Individuals with a high number of integration sites have unfavorable HCC survival (Murakami et al., 2005; Ding et al., 2012; Toh et al., 2013; Lau et al., 2014; Zhao et al., 2016).

The integrated HBV genome itself may be oncogenic (Ding et al., 2012; Fujimoto et al., 2012; Jiang et al., 2012; Li et al., 2013; Toh et al., 2013). Upon integration, the 3′-end of the HBx is often deleted, resulting in C-terminal truncated HBx (ct-HBx) protein, which contributes to HCC initiation and progression (Tu et al., 2001; Ma et al., 2008; Sze et al., 2013; Yin et al., 2013; Wang et al., 2014; Zhu et al., 2015; Li et al., 2016). The truncated HBx protein is reported to promote the transforming ability of hepatocytes (Tu et al., 2001), induce C-Jun/MMP10 activation to increase cellular proliferation (Ma et al., 2008; Sze et al., 2013), as well as enhance hepatoma cell invasion and metastasis (Sze et al., 2013; Li et al., 2016). Ct- HBx is present significantly more in tumors compared to adjacent non-tumorous tissues in several studies (Yin et al., 2013; Wang et al., 2014; Zhu et al., 2015; Li et al., 2016) and Ct-HBx expression in HCC tissue correlates with decreased patient survival (Yin et al., 2013).

Quantification of HBV integration sites may have prognostic value in predicting HCC survival. In a genome-wide survey of 88 HCC patients, increasing number of HBV integrations was correlated with HCC occurrence at younger age and shorter survival (Sung et al., 2012). A viral-human chimeric HBx-LINE1 RNA hybrid, detected in 23% of HCC tumors, was also predictive of poorer survival (Lau et al., 2014).

Somatic Mutations and Copy Number Alteration in HCC

Most somatic mutations are harmless passenger mutations accumulated in the process of tumor growth, which occur at random and confer no selective advantage for tumor cells. Driver mutations confer selective growth advantage and cause transformation of a normal cell to a cancer cell, which are clinically relevant. Recurrent coding changes in multiple tumor

TABLE 3 | HBV integration into host genes in HCC tissues from next generation sequencing studies.

Frequency	Host gene	References
Common	*TERT*	Paterlini-Brechot et al., 2003; Murakami et al., 2005; Ding et al., 2012; Fujimoto et al., 2012; Sung et al., 2012; Li et al., 2013; Toh et al., 2013; Lau et al., 2014; Kawai-Kitahata et al., 2016
Less Common	*MLL4*, *CCNE1*	Saigo et al., 2008; Ding et al., 2012; Jiang et al., 2012; Sung et al., 2012; Li et al., 2013
Infrequent	*SMAD5, SENP5, ROCK1, PDGFRB, MAPK1, ANGPT1, CYP2C8, CCNA2, MSMB, AIP, NTN1, FAS, CCNG1, P62*	Murakami et al., 2005; Tao et al., 2011; Ding et al., 2012; Jiang et al., 2012; Sung et al., 2012; Toh et al., 2013
	Viral gene	
Common	*ct-HBx,* HBx-LINE1 RNA hybrid	Yin et al., 2013; Lau et al., 2014; Wang et al., 2014; Zhu et al., 2015; Li et al., 2016
	Chromosome	
Common	Chromosome 10, 17, 8p11	Murakami et al., 2005; Ding et al., 2012; Toh et al., 2013; Lau et al., 2014

cases may identify putative cancer driver mutations (Bozic et al., 2010). Recent whole-genome and whole-exome deep sequencing of tumor and non-tumor tissues have revealed the importance of somatic mutations and structural variations in tumor development across cancer types and has led to more efficacious treatment modalities based on molecular changes or genomic classification rather than target organs of cancer (e.g., *BRAF* V600E, *KIT*, *EGFR*, *ERBB2*) (Swanton et al., 2016).

Recurrent somatic mutations in HCC have been identified in several known cancer-related genes and pathways. These include genes required for telomere maintenance, the Wnt signaling pathway, which regulates cell proliferation, cell cycle regulation, epigenetic modification, and the PI3K/Akt/mTOR, Ras/Raf/MAP, oxidative stress, and JAK/STAT pathways (Li et al., 2011; Woo et al., 2011; Fujimoto et al., 2012; Guichard et al., 2012; Huang et al., 2012; Cleary et al., 2013; Kan et al., 2013; Nault et al., 2013; Ahn et al., 2014; Meng et al., 2014; Totoki et al., 2014; Schulze et al., 2015; Kawai-Kitahata et al., 2016; Yao S. et al., 2016). The perturbed genes identified in HCC tumor genomes are listed in **Table 4**. Copy number alterations result from chromosomal focal amplifications of some oncogenes and less frequently from homozygous deletions of tumor suppressors (Sawey et al., 2011; Guichard et al., 2012; Wang et al., 2013; Totoki et al., 2014; Schulze et al., 2015). Recurrent focal amplifications have been observed for *TERT*, *MET*, and others (Sawey et al., 2011; Guichard et al., 2012; Wang et al., 2013; Totoki et al., 2014; Schulze et al., 2015), while recurrent homozygous deletions have been reported for *CDKN2A, ARID1A*, and others (**Table 4**; Guichard et al., 2012; Wang et al., 2013; Totoki et al., 2014; Schulze et al., 2015).

Recurrent Somatic Mutations

Telomere Maintenance

The *TERT* gene encodes a catalytic subunit of telomerase that maintains genomic integrity. *TERT* expression is repressed in somatic cells, but not in proliferative cells in self-renewing tissues and cancers. Somatic mutations in the *TERT* promoter are found across multiple cancer types. Immortality associated with cancer cells has been attributed to telomerase over-expression. *TERT* promoter mutations create a potential binding site for E-twenty-six/ternary complex factors (ETS/TCF) transcription factors and are associated with increased promoter activity, increased expression of *TERT* and increased telomerase activity (Heidenreich et al., 2014; Bell et al., 2015; Borah et al., 2015).

TERT promoter mutations are the most frequent somatic genetic alterations observed in HCC, with an overall prevalence of approximately 60%, with ranges from 30 to 40% for HBV-related HCC to 60 to 80% for HCV-related HCC (Nault et al., 2013; Totoki et al., 2014; Fujimoto et al., 2015; Schulze et al., 2015; Kawai-Kitahata et al., 2016; Yang et al., 2016a). HCC with HCV infection and alcohol intake more often harbor TERT promoter mutations than those with HBV infection (Nault et al., 2013). The lower rate of *TERT* promoter mutations in HBV-related HCC could be partially explained by the frequent insertion of HBV DNA in the *TERT* promoter serving as additional mechanism inducing telomerase transcription (Nault et al., 2013).

Somatic *TERT* promoter mutations may represent an early event in liver carcinogenesis in a setting of cirrhosis leading to malignant transformation (Nault et al., 2013, 2014). Mutations in the *TERT* promoter but not in classical liver cancer driver genes such as *CTNNB1* and *TP53* can be found in cirrhotic preneoplasia (Nault et al., 2013). *TERT* promoter mutations have been identified in 6% of low-grade dysplastic nodules, 19% of high-grade dysplastic nodules, 61% of early hepatocellular carcinomas, and 42% of small and progressed HCC, correlating with step-wise development of hepatocarcinogenesis. *TERT* promoter mutations may have utility as a marker for high risk of malignant transformation in cirrhotic tissue (Nault et al., 2014). *TERT* promoter mutations were more frequent in those with lower AFP serum levels, usually in small tumors (Nault et al., 2013; Yang et al., 2016a). Thus, detection of *TERT* promoter

TABLE 4 | Recurrent somatic mutations in HCC tissues.

Pathway	Gene	Frequency of Mutations				References
		HBV-HCC	HCV-HCC	Alcoholic HCC	Combined etiologies*	
Telomere maintenance	*TERT*	31%∼43%	64%∼80%	68%∼83%	31%∼65%	Nault et al., 2013; Totoki et al., 2014; Fujimoto et al., 2015; Schulze et al., 2015; Kawai-Kitahata et al., 2016; Yang Z. et al., 2016
Wnt/beta-catenin pathway	*CTNNB1*	10%∼16%	24%∼42%	33%∼50%	11%∼46%	Satoh et al., 2000; Li et al., 2011; Fujimoto et al., 2012; Guichard et al., 2012; Cleary et al., 2013; Kan et al., 2013; Ahn et al., 2014; Totoki et al., 2014; Schulze et al., 2015; Kawai-Kitahata et al., 2016; Rebouissou et al., 2016; Yao S. et al., 2016
	AXIN1	8%			2%∼21%	Satoh et al., 2000; Guichard et al., 2012; Kan et al., 2013; Ahn et al., 2014; Totoki et al., 2014; Schulze et al., 2015; Kawai-Kitahata et al., 2016
Cell cycle	*TP53*	32%∼68%	12%∼23%	25%	13%∼52%	Li et al., 2011; Woo et al., 2011; Fujimoto et al., 2012; Guichard et al., 2012; Huang et al., 2012; Cleary et al., 2013; Kan et al., 2013; Nault et al., 2013; Ahn et al., 2014; Meng et al., 2014; Totoki et al., 2014; Schulze et al., 2015; Kawai-Kitahata et al., 2016; Yao S. et al., 2016
	IRF2				2%∼5%	Guichard et al., 2012; Ahn et al., 2014
	RB1	10%			3%∼10%	Kan et al., 2013; Ahn et al., 2014; Totoki et al., 2014; Yao S. et al., 2016
	CCND1	5%			0%∼6%	Ahn et al., 2014; Totoki et al., 2014; Schulze et al., 2015
	CDKN2A	5%			2%∼8%	Guichard et al., 2012; Ahn et al., 2014; Totoki et al., 2014; Schulze et al., 2015; Kawai-Kitahata et al., 2016
Epigenetic modifier	*ARID1A*	7%			1%∼17%	Fujimoto et al., 2012; Guichard et al., 2012; Huang et al., 2012; Cleary et al., 2013; Ahn et al., 2014; Totoki et al., 2014; Schulze et al., 2015; Kawai-Kitahata et al., 2016; Yao S. et al., 2016
	ARID2	2%∼3%	14%∼18%		1%∼18%	Li et al., 2011; Fujimoto et al., 2012, 2015; Guichard et al., 2012; Huang et al., 2012; Cleary et al., 2013; Ahn et al., 2014; Totoki et al., 2014; Schulze et al., 2015; Kawai-Kitahata et al., 2016; Yao S. et al., 2016
	MLL	4%			2%∼7%	Fujimoto et al., 2012; Cleary et al., 2013; Ahn et al., 2014
	MLL2	5%			5%∼6%	Cleary et al., 2013; Ahn et al., 2014; Schulze et al., 2015
	MLL3	8%			1%∼7%	Fujimoto et al., 2012; Cleary et al., 2013; Ahn et al., 2014; Schulze et al., 2015
	MLL4				3%∼7%	Cleary et al., 2013; Schulze et al., 2015
PI3K/Akt/mTOR and Ras/Raf/MAP kinase pathways	*RPS6KA3*	5%			2%∼10%	Guichard et al., 2012; Ahn et al., 2014; Totoki et al., 2014; Schulze et al., 2015
	PIK3CA				1%∼2%	Guichard et al., 2012; Totoki et al., 2014; Schulze et al., 2015; Kawai-Kitahata et al., 2016
	FGF19	5%			0%∼6%	Ahn et al., 2014; Totoki et al., 2014; Schulze et al., 2015
Stress oxidative pathway	*NFE2L2*				1%∼6%	Guichard et al., 2012; Totoki et al., 2014; Schulze et al., 2015; Kawai-Kitahata et al., 2016
	KEAP1				2%∼8%	Cleary et al., 2013; Totoki et al., 2014; Schulze et al., 2015
JAK/STAT pathway	*JAK1*				1%∼9%	Kan et al., 2013; Ahn et al., 2014; Totoki et al., 2014

(Continued)

TABLE 4 | Continued

Pathway	Gene	Frequency of Mutations				References
		HBV-HCC	HCV-HCC	Alcoholic HCC	Combined Etiologies*	
Somatic copy number alteration	**Gene**					
Recurrent focal amplifications	*TERT*, *FGF19*, *CCND1*, *MET, MTDH*, *BCL9*, *VEGFA*					Sawey et al., 2011; Guichard et al., 2012; Wang et al., 2013; Totoki et al., 2014; Schulze et al., 2015
Homozygous deletions	*CDKN2A, CDKN2B*, *CDKN2B*, *AXIN1*, *IRF2*, *ARID1A*, *RPS6KA3*					Guichard et al., 2012; Wang et al., 2013; Totoki et al., 2014; Schulze et al., 2015

HBV, hepatitis B virus; HCC, hepatocellular carcinoma; HCV, hepatitis C virus.

mutations may aid in diagnosis of atypical or early HCC cases with lower serum AFP levels.

Wnt/β-Catenin Pathway

Catenin beta 1 (*CTNNB1*), a key signaling transducer in the Wnt pathway, regulates cellular proliferation and differentiation. *CTNNB1* is the most frequently mutated oncogene in HCCs (10–50%) (Satoh et al., 2000; Li et al., 2011; Fujimoto et al., 2012; Guichard et al., 2012; Cleary et al., 2013; Kan et al., 2013; Ahn et al., 2014; Totoki et al., 2014; Schulze et al., 2015; Kawai-Kitahata et al., 2016; Rebouissou et al., 2016; Yao S. et al., 2016). Most mutated residues are in or near phosphorylation sites and prevent phosphorylation-dependent ubiquitination, resulting in abnormal accumulation of β-catenin protein that in turn causes abnormal expression of cell proliferation genes (Klaus and Birchmeier, 2008). Like *TERT* promoter mutations, *CTNNB1* mutation frequency varies in HCC cases by etiological factors, with ranges from 10 to 16% in HBV-related HCC, 20 to 40% in HCV-related HCC, and 30 to 50% in alcoholic HCC (Li et al., 2011; Ahn et al., 2014; Kawai-Kitahata et al., 2016; Rebouissou et al., 2016). *CTNNB1* mutations were associated with lower AFP levels (Rebouissou et al., 2016), indicating detection of *CTNNB1* mutations may also have diagnostic value for HCC with atypical presentation.

AXIN1 is the second most frequently mutated gene in the Wnt pathway (occurring in 2–20% of HCC cases) (Satoh et al., 2000; Guichard et al., 2012; Kan et al., 2013; Ahn et al., 2014; Totoki et al., 2014; Schulze et al., 2015; Kawai-Kitahata et al., 2016). Axin may be an effective therapeutic target for suppressing growth of HCC tumors (Satoh et al., 2000).

p53/Cell Cycle Control Pathway

As a tumor suppressor and transcription factor, TP53 can both activate and repress gene expression to initiate cell-cycle arrest, apoptosis, and senescence in response to cellular stresses, including DNA damage, oncogene activation, and hypoxia, to maintain the integrity of the genome (Lee, 2015). *TP53* mutations occurred in approximately 10% to 50% of HCC cases (Li et al., 2011; Woo et al., 2011; Fujimoto et al., 2012; Guichard et al., 2012; Huang et al., 2012; Cleary et al., 2013; Kan et al., 2013; Nault et al., 2013; Ahn et al., 2014; Meng et al., 2014; Totoki et al., 2014; Schulze et al., 2015; Kawai-Kitahata et al., 2016; Yao S. et al., 2016). The mutation spectrum of *TP53* varies depending on etiological and environmental factors. The *TP53* R249S hotspot mutation is particularly associated with aflatoxin B1 exposure, which interacts synergistically with HBV infection to promote hepatocarcinogenesis (Kew, 2003; Hussain et al., 2007). *TP53* mutations occurred more frequently in HBV-related HCC (∼30 to 70%) than in non-HBV HCC (Li et al., 2011; Ahn et al., 2014; Kawai-Kitahata et al., 2016). *TP53* mutation is also associated with tumor histological grade. HCCs with a high histological grade have a higher *TP53* mutation rate (40%) than those with a low histological grades (10%) (Ahn et al., 2014).

Abrogation of the *IRF2* (encoding interferon regulatory factor 2), occurring in ∼2–5% of HCCs, also leads to impaired TP53 function (Guichard et al., 2012).

Somatic mutations in HCC tumors have also been observed in other cell cycle genes, including the tumor suppressor genes *RB1* (∼3–10%) (Kan et al., 2013; Ahn et al., 2014; Totoki et al., 2014; Yao S. et al., 2016) and *CDKN2A* (2∼8%) (Guichard et al., 2012; Ahn et al., 2014; Totoki et al., 2014; Schulze et al., 2015; Kawai-Kitahata et al., 2016).

Epigenetic Modification

Alterations of chromatin regulator genes are recurrently observed in HCC cases. Of 27 HCC tumors with WGS, 52% had somatic mutations or indels in at least one chromatin regulator genes (e.g., *ARID1A*, *ARID1B*, *ARID2*, *MLL*, and *MLL3*; Fujimoto et al., 2012). ARID1A and ARID2 are chromatin remodeling factors, which regulate DNA accessibility to transcription, DNA replication, and repair machineries. *ARID2* mutations were significantly enriched in HCV-associated HCC (18%) compared with HBV-related HCC (2%) (Li et al., 2011). *MLL*, *MLL2*, *MLL3*, and *MLL4* genes encode H3K4 methyltransferases that regulate methylation, acetylation and remodeling of nucleosomes. The mutation rates at these genes are presented in (**Table 4**; Li et al., 2011; Fujimoto et al., 2012, 2015; Guichard et al., 2012; Huang et al., 2012; Cleary et al., 2013; Ahn et al., 2014; Totoki et al., 2014; Schulze et al., 2015; Kawai-Kitahata et al., 2016; Yao S. et al., 2016). Less common mutations (<10%) were detected in genes involved in PI3K/Akt/mTOR and Ras/Raf/MAP pathways, stress

oxidative pathway (Guichard et al., 2012; Cleary et al., 2013; Totoki et al., 2014; Schulze et al., 2015; Kawai-Kitahata et al., 2016) and JAK/STAT pathway (Kan et al., 2013; Nault et al., 2013; Ahn et al., 2014; Totoki et al., 2014) (**Table 4**).

Relationships Between Mutated Genes

Certain subsets of altered genes share the same pathways or interact, contributing to the complexity and heterogeneity of hepatocarcinogenesis. Activated mutations of *CTNNB1* are significantly associated with mutations in the *TERT* promoter (Nault et al., 2013; Totoki et al., 2014). It has been proposed that *TERT* might be a direct target of *CTNNB1* (Hoffmeyer et al., 2012; Zhang et al., 2012). Alterations in *RPS6KA3* are frequently associated with *AXIN1* mutations, suggesting cooperation between RPS6KA3 inactivation and Wnt/β-catenin activation in tumorigenesis (Guichard et al., 2012). On the other hand, a number of mutations appear to be mutually exclusive and rarely appear together in the same tumor, such as *CTNNB1* mutations with *TP53* mutations (Guichard et al., 2012; Ahn et al., 2014) and *AXIN1* mutations with *CTNNB1* mutations (Satoh et al., 2000). *ARID1A*/*ARID2* mutations are negatively associated with mutations in *TP53* (Lee, 2015). The consequences of network interactions between driver mutations may offer deeper insight into tumorigenesis.

HCC GENETICS AND PRECISION MEDICINE

Somatic Mutations and Therapeutic Targets of HCC

Targeted therapy based on genomic alterations is a core tenet of precision treatment. Exome sequencing analysis of 243 liver tumors found that 28% of patients harbor at least one alteration potentially targetable by an FDA-approved drug, and 86% harbored a mutation targetable by a drug studied in phase I to phase III clinical trials (Schulze et al., 2015). β-catenin reduction in *CTNNB1*-mutated HCCs in a murine model led to complete tumor response, showing a clear benefit of therapeutic targeting of this molecule (Delgado et al., 2015). Adenovirus mediated gene transfer of wild-type *AXIN1* induced apoptosis in hepatocellular cancer cells that had accumulated β-catenin as a consequence of mutations in *APC*, *CTNNB1,* or *AXIN1* genes, suggesting that AXIN1 may be an effective therapeutic molecule for suppressing HCC growth (Satoh et al., 2000).

Somatic Mutations and HCC Prognosis

Somatic mutations of driver genes may be predictive of HCC prognosis. In a study of over 300 HCC Chinese patients, *TP53* hotspot mutations (R249S and V157F were strongly associated with decreased overall survival, indicating that these mutations can be used as prognostic markers in HCC in patients at risk for high aflatoxin exposures (Woo et al., 2011). Mechanistically, a synergistic interaction of aflatoxin B1 induced *TP53* mutations together with HBV chronic inflammation may advance the development of HCC. In a multivariate analysis of 231 Korean HCC patients, the *RB1* somatic mutation was the only independent prognostic factor for reduced cancer-specific survival and accelerated recurrence (Ahn et al., 2014). In a cohort of resected HCCs, *CDKN2A* inactivation was associated with poor prognosis (Schulze et al., 2015). These predictive and prognostic molecular markers may have clinical utility for personalized treatment plans.

CONCLUSION, CHALLENGES AND FUTURE DIRECTIONS

The development of HCC is multifactorial with viral, host and environmental factors contributing to chronic inflammation, cirrhosis and ultimately, hepatocarcinogenesis (**Figure 1**). Interplay between host germline variants, persistent high HBV viral load, viral genotypes and mutations, HBV integration into host chromosomes, the oncogenic potential of the HBx protein, and the occurrence of somatic cancer driver mutations may contribute independently or jointly to the oncogenesis of HBV-related HCC (**Figure 1**). We hope that eventually genetic profiling of the virus and host will identify the individuals who are at higher risk of HCC and those who will benefit most from HCC treatment options. Since early HCC is largely asymptomatic and biopsies are rarely performed; there is a paucity of pre-tumor and early-stage tumor tissue available, a major impediment for genetic interrogation. This is in contrast to breast, colon, and prostate cancers where biopsies are standard of care for patients with abnormal findings during routine screening. Validated genetic biomarkers would have utility for early diagnosis, molecular classification of tumors, and prognostics as well as identify new targets for drug interventions. With the advent of ever larger HCC cohorts, denser, population-specific genotyping arrays, and next generation whole exome/genome sequencing of HCC family clusters, it may be possible to provide earlier diagnosis of HCC and to develop bespoke treatment for persons with HCC to improve outcomes.

AUTHOR CONTRIBUTIONS

PA and CW: conceived and wrote the paper; JX: wrote and revision of the manuscript; YY: revision of the manuscript.

FUNDING

This project has been funded in whole or in part with federal funds from the National Cancer Institute, National Institutes of health, under contract HHSN26120080001E. This Research was supported in part by the Intramural Research Program of the NIH, National Cancer Institute, Center for Cancer Research. The content of this publication does not necessarily reflect the views or policies of the Department of Health and Human Services, nor does mention of trade names, commercial products, or organizations imply endorsement by the U.S. Government.

ACKNOWLEDGMENTS

We thank George Nelson and Victor David for proofreading.

REFERENCES

Ahn, S. M., Jang, S. J., Shim, J. H., Kim, D., Hong, S. M., Sung, C. O., et al. (2014). Genomic portrait of resectable hepatocellular carcinomas: implications of RB1 and FGF19 aberrations for patient stratification. *Hepatology* 60, 1972–1982. doi: 10.1002/hep.27198

Baptista, M., Kramvis, A., and Kew, M. C. (1999). High prevalence of 1762(T) 1764(A) mutations in the basic core promoter of hepatitis B virus isolated from black Africans with hepatocellular carcinoma compared with asymptomatic carriers. *Hepatology* 29, 946–953. doi: 10.1002/hep.510290336

Beasley, R. P., Hwang, L. Y., Lin, C. C., and Chien, C. S. (1981). Hepatocellular carcinoma and hepatitis B virus. A prospective study of 22 707 men in Taiwan. *Lancet* 2, 1129–1133.

Bell, R. J., Rube, H. T., Kreig, A., Mancini, A., Fouse, S. D., Nagarajan, R. P., et al. (2015). The transcription factor GABP selectively binds and activates the mutant TERT promoter in cancer. *Science* 348, 1036–1039. doi: 10.1126/science.aab0015

Block, T. M., Guo, H., and Guo, J. T. (2007). Molecular virology of hepatitis B virus for clinicians. *Clin. Liver Dis.* 11, 685–706. doi: 10.1016/j.cld.2007.08.002

Borah, S., Xi, L., Zaug, A. J., Powell, N. M., Dancik, G. M., Cohen, S. B., et al. (2015). Cancer. TERT promoter mutations and telomerase reactivation in urothelial cancer. *Science* 347, 1006–1010. doi: 10.1126/science.1260200

Bozic, I., Antal, T., Ohtsuki, H., Carter, H., Kim, D., Chen, S., et al. (2010). Accumulation of driver and passenger mutations during tumor progression. *Proc. Natl. Acad. Sci. U.S.A.* 107, 18545–18550. doi: 10.1073/pnas.1010978107

Brennan, P., Hainaut, P., and Boffetta, P. (2011). Genetics of lung-cancer susceptibility. *Lancet Oncol.* 12, 399–408. doi: 10.1016/S1470-2045(10)70126-1

Bruix, J., Reig, M., and Sherman, M. (2016). Evidence-based diagnosis, staging, and treatment of patients with Hepatocellular Carcinoma. *Gastroenterology* 150, 835–853. doi: 10.1053/j.gastro.2015.12.041

Bruix, J., Sherman, M., and American Association for the Study of Liver, D. (2011). Management of hepatocellular carcinoma: an update. *Hepatology* 53, 1020–1022. doi: 10.1002/hep.24199

Buckwold, V. E., Xu, Z., Chen, M., Yen, T. S., and Ou, J. H. (1996). Effects of a naturally occurring mutation in the hepatitis B virus basal core promoter on precore gene expression and viral replication. *J. Virol.* 70, 5845–5851.

Budhu, A., and Wang, X. W. (2011). Power play: scoring our goals for liver cancer with better GWAS study design. *J. Hepatol.* 54, 823–824. doi: 10.1016/j.jhep.2010.10.035

Chan, H. L., Hui, A. Y., Wong, M. L., Tse, A. M., Hung, L. C., Wong, V. W., et al. (2004). Genotype C hepatitis B virus infection is associated with an increased risk of hepatocellular carcinoma. *Gut* 53, 1494–1498. doi: 10.1136/gut.2003.033324

Chan, K. Y., Wong, C. M., Kwan, J. S., Lee, J. M., Cheung, K. W., Yuen, M. F., et al. (2011). Genome-wide association study of hepatocellular carcinoma in Southern Chinese patients with chronic hepatitis B virus infection. *PLoS ONE* 6:e28798. doi: 10.1371/journal.pone.0028798

Chen, C. H., Hung, C. H., Lee, C. M., Hu, T. H., Wang, J. H., Wang, J. C., et al. (2007). Pre-S deletion and complex mutations of hepatitis B virus related to advanced liver disease in HBeAg-negative patients. *Gastroenterology* 133, 1466–1474. doi: 10.1053/j.gastro.2007.09.002

Chen, C. J., Yang, H. I., Su, J., Jen, C. L., You, S. L., Lu, S. N., et al. (2006a). Risk of hepatocellular carcinoma across a biological gradient of serum hepatitis B virus DNA level. *JAMA* 295, 65–73. doi: 10.1001/jama.295.1.65

Chen, G., Lin, W., Shen, F., Iloeje, U. H., London, W. T., and Evans, A. A. (2006b). Past HBV viral load as predictor of mortality and morbidity from HCC and chronic liver disease in a prospective study. *Am. J. Gastroenterol.* 101, 1797–1803. doi: 10.1111/j.1572-0241.2006.00647.x

Ching, L. K., Gounder, P. P., Bulkow, L., Spradling, P. R., Bruce, M. G., Negus, S., et al. (2016). Incidence of hepatocellular carcinoma according to hepatitis B virus genotype in Alaska Native people. *Liver Int.* 36, 1507–1515. doi: 10.1111/liv.13129

Cho, L. Y., Yang, J. J., Ko, K. P., Park, B., Shin, A., Lim, M. K., et al. (2011). Coinfection of hepatitis B and C viruses and risk of hepatocellular carcinoma: systematic review and meta-analysis. *Int. J. Cancer* 128, 176–184. doi: 10.1002/ijc.25321

Chotiyaputta, W., and Lok, A. S. (2009). Hepatitis B virus variants. *Nat. Rev. Gastroenterol. Hepatol.* 6, 453–462. doi: 10.1038/nrgastro.2009.107

Chu, C. J., Hussain, M., and Lok, A. S. (2002). Hepatitis B virus genotype B is associated with earlier HBeAg seroconversion compared with hepatitis B virus genotype C. *Gastroenterology* 122, 1756–1762. doi: 10.1053/gast.2002.33588

Cleary, S. P., Jeck, W. R., Zhao, X., Chen, K., Selitsky, S. R., Savich, G. L., et al. (2013). Identification of driver genes in hepatocellular carcinoma by exome sequencing. *Hepatology* 58, 1693–1702. doi: 10.1002/hep.26540

Delgado, E., Okabe, H., Preziosi, M., Russell, J. O., Alvarado, T. F., Oertel, M., et al. (2015). Complete response of Ctnnb1-mutated tumours to beta-catenin suppression by locked nucleic acid antisense in a mouse hepatocarcinogenesis model. *J. Hepatol.* 62, 380–387. doi: 10.1016/j.jhep.2014.10.021

Di Bisceglie, A. M. (2009). Hepatitis B and hepatocellular carcinoma. *Hepatology* 49, S56–60. doi: 10.1002/hep.22962

Ding, D., Lou, X., Hua, D., Yu, W., Li, L., Wang, J., et al. (2012). Recurrent targeted genes of hepatitis B virus in the liver cancer genomes identified by a next-generation sequencing-based approach. *PLoS Genet.* 8:e1003065. doi: 10.1371/journal.pgen.1003065

EASL (2012). EASL clinical practice guidelines: management of chronic hepatitis B virus infection. *J. Hepatol.* 57, 167–185. doi: 10.1016/j.jhep.2012.02.010

El-Serag, H. B. (2011). Hepatocellular carcinoma. *N. Engl. J. Med.* 365, 1118–1127. doi: 10.1056/NEJMra1001683

Erhardt, A., Blondin, D., Hauck, K., Sagir, A., Kohnle, T., Heintges, T., et al. (2005). Response to interferon alfa is hepatitis B virus genotype dependent: genotype A is more sensitive to interferon than genotype D. *Gut* 54, 1009–1013. doi: 10.1136/gut.2004.060327

Fang, Z. L., Sabin, C. A., Dong, B. Q., Ge, L. Y., Wei, S. C., Chen, Q. Y., et al. (2008). HBV A1762T, G1764A mutations are a valuable biomarker for identifying a subset of male HBsAg carriers at extremely high risk of hepatocellular carcinoma: a prospective study. *Am. J. Gastroenterol.* 103, 2254–2262. doi: 10.1111/j.1572-0241.2008.01974.x

Fang, Z. L., Sabin, C. A., Dong, B. Q., Wei, S. C., Chen, Q. Y., Fang, K. X., et al. (2009). The association of HBV core promoter double mutations (A1762T and G1764A) with viral load differs between HBeAg positive and anti-HBe positive individuals: a longitudinal analysis. *J. Hepatol.* 50, 273–280. doi: 10.1016/j.jhep.2008.09.014

Fattovich, G., Bortolotti, F., and Donato, F. (2008). Natural history of chronic hepatitis B: special emphasis on disease progression and prognostic factors. *J. Hepatol.* 48, 335–352. doi: 10.1016/j.jhep.2007.11.011

Fattovich, G., Giustina, G., Christensen, E., Pantalena, M., Zagni, I., Realdi, G., et al. (2000). Influence of hepatitis delta virus infection on morbidity and mortality in compensated cirrhosis type B. The European Concerted Action on Viral Hepatitis (Eurohep). *Gut* 46, 420–426. doi: 10.1136/gut.46.3.420

Franceschini, N., van Rooij, F. J., Prins, B. P., Feitosa, M. F., Karakas, M., Eckfeldt, J. H., et al. (2012). Discovery and fine mapping of serum protein loci through transethnic meta-analysis. *Am. J. Hum. Genet.* 91, 744–753. doi: 10.1016/j.ajhg.2012.08.021

Fujimoto, A., Furuta, M., Shiraishi, Y., Gotoh, K., Kawakami, Y., Arihiro, K., et al. (2015). Whole-genome mutational landscape of liver cancers displaying biliary phenotype reveals hepatitis impact and molecular diversity. *Nat. Commun.* 6:6120. doi: 10.1038/ncomms7120

Fujimoto, A., Totoki, Y., Abe, T., Boroevich, K. A., Hosoda, F., Nguyen, H. H., et al. (2012). Whole-genome sequencing of liver cancers identifies etiological influences on mutation patterns and recurrent mutations in chromatin regulators. *Nat. Genet.* 44, 760–764. doi: 10.1038/ng.2291

Gounder, P. P., Bulkow, L. R., Snowball, M., Negus, S., Spradling, P. R., and McMahon, B. J. (2016). Hepatocellular Carcinoma Risk in Alaska Native Children and Young Adults with Hepatitis B Virus: Retrospective Cohort Analysis. *J. Pediatr.* 178, 206–213. doi: 10.1016/j.jpeds.2016.08.017

Guichard, C., Amaddeo, G., Imbeaud, S., Ladeiro, Y., Pelletier, L., Maad, I. B., et al. (2012). Integrated analysis of somatic mutations and focal copy-number changes identifies key genes and pathways in hepatocellular carcinoma. *Nat. Genet.* 44, 694–698. doi: 10.1038/ng.2256

Hai, H., Tamori, A., and Kawada, N. (2014). Role of hepatitis B virus DNA integration in human hepatocarcinogenesis. *World J. Gastroenterol.* 20, 6236–6243. doi: 10.3748/wjg.v20.i20.6236

Heidenreich, B., Rachakonda, P. S., Hemminki, K., and Kumar, R. (2014). TERT promoter mutations in cancer development. *Curr. Opin. Genet. Dev.* 24, 30–37. doi: 10.1016/j.gde.2013.11.005

Hoffmeyer, K., Raggioli, A., Rudloff, S., Anton, R., Hierholzer, A., Del Valle, I., et al. (2012). Wnt/beta-catenin signaling regulates telomerase in stem cells and cancer cells. *Science* 336, 1549–1554. doi: 10.1126/science.1218370

Hu, L., Zhai, X., Liu, J., Chu, M., Pan, S., Jiang, J., et al. (2012). Genetic variants in human leukocyte antigen/DP-DQ influence both hepatitis B virus clearance and hepatocellular carcinoma development. *Hepatology* 55, 1426–1431. doi: 10.1002/hep.24799

Huang, J., Deng, Q., Wang, Q., Li, K. Y., Dai, J. H., Li, N., et al. (2012). Exome sequencing of hepatitis B virus-associated hepatocellular carcinoma. *Nat. Genet.* 44, 1117–1121. doi: 10.1038/ng.2391

Hung, I. F., Poon, R. T., Lai, C. L., Fung, J., Fan, S. T., and Yuen, M. F. (2008). Recurrence of hepatitis B-related hepatocellular carcinoma is associated with high viral load at the time of resection. *Am. J. Gastroenterol.* 103, 1663–1673. doi: 10.1111/j.1572-0241.2008.01872.x

Hung, T. H., Liang, C. M., Hsu, C. N., Tai, W. C., Tsai, K. L., Ku, M. K., et al. (2017). Association between complicated liver cirrhosis and the risk of hepatocellular carcinoma in Taiwan. *PLoS ONE* 12:e0181858. doi: 10.1371/journal.pone.0181858

Hussain, S. P., Schwank, J., Staib, F., Wang, X. W., and Harris, C. C. (2007). TP53 mutations and hepatocellular carcinoma: insights into the etiology and pathogenesis of liver cancer. *Oncogene* 26, 2166–2176. doi: 10.1038/sj.onc.1210279

Ji, J., Sundquist, K., and Sundquist, J. (2012). A population-based study of hepatitis D virus as potential risk factor for hepatocellular carcinoma. *J. Natl. Cancer Inst.* 104, 790–792. doi: 10.1093/jnci/djs168

Jiang, D. K., Sun, J., Cao, G., Liu, Y., Lin, D., Gao, Y. Z., et al. (2013). Genetic variants in STAT4 and HLA-DQ genes confer risk of hepatitis B virus-related hepatocellular carcinoma. *Nat. Genet.* 45, 72–75. doi: 10.1038/ng.2483

Jiang, Z., Jhunjhunwala, S., Liu, J., Haverty, P. M., Kennemer, M. I., Guan, Y., et al. (2012). The effects of hepatitis B virus integration into the genomes of hepatocellular carcinoma patients. *Genome Res.* 22, 593–601. doi: 10.1101/gr.133926.111

Kan, Z., Zheng, H., Liu, X., Li, S., Barber, T. D., Gong, Z., et al. (2013). Whole-genome sequencing identifies recurrent mutations in hepatocellular carcinoma. *Genome Res.* 23, 1422–1433. doi: 10.1101/gr.154492.113

Kanwal, F., Kramer, J. R., Ilyas, J., Duan, Z., and El-Serag, H. B. (2014). HCV genotype 3 is associated with an increased risk of cirrhosis and hepatocellular cancer in a national sample of U.S. Veterans with HCV. *Hepatology* 60, 98–105. doi: 10.1002/hep.27095

Kao, J. H., Chen, P. J., Lai, M. Y., and Chen, D. S. (2004). Hepatitis B virus genotypes and spontaneous hepatitis B e antigen seroconversion in Taiwanese hepatitis B carriers. *J. Med. Virol.* 72, 363–369. doi: 10.1002/jmv.10534

Kawai-Kitahata, F., Asahina, Y., Tanaka, S., Kakinuma, S., Murakawa, M., Nitta, S., et al. (2016). Comprehensive analyses of mutations and hepatitis B virus integration in hepatocellular carcinoma with clinicopathological features. *J. Gastroenterol.* 51, 473–486. doi: 10.1007/s00535-015-1126-4

Kew, M. C. (2003). Synergistic interaction between aflatoxin B1 and hepatitis B virus in hepatocarcinogenesis. *Liver Int.* 23, 405–409. doi: 10.1111/j.1478-3231.2003.00869.x

Klaus, A., and Birchmeier, W. (2008). Wnt signalling and its impact on development and cancer. *Nat. Rev. Cancer* 8, 387–398. doi: 10.1038/nrc2389

Kremsdorf, D., Soussan, P., Paterlini-Brechot, P., and Brechot, C. (2006). Hepatitis B virus-related hepatocellular carcinoma: paradigms for viral-related human carcinogenesis. *Oncogene* 25, 3823–3833. doi: 10.1038/sj.onc.1209559

Kushner, T., Serper, M., and Kaplan, D. E. (2015). Delta hepatitis within the Veterans Affairs medical system in the United States: prevalence, risk factors, and outcomes. *J. Hepatol.* 63, 586–592. doi: 10.1016/j.jhep.2015.04.025

Lai, M. W., and Yeh, C. T. (2008). The oncogenic potential of hepatitis B virus rtA181T/ surface truncation mutant. *Antivir. Ther. (Lond).* 13, 875–879.

Lai, M. W., Huang, S. F., Hsu, C. W., Chang, M. H., Liaw, Y. F., and Yeh, C. T. (2009). Identification of nonsense mutations in hepatitis B virus S gene in patients with hepatocellular carcinoma developed after lamivudine therapy. *Antivir. Ther. (Lond).* 14, 249–261.

Lau, C. C., Sun, T., Ching, A. K., He, M., Li, J. W., Wong, A. M., et al. (2014). Viral-human chimeric transcript predisposes risk to liver cancer development and progression. *Cancer Cell* 25, 335–349. doi: 10.1016/j.ccr.2014.01.030

Lee, J. H., Han, K. H., Lee, J. M., Park, J. H., and Kim, H. S. (2011). Impact of hepatitis B virus (HBV) x gene mutations on hepatocellular carcinoma development in chronic HBV infection. *Clin. Vaccine Immunol.* 18, 914–921. doi: 10.1128/CVI.00474-10

Lee, J. S. (2015). The mutational landscape of hepatocellular carcinoma. *Clin. Mol. Hepatol.* 21, 220–229. doi: 10.3350/cmh.2015.21.3.220

Li, M., Zhao, H., Zhang, X., Wood, L. D., Anders, R. A., Choti, M. A., et al. (2011). Inactivating mutations of the chromatin remodeling gene ARID2 in hepatocellular carcinoma. *Nat. Genet.* 43, 828–829. doi: 10.1038/ng.903

Li, N., Lai, E. C., Shi, J., Guo, W. X., Xue, J., Huang, B., et al. (2010). A comparative study of antiviral therapy after resection of hepatocellular carcinoma in the immune-active phase of hepatitis B virus infection. *Ann. Surg. Oncol.* 17, 179–185. doi: 10.1245/s10434-009-0694-z

Li, S., Qian, J., Yang, Y., Zhao, W., Dai, J., Bei, J. X., et al. (2012). GWAS identifies novel susceptibility loci on 6p21.32 and 21q21.3 for hepatocellular carcinoma in chronic hepatitis B virus carriers. *PLoS Genet.* 8:e1002791. doi: 10.1371/journal.pgen.1002791

Li, W., Li, M., Liao, D., Lu, X., Gu, X., Zhang, Q., et al. (2016). Carboxyl-terminal truncated HBx contributes to invasion and metastasis via deregulating metastasis suppressors in hepatocellular carcinoma. *Oncotarget.* 7, 55110–55127. doi: 10.18632/oncotarget.10399

Li, W., Zeng, X., Lee, N. P., Liu, X., Chen, S., Guo, B., et al. (2013). HIVID: an efficient method to detect HBV integration using low coverage sequencing. *Genomics* 102, 338–344. doi: 10.1016/j.ygeno.2013.07.002

Liang, T. J. (2009). Hepatitis B: the virus and disease. *Hepatology* 49, S13–S21. doi: 10.1002/hep.22881

Lin, C. L., and Kao, J. H. (2015). Hepatitis B virus genotypes and variants. *Cold Spring Harb. Perspect. Med.* 5:a021436. doi: 10.1101/cshperspect.a021436

Liu, S., Zhang, H., Gu, C., Yin, J., He, Y., Xie, J., et al. (2009). Associations between hepatitis B virus mutations and the risk of hepatocellular carcinoma: a meta-analysis. *J. Natl. Cancer Inst.* 101, 1066–1082. doi: 10.1093/jnci/djp180

Livingston, S. E., Simonetti, J. P., McMahon, B. J., Bulkow, L. R., Hurlburt, K. J., Homan, C. E., et al. (2007). Hepatitis B virus genotypes in Alaska Native people with hepatocellular carcinoma: preponderance of genotype F. *J. Infect. Dis.* 195, 5–11. doi: 10.1086/509894

Ma, N. F., Lau, S. H., Hu, L., Xie, D., Wu, J., Yang, J., et al. (2008). COOH-terminal truncated HBV X protein plays key role in hepatocarcinogenesis. *Clin. Cancer Res.* 14, 5061–5068. doi: 10.1158/1078-0432.CCR-07-5082

Maldarelli, F., Wu, X., Su, L., Simonetti, F. R., Shao, W., Hill, S., et al. (2014). HIV latency. Specific HIV integration sites are linked to clonal expansion and persistence of infected cells. *Science* 345, 179–183. doi: 10.1126/science.1254194

Meng, X., Franklin, D. A., Dong, J., and Zhang, Y. (2014). MDM2-p53 pathway in hepatocellular carcinoma. *Cancer Res.* 74, 7161–7167. doi: 10.1158/0008-5472.CAN-14-1446

Michailidou, K., Beesley, J., Lindstrom, S., Canisius, S., Dennis, J., Lush, M. J., et al. (2015). Genome-wide association analysis of more than 120,000 individuals identifies 15 new susceptibility loci for breast cancer. *Nat. Genet.* 47, 373–380. doi: 10.1038/ng.3242

Murakami, Y., Saigo, K., Takashima, H., Minami, M., Okanoue, T., Bréchot, C., et al. (2005). Large scaled analysis of hepatitis B virus (HBV) DNA integration in HBV related hepatocellular carcinomas. *Gut* 54, 1162–1168. doi: 10.1136/gut.2004.054452

Muroyama, R., Kato, N., Yoshida, H., Otsuka, M., Moriyama, M., Wang, Y., et al. (2006). Nucleotide change of codon 38 in the X gene of hepatitis B virus genotype C is associated with an increased risk of hepatocellular carcinoma. *J. Hepatol.* 45, 805–812. doi: 10.1016/j.jhep.2006.07.025

Nault, J. C., Calderaro, J., Di Tommaso, L., Balabaud, C., Zafrani, E. S., Bioulac-Sage, P., et al. (2014). Telomerase reverse transcriptase promoter mutation is an early somatic genetic alteration in the transformation of premalignant nodules in hepatocellular carcinoma on cirrhosis. *Hepatology* 60, 1983–1992. doi: 10.1002/hep.27372

Nault, J. C., Mallet, M., Pilati, C., Calderaro, J., Bioulac-Sage, P., Laurent, C., et al. (2013). High frequency of telomerase reverse-transcriptase promoter somatic mutations in hepatocellular carcinoma and preneoplastic lesions. *Nat. Commun.* 4:2218. doi: 10.1038/ncomms3218

Ni, Y.-H., Chang, M.-H., Wang, K.-J., Hsu, H.-Y., Chen, H.-L., Kao, J.-H., et al. (2004). Clinical relevance of hepatitis B virus genotype in children with chronic infection and hepatocellular carcinoma. *Gastroenterology* 127, 1733–1738. doi: 10.1053/j.gastro.2004.09.048

Njei, B., Rotman, Y., Ditah, I., and Lim, J. K. (2015). Emerging trends in hepatocellular carcinoma incidence and mortality. *Hepatology* 61, 191–199. doi: 10.1002/hep.27388

Paraskevis, D., Magiorkinis, G., Magiorkinis, E., Ho, S. Y., Belshaw, R., Allain, J. P., et al. (2013). Dating the origin and dispersal of hepatitis B virus infection in humans and primates. *Hepatology* 57, 908–916. doi: 10.1002/hep.26079

Paterlini-Brechot, P., Saigo, K., Murakami, Y., Chami, M., Gozuacik, D., Mugnier, C., et al. (2003). Hepatitis B virus-related insertional mutagenesis occurs frequently in human liver cancers and recurrently targets human telomerase gene. *Oncogene* 22, 3911–3916. doi: 10.1038/sj.onc.1206492

Pollicino, T., Cacciola, I., Saffioti, F., and Raimondo, G. (2014). Hepatitis B virus PreS/S gene variants: pathobiology and clinical implications. *J. Hepatol.* 61, 408–417. doi: 10.1016/j.jhep.2014.04.041

Raffetti, E., Fattovich, G., and Donato, F. (2016). Incidence of hepatocellular carcinoma in untreated subjects with chronic hepatitis B: a systematic review and meta-analysis. *Liver Int.* 36, 1239–1251. doi: 10.1111/liv.13142

Rebouissou, S., Franconi, A., Calderaro, J., Letouze, E., Imbeaud, S., Pilati, C., et al. (2016). Genotype-phenotype correlation of CTNNB1 mutations reveals different ß-catenin activity associated with liver tumor progression. *Hepatology* 64, 2047–2061. doi: 10.1002/hep.28638

Romeo, R., Del Ninno, E., Rumi, M., Russo, A., Sangiovanni, A., de Franchis, R., et al. (2009). A 28-year study of the course of hepatitis Delta infection: a risk factor for cirrhosis and hepatocellular carcinoma. *Gastroenterology* 136, 1629–1638. doi: 10.1053/j.gastro.2009.01.052

Saigo, K., Yoshida, K., Ikeda, R., Sakamoto, Y., Murakami, Y., Urashima, T., et al. (2008). Integration of hepatitis B virus DNA into the myeloid/lymphoid or mixed-lineage leukemia (MLL4) gene and rearrangements of MLL4 in human hepatocellular carcinoma. *Hum. Mutat.* 29, 703–708. doi: 10.1002/humu.20701

Sanchez-Tapias, J. M., Costa, J., Mas, A., Bruguera, M., and Rodes, J. (2002). Influence of hepatitis B virus genotype on the long-term outcome of chronic hepatitis B in western patients. *Gastroenterology* 123, 1848–1856. doi: 10.1053/gast.2002.37041

Satoh, S., Daigo, Y., Furukawa, Y., Kato, T., Miwa, N., Nishiwaki, T., et al. (2000). AXIN1 mutations in hepatocellular carcinomas, and growth suppression in cancer cells by virus-mediated transfer of AXIN1. *Nat. Genet.* 24, 245–250. doi: 10.1038/73448

Sawai, H., Nishida, N., Mbarek, H., Matsuda, K., Mawatari, Y., Yamaoka, M., et al. (2012). No association for Chinese HBV-related hepatocellular carcinoma susceptibility SNP in other East Asian populations. *BMC Med. Genet.* 13:47. doi: 10.1186/1471-2350-13-47

Sawey, E. T., Chanrion, M., Cai, C., Wu, G., Zhang, J., Zender, L., et al. (2011). Identification of a therapeutic strategy targeting amplified FGF19 in liver cancer by Oncogenomic screening. *Cancer Cell* 19, 347–358. doi: 10.1016/j.ccr.2011.01.040

Schulze, K., Imbeaud, S., Letouzé, E., Alexandrov, L. B., Calderaro, J., Rebouissou, S., et al. (2015). Exome sequencing of hepatocellular carcinomas identifies new mutational signatures and potential therapeutic targets. *Nat. Genet.* 47, 505–511. doi: 10.1038/ng.3252

Shen, F. M., Lee, M. K., Gong, H. M., Cai, X. Q., and King, M. C. (1991). Complex segregation analysis of primary hepatocellular carcinoma in Chinese families: interaction of inherited susceptibility and hepatitis B viral infection. *Am. J. Hum. Genet.* 49, 88–93.

Shi, Y., Wang, J., Wang, Y., Wang, A., Guo, H., Wei, F., et al. (2016). A novel mutant 10Ala/Arg together with mutant 144Ser/Arg of hepatitis B virus X protein involved in hepatitis B virus-related hepatocarcinogenesis in HepG2 cell lines. *Cancer Lett* 371, 285–291. doi: 10.1016/j.canlet.2015.12.008

Sopipong, W., Tangkijvanich, P., Payungporn, S., Posuwan, N., and Poovorawan, Y. (2013). The KIF1B (rs17401966) Single Nucleotide Polymorphism is not Associated with the Development of HBV-related Hepatocellular Carcinoma in Thai Patients. *Asian Pacific J. Cancer Prevent.* 14, 2865–2869. doi: 10.7314/apjcp.2013.14.5.2865

Su, M., Guo, J., and Huang, J. (2017). Meta-analysis of the correlation between the rs17401966 polymorphism in kinesin family member 1B and susceptibility to hepatitis B virus related hepatocellular carcinoma. *Clin. Mol. Hepatol.* 23, 138–146. doi: 10.3350/cmh.2016.0083

Sung, W. K., Zheng, H., Li, S., Chen, R., Liu, X., Li, Y., et al. (2012). Genome-wide survey of recurrent HBV integration in hepatocellular carcinoma. *Nat. Genet.* 44, 765–769. doi: 10.1038/ng.2295

Swanton, C., Soria, J. C., Bardelli, A., Biankin, A., Caldas, C., Chandarlapaty, S., et al. (2016). Consensus on precision medicine for metastatic cancers: a report from the MAP conference. *Ann. Oncol.* 27, 1443–1448. doi: 10.1093/annonc/mdw192

Sze, K. M., Chu, G. K., Lee, J. M., and Ng, I. O. (2013). C-terminal truncated hepatitis B virus x protein is associated with metastasis and enhances invasiveness by C-Jun/matrix metalloproteinase protein 10 activation in hepatocellular carcinoma. *Hepatology* 57, 131–139. doi: 10.1002/hep.25979

Tao, Y., Ruan, J., Yeh, S. H., Lu, X., Wang, Y., Zhai, W., et al. (2011). Rapid growth of a hepatocellular carcinoma and the driving mutations revealed by cell-population genetic analysis of whole-genome data. *Proc. Natl. Acad. Sci. U.S.A.* 108, 12042–12047. doi: 10.1073/pnas.1108715108

Terrault, N. A., Bzowej, N. H., Chang, K. M., Hwang, J. P., Jonas, M. M., Murad, M. H., et al. (2016). AASLD guidelines for treatment of chronic hepatitis B. *Hepatology* 63, 261–283. doi: 10.1002/hep.28156

Thomas, D. L., Thio, C. L., Martin, M. P., Qi, Y., Ge, D., O'Huigin, C., et al. (2009). Genetic variation in IL28B and spontaneous clearance of hepatitis C virus. *Nature* 461, 798–801. doi: 10.1038/nature08463

Toh, S. T., Jin, Y., Liu, L., Wang, J., Babrzadeh, F., Gharizadeh, B., et al. (2013). Deep sequencing of the hepatitis B virus in hepatocellular carcinoma patients reveals enriched integration events, structural alterations and sequence variations. *Carcinogenesis* 34, 787–798. doi: 10.1093/carcin/bgs406

Torre, L. A., Bray, F., Siegel, R. L., Ferlay, J., Lortet-Tieulent, J., and Jemal, A. (2015). Global cancer statistics, 2012. *CA Cancer J. Clin.* 65, 87–108. doi: 10.3322/caac.21262

Totoki, Y., Tatsuno, K., Covington, K. R., Ueda, H., Creighton, C. J., Kato, M., et al. (2014). Trans-ancestry mutational landscape of hepatocellular carcinoma genomes. *Nat. Genet.* 46, 1267–1273. doi: 10.1038/ng.3126

Tseng, T. C., Liu, C. J., Yang, H. C., Su, T. H., Wang, C. C., Chen, C. L., et al. (2012). High levels of hepatitis B surface antigen increase risk of hepatocellular carcinoma in patients with low HBV load. *Gastroenterology* 142, 1140–1149 e1143; quiz e1113–1144. doi: 10.1053/j.gastro.2012.02.007

Tu, H., Bonura, C., Giannini, C., Mouly, H., Soussan, P., Kew, M., et al. (2001). Biological impact of natural COOH-terminal deletions of hepatitis B virus X protein in hepatocellular carcinoma tissues. *Cancer Res.* 61, 7803–7810.

van der Meer, A. J., Veldt, B. J., Feld, J. J., Wedemeyer, H., Dufour, J. F., Lammert, F., et al. (2012). Association between sustained virological response and all-cause mortality among patients with chronic hepatitis C and advanced hepatic fibrosis. *JAMA* 308, 2584–2593. doi: 10.1001/jama.2012.144878

Vutien, P., Trinh, H. N., Nguyen, K., Garcia, R. T., Nguyen, H. A., Levitt, B. S., et al. (2013). Precore and basal core promoter mutations in Asian American patients with hepatitis B e antigen-positive chronic hepatitis B. *Aliment. Pharmacol. Ther.* 37, 464–472. doi: 10.1111/apt.12193

Wang, D., Cai, H., Yu, W. B., and Yu, L. (2014). Identification of hepatitis B virus X gene variants between hepatocellular carcinoma tissues and pericarcinoma liver tissues in Eastern China. *Int. J. Clin. Exp. Pathol.* 7, 5988–5996.

Wang, K., Lim, H. Y., Shi, S., Lee, J., Deng, S., Xie, T., et al. (2013). Genomic landscape of copy number aberrations enables the identification of oncogenic drivers in hepatocellular carcinoma. *Hepatology* 58, 706–717. doi: 10.1002/hep.26402

Wang, Q., Zhang, T., Ye, L., Wang, W., and Zhang, X. (2012). Analysis of hepatitis B virus X gene (HBx) mutants in tissues of patients suffered from hepatocellular carcinoma in China. *Cancer Epidemiol.* 36, 369–374. doi: 10.1016/j.canep.2011.11.006

WHO. (2017). *WHO Global Hepatitis Report 2017*. Available online at: http://www.who.int/hepatitis/publications/global-hepatitis-report2017/en/ [Accessed July 22, 2017].

Woo, H. G., Wang, X. W., Budhu, A., Kim, Y. H., Kwon, S. M., Tang, Z. Y., et al. (2011). Association of TP53 mutations with stem cell-like gene expression and survival of patients with hepatocellular carcinoma. *Gastroenterology* 140, 1063–1070. doi: 10.1053/j.gastro.2010.11.034

Wu, J. C., Huang, Y. H., Chau, G. Y., Su, C. W., Lai, C. R., Lee, P. C., et al. (2009). Risk factors for early and late recurrence in hepatitis B-related hepatocellular carcinoma. *J. Hepatol.* 51, 890–897. doi: 10.1016/j.jhep.2009.07.009

Xu, C., Zhou, W., Wang, Y., and Qiao, L. (2014). Hepatitis B virus-induced hepatocellular carcinoma. *Cancer Lett.* 345, 216–222. doi: 10.1016/j.canlet.2013.08.035

Yang, H. I., Yeh, S. H., Chen, P. J., Iloeje, U. H., Jen, C. L., Su, J., et al. (2008). Associations between hepatitis B virus genotype and mutants and the risk of hepatocellular carcinoma. *J. Natl. Cancer Inst.* 100, 1134–1143. doi: 10.1093/jnci/djn243

Yang, X., Guo, X., Chen, Y., Chen, G., Ma, Y., Huang, K., et al. (2016a). Telomerase reverse transcriptase promoter mutations in hepatitis B virus-associated hepatocellular carcinoma. *Oncotarget* 7, 27838–27847. doi: 10.18632/oncotarget.8539

Yang, X., Yu, D., Ren, Y., Wei, J., Pan, W., Zhou, C., et al. (2016b). Integrative Functional Genomics Implicates EPB41 Dysregulation in Hepatocellular Carcinoma Risk. *Am. J. Hum. Genet.* 99, 275–286. doi: 10.1016/j.ajhg.2016.05.029

Yang, Y., Sun, J. W., Zhao, L. G., Bray, F., and Xiang, Y. B. (2015). Quantitative evaluation of hepatitis B virus mutations and hepatocellular carcinoma risk: a meta-analysis of prospective studies. *Chin. J. Cancer Res.* 27, 497–508. doi: 10.3978/j.issn.1000-9604.2015.10.05

Yang, Z., Zhuang, L., Lu, Y., Xu, Q., Tang, B., and Chen, X. (2016). Naturally occurring basal core promoter A1762T/G1764A dual mutations increase the risk of HBV-related hepatocellular carcinoma: a meta-analysis. *Oncotarget* 7, 12525–12536. doi: 10.18632/oncotarget.7123

Yao, S., Johnson, C., Hu, Q., Yan, L., Liu, B., Ambrosone, C. B., et al. (2016). Differences in somatic mutation landscape of hepatocellular carcinoma in Asian American and European American populations. *Oncotarget*. 7, 40491–40499. doi: 10.18632/oncotarget.9636

Yeh, C. T., Chen, T., Hsu, C. W., Chen, Y. C., Lai, M. W., Liang, K. H., et al. (2011). Emergence of the rtA181T/sW172* mutant increased the risk of hepatoma occurrence in patients with lamivudine-resistant chronic hepatitis B. *BMC Cancer* 11:398. doi: 10.1186/1471-2407-11-398

Yim, H. J., and Lok, A. S. (2006). Natural history of chronic hepatitis B virus infection: what we knew in 1981 and what we know in 2005. *Hepatology* 43(2 Suppl. 1), S173–S181. doi: 10.1002/hep.20956

Yin, J., Li, N., Han, Y., Xue, J., Deng, Y., Shi, J., et al. (2013). Effect of antiviral treatment with nucleotide/nucleoside analogs on postoperative prognosis of hepatitis B virus-related hepatocellular carcinoma: a two-stage longitudinal clinical study. *J. Clin. Oncol.* 31, 3647–3655. doi: 10.1200/JCO.2012.48.5896

Yin, J., Xie, J., Zhang, H., Shen, Q., Han, L., Lu, W., et al. (2010). Significant association of different preS mutations with hepatitis B-related cirrhosis or hepatocellular carcinoma. *J. Gastroenterol.* 45, 1063–1071. doi: 10.1007/s00535-010-0253-1

Yu, M. W., Yeh, S. H., Chen, P. J., Liaw, Y. F., Lin, C. L., Liu, C. J., et al. (2005). Hepatitis B virus genotype and DNA level and hepatocellular carcinoma: a prospective study in men. *J. Natl. Cancer Inst.* 97, 265–272. doi: 10.1093/jnci/dji043

Zhang, H., Zhai, Y., Hu, Z., Wu, C., Qian, J., Jia, W., et al. (2010). Genome-wide association study identifies 1p36.22 as a new susceptibility locus for hepatocellular carcinoma in chronic hepatitis B virus carriers. *Nat. Genet.* 42, 755–758. doi: 10.1038/ng.638

Zhang, Y., Toh, L., Lau, P., and Wang, X. (2012). Human telomerase reverse transcriptase (hTERT) is a novel target of the Wnt/beta-catenin pathway in human cancer. *J. Biol. Chem.* 287, 32494–32511. doi: 10.1074/jbc.M112.368282

Zhao, L. H., Liu, X., Yan, H. X., Li, W. Y., Zeng, X., Yang, Y., et al. (2016). Genomic and oncogenic preference of HBV integration in hepatocellular carcinoma. *Nat. Commun.* 7:12992. doi: 10.1038/ncomms12992

Zhu, R., Mok, M. T., Kang, W., Lau, S. S., Yip, W. K., Chen, Y., et al. (2015). Truncated HBx-dependent silencing of GAS2 promotes hepatocarcinogenesis through deregulation of cell cycle, senescence and p53-mediated apoptosis. *J. Pathol.* 237, 38–49. doi: 10.1002/path.4554

Conflict of Interest Statement: The authors declare that the research was conducted in the absence of any commercial or financial relationships that could be construed as a potential conflict of interest.

Copyright © 2018 An, Xu, Yu and Winkler. This is an open-access article distributed under the terms of the Creative Commons Attribution License (CC BY). The use, distribution or reproduction in other forums is permitted, provided the original author(s) and the copyright owner(s) are credited and that the original publication in this journal is cited, in accordance with accepted academic practice. No use, distribution or reproduction is permitted which does not comply with these terms.

frontiers in Immunology

ORIGINAL RESEARCH
published: 10 August 2018
doi: 10.3389/fimmu.2018.01855

KIR3DL1-Negative CD8 T Cells and KIR3DL1-Negative Natural Killer Cells Contribute to the Advantageous Control of Early Human Immunodeficiency Virus Type 1 Infection in *HLA-B Bw4* Homozygous Individuals

Xin Zhang[1,2†], Xiaofan Lu[1,2†], Christiane Moog[3,4], Lin Yuan[1,2], Zhiying Liu[1,2], Zhen Li[1,2], Wei Xia[1,2], Yuefang Zhou[1,2], Hao Wu[1,2], Tong Zhang[1,2*] and Bin Su[1,2*]*

[1] Center for Infectious Diseases, Beijing You'an Hospital, Capital Medical University, Beijing, China, [2] Beijing Key Laboratory for HIV/AIDS Research, Beijing, China, [3] INSERM U1109, Fédération Hospitalo-Universitaire (FHU) OMICARE, Fédération de Médecine Translationnelle de Strasbourg (FMTS), Université de Strasbourg, Strasbourg, France, [4] Vaccine Research Institute (VRI), Créteil, France

Bw4 homozygosity in human leukocyte antigen class B alleles has been associated with a delayed acquired immunodeficiency syndrome (AIDS) development and better control of human immunodeficiency virus type 1 (HIV-1) viral load (VL) than *Bw6* homozygosity. Efficient CD8 T cell and natural killer (NK) cell functions have been described to restrain HIV-1 replication. However, the role of KIR3DL1 expression on these cells was not assessed in *Bw4*-homozygous participants infected with HIV-1 CRF01_A/E subtype, currently the most prevalent subtype in China. Here, we found that the frequency of KIR3DL1-expressing CD8 T cells of individuals homozygous for *Bw6* [1.53% (0–4.56%)] was associated with a higher VL set point (Spearman $r_s = 0.59$, $P = 0.019$), but this frequency of KIR3DL1$^+$CD8$^+$ T cells [1.37% (0.04–6.14%)] was inversely correlated with CD4 T-cell count in individuals homozygous for *Bw4* ($r_s = -0.59$, $P = 0.011$). Moreover, CD69 and Ki67 were more frequently expressed in KIR3DL1$^-$CD8$^+$ T cells in individuals homozygous for *Bw4* than *Bw6* ($P = 0.046$ for CD69; $P = 0.044$ for Ki67), although these molecules were less frequently expressed in KIR3DL1$^+$CD8$^+$ T cells than in KIR3DL1$^-$CD8$^+$ T cells in both groups (all $P < 0.05$). KIR3DL1$^-$CD8$^+$ T cells have stronger p24-specific CD8$^+$ T-cell responses secreting IFN-γ and CD107a than KIR3DL1$^+$CD8$^+$ T cells in both groups (all $P < 0.05$). Thus, KIR3DL1 expression on CD8 T cells were associated with the loss of multiple functions. Interestingly, CD69$^+$NK cells lacking KIR3DL1 expression were inversely correlated with HIV-1 VL set point in *Bw4*-homozygous individuals ($r_s = -0.52$, $P = 0.035$). Therefore, KIR3DL1$^-$CD8$^+$ T cells with strong early activation and proliferation may, together with KIR3DL1$^-$CD69$^+$NK cells, play a protective role during acute/early HIV infection in individuals homozygous for *Bw4*. These findings highlight the superior functions of KIR3DL1$^-$CD8$^+$ T cells and KIR3DL1$^-$CD69$^+$NK cells being a potential factor contributing to delayed disease progression in the early stages of HIV-1 infection.

Keywords: human immunodeficiency virus type 1, immunity, KIR3DL1 receptor, acute/early infection, *Bw4* homozygotes

OPEN ACCESS

Edited by:
Ping An,
Frederick National Laboratory for Cancer Research (NIH), United States

Reviewed by:
Paul Urquhart Cameron, University of Melbourne, Australia
Eric O. Long, National Institute of Allergy and Infectious Diseases (NIAID), United States
Guido Ferrari, Duke University, United States

***Correspondence:**
Bin Su
binsu.paris7@hotmail.com;
Tong Zhang
zt_doc@163.com;
Hao Wu
whdoc@sina.com

†These authors have contributed equally to this work.

Specialty section:
This article was submitted to Viral Immunology, a section of the journal Frontiers in Immunology

Received: *25 January 2018*
Accepted: *27 July 2018*
Published: *10 August 2018*

Citation:
Zhang X, Lu X, Moog C, Yuan L, Liu Z, Li Z, Xia W, Zhou Y, Wu H, Zhang T and Su B (2018) KIR3DL1-Negative CD8 T Cells and KIR3DL1-Negative Natural Killer Cells Contribute to the Advantageous Control of Early Human Immunodeficiency Virus Type 1 Infection in HLA-B Bw4 Homozygous Individuals. Front. Immunol. 9:1855. doi: 10.3389/fimmu.2018.01855

INTRODUCTION

CD8 T cells and natural killer (NK) cells contribute to the host immune response to human immunodeficiency virus (HIV) infection, but the functions of these cells can be repressed by the inhibitory molecules on their surface. The principal NK cell receptors are natural cytotoxicity receptors, C-type lectin-like receptors, and killer cell immunoglobulin-like receptors (KIRs). Of these molecules, natural cytotoxicity receptors are the most specific NK cell marker. C-type lectin-like receptors and KIRs are also expressed on CD8 T lymphocytes (1–3). The KIR3DL1 receptor, a member of the KIR family, interacts with its ligand to transmit inhibitory signals that suppress the NK cell-mediated lysis of target cells *via* cytoplasmic immunoreceptor tyrosine-based inhibitory motifs (ITIMs). KIR3DL1 recognizes the Bw4 motif on human leukocyte antigen (HLA) class B molecules, which may be classified as Bw4 or Bw6 allotypes, according to the serological epitopes spanning residues 77–83 on the α1-helix of the HLA-I molecule (4).

The CD8 T cells that can be activated to induce anti-HIV-1-specific responses are restricted by HLA antigens, including HLA-B alleles in particular, which play a much greater role in mediating antiviral cytotoxic T-lymphocyte (CTL) responses than HLA-A and HLA-C alleles (5, 6). The *HLA-B*27* and *-B*57* alleles, both of which carry the Bw4 motif, are associated with low HIV-1 viremia and slower progression to acquired immunodeficiency syndrome (AIDS). *HLA-B*44* and *-B*51* have not consistently been shown to play a protective role in HIV-1 infection, and the *HLA-B*05*, *-B*13*, *-B*17*, *-B*37*, and *-B*38* alleles and some other non-protective HLA antigens, also express the Bw4 public motif. Other alleles, such as *HLA-B*07*, *-B*08*, *-B*14*, *-B*35*, *-B*40*, *-B*41*, *-B*53*, *-B*56*, carry the Bw6 motif. The *HLA-B*08*, *-B*35*, *-B*53*, *-B*55*, and *-B*56* alleles are associated with rapid progression to AIDS (7). *HLA-Bw4* homozygosity is associated with a lower risk of HIV transmission (8), better control of HIV-1 viremia and protection against AIDS (9, 10) whereas *HLA-Bw6* homozygosity accelerates HIV-1 disease progression (11, 12), but the precise mechanisms underlying this protection remain unknown.

KIRs, some inhibitory and others activating, are expressed on the surface of a subpopulation of CD8 T cells with a memory and effector phenotype (13). KIR expression is relatively stable on NK cells, and the frequency of KIR-positive CD8 T cells increases with age, mostly due to the accumulation of terminally differentiated T cells (14). KIR-positive CD8 T cells are particularly abundant in participants with HIV-1 (15) or cytomegalovirus (CMV) (16) infection. By contrast, very few HIV-specific, CMV-specific CD8 T cells (17–19) in HIV-1-infected or healthy individuals express KIR receptors, including KIR3DL1. It has, therefore, been suggested that KIR3DL1-positive CD8 T cells function poorly in HIV-1-infected individuals displaying homozygosity for *Bw4*. By contrast, *Bw4* homozygosity may strengthen the functions of KIR3DL1-negative CD8 T cells, resulting in enhanced immune surveillance and playing a predominant role in protection against HIV-1 infection. Besides, KIR3DL1-expressing NK cells can play its role through the ligand of Bw4 motif *via* a known process of NK cell licensing, but it was not uncertain whether NK cells especially KIR3DL1-negative NK cells activity from *HLA-Bw4* homozygous individuals were helpful for restraining HIV-1 replication compared with *HLA-Bw6* homozygous carriers.

In this study, we observed, in the Beijing PRIMO prospective acute HIV-1 infection cohort, early activation, proliferation capacity, and the HIV-1-specific responses of KIR3DL1-positive CD8 T cells were significantly weaker than those of KIR3DL1-negative CD8 T cells in individuals homozygous for *Bw4*. More interestingly, KIR3DL1-negative NK cell activation capacity was negatively related to the viral load (VL) set point and the number of HIV-1-specific KIR3DL1^{-}CD8^{+} T cells responses in individuals homozygous for *Bw4* during acute/early HIV-1 infection. These findings improve our understanding of KIR-mediated control and CD8 T/NK-cell response mechanisms in primary HIV infection.

MATERIALS AND METHODS

Study Subjects

The study subjects were recruited from the Beijing PRIMO clinical cohort, a prospective study cohort of HIV-1-negative men who have sex with men (MSM) designed to identify cases of acute HIV-1 infection at Beijing You'an Hospital, Beijing, China, which has been running since October 2006. The enrolled participants were monitored every 2 months for HIV antibodies, HIV RNA levels, and clinical signs of acute/early infection, as previously described (20). The progression of early HIV-1 infection can be depicted as six discrete stages, as proposed by Fiebig et al. (21). In total, 17 of 24 participants homozygous for *Bw4* and 17 of 40 participants homozygous for *Bw6* were between the Fiebig stage VI and 6 months after infection, all in acute/early stages of HIV infection, and without antiretroviral therapy (ART), were enrolled in this study. These 34 participants were infected with a circulating recombinant form CRF01_A/E subtype based on *pol* sequence (22–24), currently the most prevalent subtype in China, as shown by our results for the Beijing PRIMO cohort (23, 25, 26). The opportunistic infections, tuberculosis, autoimmune diseases, or HBV/HCV co-infection were excluded and this exclusion criteria was displayed in the flow chart (Figure S1 in Supplementary Material). These enrolled participants were followed up for 3 years. During follow-up, we recorded whether CD4 T-cell count fell below 350/μl for three consecutive measurements, the first date of measurement being fixed as the time at which CD4 count dropped below 350/μl. CD4 T-cell count did not subsequently rise above 350/μl before the initiation of ART or remained below 350/μl after the initiation of ART (10). Blood samples were collected, and peripheral blood mononuclear cells (PBMCs) and plasma were isolated and cryopreserved. We enrolled 33 age-matched HIV-1-negative individuals from the MSM population with high-risk behaviors as controls.

HLA Class I Allele Genotyping

Genotypes including those for *HLA-A*, *HLA-B*, and *HLA-C* were determined by sequence-specific primer (SSP)-PCR (at the Weatherall Institute of Molecular Medicine, John Radcliffe Hospital, Oxford University, Oxford, UK). Genomic DNA was

extracted from PBMCs with the QIAamp DNA Blood MiniKit (Qiagen, Valencia, CA, USA) according to the manufacturer's instructions. The Bw4 and Bw6 motifs of the *HLA-B* alleles were identified by SSP-PCR, as previously described (10).

Cell Staining and Flow Cytometry Analysis

Cryopreserved PBMCs were thawed in RPMI 1640 medium (Hyclone, Logan, UT, USA) supplemented with 10% fetal bovine serum (Hyclone), 50 IU/ml penicillin–streptomycin (Hyclone), and 2 mM L-glutamine (Hyclone). They were then stained with fluorescence-conjugated human monoclonal antibodies (mAbs) including APC-CD3 (clone HIT3a; BioLegend, San Diego, CA, USA), PE-CD8 (clone IM0452U; Beckman Coulter, Brea, CA, USA), APC-Cy7-CD69 (clone FN50; BioLegend), Percp-Cy5.5-KIR3DL1 (clone DX9; BioLegend), FITC-CCR7 (clone G043H7; BioLegend), and Pacific blue-CD45RA (clone HI100; BioLegend). The PBMCs were then fixed and permeabilized (Cat. No: 00-5523-00; eBiosciences, San Diego, CA, USA) and were subjected to intracellular staining with PE-Cy7-Ki67 antibodies (cloneKi-67; BioLegend). NK cells were stained with a panel of NK cell-specific antibodies including PE-Cy7-CD3 (clone HIT3a; BioLegend), FITC-CD16 (clone 3G8; BioLegend), PE-CD56 (clone HCD56; BioLegend), and Percp-Cy5.5-KIR3DL1 (clone DX9; BioLegend), APC-Cy7-CD69 (clone FN50; BioLegend). The isotype control mAbs were purchased from the corresponding companies. Cytometer setup and tracking calibration particles were used to ensure that fluorescence intensity measurements were consistent in all experiments. Flow cytometry Comp-Beads kits (BD Bioscience, San Jose, CA, USA) were used for compensation. Gating on forward scatter and side scatter light was used to exclude cell debris from the analysis; forward height and forward area were used to exclude doublet cells, and dead cells were excluded by staining with Live/Dead fixable viability stain 510 (BD Biosciences, San Jose, CA, USA). At least 200,000 PBMCs were acquired with a BD CantoII flow cytometer, as previously described (27, 28), and the data were analyzed with Flowjo Software version 10.0 (Treestar, Ashland, OR, USA). The strategies for the analysis of flow cytometry data are detailed in **Figure 1**.

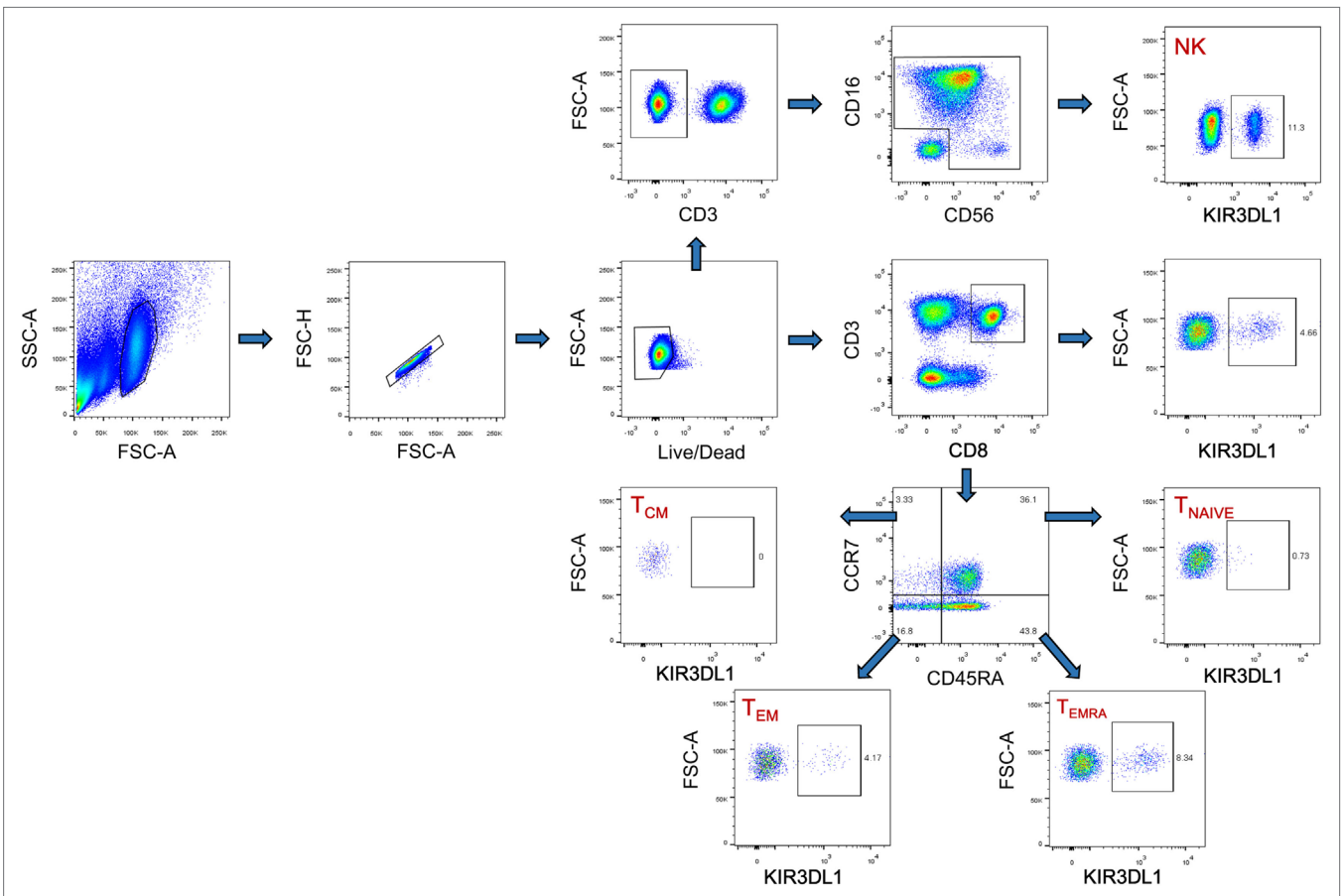

FIGURE 1 | The gating strategy for flow cytometric analysis of KIR3DL1 expressing on CD8 T cells and NK cells. Among all events, forward angle and SSC light gating were gated on lymphocytes and were used to exclude cell debris from the analysis. Forward height and forward area were used to exclude doublet cells, and cells were labeled with Live/Dead fixable viability stain 510, and dead cells were excluded. Then CD3^{+}CD8^{+} T cells, KIR3DL1^{+}CD8^{+} T cells, CD8^{+} T cell subsets (T_{NAIVE}, T_{CM}, T_{EM}, and T_{EMRA}), and KIR3DL1 expressing on different CD8^{+} T cell subsets were gated; CD3^{-} cells, CD16^{+}CD56^{+} NK cells, and KIR3DL1-expressing on NK cells were also analyzed simultaneously. The final analysis was performed with FlowJo software, which generated a graphical output. FSC, forward scatter; SSC, side scatter; NK, natural killer.

Intracellular Cytokine Staining and Cell Degranulation Staining Assays

Thawed and incubated overnight PBMCs from participants infected with subtype CRF01_A/E virus were stimulated with 2 μg/ml pooled CRF01_A/E p24 peptides, 1 μg/ml purified antibodies against CD28/CD49d (Cat. No. 347690; BD Biosciences, San Jose, CA, USA) and PE-anti-CD107a antibody (clone H4A3; BioLegend). After 1 h, 3 μg/ml brefeldin A and 2 μM monensin agents (eBioscience™ 1,000×) were added to the cells, which were incubated for 5 h. Control cells were stimulated with 1 μg/ml purified anti-CD28/CD49d antibody in the absence of peptide. Positive control cells were stimulated with 20 ng/ml phorbol 12-myristate 13-acetate (Sigma-Aldrich, St. Louis, MO, USA) and 1 μg/ml ionomycin (Sigma), and cultured for 6 h at 37°C. The PBMCs were then stained with PE-Cy7-CD3 (clone HIT3a; BioLegend), FITC-CD8 (clone IM0451U; Beckman), APC-CD69 (clone FN50; BioLegend), and Percp-Cy5.5-KIR3DL1 (clone DX9; BioLegend) antibodies for 20 min at room temperature. The PBMCs were fixed and permeabilized with BD FACS™ permeabilizing solution (Cat. No. 340457), and intracellular staining was performed for interferon gamma (IFN-γ) (Brilliant Violet 421™-conjugated; Cat. No. 502532; BioLegend) for 30 min at 4°C. The cells were then analyzed in a BD CantoII flow cytometer as described above.

Detection of IFN-γ-Producing Cells in Enzyme-Linked Immunosorbent Spot (ELISPOT) Assays

Frozen PBMCs from participants infected with HIV-1 subtype CRF01_A/E were thawed and incubated overnight at 37°C under an atmosphere containing 5% CO_2. PBMCs were pulsed with 2 μg/ml CRF01_A/E p24 peptides (same as above) for 18–24 h. The peptides used were 18 amino acids long and overlapped by 10 amino acids (Table S1 in Supplementary Material). 5 μg/ml phytohemagglutinin was used as experimental positive control and 2 μg/ml EBV/Flu/CMV (EFC) peptides were used as quality control (29); negative control was used with RPMI 1640 medium. HIV-1-specific CD8 T-cell responses were measured by quantifying IFN-γ release with an ELISPOT assay (30), using the anti-IFN-γ mAb 1-D1K (Mabtech AB, Nacka, Sweden), the biotinylated anti-IFN-γ mAb 7-B6-1 (Mabtech AB), and streptavidin-alkaline phosphatase conjugate (Mabtech AB). IFN-γ-producing cells were counted with an ELISPOT reader (Antai Yongxin Medical Technology, Beijing, China), and the results are expressed as the number of spot-forming cells per million PBMCs. ELISPOT results were shown in Figure S2 in Supplementary Material. Results were considered positive only if there were more than 50 spot-forming cells/million PBMCs and if there were at least three times as many spot-forming cells than in the negative control as reported in our previous study (31).

CD4 T-Cell Count and VL Measurement

Routine blood CD4 T-cell counts (cells/μl) were measured by four-color flow cytometry with human CD45$^+$, CD3$^+$, CD4$^+$, and CD8$^+$ cell markers (BD Biosciences), on peripheral whole-blood samples from each patient, in FACS lysing solution (BD Biosciences), according to the manufacturer's instructions. Plasma HIV-1 VL (copies/ml of plasma) was quantified by real-time PCR (Abbott Molecular Inc., Des Plaines, IL, USA). This assay has a sensitivity of 40 copies/ml of plasma for viral RNA detection. The VL set point at the very early stage of HIV-1 infection was calculated and reported in our previous study (20).

Statistical Analysis

Data are expressed as mean ± SD. Statistical analysis was performed with GraphPad Prism software version 5.03 (GraphPad Software, San Diego, CA, USA). Differences were analyzed in Student's *t*-tests (unpaired *t*-test for unpaired variables and paired *t*-test for paired variables) or non-parametric Mann–Whitney *U* tests for non-parametric samples. Spearman's rank correlation coefficient, denoted as r_s, is a statistical value that measures the monotonic relationship between two variables. Differences were considered statistically significant if $P < 0.05$ in two-tailed tests. The detailed statistical analysis is described in the figure legends.

RESULTS

Demographics of Individuals in the Acute/Early Phase of HIV-1 Infection

Bw4 homozygosity has been reported to be associated with the control of HIV-1 viremia and protection against AIDS, and with a less marked decline in CD4 T-cell counts in HIV-1-infected individuals (9). We investigated the early effects of KIR3DL1 expression on CD8 T cells in individuals homozygous for the *Bw4* or *Bw6* genotype included during the acute/early phase of HIV-1 infection. The demographic features of these individuals are described in **Table 1**. VL set point was significantly lower in individuals homozygous for *Bw4* than in individuals homozygous for *Bw6* ($P = 0.002$, **Table 1**), whereas CD4 T-cell count appeared to trend higher in individuals homozygous for *Bw4*, although it was not statistically significant ($P = 0.083$, **Table 1**). Furthermore, CD4 T-cell count fell below 350/μl during the first 3 years of HIV-1 infection more frequently in individuals homozygous for *Bw6* than in individuals homozygous for *Bw4* ($P = 0.013$). KIR3DL1 expression and the functions of KIR3DL1$^+$CD8$^+$ and KIR3DL1$^-$CD8$^+$ T cells were investigated, to explore the effects of KIR3DL1 expression on CD8 T cells in the presence and absence of *Bw4* homozygosity.

Higher Percentage of KIR3DL1 Expression on CD8 T_{EMRA} Cells Was Correlated With HIV-1 VL Set Point in *Bw6*-Homozygous Individuals

Figure 1 displayed the flow cytometric gating strategies for the analysis of KIR3DL1 expression on different CD8 T cells and NK cells. In HIV-1-infected individuals, the percentages of KIR3DL1$^+$CD8$^+$ T cells and KIR3DL1$^+$NK cells were 1.49% (0–6.14%) and 12.64% (0–60.6%), respectively, versus 2.03% (0–6.74%) and 14.96% (0–30.18%) in individuals negative for HIV-1 antibody, and this difference was not statistically

TABLE 1 | Demographics of HIV-1-infected individuals.

	Age	VL set point, Log_{10} (copies/ml)	CD4 T-cell count (cells/μl)	*HLA-*B* alleles	VL at 3 years after infection, Log_{10} (copies/ml)	CD4 decline to <350 within 3 years
Bw4/4						
1	34	4.37	374	*B*37, B*51*	4.29	Y
2	23	3.84	1,058	*B*51, B*51*	4.54	N
3	25	2.94	919	*B*57, B*27*	3.10	N
4	26	5.19	117	*B*58, B*51*	ND[a]	Y
5	27	4.43	602	*B*13, B*27*	5.06	N
6	28	3.87	455	*B*13, B*13*	ND[a]	Y
7	47	4.04	561	*B*13, B*13*	4.43	N
8	26	3.62	820	*B*37, B*58*	5.02	Y
9	24	3.41	668	*B*44, B*52*	4.04	N
10	41	3.68	345	*B*27, B*52*	3.94	Y
11	24	2.50	345	*B*44, B*58*	3.75	N
12	22	4.82	546	*B*44, B*38*	5.02	Y
13	21	3.09	505	*B*44, B*57*	3.23	N
14	46	2.81	505	*B*44, B*13*	3.07	N
15	47	3.85	498	*B*44, B*13*	4.77	N
16	34	2.95	933	*B*52, B*52*	3.21	N
17	31	3.94	530	*B*44, B*13*	1.88[a]	N
Mean ± SD	30.9 ± 9.0	3.73 ± 0.73	575 ± 242.2			
Bw6/6						
18	39	4.24	358	*B*15, B*15*	3.65	Y
19	42	4.90	222	*B*15, B*35*	3.71[a]	Y
20	56	4.40	513	*B*08, B*54*	4.39	Y
21	25	3.27	827	*B*39, B*15*	3.82	N
22	24	3.40	303	*B*40, B*67*	4.67	Y
23	27	4.66	899	*B*15, B*67*	4.17	Y
24	38	5.24	258	*B*40, B*15*	5.16	N
25	39	4.30	196	*B*40, B*15*	4.07	Y
26	39	4.04	454	*B*07, B*15*	3.95	N
27	49	5.07	281	*B*08, B*15*	4.84	Y
28	25	4.88	351	*B*46, B*15*	4.35	Y
29	23	4.85	205	*B*55, B*15*	ND[a]	Y
30	36	5.23	554	*B*40, B*46*	5.28	Y
31	34	4.60	516	*B*48, B*40*	5.40	Y
32	27	4.42	770	*B*08, B*45*	4.18	Y
33	54	4.30	308	*B*07, B*35*	NA	–[b]
34	25	4.46	353	*B*07, B*48*	3.15[a]	Y
Mean ± SD	35.4 ± 10.6	4.48 ± 0.56	433 ± 219.6	–	–	
P value	0.195[c]	0.002[d]	0.083[e]		0.183[f]	0.013[g]

[a]*Patients initiating ART.*

[b]*This patient had less than 3 years of follow-up visits after HIV-1 infection.*

The significance of the difference in age[c], VL set point[d], CD4 T-cell count[e], VL at 3 years after infection[f] (patients initiating ART were excluded) between the two groups of individuals was assessed in Student's t-test. Differences were considered statistically significant at $P < 0.05$.

[g]*Fisher's exact test.*

Y, yes; N, no; NA, not applicable; ND, not detected; HIV-1, human immunodeficiency virus type 1; HLA, human leukocyte antigen; ART, antiretroviral therapy; VL, viral load.

significant, as shown in **Figure 2A**. The percentage of CD8 T_{EM} ($CD45RA^{-}CCR7^{-}$, effector memory) cells was significantly higher than that of CD8 T_{EMRA} cells ($CD45RA^{+}CCR7^{-}$, terminally differentiated effector memory) in HIV-1-infected individuals (**Figure 2B**). KIR3DL1 was expressed principally on the cells of the CD8 T_{EMRA} subset, and also on those of the CD8 T_{EM} subset, as shown in **Figure 2C**. The percentage of $KIR3DL1^{+}CD8^{+}$ T_{EM} cells in the total CD8 T-cell population was much lower than that of $KIR3DL1^{+}CD8^{+}$ T_{EMRA} cells ($P < 0.05$), in both HIV-1-positive and HIV-1-negative individuals (**Figure 2D**). Furthermore, the frequency of $KIR3DL1^{+}CD8^{+}$ T cells in *Bw4*-homozygous individuals was similar to that in *Bw6*-homozygous individuals [1.37% (0.04–6.14%) versus 1.53% (0–4.56%)]. The percentage of $KIR3DL1^{+}$NK cells was 12.5% (3.15–37.67%) in individuals homozygous for *Bw4* and 12.76% (0–60.60%) in individuals homozygous for *Bw6*, as shown in **Figure 2E**. KIR3DL1 expression on NK and CD8 T cells was independent of homozygosity for *Bw4* or *Bw6* in *HLA-B* alleles (**Figure 2E**). The percentage of CD8 T_{EM} cells was higher than that of CD8 T_{EMRA} cells in both individuals homozygous for *Bw4* and those homozygous for *Bw6* (**Figure 2F**). KIR3DL1 was more frequently expressed on CD8 T_{EMRA} cells than on CD8 T_{EM} cells and was independent of *HLA-B* locus-specific Bw4 or Bw6 motifs (**Figure 2G**). In individuals homozygous for *Bw6*, $KIR3DL1^{+}CD8^{+}$ T_{EMRA} cells had a higher frequency than $KIR3DL1^{+}CD8^{+}$ T_{EM} cells among total CD8 T cells ($P = 0.027$, **Figure 2H**). In addition, the percentage of

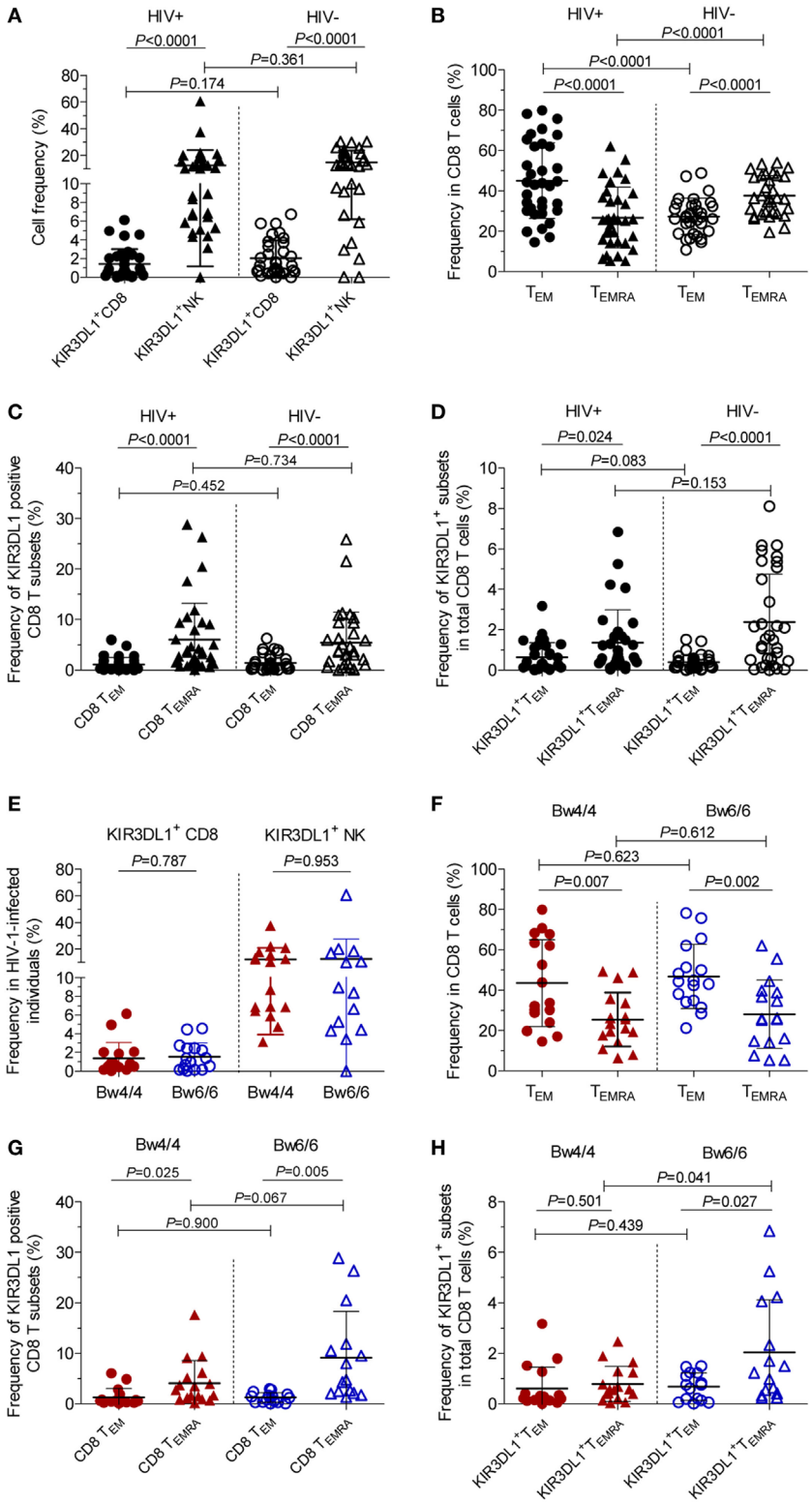

FIGURE 2 | KIR3DL1 expression on natural killer (NK) cells, total CD8 T cells, and CD8 T-cell subsets. Differences in KIR3DL1 expression on total CD8 T cells or NK cells **(A)**, CD8 T_{EM} ($CD45RA^{-}CCR7^{-}$) and CD8 T_{EMRA} ($CD45RA^{+}CCR7^{-}$) subsets from total CD8 T cells **(B,C)**, and $KIR3DL1^{+}$ T_{EM} and $KIR3DL1^{+}$ T_{EMRA} from total CD8 T cells between human immunodeficiency virus type 1 (HIV-1)-positive patients at the acute/early stage and HIV-1-negative individuals **(D)**. KIR3DL1 expression on CD8 T cells or NK cells **(E)**, CD8 T_{EM} and CD8 T_{EMRA} subsets **(F,G)**, and $KIR3DL1^{+}$ T_{EM} and $KIR3DL1^{+}$ T_{EMRA} from total CD8 T cells **(H)** in HIV-1-infected patients homozygous for *Bw4* or *Bw6*. Data are expressed as mean ± SD. The significance of differences was analyzed in unpaired *t*-tests, with $P < 0.05$ considered significant. Bw4/4: *Bw4* homozygotes (red); Bw6/6: *Bw6* homozygotes (blue).

KIR3DL1$^+$CD8$^+$ T_{EMRA} cells among total CD8 T cells was higher in HIV-1-infected individuals homozygous for *Bw6* than in those homozygous for *Bw4* ($P = 0.041$, **Figure 2H**).

KIR3DL1$^+$CD8$^+$ T-cell percentage and VL set point were positively correlated in *Bw6*-homozygous individuals ($r_s = 0.59$, $P = 0.019$, **Figure 3A**), but not in *Bw4*-homozygous individuals ($r_s = 0.12$, $P = 0.646$, **Figure 3A**). Conversely, the inverse association between KIR3DL1$^+$CD8$^+$ T-cell levels and CD4 T-cell count was observed only in individuals homozygous for *Bw4* ($r_s = -0.59$, $P = 0.011$, **Figure 3B**). In individuals homozygous for *Bw6*, the percentage of CD8 T_{EMRA} cells expressing KIR3DL1 was positively correlated with VL set point ($r_s = 0.77$, $P = 0.0008$, **Figure 3C**), but not with CD4 T-cell count (**Figure 3D**).

In addition, a positive association between the percentage of KIR3DL1$^+T_{EMRA}$ cells among total CD8 T cells and HIV-1 VL set point was observed in individuals homozygous for *Bw6* ($r_s = 0.65$, $P = 0.008$, **Figure 3E**), whereas a trend toward a negative relationship between KIR3DL1$^+T_{EMRA}$ levels and CD4 T-cell count was observed in individuals homozygous for *Bw4* ($r_s = -0.44$, $P = 0.074$, **Figure 3F**).

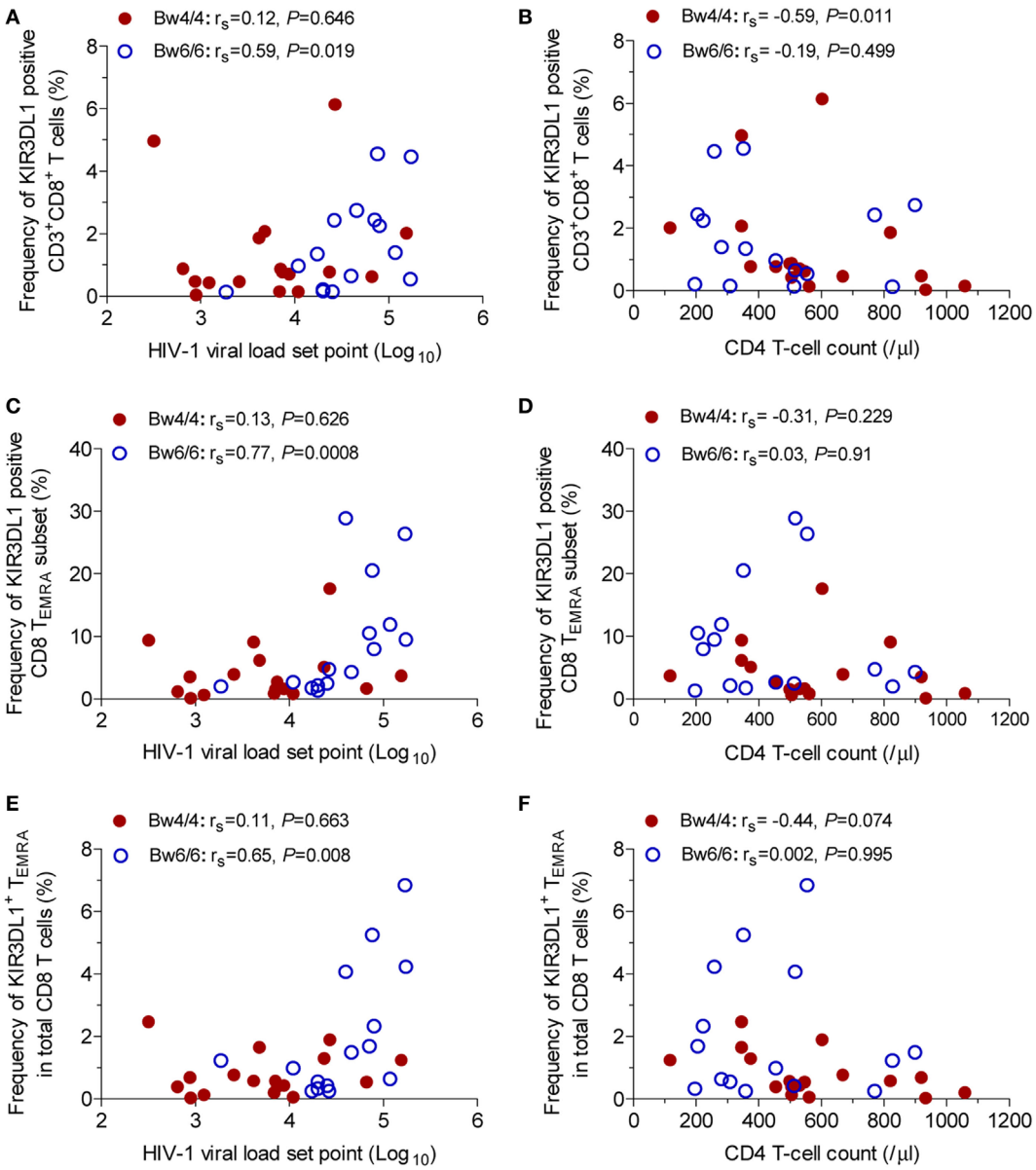

FIGURE 3 | Correlation between KIR3DL1 expression on CD8 T cells with human immunodeficiency virus type 1 (HIV-1) viral load (VL) set point and CD4 T-cell count in individuals with different *HLA-B* serological genotypes. Correlation of KIR3DL1 expression on CD8 T cells with HIV-1 VL set point **(A)** and CD4 T-cell count **(B)**, of the percentage of CD8 T_{EMRA} cells expressing KIR3DL1 with HIV-1 VL set point **(C)** and CD4 T-cell count **(D)**, and of KIR3DL1$^+$ T_{EMRA} levels as a proportion of total CD8 T cells with HIV-1 VL set point **(E)** and CD4 T-cell count **(F)**. Correlations between two variables were analyzed in non-parametric Spearman's rank correlation tests, with $P < 0.05$ considered significant.

Higher Frequencies of KIR3DL1⁻CD69⁺CD8⁺ T Cells and KIR3DL1⁻Ki67⁺CD8⁺ T Cells Were Associated With Homozygosity for *Bw4* in *HLA-B* Alleles

Following infection with HIV-1, immune cells, including CD8 T cells, are activated to fight this pathogen. CD69 is one of the earliest T-cell activation markers detected, due to its rapid appearance on the surface of the plasma membrane after stimulation (32). **Figure 4A** displayed the flow cytometric profiles of KIR3DL1 and CD69 expression on CD8 T cells. In this study, the levels of CD69 expression on CD8 T cells during acute/early HIV-1 infection were significantly higher in *Bw4*-homozygous individuals than in *Bw6*-homozygous individuals ($P = 0.033$, **Figure 4B**). When individuals encounter the HIV-1, their immune cell populations, including CD8 T cells, expand to protect the host against viral infection after activation. Ki67 antigen is required for cell proliferation and used as an excellent marker of cell proliferation (33).

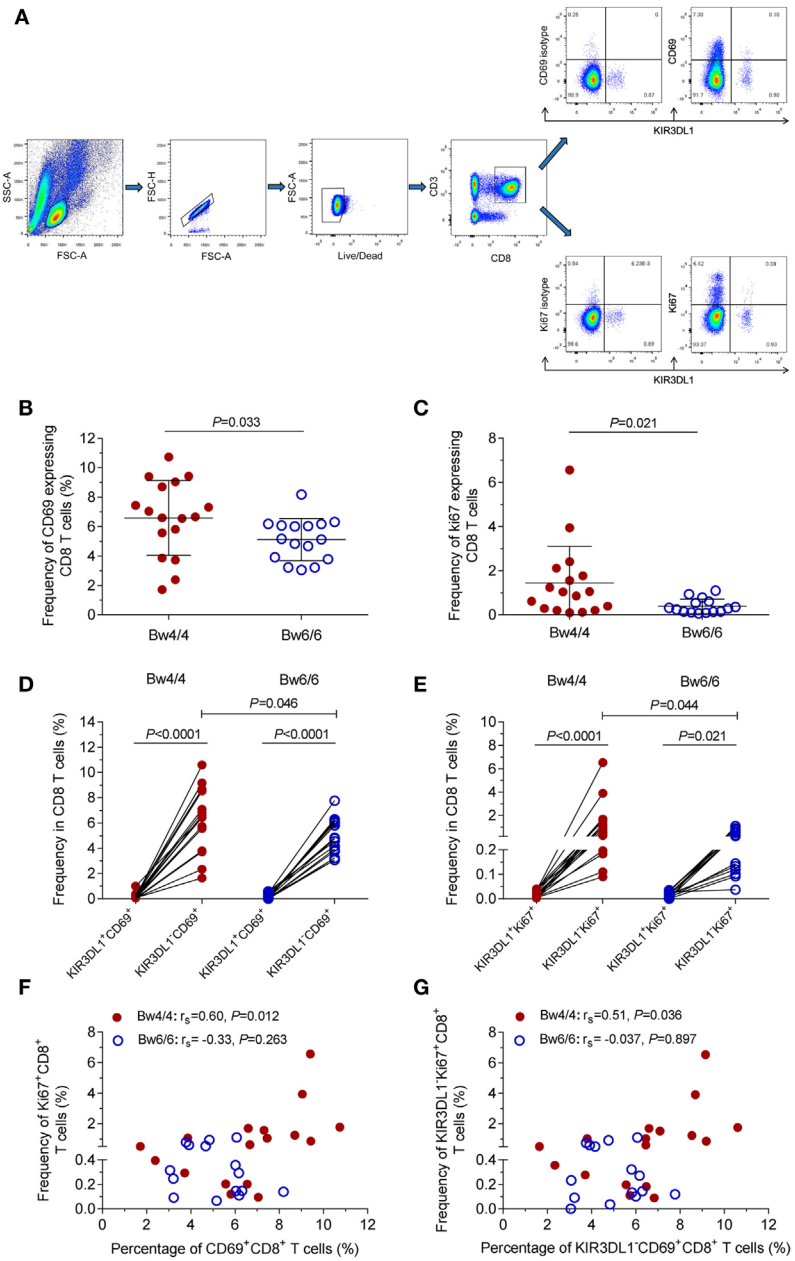

FIGURE 4 | Early activation and proliferation of CD8 T cells in individuals with different *HLA-B* serological genotypes. **(A)** Gating strategy for flow cytometric analysis of CD69 and Ki67 expression on CD8 T cells; **(B)** early activation capacity of CD8 T cells; **(C)** proliferation capacity of CD8 T cells; **(D)** proportion of KIR3DL1⁺CD69⁺ cells and KIR3DL1⁻CD69⁺ cells in total CD8 T cells; **(E)** proportion of KIR3DL1⁺Ki67⁺ cells and KIR3DL1⁻Ki67⁺ cells in total CD8 T cells. Relationship between the early activation and proliferation capacity of total CD8 T cells **(F)** and KIR3DL1⁻CD8⁺ T cells **(G)**. Comparisons between two groups were performed with unpaired Student's *t*-tests, and correlations between two variables were analyzed in Spearman's rank correlation tests, with $P < 0.05$ considered significant.

The proliferative capacity of CD8 T cells was significantly higher in HIV-1-infected individuals homozygous for the *Bw4* allele than in those homozygous for *Bw6* ($P = 0.021$, **Figure 4C**). However, the levels of CD69$^+$CD8$^+$ T cells or Ki67$^+$CD8$^+$ T cells were not associated with HIV-1 VL set point or CD4 T-cell count (data not shown).

In addition, the frequency of KIR3DL1$^+$CD69$^+$CD8$^+$ T cells was much lower than that of KIR3DL1$^-$CD69$^+$CD8$^+$ T cells in HIV-1-infected individuals, regardless of *Bw4* or *Bw6* homozygosity (all $P < 0.0001$, **Figure 4D**). Nevertheless, the proportion of KIR3DL1$^-$CD69$^+$CD8$^+$ T cells in HIV-1-infected individuals homozygous for *Bw4* was significantly higher than that in individuals homozygous for *Bw6* ($P = 0.046$, **Figure 4D**). The percentage of KIR3DL1$^+$Ki67$^+$CD8$^+$ T cells was significantly lower than that of KIR3DL1$^-$Ki67$^+$CD8$^+$ T cells in both individuals homozygous for *Bw4* and in those homozygous for *Bw6* (all $P < 0.05$, **Figure 4E**). By contrast, the proportion of KIR3DL1$^-$Ki67$^+$CD8$^+$ T cells was significantly higher in individuals homozygous for *Bw4* than in those homozygous for *Bw6* ($P = 0.044$, **Figure 4E**). Thus, a minority of KIR3DL1$^+$CD8$^+$ T cells and the majority of KIR3DL1$^-$CD8$^+$ T cells constituted the expanded CD8 T-cell population, and this specificity was not associated with *Bw4* or *Bw6* homozygosity. Here, the levels of KIR3DL1$^-$CD69$^+$CD8$^+$ T cells or KIR3DL1$^-$Ki67$^+$CD8$^+$ T cells were not associated with HIV-1 VL set point or CD4 T-cell count (data not shown). Furthermore, the numbers of CD69$^+$CD8$^+$ T cells and KIR3DL1$^-$CD69$^+$CD8$^+$ T cells were positively correlated with the percentages of Ki67$^+$CD8$^+$ T cells ($r_s = 0.60$, $P = 0.012$, **Figure 4F**) and KIR3DL1$^-$Ki67$^+$CD8$^+$ T cells ($r_s = 0.51$, $P = 0.036$, **Figure 4G**), respectively, in individuals homozygous for *Bw4*.

HIV-1-Specific CD8$^+$ T-Cell Responses Were Stronger for KIR3DL1$^-$CD8$^+$ T Cells

We studied HIV-1-specific cytokine secretion and the degranulation of CD8 T cells in acute/early HIV-1 infection, by stimulating PBMCs with the p24 peptides pool and measuring the amounts of IFN-γ and CD107a produced by CD8 T cells (**Figure 5**). The flow cytometry gating strategy for the analysis of IFN-γ and CD107a secretions by CD8 T cells was displayed in **Figure 5A**. The levels of HIV-1-specific CD8 T cells secreting IFN-γ and CD107a were similar in individuals homozygous for *Bw4* and those homozygous for *Bw6*. The frequencies of KIR3DL1$^+$IFN-γ$^+$ cells and KIR3DL1$^+$CD107a$^+$ cells as a proportion of total CD8 T cells were lower than those of KIR3DL1$^-$IFN-γ$^+$ cells and KIR3DL1$^-$CD107a$^+$ cells, respectively, in HIV-1-infected individuals, regardless of homozygosity for *Bw4* or *Bw6* (all $P < 0.05$, **Figures 5B,C**). Furthermore, the fluorescence intensity obtained for IFN-γ secretion by KIR3DL1$^+$CD8$^+$ T cells was significantly lower than that for secretion by KIR3DL1$^-$CD8$^+$ T cells in these two groups of individuals (all $P < 0.0001$, **Figure 5D**). Likewise, the fluorescence intensity obtained for CD107a degranulation by KIR3DL1$^+$CD8$^+$ T cells was also significantly lower than that for KIR3DL1$^-$CD8$^+$ T cells ($P = 0.0012$ for *Bw4* homozygotes; $P < 0.0001$ for *Bw6* homozygotes, **Figure 5E**) for these two genotypes of individuals. These data suggest that KIR3DL1$^-$CD8$^+$ T cells play a predominant role in HIV-1-specific CD8 T-cell cytokine secretion and degranulation in acute/early HIV-1 infection, independent of *Bw4* homozygosity.

The Levels of HIV-1-Specific KIR3DL1$^-$CD8$^+$ T Cells Secreting IFN-γ Were Inversely Correlated With the Early Activation of KIR3DL1$^-$CD8$^+$ T Cells

CD8 T cells are activated by HIV-1, leading to their production of cytokines, such as IFN-γ, to suppress virus replication. In this study, the levels of HIV-1-specific CD8 T cells secreting IFN-γ were inversely correlated with the early activation of CD8 T cells in individuals homozygous for *Bw4* ($r_s = -0.81$, $P = 0.0007$, Figure S3A in Supplementary Material), but not in those homozygous for *Bw6* ($r_s = -0.23$, $P = 0.385$, Figure S3A in Supplementary Material). Interestingly, the number of HIV-1-specific KIR3DL1$^-$IFN-γ$^+$CD8$^+$ T cells in *Bw4*-homozygous individuals was also inversely correlated with the frequency of KIR3DL1$^-$CD69$^+$CD8$^+$ T cells ($r_s = -0.54$, $P = 0.050$, Figure S3B in Supplementary Material). These findings suggest that higher levels of CD69 expression on CD8 T cells are correlated with lower levels of HIV-1-specific IFN-γ release by CD8 T cells in *Bw4* homozygotes. This was further confirmed by the observation that very few HIV-1-specific CD8$^+$ T cells expressed CD69 (Figure S3C in Supplementary Material). By contrast, CD69$^-$CD8$^+$ T cells could be induced specifically by HIV-1 to produce specific IFN-γ and CD107a (Figure S3C in Supplementary Material).

Similar Strength and Breadth of p24-Specific CD8 T Cell Responses Were Induced in *Bw4*- and *Bw6*-Homozygous Individuals

As the levels of HIV-1-specific CD8 T cells secreting IFN-γ in *Bw4*-homozygous individuals were similar to those in *Bw6*-homozygous individuals, we investigated whether the strength and breadth of HIV-1-specific CD8 T-cell responses induced by individual p24 peptides were similar in the two groups of individuals. The median magnitude of the p24-specific CD8 T-cell responses elicited in individuals homozygous for *Bw4* was 375 (0–3,135) SFCs/10^6 PBMCs, a value similar to the 1,065 (0–3,890) SFCs/10^6 PBMCs in *Bw6*-homozygous individuals ($P = 0.183$, **Figure 6A**). Furthermore, the breadth of the CD8 T-cell responses induced by individual p24 peptides in *Bw4*-homozygous individuals was 1 (range, 0–4), a value tending toward significance to that obtained for *Bw6*-homozygous individuals (2; range: 0–5; $P = 0.067$, **Figure 6B**). The difference in p24 peptide mapping between individuals homozygous for *Bw4* and those homozygous for *Bw6* is shown in **Figure 6C**. The ELISPOT assays confirmed the similar magnitude and breadth of the HIV-1-specific CD8 T-cell responses elicited by individual p24 peptides in individuals homozygous for *Bw4* and individuals homozygous for *Bw6* in the acute/early stage of HIV-1 infection.

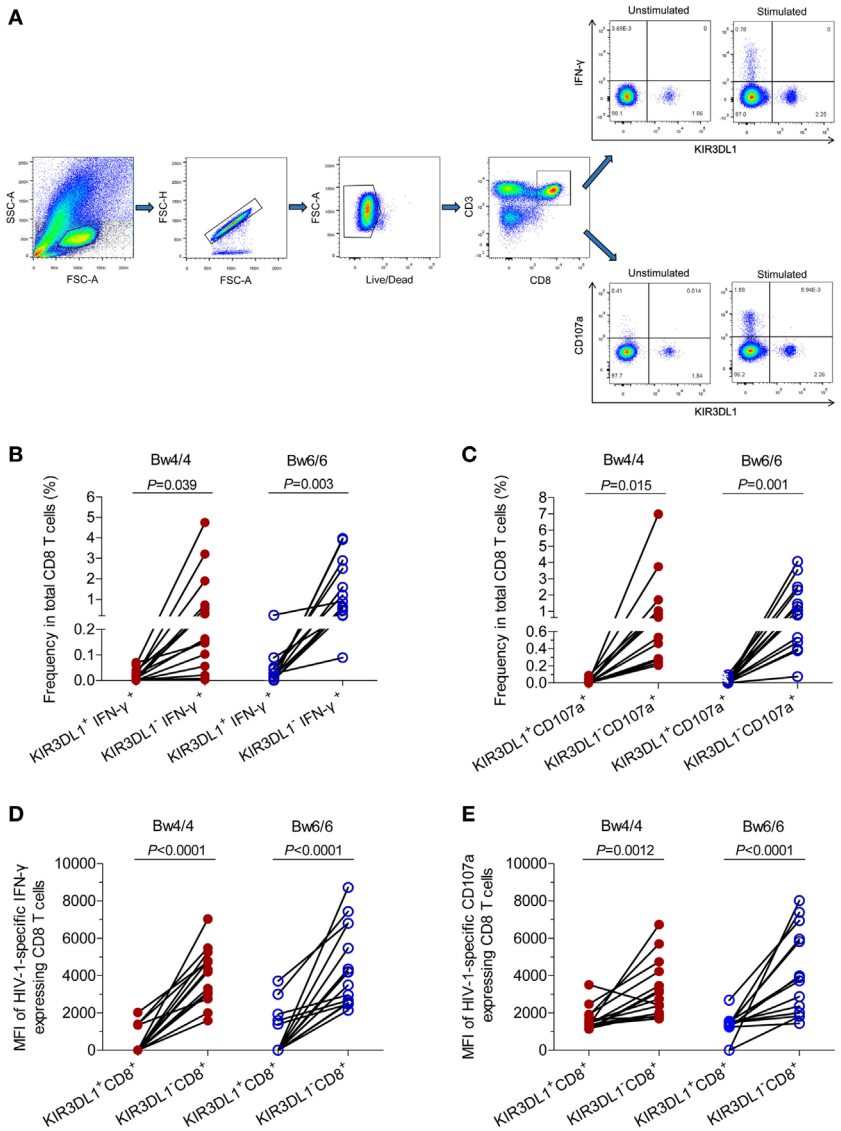

FIGURE 5 | Median fluorescence intensity and levels of human immunodeficiency virus type 1 (HIV-1)-specific IFN-γ and CD107a produced by CD8 T cells, in *Bw4* and *Bw6* homozygotes. **(A)** Gating strategy for flow cytometric analysis of IFN-γ and CD107a expressing in CD8 T cells; **(B)** frequency of KIR3DL1⁺IFN-γ⁺ cells and KIR3DL1⁻IFN-γ⁺ cells among total CD8 T cells stimulated with HIV-1 p24 peptides; **(C)** frequency of KIR3DL1⁺CD107a⁺ and KIR3DL1⁻CD107a⁺ cells among total CD8 T cells stimulated with HIV-1 p24 peptides. The difference in median fluorescence intensity for the HIV-1-specific IFN-γ **(D)** and CD107a **(E)** released by KIR3DL1⁺CD8⁺ and KIR3DL1⁻CD8⁺ T cells. The Bw4/4 and Bw6/6 motifs are shown in red and blue, respectively. Paired Student's *t*-tests were used to compare groups, with $P < 0.05$ considered significant.

KIR3DL1⁻NK Cell Activation and HIV-1-Specific KIR3DL1⁻CD8 T-Cell Responses Were Inversely Correlated With HIV-1 VL Set Point in *Bw4*-Homozygous Individuals

As no advantageous effect of the p24-specific CD8 T-cell responses induced in *Bw4*-homozygous individuals was observed (**Figures 5** and **6**), we hypothesized that the inhibition of viral replication in these individuals might be due to an increase in NK cell activity. The compound expression profiles of KIR3DL1 and CD69 molecules on NK cells showed that CD69 predominantly expressed on KIR3DL1⁻NK cells (**Figure 7A**). The early activation levels for both total NK cells and KIR3DL1⁻NK cells did not differ between *Bw4*- and *Bw6*-homozygous individuals ($P > 0.05$, **Figure 7B**). However, the activation capacity of total NK cells ($r_s = -0.53$, $P = 0.030$, **Figure 7C**) and KIR3DL1⁻NK cells ($r_s = -0.52$, $P = 0.035$, **Figure 7D**) was, respectively, inversely related to HIV-1 VL set point in *Bw4*-homozygous individuals, but not in *Bw6*-homozygous individuals. Interestingly, this NK cell activation capacity was also negatively related to the levels of HIV-1 VL at 3 years after infection in *Bw4*-homozygous individuals ($r_s = -0.63$, $P = 0.016$ for total NK cells; $r_s = -0.54$, $P = 0.047$

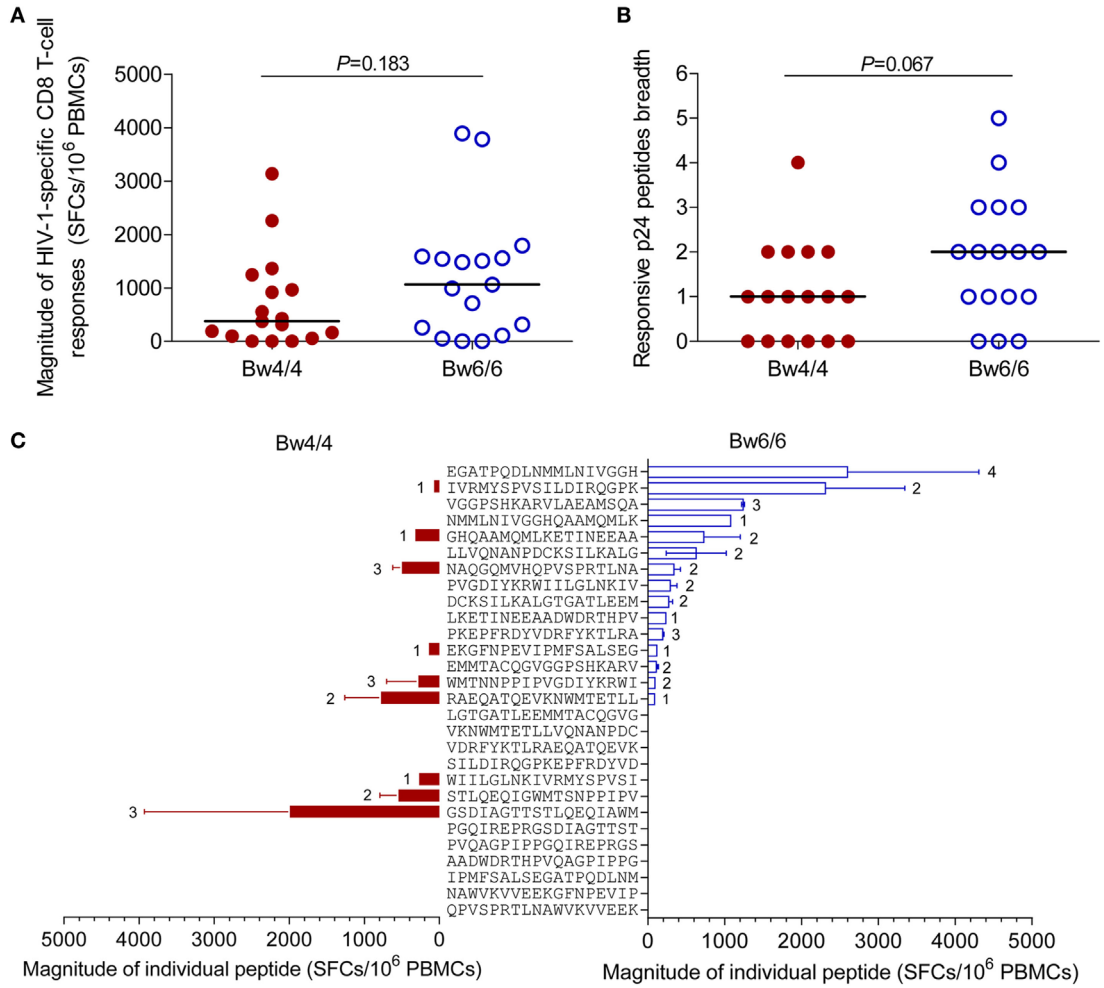

FIGURE 6 | Comparison of human immunodeficiency virus type 1 (HIV-1)-specific CD8 T-cell responses. Comparison of the magnitude **(A)** and the breadth **(B)** of the p24-specific CD8 T-cell responses induced in patients homozygous for *Bw4* or *Bw6*; **(C)** Differences in peptide mapping for patients homozygous for *Bw4* (red) and *Bw6* (blue). The location of individual peptide was shown in Table S1 in Supplementary Material. The number beside the bar indicates the number of patients responding to the peptide concerned. Unpaired, non-parametric Mann–Whitney *U* tests were used to compare groups, with $P < 0.05$ considered significant.

for KIR3DL1⁻NK cells; **Figure 7E**), but not in *Bw6*-homozygous individuals (data not shown). These results suggest that NK cell, principally KIR3DL1⁻NK cell activation may decrease HIV-1 VL in *Bw4*-homozygous individuals.

In addition, the numbers of HIV-1-specific KIR3DL1⁻CD107a⁺CD8⁺ T cells was inversely associated with the VL set point ($r_s = -0.49$, $P = 0.048$, **Figure 7F**) and even the levels of VL at 3 years after infection ($r_s = -0.62$, $P = 0.023$, **Figure 7G**) in individuals homozygous for *Bw4*, but not for *Bw6*. These results suggest that KIR3DL1⁻CD107a⁺CD8⁺ T cells and activated KIR3DL1⁻NK cells simultaneously inhibited HIV-1 viral replication in *Bw4*-homozygous individuals, but the KIR3DL1⁻NK cell activation levels had no correlation with the numbers of HIV-1-specific KIR3DL1⁻CD107a⁺CD8⁺ T cells ($r_s = -0.41$, $P = 0.128$, **Figure 7H**) in *Bw4*-homozygous individuals.

Interestingly, total NK cell activation capacity was negatively related to the numbers of HIV-1-specific IFN-γ⁺CD8⁺ T cells ($r_s = -0.68$, $P = 0.004$, **Figure 7I**) in *Bw4*-homozygous individuals. Likewise, this inverse relationship was exhibited between KIR3DL1⁻NK cell activation capacity and the amounts of HIV-1-specific KIR3DL1⁻IFN-γ⁺CD8⁺ T cells ($r_s = -0.66$, $P = 0.005$, **Figure 7J**). Thus, strong KIR3DL1⁻NK cell activation capacity, which is related to the control of HIV-1 disease progression, was associated with the weak HIV-1-specific CD8 T-cell responses in *Bw4*-homozygous individuals from our Beijing PRIMO Cohort.

DISCUSSION

In this study, KIR3DL1-positive CD8 T cells, was not related to the percentage of NK cells expressing KIR3DL1, in either HIV-1-positive or HIV-1-negative individuals, indicating the presence of different pathways regulating KIR3DL1 expression on NK and CD8 T cells. KIR3DL1-positive CD8 T cells did not increase in acute/early HIV-1 infection (**Figure 2**), whereas the KIRs-positive CD8 T cells, including KIR3DL1, has been shown

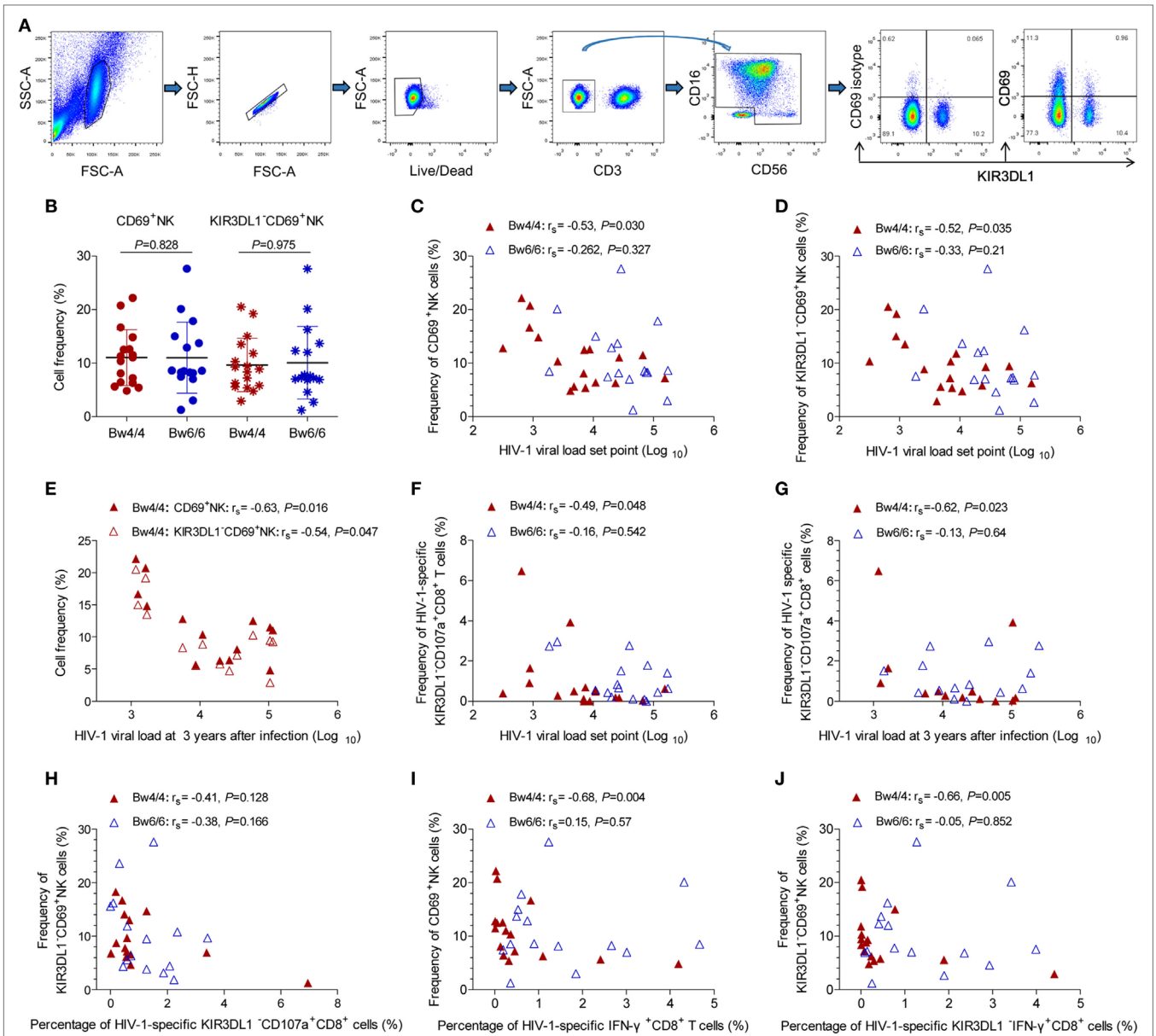

FIGURE 7 | Inverse correlation between KIR3DL1⁻ natural killer (NK) cell activation or human immunodeficiency virus type 1 (HIV-1)-specific KIR3DL1⁻CD8 T-cell responses and viral load (VL) set point in *Bw4*-homozygous individuals. **(A)** Gating strategy for flow cytometric analysis of CD69 and KIR3DL1 expressing on NK cells; **(B)** comparison of the proportion of CD69⁺NK and KIR3DL1⁻CD69⁺NK cells between HIV-1-infected individuals homozygous for *Bw4* (red) and *Bw6* (blue). Inverse correlation between the frequency of CD69⁺NK cells **(C)**, KIR3DL1⁻CD69⁺NK cells **(D)** and HIV-1 VL set point, and even HIV-1 VL at 3 years after infection **(E)** in *Bw4*-homozygous individuals; negative correlation of the frequency of HIV-1-specific KIR3DL1⁻CD107a⁺CD8⁺ T cells with HIV-1 VL set point **(F)** and HIV-1 VL at 3 years after infection **(G)** in *Bw4*-homozygous participants; correlation between the KIR3DL1⁻NK cells activation capacity and the frequency of HIV-1-specific KIR3DL1⁻CD107a⁺CD8⁺ T cells **(H)**; inverse correlation between the frequency of CD69⁺NK cells and the amounts of HIV-1-specific IFN-γ⁺CD8⁺ T cells **(I)**, between the frequency of KIR3DL1⁻CD69⁺NK cells and the amounts of HIV-1-specific KIR3DL1⁻IFN-γ⁺CD8⁺ T cells **(J)** were shown. Comparisons between two groups were performed with unpaired Student's *t*-tests and correlations between two variables were assessed in non-parametric Spearman's rank correlation tests, with $P < 0.05$ considered significant.

to increase in untreated individuals with chronic HIV-1 infection (17). The higher proportion of KIR3DL1-expressing CD8 T_{EMRA} cells in *Bw6*-homozygous individuals than in *Bw4*-homozygous individuals suggested that the weak antiviral activity observed in individuals homozygous for *Bw6* was due to 76.5 (71.5–92.6%) of KIR3DL1⁺CD8⁺ T cells expressing CD57 (19), a marker of cell immunosenescence.

Indeed, the early activation and proliferation of KIR3DL1⁺CD8⁺ T cells were very weak, and the levels of HIV-1-specific KIR3DL1-expressing CD8 T cells secreting IFN-γ and expressing CD107a

were very low, regardless of whether the individuals was homozygous for *Bw4* or *Bw6* (**Figures 4** and **5**). Similarly, several studies have demonstrated that most HIV-1-specific CD8 T cells lack KIR expression (17, 19). Together, these results suggest that the KIR3DL1$^+$CD8$^+$ T cells do not play a crucial role in controlling HIV-1 infection and these CD8 T cells are not responsible for the beneficial effects observed in *Bw4* homozygotes.

HLA-B Bw4-homozygous individuals displayed stronger CD8 T-cell early activation and proliferation, particularly for KIR3DL1$^-$CD8$^+$ T cells, than *Bw6* homozygotes (**Figure 4**), suggesting that the favorable effects of *Bw4* homozygosity are associated with KIR3DL1-negative CD8 T cells. Surprisingly, the intracellular cytokine staining and ELISPOT assays showed that the HIV-1-specific CD8 T-cell responses induced in *HLA-B Bw4*-homozygous individuals were no stronger than those induced in *Bw6*-homozygous individuals (**Figure 6**). As shown in **Figure 6C** and Table S1 in Supplementary Material, several peptides were recognized by both *Bw4* and *Bw6*-homozygous individuals, but others were only recognized and induced stronger responses in individuals homozygous for *Bw4* ($gag_{233–250}$, which contained the CTL epitope TSTLQEQIAW restricted by B*57 and B*58) or *Bw6* ($gag_{177–194}$, which contained the CTL epitope TPQDLNMMLN restricted by B*07 and B*42). Nonetheless, the overall p24-specific responses did not differ between these two groups (**Figure 6C**). Our findings were inconsistent with other studies reporting the elicitation of strong HIV-1-specific CD8 T-cell responses in *HLA-B*57* and/or-*B*27* individuals (34, 35). It would have been desirable to compare the HIV-1-specific responses induced on *Bw4*-homozygous individuals harboring *HLA-B*27* and/or *-B*57* individuals to those homozygous for *Bw6* in this study. Unfortunately, only three individuals carried *HLA-B*27* and/or *-B*57* alleles (**Table 1**). Indeed, *HLA-B*57* is rare in the Chinese population (10, 12). Another reason may relate to the *HLA-B*27* allele, which has been reported to prevent disease progression only for late-stage disease and was not linked to a strong CD8 T-cell antiviral response (36, 37). The individuals enrolled in this study were in the acute/early stage of HIV-1 infection. Moreover, in this study, isolated CD8$^+$ T cells induced about 95% of the p24-specific T-cell responses (**Figure 6**; Table S1 in Supplementary Material), but isolated CD4$^+$ T cells induced very little of the p24-specific T-cell responses recognized against the 18 amino acids length peptides pool (data not shown) in ELISPOT assay. Given the magnitude and breadth of HIV-1-specific CD8 T-cell responses was not stronger in *Bw4*-homozygous individuals than in *Bw6*-homozygous individuals, so the polyfunctionality, functional avidity, and cross-reactivity to epitope variants (38, 39) of HIV-1-specific CD8 T-cell responses requires further investigation to account for the advantageous effect of *Bw4* homozygosity in *HLA-B* alleles.

Interestingly, the effector responses of HIV-1-specific CD8 T cells particularly KIR3DL1$^-$CD8$^+$ T cells secreting IFN-γ were not increased in *Bw4*-homozygous individuals, but this effector responses were inversely correlated with early activation (Figure S2 in Supplementary Material). Indeed, early activated CD8 T cells produce very little IFN-γ and CD107a specifically in response to HIV-1, but CD69-positive CD8 cells in tissue can secrete other chemokines, such as transforming growth factor-β and IL-10 (32, 40, 41), to regulate immune responses. Besides, CD69 is involved in early events of lymphocyte activation, and plays a functional role in the redirected lysis mediated by activated NK cells, and we found that the level of CD69 expression on NK cells in *Bw4*-homozygous individuals was inversely correlated with HIV-1 VL set point (**Figure 7**). HIV-1 VL set point reflects the equilibrium between HIV-1 replication level and efficacy of immunologic response and has long been used as a prognostic marker of disease progression (42, 43). The early activation of NK cells particularly KIR3DL1$^-$NK cells therefore appeared to be beneficial for HIV-1 viremia control especially in individuals homozygous for *Bw4*. An inverse relationship was observed between KIR3DL1$^-$NK cell activation and HIV-1-specific KIR3DL1$^-$CD8 T-cell responses, especially the production of IFN-γ (**Figure 6**), consistent with the findings of Tomescu's study (44). Strong NK cell responses are associated with protective *KIR3DL1**h/*y receptor and *HLA-I* allele (such as *HLA-B*57*), independently of the lack of increase in HIV-1 gag-specific T-cell responses in HIV-1-infected elite controllers. Waggoner et al. described a role for NK cells in the inverse modulation of antiviral CD8 T cells (45). Our findings indicate that KIR3DL1$^-$NK activation was inversely related to HIV-1-specific KIR3DL1$^-$CD8$^+$ T-cell responses in *Bw4*-homozygous individuals, suggesting higher levels of activated KIR3DL1$^-$NK cells might decrease the levels of HIV-1-specific KIR3DL1$^-$CD8$^+$ T cell responses, but all these cells were potent in controlling HIV-1 infection.

Kim et al. reported that KIR3DL1$^+$NK cells in *HLA-Bw4* homozygous healthy individuals were more responsive to autologous target cells than in *HLA-Bw6* homozygous healthy donors (46), while the functionality of KIR3DL1$^+$NK cells did not differ in *HLA-Bw4* carriers and *HLA-Bw6* homozygous individuals in HIV-1 infection (47). No differences in NK cell functionality of mediating anti-HIV ADCC responses was observed between KIR3DL1$^+$NK cells and KIR3DL1$^-$NK cells in *HLA-Bw4* individuals infected with HIV-1 (47), though KIR3DL1$^+$NK cells from *HLA-Bw4* healthy controls were more functional than KIR3DL1$^-$NK cells (46). These data suggested the functionality of KIR3DL1$^+$NK cells could be attenuated due to HIV-1 infection in *HLA-Bw4* homozygous individuals. NK cells from HIV-1-uninfected *Bw6*-homozygous individuals inhibited HIV-1 replication in infected autologous CD4 cells less potently than those from protective *KIR/HLA* genotypes including *KIR3DL1**h/*y and *B*57* combined genotypes (48), which secreted higher levels of CC-chemokines (CCL-3 and CCL-4). Based on these reports and the outcomes of the vast majority of activated NK cells were KIR3DL1-negative NK cells, and the negative relationship between KIR3DL1$^-$NK cell activation and VL set point in *Bw4*-homozygous individuals, we speculate that KIR3DL1$^-$NK cells may be more active in HIV-1-infected individuals homozygous for the *Bw4* allele, although no increase in HIV-1-specific CD8 T-cell responses was observed in this study. In addition, the higher frequency of early activated and proliferated CD8 T cells, and particularly of KIR3DL1-negative CD8 T cells in *Bw4*-homozygous individuals, would have greater antiviral potential during acute/early HIV-1 infection.

In general, KIR3DL1 expression on CD8 T cells was associated with the loss of multiple functions, including the limitation of viral replication and the slowing of CD4 decline, early activation, proliferation, HIV-1-specific cytokine secretion, and degranulation *in vitro*. KIR3DL1⁻CD8⁺ T cells and KIR3DL1⁻NK cells in individuals homozygous for *Bw4* were related to inhibiting HIV-1 infection as summarized in **Figure 8**, but the underlying mechanisms are not fully clear. Thus, further studies are required to determine whether other inhibitory KIRs and other immune inhibitory receptors containing the ITIMs such as PD-1 and TIGIT (49, 50) are involved in regulating KIR3DL1⁻CD8⁺ T-cell and KIR3DL1⁻NK cell functions. Furthermore, only 34

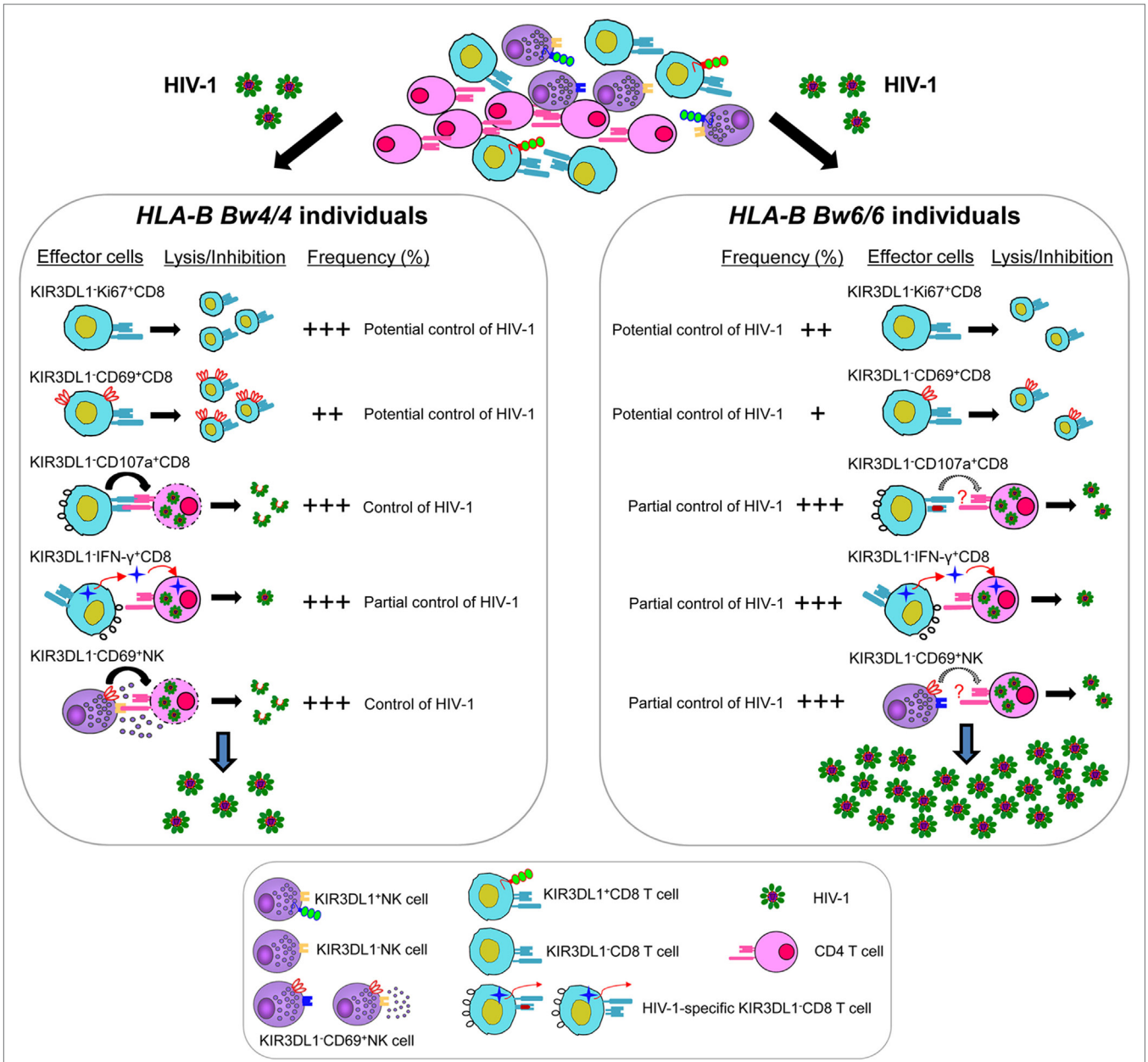

FIGURE 8 | Model for KIR3DL1⁻CD8⁺ T cell and KIR3DL1⁻ natural killer (NK) cell controlling human immunodeficiency virus type 1 (HIV-1) infection in individuals with distinct *HLA-B* serological genotypes. HIV-1-specific KIR3DL1⁻CD107a⁺CD8⁺ T cells and KIR3DL1⁻CD69⁺NK cells were associated with inhibiting HIV-1 replication in *Bw4*-homozygous individuals, but not efficient in *Bw6*-homozygous individuals. The levels of HIV-1-specific KIR3DL1⁻IFN-γ⁺CD8⁺ T cells were similar in both individuals homozygous for *Bw4* and *Bw6*, may be associated with partial control of HIV-1 infection. Moreover, the proliferative capacity of KIR3DL1⁻Ki67⁺CD8⁺ T and the early activation of KIR3DL1⁻CD69⁺CD8⁺ T cells, which can potential control of HIV-1 infection, were significantly higher in HIV-1-infected individuals homozygous for the *Bw4* than in those homozygous for *Bw6*. Nevertheless, the frequency and function of KIR3DL1-expressing CD8⁺ T/NK cells was much lower than that of KIR3DL1-negative CD8⁺ T/NK cells in HIV-1-infected individuals, regardless of *Bw4* or *Bw6* homozygosity. Thus, KIR3DL1-expressing CD8⁺ T/NK cells, which associated with the loss of multiple functions, may do not play a crucial role in controlling HIV-1 infection in the early stages of HIV-1 infection.

participants infected with HIV-1 CRF01_A/E subtype were enrolled in this current study, because CRF01_A/E subtype is the most dominant strain in most regions of China. Thus, it will be worthwhile for further studies to investigate the mechanisms of advantageous effects of *Bw4* homozygosity based on other HIV-1 subtypes, and a larger number of individuals with *HLA-B Bw4* homozygotes will be also required.

Taken together, our findings demonstrate for the first time that the KIR3DL1−CD8 T/NK cell functions of *Bw4* homozygotes are associated with the control of early HIV-1 replication in the absence of antiretroviral treatment. These results open up new insights into the design of an effective vaccine against HIV.

ETHICS STATEMENT

This study and all the relevant experiments were approved by the Beijing You'an Hospital Research Ethics Committee, and written informed consent was obtained from each participant in accordance with the Declaration of Helsinki. All participants provided written informed consent for the collection of information, and their clinical samples were stored and used for research. The methods used conformed to approved guidelines and regulations.

AUTHOR CONTRIBUTIONS

XZ, HW, TZ, and BS conceived and designed the experiments; WX, and YZ collected the sample information, contributed to reagents and materials; XZ, XL, LY, ZLi, and ZLiu performed the experiments; XZ, CM, HW, TZ, and BS analyzed the data; and XZ, CM, and BS wrote the manuscript. All authors read and approved the final manuscript.

ACKNOWLEDGMENTS

We thank Yunxia Ji, Rui Wang for cell counting and viral load detecting, and the HIV-1-infected individuals participated in our study. This work was supported by the National Natural Science Foundation of China (NSFC, 81772165 to BS, 81571973 to HW, 81501732 to XL, 81501731 to ZL), the NSFC-NIH Biomedical collaborative research program (81761128001 to HW), the National 13th Five-Year Grand Program on Key Infectious Disease Control (2017ZX10202102-005-003 to BS, 2017ZX10202101-004-001 to TZ), the Beijing Municipal of Science and Technology Major Project (D161100000416003 to HW), the Funding for Chinese overseas talents returning to China in 2016 (to BS), the Basic-Clinical Research Cooperation Fund of Capital Medical University (17JL20 to BS), the Beijing Key Laboratory for HIV/AIDS Research (BZ0089), the French Agency for Research on AIDS and Viral Hepatitis (ANRS), the Vaccine Research Institute, SIDACTION Pierre Bergé, and the Investissements d'Avenir program managed by the ANR under reference ANR-10-LABX-77 (to CM). The funders had no role in study design, data collection and analysis, decision to publish, or preparation of the manuscript.

SUPPLEMENTARY MATERIAL

The Supplementary Material for this article can be found online at https://www.frontiersin.org/articles/10.3389/fimmu.2018.01855/full#supplementary-material.

FIGURE S1 | Flow chart of human immunodeficiency virus type 1 (HIV-1) participants at enrollment. Screening and follow-up of participants in the acute/early phase of HIV-1 infection. In total, 17 of 24 participants homozygous for *Bw4* and 17 of 40 participants homozygous for *Bw6* were enrolled in this study. These 34 participants without antiretroviral therapy were infected with a CRF01_A/E subtype based on *pol* sequence and between the Fiebig stage VI and 6 months after infection. The opportunistic infections, tuberculosis, autoimmune diseases, or HBV/HCV co-infection were excluded.

FIGURE S2 | ELISOPT assays. Representative experiments showing peripheral blood mononuclear cells from eight individuals infected with human immunodeficiency virus type 1 subtype CRF01_A/E were stimulated with CRF01_A/E p24 peptides pool. Phytohemagglutinin (PHA) was used as experimental positive control and EBV/Flu/CMV (EFC) peptides were used as quality control; negative control was used with RPMI 1640 medium.

FIGURE S3 | Relationship between the early activation capacity of CD8 T cells and the levels of human immunodeficiency virus type 1 (HIV-1)-specific IFN-γ or CD107a released by CD8 T cells. Inverse relationship between early activation capacity and levels of HIV-1-specific IFN-γ-secreting total CD8 T cells **(A)**, and **(B)** KIR3DL1-negative CD8 T cells; **(C)** gating strategy for flow cytometric analysis of CD69, IFN-γ and CD107a combined expressing on CD8 T cells after stimulation with p24 peptides. Graphs are shown for gating on the CD8 T-cell population. Correlation between two variables was analyzed with Spearman's rank correlation tests, with $P < 0.05$ considered significant.

REFERENCES

1. Thomas R, Low HZ, Kniesch K, Jacobs R, Schmidt RE, Witte T. NKG2C deletion is a risk factor of HIV infection. *AIDS Res Hum Retroviruses* (2012) 28:844–51. doi:10.1089/AID.2011.0253
2. Zeddou M, Rahmouni S, Vandamme A, Jacobs N, Frippiat F, Leonard P, et al. Downregulation of CD94/NKG2A inhibitory receptors on CD8+ T cells in HIV infection is more pronounced in subjects with detected viral load than in their aviraemic counterparts. *Retrovirology* (2007) 4:72. doi:10.1186/1742-4690-4-72
3. Warren HS, Rana PM, Rieger DT, Hewitt KA, Dahlstrom JE, Kent AL. CD8 T cells expressing killer Ig-like receptors and NKG2A are present in cord blood and express a more naive phenotype than their counterparts in adult blood. *J Leukoc Biol* (2006) 79:1252–9. doi:10.1189/jlb.0905536
4. Ayres J, Cresswell P. HLA-B specificities and w4, w6 specificities are on the same polypeptide. *Eur J Immunol* (1976) 6:794–9. doi:10.1002/eji.1830061108
5. Kiepiela P, Leslie AJ, Honeyborne I, Ramduth D, Thobakgale C, Chetty S, et al. Dominant influence of HLA-B in mediating the potential co-evolution of HIV and HLA. *Nature* (2004) 432:769–75. doi:10.1038/nature03113
6. Bihl F, Frahm N, Di Giammarino L, Sidney J, John M, Yusim K, et al. Impact of HLA-B alleles, epitope binding affinity, functional avidity, and viral coinfection on the immunodominance of virus-specific CTL responses. *J Immunol* (2006) 176:4094–101. doi:10.4049/jimmunol.176.7.4094
7. Crux NB, Elahi S. Human leukocyte antigen (HLA) and immune regulation: how do classical and non-classical HLA alleles modulate immune response to human immunodeficiency virus and hepatitis C virus infections? *Front Immunol* (2017) 8:832. doi:10.3389/fimmu.2017.00832
8. Welzel TM, Gao X, Pfeiffer RM, Martin MP, O'Brien SJ, Goedert JJ, et al. HLA-B Bw4 alleles and HIV-1 transmission in heterosexual couples. *AIDS* (2007) 21:225–9. doi:10.1097/QAD.0b013e3280123840
9. Flores-Villanueva PO, Yunis EJ, Delgado JC, Vittinghoff E, Buchbinder S, Leung JY, et al. Control of HIV-1 viremia and protection from AIDS are

associated with HLA-Bw4 homozygosity. *Proc Natl Acad Sci U S A* (2001) 98:5140–5. doi:10.1073/pnas.071548198

10. Zhang X, Huang X, Xia W, Li W, Zhang T, Wu H, et al. HLA-B*44 is associated with a lower viral set point and slow CD4 decline in a cohort of Chinese homosexual men acutely infected with HIV-1. *Clin Vaccine Immunol* (2013) 20:1048–54. doi:10.1128/CVI.00015-13
11. Qing M, Li T, Han Y, Qiu Z, Jiao Y. Accelerating effect of human leukocyte antigen-Bw6 homozygosity on disease progression in Chinese HIV-1-infected patients. *J Acquir Immune Defic Syndr* (2006) 41:137–9. doi:10.1097/01.qai.0000195607.25262.92
12. Huang X, Ling H, Mao W, Ding X, Zhou Q, Han M, et al. Association of HLA-A, B, DRB1 alleles and haplotypes with HIV-1 infection in Chongqing, China. *BMC Infect Dis* (2009) 9:201. doi:10.1186/1471-2334-9-201
13. Arlettaz L, Degermann S, De Rham C, Roosnek E, Huard B. Expression of inhibitory KIR is confined to CD8+ effector T cells and limits their proliferative capacity. *Eur J Immunol* (2004) 34:3413–22. doi:10.1002/eji.200324756
14. Li G, Yu M, Weyand CM, Goronzy JJ. Epigenetic regulation of killer immunoglobulin-like receptor expression in T cells. *Blood* (2009) 114:3422–30. doi:10.1182/blood-2009-01-200170
15. Anfossi N, Doisne JM, Peyrat MA, Ugolini S, Bonnaud O, Bossy D, et al. Coordinated expression of Ig-like inhibitory MHC class I receptors and acquisition of cytotoxic function in human CD8+ T cells. *J Immunol* (2004) 173:7223–9. doi:10.4049/jimmunol.173.12.7223
16. McMahon CW, Zajac AJ, Jamieson AM, Corral L, Hammer GE, Ahmed R, et al. Viral and bacterial infections induce expression of multiple NK cell receptors in responding CD8(+) T cells. *J Immunol* (2002) 169:1444–52. doi:10.4049/jimmunol.169.3.1444
17. Alter G, Rihn S, Streeck H, Teigen N, Piechocka-Trocha A, Moss K, et al. Ligand-independent exhaustion of killer immunoglobulin-like receptor-positive CD8+ T cells in human immunodeficiency virus type 1 infection. *J Virol* (2008) 82:9668–77. doi:10.1128/JVI.00341-08
18. van der Veken LT, Diez Campelo M, van der Hoorn MA, Hagedoorn RS, van Egmond HM, van Bergen J, et al. Functional analysis of killer Ig-like receptor-expressing cytomegalovirus-specific CD8+ T cells. *J Immunol* (2009) 182:92–101. doi:10.4049/jimmunol.182.1.92
19. Zipperlen K, Gallant M, Stapleton S, Heath J, Barrett L, Grant M. Protective genotypes in HIV infection reflect superior function of KIR3DS1+ over KIR3DL1+ CD8+ T cells. *Immunol Cell Biol* (2015) 93:67–76. doi:10.1038/icb.2014.68
20. Huang X, Chen H, Li W, Li H, Jin X, Perelson AS, et al. Precise determination of time to reach viral load set point after acute HIV-1 infection. *J Acquir Immune Defic Syndr* (2012) 61:448–54. doi:10.1097/QAI.0b013e31827146e0
21. Fiebig EW, Wright DJ, Rawal BD, Garrett PE, Schumacher RT, Peddada L, et al. Dynamics of HIV viremia and antibody seroconversion in plasma donors: implications for diagnosis and staging of primary HIV infection. *AIDS* (2003) 17:1871–9. doi:10.1097/00002030-200309050-00005
22. Huang X, Lodi S, Fox Z, Li W, Phillips A, Porter K, et al. Rate of CD4 decline and HIV-RNA change following HIV seroconversion in men who have sex with men: a comparison between the Beijing PRIMO and CASCADE cohorts. *J Acquir Immune Defic Syndr* (2013) 62:441–6. doi:10.1097/QAI.0b013e31827f5c9a
23. Li X, Xue Y, Lin Y, Gai J, Zhang L, Cheng H, et al. Evolutionary dynamics and complicated genetic transmission network patterns of HIV-1 CRF01_AE among MSM in Shanghai, China. *Sci Rep* (2016) 6:34729. doi:10.1038/srep34729
24. Li X, Liu H, Liu L, Feng Y, Kalish ML, Ho SYW, et al. Tracing the epidemic history of HIV-1 CRF01_AE clusters using near-complete genome sequences. *Sci Rep* (2017) 7:4024. doi:10.1038/s41598-017-03820-8
25. Zhang Z, Dai L, Jiang Y, Feng K, Liu L, Xia W, et al. Transmission network characteristics based on env and gag sequences from MSM during acute HIV-1 infection in Beijing, China. *Arch Virol* (2017) 162:3329–38. doi:10.1007/s00705-017-3485-z
26. Wang X, Wu Y, Mao L, Xia W, Zhang W, Dai L, et al. Targeting HIV prevention based on molecular epidemiology among deeply sampled subnetworks of men who have sex with men. *Clin Infect Dis* (2015) 61:1462–8. doi:10.1093/cid/civ526
27. Li Z, Lu X, Hu Z, Luo Z, Jiang W, Wu H, et al. Syphilis infection differentially regulates the phenotype and function of gammadelta T cells in HIV-1-infected patients depends on the HIV-1 disease stage. *Front Immunol* (2017) 8:991. doi:10.3389/fimmu.2017.00991
28. Chen P, Su B, Zhang T, Zhu X, Xia W, Fu Y, et al. Perturbations of monocyte subsets and their association with T helper cell differentiation in acute and chronic HIV-1-infected patients. *Front Immunol* (2017) 8:272. doi:10.3389/fimmu.2017.00272
29. Currier JR, Kuta EG, Turk E, Earhart LB, Loomis-Price L, Janetzki S, et al. A panel of MHC class I restricted viral peptides for use as a quality control for vaccine trial ELISPOT assays. *J Immunol Methods* (2002) 260:157–72. doi:10.1016/S0022-1759(01)00535-X
30. Zhang X, Xing H, Feng X, Zhang H, Wang Y, Yan H. Hepatitis B virus (HBV)-specific T-cell responses to recombinant HBV core protein in patients with normal liver function and co-infected with chronic HBV and human immunodeficiency virus 1 (HIV-1). *Virol J* (2013) 10:232. doi:10.1186/1743-422X-10-232
31. Zhang Y, Peng Y, Yan H, Xu K, Saito M, Wu H, et al. Multilayered defense in HLA-B51-associated HIV viral control. *J Immunol* (2011) 187:684–91. doi:10.4049/jimmunol.1100316
32. Gonzalez-Amaro R, Cortes JR, Sanchez-Madrid F, Martin P. Is CD69 an effective brake to control inflammatory diseases? *Trends Mol Med* (2013) 19:625–32. doi:10.1016/j.molmed.2013.07.006
33. Sun X, Kaufman PD. Ki-67: more than a proliferation marker. *Chromosoma* (2018) 127:175–86. doi:10.1007/s00412-018-0659-8
34. Brennan CA, Ibarrondo FJ, Sugar CA, Hausner MA, Shih R, Ng HL, et al. Early HLA-B*57-restricted CD8+ T lymphocyte responses predict HIV-1 disease progression. *J Virol* (2012) 86:10505–16. doi:10.1128/JVI.00102-12
35. den Uyl D, van der Horst-Bruinsma IE, van Agtmael M. Progression of HIV to AIDS: a protective role for HLA-B27? *AIDS Rev* (2004) 6(2):89–96.
36. Gao X, Bashirova A, Iversen AK, Phair J, Goedert JJ, Buchbinder S, et al. AIDS restriction HLA allotypes target distinct intervals of HIV-1 pathogenesis. *Nat Med* (2005) 11:1290–2. doi:10.1038/nm1333
37. Emu B, Sinclair E, Hatano H, Ferre A, Shacklett B, Martin JN, et al. HLA class I-restricted T-cell responses may contribute to the control of human immunodeficiency virus infection, but such responses are not always necessary for long-term virus control. *J Virol* (2008) 82:5398–407. doi:10.1128/JVI.02176-07
38. Kosmrlj A, Read EL, Qi Y, Allen TM, Altfeld M, Deeks SG, et al. Effects of thymic selection of the T-cell repertoire on HLA class I-associated control of HIV infection. *Nature* (2010) 465:350–4. doi:10.1038/nature08997
39. Neumann-Haefelin C. HLA-B27-mediated protection in HIV and hepatitis C virus infection and pathogenesis in spondyloarthritis: two sides of the same coin? *Curr Opin Rheumatol* (2013) 25:426–33. doi:10.1097/BOR.0b013e328362018f
40. Sancho D, Gomez M, Sanchez-Madrid F. CD69 is an immunoregulatory molecule induced following activation. *Trends Immunol* (2005) 26:136–40. doi:10.1016/j.it.2004.12.006
41. Marazuela M, Garcia-Lopez MA, Figueroa-Vega N, de la Fuente H, Alvarado-Sanchez B, Monsivais-Urenda A, et al. Regulatory T cells in human autoimmune thyroid disease. *J Clin Endocrinol Metab* (2006) 91:3639–46. doi:10.1210/jc.2005-2337
42. Ho DD. Viral counts count in HIV infection. *Science* (1996) 272:1124–5. doi:10.1126/science.272.5265.1124
43. Mellors JW, Margolick JB, Phair JP, Rinaldo CR, Detels R, Jacobson LP, et al. Prognostic value of HIV-1 RNA, CD4 cell count, and CD4 Cell count slope for progression to AIDS and death in untreated HIV-1 infection. *JAMA* (2007) 297:2349–50. doi:10.1001/jama.297.21.2349
44. Tomescu C, Duh FM, Hoh R, Viviani A, Harvill K, Martin MP, et al. Impact of protective killer inhibitory receptor/human leukocyte antigen genotypes on natural killer cell and T-cell function in HIV-1-infected controllers. *AIDS* (2012) 26:1869–78. doi:10.1097/QAD.0b013e32835861b0
45. Waggoner SN, Cornberg M, Selin LK, Welsh RM. Natural killer cells act as rheostats modulating antiviral T cells. *Nature* (2011) 481:394–8. doi:10.1038/nature10624
46. Kim S, Sunwoo JB, Yang L, Choi T, Song YJ, French AR, et al. HLA alleles determine differences in human natural killer cell responsiveness and potency. *Proc Natl Acad Sci U S A* (2008) 105:3053–8. doi:10.1073/pnas.0712229105
47. Parsons MS, Wren L, Isitman G, Navis M, Stratov I, Bernard NF, et al. HIV infection abrogates the functional advantage of natural killer cells educated

through KIR3DL1/HLA-Bw4 interactions to mediate anti-HIV antibody-dependent cellular cytotoxicity. *J Virol* (2012) 86:4488–95. doi:10.1128/JVI.06112-11

48. Song R, Lisovsky I, Lebouche B, Routy JP, Bruneau J, Bernard NF. HIV protective KIR3DL1/S1-HLA-B genotypes influence NK cell-mediated inhibition of HIV replication in autologous CD4 targets. *PLoS Pathog* (2014) 10:e1003867. doi:10.1371/journal.ppat.1003867
49. Chew GM, Fujita T, Webb GM, Burwitz BJ, Wu HL, Reed JS, et al. TIGIT marks exhausted T cells, correlates with disease progression, and serves as a target for immune restoration in HIV and SIV infection. *PLoS Pathog* (2016) 12:e1005349. doi:10.1371/journal.ppat.1005349
50. Zhang Q, Bi J, Zheng X, Chen Y, Wang H, Wu W, et al. Blockade of the checkpoint receptor TIGIT prevents NK cell exhaustion and elicits potent anti-tumor immunity. *Nat Immunol* (2018) 19:723–32. doi:10.1038/s41590-018-0132-0

Conflict of Interest Statement: The authors declare that the research was conducted in the absence of any commercial or financial relationships that could be construed as a potential conflict of interest.

Copyright © 2018 Zhang, Lu, Moog, Yuan, Liu, Li, Xia, Zhou, Wu, Zhang and Su. This is an open-access article distributed under the terms of the Creative Commons Attribution License (CC BY). The use, distribution or reproduction in other forums is permitted, provided the original author(s) and the copyright owner(s) are credited and that the original publication in this journal is cited, in accordance with accepted academic practice. No use, distribution or reproduction is permitted which does not comply with these terms.

frontiers in Immunology

ORIGINAL RESEARCH
published: 14 September 2018
doi: 10.3389/fimmu.2018.02025

Chickens Expressing IFIT5 Ameliorate Clinical Outcome and Pathology of Highly Pathogenic Avian Influenza and Velogenic Newcastle Disease Viruses

*Mohammed A. Rohaim[1,2,3], Diwakar Santhakumar[3], Rania F. El Naggar[4], Munir Iqbal[2], Hussein A. Hussein[1] and Muhammad Munir[3]**

[1] Department of Virology, Faculty of Veterinary Medicine, Cairo University, Giza, Egypt, [2] The Pirbright Institute, Woking, United Kingdom, [3] Division of Biomedical and Life Sciences, Faculty of Health and Medicine, Lancaster University, Lancaster, United Kingdom, [4] Department of Virology, Faculty of Veterinary Medicine, University of Sadat City, Sadat, Egypt

Innate antiviral immunity establishes first line of defense against invading pathogens through sensing their molecular structures such as viral RNA. This antiviral potential of innate immunity is mainly attributed to a myriad of IFN-stimulated genes (ISGs). Amongst well-characterized ISGs, we have previously shown that antiviral potential of chicken IFN-induced proteins with tetratricopeptides repeats 5 (chIFIT5) is determined by its interaction potential with 5′ppp containing viral RNA. Here, we generated transgenic chickens using avian sarcoma-leukosis virus (RCAS)-based gene transfer system that constitutively and stably express chIFIT5. The transgenic chickens infected with clinical dose (EID_{50} 10^4 for HPAIV and 10^5 EID_{50} for vNDV) of high pathogenicity avian influenza virus (HPAIV; H5N1) or velogenic strain of Newcastle disease virus (vNDV; Genotype VII) showed marked resistance against infections. While transgenic chickens failed to sustain a lethal dose of these viruses (EID_{50} 10^5 for HPAIV and 10^6 EID_{50} for vNDV), a delayed and lower level of clinical disease and mortality, reduced virus shedding and tissue damage was observed compared to non-transgenic control chickens. These observations suggest that stable expression of chIFIT5 alone is potentially insufficient in providing sterile protection against these highly virulent viruses; however, it is sufficient to ameliorate the clinical outcome of these RNA viruses. These findings propose the potential of innate immune genes in conferring genetic resistance in chickens against highly pathogenic and zoonotic viral pathogens causing sever disease in both animals and humans.

Keywords: innate immunity, antiviral response, transgenic, viruses, host registance

OPEN ACCESS

Edited by:
Ping An,
Frederick National Laboratory for Cancer Research (NIH), United States

Reviewed by:
Hiroyuki Oshiumi,
Kumamoto University, Japan
Jianzhong Zhu,
Yangzhou University, China

***Correspondence:**
Muhammad Munir
muhammad.munir@lancaster.ac.uk

Specialty section:
This article was submitted to Viral Immunology, a section of the journal Frontiers in Immunology

Received: *24 April 2018*
Accepted: *16 August 2018*
Published: *14 September 2018*

Citation:
Rohaim MA, Santhakumar D, Naggar RFE, Iqbal M, Hussein HA and Munir M (2018) Chickens Expressing IFIT5 Ameliorate Clinical Outcome and Pathology of Highly Pathogenic Avian Influenza and Velogenic Newcastle Disease Viruses. Front. Immunol. 9:2025. doi: 10.3389/fimmu.2018.02025

INTRODUCTION

Virus recognition by germ-line-encoded intracellular receptors underlines the potency of innate immune responses in restricting virus infections and disease progressions (1, 2). These intracellular receptors discriminate the host (self) nucleic acid from the virus (non-self) nucleic acid by the presence of molecular signatures in the viral genomic material. One of the well-characterized

signatures of innate immune induction is the presence of triphosphate group (5′-ppp) in viral RNA which is absent in any RNA species of the host (3). Beside canonical cellular receptors including Toll-like receptors, retinoic-acid-inducible protein 1 (RIG-I)-like receptors, and nucleotide oligomerization domain-like receptors, recently a novel class of IFN-effectors, known as IFN-induced proteins with tetratricopeptides repeats (IFITs) which has been identified to directly engage with 5′-ppp viral RNA (4, 5).

Amongst viral RNA-recognizing cellular factors, IFITs proteins are the most transcribed and translated family of virus- and IFN-regulated proteins (6–8). These proteins are evolutionary conserved with at least four well-characterized paralogs in humans; IFIT1 (ISG56), IFIT2 (ISG54), IFIT3 (ISG60), and IFIT5 (also known as ISG58) (7–9). These IFNs and virus-responsive proteins are implicated in the regulation of several physiological (protein translation and cell proliferation) and pathological (inhibition of viruses) processes in mammals (7, 10). Among these functions, the implication of IFIT proteins in establishing host resistance against viruses has been well documented (4, 10, 11). Different biological, biochemical, and structural approaches have mapped the nature of RNA that is recognized by IFIT proteins including 5′-ppp, AU-rich elements, and initiator tRNAs (4, 9, 11, 12). Additional evidences suggested that IFIT5 proteins can perform their antiviral activities by two possible ways; sequestration of viral RNA translation and initiation of innate immune responses (9, 13). Both these activities augment the antiviral potential of IFIT5 against RNA viruses such as orthomyxoviruses (e.g., avian influenza viruses, AIV) and paramyxoviruses (e.g., Newcastle disease virus, NDV).

Highly pathogenic IAV (HPAIV) and velogenic NDV (vNDV) are causing devastating economical and welfare impacts on the poultry, and HPAIV are posing significant human health implications, around the globe (14, 15). Majority of negative sense single stranded RNA viruses, including HPIAV and vNDV, produce 5′-ppp containing RNA during the course of virus replication (16–18). Interaction of 5′ppp RNA and cellular receptors (e.g., IFIT5) leads to the induction of cytokines and may underline the antiviral state of the host with variable clinical or pathological outcomes. Understanding host factors that contribute in the pathobiology of viruses in their natural hosts may help to devise effective intervention strategies and to define the genetic markers of disease resistance. In the present study, we investigated the *in vivo* impact of chicken IFIT5 (chIFIT5) against HPAIV and vNDV-induced infections in transgenic chickens generated by the RCAS-based retroviral gene transfer system.

MATERIALS AND METHODS

Viruses and Virus Titration Assays (EID_{50})

HPAIV H5N1 (strain A/chicken/Egypt_128s_2012) and vNDV (strain NDV-B7-RLQP-CH-EG-12 were kindly provided by Prof Hussein Ahmed (Virology Department, Faculty of Veterinary Medicine, Cairo University, Egypt). Both viruses were propagated in 9 days old specific pathogen free (SPF) chicken eggs. Infective allantoic fluid from the inoculated eggs was diluted in brain-heart infusion buffer (BHIB) and the median egg infectious doses 50 (EID_{50}) were determined in SPF eggs using the Reed and Muench method (19).

Construction of Transgene Expressing RCAS Reverse Genetic Systems

The ORF of chicken IFIT5 was amplified from RNA extracted from the NDV-infected primary chicken embryo fibroblasts (CEFs), was sequence verified, codon optimized and chemically synthesized in-fusion with V5-tag, and sub-cloned into an improved version of RCASBP(A)-ΔF1 (kindly provided by Stephen H. Hughes, National Cancer Institute, MD, USA) via the *ClaI* and *MulI* restriction sites which replace the *src* gene while maintaining the splice accepter signals. The resultant constructs were named as RCASBP(A)-chIFIT5. Similarly, a GFP encoding RCASBP(A), referred as RCASBP(A)-eGFP, was generated by introducing the coding sequence of the GFP in between the *ClaI* and *MulI* sites. The inserted gene orientation and sequence validity were confirmed by DNA sequencing.

Rescue of RCAS Viruses and Validation of Transgene Expression

To rescue recombinant RCASBP(A) viruses, a total of 2.5×10^5 DF-1 cells were seeded in 25 cm^2 flasks and maintained at 37°C, 5% (vol/vol) CO_2 for 24 h (∼80% confluent). Cells were washed with PBS and transfected with 2.5 μg of each of the RCASBP(A)-eGFP, and RCASBP(A)-chIFIT5 plasmids using Lipofectamine 2000 in OptiMEM with a pre-determined optimized ratio of 1:6 (Invitrogen, Carlsbad, CA, USA). Media were changed 6 h post transfection and the cells were maintained in DMEM supplemented with 10% FCS and 1% penicillin/streptomycin for 48 h. Expression of the reporter gene (GFP) was monitored using fluorescence microscopy whereas replication efficiencies of chIFIT5 expressing retroviruses were assessed by staining the structural protein of RCASBP(A) and V5 tag. The GFP/gag expression-confirmed cell cultures were split into 25 cm^2 flasks and were passaged again into 75 cm^2 flasks after 3 days. Finally, cells were expanded into 150 cm^2 flasks until the desired number (10^6 cells/egg) was achieved.

Confocal Microscopy

Chicken cells were transfected with individual or combined plasmids for indicated time points using Lipofectamine 2000 (Invitrogen) at a ratio of 1:3 or were infected with lentiviruses, retroviruses or NDV-GFP for indicated time points. These cells were then fixed for 1 h in 4% paraformaldehyde and permeabilised using 0.1% Triton-X100 before incubation with primary antibodies raised against V5 tag, or *gag* protein of retroviruses. Additionally, depending upon the experimental needs, different fluorescent markers (RFP, GFP) were used. Afterwards, cells were incubated with corresponding secondary antibodies at 37°C for 2 h. After brief staining with 4′, 6-diamidino-2-phenylindole (DAP1) (nuclear), slides were visualized using a Leica SP5 confocal laser-scanning microscope.

Animals

SPF eggs were acquired from a local supplier in co-operation with Virology Department, Faculty of Veterinary Medicine, Cairo University, and the Central Lab for Evaluation of Veterinary Biologics Abbassia, Egypt. Transgenic chickens were generated as described below and each group of birds was housed separately at containment level 4 isolators. Food and water were provided *ad libitum*, and general animal care was provided by the animal house staff as required for each groups.

Generation of Transgenic Chickens

Mosaic-transgenic chicken embryos were generated by inoculation of 1 million RCASBP(A)-chIFIT5-infected DF-1 cells or non-infectious DF-1 cells using 24G needs at day 2 post-embryonation in SPF chicken eggs. Embryos were fixed for 2 h post-inoculation before incubation at 37°C with 60–80% humidity in rotating incubator (twice daily). Transgenic embryos were allowed to hatch naturally at 21 days of incubation or were manually hatched on 22 days of embryonation.

Challenge Experimental Design

Experiment 1: Virus Dose Optimization

To effectively monitor the dose of viruses that can either induce clinical signs or mortality, a total of 10 SPF chicks (12 days old) were individual challenged with a dose of 10^4, 10^5, 10^6 EID_{50} of HPAIV-H5N1. Similarly, vNDV was used to challenge 10 SPF chicks with a dose of 10^4, 10^5, 10^6 EID_{50} in isolation units under biosafety level 4 conditions, and disease was monitored in all groups for 11 days for the appearance of clinical signs, weight gain, feed intake and mortalities in all groups. Birds were monitored for the presence of clinical sign and symptoms twice daily which were recorded as clinical scores 1 (no clinical signs), 2 (mild clinical signs), 3 (severe clinical signs), or 4 (dead/mortalities), as described previously (20, 21). At day 11 post-infection, the remaining animals were humanly euthanized.

Experiment 2: Transgenic Chickens and Virus Challenge

A total of 11 RCASBP(A)-chIFIT5 transgenic chicks (chIFIT5-HPAIV/vNDV +ve), 20 mock-inoculated chicks (mock-HPAIV/vNDV +ve) were either challenged with 10^4 EID_{50} HPAIV or 10^5 EID_{50} vNDV (clinical doses) on 12 days of age (1st day virus infection). Correspondingly, 10 chicks were kept as a naïve control group that were neither inoculated with retroviruses nor challenged with HPAIV or vNDV (mock-HPAIV/vNDV –ve). Before second challenge, a naïve group (Naïve-HPAIV/vNDV +ve) containing 4 chicks for HPAIV group and 3 chicks for NDV group was introduced. Except mock-HPAIV/vNDV –ve, individual birds in all groups were challenged with 10^6 EID_{50} of HPAIV and vNDV. Disease was monitored for next 10 days for the appearance of clinical signs, weight gain, feed intake and mortalities in all groups. Birds were monitored for the presence of symptoms twice daily, and clinical signs were recorded as clinical scores 1 (no clinical signs), 2 (mild clinical signs), 3 (severe clinical signs), 4 (dead), as was described previously (20). Three birds from chIFIT5-HPAIV/vNDV +ve and two chicks from mock-HPAIV/vNDV +ve were sacrificed for comparison between transgenic and wild type birds. The experiment was terminated at day 17 post-challenge and all remaining animals were euthanized.

Confirmation of Transgene Expression

Total RNA was extracted from trachea, which were collected from transgenic and non-transgenic chickens using TRIzol reagents (Invitrogen, Carlsbad, CA, USA). A total of 200 ng of RNA was used in PCR reactions using SuperScript® III Platinum® SYBR® Green One-Step qRT-PCR Kit (Invitrogen, Carlsbad, CA, USA) as we demonstrated earlier (5). The abundance of specific chIFIT5 mRNA was compared to the 28S rRNA in the Applied Biosystems Prism 7500 system. The reaction was carried out using the thermo profile reported earlier (5).

Expression of Innate Immune Genes

In order to determine the expression of innate immune genes, total RNA was extracted as described above using TRIzol reagents (Invitrogen, Carlsbad, CA, USA). A total of 200 ng of RNA was used in PCR reactions using SuperScript® III Platinum® SYBR® Green One-Step qRT-PCR Kit (Invitrogen, Carlsbad, CA, USA). The abundances of specific innate immune gene mRNA in trachea from transgenic ($n = 05$) and non-transgenic ($n = 05$) from both virus (HPAIV and vNDV) and mock-infected birds were compared to corresponding 28S rRNA and the average fold changes were determined (**Supplementary Table 1**). The reaction was carried out in ABI 7500 light cycler using the thermo profile described earlier (5). Primers for innate immune genes are provided in Supplementary Material.

Processing of Swab Samples

Cloacal and oropharyngeal swabs were collected in 1 mL of 15% BHIB with antibiotics (10,000 IU/mL Penicillin G + 100 µg/mL Gentamycin + 20 µg/mL Amphotericin B) and were kept on ice, and then filtered through a 0.2 µm filter. The filtered material was stored at −80°C until all samples were collected, and then were subjected to HA as described previously (22).

Histopathology

Selected tissues including trachea, brain, spleen, kidney and liver were collected and fixed by immersion in 10% neutral buffered formalin at room temperature for 48 h followed by processing and embedding in paraffin wax. Tissue sections of 5 µm were stained with Haematoxylin & Eosin and examined for microscopic lesions under light microscope.

Statistical Analysis

Pairwise comparisons of treated and control groups were performed using Student's *t*-test. Kaplan-Meier analysis was performed to calculate the survival rates. All statistical tests were conducted in the GraphPad Prism 7 (GraphPad Software, La Jolla, CA, USA).

Ethics Statement

All animal studies and procedures were carried out in strict accordance with the guidance and regulations of European and United Kingdom Home Office regulations. As part of this process, the work has undergone scrutiny and approval by the Animal Welfare and Ethical Review Body (AWERB) at The Pirbright Institute, UK.

RESULTS

Effective and Constitutive Expression of Transgene Using RCAS Vector System

We have recently demonstrated that chicken IFIT5 is a crucial host restriction factor and can effectively subvert the replication of negative sense single stranded RNA viruses *in vitro* and *in ovo* (5). We next sought to investigate the potential of this antiviral protein in interfering virus replication *in vivo* and to propose a genetic marker of resistance against RNA viruses in poultry. For this purpose, efforts were made to generate transgenic chickens stably expressing chIFIT5, and to determine the antiviral potential of chIFIT5. For this purpose, we applied avian retroviruses (avian leukosis virus, ALV) vector-based expression system to assess impact of chIFIT5 gene against virus challenges in developing chicks. Specifically, the replication-competent and avian-origin RCAS (replication competent ALV long terminal repeats with a splice acceptor) system was applied to generate mosaic transgenic chicken (20, 23). The transgenes (GFP and chIFIT5) were expressed by the splice acceptor (SA) signal of the *src* viral oncogene, which were inserted between the unique polylinker sites as depicted in **Figure 1A**.

Initially, a reporter virus construct (RCASBP(A)-eGFP) was generated to monitor *in vitro* rescuing and progression of the virus. In addition, we constructed RCASBP(A)-chIFIT5 recombinant virus to generate mosaic-transgenic chicken embryos that are constitutively expressing chIFIT5.

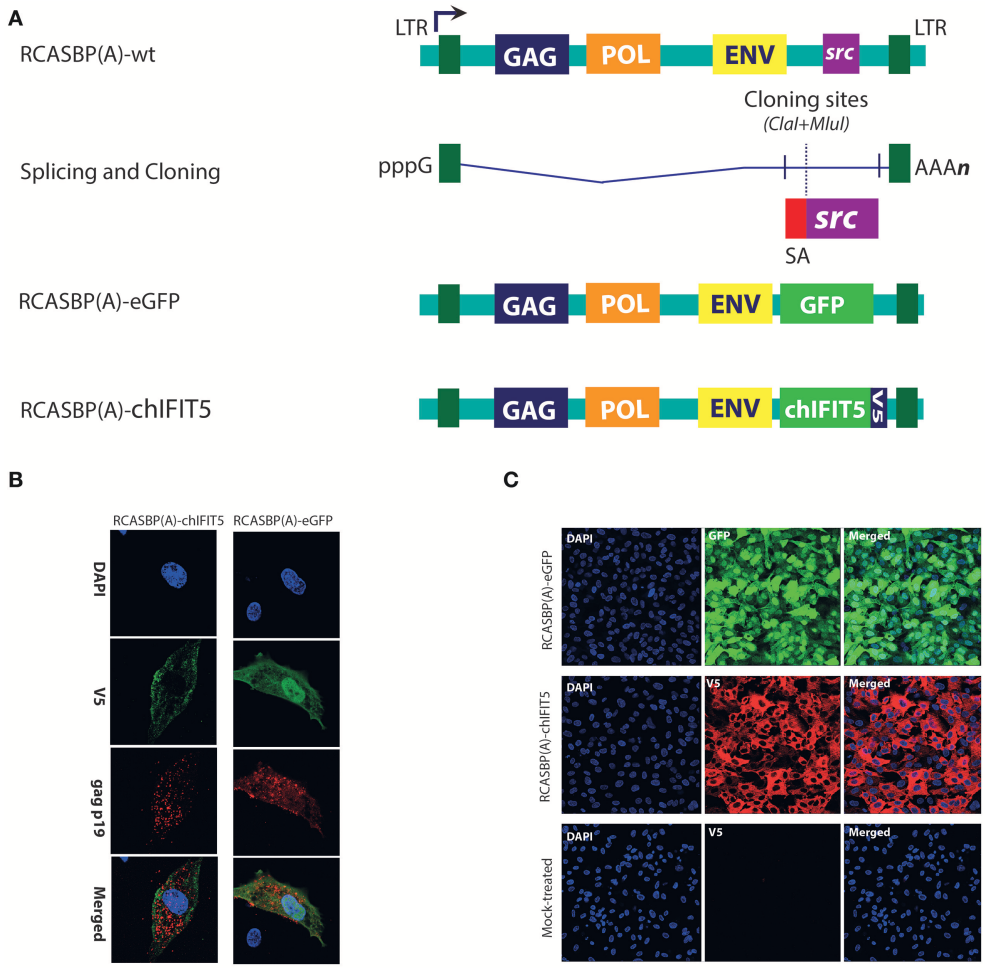

FIGURE 1 | Generation and rescue of recombinant retroviruses expressing marker gene (GFP), and chIFIT5. **(A)** A schema for the generation of recombinant RCAS viruses in which *src* gene was replaced with either GFP, or chIFIT5. **(B)** Retroviruses were rescued in DF-1 cells and stained for retroviral structural gag protein and V5-taged fused to the chIFIT5, indicating the specific replication-competency of these retroviruses. **(C)** Immunofluorescence staining of the transgene in chicken fibroblasts expanded from individual clones expressing RCAS-mediated GFP and IFIT5 indicating stable and substantial expression of these proteins.

Both viruses were rescued in chicken embryo fibroblasts (DF-1) and replication was assessed by monitoring viral structural protein (gag) and transgene; GFP and V5-tagged chIFIT5, simultaneously (**Figure 1B**). Cell clones expressing RCAS-mediated GFP and chIFIT5 were individually and clonally expanded to obtain require stock density for transgenic embryo generation. Immunofluorescence staining of the transgene in chicken fibroblasts (**Figure 1C**) indicate stable and substantial expression of these proteins. These validated infectious chicken fibroblasts were used to generate transgenic chicken embryos.

Clinical and Lethal Dose Assessment for HPAIV and vNDV

HPAIV and vNDV strains cause severe infections and the clinical outcome of infection depends upon several factors including nature of the virus and genetics of the host (24). Based on the surface glycoprotein genes (haemagglutinin (HA) and fusion (F) genes), influenza and NDV can be divided into different subtypes, pathotypes, clades (**Figure 2A**) and genotypes (**Figure 2B**), respectively. Viruses belonging to H5-subtype that possess polybasic residues at the hemagglutinin protein cleavage site are reported to be highly pathogenic for both chickens and human (15), whereas Genotype VII strains of NDV are most prevalent and one of the major pathogen for clinical ND infections in chickens, around the globe (14).

Owing to direct correlation of virus dose with the severity of the clinical infections, we first determined the titre of HPAIV and vNDV inoculum, which induce clinical disease in chickens. Groups of ten SPF-chickens (12 days old) were challenged with different dosses (10^4, 10^5, or 10^6 EID_{50}) of HPAIV or vNDV and clinical disease scores were recorded until 11 days post-infection. Based on the level of disease severity, 10^4 EID_{50} inoculum of H5N1 HPAIV induced clinical signs and was therefore considered as clinical dose. However, rapid death (lethal dose) was observed in birds inoculated with 10^6 EID_{50} dose of H5N1 HPAIV (**Figure 2C**). For vNDV, most clinical signs were observed when 10^5 EID_{50} virus particles (clinical dose) were used whereas a substantial mortality was observed in chickens, which were inoculated with 10^6 EID_{50} virus dose (lethal dose) (**Figure 2D**). Prototype strains of H5N1 clade 2.2.1.2 (A/chicken/Egypt_128s_2012) and vNDV genotype VIId (NDV-B7-RLQP-CH-EG-12) with optimized doses 10^4 EID_{50} and 10^5 EID_{50} were used as inoculum to challenge transgenic chickens to demonstrate antiviral potential of IFIT5.

Improved Survivability of Transgenic Chickens Expressing ChIFIT5 Following Infection With HPAIV and vNDV

Mosaic transgenic chickens were generated by inoculating 2-day-old embryonated SPF eggs with recombinant RCAS virus-infected CEF expressing chIFIT5 (as shown in **Figure 1C**) or were inoculated with non-infectious CEF. Chicks hatched from infected embryonated eggs were reared in isolators until 12 days of age before challenge with clinical dose of HPAIV or vNDV at 12 days of age followed by lethal dose on 20 days of chick's age (8 days post first infection) (**Figure 3A**). Onset of clinical disease and health parameters were assessed until the end of experiment in IFIT5-expressing virus-challenged (chIFIT5-HPAIV/vNDV +ve), mock-inoculated and virus-challenged (mock-HPAIV/vNDV +ve) and mock-inoculated and non-virus-challenged groups (mock-HPAIV/vNDV –ve). Additionally, in order to delineate priming effect of clinical dose of the virus on the lethal dose, a naïve SPF group of chicken was included and challenged with lethal dose only.

While no detrimental effect of the chIFIT5 expression was observed on the embryonic development, hatchability of RCAS-chIFIT5 transgenic eggs was compromised compared to mock groups in two independently performed experiments. A total of 3 manually hatched and 6 naturally hatched chicks in RCAS-chIFIT5 group were weak and unhealthy, unable to drink, dehydrated and shown visceral gout, and all were humanly euthanized due to welfare reasons before the clinical challenge (12 days of hatching). No further macroscopic lesions or pathologies were noticed on necropsy investigation of these euthanized birds (data not shown). Interestingly, all RCAS-chIFIT5 transgenic chicks were hatched with substantially reduced body weight (**Figure 3B**). Except chicks ($n = 6$) that were died at 2nd, 7th or 9th day of hatching, RCAS-chIFIT5 transgenic chicks progressively regained the body weight and shown comparable weight with mock controls before first virus challenge at day 12 post hatch (**Figure 3C**).

A total of 30% mock-inoculated chicks were succumbed to HPAIV infection within 4 days of infection. However, RCAS-chIFIT5 transgenic chicks were fully protected with the clinical dose of HPAIV (chIFIT5-HPAIV +ve) as was observed in negative control (Mock-HPAIV –ve) (**Figure 3D**). Correspondingly, overexpression of IFIT5 protected all birds whereas 90% mock-inoculated chickens showed no apparent clinical disease when inoculated with clinical dose of vNDV (**Figure 3E**). In comparison, the group challenged with lethal dose of HPAIV showed rapid and sever disease signs and were humanly euthanized. Suggesting lethal dose of HPAI override endogenous levels of host innate responses including overexpression of IFIT5 (**Figure 3F**). Albeit corresponding mortality was observed in chicks challenged with lethal dose of vNDV, the lethality of the virus was meliorated for 4 days in RCAS-chIFIT5 transgenic chicks (**Figure 3G**). In order to exclude the possibility of priming effect of clinical dose on the protective efficacy of IFIT5 against lethal dose, naïve chicks of same age were challenged with corresponding lethal doses of HPAIV and vNDV (Naïve-HPAIV/vNDV +ve). As expected, 100% HPIAV and 66% vNDV challenged naïve chicks showed sever clinical signs and were culled or suddenly died due to infection within three days of challenge (**Figures 3F,G**). Taken together, the results demonstrate the functional role of IFIT5 to progressively protect chicks from clinical doses of both RNA viruses; however, overexpression of IFIT5 is insufficient as a stand-alone antiviral host factor that could completely protect chickens from the lethal dose of HPAIV and vNDV.

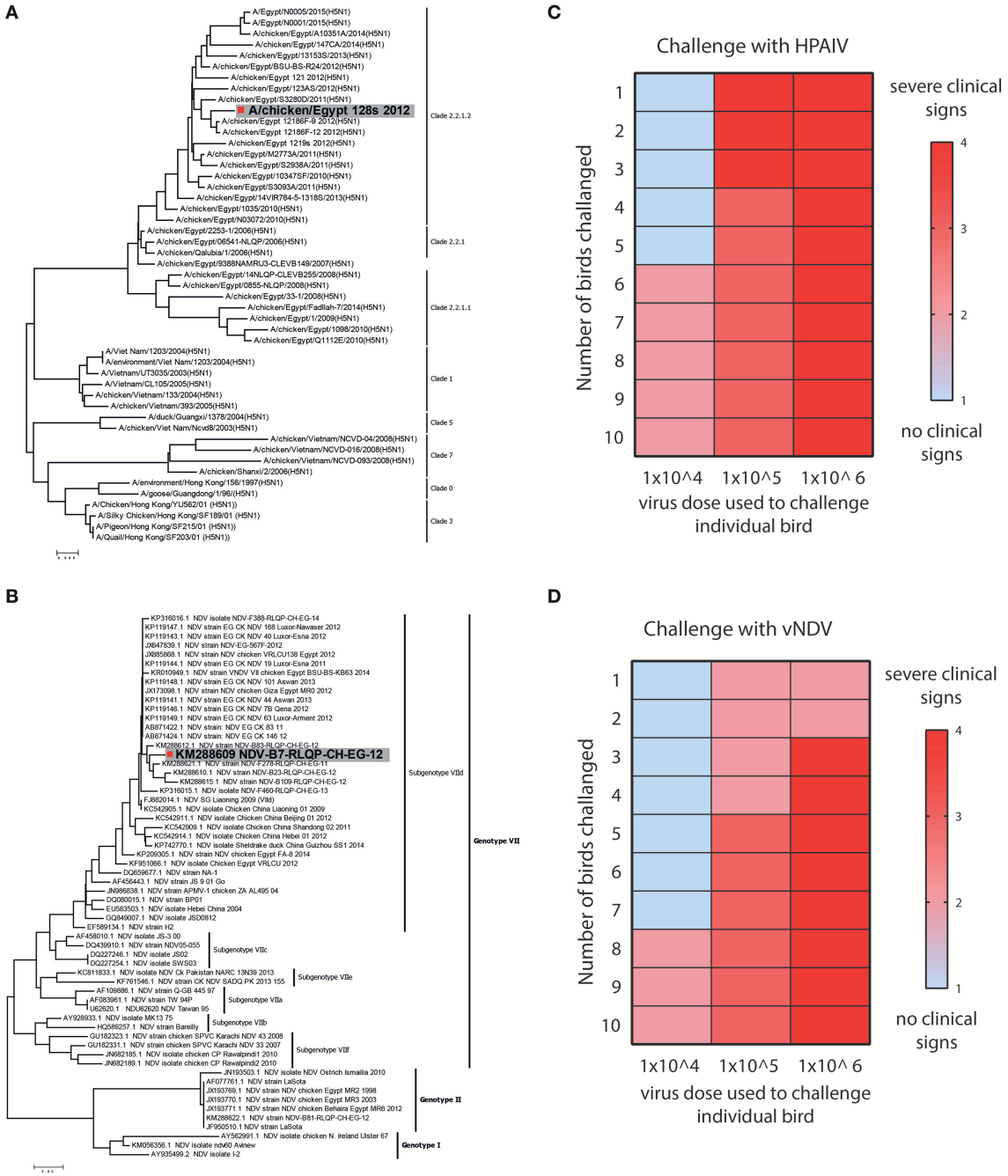

FIGURE 2 | Strain selection and clinical and lethal doses assessment for HPAIV and vNDV. **(A)** Bioinformatics analysis of representative strains of H5N1 and **(B)** velogenic strains of NDV. Strains used in this study are colored gray. **(C)** Twelve days old SPF-chickens were challenged with the EID_{50} of 10^4, 10^5, and 10^6 HPAIV or **(D)** vNDV and the disease was monitored until 11 days post-infection. Color gradient represent the severity of clinical signs.

Transgenic Chickens Expressing ChIFIT5 Showed Protection From Clinical Disease Signs When Challenged With Sub-lethal Dose of HPAIV and vNDV

Intriguingly, IFIT5 fully protected transgenic chicks from morbid clinical signs when exposed to sub-lethal dose (10^4 EID_{50}) of HPAIV (**Figure 4**). In contrast, mock group (Mock-HPAIV +ve) showed sever clinical signs as early as third day following inoculation with clinical virus dose (10^4 EID_{50}). The clinical signs were further exacerbated when birds were follow-on exposed to lethal dose of HPAIV. While chicks in negative control (Mock-HPAIV –ve) remained healthy and corresponding challenged group shown the most clinical signs, overexpression of IFIT5

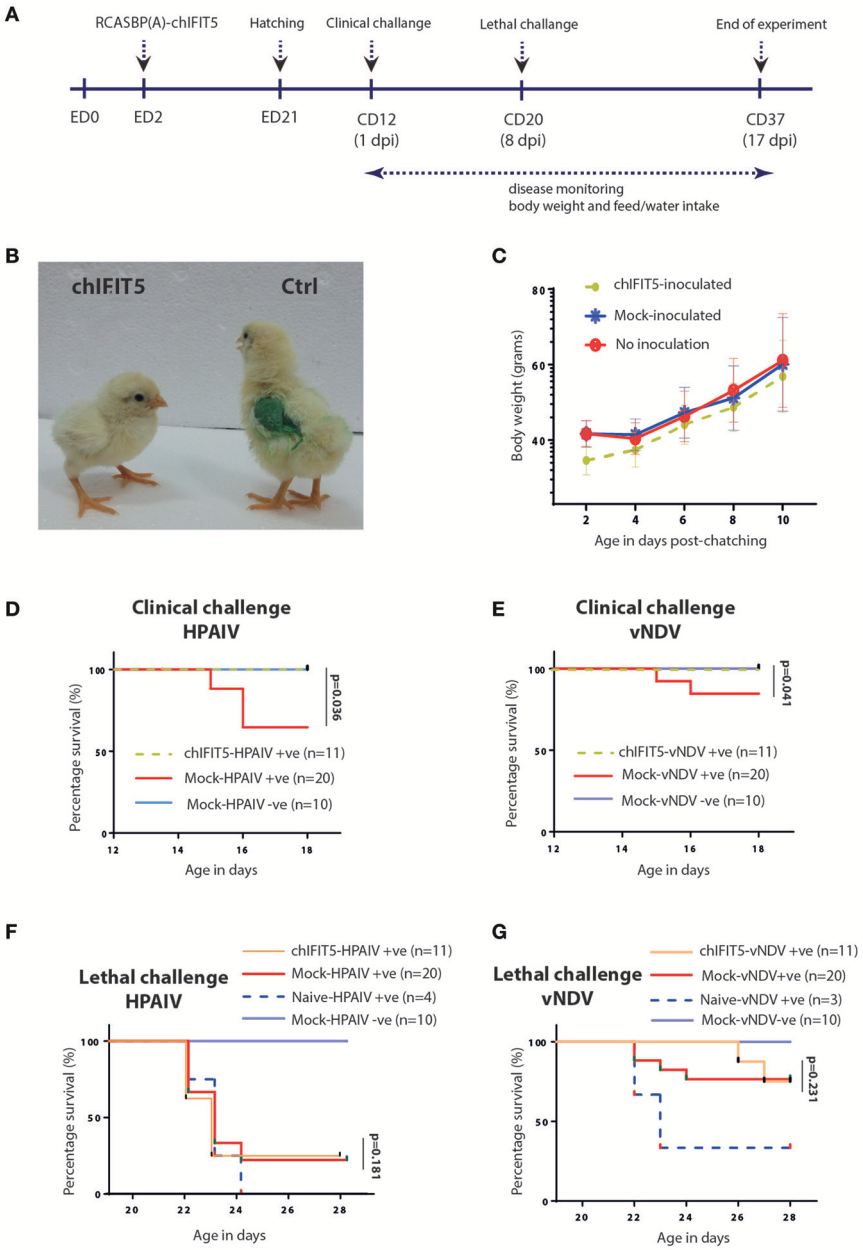

FIGURE 3 | Generation of transgenic chickens and impact of chIFIT5 on physiological parameters of chicken. **(A)** Schema representing the time of transgenesis and challenge experiment. **(B)** Comparison of the body mass of chIFIT5 expressing transgenic chicken and control chicken. **(C)** Wait gain in transgenic and control chickens post-hatching and pre-challenge. **(D)** Survival curve of chickens against clinical dose of HPAIV, **(E)** vNDV, **(F)** lethal dose of HPAIV and **(G)** vNDV.

has substantially reduced the appearance of the clinical outcomes of HPAIV infections. These effects were markedly observed in vNDV infected RCAS-chIFIT5 transgenic chicks. Not only that IFIT5 expressing chicks were protected from the clinical challenge but substantially from the lethal challenge (**Figure 4**). Importantly, the clinical signs, which appeared in the RCAS-chIFIT5 transgenic chicks, were delayed by at least by 10 days (**Figure 5**). These results highlight the possible roles of IFIT5 in meliorating the clinical outcome of two highly pathogenic viruses in the poultry, influenza and NDV.

Confirmation of Transgene Expression and Reduced Virus Shedding in IFIT5-Expressing Transgenic Chickens Challenged With HPAIV and vNDV

In order to demonstrate the successful expression of chIFIT5 in transgenic chickens, we exploited the codon-optimized version of RCAS-mediated chIFIT5 gene (5). A quantitative PCR that specifically detect codon-optimized chIFIT5 was established to demonstrate the expression of chIFIT5 as transgene and

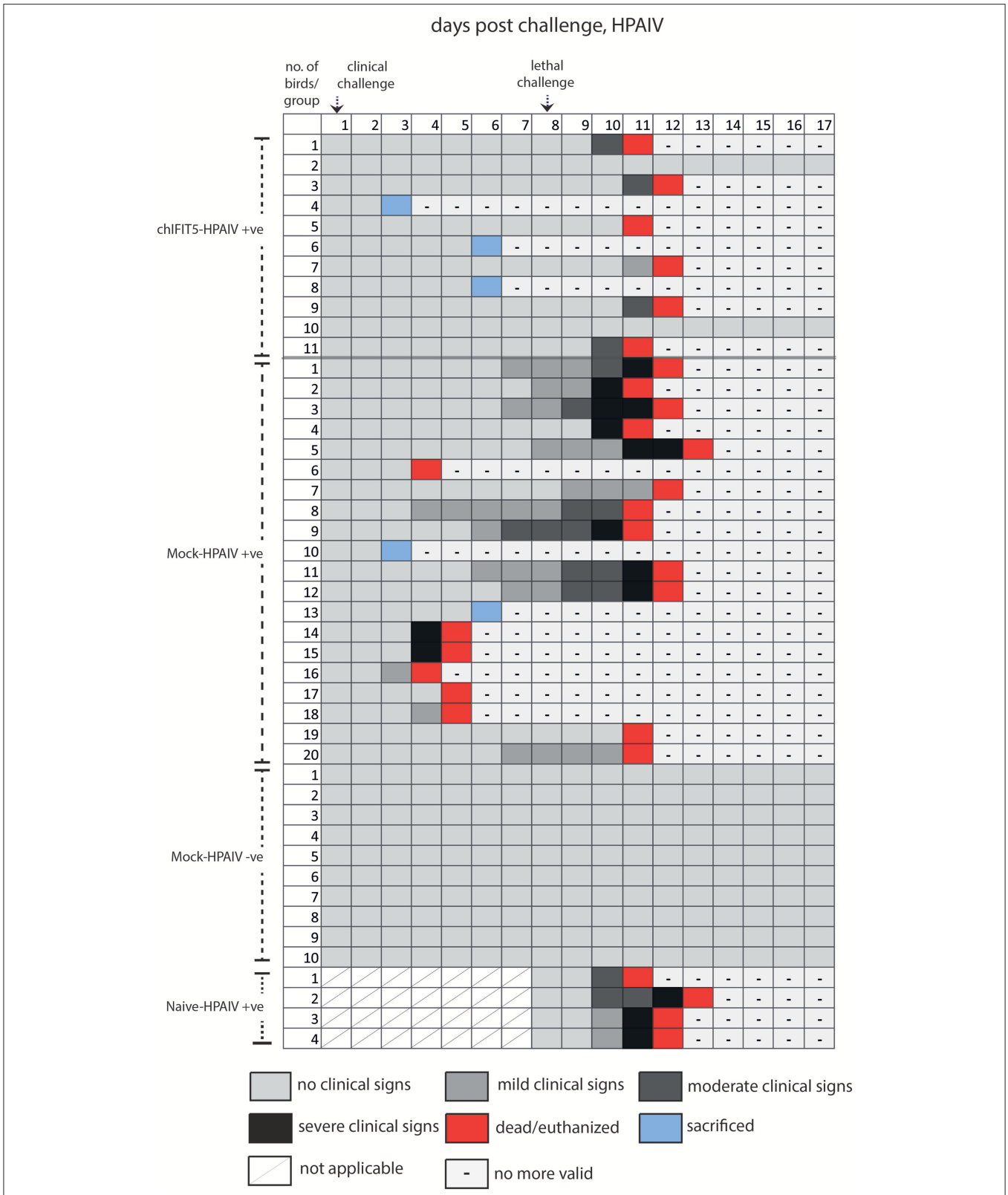

FIGURE 4 | Clinical signs of individual chicken in different groups pre- and post-clinical and lethal challenge induced by the HPAIV.

to differentiate the transgene from endogenously expressed chIFIT5. Using this assay, we detected a significantly higher level of IFIT5 in tracheal RNA collected from transgenic chicken compared to corresponding non-transgenic RNA. Relative to HPAIV-infected transgenic chicken (**Figure 6A**), the expression of chIFIT5 was significantly higher in vNDV-infected transgenic chickens (**Figure 6B**). Collectively, these data demonstrate the successful generation of transgenic chicken and the expression of transgene.

We next assessed if chIFIT5-mediated reduction in the clinical picture reflect upon the virus shedding in two most common routes of virus transmission and shedding; oral and cloacal routes. For this purpose, both cloacal and oropharyngeal swabs were collected from all three groups (chIFIT5-vNDV+ve, and mock-vNDV +ve, and mock-vNDV –ve) before the challenge and every day post-clinical and post-lethal dose challenges. Assessment of virus titres in the swab samples indicated a substantial shedding of both vNDV and HPAIV in cloacal secretions (**Figures 6C,D**). However, transgenic chickens, constitutively expressing chIFIT5 showed substantial reduction in both shedding titres (NDV: 8 log2 vs. 4 log2 in control, HPIAV; 3 log2 vs. 12 log2 in control) and the duration of shedding period following challenge with vNDV and HPAIV. In comparison to vNDV challenged chickens, the virus shedding was markedly reduced in cloacal swabs of HPAIV-challenged chicks.

Since shedding of both under-study viruses reported by the respiratory route of the chicken (22), we next assessed the magnitude of virus shedding in oropharyngeal swabs. Virus quantification analysis indicated secretion of both viruses (vNDV and HPAIV) in mock-transgenic and viruses-infected animals. However, intriguingly, the shedding of the viruses was fully blocked in chickens, which were engineered to constitutively express chIFIT5 in both clinical and lethal doses challenge (**Figures 6E,F**). A relatively low surge in virus shedding (1 log2) was observed in chickens that were challenged with lethal dose of HPAIV, which was subsided in 2 days. Collectively, these finding suggest that chIFIT5 play decisive roles in virus replication especially in the respiratory epithelial cells resulting in lower shedding levels in of viruses in the buccal cavity.

The ChIFIT5-Expressing Transgenic Chickens Show Improved Virus-Induced Microscopic Pathologies and These Are Not Associated With Enhanced Innate Immunity

In order to estimate the magnitude of histopathological changes induced by these pathogenic viruses and the level of protection afforded by the stably expressing chIFIT5, organs (trachea, brain, spleen, kidneys and liver) were collected and histopathologically examined both at the clinical and lethal doses and compared with non-treated and mock controls. As expected, examination of trachea showed marked pathological lesions in mocked-transgenic and HPAIV and vNDV-challenged chickens including focal necrosis of lamina epithelialis mucosa, oedema in the lamina propria and congestion of mucosal blood vessels (after clinical-challenge). Severe histopathological alterations were also noticed after lethal-challenge including focal necrosis of the mucosa and accumulation of mucous exudate in the tracheal lumen. On the other hand, trachea collected from chickens, which were transgenically expressing chIFIT5 and infected with HPAIV and vNDV showed no histopathological changes except slight congested blood vessels, slight edema in the lamina propria/submucosa layers (**Figures 7A–T**). Congestion of cerebral blood vessel, necrosis of neurons and neuronophagia were observed in brain collected from mocked-transgenic and vNDV and HPAIV-challenged chickens. In brain examined from chicken, which were transgenically expressing chIFIT5 and infected with vNDV and HPAIV, showed lesions of slight cellular oedema and necrosis of sporadic neurons (**Figures 7A–T**). Corresponding histopathological lesions were observed in spleen, kidneys and liver (**Supplementary Figure 1**). Taken together, these results demonstrate that constitutive expression of chIFIT5 protects different organs against virus replication, which collectively reflect upon virus shedding, ameliorated clinical outcome and improved health status.

Owing to association of IFIT5 mediated induction of innate immunity (10, 13), we next investigated whether the improved protection in transgenic chickens was mediated by the innate immunity. For this purpose, total RNA was extracted from trachea, because both viruses can cause respiratory signs, and expression levels of five innate immune genes were determined. These genes were chosen based on their expression dynamics against viruses, and existing assays (1). Direct comparison of expression of innate immune genes indicated non-significant differences between transgenic (over-expressing chIFIT5) and non-transgenic (mock expressing) (**Supplementary Table 1**). These differences were not only noticed in vNDV challenged birds, which show enhanced protection but also in HPAIV-challenged birds, that were susceptible to influenza infections. These results propose that chIFIT5-confered protection was not associated with the induced innate immune responses and may link to direct antiviral affect of chIFIT5 (5, 9).

DISCUSSION

Poultry production is crucial for economy and food security for growing global human population. While the productivity of poultry has increased significantly over the years through selective breeding and improved genetics, the threats imposed by emerging and re-emerging pathogens have increased significantly especially since the introduction of intensive poultry-raising systems (25). Among these pathogens, avian viruses are at the forefront of constraints to enhanced productivity including avian influenza virus, NDV and infectious bronchitis virus amongst others. Upon infection with viruses, the innate immune responses mainly mediated by IFN-regulated proteins establish profound antiviral state in the host, and defines the gravity clinical disease outcome and associated decrease in productivity and mortalities. Avian species, especially chicken, are unique in the nature and dynamics of innate immunity (1) and are known to play crucial roles in the evolution and emergence of influenza viruses and their potential to cause infections in human (26).

Interestingly, chickens are lacking essential components of innate immune system (e.g., RIG-I, IRF3, IRF9); they yet mount profound innate immune responses against virus infections

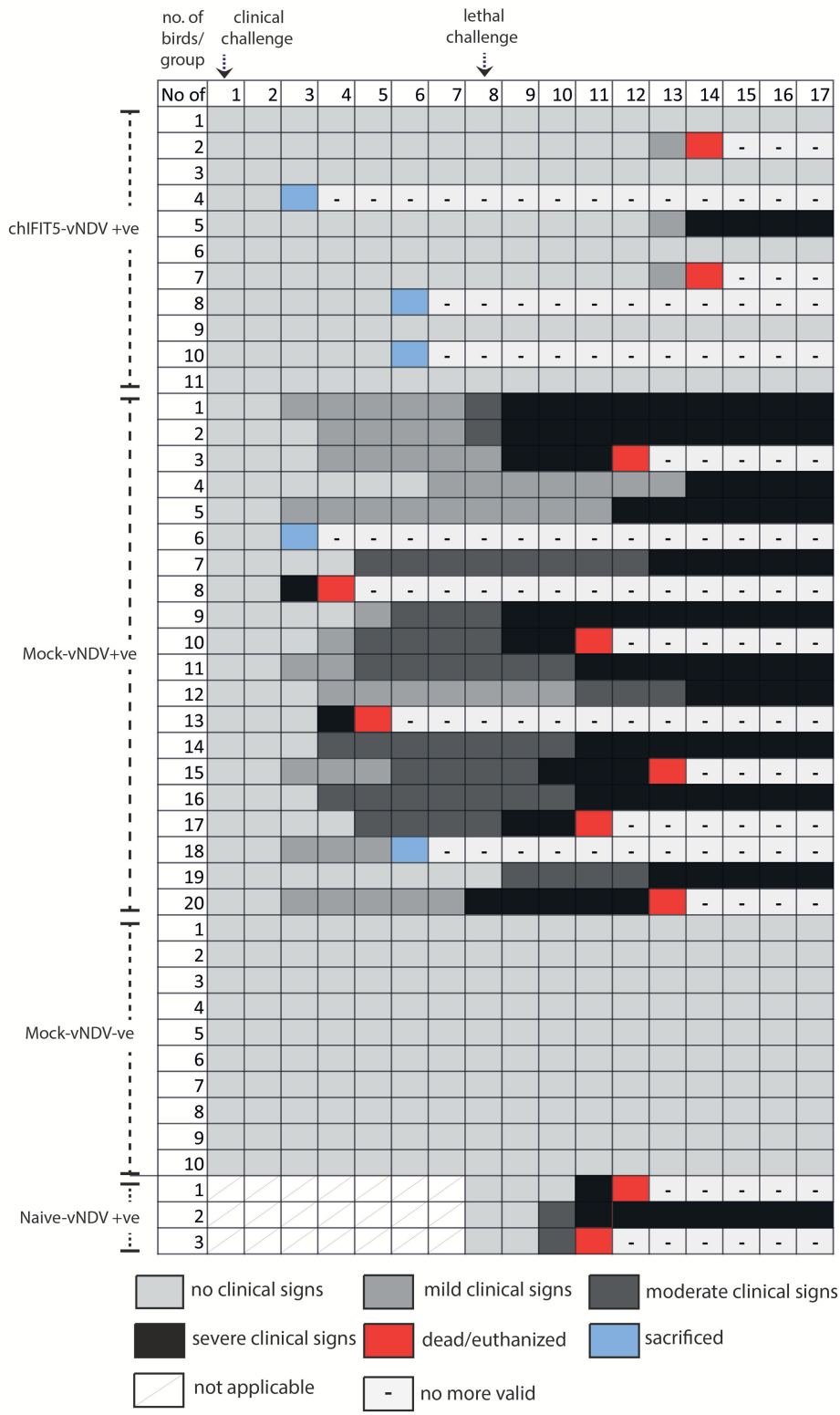

FIGURE 5 | Clinical signs of individual chicken in different groups pre- and post-clinical and lethal challenge induced by the vNDV.

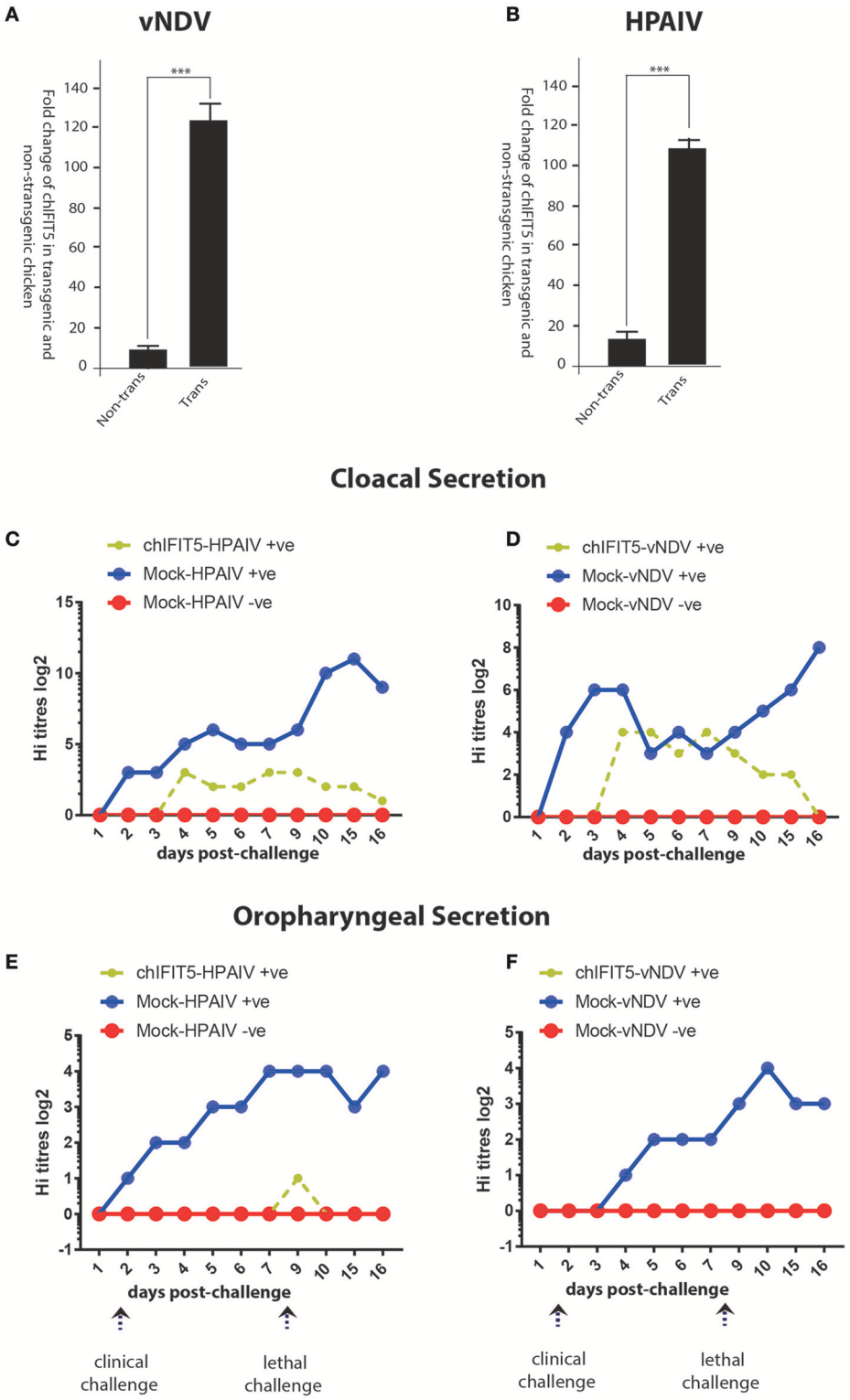

FIGURE 6 | Expression of the transgene (chIFIT5), in vNDV-infected transgenic **(A)** and HPAIV-infected transgenic **(B)**, compared to non-transgenic chicken. Quantitative assessment of virus shedding in cloacal section for the **(C)** vNDV, **(D)** HPAIV and in oropharyngeal secretion for the **(E)** vNDV and **(F)** HPAIV in transgenic chickens expressing chIFIT5-challenged with virus (chIFIT5-vNDV/HPAIV +ve), mock-transgenic-virus challenged (mock-vNDV/HPAIV+ve) and mock control (mock-vNDV/HPAIV –ve). Days of clinical and lethal challenges are marked with arrows. *** indicate the level of significance at $p > 0.05$.

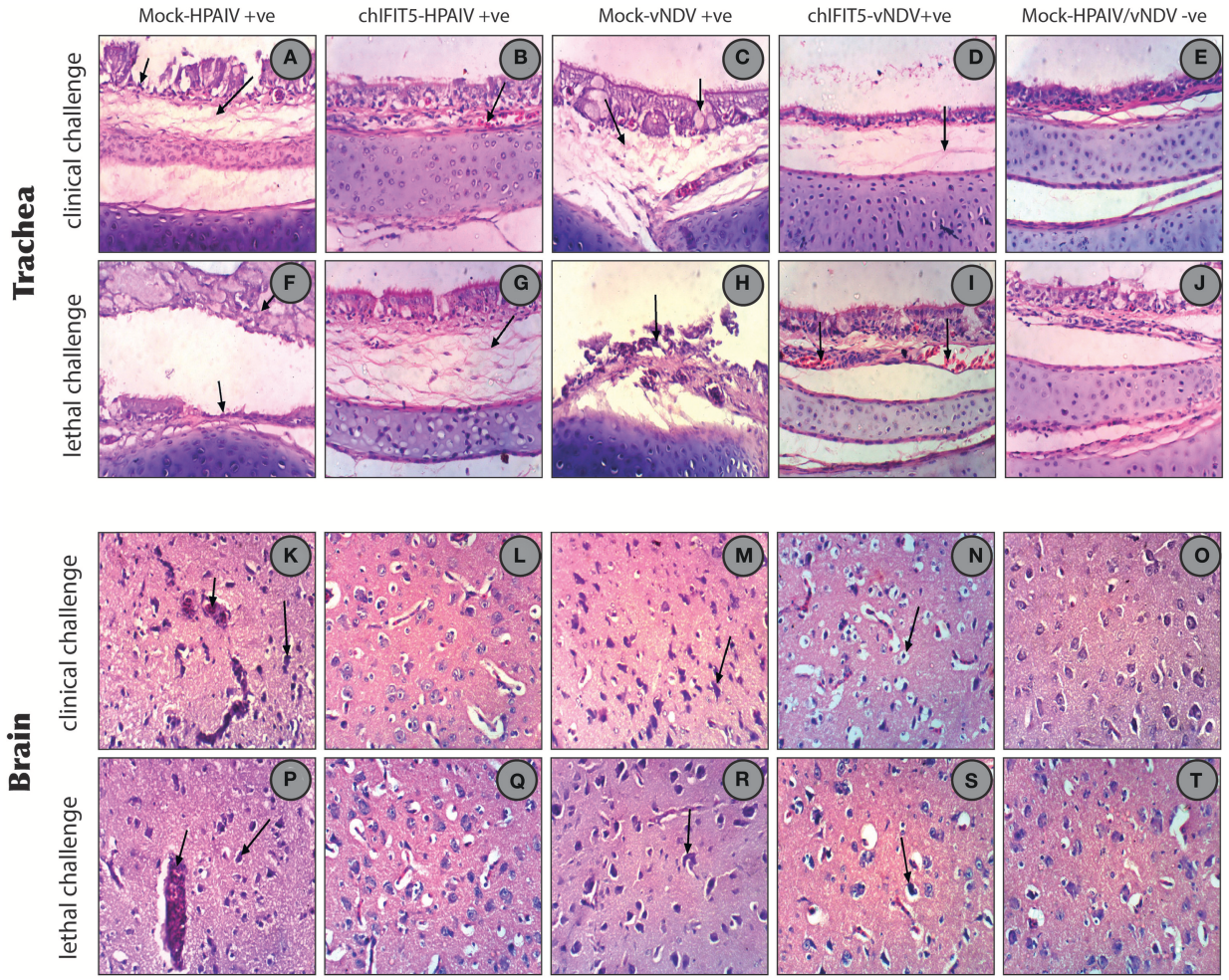

FIGURE 7 | (A) Trachea of chicken infected with HPAIV (clinical challenged) showing focal necrosis of lamina epithelialis (small arrow) and oedema in the lamina propria/submucosa layer (large arrow). **(B)** Trachea of chicken expressing chIFIT5 and infected with HPAIV showing slight congested blood vessel. **(C)** Trachea of chicken infected with vNDV (clinical challenged) showing activation of mucous secreting glands (small arrow) and oedema in the lamina propria/submucosa layers (large arrow). **(D)** Trachea of chicken expressing chIFIT5 and infected with vNDV showing slight oedema in the lamina propria/submucosa layers. **(E)** Trachea of control chicken showing the normal histological layers. **(F)** Trachea of chicken infected with HPAIV (lethal challenged) showing focal necrosis of the mucosa (small arrow) and accumulation of mucous exudate in the lumen (large arrow). **(G)** Trachea of chicken injected expressing chIFIT5 and infected with HPAIV (lethal challenge) showing oedema in the lamina propria/submucosa layers. **(H)** Trachea of chicken infected with vNDV (lethal challenge) showing necrosis of the mucosa (arrow). **(I)** Trachea of chicken expressing chIFIT5 and infected with vNDV (lethal challenge) showing congested blood vessels. **(J)** Trachea of control chicken showing the normal histological layers. **(K)** Brain of chicken expressing chIFIT5 and infected with HPAIV (clinical challenge) showing congestion of cerebral blood vessel (small arrow) and necrosis of neurons (large arrow). **(L)** Brain of chicken expressing chIFIT5 and infected with HPAIV (clinical challenged) showing no histopathological changes. **(M)** Brain of chicken expressing chIFIT5 and infected with HPAIV (clinical challenged) showing necrosis of neurons (arrow). **(N)** Brain of chicken expressing chIFIT5 and infected with vNDV (clinical challenge) showing cellular oedema. **(O)** Brain of control chicken showing no histopathological changes. (**P**) Brain of chicken expressing chIFIT5 and infected with HPAI (lethal challenge) showing congestion of cerebral blood vessel (small arrow) and necrosis of neurons (large arrow). **(Q)** Brain of chicken expressing chIFIT5 and infected with HPAIV (lethal challenged) showing no histopathological changes. **(R)** Brain of chicken expressing chIFIT5 and infected with vNDV (lethal challenged) showing necrosis of neurons and neuronophagia (arrow). **(S)** Brain of chicken expressing chIFIT5 and infected with vNDV (lethal challenged) showing necrosis of some neurons and neuronophagia. **(T)** Brain of control chicken showing no histopathological changes. (All images were stained with H&E and are imaged at x400).

(1). Efforts have been made to delineate underlying molecular factors that uniquely control the virus-mediated innate immune-induction and have provided mechanistic insights, which differ between avian and mammals. Further understanding the alternative means immune regulation and antiviral defenses in chicken could establish the foundation to control avian viral disease and the chicken-mediated emergence of zoonotic infections such as influenza viruses (26).

Recently, in an effort to explore the functional implication of IFIT proteins in chickens, we reported that chicken encodes single IFIT5 proteins compared to several in humans and mice. This highly virus- and IFN-inducible protein interacted with RNA carrying a triphosphate group on its 5′ terminus (ppp-RNA) (5). These structures are present in the native form of negative sense viral genomics RNA. It is hypothesized that the interaction of IFIT5 with the 5′-ppp containing viral RNA potentially

interferes with the transcription and subsequent translation of viral proteins (5). These interferences cooperatively impact negatively on the replication kinetics of RNA viruses. Most of these studies we conducted either in the cell culture models or *in ovo*, highlighting the potential of chIFIT5 as essential host antiviral restriction factor. To further investigate the antiviral activity of IFIT5 *in vivo*, we generated mosaic transgenic chicken that stably and constitutively express chIFIT5. These chickens were used to test the antiviral impact of IFIT5 on two highly pathogenic viruses; HPAIV and vNDV.

The mosaic transgenic chickens overexpressing chIFIT5 provided strong evidences that this cytokine possesses profound antiviral activities *in vivo*. These antiviral actions were sufficient to fully protect chicken against dose of viruses that otherwise cause clinical disease signs in chickens. Since the virus load in the field condition varies and the exposure of chickens to environmental stress contributes to the virus-induce pathologies, we additionally assess the impact of chIFIT5 overexpression on the pre-determined lethal dose (an amount virus dose that cause server disease and mortality in chickens). While over expression of chIFIT5 alone seems insufficient in affording complete protection from morbidity and mortality when challenged with "lethal dose (10^5-10^6 EID_{50})" of viruses. Nevertheless, the clinical outcome was substantially ameliorated when transgenic chickens were challenged with "clinal dose 10^4-10^5 EID_{50}." Furthermore, the results clearly ruled out the possibility that pre-exposure with "clinical dose" may have induced adaptive immune responses masking the impact of "lethal dose" on clinical outcome. These evidences clearly highlight the potential of innate immune in conferring resistance against HPAIV and vNDV.

It is noteworthy to mention that the protective role of chIFIT5 was assessed against two highly virulent viruses; highly pathogenic IAV and velogenic NDV. Both can cause up to 100% mortality in infected flocks. Therefore, it is plausible to hypothesize that the chIFIT5-alleviated morbidity against these highly pathogenic viruses may propose relatively profound impacts against viruses that are relatively less virulent, cause only clinical disease and low mortality. Additionally, vaccination of chIFIT5-expressing transgenic chicken may provide additional resistance to viruses, which warrant future investigation.

The challenge to generate transgenic chickens was mitigated by the use of RCAS-based retroviral gene transfer system. Based on previous studies (20, 27) and our recent report (5), retroviral-mediated transgene expression has been proposed as a convenient, economical and less laboratory-intensive system. Our *in vitro* investigation and *in ovo* assessments further confirmed the expression of transgenes in developing embryos and chicks. Additionally, we used qPCR to specifically detect chIFIT5 in tracheal RNA which is not only demonstrating the successful transgenesis but also re-enforcing our previous finding (5) that dictate the predominant expression of RCAS-mediated gene delivery in epithelial-enriched organs. While the RCAS-vector system is an efficient approach, it is by no means substitute for the genome edited-based (TALEN or CRISPR) transgenesis. It is therefore feasible that the phenotypic effect of chIFIT5 as antiviral may be profound in knocked-in primordial germinal cells and CRISPR/Cas9-generated transgenic chickens.

Overexpression of chIFIT5 has not only alleviated the manifestation of clinical disease signs in HPAIV and vNDV infected chickens but also reduced the viruses-induced pathological lesions and virus shedding. Since RCAS-based retroviral gene transfer system is predominantly effective in organs that are rich in endothelial cells (20, 27), we reasoned the complete blockage of virus shedding in trachea. This substantially reduced virus shedding correlated with the improved tracheal tissue health, which may highlight the expression and functional importance of chIFIT5 in mucosal surfaces. However, further investigations are warranted to ensure the enriched expression of this host factor in tracheal lining and its subsequent impact on virus replication. While a reduced body weight in transgenic chicks at hatching was observed, hatched chicks regained the weight swiftly and obtained comparable sizes to non-transgenic chicks. It requires additional investigations to fully delineate the mechanisms of this retarded embryo development; there are feasibilities that transgenically over-expression of the IFIT5 may interfere physiological and developmental processes of the chick. A single IFIT5 in chicken, compared to four or more in mammals, may likely to be restricted with its biological activities or may propose unconventional functions, which require future investigations.

Since previous reports (10, 13) indicate that human IFIT5 can positively regulate innate immune responses and hence inhibits viruses, we mapped chicken innate immune genes ($n = 5$; Mx, IFN-β, Viperin, IFI35, ADAP2) in transgenic chickens that were over-expressing chIFIT5. A non-significant difference was observed between transgenic and non-transgenic chicken. These finding propose existence of additional mechanisms that dictate the antiviral actions of chIFIT5 such as interaction with 5'-RNA and sequestration of viral RNA (5, 9, 10). Moreover, due to missing of additional IFIT genes in chicken (5), it is also plausible that chicken IFIT5 might carry functional plasticity for antiviral activities compared to human IFIT5, which require further research to delineate these mechanisms.

Taken together, we characterized the function of chIFIT5 in chicken and systemically analyzed the functional rationale for antiviral activities of chIFIT5 against RNA viruses using transgenic animal model. These finding propose the potential of innate immune in conferring resistance in chicken against viruses and provide evidences to generate future virus-resistance transgenic chicken for food security and to hamper transmission of zoonotic viruses to human.

AUTHOR CONTRIBUTIONS

MM conceived the project and wrote the manuscript. MM, MI, DS, MR, and HH designed experiments. MR, DS, and RE performed experiments. MM, MR, DS, RN, MI, and HH participated in data analyses and reviewed the manuscript.

FUNDING

This study was supported by the Biotechnology and Biological Sciences Research Council (BBSRC) (grant

numbers BB/M008681/1, BB/R012695/1, BB/L018853/1, BBS/E/I/00007034, BBS/E/I/00007035), and Culture Affairs and Mission Sector, Ministry of Higher Education, Government of Egypt. Additional financial support was provided by the British Council's Institutional Links programme between UK and Egypt (grant number 332228521) and Science and Technology Development Fund-Research Scientific Grant (STDF-STF, Project ID: 24231).

ACKNOWLEDGMENTS

We would like to thank Stephen H. Hughes for providing RCASBP(A)-ΔF1. MR was supported via PhD scholarship from Culture Affairs and Mission Sector, Ministry of Higher Education, Government of Egypt. We thank Risks Assessment Committee of The Pirbright Institute, for reviewing and approving the protocol to conduct animal experiments.

SUPPLEMENTARY MATERIAL

The Supplementary Material for this article can be found online at: https://www.frontiersin.org/articles/10.3389/fimmu.2018.02025/full#supplementary-material

Supplementary Figure 1 | Histopathological lesions in different organs collected from transgenic or non-stransgenic chickens and challenged or not with HPAIV or vNDV. Labeling on the X-axes indicates the treatment and on the Y-axes are levels of virus challenge (clinical or lethal). Please refer to figure 7 in the main manuscript for detailed descriptions on the lesions.

Supplementary Table 1 | Expression of innate immune genes in transgenic and non-transgenic chicken infected with under-study viruses.

REFERENCES

1. Santhakumar D, Rubbenstroth D, Martinez-Sobrido L, Munir M. Avian interferons and their antiviral effectors. *Front Immunol*. (2017) 8:49. doi: 10.3389/fimmu.2017.00049
2. Randall RE, Goodbourn S. Interferons and viruses: an interplay between induction, signalling, antiviral responses and virus countermeasures. *J Gen Virol*. (2008) 89:1–47. doi: 10.1099/vir.0.83391-0
3. Leung DW, Amarasinghe GK. When your cap matters: structural insights into self vs non-self-recognition of 5 ' RNA by immunomodulatory host proteins. *Curr Opin Struc Biol*. (2016) 36:133–41. doi: 10.1016/j.sbi.2016.02.001
4. Abbas YM, Pichmair A, Gorna MW, Superti-Furga G, Nagar B, Structural basis for viral 5 '-PPP-RNA recognition by human IFIT proteins. *Nature* (2013) 494:60–4. doi: 10.1038/nature11783.
5. Santhakumar D, Rohaim MAS, Hussein HA, Hawes P, Ferreira HL, Behboudi S, et al. Chicken interferon-induced protein with Tetratricopeptide repeats 5 antagonizes replication of RNA viruses. *Sci Rep*. (2018) 8:6794. doi: 10.1038/s41598-018-24905-y
6. Habjan M, Hubel PL. Lacerda L, Benda C, Holze C, Eberl CH, et al. Sequestration by IFIT1 impairs translation of 2 ' O-unmethylated capped RNA. *Plos Pathog*. (2013) 9:e1003663. doi: 10.1371/journal.ppat.1003663
7. Ganes S, Fensterl V. Interferon-induced Ifit proteins: their role in viral pathogenesis. *Cytokine* (2015) 89:2462–8. doi: 10.1128/JVI.02744-14
8. Liu Y, Zhang YB, Liu TK, Gui JF. Lineage-specific expansion of IFIT gene family: an insight into coevolution with IFN gene family. *PLoS ONE* (2013) 8:e66859. doi: 10.1371/journal.pone.0066859
9. Pichlmair A, Lassnig C, Eberle CA, Gorna MW, Baumann CL, Burkard TR, et al. IFIT1 is an antiviral protein that recognizes 5 '-triphosphate RNA. *Nat Immunol*. (2011) 12:624–30. doi: 10.1038/ni.2048
10. Diamond MS, Farzan M. The broad-spectrum antiviral functions of IFIT and IFITM proteins. *Nat Rev Immunol*. (2013) 13:46–57. doi: 10.1038/nri3344.
11. Feng F, Yuan LM, Wang YE, Crowley C, Lv ZY, Li JJ, et al. Crystal structure and nucleotide selectivity of human IFIT5/ISG58. *Cell Res*. (2013) 23:1055–8. doi: 10.1038/cr.2013.80
12. Katibah GE, Lee HJ, Huizar JP, Vogan JM, Alber T, Collins K. tRNA binding, structure, and localization of the human interferon-induced protein IFIT5. *Mol Cell* (2013) 49:743–50. doi: 10.1016/j.molcel.2012.12.015
13. Zhang BH, Liu XY, Chen W, Chen L. IFIT5 potentiates anti-viral response through enhancing innate immune signaling pathways. *Acta Bioch Bioph Sin*. (2013) 45:867–74. doi: 10.1093/abbs/gmt088
14. Munir M, Cortey M, Abbas A, Qureshi ZU, Afzal F, Shabbir MZ, et al. Biological characterization and phylogenetic analysis of a novel genetic group of Newcastle disease virus isolated from outbreaks in commercial poultry and from backyard poultry flocks in Pakistan. *Infect Genet Evol*. (2012) 12:1010–9. doi: 10.1016/j.meegid.2012.02.015.
15. Reperant LA, Kuiken T, Osterhaus ADME. Adaptive pathways of zoonotic influenza viruses: from exposure to establishment in humans. *Vaccine* (2012) 30:4419–34. doi: 10.1016/j.vaccine.2012.04.049
16. Goubau D, Deddouche S, Reis e Sousa C, Cytosolic sensing of viruses. *Immunity* (2013) 38:855–69. doi: 10.1016/j.immuni.2013.05.007
17. Son KN, Liang Z, Lipton HL. Double-stranded RNA is detected by immunofluorescence analysis in RNA and DNA virus infections, including those by negative-stranded RNA viruses. *J Virol*. (2015) 89:9383–92. doi: 10.1128/JVI.01299-15
18. Zhang S, Sun Y, Chen H, Dai Y, Zhan Y, Yu S, et al. Activation of the PKR/eIF2α signaling cascade inhibits replication of Newcastle disease virus. *Virol J*. (2014) 11:62. doi: 10.1186/1743-422X-11-62
19. Reed LJ, Muench H. A simple method for estimating fifty percent enpoints. *Am J Epidemiol*.. 27 (1938) 27:493–7. doi: 10.1093/oxfordjournals.aje.a118408
20. Reuter A, Soubies S, Hartle S, Schusser B, Kaspers B, Staeheli P, et al. Antiviral activity of lambda interferon in chickens. *J Virol*. (2014) 88:2835–43. doi: 10.1128/JVI.02764-13
21. Penski N, Hartle S, Rubbenstroth D, Krohmann C, Ruggli N, Schusser B, et al. Highly pathogenic avian influenza viruses do not inhibit interferon synthesis in infected chickens but can override the interferon-induced antiviral state. *J Virol*. (2011) 85:7730–41. doi: 10.1128/JVI.00063-11
22. Iqbal M, Yaqub T, Mukhtar N, Shabbir MZ, McCauley JW. Infectivity and transmissibility of H9N2 avian influenza virus in chickens and wild terrestrial birds. *Vet Res.* (2013) 44:100. doi: 10.1186/1297-9716-44-100
23. Hughes SH. The RCAS vector system. *Folia Biol.* (2004) 50:107–19
24. Tellier R. Review of aerosol transmission of influenza A virus. *Emerg Infect Dis*. (2006) 12:1657–62. doi: 10.3201/eid1211.060426
25. Sims LD. *Risks Associated With Poultry Production Systems. Poultry in the 21st 2 Century*. Available online at: https://pdfs.semanticscholar.org/905c/8f04d8d29f29d4e65f6ce599497c969e01f0.pdf
26. Barber MRW, Aldridge JR, Webster RG, Magor KE. Association of RIG-I with innate immunity of ducks to influenza. *Proc Natl Acad Sci USA* (2010) 107:5913–8. doi: 10.1073/pnas.1001755107
27. Kothlow S, Schenk-Weibhauser K, Ratcliffe MJ, Kaspers B. Prolonged effect of BAFF on chicken B cell development revealed by RCAS retroviral gene transfer *in vivo*. *Mol Immunol*. (2010) 47:1619–28. doi: 10.1016/j.molimm.2010.01.011

Conflict of Interest Statement: The authors declare that the research was conducted in the absence of any commercial or financial relationships that could be construed as a potential conflict of interest.

Copyright © 2018 Rohaim, Santhakumar, Naggar, Iqbal, Hussein and Munir. This is an open-access article distributed under the terms of the Creative Commons Attribution License (CC BY). The use, distribution or reproduction in other forums is permitted, provided the original author(s) and the copyright owner(s) are credited and that the original publication in this journal is cited, in accordance with accepted academic practice. No use, distribution or reproduction is permitted which does not comply with these terms.

frontiers in Microbiology

ORIGINAL RESEARCH
published: 12 November 2018
doi: 10.3389/fmicb.2018.02724

Chaperones, Membrane Trafficking and Signal Transduction Proteins Regulate Zaire Ebola Virus trVLPs and Interact With trVLP Elements

Dong-Shan Yu[1,2†], Tian-Hao Weng[1,2†], Chen-Yu Hu[1,2†], Zhi-Gang Wu[1,2], Yan-Hua Li[1,2], Lin-Fang Cheng[1,2], Nan-Ping Wu[1,2], Lan-Juan Li[1,2] and Hang-Ping Yao[1,2*]*

[1] State Key Laboratory for Diagnosis and Treatment of Infectious Diseases, The First Affiliated Hospital, School of Medicine, Zhejiang University, Hangzhou, China, [2] Collaborative Innovation Center for Diagnosis and Treatment of Infectious Diseases, The First Affiliated Hospital, School of Medicine, Zhejiang University, Hangzhou, China

OPEN ACCESS

Edited by:
Ping An,
Frederick National Laboratory for Cancer Research (NIH), United States

Reviewed by:
Junji Xing,
Houston Methodist Research Institute, United States
Fatah Kashanchi,
George Mason University, United States
Axel T. Lehrer,
University of Hawai'i at Mānoa, United States

***Correspondence:**
Lan-Juan Li
ljli@zju.edu.cn
Hang-Ping Yao
yaohangping@zju.edu.cn

[†] These authors have contributed equally to this work

Specialty section:
This article was submitted to Virology, a section of the journal Frontiers in Microbiology

Received: 21 June 2018
Accepted: 24 October 2018
Published: 12 November 2018

Citation:
Yu D-S, Weng T-H, Hu C-Y, Wu Z-G, Li Y-H, Cheng L-F, Wu N-P, Li L-J and Yao H-P (2018) Chaperones, Membrane Trafficking and Signal Transduction Proteins Regulate Zaire Ebola Virus trVLPs and Interact With trVLP Elements. Front. Microbiol. 9:2724. doi: 10.3389/fmicb.2018.02724

Ebolavirus (EBOV) life cycle involves interactions with numerous host factors, but it remains poorly understood, as does pathogenesis. Herein, we synthesized 65 siRNAs targeting host genes mostly connected with aspects of the negative-sense RNA virus life cycle (including viral entry, uncoating, fusion, replication, assembly, and budding). We produced EBOV transcription- and replication-competent virus-like particles (trVLPs) to mimic the EBOV life cycle. After screening host factors associated with the trVLP life cycle, we assessed interactions of host proteins with trVLP glycoprotein (GP), VP40, and RNA by co-immunoprecipitation (Co-IP) and chromatin immunoprecipitation (ChIP). The results demonstrate that RNAi silencing with 11 siRNAs (ANXA5, ARFGAP1, FLT4, GRP78, HSPA1A, HSP90AB1, HSPA8, MAPK11, MEK2, NTRK1, and YWHAZ) decreased the replication efficiency of trVLPs. Co-IP revealed nine candidate host proteins (FLT4, GRP78, HSPA1A, HSP90AB1, HSPA8, MAPK11, MEK2, NTRK1, and YWHAZ) potentially interacting with trVLP GP, and four (ANXA5, GRP78, HSPA1A, and HSP90AB1) potentially interacting with trVLP VP40. Ch-IP identified nine candidate host proteins (ANXA5, ARFGAP1, FLT4, GRP78, HSPA1A, HSP90AB1, MAPK11, MEK2, and NTRK1) interacting with trVLP RNA. This study was based on trVLP and could not replace live ebolavirus entirely; in particular, the interaction between trVLP RNA and host proteins cannot be assumed to be identical in live virus. However, the results provide valuable information for further studies and deepen our understanding of essential host factors involved in the EBOV life cycle.

Keywords: Ebola virus life cycle, trVLPs, RNAi screening, glycoprotein, protein 40, immunoprecipitation

Abbreviations: ChIP, chromatin immunoprecipitation; Co-IP, co-immunoprecipitation; CPE, cytopathic effect; DAPI, 4′,6-diamidino-2-phenylindole; DiI, 1,1′-Dioctadecyl-3,3,3′,3′-Tetramethylindocarbocyanine Perchlorate; DMEM, Dulbecco's modified Eagle's medium; EM, electron microscopy; EVD, Ebola virus disease; FBS, fetal calf serum; GP, glycoprotein; HEK, human embryonic kidney; PAGE, polyacrylamide gel electrophoresis; PBS, phosphate-buffered saline; PVDF, polyvinylidene fluoride; qRT-PCR, quantitative real-time reverse transcription polymerase chain reaction; RNAi, RNA interference; RNP, ribonucleoprotein; SDS, sodium dodecyl sulfate; TCID50, 50% tissue culture infective dose; trVLPs, transcription- and replication-competent virus-like particles; VP40, matrix protein 40; Zaire EBOV, Zaire Ebola virus.

INTRODUCTION

Ebolavirus (EBOV) is a single-stranded, negative-sense RNA virus with a heterogeneous filamentous structure (Jun et al., 2015) that was first reported in 1976 as the cause of Ebola viral disease (EVD) in humans and other primates (Johnson et al., 1977). Five different EBOVs have been defined: Ebola virus (EBOV, previously known as Zaire ebolavirus), Sudan virus (SUDV), Bundibugyo virus (BDBV), Taï Forest virus (TAFV) and Reston virus (RESTV) (Kuhn, 2017). The EVD epidemic from December 2013 to March 2016 in Western Africa was caused by EBOV, and was associated with >28,000 cases and >11,000 deaths in 11 countries (Ajisegiri et al., 2018).

Although numerous studies have been devoted to EVD therapeutics, such as immune-based treatments and small molecule inhibitors, and considerable progress has been made (Fabozzi et al., 2011; Oestereich et al., 2014; Wolf et al., 2015; Sissoko et al., 2016), the molecular basis of the EBOV life cycle and its relevance to pathogenesis remain poorly understood. For example, the mechanisms, proteins and receptors mediating viral entry, the host enzymes triggering and accelerating uncoating and virus fusion, and the host factors facilitating VP40 oligomerisation and association of VP40 with the inner leaflet remain largely unknown (Johnson et al., 2016; Gc et al., 2017; Younan et al., 2017; Kurosaki et al., 2018).

To model the EBOV life cycle using a safe method, a series of trVLPs have been developed (Hoenen et al., 2014). These trVLPs could express the EBOV proteins required for genome replication and transcription to model EBOV life cycles under biosafety level 2 conditions. Based on the EBOV life cycle in host cells, and on previous RNAi screening that identified filovirion-associated and secretory pathway-related host factors (Spurgers et al., 2010; Simpson et al., 2012; Sakurai et al., 2015), we herein synthesized siRNAs targeting host genes connected to membrane traffic machinery, endoplasmic reticulum-Golgi recycling, inhibition of secretion, and lipid droplet formation, and assessed their role in the EBOV life cycle. These genes are mostly connected with virus life cycle, specifically viral entry, uncoating, fusion, replication, assembly and budding.

In the EBOV life cycle, GP is critical for EBOV entry, uncoating and fusion processes (Nanbo et al., 2010; Takada, 2012), while VP40 also plays a crucial role in EBOV assembly and budding (Dessen et al., 2000; Balmith and Soliman, 2017), and both proteins engage in important interactions with host cellular and plasma membranes. Thus, host factors that exert a significant influence on the EBOV life cycle were identified by RNAi silencing, and interactions between EBOV GP, VP40, and nucleic acids were evaluated by Co-IP or ChIP. This is the first systematic survey of host factors that affect the EBOV life cycle, demonstrating interactions between host proteins and EBOV GP, VP40 and RNA.

MATERIALS AND METHODS

Cell Line and Plasmids

Human embryonic kidney (HEK) 293T cells were cultured in DMEM (Thermo Fisher, Waltham, MA, United States; Cat# 10566016) containing 10% FBS (Gibco, Waltham, MA, United States; Cat# 10099141), 2 mM L-glutamine (Life Technologies, Waltham, MA, United States; Cat# 25030081), and 1% penicillin- streptomycin (Life Technologies; Cat# 10378016) at 37°C with 5% CO_2. Plasmids pCAGGS-VP30, pCAGGS-VP35, pCAGGS-NP, pCAGGS-L, p4cis-vRNA-RLuc, pCAGGS-Tim1, and pCAGGS-T7 were kindly provided by Drs. Heinz Feldmann and Thomas Hoenen, Rocky Mountain Laboratories, National Institute of Health (NIH). Plasmid p4cis-vRNA-RLuc containing EBOV non-coding regions, a reporter gene, and three genes (VP40, GP1, 2 and VP24) involved in morphogenesis, budding and cell entry, was used to produce trVLPs. In the following experiments, all tests were carried out with EBOV trVLPs.

Production of trVLPs

Producer 293T cells (p0) in 6-well plates were transfected with plasmids encoding each EBOV structural protein (75 ng pCAGGS-VP30, 125 ng pCAGGS-VP35, 125 ng pCAGGS-NP, 1,000 ng pCAGGS-L, 250 ng p4cis-vRNA-RLuc), and pCAGGS-T7 (250 ng) encoding a Renilla luciferase reporter (Hoenen et al., 2014). Cell supernatants (200 ml) from 10 6-well plates containing released trVLPs were harvested at 72 h post-transfection, and cells and cellular debris were pelleted by gentle centrifugation at 175 × *g*. The supernatant was then used to infect target 293T cells (p1) previously transfected with RNP components (125 ng pCAGGS-NP, 125 ng pCAGGS-VP35, 75 ng pCAGGS-VP30, 1,000 ng pCAGGS-L, 250 ng pCAGGS-Tim1) (Hoenen et al., 2014). Target 293T cells (p2–p5) were treated in a similar manner. Cleared supernatants (33 ml) in 2 ml of 20% sucrose from the bottom of each tube were centrifuged at 125,000 × *g* in a SW-28 rotor for 3 h at 4°C. The resulting pellets were resuspended in 100 μl ice-cold NTE buffer (10 mM Tris pH 7.5, 100 mM NaCl, 1 mM EDTA) by tapping gently about 100 times, and trVLPs were stored on ice or in a refrigerator at 4°C until use.

Determining the 50% Tissue Culture Infective Dose (TCID50) of trVLPs

To determine the TCID50 values of trVLPs, CPEs were observed using microscopy, and the results from each dilution were used to calculate TCID50 values using the Reed–Muench method (Ramakrishnan, 2016). After harvest, trVLPs were 10-fold serially diluted with DMEM at concentrations ranging from 10^{-1} to 10^{-10}. Attenuated trVLPs (100 μl) were added to eight wells in each row of a 96-well plate, and 293T cell suspension (100 μl) was added to each well to a final cell density of 2×10^5 cells/ml. Additionally, 293T cells not infected with trVLPs were included as controls. CPEs were observed and recorded each day for 7 days, and TCID50 values were calculated according the Reed–Muench method, giving a value of $10^{3.76}$/0.1 ml (detailed data are listed in **Supplementary Table S1**).

Electron Microscopy (EM) Analysis of trVLPs

Purified trVLPs were pipetted onto a 300-mesh copper grid coated with carbon film, incubated for 5 min at room temperature, and grids were washed twice with distilled water and negatively stained for 15 s with 1% uranyl acetate. Excess liquid was removed with a filter paper and trVLPs were visualized under a Hitachi H7000 transmission electron microscope.

Imaging of DiI-Labeled trVLP Internalization in Live 293T Cells

Purified trVLPs (∼100 μg viral protein) were resuspended in NTE buffer a final volume of 1 ml and 1,1′-dioctadecyl-3,3,3′,3′-tetramethylindocarbocyanine perchlorate (DiI, dissolved in ethanol to a final concentration of 10 μM; Invitrogen, Waltham, MA, United States; Cat# D282) was added and mixed thoroughly. The mixture was shaken gently for 1 h at room temperature then passed through a 0.22 μm filter (Millipore, Darmstadt, Germany; Cat# SLGP033RB). HEK 293T cells cultured in 8-well chamber slides with removable wells were mixed with 4′,6-diamidino-2-phenylindole (DAPI; Invitrogen; Cat# P36931) at 10 μg/ml for 10 min to stain nuclei, and 293T cells were then incubated with DiI-labeled trVLPs at 4°C for 10 min and washed with PBS. The internalization of DiI-labeled trVLPs in 293T cells was imaged at different times from 10 to 60 min at 37°C on the stage of a fluorescence microscope.

Selection of Candidate Genes

To select host factors that are potentially related to various stages of the EBOV life cycle (including viral entry, uncoating, fusion, replication, assembly and budding), we chose host genes that are associated with membrane traffic machinery, endoplasmic reticulum-Golgi recycling, inhibition of secretion, and lipid droplet formation. For example, the knockdown of FLT4, RAB11B, and PLCH1 resulted in high-level secretion inhibition; GOSR1, LTK, and CNKSR1 are linked to endoplasmic reticulum-Golgi recycling; VAMP2, RAB11B, and COPG are membrane traffic machinery-related molecules (Simpson et al., 2012); HSPA8, HSP90AB1, and ANXA5 are believed to be related to filamentous virus (Spurgers et al., 2010). A total of 65 genes probably associated with the EBOV life cycle or virus life cycle-related functions (Spurgers et al., 2010; Simpson et al., 2012; Sakurai et al., 2015) were selected according to preliminary screening. Details and references for these genes are listed in **Supplementary Table S3**.

SiRNA Screening and trVLP Infection

SiRNAs targeting the 65 selected genes were designed and three sequences were synthesized for each gene. To choose the most efficient sequence for RNA interfere (RNAi), the gene knockdown efficiency of each sequence was evaluated by quantitative PCR, with the 18sRNA gene as a control. Values were calculated using the $2^{-\Delta\Delta Ct}$ method, and the smaller the value, the higher the knockdown efficiency. The most efficient siRNAs were chosen for RNAi screening tests (data listed in **Supplementary Table S2**), and details of each chosen siRNA are included in **Supplementary Table S3**. In 24-well plates, 100 μl of opti-MEM medium (Invitrogen; Cat# 31985070) containing 1.4 μl siRNA and 4.5 μl HiPerFect transfection reagent (Qiagen, Dusseldorf, Germany; Cat# 301705) was added to each well and plates were shaken gently for 1 min. After 10 min incubation at room temperature, a cell suspension (400 μl) containing 1×10^5 cells was added to give a final siRNA concentration of 75 nM. Cells were incubated at 37°C and 5% CO_2 for 48 h, washed with PBS, and infected with trVLPs (TCID50 = $10^{2.76}$/0.01 ml) for 48 h. Negative control siRNA (Qiagen; Cat# 1027310) served as a control.

RNA Extraction and Quantitative Real-Time Reverse Transcription PCR (qRT-PCR)

After trVLP infection, 293T cells in 24-well plates were washed with PBS, and total RNA was extracted from cells using TRIzol (Invitrogen; Cat# 15596018) according to the manufacturer's instructions. qRT-PCR was performed with a EBOV nucleic acid test kit (Zhijiang Bio-tech, Shanghai, China; Cat# QR-0220-02) on an ABI 7500 qPCR system (45°C for 10 min and 95°C for 15 min, followed by 45 cycles at 95°C for 15 s and 60°C for 30 s). The positive control, provided in the kit, was serially diluted over three orders of magnitude, and the absolute quantity of EBOV RNA (copy/ml) was calculated using the comparative Ct method and a standard curve. All qRT-PCR experiments were performed in triplicate and repeated independently three times.

Antibodies

Antibodies recognizing HSP70 (HSPA1A; Cat# 4873S), HSP90β (HSP90AB1; Cat# 5087S), MEK1/2 (Cat# 9122S), ARFGAP1 (Cat# 14522S) and Trk (NTRK1; Cat# 92991S) were purchased from Cell Signaling Technology (Danvers, MA, United States). Antibodies recognizing MAPK11 (Cat# ab183208), VEGF Receptor 3 (FLT4; Cat# ab10284), Annexin V (ANXA5; Cat# ab54775), GRP78 (HSPA5; Cat# ab21685), GAPDH (Cat# ab8245), and Ebola virus GP (Cat# ab1918) were purchased from Abcam (Cambridge, United Kingdom). Antibodies recognizing 14-3-3 zeta/beta (YWHAZ; Cat# NB100-1964) and Hsc70 (HSPA8; Cat# NBP2-12880) were purchased from Novus Biologicals (Littleton, CO, United States). Antibody recognizing Ebola virus VP40 (Cat# sc-51872) was purchased from Santa Cruz Biotechnology (Dallas, TX, United States). Antibodies against HSPA1A, HSP90AB1, MEK1/2, ARFGAP1, NTRK1, MAPK11, FLT4, and GRP78 were rabbit-derived IgGs. Antibodies against ANXA5, YWHAZ, and HSPA8 were mouse-derived IgGs. Normal mouse IgG (Cat# SC-2025) and normal rabbit IgG (Cat# SC-2027) were obtained from Santa Cruz Biotechnology and used as isotype controls in immunoprecipitation tests.

Co-IP and Immunoblot Analysis

HEK 293T cells in 12-well plates were infected with trVLPs (TCID50 = $10^{3.76}$/0.1 ml) for 48 h and whole-cell extracts were prepared followed by incubation overnight with appropriate antibodies recognizing host proteins plus Protein G beads (GE Healthcare, Uppsala, Sweden; Cat# 28-9440-08). Antibodies

mixed with Protein G beads and normal cell/extracts without trVLPs, and Protein G beads mixed with trVLP-treated cell extracts without antibodies, were included as control groups. Beads were then washed five times with low-salt lysis buffer, and immunoprecipitates were eluted with 2× SDS Loading Buffer and resolved by SDS-PAGE. Proteins were transferred to PVDF membranes and further incubated with anti-GP or VP40 antibodies. Proteins of interest were detected with the Super Signal West Pico chemiluminescent substrate (Thermo Fisher; Cat# 34580). To confirm that siRNAs interfered with the expression of target proteins in a specific manner, immunoblot analysis of target host proteins was performed after siRNA transfection. Meanwhile, to confirm the specificity of the antibodies, target host proteins, GP, and VP40 proteins from the above extracts were tested before and after Co-IP separately (normal mouse or rabbit IgG served as isotype controls). The housekeeping protein GAPDH was used as an internal control for immunoblot analyses.

Chromatin Immunoprecipitation (ChIP)

After infection of trVLPs (TCID50 = $10^{2.76}$/0.01 ml) for 48 h, HEK 293T cells in 12-well plates were fixed with 1% formaldehyde for 10 min, and glycine (Thermo Fisher; Cat# 28363) was added to terminate the cross-linking reaction. Whole-cell extracts were then prepared using a Simple ChIP Enzymatic Chromatin IP Kit (Cell Signaling Technology; Cat# 9003) following the manufacturer's instructions with appropriate antibodies recognizing host proteins, and normal mouse or rabbit IgGs served as isotype controls. Beads were then washed and cross-linking substances were unlocked according the ChIP kit instructions. Purified nucleic acids were then amplified by qPCR with a qPCR Probe Kit (Vazyme Biotech, Nanjing, China; Cat# Q2223-01). Primers and probe were designed according to the sequence of *Zaire ebolavirus* isolate *Homo sapiens*-wt/GIN/2014/Gueckedou-C05 (GenBank No. KJ660348.2) as follows: EN-Z-F, ATGATGGARGCTACGGCG; EN-Z-R, TGCCCTCTGTATGCTGGCCCT; EN-Z-P, CCARA GTTACTCGGAAAACGGCATG.

Sequencing Analysis

The PCR products amplified from ChIP samples were purified by agarose gel electrophoresis, recycled, and sequenced by the Sanger chain termination method. Genotypes were attributed using BioEdit software (Ibis Biosciences, Carlsbad, CA, United States) for allelic discrimination.

Statistical Analysis

Data in normal distributions are presented as the mean ± standard deviation (Kim et al., 2018). Student's *t*-tests (two-tailed, paired or unpaired *t*-tests with Welch's correction), and multiple comparisons were performed where appropriate. All analysis was performed with Graphpad Prism 5 (GraphPad Software, United Kingdom) and differences between group means with $p < 0.05$ were considered statistically significant.

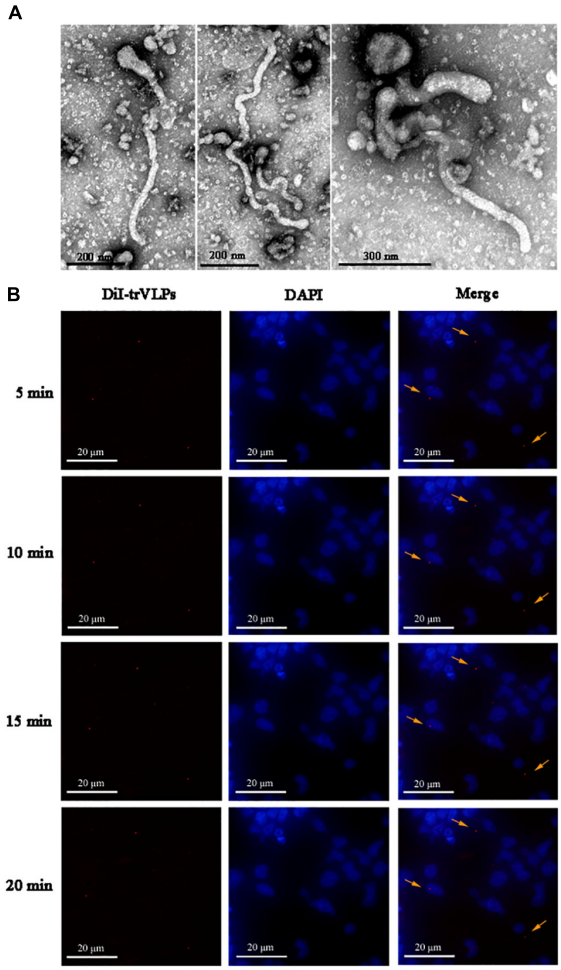

FIGURE 1 | Visualization and identification of ebolavirus transcription- and replication-competent virus-like particle (EBOV-trVLP). **(A)** Visualization of ebolavirus (EBOV) transcription- and replication-competent virus-like particles (trVLPs) by electron microscopy (EM). trVLPs were purified by ultracentrifugation using a 20% sucrose gradient and particles were visualized by EM after negative staining. The arrow indicates filamentous-like viral particles. **(B)** Internalization and tracing of 1,1′-dioctadecyl-3,3,3′,3′-tetramethylindocarbocyanine perchlorate (DiI)-labeled trVLPs at 5, 10, 15, and 20 min after infecting 293T cells by fluorescence microscopy (indicated by yellow arrows).

RESULTS

EBOV-trVLPs Successfully Simulate Authentic Ebola Virions

EBOV-trVLPs synthesized as described above displayed a filamentous-like morphology with a diameter of 100–500 μm as visualized by EM (**Figure 1A**). Meanwhile, internalization and tracking of DiI-labeled trVLPs in live 293T cells visualized by fluorescent microscopy indicated that trVLPs gradually translocated into the cytoplasm over time (**Figure 1B**). It has been reported that filamentous viruses, including authentic EBOV, are internalized into cells following stimulation of the

macropinocytosis pathway, while spherical pseudotype virions are internalized via the endocytosis pathway (Nanbo et al., 2010). In our present study, trVLPs are filamentous virions, hence we presumed that trVLPs would be internalized via the macropinocytosis pathway.

SiRNA Knockdown of Host Factors Decreases Replication of trVLPs

To identify factors associated with the life cycle of trVLPs, siRNAs targeting 65 selected genes were tested in 293T cells infected with trVLPs in triplicate by qRT-PCR. The results showed that siRNA knockdown of ANXA5, ARFGAP1, FLT4, GRP78, HSPA1A, HSP90AB1, HSPA8, MAPK11, MEK2, NTRK1, and YWHAZ efficiently inhibited trVLP replication ($p < 0.05$; **Figure 2A**). To confirm that these siRNAs interfered with the expression of target proteins in a specific manner, we measured the levels of target proteins by western blot analysis, and this demonstrated significant interference for each target protein as expected (**Figure 2B**). The results suggest that these host proteins are highly likely to participate in the trVLP life cycle, and may perform critical roles. In addition, the results from the siRNA knockdowns of other host proteins suggest that they do not interfere with trVLP replication (**Supplementary Figure S1**).

Among these selected candidate host factors, four are chaperones (HSPA1A, HSP90AB1, HSPA8, and GRP78), four are involved in plasma and/or endosome membrane trafficking (ANXA5, ARFGAP1, FLT4, and NTRK1), and three play important roles in signal transduction pathways (MAPK11, MEK2, and YWHAZ). Further bioinformatic analysis by GeneMANIA revealed that these candidate host factors were markedly enriched in gene categories associated with 14-3-3 protein families [such as YWHAZ, YWHAE and YWHAQ)], annexin families (including ANXA1, ANXA4, and ANXA5), heat shock protein (HSP) families (e.g., HSPA1A, HSP90AB1, GRP78, and HSPA8), and MAP kinase families (including MAPK11 and MAP2K2; **Figure 2C**). The analysis also indicated that candidate host factors are associated with cytoplasmic vesicle membranes, mitochondrial membranes, mitochondria, the COP9 signalosome, and phospholipid binding, and strongly connected with antigen binding, viral endocytosis, transportation, anti-virus responses, and viral budding.

Since GP and VP40 proteins perform critical functions in the EBOV life cycle and since both interact with host cell membranes, we performed Co-IP and Ch-IP assays to validate host protein-GP/VP40 and host protein-trVLP nucleic acid interactions.

Candidate Host Proteins Interact With trVLP GP

Antibodies recognizing the 11 host proteins were incubated overnight with Protein G beads and cell extracts infected with trVLPs described above. Immunoblot analysis was then carried out with anti-GP antibody, and the results demonstrated that nine host proteins (FLT4, GRP78, HSPA1A, HSP90AB1, HSPA8, MAPK11, MEK2, NTRK1, and YWHAZ) interacted with GP, whereas ARFGAP1 and ANXA5 did not appear to interact with GP (normal mouse or rabbit IgG served as isotype controls; **Figure 3A**). Meanwhile, immunoblot analyses of the 11 target host proteins before and after IP indicated a high degree of specificity for those antibodies, further verifying the interactions between GP and candidate host proteins (**Figures 3B,C**).

Candidate Host Proteins Interact With trVLP VP40

Next, interactions of the 11 candidate host proteins with VP40 were tested by incubating antibodies recognizing the 11 host proteins overnight with Protein G beads and trVLPs-treated cell extracts. Western blotting with anti-VP40 antibody indicated that ANXA5, GRP78, HSPA1A, and HSP90AB1 interacted with VP40, whereas ARFGAP1, HSPA8, MAPK11, MEK2, FLT4, NTRK1, and YWHAZ did not interact with VP40 (normal mouse or rabbit IgG served as isotype controls; **Figure 4A**). Immunoblot analyses of the 11 candidate host proteins before and after IP confirmed the specificity of those antibodies, as well as interactions between VP40 and candidate host proteins (**Figures 4B,C**).

Candidate Host Proteins Interact With trVLP RNA

Since interactions between virus RNA and host proteins are likely to be essential for viral replication, we next investigated whether trVLP RNA interacts with the candidate host proteins using Ch-IP assays and purified nucleic acids by qPCR and DNA sequencing. BLAST analysis of the sequencing results indicated that sequences from nine antibodies recognizing candidate host proteins (HSP90AB1, ANXA5, ARFGAP1, FLT4, GRP78, HSPA1A, MEK2, NTRK1, and MAPK11) were consistent with *Zaire ebolavirus* (GenBank No. KJ660348.2; **Figure 5**). HSPA8, YWHAZ, and isotype controls did not recognize trVLP RNA.

DISCUSSION

A better understanding of the mechanisms of the EBOV life cycle and host–virus interactions (including protein–protein and protein–RNA interactions) would greatly assist the elucidation of EBOV pathogenesis and therapeutic development. Herein, we identified 11 candidate host proteins by RNAi silencing that appear to function in the EBOV-trVLP life cycle among 65 host factors presumed to be associated with the virus life cycle and secretary pathways. Meanwhile, we measured candidate host protein levels after RNAi by western blot analysis, and the results revealed significant interference effects and confirmed the specificity of RNAi silencing. Bioinformatic analysis by GeneMANIA indicated that these candidate host proteins belong to the following families: (1) HSPs that participate in a wide variety of cellular processes, including activation of proteolysis, protecting the proteome against stress, infection, and transport of newly synthesized polypeptides (Alvarez-Sanchez et al., 2015; Chaudhary et al., 2016; Heck et al., 2017); (2) 14-3-3 protein families that bind a number of signaling proteins including kinases, phosphatases and transmembrane receptors (Radhakrishnan et al., 2012; Obsilova et al., 2014;

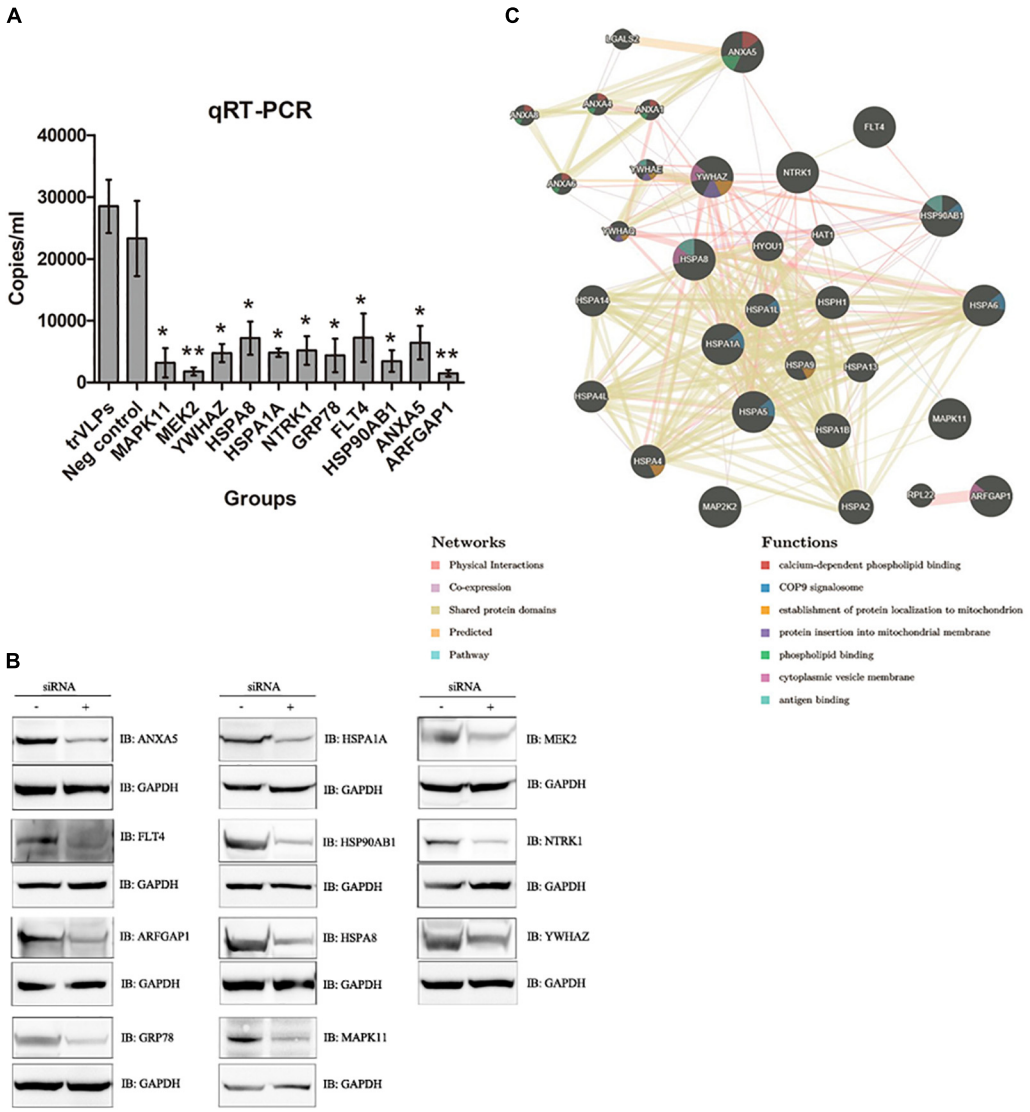

FIGURE 2 | RNAi screening of host factors related to EBOV-trVLP life cycle and further validation and analysis. **(A)** RNAi silencing analysis of host factors required for the EBOV trVLP life cycle. A 100 μl sample of opti-MEM medium containing 1.4 μl siRNA and 4.5 μl HiPerFect was placed in 24-well plates, and a cell suspension (400 μl) containing 1×10^5 cells was added to give a final siRNA concentration of 75 nM. After incubation for 48 h, cells were infected with trVLPs for another 48 h, total RNA was extracted, and the absolute quantity of EBOV RNA was measured using a EBOV nucleic acid test kit. All qRT-PCR experiments were performed in triplicate and repeated three times independently. Cells not transfected with siRNA but infected with trVLPs served as a blank control; cells transfected with isotype siRNA and infected with trVLPs served as a negative control. Eleven siRNAs targeting HSPA1A, HSP90AB1, ARFGAP1, ANXA5, YWHAZ, MAPK11, NTRK1, FLT4, GRP78, MEK2, and HSPA8 inhibited trVLP replication effectively. $^*p < 0.05$, $^{**}p < 0.01$. **(B)** Western blot analysis of each target protein after siRNA transfection. The 11 target proteins were all expressed at much lower levels following transfection with the relevant siRNA. Normal 293T cells and cells transfected with isotype siRNAs served as controls. **(C)** Characterization of selected networks of candidate host proteins that may be important for regulating the trVLP life cycle. Interactions of the 11 host proteins were assessed using the GeneMANIA interaction database, and their functions were evaluated in association with cytoplasmic vesicle membranes, mitochondrial membranes, mitochondria, antigen binding, the COP9 signalosome, and phospholipid binding.

Aghazadeh and Papadopoulos, 2016); (3) Annexin families that are involved in trafficking and organization of endocytosis, vesicles, exocytosis, and calcium ion channel formation (Grieve et al., 2012; Kuehnl et al., 2016); (4) MAP kinase families, which play critical roles in signal transduction, phosphorylation and activation of MAPK1/ERK2 and MAPK3/ERK1 pathways (Vomastek et al., 2008; Robinson and Pitcher, 2013; Cook et al., 2017). Further functional analysis confirmed that the candidate host proteins were strongly associated with cytoplasmic vesicle membranes, mitochondrial membranes, mitochondria, the COP9 signalosome, and phospholipid binding, and connected with antigen binding, viral endocytosis, transportation, anti-virus responses, and viral budding (Bech-Otschir et al., 2001; Horner et al., 2011; van Zuylen et al., 2012; Richard et al., 2015).

Heat shock protein family proteins are known to be associated with many viruses. For example, the Hsp70 chaperone network

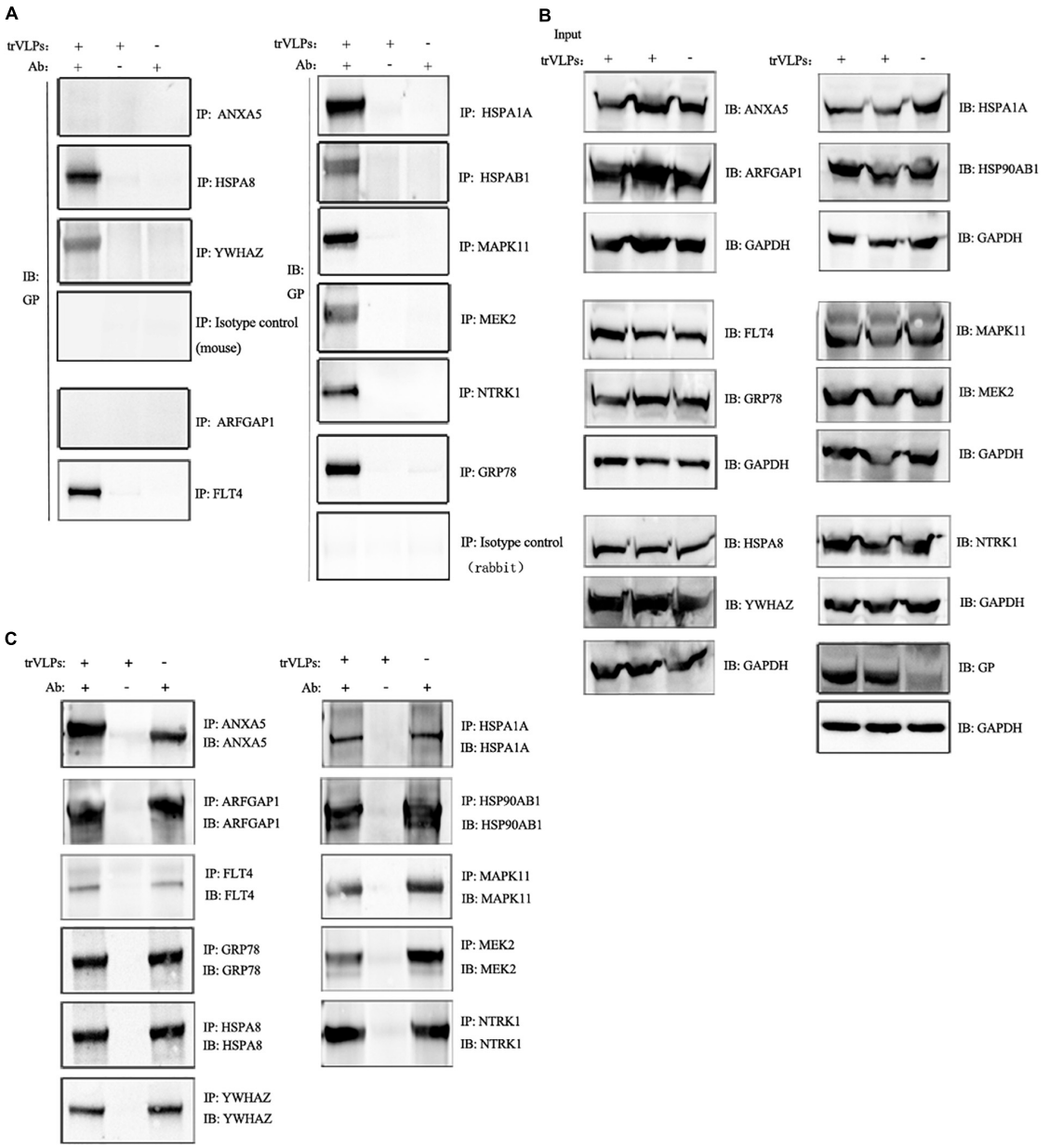

FIGURE 3 | Co-immunoprecipitation (Co-IP) and immunoblot analysis of interaction between target proteins and EBOV-trVLP glycoprotein (GP). **(A)** Co-IP and immunoblot analysis of EBOV trVLP GP. Extracts from HEK 293T cells infected with trVLPs were incubated with antibodies recognizing candidate host proteins plus Protein G beads; pulled-down proteins were detected by western blotting using anti-GP antibody. HSPA1A, MAPK11, NTRK1, GRP78, FLT4, HSPA8, MEK2, HSP90AB1, and YWHAZ interact with GP, whereas ARFGAP1, ANXA5, and isotype controls do not. Extracts incubated with Protein G beads without antibody, and antibodies mixed with Protein G beads and normal cell extracts without trVLPs served as controls. **(B)** Immunoblot analysis of the 11 target proteins before IP and **(C)** after IP. Samples were prepared as described above.

mediates the dengue virus life cycle, GRP78 is a potential defensive molecule against hepatitis A virus replication, and Hsp90 controls reactivation of human immunodeficiency virus type 1 from latency (Anderson et al., 2014; Taguwa et al., 2015; Vashist et al., 2015; Jiang et al., 2017). Meanwhile, filovirion studies showed that HSP70 family proteins are associated with Ebola virus (Nelson et al., 2017), consistent with our current results. Members of 14-3-3 protein families are also connected with viral infection, since they mediate signaling pathways and interactions during viral dsRNA stimulation and advanced antiviral innate immune responses (Ohman et al., 2010; Ohman et al., 2014). However, interactions of 14-3-3 proteins with EBOV have not been reported previously. Similarly, annexin family proteins also interact closely with RNA viruses such as measles virus and H5N1 avian influenza virus (Ma et al., 2017; Koga et al., 2018), but interactions with EBOV

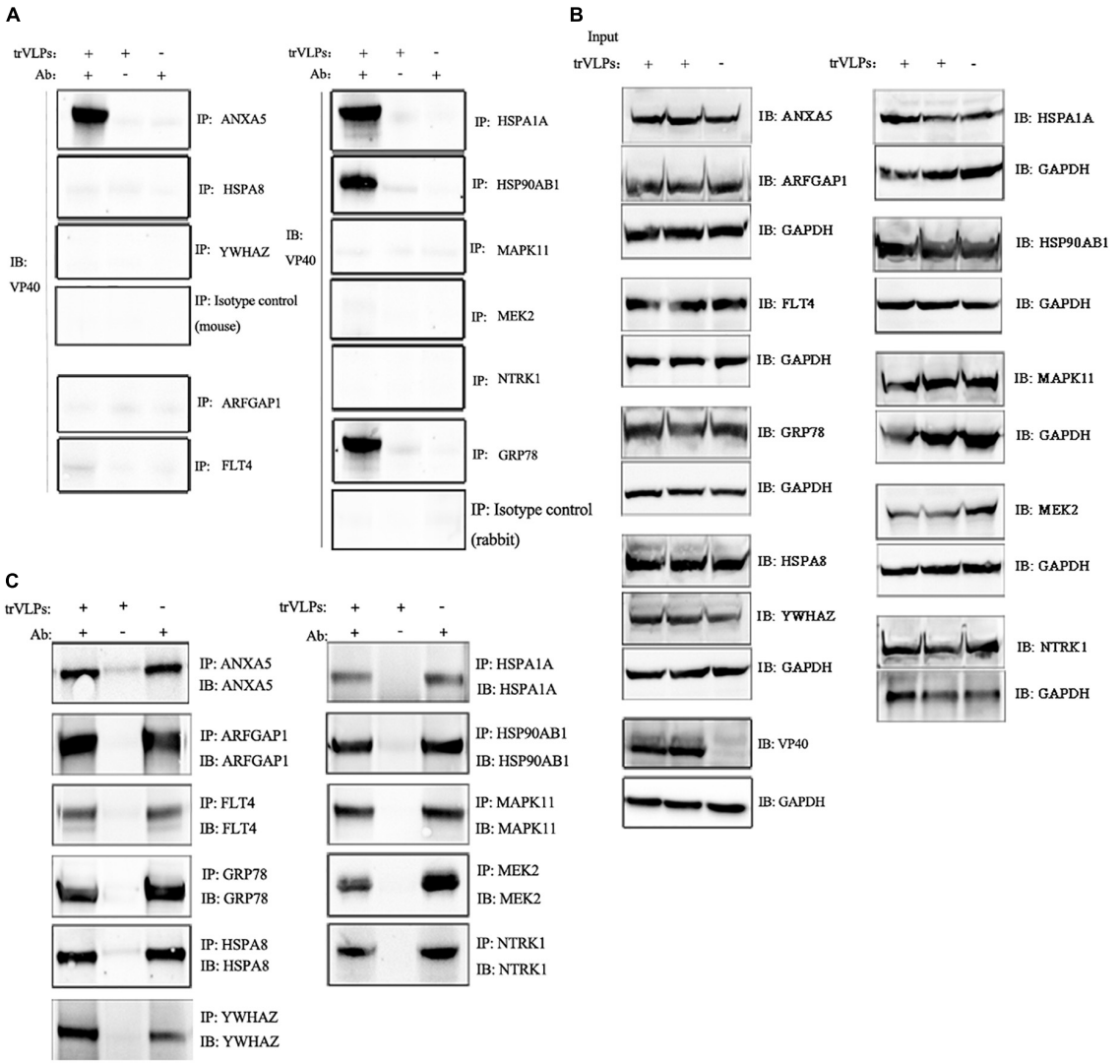

FIGURE 4 | Co-immunoprecipitation and immunoblot analysis of interaction between target proteins and EBOV-trVLP VP40. **(A)** Co-IP and immunoblot analysis of EBOV trVLP protein 40 (VP40). Extracts from HEK 293T cells infected with trVLPs were incubated with antibodies recognizing candidate host proteins plus Protein G beads, and pulled-down proteins were detected by western blotting using anti-VP40 antibody. HSP90AB1, ANXA5, HSPA1A, and GRP78 interact with VP40, whereas ARFGAP1, YWHAZ, MAPK11, NTRK1, FLT4, MEK2, HSPA8, and isotype controls do not. Extracts incubated with Protein G beads without antibody, and antibodies mixed with Protein G beads and normal cell extracts without trVLPs served as controls. **(B)** Immunoblot analysis of the 11 target proteins before IP and **(C)** after IP. Samples were treated as described above.

have not been reported previously. MAP kinases are essential in signal transduction and involved in numerous virus life cycle events, including in EBOV (Strong et al., 2008; Johnson et al., 2014), but the detailed mechanisms of interactions between MAP kinases and EBOV remain ambiguous.

To confirm the interactions of candidate host proteins with EBOV, Co-IP, and Ch-IP were performed. The results revealed that HSPA1A, HSP90AB1, HSPA8, MAPK11, NTRK1, MEK2, FLT4, GRP78, and YWHAZ interacted with EBOV GP. Meanwhile, immunoblot analyses of the 11 target host proteins before and after IP confirmed the high degree of specificity for those antibodies, and specific interactions between GP and candidate host proteins. Four of these proteins belong to HSP families, which are involved in a variety of cellular functions, and some of the others function in plasma and/or endosome membrane trafficking and signal transduction pathways. These results are consistent with the functions of EBOV GP, which is critical for EBOV cell entry, and uncoating and fusion processes occurring at the cell membrane through the endosomal pathway. Protein interactions can involve various mechanisms including subunit polymerization, cross polymerization, and molecular recognition. However, the detailed mechanisms of the interactions between GP and host proteins remain unclear. Meanwhile, it is worth noting that additional factors likely act as a bridge between the candidate host proteins and GP.

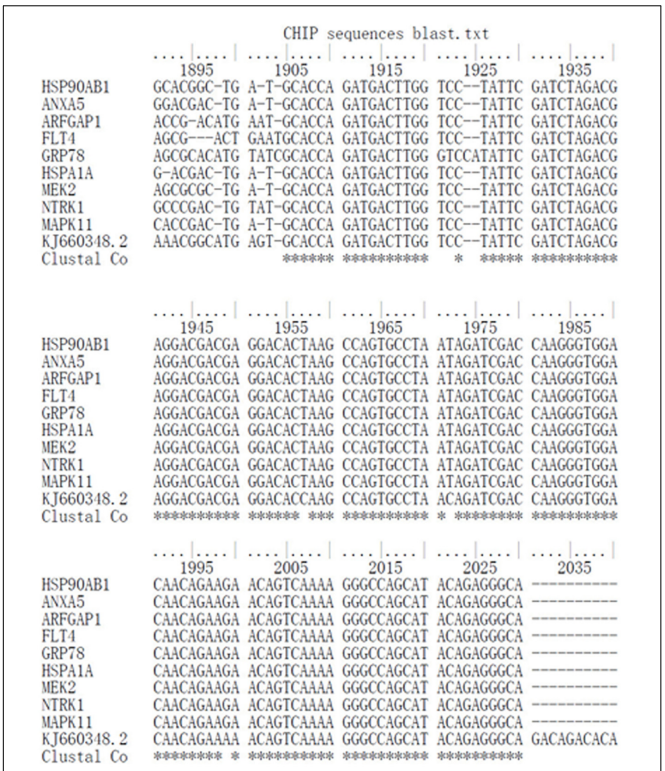

FIGURE 5 | Chromatin immunoprecipitation (ChIP) and DNA sequencing analysis of EBOV trVLP nucleic acids. Extracts from HEK 293T cells infected with trVLPs were processed and pulled down using a Chromatin IP Kit with antibodies recognizing candidate host proteins. Purified nucleic acids were amplified by qPCR, and products were sequenced by the Sanger chain termination method. Genotypes were attributed and compared with the Zaire ebolavirus sequence (GenBank No. KJ660348.2) using BioEdit software. Samples from HSP90AB1, ANXA5, ARFGAP1, FLT4, GRP78, HSPA1A, MEK2, NTRK1, and MAPK11 are consistent with sequences from EBOV, while HSPA8 and YWHAZ are not. Isotype negative controls were included.

Co-immunoprecipitation and immunoblot analyses also revealed that ANXA5, GRP78, HSPA1A, and HSP90AB1 interact with VP40, and bioinformatic analysis indicated that ANXA5 engages in phospholipid binding, while GRP78 and HSP90AB1 are associated with the COP9 signalosome, which is believed to act as a scaffold to facilitate spatial sequestration for multiple interacting molecules that regulate protein stability, transcription, protein phosphorylation and intracellular distribution (Lee et al., 2013; Mosadeghi et al., 2016). The functions of these candidate host proteins are consistent with the role of VP40 in the EBOV life cycle, which presides over association with plasma membrane phosphatidylserine, the inner leaflet, and translocation of virions through the plasma membrane (Dessen et al., 2000; Balmith and Soliman, 2017). Regardless of whether the modes of interaction between the candidate host proteins and VP40 are direct, indirect, or complex, these proteins appear to be linked to the EBOV life cycle.

Interactions of host proteins with trVLP RNA were assessed, and the results indicated that HSP90AB1, HSPA1A, GRP78, ANXA5, ARFGAP1, FLT4, MAPK11, MEK2, and NTRK1 interact with trVLP RNA. Protein-RNA interactions are important for various cellular process including transcriptional and post-transcriptional regulation, and activating immune responses against virus infection (Bidet and Garcia-Blanco, 2014; Cheng et al., 2015; Borodavka et al., 2017; Cipriano and Ballarino, 2018). In the EBOV life cycle, viral nucleic acids are exposed after uncoating in the late endosome, and negative-sense RNA then acts as a template for the synthesis of positive-sense RNA, which guides transcription of viral mRNA. Host protein-virus RNA interactions are presumably crucial during the EBOV life cycle, as indicated by our results.

There were some limitations to our study. Firstly, all the experiments were based on EBOV trVLPs and HEK 293T cells, the interactions may not reflect the physiology of live EBOV. Further experiments using EBOV are therefore required to confirm these current findings. Secondly, the interaction patterns are unclear, which may work either through direct binding or through the indirect action of one or more intermediate molecules, or through the formation of protein complexes by bridge proteins. Furthermore, it is unclear which region or segment of the GP or VP40 protein interacts with the host proteins. Finally, as ebolavirus probably infects different cell types via different mechanisms, the interactions we found in 293T cells may not be relevant in other host cells, such as monocytes and hepatocytes (Kindrachuk et al., 2014; Rogers and Maury, 2018). Subsequent experiments will attempt to define the patterns of interactions, clarify the specificity and binding sites.

CONCLUSION

Analysis of EBOV life cycle-associated host factors by RNAi silencing identified four chaperones (HSPA1A, HSP90AB1, HSPA8, and GRP78), four plasma and endosome membrane trafficking molecules (ANXA5, ARFGAP1, FLT4, and NTRK1) and three signal transduction elements (MAPK11, MEK2, and YWHAZ) that may be essential for EBOV replication. Among these host proteins, nine (FLT4, GRP78, HSPA1A, HSP90AB1, HSPA8, MAPK11, MEK2, NTRK1, and YWHAZ) potentially interact with trVLP GP, four (ANXA5, GRP78, HSPA1A, and HSP90AB1) potentially interact with trVLP VP40, and nine (ANXA5, ARFGAP1, FLT4, GRP78, HSPA1A, HSP90AB1, MAPK11, MEK2, and NTRK1) participate in host protein-trVLP RNA interactions. Although EBOV trVLP cannot replace live ebolavirus entirely, and these interactions cannot be assumed to be identical in live virus, the study provides valuable foundations for further research.

AUTHOR CONTRIBUTIONS

D-SY, T-HW, C-YH, Z-GW, Y-HL, and L-FC performed the experiments. H-PY and D-SY performed the statistical analysis. H-PY, N-PW, and L-JL designed the study and drafted the manuscript. All authors participated in writing the manuscript.

FUNDING

This work was supported by the Major Program of National Natural Science Foundation of China [Grant Number 81590763].

ACKNOWLEDGMENTS

We greatly appreciate the Elixigen Corporation which is a professional scientific editing company for proofreading the manuscript.

SUPPLEMENTARY MATERIAL

The Supplementary Material for this article can be found online at: https://www.frontiersin.org/articles/10.3389/fmicb.2018.02724/full#supplementary-material

FIGURE S1 | RNAi silencing analysis of host factors that failed to inhibit ebolavirus transcription- and replication-competent virus-like particle (EBOV-trVLP) replication. Samples (100 μl) of opti-MEM medium containing 1.4 μl siRNA and 4.5 μl HiPerFect were placed in 24-well plates, and a cell suspension (400 μl) containing 1×10^5 293T cells was added to give a final siRNA concentration of 75 nM. After incubation for 48 h, cells were infected with trVLPs for another 48 h, then total RNA was extracted, and the absolute quantity of EBOV RNA was measured using an EBOV nucleic acid test kit. All qRT-PCR experiments were performed in triplicate and repeated three times independently. Cells not transfected with siRNA but infected with trVLPs served as a blank control, and cells transfected with isotype siRNA and infected with trVLPs served as a negative control.

TABLE S1 | TCID50 of trVLPs calculated by Reed–Muench method.

TABLE S2 | The gene knock-down efficiency of the most efficient siRNAs chosen for RNAi screening tests.

TABLE S3 | Information of each gene chosen for RNA interference screening tests.

REFERENCES

Aghazadeh, Y., and Papadopoulos, V. (2016). The role of the 14-3-3 protein family in health, disease, and drug development. *Drug Discov. Today* 21, 278–287. doi: 10.1016/j.drudis.2015.09.012

Ajisegiri, W. S., Chughtai, A. A., and MacIntyre, C. R. (2018). A risk analysis approach to prioritizing epidemics: ebola virus disease in West Africa as a case study. *Risk Anal.* 38, 429–441. doi: 10.1111/risa.12876

Alvarez-Sanchez, C., Cancio-Lonches, C., Mora-Heredia, J. E., Santos-Valencia, J. C., Barrera-Vazquez, O. S., Yocupicio-Monroy, M., et al. (2015). Negative effect of heat shock on feline calicivirus release from infected cells is associated with the control of apoptosis. *Virus Res.* 198, 44–52. doi: 10.1016/j.virusres.2015.01.003

Anderson, I., Low, J. S., Weston, S., Weinberger, M., Zhyvoloup, A., Labokha, A. A., et al. (2014). Heat shock protein 90 controls HIV-1 reactivation from latency. *Proc. Natl. Acad. Sci. U.S.A.* 111, E1528–E1537. doi: 10.1073/pnas.1320178111

Balmith, M., and Soliman, M. E. (2017). VP40 of the ebola virus as a target for EboV therapy: comprehensive conformational and inhibitor binding landscape from accelerated molecular dynamics. *Cell Biochem. Biophys.* 75, 65–78. doi: 10.1007/s12013-017-0783-8

Bech-Otschir, D., Kraft, R., Huang, X., Henklein, P., Kapelari, B., Pollmann, C., et al. (2001). COP9 signalosome-specific phosphorylation targets p53 to degradation by the ubiquitin system. *EMBO J.* 20, 1630–1639. doi: 10.1093/emboj/20.7.1630

Bidet, K., and Garcia-Blanco, M. A. (2014). Flaviviral RNAs: weapons and targets in the war between virus and host. *Biochem. J.* 462, 215–230. doi: 10.1042/bj20140456

Borodavka, A., Dykeman, E. C., Schrimpf, W., and Lamb, D. C. (2017). Protein-mediated RNA folding governs sequence-specific interactions between rotavirus genome segments. *eLife* 6:e27453. doi: 10.7554/eLife.27453

Chaudhary, P., Khan, S. Z., Rawat, P., Augustine, T., Raynes, D. A., Guerriero, V., et al. (2016). HSP70 binding protein 1 (HspBP1) suppresses HIV-1 replication by inhibiting NF-kappaB mediated activation of viral gene expression. *Nucleic Acids Res.* 44, 1613–1629. doi: 10.1093/nar/gkv1151

Cheng, Z., Zhou, S., and Guan, J. (2015). Computationally predicting protein-RNA interactions using only positive and unlabeled examples. *J. Bioinform. Comput. Biol.* 13:1541005. doi: 10.1142/s021972001541005x

Cipriano, A., and Ballarino, M. (2018). The ever-evolving concept of the gene: the use of RNA/Protein experimental techniques to understand genome functions. *Front. Mol. Biosci.* 5:20. doi: 10.3389/fmolb.2018.00020

Cook, S. J., Stuart, K., Gilley, R., and Sale, M. J. (2017). Control of cell death and mitochondrial fission by ERK1/2 MAP kinase signalling. *FEBS J.* 284, 4177–4195. doi: 10.1111/febs.14122

Dessen, A., Volchkov, V., Dolnik, O., Klenk, H. D., and Weissenhorn, W. (2000). Crystal structure of the matrix protein VP40 from Ebola virus. *EMBO J.* 19, 4228–4236. doi: 10.1093/emboj/19.16.4228

Fabozzi, G., Nabel, C. S., Dolan, M. A., and Sullivan, N. J. (2011). Ebolavirus proteins suppress the effects of small interfering RNA by direct interaction with the mammalian RNA interference pathway. *J. Virol.* 85, 2512–2523. doi: 10.1128/jvi.01160-10

Gc, J. B., Gerstman, B. S., and Chapagain, P. P. (2017). Membrane association and localization dynamics of the Ebola virus matrix protein VP40. *Biochim. Biophys. Acta* 1859, 2012–2020. doi: 10.1016/j.bbamem.2017.07.007

Grieve, A. G., Moss, S. E., and Hayes, M. J. (2012). Annexin A2 at the interface of actin and membrane dynamics: a focus on its roles in endocytosis and cell polarization. *Int. J. Cell Biol.* 2012:852430. doi: 10.1155/2012/852430

Heck, T. G., Scomazzon, S. P., Nunes, P. R., Scholer, C. M., da Silva, G. S., Bittencourt, A., et al. (2017). Acute exercise boosts cell proliferation and the heat shock response in lymphocytes: correlation with cytokine production and extracellular-to-intracellular HSP70 ratio. *Cell Stress Chaperones* 22, 271–291. doi: 10.1007/s12192-017-0771-3

Hoenen, T., Watt, A., Mora, A., and Feldmann, H. (2014). Modeling the lifecycle of Ebola virus under biosafety level 2 conditions with virus-like particles containing tetracistronic minigenomes. *J. Vis. Exp.* 91:52381. doi: 10.3791/52381

Horner, S. M., Liu, H. M., Park, H. S., Briley, J., and Gale, M. Jr. (2011). Mitochondrial-associated endoplasmic reticulum membranes (MAM) form innate immune synapses and are targeted by hepatitis C virus. *Proc. Natl. Acad. Sci. U.S.A.* 108, 14590–14595. doi: 10.1073/pnas.1110133108

Jiang, X., Kanda, T., Haga, Y., Sasaki, R., Nakamura, M., Wu, S., et al. (2017). Glucose-regulated protein 78 is an antiviral against hepatitis A virus replication. *Exp. Ther. Med.* 13, 3305–3308. doi: 10.3892/etm.2017.4407

Johnson, J. C., Martinez, O., Honko, A. N., Hensley, L. E., Olinger, G. G., and Basler, C. F. (2014). Pyridinyl imidazole inhibitors of p38 MAP kinase impair viral entry and reduce cytokine induction by Zaire ebolavirus in human dendritic cells. *Antiviral Res.* 107, 102–109. doi: 10.1016/j.antiviral.2014.04.014

Johnson, K. A., Taghon, G. J., Scott, J. L., and Stahelin, R. V. (2016). The Ebola Virus matrix protein, VP40, requires phosphatidylinositol 4,5-bisphosphate (PI(4,5)P2) for extensive oligomerization at the plasma membrane and viral egress. *Sci. Rep.* 6:19125. doi: 10.1038/srep19125

Johnson, K. M., Lange, J. V., Webb, P. A., and Murphy, F. A. (1977). Isolation and partial characterisation of a new virus causing acute haemorrhagic fever in Zaire. *Lancet* 1, 569–571.

Jun, S. R., Leuze, M. R., Nookaew, I., Uberbacher, E. C., Land, M., Zhang, Q., et al. (2015). Ebolavirus comparative genomics. *FEMS Microbiol. Rev.* 39, 764–778. doi: 10.1093/femsre/fuv031

Kim, Y. H., Lee, J., Kim, Y. E., Chong, C. K., Pinchemel, Y., Reisdorfer, F., et al. (2018). Development of a rapid diagnostic test kit to detect IgG/IgM antibody against zika virus using monoclonal antibodies to the envelope and non-structural protein 1 of the virus. *Korean J. Parasitol.* 56, 61–70. doi: 10.3347/kjp.2018.56.1.61

Kindrachuk, J., Wahl-Jensen, V., Safronetz, D., Trost, B., Hoenen, T., Arsenault, R., et al. (2014). Ebola virus modulates transforming growth factor beta signaling and cellular markers of mesenchyme-like transition in hepatocytes. *J. Virol.* 88, 9877–9892. doi: 10.1128/jvi.01410-14

Koga, R., Kubota, M., Hashiguchi, T., Yanagi, Y., and Ohno, S. (2018). Annexin A2 mediates the localization of measles virus matrix protein at the plasma membrane. *J. Virol.* 92:e00181-18. doi: 10.1128/jvi.00181-18

Kuehnl, A., Musiol, A., Raabe, C. A., and Rescher, U. (2016). Emerging functions as host cell factors - an encyclopedia of annexin-pathogen interactions. *Biol. Chem.* 397, 949–959. doi: 10.1515/hsz-2016-0183

Kuhn, J. H. (2017). Guide to the correct use of filoviral nomenclature. *Curr. Top. Microbiol. Immunol.* 411, 447–460. doi: 10.1007/82_2017_7

Kurosaki, Y., Ueda, M. T., Nakano, Y., Yasuda, J., Koyanagi, Y., Sato, K., et al. (2018). Different effects of two mutations on the infectivity of Ebola virus glycoprotein in nine mammalian species. *J. Gen. Virol.* 99, 181–186. doi: 10.1099/jgv.0.000999

Lee, J. H., Yi, L., Li, J., Schweitzer, K., Borgmann, M., Naumann, M., et al. (2013). Crystal structure and versatile functional roles of the COP9 signalosome subunit 1. *Proc. Natl. Acad. Sci. U.S.A.* 110, 11845–11850. doi: 10.1073/pnas.1302418110

Ma, Y., Sun, J., Gu, L., Bao, H., Zhao, Y., Shi, L., et al. (2017). Annexin A2 (ANXA2) interacts with nonstructural protein 1 and promotes the replication of highly pathogenic H5N1 avian influenza virus. *BMC Microbiol.* 17:191. doi: 10.1186/s12866-017-1097-0

Mosadeghi, R., Reichermeier, K. M., Winkler, M., Schreiber, A., Reitsma, J. M., Zhang, Y., et al. (2016). Structural and kinetic analysis of the COP9-signalosome activation and the cullin-RING ubiquitin ligase deneddylation cycle. *eLife* 5:e12102. doi: 10.7554/eLife.12102

Nanbo, A., Imai, M., Watanabe, S., Noda, T., Takahashi, K., Neumann, G., et al. (2010). Ebolavirus is internalized into host cells via macropinocytosis in a viral glycoprotein-dependent manner. *PLoS Pathog.* 6:e1001121. doi: 10.1371/journal.ppat.1001121

Nelson, E. V., Pacheco, J. R., Hume, A. J., Cressey, T. N., Deflube, L. R., Ruedas, J. B., et al. (2017). An RNA polymerase II-driven Ebola virus minigenome system as an advanced tool for antiviral drug screening. *Antiviral Res.* 146, 21–27. doi: 10.1016/j.antiviral.2017.08.005

Obsilova, V., Kopecka, M., Kosek, D., Kacirova, M., Kylarova, S., Rezabkova, L., et al. (2014). Mechanisms of the 14-3-3 protein function: regulation of protein function through conformational modulation. *Physiol. Res.* 63(Suppl. 1), S155–S164.

Oestereich, L., Rieger, T., Neumann, M., Bernreuther, C., Lehmann, M., Krasemann, S., et al. (2014). Evaluation of antiviral efficacy of ribavirin, arbidol, and T-705 (favipiravir) in a mouse model for crimean-congo hemorrhagic fever. *PLoS Negl. Trop. Dis.* 8:e2804. doi: 10.1371/journal.pntd.0002804

Ohman, T., Lietzen, N., Valimaki, E., Melchjorsen, J., Matikainen, S., and Nyman, T. A. (2010). Cytosolic RNA recognition pathway activates 14-3-3 protein mediated signaling and caspase-dependent disruption of cytokeratin network in human keratinocytes. *J. Proteome Res.* 9, 1549–1564. doi: 10.1021/pr901040u

Ohman, T., Soderholm, S., Hintsanen, P., Valimaki, E., Lietzen, N., MacKintosh, C., et al. (2014). Phosphoproteomics combined with quantitative 14-3-3-affinity capture identifies SIRT1 and RAI as novel regulators of cytosolic double-stranded RNA recognition pathway. *Mol. Cell. Proteomics* 13, 2604–2617. doi: 10.1074/mcp.M114.038968

Radhakrishnan, V. M., Putnam, C. W., and Martinez, J. D. (2012). Activation of phosphatidylinositol 3-kinase (PI3K) and mitogen-activated protein kinase (MAPK) signaling and the consequent induction of transformation by overexpressed 14-3-3gamma protein require specific amino acids within 14-3-3gamma N-terminal variable region II. *J. Biol. Chem.* 287, 43300–43311. doi: 10.1074/jbc.M112.397877

Ramakrishnan, M. A. (2016). Determination of 50% endpoint titer using a simple formula. *World J. Virol.* 5, 85–86. doi: 10.5501/wjv.v5.i2.85

Richard, A. S., Zhang, A., Park, S. J., Farzan, M., Zong, M., and Choe, H. (2015). Virion-associated phosphatidylethanolamine promotes TIM1-mediated infection by Ebola, dengue, and *West Nile viruses*. *Proc. Natl. Acad. Sci. U.S.A.* 112, 14682–14687. doi: 10.1073/pnas.1508095112

Robinson, J. D., and Pitcher, J. A. (2013). G protein-coupled receptor kinase 2 (GRK2) is a Rho-activated scaffold protein for the ERK MAP kinase cascade. *Cell. Signal.* 25, 2831–2839. doi: 10.1016/j.cellsig.2013.08.031

Rogers, K. J., and Maury, W. (2018). The role of mononuclear phagocytes in Ebola virus infection. *J. Leukoc. Biol.* 104, 717–727. doi: 10.1002/jlb.4ri0518-183r

Sakurai, Y., Kolokoltsov, A. A., Chen, C. C., Tidwell, M. W., Bauta, W. E., Klugbauer, N., et al. (2015). Ebola virus. Two-pore channels control Ebola virus host cell entry and are drug targets for disease treatment. *Science* 347, 995–998. doi: 10.1126/science.1258758

Simpson, J. C., Joggerst, B., Laketa, V., Verissimo, F., Cetin, C., Erfle, H., et al. (2012). Genome-wide RNAi screening identifies human proteins with a regulatory function in the early secretory pathway. *Nat. Cell Biol.* 14, 764–774. doi: 10.1038/ncb2510

Sissoko, D., Laouenan, C., Folkesson, E., M'Lebing, A. B., Beavogui, A. H., Baize, S., et al. (2016). Experimental treatment with favipiravir for ebola virus disease (the JIKI Trial): a historically controlled, single-arm proof-of-concept trial in Guinea. *PLoS Med.* 13:e1001967. doi: 10.1371/journal.pmed.1001967

Spurgers, K. B., Alefantis, T., Peyser, B. D., Ruthel, G. T., Bergeron, A. A., Costantino, J. A., et al. (2010). Identification of essential filovirion-associated host factors by serial proteomic analysis and RNAi screen. *Mol. Cell. Proteomics* 9, 2690–2703. doi: 10.1074/mcp.M110.003418

Strong, J. E., Wong, G., Jones, S. E., Grolla, A., Theriault, S., Kobinger, G. P., et al. (2008). Stimulation of Ebola virus production from persistent infection through activation of the Ras/MAPK pathway. *Proc. Natl. Acad. Sci. U.S.A.* 105, 17982–17987. doi: 10.1073/pnas.0809698105

Taguwa, S., Maringer, K., Li, X., Bernal-Rubio, D., Rauch, J. N., Gestwicki, J. E., et al. (2015). Defining Hsp70 subnetworks in dengue virus replication reveals key vulnerability in flavivirus infection. *Cell* 163, 1108–1123. doi: 10.1016/j.cell.2015.10.046

Takada, A. (2012). Filovirus tropism: cellular molecules for viral entry. *Front. Microbiol.* 3:34. doi: 10.3389/fmicb.2012.00034

van Zuylen, W. J., Doyon, P., Clement, J. F., Khan, K. A., D'Ambrosio, L. M., Do, F., et al. (2012). Proteomic profiling of the TRAF3 interactome network reveals a new role for the ER-to-Golgi transport compartments in innate immunity. *PLoS Pathog.* 8:e1002747. doi: 10.1371/journal.ppat.1002747

Vashist, S., Urena, L., Gonzalez-Hernandez, M. B., Choi, J., de Rougemont, A., Rocha-Pereira, J., et al. (2015). Molecular chaperone Hsp90 is a therapeutic target for noroviruses. *J. Virol.* 89, 6352–6363. doi: 10.1128/jvi.00315-15

Vomastek, T., Iwanicki, M. P., Burack, W. R., Tiwari, D., Kumar, D., Parsons, J. T., et al. (2008). Extracellular signal-regulated kinase 2 (ERK2) phosphorylation sites and docking domain on the nuclear pore complex protein Tpr cooperatively regulate ERK2-Tpr interaction. *Mol. Cell. Biol.* 28, 6954–6966. doi: 10.1128/mcb.00925-08

Wolf, T., Kann, G., Becker, S., Stephan, C., Brodt, H. R., de Leuw, P., et al. (2015). Severe ebola virus disease with vascular leakage and multiorgan failure: treatment of a patient in intensive care. *Lancet* 385, 1428–1435. doi: 10.1016/s0140-6736(14)62384-9

Younan, P., Iampietro, M., Nishida, A., Ramanathan, P., Santos, R. I., Dutta, M., et al. (2017). Ebola virus binding to Tim-1 on T lymphocytes induces a cytokine storm. *mBio* 8:e00845-17. doi: 10.1128/mBio.00845-17

Conflict of Interest Statement: The authors declare that the research was conducted in the absence of any commercial or financial relationships that could be construed as a potential conflict of interest.

Copyright © 2018 Yu, Weng, Hu, Wu, Li, Cheng, Wu, Li and Yao. This is an open-access article distributed under the terms of the Creative Commons Attribution License (CC BY). The use, distribution or reproduction in other forums is permitted, provided the original author(s) and the copyright owner(s) are credited and that the original publication in this journal is cited, in accordance with accepted academic practice. No use, distribution or reproduction is permitted which does not comply with these terms.

frontiers in Microbiology

ORIGINAL RESEARCH
published: 13 November 2018
doi: 10.3389/fmicb.2018.02734

EGFR as a Negative Regulatory Protein Adjusts the Activity and Mobility of NHE3 in the Cell Membrane of IPEC-J2 Cells With TGEV Infection

*Zhou Yang†, Ling Ran†, Peng Yuan, Yang Yang, Kai Wang, Luyi Xie, Shilei Huang, Jia Liu and Zhenhui Song**

Department of Veterinary Medicine, Southwest University, Chongqing, China

OPEN ACCESS

Edited by:
Ping An,
Frederick National Laboratory for Cancer Research (NIH), United States

Reviewed by:
Dongbo Sun,
Heilongjiang Bayi Agricultural University, China
Xiuqing Wang,
South Dakota State University, United States

****Correspondence:***
Zhenhui Song
szh7678@126.com

†These authors have contributed equally to this work

Specialty section:
This article was submitted to Virology, a section of the journal Frontiers in Microbiology

Received: *29 August 2018*
Accepted: *25 October 2018*
Published: *13 November 2018*

Citation:
Yang Z, Ran L, Yuan P, Yang Y, Wang K, Xie L, Huang S, Liu J and Song Z (2018) EGFR as a Negative Regulatory Protein Adjusts the Activity and Mobility of NHE3 in the Cell Membrane of IPEC-J2 Cells With TGEV Infection. Front. Microbiol. 9:2734. doi: 10.3389/fmicb.2018.02734

Transmissible gastroenteritis (TGE) has caused devastating economic losses to the swine industry worldwide, despite extensive research focusing on the pathogenesis of virus infection. The molecular pathogenic mechanism of TGEV-induced diarrhea in piglets is unknown. Intestinal diarrhea is closely related to the function of the Na^+/H^+ exchanger protein NHE3 in the brush border membrane of small intestine epithelial cells. The epidermal growth factor receptor (EGFR) may act to regulate NHE3 expression. In addition, EGFR may promote viral invasion of host cells. The present study aimed to determine whether NHE3 activity is regulated by altering EGFR expression to affect Na^+ absorption in TGEV-infected intestinal epithelial cells. Porcine intestinal epithelial cells were used as models for TGEV infection. The results showed that Na^+ absorption and NHE3 expression levels decreased in TGEV-infected cells. Proliferation of TGEV within IPEC-J2 cells could be inhibited by treatment with the EGFR inhibitor AG1478 and knockdown; resulting in recovery of Na^+ absorption in TGEV infected cells and increasing the activity and expression of NHE3. Moreover, we demonstrated that NHE3 activity was regulated through the EGFR/ERK pathway. Importantly, NHE3 mobility on the plasma membrane of TGEV infected cells was significantly weaker than that in normal cells, and EGFR inhibition and knockdown recovered this mobility. Our research indicated that NHE3 activity was negatively regulated by EGFR in TGEV-infected intestinal epithelial cells.

Keywords: transmissible gastroenteritis virus, NHE3, EGFR, infection, regulation

INTRODUCTION

Transmissible gastroenteritis (TGE), caused by transmissible gastroenteritis virus (TGEV), is one many gastrointestinal infections in piglets, characterized by diarrhea and high mortality (Wu et al., 2003). The villi of jejunum and ileum become shorter after TGEV infection, which destroys the absorption function of intestinal epithelial cells, affecting the transport of nutrients and electrolytes, and increasing the osmotic pressure in the intestinal lumen, finally leading to severe diarrhea and dehydration. Nowadays, TGEV is one of the most important diseases threatening pork production

worldwide. Diarrhea in piglets is accompanied by malnutrition, low immunity, serious stunting of growth and development, and a significant reduction in survival, with a mortality rate of up to 100% (Chae et al., 2000; Kim and Chae, 2001). Therefore, a study on pathogenesis of diarrhea caused by TGEV in piglets would be beneficial to improve treatments and coping strategies to reduce the economic losses in the pig industry.

Transmissible gastroenteritis virus belongs to the coronavirus pathogens that naturally infect pigs (Goh et al., 2012). The virus is transmitted by the mouth–nose route, and appears in the epithelial cells of the intestinal mucosa and alveolar macrophages in piglets, resulting in extensive injury of the lungs under severe conditions (Sestak et al., 2008). The virus sequentially spreads in the nasal mucosa, lungs, digestive tract, and small intestine. The microvilli of the jejunum and ileum shrink sharply or even break down, decreasing the absorption area of the intestinal villi (Zhao et al., 2014). Cell membrane transporter and ion channel transporter activities in intestinal epithelial decrease, resulting in disrupted Na^+ transport or an imbalance of absorption and secretion, causing substantial losses of nutrients and water-electrolytes in intestinal epithelial cells (Sun et al., 2014). As Na^+ absorption decreases, the osmotic pressure of the intestine increases abnormally, resulting in malabsorption diarrhea.

Malabsorption diarrhea includes abnormal Na^+ transporter activity in the brush border membrane of intestinal cells, which results in serious inhibition of Na^+ absorption (Liu et al., 2014). Na^+ absorption at the top of the brush border in intestinal epithelial cells of mammals is accomplished by two main pathways, including the functions of an Na^+/H^+ exchanger (NHE3) and an Na^+/glucose co-transporter (SGLT1), in which NHE3 plays a dominant role (Coon et al., 2011). A large amount of NHE3 promotes Na^+ absorption in the intestinal epithelium via an electroneutral pathway (Malakooti et al., 2014). Diarrhea is accompanied by disordered NHE3 activity.

NHE3 is a member of the third subtype of the Na^+/H^+ exchanger family, responsible for the stable absorption of water and Na^+ in cells, and is highly expressed in the gastrointestinal tract and kidney (Zachos et al., 2005). NHE3 promotes the alternative transport of Na^+/H^+ between the small intestine and the apical membrane of the proximal tubule (Biemesderfer et al., 1993; Amemiya et al., 1995; Biemesderfer et al., 1997), and is responsible for the maintenance of Na^+ resorption and the acid–base balance in mammals, mediating the exchange pathway of extracellular Na^+ and intracellular H^+ in normal physiology to promote the absorption of water in the intestinal tract (Yin et al., 2015). Knockout of the *Nhe3* gene in mice resulted in a reduction of NaHCO3 resorption by proximal tubules of up to 60% (Wang et al., 2004); thus, the main source of Na^+/H^+ absorption in the intestinal tract of mice was ablated (Schultheis et al., 1998; Gawenis et al., 2002).

Membrane proteins on mammalian cell membranes play important roles in the uptake of water-electrolytes and nutrients. The membrane proteins on the plasma membrane are mobile within the membrane (Lin and Nie, 1985), allowing them to diffuse laterally in the lipid bilayer and move to the microvillus of the brush border membrane to perform their functions in nutrients absorption and material transport. The dynamic transport of membrane protein NHE3 has been studied using fluorescence bleaching recovery (FRAP) technology, which showed that the lysophosphatidic acid (LPA)/LPA5R signaling pathway, mediated by the epidermal growth factor receptor (EGFR), is involved in the regulation of NHE3 activity in microvilli. LPA, as an inflammatory factor, directly induces intestinal anti-secretion, and intensively stimulated NHE3 activity to inhibit secretory diarrhea induced by cholera. The FRAP results showed that LPA could increase NHE3 mobility in inflammatory bowel disease. The dynamic transport of NHE3 on intestinal microvillus was regulated by stimulating an increase in extracellular secretion (Lin et al., 2010).

To date, there have been many studies on vaccines and drugs targeted to TGEV in China; however, there have been fewer studies on the pathogenesis of TGEV, and the factors affecting diarrhea caused by TGEV in piglets remain unclear. Studies showed that diarrhea could decrease the activity and mobility of NHE3 in the intestinal microvillus (Cha et al., 2010; Lin et al., 2010), and the amount of NHE3 decreased rapidly. A few studies on the regulation of NHE3 activity have been performed under normal physiological conditions; however, the effects on the activity of NHE3 during diarrhea caused by TGEV infection have not been reported. EGFR may influence TGEV entrance, enhancing the ability of the virus to infect intestinal epithelial cells (Hu et al., 2016). In addition, EGFR is involved in the regulation of NHE3 activity during its dynamic transport. We hypothesized that in TGEV-infected cells, the dynamic transport of NHE3 would be regulated by TGEV infection. NHE3 mobility on the microvillus of the brush border membrane would be altered and NHE3 activity would be inhibited, ultimately affecting Na^+ absorption in intestinal epithelial cells. It is important to explore this possible regulatory mechanism of the pathogenesis of diarrhea caused by TGEV infection in piglets.

MATERIALS AND METHODS

Cells, Viruses, and Reagents

Porcine jejunum intestinal cells (IPEC-J2) were grown at 37°C and 5% CO_2 in Roswell Park Memorial Institute (RPMI) 1640 medium (Gibco, United States) supplemented with 4% fetal bovine serum (FBS, Gibco), respectively. IPEC-J2 cells were purchased from Shanghai Zishi Biotechnology. The Miller strain of TGEV was preserved in our laboratory. We selected the tyrosine kinase inhibitor AG1478 as the inhibitor of EGFR, based on amino acid sequence of EGFR from NCBI.

Experiment of Gene Silencing

Lentivival vectors (pLKO.1) purchased from Wuhan Miaoling Biotechnology designed to express short hairpin RNA (shRNA). shRNA lentiviral particles were used to designate EGFR (pLKO.1-EGFR-p-shRNA) for silencing of EGFR expression. pLKO.1-TRC was used to generate control lentivival. IPEC-J2 cells in TGEV-Infected groups and un-infected groups were prepared, respectively, to be transfected with the EGFR-specific shRNA plasmid using Lipofectamine^{TM} 3000 (Invitrogen, United States), according to the manufacturer's instructions.

Construction of the Expression Vector

To measure NHE3 mobility in IPEC-J2 cells, the coding sequence of NHE3 (GenBank ID: XM_021077062.1) was used. On the basis of no change occurring to the amino acid sequence of NHE3, the coding sequence was amplified as a 2,511 bp fragment, with Nhe I and Hind III restriction sites inserted at the 5′ and 3′ ends, respectively. The NHE3 gene fragment was synthesized by Wuhan Miaoling Biotechnology and then cloned into vector pEGFP-N3 vector (Clontech, Mountain View, CA, United States) to assemble the full-length pEGFP-NHE3 recombinant fluorescence plasmid for FRAP measurements.

Transfection of the Recombinant Plasmid

IPEC-J2 cells were cultured on glass-bottomed 35-mm plastic culture dishes in RPMI 1640 medium (Gibco), supplemented with 5% FBS, 1% penicillin–streptomycin at 37°C in a 5% CO_2. Cells were incubated in a 6-well plate for at least 24 h before transfection (60–70% confluency), and then incubated with the transfection complex containing 2.5 μg of pEGFP-NHE3 and pEGFP-N3 (Vector) in 125 μL of Opti-MEM medium mixed with Lipofectamine^{TM} 3000 (Invitrogen, United States), which was added to the cells in a dropwise manner, according to the manufacturer's instructions. After observation under a fluorescence microscope, we determined the stable expression of the fluorescence protein. For FRAP detection, a premix comprising RPMI 1640 and 30 μM AG1478 was evenly covered on surface of the cells. After incubation for 24 h, the cells were infected with 0.1 multiplicity of infection (MOI) of TGEV per well in 6-well plates.

$TCID_{50}$ Analysis

TGEV-infected cells were collected 48 h after treatment with AG1478, subjected to three cycles of freezing and thawing, diluted sevenfold from 10^{-1} to 10^{-7} consistently, and added to 96-well plates. Each dilution was added to eight replicated wells. The method of Reed and Muench was then used to calculate $TCID_{50}$ of the virus for the different groups.

Flame Atomic Absorption Spectrometry

Samples to determine the intracellular and extracellular Na^+ levels of IPEC-J2 were collected from the cell lysate after treatment with radioimmunoprecipitation assay (RIPA) solution and from the cell culture supernatant, respectively. Deionized water was used for all dilutions. A Na^+ standard solution (10 μg/mL) was prepared by dissolving 1 mL of Na^+ standard solution (1,000 μg/mL) in 100 mL of deionized water. The potassium (K) blank solution was prepared by dissolving 2.593 g of KNO3 in 50 mL of 5% HNO3, and then diluting to 500 mL with deionized water to get a 5% HNO_3+K solution containing 2 mg/mL of K. The Na^+ standard solution was then diluted as standard working solutions to 0.05, 0.1, 0.2, and 0.4 μg/mL. The intracellular and extracellular samples were diluted by 9.5×10^4-fold and 6×10^3-fold, respectively, to prepare for Na^+ detection. The instrument conditions of the TAS-990 atomic absorption spectrometer were set as follows: Wavelength of 589 nm, negative high-voltage of 297 V, current of 2 mA, and a gas flow of 1,200 mL min^{-1}, to measure the Na^+ concentration of samples collected from different groups.

Quantitative Real-Time Reverse Transcription Polymerase Chain Reaction (qRT-PCR)

Quantitative analysis of *NHE3* mRNA levels in TGEV-infected cells was performed using qRT-PCR with specific primers. Samples to be tested were collected from IPEC-J2 cells after TGEV infection for different times. Total RNA was extracted using the RNAiso plus reagent (Takara, Tokyo, Japan), and single-stranded cDNA was synthesized by reverse transcription using RNA PCR^{TM} Kit (AMV) Ver 3.0 Kit (Takara) according to the manufacturer's instructions. Quantitative real-time PCR was then performed using SYBR Premix EX Taq II (Takara), with the following specific primers: NHE3 (Forward: 5′-GACCATCAAGCCTCTGGTGC-3′and Reverse: 5′-AATGTCCTCGATGGCCGAGA-3′), β-Actin (Forward: 5′-CTCTTCCAGCCCTCCTTCC-3′and Reverse: 5′-GGTCCTTGCGGATGTCG-3′), under the following conditions: 30 s at 95°C, and then 39 cycles of 5 s at 95°C, followed by 30 s at 60°C. Triplicate measurements were applied to calculate the average cycle threshold (Ct) for each individual test using the QuantStudio^{TM} 3 System software (Applied Biosystems, Carlsbad, CA, United States).

Western Blot Analysis

Protein samples separated by SDS-PAGE were transferred to nitrocellulose membranes (Bio-Rad). The membranes were incubated with the following primary antibodies: rabbit polyclonal anti-NHE3 (Affinity), rabbit polyclonal anti-EGFR (Biorbyt), rabbit polyclonal anti-phospho-EGF (Tyr1068) (Cell Signaling), rabbit polyclonal anti-phospho-ERK1/2 (Thr202+Tyr204) (Bioss), rabbit polyclonal anti-β-tubulin (Proteintech), with goat anti-rabbit IgG (H+L) antibodies (Sangon Biotech) as the secondary antibody. Images of blots were obtained using a VILBER Fusion FX5 imaging system (VILBER) and the gray levels of all bands were analyzed.

Fluorescence Recovery After Photobleaching (FRAP)

Fluorescence recovery after photobleaching was used to determine the lateral mobility of pEGFP-NHE3 at the apical domain of polarized IPEC-J2 cells. IPEC-J2 cells were cultured on glass-bottomed 35-mm plastic culture dishes in RPMI 1640 medium without phenol red. The cells were then transfected using Lipofectamine^{TM} 3000 with pEGFP-NHE3, and then infected with TGEV, during which time the cells were not exposed to serum. The glass-bottomed culture dish was then placed on the microscope stage for FRAP measurement. The region of interest (ROI) used to collect signal was located in a square of the apical domain (0.3 μm) of the target cell. The mobile fraction and diffusion rate were then calculated. High laser power (100% power, 100% transmission) was used for photobleaching. Before and after bleaching, we used 20%

laser power with 1% transmission to measure the fluorescence. During the measurement, the 488 nm line of a 400 mW Kr/Ar laser was used. One image was collected every 60 s, and the bleaching and recovery were set with 10 time series. The images were saved after capturing of all the time series. The fluorescence intensity of the anchoring bleached region during the whole recovery process of fluorescence bleaching was detected and analyzed by the image analysis system of the Zen blue software (ZEISS, Germany). The percentage of maximal bleached fluorescence could be calculated from the recovery rates. The intensity ratio of the fluorescence intensity before bleaching (Fi), after bleaching (F0), and during full recovery (F∞) in the bleached region were compared, and the mobile and immobile fractions of the ROI were calculated using the equation: Mf = (F∞ − F0)/(Fi − F0) × 100%. In each treatment group, the data from at least five cells were used for quantification and were measured repeatedly.

Statistical Analyses

All results in the figures are presented as the mean ± the standard deviation (SD) from three independent experiments, and were analyzed using GraphPad Prism 6 software (GraphPad Inc.). For each assay, a *t*-test was used for statistical comparison and a *p*-value < 0.05 was considered statistically significant.

RESULTS

NHE3 Expression Is Related to Na^+ Absorption in TGEV-Infected Cells

Research on the mechanism of diarrhea has mainly focused on the physiological activity of Na^+/H^+ exchange proteins (Singh et al., 2014). Under normal physiological conditions, Na^+/H^+ exchanger NHE3 is generally responsible for the intake of Na^+ in intestinal epithelial cells. Thus, cellular Na^+ absorption is determined by the NHE3 activity. In mammals, the deletion of the NHE3 gene profoundly weakened Na^+ absorption. Therefore, we examined the changes in the intra- and extracellular Na^+ concentration in intestinal epithelial cells using flame atomic absorption spectrometry at 0, 48, and 72 h post-TGEV infection. Compared with the control group, the extracellular

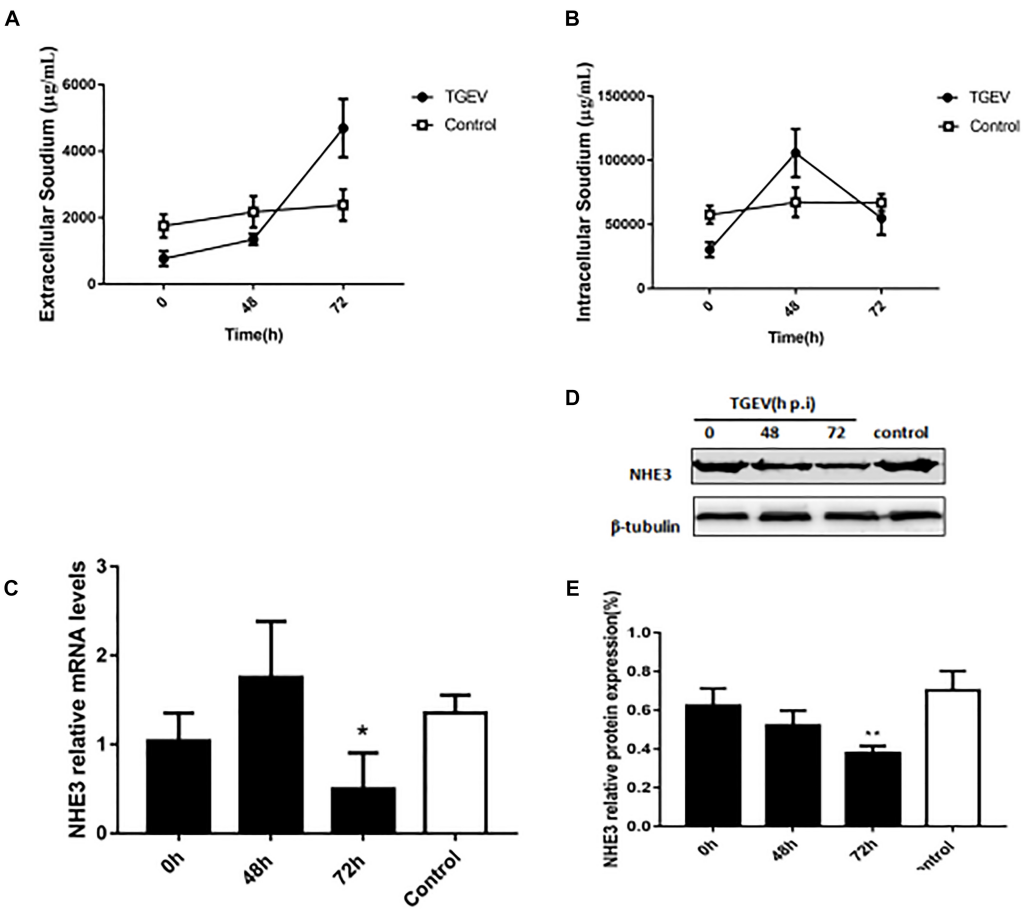

FIGURE 1 | The effect of TGEV on Na^+ concentration and the relative expression of NHE3 in IPEC-J2 cells. **(A,B)** Intra and extracellular Na^+ concentration in cells infected with TGEV at 0, 48, and 72 h post infection. **(C)** NHE3 mRNA expression levels were detected using qRT-PCR and normalized by the β-actin mRNA level. **(D)** NHE3 protein levels were analyzed by Western blotting. **(E)** Grayscale analysis of NHE3 relative abundance changes. $*0.01 < p < 0.05$, $**p < 0.01$.

Na^+ concentration of the TGEV-infected group continued to increase, reaching its highest levels at 72 h post-infection (p.i.) (**Figure 1A**). The intracellular Na^+ concentration gradually increased up to 48 h p.i., and then began to decrease in the last period (**Figure 1B**). By contrast, the intra and extracellular Na^+ levels in the control showed almost no change, suggesting that TGEV infection affected the intra- and extracellular Na^+ concentration in piglet intestinal epithelial cells. Subsequently, we examined the expression level of the NHE3 gene (**Figure 1C**). In IPEC-J2 cells during 72 h of TGEV infection, after an initial increase in expression, the mRNA level of *NHE3* decreased to a level lower than that of the control. We then used Western

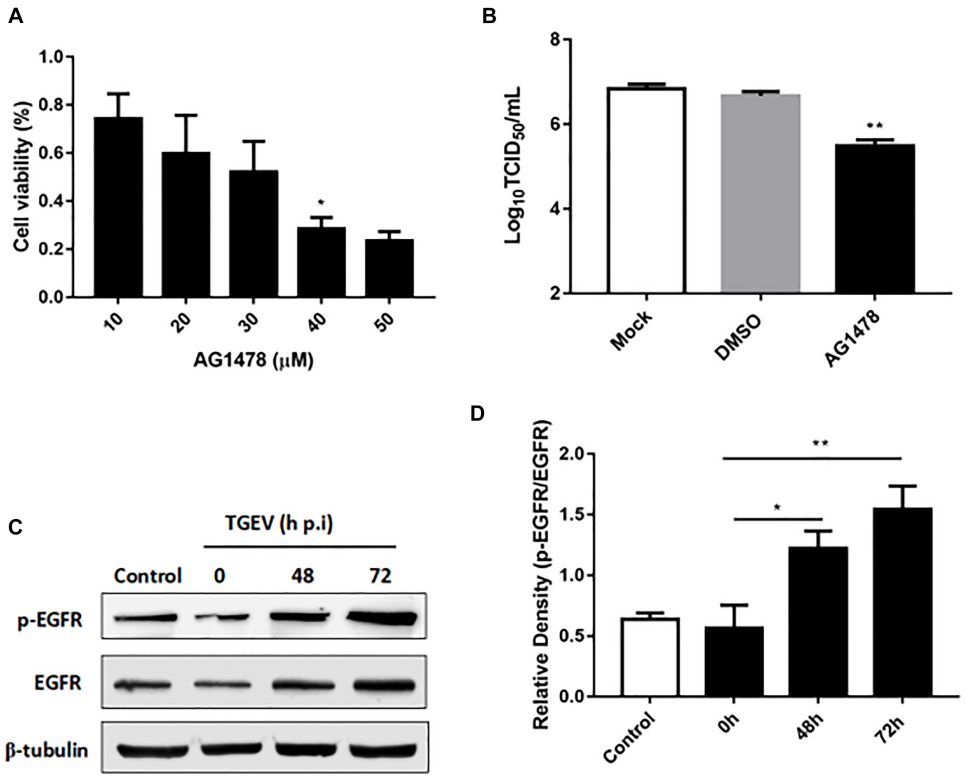

FIGURE 2 | The role of EGFR in IPEC-J2 cells infected with TGEV. **(A)** MTT detection of cell viability after treatment with AG1478 at different concentrations in IPEC-J2 cells. **(B)** The propagation of TGEV in IPEC-J2 cells after treatment with 30 μM AG1478. **(C)** EGFR protein expression levels were analyzed by Western blotting. **(D)** Grayscale analysis for the level of phosphorylated EGFR in IPEC-J2 cells infected with TGEV at 0, 48, and 72 h post-infection. $*0.01 < p < 0.05$, $**p < 0.01$.

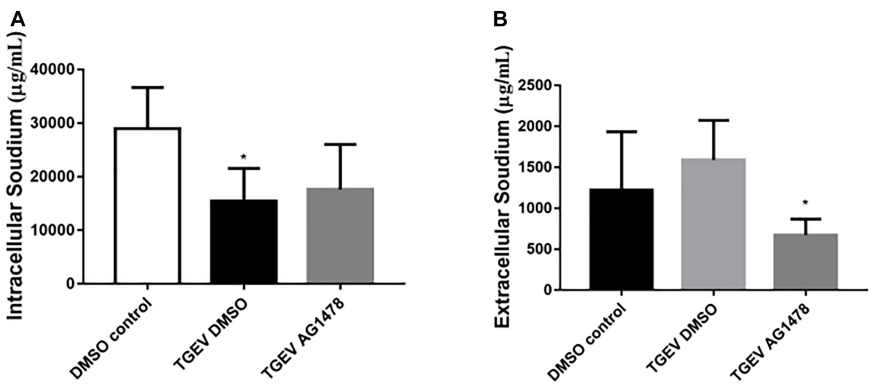

FIGURE 3 | Effect of inhibition of EGFR on the intracellular and extracellular Na^+ concentration in TGEV-infected cells. **(A)** Intracellular Na^+ concentration in IPEC-J2 cells after treatment with 30 μM AG1478 or DMSO for 24 h; samples collected from the cell lysate were tested. **(B)** Extracellular Na^+ concentration in IPEC-J2 cells after treatment with AG1478 or DMSO for 24 h; samples collected from the cell culture medium were tested. $*0.01 < p < 0.05$.

blotting to study the effect of TGEV infection on level of the NHE3 protein in IPEC-J2 cell at 0, 48, and 72 h p.i. The results suggested that TGEV infection caused consistent downregulation of NHE3 levels, most significant at 72 h p.i. compared with 0 h p.i. (**Figures 1D,E**).

TGEV Invasion Is Suppressed via Inhibition of EGFR

Epidermal growth factor receptor is regarded as a transmembrane receptor for multiple viruses, including TGEV (Eppstein et al., 1985; Hu et al., 2016). To determine whether EGFR affects the process of TGEV invasion and infection of IPEC-J2 cells, we used Western blotting to assess its levels in TGEV-infected cells. We observed that the level of phosphorylated EGFR increased during TGEV infection (**Figures 2C,D**), especially at 72 h p.i. We then used AG1478 as an EGFR inhibitor to suppress EGFR in IPEC-J2 cells. The 3-(4,5-dimethylthiazol-2-yl)-2,5-diphenyltetrazolium bromide (MTT) assay showed that cell viability was not reduced after EGFR inhibition (**Figure 2A**), and that 30 μM was the best toxic dosage of AG1478 for IPEC-J2 cells. To study whether AG1478 could inhibit TGEV proliferation in cells, we used 30 μM AG1478 to treat cells for 24 h, followed by incubation with 10^4 $TCID_{50}$ TGEV for 48 h. The results showed that the average viral titer of the DMSO group (infected with TGEV after treatment with 30 μM DMSO) was $10^{6.84}$ $TCID_{50}$/mL, and the titer of the AG1478 group (infected with TGEV after treatment with 30 μM AG1478) was $10^{5.49}$ $TCID_{50}$/mL, representing a reduction of 93.3% compared with that of the DMSO group (**Figure 2B**). These data showed that proliferation of TGEV in IPEC-J2 cells could be reduced by inhibiting EGFR.

Inhibition of EGFR Promotes Na^+ Absorption in TGEV-Infected Cells

To further investigate the role of EGFR in Na^+ absorption in TGEV-infected IPEC-J2 cells, we examined the effects of AG1478 treatment on Na^+ absorption. As shown in **Figure 3A**, the intracellular Na^+ concentration of IPEC-J2 cells was significantly increased by treatment with the EGFR inhibitor AG1478 during TGEV infection. By contrast, treatment with AG1478 significantly reduced the extracellular Na^+ concentration (**Figure 3B**). These data showed that EGFR inhibition could restore the function of Na^+ absorption in IPEC-J2 cells during TGEV infection.

NHE3 Protein Levels Are Regulated Though the EGFR/ERK Pathway

During viral invasion of host cells, the first step is to combine with receptors on the cell membrane, and then transfer signals into cells to stimulate a series of downstream signal cascade reactions (Homma and Yasui, 1968). The transmembrane receptor EGFR can promote virus invasion of host cells and activate downstream signaling pathways, of which the most common pathway is the MAPK signaling pathway. Diarrhea weakens the Na^+ absorption function of intestinal epithelial cells. Na^+ absorption is primarily mediated by NHE3 in the cell membrane. Therefore, we assessed

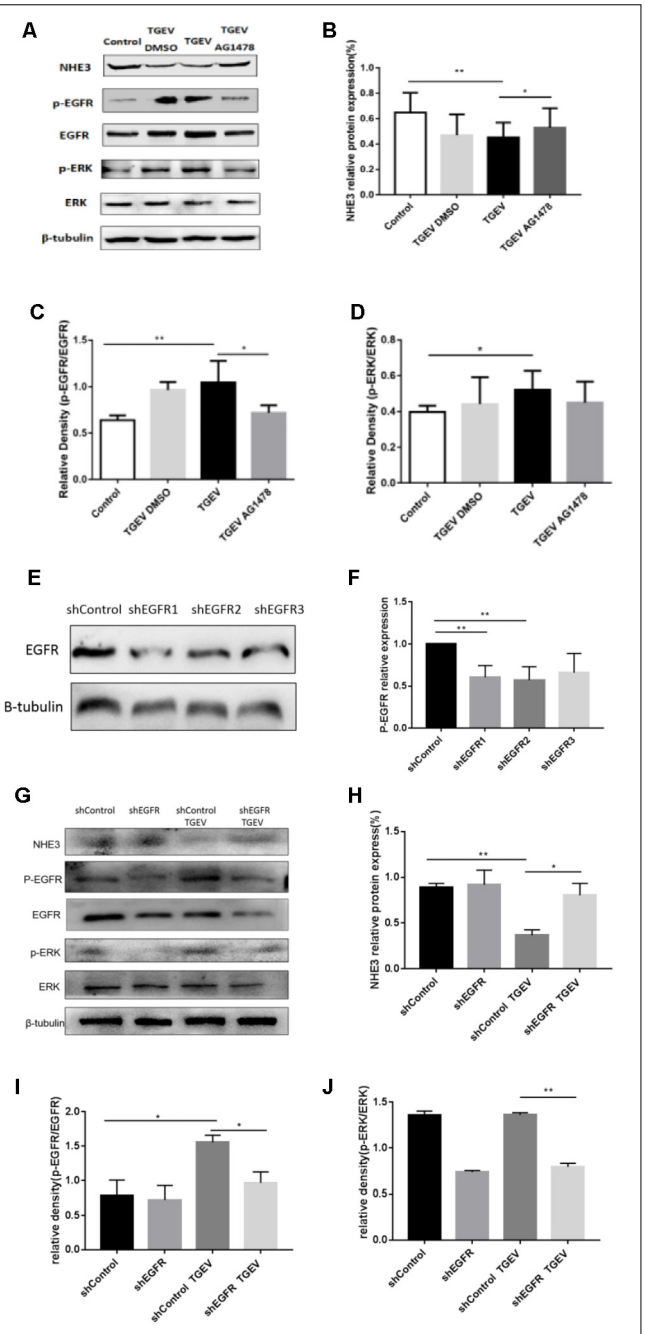

FIGURE 4 | TGEV regulated the inhibition of NHE3 via the EGFR/ERK pathway. **(A)** IPEC-J2 cells in corresponding groups were treated with AG1478, protein levels of NHE3, p-EGFR, EGFR, p-ERK, and ERK in TGEV-infected cells or uninfected cells were analyzed by Western blotting using specific antibodies. **(B–D)** Grayscale analysis of the changes in NHE3, p-EGFR/EGFR, and p-ERK/ERK levels, as analyzed using the spass software. **(E,F)** Knockdown of EGFR expression in IPEC-J2 cells by short hairpin shEGFR lentivirus was decreased by 57–66% in shEGFR-infected cells compared with control cells. **(G)** IPEC-J2 cells in corresponding groups were treated with EGFR-specific shRNA, expression levels of p-EGFR, EGFR, p-ERK, ERK, and NHE3 proteins were evaluated by Western blotting analysis. **(H–J)** Grayscale analysis of the changes in p-EGFR/EGFR, p-ERK/ERK, and NHE3 levels, as analyzed using the spass software. Each experiment was performed in triplicate. $*0.01 < p < 0.05$, $**p < 0.01$.

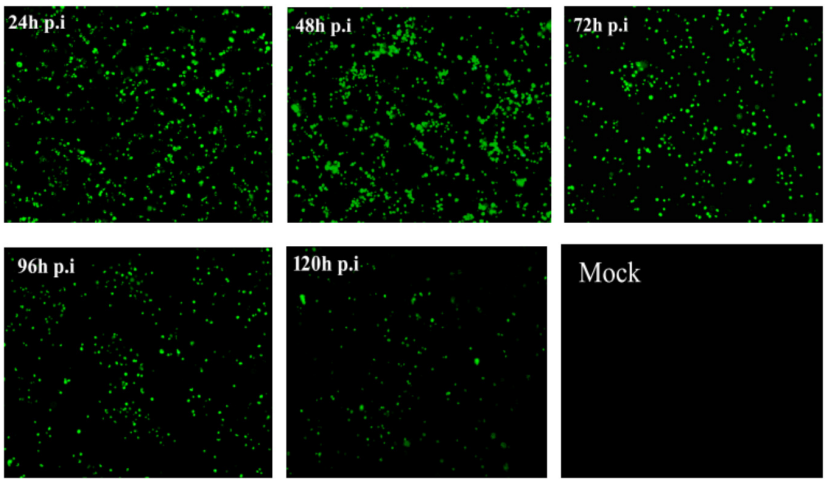

FIGURE 5 | Fluorescence observation of IPEC-J2 cells transfected with pEGFP-NHE3 (10×). IPEC-J2 cells were transfected with recombinant vector (pEGFP-NHE3) for different times (24, 48, 72, and 120 h), and examined using fluorescence/phase-contrast microscopy.

whether the activity and expression of NHE3 was regulated via activation of the EGFR/ERK signaling pathway in IPEC-J2 cells during TGEV infection. As shown in **Figure 4**, we chose 30 μM AG1478 and DMSO to treat cells for 24 h, respectively, and then infected them with TGEV. Meanwhile, normal cells without any treatment were regarded as the control group. As shown in **Figure 4B**, the NHE3 protein level in the TGEV-infected group was significantly decreased compared with that in normal cells group, and its level in the TGEV plus AG1478 group was increased compared with that in the TGEV-infected group. Compared with the control group, the level of phosphorylated EGFR or ERK in the TGEV-infected group was significantly increased (**Figure 4A**). However, the level of p-EGFR in the TGEV plus AG1478 group was significantly lower than that in the TGEV-infected group (**Figure 4C**). The level of p-ERK was also downregulated (**Figure 4D**). We confirmed the knockdown efficiency of EGFR (**Figures 4E,F**). As well as the effect of EGFR inhibitor AG1478 on NHE3 via EGFR interference, transfection of PLKO.1-EGFR-p-shRNA in IPEC-J2 cells resulted in a significant increase in NHE3 activity, comparing with the TGEV-infected group (**Figure 4H**), suggesting that EGFR played a role in the regulation of NHE3 activity in IPEC-J2 cells, NHE3 activity could recover in TGEV-infected group after inhibition of EGFR. On the contrary, both phosphorylation levels of EGFR and ERK were significantly decreased compared with TGEV-infected group (**Figures 4I,J**), as well as knockdown of EGFR reduced the phosphorylation of EGFR and ERK in the TGEV-infected cells. These results suggested that the EGFR/ERK pathway is one of the pathways that regulate NHE3 protein activity in TGEV-infected cells.

EGFR as a Crucial Protein Controls NHE3 Mobility in Cytomembrane

Stable mobility of the brush border membrane is very important for the uptake of Na^+ and water-electrolytes in the intestinal epithelium. The membrane transporter NHE3 is mainly responsible for the electrically neutral translocation of Na^+/H^+ in intestinal epithelial cells, and changes in the transport capacity of Na^+/H^+ on the brush border membrane is determined by changes in NHE3 activity. In general, NHE3 on the plasma membrane diffuses to the top of the brush border to exert its function and stimulate the Na^+ absorption in the intestinal epithelium. To further identify the dynamic changes of NHE3 on the brush border membrane caused by TGEV infection in small intestinal epithelial cells, NHE3 mobility on the membrane of TGEV-infected cells after treatment with EGFR was analyzed using FRAP.

The recombinant expression plasmid pEGFP-NHE3 was transfected into IPEC-J2 cells and cultured at 37°C with 5% CO_2. The stable expression of the recombinant plasmid was observed under an inverted fluorescence microscope. The transient expression of green fluorescent protein (GFP) was observed under the control of a CMV promoter. Green fluorescence was produced using a 490 nm blue wavelength under the fluorescence microscope. The recombinant fluorescent-protein was expressed stably for 48 h and reached a peak at 24–120 h after transfection, as shown in **Figure 5**. Untransfected normal cells showed no fluorescence. The above results indicated that recombinant fluorescent plasmid pEGFP-NHE3 was transfected into IPEC-J2

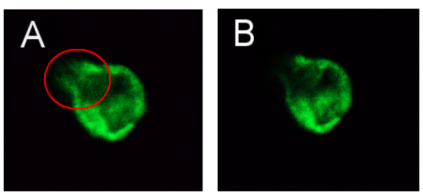

FIGURE 6 | LSCM images captured before **(A)** and after **(B)** bleaching (63×/1.4 NA).

cells and expressed the EGFP-NHE3 fusion protein successfully. The period of stable EGFP-NHE3 expression was about 5 days.

After transfection of the eukaryotic expression plasmid pEGFP-N3 into normal cells, this group was set as control vector group. FRAP analysis of eight cells was then used to determine the best time of fluorescence bleaching and recovery (**Figure 6**). After bleaching, the fluorescence intensity at the bleached region tended to be stable after 5 min. **Figure 6** show the images captured before and after bleaching, and 5 min was chosen as the best time of bleaching. After bleaching using an intense laser, the change in fluorescence intensity recovery was observed in the bleached area. The fluorescence recovery curve showed that the fluorescence intensity of the bleached area gradually recovered with prolonged time, and the fluorescence intensity of the bleached region tended to stabilize after 8 min. Therefore, 8 min was chosen as the best time to detect the fluorescence recovery rate in each group. The recovery rate of fluorescence bleaching and mobile fractions were measured in the same time period.

Subsequently, the fluorescence images at five time points (0, 2, 4, 6, and 8 min) were selected to reflect the dynamic change of fluorescence bleaching and recovery in each group (**Figure 7**). The formula used to calculate the FRAP rate in each group was as follows: $Kt = (Ft - F0)/(Fi - F0) \times 100\%$, where Kt represents the fluorescence recovery rate at each time point, Ft stands for the fluorescence intensity after bleaching, F0 stands for the fluorescence at time 0, and Fi stands for the fluorescence intensity before bleaching. The fluorescence recovery curves according to the fluorescence recovery rate at different time points for different groups of cells were then drawn (**Figure 8**). The results showed that the fluorescence recovery rate of NHE3 in cells infected with TGEV was significantly lower than that in the control group. The fluorescence recovery rate of NHE3 in TGEV-infected cells after treatment with AG1478 was significantly higher than that in cells infected with TGEV, but was lower than that in the control group without TGEV infection. The fluorescence recovery rate in cells transfected with the empty vector was the lowest compared with the other three groups, showing almost no recovery.

According to the analysis, the average value of stable fluorescence intensity restored before and after bleaching, and the mobile fraction of NHE3 in the four groups, was calculated using the following formula $M_f = (F_\infty - F_0)/(F_i - F_0) \times 100\%$, where, F_∞ was the fluorescence intensity returned to stability after bleaching, Fi was the fluorescence intensity before bleaching, and F0 was the fluorescence intensity at 0 min after bleaching. According to the analysis of the calculation results (**Figure 9**), the mobile fraction of the empty carrier group was reduced by 96% compared with the control group, and the difference was very significant ($p < 0.01$). The mobile fraction of NHE3 in TGEV-infected group decreased significantly by 54% ($0.01 < p < 0.05$). The mobile fraction of NHE3 in the TGEV plus AG1478 group increased by 33% compared with that in the TGEV group. The results showed that the non-quenched fluorescence molecules gradually diffused from the unbleached region to the bleached area with increasing time, and the fluorescence of the bleached region gradually recovered. Therefore, we believe that the membrane transporter NHE3 is mobile on the cell surface, and the different treatment groups had different NHE3 mobilities. NHE3 mobility on the plasma membrane was decreased in cells infected with TGEV compared with normal cells, and NHE3 mobility in cells infected with TGEV after treatment with AG1478 increased. These results indicated that decreased EGFR activity in intestinal epithelial cells was accompanied by increased NHE3 mobility after TGEV infection. Thus, EGFR negatively regulates NHE3 mobility on the plasma membrane in TGEV-infected cells.

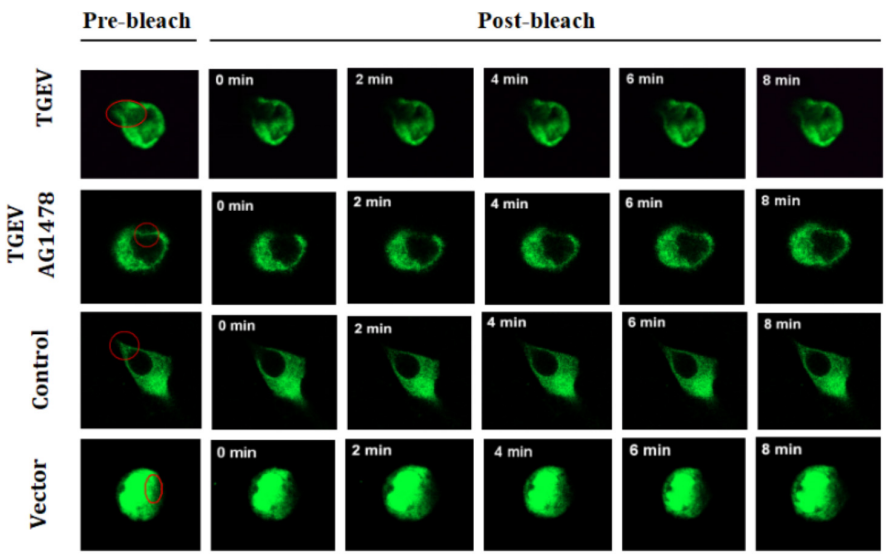

FIGURE 7 | Dynamic changes of fluorescent molecules within bleached regions during fluorescence recovery after photobleaching (63×/1.4 NA). Representative images of FRAP experiments in different groups of IPEC-J2 cells with TGEV infection or not, and for those treated with AG1478. The first images on the left are from before photo-bleaching, subsequent images were taken immediately or at 0, 2, 4, 6, and 8 min after bleaching.

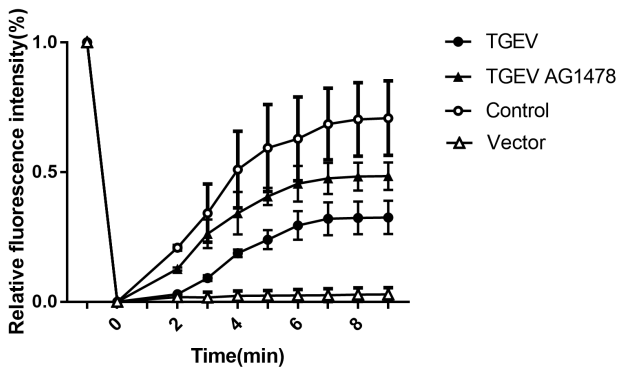

FIGURE 8 | Fluorescence recovery rate on the surface of IPEC-J2 cell (2 mW, 63×/1.4 NA). FRAP recovery curves of pEGFP-NHE3 in different groups are shown. Error bars represent the mean ± SD.

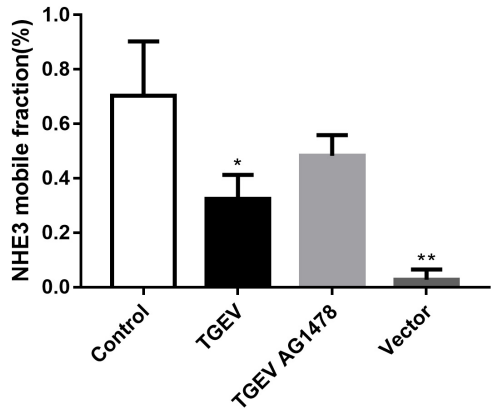

FIGURE 9 | Analysis of NHE3 mobile fraction (2 mW, 63×/1.4 NA). Each test was replicated three times. FRAP data from eight different cells in each group were used for the calculation and analysis. *$0.01 < p < 0.05$, **$p < 0.01$.

DISCUSSION

Previous studies showed that the absorption of Na^+ and water in the intestines dropped sharply and led to severe diarrhea in NHE3 deficient mice. The expression and activity of NHE3 were significantly inhibited under conditions of diarrhea and severe intestinal inflammation induced by cholera toxin (Coon et al., 2011; Yang et al., 2015). According to results of flame atomic absorption spectrometry, during TGEV infection, the intracellular Na^+ concentration increased before 48 h p.i., but decreased from 48 to 72 h p.i. The extracellular Na^+ concentration also increased, with a peak at 72 h p.i.

It is believed that the Na^+/H^+ exchanger protein NHE3 has two main functions. One is to transport extracellular Na^+ into cells and the other is to secrete intracellular H^+ to the extracellular area. Under normal physiological conditions, homeostasis is maintained between the intra and extra-cellular Na^+ concentration. Na^+/H^+ exchanger 3 (NHE3) and Na-glucose cotransporter-2 can deliver Na^+ from the extracellular medium into cells. At the same time, an intracellular Na–K pump will pump out the intracellular Na^+, thus to maintaining a normal Na^+ concentration gradient on both sides of the plasma membrane. Thus, the Na^+ concentration in inside and outside of uninfected cells seemed to be stable, without any obvious increases or decreases, which was in accordance with the theoretical basis. By contrast, TGEV infection resulted in a decrease in Na^+ absorption and reduced Na^+ transportation from the outside to inside of cells by NHE3, leading to a gradual increase in the extracellular Na^+ concentration and a decrease in the intracellular Na^+ concentration. Sodium/glucose cotransporter 1 (SGLT1) also plays a role in intracellular Na^+ absorption, acting as a Na^+-glucose co-transporter, which transports Na^+ across the plasma membrane of animal cells down an electrochemical gradient. Glucose is "dragged" into the cells against the concentration gradient. Meanwhile, SGLT1 can promote Na^+ absorption and glucose uptake of epithelial cells. Research has shown that SGLT1 plays a critical role during the process of TGEV infection in cells. Dai et al. (2016) reported that SGLT1 protein levels were upregulated and glucose uptake in the small intestine was enhanced in the early stage of TGEV infection of IPEC-J2 cells. However, later, the glucose intake of the intestinal epithelium decreased (Dai et al., 2016).

Our results showed that the intracellular Na^+ concentration in TGEV-infected cells increased before 48 h p.i. One of the likely explanations was that in IPEC-J2 cells with TGEV infection, SGLT1 could transport extracellular Na^+ into the cells down a concentration gradient during the early phase of infection with TGEV, to increase intracellular glucose intake. The subsequent decrease in the intracellular Na^+ concentration likely reflected the continuous infection with TGEV into the cells promoted by the increase of intracellular glucose intake, resulting in atrophy and rupture of intestinal epithelial microvillus. As the absorption area of intestinal villi decreases (Zhao et al., 2014), the quantity of NHE3 and mobility of in the brush border would also decrease. As the NHE3-mediated Na^+ transportation decreased, the intracellular Na^+ decreased and the extracellular Na^+ concentration increased.

We next investigated whether TGEV infection regulated the activity, abundance, and mobility of NHE3 through EGFR in IPEC-J2 cells. The spike protein (S) of TGEV combines with

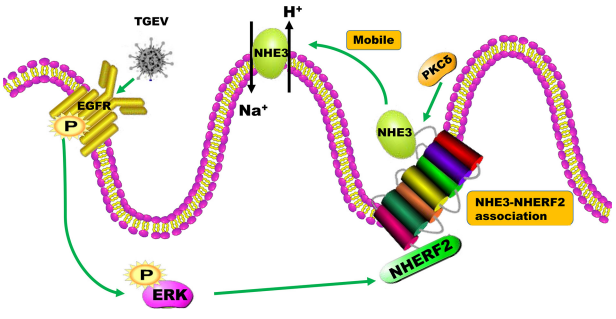

FIGURE 10 | The mechanism of the regulation of NHE3 activity by the EGFR/ERK signaling pathway in intestinal epidermal cells after TGEV infection.

EGFR to activate the downstream PI3K signaling pathway, allowing TGEV to invade small intestinal epithelial cells (Dai et al., 2016). Our results showed that the levels of p-EGFR and p-ERK were significantly upregulated in porcine intestinal epithelial cells after TGEV infection. In addition, the EGFR inhibitor AG1478 and kockdown of EGFR downregulated the levels of p-EGFR and p-ERK. Compared with TGEV-infected cells, the NHE3 levels in cells with TGEV infection after using EGFR inhibition and shRNA lentiviral particles were upregulated. These results showed that TGEV infection regulated NHE3 via the EGFR/ERK signaling pathway, and there was a negative correlation between EGFR and NHE3. EGFR and ERK are activated by TGEV infection in IPEC-J2 cells; however, AG1478 and PLKO.1-EGFR-p-shRNA could significantly reduce the proliferation of TGEV by inhibiting EGFR. Inhibition of EGFR reduced the damage caused by TGEV to intestinal epithelial cells, ameliorated the loss of intracellular Na^+ caused by TGEV infection, restored the normal function of membrane transporter NHE3, and promoted the transport of extracellular Na^+ into cells. The results indicated that TGEV could bind and activate the specific receptor EGFR in porcine intestinal epithelial cells after infection, leading to phosphorylation of ERK and regulation of the expression and activity NHE3, which resulted in dysfunctional NHE3 transport in intestinal epithelial cells. Extracellular Na^+ could not flow into the cells because of continuous accumulation of an Na^+ concentration gradient and the absorption of water and electrolyte-generated disorders.

NHE3 is mainly found in the brush border membrane of intestinal epithelial cells. The brush border consists of a large number of long microvilli. The number of NHE3 on the brush border membrane and the mobility of NHE3 on microvilli were significantly decreased under diarrheal conditions (Cha et al., 2010; Lin et al., 2010). Researchers found that LPA could promote the rapid movement of NHE3 from the bottom to the top of the microvillus to facilitate Na^+ absorption, promoting the absorption of water-electrolytes and relieving the symptoms of diarrhea. The main mechanism of this regulation is that PKCδ-dependent LPA could recognize LPA5R to activate EGFR and ERK, resulting in their phosphorylation. NHE3 is released from the bottom of the microvilli to the top by PKCδ, which would enhance NHE3 mobility on brush border membrane (Yoo et al., 2011; Cha et al., 2014).

We used FRAP to study whether the mobility of NHE3 on the plasma membrane changes in intestinal epithelial cells after TGEV infection. The results showed that the mobile fraction of pEGFP-NHE3 in the uninfected cells was the highest and had the strongest mobility. We inferred that NHE3 is very mobile on the microvillus of the brush border membrane of small intestinal epithelial cells under normal physiological conditions. Continuous Na^+ absorption is accomplished through NHE3 at the top of the plasma membrane by way of the lateral movement of the brush border membrane.

The mobile fractions of pEGFP-NHE3 decreased obviously in TGEV-infected cells, which might be due to the atrophy and rupture of intestinal epithelial microvillus in the small intestine, which would decrease the abundance and mobility of NHE3 on the brush border membrane. Compared with that in the TGEV-infected cells, NHE3 mobility in the TGEV-infected cells after EGFR inhibition was significantly increased. This result suggested that inhibition of EGFR activity could attenuate the damage to the brush border membrane microvilli caused by TGEV invasion and reduce intracellular virus proliferation in intestinal epithelial cells. In addition, NHE3 activity would be enhanced on the brush border membrane. Therefore, we speculated that the intensive mobility of NHE3 on the plasma membrane is beneficial for Na^+ absorption in porcine intestinal epithelial cells. This speculation needs to be proven in further experiments.

Based on the above results, the present study revealed that the activity and mobility of NHE3, regulated through the EGFR/ERK pathway on the brush border membrane of small intestinal epithelial cells, decreased after TGEV infection (**Figure 10**). This decreased the Na^+/H^+ transport mediated by NHE3 on the brush border membrane. Furthermore, the inhibition of EGFR was beneficial to the recovery of Na^+ absorption in TGEV-infected cells.

AUTHOR CONTRIBUTIONS

ZY, YY, and ZS conceived and designed the experiments. ZY, LR, YY, KW, and PY performed the experiments. ZY, LX, SH, and JL analyzed the data. ZY, LR, and ZS wrote the manuscript.

FUNDING

This work was supported by the Fundamental Research Funds for the Central Universities (XDJK2018B023 and XDJK2017D082), and the Chongqing Basic Research Program (cstc2016jcyA0235).

ACKNOWLEDGMENTS

The authors gratefully acknowledge PY, YY, KW, and other veterinary medicine students from Southwest University for valuable suggestions and assistance.

REFERENCES

Amemiya, M., Loffing, J., Amemiya, M., Loffing, J., Lötscher, M., Kaissling, B., et al. (1995). Expression of NHE3 in the apical membrane of rat renal proximal tubule and thick ascending limb. *Kidney Int.* 48, 1206–1215. doi: 10.1038/ki.1995.404

Biemesderfer, D., Pizzonia, J., Abu-Alfa, A., Exner, M., Reilly, R., Igarashi, P., et al. (1993). NHE3: a Na^+ /H^+ exchanger isoform of renal brush border. *Am. J. Physiol.* 265(5 Pt 2):F736. doi: 10.1152/ajprenal.1993.265.5.F736

Biemesderfer, D., Rutherford, P. A., Nagy, T., Pizzonia, J. H., Abualfa, A. K., and Aronson, P. S. (1997). Monoclonal antibodies for high-resolution localization

of NHE3 in adult and neonatal rat kidney. *Am. J. Physiol.* 273, 289–299. doi: 10.1152/ajprenal.1997.273.2.F289

Cha, B., Chen, T., Sarker, R., Yang, J., Raben, D., Tse, C. M., et al. (2014). Lysophosphatidic acid stimulation of NHE3 exocytosis in polarized epithelial cells occurs with release from NHERF2 via ERK-PLC-PKCδ signaling. *Am. J. Physiol. Cell Physiol.* 307, 55–65. doi: 10.1152/ajpcell.00045.2014

Cha, B., Zhu, X. C., Chen, W., Jones, M., Ryoo, S., and Zachos, N. C. (2010). NHE3 mobility in brush borders increases upon nherf2-dependent stimulation by lyophosphatidic acid. *J. Cell Sci.* 123, 2434–2443. doi: 10.1242/jcs.056713

Chae, C., Kim, O., Choi, C., Min, K., Cho, W. S., and Kim, J. (2000). Prevalence of porcine epidemic diarrhoea virus and transmissible gastroenteritis virus infection in Korean pigs. *Vet. Record* 147, 606–608. doi: 10.1136/vr.147.21.606

Coon, S., Kekuda, R., Saha, P., and Sundaram, U. (2011). Reciprocal regulation of the primary sodium absorptive pathways in rat intestinal epithelial cells. *Am. J. Physiol. Cell Physiol.* 300, 496–505. doi: 10.1152/ajpcell.00292.2010

Dai, L., Hu, W. W., Xia, L., Xia, M., and Yang, Q. (2016). Transmissible gastroenteritis virus infection enhances SGLT1 and GLUT2 expression to increase glucose uptake. *PLoS One* 11:e0165585. doi: 10.1371/journal.pone.0165585

Eppstein, D. A., Marsh, Y. V., and Schreiber, A. B. (1985). Epidermal growth factor receptor occupancy inhibits vaccinia virus infection. *Nature* 318, 663–665. doi: 10.1038/318663a0

Gawenis, L. R., Stien, X., Shull, G. E., Schultheis, P. J., Woo, A. L., and Walker, N. M. (2002). Intestinal NaCl transport in NHE2 and NHE3 knockout mice. *Am. J. Physiol. Gastrointest. Liver Physiol.* 282, G776–G784. doi: 10.1152/ajpgi.00297.2001

Goh, K. M., Dunker, A. K., and Uversky, V. N. (2012). Understanding viral transmission behavior via protein intrinsic disorder prediction: coronaviruses. *J. Pathog.* 11:738590. doi: 10.1155/2012/738590

Homma, R., and Yasui, K. (1968). Cellular receptors for animal viruses. *Tanpakushitsu Kakusan Koso* 13, 543–553.

Hu, W. W., Zhu, L. Q., Yang, X., Lin, J., and Yang, Q. (2016). The epidermal growth factor receptor regulates cofilin activity and promotes transmissible gastroenteritis virus entry into intestinal epithelial cells. *Oncotarget* 7, 12206–12221. doi: 10.18632/oncotarget.7723

Kim, B., and Chae, C. (2001). In situ hybridization for the detection of transmissible gastroenteritis virus in pigs and comparison with other methods. *Can. J. Vet. Res.* 65, 33–37.

Lin, K., and Nie, S. Q. (1985). Membrane fluidity. *Adv. Physiol.* 16, 85–91.

Lin, S., Yeruva, S., He, P., Singh, A. K., Zhang, H., and Chen, M. (2010). Lysophosphatidic acid stimulates the intestinal brush border Na^+/H^+ exchanger 3 and fluid absorption via LPA(5) and NHERF2. *Gastroenterology* 138, 649–658. doi: 10.1053/j.gastro.2009.09.055

Liu, F. J., Wang, Y., and Yang, G. Y. (2014). NHEs gene expression in the intestine of mice diarrhea induced by LPS. *Anim. Husb. Vet.* 46, 255–256.

Malakooti, J., Saksena, S., Ravinder, K. G., and Dudeja, P. K. (2014). Transcriptional regulation of the intestinal luminal Na^+ and Cl^- transporters. *Biochem. J.* 435, 313–325. doi: 10.1042/BJ20102062

Schultheis, P. J., Clarke, L. L., Meneton, P., Miller, M. L., Soleimani, M., and Gawenis, L. R. (1998). Renal and intestinal absorptive defects in mice lacking the NHE3 Na^+/H^+ exchanger. *Nat. Genet.* 19, 282–285. doi: 10.1038/969

Sestak, K., Saif, L. J., Morilla, A., Sestak, K., Saif, L. J., Morilla, A., et al. (2008). *Porcine Coronaviruses. Trends in Emerging Viral Infections of Swine*. Ames, IA: Iowa State Press, 321–330. doi: 10.1002/9780470376812.ch10a

Singh, V., Yang, J., Chen, T. E., Zachos, N. C., Kovbasnjuk, O., and Verkman, A. S. (2014). Translating molecular physiology of intestinal transport into pharmacologic treatment of diarrhea: stimulation of Na^+ absorption. *Clin. Gastroenterol. Hepatol.* 12, 27–31. doi: 10.1016/j.cgh.2013.10.020

Sun, X., Zhang, H., Sheikhahmadi, A., Wang, Y., Jiao, H., and Lin, H. (2014). Erratum to: effects of heat stress on the gene expression of nutrient transporters in the jejunum of broiler chickens (*Gallus gallus* domesticus). *Int. J. Biometeorol.* 59, 127–135. doi: 10.1007/s00484-014-0829-1

Wang, W., Li, C., Kwon, T. H., Miller, R. T., Knepper, M. A., and Frøkiaer, J. (2004). Reduced expression of renal Na^+ transporters in rats with PTH-induced hypercalcemia [J]. *Am. J. Physiol. Renal Physiol.* 286:F534. doi: 10.1152/ajprenal.00044.2003

Wu, G. P., Yin, Y. B., and Wu, S. Y. (2003). Research progress of porcine transmissible gastroenteritis virus. *Chin. J. Vet. Med.* 39, 29–32.

Yang, J., Zhao, X., Patel, A., Potru, R., Azizighannad, S., Dolinger, M., et al. (2015). Rapamycin inhibition of mTOR reduces levels of the Na^+/H^+ exchanger 3 in intestines of mice and humans. Leading to Diarrhea. *Gastroenterology* 149, 151–162. doi: 10.1053/j.gastro.2015.03.046

Yin, L., Vaught, L., Zhang, A., Okunieff, P., and Vidyasagar, S. (2015). Mo2029 differential activity of NHE3 and NHE2 in the small intestine of irradiated mice. *Gastroenterology* 148:S-774. doi: 10.1016/S0016-5085(15)32638-X

Yoo, B. K., He, P. J., Lee, S. J., and Yun, C. C. (2011). Lysophophatidic acid 5 receptor induces activation of Na^+/H^+ exchanger 3 via apical epidermal growth factor receptor in intestinal epithelial cells. *Am. J. Physiol. Cell Physiol.* 301, 1008–1016. doi: 10.1152/ajpcell.00231.2011

Zachos, N. C., Tse, M., and Donowitz, M. (2005). Molecular physiology intestinal Na^+/H^+ exchange. *Annu. Rev. Physiol.* 67, 411–443. doi: 10.1146/annurev.physiol.67.031103.153004

Zhao, S., Gao, J., Zhu, L., and Yang, Q. (2014). Transmissible gastroenteritis virus and porcine epidemic diarrhoea virus infection induces dramatic changes in the tight junctions and microfilaments of polarized IPEC-J2 cells. *Virus Res.* 192, 34–45. doi: 10.1016/j.virusres.2014.08.014

Conflict of Interest Statement: The authors declare that the research was conducted in the absence of any commercial or financial relationships that could be construed as a potential conflict of interest.

Copyright © 2018 Yang, Ran, Yuan, Yang, Wang, Xie, Huang, Liu and Song. This is an open-access article distributed under the terms of the Creative Commons Attribution License (CC BY). The use, distribution or reproduction in other forums is permitted, provided the original author(s) and the copyright owner(s) are credited and that the original publication in this journal is cited, in accordance with accepted academic practice. No use, distribution or reproduction is permitted which does not comply with these terms.

frontiers in Microbiology

ORIGINAL RESEARCH
published: 14 November 2018
doi: 10.3389/fmicb.2018.02685

Comparative Transcriptomic and Metagenomic Analyses of Influenza Virus-Infected Nasal Epithelial Cells From Multiple Individuals Reveal Specific Nasal-Initiated Signatures

Kai Sen Tan[1†], Yan Yan[1,2†], Wai Ling Hiromi Koh[3†], Liang Li[4], Hyungwon Choi[3,5], Thai Tran[6], Richard Sugrue[7], De Yun Wang[1] and Vincent T. Chow[8*]*

[1] Department of Otolaryngology, National University of Singapore, Singapore, Singapore, [2] Center for Interventional Medicine, The Fifth Affiliated Hospital of Sun Yat-sen University, Zhuhai, China, [3] Saw Swee Hock School of Public Health, National University of Singapore, Singapore, Singapore, [4] Institute of Biomedicine and Biotechnology, Shenzhen Institutes of Advanced Technology, Chinese Academy of Sciences, Shenzhen, China, [5] Institute of Molecular and Cell Biology, A*STAR, Singapore, Singapore, [6] Department of Physiology, National University of Singapore, Singapore, Singapore, [7] School of Biological Sciences, Nanyang Technological University, Singapore, Singapore, [8] Department of Microbiology and Immunology, Yong Loo Lin School of Medicine, National University of Singapore, Singapore, Singapore

In vitro and *in vivo* research based on cell lines and animals are likely to be insufficient in elucidating authentic biological and physiological phenomena mimicking human systems, especially for generating pre-clinical data on targets and biomarkers. There is an obvious need for a model that can further bridge the gap in translating pre-clinical findings into clinical applications. We have previously generated a model of *in vitro* differentiated human nasal epithelial cells (hNECs) which elucidated the nasal-initiated repertoire of immune responses against respiratory viruses such as influenza A virus and rhinovirus. To assess their clinical utility, we performed a microarray analysis of influenza virus-infected hNECs to elucidate nasal epithelial-initiated responses. This was followed by a metagenomic analysis which revealed transcriptomic changes comparable with clinical influenza datasets. The primary target of influenza infection was observed to be the initiator of innate and adaptive immune genes, leaning toward type-1 inflammatory activation. In addition, the model also elucidated a down-regulation of metabolic processes specific to the nasal epithelium, and not present in other models. Furthermore, the hNEC model detected all 11 gene signatures unique to influenza infection identified from a previous study, thus supporting the utility of nasal-based diagnosis in clinical settings. In conclusion, this study highlights that hNECs can serve as a model for nasal-based clinical translational studies and diagnosis to unravel nasal epithelial responses to influenza in the population, and as a means to identify novel molecular diagnostic markers of severity.

Keywords: influenza, transcriptomics, meta-analysis, human nasal epithelial cells, pre-clinical model

OPEN ACCESS

Edited by:
John W. A. Rossen, University Medical Center Groningen, Netherlands

Reviewed by:
Sarah Julia Reiling, Health Canada, Canada
Frank van der Meer, University of Calgary, Canada

****Correspondence:***
De Yun Wang
entwdy@nus.edu.sg
Vincent T. Chow
micctk@nus.edu.sg

† These authors have contributed equally to this work

Specialty section:
This article was submitted to Infectious Diseases, a section of the journal Frontiers in Microbiology

Received: *18 July 2018*
Accepted: *22 October 2018*
Published: *14 November 2018*

Citation:
Tan KS, Yan Y, Koh WLH, Li L, Choi H, Tran T, Sugrue R, Wang DY and Chow VT (2018) Comparative Transcriptomic and Metagenomic Analyses of Influenza Virus-Infected Nasal Epithelial Cells From Multiple Individuals Reveal Specific Nasal-Initiated Signatures. Front. Microbiol. 9:2685. doi: 10.3389/fmicb.2018.02685

INTRODUCTION

Annually, influenza virus infection causes a large number of vaccine-preventable deaths worldwide (Poland et al., 2007). Despite global efforts to curb ongoing transmission, novel strains of influenza viruses are emerging at a rapid rate, and threaten to escalate into epidemics or pandemics (Hui et al., 2017). Therefore, there is an urgent need to enhance our understanding of influenza pathogenesis to discover means to ameliorate the global burden of influenza virus infection.

The nasal epithelium is the primary portal of entry for respiratory viruses such as influenza viruses, and serves as an immediate target for viral replication in the respiratory tract (Braciale et al., 2012; Kolesnikova et al., 2013; Yan et al., 2013, 2016; Wang D.Y. et al., 2015). The nasal epithelium was initially thought to function as a mechanical barrier that filters external agents, preventing their entry into the respiratory system; but recent studies have revealed that it functions beyond just being a physical barrier (Watelet et al., 2006; Wang D.Y. et al., 2015). Nasal epithelial cells are shown to elicit their own repertoire of immune responses and actively prevent pathogens from damaging the airway (Yan et al., 2013, 2016). Upon infection, they not only release anti-microbial surfactants and mucus to mitigate pathogen transmission in the airway (Watelet et al., 2006; Wang D.Y. et al., 2015), but also express and secrete various cytokines and chemokines to drive immune responses against these pathogens (Watelet et al., 2006; Yan et al., 2016). Therefore, the interactions between the nasal epithelium and invading pathogens play key roles in the disease progression and subsequent immune responses against the virus.

Despite direct interaction with the virus at host contact sites, studies on influenza viruses often overlook the nasal epithelia, but focus on the lungs where the more serious influenza-induced pneumonitis occurs. As a result, there is a lack of suitable nasal epithelial models in the current literature (Sutejo et al., 2012; Watanabe et al., 2013; Clay et al., 2014; Wu et al., 2014; Wang Z. et al., 2015). Therefore, it is of interest to profile nasal epithelial responses to influenza virus at the actual contact site, and to characterize the nasal epithelium as an intermediate checkpoint for downstream immune responses by immune cells (e.g., secretome). Furthermore, it is important to determine whether molecular factors that confer differential susceptibility among individuals with different genetic backgrounds exist in the nasal epithelium, thereby impacting influenza transmission in the host population. The investigation of nasal-based markers and susceptibility factors may also encourage nasal-based diagnosis that can be developed into a rapid tool for influenza management.

To investigate the feasibility of nasal models in elucidating influenza signatures, we have developed an *in vitro* model of fully differentiated, multi-layered nasal epithelial cells derived from stem cells of different individuals in an air-liquid interface (ALI) culture (Li et al., 2014; Yan et al., 2016). This model fully mimics nasal epithelium with the presence of ciliated, goblet and basal cells. The model also facilitates focused analysis of epithelial responses, and their contribution to anti-influenza responses (Yan et al., 2016). Using this *in vitro* ALI model, we studied the transcriptomic signature of the nasal epithelium in response to influenza virus infection. We hypothesized that the *in vitro* differentiated nasal epithelium closely mimics immune responses in cell lines and blood samples from clinical studies, and serves as the initial checkpoint of these responses. We compared the infected nasal epithelial transcriptomic signature against influenza infection signatures derived from other studies that employ epithelial cell lines or patient blood samples through meta-analysis to highlight responses triggered by the nasal epithelium. The objective of this study is to evaluate the utility of the hNEC model as a bridge between pre-clinical data and clinical settings, in order to achieve its potential application in clinical influenza and infectious diseases.

MATERIALS AND METHODS

Derivation of hNESPCs and *in vitro* Differentiation of hNECs

This study was approved by the Ethical Committees (National Healthcare Group of Singapore Domain-Specific Review Board, DSRB Reference no. D/11/228, and National University of Singapore Institutional Review Board, IRB code 13-509). Under the DSRB and IRB, written informed consent was obtained from each subject. The human nasal epithelial stem and progenitor cells (hNESPCs) were derived from the inferior turbinate of five patients with septal deviation (SD) who underwent septal plastic surgery at the National University Hospital, Singapore. All subjects were free of symptoms of upper respiratory infection, and had not used corticosteroids and antibiotics within 3 months before the surgery. The medical background of the donors' samples is summarized in **Supplementary Table S1**. Cell culture method has been described previously (Zhao et al., 2012; Li et al., 2014; Wang et al., 2014). Fully differentiated hNECs, including beating ciliated cells and mucus-producing goblet cells, were obtained after 32–35 days of ALI culture. The hNECs were previously characterized by immunofluorescence (IF) staining of ciliated and goblet cell markers, i.e., mouse anti-human βIV-tubulin (Zhao et al., 2012; Li et al., 2014), rabbit anti-human acetylated α-tubulin and rabbit anti-human mucin5AC (Wang et al., 2014).

Influenza A Virus (H3N2) Infection of Fully Differentiated hNECs

The human influenza A virus Aichi/2/1968 H3N2 strain was purchased from the American Type Culture Collection (ATCC, Manassas, VA, United States), propagated in eggs, and titrated by plaque assay using Madin-Darby canine kidney (MDCK, NBL-2) cells (ATCC, Manassas, VA, United States). The virus was thawed on ice and immediately diluted in 100 μL of B-ALI^{TM} differentiation medium at a multiplicity of infection (MOI) of 0.1, inoculated into the apical chamber of Transwells, and incubated at 35°C for 1 h. B-ALI^{TM} differentiation medium was added into the control well at 0 h post-infection (hpi) without the virus. The H3N2-infected and mock-infected hNECs were

then incubated at 35°C with 5% CO_2 for 8, 24, and 48 hpi, respectively.

Virus Plaque Assay

At serial time-points, 150 μL of DPBS was added and incubated in the apical chamber at 35°C for 10 min to recover progeny viruses, and the aliquots of inoculated virus were stored at −80°C until titration by plaque assay. MDCK cells at 85–95% confluence in 24-well plates were incubated with 100 μL of serial dilutions (from 10^{-1} to 10^{-4}) of virus from infected hNECs at 35°C for 1 h. The plates were rocked every 15 min to ensure equal distribution of virus. The inocula were removed and replaced with 1 mL of Avicel overlay (FMC Biopolymer, Philadelphia, PA, United States) to each well, and incubated at 35°C with 5% CO_2 for 65–72 h. Avicel overlay was then removed, and cells were fixed with 4% formaldehyde in PBS for 1 h. Formaldehyde was removed, and cells were washed with PBS. The fixed cells were stained with 1% crystal violet for 15 min, and washed. The plaque-forming units (PFU) were calculated as follows: number of plaques × dilution factor = number of PFU per 100 μL. The final data were presented as PFU per 100 μL (innoculation volume).

Total RNA Extraction and Gene Microarray

Total RNA was extracted from hNECs using mirVana^{TM} miRNA isolation kit (Life Technologies, Carlsbad, CA, United States) following the manufacturer's protocol. The concentration and quality of total RNA were determined by a bio-analyzer, and only total RNA samples deemed of good quality were subjected to microarray analyses. Gene microarrays for the infected and control hNEC samples were performed using Affymetrix human transcriptome array (HTA) microarray platform.

Reverse Transcription and Real-Time Quantitative PCR

RNA (2 μg) was subjected to cDNA synthesis using the Maxima first-strand cDNA synthesis kit (ThermoScientific, Pittsburgh, PA, United States). The qPCR analysis was performed to evaluate the transcriptional levels of host response genes selected based on the microarray analysis using pre-designed primers (Sigma Aldrich, St. Louis, MO, United States). The qPCR assays were performed in duplicate using GoTaq-qPCR Master Mix kit (Promega, San Luis Obispo, CA, United States), and the median values and interquartile ranges were generated. Relative gene expression was calculated using the comparative method of $2^{-\Delta\Delta Ct}$, i.e., $2^{(\Delta Ctofgene\ -\ \Delta CtofPGK1)}$, and normalized to the mRNA level of the housekeeping gene PGK1.

Bioinformatics Analysis for Gene Expression Data in hNEC Samples

Affymetrix microarray data for hNEC samples were processed using the "affy" package in R Bioconductor (Gautier et al., 2004). A Bayesian model-based method was to detect differential expression between post-infection time-points and baseline (Teo et al., 2015). A gene was considered differentially expressed if the probability score for differential expression was above the threshold associated with 1% FDR. Pathway-level analysis was conducted in two ways, using the Ingenuity Pathway Analysis (IPA; Qiagen, Hilden, Germany) and an in-house program for testing enrichment of biological functions (hypergeometric tests) against a database consisting of Gene Ontology (Ashburner et al., 2000) and CPDB (Kamburov et al., 2009).

Metagenomics Analysis of hNEC Transcriptome With Multiple Influenza Transcriptomic Studies

The studies used in the meta-analysis are summarized in **Supplementary Table S2**. All processed data sets were downloaded from the Gene Expression Omnibus (GEO) database after literature search. The same model-based differential expression analysis was used for comparison between infection peak time and the baseline. For each and every data set, systematic shifts in the expression values were examined by boxplots and it was deemed unnecessary to apply further normalization procedures. The list of up- and down-regulated genes was also annotated in terms of biological functions in each study, and compared across the studies along with the hNEC data (−log10 *p*-value for up-regulation and log10 *p*-value for down-regulation to account for direction of change).

RESULTS

The hNECs of Multiple Subjects Reveal Similar Temporal Responses Against Influenza Infection With Varying Magnitude of Expression

To establish a common transcriptomic response signature, the post-infection gene expression profiles (8, 24, and 48 hpi) were compared against the baseline profile from the gene expression microarray data for five donors. **Figure 1A** and **Supplementary Figure S1** show that the response of the nasal epithelium of all five donors followed a similar trend over time. There were potentially also slight differences in the temporal induction and magnitude of response genes expressed across individuals, such as type III IFNs (IFNλ/IFNL), IL36γ, IL-1A and ICAM-1. The details of the individual expression profiles of the genes are provided in **Supplementary Table S3**. The principal component analysis (PCA) of significantly altered genes (FDR < 0.01) (**Figure 1B**) showed that the changes in gene expression over the course of infection followed a specific pattern over time, with potentially variable responses across donors. In addition, while the range of virus progeny production in different samples varied by as much as a hundred-fold (**Figure 1C**), it was deemed not clinically significant in the case of H3N2 infection since all samples led to sufficiently high viral titers post-infection to exert the gene expression changes (Granados et al., 2017).

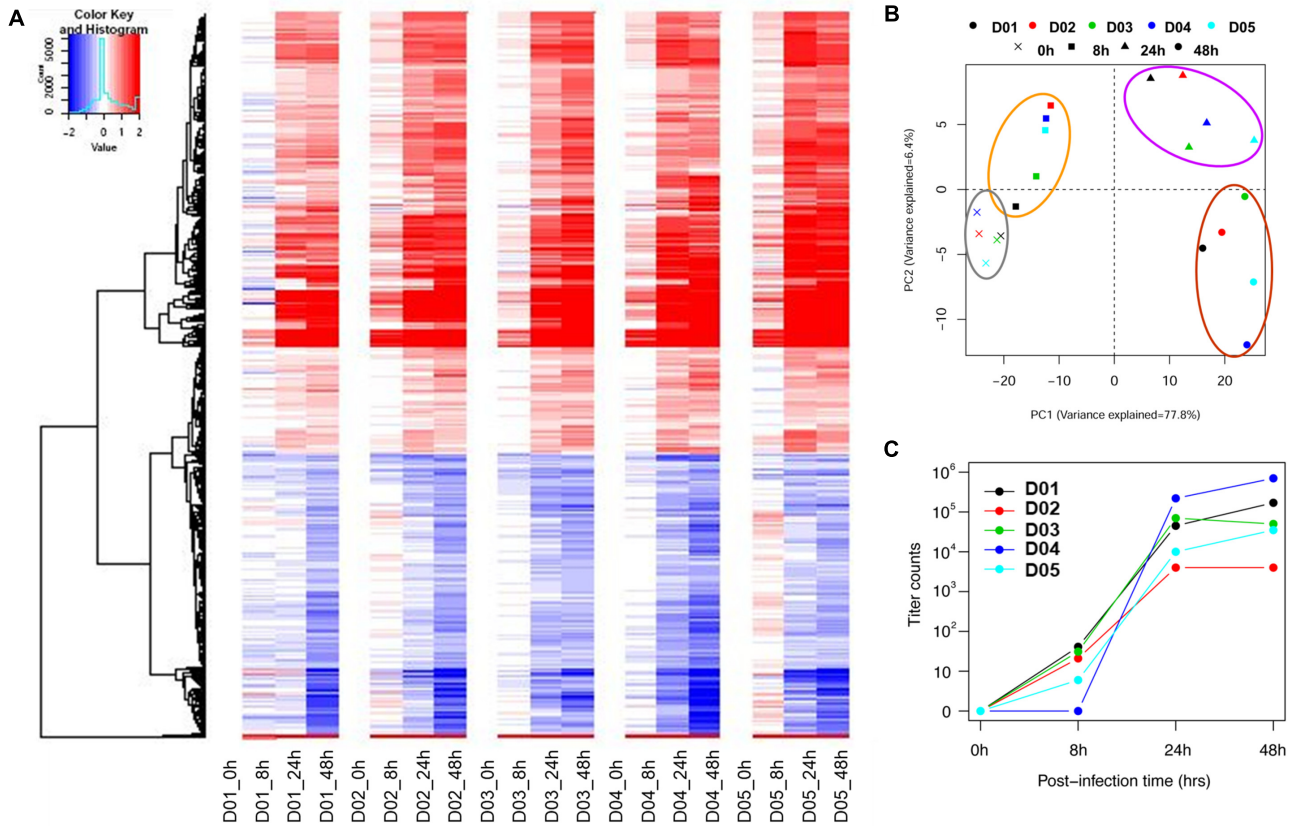

FIGURE 1 | Individual heat-map and PCA analysis of five individual subjects show similar trends but potentially retained some degree of variability in temporal induction and magnitude between donors. **(A)** Individual heat-maps of different subjects revealed largely similar patterns with potential differences in temporal induction from 8 to 48 hpi, including the magnitude of induction. **(B)** Individual PCA plot showed that the transcriptomes across different subjects were not clustered as tightly since the hNEC samples were of different genetic backgrounds. The PCA plot showed a distinct progression of differential gene changes across time-points even at 0 hpi. **(C)** Individual viral titers increased over time to reach high viral loads in samples from all donors. The individual variation was deemed not clinically significant given that a sufficiently high virus titer was attained to induce a consistent response.

Influenza Virus Infection of hNECs Leads to Elevated Expression of Both Innate and Adaptive Response Genes, and Reduced Expression of Metabolism Genes

We established that the nasal epithelium interaction with influenza virus was complex but observable *in vitro*, and may reflect the differences in subsequent host response and disease progression. To follow up, we further identified the pathways in which the differentially expressed genes were involved, since their differing expression between individuals may affect these pathways and account for varying susceptibility toward influenza infection. We analyzed the numbers and categories of differentially regulated genes during the increase of viral titers as these genes may constitute the susceptibility factors contributing to differences in pathogenesis. There was an earlier up-regulation of genes at 24 hpi, numbering about 250–350 genes; while the down-regulation of genes was only observed later at 48 hpi (**Figure 2A**). These genes were subjected to hypergeometric analysis for gene set enrichment based on gene ontology database ($p < 0.01$), and mainly belong to immune response pathways which were up-regulated; and metabolic pathways which were down-regulated following infection (**Figure 2B**). The analysis revealed that the major pathway changes in the nasal epithelium following influenza infection were predominantly increased antiviral immune responses, and decreased metabolic functions.

Ingenuity Pathway Analysis Reveals Pathways Initiated at the Nasal Epithelium Following Influenza Infection

Upon establishing the nasal changes following influenza infection, we further categorized these pathways using Ingenuity pathway analysis (IPA) software (**Figures 3A–C**; **Supplementary Tables S4A–C**). From the analysis of canonical pathways using genes at FDR < 0.01, the major up-regulated pathways ($p < 0.05$) involved in the nasal epithelium gradually shifted from antiviral responses and inflammasome activation (**Figure 3A**), to early adaptive immune responses involving antigen presentation and suppression of homeostatic activities (**Figures 3B,C**). On the other hand, downregulation was observed in DNA damage

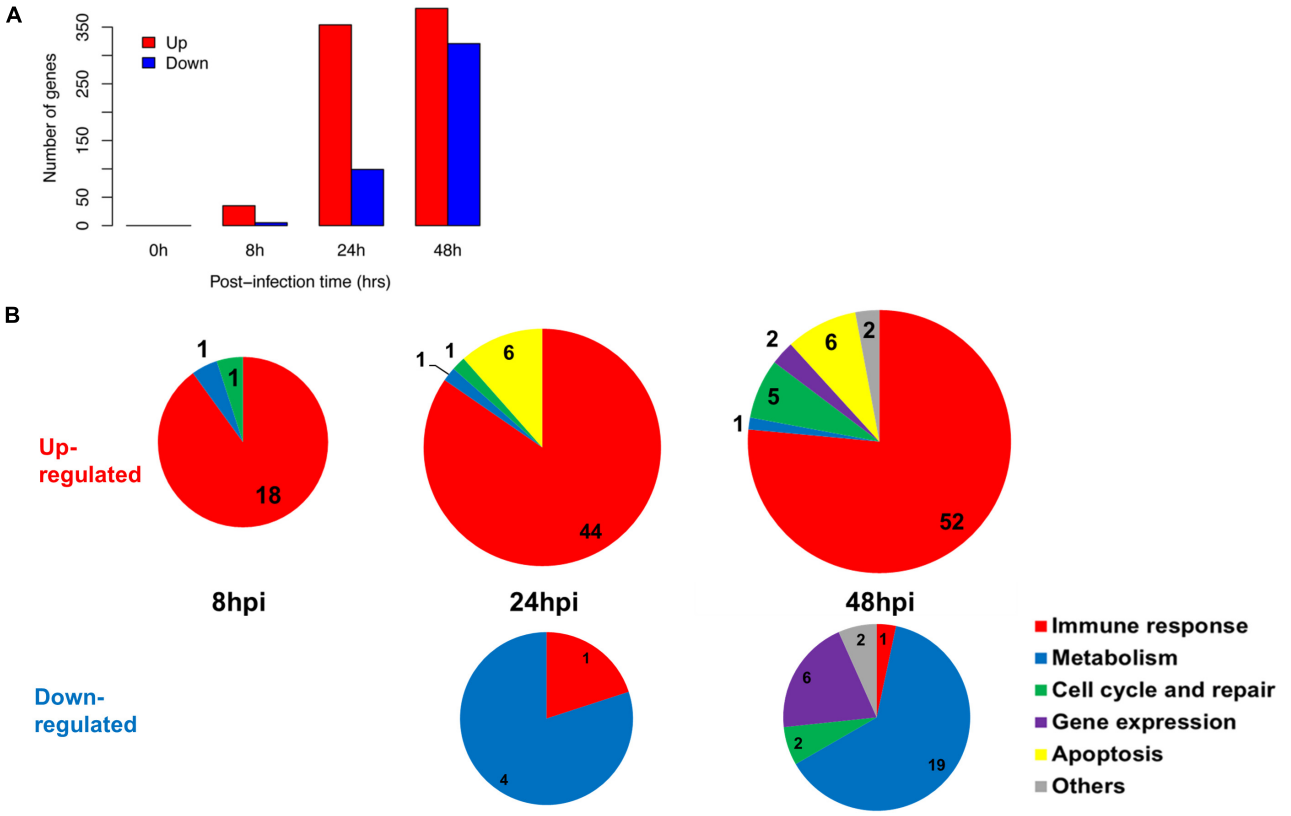

FIGURE 2 | Summary of gene changes in hNECs which correlate with increasing viral titer. **(A)** Gene changes corresponding to increasing viral titer exhibited maximal up-regulation and maximal down-regulation at 48 hpi. **(B)** Temporal analysis demonstrated key up-regulated (upper three pie charts) and down-regulated (bottom two pie charts) gene ontology (GO) terms in the nasal epithelium corresponding to increasing viral titer. The majority of up-regulated GO terms were immune-related, whereas down-regulated GO terms were metabolism-related.

pathways, as well as in metabolic and biosynthetic pathways ($p < 0.05$) (**Figure 3C**).

Comparison of hNEC Infection With Other *in vitro* and Human Studies Indicate That hNEC Responses Closely Mimic *in vivo* Systems

We compared the transcriptomic responses of our infected hNECs with 15 other *in vitro* and *in vivo* influenza infection transcriptomic studies, at their peak responses against influenza. Across all studies, the transcriptome data at the peak of infection were compared against the corresponding baseline data, and the transcriptomic changes were compared across the studies, with FDR < 0.01 being assigned as the baseline for significance (see section "Materials and Methods"). The differential transcriptome signature in hNECs was highly similar to the signatures from other influenza infection models (**Figure 4A**). Interestingly, compared to the homogenous cell lines tested during *in vitro* studies, our heterogenous hNEC model exhibited a more comparable response to the clinical influenza studies. This is shown by hierarchical clustering where the hNECs are clustered closer to clinical studies in their responses against influenza infection. Furthermore, when the studies were clustered according to functional changes arising from the transcriptomic changes, our hNEC model was also found to cluster closer to large-scale clinical influenza studies based on blood or peripheral blood mononuclear cells (PBMCs), rather than with cell line studies (**Figure 4B** and **Supplementary Figure S2**).

Functional Comparison of Infected hNEC Responses With Other Infection Models Reveals Key Factors Initiated by the Nasal Epithelium

We further compared the hypergeometric gene ontology (GO) analysis of hNECs with those in other studies to identify functional changes associated with the transcriptomic changes elicited by the nasal epithelium, using a cutoff of $p < 0.01$ to elucidate the common and unique pathways with greater confidence (**Supplementary Table S5**). Our model representing the human nasal epithelium displayed transcriptomic changes that mainly clustered with immune responses and metabolic processes. Compared to the other studies, the infected hNEC model induced comparable increases (FDR_up < 0.01) in

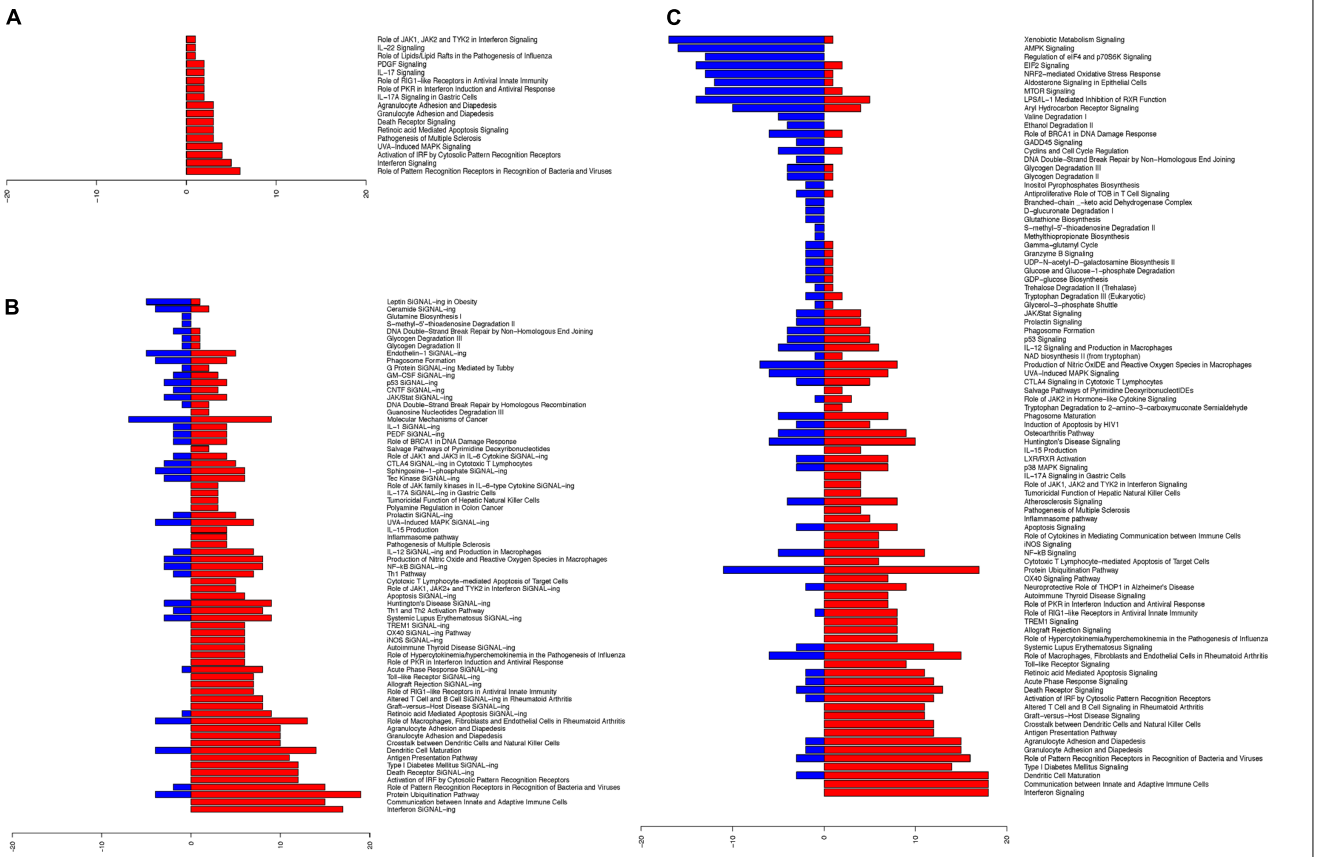

FIGURE 3 | Ingenuity pathway analysis revealed upregulated changes of pathways in hNECs over time and became more diverse. The significant pathway changes following influenza infection and the number of genes (x-axis) significantly up-regulated (red) or down-regulated (blue) in each pathway are shown. **(A)** At 8 hpi, all significant pathways ($p < 0.05$) exhibited up-regulation of components which are all immune-related. **(B)** At 24 hpi, a combination of pathways were significantly altered ($p < 0.05$), with down-regulation of certain biosynthesis pathways. **(C)** At 48 hpi, more of the significant pathways ($p < 0.05$) were down-regulated, while immune response genes shifted toward cytokine production and cross-talk with adaptive immune cells.

immune responses (highlighted in red in **Supplementary Table S5**), i.e., 47 out of 67 significant immune functions that overlapped with at least one other study, and 37 out of 41 with at least 3 other studies. Therefore, this strong overlap highlights that most immune processes against influenza are locally initiated at the nasal epithelium, which are subsequently propagated, and can be detected systemically. Furthermore, given that they are the primary target cells for influenza infection, the hNECs also exhibited reduction (FDR_down < 0.01) in metabolic processes (highlighted in blue in **Supplementary Table S5**). The overlap in this reduction was 20 out of 32 with at least one other study; and 6 out of 8 with at least 3 other studies. These reductions in nitrogen compounds, carbohydrates and lipids may be a direct consequence of the infection; or may be part of a signaling mechanism in antiviral responses, which remain to be further explored. On the other hand, the infected hNEC model does not reflect most changes at the cell cycle and tissue repair pathways (highlighted in green in **Supplementary Table S5**; 11 out of 73), which are likely to be initiated only upon viral clearance. There was also only slight overlap in gene expression mechanisms (highlighted in purple in **Supplementary Table S5**), i.e., 3 out of 37.

Quantitative Real-Time PCR Verification With Independent hNEC Infections to Identify Key and Novel Pathways in Influenza Infection

To confirm the validity of the microarray analysis and the similarity of hNEC responses to *in vivo* clinical models, we performed independent infection experiments on another batch of hNEC donors to compare their responses to the transcriptomic analysis. By selecting genes involved in viral sensing, interferon (IFN), antiviral, type-1 inflammatory response, metabolic and homeostatic pathways, we compared the expression profiles between the microarray and the independent infections. In the independent infections, the qPCR analyses revealed close agreement with the microarray expression, and confirmed the expression of viral sensing via TLR7, which activates the JAK-STAT pathways via type I and type III IFN activation to initiate type-1 inflammatory responses (**Figure 5**). Additionally, antiviral

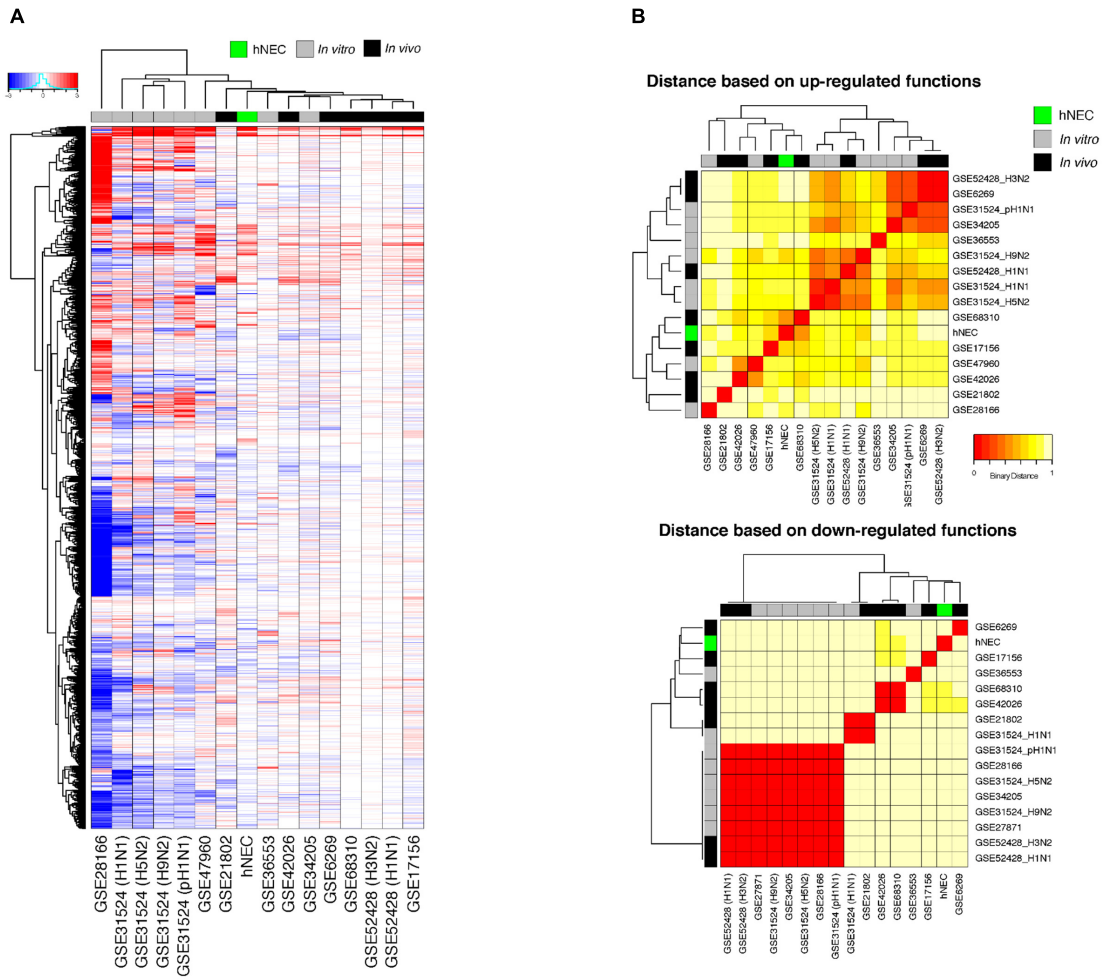

FIGURE 4 | Meta-analysis of genes and functions across *in vitro* and *in vivo* influenza transcriptomic studies at peak responses reveal similarities of hNECs to human studies. **(A)** Transcriptomic signatures (FDR < 0.01) revealed that the differential changes in infected hNECs were more similar to human studies due to heterogeneity of hNECs. **(B)** Using functional clustering of meta-genomic data, hNECs were observed to tightly cluster functionally with most human studies (*in vivo*) at the peak of viral-induced changes of each individual study.

genes were also activated during the infection process with the exception of MUC5AC (**Supplementary Figure S3**), which concurs with our previous finding where influenza does not alter MUC5AC expression (Yan et al., 2016). Furthermore, we also analyzed genes involved in homeostatic and metabolic activities (**Figure 6**), and observed reduced expression of genes governing lipid metabolism (ALOX15), retinoic acid synthesis (RDH10), peroxisome transport (ABCD3), and pH regulation (SLC4A4). Interestingly, the mRNA encoding peptidase inhibitor 3 (PI3), which plays a role in anti-bacterial and anti-fungal activity, was up-regulated in the nasal epithelium, implying that this gene may help to prevent secondary bacterial infection.

DISCUSSION

Evidence is accumulating that the nasal epithelium, the first contact site of respiratory viruses, plays crucial defense functions beyond being host cells for influenza infection. Many studies indicate that the nasal epithelium actively triggers innate immune responses and also modulates adaptive immunity against these viruses (Vareille et al., 2011; Braciale et al., 2012; Yan et al., 2016). However, the scarcity of human nasal cell models impeded in-depth studies on this aspect. The role of nasal epithelium was also unclear since most human studies focused on systemic signals from the blood (Bermejo-Martin et al., 2010; Herberg et al., 2013; Zhai et al., 2015); thereby masking the immune effects of the nasal epithelium and their utility in clinical settings. Therefore, using our hNEC culture differentiated from enriched nasal stem cells, we elucidated the initial changes in the infected nasal epithelium that likely generate most of the signals that ultimately lead to the cascading immune responses mediated by immune cells. Since the nasal epithelium can mount distinct responses that eventually lead to type-1 and type-2 inflammatory responses against influenza, such responses may be crucial in controlling viral pathogenesis and in modulating

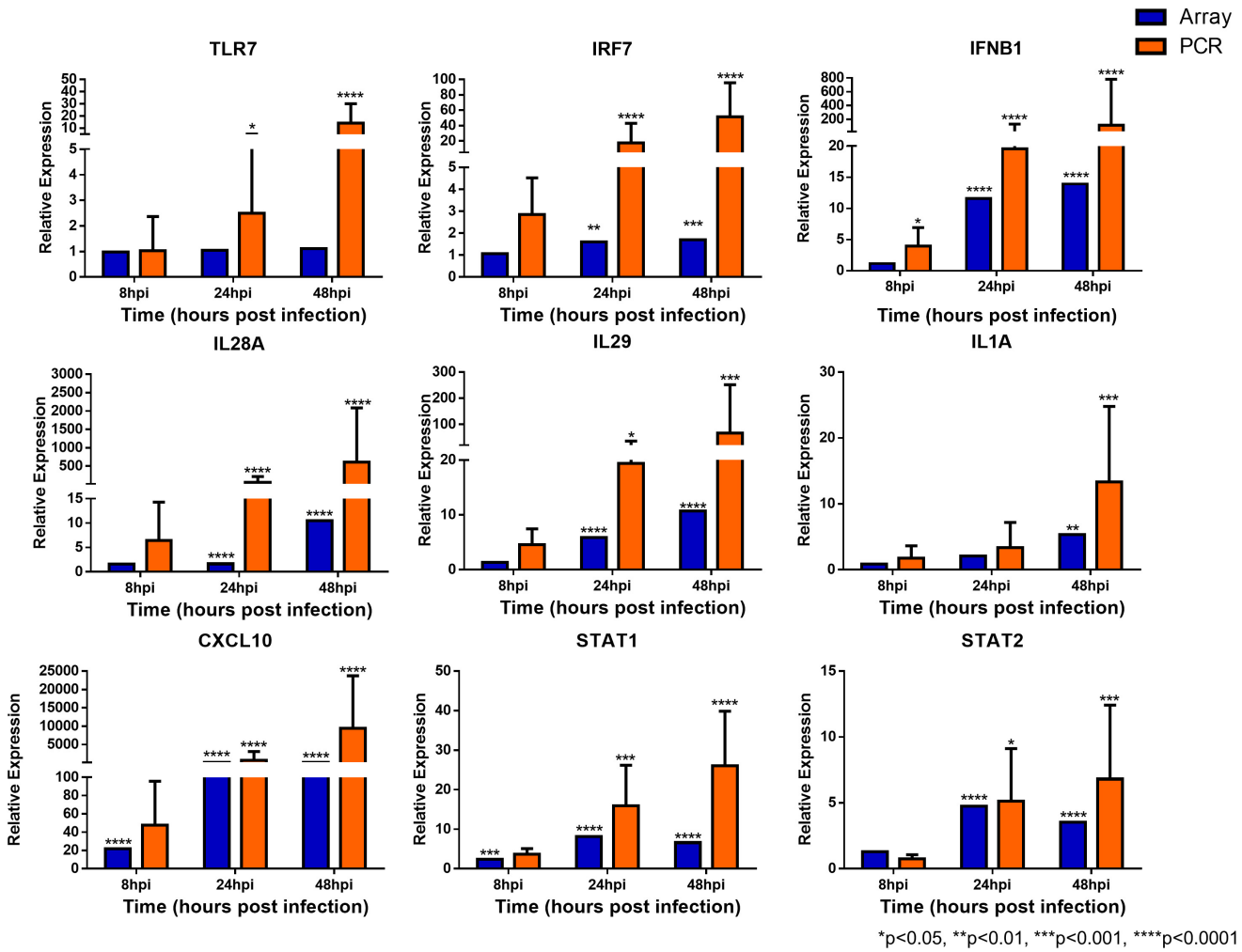

FIGURE 5 | Expression of immune response genes in nasal epithelial cells following influenza infection. Expression of host genes in response to influenza in sequence: TLR7, IRF7, IFNB1, IL28A, IL29, IL1A, CXCL10, STAT1, and STAT2 (n = 4–12). The statistical significance level of the RT-qPCR expression was calculated using one-way ANOVA, nonparametric, grouped, Dunn multiple comparison test, with the p-value derived by comparison against uninfected control cells. *$p < 0.05$; **$p < 0.01$; ***$p < 0.001$; ****$p < 0.0001$. The RT-qPCR data were presented as medians with inter-quartile range.

local antiviral responses (Tan et al., 2017; Edwards et al., 2018).

Our study evaluated nasal epithelial cells differentiated from five different donors, which mounted a consistent response against influenza, with potential differential responses between individuals in antiviral response genes such as IFNλs, IL36γ, IL-1A, and ICAM-1. These genes, while not strongly induced, may play roles in modulating the immune defense against influenza infection to prevent damage to the surrounding tissues (Galani et al., 2017; Klinkhammer et al., 2018; Wein et al., 2018). We also observed that, in the absence of immune cells, the nasal epithelial response skewed heavily toward type-1 inflammatory activation with minimal type-2 inflammatory activating responses. This suggests that naïve epithelial cells primarily evoke a type-1 inflammatory response against invading viruses, especially in the context of influenza. Furthermore, the nasal cells could initiate cross-talk between innate and adaptive immunity via robust production of adaptive immune-activating cytokines and chemokines such as IL-6, CXCL10, and IFNλs including IFNL2 (IL28A) and IFNL1 (IL29). Compared with the other clinical studies involving peripheral blood mononuclear cells (PBMCs), blood or serum from patients, the hNECs exhibited similar transcriptomic changes in up-regulated immune responses, thus identifying nasal-initiated immune functions (JAK-STAT-mediated type-1 inflammatory response activation).

On the other hand, there were critical down-regulated functions in hNECs related to multiple metabolic and DNA damage responses against influenza that were mostly not observed in blood or serum samples (Ivan et al., 2012, 2013; Raval and Nikolajczyk, 2013; Li et al., 2015; Cui et al., 2016). Such reductions in metabolic functions and related metabolites at the primary infection site of influenza may be an interesting area for future investigation to understand their relationships

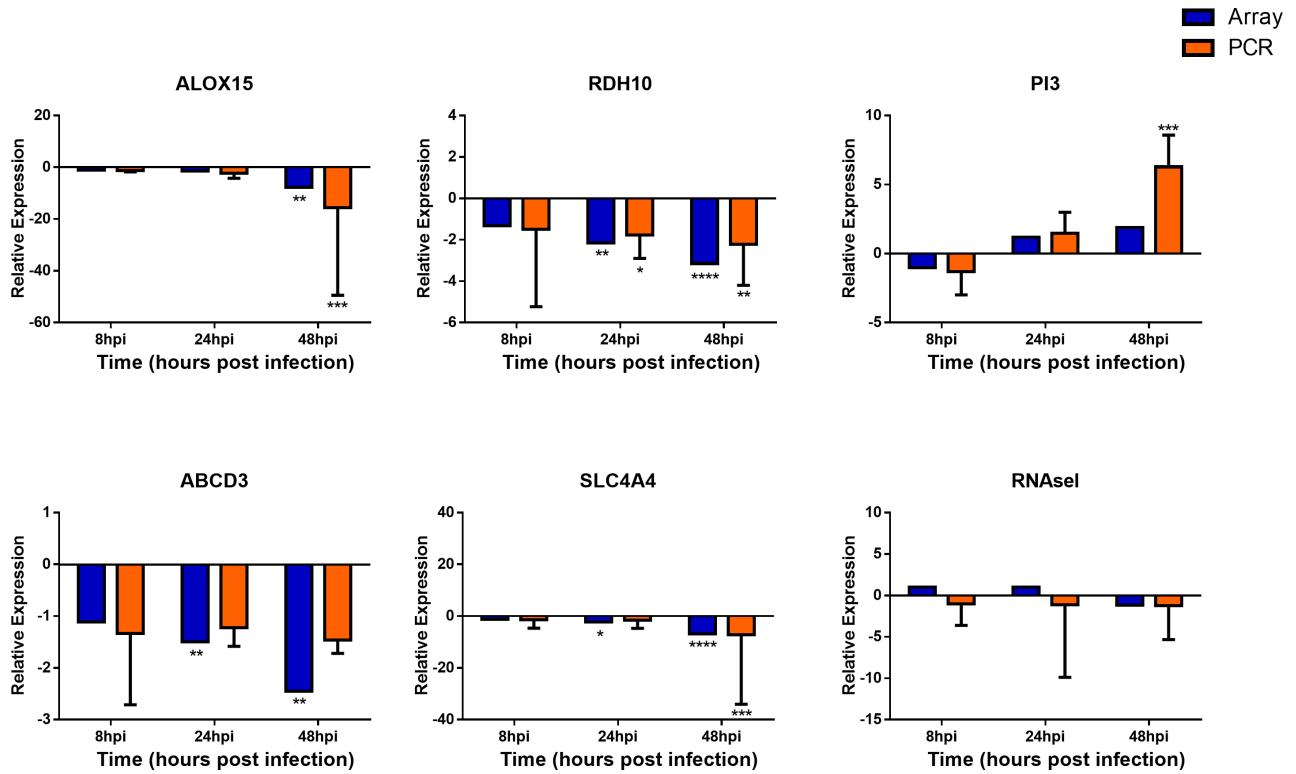

FIGURE 6 | Expression of homeostatic and metabolic genes in nasal epithelial cells following influenza infection. Expression of host genes in response to influenza in sequence: ALOX15, RDH10, PI3, ABCD3, SLC4A4, and RNASel (n = 4–12). The statistical significance level of the RT-qPCR expression was calculated using one-way ANOVA, nonparametric, grouped, Dunn multiple comparison test, with the p-value derived by comparison against uninfected control cells. *$p < 0.05$; **$p < 0.01$; ***$p < 0.001$; ****$p < 0.0001$. The RT-qPCR data were presented as medians and inter-quartile range.

with viral replication and immune functions (Cui et al., 2016; Gonzalez Plaza et al., 2016; Boergeling and Ludwig, 2017; Cui et al., 2017; Smallwood et al., 2017). In addition, these changes in the metabolic and homeostatic pathways are unique to the nasal epithelium, and were not documented in other *in vitro* and clinical studies. Dampening of these homeostatic pathways may impact downstream immune and non-immune responses or cause complications that contribute to the pathogenesis of influenza or other metabolic disorders (Gonzalez Plaza et al., 2016; Smallwood et al., 2017). One such example of altered gene expression related to lipid and peroxisomal metabolism during influenza (Tanner et al., 2014), was also revealed in our study, i.e., ABCD3. Moreover, certain homeostatic proteins serve dual roles, such as BPIFA1 and CD151, which possess pro- or anti-viral, homeostatic and signaling functions in the airway (Akram et al., 2018; Kim et al., 2018; Qiao et al., 2018). Therefore, this study highlighted perturbations in homeostatic and metabolic pathways which warrant further exploration into their underlying mechanisms associated with influenza pathogenesis.

The comparable responses of hNECs with clinical datasets suggest that most influenza-related responses can be detected within the nasal eptithelium. Furthermore, the transcriptomic changes of infected nasal epithelial cells revealed differential regulation of all 11 targets (CD38, HERC5, HERC6, IFI6, IFIH1, LGALS3BP, LY6E, MX1, PARP12, RTP4, and ZBP1) previously thought to be influenza-specific signatures (Andres-Terre et al., 2015). Hence, the fact that these key transcriptomic signatures during influenza were nasal-initiated, underscores the clinical utility of the hNEC model. The signature changes revealed in this study can be exploited to identify and verify potential markers that contribute to severe infection via the human nasal transcriptome *in vitro* and *in vivo*. These markers can then be further applied using molecular diagnostics to detect these signatures during early infection to distinguish patients who may progress to severe disease, especially during outbreaks such as the 2009 H1N1 pandemic in which the severity of infection varied widely among patients. For example, markers such as IFNλs represent factors exerting antiviral responses that are less damaging to the surrounding tissues (Davidson et al., 2016; Galani et al., 2017). This is clinically significant in view of the proximity of the nasal epithelium to the infection; hence nasal diagnosis would facilitate more rapid detection of the severity markers compared to blood or serum specimens. In addition, intervention studies can also be performed using this model in studying local antiviral or immunomodulatory compounds. However, this model is not without its limitations. One disadvantage of this *in vitro* model is its inability to achieve complete viral clearance. It is thus unable to study the responses and repair of the nasal epithelium after viral clearance, for which

in vivo models would still be necessary. Another limitation is that this study only evaluated infection with a H3N2 strain. Given that hNECs infected with currently circulating strains belonging to H1N1 and B subtypes may respond differently, future studies are warranted to establish a more complete picture of influenza infection signatures in the nasal epithelium.

CONCLUSION

In conclusion, the nasal epithelium is an active component of initial host responses against influenza infection, and the nasal epithelial-specific transcriptomic changes may significantly influence the downstream immune responses and homeostasis that define the pathology of influenza in different individuals. Epithelial cells from different donors sustained infection differently; thus potential variations in nasal epithelial transcriptomic changes during influenza may result in differential pathogenesis between individuals. While infected nasal epithelial cells clearly elicited immune responses, the microarray analyses revealed that metabolism and antioxidant processes were also enriched among the transcriptomic changes. Future studies are warranted in the population to investigate nasal-associated factors identified in this study to ensure reproducibility of these factors in contributing to differential influenza pathogenesis amongst different individuals. This can be achieved through replicate infection studies of cells obtained from the same individual. In addition, being the site of closest proximity to the infection as well as exerting most responses observed in blood/serum may encourage the development of rapid molecular diagnostic tools based on the detection of nasal epithelial signatures that may predict the severity of influenza.

AUTHOR CONTRIBUTIONS

KT, YY, HC, TT, RS, VC, and DW conceived and designed the study, including selection of online transcriptomic datasets. KT, YY, WK, LL, and HC carried out the experiments and bioinformatics analysis and performed the statistical analyses. KT, HC, and VC co-wrote the original draft of the paper. All authors contributed to data interpretation, reviewed and edited the drafts, and approved the final version for submission.

FUNDING

This study was supported by grants from the National Medical Research Council, Singapore (NMRC/CIRG/1362/2013, NMRC/CIRG/1458/2016 and NMRC/CG/M009). Part of this work was presented at the Nature Conference on Viral Infection and Immune Response, Wuhan, China, October 21–24, 2016; European Academy of Allergy and Clinical Immunology Conference, Helsinki, Finland, June 17–21, 2017; and International Union of Microbiological Societies Congress, Singapore, July 17–21, 2017.

ACKNOWLEDGMENTS

We thank the surgeons and staff in the Department of Otolaryngology, National University Hospital, Singapore. We also thank M. C. Phoon and S. H. Lau for technical assistance.

SUPPLEMENTARY MATERIAL

The Supplementary Material for this article can be found online at: https://www.frontiersin.org/articles/10.3389/fmicb.2018.02685/full#supplementary-material

FIGURE S1 | Individual heat-maps of all differentially expressed genes following influenza infection of five donor hNECs.

FIGURE S2 | Meta-analysis and hierarchical functions across *in vitro* and *in vivo* influenza transcriptomic studies.

FIGURE S3 | Expression of host response genes in nasal epithelium following influenza infection.

TABLE S1 | Information and source of hNECs from five donors.

TABLE S2 | Details of transcriptomic studies included in meta-analysis.

TABLE S3 | Complete gene list output from microarray analysis.

TABLE S4 | Canonical pathways of the nasal epithelium following influenza virus infection. **(A)** 8 hpi; **(B)** 24 hpi; **(C)** 48 hpi.

TABLE S5 | Functional pathways (gene ontology terms) that are differentially regulated across all 15 studies analyzed.

REFERENCES

Akram, K. M., Moyo, N. A., Leeming, G. H., Bingle, L., Jasim, S., Hussain, S., et al. (2018). An innate defense peptide BPIFA1/SPLUNC1 restricts influenza A virus infection. *Mucosal Immunol.* 11, 71–81. doi: 10.1038/mi.2017.45

Andres-Terre, M., McGuire, H. M., Pouliot, Y., Bongen, E., Sweeney, T. E., Tato, C. M., et al. (2015). Integrated, multi-cohort analysis identifies conserved transcriptional signatures across multiple respiratory viruses. *Immunity* 43, 1199–1211. doi: 10.1016/j.immuni.2015.11.003

Ashburner, M., Ball, C. A., Blake, J. A., Botstein, D., Butler, H., Cherry, J. M., et al. (2000). Gene ontology: tool for the unification of biology. The Gene Ontology Consortium. *Nat. Genet.* 25, 25–29. doi: 10.1038/75556

Bermejo-Martin, J. F., Martin-Loeches, I., Rello, J., Anton, A., Almansa, R., Xu, L., et al. (2010). Host adaptive immunity deficiency in severe pandemic influenza. *Crit. Care* 14:R167. doi: 10.1186/cc9259

Boergeling, Y., and Ludwig, S. (2017). Targeting a metabolic pathway to fight the flu. *FEBS J.* 284, 218–221. doi: 10.1111/febs.13997

Braciale, T. J., Sun, J., and Kim, T. S. (2012). Regulating the adaptive immune response to respiratory virus infection. *Nat. Rev. Immunol.* 12, 295–305. doi: 10.1038/nri3166

Clay, C. C., Reader, J. R., Gerriets, J. E., Wang, T. T., Harrod, K. S., and Miller, L. A. (2014). Enhanced viral replication and modulated innate immune responses in infant airway epithelium following H1N1 infection. *J. Virol.* 88, 7412–7425. doi: 10.1128/JVI.00188-14

Cui, L., Fang, J., Ooi, E. E., and Lee, Y. H. (2017). Serial metabolome changes in a prospective cohort of subjects with influenza viral infection and comparison with dengue fever. *J. Proteome Res.* 16, 2614–2622. doi: 10.1021/acs.jproteome.7b00173

Cui, L., Zheng, D., Lee, Y. H., Chan, T. K., Kumar, Y., Ho, W. E., et al. (2016). Metabolomics investigation reveals metabolite mediators associated with acute lung injury and repair in a murine model of influenza pneumonia. *Sci. Rep.* 6:26076. doi: 10.1038/srep26076

Davidson, S., McCabe, T. M., Crotta, S., Gad, H. H., Hessel, E. M., Beinke, S., et al. (2016). IFNlambda is a potent anti-influenza therapeutic without the inflammatory side effects of IFNalpha treatment. *EMBO Mol. Med.* 8, 1099–1112. doi: 10.15252/emmm.201606413

Edwards, M. R., Walton, R. P., Jackson, D. J., Feleszko, W., Skevaki, C., Jartti, T., et al. (2018). The potential of anti-infectives and immunomodulators as therapies for asthma and asthma exacerbations. *Allergy* 73, 50–63. doi: 10.1111/all.13257

Galani, I. E., Triantafyllia, V., Eleminiadou, E. E., Koltsida, O., Stavropoulos, A., Manioudaki, M., et al. (2017). Interferon-lambda mediates non-redundant front-line antiviral protection against influenza virus infection without compromising host fitness. *Immunity* 46, 875–890. doi: 10.1016/j.immuni.2017.04.025

Gautier, L., Cope, L., Bolstad, B. M., and Irizarry, R. A. (2004). affy - analysis of affymetrix genechip data at the probe level. *Bioinformatics* 20, 307–315. doi: 10.1093/bioinformatics/btg405

Gonzalez Plaza, J. J., Hulak, N., Kausova, G., Zhumadilov, Z., and Akilzhanova, A. (2016). Role of metabolism during viral infections, and crosstalk with the innate immune system. *Intractable Rare Dis. Res.* 5, 90–96. doi: 10.5582/irdr.2016.01008

Granados, A., Peci, A., McGeer, A., and Gubbay, J. B. (2017). Influenza and rhinovirus viral load and disease severity in upper respiratory tract infections. *J. Clin. Virol.* 86, 14–19. doi: 10.1016/j.jcv.2016.11.008

Herberg, J. A., Kaforou, M., Gormley, S., Sumner, E. R., Patel, S., Jones, K. D., et al. (2013). Transcriptomic profiling in childhood H1N1/09 influenza reveals reduced expression of protein synthesis genes. *J. Infect. Dis.* 208, 1664–1668. doi: 10.1093/infdis/jit348

Hui, D. S. C., Lee, N., and Chan, P. K. S. (2017). A clinical approach to the threat of emerging influenza viruses in the Asia-Pacific region. *Respirology* 22, 1300–1312. doi: 10.1111/resp.13114

Ivan, F. X., Rajapakse, J. C., Welsch, R. E., Rozen, S. G., Narasaraju, T., Xiong, G. M., et al. (2012). Differential pulmonary transcriptomic profiles in murine lungs infected with low and highly virulent influenza H3N2 viruses reveal dysregulation of TREM1 signaling, cytokines, and chemokines. *Funct. Integr. Genomics* 12, 105–117. doi: 10.1007/s10142-011-0247-y

Ivan, F. X., Tan, K. S., Phoon, M. C., Engelward, B. P., Welsch, R. E., Rajapakse, J. C., et al. (2013). Neutrophils infected with highly virulent influenza H3N2 virus exhibit augmented early cell death and rapid induction of type I interferon signaling pathways. *Genomics* 101, 101–112. doi: 10.1016/j.ygeno.2012.11.008

Kamburov, A., Wierling, C., Lehrach, H., and Herwig, R. (2009). ConsensusPathDB - a database for integrating human functional interaction networks. *Nucleic Acids Res.* 37, D623–D628. doi: 10.1093/nar/gkn698

Kim, C. S., Ahmad, S., Wu, T., Walton, W. G., Redinbo, M. R., and Tarran, R. (2018). SPLUNC1 is an allosteric modulator of the epithelial sodium channel. *FASEB J.* 32, 2478–2491. doi: 10.1096/fj.201701126R

Klinkhammer, J., Schnepf, D., Ye, L., Schwaderlapp, M., Gad, H. H., Hartmann, R., et al. (2018). IFN-lambda prevents influenza virus spread from the upper airways to the lungs and limits virus transmission. *eLife* 7:e33354. doi: 10.7554/eLife.33354

Kolesnikova, L., Heck, S., Matrosovich, T., Klenk, H. D., Becker, S., and Matrosovich, M. (2013). Influenza virus budding from the tips of cellular microvilli in differentiated human airway epithelial cells. *J. Gen. Virol.* 94, 971–976. doi: 10.1099/vir.0.049239-0

Li, N., Parrish, M., Chan, T. K., Yin, L., Rai, P., Yoshiyuki, Y., et al. (2015). Influenza infection induces host DNA damage and dynamic DNA damage responses during tissue regeneration. *Cell. Mol. Life Sci.* 72, 2973–2988. doi: 10.1007/s00018-015-1879-1

Li, Y. Y., Li, C. W., Chao, S. S., Yu, F. G., Yu, X. M., Liu, J., et al. (2014). Impairment of cilia architecture and ciliogenesis in hyperplastic nasal epithelium from nasal polyps. *J. Allergy Clin. Immunol.* 134, 1282–1292. doi: 10.1016/j.jaci.2014.07.038

Poland, G. A., Jacobson, R. M., and Targonski, P. V. (2007). Avian and pandemic influenza: an overview. *Vaccine* 25, 3057–3061. doi: 10.1016/j.vaccine.2007.01.050

Qiao, Y., Yan, Y., Tan, K. S., Tan, S. S. L., Seet, J. E., Arumugam, T. V., et al. (2018). CD151, a novel host factor of nuclear export signaling in influenza virus infection. *J. Allergy Clin. Immunol.* 141, 1799–1817. doi: 10.1016/j.jaci.2017.11.032

Raval, F. M., and Nikolajczyk, B. S. (2013). The bidirectional relationship between metabolism and immune responses. *Discoveries* 1:e6. doi: 10.15190/d.2013.6

Smallwood, H. S., Duan, S., Morfouace, M., Rezinciuc, S., Shulkin, B. L., Shelat, A., et al. (2017). Targeting metabolic reprogramming by influenza infection for therapeutic intervention. *Cell Rep.* 19, 1640–1653. doi: 10.1016/j.celrep.2017.04.039

Sutejo, R., Yeo, D. S., Myaing, M. Z., Hui, C., Xia, J., Ko, D., et al. (2012). Activation of type I and III interferon signalling pathways occurs in lung epithelial cells infected with low pathogenic avian influenza viruses. *PLoS One* 7:e33732. doi: 10.1371/journal.pone.0033732

Tan, K. S., Yan, Y., Ong, H. H., Chow, V. T. K., Shi, L., and Wang, D. Y. (2017). Impact of respiratory virus infections in exacerbation of acute and chronic rhinosinusitis. *Curr. Allergy Asthma Rep.* 17:24. doi: 10.1007/s11882-017-0693-2

Tanner, L. B., Chng, C., Guan, X. L., Lei, Z., Rozen, S. G., and Wenk, M. R. (2014). Lipidomics identifies a requirement for peroxisomal function during influenza virus replication. *J. Lipid Res.* 55, 1357–1365. doi: 10.1194/jlr.M049148

Teo, G., Kim, S., Tsou, C. C., Collins, B., Gingras, A. C., Nesvizhskii, A. I., et al. (2015). mapDIA: preprocessing and statistical analysis of quantitative proteomics data from data independent acquisition mass spectrometry. *J. Proteomics* 129, 108–120. doi: 10.1016/j.jprot.2015.09.013

Vareille, M., Kieninger, E., Edwards, M. R., and Regamey, N. (2011). The airway epithelium: soldier in the fight against respiratory viruses. *Clin. Microbiol. Rev.* 24, 210–229. doi: 10.1128/CMR.00014-10

Wang, D. Y., Li, Y., Yan, Y., Li, C., and Shi, L. (2015). Upper airway stem cells: understanding the nose and role for future cell therapy. *Curr. Allergy Asthma Rep.* 15:490. doi: 10.1007/s11882-014-0490-0

Wang, W., Yan, Y., Li, C. W., Xia, H. M., Chao, S. S., Wang de, Y., et al. (2014). Live human nasal epithelial cells (hNECs) on chip for in vitro testing of gaseous formaldehyde toxicity via airway delivery. *Lab Chip* 14, 677–680. doi: 10.1039/C3LC51208H

Wang, Z., Wan, Y., Qiu, C., Quinones-Parra, S., Zhu, Z., Loh, L., et al. (2015). Recovery from severe H7N9 disease is associated with diverse response mechanisms dominated by CD8(+) T cells. *Nat. Commun.* 6:6833. doi: 10.1038/ncomms7833

Watanabe, T., Kiso, M., Fukuyama, S., Nakajima, N., Imai, M., Yamada, S., et al. (2013). Characterization of H7N9 influenza A viruses isolated from humans. *Nature* 501, 551–555. doi: 10.1038/nature12392

Watelet, J. B., Van Zele, T., Gjomarkaj, M., Canonica, G. W., Dahlen, S. E., Fokkens, W., et al. (2006). Tissue remodelling in upper airways: where is the link with lower airway remodelling? *Allergy* 61, 1249–1258. doi: 10.1111/j.1398-9995.2006.01226.x

Wein, A. N., Dunbar, P. R., McMaster, S. R., Li, Z. T., Denning, T. L., and Kohlmeier, J. E. (2018). IL-36gamma protects against severe influenza infection by promoting lung alveolar macrophage survival and limiting viral replication. *J. Immunol.* 201, 573–582. doi: 10.4049/jimmunol.1701796

Wu, D., Huang, W., Wang, Y., Guan, W., Li, R., Yang, Z., et al. (2014). Gene silencing of beta-galactosamide alpha-2,6-sialyltransferase 1 inhibits human influenza virus infection of airway epithelial cells. *BMC Microbiol.* 14:78. doi: 10.1186/1471-2180-14-78

Yan, Y., Gordon, W. M., and Wang, D. Y. (2013). Nasal epithelial repair and remodeling in physical injury, infection, and inflammatory diseases. *Curr. Opin. Otolaryngol. Head Neck Surg.* 21, 263–270. doi: 10.1097/MOO.0b013e32835f80a0

Yan, Y., Tan, K. S., Li, C., Tran, T., Chao, S. S., Sugrue, R. J., et al. (2016). Human nasal epithelial cells derived from multiple subjects exhibit differential responses to H3N2 influenza virus infection in vitro. *J. Allergy Clin. Immunol.* 138, 276–281. doi: 10.1016/j.jaci.2015.11.016

Zhai, Y., Franco, L. M., Atmar, R. L., Quarles, J. M., Arden, N., Bucasas, K. L., et al. (2015). Host transcriptional response to influenza and other acute respiratory viral infections - a prospective cohort study. *PLoS Pathog* 11:e1004869. doi: 10.1371/journal.ppat.1004869

Zhao, X., Yu, F., Li, C., Li, Y., Chao, S.-S., Loh, W.-S., et al. (2012). The use of nasal epithelial stem/progenitor cells to produce functioning ciliated cells in vitro. *Am. J. Rhinol. Allergy* 26, 345–350. doi: 10.2500/ajra.2012.26.3794

Conflict of Interest Statement: The authors declare that the research was conducted in the absence of any commercial or financial relationships that could be construed as a potential conflict of interest.

Copyright © 2018 Tan, Yan, Koh, Li, Choi, Tran, Sugrue, Wang and Chow. This is an open-access article distributed under the terms of the Creative Commons Attribution License (CC BY). The use, distribution or reproduction in other forums is permitted, provided the original author(s) and the copyright owner(s) are credited and that the original publication in this journal is cited, in accordance with accepted academic practice. No use, distribution or reproduction is permitted which does not comply with these terms.

frontiers in Immunology

ORIGINAL RESEARCH
published: 21 November 2018
doi: 10.3389/fimmu.2018.02631

Dysregulated miRNAome and Proteome of PPRV Infected Goat PBMCs Reveal a Coordinated Immune Response

Alok Khanduri[1†], Amit Ranjan Sahu[1,2†], Sajad Ahmad Wani[1,3], Raja Ishaq Nabi Khan[1†], Aruna Pandey[1], Shikha Saxena[1], Waseem Akram Malla[1], Piyali Mondal[1], Kaushal Kishor Rajak[4], D. Muthuchelvan[5], Bina Mishra[4], Aditya P. Sahoo[6], Yash Pal Singh[7], Raj Kumar Singh[1], Ravi Kumar Gandham[1,2] and Bishnu Prasad Mishra[1*]*

[1] Division of Veterinary Biotechnology, ICAR-Indian Veterinary Research Institute (IVRI), Bareilly, India, [2] DBT-National Institute of Animal Biotechnology, Hyderabad, India, [3] The Ohio State University, Columbus, Ohio, OH, United States, [4] Division of Biological Products, ICAR-Indian Veterinary Research Institute (IVRI), Bareilly, India, [5] Division of Virology, ICAR-Indian Veterinary Research Institute (IVRI), Mukteswar, India, [6] ICAR- Directorate of Foot and Mouth Disease, Mukteswar, India, [7] ARIS Cell, ICAR-Indian Veterinary Research Institute (IVRI), Bareilly, India

In this study, the miRNAome and proteome of virulent Peste des petits ruminants virus (PPRV) infected goat peripheral blood mononuclear cells (PBMCs) were analyzed. The identified differentially expressed miRNAs (DEmiRNAs) were found to govern genes that modulate immune response based on the proteome data. The top 10 significantly enriched immune response processes were found to be governed by 98 genes. The top 10 DEmiRNAs governing these 98 genes were identified based on the number of genes governed by them. Out of these 10 DEmiRNAs, 7 were upregulated, and 3 were downregulated. These include miR-664, miR-2311, miR-2897, miR-484, miR-2440, miR-3533, miR-574, miR-210, miR-21-5p, and miR-30. miR-664 and miR-484 with proviral and antiviral activities, respectively, were upregulated in PPRV infected PBMCs. miR-210 that inhibits apoptosis was downregulated. miR-21-5p that decreases the sensitivity of cells to the antiviral activity of IFNs and miR-30b that inhibits antigen processing and presentation by primary macrophages were downregulated, indicative of a strong host response to PPRV infection. miR-21-5p was found to be inhibited on IPA upstream regulatory analysis of RNA-sequencing data. This miRNA that was also highly downregulated and was found to govern 16 immune response genes in the proteome data was selected for functional validation vis-a-vis *TGFBR2* (TGF-beta receptor type-2). *TGFBR2* that regulates cell differentiation and is involved in several immune response pathways was found to be governed by most of the identified immune modulating DEmiRNAs. The decreased luciferase activity in Dual Luciferase Reporter Assay indicated specific binding of miR-21-5p and miR-484 to their target thus establishing specific binding of the miRNAs to their targets.This is the first report on the miRNAome and proteome of virulent PPRV infected goat PBMCs.

Keywords: miRNAome, proteome, PPR, goats, host-pathogen interaction, immunopathogenesis

OPEN ACCESS

Edited by:
Ju-Tao Guo,
Baruch S. Blumberg Institute, United States

Reviewed by:
Jianzhong Zhu,
Yangzhou University, China
Noemi Sevilla,
Instituto Nacional de Investigación y Tecnología Agraria y Alimentaria (INIA), Spain

***Correspondence:**
Bishnu Prasad Mishra
bpmishra_1@hotmail.com
Ravi Kumar Gandham
gandham71@gmail.com

[†] These authors have contributed equally to this work

Specialty section:
This article was submitted to Comparative Immunology, a section of the journal Frontiers in Immunology

Received: *02 April 2018*
Accepted: *25 October 2018*
Published: *21 November 2018*

Citation:
Khanduri A, Sahu AR, Wani SA, Khan RIN, Pandey A, Saxena S, Malla WA, Mondal P, Rajak KK, Muthuchelvan D, Mishra B, Sahoo AP, Singh YP, Singh RK, Gandham RK and Mishra BP (2018) Dysregulated miRNAome and Proteome of PPRV Infected Goat PBMCs Reveal a Coordinated Immune Response. Front. Immunol. 9:2631. doi: 10.3389/fimmu.2018.02631

INTRODUCTION

MicroRNAs (miRNAs) are small non-coding RNAs (22 nucleotides) found to regulate the expression of genes post-transcriptionally in animals, plants, and some viruses (1). They regulate different cellular processes, including reproduction, development, pathogenesis, and apoptosis (2–4). miRNAs are also effective in regulating immune response and cellular differentiation (5–7). The regulation process generally takes place by binding of miRNA at its seed sequence (2–8 nucleotides from 5′-end) to the 3′ untranslated region (3′UTR) of specific mRNAs of the genes that govern the biological processes. However, several instances of miRNAs binding to 5' UTR or coding regions in the regulation process have also been reported (8, 9).

Viral pathogenesis is greatly influenced by cellular miRNAs (10–12). Several cellular miRNAs have been demonstrated to play a regulatory role in the host-virus interaction networks (13, 14). Cellular miRNA expression profile is profoundly influenced by viral infections and vice-versa (15). For example, miR-122 is reported to enhance replication of Hepatitis C virus (16) and miR-142 suppresses replication of Eastern Equine Encephalitis virus (17). The HIV-1 virus has been found to increase the expression of various host miRNAs, including miR-370, miR-122, miR-297, and miR-373, and suppress the expression of miR-17-92 cluster (18). With the advent of deep sequencing technology, it has become possible to explore changes in miRNA expression in the host, in response to various viral infections like enterovirus 71, avian influenza, PPRV, Japanese Encephalitis virus and hepatitis C virus (19–23).

Peste des petits ruminants (PPR) characterized by fever, sore mouth, conjunctivitis, gastroenteritis, and pneumonia, is an acute, highly contagious viral disease of sheep and goats. However, a more severe form of the clinical disease has been reported in goats than in sheep, since goats are more susceptible (24–29). The recovery is also slower in goats than in sheep (27). However, regions having large sheep populations have reported severe outbreaks of PPR (27, 30, 31). Our earlier *in-vitro* transcriptome analysis studies to evaluate host response of goat PBMCs to PPR live attenuated vaccine virus uncovered several transcription factors that modulate immune response (32, 33). Also, dysregulation in the host miRNAome in lung and spleen of experimentally infected goats and sheep by virulent PPRV suggests a strong host immune response in sheep and goats (21). However, the host miRNAome of PPRV infected goat and sheep PBMCs has not been explored to date. Lymphocytes are the primary targets of PPRV infection from where it reaches different tissues by piggybacking on PBMCs (34). A higher viral load is reported to be at 9 days post-infection (dpi), which coincides with the peak clinical signs of the disease (22, 35). In the present study, control (0 day) and PPRV infected PBMCs (9 dpi) of goats were isolated and subjected to microRNA sequencing (miRNA-seq) and proteome profiling. DEmiRNAs were identified from miRNA-seq data and correlated with the proteome data to identify the miRNAs that govern the immune processes. Among the miRNAs, miR-21-5p was found to be highly downregulated in miRNA-seq data, inhibited in RNA sequencing (RNA-seq) data (unpublished) and involved in regulation of various immune response genes. This miR-21-5p was selected for annotation and functional validation. Additionally, one more miR, miR-484 was randomly chosen from top 10 immunoregulating DEmiRNAs for functional validation.

MATERIALS AND METHODS

Ethics Statement and Animal Experiment

The study is a part of vaccine potency testing experiment conducted at ICAR-Indian Veterinary Research Institute Mukteshwar Campus as per the guidelines of Indian pharmacopeia-2014. The permission to conduct the experiment was sought from Indian Veterinary Research Institute–Institutional Animal Ethics Committee (IVRI–IAEC) under the Committee for the Purpose of Control and Supervision of Experiments on Animals (CPCSEA), India and was approved vide letter no 387/CPCSEA. The animals that were apparently healthy and negative for the presence of PPRV antibody by competitive ELISA and serum neutralization test (SNT) were used in this study. Virulent PPRV [accession number KR140086.1 (36)], a lineage IV isolate and strain Izatnagar/94, was used as a challenge virus and infection was confirmed in goats by RT–PCR, qRT-PCR, and sandwich ELISA. PBMCs were isolated from the blood collected from PPRV (Izatnagar/94) infected goats at 9 dpi (The animals succumbed to the disease at 10 dpi). The PBMCs isolated from blood collected from apparently healthy animals (0 day) acted as a control. PBMCs were isolated using Histopaque-1077 (Sigma), USA.

MicroRNA Sequencing

Total RNA from the PBMCs of goats was isolated using the RNeasy Mini kit (Qiagen GmbH, Germany) following the manufacturer's protocol. To access integrity and quality of the RNA, RNA integrity number (RIN) value of each sample was measured on Bioanalyzer (Agilient Technologies, Inc.). The RIN value was found to be >8, which is considered suitable for further processing (37). The library was prepared using NEBNext Multiplex Small RNA Library Prep Kit (New England Biolabs Inc.) as per the manufacturer's protocol. Hundred nanogram of total RNA from each sample was used for small RNA library preparation. The quality of the libraries was assessed on Bioanalyzer. Libraries were quantified using Qubit 2.0 Fluorometer (Life Technologies) and by qPCR (38).The high-throughput sequencing was performed on Illumina–NextSeq500 platform to generate 75 bp single-end reads as per manufacturer's protocol. The data was submitted to the GEO database with accession number GSE109799.

Processing miRNA-seq Data

The miRNA reads trimming and preprocessing was performed with CLC Genomic workbench v6.0 (CLC bio, Denmark) to remove adaptor sequences and low quality reads using default parameters. Since the cattle genome (mirBase–Release 21) is relatively better annotated and as the miRNAs are conserved across species, cattle genome was used to map these clean reads. The map files for the infected and control samples were

created independently. From the toolbox of CLC workbench, an experiment was created, the read count was quantitatively normalized and the expression values were obtained. Proportion based statistics–Kal's test was used to identify differentially expressed miRNAs at 9dpi PPRV infected PBMCs of goat.

Proteomics Data Generation and Analysis

The proteomic data was generated from control and PPRV infected 9 dpi goats PBMCs and analyzed following the standard procedure as described in the previous study (21). Briefly, proteome from goat PBMCs was quantitatively analyzed using trypsin in conjugation with C18 Nano-LC column separation, followed by analysis on the Waters Synapt G2 Q-TOF instrument for MS. The raw data was processed by MassLynx 4.1 WATERS, and MSMS spectra were matched to the database sequence using PLGS software. The identified proteins in the three runs of each sample were compared with each other as control (healthy) and infected samples. Quantification was done using expression analysis package of the PLGS software. The ion counts matching with the peptides of a specific protein corresponding between the two samples in the three runs

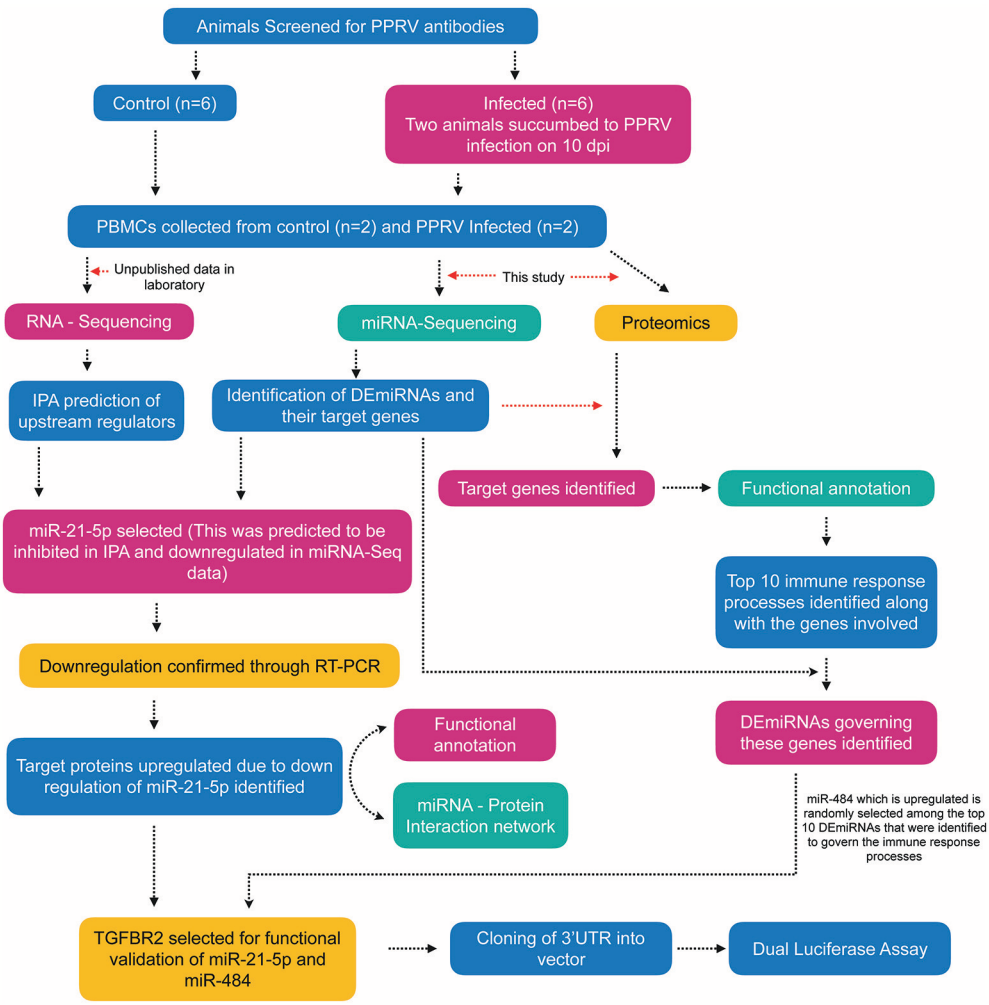

FIGURE 1 | Overview of the experiment. Apparently healthy goats ($n = 6$) that were negative for the presence of PPRV antibody by competitive ELISA and serum neutralization test (SNT) were infected with virulent PPRV strain Izatnagar/94. These animals acted as control in the vaccine potency experiment. Two animals in the group succumbed to disease on 10 dpi. PBMCs from blood collected at 9dpi from these two succumbed animals and PBMCs isolated from blood collected on 0 day (control) were sent for miRNA-Sequencing, RNA-Sequencing (unpublished data in the lab) and Proteome profiling. Differentially expressed miRNAs (DEmiRNAs) and proteins were identified from the miRNA-Seq and proteome data, repectively. The DEmiRNAs were functionally annotated w.r.t the proteins governed in the proteome data. The top 10 DEmiRNAs governing the top 10 immune response processes were identified. miR-21-5p which was found to be inhibited on IPA upstream regulatory analysis of RNA-Sequencing data, highly downregulated in miRNA-Seq data (validated by qRT-PCR) and found to govern 16 immune response genes in the proteome data was selected for functional validation vis-a-vis *TGFBR2* (TGF-beta receptor type-2). *TGFBR2* regulates cell differentiation and is involved in several immune response pathways was found to be governed by most of the identified immune modulating DEmiRNAs. Dual luciferase assay was done using mimics of miR-21-5p and miR-484 and 3′UTR of the target gene *TGFBR2* to establish the specificity of binding.

were averaged and the ratio was calculated for the whole protein.

Functional Annotation of Differentially Expressed miRNAs

To explore the regulatory role of the differentially expressed miRNAs, the target genes governed by each of the DEmiRNAs were obtained using TargetScan tool (39)[1] All these target genes were pooled up and compared to the dysregulated proteins identified in proteomics data. The genes common to both data were selected for functional annotation via ClueGo (ver. 2.3.3) and CluePedia (ver. 1.3.3) (40) in Cytoscape (ver. 3.2.1) (41). The genes involved in top 10 significantly enriched immune response processes were identified. Out of these immune response genes, the genes governed by each of the DEmiRNAs were identified and top 10 DEmiRNAs were selected.

TABLE 1 | Co-transfection complex for the target gene against miRNAs.

	Well 1	Well 2	Well 3	Well 4
Tube A	TGFBR2 Wild (1 μg)	TGFBR2 Wild (1 μg)	TGFBR2 Mutant (1 μg)	TGFBR2 Mutant (1 μg)
	pGL4.74 (5 ng)	pGL4.74 (5 ng)	pGL4.74 (5 ng)	pGL4.74 (5 ng)
	miR-21-5p/484 mimic (25 μM)	miR-67-3p (25 μM)	miR-21-5p/484 mimic (25 μM)	miR-67-3p (25 μM)
	P3000 Reagent (1 μl)	P3000 Reagent (1 μl)	P3000 Reagent (1 μl)	P3000 Reagent (1 μl)
	Opti-MEM (50 μl)	Opti-MEM (50 μl)	Opti-MEM (50 μl)	Opti-MEM (50 μl)
Tube B	Lipofectamine 3000 (1.5 μl)	Lipofectamine 3000 (1.5 μl)	Lipofectamine 3000 (1.5 μl)	Lipofectamine 3000 (1.5 μl)
	Opti-MEM (50 μl)	Opti-MEM (50 μl)	Opti-MEM (50 μl)	Opti-MEM (50 μl)

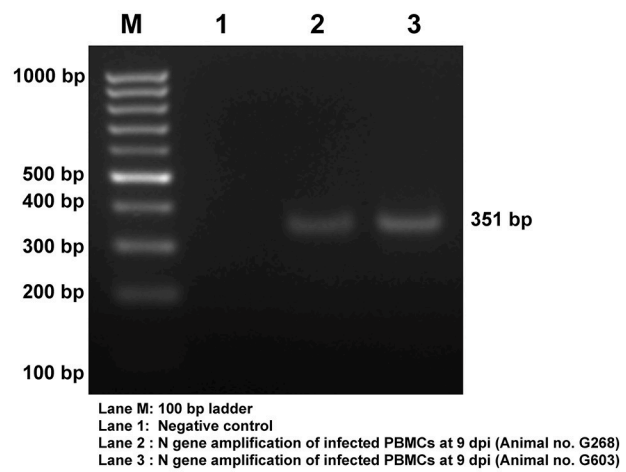

FIGURE 2 | Confirmation of PPRV infection in PBMCs of goats. Amplification of 351 bp N gene by RT- PCR. Lane M, 100 bp ladder; Lane 1, NTC; Lane 2, Infected Goat PBMCs (Animal no: G268) Lane 3, Infected Goat PBMCs (Animal No: G603).

Processing RNA-seq Data

From IPA analysis (Ingenuity Pathway Analysis)[2] of the RNA-sequencing data generated in our lab (unpublished), the upstream miRNA regulators governing the differentially expressed genes (data not shown) were identified. The overview of the entire analysis is given in **Figure 1.**

Downregulation of miR-21-5p in qRT-PCR

The expression of the miR-21-5p in PPRV infected PBMCs was validated by qRT-PCR. Total RNA, including small RNA

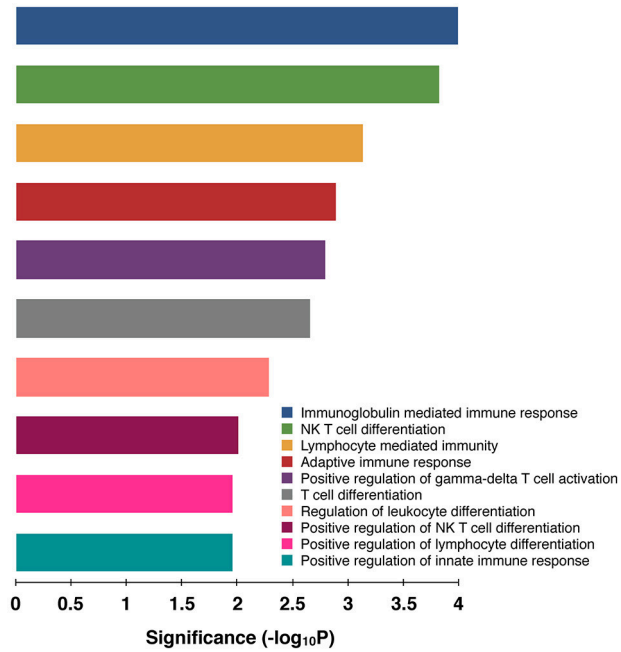

FIGURE 3 | Top 10 Significant ($P < 0.05$) Immunological processes involved in virulent PPRV goats PBMCs. Color differentiates the immune processes.

TABLE 2 | Ten DEmiRNAs based on the number of immune response genes, involvement of *TGFBR2* and fold-change values.

	miRNAs	No. of Immune response genes	*TGFBR2*	log_2FC
1	miR-664	33	Yes	1.37
2	miR-2311	31	Yes	1.15
3	miR-2897	27	-	1.85
4	miR-484	27	Yes	1.14
5	miR-2440	22	Yes	0.13
6	miR-3533	19	-	1.87
7	miR-574	18	Yes	0.83
8	miR-210	17	Yes	−2.70
9	miR-21-5p	16	Yes	−7.20
10	miR-30	15	-	−6.97

[1]http://www.targetscan.org/vert_71/.

[2]https://www.qiagenbioinformatics.com/products/ingenuity-pathway-analysis/

from the PBMCs of control and infected goats, was isolated using mirVana™ miRNA isolation kit (Invitrogen). Reverse transcriptase reactions were performed using RT specific primers of miR-21-5p and U6snRNA by TaqMan® MicroRNA Reverse Transcription Kit (Applied Biosystems, USA, #4366596). Total RNA from the PBMCs was diluted to a concentration of 10 ng/μl and 1 μl of RNA was added to the reaction mix containing 0.15 μl 100 mM dNTPs, 1 μl of RT enzyme (50 U/μl), 1.5 μl 10× RT buffer, 0.19 μl RNase inhibitor (20 U/μl), 3 μl 5 × RT specific-primer and 8.16 μl DEPC-treated water to obtain a final volume of 15 μl. The reaction conditions were 16°C for 30 min followed by 42°C at 30 min and 85°C for 5 min to stop the reaction. The cDNA was then used for the Real-time PCR. Real-time PCR was performed using a standard TaqMan PCR kit protocol on Applied Biosystems 7,500 fast Sequence Detection System. The 10 μl PCR included 5 μl of 2× Taqman Gene Expression Mastermix (Thermo Fisher Scientific Inc., Wilmington, DE, USA), 0.5 ul of 20× Taqman probe (Assay ID 005982-mat), 2 μl (0.134 ng) of RT product and 2.5 μl of NFW. The reactions were incubated in a 96-well plate at 95°C for 10 min, followed by 40 cycles of 95°C for 15 s and 60°C for 1 min. All reactions were run in triplicate. The expression of miRNA-21-5p was assayed taking the expression of U6snRNA as an internal control. The relative expression of miR-21-5p was calculated using the $2^{-\Delta\Delta CT}$ method with the control group as calibrator (42). Student's *t*-test was done in JMP9 (SAS Institute Inc., Cary, USA) to test the significance of difference and difference between groups was considered significant at $P \leq 0.05$.

Prediction of miR-21-5p Target Genes and Functional Annotation

The target genes governed by miRNA-21-5p were obtained using TargetScan tool to explore its regulatory role (39). The target genes obtained were compared to the upregulated proteins from proteome data to identify the proteins that are upregulated because of downregulation of miR-21-5p. The miRNA-protein-network was created based on the expression profile of target genes and miR-21-5p using Cytoscape (ver. 3.2.1). Functional annotation of these genes was performed by ClueGo (ver. 2.3.3) and CluePedia (ver. 1.3.3) (40) in Cytoscape (ver. 3.2.1) (41).

Functional Validation of miR-21-5p and miR-484

Prediction of miR Target Site in 3′ UTR

TGFBR2 that is governed by miR-21-5p and miR-484, and found connected to most significantly enriched GO terms, was selected for further validation of the miRNAs. The 3'UTR target site of this gene and mature miRNA were extracted from NCBI and analyzed in miRanda (43) tool to evaluate the strength of interaction using the parameters ΔG and total score value.

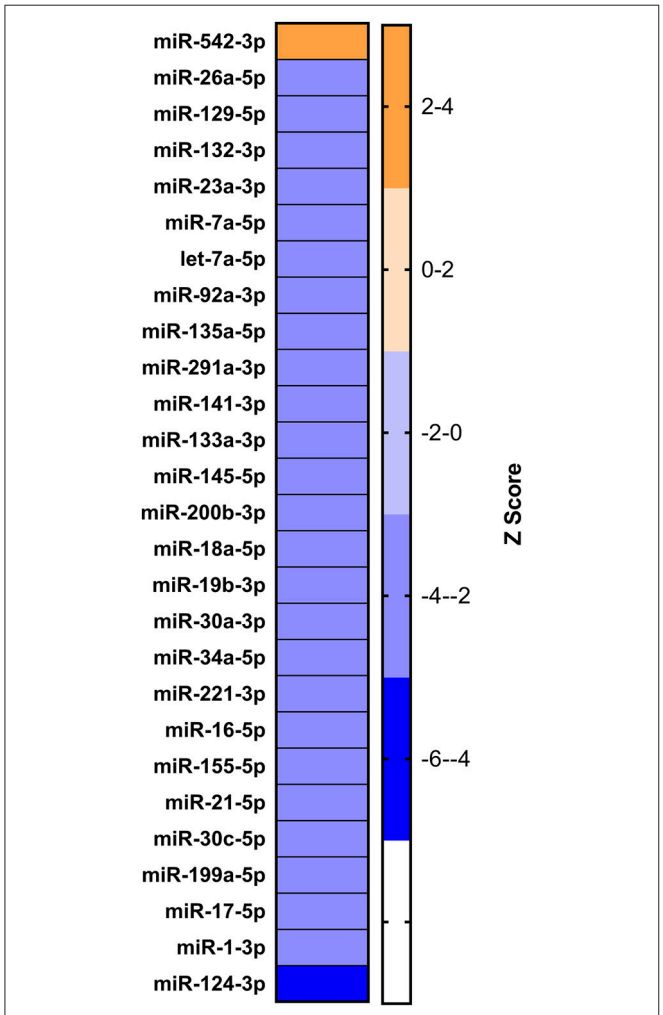

FIGURE 4 | Identification of dysregulated miRNA from RNA sequencing data. IPA analysis to identify the upstream regulators governing the differentially expressed genes yielded 27 miRNAs.

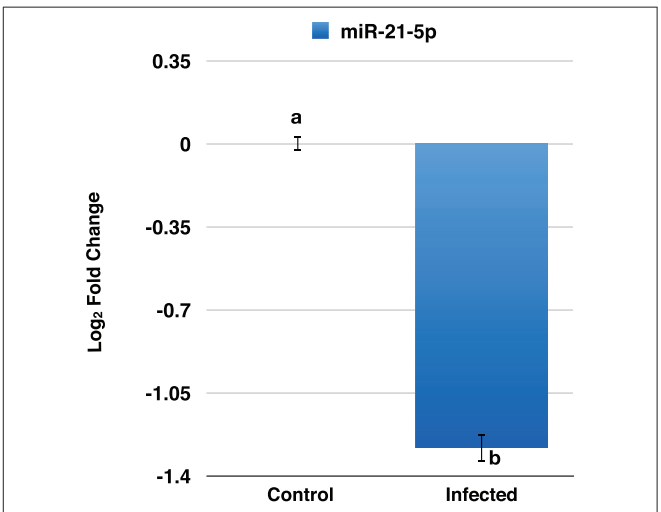

FIGURE 5 | RT-qPCR analysis of miR-21-5p in PPRV infected goats PBMCs. The miR-21-5p was found to be downregulated in PPRV infected goat PBMCs.

Design of Wild Type and Mutant Type miR Target Sites and miRNA Mimic and Control

While two wild-type oligonucleotides (62 bp) were constructed from 3′UTR of *TGFBR2* mRNA flanking the miR-21-5p and miR-484 target sites, respectively, the mutant of both was created by replacing the target site either with poly A or poly T sequence. pGL4.13 vector (Promega) was used to clone the oligonucleotide sequences (wild-type and mutant-type separately) at XbaI RE site of this vector. pGL4.74 was used as a control vector for the normalization of the transfection efficiency. Likewise, mimics of miR-21-5p and miR-484 were chemically synthesized. miR-67-3p was used as control for it is reported to have least sequence identity with known miRNAs in humans, rat, and mouse (44).

Co-transfection Strategy for Carrying Out Dual-Luciferase Reporter Assay

HEK293 cells were used for the co-transfection of the vectors, pGL4.13, and pGL4.74. The cells were maintained in MEM medium with 10% FBS, antibiotic and antimycotic (Himedia), and placed in an incubator at 37°C with 5% CO_2. The experiment was performed in triplicates. Briefly, the co-transfection complex for each vector was prepared in 2 tubes, one containing Opti-MEM + Lipofectamine and the other tube containing Opti-MEM + Vectors + Mimic. The complex was formulated as shown in **Table 1.** Contents of tube A and B were mixed and incubated for 15 min at room temperature to allow the formation of transfection complex. After the formation of the complex, Opti-MEM was added to the complex to make the volume up to

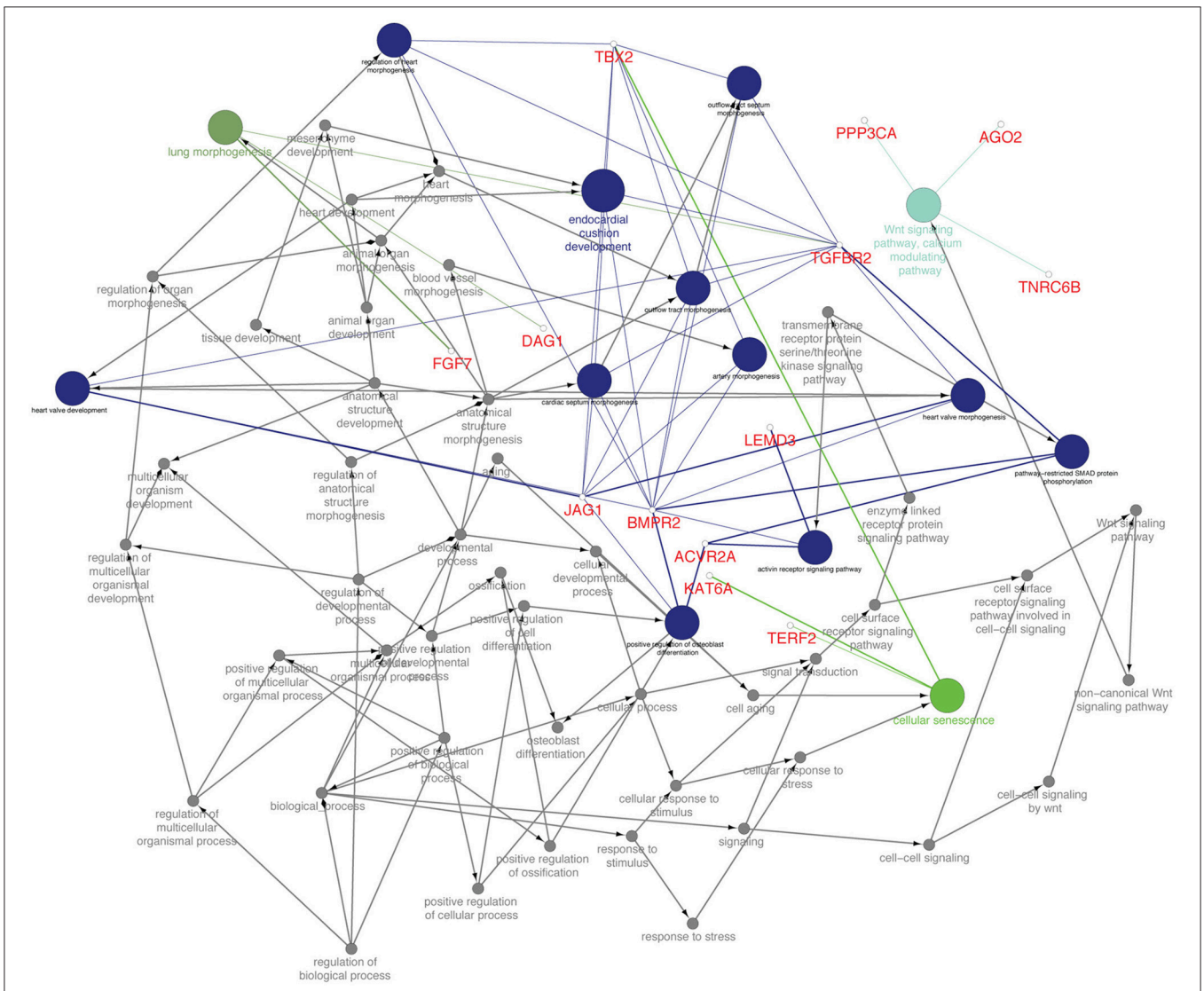

FIGURE 6 | Functionally annotation of miR-21-5p based on the upregulated target genes (45). Gene ontology was visualized in these genes visualized in ClueGo (ver. 2.3.3) + CluePedia (ver. 1.3.3) plugin of Cytoscape (ver. 3.2.1).

400 µl. The medium from the 24 well plate was removed and the co-transfection complexes were gently loaded into each well of the plate. The plate was kept in an incubator for 4 h. After 4 h, the medium with the complex was removed from the wells and fresh 1% MEM (500 µl) was added to the wells. The cells were lysed 48 h post co-transfection and the luciferase activity was measured using Dual Luciferase Assay kit (Promega) according to the manufacturer's protocol. The assay results were represented as relative luciferase activity. Student's *t*-test was done in JMP9 (SAS Institute Inc, Cary, USA) to test the significance of difference, and differences between groups were considered significant at $P \leq 0.05$.

RESULTS

Confirmation of PPRV Infection

Viral infection in the PBMCs of goats infected with PPRV was confirmed by RT-PCR amplification of 351 bp N gene fragment (**Figure 2**). The viral infection was further confirmed by sandwich ELISA and qRT-PCR (data not shown).

miRNAs Governing the Immune Processes Were Identified

In goat PBMCs infected with PPRV, a total of 68 miRNAs were significantly ($P < 0.05$) differentially expressed (42 down-regulated and 26 up-regulated) (**Table S1**). From the proteomics data (**Table S2**) generated from PPRV infected goat PBMCs, 1,965 and 3,509 proteins were identified to be downregulated and upregulated, respectively. From the TargetScan data, 15,341 genes were found to be governed by the 68 DEmiRNAs, out of which 4,027 proteins were found to be dysregulated in the proteomics data. On ClueGo analysis of these genes, the top 10 significantly enriched immunological processes included immunoglobulin mediated immune response, NK T cell differentiation lymphocyte mediated immunity, adaptive immune response, positive regulation of gamma-delta T

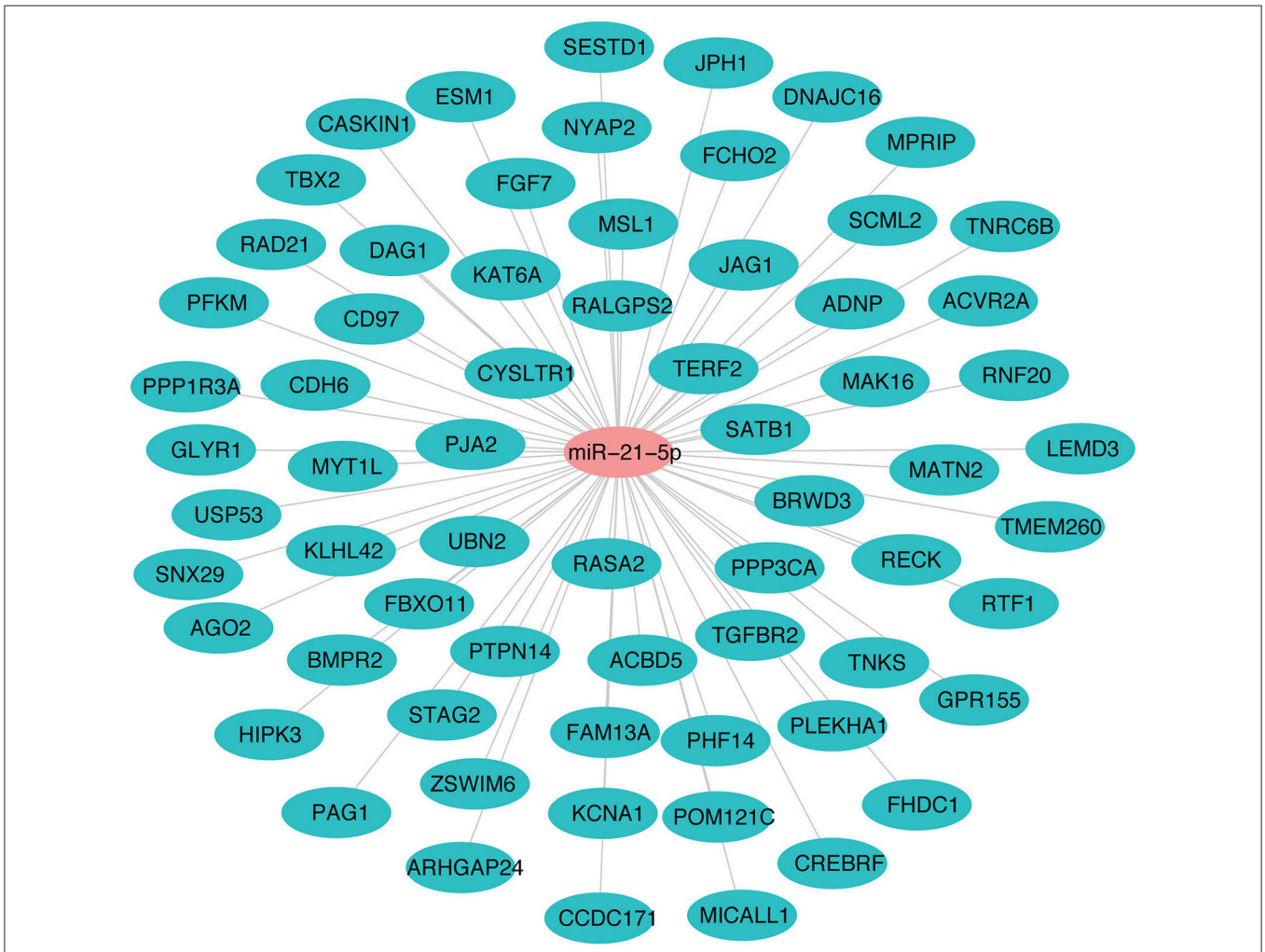

FIGURE 7 | miRNA-protein interaction network of target proteins upregulated due to downregulation of miR-21-5p. Student's t-test was done in JMP9 (SAS Institute Inc, Cary, USA) to test the significance of difference and difference between groups was considered significant at $P \leq 0.05$.

cell activation, T cell differentiation, regulation of leukocyte differentiation, positive regulation of NK T cell differentiation, positive regulation of lymphocyte differentiation, positive regulation of innate immune response (**Figure 3**). The genes (from the proteomics data) enriched under these GO terms are given in **Table S3.** A total of 98 genes were found to be enriched in these top 10 significant immune response processes governed by 42 DEmiRNAs (18 upregulated and 24 downregulated) (**Tables S4**, **S5**). The top 10 DEmiRNAs based on the number of immune response genes governed are given in **Table 2.** On comparing the DEmiRNAs of PPRV infected PBMCs with DEmiRNAs of the PPRV infected lung and spleen, reported in our earlier study (21), we found there are 3 DEmiRNAs common among the lung, spleen and PBMCs and 9 DEmiRNAs common between the lung and PBMCs. However, there was no DEmiRNA exclusively common between PBMCs and spleen (**Table S6**). Of the 9 DEmiRNAs common between lung and PBMCs, miR-378b, miR-342, miR-30f, miR-339a were found to be downregulated while miR-1246 and miR-2440 were upregulated in both. In addition, miR-181a-1, miR-181a-2 and miR-7-1 were found upregulated in lung but downregulated in PBMCs. Of the 3 DEmiRNAs common to each, miR-574 was found upregulated. miR-21-5p was found upregulated in spleen and lung but downregulated in PBMCs and vice-versa in case of miR-744.

miR-21-5p Was Selected for Functional Annotation and Validation

On analyzing RNA-seq data (from the lab) of the 9 dpi PBMCs, 5,150 differentially expressed genes (DEGs) were identified in PPRV infected goats. These genes were further subjected to IPA using various modules based on knowledge database to predict the biological function of DEGs, the role of the molecules in various disease processes, upstream regulators (transcription factors, miRNAs, and drugs) that regulate the function of the downstream target genes and possible interactions among them. In the present study, we concentrated only on those miRNAs, which act as upstream regulators for DEGs. Twenty-seven miRNAs were identified regulating these DEGs. Of the 27 identified miRNAs, 26 were inhibited (z score <-2) and only 1 was activated (z score >2) (**Figure 4**). Further, out of these 27, only four miRNAs viz miR-129, miR-21-5p, Let-7a, and miR-200 were found be differentially expressed in the miRNA-seq data. miR-21-5p was found highly downregulated in miRNA-seq data (**Table 2**), inhibited in RNA-seq data and involved in regulation of various immune response genes. This miR-21-5p was further selected for annotation and functional validation.

Validation of miR-21-5p by qRT-PCR

To confirm the downregulation of miR-21-5p, qRT-PCR was used to validate its expression in PPRV infected goat PBMCs. This miRNA was found to be downregulated and was in concordance with the miRNA-seq results (**Figure 5**).

Prediction of miRNA-21-5p Targets, Gene Ontology Analysis, and Target Selection for Functional Validation

From the TargetScan data, 356 genes were found to be governed by miR-21-5p, out of which 66 proteins were found to be upregulated (since miR-21-5p was downregulated, the study was

TABLE 3 | Immune-related functions of proteins upregulated due to downregulation of miR-21-5p.

Protein symbol	Protein Name	Function
ACBD5	Acyl-CoA binding domain containing 5	It acts as the peroxisome receptor for degradation of damaged peroxisomes and proteins (46). Mutation in the gene is associated with Thrombocytopenia (47).
ADNP	Activity-dependent neuroprotector homeobox	It is a neuroprotective molecule (45).
CD97	Adhesion G protein-coupled receptor E5	Leukocyte receptor involved in wide range of functions including cell adhesion and migration (48, 49).
CDH6	Cadherin 6	Role in Homophilic cell adhesion (50).
CREBRF	CREB3 regulatory factor	It assists unfolded protein response during endoplasmic reticulum stress (51).
CYSLTR1	Cysteine leukotriene receptor 1	It is involved in stimulating the activity of mast cells, eosinophil, dendritic cells and neutrophils (52, 53).
DNAJC16	DnaJ heat shock protein family (Hsp40) member C16	It belongs to DnaJ/Hsp40 family that acts as co-chaperone for Hsp70 proteins mediating folding of substrates in cytosol during cell stress (54).
FBXO11	F-box protein 11	It regulates Pr-Set7/Set8-Mediated Cellular Migration (55).
HIPK3	Homeodomain-interacting protein kinase 3	It promotes Resistance to Fas-mediated Apoptosis in DU 145 Prostate Carcinoma Cells (56).
JAG1	Jagged 1	It binds with the CD46 receptor and mediates induction of interferon-γ (IFN-γ)-secreting effector T helper type 1 (TH1) cells and their subsequent switch into interleukin 10 (IL-10)-producing regulatory T cells (57).
KAT6A	Lysine acetyltransferase 6A	Increases effector-like memory CD8+ T cells and cell surface CD8 and TCR levels (58).
PAG1	Phosphoprotein membrane anchor with glycosphingolipid microdomains 1	The complex of PAG with tyrosine kinase (Csk) transmits negative regulatory signals and thus may help to keep resting T cells in a quiescent state (59).
PJA2	Praja ring finger ubiquitin ligase 2	It regulates transcription of HIV Virus by degrading Tat (60).
RAD21	RAD21 cohesin complex component	Plays a role in apoptosis, via its cleavage by caspase-3/CASP3 or caspase-7/CASP7 during early steps of apoptosis (61).

concentrated only on upregulated proteins) in the proteomics data. These target proteins on GO analysis were enriched in Wnt signaling pathway, cell surface receptor signaling pathway, pathway-restricted SMAD phosphorylation, morphogenesis processes, positive regulation of cellular processes, multicellular organismal development, etc., (**Figure 6**). *TGFBR2* gene, which is connected to most of the GO terms viz pathway-restricted SMAD phosphorylation, activin receptor signaling pathway, Wnt signaling pathway, morphogenesis of lung and heart and blood vessels, and osteoclast differentiation was selected as the target of miR-21-5p. *TGFBR2* was also found to be governed by 21 identified immune regulating DEmiRNAs (**Table 2** and **Table S7**).

miRNA-Protein Regulatory Network of miR-21-5p

The miR-21-5p and 66 upregulated proteins interacting with it are represented in a network (**Figure 7**). Among the 66, 15 proteins (ACBD5, ADNP, CD97, CDH6, CREBRF, CYSLTR1, DNAJC16, FBXO11, HIPK3, JAG1, KAT6A, PAG1, PJA2, RAD21, *TGFBR2*) were found to be involved in immune response processes (**Table 3**). This suggested the involvement of miR-21-5p in the regulation of immune response in PPRV infected PBMCs.

miR-21-5p and miR-484 Were Functionally Validated Using Dual-Luciferase Reporter Assay

The miR-21-5p and miR-484 sequences were found to be complementary to sequences from 329-349 and 613-634 at 3′ UTR of *TGFBR2* gene, respectively. Further, the strength of interaction between the target site on *TGFBR2* for miR-21-5p as evaluated on the basis of ΔG value and total score value was−18.70 kCal/Mol and 152, respectively. The parameters of the interaction for the miR-484 and its target site at 3′ UTR of

FIGURE 8 | Construction of wild type and mutant type sequences flanking the miRNA target sequence. 3'UTR target site of *TGFBR2* gene was retrieved from NCBI **(a)** and analyzed in miRanda **(b1,b2)**. The complementary binding (in red), ΔG value (−18.70 and−18.16) and total score value (152 and 148) indicated the strength of interaction between miR-21-5p and *TGFBR2* (329-349 3'UTR), and miR-484 and *TGFBR2* (613-634 3'UTR) respectively **(b1, c1, b2, c2)**. While wild type oligonucleotide (62 bp) was constructed from 3'UTR of *TGFBR2* mRNA flanking the miRNA target site **(d1, d2)**, the mutant was created by replacing the target site either with poly A or poly T sequence (red) **(e1, e2)**.

TGFBR2 were−18.16 kCal/Mol and 148 (**Figure 8**). The wild-type and mutated type target sequences of *TGFBR2* were cloned into XbaI site of the vector pGL4.13. The transfection results showed complementary binding between miRNA mimics and their specific target sites expressed in the form of decreased expression of the luciferase gene in case of wild-type construct and increased expression in case of mutant type (**Figure 9**). The overview of abstract form of results is given in **Data Sheet 1**.

DISCUSSION

In an attempt to explore the role of microRNAs in modulating the host immune response against PPRV infection**,** we studied the differential expression of miRNAs in PPRV infected PBMCs, evaluated the influence of these DEmiRNAs on immune response processes from the proteomics data and functionally validated two miRNAs through Dual-Luciferase Reporter Assay.

The miRNA-seq data was analyzed in CLC genomics[3] The analysis tools in CLC Genomics Workbench are designed to facilitate trimming of reads, and counting and annotation of the resulting tags using miRBase in general and microRNA of reference organism in particular. Functional analyses of miRNAs or miRNA high-throughput datasets commonly use the Gene Ontology annotations associated with the genes or gene products that the miRNAs are predicted to regulate. Therefore, it is critical to identify targets for understanding their biological function and molecular mechanism (62). TargetScan, an online tool allows the user to extract target genes against broadly conserved or poorly conserved miRNA families across several species or target miRNAs against a particular gene. Thus, it is imperative to identify proteins that are regulated by miRNAs.

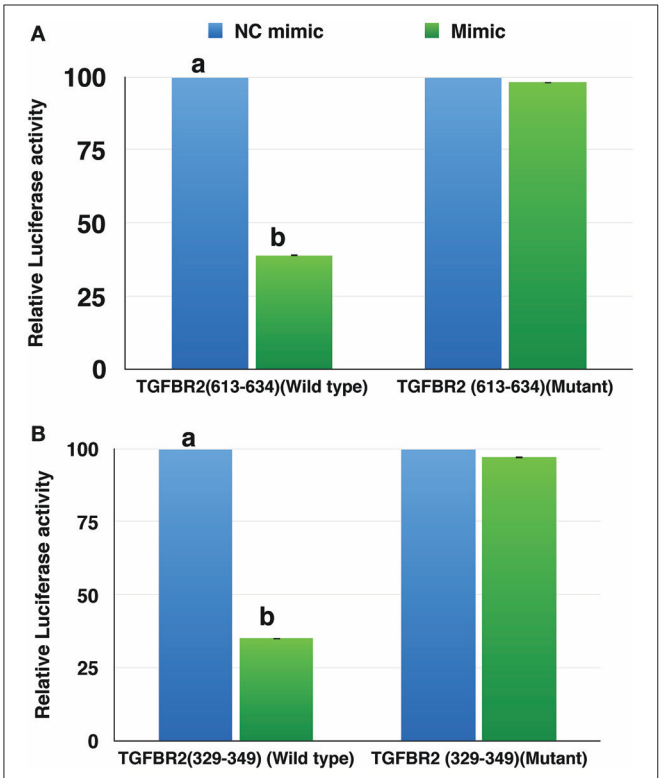

FIGURE 9 | Relative luciferase activity in wild type and mutant of *TGFBR2* gene. The decrease in luciferase activity in the wild type indicated specific binding of miR-484 **(A)** and miR-21-5p **(B)** to their target site. Student's *t*-test was done in JMP9 (SAS Institute Inc, Cary, USA) to test the significance of difference and differences between groups were considered significant at $P \leq 0.05$.

[3]https://www.qiagenbioinformatics.com/products/clc-genomics-workbench/.

The miRNA-protein network analysis suggests that one miRNA could participate in several biological processes by targeting different mRNAs, and one biological process could be influenced by multiple miRNAs (2). The DEmiRNAs identified were found to govern 98 genes that regulate several immune response pathways. miR-664, miR-2311, miR-484, miR-2440, miR-574, miR-210, miR-21-5p, miR-2897, miR-3533, and miR-30 were the top 10 miRNAs governing the immune response processes. miR-664 has been demonstrated to be upregulated during influenza A infection of A549 cells and was found to have proviral activity (63). Similarly, overexpression of miR-484 has been found to inhibit Dengue viral infection *in-vitro* (64). These miRNAs—miR-664 and miR-484 were found to be upregulated in our study indicating their possible role in the immune response in PPRV infected PBMCs. miR-210 has been reported to inhibit apoptosis (65). This miR-210 was downregulated in PPRV infected PBMCs thus promoting apoptosis in animals that succumbed to the disease. PPRV has been reported to cause apoptosis in PBMCs (66)**.** miR-21-5p has been found to decrease the sensitivity of the cell to the antiviral activity of IFNs, decrease the production of the Th1 cytokine IFN γ and inactivate the T-cell (67), thus facilitating viral replication. In our previous study, IFN γ has been found to increase in PBMCs infected with PPRV infection (35)**.** So, the downregulation of miR-21-5p could be a contributing factor for the increase in IFN γ level during PPRV infection. miR-30b plays an inhibitory role in antigen processing and presentation by primary macrophages and dendritic cells (68) and suppresses TLR/MyD88 activation and cytokine expression in THP-1 cells during MTB H37Rv infection (69). The downregulation of miR-21-5p and miR-30 in our study is indicative of strong host response to PPRV infection.

To investigate the role of immune regulating DEmiRNAs in regulating immune response genes in goat, we choose to confirm the binding between miRNAs and a common gene to evaluate the effect of the interaction. Here, we selected miR-21-5p for functional validation vis-à-vis *TGFBR2* as a target gene. *TGFBR2* along with TGFBR1 transduces signals of cytokines like TGFB1, TGFB2, and TGFB3 from the cell surface to cytoplasm (70). TGFB signaling pathway plays an important role not only in tissue development and morphogenesis (71, 72) but also in wound healing (73). In this study, *TGFBR2* was found to be regulated by 21 identified DEmiRNAs including most of the top 10 immune regulating miRNAs. We identified *TGFBR2* to be connected to various development processes

like lung morphogenesis and cardiovascular system in GO analysis, suggesting its role in restoring host physiology under PPRV infection. Further, the development, differentiation, and tolerance of T cells and homeostasis of T and B cells are regulated separately by TGFB signaling pathway and Wnt signaling pathway (74–76). Activin receptor signaling pathway shares the SMAD proteins with TGFB signaling pathway (77, 78) and plays a crucial role in inflammation (79). The involvement of *TGFBR2* in TGFB signaling pathway and its direct association with Activin receptor signaling pathway and indirect association with Wnt signaling pathway, as predicted in the GO analysis in this study, highlights how TGFBR2 regulates immune response under PPRV infection. Moreover, miR-484 was selected at random from the top 10 immune regulating DEmiRNAs for functional validation against *TGFBR2* to provide further evidence of interaction between miRs and genes.

Genetic reporter systems provide efficient means of studying the regulation of eukaryotic gene expression by exploiting the "biochemical requirements" for luminescence of reporter molecules (80). In Dual Luciferase Reporter (DLR) Assay, the target sites of the *TGFBR2* for miR-21-5p and for miR-484 were cloned into pGL4.13 vector having luciferase reporter. The interaction between the target mRNA and the specific miRNA mimic lead to an inevitable knockdown in expression of the target mRNA. The ligation of the target site (3'UTR) of *TGFBR2* to the luciferase reporter gene in the vector pGL4.13 prevent the luciferase gene from getting translated whenever miRNA-21-5p and miR-484 mimics were cotransfected with the vector. Hence, the significant reduction in expression of luciferase activity in wild-type *TGFBR2* in comparison to mutant type *TGFBR2* was observed.

In this study, we identified miRNAs that are instrumental in regulating immune response to PPRV infection following integrative analysis of miRNA-seq data and proteome profiling data.

AUTHOR CONTRIBUTIONS

RS, BPM, and RG conceived and designed the research. KR and DM performed the vaccine potency experiment. YS and RG maintained the server for analysis. AK, ARS, SW, and SS conducted the wet lab work. AK, ARS, RK, AP, and RG analyzed the data. RK, WM, RG, APS, PM, and BM helped in manuscript drafting and editing. RS, BPM, and RG proofread the manuscript.

ACKNOWLEDGMENTS

This study was supported in part by Centre for Agricultural Bioinformatics (ICAR-IASRI) and SubDIC (BTISnet), ICAR-IVRI. We also thank Department of Biotechnology for providing fellowship and contingency for students - Amit Ranjan Sahu (DBT Fellow No. DBT/2014/IVRI/170) and Raja Ishaq Nabi Khan (DBT Fellow No. DBT/2017/IVRI/768).

SUPPLEMENTARY MATERIAL

The Supplementary Material for this article can be found online at: https://www.frontiersin.org/articles/10.3389/fimmu.2018.02631/full#supplementary-material

Table S1 | Summary of miRNA sequencing data.

Table S2 | Proteome data.

Table S3 | Gene Symbol of proteins identified in GO terms pertinent to immune response.

Table S4 | Total immune response genes governed by various upregulated miRNAs.

Table S5 | Total immune response genes governed by various downregulated miRNAs.

Table S6 | Comaprsion of DEmiRNA from PPRV infected PBMCs with DEmiRNA from PPRV infected lung and spleen.

Table S7 | DEmiRNAs that regulates the expression of *TGFBR2*.

Data Sheet 1 | Overview of results.

REFERENCES

1. Sevignani C, Calin GA, Siracusa LD, Croce CM. Mammalian microRNAs: a small world for fine-tuning gene expression. *Mamm Genome* (2006) 17:189–202. doi: 10.1007/s00335-005-0066-3
2. Bartel DP. MicroRNAs: genomics, biogenesis, mechanism, and function. *Cell* (2004) 116:281–97. doi: 10.1016/S0092-8674(04)00045-5
3. Sahu AR. Host-virus interaction: role of miRNA and bioinformatics tools for miRNA target prediction. *Adv Animal Vet Sci.* (2015) 3:30–6. doi: 10.14737/journal.aavs/2015/3.4s.30.36
4. Ambros V. The functions of animal microRNAs Nature 431: 350–355. *Proc Natl Acad Sci USA*. (2004) 103:3687–92. doi: 10.1038/nature02871
5. Rodriguez A, Vigorito E, Clare S, Warren MV, Couttet P, Soond DR, et al. Requirement of bic/microRNA-155 for normal immune function. *Science* (2007) 316:608–11. doi: 10.1126/science.1139253
6. Thai T-H, Calado DP, Casola S, Ansel KM, Xiao C, Xue Y, et al. Regulation of the germinal center response by microRNA-155. *Science* (2007) 316:604–8. doi: 10.1126/science.1141229
7. Johnnidis JB, Harris MH, Wheeler RT, Stehling-Sun S, Lam MH, Kirak O, et al. Regulation of progenitor cell proliferation and granulocyte function by microRNA-223. *Nature* (2008) 451:1125–9. doi: 10.1038/nature06607
8. Roberts AP, Lewis AP, Jopling CL. miR-122 activates hepatitis C virus translation by a specialized mechanism requiring particular RNA components. *Nucleic Acids Res.* (2011) 39:7716–29. doi: 10.1093/nar/gkr426
9. Tay Y, Zhang J, Thomson AM, Lim B, Rigoutsos I. MicroRNAs to Nanog, Oct4 and Sox2 coding regions modulate embryonic stem cell differentiation. *Nature* (2008) 455:1124–8. doi: 10.1038/nature07299
10. Guo XK, Zhang Q, Gao L, Li N, Chen XX, Feng WH. Increasing expression of microRNA 181 inhibits porcine reproductive and respiratory syndrome virus replication and has implications for controlling virus infection. *J Virol.* (2013) 87:1159–71. doi: 10.1128/JVI.02386-12
11. Li S, Duan X, Li Y, Liu B, McGilvray I, Chen L. MicroRNA-130a inhibits HCV replication by restoring the innate immune response. *J Viral Hepat.* (2014) 21:121–8. doi: 10.1111/jvh.12131
12. Mizuguchi Y, Takizawa T, Uchida E. Host cellular microRNA involvement in the control of hepatitis B virus gene expression and replication. *World J Hepatol.* (2015) 7:696–702. doi: 10.4254/wjh.v7.i4.696
13. Grassmann R, Jeang KT. The roles of microRNAs in mammalian virus infection. *Biochim Biophys Acta* (2008) 1779:706–11. doi: 10.1016/j.bbagrm.2008.05.005

14. Scaria V, Hariharan M, Maiti S, Pillai B, Brahmachari SK. Host-virus interaction: a new role for microRNAs. *Retrovirology* (2006) 3:68. doi: 10.1186/1742-4690-3-68
15. Skalsky RL, Cullen BR. Viruses, microRNAs, and host interactions. *Annu Rev Microbiol.* (2010) 64:123–41. doi: 10.1146/annurev.micro.112408.134243
16. Chang J, Guo JT, Jiang D, Guo H, Taylor JM, Block TM. Liver-specific microRNA miR-122 enhances the replication of hepatitis C virus in nonhepatic cells. *J Virol.* (2008) 82:8215–23. doi: 10.1128/JVI.02575-07
17. Trobaugh DW, Gardner CL, Sun C, Haddow AD, Wang E, Chapnik E, et al. RNA viruses can hijack vertebrate microRNAs to suppress innate immunity. *Nature* (2014) 506:245–8. doi: 10.1038/nature12869
18. Roberts AP, Lewis AP, Jopling CL. The role of microRNAs in viral infection. *Progr Molecul Biol Transl Sci.* (2011). 102.101–39. doi: 10.1016/B978-0-12-415795-8.00002-7
19. Cui L, Guo X, Qi Y, Qi X, Ge Y, Shi Z, et al. Identification of microRNAs involved in the host response to enterovirus 71 infection by a deep sequencing approach. *J Biomed Biotechnol.* (2010) 2010:425939. doi: 10.1155/2010/425939
20. Wang Y, Brahmakshatriya V, Zhu H, Lupiani B, Reddy SM, Yoon BJ, et al. Identification of differentially expressed miRNAs in chicken lung and trachea with avian influenza virus infection by a deep sequencing approach. *BMC Genomics* (2009) 10:512. doi: 10.1186/1471-2164-10-512
21. Pandey A, Sahu AR, Wani SA, Saxena S, Kanchan S, Sah V, et al. Modulation of Host miRNAs transcriptome in lung and spleen of peste des petits ruminants virus infected sheep and goats. *Front Microbiol.* (2017) 8:1146. doi: 10.3389/fmicb.2017.01146
22. Patel A, Rajak KK, Balamurugan V, Sen A, Sudhakar SB, Bhanuprakash V, et al. Cytokines expression profile and kinetics of Peste des petits ruminants virus antigen and antibody in infected and vaccinated goats. *Virologica Sinica* (2012) 27:265–71. doi: 10.1007/s12250-012-3240-2
23. Kumari B, Jain P, Das S, Ghosal S, Hazra B, Trivedi AC, et al. Dynamic changes in global microRNAome and transcriptome reveal complex miRNA-mRNA regulated host response to Japanese Encephalitis Virus in microglial cells. *Sci Rep.* (2016) 6:20263. doi: 10.1038/srep20263
24. Lefèvre P-C, Diallo A. Peste des petits ruminants. *Rev Sci Tech.* (1990) 9:935–81.
25. Nanda Y, Chatterjee A, Purohit A, Diallo A, Innui K, Sharma R, et al. The isolation of peste des petits ruminants virus from Northern India. *Vet Microbiol.* (1996) 51:207–16.
26. Dhar P, Sreenivasa B, Barrett T, Corteyn M, Singh R, Bandyopadhyay S. Recent epidemiology of peste des petits ruminants virus (PPRV). *Vet Microbiol.* (2002) 88:153–9. doi: 10.1016/S0378-1135(02)00102-5
27. Singh R, Saravanan P, Sreenivasa B, Singh R, Bandyopadhyay S. Prevalence and distribution of peste des petits ruminants virus infection in small ruminants in India. *Rev Sci Tech.* (2004) 23:807–19. doi: 10.20506/rst.23.3.1522
28. Delil F, Asfaw Y, Gebreegziabher B. Prevalence of antibodies to peste des petits ruminants virus before and during outbreaks of the disease in Awash Fentale district, Afar, Ethiopia. *Trop Anim Health Produc.* (2012) 44:1329–30. doi: 10.1007/s11250-012-0110-8
29. Truong T, Boshra H, Embury-Hyatt C, Nfon C, Gerdts V, Tikoo S, et al. Peste des petits ruminants virus tissue tropism and pathogenesis in sheep and goats following experimental infection. *PLoS ONE* (2014) 9:e87145. doi: 10.1371/journal.pone.0087145
30. Raghavendra A, Gajendragad M, Sengupta P, Patil S, Tiwari C, Balumahendiran M, et al. Seroepidemiology of peste des petits ruminants in sheep and goats of southern peninsular India. *Revue Sci et Tech.* (2008) 27:861. doi: 10.1007%2Fs13337-013-0177-5
31. Maganga GD, Verrier D, Zerbinati RM, Drosten C, Drexler JF, Leroy EM. Molecular typing of PPRV strains detected during an outbreak in sheep and goats in south-eastern Gabon in 2011. *Virol J.* (2013) 10:82. doi: 10.1186/1743-422X-10-82
32. Manjunath S, Mishra BP, Mishra B, Sahoo AP, Tiwari AK, Rajak KK, et al. Comparative and temporal transcriptome analysis of peste des petits ruminants virus infected goat peripheral blood mononuclear cells. *Virus Res.* (2017) 229:28–40. doi: 10.1016/j.virusres.2016.12.014
33. Manjunath S, Kumar GR, Mishra BP, Mishra B, Sahoo AP, Joshi CG, et al. Genomic analysis of host - Peste des petits ruminants vaccine viral transcriptome uncovers transcription factors modulating immune regulatory pathways. *Vet Res.* (2015) 46:15. doi: 10.1186/s13567-015-0153-8
34. Pope RA, Parida S, Bailey D, Brownlie J, Barrett T, Banyard AC. Early events following experimental infection with peste-des-petits ruminants virus suggest immune cell targeting. *PLoS ONE* (2013) 8:e55830. doi: 10.1371/journal.pone.0055830
35. Wani SA, Sahu AR, Saxena S, Rajak KK, Saminathan M, Sahoo AP, et al. Expression kinetics of ISG15, IRF3, IFNγ, IL10, IL2 and IL4 genes vis-a-vis virus shedding, tissue tropism and antibody dynamics in PPRV vaccinated, challenged, infected sheep and goats. *Microb Pathog.* (2018) 117:206–18. doi: 10.1016/j.micpath.2018.02.027
36. Sahu AR, Wani SA, Saminathan M, Rajak KK, Sahoo AP, Pandey A, et al. Genome sequencing of an Indian peste des petits ruminants virus isolate, Izatnagar/94, and its implications for virus diversity, divergence and phylogeography. *Arch Virol.* (2017) 162:1677–93. doi: 10.1007/s00705-017-3288-2
37. Kukurba KR, Montgomery SB. RNA Sequencing and Analysis. *Cold Spring Harb Protoc.* (2015) 2015:951–69. doi: 10.1101/pdb.top084970
38. Robin JD, Ludlow AT, LaRanger R, Wright WE, Shay JW. Comparison of DNA quantification methods for next generation sequencing. *Sci Rep.* (2016) 6:24067. doi: 10.1038/srep24067
39. Agarwal V, Bell GW, Nam JW, Bartel DP. Predicting effective microRNA target sites in mammalian mRNAs. *Elife* (2015) 12:4. doi: 10.7554/eLife.05005
40. Bindea G, Mlecnik B, Hackl H, Charoentong P, Tosolini M, Kirilovsky A, et al. ClueGO: a Cytoscape plug-in to decipher functionally grouped gene ontology and pathway annotation networks. *Bioinformatics* (2009) 25:1091–3. doi: 10.1093/bioinformatics/btp101
41. Shannon P, Markiel A, Ozier O, Baliga NS, Wang JT, Ramage D, et al. Cytoscape: a software environment for integrated models of biomolecular interaction networks. *Genome Res.* (2003) 13:2498–504. doi: 10.1101/gr.1239303
42. Schmittgen TD, Livak KJ. Analyzing real-time PCR data by the comparative C T method. *Nature Protoc.* (2008) 3:1101. doi: 10.1038/nprot.2008.73
43. Enright AJ, John B, Gaul U, Tuschl T, Sander C, Marks DS. MicroRNA targets in *Drosophila*. *Genome Biol.* (2003) 5:R1. doi: 10.1186/gb-2003-5-1-r1
44. Jin Y, Chen Z, Liu X, Zhou X. Evaluating the microRNA targeting sites by luciferase reporter gene assay. *Methods Mol Biol.* (2013) 936:117–27. doi: 10.1007/978-1-62703-083-0_10
45. Mandel S, Rechavi G, Gozes I. Activity-dependent neuroprotective protein (ADNP) differentially interacts with chromatin to regulate genes essential for embryogenesis. *Dev Biol.* (2007) 303:814–24. doi: 10.1016/j.ydbio.2006.11.039
46. Nazarko TY, Ozeki K, Till A, Ramakrishnan G, Lotfi P, Yan M, et al. Peroxisomal Atg37 binds Atg30 or palmitoyl-CoA to regulate phagophore formation during pexophagy. *J Cell Biol.* (2014) 204:541–57. doi: 10.1083/jcb.201307050
47. Punzo F, Mientjes E, Rohe C, Scianguetta S, Amendola G, Oostra B, et al. A mutation in the acyl-coenzyme A binding domain-containing protein 5 gene (ACBD5) identified in autosomal dominant thrombocytopenia. *J Thrombosis Haemostasis* (2010) 8:2085–7. doi: 10.1111/j.1538-7836.2010.03979.x
48. Safaee M, Clark AJ, Ivan ME, Oh MC, Bloch O, Sun MZ, et al. CD97 is a multifunctional leukocyte receptor with distinct roles in human cancers. *Intl J Oncol.* (2013) 43:1343–50. doi: 10.3892/ijo.2013.2075
49. Leemans JC, te Velde AA, Florquin S, Bennink RJ, de Bruin K, van Lier RA, et al. The epidermal growth factor-seven transmembrane (EGF-TM7) receptor CD97 is required for neutrophil migration and host defense. *J Immunol.* (2004) 172:1125–31. doi: 10.4049/jimmunol.172.2.1125
50. Shimoyama Y, Gotoh M, Terasaki T, Kitajima M, Hirohashi S. Isolation and sequence analysis of human cadherin-6 complementary DNA for the full coding sequence and its expression in human carcinoma cells. *Cancer Res.* (1995) 55:2206–11.
51. Yang Y, Jin Y, Martyn AC, Lin P, Song Y, Chen F, et al. Expression pattern implicates a potential role for LRF in the process of implantation in uteri and development of preimplantation embryos in mice. *J Reprod Dev.* (2012) 59:245–51. doi: 10.1262%2Fjrd.2012-137
52. Audas TE, Hardy-Smith PW, Penney J, Taylor T, Lu R. Characterization of nuclear foci-targeting of Luman/CREB3 recruitment factor (LRF/CREBRF) and its potential role in inhibition of herpes simplex virus-1 replication. *Eur J Cell Biol.* (2016) 95:611–22. doi: 10.1016/j.ejcb.2016.10.006

53. Theron AJ, Steel HC, Tintinger GR, Gravett CM, Anderson R, Feldman C. Cysteinyl leukotriene receptor-1 antagonists as modulators of innate immune cell function. *J Immunol Res.* (2014) 2014:608930. doi: 10.1155/2014/608930
54. Qiu X-B, Shao Y-M, Miao S, Wang L. The diversity of the DnaJ/Hsp40 family, the crucial partners for Hsp70 chaperones. *Cell Molecul Life Sci.* (2006) 63:2560–70. doi: 10.1007/s00018-006-6192-6
55. Abbas T, Mueller AC, Shibata E, Keaton M, Rossi M, Dutta A. CRL1-FBXO11 promotes Cdt2 ubiquitylation and degradation and regulates Pr-Set7/Set8-mediated cellular migration. *Molecul Cell* (2013) 49:1147–58. doi: 10.1016/j.molcel.2013.02.003
56. Curtin JF, Cotter TG. JNK regulates HIPK3 expression and promotes resistance to Fas-mediated apoptosis in DU 145 prostate carcinoma cells. *J Biol Chem.* (2004) 279:17090–100. doi: 10.1074/jbc.M307629200
57. Le Friec G, Sheppard D, Whiteman P, Karsten CM, Shamoun SA-T, Laing A, et al. The CD46-Jagged1 interaction is critical for human T H 1 immunity. *Nat Immunol.* (2012) 13:1213. doi: 10.1038/ni.2454
58. Newman DM, Sakaguchi S, Lun A, Preston S, Pellegrini M, Khamina K, et al. Acetylation of the Cd8 locus by KAT6A determines memory T cell diversity. *Cell Rep.* (2016) 16:3311–21. doi: 10.1016/j.celrep.2016.08.056
59. Brdicka T, Pavlistová D, Leo A, Bruyns E, Korínek V, Angelisová P, et al. Phosphoprotein associated with glycosphingolipid-enriched microdomains (PAG), a novel ubiquitously expressed transmembrane adaptor protein, binds the protein tyrosine kinase csk and is involved in regulation of T cell activation. *J Exp Med.* (2000) 191:1591–604. doi: 10.1084/jem.191.9.1591
60. Faust TB, Li Y, Jang GM, Johnson JR, Yang S, Weiss A, et al. PJA2 ubiquitinates the HIV-1 Tat protein with atypical chain linkages to activate viral transcription. *Sci Rep.* (2017) 7:45394. doi: 10.1038/srep45394
61. Pati D, Zhang N, Plon SE. Linking sister chromatid cohesion and apoptosis: role of Rad21. *Molecul Cell Biol.* (2002) 22:8267–77. doi: 10.1128%2FMCB.22.23.8267-8277.2002
62. Tang Z, Yang Y, Wang Z, Zhao S, Mu Y, Li K. Integrated analysis of miRNA and mRNA paired expression profiling of prenatal skeletal muscle development in three genotype pigs. *Sci Rep.* (2015) 5:15544. doi: 10.1038/srep15544
63. Wolf S, Wu W, Jones C, Perwitasari O, Mahalingam S, Tripp RA. MicroRNA regulation of human genes essential for influenza A (H7N9) replication. *PLoS ONE* (2016) 11:e0155104. doi: 10.1371/journal.pone.0155104
64. Castrillón-Betancur JC, Urcuqui-Inchima S. Overexpression of miR-484 and miR-744 in Vero cells alters Dengue virus replication. *Memórias do Instituto Oswaldo Cruz* (2017) 112:281–91. doi: 10.1590%2F0074-02760160404
65. Hu S, Huang M, Li Z, Jia F, Ghosh Z, Lijkwan MA, et al. MicroRNA-210 as a novel therapy for treatment of ischemic heart disease. *Circulation* (2010) 122(Suppl. 11):S124–31. doi: 10.1161/CIRCULATIONAHA.109.928424
66. Mondal B, Sreenivasa B, Dhar P, Singh R, Bandyopadhyay S. Apoptosis induced by peste des petits ruminants virus in goat peripheral blood mononuclear cells. *Virus Res.* (2001) 73:113–9. doi: 10.1016/S0168-1702(00)00214-8
67. Yang CH, Li K, Pfeffer SR, Pfeffer LM. The type I IFN-induced miRNA, miR-21. *Pharmaceuticals* (2015) 8:836–47. doi: 10.3390%2Fph8040836
68. Naqvi AR, Fordham JB, Ganesh B, Nares S. miR-24, miR-30b and miR-142-3p interfere with antigen processing and presentation by primary macrophages and dendritic cells. *Sci Rep.* (2016) 6:32925. doi: 10.1038%2Fsrep32925
69. Wu Y, Sun Q, Dai L. Immune regulation of miR-30 on the Mycobacterium tuberculosis-induced TLR/MyD88 signaling pathway in THP-1 cells. *Exp Therapeutic Med.* (2017) 14:3299–303. doi: 10.3892/etm.2017.4872
70. Wieser R, Wrana J, Massague J. GS domain mutations that constitutively activate T beta R-I, the downstream signaling component in the TGF-beta receptor complex. *EMBO J.* (1995) 14:2199–208. doi: 10.1002/j.1460-2075.1995.tb07214.x
71. Ogata S, Morokuma J, Hayata T, Kolle G, Niehrs C, Ueno N, et al. TGF-β signaling-mediated morphogenesis: modulation of cell adhesion via cadherin endocytosis. *Genes Dev.* (2007) 21:1817–31. doi: 10.1101/gad.1541807
72. Buschke S, Stark H-J, Cerezo A, Prätzel-Wunder S, Boehnke K, Kollar J, et al. A decisive function of transforming growth factor-β/Smad signaling in tissue morphogenesis and differentiation of human HaCaT keratinocytes. *Molecul Biol Cell* (2011) 22:782–94. doi: 10.1091/mbc.E10-11-0879
73. Finnson KW, McLean S, Di Guglielmo GM, Philip A. Dynamics of transforming growth factor beta signaling in wound healing and scarring. *Adv Wound Care* (2013) 2:195–214. doi: 10.1089/wound.2013.0429
74. Spender L, O'Brien D, Simpson D, Dutt D, Gregory C, Allday M, et al. TGF-β induces apoptosis in human B cells by transcriptional regulation of BIK and BCL-X L. *Cell Death Diff.* (2009) 16:593. doi: 10.1038/cdd.2008.183
75. Roes J, Choi BK, Cazac BB. Redirection of B cell responsiveness by transforming growth factor β receptor. *Proc Natl Acad Sci. USA.* (2003) 100:7241–6. doi: 10.1073/pnas.0731875100
76. Reya T, O'Riordan M, Okamura R, Devaney E, Willert K, Nusse R, et al. Wnt signaling regulates B lymphocyte proliferation through a LEF-1 dependent mechanism. *Immunity* (2000) 13:15–24. doi: 10.1016/S1074-7613(00)00004-2
77. Lebrun J-J, Takabe K, Chen Y, Vale W. Roles of pathway-specific and inhibitory Smads in activin receptor signaling. *Molecul Endocrinol.* (1999) 13:15–23.
78. Deacu E, Mori Y, Sato F, Yin J, Olaru A, Sterian A, et al. Activin type II receptor restoration in ACVR2-deficient colon cancer cells induces transforming growth factor-β response pathway genes. *Cancer Res.* (2004) 64:7690–6. doi: 10.1158/0008-5472.CAN-04-2082
79. Palin NK, Savikko J, Pasternack A, Rintala JM, Kalra B, Mistry S, et al. Activin inhibition limits early innate immune response in rat kidney allografts-a pilot study. *Transpl Int.* (2017) 30:96–107. doi: 10.1111/tri.12876
80. McNabb DS, Reed R, Marciniak RA. Dual luciferase assay system for rapid assessment of gene expression in Saccharomyces cerevisiae. *Eukaryotic Cell* (2005) 4:1539–49. doi: 10.1128/EC.4.9.1539-1549.2005

Conflict of Interest Statement: The authors declare that the research was conducted in the absence of any commercial or financial relationships that could be construed as a potential conflict of interest.

Copyright © 2018 Khanduri, Sahu, Wani, Khan, Pandey, Saxena, Malla, Mondal, Rajak, Muthuchelvan, Mishra, Sahoo, Singh, Singh, Gandham and Mishra. This is an open-access article distributed under the terms of the Creative Commons Attribution License (CC BY). The use, distribution or reproduction in other forums is permitted, provided the original author(s) and the copyright owner(s) are credited and that the original publication in this journal is cited, in accordance with accepted academic practice. No use, distribution or reproduction is permitted which does not comply with these terms.

frontiers in Microbiology

REVIEW
published: 08 January 2019
doi: 10.3389/fmicb.2018.03228

IFITM Genes, Variants, and Their Roles in the Control and Pathogenesis of Viral Infections

*Xuesen Zhao[1,2], Jiarui Li[1,2], Cheryl A. Winkler[3], Ping An[3] and Ju-Tao Guo[4]**

[1] Institute of Infectious Disease, Beijing Ditan Hospital, Capital Medical University, Beijing, China, [2] Beijing Key Laboratory of Emerging Infectious Disease, Beijing, China, [3] Basic Research Laboratory, Frederick National Laboratory for Cancer Research, National Cancer Institute, Leidos Biomedical Research, Inc., Frederick, MD, United States, [4] Baruch S. Blumberg Institute, Hepatitis B Foundation, Doylestown, PA, United States

Interferon-induced transmembrane proteins (IFITMs) are a family of small proteins that localize in the plasma and endolysosomal membranes. IFITMs not only inhibit viral entry into host cells by interrupting the membrane fusion between viral envelope and cellular membranes, but also reduce the production of infectious virions or infectivity of progeny virions. Not surprisingly, some viruses can evade the restriction of IFITMs and even hijack the antiviral proteins to facilitate their infectious entry into host cells or promote the assembly of virions, presumably by modulating membrane fusion. Similar to many other host defense genes that evolve under the selective pressure of microorganism infection, IFITM genes evolved in an accelerated speed in vertebrates and many single-nucleotide polymorphisms (SNPs) have been identified in the human population, some of which have been associated with severity and prognosis of viral infection (e.g., influenza A virus). Here, we review the function and potential impact of genetic variation for IFITM restriction of viral infections. Continuing research efforts are required to decipher the molecular mechanism underlying the complicated interaction among IFITMs and viruses in an effort to determine their pathobiological roles in the context of viral infections *in vivo*.

Keywords: host susceptibility, interferon-induced transmembrane proteins, IFITM, single nucleotide polymorphisms, viral infection

OPEN ACCESS

Edited by:
Jianrong Li,
The Ohio State University,
United States

Reviewed by:
Arnaud Moris,
Center for the National Scientific Research (CNRS), France
Shitao Li,
Oklahoma State University,
United States

***Correspondence:**
Ju-Tao Guo
ju-tao.guo@bblumberg.org

Specialty section:
This article was submitted to Virology, a section of the journal Frontiers in Microbiology

Received: *08 October 2018*
Accepted: *12 December 2018*
Published: *08 January 2019*

Citation:
Zhao X, Li J, Winkler CA, An P and Guo J-T (2019) IFITM Genes, Variants, and Their Roles in the Control and Pathogenesis of Viral Infections. Front. Microbiol. 9:3228. doi: 10.3389/fmicb.2018.03228

Interferon-induced transmembrane proteins (IFITMs) are a family of small proteins that can be found in single cell organisms and are evolutionally conserved across vertebrates (Siegrist et al., 2011; Zhang et al., 2012). The human IFITM family comprises five members, including immune-related IFITM1, IFITM2, and IFITM3, as well as IFITM5 and IFITM10 with no known role in immunity. As key host defense genes, IFITMs evolved under the selective pressure of microorganism infection (Compton et al., 2016). IFITM proteins are involved in many aspects of virus–host interaction and play important roles in viral pathogenesis. Among the number of single-nucleotide polymorphisms (SNPs) in *IFITM3* gene that have been identified in human populations, several are associated with disease severity and prognosis of influenza A virus (IAV) and other viral infections (Everitt et al., 2012; Zhang et al., 2015; Xu-Yang et al., 2016; Allen et al., 2017). Mechanistically, these SNPs either alter the expression of IFITM3 or result in expression of N-terminally truncated IFITM3 isoform, Δ21-IFITM3, with reduced antiviral activity against different viruses (Everitt et al., 2012; Allen et al., 2017). In this review, we will summarize the findings on human IFITM structural features related with antiviral activity, and impact of genetic variation on IFITM antiviral function in the control and pathogenesis of viral infections in humans.

IFITMS RESTRICT A BROAD SPECTRUM OF VIRUSES IN CULTURED CELLS AND *IN VIVO*

To date, IFITMs have been shown to inhibit the infection of enveloped RNA viruses from 9 viral families (Perreira et al., 2013), non-enveloped RNA viruses, e.g., reovirus (Anafu et al., 2013) and foot-and-mouth disease virus (Xu et al., 2014), and several DNA viruses (Li et al., 2018). IFITMs efficiently inhibit a number of medically important human pathogenic viruses, including IAV (Brass et al., 2009; Bailey et al., 2012), dengue virus (DENV) (Brass et al., 2009; Jiang et al., 2010), West Nile virus (WNV) (Brass et al., 2009; Jiang et al., 2010), Zika Virus (ZIKV) (Savidis et al., 2016), Ebola virus (EBOV) (Huang et al., 2011; Wrensch et al., 2015), Marburg virus (MARV) (Huang et al., 2011), severe acute respiratory syndrome coronavirus (SARS-CoV) (Huang et al., 2011), Rift Valley fever virus (RVFV) (Mudhasani et al., 2013), Hantaan virus (HTNV) (Mudhasani et al., 2013; Xu-Yang et al., 2016), hepatitis C virus (HCV) (Wilkins et al., 2013), and human immunodeficiency virus (HIV) (Lu et al., 2011; Compton et al., 2014; Yu et al., 2015; Compton et al., 2016; Foster et al., 2016; Chesarino et al., 2017; Tartour et al., 2017; Wang et al., 2017). *In vivo* studies in *IFITM3* knockout mice demonstrate the critical role of IFITM3 in restricting infection and reducing disease severity of infection by IAV (Bailey et al., 2012; Everitt et al., 2012), WNV (Gorman et al., 2016), Chikungunya virus and Venezuelan equine encephalitis virus (Poddar et al., 2016), and respiratory syncytial virus (Everitt et al., 2013). IFITM3 in mice not only protects lung epithelia cells from IAV infection, but it was also shown to restricts IAV infection of lung dendritic cells, which traffic to lymph nodes to prime $CD8^+$ T cell anti-viral response (Infusini et al., 2015). Moreover, lung resident memory $CD8^+$ T cells in mice were programmed to retain IFITM3 expression, facilitating their survival and protection from viral infection during subsequent exposures (Wakim et al., 2013).

IFITMS MAINLY RESTRICT VIRUS INFECTION AT CELL ENTRY

IFITM proteins localize at the plasma membrane as well as the membranes of endocytic vesicles and lysosomes (Bailey et al., 2014). IFITMs can also be incorporated into envelope membranes of many viruses (Yu et al., 2015; Tartour et al., 2017). Emerging evidence suggests that IFITM proteins on both viral and cellular membranes can restrict the infectious entry of diverse envelope viruses by inhibiting viral fusion at cell plasma or endolysosomal membranes, but IFITM does not impede endocytosis of virions into cells (Weidner et al., 2010; Li et al., 2013; Perreira et al., 2013; Compton et al., 2014; Desai et al., 2014). As extensively discussed in a previous review (Perreira et al., 2013), the potency of IFITM restriction of viral cell entry is generally correlated to the co-localization of IFITM proteins at the sites of viral fusion. For instance, IFITM1 more efficiently restricts the viruses that enter the cytoplasm *via* direct fusion with plasma membrane *or via Rab-5 positive early endosomes*, whereas IFITM3 more efficiently inhibits viruses that enter *via* Rab7-positive late endosomes or lysosomes. This rule is highlighted by the finding that mutation of IFITM3 endocytic signal results in its cell surface accumulation and gains a function to restrict the infection of human parainfluenza virus 3 (HPIV-3), which enters cells *via* direct fusion with the plasma membrane (Rabbani et al., 2016; Zhao et al., 2018). Another example is that the sensitivity of IAVs to IFITM3 appears to depend on the pH value at which the IAV hemagglutinin triggers membrane fusion and thus the endocytic compartments where the membrane fusion take place (Gerlach et al., 2017). However, exceptions of this rule do exist. For instance, it remains to know how Moloney leukemia virus (MLV) and Sendai virus that fuse at cell plasma membrane (Brass et al., 2009; Hach et al., 2013) as well as Lassa fever virus (LASV) and lymphocytic choriomeningitis virus (LCMV) that fuse at Rab7-positive late endosomes (Brass et al., 2009; Mudhasani et al., 2013) to escape IFITM1 and IFITM3 restriction, respectively.

The mechanism of IFITM inhibition of viral fusion and cell entry is not yet resolved. One study reported that IFITM inhibited Jaagsiekte sheep retrovirus envelope and IAV hemagglutinin fusion of viral envelope to cellular membranes prior to coalescence of lipid-bilayers, a process known as hemifusion (Li et al., 2013). However, another study using a direct virus-cell fusion assay in viable cells to investigate IAV entry found that overexpression of IFITM3 protein in late endosomes did not alter lipid mixing, but rather inhibited the release of viral contents into the cytoplasm, suggesting that IFITM3 inhibits the transition from hemifusion to full fusion of the respective lipid membranes (Desai et al., 2014). Others studies suggested that IFITM multimerization decreases membrane flexibility by altering membrane curvature, with the consequence of interruption of the virus-cell membrane fusion (John et al., 2013; Lin et al., 2013). Another group reported that IFITM expression increased cholesterol content in the endosome or lysosome *via* an interaction with vesicle-associated membrane protein-associated protein A (VAPA), which abrogated endolysosomal fusion with the viral envelop (Amini-Bavil-Olyaee et al., 2013). However, this later observation was not confirmed by other studies (Desai et al., 2014; Wrensch et al., 2014). In addition, IFITMs were reported to affect the trafficking of vacuolar ATPase (v-ATPase), implying that IFITMs may indirectly restrict viral entry by modulating endosomal acidity (Wee et al., 2012). It is also well documented that the antiviral potency of IFITM proteins varies among different cell types (Huang et al., 2011; Zhao et al., 2018), suggesting that IFITMs work together with other cellular proteins to modulate viral fusion. In support of this notion, zinc metallopeptidase STE24 (ZMPSTE24), a transmembrane metalloprotease localized in the inner nuclear membrane and cytoplasmic organelles, had been identified as a downstream partner of IFITM3 to restrict the entry of enveloped RNA and DNA viruses (Fu et al., 2017).

In addition to the protective function of IFITM proteins to reduce viral infection of host cells, IFITM proteins, particularly IFITM2 and 3, can lead to the production of virions that package IFITMs and display reduced entry into target cells (Compton et al., 2014; Tartour et al., 2014, 2017). One study found that

IFITM proteins interact with HIV envelope protein in viral producer cells to disrupt envelope protein processing and virion incorporation, which impairs virion infectivity (Yu et al., 2015); however, another found that IFITM3 expression in producing cells did not affect the amount of envelope protein incorporation into progeny HIV-1 virions (Appourchaux et al., 2018). Both studies reported that the level of IFITM protein incorporation into progeny virions does not correlate with the extent of infectivity reduction.

Moreover, recent studies have also shown that IFITMs can modulate viral infection and pathogenesis *via* mechanisms that are not directly related to the restriction of virus entry. For example, given the resistance of human papillomaviruses (HPV) to IFITMs, HPV infection of keratinocytes inhibits the expression of IFITM1 and RIPK3 to escape from IFN-γ and TNF-α-mediated antiproliferation and necroptosis, which is essential for establishing a persistent infection (Ma et al., 2016). In addition, it was demonstrated in IFITM3 knockout mice that IFITM3 limited murine CMV (MCMV) pathogenesis without directly preventing virus replication (Stacey et al., 2017). Instead, IFITM3 contributed to the antiviral cellular immunity by abrogating inflammatory cytokine-driven lymphopenia including apoptosis-independent NK cell death and T cells depletion (Stacey et al., 2017).

VIRAL COUNTERACTION FOR EVADING IFITMS

Not surprisingly, in the arms race between pathogen and host, many viruses have evolved strategies to evade the antiviral function of host restriction proteins. For instance, transmitted founder HIV-1 strains establishing *de novo* infection are generally capable of evading IFITM restriction (Foster et al., 2016; Wang et al., 2017). Mutations allow the virus to escape adaptive immune responses, and/or switches in the HIV-1 co-receptor tropism from CCR5 to CXCR4 increases viral sensitivity to inhibition by IFITM2 and IFITM3 in endosomal compartments (Foster et al., 2016). Moreover, IAV facilitates its infection by activating p53 or degrading eukaryotic translation initiation factor 4B (eIF4B) to inhibit the expression of IFITM proteins (Wang S. et al., 2014; Wang et al., 2018). In contrast, human coronavirus OC43 (HCoV-OC43) and human cytomegalovirus (HCMV) hijack IFITM3 to promote its infectious entry and progeny virions assembly, respectively (Zhao et al., 2014; Xie et al., 2015).

STRUCTURE AND POLYMORPHISM OF IFITM GENE LOCUS

The human *IFITM* locus, approximately 18kb long, is located on chromosome 11 and comprises five genes: *IFITM1*, *IFITM2*, *IFITM3*, *IFITM5,* and *IFITM10* (**Figure 1**). As an IFN-stimulated gene (ISG), *IFITM1*, *IFITM2*, *IFITM3* genes each has an interferon stimulated response element (ISRE) in its promoter region besides the additional gamma-activated sequence (GAS) in the promoter region of *IFITM1* gene (Siegrist et al., 2011). However, the protein expression of IFITM5 and IFITM10 are not induced by IFNs (Zhang et al., 2012). Though IFITM1-3 proteins are ubiquitously expressed in human tissues in the absence of IFN induction, they can be robustly up-regulated by all three types of IFNs (Zhao et al., 2014). The *IFITM3* promoter has binding sites for dozens of transcription factors, including POLR2A, MYC, ELF1, PHF8, CHD1, TAF1, REST, SIN3AK20, SIN3A, IRF1, STAT1, TBP, STAT3, STAT2, ZBTB7A, and CTCF, some of which may affect IFITM3 expression (Allen et al., 2017).

As illustrated in **Figure 1**, all *IFITM* genes contain two coding exons interspersed by one intron. Both *IFITM2* and *IFITM3* were predicated to encode a wild typed full-length form and a truncated isoform with 20/21 amino acid residues deletion from N-terminus. Most vertebrate animals have two or more IFITM genes. In many primate species, gene duplication, and divergence of *IFITM3* has been identified (Zhang et al., 2012; Compton et al., 2016). *IFITM* locus in many modern primate species contains multiple copies of *IFITM3*-like genes due to gene duplication (Compton et al., 2016). For instance, Marmoset, Macaque, and Africa Green Monkey (AGM) each has five, six and eight copies of *IFITM3 genes*, respectively (Compton et al., 2016). Comparative genomics studies indicate that *IFITM3* is the most ancient member in the *IFITM* family and *IFITM2* emerges as a rather recent genetic event in human, chimpanzee, and gorilla (Compton et al., 2016). The multiplicity and diversity of *IFITM2/3* indicates that there is a positive selection in *IFITM* evolution, which is consistent with their role in restricting pathogen invasion (Compton et al., 2016).

STRUCTURAL FUNCTION RELATIONSHIP OF IFITM PROTEINS

IFITM proteins have several topologies that may affect their function. As shown in **Figure 2A**, although IFITM3 may adopt three different membrane topologies (Bailey et al., 2014), it exists predominantly as a type II transmembrane protein with the N-terminus in cytosol and the short C-terminus exposed to cellular exterior or in the lumen of endolysosome (Bailey et al., 2013). Although IFITM1 was also reported to predominately adopt a type II transmembrane topology, other membrane topologies may exist (**Figure 2B**; Li et al., 2015).

As depicted in **Figure 3**, IFITMs consist of intramembrane (IMD) and transmembrane (TMD) domains separated by an intracellular loop (CIL) and variable N and C terminal domains (NTD and CTD), respectively (Bailey et al., 2013, 2014; Chesarino et al., 2017). While the NTD and CTD are highly variable in length and sequence among IFITM orthologs and paralogs, the canonical CD225 domain spanning IMD to CIL domains is evolutionally more conserved (Bailey et al., 2014). Critical structure motifs and amino acid residues undergoing post-translational modifications required for IFITM oligomerization as well as their biological and antiviral functions are discussed below.

NTD of IFITM2 and IFITM3

Compared to IFITM1, IFITM2 and IFITM3 have N-terminal 20-aa or 21-aa extension which was previously regarded to

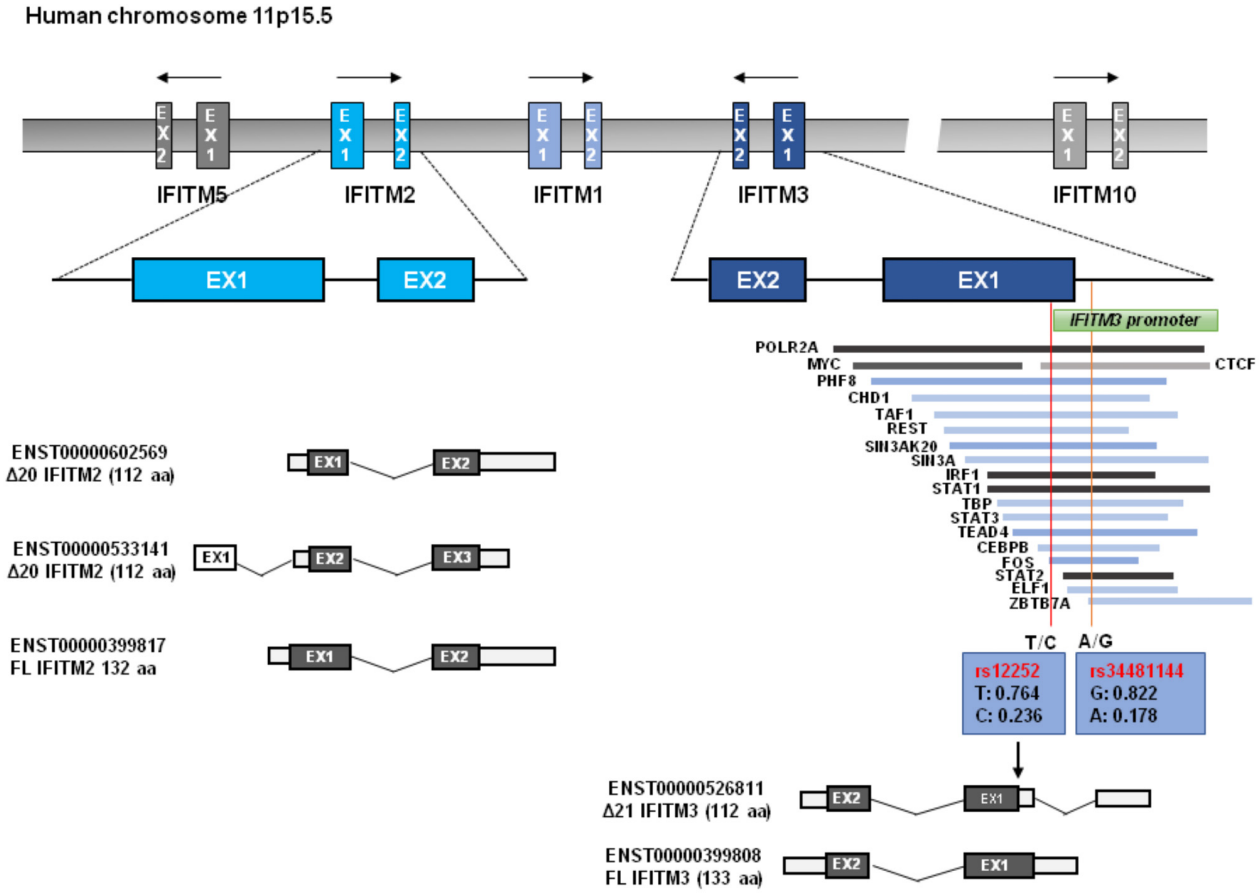

FIGURE 1 | *IFITM* gene structure. Human *IFITM* genes located in chromosome 11p15.5 are indicated, and the exons of immunity-related *IFITM* genes (*IFITM1, IFITM2,* and *IFITM3*) are indicated in blue color. The putative transcripts of *IFITM2* and *IFITM3* are also shown below. The transcription factor binding regions derived from UCSC Genome Browser are shown, which is verified by Chip-seq from the 161 proteins tested through ENCODE; GRCh37/hg19. Two red vertical lines across transcription factor binding sites represent the Influenza associated SNPs of rs12252 and rs34481144 with allele frequencies, respectively. N-terminally truncated IFITM3 isoform (Δ21 IFITM3) that is presumably generated by rs12252 is indicated.

be absent in rs12252-C encoding IFITM3 isoform. Although deletion of this N-terminal 21-aa region significantly impaired its ability to inhibit the infection by IAV, VSV, and DENV, the deletion apparently did not affect its ability to enhance HCoV-OC43pp infection (Weidner et al., 2010; John et al., 2013). Interestingly, Δ21-IFITM3 enhanced inhibition of HIV-1 fusion (Compton et al., 2016). Moreover, Δ20-IFITM2, a N-terminal 20-aa truncated isoform of IFITM2, which is derived from an alternatively initiated RNA transcript (**Figure 1**), demonstrated a more potent suppression on HIV-1 infection than that by full-length wild-type IFITM2 (Wu et al., 2017). In fact, a recent study argues that the Δ20-IFITM2, rather than the full-length IFITM2 and IFITM3, is the effective restriction factor of HIV-1 with CXCR4-tropism (Wu et al., 2017).

The ^{20}YXXΦ^{23} motif of IFITM3 is an endocytic signal essential for endocytosis and localization of IFITM3 to endocytic vesicles and lysosomes (Jia et al., 2014). Artificial mutations of ^{20}YEML^{23} motif (Y20D, Y20A, or L23A) result in an accumulation of IFITM3 in the plasma membrane and reduced inhibition of viruses that enter the cytoplasm at endocytic vesicles/lysosomes, such as IAV, human coronaviruses NL63 and -229E (Chesarino et al., 2014a; Jia et al., 2014; Williams et al., 2014; Zhao et al., 2018), but enhanced inhibition of viruses that directly enter cells at the plasma membranes, such as HPIV-3 and HIV-1 (Jia et al., 2012; Compton et al., 2016; Rabbani et al., 2016). Intriguingly, replacement of IFITM3 tyrosine (Y) 20 with either alanine (A) or aspartic acid (D) to mimic unphosphorylated or phosphorylated IFITM3 converted the antiviral protein to enhance the entry of SARS-CoV and MERS-CoV (Zhao et al., 2018). These studies suggest that the NTD, particularly ^{20}YXXΦ^{23} motif, plays important roles in IFITM2/3 subcellular localization and antiviral activity. IFITM3 are phosphorylated by the protein-tyrosine kinase Fyn on tyrosine 20 (Y20), which results in its plasma membrane accumulation and decreased antiviral activity against influenza viruses (Jia et al., 2012, 2014; Chesarino et al., 2014a). This result is consistent with the mutagenesis studies of ^{20}YXXΦ^{23} motif, where Y20 is part of an endocytosis signal that can be blocked by phosphorylation (Chesarino et al., 2014a). Additionally, phosphorylation of IFITM3 by Fyn and mutagenesis of Y20 also lead to decreased

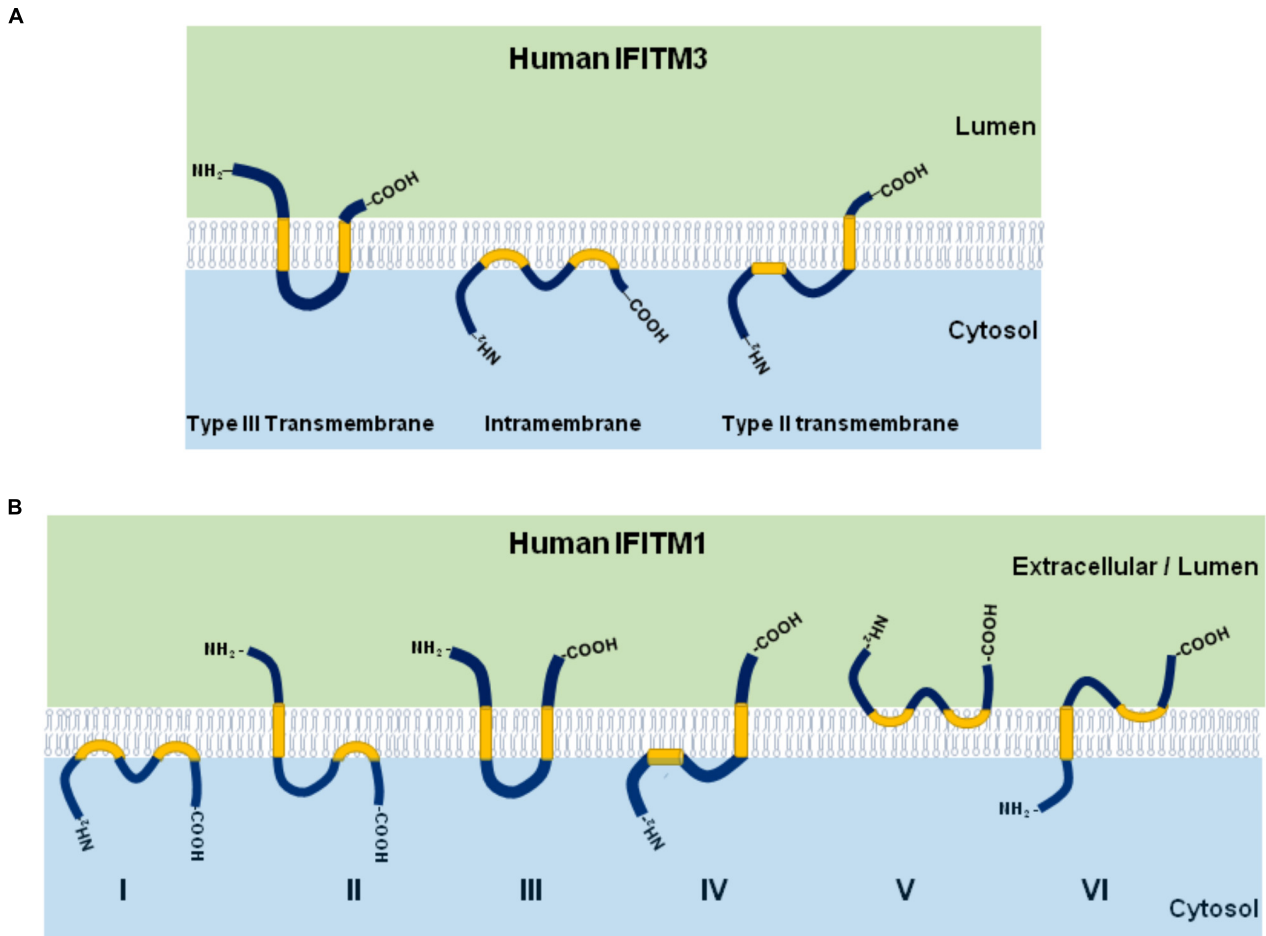

FIGURE 2 | Illustration of IFITM protein membrane topology. The three possible membrane topologies of IFITM3 **(A)** and six possible membrane topological forms of IFITM1 **(B)** are presented. The two transmembrane (or intramembrane) regions were highlighted in yellow.

IFITM3 ubiquitination, suggesting modification of Y20 as an important mechanism to control IFITM3 trafficking and degradation (Chesarino et al., 2014a).

CTD of IFITM1

Compared to IFITM2 and IFITM3, human IFITM1 has a relatively long C-terminal region of 18 amino acid residues. The ^{122}KRXX^{125} motif serves as a sorting signal for IFITM1. Substitution of two basic residues ^{122}KR^{123} with alanine (KR/AA) in IFITM1 reduced its distribution in LAMP1-positive lysosomes but enriched its localization in CD63-positive multivesicular bodies (Li et al., 2015). The KR/AA mutant IFITM1 executed increased activity to inhibit the infection by Jaagsiekte sheep retrovirus (JSRV) and 10A1 amphotropic murine leukemia virus (MLV) (Li et al., 2015). Interestingly, although SARS-CoV and HCoV-NL63 share the ACE2 receptor for infection of host cells, deletion of the C-terminal 3, 6, or 9 amino acids did not apparently affect the activity of IFITM1 to inhibit SARS-CoV entry but enhanced the activity of IFITM1 to inhibit the entry of HCoV-NL63 (Zhao et al., 2018). However, further deletion of the C-terminal 12, 15, or 18 amino acids significantly attenuated or even abolished the ability of IFITM1 to inhibit the entry of SARS-CoV, but did not apparently affect the entry of NL63 (Zhao et al., 2018). More strikingly, deletion of C-terminal 12-aa or 18-aa converted IFITM1 to a potent enhancer of MERS-CoV and HCoV-OC43 entry (Zhao et al., 2014, 2018). A recent mutagenesis study indicated that amino acid residues 127–132 in the CTD domain of IFITM3 differentially modulates its activities in target cell protection and negative imprinting of progeny HIV-1 infectivity (Appourchaux et al., 2018). These studies clearly indicate that the CTD of IFITMs contains multiple structure motifs that regulate the subcellular localization and antiviral functions.

CD225 Domain

The canonical CD225 domain comprises IMD to CIL domains and is evolutionally conserved (Bailey et al., 2014). IMD domain (residues 58–80) is a hydrophobic region and possesses an amphipathic alpha helix spanning residues 59–68 (Chesarino et al., 2017). It was demonstrated recently that either deletion of this alpha helices or mutations altering amphipathicity largely impaired or even abolished IFITM antiviral activity, suggesting

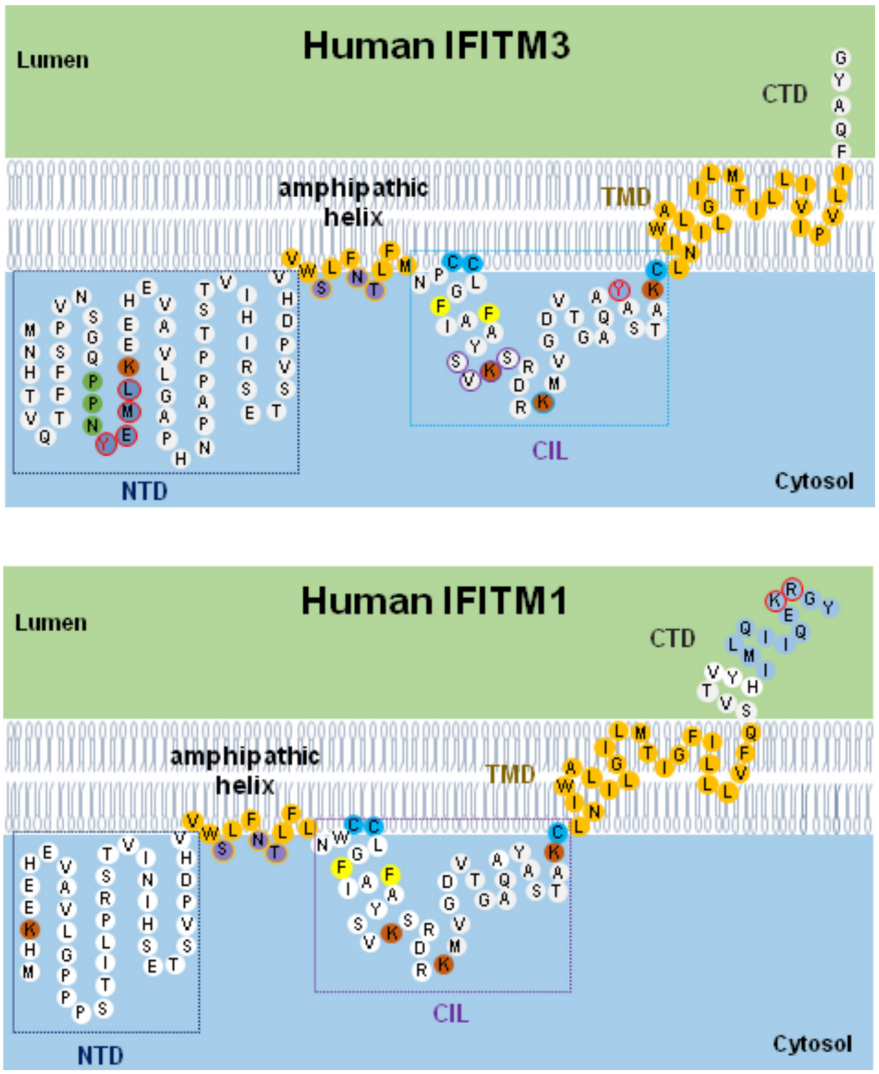

FIGURE 3 | Schematic diagram of IFITM1/3 topology and structural determinants essential for their modulation of viral entry. Five structural domains, including the N-terminal domain (NTD), amphipathic helix domain (AHD), intracellular loop (CIL), transmembrane domain (TMD), and C-terminal domain (CTD), are illustrated. Two membrane-associated domains (AHD and TMD) are embodied in light orange. In IFITM3, three hydrophilic residues (S61, N64, and T65) in amphipathic helix are labeled in violet. In NTD domain, ^{20}YEML^{23} motif required for IFITM3 endocytosis are depicted in blue with red circle and ^{17}PPNY^{20} motif recruiting NEDD4 E3 ligase are shown in green. In CIL domain, ^{81}SVKS^{84} motif required for IFITM3 to inhibit IAV, DENV, and LLOV infection is indicated with purple circle. The residues with post-translational modification, including phosphorylation (Y20 and Y99 labeled with red circle), palmitoylation (C71, C72, and C105 marked with light blue), and ubiquitination (highlighted in orange), are indicated. In addition, two residues (F75 and F78) essential for oligomerization are marked with yellow. In IFITM1, C-terminal 12-aa residues critical for modulating human coronaviruses entry is indicated in blue, and ^{122}KR^{123} dibasic motif constituted as IFITM1 sorting signal is depicted with red circle.

a critical role in IFITM antiviral function, presumably through affecting membrane physical properties (Chesarino et al., 2017). In addition, the ^{81}SVKS^{84} motif residing in CIL domain is essential for IFITM3 to inhibit IAV and DENV infection, but replacement of this motif with four residues of alanine promoted cellular entry driven by Lloviu virus (LLOV) glycoprotein (Wrensch et al., 2015).

Palmitoylation of IFITM

IFITM proteins can be palmytoylated at three cystines in CD225 domain by multiple zinc finger DHHC domain-containing palmitoyltransferases (ZDHHCs) (McMichael et al., 2017). While Cys105 localizes close to the amphipathic alpha helix in the IMD domain, Cys71 and Cys72 are adjacent to the TMD domain. Mutagenesis studies indicated that substitution of those three cysteine residues with alanine alters the IFITM3 distribution from punctate clusters in the cellular membrane to a more diffused pattern and the resulting palmitoylation-deficient mutant showed impaired or even abolished antiviral activity (Yount et al., 2010). Interestingly, when other lipid modification sites, such as myristoylation and prenylation, were introduced in IFITM NTD or CTD domains, the antiviral function of

palmitoylation-deficient IFITM3 mutant could be restored. These findings imply that anchoring IFITM protein to membranes, but not structure alteration by S-palmitoylation, is important for IFITM restriction of virus entry (Yount et al., 2012; Chesarino et al., 2014b).

Ubiquitination of IFITM

Human IFITM proteins possess four conserved lysine residues (**Figure 2**) that can be ubiquitinated by E3 ubiquitin ligase such as NEDD4 (Yount et al., 2012; Chesarino et al., 2015). Previous studies demonstrated that each lysine residue can be modified with mono- and poly-ubiquitination through Lys-48 and Lys-63 linkages (Yount et al., 2012). By replacing all four residues of lysine with alanine, the mutant IFITM3 demonstrated endolysosomal distribution and execute hyperactivity to restrict IAV infection than wild type (Yount et al., 2012). However, our studies demonstrated that ubi-deficient IFITM3 lost antiviral activity against all the viruses tested, including IAV (Zhao et al., 2014, 2018). The discrepancy of those studies is not clear. Importantly, ubiquitination and endocytosis of IFITM3 is required for mTOR inhibitor-induced degradation of IFITM3 (Shi et al., 2018). In addition, IFITM3 K88 can be monomethylated by lysine methyltransferase SET7 and demethylated by histone demethylase LSD1 (Shan et al., 2013, 2017). While vesicular stomatitis virus (VSV) and IAV infection increased IFITM3-K88me1 levels by promoting the interaction between IFITM3 and SET7 and disassociation from LSD1 to attenuate IFITM3 antiviral activity, IFN-α reduced IFITM3-K88me1 levels and increased its antiviral activity (Shan et al., 2013, 2017).

Oligomerization of IFITMs

IFITM proteins function as homo- or hetero-oligomers. Two phenylalanine residues (F75 and F78) are essential for IFITM homo- and hetero-oligomerization (John et al., 2013). IFITM3 bearing F75A and F78A mutations (IFITM3/2FA) showed reduced ability to inhibit the entry of HCoV-NL63, but lost ability to inhibit or enhance the entry of all other tested viruses (Zhao et al., 2014, 2018).

ANTIVIRAL ACTIVITY OF HUMAN IFITM VARIANTS

The antiviral activity of many naturally existing human IFITM variants has been tested in cell cultures. As shown in **Table 1** and mentioned in previous sections, although SNP rs12252 is predicted to encode a splice variant specifying a N-terminally truncated isoform IFITM3 (Everitt et al., 2012), the putative Δ21-IFITM3 protein has not been detected in the tissues or cells of affected subjects (Wu et al., 2017; Makvandi-Nejad et al., 2018). However, subcellular localization and antiviral activity of genetically engineered Δ21-IFITM3 have been extensively investigated in cultured cells (John et al., 2013; Compton et al., 2016). Interestingly, IFITM2 was reported recently to have a similar N-terminally truncated isoform (Δ20-IFITM2) expressed in human innate immune cells and $CD4^+$ T cells (Wu et al., 2017). Compared with the full-length wild-type IFITM2, Δ20-IFITM2 demonstrated an increased plasma membrane accumulation and enhanced antiviral activity against HIV-1, particularly, HIV-1 with CXCR4 tropism (Compton et al., 2016; Wu et al., 2017). In addition, expression and antiviral activity of some human nonsynonymous IFITM3 variants have also been investigated in cell cultures (John et al., 2013). While many of the SNPs results in undetectable levels of IFITM3 in the transfected cells, presumably due to the reduced stability of mutant proteins, and thus loss of antiviral activity against IAV, a few SNPs did not apparently alter the amount of IFITM proteins but impaired the antiviral activity against IAV. It will be interesting to test all the IFITM variants against a group of viruses and identify the SNPs that potentially impact the control and pathogenesis of specific viral infections in humans.

IFITM VARIANTS AND DISEASES

IFITM Variants in Human Populations

As a potent viral restriction factor, IFITMs play a pivotal role in limiting the infection by multiple viruses and any genetic variation affecting the IFITM expression or function might contribute to viral pathogenesis. Thus, natural variation in *IFITM* genes and its association with illness severity has been extensively investigated. Currently, a dozen of SNP in *IFITM3* have been reported, some of which may modulate IFITM expression, affect RNA splicing, or result in nonsynonymous or synonymous variants (**Table 1**). Several SNPs affecting function of IFITMs have been investigated for their association with morbidity, severity and prognosis of microorganism infection (Everitt et al., 2012; Shen et al., 2013; Zhang et al., 2013, 2015; Wang Z. et al., 2014; Allen et al., 2017).

The most studied SNP associated with severe outcomes of IAV infection is SNP rs12252, which is a nonsynonymous variation in the first exon of *IFITM3* (Everitt et al., 2012). The substitution of the major allele of T with alternative allele of C was predicted to alter IFITM3 mRNA splicing and generate a N-terminally truncated variant of IFITM3 with 21 amino acid residues deletion (Δ21-IFITM3) (Everitt et al., 2012). The SNP rs12252 has a higher prevalence in the population of East Asia than Europe (0.528 vs. 0.041) (Everitt et al., 2012). Moreover, the homozygous CC genotype and heterozygous TC genotype have significantly higher frequency in East Asia than that in Europe (0.300 vs. 0.000 and 0.456 vs. 0.082, respectively) (Everitt et al., 2012).

rs34481144 located at the *IFITM3* promoter is associated with severe influenza in three human cohorts (Allen et al., 2017). SNP rs34481144, wherein the majority G allele is replaced with a minor A allele, controls *IFITM3* promoter activity and determines the expression level. Compared to the G allele, A allele has activities of decreased IRF3 binding and increased CTCF binding, thus resulting in lower *IFITM3* expression. SNP rs34481144 has diverse allele and genotypic frequencies in different human populations (**Table 1**). The allele frequency of rs34481144-G is higher in the population of East Asia and Africa than that in Europe (0.957 and 0.994 vs. 0.538, respectively) (Allen et al., 2017). Also, the homozygous GG genotype has

TABLE 1 | Human IFITM variants and their biological functions.

Gene	Variant	Allele Frequency		Protein expression or steady	Subcellular distribution	Restriction of IAV	Restriction of HIV-1
IFITM3	rs34481144	All:	G:0.822; A:0.178	IFITM3 Expression is downregulated	Endosome and lysosome	Largely attenuated Lower $CD8^+$ T cells	Not available
		AFR:	G:0.957; A:0.043				
		AMR:	G:0.767; A:0.233				
		EAS:	G:0.994; A:0.006				
		EUR:	G:0.538; A:0.462				
		SAS:	G:0.793; A: 0.207				
IFITM3	Δ21 IFITM3/rs12252	All:	T: 0.764; C:0.236	Similar to wild type	Endolysosome and periphery of plasm membrane	Attenuated	Enhanced
		AFR:	T: 0.760; C:0.260				
		AMR:	T: 0.823; C:0.177				
		EAS:	T: 0.472; C:0.528				
		EUR:	T: 0.959; C:0.041				
		SAS:	T: 0.853; C:0.147				
IFITM3	H3Q/rs1136853	All:	C:0.961; A:0.039	Not available	Not available	Similar to wild type	Not available
		AFR:	C:0.948; A:0.052				
		AMR:	C:0.970; A:0.030				
		EAS:	C:1.000				
		EUR:	C:0.971; A:0.029				
		SAS:	C:0.920; A:0.080				
IFITM2	Δ20 IFITM2	Alternative transcription start site		Similar to wild type	Endolysosome and plasm membrane	Not available	Enhanced inhibition of X4 HIV-1

AFR, African; AMR, Admixed American; EAS, East Asian; EUR, European; SAS, South Asian.

significantly higher frequency in East Asia than Europe (0.988 vs. 0.294) (Allen et al., 2017).

IFITM3 Variants and Influenza A Virus Infection

Several groups previously reported that *IFITM3* SNP of rs12252 is associated with the susceptibility and severity of patients with seasonal influenza and pandemic H1N1 and H7N9 IAV infection (Everitt et al., 2012; Zhang et al., 2013; Wang Z. et al., 2014; Pan et al., 2017). As summarized in **Table 2**, Everitt et al. (2012) first discovered that a higher allelic frequency of rs12252-C exists in Caucasian hospitalized influenza patients than healthy control. Moreover, they observed a remarkably higher frequency of the homologous CC genotype in hospitalized influenza patients compared to the normal European population (5.7% vs. 0.3%) (Everitt et al., 2012). Importantly, another group reported that the minor C allele of rs12252 in the Caucasian population is much more prevalent in Han Chinese and Japanese and is associated with disease severity in patients with pH1N1/09 IAV infection (Zhang et al., 2013). In line with this observation, results obtained from study of H7N IAV infection revealed that H7N9 infected patients with rs12252-CC genotype exhibited accelerated disease progression and increased mortality rate than patients with the TC and TT genotype (Wang Z. et al., 2014). These studies collectively suggest that rs12252-C is a risk allele associated with severe IAV infection. However, several recent studies from European or Africa-American ethnic groups did not support the association of rs12252 with severe influenza infection (Mills et al., 2014; Lopez-Rodriguez et al., 2016; Randolph et al., 2017). The rare frequency of rs12252-C in European population may account for this discrepancy. Through meta-analysis of 11 studies, rs12252 T > C was associated with risk to severe influenza infection with odds ratio of 1.69 (95% CI 1.23, 2.33) in both European and East Asian populations, but for the mild infection, the results remained uncertain (Prabhu et al., 2018).

Although the association of rs12252 with the susceptibility to influenza infection and disease severity was observed by many studies, the mechanism for this association is largely unknown. As mentioned above, although rs12252-C is speculated to encode a N-terminal truncated IFITM3 with attenuated antiviral activity to impede IAV entry, the truncated variant has not been detected so far (Everitt et al., 2012; Makvandi-Nejad et al., 2018). Moreover, the homozygous CC genotype was demonstrated to only express full-length IFITM3 at a similar level to TT genotype (Wu et al., 2017). Thus rs12252-C genetic variant does not appear to affect the biochemical nature and expression of IFITM3. Obviously, further investigation to determine whether rs12252-C influences IFITM3 gene splicing or protein levels in a cell type-specific manner and whether this SNP co-segregates with a different causative allele is warranted.

A recent study found that another *IFITM3* SNP rs34481144 has a strong association with disease severity in three influenza cohorts (Allen et al., 2017). rs34481144 is located in the promoter region of *IFITM3* (**Figure 1**). The substitution of the majority allele of G with minority allele of C reduces IFITM3 expression level and consequently results in the reduced number of antiviral $CD8^+$ T cells in lung tissue upon IAV infection (Allen et al., 2017). In cohort FLU09, a cohort of naturally acquired influenza infection, a higher frequency of homozygosity of risk A allele was observed in patients with severe illness than the mild cases (33.3% vs. 1.3%) (**Table 3**; Allen et al., 2017). Also, an increased frequency

TABLE 2 | Association of IFITM rs12252 alleles on viral pathogenesis in humans.

Study of rs12252		Allele Frequency		Genotype Frequency (%)			Allelic *P*-value (patients vs. Control.)
	Population	C	T	CC	TC	TT	
Influenza study by Everitt et al. (2012)	Welcome Trust Case Control Consortium 1 (WTCCC1, United Kingdom) (*N* = 2,938)	0.034	0.966	0.3	6.7	93.0	0.00006
	British hospitalized patients with seasonal influenza A or B virus or pandemic influenza A pH1N1/09 infection (N = 53)	0.094	0.906	5.7	7.5	86.8	
Influenza study by Zhang et al. (2013)	Han Chinese 1000 Genomes (*N* = 197)	0.502	0.498	25.4	49.8	24.9	0.0001
	All hospitalized pH1N1-infected patients (*N* = 83)	0.657	0.343	42.2	47.0	10.8	
	Mild Infection (*N* = 51)	0.559	0.441	25.5	60.8	13.7	0.0006
	Severe Infection (*N* = 32)	0.813	0.187	68.7	25	6.3	
Influenza study by Wang Z. et al. (2014)	Chinese 1000 Genomes	0.445	0.555	26	37	37	<0.05
	Hospitalized H7N9 influenza patients (*N* = 16)	0.59	0.41	37	44	19	
Influenza study by Mills et al. (2014)	GRACE healthy control (*N* = 2623)	0.035	0.965	0.15	7.7	92.1	0.753
	GAinS hospitalized patients with severe H1N1 infection (*N* = 34)	0.044	0.956	0	8.8	91.2	
Influenza study by Lopez-Rodriguez et al. (2016)	General Spanish population (*N* = 246)	0.0345	0.965	0.0	6.9	93.1	
	Patients with influenza virus infection (*N* = 118)	0.063	0.936	0.84	11.0	88.1	0.074
	Patients with mild influenza virus infection (*N* = 58)	0.069	0.931	1.7	10.3	88.0	0.11
	Hospitalized patients with primary viral pneumonia (*N* = 60)	0.058	0.942	0.0	11.7	88.3	0.171
Influenza study by Randolph et al. (2017)	European 1000 Genomes (*N* = 503)	0.041	0.959	0	8.2	91.8	0.80
	PICFLU-White non-Hispanic (*N* = 185)	0.038	0.962	1.1	5.4	93.5	
	African 1000 Genomes (*N* = 661)	0.26	0.74	7	38.1	54.9	0.97
	PICFLU-African American (*N* = 56)	0.258	0.742	7.1	37.5	55.4	
AIDS (Zhang et al., 2015)	Chinese MSM HIV-1-negative control (*N* = 196)	0.528	0.472	35.20	43.88	20.92	0.441
	Acute HIV infection with rapid progression in MSM cohort (*N* = 74)	0.608	0.392	29.73	62.16	8.11	
HFRS (Xu-Yang et al., 2016)	Han Chinese 1000 Genomes (*N* = 208)	0.522	0.478	26.92	50.48	22.60	0.0076
	Chinese patients with severe HFRS (*N* = 41)	0.683	0.317	43.90	48.78	7.32	

P-value refers to the differences of allele frequencies between patients infected with different viruses and the control group (general population, healthy population or virus-negatives as used in the specific studies).

TABLE 3 | Impacts of IFITM variant rs34481144 on viral pathogenesis in humans.

Study of rs34481144 with influenza (Allen et al., 2017)		Allele frequency		Genotype frequency (%)			Allelic *P*-value (severe vs. mild)
	Population	A	G	AA	AG	GG	
Cohort FLU09 (naturally acquired influenza infection) (*N* = 86)	Mild (*N* = 77)	0.169	0.831	1.3	31.2	67.5	0.037
	Severe (*N* = 9)	0.500	0.500	33.3	33.3	33.3	
Cohort of genentech challenge study (*N* = 42)	Mild (*N* = 23)	0.282	0.718	4.3	47.8	47.8	0.01
	Severe (*N* = 19)	0.553	0.447	21.1	68.4	10.5	
PICFlu cohort (pediatric influenza cohort of critically ill children) (*N* = 265)	Mild (*N* = 247)	0.333	0.667	14.1	38.3	47.6	0.047
	Severe (*N* = 18)	0.500	0.500	17.6	64.7	17.6	

P-value refers to the differences of allele frequencies between mild influenza patients and severe influenza patients.

of the A allele was found in patients who suffered with severe influenza in other two cohorts (**Table 3**; Allen et al., 2017). Thus, rs34481144-A is a risk allele associated with severe IAV infection and its association with other viral infection disease deserves to be investigated in future.

IFITM3 Variants and Other Viral Infections

In addition to influenza, SNP of rs12252 was also observed to have association with development of AIDS and Hantaan virus associated hemorrhagic fever with renal syndrome (HFRS) (Zhang et al., 2015; Xu-Yang et al., 2016). Zhang et al. (2015) reported that rs12252 is associated with rapid progression of AIDS, but not the susceptibility to HIV infection. Patients of AIDS rapid progressors had a higher frequency of rs12252 CC and CT genotype than non-progressors (Zhang et al., 2015). Compared with TT genotype, more patients with CC/CT genotypes were characterized with higher viremia level and more significantly reduced CD4 T^+ cells (Zhang et al., 2015). In addition, the association of rs12252-C and homozygous CC genotype with disease severity in HFRS patients infected by Hantaan virus was reported recently (Xu-Yang et al., 2016). A higher allelic frequency of rs12252-C was observed in severe HFRS patients hospitalized than healthy Han Chinese controls (68.29% vs. 52.16%). Also, severe HFRS patients had a higher frequency of rs12252 CC than patients with mild HFRS and healthy Han Chinese. Along these lines, this group also reported that the viral titer detected in the plasma of HFRS patients with rs12252-CC genotype was more significantly alleviated than those with the TC and TT genotype (Xu-Yang et al., 2016). Thus, rs12252 C is a risk allele associated with severity of AIDS and HFRS, indicating that SNP rs12252 may have a profound impact on the pathogenesis of multiple viral diseases.

FUTURE DIRECTIONS

IFITMs are a group of small fusogenic proteins that restrict the infection of broad spectrum of viruses by inhibiting the fusion of viral and cellular membranes. However, whether IFITMs inhibit hemifusion, the process whereby the outer, but not the inner, leaflet of the viral and cellular membranes merge, or the transition from hemifusion to pore formation remains to be rigorously determined. It is also important to note that IFITMs do not always inhibit virus entry, but may promote membrane fusion under selected conditions, such as in the case of HCoV-OC43 infection (Zhao et al., 2014). Moreover, our recent studies indicated that specific mutations can flip the biological activity of IFITMs, from inhibiting to promoting the infection of selected human coronaviruses (Zhao et al., 2018). Those later findings strongly suggest that the fusogenic activity of IFITMs might be bidirectional and could be regulated by viral and host factors. The elucidation of molecular mechanisms underlying IFITM-mediated innate immunity via modulation of viral entry into host cells as well as the negative imprinting of progeny virions (virions incorporating IFITMs display decreased infectivity) will open new avenues for future research. We have only just begun to appreciate the role of IFITM proteins in innate antiviral defenses. Genetic association studies of rare and common variants may explain population-specific and individual variance in susceptibility to common viral pathogens and identify specific IFITM – virus interactions. Expansion of genetic studies incorporating gene knock-down or knock-off screens, single cell transcriptomics, epigenetic modification, and targeted sequencing for different viral infections will provide needed insights into cellular mechanisms and pathways involved in IFITM-mediated host response to viral exposure and infection.

AUTHOR CONTRIBUTIONS

All the authors participated in the draft and revision of this review article.

FUNDING

The project was supported by grants from the U.S. National Institutes of Health (AI113267), the National Natural Science Foundation of China (81571976 and 81772173), the Commonwealth of Pennsylvania through the Hepatitis B Foundation as well as federal funds from the National Cancer Institute, National Institutes of health, under contract HHSN26120080001E. This project was supported in part by the Intramural Research Program of the NIH, National Cancer Institute, Center for Cancer Research. The content of this publication does not necessarily reflect the views or policies of the Department of Health and Human Services, nor do mention of trade names, commercial products, or organizations imply endorsement by the U.S. Government.

ACKNOWLEDGMENTS

We want to thank the critical comments and suggestions by Dr. Jinhong Chang and Julia Ma on this manuscript.

REFERENCES

Allen, E. K., Randolph, A. G., Bhangale, T., Dogra, P., Ohlson, M., Oshansky, C. M., et al. (2017). SNP-mediated disruption of CTCF binding at the IFITM3 promoter is associated with risk of severe influenza in humans. *Nat. Med.* 23, 975–983. doi: 10.1038/nm.4370

Amini-Bavil-Olyaee, S., Choi, Y. J., Lee, J. H., Shi, M., Huang, I. C., Farzan, M., et al. (2013). The antiviral effector IFITM3 disrupts intracellular cholesterol homeostasis to block viral entry. *Cell Host Microbe* 13, 452–464. doi: 10.1016/j.chom.2013.03.006

Anafu, A. A., Bowen, C. H., Chin, C. R., Brass, A. L., and Holm, G. H. (2013). Interferon-inducible transmembrane protein 3 (IFITM3) restricts reovirus cell entry. *J. Biol. Chem.* 288, 17261–17271. doi: 10.1074/jbc.M112.438515

Appourchaux, R., Delpeuch, M., Zhong, L., Burlaud-Gaillard, J., Tartour, K., Savidis, G., et al. (2018). Functional mapping of regions involved in the negative imprinting of virion particles infectivity and in target cell protection

by the Interferon-Induced Transmembrane Protein 3 (IFITM3) against HIV-1. *J. Virol.* doi: 10.1128/JVI.01716-18 [Epub ahead of print].

Bailey, C. C., Huang, I. C., Kam, C., and Farzan, M. (2012). Ifitm3 limits the severity of acute influenza in mice. *PLoS Pathog.* 8:e1002909. doi: 10.1371/journal.ppat.1002909

Bailey, C. C., Kondur, H. R., Huang, I. C., and Farzan, M. (2013). Interferon-induced transmembrane protein 3 is a type II transmembrane protein. *J. Biol. Chem.* 288, 32184–32193. doi: 10.1074/jbc.M113.514356

Bailey, C. C., Zhong, G., Huang, I. C., and Farzan, M. (2014). IFITM-family proteins: the cell's first line of antiviral defense. *Ann. Rev. Virol.* 1, 261–283. doi: 10.1146/annurev-virology-031413-085537

Brass, A. L., Huang, I. C., Benita, Y., John, S. P., Krishnan, M. N., Feeley, E. M., et al. (2009). The IFITM proteins mediate cellular resistance to influenza A H1N1 virus, West Nile virus, and dengue virus. *Cell* 139, 1243–1254. doi: 10.1016/j.cell.2009.12.017

Chesarino, N. M., Compton, A. A., McMichael, T. M., Kenney, A. D., Zhang, L., Soewarna, V., et al. (2017). IFITM3 requires an amphipathic helix for antiviral activity. *EMBO Rep.* 18, 1740–1751. doi: 10.15252/embr.201744100

Chesarino, N. M., McMichael, T. M., Hach, J. C., and Yount, J. S. (2014a). Phosphorylation of the antiviral protein interferon-inducible transmembrane protein 3 (IFITM3) dually regulates its endocytosis and ubiquitination. *J. Biol. Chem.* 289, 11986–11992. doi: 10.1074/jbc.M114.557694

Chesarino, N. M., McMichael, T. M., and Yount, J. S. (2014b). Regulation of the trafficking and antiviral activity of IFITM3 by post-translational modifications. *Future Microbiol.* 9, 1151–1163. doi: 10.2217/fmb.14.65

Chesarino, N. M., McMichael, T. M., and Yount, J. S. (2015). E3 ubiquitin ligase NEDD4 promotes influenza virus infection by decreasing levels of the antiviral protein IFITM3. *PLoS Pathog.* 11:e1005095. doi: 10.1371/journal.ppat.1005095

Compton, A. A., Bruel, T., Porrot, F., Mallet, A., Sachse, M., Euvrard, M., et al. (2014). IFITM proteins incorporated into HIV-1 virions impair viral fusion and spread. *Cell Host Microbe* 16, 736–747. doi: 10.1016/j.chom.2014.11.001

Compton, A. A., Roy, N., Porrot, F., Billet, A., Casartelli, N., Yount, J. S., et al. (2016). Natural mutations in IFITM3 modulate post-translational regulation and toggle antiviral specificity. *EMBO Rep.* 17, 1657–1671. doi: 10.15252/embr.201642771

Desai, T. M., Marin, M., Chin, C. R., Savidis, G., Brass, A. L., and Melikyan, G. B. (2014). IFITM3 restricts influenza A virus entry by blocking the formation of fusion pores following virus-endosome hemifusion. *PLoS Pathog.* 10:e1004048. doi: 10.1371/journal.ppat.1004048

Everitt, A. R., Clare, S., McDonald, J. U., Kane, L., Harcourt, K., Ahras, M., et al. (2013). Defining the range of pathogens susceptible to Ifitm3 restriction using a knockout mouse model. *PLoS One* 8:e80723. doi: 10.1371/journal.pone.0080723

Everitt, A. R., Clare, S., Pertel, T., John, S. P., Wash, R. S., Smith, S. E., et al. (2012). IFITM3 restricts the morbidity and mortality associated with influenza. *Nature* 484, 519–523. doi: 10.1038/nature10921

Foster, T. L., Wilson, H., Iyer, S. S., Coss, K., Doores, K., Smith, S., et al. (2016). Resistance of transmitted founder HIV-1 to IFITM-mediated restriction. *Cell Host Microbe* 20, 429–442. doi: 10.1016/j.chom.2016.08.006

Fu, B., Wang, L., Li, S., and Dorf, M. E. (2017). ZMPSTE24 defends against influenza and other pathogenic viruses. *J. Exp. Med.* 214, 919–929. doi: 10.1084/jem.20161270

Gerlach, T., Hensen, L., Matrosovich, T., Bergmann, J., Winkler, M., Peteranderl, C., et al. (2017). pH optimum of hemagglutinin-mediated membrane fusion determines sensitivity of influenza a viruses to the interferon-induced antiviral state and IFITMs. *J. Virol.* 91:e00246-17. doi: 10.1128/JVI.00246-17

Gorman, M. J., Poddar, S., Farzan, M., and Diamond, M. S. (2016). The interferon-stimulated gene ifitm3 restricts west nile virus infection and pathogenesis. *J. Virol.* 90, 8212–8225. doi: 10.1128/JVI.00581-16

Hach, J. C., McMichael, T., Chesarino, N. M., and Yount, J. S. (2013). Palmitoylation on conserved and nonconserved cysteines of murine IFITM1 regulates its stability and anti-influenza A virus activity. *J. Virol.* 87, 9923–9927. doi: 10.1128/JVI.00621-13

Huang, I. C., Bailey, C. C., Weyer, J. L., Radoshitzky, S. R., Becker, M. M., Chiang, J. J., et al. (2011). Distinct patterns of IFITM-mediated restriction of filoviruses, SARS coronavirus, and influenza A virus. *PLoS Pathog.* 7:e1001258. doi: 10.1371/journal.ppat.1001258

Infusini, G., Smith, J. M., Yuan, H., Pizzolla, A., Ng, W. C., Londrigan, S. L., et al. (2015). Respiratory DC Use IFITM3 to avoid direct viral infection and safeguard virus-specific CD8+ T cell priming. *PLoS One* 10:e0143539. doi: 10.1371/journal.pone.0143539

Jia, R., Pan, Q., Ding, S., Rong, L., Liu, S. L., Geng, Y., et al. (2012). The N-terminal region of IFITM3 modulates its antiviral activity by regulating IFITM3 cellular localization. *J. Virol.* 86, 13697–13707. doi: 10.1128/JVI.01828-12

Jia, R., Xu, F., Qian, J., Yao, Y., Miao, C., Zheng, Y. M., et al. (2014). Identification of an endocytic signal essential for the antiviral action of IFITM3. *Cell. Microbiol.* 16, 1080–1093. doi: 10.1111/cmi.12262

Jiang, D., Weidner, J. M., Qing, M., Pan, X. B., Guo, H., Xu, C., et al. (2010). Identification of five interferon-induced cellular proteins that inhibit west nile virus and dengue virus infections. *J. Virol.* 84, 8332–8341. doi: 10.1128/JVI.02199-09

John, S. P., Chin, C. R., Perreira, J. M., Feeley, E. M., Aker, A. M., Savidis, G., et al. (2013). The CD225 domain of IFITM3 is required for both IFITM protein association and inhibition of influenza A virus and dengue virus replication. *J. Virol.* 87, 7837–7852. doi: 10.1128/JVI.00481-13

Li, C., Du, S., Tian, M., Wang, Y., Bai, J., Tan, P., et al. (2018). The host restriction factor interferon-inducible transmembrane protein 3 inhibits *Vaccinia virus* infection. *Front. Immunol.* 9:228. doi: 10.3389/fimmu.2018.00228

Li, K., Jia, R., Li, M., Zheng, Y. M., Miao, C., Yao, Y., et al. (2015). A sorting signal suppresses IFITM1 restriction of viral entry. *J. Biol. Chem.* 290, 4248–4259. doi: 10.1074/jbc.M114.630780

Li, K., Markosyan, R. M., Zheng, Y. M., Golfetto, O., Bungart, B., Li, M., et al. (2013). IFITM proteins restrict viral membrane hemifusion. *PLoS Pathog.* 9:e1003124. doi: 10.1371/journal.ppat.1003124

Lin, T. Y., Chin, C. R., Everitt, A. R., Clare, S., Perreira, J. M., Savidis, G., et al. (2013). Amphotericin B increases influenza A virus infection by preventing IFITM3-mediated restriction. *Cell Rep.* 5, 895–908. doi: 10.1016/j.celrep.2013.10.033

Lopez-Rodriguez, M., Herrera-Ramos, E., Sole-Violan, J., Ruiz-Hernandez, J. J., Borderias, L., Horcajada, J. P., et al. (2016). IFITM3 and severe influenza virus infection. No evidence of genetic association. *Eur. J. Clin. Microbiol. Infect. Dis.* 35, 1811–1817. doi: 10.1007/s10096-016-2732-7

Lu, J., Pan, Q., Rong, L., He, W., Liu, S. L., and Liang, C. (2011). The IFITM proteins inhibit HIV-1 infection. *J. Virol.* 85, 2126–2137. doi: 10.1128/JVI.01531-10

Ma, W., Tummers, B., van Esch, E. M., Goedemans, R., Melief, C. J., Meyers, C., et al. (2016). Human papillomavirus downregulates the expression of IFITM1 and RIPK3 to escape from IFNgamma- and TNFalpha-mediated antiproliferative effects and necroptosis. *Front. Immunol.* 7:496. doi: 10.3389/fimmu.2016.00496

Makvandi-Nejad, S., Laurenson-Schafer, H., Wang, L., Wellington, D., Zhao, Y., Jin, B., et al. (2018). Lack of truncated IFITM3 transcripts in cells homozygous for the rs12252-C variant that is associated with severe influenza infection. *J. Infect. Dis.* 217, 257–262. doi: 10.1093/infdis/jix512

McMichael, T. M., Zhang, L., Chemudupati, M., Hach, J. C., Kenney, A. D., Hang, H. C., et al. (2017). The palmitoyltransferase ZDHHC20 enhances interferon-induced transmembrane protein 3 (IFITM3) palmitoylation and antiviral activity. *J. Biol. Chem.* 292, 21517–21526. doi: 10.1074/jbc.M117.800482

Mills, T. C., Rautanen, A., Elliott, K. S., Parks, T., Naranbhai, V., Ieven, M. M., et al. (2014). IFITM3 and susceptibility to respiratory viral infections in the community. *J. Infect. Dis.* 209, 1028–1031. doi: 10.1093/infdis/jit468

Mudhasani, R., Tran, J. P., Retterer, C., Radoshitzky, S. R., Kota, K. P., Altamura, L. A., et al. (2013). IFITM-2 and IFITM-3 but not IFITM-1 restrict Rift Valley fever virus. *J. Virol.* 87, 8451–8464. doi: 10.1128/JVI.03382-12

Pan, Y., Yang, P., Dong, T., Zhang, Y., Shi, W., Peng, X., et al. (2017). IFITM3 Rs12252-C variant increases potential risk for severe influenza virus infection in chinese population. *Front. Cell Infect. Microbiol.* 7:294. doi: 10.3389/fcimb.2017.00294

Perreira, J. M., Chin, C. R., Feeley, E. M., and Brass, A. L. (2013). IFITMs restrict the replication of multiple pathogenic viruses. *J. Mol. Biol.* 425, 4937–4955. doi: 10.1016/j.jmb.2013.09.024

Poddar, S., Hyde, J. L., Gorman, M. J., Farzan, M., and Diamond, M. S. (2016). The interferon-stimulated gene IFITM3 restricts infection and pathogenesis of arthritogenic and encephalitic alphaviruses. *J. Virol.* 90, 8780–8794. doi: 10.1128/JVI.00655-16

Prabhu, S. S., Chakraborty, T. T., Kumar, N., and Banerjee, I. (2018). Association between IFITM3 rs12252 polymorphism and influenza susceptibility and severity: a meta-analysis. *Gene* 674, 70–79. doi: 10.1016/j.gene.2018.06.070

Rabbani, M. A., Ribaudo, M., Guo, J. T., and Barik, S. (2016). Identification of interferon-stimulated gene proteins that inhibit human parainfluenza virus type 3. *J. Virol.* 90, 11145–11156. doi: 10.1128/JVI.01551-16

Randolph, A. G., Yip, W. K., Allen, E. K., Rosenberger, C. M., Agan, A. A., Ash, S. A., et al. (2017). Evaluation of IFITM3 rs12252 association with severe pediatric influenza infection. *J. Infect. Dis.* 216, 14–21. doi: 10.1093/infdis/jix242

Savidis, G., Perreira, J. M., Portmann, J. M., Meraner, P., Guo, Z., Green, S., et al. (2016). The IFITMs Inhibit Zika Virus Replication. *Cell Rep.* 15, 2323–2330. doi: 10.1016/j.celrep.2016.05.074

Shan, J., Zhao, B., Shan, Z., Nie, J., Deng, R., Xiong, R., et al. (2017). Histone demethylase LSD1 restricts influenza A virus infection by erasing IFITM3-K88 monomethylation. *PLoS Pathog.* 13:e1006773. doi: 10.1371/journal.ppat.1006773

Shan, Z., Han, Q., Nie, J., Cao, X., Chen, Z., Yin, S., et al. (2013). Negative regulation of interferon-induced transmembrane protein 3 by SET7-mediated lysine monomethylation. *J. Biol. Chem.* 288, 35093–35103. doi: 10.1074/jbc.M113.511949

Shen, C., Wu, X. R., Jiao, W. W., Sun, L., Feng, W. X., Xiao, J., et al. (2013). A functional promoter polymorphism of IFITM3 is associated with susceptibility to pediatric tuberculosis in Han Chinese population. *PLoS One* 8:e67816. doi: 10.1371/journal.pone.0067816

Shi, G., Ozog, S., Torbett, B. E., and Compton, A. A. (2018). mTOR inhibitors lower an intrinsic barrier to virus infection mediated by IFITM3. *Proc. Natl. Acad. Sci. U.S.A.* 115, E10069–E10078. doi: 10.1073/pnas.1811892115

Siegrist, F., Ebeling, M., and Certa, U. (2011). The small interferon-induced transmembrane genes and proteins. *J. Interferon Cytokine Res.* 31, 183–197. doi: 10.1089/jir.2010.0112

Stacey, M. A., Clare, S., Clement, M., Marsden, M., Abdul-Karim, J., Kane, L., et al. (2017). The antiviral restriction factor IFN-induced transmembrane protein 3 prevents cytokine-driven CMV pathogenesis. *J. Clin. Invest.* 127, 1463–1474. doi: 10.1172/JCI84889

Tartour, K., Appourchaux, R., Gaillard, J., Nguyen, X. N., Durand, S., Turpin, J., et al. (2014). IFITM proteins are incorporated onto HIV-1 virion particles and negatively imprint their infectivity. *Retrovirology* 11:103. doi: 10.1186/s12977-014-0103-y

Tartour, K., Nguyen, X. N., Appourchaux, R., Assil, S., Barateau, V., Bloyet, L. M., et al. (2017). Interference with the production of infectious viral particles and bimodal inhibition of replication are broadly conserved antiviral properties of IFITMs. *PLoS Pathog.* 13:e1006610. doi: 10.1371/journal.ppat.1006610

Wakim, L. M., Gupta, N., Mintern, J. D., and Villadangos, J. A. (2013). Enhanced survival of lung tissue-resident memory CD8(+) T cells during infection with influenza virus due to selective expression of IFITM3. *Nat. Immunol.* 14, 238–245. doi: 10.1038/ni.2525

Wang, B., Lam, T. H., Soh, M. K., Ye, Z., Chen, J., and Ren, E. C. (2018). Influenza A virus facilitates its infectivity by activating p53 to inhibit the expression of interferon-induced transmembrane proteins. *Front. Immunol.* 9:1193. doi: 10.3389/fimmu.2018.01193

Wang, S., Chi, X., Wei, H., Chen, Y., Chen, Z., Huang, S., et al. (2014). Influenza A virus-induced degradation of eukaryotic translation initiation factor 4B contributes to viral replication by suppressing IFITM3 protein expression. *J. Virol.* 88, 8375–8385. doi: 10.1128/JVI.00126-14

Wang, Y., Pan, Q., Ding, S., Wang, Z., Yu, J., Finzi, A., et al. (2017). The V3 Loop of HIV-1 Env determines viral susceptibility to ifitm3 impairment of viral infectivity. *J. Virol.* 91:e02441-16. doi: 10.1128/JVI.02441-16

Wang, Z., Zhang, A., Wan, Y., Liu, X., Qiu, C., Xi, X., et al. (2014). Early hypercytokinemia is associated with interferon-induced transmembrane protein-3 dysfunction and predictive of fatal H7N9 infection. *Proc. Natl. Acad. Sci. U.S.A.* 111, 769–774. doi: 10.1073/pnas.1321748111

Wee, Y. S., Roundy, K. M., Weis, J. J., and Weis, J. H. (2012). Interferon-inducible transmembrane proteins of the innate immune response act as membrane organizers by influencing clathrin and v-ATPase localization and function. *Innate Immun.* 18, 834–845. doi: 10.1177/1753425912443392

Weidner, J. M., Jiang, D., Pan, X. B., Chang, J., Block, T. M., and Guo, J. T. (2010). Interferon-induced cell membrane proteins, IFITM3 and tetherin, inhibit vesicular stomatitis virus infection via distinct mechanisms. *J. Virol.* 84, 12646–12657. doi: 10.1128/JVI.01328-10

Wilkins, C., Woodward, J., Lau, D. T., Barnes, A., Joyce, M., McFarlane, N., et al. (2013). IFITM1 is a tight junction protein that inhibits hepatitis C virus entry. *Hepatology* 57, 461–469. doi: 10.1002/hep.26066

Williams, D. E., Wu, W. L., Grotefend, C. R., Radic, V., Chung, C., Chung, Y. H., et al. (2014). IFITM3 polymorphism rs12252-C restricts influenza A viruses. *PLoS One* 9:e110096. doi: 10.1371/journal.pone.0110096

Wrensch, F., Karsten, C. B., Gnirss, K., Hoffmann, M., Lu, K., Takada, A., et al. (2015). Interferon-induced transmembrane protein-mediated inhibition of host cell entry of ebolaviruses. *J. Infect. Dis.* 212(Suppl. 2), S210–S218. doi: 10.1093/infdis/jiv255

Wrensch, F., Winkler, M., and Pohlmann, S. (2014). IFITM proteins inhibit entry driven by the MERS-coronavirus spike protein: evidence for cholesterol-independent mechanisms. *Viruses* 6, 3683–3698. doi: 10.3390/v6093683

Wu, W. L., Grotefend, C. R., Tsai, M. T., Wang, Y. L., Radic, V., Eoh, H., et al. (2017). Delta20 IFITM2 differentially restricts X4 and R5 HIV-1. *Proc. Natl. Acad. Sci. U.S.A.* 114, 7112–7117. doi: 10.1073/pnas.1619640114

Xie, M., Xuan, B., Shan, J., Pan, D., Sun, Y., Shan, Z., et al. (2015). Human cytomegalovirus exploits interferon-induced transmembrane proteins to facilitate morphogenesis of the virion assembly compartment. *J. Virol.* 89, 3049–3061. doi: 10.1128/JVI.03416-14

Xu, J., Qian, P., Wu, Q., Liu, S., Fan, W., Zhang, K., et al. (2014). Swine interferon-induced transmembrane protein, sIFITM3, inhibits foot-and-mouth disease virus infection in vitro and in vivo. *Antiviral Res.* 109, 22–29. doi: 10.1016/j.antiviral.2014.06.008

Xu-Yang, Z., Pei-Yu, B., Chuan-Tao, Y., Wei, Y., Hong-Wei, M., Kang, T., et al. (2016). Interferon-induced transmembrane protein 3 inhibits hantaan virus infection, and its single nucleotide polymorphism rs12252 influences the severity of hemorrhagic fever with renal syndrome. *Front. Immunol.* 7:535. doi: 10.3389/fimmu.2016.00535

Yount, J. S., Karssemeijer, R. A., and Hang, H. C. (2012). S-palmitoylation and ubiquitination differentially regulate interferon-induced transmembrane protein 3 (IFITM3)-mediated resistance to influenza virus. *J. Biol. Chem.* 287, 19631–19641. doi: 10.1074/jbc.M112.362095

Yount, J. S., Moltedo, B., Yang, Y. Y., Charron, G., Moran, T. M., López, C. B., et al. (2010). Palmitoylome profiling reveals S-palmitoylation-dependent antiviral activity of IFITM3. *Nat. Chem. Biol.* 6, 610–614. doi: 10.1038/nchembio.405

Yu, J., Li, M., Wilkins, J., Ding, S., Swartz, T. H., Esposito, A. M., et al. (2015). IFITM proteins restrict HIV-1 infection by antagonizing the envelope glycoprotein. *Cell Rep.* 13, 145–156. doi: 10.1016/j.celrep.2015.08.055

Zhang, Y., Makvandi-Nejad, S., Qin, L., Zhao, Y., Zhang, T., Wang, L., et al. (2015). Interferon-induced transmembrane protein-3 rs12252-C is associated with rapid progression of acute HIV-1 infection in Chinese MSM cohort. *AIDS* 29, 889–894. doi: 10.1097/QAD.0000000000000632

Zhang, Y. H., Zhao, Y., Li, N., Peng, Y. C., Giannoulatou, E., Jin, R. H., et al. (2013). Interferon-induced transmembrane protein-3 genetic variant rs12252-C is associated with severe influenza in Chinese individuals. *Nat. Commun.* 4:1418. doi: 10.1038/ncomms2433

Zhang, Z., Liu, J., Li, M., Yang, H., and Zhang, C. (2012). Evolutionary dynamics of the interferon-induced transmembrane gene family in vertebrates. *PLoS One* 7:e49265. doi: 10.1371/journal.pone.0049265

Zhao, X., Guo, F., Liu, F., Cuconati, A., Chang, J., Block, T. M., et al. (2014). Interferon induction of IFITM proteins promotes infection by human coronavirus OC43. *Proc. Natl. Acad. Sci. U.S.A.* 111, 6756–6761. doi: 10.1073/pnas.1320856111

Zhao, X., Sehgal, M., Hou, Z., Cheng, J., Shu, S., Wu, S., et al. (2018). Identification of residues controlling restriction versus enhancing activities of IFITM proteins on entry of human coronaviruses. *J. Virol.* 92:e01535-17. doi: 10.1128/JVI.01535-17

Conflict of Interest Statement: The authors declare that the research was conducted in the absence of any commercial or financial relationships that could be construed as a potential conflict of interest.

Copyright © 2019 Zhao, Li, Winkler, An and Guo. This is an open-access article distributed under the terms of the Creative Commons Attribution License (CC BY). The use, distribution or reproduction in other forums is permitted, provided the original author(s) and the copyright owner(s) are credited and that the original publication in this journal is cited, in accordance with accepted academic practice. No use, distribution or reproduction is permitted which does not comply with these terms.

frontiers in Genetics

REVIEW
published: 23 January 2019
doi: 10.3389/fgene.2018.00720

Interaction of the Host and Viral Genome and Their Influence on HIV Disease

Riley H. Tough[1,2] *and Paul J. McLaren*[1,2]*

[1] JC Wilt Infectious Diseases Research Centre, Public Health Agency of Canada, Winnipeg, MB, Canada, [2] Department of Medical Microbiology and Infectious Diseases, University of Manitoba, Winnipeg, MB, Canada

The course of Human Immunodeficiency Virus type 1 (HIV) infection is a dynamic interplay in which both host and viral genetic variation, among other factors, influence disease susceptibility and rate of progression. HIV set-point viral load (spVL), a key indicator of HIV disease progression, has an estimated 30% of variance attributable to common heritable effects and roughly 70% attributable to environmental factors and/or additional non-genetic factors. Genome-wide genotyping and sequencing studies have allowed for large-scale association testing studying host and viral genetic variants associated with infection and disease progression. Host genomics of HIV infection has been studied predominantly in Caucasian populations consistently identifying human leukocyte antigen (HLA) genes and C-C motif chemokine receptor 5 as key factors of HIV susceptibility and progression. However, these studies don't fully assess all classes of genetic variation (e.g., very rare polymorphisms, copy number variants etc.) and do not inform on non-European ancestry groups. Additionally, viral sequence variability has been demonstrated to influence disease progression independently of host genetic variation. Viral sequence variation can be attributed to the rapid evolution of the virus within the host due to the selective pressure of the host immune response. As the host immune system responds to the virus, e.g., through recognition of HIV antigens, the virus is able to mitigate this response by evolving HLA-specific escape mutations. Diversity of viral genotypes has also been correlated with moderate to strong effects on CD4+ T cell decline and some studies showing weak to no correlation with spVL. There is evidence to support these viral genetic factors being heritable between individuals and the evolution of these factors having important consequences in the genetic epidemiology of HIV infection on a population level. This review will discuss the host-pathogen interaction of HIV infection, explore the importance of host and viral genetics for a better understanding of pathogenesis and identify opportunities for additional genetic studies.

Keywords: HIV infection, genetic variation, set point viral load, genome-wide studies, genetic epidemiology, host–pathogen interaction

OPEN ACCESS

Edited by:
Ping An,
Frederick National Laboratory for Cancer Research (NIH), United States

Reviewed by:
Taisuke Izumi,
Henry M. Jackson Foundation, United States
Mark Z. Kos,
University of Texas Rio Grande Valley Edinburg, United States

***Correspondence:**
Paul J. McLaren
paul.mclaren@canada.ca

Specialty section:
This article was submitted to Applied Genetic Epidemiology, a section of the journal Frontiers in Genetics

Received: *12 October 2018*
Accepted: *21 December 2018*
Published: *23 January 2019*

Citation:
Tough RH and McLaren PJ (2019) Interaction of the Host and Viral Genome and Their Influence on HIV Disease. Front. Genet. 9:720. doi: 10.3389/fgene.2018.00720

INTRODUCTION

Since the discovery of Human Immunodeficiency Virus type 1 (HIV) in the 1980s, a major goal of the infectious disease research community has been to study the pathogenesis of HIV disease to guide the development of therapeutics and, more recently, a functional cure. Since the start of the epidemic there have been an estimated 77.3 million (59.9–100 million) individuals infected with HIV and, in 2017, an estimated 36.9 million (31.1–43.9 million) individuals living with HIV globally (UNAIDS, 2018). More than 25 therapeutics have been developed for the treatment of HIV, although there is still no preventative vaccine and no functional cure (Tseng et al., 2015). The use of combination antiretroviral therapy (cART) has been shown to drastically improve the longevity and quality of life in people living with HIV infection.

While the vast majority of the infected population requires cART to achieve suppressed viral load, it has become widely accepted that some individuals are able to maintain suppression without the use of cART (reviewed in Deeks and Walker, 2007) and those who are entirely resistant to infection (Horton et al., 2010). The significance of a suppressed viral load was underscored in 2016 when it was determined that an undetectable viral load significantly reduced the risk of HIV transmission which has led to the statement "undetectable equals untransmittable" (U = U) (Cohen et al., 2011; Rodger et al., 2016). Therefore, achieving viral suppression in the majority of the infected population has become a major goal in ending the HIV epidemic. This is the motivation behind the UNAIDS (90-90-90) initiative which aims to have 90% of the global infected population diagnosed for HIV, 90% of diagnosed individuals on appropriate treatment, and 90% of individuals on treatment having viral suppression (UNAIDS, 2018). Meeting this goal by the year 2020 is a major ongoing effort by the global community with the hopes of ending the AIDS epidemic by 2030. It is likely that both existing and novel anti-HIV interventions will be required to meet this goal.

In this review, we will outline new advances in HIV host and viral genetic/genomic studies and discuss how genetic variability can modify susceptibility, disease progression and the dynamics of the host–pathogen interaction. We will also identify gaps in the current HIV genomics research and opportunities for future investigations.

BACKGROUND ON HIV AND DISEASE PROGRESSION

HIV Disease Progression

HIV disease progression consists of an acute phase where, after the initial infection, there is a peak of viral RNA and a drastic decrease of host CD4+ T cells (**Figure 1**), which can be accompanied with flu-like symptoms. The acute phase generally corresponds to a high viral titer and therefore increased transmissibility so early detection of individuals suspected of infection is important. Following acute infection, there is a brief recovery phase where there is some recovery of CD4+ T cells and a decrease of viral RNA, but then progressing into a persistent decrease of CD4+ T cells and increase of viral RNA associated with chronic stages of infection. The chronic phase can last over 10 years before an individual develops acquired immunodeficiency syndrome (AIDS) although rate of progression can vary dramatically. AIDS is defined as a CD4+ T cell count of less than 200 cells/mm^3, taken from an individual living with HIV.

During chronic, untreated infection, the amount of viral RNA in blood can remain relatively constant in an individual and is referred to as the set-point viral load (spVL). SpVL can change quite drastically between individuals but has been shown to be relatively constant within a person with a higher viral load being strongly associated with a faster disease progression (Mellors et al., 1996; O'Brien et al., 1996). Rate of disease progression is also variable in the infected population, with the majority of untreated individuals progressing to AIDS in 5–10 years (**Figure 1**). Although research has shown there are some viral and host factors which can influence the rate of progression and spVL of an individual, much of the variance in these traits remains unknown (McLaren et al., 2015).

High spVL is a public health concern due to increased transmission risk in all risk groups including intravenous drug users, men who have sex with men (MSM), and heterosexual transmission (Crepaz et al., 2016). Although most individuals undergo viral suppression during ART, small populations of individuals, called HIV controllers, are able to achieve this suppression in the absence of therapy (Cao et al., 1995). There is substantial variance in viremia between HIV controllers and progressors, as well as rate of disease progression between the two groups. There have also been several observations of both extreme long-term non-progression and extreme rapid progression, although their definitions are not consistently held (Gurdasani et al., 2014; Olson et al., 2014). HIV controllers and progressors have been important populations of study to determine the effects of viral, host, and environmental factors which contribute to the variance in viral load and disease progression.

The ability of an individual to suppress their viral load, in the absence or with the assistance of cART, can significantly decrease HIV disease progression and greatly improve quality of life. This phenomenon has warranted a large amount of time to research the variability of HIV disease progression and has resulted in a wealth of knowledge regarding the complex interaction of HIV and host proteins. There are many factors which impact HIV disease progression such as viral and host genetic diversity, host–pathogen interaction and environmental factors. Although the root causes of variability in spVL and rates of progression are not fully understood, one area that has received significant attention, and produced significant discoveries, is the role of viral and host genetic variability, and the dynamics of host–pathogen interaction.

Methods for Studying Genetic Diversity

Genome-wide genotyping and sequencing studies have marked a shift in the direction of human genetic research from the use of

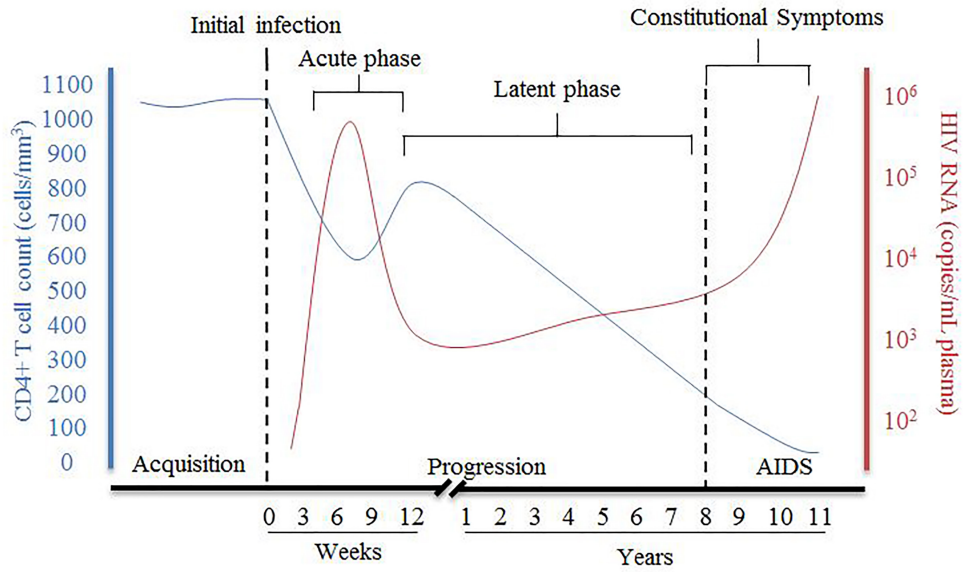

FIGURE 1 | Summary of pathogenesis of HIV infection in the presence of combined antiretroviral therapy. The disease progression of HIV in this figure is represented by the relative CD4+ T cell count in cells/mm^3 (blue) and HIV viral RNA in copies/mL plasma (red) and their relationship during HIV from acquisition to the development of AIDS [Figure was adapted from An and Winkler (2010)].

candidate gene studies to genome-wide approaches allowing for the identification of large number of genetic variants associated with control of HIV infection. Genome-wide association studies (GWAS) provide an unbiased scan of the genome for common single nucleotide polymorphisms (SNPs) and small insertions and deletions (indels) associated with a particular trait (e.g., viral load). While these types of studies do not provide any causal information, they direct researchers to a region of interest which requires further studies to determine causality. However, GWAS require strict statistical standards and require large sample sizes which can make study designs difficult (Ioannidis et al., 2011).

HIV GENETIC IMPACT ON HIV PATHOGENESIS

HIV Viral Diversity

The global HIV pandemic originated from the independent zoonotic transmission events between non-human primates and humans which resulted in four different groups of HIV M, N, O, and P (Keele et al., 2006; reviewed in Taylor et al., 2008; Vallari et al., 2011). HIV group M, which is responsible for the majority of global infections, can be separated into eight genetically distinct subtypes: A, B, C, D, F, G, H, J, and K with additional circulating recombinant forms (CRFs) that have also been observed. Due to the high error rate of the reverse transcriptase (RT) enzyme and the rapid replication rate of HIV, the virus is able to generate large numbers of mutations within its genome (Fryer et al., 2010; Cuevas et al., 2015; Roberts et al., 2016). These viral mutations, if beneficial for survival, can create quasispecies that are resistant to immune responses (Crawford et al., 2009; Bronke et al., 2013) and antiretroviral therapy (Roche et al., 2011; Hayashida et al., 2016). If these mutations enhance the viruses' ability to circumvent cART or host defense mechanisms, they are termed escape mutations. Escape mutations may be at a cost of viral fitness resulting in a more resistant virus but with decreased virulence within the host (Fryer et al., 2012; Song et al., 2012; Shahid et al., 2015). There have also been reports of specific escape mutations causing decreased viral fitness during transmission to a new host (Chopera et al., 2008). While the host immune system exerts strong selective pressure on HIV to develop escape mutations, evidence shows that this process is slowed in the presence of cART (Knapp et al., 2012).

Viral Sequencing

Since HIV has such a high mutation rate, viral sequencing is an essential process for determining potential drug resistance at the beginning of treatment. Early detection of drug resistance is necessary to help guide treatments options which are most suitable for a particular patient. This process is traditionally performed by sequencing plasma HIV RNA and looking for known variants in the RT, protease (PR), and integrase (IN) genes that are associated with resistance. Recently, the field of HIV sequencing has started a shift from traditional Sanger sequencing methods toward next generation sequencing (NGS) for the detection of low frequency viral variants. While NGS is able to detect more variants than traditional RNA or DNA Sanger sequencing, the clinical relevance of low frequency viral variants still requires more investigation before use in a clinical setting (Alidjinou et al., 2017; Inzaule et al., 2018). Particularly, HIV exists as a number of quasispecies within a host resulting

in a large amount of intra-host genetic diversity which can make interpretation of sequencing results challenging.

Impact of HIV Viral Subtype and Sequence Diversity on Pathogenesis

Viral sequence diversity has been shown to affect disease progression independently of host factors (Pai et al., 2012). Current evidence suggests subtype D is associated with faster disease progression when compared to subtype A. In Africa, subtype D had a faster disease progression than subtype A during the pre-ART period (Vasan et al., 2006; Kiwanuka et al., 2008; Ssemwanga et al., 2013). In a large study using data from the CASCADE collection (3364 seroconverting individuals of known subtype), they observed slower CD4+ T cell decline in individuals infected by subtypes A, C, and CRF02 compared to those infected with subtype B (Touloumi et al., 2013). However, in an analysis adjusting for demographic factors there was no significant difference in time to AIDS or median viral load set point between individuals infected by different subtypes. The results of the study also show that recombinant CRF01 and CRF02 are not more virulent than parent isolates (Touloumi et al., 2013).

Investigations of within subtype diversity have also identified some differences in rates of progression. In a study looking at 8483 United Kingdom patients prior to antiretroviral therapy, genetic diversity in the polymerase gene explained roughly 5.7% of the variance of spVL in subtype B infected individuals (Hodcroft et al., 2014). More recently, studies of near full-length HIV sequences in the Swiss HIV Cohort Study have suggested that the viral genome can explain up to 30% of the observed variance in spVL (Bartha et al., 2017; Bertels et al., 2018). Additional studies in clade B and across multiple clades, have resulted in similar heritability estimates with viral genotype explaining between 26 and 44% of observed variance in spVL (reviewed in Bonhoeffer et al., 2015).

While viral sequence variation can have a direct impact on disease progression causing increased or decreased viral load, this may be reflecting host genetic pressure on spVL as variation of viral sequences can be attributed to escape mutations. In a joint host/viral genetic analysis, 23.6% of the variability in HIV spVL mapped to known epitope regions, suggesting that this variability is the result of pathogen evolution away from host HLA (Bartha et al., 2017). Furthermore, the authors showed that by not accounting for viral genetics that reliability of heritability estimates by host genetic studies may be impacted.

At the population level, adaptation of the viral genome to host HLA can impact the rate of disease progression to prevent detection and elimination of the virus by CD8+ T cells. There are many HLA alleles which have been associated with control of HIV infection. HLA-B*57:01 is known to strongly decrease the rate of disease progression, however, across multiple continents; it has been shown that HIV is developing an escape mutation, I135X, which attenuates control (Kawashima et al., 2009). Similarly, the protective allele HLA-B*52:01-C*12:02 is associated with decreased viral load in Japan due to the development of escape mutations in the *pol* gene of HIV which causes poor viral fitness (Murakoshi et al., 2017). These escape mutations allow the virus to evade HLA detection and change the dynamics of disease progression, albeit at the cost of viral fitness. Additional studies in Africa (Payne et al., 2014) and North America (Brumme et al., 2018) have also demonstrated local adaptation of HIV to common HLA alleles, with a potential impact on disease progression rates in the population.

While the impact of HIV sequence variation on disease progression can be an important factor for determining the prognosis of disease and for the development of therapeutics, the impact of host genetics should not be ignored due to the complex interaction of host and viral proteins during disease progression.

HOST GENETICS IMPACT ON HIV PATHOGENESIS

Influence of Human Genetic Diversity on HIV

Previous research has shown that some individuals of European ancestry have homozygous loss-of-function of the C-C motif chemokine receptor 5 (*CCR5)* gene, the only genotype which has consistently associated with protection against acquisition of HIV infection (Samson et al., 1996). Several other genes have been claimed to confer resistance to infection, usually through candidate gene studies, however, these have not been replicated by large GWAS (McLaren et al., 2013). The class 1 human leukocyte antigen (HLA) genes, in particular HLA-B, have been consistently replicated as the major host genetic determinant of HIV viral load and rate of disease progression (McLaren et al., 2015). Similarly, -35 HLA-C variant has been shown to strongly influence spVL and that high HLA-C expression is associated with better control of HIV disease than individuals with lower expression (Thomas et al., 2009). While other genes have been proposed, it is uncertain whether common genetic variants outside of the *HLA* and *CCR5* regions have significant impact on HIV disease progression.

Effect of Host Genetics on Acquisition

Before the use of GWAS, candidate genes studies were the primary method for identifying genes involved in the acquisition and progression of HIV. These types of studies required understanding of the biological mechanisms of infection, such as gp120 binding to cell surface receptors, for the identification of potential therapeutic or vaccine targets. In a study of HIV-exposed seronegative (HESN) patients in 1996, it was discovered that a 32-bp deletion in the gene CCR5 was able to greatly reduce or prevent infection in HIV-exposed individuals homozygous for the deletion allele (Dean et al., 1996). The CCR5Δ32 variant causes the truncated protein to no longer be expressed on the cell surface (Agrawal et al., 2004) and also associated with reduced disease progression in heterozygous individuals. To date, this deletion variant has not been observed at high frequency in any populations other than Europeans and is the only host genetic variant that has been consistently observed at preventing the acquisition of HIV.

Since the discovery CCR5Δ32, substantial research has been done to identify other genetic variants associated with reduction of HIV susceptibility. Many of these studies have focused on highly HIV exposed seronegative individuals and high-risk populations for identification of susceptibility factors. One large study attempting to determine genetic variants associated with acquisition of HIV examined 848 HIV-negative cases and 531 HIV-positive controls and tested approximately 800,000 SNPs (Petrovski et al., 2011). However, they did not detect any regions which met genome-wide significance following quality control and correction for multiple comparisons.

Recently, a study of the Urban Health Study (UHS) cohort of individuals of African (628 cases and 1376 controls) and European (327 cases and 805 controls) ancestry used a large population size in a high risk population to identify susceptibility variants (Johnson et al., 2015). They reported a region in chromosome 19 which met genome-wide significance ($P < 5 \times 10^{-8}$) and six other regions which had suggestive significance ($P < 1 \times 10^{-6}$). However, these results require further investigation as a 2013 study of 6334 patients and 7247 controls of European ancestry was unable to detect any SNPs, outside the major histocompatibility complex (MHC) region of chromosome 6, that met genome-wide significance (McLaren et al., 2013). Thus, the consistent identification of genes that limit HIV susceptibility remains an active area of research.

Effect of Host Genetics on Viral Load

Upon infection with HIV, the immune system recognizes the presence of the virus through the use of the MHC encoded by HLA genes. These proteins are highly variable and certain *HLA* variants have been implicated in control of HIV infection in diverse populations (Fellay et al., 2009; Pereyra et al., 2010; Leszczyszyn-Pynka et al., 2015). Specifically, *HLA-B* alleles have been identified in several populations as being significantly associated with viral load (Fellay et al., 2009; McLaren et al., 2015). These variants are thought to modify specificity of antigen presentation which can allow differential targeting of HIV-infected cells.

An international consortium study looking at 974 HIV controllers (cases) and 2648 progressors (controls), determined that in European samples (1712 individuals) and African American samples there were no variants that met genome-wide significance outside of the MHC region of chromosome 6 (Pereyra et al., 2010). This study emphasized that the major host genetic determinant of HIV control, in the context of the whole genome, are the *HLA* alleles and *CCR5* genes. When considering the European subset, they identified 313 significant variants all in the MHC region and showed that four of these SNPs explained 19% of the variance in the HIV controller trait.

In a study of African HIV serodiscordant couples from Partners in Prevention HSC/HIV Transmission Study and Couples Observational Study cohorts to determine the effect of host genetics and genital factors (i.e., male circumcision, bacterial vaginosis, or use of acyclovir) of the transmitter on spVL (Mackelprang et al., 2015). *HLA* variants (B*53:01, B*14:01, and B*27:03) and Toll-like receptors (TLR) polymorphisms (TLR2 rs3804100 and TLR7 rs179012) explained 13% and 5% of the variance in viral load, respectively. Other factors, such as plasma HIV levels of the transmitting partner and HLA-concordance between partners were able to explain 10% and 6% of the variance, respectively. Additionally, incorporation of genital factors of the transmitting partner was able to explain 46% of the variation of spVL in this population (Mackelprang et al., 2015).

In the largest spVL genome-wide association study to date including 6315 individuals of European ancestry, it was determined that 24.6% of the observed variability in spVL could be attributed to common human genetic polymorphisms (McLaren et al., 2015). This study again identified *HLA* alleles and *CCR5Δ32* as the only two regions associated with viral load, with no other variants surpassing statistical significance. However, there was a small but measurable contribution (∼5%) from combined common additive effects outside the MHC and CCR5 regions (McLaren et al., 2015).

The MHC region was also observed in a study 538 individuals across three diverse Chinese populations (HAN, YUN, XIN) where it was the only region that met genome-wide significance (Wei et al., 2015). In this study, the authors note that, although the same region has been implicated in other populations (European and African American), the identification and significance of variants varied greatly. The authors proposed that this is because linkage patterns between tagged SNPs and causal variants may differ per population, and that there may be different causal variants in these Chinese populations compared to Europeans and African populations, and/or minor allele frequency in the populations may result in different associated SNPs (Wei et al., 2015).

Taken together, these studies show that host genetics can explain roughly 30% of variance in viral load, however, a majority of the remaining variance is still unknown but is thought to be environmental factors and/or unidentified host factors. Therefore, to better understand variation in HIV disease progression related to spVL, more research is needed in larger samples using novel analytical methods that provide more power for detecting smaller genetic effects and additional ancestry groups for identifying non-European variants.

CHARACTERIZING THE HOST–PATHOGEN INTERACTION THROUGH HIV HOST DEPENDENCY FACTORS

In order to understand the pathogenesis of HIV infection, it is important to explore how viral and host proteins interact. HIV only encodes nine genes and requires the use of host proteins to establish and maintain infection, termed HIV host dependency factors (HDFs) (Brass et al., 2008). Generally, there have been two different genome-wide methods employed to identify these interactions including: genome-wide siRNA knockout screens and more recently genome-wide CRISPR knockouts. These methods have identified multiple HDFs, however, the precise pathways involved often differ, possibly dependent on the specific methods used.

RNA-interference (RNAi) based studies are popular for identifying large numbers of HDFs required for establishing and maintaining infectious diseases and three initial studies proposed over 800 HDFs required during HIV infection (Brass et al., 2008; König et al., 2008; Zhou et al., 2008). The first RNAi-based HIV HDF study aimed to characterize HDFs involved in pathogenesis through two different screens (Brass et al., 2008). The first screen used HIV-IIIB to identify host proteins involved with viral entry and Gag translation but was unable to identify proteins involved in viral assembly and budding. This was subsequently addressed by a second screen performed in HeLa-derived TZM-bl cells, expressing transgenic CD4 and CCR5, to identify factors involved in viral assembly and budding (Brass et al., 2008). While HeLa cells are not physiologically relevant to HIV pathogenesis, they provide insight into some potential cellular functions that can be replicated or confirmed using primary CD4+ T cells.

Shortly after, König et al. (2008) used a similar RNAi method to determine host factors associated with early infection (König et al., 2008). This study identified 295 genes and, when compared to the 283 genes determined by Brass et al. (2008), discovered 13 genes that were statistically significant in both screens (Brass et al., 2008; König et al., 2008). The difference may be due to the different cell lines used between the studies or variation of the lentiviral vector used for transfection of the study (**Table 1**).

Zhou et al. (2008) used β-gal activity after 48 h, to identify host factors associated with viral entry, or at 96 h to identify factors responsible at all stages of infection (Zhou et al., 2008). Of the 232 HDFs identified in this screen, 15 overlapped with Brass et al. (2008) (Zhou et al., 2008). Although, limited, it was determined that this overlap was higher than what would be expected by chance alone. The authors acknowledged that the differences between genes identified in their study and the previous Brass et al. (2008) study may be due to transfection time, type of reporter (Tat-driven or p24), and/or the nature of the algorithm-generated siRNA libraries (Brass et al., 2008; Zhou et al., 2008). While these screens have little consistency of identified genes, they do detect genes within the same biological processes. For example the SP1/mediator complex and the NF-κB signaling pathways (Zhou et al., 2008). Subsequently, a meta-analysis of these three screens determined that there was significant functional overlap of the implicated genes at the pathway level, implicating Nuclear Pore/Transport, GTP Binding, Protein Complex Assembly, and DNA repair (Bushman et al., 2009). These studies propose that ∼9.5% of human protein coding genes are now implicated in HIV replication (Brass et al., 2008; König et al., 2008; Zhou et al., 2008; Bushman et al., 2009).

TABLE 1 | Summary of RNAi and CRISPR-Cas9 genome-wide knockout experiment characteristics for the study of HIV disease.

Study (Year)	Type of screen	Cell types[1]	HIV-1 strains[2]	Reference
Brass et al., 2008	RNAi	HeLa-derived TZM-bl cells	HIV-1 IIIB	Brass et al., 2008
König et al., 2008	RNAi	HEK-293 T cells	HIV-1 VSV-G	König et al., 2008
Zhou et al., 2008	RNAi	HeLa P4-R5	HIV-1 HXB2	Zhou et al., 2008
Zhu et al., 2014	RNAi	HeLa MAGI	HIV-1 IIIB	Zhu et al., 2014
Park et al., 2017	CRISPR	GXRCas9	HIV-1 JR-CSF	Park et al., 2017

[1]Cell types used for RNAi or CRISPR screening. [2]HIV-1 strains used for RNAi screens.

In a more recent study by Zhu et al. (2014), they used Multiple Orthologous RNAi Reagent (MORR) screens as well as an RNAi Gene Enrichment Ranking (RIGER) method in order to minimize false positives and negatives (Zhu et al., 2014). This study identified c3orf58 (renamed GOLGI49*), SEC13, COG, and THOC2 as key HDFs and characterized the roles of these genes *in vitro*. Notably, GOLGI49 was identified as a Golgi protein and during knock-down shown to decrease replication of both HIV IIIB (X4-tropic) and BaL (R5-tropic) viruses (Zhu et al., 2014). THOC2, and by association the THO/TREX complex, was identified as a potential key complex involved in regulation of HIV replication, however, more studies are needed to determine the mechanism of action (Zhu et al., 2014). SUPT16H was identified by the RNAi screen and later confirmed to play a key role in HIV transcription (Zhu et al., 2014; Huang et al., 2015). SEC13 was determined to play an essential role in viral replication prior to viral integration but after nuclear import in both Jurkat and primary CD4+ T cells.

Although strategies like MORR-RIGER and Genome-wide Enrichment of Seed Sequence (GESS) analysis can reduce false positives and off target effects, further techniques and standardizations are required. There is currently no standard cell line for HDF work with groups which may explain the variable results observed in these studies. HeLa-derived cell lines and MAGI cells require the addition of CCR5 to become susceptible to R5-tropic HIV infection which strains their physiological relevance. Therefore, without consistent use of cell-types, the physiological landscape of protein expression may cause increased variation and further deviation from the expected in primary cell lines.

Recently, genome-wide CRISPR knockouts screens have become more popular for generation of loss-of-function variants as they have increased knock-out reliability and decreased off target effects compared to siRNA methods (Shalem et al., 2014; Wang et al., 2014). This technology allows for targeting of various host cells with increased efficacy to address concerns that RNAi based screening can allow for low-level protein expression. Indeed, it has been shown that the use of CRISPR-Cas9 lentiviral single-guide RNA constructs can achieve greater specificity and sensitivity than the use of RNAi-based screens previously allowed (Park et al., 2017).

In a genome-wide CRISPR knockout study, novel host–pathogen interactions involving *TPST2*, *SLC35B2*, and *ALCAM* during HIV pathogenesis were identified, not seen by the previous RNAi-based screens (Park et al., 2017). They showed infection inhibition in primary human CD4+ T cells supporting these factors as key genes in HIV infection with loss-of-function variants without impairing cell viability. *TPST2* and *SLC35B2* were shown to be involved in sulfation of CCR5 on extracellular tyrosine residues (Park et al., 2017). Knockdown of TPST2

and SLC35B2 prevented proper extracellular folding of CCR5, thereby inhibiting interaction with viral gp120. While the role of *ALCAM* is not fully understood, Park et al. showed it was required for effective cell-to-cell transmission of HIV. Importantly, the genome-wide CRISPR knockout approach of Park et al. can be modified for use of studying entry of other viruses (Schott and König, 2017).

While CRISPR and RNAi technology has identified large numbers of potential HDFs in model systems, the relevance in humans is still unclear. While cell lines may be able to survive with a particular gene knockdown, whether the gene is essential for human life cannot be determined from the present screening data. However, the Genome Aggregation Database (gnomAD)[a], has over 15,000 whole-genome and over 120,000 exome sequences which can be used to identify individuals with predicted homozygous loss-of-function alleles. If an individual is healthy with a homozygous loss-of-function allele, the gene is likely not essential for human life and may make a valuable drug therapy target.

CONCLUSION

It has been clearly demonstrated that both host and viral genetics play a vital role in determining HIV acquisition and disease progression. Current evidence supports the role that viral subtype has an effect on disease progression, however, there is also evidence against this claim. Overall, viral diversity has been demonstrated to have an impact of disease progression and therefore, it is important to study disease progression in the context of both host and viral genetics.

As GWAS have become a useful tool for discovering novel variants associated with a particular trait, it is important to recognize that their use is limited by the diversity of the target population. In 2016, it was reported that "genomics is failing on diversity" with the vast majority (81% over 2511 studies) of GWAS, in all disciplines, being performed in individuals of European ancestry in 2016 (Popejoy and Fullerton, 2016). These tools have not been used to their full potential and replication of studies within large, diverse populations may yield novel associations. While GWAS of other phenotypes have benefitted from cohorts of over 100,000, the largest cohort of HIV was only 6315 individuals. Larger sample sizes are required for the detection of genetic variants outside of the MHC and CCR5 regions, and this will require additional investment in developing new and diverse cohorts and acquiring the required clinical and genetic data.

Genome-wide knockout studies have great potential for studying the effects of HDFs for a variety of infectious diseases; however, translation of their physiological relevance in primary cells or *in vivo* remains an area of active research. Cross-referencing the genes from RNAi and CRISPR genome-wide studies with large databases such as gnomAD for identification of genes which have homozygous loss-of-function in individuals of various populations could provide interesting avenues for new therapeutics. This is akin to reading the *natural experiment* where healthy individuals with a homozygous loss-of-function gene purported to be necessary for HIV replication could act as valuable resources to determine the gene's action *in vivo*.

As the field of genomics continues to evolve, there is opportunity to leverage the growing wealth of information available to better understand disease acquisition and progression.

AUTHOR CONTRIBUTIONS

RT and PM conceived and wrote the manuscript.

REFERENCES

Agrawal, L., Lu, X., Qingwen, J., VanHorn-Ali, Z., Nicolescu, I. V., McDermott, D. H., et al. (2004). Role for CCR5Delta32 protein in resistance to R5, R5X4, and X4 human immunodeficiency virus type 1 in primary CD4+ cells. *J. Virol.* 78, 2277–2287. doi: 10.1128/JVI.78.5.2277

Alidjinou, E. K., Deldalle, J., Hallaert, C., Robineau, O., Ajana, F., Choisy, P., et al. (2017). RNA and DNA sanger sequencing versus next-generation sequencing for HIV-1 drug resistance testing in treatment-naive patients. *J. Antimicrob. Chemother.* 72, 2823–2830. doi: 10.1093/jac/dkx232

An, P., and Winkler, C. A. (2010). Host genes associated with HIV/AIDS: advances in gene discovery. *Trends Genet.* 26, 119–131. doi: 10.1016/j.tig.2010.01.002

Bartha, I., McLaren, P. J., Brumme, C., Harrigan, R., Telenti, A., and Fellay, J. (2017). Estimating the respective contributions of human and viral genetic variation to HIV control. *PLoS Comput. Biol.* 13:e05339. doi: 10.1371/journal.pcbi.1005339

Bertels, F., Marzel, A., Leventhal, G., Mitov, V., Fellay, J., Günthard, H. F., et al. (2018). Dissecting HIV virulence: heritability of setpoint viral load, CD4+ T-cell decline, and per-parasite pathogenicity. *Mol. Biol. Evol.* 35, 27–37. doi: 10.1093/molbev/msx246

Bonhoeffer, S., Fraser, C., and Leventhal, G. E. (2015). High heritability is compatible with the broad distribution of set point viral load in HIV carriers. *PLoS Pathog.* 11:e1004634. doi: 10.1371/journal.ppat.1004634

Brass, A. L., Dykxhoorn, D. M., Benita, Y., Yan, N., Engelman, A., Xavier, R. J., et al. (2008). Identification of host proteins required for HIV infection through a functional genomic screen. *Science (80-)* 319, 921–926. doi: 10.1126/science.1152725

Bronke, C., Almeida, C. A. M., Mckinnon, E., Roberts, S. G., Keane, N. M., Chopra, A., et al. (2013). HIV escape mutations occur preferentially at HLA-binding sites of CD8 T-cell epitopes. *Aids* 27, 899–905. doi: 10.1097/QAD.0b013e32835e1616

Brumme, Z. L., Kinloch, N. N., Sanche, S., Wong, A., Martin, E., Cobarrubias, K. D., et al. (2018). Extensive host immune adaptation in a concentrated North American HIV epidemic. *AIDS* 32, 1927–1938. doi: 10.1097/QAD.0000000000001912

Bushman, F. D., Malani, N., Fernandes, J., D'Orso, I., Cagney, G., Diamond, T. L., et al. (2009). Host cell factors in HIV replication: meta-analysis of genome-wide studies. *PLoS Pathog.* 5:e1000437. doi: 10.1371/journal.ppat.1000437

Cao, Y., Qin, L., Zhang, L., Safrit, J., and Ho, D. D. (1995). Virologic and immunologic characterization of long-term survivors of human immunodeficiency virus type 1 infection. *N. Engl. J. Med.* 332, 201–208. doi: 10.1056/NEJM199501263320401

Chopera, D. R., Woodman, Z., Mlisana, K., Mlotshwa, M., Martin, D. P., Seoighe, C., et al. (2008). Transmission of HIV-1 CTL escape variants provides HLA-mismatched recipients with a survival advantage. *PLoS Pathog.* 4:e1000033. doi: 10.1371/journal.ppat.1000033

Cohen, M. S., Chen, Y. Q., McCauley, M., Gamble, T., Hosseinipour, M. C., Kumarasamy, N., et al. (2011). Prevention of HIV-1 infection with early

antiretroviral therapy. *N. Engl. J. Med.* 365, 493–505. doi: 10.1056/NEJMoa1105243

Crawford, H., Lumm, W., Leslie, A., Schaefer, M., Boeras, D., Prado, J. G., et al. (2009). Evolution of HLA-B*5703 HIV-1 escape mutations in HLA-B*5703–positive individuals and their transmission recipients. *J. Exp. Med.* 206, 909–921. doi: 10.1084/jem.20081984

Crepaz, N., Tang, T., Marks, G., Mugavero, M. J., Espinoza, L., and Hall, H. I. (2016). Durable viral suppression and transmission risk potential among persons with diagnosed HIV infection: United States, 2012-2013. *Clin. Infect. Dis.* 63, 976–983. doi: 10.1093/cid/ciw418

Cuevas, J. M., Geller, R., Garijo, R., López-Aldeguer, J., and Sanjuán, R. (2015). Extremely high mutation rate of HIV-1 in vivo. *PLoS Biol.* 13:e1002251. doi: 10.1371/journal.pbio.1002251

Dean, M., Carrington, M., Winkler, C., Huttley, G. A., Smith, M. W., Allikmets, R., et al. (1996). Genetic restriction of HIV-1 infection and progression to AIDS by a deletion allele of the CKR5 structural gene. *Science* 273, 1856–62. doi: 10.1126/science.273.5283.1856

Deeks, S. G., and Walker, B. D. (2007). Human immunodeficiency virus controllers: mechanisms of durable virus control in the absence of antiretroviral therapy. *Immunity* 27, 406–416. doi: 10.1016/j.immuni.2007.08.010

Fellay, J., Ge, D., Shianna, K. V., Colombo, S., Ledergerber, B., Cirulli, E. T., et al. (2009). Common genetic variation and the control of HIV-1 in humans. *PLoS Genet.* 5:e1000791. doi: 10.1371/journal.pgen.1000791

Fryer, H. R., Frater, J., Duda, A., Palmer, D., Phillips, R. E., and McLean, A. R. (2012). Cytotoxic T-lymphocyte escape mutations identified by HLA association favor those which escape and revert rapidly. *J. Virol.* 86, 8568–8580. doi: 10.1128/JVI.07020-11

Fryer, H. R., Frater, J., Duda, A., Roberts, M. G., Phillips, R. E., and McLean, A. R. (2010). Modelling the evolution and spread of HIV immune escape mutants. *PLoS Pathog.* 6:e1001196. doi: 10.1371/journal.ppat.1001196

Gurdasani, D., Iles, L., Dillon, D. G., Young, E. H., Olson, A. D., Naranbhai, V., et al. (2014). A systematic review of definitions of extreme phenotypes of HIV control and progression. *AIDS* 28, 149–162. doi: 10.1097/QAD.0000000000000049

Hayashida, T., Hachiya, A., Ode, H., Nishijima, T., Tsuchiya, K., Sugiura, W., et al. (2016). Rilpivirine resistance mutation E138K in HIV-1 reverse transcriptase predisposed by prevalent polymorphic mutations. *J. Antimicrob. Chemother.* 71, 2760–2766. doi: 10.1093/jac/dkw224

Hodcroft, E., Hadfield, J. D., Fearnhill, E., Phillips, A., Dunn, D., O'Shea, S., et al. (2014). The contribution of viral genotype to plasma viral set-point in HIV infection. *PLoS Pathog.* 10:e1004112. doi: 10.1371/journal.ppat.1004112

Horton, R. E., McLaren, P. J., Fowke, K., Kimani, J., and Ball, T. B. (2010). Cohorts for the study of HIV-1–Exposed but uninfected individuals: benefits and limitations. *J. Infect. Dis.* 202, S377–S381. doi: 10.1086/655971

Huang, H., Santoso, N., Power, D., Simpson, S., Dieringer, M., Miao, H., et al. (2015). FACT proteins, SUPT16H and SSRP1, are transcriptional suppressors of HIV-1 and HTLV-1 that facilitate viral latency. *J. Biol. Chem.* 290, 27297–27310. doi: 10.1074/jbc.M115.652339

Inzaule, S. C., Hamers, R. L., Noguera-Julian, M., Casadellà, M., Parera, M., Kityo, C., et al. (2018). Clinically relevant thresholds for ultrasensitive HIV drug resistance testing: a multi-country nested case-control study. *Lancet HIV* 5, e638–e646. doi: 10.1016/S2352-3018(18)30177-2

Ioannidis, J. P. A., Tarone, R., and McLaughlin, J. K. (2011). The false-positive to false-negative ratio in epidemiologic studies. *Epidemiology* 22, 450–456. doi: 10.1097/EDE.0b013e31821b506e

Johnson, E. O., Hancock, D. B., Gaddis, N. C., Levy, J. L., Page, G., Novak, S. P., et al. (2015). Novel genetic locus implicated for HIV-1 acquisition with putative regulatory links to HIV replication and infectivity: a genome-wide association study. *PLoS One* 10:e0118149. doi: 10.1371/journal.pone.0118149

Kawashima, Y., Pfafferott, K., Frater, J., Matthews, P., Payne, R., Addo, M., et al. (2009). Adaptation of HIV-1 to human leukocyte antigen class I. *Nature* 458, 641–645. doi: 10.1038/nature07746

Keele, B. F., Van Heuverswyn, F., Li, Y., Bailes, E., Takehisa, J., Santiago, M. L., et al. (2006). Chimpanzee reservoirs of pandemic and nonpandemic HIV-1. *Science (80-)* 313, 523–526. doi: 10.1126/science.1126531

Kiwanuka, N., Laeyendecker, O., Robb, M., Kigozi, G., Arroyo, M., McCutchan, F., et al. (2008). Effect of human immunodeficiency virus type 1 (HIV-1) subtype on disease progression in persons from rakai, Uganda, with Incident HIV-1 Infection. *J. Infect. Dis.* 197, 707–713. doi: 10.1086/527416

Knapp, D. J., Brumme, Z. L., Huang, S. Y., Wynhoven, B., Dong, W. W., Mo, T., et al. (2012). Increasingly successful highly active antiretroviral therapy delays the emergence of new HLA class I-associated escape mutations in HIV-1. *Clin. Infect. Dis.* 54, 1652–1659. doi: 10.1093/cid/cis253

König, R., Zhou, Y., Elleder, D., Diamond, T. L., Bonamy, G. M. C., Irelan, J. T., et al. (2008). Global analysis of host-pathogen interactions that regulate early-stage HIV-1 replication. *Cell* 135, 49–60. doi: 10.1016/j.cell.2008.07.032

Leszczyszyn-Pynka, M., Aksak-Was, B., Urbańska, A., and Parczewski, M. (2015). Protective effect of HLA-B* 5701 and HLA-C-35 genetic variants in HIV-positive caucasians from northern poland. *PLoS One* 10:e0127867. doi: 10.1371/journal.pone.0127867

Mackelprang, R. D., Carrington, M., Thomas, K. K., Hughes, J. P., Baeten, J. M., Wald, A., et al. (2015). Host genetic and viral determinants of HIV-1 RNA set point among HIV-1 seroconverters from sub-saharan africa. *J. Virol.* 89, 2104–2111. doi: 10.1128/JVI.01573-14

McLaren, P. J., Coulonges, C., Bartha, I., Lenz, T. L., Deutsch, A. J., Bashirova, A., et al. (2015). Polymorphisms of large effect explain the majority of the host genetic contribution to variation of HIV-1 virus load. *Proc. Natl. Acad. Sci. U.S.A.* 112, 14658–14663. doi: 10.1073/pnas.1514867112

McLaren, P. J., Coulonges, C., Ripke, S., van den Berg, L., Buchbinder, S., Carrington, M., et al. (2013). Association study of common genetic variants and HIV-1 acquisition in 6,300 infected cases and 7,200 controls. *PLoS Pathog.* 9:e1003515. doi: 10.1371/journal.ppat.1003515

Mellors, J. W., Rinaldo, C. R., Gupta, P., White, R. M., Todd, J. A., and Kingsley, L. A. (1996). Prognosis in HIV-1 infection predicted by the quantity of virus in plasma. *Science* 272, 1167–1170. doi: 10.1126/science.272.5265.1167

Murakoshi, H., Koyanagi, M., Chikata, T., Rahman, M. A., Kuse, N., Sakai, K., et al. (2017). Accumulation of pol mutations selected by HLA-B*52:01-C*12:02 protective haplotype-restricted cytotoxic T lymphocytes causes low plasma viral load due to low viral fitness of mutant viruses. *J. Virol.* 91, 1–13. doi: 10.1128/JVI.02082-16

O'Brien, T. R., Blattner, W. A., Waters, D., Eyster, E., Hilgartner, M. W., Cohen, A. R., et al. (1996). Serum HIV-1 RNA levels and time to development of AIDS in the multicenter hemophilia cohort study. *JAMA* 276, 105–110. doi: 10.1001/jama.1996.03540020027025

Olson, A. D., Guiguet, M., Zangerle, R., Gill, J., Perez-Hoyos, S., Lodi, S., et al. (2014). Evaluation of rapid progressors in HIV infection as an extreme phenotype. *J. Acquir. Immune Defic. Syndr.* 67, 15–21. doi: 10.1097/QAI.0000000000000240

Pai, N. P., Shivkumar, S., and Cajas, J. M. (2012). Does genetic diversity of HIV-1 non-B subtypes differentially impact disease progression in treatment-naive HIV-1-infected individuals? A systematic review of evidence: 1996-2010. *J. Acquir. Immune Defic. Syndr.* 59, 382–388. doi: 10.1097/QAI.0b013e31824a0628

Park, R. J., Wang, T., Koundakjian, D., Hultquist, J. F., Lamothe-Molina, P., Monel, B., et al. (2017). A genome-wide CRISPR screen identifies a restricted set of HIV host dependency factors. *Nat. Genet.* 49, 193–203. doi: 10.1038/ng.3741

Payne, R., Muenchhoff, M., Mann, J., Roberts, H. E., Matthews, P., Adland, E., et al. (2014). Impact of HLA-driven HIV adaptation on virulence in populations of high HIV seroprevalence. *Proc. Natl. Acad. Sci. U.S.A.* 111, E5393–E5400. doi: 10.1073/pnas.1413339111

Pereyra, F., Jia, X., Mclaren, P. J., Kadie, C. M., Carlson, J. M., Heckerman, D., et al. (2010). The major genetic determinants of HIV-1 control affect HLA class I peptide presentation. *Science (80-)* 330, 1551–1557. doi: 10.1126/science.1195271

Petrovski, S., Fellay, J., Shianna, K. V., Carpenetti, N., Kumwenda, J., Kamanga, G., et al. (2011). Common human genetic variants and HIV-1 susceptibility: a genome-wide survey in a homogeneous African population. *AIDS* 25, 513–518. doi: 10.1097/QAD.0b013e328343817b

Popejoy, A. B., and Fullerton, S. M. (2016). Genomics is failing on diversity. *Nature* 538, 161–164. doi: 10.1038/538161a

Roberts, J. D., Bebenek, K., and Kunkel, T. A. (2016). The accuracy of reverse transcriptase. *Am. Assoc. Adv. Sci.* 242, 1171–1173.

Roche, M., Jakobsen, M. R., Sterjovski, J., Ellett, A., Posta, F., Lee, B., et al. (2011). HIV-1 escape from the CCR5 antagonist maraviroc associated with an altered and less-efficient mechanism of gp120-CCR5 engagement that attenuates macrophage tropism. *J. Virol.* 85, 4330–4342. doi: 10.1128/JVI.00106-11

Rodger, A. J., Cambiano, V., Bruun, T., Vernazza, P., Collins, S., Van Lunzen, J., et al. (2016). Sexual activity without condoms and risk of HIV transmission in serodifferent couples when the HIV-positive partner is using suppressive antiretroviral therapy. *JAMA - J. Am. Med. Assoc.* 316, 171–181. doi: 10.1001/jama.2016.5148

Samson, M., Libert, F., Doranz, B. J., Rucker, J., Liesnard, C., Farber, C.-M., et al. (1996). Resistance to HIV-1 infection in Caucasian individuals bearing mutant alleles of the CCR-5 chemokine receptor gene. *Nature* 382, 722–725. doi: 10.1038/382722a0

Schott, K., and König, R. (2017). Picking the survivor! CRISPR reveals HIV dependency factors. *Trends Microbiol.* 25, 243–245. doi: 10.1016/j.tim.2017.02.004

Shahid, A., Olvera, A., Anmole, G., Kuang, X. T., Cotton, L. A., Plana, M., et al. (2015). Consequences of HLA-B*13-associated escape mutations on HIV-1 replication and Nef function. *J. Virol.* 89:JVI.01955-15. doi: 10.1128/JVI.01955-15

Shalem, O., Sanjana, N. E., Hartenian, E., Shi, X., Scott, D. A., Mikkelsen, T. S., et al. (2014). Genome-scale CRISPR-Cas9 knockout screening in human cells. *Science (80-)* 343, 84–87. doi: 10.1126/science.1247005

Song, H., Pavlicek, J. W., Cai, F., Bhattacharya, T., Li, H., Iyer, S. S., et al. (2012). Impact of immune escape mutations on HIV-1 fitness in the context of the cognate transmitted/founder genome. *Retrovirology* 9:1. doi: 10.1186/1742-4690-9-89

Ssemwanga, D., Nsubuga, R. N., Mayanja, B. N., Lyagoba, F., Magambo, B., Yirrell, D., et al. (2013). Effect of HIV-1 subtypes on disease progression in rural uganda: a prospective clinical cohort study. *PLoS One* 8:e0071768. doi: 10.1371/journal.pone.0071768

Taylor, B. S., Sobieszczyk, M. E., McCutchan, F. E., and Hammer, S. M. (2008). The challenge of HIV-1 subtype diversity. *N. Engl. J. Med.* 358, 1590–1602. doi: 10.1056/NEJMra0706737

Thomas, R., Apps, R., Qi, Y., Gao, X., Male, V., O'hUigin, C., et al. (2009). HLA-C cell surface expression and control of HIV/AIDS correlate with a variant upstream of HLA-C. *Nat. Genet.* 41, 1290–1294. doi: 10.1038/ng.486

Touloumi, G., Pantazis, N., Pillay, D., Paraskevis, D., Chaix, M. L., Bucher, H. C., et al. (2013). Impact of HIV-1 subtype on CD4 count at HIV seroconversion, rate of decline, and viral load set point in European seroconverter cohorts. *Clin. Infect. Dis.* 56, 888–897. doi: 10.1093/cid/cis1000

Tseng, A., Seet, J., and Phillips, E. J. (2015). The evolution of three decades of antiretroviral therapy: challenges, triumphs and the promise of the future. *Br. J. Clin. Pharmacol.* 79, 182–194. doi: 10.1111/bcp.12403

UNAIDS (2018). *UNAIDS Data 2018*. Geneva: UNAIDS, 370. doi: 10.15713/ins.mmj.3

Vallari, A., Holzmayer, V., Harris, B., Yamaguchi, J., Ngansop, C., Makamche, F., et al. (2011). Confirmation of putative HIV-1 group P in cameroon. *J. Virol.* 85, 1403–1407. doi: 10.1128/JVI.02005-10

Vasan, A., Renjifo, B., Hertzmark, E., Chaplin, B., Msamanga, G., Essex, M., et al. (2006). Different rates of disease progression of HIV type 1 infection in tanzania based on infecting subtype. *Clin. Infect. Dis.* 42, 843–852. doi: 10.1086/499952

Wang, T., Wei, J. J., Sabatini, D. M., and Lander, E. S. (2014). Genetic screens in human cells using the CRISPR-Cas9 system. *Science (80-).* 343, 80–84. doi: 10.1126/science.1246981

Wei, Z., Liu, Y., Xu, H., Tang, K., Wu, H., Lu, L., et al. (2015). Genome-wide association studies of HIV-1 host control in ethnically diverse chinese populations. *Sci. Rep.* 5, 1–9. doi: 10.1038/srep10879

Zhou, H., Xu, M., Huang, Q., Gates, A. T., Zhang, X. D., Castle, J. C., et al. (2008). Genome-scale RNAi screen for host factors required for HIV replication. *Cell Host Microbe* 4, 495–504. doi: 10.1016/j.chom.2008.10.004

Zhu, J., Davoli, T., Perriera, J. M., Chin, C. R., Gaiha, G. D., John, S. P., et al. (2014). Comprehensive identification of host modulators of HIV-1 replication using multiple orthologous RNAi reagents. *Cell Rep.* 9, 752–766. doi: 10.1016/j.celrep.2014.09.031

Conflict of Interest Statement: The authors declare that the research was conducted in the absence of any commercial or financial relationships that could be construed as a potential conflict of interest.

Copyright © 2019 Tough and McLaren. This is an open-access article distributed under the terms of the Creative Commons Attribution License (CC BY). The use, distribution or reproduction in other forums is permitted, provided the original author(s) and the copyright owner(s) are credited and that the original publication in this journal is cited, in accordance with accepted academic practice. No use, distribution or reproduction is permitted which does not comply with these terms.

frontiers in Immunology

ORIGINAL RESEARCH
published: 24 January 2019
doi: 10.3389/fimmu.2019.00053

Impact of *APOL1* Genetic Variants on HIV-1 Infection and Disease Progression

Ping An[1], Gregory D. Kirk[2], Sophie Limou[1,3,4], Elizabeth Binns-Roemer[1], Jeffrey B. Kopp[5] and Cheryl A. Winkler[1]**

[1] Molecular Genetic Epidemiology Section, Basic Science Program, Basic Research Laboratory, Frederick National Laboratory for Cancer Research, National Cancer Institute, Frederick, MD, United States, [2] Departments of Epidemiology and Medicine, Johns Hopkins University, Baltimore, MD, United States, [3] CRTI UMR1064, Inserm, Université de Nantes & ITUN, CHU Nantes, Nantes, France, [4] Ecole Centrale de Nantes, Nantes, France, [5] Kidney Disease Section, National Institute of Diabetes and Digestive and Kidney Diseases, NIH, Bethesda, MD, United States

Apolipoprotein L1 (APOL1) has broad innate immune functions and has been shown to restrict HIV replication *in vitro* by multiple mechanisms. Coding variants in *APOL1* are strongly associated with HIV-associated nephropathy (HIVAN) in persons with untreated HIV infection; however, the mechanism by which *APOL1* variant protein potentiates renal injury in the presence of high viral load is not resolved. Little is known about the association of *APOL1* genotypes with HIV viral load, HIV acquisition, or progression to AIDS. We assessed the role of *APOL1* coding variants on HIV-1 acquisition using the conditional logistic regression test, on viral load using the *t*-test or ANOVA, and on progression to AIDS using Cox proportional hazards models among African Americans enrolled in the ALIVE HIV natural history cohort ($n = 775$). *APOL1* variants were not associated with susceptibility to HIV-1 acquisition by comparing genotype frequencies between HIV-1 positive and exposed or at-risk HIV-1 uninfected groups (recessive model, 12.8 vs. 12.5%, respectively; OR 1.02, 95% CI 0.62–1.70). Similar null results were observed for dominant and additive models. *APOL1* variants were not associated with HIV-1 viral load or with risk of progression to AIDS [Relative hazards (RH) 1.33, 95% CI 0.30–5.89 and 0.96, 95% CI 0.49–1.88, for recessive and additive models, respectively]. In summary, we found no evidence that *APOL1* variants are associated with host susceptibility to HIV-1 acquisition, set-point HIV-1 viral load or time to incident AIDS. These results suggest that APOL1 variants are unlikely to influence HIV infection or progression among individuals of African ancestry.

Keywords: HIV-1, AIDS, APOL1, host susceptibility, genetic epidemiology

OPEN ACCESS

Edited by:
Guido Poli,
Vita-Salute San Raffaele University, Italy

Reviewed by:
Jacques Fellay,
École Polytechnique Fédérale de Lausanne, Switzerland
Joanna Mikulak,
Humanitas Research Hospital, Italy

****Correspondence:***
Ping An
ping.an@nih.gov
Cheryl A. Winkler
winklerc@mail.nih.gov

Specialty section:
This article was submitted to Viral Immunology, a section of the journal Frontiers in Immunology

Received: *26 October 2018*
Accepted: *09 January 2019*
Published: *24 January 2019*

Citation:
An P, Kirk GD, Limou S, Binns-Roemer E, Kopp JB and Winkler CA (2019) Impact of APOL1 Genetic Variants on HIV-1 Infection and Disease Progression. Front. Immunol. 10:53. doi: 10.3389/fimmu.2019.00053

INTRODUCTION

Apolipoprotein L1 (APOL1) is a human innate immune factor against African trypanosomes responsible for human African trypanosomiasis (or sleeping sickness) (1). Two common *APOL1* variants, G1 (rs73885319, p.S342G) and G2 (a 6-bp in-frame deletion removing two amino acids, rs71785313, p.N388_Y389del), extend APOL1 restriction to *T.b.rhodesiense,* the cause of acute human African trypanosomiasis. These variants are found only in individuals with recent African ancestry. The 12–14% of African Americans carrying two *APOL1* renal risk alleles in

the compound heterozygous or homozygous state (referred to as *APOL1* high risk [HR] genotypes) have a 3-, 7-, and 17-fold increased risk for developing hypertension-attributed nephropathy, non-diabetic end-stage kidney disease, and focal segmental glomerulosclerosis, respectively, (2–4). *APOL1* is most strongly associated with HIV-associated nephropathy (HIVAN), with odds ratio (OR) 29 in African Americans and OR 89 in South Africans (3, 5), suggesting a strong interaction between APOL1 and the HIV-1 virus. The lifetime risk of HIVAN, a form of collapsing focal segmental glomerulosclerosis associated with rapid progression to end-stage renal disease, is ∼10% in African Americans with untreated HIV infection (6, 7). The pathogenesis of HIVAN is likely due to direct HIV infection of kidney epithelial cells, which leads to podocyte proliferation and APOL1-mediated podocyte injury and loss (8–11). *APOL1* transcription is up-regulated by interferons and other pro-inflammatory cytokines (12).

Recently, Taylor et al. reported that APOL1 restricts HIV-1 replication in macrophages and differentiated monocytes (12). APOL1 was shown to target HIV-1 Gag for degradation by the endolysosomal pathway and to deplete HIV-1 Vif, which counteracts the APOBEC3G host restriction factor in lysosomes (12). However, it remains unknown if variant APOL1 affects HIV acquisition, viral replication, or HIV disease progression.

APOL1 renal risk variants are most common in West Africa, where the prevalence of *APOL1* HR genotypes approaches 25% but are also found throughout sub-Saharan Africa (4, 13) where HIV-1 infection is notably prevalent. Although *APOL1* renal risk variants are a risk factor for kidney disease in HIV-1 infected persons, it is unknown if *APOL1* renal risk variants are associated with other HIV-1 phenotypes. In the present study, we evaluate the genetic associations between *APOL1* variants and HIV-1 acquisition, set-point viral load, and rate of progression to AIDS among African Americans enrolled in the ALIVE HIV-1 cohort.

MATERIALS AND METHODS

Ethics Statement

Ethical approval for the study was obtained from the National Institute of Health Office of Human Subjects Research Protections (OHSRP #3314). Review Boards of participating institutions approved the study protocols, and written informed consent was obtained from all study participants.

Study Participants

Since *APOL1* G1-G2 alleles are found only on African-origin chromosomes, we studied only African American participants enrolled in the ALIVE (AIDS Link to the Intravenous Experience) cohort.

The ALIVE Cohort

The epidemiological and clinical characteristics of the ALIVE cohort have been previously described (14). ALIVE is a prospective longitudinal natural cohort originally designed to characterize the incidence and natural history of HIV infection among injection drug users (IDUs) in Baltimore, MD, initiated in 1988 (14). At study entry, 88% of participants were African Americans. The participants were followed up semi-annually with blood draws for viral load and CD4+ T cell measurements and physical exam at each visit.

The study group comprises 227 African American incident HIV-1 seroconverters, 213 HIV-1 seroprevalent participants, and 335 uninfected, IDU participants. Seroconversion date was estimated as the midpoint between the last seronegative and the first seropositive HIV-1 antibody test date (mean interval 0.66 years, range 0.11–3.4 years) (15).

Genotyping of APOL1 G1-G2 Risk Variants

APOL1 renal risk variants G1 (rs73885319, p.S342G) and G2 (rs71785313, p.N388_Y389del) were genotyped by TaqMan genotyping assays (Applied Biosystems, Foster City, CA). The TaqMan allele discrimination assays were carried out on an ABI 7900HT sequencer detector system (Applied Biosystems, Foster City, CA, USA), according to the manufacturer's protocol as previously described (3). For quality control, water controls were included on each plate and 10% of samples were duplicated. No water contamination or genotype mismatches between duplicates was observed. The genotype results were also further validated by the Sanger sequencing, following the protocol previously described (16).

Defining APOL1 Risk Haplotypes

The G1 risk allele is defined by the presence of the G allele at rs73885319 (342G) and the G2 (6-del) risk allele by the 6 base pair deletion at rs71785313 (-/TTATAA), which leads to the loss of two amino acids (388–389NYK>K) (2, 3). The G1 and G2 risk alleles are in absolute negative disequilibrium and never occur together on the same chromosome (17)). *APOL1* follows a recessive inheritance model for HIVAN and other kidney diseases: *APOL1* HR status for kidney disease is defined by carriage of 2 risk alleles (G1/G1, G1/G2, and G2/G2) and low-risk (LR) status is defined by carriage of 1 or 0 renal risk alleles (18).

Statistical Analysis

We assessed the potential effects of *APOL1* risk genotypes using additive (2 vs. 1 vs. 0 risk alleles), dominant (2 or 1 vs. 0), and recessive (2 vs. 1 or 0 risk alleles) models. All analyses were performed using SAS version 9.12 (SAS Institute, Cary, NC).

Analysis of Risk to HIV-1 Acquisition

We assessed the impact of *APOL1* G1-G2 variants on HIV-1 infection susceptibility by comparing frequencies between the HIV-1 infected group comprising HIV-1 seroincident and seroprevalent subjects and the HIV-1 at-risk, uninfected group. Odds ratios (OR) and *P*-values were obtained by using a conditional logistic regression test. Statistical power was calculated with GAS-power-calculator available at http://csg.sph.umich.edu/abecasis/gas_power_calculator/.

Abbreviations: HIV-1, HIV type 1; OR, Odds ratio; RH, Relative Hazards; SNP, Single Nucleotide Polymorphism.

Analysis of Viral Load

For the seroincident participants, HIV-1 viral load set-point was defined as the mean $\log_{10}$-transformed HIV-1 RNA plasma copies measured between 6 and 33 months after seroconversion (2–5 measurements). Viral load measurements exceeding 3-fold (0.5 $\log_{10}$) from the average of all remaining points were excluded, as previously suggested (19). We ran *t*-tests to estimate the difference of viral load means between *APOL1* HR and LR subgroups. We used the one-way analysis of variance (ANOVA) to determine whether there were any statistically significant differences among the means for carriage of 2, 1, or 0 *APOL1* risk alleles.

Analysis of Disease Progression to AIDS

In the ALIVE cohort, we tested the association of *APOL1* risk alleles on disease progression to AIDS using Cox proportional hazards model (Cox model) and Kaplan-Meier survival curve analyses for incident HIV seroconverters. The disease progression endpoints were: CD4 T-cell <200 cells/mm^3, or clinical AIDS diagnosis (20). The median time from seroconversion to AIDS was 7 years. To avoid the confounding effect of anti-retroviral therapy (ART) on disease progression, we censored the data after July 31, 1997 as few ALIVE participants received ART prior to this date (21). We included known genetic factors modifying AIDS progression as covariates in the adjusted Cox model analysis: *HLA-B**57 and *HLA* Class I homozygosity (22). The analyses were stratified by sex and by age at seroconversion: 0–20, 20–40, and >40 years. Two-tailed *P*-values were computed using Wald tests.

RESULTS

Association of *APOL1* Risk Alleles on the Risk of HIV-1 Acquisition

To determine whether *APOL1* G1 or G2 variants affect host susceptibility to HIV-1 acquisition, we compared the distribution of G1 and G2 variants in HIV-1 seroincident subjects ($n = 227$) with at risk, seronegative individuals ($n = 335$) (**Table 1**). No associations with HIV-1 acquisition were observed for the additive ($P = 0.61$), dominant ($P = 0.56$) or recessive genetic models ($P = 0.87$) (**Table 1**). To increase power, we combined seroconverters and seroprevalents) but results remained non-significant (**Table 1**). Adjusting for sex and age did not affect the results (**Table 1**). These results suggest that *APOL1* risk variants have no impact on host susceptibility to HIV-1 acquisition.

Association of *APOL1* Risk Alleles on HIV-1 Viral Load

Among HIV-1 seroincident participants, set-point HIV-1 viral load levels were found to be similar for carriers of 2, 1, or 0 *APOL1* risk alleles ($P = 0.79$, ANOVA). In the recessive model comparing viral load between carriers of HR genotypes (VL $= 4.23 \pm 0.64$, $N = 27$) and those with LR APOL1 genotypes (VL $= 4.20 \pm 0.73$, $N = 177$), we also observed no differences in viral load ($P = 0.48$, **Table 2**).

Association of *APOL1* Risk Alleles on HIV-1 Disease Progression

To assess the impact of *APOL1* HR on disease progression in untreated individuals from date of seroconversion to

TABLE 1 | Association of APOL1 G1-G2 variants with HIV-1 acquisition.

HIV-1 status	*n*	Age (years)$	Female& (%)	No. G1-G2 risk alleles			Comparison	Model*	OR (95% CI)*	*P**
				0	1	2				
Seroincident (SI)	227	39.9 ± 6.3	25.1	88 (38.8%)	110 (48.5%)	29 (12.8%)	SI vs. SN	Add	1.07 (0.84–1.38)	0.57
								Add_{adj}	1.07 (0.83–1.37)	0.61
								Dom	1.13 (0.80–1.60)	0.47
								Dom_{adj}	1.10 (0.78–1.57)	0.56
								Rec	1.02 (0.62–1.70)	0.98
								Rec_{adj}	1.04 (0.63–1.74)	0.87
Seroincident (SI) + seroprevalent (SP)	441	40.5 ± 6.2	25.0	177 (41.8%)	217 (49.2%)	47 (10.7%)	SI+SP vs. SN	Add	0.99 (0.80–1.23)	0.96
								Add_{adj}	1.00 (0.81–1.24)	0.99
								Dom	1.07 (0.80–1.43)	0.64
								Dom_{adj}	1.07 (0.80–1.43)	0.64
								Rec	0.83 (0.54–1.30)	0.42
								Rec_{adj}	0.84 (0.54–1.31)	0.45
Seronegative (SN)	335	41.5 ± 7.4	29.3	140 (41.8%)	153 (45.7%)	42 (12.5%)	Reference		-	-

*There were no associations between APOL1 kidney risk allele status and HIV-1-infection status. $P > 0.05 for SN vs. SI + SP; P < 0.05 for SN vs. SI; & P > 0.05 for SN vs. SI+SP or SN vs. SI. *Logistic regression for additive (Add, 2 vs. 1 vs. 0), dominant (Dom, 2 or 1 vs. 0), and recessive (Rec, 2 vs. 1 or 0) genetic models, adjusted (adj) for age (years) and stratified on sex.*

CD4 <200 cell/mm^3 and to incident AIDS, we performed time-to-event analysis for 227 African American seroincident participants. *APOL1* genotypes were not associated with the rate of progression to CD4 <200 cells/mm^3 (**Figure 1A**) or AIDS in Kaplan-Meier survival analyses (**Figure 1B**, additive model, $P > 0.12$ for log-rank or Wilcoxon tests). In the crude (data not shown) and adjusted Cox models, *APOL1* HR genotype (recessive model), *APOL1* risk allele number (additive) or risk allele carriage (dominant model) were not associated with the rate of progression to AIDS ($P > 0.70$, **Table 3**).

TABLE 2 | Association between *APOL1* G1-G2 variant alleles and HIV-1 viral load.

No. *APOL1* G1-G2 risk alleles	*n*	Viral load (SD)	Comparison	*P**
0 or 1	177	4.20± 0.73	ref	1
0	82	4.26 ± 0.68	ref	1
1	95	4.19 ± 0.77		0.52
2	27	4.23 ± 0.65		0.67
			Additive (2 vs. 1. vs. 0)	0.79
			Dominant (2 or 1 vs. 0)	0.50
			Recessive (2 vs. 1 or 0)	0.86

*There were no associations between number of APOL1 kidney risk alleles and HIV-1 viral load, presented as log base 10, copies/ml. *From t-tests or ANOVA (additive); SD, Standard Deviation.*

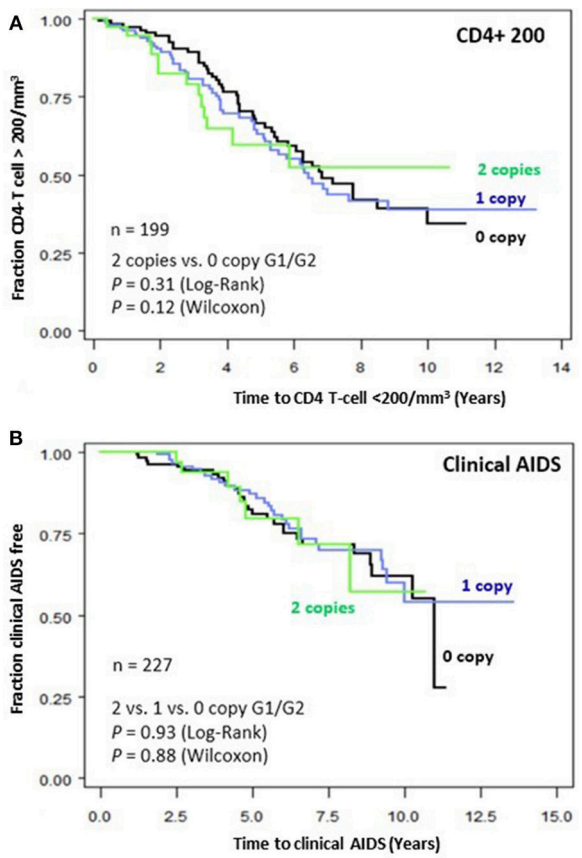

FIGURE 1 | Genetic effects of APOL1 G1-G2 variants on progression of HIV disease. Kaplan-Meier survival curves for carriage of 0, 1, and 2 *APOL1* risk allele for progression to **(A)** CD4+ T-cell <200/mm^3 and **(B)** clinical AIDS. RH and adjusted *P*-values were estimated from Cox proportional hazards models. *P*-values for survival curves were obtained from a log-rank test.

DISCUSSION

In this genetic epidemiological study of an HIV-1 at-risk and natural progression cohort, we observed no evidence of association between *APOL1* renal risk alleles and HIV-1 acquisition, HIV-1 viral load, and rate of progression to CD4 <200, AIDS, or the composite outcome. Our results indicate that *APOL1* renal risk variants, which are highly prevalent among African Americans and sub-Saharan Africans, do not significantly contribute to the HIV-1 epidemic by increasing viral burden or potentiating HIV-1 transmission.

A recent *in vitro* study reported that APOL1 protein can inhibit HIV-1 infection of macrophage and monocytes by multiple mechanisms, including inhibition of transcription and degradation of HIV-1 Gag and Vif proteins (12). If APOL1 protein effectively inhibits HIV-1 *in vitro*, *APOL1* coding variants might confer differential impact on HIV replication or disease progression by enhancing or attenuating the anti-HIV properties of APOL1 protein. However, our genetic association study revealed no *in vivo* evidence of association of *APOL1* renal risk alleles with HIV-1 infection acquisition or disease progression. Our findings are supported by the observation that *APOL1* gene expression is undetectable in CD4+ T cells, the primary target of HIV infection even with IFN-γ stimulation (12). In contrast, *APOL1* gene expression is highly inducible by IFN-γ stimulation in monocytes and macrophages, which were used in the *in vitro* experiments testing for APOL1 restriction of HIV replication (12). CD4$^+$ T lymphocytes are the principal target of HIV, while infected macrophages play a supportive role in viral pathogenesis involving HIV cell-to-cell spread, and certain tissue infections including lungs, gut and brain (23, 24). The *in vivo* role of APOL1 in HIV-1 pathogenesis thus warrants further investigation. An implication of this study is that development of HIVAN and eGFR decline among those with *APOL1* HR status (18, 25, 26), is likely due to local podocyte injury in a setting of high viral load in patients with untreated HIV infection. A

TABLE 3 | Association between *APOL1* G1-G2 variant alleles and incident clinical AIDS.

No. *APOL1* G1-G2 risk alleles	*n*	RH	95% CI	*P*
0 (reference)	88	1	–	1
1 (1 vs. 0)	110	1.11	0.52–2.34	0.79
2 (2 vs. 0)	29	0.87	0.16–4.74	0.87
Additive (2 vs. 1. vs. 0)		1.09	0.59–2.02	0.79
Dominant (2 or 1 vs. 0)		1.07	0.51–2.24	0.85
Recessive (2 vs. 1 or 0)		1.24	0.28–5.40	0.78

*There were no associations between APOL1 kidney risk alleles and incident AIDS. Cox model results, adjusted for age, sex, HLA-B*57, and HLA Class I homozygosity.*

recent study demonstrated that variant APOL1 protein increases accumulation of HIV-1 in podocytes, inducing inflammatory responses via IL-1β priming (11).

This study has both strengths and limitations. A strength is that the ALIVE cohort is one of few well-characterized HIV natural history cohorts enrolling African Americans prior to the ART era, and the large number of treatment-naïve seroconverters makes it a choice cohort for unbiased exploration of HIV-related outcomes. The relatively modest sample size is balanced by the combined high frequency of these variants in the African American population. We had 80% power to detect a potential association of *APOL1* G1-G2 with HIV-1 infection, with an OR 1.35 for additive model and 1.93 for recessive model. We were unable to control for mortality due to *APOL1*-associated ESKD or to HIVAN since biopsy data were unavailable; however, only 1 death was observed among 29 APOL1 HR individuals prior to censoring on July 31, 1997, suggesting that our null results are not due to frailty bias resulting from excess HIVAN or ESKD-related deaths in the HR group.

In summary, this population genetic study found no evidence that *APOL1* renal risk variants contribute to the risk of HIV-1 acquisition or progression of HIV-1 disease progression to AIDS. *APOL1* variants are unlikely to contribute to the prevalence of HIV infection in subSaharan Africa or among African Americans.

AUTHOR CONTRIBUTIONS

PA and CW conceived the study, designed the analyses, and wrote the manuscript. PA performed the analyses. EB-R performed genotyping. GK provided clinical data and DNA samples. GK, SL, and JK contributed to data interpretation and manuscript revisions. All authors reviewed the manuscript.

FUNDING

This project has been funded in whole or in part with federal funds from the National Cancer Institute, National Institutes of health, under contract HHSN26120080001E. This Research was supported in part by the Intramural Research Program of the NIH, National Cancer Institute, Center for Cancer Research and of the Kidney Disease Section, National Institute of Diabetes and Digestive and Kidney Diseases. The content of this publication does not necessarily reflect the views or policies of the Department of Health and Human Services, nor does mention of trade names, commercial products, or organizations imply endorsement by the U.S. Government. ALIVE is supported by National Institute on Drug Abuse (U01-036297 and R01-12586). SL's work was realized in the context of the LabEx IGO program that is supported by the National Research Agency via the Investment Into The Future program (ANR-11-LABX-0016-01).

REFERENCES

1. Pays E, Vanhollebeke B, Vanhamme L, Paturiaux-Hanocq F, Nolan DP, Perez-Morga D. The trypanolytic factor of human serum. *Nat Rev Microbiol.* (2006) 4:477–86. doi: 10.1038/nrmicro1428
2. Genovese G, Friedman DJ, Ross MD, Lecordier L, Uzureau P, Freedman BI, et al. Association of trypanolytic ApoL1 variants with kidney disease in African Americans. *Science* (2010) 329:841–5. doi: 10.1126/science.1193032
3. Kopp JB, Nelson GW, Sampath K, Johnson RC, Genovese G, An P, et al. APOL1 genetic variants in focal segmental glomerulosclerosis and HIV-associated nephropathy. *J Am Soc Nephrol.* (2011) 22:2129–37. doi: 10.1681/ASN.2011040388
4. Limou S, Dummer PD, Nelson GW, Kopp JB, Winkler CA. APOL1 toxin, innate immunity, and kidney injury. *Kidney Int.* (2015) 88:28–34. doi: 10.1038/ki.2015.109
5. Kasembeli AN, Duarte R, Ramsay M, Mosiane P, Dickens C, Dix-Peek T, et al. APOL1 risk variants are strongly associated with HIV-associated nephropathy in black South Africans. *J Am Soc Nephrol.* (2015) 26:2882–90. doi: 10.1681/ASN.2014050469
6. Shahinian V, Rajaraman S, Borucki M, Grady J, Hollander WM, Ahuja TS. Prevalence of HIV-associated nephropathy in autopsies of HIV-infected patients. *Am J kidney Dis.* (2000) 35:884–8. doi: 10.1016/s0272-6386(00)70259-9
7. Lucas GM, Eustace JA, Sozio S, Mentari EK, Appiah KA, Moore RD. Highly active antiretroviral therapy and the incidence of HIV-1-associated nephropathy: a 12-year cohort study. *AIDS* (2004) 18:541–6. doi: 10.1097/00002030-200402200-00022
8. Chandel N, Sharma B, Husain M, Salhan D, Singh T, Rai P, et al. HIV compromises integrity of the podocyte actin cytoskeleton through downregulation of the vitamin D receptor. *Am J Physiol Renal Physiol.* (2013) 304:F1347–57. doi: 10.1152/ajprenal.00717.2012
9. Doyle T, Goujon C, Malim MH. HIV-1 and interferons: who's interfering with whom? *Nat Rev Microbiol.* (2015) 13:403–13. doi: 10.1038/nrmicro3449
10. Kopp JB, Heymann J, Winkler CA. APOL1 renal risk variants: fertile soil for hiv-associated nephropathy. *Semin Nephrol.* (2017) 37:514–9. doi: 10.1016/j.semnephrol.2017.07.004
11. Mikulak J, Oriolo F, Portale F, Tentorio P, Lan X, Saleem MA, et al. Impact of APOL1 polymorphism and IL-1beta priming in the entry and persistence of HIV-1 in human podocytes. *Retrovirology* (2016) 13:63. doi: 10.1186/s12977-016-0296-3
12. Taylor HE, Khatua AK, Popik W. The innate immune factor apolipoprotein L1 restricts HIV-1 infection. *J Virol.* (2014) 88:592–603. doi: 10.1128/JVI.02828-13
13. Limou S, Nelson GW, Kopp JB, Winkler CA. APOL1 kidney risk alleles: population genetics and disease associations. *Adv Chronic Kidney Dis.* (2014) 21:426–33. doi: 10.1053/j.ackd.2014.06.005
14. Vlahov D, Graham N, Hoover D, Flynn C, Bartlett JG, Margolick JB, et al. Prognostic indicators for AIDS and infectious disease death in HIV-infected injection drug users: plasma viral load and CD4+ cell count. *JAMA* (1998) 279:35–40.
15. An P, Duggal P, Wang LH, O'Brien SJ, Donfield S, Goedert JJ, et al. Polymorphisms of CUL5 are associated with CD4+ T cell loss in HIV-1 infected individuals. *PLoS Genet.* (2007) 3:e19. doi: 10.1371/journal.pgen.0030019
16. Ko WY, Rajan P, Gomez F, Scheinfeldt L, An P, Winkler CA, et al. Identifying Darwinian selection acting on different human APOL1 variants among diverse African populations. *Am J Hum Genet.* (2013) 93:54–66. doi: 10.1016/j.ajhg.2013.05.014
17. Kruzel-Davila E, Shemer R, Ofir A, Bavli-Kertselli I, Darlyuk-Saadon I, Oren-Giladi P, et al. APOL1-mediated cell injury involves disruption of conserved trafficking processes. *J Am Soc Nephrol.* (2017) 28:1117–30. doi: 10.1681/ASN.2016050546
18. Estrella MM, Li M, Tin A, Abraham AG, Shlipak MG, Penugonda S, et al. The association between APOL1 risk alleles and longitudinal kidney function differs by HIV viral suppression status. *Clin Infect Dis.* (2015) 60:646–52. doi: 10.1093/cid/ciu765

19. Fellay J, Ge D, Shianna KV, Colombo S, Ledergerber B, Cirulli ET, et al. Common genetic variation and the control of HIV-1 in humans. *PLoS Genet*. (2009) 5:e1000791. doi: 10.1371/journal.pgen.1000791
20. CDC. Revision of the CDC surveillance case definition for acquired immunodeficiency syndrome. *MMWR* (1987) 36(Suppl. 1):1S−15S.
21. Celentano DD, Galai N, Sethi AK, Shah NG, Strathdee SA, Vlahov D, et al. Time to initiating highly active antiretroviral therapy among HIV-infected injection drug users. *AIDS* (2001) 15:1707–15. doi: 10.1097/00002030-200109070-00015
22. O'Brien SJ, Nelson GW. Human genes that limit AIDS. *Nat Genet*. (2004) 36:565–74. doi: 10.1038/ng1369
23. Sattentau QJ, Stevenson M. Macrophages and HIV-1: an unhealthy constellation. *Cell Host Microbe* (2016) 19:304–10. doi: 10.1016/j.chom.2016.02.013
24. Koppensteiner H, Brack-Werner R, Schindler M. Macrophages and their relevance in Human Immunodeficiency Virus Type I infection. *Retrovirology* (2012) 9:82. doi: 10.1186/1742-4690-9-82
25. Jotwani V, Shlipak MG, Scherzer R, Parekh RS, Kao WH, Bennett M, et al. APOL1 genotype and glomerular and tubular kidney injury in women with HIV. *Am J Kid Dis*. (2015) 65:889–98. doi: 10.1053/j.ajkd.2015.02.329
26. Swanepoel CR, Atta MG, D'Agati VD, Estrella MM, Fogo AB, Naicker S, et al. Kidney disease in the setting of HIV infection: conclusions from a Kidney Disease: improving Global Outcomes (KDIGO) Controversies Conference. *Kidney Int*. (2018) 93:545–59. doi: 10.1016/j.kint.2017.11.007

Conflict of Interest Statement: The authors declare that the research was conducted in the absence of any commercial or financial relationships that could be construed as a potential conflict of interest.

Copyright © 2019 An, Kirk, Limou, Binns-Roemer, Kopp and Winkler. This is an open-access article distributed under the terms of the Creative Commons Attribution License (CC BY). The use, distribution or reproduction in other forums is permitted, provided the original author(s) and the copyright owner(s) are credited and that the original publication in this journal is cited, in accordance with accepted academic practice. No use, distribution or reproduction is permitted which does not comply with these terms.

frontiers in Microbiology

ORIGINAL RESEARCH
published: 13 February 2019
doi: 10.3389/fmicb.2019.00209

Inhibitor of Sarco/Endoplasmic Reticulum Calcium-ATPase Impairs Multiple Steps of Paramyxovirus Replication

Naveen Kumar[1†], Nitin Khandelwal[1†], Ram Kumar[1], Yogesh Chander[1], Krishan Dutt Rawat[1], Kundan Kumar Chaubey[2], Shalini Sharma[3], Shoor Vir Singh[2], Thachamvally Riyesh[1], Bhupendra N. Tripathi[1*] and Sanjay Barua[1*]*

[1]National Centre for Veterinary Type Cultures, ICAR-National Research Centre on Equines, Hisar, India, [2]Department of Biotechnology, GLA University, Mathura, India, [3]Department of Veterinary Physiology and Biochemistry, Lala Lajpat Rai University of Veterinary and Animal Sciences, Hisar, India

OPEN ACCESS

Edited by:
Cheryl Ann Winkler,
Frederick National Laboratory for Cancer Research (NIH), United States

Reviewed by:
Sara Louise Cosby, Queen's University Belfast, United Kingdom
Masato Tsurudome, Chubu University, Japan

***Correspondence:**
Naveen Kumar
naveenkumar.icar@gmail.com
Bhupendra N. Tripathi
bntripathi1@yahoo.co.in
Sanjay Barua
sbarua06@gmail.com

[†]These authors have contributed equally to this work

Specialty section:
This article was submitted to Virology, a section of the journal Frontiers in Microbiology

Received: 29 September 2018
Accepted: 24 January 2019
Published: 13 February 2019

Citation:
Kumar N, Khandelwal N, Kumar R, Chander Y, Rawat KD, Chaubey KK, Sharma S, Singh SV, Riyesh T, Tripathi BN and Barua S (2019) Inhibitor of Sarco/Endoplasmic Reticulum Calcium-ATPase Impairs Multiple Steps of Paramyxovirus Replication. Front. Microbiol. 10:209. doi: 10.3389/fmicb.2019.00209

Sarco/endoplasmic reticulum calcium-ATPase (SERCA) is a membrane-bound cytosolic enzyme which is known to regulate the uptake of calcium into the sarco/endoplasmic reticulum. Herein, we demonstrate for the first time that SERCA can also regulate virus replication. Treatment of Vero cells with SERCA-specific inhibitor (Thapsigargin) at a concentration that is nontoxic to the cells significantly reduced Peste des petits ruminants virus (PPRV) and Newcastle disease virus (NDV) replication. Conversely, overexpression of SERCA rescued the inhibitory effect of Thapsigargin on virus replication. PPRV and NDV infection induced SERCA expression in Vero cells, which could be blocked by Thapsigargin. Besides inducing enhanced formation of cytoplasmic foci, Thapsigargin was shown to block viral entry into the target cells as well as synthesis of viral proteins. Furthermore, NDV was shown to acquire significant resistance to Thapsigargin upon long-term passage (P) in Vero cells. As compared to the P0 and P70-Control, the fusion (F) protein of P70-Thapsigargin virus exhibited a unique mutation at amino acid residue 104 (E104K), whereas no Thapsigargin-associated mutations were observed in HN gene. To the best of our knowledge, this is the first report describing the virus-supportive role of SERCA and a rare report suggesting that viruses may acquire resistance even in the presence of an inhibitor that targets a cellular factor.

Keywords: SERCA, virus replication, paramyxovirus, antiviral drug resistance, host-targeting antiviral agents

INTRODUCTION

The control strategies against pathogens have classically relied upon targeting essential proteins of the pathogens (Kumar et al., 2011b). High mutation rates in viral genome allows the virus to become resistant to antiviral drugs and preexisting immunity (Andino and Domingo, 2015). Classically, antiviral drugs have been developed by directly targeting viral proteins (Chen et al., 2016). Due to high mutation rates, viruses with mutations at the druggable targets are selected for resistance. The rise in incidence of drug resistance has prompted a shift in the development

of novel antiviral drugs (Ludwig et al., 2006). Viruses are obligate intracellular parasites that are highly dependent on the host. Host responses are equally important in determining the actual outcome of a disease. Upon viral infection, numerous cellular factors are dysregulated (increased or decreased expression); some of these host factors facilitate virus replication (proviral), whereas others may have antiviral function (Griffiths et al., 2013). Proviral host factors may serve as targets for the development of novel antiviral therapeutics (Kumar et al., 2008, 2011a,b).

Protein phosphorylation and dephosphorylation, mediated respectively *via* kinases and phosphatases, are ubiquitous cellular regulatory mechanisms during signal transduction which determines key cellular processes such as growth, development, transcription, metabolism, apoptosis, immune response, and cell differentiation (Coito et al., 2004). Kinome, the protein kinase complement of the human genome, completed in 2002, identified 518 protein kinase genes. These kinases have been shown to play a key role in cancer and many other diseases (Coito et al., 2004) including viral infections (Nousiainen et al., 2013), making these proteins potential drug targets.

In vertebrates, there are three families of P-type Ca^{2+}-ATPases, which regulate homeostasis of intracellular Ca^{2+} level. Plasma membrane Ca^{2+}-ATPase (PMCA), sarco/endoplasmic reticulum calcium-ATPase (SERCA), and secretory pathway calcium ATPAse (SPCA) are located in the plasma membrane, endoplasmic reticulum, and Golgi apparatus, respectively (Feng and Rao, 2013). SERCA transports Ca^{2+} from cytosol to the double membrane-bound (endoplasmic reticulum) intracellular compartments (Inesi et al., 2005; Arruda et al., 2007; Clapham, 2007; Primeau et al., 2018). SERCA is also involved in other cellular functions such as signal transduction, apoptosis, exocytosis (Kudla et al., 2010), cell motility (Qi et al., 2007), and transcription (Flavell and Greenberg, 2008). There are three genes (ATP2A1–3) in vertebrates that code for three SERCA isoforms, namely SERCA1–3 (Wuytack et al., 2002; Altshuler et al., 2012). Each of these genes undergoes alternative splicing and hence results in 10 SERCA proteins (two each from SERCA1 and 2 and six from SERCA3) (Martin et al., 2002). While some of these isoforms/variants are ubiquitously expressed in most cell types (SERCA2), others show a range of cell type-specific expression patterns (de Meis et al., 2005; Arruda et al., 2007; Altshuler et al., 2012). The role of these Ca^{2+}-ATPases in virus replication is only beginning to be appreciated. Whereas the role of SERCA and PMCA in virus replication remains unknown, a recent study suggests that SPCA1 supports virus replication (Hoffmann et al., 2017).

Previously, we screened a library of kinase and phosphate inhibitors for their antiviral potential and identified several hits against influenza A viruses (Kumar et al., 2011a). Herein, we also screened a library of these chemical inhibitors for their antiviral effects against paramyxovirus-morbillivirus [(peste des petits ruminants virus (PPRV)] and avulavirus [(Newcastle disease virus (NDV)]. SERCA inhibitor (Thapsigargin) was identified as one candidate that blocked NDV and PPRV replication. We show that Thapsigargin can block multiple steps of paramyxovirus replication, thus revealing SERCA as a potential target for the development of antiviral therapeutics.

MATERIALS AND METHODS

Cells and Viruses

Vero (African green monkey kidney), 293 T (human embryonic kidney), MDBK (Madin-Darby bovine kidney), HeLa, and goat kidney cells were grown in Dulbecco's Modified Eagle's Medium (DMEM) supplemented with antibiotics and 10% heat-inactivated fetal bovine serum. PPRV, NDV, buffalopox virus (BPXV), and bovine herpesvirus 1 (BHV-1) were available in our laboratory and have been described elsewhere (Kumar et al., 2016). Viral titers were determined by plaque assay, as previously described (Kumar et al., 2016).

Inhibitor

Thapsigargin (SERCA inhibitor) was procured from Sigma (Catalog Number-T9033, Steinheim, Germany). Thapsigargin is a noncompetitive inhibitor of SERCA. It is extracted from a plant *Thapsia garganica* and structurally classified as a sesquiterpene lactone (Rasmussen et al., 1978).

Antibodies

SERCA2 ATPase Antibody (MA3-919) was procured from Invitrogen (Carlsbad, USA). HA Tag Monoclonal Antibody was procured from Thermo Fisher Scientific (Rockford, USA). Anti-PPRV serum that predominantly reacts with PPRV HN, F, and M proteins and anti-NDV serum that predominantly reacts with NDV F and HN proteins (in Western blot) are described elsewhere by our group (Khandelwal et al., 2017). Secondary fluorescein isothiocyanate (FITC)-conjugated anti-rabbit antibody and secondary tetramethylrhodamine isothiocyanate (TRITC)-conjugated anti-mouse antibody were purchased from Sigma (Steinheim, Germany).

MTT Assay

Cytotoxicity of Thapsigargin was analyzed in MTT assay, as previously described (Khandelwal et al., 2017).

Antiviral Efficacy

Vero/MDBK cells were infected with respective viruses at MOI = 0.1 in the presence of 0.5 μM Thapsigargin or vehicle control (0.05% DMSO). Progeny virus particles released in the supernatants were quantified by plaque assay.

Effect of Thapsigargin on NDV Replication *in ovo*

Specific pathogen-free (SPF) embryonated chicken eggs were procured from Immunetic Life Sciences Pvt. Ltd. Una, India. LD_{50} of Thapsigargin was determined by inoculating five-fold serial dilutions of Thapsigargin (concentration ranging from 6,250–10 ng/egg) or vehicle control, in 10-day-old embryonated SPF eggs, in a total of 100 μl volumes *via* allantoic route. Eggs were examined for viability of the embryos up to 5 days post-inoculation to determine the LD_{50} by the Reed-Muench method.

To analyze the effect of Thapsigargin on NDV replication *in ovo*, SPF eggs were infected with 100 μl of NDV (HA titer = 2^7) in 10-day-old embryonated SPF eggs *via* allantoic route. The

allantoic fluid was collected at 6 and 96 h post-infection and quantified for NDV by hemagglutination assay (chicken red blood cells) as described previously (Kumar et al., 2016).

Virucidal Activity

Virus suspensions (PPRV/NDV) containing ~10^6 plaque forming units (pfu) were incubated in serum-free medium containing either DMSO or 10-fold dilutions of the Thapsigargin, for 1.5 h at 37°C. Thereafter, the samples were chilled at 4°C and diluted by 10^{-3}-, 10^{-4}-, and 10^{-5}-fold before being applied onto Vero/MDBK cells in six-well plates for plaque assaying. The results were plotted as relative infectivity of virions against concentrations of the compound used.

Overexpression of SERCA

HeLa/goat kidney cells were transfected in 24-well plates, in triplicates with either 1 μg of pCR3 (empty vector) or with pCR3-SERCA2.HA (SERCA with HA tag at 3′ end) using Lipofectamine 3000 transfection reagent as per the instructions of the manufacturer. At 48 h post-transfection, cells were infected with virus (NDV to HeLa cells and PPRV to goat kidney cells) at MOI of 1. Virus particles released in the supernatant at 24 h post-infection (hpi) (NDV) or 96 hpi (PPRV) were quantified by plaque assay.

Attachment Assay

The attachment assay was performed as described previously (Khandelwal et al., 2014). Briefly, Vero cells were preincubated with 0.5 μM Thapsigargin or vehicle control for 1 h and then infected with PPRV or NDV at MOI of 5 for 2 h at 4°C. The cells were then washed six times with PBS, and the cell lysates were prepared by rapid freeze-thaw method. The virus titers were determined by plaque assay.

Entry Assay

Vero cell monolayers were prechilled to 4°C and infected with the respective viruses at MOI of 5 in Thapsigargin-free medium for 1 h at 4°C to permit attachment, followed by washing and addition of fresh medium containing 0.5 μM Thapsigargin or vehicle control (0.05% DMSO). Entry was allowed to proceed at 37°C for 1 h after which the cells were washed again with PBS to remove any extracellular viruses and incubated with cell culture medium without any inhibitor. The progeny virus particles released in the cell culture supernatants in the treated and untreated cells were titrated by plaque assay.

qRT-PCR

The levels of viral RNA in the infected cells were quantified by quantitative real-time PCR (qRT-PCR). Viral RNA/DNA Purification Kit (Thermo Scientific, Vilnius, Lithuania) was used for extraction of viral RNA from the infected cell lysate. cDNA was synthesized as per the protocol described by the manufacturer (Fermentas, Hanover, USA) using random hexamer primer. The resulting cDNA was stored at −20°C until use. qRT-PCR was carried out with a 20 μl reaction mixture containing gene-specific primers, template and Sybr green DNA dye (Promega, Madison, USA), and run on LineGene 9600 Bioer Real-Time PCR Detection Systems. Thermal cycler conditions were as follows: a denaturation step of 5 min at 94°C followed by 40 cycles of amplification (30 s at 94°C, 30 s at 55°C, and 30 s at 72°C). The levels of viral RNA, expressed as threshold cycle (Ct) values, were analyzed to determine relative fold change in RNA copy number as described previously (Kumar et al., 2016). The primers used for qRT-PCR were as follows: NDV (F gene) (forward primer: 5′-CAGCTGCAGGGATTGTGGT-3′ and reverse primer: 5′-TCTTTGAGCAGGAGGATGTTG-3′) and PPRV (nucleoprotein gene) (forward primer: 5′-ACAGGCGCAGGTTTCATTCTT-3′ and reverse primer: 5′-GCTGAGGATATCCTTGTCGTT-3′).

Viral Protein Synthesis

Vero cells were either mock-infected or infected with PPRV or NDV at MOI of 10 for 3 h followed by washing with PBS and addition of 0.5 μM Thapsigargin or vehicle control (0.05% DMSO). The cells were scrapped at 9 and 20 hpi, respectively, for NDV and PPRV to prepare the cell lysate. Viral proteins were probed by Western blot analysis.

Virus Release Assay

Virus release assay was performed as described previously (Kumar et al., 2011a). Briefly, confluent monolayers of Vero cells were infected with PPRV or NDV, in triplicates, for 2 h at MOI of 5 followed by washing and addition of fresh media. At 36 and 10 hpi, respectively, for PPRV and NDV, cells were washed six times with chilled PBS followed by addition of fresh medium containing 0.5 μM Thapsigargin or vehicle control. Virus released at 1 and 2 h (PPRV) or 30 min and 1 h (NDV) was quantified by plaque assay.

Immunofluorescence Assay

Vero cells were grown in chamber slides at ~20% confluency and infected with PPRV/NDV at MOI of 5 for 2 h followed by washing with PBS and replacement with fresh medium. Thapsigargin was applied at 3 and 10 hpi, respectively, in NDV- and PPRV-infected cells. The intracellular localization of viral proteins in the virus-infected cells was detected by immunofluorescence assay. Briefly, cells were fixed with 4% paraformaldehyde for 15 min and blocked by 1% bovine serum albumin for 30 min at room temperature. After washing with PBS, cells were stained with primary antibody (rabbit anti-NDV/rabbit anti-PPRV or mouse SERCA2 ATPase) for 30 min in the presence of 0.2% saponin. Thereafter, cells were washed three times with PBS and incubated with a secondary fluorescein isothiocyanate-conjugated anti-rabbit antibody or secondary rhodamine-conjugated anti-mouse antibody in the presence of 0.2% saponin for 30 min. After being washed again with PBS, the cells were mounted with a medium containing 4,6-diamidino-2-phenylindole (DAPI; Sigma) and examined by fluorescence microscopy.

Selection of Thapsigargin-Resistant Viral Mutants

NDV was sequentially passaged (70 passages) in Vero cells in the presence of either 0.25 μM Thapsigargin or vehicle

control (0.05% DMSO). At each passage, confluent monolayers of Vero cells were infected with NDV, washed five times with PBS before a fresh aliquot of DMEM was added, and incubated for 72–96 h or until the appearance of cytopathic effect (CPE) in ≥75% cells. The virus released in the supernatant was termed as passage 1 (P1). The virus was quantified by plaque assay, and it (at MOI of 0.01) was used in the second round of infection, which was termed as passage 2 (P2). Seventy passages of virus infection were similarly carried out. In order to study the relative resistance against Thapsigargin at various passages, Thapsigargin-passaged and DMSO-passaged viruses were used to infect Vero cells at MOI = 0.1 and grown in the presence of either 0.05% DMSO or 0.5 μM Thapsigargin. The virus released in the supernatant was quantified by plaque assay, and fold-inhibition level was determined.

RESULTS

SERCA Inhibitor Blocks Paramyxovirus Replication

Thapsigargin is a potent inhibitor of SERCA (Rogers et al., 1995; Eastman and Fidock, 2009). It was identified from a protein kinase inhibitor library described previously (Kumar et al., 2011a). In order to determine the *in vitro* efficacy of Thapsigargin against paramyxoviruses (PPRV and NDV) and DNA viruses (BHV-1 and BPXV), we first determined its cytotoxicity in cultured Vero/MDBK cells by MTT assay. As shown in **Figures 1A,B**, Thapsigargin at concentrations between 0.00064 and 2 μM did not significantly affect the cell viability even when incubated in cell cultures for 96 h. However, at higher concentrations (>2 μM), it was found to be toxic to the cells. The CC_{50} was determined to be 3.37 and 3.30 μM, respectively, for Vero and MDBK cells. At 2 μM, Thapsigargin cytotoxicity levels varied between 0 and 18% (from experiment to experiment). However, no absolute cytotoxicity was detected at <1 μM (data not shown). Therefore, a highest sub-cytotoxic concentration of 0.5 μM was determined using subsequent experiments.

In order to determine the *in vitro* antiviral efficacy of Thapsigargin, we measured the yield of infectious PPRV and NDV in the presence of indicated concentrations of the Thapsigargin or vehicle control (0.05% DMSO). Thapsigargin significantly inhibited NDV (**Figure 1C**) and PPRV (**Figure 1D**) replication (paramyxoviruses) in a dose-dependent manner at an EC_{50} of 5.9 and 14.2 nM, respectively. The therapeutic index (CC_{50}/EC_{50}) was determined to be 571.18 and 237.32, respectively, for NDV and PPRV. Thapsigargin also inhibited BHV-1 (**Figure 1E**) but not BPXV (**Figure 1F**) replication (DNA viruses), suggesting its antiviral efficacy against paramyxoviruses and BHV-1 virus.

Furthermore, in order to determine whether the antiviral efficacy of Thapsigargin against paramyxoviruses is partially due to direct inactivation of the cell free virions, we incubated the infectious virions with either 0.5 or 5 μM Thapsigargin for 1.5 h and subsequently tested the residual infectivity on Vero/MDBK cells. Thapsigargin did not exhibit any virucidal effect on any of the prototype virus tested (**Figure 1G**), suggesting that the antiviral activity of Thapsigargin is due to the inhibitory effect on virus replication in the target cells.

We also analyzed the effect of Thapsigargin on replication of NDV in embryonated SPF chicken eggs. The lethal dose 50 (LD_{50}) of the Thapsigargin was determined to be 250 ng/egg (**Figure 1H**). At a noncytotoxic concentration of Thapsigargin (10 ng/egg) and at 96 hpi, NDV yield (allantoic fluid) was significantly lower in Thapsigargin-treated eggs, as compared to the vehicle control-treated eggs (**Figure 1I**), suggesting that Thapsigargin has the potential to inhibit virus replication *in vivo*. There was no detectable virus (HA titer <4) at 6 hpi (**Figure 1I**) in both Thapsigargin-treated and control-treated eggs, suggesting that the decreased viral titers in Thapsigargin-treated eggs at 96 hpi are actually due to inhibition in virus replication, not simply due to Thapsigargin toxicity.

SERCA Facilitates Paramyxovirus Replication

In order to further confirm the role of SERCA in virus replication, the inhibitory effect of Thapsigargin was rescued by overexpression of the SERCA. The expression of exogenous/recombinant SERCA was confirmed by probing HA Tag (present at 3′ end of the SERCA) in Western blot analysis (**Figure 2A**). As compared to the control plasmid (empty vector)-transfected cells, overexpression of SERCA2-HA not only facilitated NDV and PPRV replication but also rescued the inhibitory effect of Thapsigargin on virus replication, suggesting that SERCA2 supports paramyxovirus replication (**Figures 2B,C**).

Paramyxoviruses Induce SERCA Expression

SERCA2 is expressed by most cell types. We also evaluated whether virus infection induces any alteration in SERCA expression. PPRV infection of Vero cells resulted in enhanced SERCA2 expression. As compared to mock-infected cells, a significant induction in SERCA2 expression was observed at 3 hpi, which remained at the peak level between 24 and 72 hpi, before beginning to decline at 96 hpi (**Figure 3A, upper panel**). However, the levels of house keeping control gene (GAPDH) were similar at all the time points, suggesting that the enhanced levels of SERCA2 expression were related to viral infection (**Figure 3A, lower panel**). Besides, we also observed that NDV-induced SERCA2 expression could be blocked by Thapsigargin treatment (**Figure 3B**).

Time-of-Addition Assay

In order to ascertain the stage(s) of the viral life cycle which can be impaired by Thapsigargin, we performed a time-of-addition assay (one-step growth curve), in which the inhibitor was applied at different times post-infection, and the virus released into the supernatant was quantified by plaque assay.

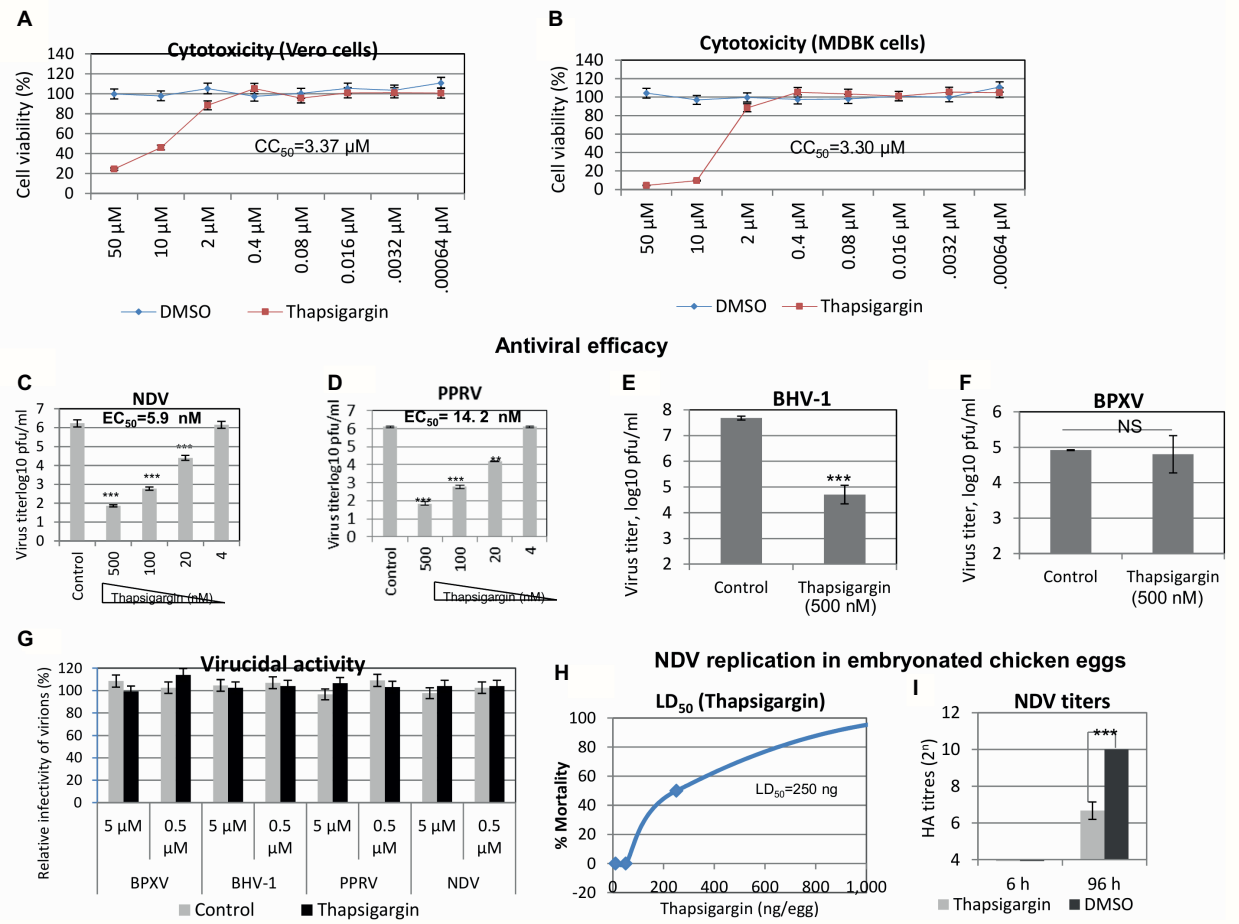

FIGURE 1 | Antiviral efficacy of Thapsigargin. *Cytotoxicity (MTT assay):* five-fold serial dilutions of Thapsigargin (50–0.00064 µM) or equivalent volume of vehicle control (0.05% DMSO) were incubated with cultured Vero/MDBK cells for 96 h, and percentage of cell *via*bility was measured by MTT assay. Cell viability of Vero **(A)** and MDBK **(B)** cells is shown. *Antiviral efficacy*: Vero/MDBK cells were infected with respective viruses at MOI = 0.1 in the presence of indicated concentration of Thapsigargin or vehicle control (0.05% DMSO). Progeny virus particles released in the supernatants were quantified by plaque assay. Antiviral efficacy of Thapsigargin against NDV **(C)**, PPRV **(D)**, BHV-1 **(E)**, and BPXV **(F)** is shown. *Virucidal activity*: 10-fold dilutions of the Thapsigargin or DMSO were mixed with ~10^6 pfu of the indicated viruses and incubated for 1.5 h at 37°C. Thereafter, the residual viral infectivity was determined by plaque assay in Vero (NDV, PPRV, and BPXV) or MDBK (BHV-1) cells **(G)**. *Effect of Thapsigargin on replication of NDV in embryonated chicken eggs.* Embryonated SPF chicken eggs, in triplicates, were inoculated with indicated concentration of Thapsigargin *via* allantoic route. At 96 h post-Thapsigargin inoculation, eggs were visualized for viability of the embryos. LD_{50} was determined by the Reed-Muench method **(H)**. To analyze the effect of Thapsigargin on NDV replication *in ovo*, embryonated SPF chicken eggs, in triplicates, were infected with NDV *via* allantoic route, along with administration of Thapsigargin (10 ng/egg). At 6 and 96 hpi, the allantoic fluid was examined for NDV yield by HA **(I)**. Error bars indicate SD. Pair-wise statistical comparisons were performed using Student's t test (** = $p < 0.01$, *** = $p < 0.001$). NS represents no statistical significance.

The NDV and PPRV vary in their length of replication cycle, ~10 and ~24 h, respectively; therefore, time-of-addition of inhibitor and time of virus harvest varied from virus to virus. As shown in **Figure 4A**, the magnitude of viral (NDV) inhibition gradually decreased. The highest inhibition was observed when the inhibitor was applied 30 min before infection. The inhibition levels progressively decreased from 1 to 6 hpi. Thapsigargin did not exhibit any inhibitory effect on virus replication if it was applied at 10 hpi, a later time point in NDV life cycle when the virus is presumably undergoing budding. Similar findings were observed with PPRV; highest inhibition in viral titers was observed when the inhibitor was applied 30 min prior to infection, magnitude of inhibition progressive decreased from 4 to 24 hpi (**Figure 4B**). The time-of-addition assay, therefore, suggested that Thapsigargin may inhibit multiple prebudding steps of paramyxovirus replication.

Effect of Thapsigargin on Specific Steps of Viral Life Cycle

Attachment

To analyze the effect of Thapsigargin on attachment of the virus on cell surface, virus was allowed to adsorb (attach) at 4°C (to restrict the entry) in the presence or absence of Thapsigargin. We did not observe any significant difference in the viral titers (adsorbed onto cell surface) between Thapsigargin and vehicle control-treated cells (data not shown), suggesting that Thapsigargin has no effect on attachment of virus to the host cells.

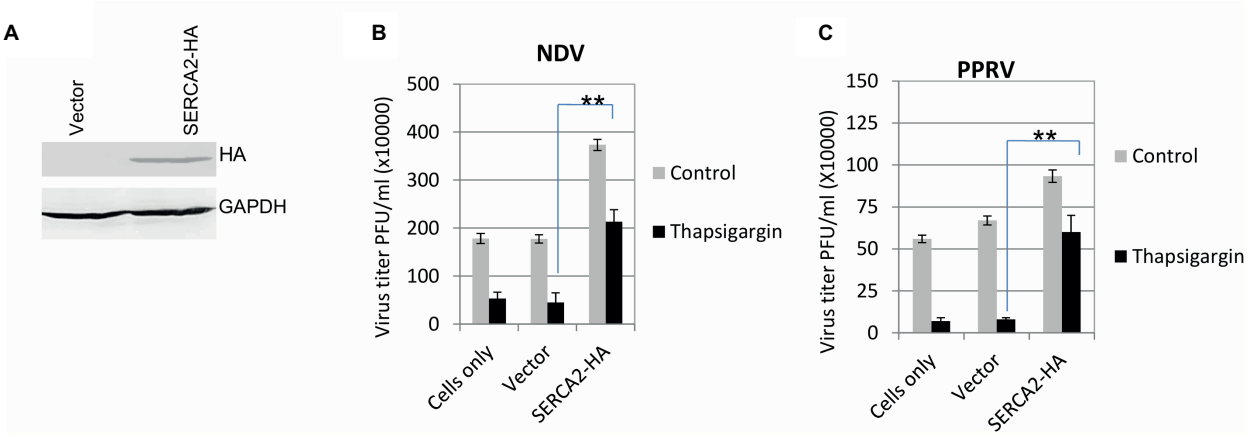

FIGURE 2 | SERCA facilitates paramyxovirus replication. Evaluation of the expression of recombinant SERCA2: HeLa cells were transfected with either an empty vector or with a construct expressing SERCA2-HA. At 48 h-post transfection, cell lysates were probed for expression of HA in Western blot analysis **(A)**. Effect of overexpression of SERCA on paramyxovirus replication: HeLa/goat kidney cells were transfected with SERCA-expressing plasmid (pCR3-SERCA2) or control plasmid (pCR3, empty vector). At 48 h post-transfection, cells were infected with virus (NDV to HeLa cells and PPRV to goat kidney cells) at MOI of 1. Virus released in the supernatant at 24 hpi (NDV) **(B)** or 96 hpi (PPRV) **(C)** was quantified by plaque assay. Error bars indicate SD. Pair-wise statistical comparisons were performed using Student's t test (** = $p < 0.01$).

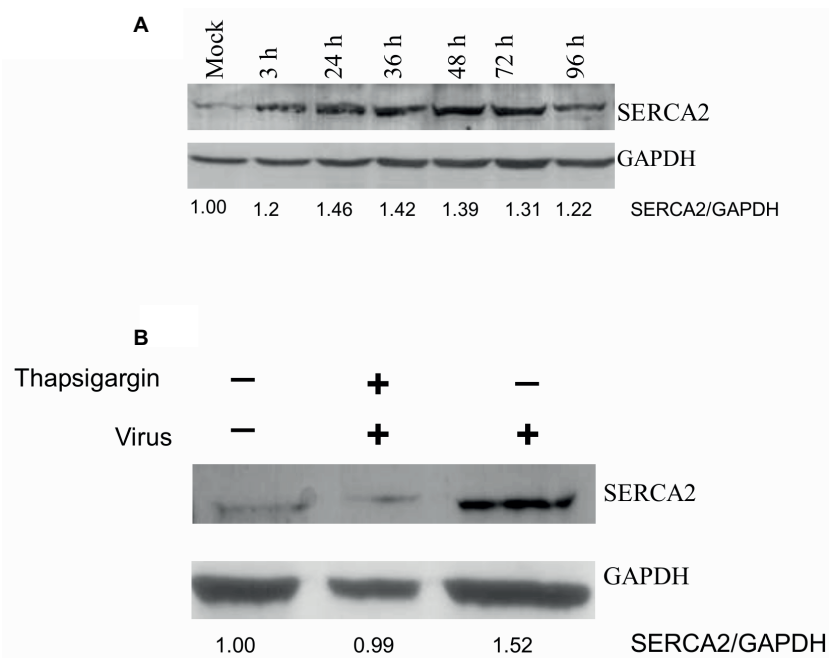

FIGURE 3 | Paramyxovirus infections induce SERCA expression. **(A)** *PPRV infection induces SERCA2 expression:* Vero cells were infected with PPRV at MOI 5, and the cell lysates were prepared at indicated time points. The levels of SERCA2 (upper panel) or house-keeping control protein (GAPDH) (lower panel) were examined by Western blot analysis. **(B)** *Thapsigargin inhibits NDV-induced SERCA2 expression in Vero cells:* Vero cells were infected with NDV at MOI of 5 for 1 h followed by washing with PBS and addition of fresh medium containing Thapsigargin or vehicle control (0.05% DMSO). Cell lysates were prepared at 16 hpi to probe SERCA2 and GAPDH by Western blot analysis. Relative fold-change in the levels of viral/cellular proteins was determined by ImageJ (NIH).

Entry

In order to determine whether the pre-attached virus was able to enter into the cells in the presence of Thapsigargin, a standard entry assay was performed. Pre-attached virus (4°C) was allowed to enter at 37°C in the presence of Thapsigargin, and infectious virus released in the cell culture supernatant was measured. Thapsigargin treatment resulted in reduced NDV (**Figure 5A**) and PPRV (**Figure 5B**) titers, suggesting that SERCA inhibitor blocks paramyxovirus entry.

In order to ascertain that SERCA functions were restored after withdrawal of the Thapsigargin from the cell culture medium (during entry assay) and did not affect post-entry steps of the viral life cycle, we performed an additional experiment where cells were pretreated with Thapsigargin

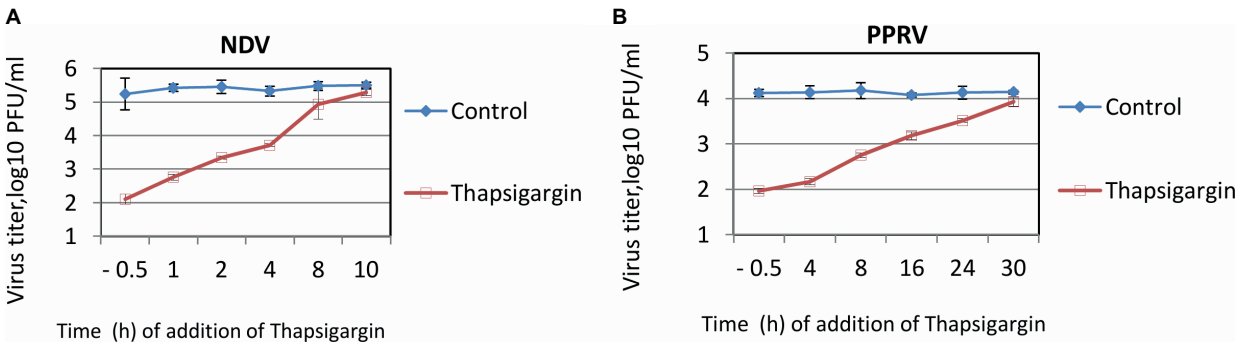

FIGURE 4 | Time-of-addition assay. Confluent monolayers of Vero cells were infected, in triplicate, with PPRV or NDV at MOI of 5, washed six times with PBS and fresh medium with either 0.5 μM Thapsigargin or 0.05% DMSO were added at indicated times. Supernatants were collected at 12 (NDV) or 48 hpi (PPRV) and quantified by plaque assay. Time-of-addition assay for NDV **(A)** and PPRV **(B)** is shown.

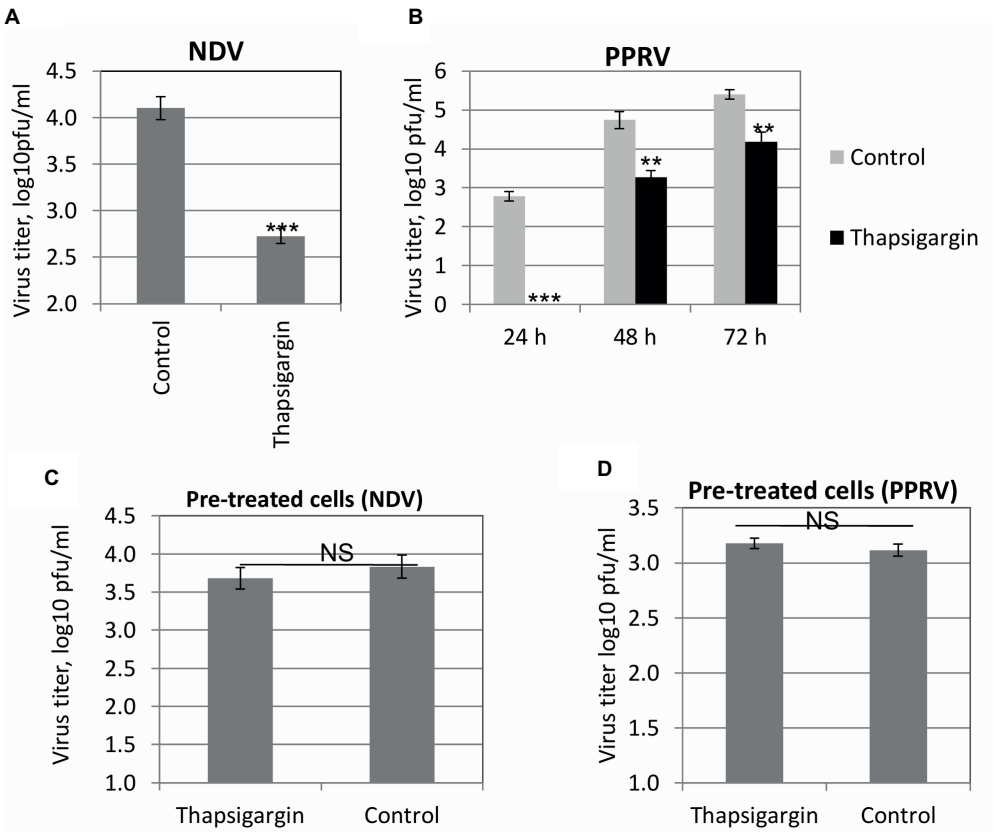

FIGURE 5 | Viral entry. Vero cell monolayers were prechilled to 4°C and infected with the respective viruses at MOI of 5 in Thapsigargin-free medium for 1 h at 4°C to permit the attachment, followed by washing and addition of fresh medium containing Thapsigargin or vehicle control. Entry was allowed to proceed at 37°C for 1 h after which the cells were washed again with PBS to remove any extracellular viruses and incubated with cell culture medium without any inhibitor. The progeny virus particles released in the cell culture supernatants in the treated and untreated cells were titrated by plaque assay. Entry assay for NDV **(A)** and PPRV **(B)** is shown. Vero cells were pretreated with Thapsigargin or DMSO for 1 h followed by washing with PBS and infection with NDV/PPRV at MOI of 5. NDV **(C)** and PPRV **(D)** released in the supernatant were quantified by plaque assay. Error bars indicate SD. Pair-wise statistical comparisons were performed using Student's t test (** = $p < 0.01$, *** = $p < 0.001$, NS = nonsignificant difference).

for 1 h at 37°C followed by its removal by washing with PBS. The cells were then infected with NDV/PPRV and grown in the absence of the inhibitor. There was no significant difference in the viral titers between Thapsigargin- and DMSO-pretreated cells in both NDV (**Figure 5C**) and PPRV (**Figure 5D**), suggesting that the SERCA functions might have been restored after the removal of Thapsigargin from the cell culture medium.

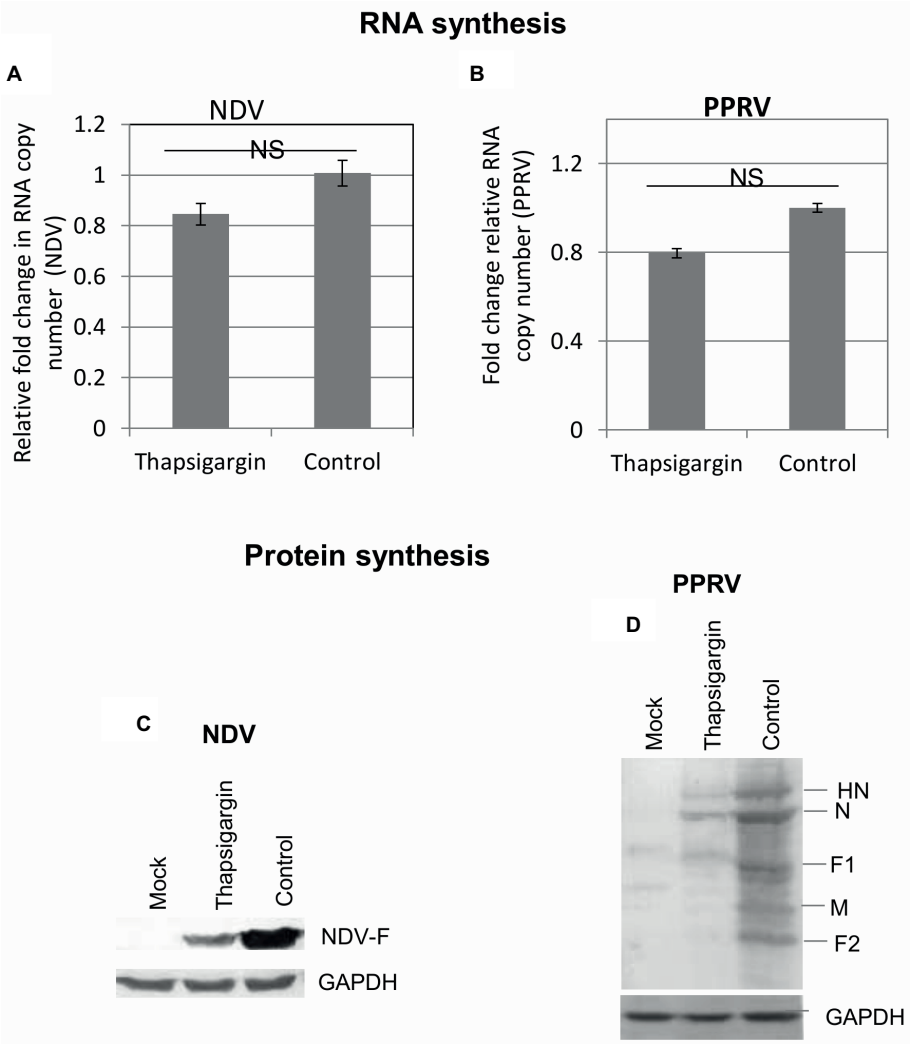

FIGURE 6 | RNA and protein synthesis. Vero cells were either mock-infected or infected with the indicated viruses at MOI of 10 for 3 h followed by washing with PBS and addition of 0.5 μM Thapsigargin or vehicle control (0.05% DMSO). The cells were scrapped at 9 and 20 hpi, respectively, for NDV and PPRV to prepare the cell lysate. Viral RNA was quantified by qRT-PCR. Ct values were normalized with β-actin house-keeping control gene, and relative fold-change was calculated by ΔΔCt method. Relative fold-change in RNA copy number of NDV **(A)** and PPRV **(B)** is shown. The levels of viral proteins were analyzed by Western blot analysis. The levels of viral proteins in NDV **(C)** and PPRV **(D)** infected cells are shown. NS = No significant difference.

RNA and Protein Synthesis

In order to determine the effect of Thapsigargin on the synthesis of viral genome/protein, Thapsigargin was applied to the virus-infected cells when early steps of the virus life cycle (attachment/entry) were expected to occur (>3 h). Cell lysates were prepared at 9 and 20 hpi, respectively, for NDV and PPRV to examine the levels of viral RNA and proteins. No significant difference was observed in viral RNA copy number between Thapsigargin- and control-treated cells (**Figures 6A,B**), suggesting that Thapsigargin has no impact on the synthesis of paramyxoviral genome. However, as compared to the vehicle control (0.05% DMSO)-treated cells, lower levels of viral [NDV (**Figure 6C**) and PPRV (**Figure 6D**)] proteins were observed in Thapsigargin-treated cells.

Budding

We also analyzed the potential effect of Thapsigargin on the release (budding) of progeny virus particles from infected cells. In budding assay, Thapsigargin was applied at the time when the virus presumably starts budding (during logarithmic phase but before attaining a stationary phase viz; 10 and 36 hpi, respectively, for NDV and PPRV). Viral titers in the supernatants were comparable in Thapsigargin-treated and control-treated cells (data not shown), suggesting that Thapsigargin has no impact on the release of the virus from infected cells.

SERCA Inhibition Results in Enhanced Formation of Cytoplasmic Foci in Virus-Infected Cells

To further examine whether SERCA inhibitor impacts other intermediate step(s) of viral replication, immunofluorescence assay

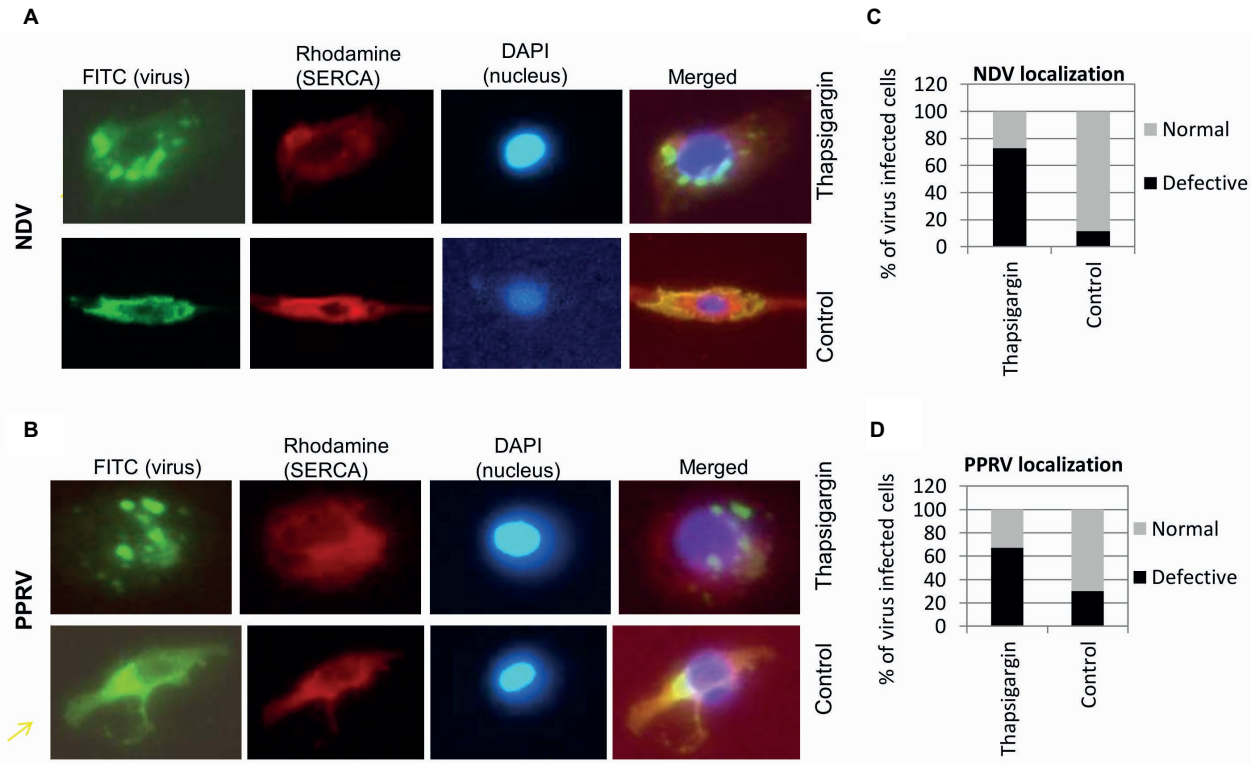

FIGURE 7 | Thapsigargin treatment induces enhanced formation of cytoplasmic foci. Vero cells at ~20% confluence were infected with NDV or PPRV at MOI of 10. At 3 (NDV) or 10 hpi (PPRV), cells were incubated with either 0.5 μM Thapsigargin or 0.05% DMSO. At 10 (NDV) or 36 hpi (PPRV), cells were fixed and subjected for immunofluorescence assay for localization of the viral proteins in the virus-infected cells. Virus was stained with FITC (green), whereas SERCA was stained with rhodamine conjugate. DAPI was used as nuclear stain. Subcellular localization of NDV **(A)** and PPRV **(B)** is shown. Virus-infected cells (FITC) were usually of two types – with or without punctuate structures. To quantitate the subcellular localization, 100 cells (under several different fields) were randomly counted. The percentage of the cells with or without punctuate structures in Thapsigargin-treated and control-treated is shown for NDV **(C)** and PPRV **(D)**.

was performed to monitor the subcellular localization of PPRV and NDV proteins in the cytoplasm of the infected cells. The inhibitor or respective vehicle control (0.05% DMSO) was applied at 3 hpi (NDV) or 10 hpi (PPRV); a time point at which the early events of virus replication (attachment, entry and RNA synthesis) are believed to occur. At 12 hpi (NDV) or 36 hpi (PPRV), when the progeny virus particles presumably bud from the plasma membrane, we observed more number of cytoplasmic foci in Thapsigargin-treated cells, as compared to DMSO-treated cells (**Figures 7A,B**). Thapsigargin treatment showed cytoplasmic foci in ~70% of the cells, as compared to DMSO control wherein this proportion was 10–30% (**Figures 7C,D**).

Selection of Thapsigargin-Resistant Viral Mutants

Due to the high genetic barrier to resistance, host-targeting agents provide an interesting perspective for novel antiviral strategies, rather than the directly acting agents. NDV, when passaged sequentially in the presence of a SERCA inhibitor (Thapsigargin, a host-targeting agent), did not generate a completely resistant phenotype against Thapsigargin, even upon 70 passages in Vero cells (**Figure 8A**). However, resistance began appearing at ~P25 and significant resistance was observed at P35 (~100-fold inhibition compared to ~10,000-fold inhibition at zero passage) after which it became stable without acquiring complete resistance (**Figure 8A**). As compared to P0 and P70-Control viruses, P70-Thapsigargin virus exhibited significantly lower sensitivity to Thapsigargin, though a completely resistant phenotype could not be observed (**Figure 8B**). Control-passaged viruses did not exhibit any significant resistance against Thapsigargin even upon 70 passages (**Figures 8B**,**C**), suggesting that resistance against Thapsigargin (NDV) is not a general phenomenon due to sequential high passages but rather a specific event acquired in the presence of Thapsigargin.

Alternatively, it is possible that the original NDV stock might have contained defective interfering (DI) particles, which suppressed the virus yield. Therefore, we plaque purified P70-Control and P70-Thapsigargin virus stocks – a process which presumably eliminated DI particles. Plaque purified viruses (4 plaques each from P70-Thapsigargin and P70-Control stocks) were again evaluated for their sensitivity to Thapsigargin, wherein P70-Thapsigargin plaques (viruses) were found to replicate at relatively higher titers (~20-fold) (compare **Figures 8D,E**), as compared to the control viruses, suggesting that the higher growth of P70-Thapsigargin virus was presumably due to mutations in the viral genome, rather than simply due to the suppression of DI particle. Furthermore, we also analyzed the mutations in the F protein of P70-Thapsigargin and P70-Control viruses. As compared

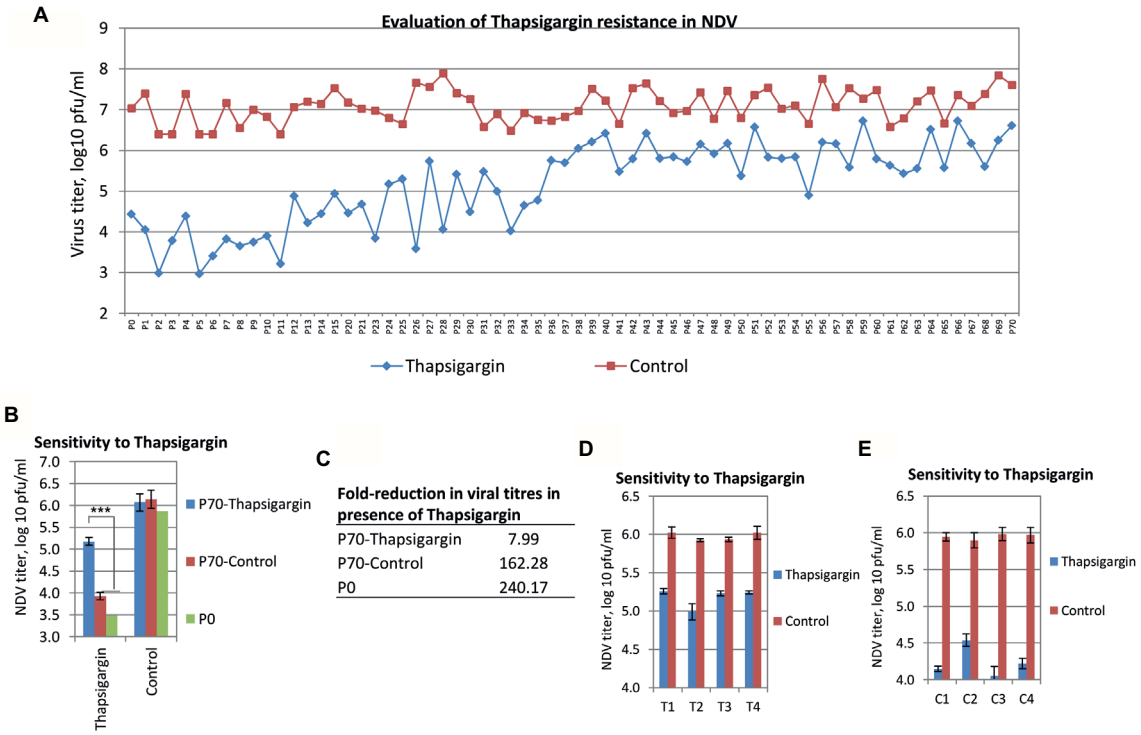

FIGURE 8 | Selection of Thapsigargin-resistant viral mutants. Vero cells were infected with NDV or PPRV at MOI of 0.01 and grown in the presence of either 0.25 μM of Thapsigargin or vehicle control (0.05% DMSO). The progeny virus particles released in the supernatant were harvested either at 72–120 hpi or when ~75% cells exhibited CPE. Seventy (70) such sequential passages were made. **(A)** The levels of NDV inhibition at various passage levels in Thapsigargin-treated and untreated cells are shown. **(B)** *Sensitivity of P70-Thapsigargin NDV to Thapsigargin:* Vero cells, in triplicate, were infected with P0, P70-Thapsigargin, or P70-Control passaged viruses at MOI of 0.1 in the presence of either 0.5 μM Thapsigargin or 0.05% DMSO, and the progeny virus particles released in the supernatant at 24 hpi were quantified. **(C)** Relative growth (fold reduction) of P0, P70-Thapsigargin, and P70-Control viruses in the presence of Thapsigargin. **(D,E)** *Sensitivity of plaque purified (P70) viruses to Thapsigargin:* P70-Thapsigargin or P70-Control viruses were plaque purified [(four plaques each of P70-Control (C1, C2, C3, and C4) and P70-Thapsigargin (T1, T2, T3, and T4)] and amplified in Vero cells. To evaluate the sensitivity to Thapsigargin, plaque purified viruses were infected at MOI of 0.1, and virus yield was measured in the presence of 0.5 μM Thapsigargin or 0.05% DMSO. Error bars indicate SD. Pair-wise statistical comparisons were performed using Student's t test (*** = $p < 0.001$).

Mapping mutations in passaged (P70) viruses (F gene)

Mutation	Virus
E104K	P70-Thapsigargin
K395R	P70-Thapsigargin & P70-Control

FIGURE 9 | *Nucleotide sequencing of passaged virus.* RNA was extracted from P70-Control and P70-Thapsigargin viruses as well as plaque purified viruses (two plaques each of P70-Control and P70-Thapsigargin) followed by amplification and sequence analysis of F gene. Nucleotide sequences were translated into amino acid sequences and compared with P0 as well as WT sequences retrieved from GenBank (n = 18). Amino acid mutations associated with Thapsigargin resistance as well as those acquired simply due to sequential cell culture passage (present in both P70-Control and P70-Thapsigargin) are shown.

to WT [(n = 18, sequences retrieved from GenBank with a global representation)], P0 and P70-Control, P70-Thapsigargin virus showed a unique mutation viz., E104K (**Figure 9**). In addition, as compared to WT, K395R mutation was present in both P70-Control and P70-Thapsigargin, which might have been simply acquired due to sequential cell culture passages (adaptation) (**Figure 9**). These mutations were invariably present in both passaged virus stock (P70) and respective plaque purified viruses (**Figure 9**). However, we could not observe any Thapsigargin-associated mutations in HN gene (data not shown).

DISCUSSION

High mutation rates in RNA viruses enable resistance to antiviral drugs and preexisting immunity to develop. The rise in incidence of drug resistance has prompted a shift towards the development of novel antiviral drugs. As compared to the viral genome, genetic variability of the host is quite low, and therefore, host-targeting agents are considered to impose a higher genetic barrier to generation of resistant viruses (Fofana et al., 2010, 2012; Lupberger et al., 2011; Khandelwal et al., 2017). Thus, a potentially better approach for the development of novel antiviral therapeutics would be to target host factors required for viral replication, although cytotoxicity of such antiviral agents is of considerable importance. Targeting host factors could have a significant impact on multiple virus genotypes

(strain/serotype) and could provide broad spectrum inhibition against different families of viruses which might use the same cellular pathway(s) for replication (Pawlotsky, 2012; Ruiz and Russell, 2012; Conteduca et al., 2014; Shahidi et al., 2014; Khandelwal et al., 2017). This novel approach has led to the development of some promising compounds for the treatment of HCV and HIV (Gilliam et al., 2011; von Hahn et al., 2011). In this study, we have shown that targeting SERCA (a Ca2+ ATPase) by a small molecule chemical inhibitor (Thapsigargin) can block paramyxovirus replication. The inhibitory effect of Thapsigargin could be rescued by overexpression of SERCA, suggesting the virus supportive role of SERCA. Therefore, SERCA may be a novel target for antiviral drug development. Hoffmann and coworkers identified that SPCA1 [a secretary pathway calcium (Ca^{2+}) transporter that facilitates Ca^{2+} and Mn^{2+} uptake into the trans-Golgi network] also facilitates replication of the members of the family, *Flaviviridae*, *Togaviridae*, and *Paramyxoviridae* (Hoffmann et al., 2017), suggesting the involvement of multiple calcium transporters in paramyxovirus replication. Mechanistically, SERCA inhibitor was shown to block viral entry and synthesis of viral proteins, besides inducing enhanced formation of cytoplasmic foci. While the precise mechanism of formation of enhanced cytoplasmic foci remains elusive, this might probably have occurred due to general dysregulation of endoplasmic reticulum/altered calcium homeostasis. Furthermore, how SERCA2 regulates both viral entry and synthesis of viral proteins is intriguing and needs further investigation.

It is generally believed that viruses do not acquire resistance against host-targeting antiviral agents (Kumar et al., 2011b, 2014; Pawlotsky, 2012; Chaudhary et al., 2015). However, in a recent study (van der Schaar et al., 2012), Schaar and colleagues identified Coxsackievirus B3 (CVB3) mutants that replicate efficiently in the presence of several potent antiviral drugs known to inhibit phosphatidylinositol-4-kinase IIIα (PI4KIIIα), a key cellular factor for CVB3 replication. The authors observed that a single point mutation in the viral 3A protein confers resistance, and the drug-resistant escape mutants of CVB3 can replicate in cells with low PI4KIIIα. Additionally, cyclosporine A (CsA)-resistant hepatitis C virus (HCV) mutant has also been identified (Coelmont et al., 2009; Chatterji et al., 2010). In our study, resistance acquired by NDV against SERCA inhibitor adds another example to a short list of viruses, which can acquire resistance to host-targeting antiviral agents. To the best of our knowledge, this is the first documented example wherein a paramyxovirus significantly bypasses its dependency on a cellular factor that is targeted by a small molecule inhibitor. While not yet understood, one possible mechanism underlying acquisition of drug resistance is due to change in host factor requirement (Hopcraft and Evans, 2015). For example, under selection pressure in CLDN1 (tight junction protein claudin-1, which serves as an entry factor for HCV) knock-out cells, CLDN1-dependent HCV evolved to use alternate host factors – CLDN6 or CLDN9 (Hopcraft and Evans, 2015). Alternatively, resistant viruses may simply have enhanced affinity for its natural substrate, thereby allowing the virus to propagate despite reduction in concentration of the cellular factors (Kaufmann et al., 2018).

We mapped at least one mutation (E104K) in F protein of Thapsigargin-resistant NDV. Further studies on recombinant NDV harboring point mutation(s) in F and/or other viral proteins are required to precisely understand the mechanism underlying acquisition of drug resistance against Thapsigargin. Though a complete Thapsigargin-resistant NDV phenotype could not be achieved even up to passage level 70, it is a matter of conjecture as to how NDV became less dependent on SERCA (under the selection pressure of Thapsigargin). In immunofluorescence assay, we could not observe a perfect co-localization of SERCA and viral proteins. A co-immunoprecipitation assay to detect a direct interaction between SERCA and virus was also unsuccessful; therefore, in this study, we could not determine any direct interaction between SERCA and viral proteins.

To conclude, we have provided strong evidence for SERCA as a crucial host factor in facilitating optimal paramyxovirus replication, thus validating this as a candidate drug target for the development of antiviral therapeutics. The drug resistance against host-targeting antiviral agents is not an unprecedented event.

AUTHOR CONTRIBUTIONS

NKu, SB, SSh, TR and BT designed the experiments. NKu, NKh, RK, YC, KR and KC performed the experiments. NKu, SB, SSh, SSi and BT wrote the manuscript.

FUNDING

This work was supported by the Science and Engineering Research Board, Department of Science and Technology, Government of India (Grant number SB/SO/AS-20/2014) and has been released as a pre-print at BioRxiv.

REFERENCES

Altshuler, I., Vaillant, J. J., Xu, S., and Cristescu, M. E. (2012). The evolutionary history of sarco(endo)plasmic calcium ATPase (SERCA). *PLoS One* 7:e52617. doi: 10.1371/journal.pone.0052617

Andino, R., and Domingo, E. (2015). Viral quasispecies. *Virology* 479–480, 46–51. doi: 10.1016/j.virol.2015.03.022

Arruda, A. P., Nigro, M., Oliveira, G. M., and de Meis, L. (2007). Thermogenic activity of Ca^{2+}-ATPase from skeletal muscle heavy sarcoplasmic reticulum: the role of ryanodine Ca^{2+} channel. *Biochim. Biophys. Acta* 1768, 1498–1505. doi: 10.1016/j.bbamem.2007.03.016

Chatterji, U., Lim, P., Bobardt, M. D., Wieland, S., Cordek, D. G., Vuagniaux, G., et al. (2010). HCV resistance to cyclosporin A does not correlate with a resistance of the NS5A-cyclophilin A interaction to cyclophilin inhibitors. *J. Hepatol.* 53, 50–56. doi: 10.1016/j.jhep.2010.01.041

Chaudhary, K., Chaubey, K. K., Singh, S. V., and Kumar, N. (2015). Receptor tyrosine kinase signaling regulates replication of the peste des petits ruminants virus. *Acta Virol.* 59, 78–83. doi: 10.4149/av_2015_01_78

Chen, Z. W., Hu, P., and Ren, H. (2016). A new challenge in clinical practice: resistance to directly acting antivirals in hepatitis C treatment. *Zhonghua Gan Zang Bing Za Zhi* 24, 165–169. doi: 10.3760/cma.j.issn.1007-3418.2016.03.002

Clapham, D. E. (2007). Calcium signaling. *Cell* 131, 1047–1058. doi: 10.1016/j.cell.2007.11.028

Coelmont, L., Kaptein, S., Paeshuyse, J., Vliegen, I., Dumont, J. M., Vuagniaux, G., et al. (2009). Debio 025, a cyclophilin binding molecule, is highly efficient in clearing hepatitis C virus (HCV) replicon-containing cells when used alone or in combination with specifically targeted antiviral therapy for HCV (STAT-C) inhibitors. *Antimicrob. Agents Chemother.* 53, 967–976. doi: 10.1128/AAC.00939-08

Coito, C., Diamond, D. L., Neddermann, P., Korth, M. J., and Katze, M. G. (2004). High-throughput screening of the yeast kinome: identification of human serine/threonine protein kinases that phosphorylate the hepatitis C virus NS5A protein. *J. Virol.* 78, 3502–3513. doi: 10.1128/JVI.78.7.3502-3513.2004

Conteduca, V., Sansonno, D., Russi, S., Pavone, F., and Dammacco, F. (2014). Therapy of chronic hepatitis C virus infection in the era of direct-acting and host-targeting antiviral agents. *J. Inf. Secur.* 68, 1–20. doi: 10.1016/j.jinf.2013.08.019

de Meis, L., Oliveira, G. M., Arruda, A. P., Santos, R., Costa, R. M., and Benchimol, M. (2005). The thermogenic activity of rat brown adipose tissue and rabbit white muscle Ca^{2+}-ATPase. *IUBMB Life* 57, 337–345. doi: 10.1080/15216540500092534

Eastman, R. T., and Fidock, D. A. (2009). Artemisinin-based combination therapies: a vital tool in efforts to eliminate malaria. *Nat. Rev. Microbiol.* 7, 864–874. doi: 10.1038/nrmicro2239

Feng, M. Y., and Rao, R. (2013). New insights into store-independent $Ca^{(2+)}$ entry: secretory pathway calcium ATPase 2 in normal physiology and cancer. *Int. J. Oral. Sci.* 5, 71–74. doi: 10.1038/ijos.2013.23

Flavell, S. W., and Greenberg, M. E. (2008). Signaling mechanisms linking neuronal activity to gene expression and plasticity of the nervous system. *Annu. Rev. Neurosci.* 31, 563–590. doi: 10.1146/annurev.neuro.31.060407.125631

Fofana, I., Fafi-Kremer, S., Carolla, P., Fauvelle, C., Zahid, M. N., Turek, M., et al. (2012). Mutations that alter use of hepatitis C virus cell entry factors mediate escape from neutralizing antibodies. *Gastroenterology* 143, 223–233. e229. doi: 10.1053/j.gastro.2012.04.006

Fofana, I., Krieger, S. E., Grunert, F., Glauben, S., Xiao, F., Fafi-Kremer, S., et al. (2010). Monoclonal anti-claudin 1 antibodies prevent hepatitis C virus infection of primary human hepatocytes. *Gastroenterology* 139, 953–964.e4. doi: 10.1053/j.gastro.2010.05.073

Gilliam, B. L., Riedel, D. J., and Redfield, R. R. (2011). Clinical use of CCR5 inhibitors in HIV and beyond. *J. Transl. Med.* 9(Suppl. 1):S9. doi: 10.1186/1479-5876-9-S1-S9

Griffiths, S. J., Koegl, M., Boutell, C., Zenner, H. L., Crump, C. M., Pica, F., et al. (2013). A systematic analysis of host factors reveals a Med23-interferon-lambda regulatory axis against herpes simplex virus type 1 replication. *PLoS Pathog.* 9:e1003514. doi: 10.1371/journal.ppat.1003514

Hoffmann, H. H., Schneider, W. M., Blomen, V. A., Scull, M. A., Hovnanian, A., Brummelkamp, T. R., et al. (2017). Diverse viruses require the calcium transporter SPCA1 for maturation and spread. *Cell Host Microbe* 22, 460–470.e465. doi: 10.1016/j.chom.2017.09.002

Hopcraft, S. E., and Evans, M. J. (2015). Selection of a hepatitis C virus with altered entry factor requirements reveals a genetic interaction between the E1 glycoprotein and claudins. *Hepatology* 62, 1059–1069. doi: 10.1002/hep.27815

Inesi, G., Hua, S., Xu, C., Ma, H., Seth, M., Prasad, A. M., et al. (2005). Studies of Ca^{2+} ATPase (SERCA) inhibition. *J. Bioenerg. Biomembr.* 37, 365–368. doi: 10.1007/s10863-005-9472-1

Kaufmann, S. H. E., Dorhoi, A., Hotchkiss, R. S., and Bartenschlager, R. (2018). Host-directed therapies for bacterial and viral infections. *Nat. Rev. Drug Discov.* 17, 35–56. doi: 10.1038/nrd.2017.162

Khandelwal, N., Chander, Y., Rawat, K. D., Riyesh, T., Nishanth, C., Sharma, S., et al. (2017). Emetine inhibits replication of RNA and DNA viruses without generating drug-resistant virus variants. *Antivir. Res.* 144, 196–204. doi: 10.1016/j.antiviral.2017.06.006

Khandelwal, N., Kaur, G., Chaubey, K. K., Singh, P., Sharma, S., Tiwari, A., et al. (2014). Silver nanoparticles impair Peste des petits ruminants virus replication. *Virus Res.* 190, 1–7. doi: 10.1016/j.virusres.2014.06.011

Kudla, J., Batistic, O., and Hashimoto, K. (2010). Calcium signals: the lead currency of plant information processing. *Plant Cell* 22, 541–563. doi: 10.1105/tpc.109.072686

Kumar, N., Barua, S., Riyesh, T., Chaubey, K. K., Rawat, K. D., Khandelwal, N., et al. (2016). Complexities in isolation and purification of multiple viruses from mixed viral infections: viral interference, persistence and exclusion. *PLoS One* 11:e0156110. doi: 10.1371/journal.pone.0156110

Kumar, N., Liang, Y., Parslow, T. G., and Liang, Y. (2011a). Receptor tyrosine kinase inhibitors block multiple steps of influenza a virus replication. *J. Virol.* 85, 2818–2827. doi: 10.1128/JVI.01969-10

Kumar, N., Maherchandani, S., Kashyap, S. K., Singh, S. V., Sharma, S., Chaubey, K. K., et al. (2014). Peste des petits ruminants virus infection of small ruminants: a comprehensive review. *Viruses* 6, 2287–2327. doi: 10.3390/v6062287

Kumar, N., Sharma, N. R., Ly, H., Parslow, T. G., and Liang, Y. (2011b). Receptor tyrosine kinase inhibitors that block replication of influenza a and other viruses. *Antimicrob. Agents Chemother.* 55, 5553–5559. doi: 10.1128/AAC.00725-11

Kumar, N., Xin, Z. T., Liang, Y., Ly, H., and Liang, Y. (2008). NF-kappaB signaling differentially regulates influenza virus RNA synthesis. *J. Virol.* 82, 9880–9889. doi: 10.1128/JVI.00909-08

Ludwig, S., Pleschka, S., Planz, O., and Wolff, T. (2006). Ringing the alarm bells: signalling and apoptosis in influenza virus infected cells. *Cell. Microbiol.* 8, 375–386. doi: 10.1111/j.1462-5822.2005.00678.x

Lupberger, J., Zeisel, M. B., Xiao, F., Thumann, C., Fofana, I., Zona, L., et al. (2011). EGFR and EphA2 are host factors for hepatitis C virus entry and possible targets for antiviral therapy. *Nat. Med.* 17, 589–595. doi: 10.1038/nm.2341

Martin, V., Bredoux, R., Corvazier, E., van Gorp, R., Kovacs, T., Gelebart, P., et al. (2002). Three novel sarco/endoplasmic reticulum Ca^{2+}-ATPase (SERCA) 3 isoforms. Expression, regulation, and function of the membranes of the SERCA3 family. *J. Biol. Chem.* 277, 24442–24452. doi: 10.1074/jbc.M202011200

Nousiainen, L., Sillanpaa, M., Jiang, M., Thompson, J., Taipale, J., and Julkunen, I. (2013). Human kinome analysis reveals novel kinases contributing to virus infection and retinoic-acid inducible gene I-induced type I and type III IFN gene expression. *Innate. Immun.* 19, 516–530. doi: 10.1177/1753425912473345

Pawlotsky, J. M. (2012). The science of direct-acting antiviral and host-targeted agent therapy. *Antivir. Ther.* 17, 1109–1117. doi: 10.3851/IMP2423

Primeau, J. O., Armanious, G. P., Fisher, M. E., and Young, H. S. (2018). The sarcoendoplasmic reticulum calcium ATPase. *Subcell. Biochem.* 87, 229–258. doi: 10.1007/978-981-10-7757-9_8

Qi, H., Moran, M. M., Navarro, B., Chong, J. A., Krapivinsky, G., Krapivinsky, L., et al. (2007). All four CatSper ion channel proteins are required for male fertility and sperm cell hyperactivated motility. *Proc. Natl. Acad. Sci. USA* 104, 1219–1223. doi: 10.1073/pnas.0610286104

Rasmussen, U., Broogger Christensen, S., and Sandberg, F. (1978). Thapsigargine and thapsigargicine, two new histamine liberators from *Thapsia garganica* L. *Acta. Pharm. Suec.* 15, 133–140.

Rogers, T. B., Inesi, G., Wade, R., and Lederer, W. J. (1995). Use of thapsigargin to study Ca^{2+} homeostasis in cardiac cells. *Biosci. Rep.* 15, 341–349. doi: 10.1007/BF01788366

Ruiz, A., and Russell, S. J. (2012). A new paradigm in viral resistance. *Cell Res.* 22, 1515–1517. doi: 10.1038/cr.2012.139

Shahidi, M., Tay, E. S., Read, S. A., Ramezani-Moghadam, M., Chayama, K., George, J., et al. (2014). Endocannabinoid CB1 antagonists inhibit hepatitis C virus production, providing a novel class of antiviral host-targeting agents. *J. Gen. Virol.* 95, 2468–2479. doi: 10.1099/vir.0.067231-0

van der Schaar, H. M., van der Linden, L., Lanke, K. H., Strating, J. R., Purstinger, G., de Vries, E., et al. (2012). Coxsackievirus mutants that can bypass host factor PI4KIIIbeta and the need for high levels of PI4P lipids for replication. *Cell Res.* 22, 1576–1592. doi: 10.1038/cr.2012.129

von Hahn, T., Ciesek, S., and Manns, M. P. (2011). Arrest all accessories—inhibition of hepatitis C virus by compounds that target host factors. *Discov. Med.* 12, 237–244.

Wuytack, F., Raeymaekers, L., and Missiaen, L. (2002). Molecular physiology of the SERCA and SPCA pumps. *Cell Calcium* 32, 279–305. doi: 10.1016/S0143416002001847

Conflict of Interest Statement: The authors declare that the research was conducted in the absence of any commercial or financial relationships that could be construed as a potential conflict of interest.

Copyright © 2019 Kumar, Khandelwal, Kumar, Chander, Rawat, Chaubey, Sharma, Singh, Riyesh, Tripathi and Barua. This is an open-access article distributed under the terms of the Creative Commons Attribution License (CC BY). The use, distribution or reproduction in other forums is permitted, provided the original author(s) and the copyright owner(s) are credited and that the original publication in this journal is cited, in accordance with accepted academic practice. No use, distribution or reproduction is permitted which does not comply with these terms.

frontiers in Immunology

ORIGINAL RESEARCH
published: 28 February 2019
doi: 10.3389/fimmu.2019.00340

Immune Activations and Viral Tissue Compartmentalization During Progressive HIV-1 Infection of Humanized Mice

Hang Su[1], Yan Cheng[1], Sruthi Sravanam[1], Saumi Mathews[1], Santhi Gorantla[1], Larisa Y. Poluektova[1], Prasanta K. Dash[1] and Howard E. Gendelman[1,2*†]*

[1] Department of Pharmacology and Experimental Neuroscience, College of Medicine, University of Nebraska Medical Center, Omaha, NE, United States, [2] Department of Pharmaceutical Sciences, College of Pharmacy, University of Nebraska Medical Center, Omaha, NE, United States

Human immunodeficiency virus type one (HIV-1) tissue compartments are established soon after viral infection. However, the timing in which virus gains a permanent foothold in tissue and the cellular factors that control early viral-immune events are incompletely understood. These are critical events in studies of HIV-1 pathogenesis and in the development of viral reservoirs after antiretroviral therapy. Moreover, factors affecting the permanence of viral-tissue interactions underlie barriers designed to eliminate HIV-1 infection. To this end we investigated the temporal and spatial viral and host factors during HIV-1 seeding of tissue compartments. Two humanized NOD.Cg-Prkdc^{scid} IL2rg^{tm1Wjl}/SzJ mouse models were employed. In the first, immune deficient mice were reconstituted with human CD34+ cord blood hematopoietic stem cells (HSC) (hu-HSC) and in the second mice were transplanted with adult mature human peripheral lymphocytes (hu-PBL). Both, in measure, reflect relationships between immune activation and viral infection as seen in an infected human host. Following humanization both mice models were infected with HIV-1$_{ADA}$ at 10^4 50% tissue culture infective doses. Viral nucleic acids and protein and immune cell profiles were assayed in brain, lung, spleen, liver, kidney, lymph nodes, bone marrow, and gut from 3 to 42 days. Peripheral CD4+ T cell loss began at 3 days together with detection of HIV-1 RNA in both mouse models after initiation of HIV-1 infection. HIV-1 was observed in all tested tissues at days 3 and 14 in hu- PBL and HSC mice, respectively. Immune impairment was most prominent in hu-PBL mice. T cell maturation and inflammation factors were linked directly to viral tissue seeding in both mouse models. We conclude that early viral tissue compartmentalization provides a roadmap for investigations into HIV-1 elimination.

Keywords: humanized mice, host immune responses, HIV-1 seeding, viral tissue compartments, immune activation, host inflammatory responses

OPEN ACCESS

Edited by:
Cheryl Ann Winkler, Frederick National Laboratory for Cancer Research (NIH), United States

Reviewed by:
Vijayakumar Velu, Emory University, United States
Paul Urquhart Cameron, The University of Melbourne, Australia

***Correspondence:**
Prasanta K. Dash
pdash@unmc.edu
Howard E. Gendelman
hegendel@unmc.edu

†Present Address:
Howard E. Gendelman, Department of Pharmacology and Experimental Neuroscience, University of Nebraska Medical Center, Omaha, NE, United States

Specialty section:
This article was submitted to Viral Immunology, a section of the journal Frontiers in Immunology

Received: *10 August 2018*
Accepted: *08 February 2019*
Published: *28 February 2019*

Citation:
Su H, Cheng Y, Sravanam S, Mathews S, Gorantla S, Poluektova LY, Dash PK and Gendelman HE (2019) Immune Activations and Viral Tissue Compartmentalization During Progressive HIV-1 Infection of Humanized Mice. Front. Immunol. 10:340. doi: 10.3389/fimmu.2019.00340

INTRODUCTION

Following the introduction of antiretroviral therapy (ART) in the mid-1990s, remarkable progress was made toward reducing disease morbidities and mortality during a life-long human immunodeficiency virus type one (HIV-1) infection (1–3). While ART efficiently controls viremia and preserves immune function (4) it does not eradicate infection (5). Recent discoveries suggested that HIV-1 persistence is established within 2 weeks of viral exposure (6). Thus, complete understanding of viral tissue compartmentalization needs be made in efforts to eliminate HIV-1 infection.

To reflect the temporal and spatial challenges of human infection, animal models must reflect essential features of HIV-1 pathobiology in its human host (7). Insights into HIV-1 transmission and tissue distribution were made through studies of simian immunodeficiency virus (SIV) infection of nonhuman primates (8, 9). However, there are limitations. *First*, SIV and HIV are genetically and biologically distinct (10). *Second*, divergent viral and host factors affect progression to the acquired immune deficiency syndrome which commonly occurs more rapidly during SIV than HIV (10). Therefore, an HIV-1 susceptible animal model would be preferable for studies that reflect human infection. To such ends, humanized mouse models were developed. These models received engraftment of human cells into immunodeficient rodents resulting in the establishment of a functional human immune systems and tissue microenvironment that support long-term HIV-1 replication in target cells and tissues (11). Studies conducted by our group and others using such humanized mice have provided new insights into HIV-1 virology, immunology, pathology, therapeutics, and modes of viral eradication (12–16). However, to date, limited studies were performed to dissect when and to what extent HIV-1 establishes persistent infection in tissue compartments. If this information is gleamed they could prove instrumental in developing improved antiretroviral therapies.

In our prior works, chronic HIV-1 infected CD34+ hematopoietic stem cell (hu-HSC) reconstituted NOD.Cg-Prkdc^{scid} Il2rg^{tm1Wjl}/SzJ (NSG) mice were investigated (17–19). They were used successfully to identify viral replication patterns and virus-induced injuries in diverse cell and tissue types. In the current study, attempts were made to better understand the temporal and spatial dynamics of viral seeding that followed HIV-1 inoculation. To this end we tracked early viral footprints in tissue compartments. To compare how the host microenvironment could affect viral seeding we used both infected adult peripheral blood lymphocyte (hu-PBL) and hu-HSC mouse models. Animals were evaluated in parallel after infection and were necropsied at days 3, 5, 7, 14, 28, and 42. Results showed that peripheral CD4+ T cells decreased rapidly in infected hu-PBL mice with viral detection in all tissues within 3 days of infection. In contrast, in hu-HSC mice virus was detected in gut, kidney, spleen, lung, liver, and lymph nodes and in brain only by 14 and 28 days. HIV-1 nucleic acids and proteins demonstrated that the viral life cycle was completed in both humanized mice. Transcriptomic analysis demonstrated substantive immune activation and pro-inflammatory signature in hu-PBL compared to HSC mice that paralleled viral tissue compartmentalization. These data, taken together, demonstrate the dynamics and extent of HIV-1 tissue infections and its link to human immunity in relevant humanized mouse models of viral infection.

MATERIALS AND METHODS

Generation and HIV-1 Infection of Humanized Mice

NSG mice were purchased from the Jackson Laboratory (Bar Harbor, ME) and housed under pathogen-free conditions in accordance with ethical guidelines for the care of laboratory animals at the National Institutes of Health and the University of Nebraska Medical Center. All experimental protocols were approved by the University of Nebraska Medical Center Institutional Animal Care and Use Committee (IACUC).

To generate human CD34+ mice, the new born NSG mice were irradiated with a RS 2,000 biological irradiator (Rad Source Technologies Inc.), followed with intrahepatic engraftment of human CD34+ HSCs that were isolated from human cord blood. Humanization of the animals was monitored monthly from peripheral blood using flow cytometry analysis on human cell markers. At 20–22 weeks of age, a total of 31 animals with replicate levels of human cell reconstitution were selected then divided into uninfected ($n = 5$) and HIV-1 infected mouse groups ($n = 26$). The latter animals were infected intraperitoneally with HIV-1_{ADA} at 10^4 $TCID_{50}$ and then randomly distributed into groups that were sacrificed at days 3 ($n = 5$), 5 ($n = 5$), 7 ($n = 5$), 14 ($n = 5$), 28 ($n = 3$), and 42 ($n = 3$) post viral challenge for further immune and viral analysis.

Adult human PBL mice were generated by intraperitoneal injection of adult human peripheral blood lymphocytes purified from HIV-1 seronegative donor leukopaks into 8-week old NSG mice at 25×10^6 PBLs/mouse. Ten days after engraftment, animal humanization was confirmed by flow cytometry. In total, 28 mice with replicate numbers of engrafted human cells were divided into uninfected ($n = 4$) and HIV-1 infected groups ($n = 24$) used for analyses. HIV-1_{ADA} challenge was given intraperitoneally at 10^4 $TCID_{50}$. Infected animals were then randomly distributed into groups that were sacrificed at days 3, 5, 7, and 17 ($n = 6$, 5, 5, and 8) after viral infection for further immune and viral evaluations.

Flow Cytometry

Peripheral blood was collected at designated time points into EDTA-coated tubes by cardiocentesis at the study end. Cellular phenotypes were analyzed for human antigens CD45, CD3, CD19, CD4, CD8, and CD14 (BD Pharmingen, San Diego, CA) using the fluorescence-activated cell sorting (FACS) system BD LSR2 (BD Immunocytometry Systems, Mountain View, CA) system. CD45+ human cells were gated from total lymphocytes. The percentages of $CD4^+$ and $CD8^+$ cells were obtained from the gate set for human CD3+ T cells. Results were analyzed using FlowJo software (BD Pharmingen, San Diego, CA).

Viral Load Analyses

Plasma samples were isolated from animal peripheral blood by centrifugation. Plasma HIV-1 RNA levels were measured using an automated COBAS Amplicor V2.0/Taqman-48 system (Roche Molecular Diagnostics, Basel, Switzerland) as per the manufacturer's instructions.

Nucleic Acid Extraction and Quantification

Animal tissues were homogenized using a Qiagen Tissue Lyser II followed total nucleic acids (DNA and RNA) extraction with Qiagen All Prep DNA/RNA Mini Kit (QIAGEN). Serial dilutions of HIV-1 DNA from the ACH-2 cell line, which contains one integrated viral copy per cell, served as the standard control (20). Tissue HIV-1 RNA was first reverse-transcribed to complementary DNA using a cDNA synthesis kit (Invitrogen, MA) (21). HIV-1 DNA and RNA were quantified by semi-nested real-time PCR as previously described (19). The first round of the PCR was performed on a conventional PCR machine (T100 Thermal Cycler, BioRad, CA). The products were subsequently applied to the second round real-time PCR using TaqMan fluorescent probes on an ABI Prism 7000 real-time PCR machine (Applied Biosystems, MA). The expression levels of tissue HIV-1 DNA and RNA were normalized to those for the human CD45 gene (Life Technology, CA). The sensitivity of our assay is around 10 copies.

RNAscope

RNA scope was performed on 5-μm thick paraffin-embedded spleen sections (Advanced Cell Diagnostics, Hayward, CA) according to the manufacturer's instructions. Anti-sense HIV-1 Clade B probe designed for targeting 854–8291 base pairs of HIV-1 sequence was used for viral detection. Positive signals were expressed as single or clusters of brown dots. Human peptidylprolyl isomerase B (PPIB) was applied as controls for human genome. All the images were captured for 40X magnification.

Immunohistochemistry

Tissue samples were collected at the time of animal autopsy, fixed with 4% paraformaldehyde, and embedded in paraffin. Tissue sections of 5-μm thickness were cut and immuno-stained with HLA-DR (clone CR3/43, 1:100, DAKO, Carpinteria, CA) and HIV-1 p24 (1:10, DAKO) antibodies. The DAKO EnVision polymer-based system was used for staining development, and all the sections were counterstained with Mayer's hematoxylin (12). Images were obtained with a Nuance EX camera fixed to a Nikon Eclipse E800 microscope using Nuance software (Cambridge Research & Instrumentation, Woburn, MA). Human HLA-DR images were taken at 20× magnifications and HIV-1p24 images were captured at 40× objective magnifications.

Human mRNA Analysis of Immune Responses

Humanized mouse spleen was harvested at animal necropsy followed with total RNA isolation using an RNease Mini Kit (QIAGEN). Complementary DNA (cDNA) was generated using a cDNA synthesis kit (Invitrogen, MA) and subscribed to RT^2 PCR arrays for T & B cell activation analysis (QIAGEN). Quantitative RT-PCR was performed on an Master cycler® ep realplex as per the manufacturer's instructions (Eppendorf) and analyzed using RT^2 Profiler PCR Array web-based data analysis software, version 3.5 (QIAGEN). Gene networks analysis was performed using Ingenuity Pathway Analysis (QIAGEN).

Statistical Analyses

Data were analyzed using GraphPad Prism 7.0 software (La Jolla, CA). The Student's *t*-test was used for two-group comparison. A value of $p < 0.05$ was considered statistically significantly different. All results were presented as the means ± the standard error of the mean (SEM). Fisher's Exact Test was used to validate the IPA data of spleen of each canonical pathway.

RESULTS

Immune Profiles in HIV-1 Infected Humanized Mice

NSG mice were irradiated at birth then were transplanted by intrahepatic injection with human CD34+ cord blood hematopoietic stem cells (hu-HSC) (12). Monthly whole blood flow cytometry showed that by 22 weeks mouse blood contained 30–60% human immunocytes. Following HIV-1_{ADA} infection at 10^4 50% tissue culture infection dose ($TCID_{50}$)/animal, assays for viral, and immune profiles were performed in blood and tissues at days 0, 3, 5, 7, 14, 28, and 42. Replicates of 3 to 5 animals were tested at each of the time points before and after infection (at the time of sacrifice) (**Figure 1A**).

Our flow cytometric gating strategy is illustrated in **Figure S1A**. Prior to HIV-1 infection, the percentages of human CD45+ cells in hu-HSC mouse blood ranged between 30 and 60% (**Figure 1B**). A significant decline was seen by 42 days (10.9% ± 0.9), but not much decline was observed in the earlier time points (**Figure 1B**). Percentages of human cells stayed consistent between HIV-1 infected and mock infected controls in hu-HSC spleen and bone marrow that ranged from 45 to 55% (**Figures S1B,C**).

Progressive loss of CD4+ T cells in blood was observed in infected hu-HSC mice. The mean decreases in CD4+ T cells were 4.7% ± 5.1, 10.2% ± 2.2, 14.0% ± 0.8, 11.9% ± 1.6, 14.0% ± 2.9, and 18.8% ± 1.8, at days 3, 5, 7, 14, 28, and 42, respectively. In parallel, CD8+ T cell counts were increased by 4.6% ± 3.8, 9.7% ± 2.0, 10.6% ± 1.6, 9.1% ± 1.3, 3.8% ± 2.6, and 14.4% ± 1.1, at respective time points (**Figure 1B**). Splenocytes and bone marrow cells were collected at necropsy and showed parallel losses and increases in CD4+ and CD8+ T cells, respectively, in HIV-1 infected vs. mock infected mice (**Figures S1B,C**).

To compare virus-host interactions during early HIV-1 infection with immunologically "mature" hu-PBL mice, replicate evaluations were performed. Due to expected graft-vs.-host disease in this model (22) testing was conducted up to 14 days. Adult NSG mice were engrafted with hu-PBL 10 days prior to HIV-1_{ADA} infection with up to eight animals/time point evaluated at days 0, 3, 5, 7, and 14 (**Figure 2A**). No significant changes of peripheral human CD45+ cell counts were observed in hu-PBL mice before and after infection. The values ranged

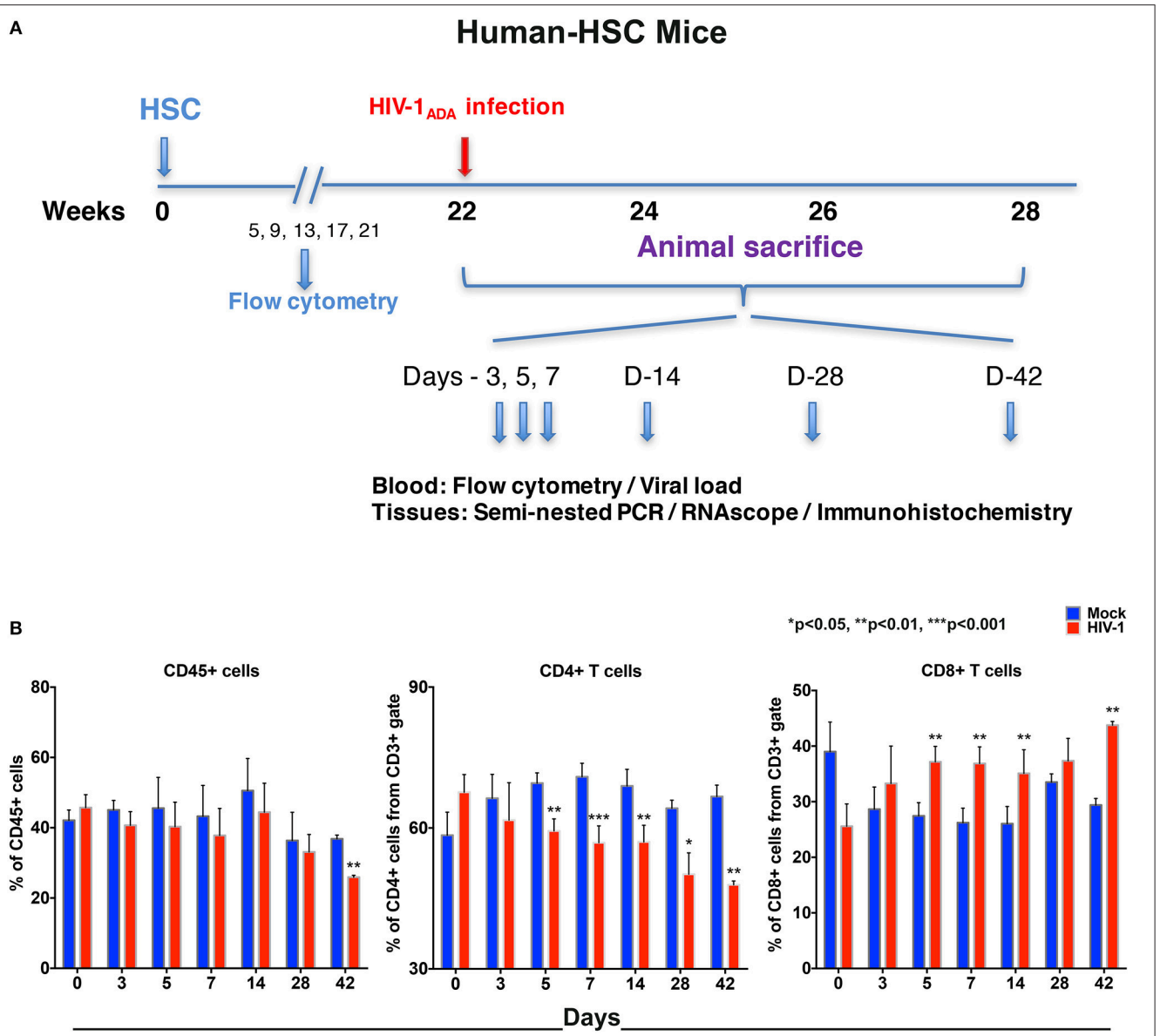

FIGURE 1 | Human lymphocyte responses following HIV-1 infection of hu-HSC mice. **(A)** The illustrated experimental design for hu-HSC mice human cell reconstitution, HIV-1 infection, and serial animal sacrifice performed at days 0, 3, 5, 7, 14, 28, and 42. Animal numbers are $N = 5, 5, 5, 5, 5, 3$, and 3 at each of the time points. **(B)** Peripheral blood CD45+, CD4+, and CD8+ cell counts before/mock infection (blue) and after HIV-1 infection (red) for each of the time points by flow cytometry tests. Data are expressed as mean ± SEM and considered *, **, *** statistically different, at $p < 0.05$, $p < 0.01$, and $p < 0.001$.

from 25 to 45% of total immunocytes (**Figure 2B**). The depletion of CD4+ T cells was robust in infected hu-PBL mice. These equaled 24.1% ± 4.6, 18.2% ± 3.0, 20.6% ± 2.6, and 37.4% ± 6.9, at days 3, 5, 7, and 14, respectively, following infection. In parallel, peripheral CD8+ T cell counts rose by 24.1% ± 4.3, 22.1% ± 3.8, 21.3% ± 3.9, and 40.5% ± 7.6, at equivalent time points (**Figure 2B**). Taken together, the early and progressive impairment of human immune cells was observed during HIV-1 infection in both hu-HSC and hu-PBL mouse models, but more vigorously in hu-PBL than in hu-HSC mice.

Plasma Viral Loads in HIV-1 Infected Humanized Mice

HIV-1 RNA appears before antiviral antibodies in blood at 10 to 14 days after viral exposure. To recapitulate these findings blood was collected from humanized mice and analyzed for viral loads by the COBAS Ampliprep V2.0 and Taqman-48 assay (**Figure 3**). In hu-HSC mice, plasma HIV-1 RNA was detected in all animals with a mean of 5.0 ± 3.4 × 10^4 copies/ml at 14 days after infection. At days 3, 5, and 7 after infection plasma viral loads were observed in 2/5 animals at or near to the detection limit of

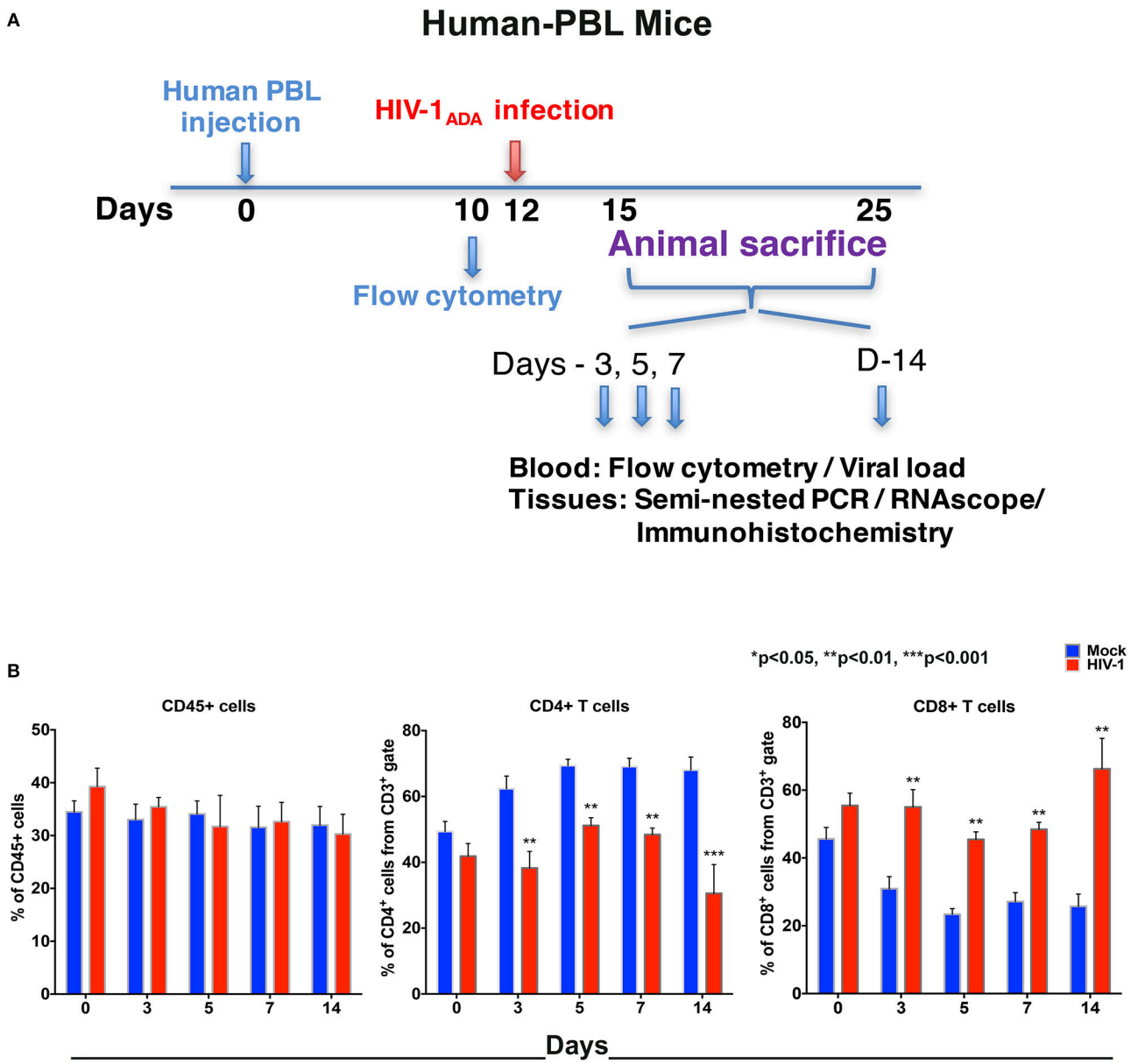

FIGURE 2 | Human lymphocyte responses following HIV-1 infection of hu-PBL mice. **(A)** The illustrated experimental design for hu-PBL mice human cell reconstitution, HIV-1 infection, and serial animal sacrifice performed at days 0, 3, 5, 7, and 14. Animal number are $N = 4$, 6, 5, 5, and 8 at each of the time points, respectively. **(B)** Peripheral blood CD45+, CD4+, and CD8+ cell counts before/mock infection (blue) and after HIV-1 infection (red) for each of the time points by flow cytometry tests. Data are expressed as mean ± SEM and considered **, *** statistically significant, at $p < 0.01$ and $p < 0.001$.

400 copies/ml. Peak viremia was recorded at day 28 at a mean of $5.9 \pm 3.4 \times 10^5$ copies/ml. At 42 days plasma viral load was at $6.6 \pm 1.4 \times 10^5$ copies/ml (**Figure 3A**).

In contrast, HIV-1 RNA was readily observed in all infected hu-PBL mice at day 3 with the mean of $4.7 \pm 0.8 \times 10^3$ copies/ml. A 2-log increase in viral copies were observed at days 5 and 7 with means of $5.4 \pm 2.6 \times 10^5$ and $8.0 \pm 3.5 \times 10^7$ copies/ml, respectively. At day 14, plasma viral load was $8.3 \pm 4.8 \times 10^7$ copies/ml (**Figure 3B**).

Tissue Compartments in HIV-1 Infected Humanized Mice

HIV-1 infection is established in target tissues before viremia can be detected (23). To determine the early distribution of HIV-1 infection in tissues, gut, spleen, lung, liver, brain, and kidney were procured then evaluated after animal sacrifices (**Figures 1A**, **2A**). Tissue HIV-1 DNA and RNA were quantified by ultrasensitive semi-nested real-time qPCR (19). In general, tissue viral levels were higher in longer infected hu-HSC

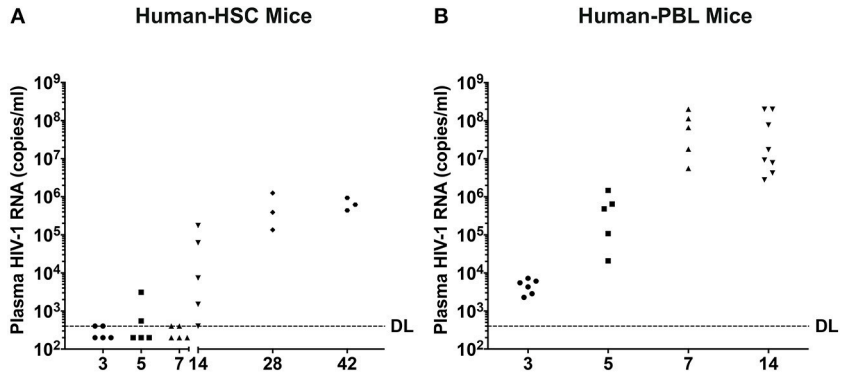

FIGURE 3 | Peripheral viral loads during the course of HIV-1 infection. Plasma samples were collected following animal sacrifice from HIV-1 infected **(A)** hu-HSC and **(B)** hu-PBL mice. Fifty microliter mouse sera was collected then diluted to 1 ml with sterile filtered healthy human sera enabling a detection limit (DL) of 400 HIV-1 RNA copies/ml that is illustrated by the dashed line. Each dot represents an individual animal. The mean HIV-1 copy value from each group of animals was labeled.

and hu-PBL mice. In addition, tissue viral DNA and RNA corresponded to what was detected in plasma in both animal models (**Figures 4A,B**, **Figures 5A,B**).

In hu-HSC mice, HIV-1 DNA, and RNA were detected at low levels within 3 days after viral challenge, from spleen, lung, and liver in 1/5 animals (**Figures 4C,D**). The same tissues examined at days 5 and 7 showed infection in 2/5 animals while HIV-1 remained undetected in other tested tissues. In the animals infected for 14 days, viral DNA, and RNA were observed in 3/5 gut, spleen, lung, and kidney tissues, and 2/5 liver samples (**Figures 4C,D**). However, HIV-1 was not detected in hu-HSC mouse brain until day 28. At 28 and 42 days, virus was readily observed throughout all tested tissues from all infected animals (**Figures 4C,D**).

HIV-1 was detected earlier and at higher levels in hu-PBL vs. hu-HSC mouse tissues at all-time points (**Figures 5C,D**). Viral DNA and RNA were seen by day 3 in 81% (29/36) gut, spleen, lung, liver, brain, and kidney tissues examined. At day 5, 93% (28/30) infected tissue were HIV nucleic acid positive. Notably, 67% (6/9) brain tissue samples from days 3 and 5 showed absent virus that supported later seeding for this tissue compartment. In the animals infected for 7 and 14 days virus was readily observed in all tissues (**Figures 5C,D**). HIV-1 DNA levels in gut were higher than that in all other tissues and supported the notion that gut serves as a prominent virus tissue compartment (**Figure 5A**). Altogether, these data suggested that both peripheral and tissue HIV-1 compartments were rapidly established in hu-HSC (day-14) and hu-PBL (day-3) mouse models, but much faster in hu-PBL than in hu-HSC mice.

Confirmatory Tests of Viral Gene Expression in Infected Humanized Mice

To confirm tissue compartmentalization in early HIV-1 infected humanized mice, spleen sections were obtained then tested by RNAscope that can detect up to 1–2 copies of viral RNA (representative images shown in **Figure 6**). An antisense HIV-1 Clade B probe was employed which covers nearly entire viral genome (except LTR region). To this end, spleen HIV-1 RNA was shown as a single or cluster of brown dots, at the earliest stage of infection in both mouse models. In hu-HSC mice, HIV-1 RNA was visualized within 3 days of infection, which reaffirmed the rapid set-up of viral tissue compartment. As infection proceeded, virus spread as shown in multiple clusters of brown dots within each tissue section. By day 42, viral burden was much more prominent with invaded cells aggregated throughout the observed field of interest (**Figure 6A**). In hu-PBL mice, HIV-1 RNA was observed in all infected animal spleens at each time point. Viral RNA levels were comparable or higher in hu-PBL than hu-HSC mice at equivalent time courses (**Figure 6B**).

Viral Protein Expression in Infected Humanized Mice

HIV-1p24 is a capsid component that is among the earliest expressed viral proteins. To assess its presence in infected tissues we employed immunohistochemistry assays to trace HIV-1p24 along with human HLA-DR staining. Representative photomicrographs were taken from each tissue sample stained with both antibodies (**Figure 7**). In hu-HSC mice, while HLA-DR+ cells were easily seen in the observation field, HIV-1p24 cells, however, were observed only in 1/5 animal spleens infected for 5 or 7 days. No infected cells were seen at 3 days. By day 14, 3/5 animals were HIV-1p24 positive. These three animals were the same ones where virus was detected by viral qPCR and RNAscope tests (**Figures 4**, **6**). At 28 and 42 days, HIV-1p24 stained cells were demonstrated in all infected animals (**Figure 7A**). In hu-HSC lymph nodes, HIV-1p24 antigens were detected starting at 14 days after infection and increased over time (**Figure 7A**).

In hu-PBL mice, HIV-1p24 antigens were captured in all infected animal spleens and lymph nodes during serial necropsies while human HLA-DR+ cells were well reconstituted (**Figure 7B**). Levels of HIV-1 p24 and nucleic acids in spleen measured by immunostaining and qPCR and RNAscope tests paralleled one another (**Figures 5**, **6B**). During the equivalent infection windows, tissue HIV-1p24 expansion was more aggressive in hu-PBL than that in hu-HSC mice (**Figure 7B**).

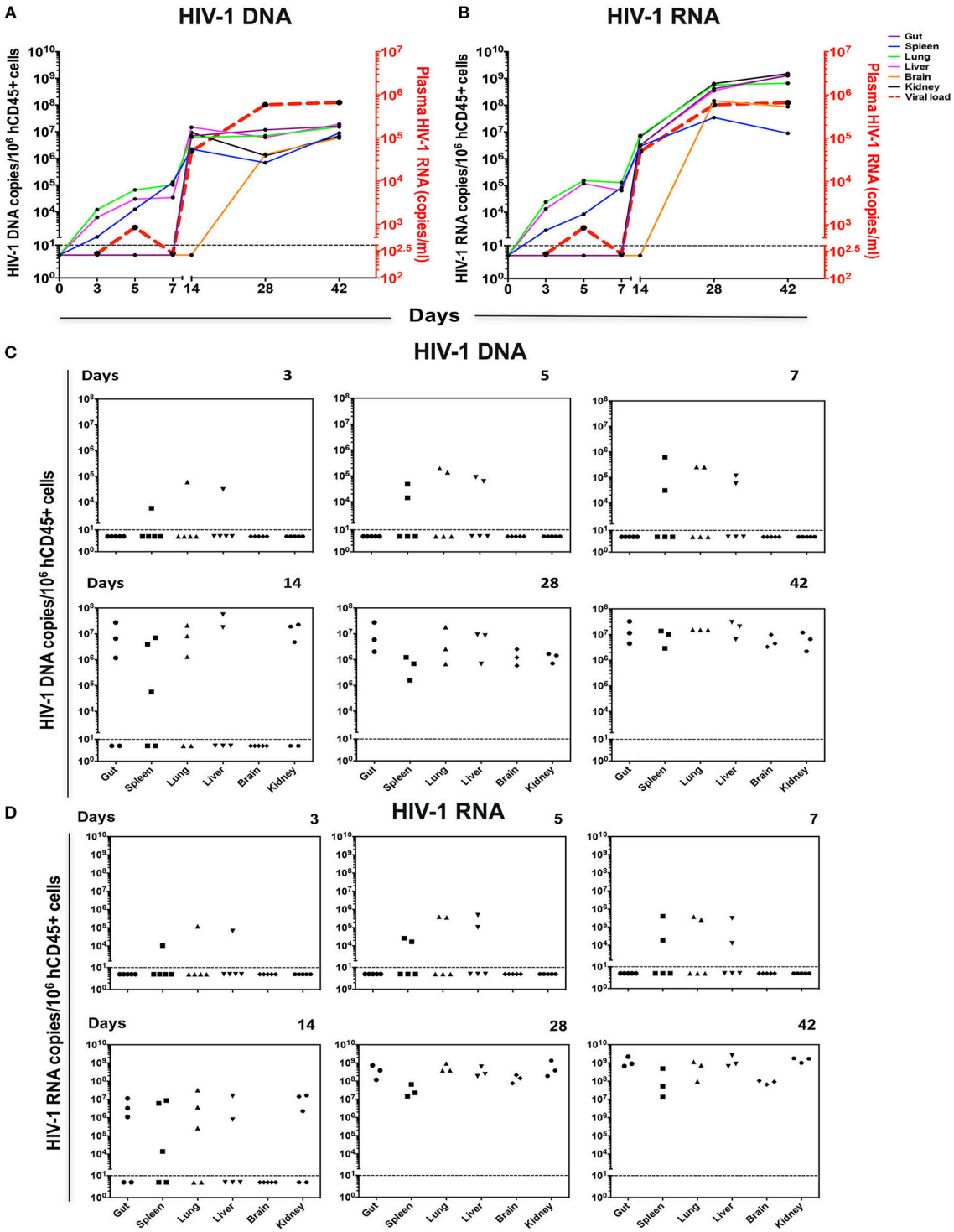

FIGURE 4 | Viral tissue compartments in HIV-1 infected hu-HSC mice. Gut, spleen, lung, liver, brain, and kidney tissues were collected at necropsy at times indicated from HIV-1 infected hu-HSC mice, followed by assay of viral DNA and RNA by qPCR. The kinetics of **(A)** HIV-1 DNA and **(B)** HIV-1 RNA in each tissue are shown by colored straight lines assigning viral copies/10^6 hCD45+ cells (left Y axis) vs. time (X axis). The temporal relationship of viral load (acquired from **Figure 3A**) was plotted in red dashed line (right Y axis). Data are expressed as the means. **(C)** HIV-1 DNA and **(D)** HIV-1 RNA in tissues at single time point were listed with each dot representing an individual animal. Values below the horizontal line indicated that viral DNA and RNA were below the DL.

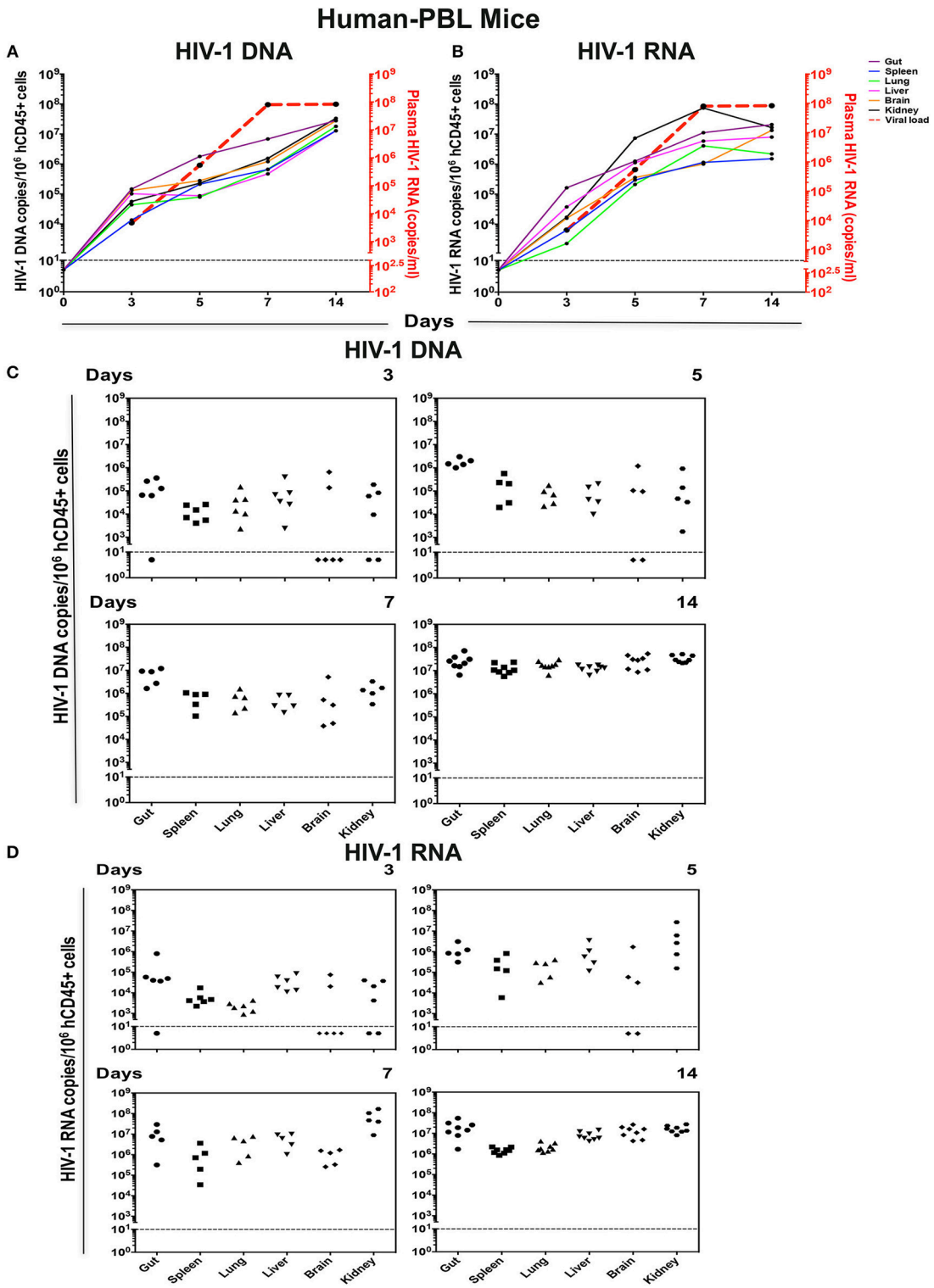

FIGURE 5 | Viral tissue compartments in HIV-1 infected hu-PBL mice. Gut, spleen, lung, liver, brain, and kidney tissues were collected at necropsy at times indicated from HIV-1 infected hu-PBL mice, followed by assay of viral DNA and RNA by real-time qPCR. The kinetics of **(A)** HIV-1 DNA and **(B)** HIV-1 RNA in each tissue are shown by colored straight lines assigning viral copies/10^6 hCD45+ cells (left Y-axis) vs. time (X axis). The temporal relationship of viral load (acquired from **Figure 3B**) was plotted in red dashed line (right Y axis). Data are expressed as the means. **(C)** HIV-1 DNA and **(D)** HIV-1 RNA in tissues at single time point were listed with each dot representing an individual animal. Values below the horizontal line indicated that viral DNA and RNA were below the limit of detection.

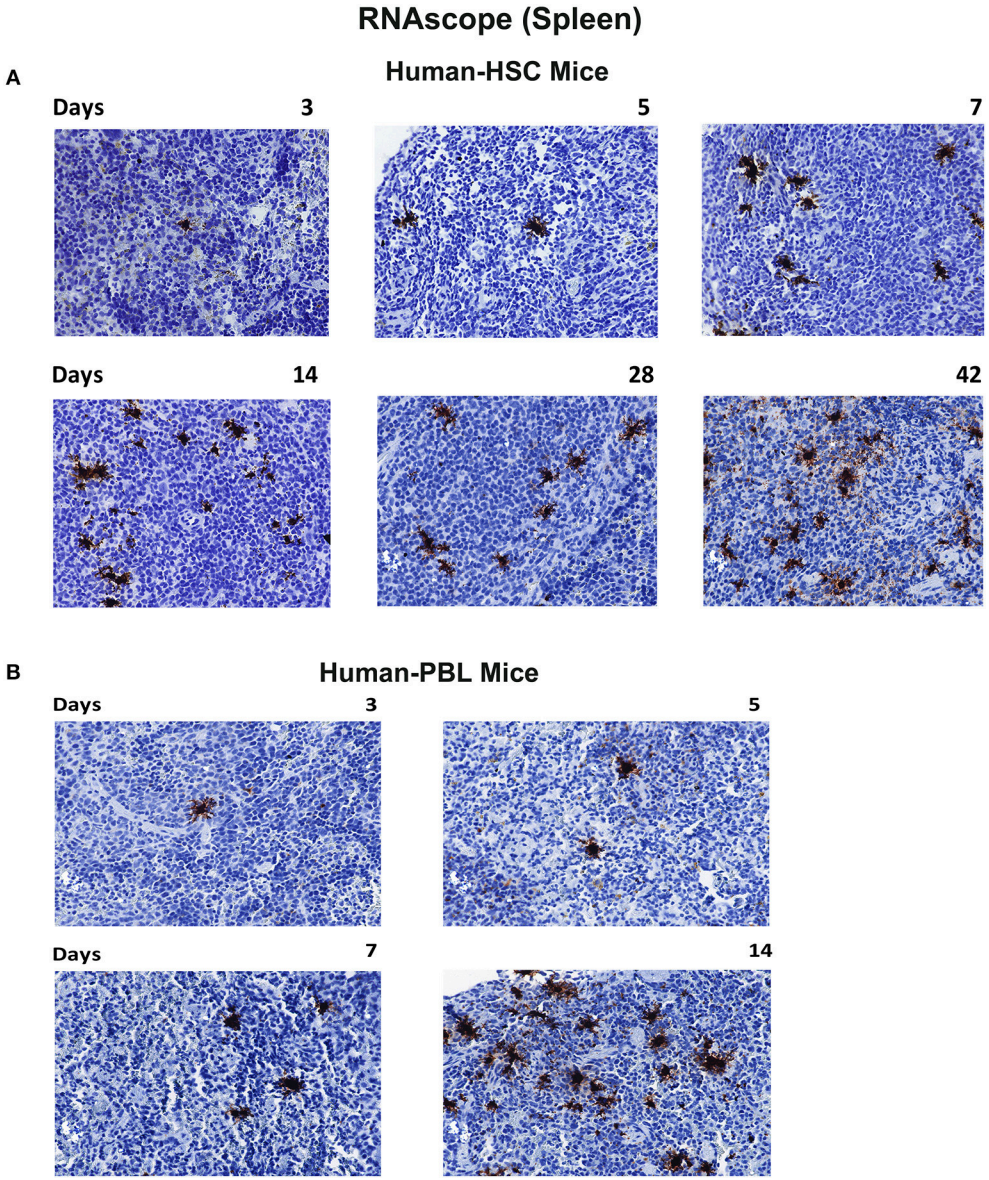

FIGURE 6 | Viral RNA tissue expression in infected humanized mice. Spleen tissues of hu-HSC **(A)** and hu-PBL **(B)** mice were collected with formalin fixed and paraffin embedded at necropsy. Five micrometer thick slices were prepared for RNAscope assays. Representative images from each group were shown with HIV-1 RNA labeled as single or cluster of brown dots. Images were taken at 40 x objective magnifications.

These data together confirmed that the quickly established HIV-1 infection in both models were replication-competent and virus spread more aggressively in hu-PBL than in hu-HSC mice.

Host Immunity in Humanized Mouse Models

Different strategies of humanization shape unique cellular integrations in humanized mice. Previous studies observed that the engrafted human T cells in hu-PBL mice expressed a predominated memory/activated (CD45RO) phenotype that supports HIV-1 infection (24) while in hu-HSC mice approximately 50% of human T cells are naive (CD45RA) that are less susceptible to HIV-1 infection (19). Therefore, viral infection is usually more aggressive in hu-PBL mice than that in hu-HSC mice (10). In the current study, we also observed a similar pattern during early HIV-1 infection where virus was seeded at accelerated rates in hu- PBL than in HSC mice. To further characterize and compare the intrinsic host environment in both mouse models that may affect HIV-1 infection, we adopted naïve hu-HSC and hu-PBL mice ($n = 3$/group) with comparable human cell reconstitutions (**Table S1**). In these animals, immune-linked host gene expression was tested. Total RNA was isolated from individual animal spleen and a total of 84 gene expressions were evaluated. Overall, increases in

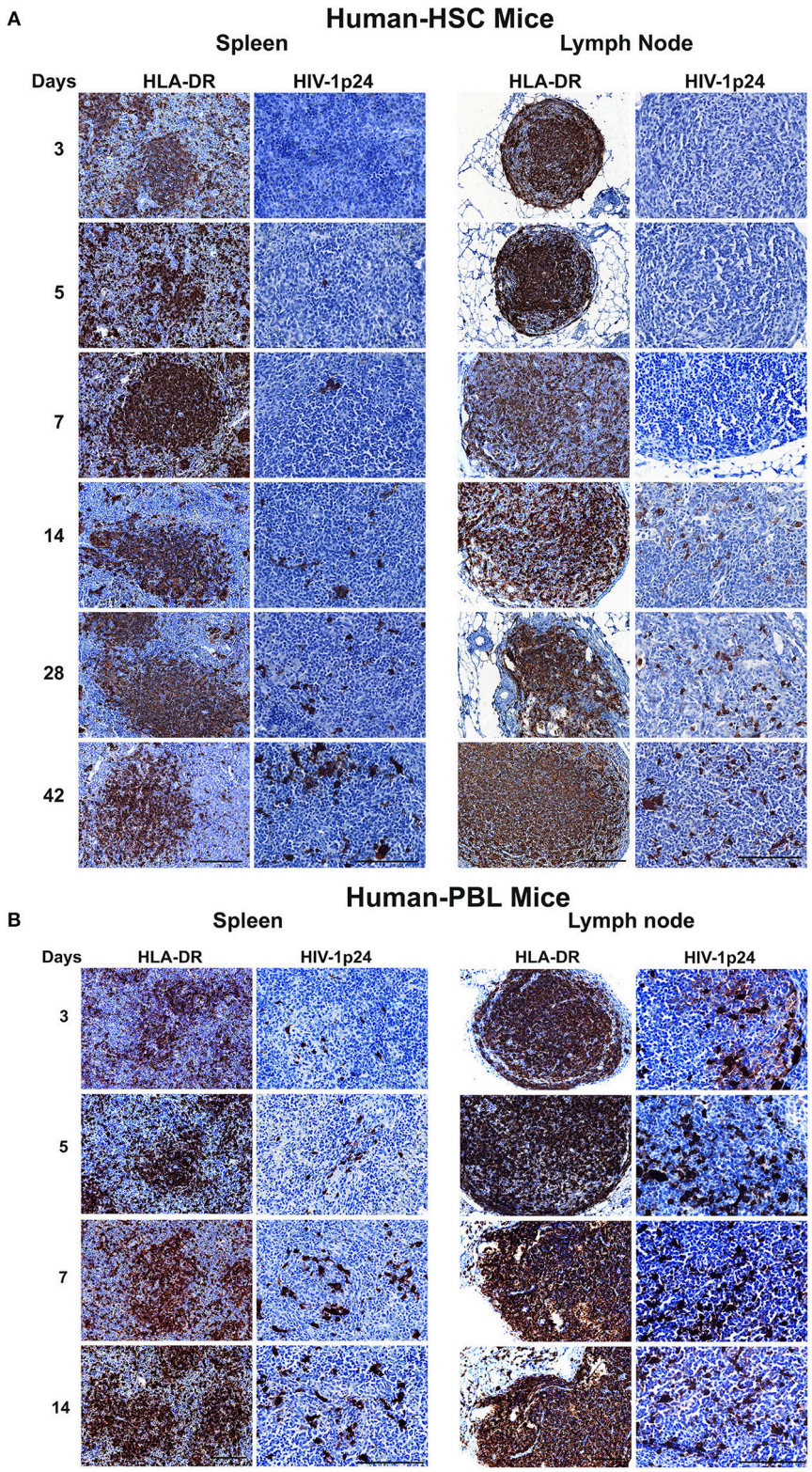

FIGURE 7 | HIV-1p24 expression in infected humanized mice. Spleen and lymph node samples were collected from **(A)** hu-HSC and **(B)** hu-PBL mice at necropsy then formalin fixed and paraffin embedded. Five micrometer thick sections were cut then stained with human HLA-DR and HIV-1p24 antibodies. Representative images from each group were selected and pictures were captured for both markers (shown as brown dots) from individual animals. Human HLA-DR images were taken at 20 x objective magnifications and HIV-1p24 images were captured at 40 x objective magnifications.

gene expressions paralleled adaptive immune activation and were most prominent in hu- PBL vs. HSC mice (**Figure 8** and **Table S2**). Upregulated T cell genes were readily observed affecting cell activation (e.g. CD2, CD3, CD4, CD8, FOXP3, and LAG3), proliferation (e.g. CD28, IL2, IL1β, IL18, and TNFSF14), and differentiation (e.g. CD27, CD80, CD86, and IL15). Two major co-receptors for HIV-1 entry, CCR5, and CXCR4, were also found to be upregulated in hu-PBL compared to HSC mice. The elevated B cell activation and proliferation markers included CD27, CD40, CD80, CD81, IL2, and IL10. To investigate how these differentially expressed molecules may impact the host environment, we subjected the genes with fold changes above 2 (81/84) to Ingenuity Pathway Analysis (IPA). These tests revealed that the top canonical pathways affected in hu-PBL over HSC mice were (1) Th1 and Th2 activation pathway ($p =$ 4.62E-56); (2) innate and adaptive immunocyte communications ($p =$ 3.03E-47); (3) Th2 ($p =$ 5.58E-43); (4) Th1 ($p =$ 2.14E-42) and (5) T-helper cell differentiation ($p =$ 1.76E-39, **Figure 9A**). All five pathways are engaged in T cell regulation. Downstream Effects Analysis was performed to assess regulatory hierarchy. A total of 500 gene-related diseases or functions each with a minimum of 10 molecules related were predicted and top 10 functions were listed (**Table S3**). The differential genetic network in the hu-PBL mice was most significantly correlated with the activation of lymphatic systems with 80% (65/81) of the input genes involved and 83% (54/65) led to systemic activation responses (**Figure 9B**). A spectrum of inflammation-associated genes was also upregulated in hu-PBL as compared to hu-HSC mice, including both pro-inflammatory (e.g., IL1, IL17, IFN γ, TNFα, CXCL3, and CXCL8) and anti-inflammatory (e.g., IL4, IL6, IL10, IL12, IL13, and TNFβ) molecules (**Figure 8** and **Table S2**). IPA analysis confirmed that this genetic pattern was associated with inflammatory responses with 67% (54/81) of the input genes involved and 81% (44/54) linked to cell activation pathways (**Table S3** and **Figure S2**). Taken together, these data support the notion that an established immune activated and inflammatory tissue environment facilitates HIV-1 infection and dissemination.

DISCUSSION

Early ART intervention restricts the HIV-1 reservoir size (25–27) and may achieve long-term viral remission in select infected individuals (28, 29). However, all patients inevitably experience viral relapse even when treatment is started as early as 14 days after infection (6). It is thus important to determine viral compartmentalization in cells and tissues. Nonetheless, it is not possible to accurately answer this question in an infected human. Therefore, in the current study we traced HIV-1 peripheral and tissue dissemination after infection in humanized mice used to reflect the temporal dynamics of tissue infection. The major advancements of this study were direct comparisons between hu- HSC and PBL mice using a dual tropic HIV-1 strain (HIV-1_{ADA}) in study (30). Multiple time points after HIV-1 infection to reflect a complete picture of early viral dynamics as well as host immune responses. By comparing the viral-host kinetics, we were able to identify the host factors that affect early events of HIV-1 infection. Limitations in accessing human samples to correlate immune responses can be achieved through the use of humanized mice.

Herein, two well-studied chimeric humanized mouse models were used in this report with divergent biologic and immune characteristics. Hu-HSC mice were made after engrafting human CD34+ HSC into new born NSG mice (31). After cell differentiation and maturation, mice are reconstituted with multiple lineages of human immune cells. The cellular type and composition in hu-HSC mice are more similar to human (T and B cells and monocyte-macrophages) with a life expectancy of more than a year. Hu-PBL mice are produced by implanting human peripheral blood lymphocytes into the adult NSG mice. This leads to dominant human lymphocyte reconstitution of up to 95% T cells within 2–3 days (32). However, as a result of GvHD, the life span of the viral immune responses in these animals can only be measured for a single month. Results from both models allowed us not only able to trace early HIV-1 infection, but investigate how host environments may affect viral-host outcomes (33). Peritoneal infections were performed to ensure reproducibility between animals.

Effector memory CD4+ T cells are the primary targets of HIV-1 and their depletion parallels the development of the acquired immune deficiency syndrome (23). CD4+ T cell loss is observed within months of HIV-1 infection from both peripheral blood and lymphoid tissues (34). In the current study, we observed modest CD4+ T depletion in blood of hu-HSC mice as early as 3 days after infection that progressed over time. A similar trend was also observed in infected splenocytes and bone marrow. Altogether, such results indicate that human immune function is impaired at the earliest stage of infection (35). CD8+ T cell percentages were elevated in parallel to CD4+ T cell losses. In hu-PBL mice, peripheral CD4+ T cell depletion was more significant than what was observed in hu-HSC mice. This reflected a highly activated cell phenotype facilitating productive HIV-1 infection and cellular degradation.

Plasma HIV-1 RNA is first seen within 3 weeks after HIV-1 infection in humans (36, 37). Due to the difficulty of early HIV-1 screen in the clinic, a gap between initial viral exposure, and estimated infection period is inevitable, which can be bridged using suitable animal models. In the current study, peripheral viral load was detected in 40% (2/5) of hu-HSC animals by days 3, 5, and 7 after infection each and 100% by day 14. It implied that peripheral viral replication might be established earlier than what is usually observed in humans given the possibility that highly sensitive techniques may further improve detection limit. In hu-PBL mice peripheral viral load was fully expressed in all monitored animals within 3 days of infection with a peak viremia seen at day 7. The data clearly support the notion that viral replication is linked to immune activation.

Tissue HIV-1 DNA and RNA was first detected by semi-nested qPCR at 3 days after infection in hu-HSC mouse spleen, lung, and liver, demonstrating that infection was established and disseminated to multiple tissues rapidly while plasma viral load is extremely low or undetectable. Interestingly, at 5 and 7 days after infection, viral nuclear acids were recovered from each

A

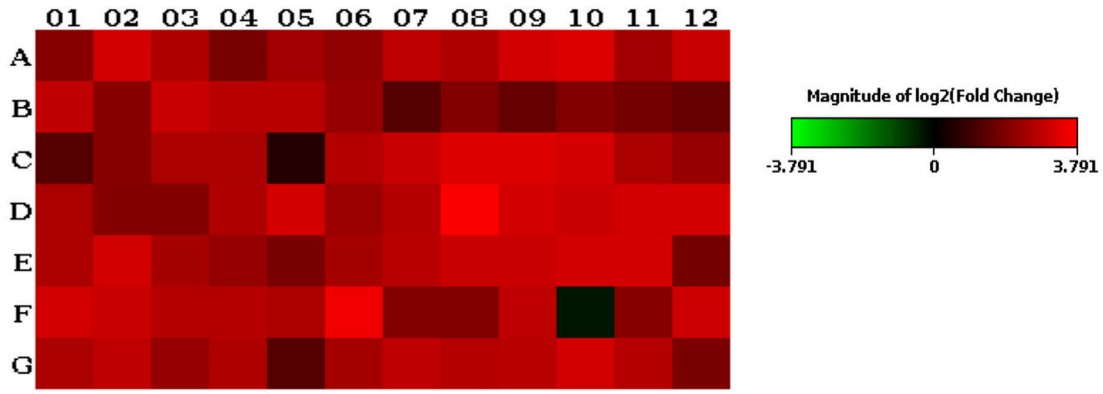

Layout	01	02	03	04	05	06	07	08	09	10	11	12
A	ADA 2.06	AICDA 3.11	APC 2.61	BCL2 1.77	BLM 2.39	BLNK 2.17	CCL3 2.82	CCR1 2.62	CCR2 3.15	CCR3 3.24	CCR4 2.43	CCR5 3.04
B	CD1D 2.88	CD2 2.05	CD27 3.00	CD274 2.77	CD276 2.76	CD28 2.25	CD3D 1.29	CD3E 1.90	CD3G 1.50	CD4 1.89	CD40 1.70	CD40LG 1.53
C	CD47 1.28	CD5 2.01	CD7 2.52	CD80 2.55	CD81 0.54	CD86 2.66	CD8A 2.99	CD8B 3.24	CSF2 3.27	CX3CL1 3.18	CXCR3 2.54	CXCR4 2.24
D	CXCR5 2.52	DPP4 2.00	EGR1 1.95	FAS 2.63	FASLG 3.17	FOXP3 2.32	ICOSLG 2.70	IFNG 3.79	IL10 3.18	IL11 2.98	IL12A 3.11	IL12B 3.18
E	IL12RB1 2.56	IL12RB2 3.13	IL13 2.51	IL15 2.24	IL18 1.86	IL18R1 2.49	IL1B 2.77	IL2 3.04	IL2RA 3.00	IL3 3.17	IL4 3.20	IL4R 1.74
F	IL5 3.12	IL6 2.99	IL7 2.74	CXCL8 2.72	IRF4 2.52	LAG3 3.54	LCK 1.93	MAP3K7 1.89	MICB 2.79	MS4A1 -0.34	NCK1 2.02	NOS2 3.07
G	PTPRC 2.56	RAG1 2.82	RIPK2 2.24	SOCS1 2.61	TGFB1 1.25	TLR1 2.50	TLR2 2.85	TLR4 2.66	TLR6 2.76	TLR9 3.13	TNFSF14 2.72	VAV1 1.85

B

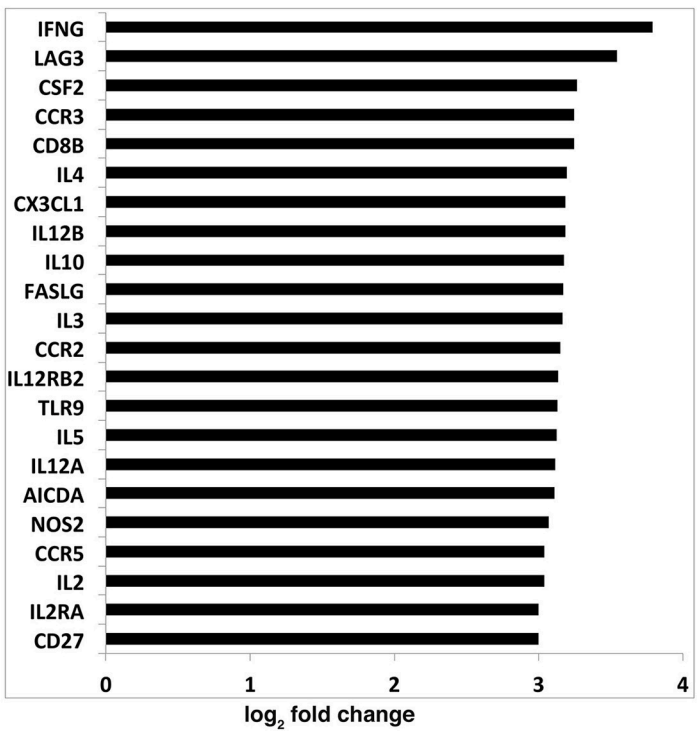

FIGURE 8 | Expression of human immune activation markers in humanized mice. Total RNA was isolated from uninfected humanized mouse spleens and analyzed for the expression of markers for human immune activation. A total of 84 genes were evaluated and compared between the two animal models. **(A)** Heatmap depicted the differentially expressed genes (for 1–12) associated with immune activation in hu- PBL compared against HSC mice (for A–G)**.** The $\log_2$ fold change of the individual gene is listed in the bottom panel. **(B)** Differentially expressed genes with $\log_2$ fold change of $\geq$3 are outlined that are expressed in hu-PBL spleens over what was found in HSC mice. A complete gene list can be found in **Table S2**.

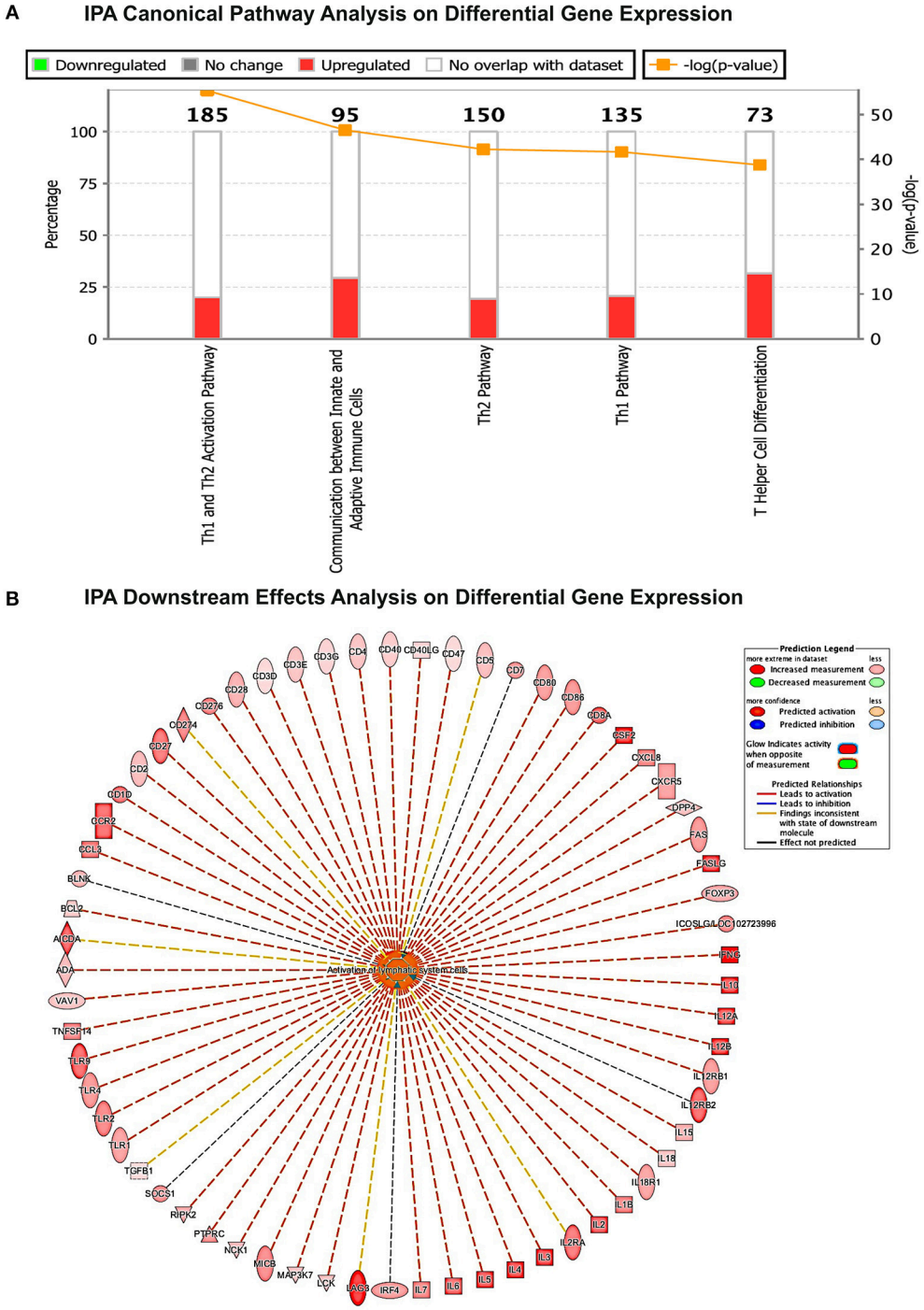

FIGURE 9 | Gene expression patterns analysis by IPA in humanized mice. **(A)** Canonical pathway gene analyses. The stacked bar chart demonstrates the percentage of upregulated (red) and downregulated (green), as well as non-overlapped (white) genes from the prestored genebank in IPA (numbers listed at the top of each bar). The right y-axis displays the –log of *p*-Value calculated by Fisher's Exact Test illustrates the significance of each canonical pathway. **(B)** Downstream biological effects prediction. The most relevant downstream effect predicted by IPA was lymphoid activation. A set of 65 genes that were differentially expressed between hu-PBL and hu-HSC mice co-regulate this pathway. The putative function was located in the center while the related regulator listed at the periphery. The type of interaction is indicated by red (prediction of activation), blue (prediction of inhibition), yellow (inconsistent), and gray (related, not predicted).

of these tissues in 2/5 animals and supported the fact that all three tissue compartments were seeded by virus at the earliest stage of infection. The observation of HIV-1 RNA and HIV-1p24 antigen on spleen sections supported that it could serve as a major anatomical infectious site (38). In addition, infected cells were highly enriched within the lymphoid follicles. This is likely due to

known higher numbers of reconstituted human cells in follicular regions and indicates that this lymphoid subregion may play a major role during early establishment of tissue infections. As the germinal centers are poorly developed in humanized mice, their role in viral compartmentalization, and as potential reservoirs for infection requires further research if a potential viral sanctuary can be realized and most notably during effective ART (39). At 14 days after HIV-1 infection, virus was easily seen in spleen, lung, liver, gut, and kidney. Tissue viral DNA and RNA levels were dramatically increased compared to the early time points, accordant with plasma HIV-1 RNA. One can speculate that multiple peripheral and tissue sanctuaries have been established at early points after viral infection, which may illustrate the hurdles that need be overcome to achieve viral eradication (6). These observations highlight hu-HSC mice as a robust model for studying the earlier stages of HIV-1 infection and support our own prior works using the model to investigate viral cellular and tissue replication patterns during chronic infections (19). Indeed in hu-HSC mice, HIV-1 replication is readily identified in a broad range of bone marrow, spleen, lung, gut, brain, kidney, and liver tissues as well as CD34+ progenitors, monocyte-macrophages, dendritic cells, and CD4+ stem cell memory, naïve memory, central memory, effector memory, and regulatory T cells. All were identified in animals after 5 to 14 weeks of viral infection.

Lymph nodes are major tissue compartments that harbor HIV-1 (40). In the current study, we did not detect HIV-1p24 in hu-HSC mouse lymph nodes until 14 days after infection. This reflected, in measure, the underdeveloped lymph nodes in immune deficient animals (41). While gut-associated lymphoid tissue or GALT is one of the earliest observed infected tissue during acute HIV-1 infection (42) we also were not able to detect HIV-1 infection in hu-HSC mouse GALT until day 14. This was later than what was observed from spleen, lung, and liver. These data reflect the relatively low humanization operative in hu-HSC mouse GALT (43). This limitation restricts studies of viral transmission (44). However, even considering the limitations of the model infection of GALT showed high levels of infection at later time points. The low reconstitution of human immune cells may also explain delayed HIV-1 infection in hu-HSC mouse brains. A recent study reported that within early infected individuals (median 15 days), HIV-1 RNA was observed in cerebrospinal fluid from 83%, 15/18 infected subjects, with the earliest detection by 8 days (37). However, according to variant humanized mouse models studied, HIV-1 seeding in the central neural system was generally much more delayed (16, 19, 45). This discordance demonstrates some of the limitation of our current humanized mouse models. Of interest to the current studies are our prior experiences in using hu-HSC mice that showed sustained bone marrow viral burden (19, 46). Although bone marrow HIV-1 infection was not measured in the current study, the progressive decline of CD4+ T cells indicated that active viral replication was rapidly established in the hu-HSC mouse bone marrow. Notably and distinct from hu-HSC mice, HIV-1 was seeded into tissue compartments more rapidly in hu-PBL mice. At 3 days post-infection, HIV-1 DNA and RNA were readily detected across a wide range of tested tissues, including brains. HIV-1p24 was also observed in the 3-day infected lymph node sections. Viral levels were higher in hu-PBL mice at the same time courses compared to that in hu-HSC mice. Altogether, these results strengthen the notion that the host microenvironment is closely linked to early HIV-1 replication dynamics.

Previous studies by others showed that low levels of T cell activation and proliferation lead to reduced HIV-1 susceptibility (47, 48). Nevertheless, comorbid factors such as sexually transmitted infectious diseases substantially increased the risks of HIV-1 acquisition and transmission as well as affecting viral load. All are known to be associated with inflammation and immune activation (49–51). Our data support the idea that immune activation markers predict viral susceptibility in mouse models of human disease. Comparisons in host tissue environments were made at the transcriptional level in tissues from both models. After identifying viral dynamics after HIV-1 infection of hu-PBL mice, immune-activated genes linked to T and B cells were upregulated when compared to hu-HSC mice. These data support the idea that immune activation that occurs prior to infection could predict early HIV-1 infection dynamics in these animal models. In addition, a wide range of inflammation-associated genes was upregulated in the hu- PBL compared to HSC mice. While pro-inflammatory conditions facilitate viral acquisition, and promote T cell activation (52) anti-inflammatory factors serve to maintain systemic homeostasis. Noteworthy, a recent report demonstrated that a systemic proinflammatory signature was established by as early as 24 h after SIV infection of rhesus macaques (9). It will be interesting to evaluate how early inflammasome activated in HIV-1 infection affects early viral dynamics. We posit that immune-activation and inflammation explains early HIV-1 infection, rapid viral dissemination, and accelerated CD4+ T cell loss in the hu-HSC mice.

Recently we demonstrated that hu-HSC mice infected with HIV-1_{NL4-3} strain (53) expressed high levels of HIV-1 replication in peripheral blood, gut, spleen, lung, liver, brain, kidney, lymph node, and bone marrow. These results illustrated that viral factors also affect the formation of HIV-1 infection in tissue compartments. In addition, a recent report found that after acute intravaginal challenge of HIV-1_{BaL} on humanized Rag1KO.IL2RγcKO.NOD mice expressing HLA class II (DR4) molecule (DRAG) mice (16), virus was detected at certain tissues by day 4 while brain was lastly infected until day 21. This also suggested that different infection routes and genetic background should be considered in reflecting what would be operative in an infected human host. While we understand that the intraperitoneal route used to establish viral infection does not reflect what is operative during natural conditions. However, we performed this route to ensure infection was operative in 100% of challenged animals and was able to explore viral compartmentalization during the evolution of persistent viral infection. While early HIV-1 infection remains challenging to identify and investigate in the clinic, humanized mouse models allow researchers to determine how, where and at what levels virus gains a foot hold in tissue sites and prior to any or all therapeutic or cure strategies. Indeed, based on this work, our group has shown that combinations of long acting slow effective

release antiretroviral therapy (LASER ART) and CRISPR-Cas9 for viral excision can lead to permanent HIV-1 elimination. In up to one third of infected humanized mice (our unpublished observations) and supports the use of this model in viral eradication schemes.

In conclusion, by using humanized mouse models, our study identified a wide range of tissue compartments, and their temporal and spatial dynamics during early HIV-1 infection. The four major findings from this study are summarized as *First,* HIV-1 infection was identified in multiple tissue compartments as early as 3 days post-infection using highly sensitive detection techniques in two different humanized animal models. Second HIV-1 was detected in all tissue by day 14 in hu-HSC mice. *Third,* tissue viral replication patterns were linked to markers of immune activation and immunity for each animal model that included T cell maturation and inflammation. *Fourth,* spleen, lung, and liver were among the earliest infected tissues and sustained heavy viral burden throughout the monitoring period as shown in proviral DNA amplifications. It is noteworthy that the tissue types listed above do not cover all the human anatomical viral sanctuaries. Others tissues that require analyses in humanized mice include but not limited by thymus, male and female reproductive tract, skin, and adipose tissue (54, 55). Even accepting the limitation of both models and underdevelopment of secondary lymphoid tissues this information will instruct us on the guideline of early ART intervention and development of tissue-specific ART. It has been an intriguing question that whether a window exists for "HIV-1 cure," if ART is administrated soon after viral exposure to maximize the restriction of viral replication followed by combinational strategies targeting the residual proviral DNA. Using humanized mouse model under controlled conditions, we will be able to answer this question, which will benefit the translation of clinical investigation.

AUTHOR CONTRIBUTIONS

PD and HG conceived and designed the experiments and interpreted the data sets. PD and HS performed the virologic, immunologic, molecular biology and transcriptomic experiments, and interpreted and plotted the datasets. Both prepared the figures for publication and wrote the manuscript. YC, SS, and SM generated the mice used in the study and performed immunologic testing. Manuscript editing was performed by HG with the assistance of PD, SG, and LP.

ACKNOWLEDGMENTS

We acknowledge the technical support given in this project by Celina Prince, Tian Zhou, Katherine Olson, Edward Makarov, and Amanda Branch Woods. Each provided outstanding technical assistance for preparing the humanized mice and tissue acquisition and processing. We also acknowledge Dr. R. Lee Mosley for statistical assistance. This work was supported by the University of Nebraska Foundation, the Carol Swarts, M.D. Emerging Neuroscience Research Laboratory, the Margaret R. Larson Professorship, the Frances and Louie Blumkin and Harriet Singer Endowments and by the National Institute of Health grants awarded to University of Nebraska Medical Center including R01NS36126, R01NS034239, P30MH062261, R01AG043540, P01DA037830, R01MH110360, R01MH115860, and R24OD018546.

SUPPLEMENTARY MATERIAL

The Supplementary Material for this article can be found online at: https://www.frontiersin.org/articles/10.3389/fimmu.2019.00340/full#supplementary-material

REFERENCES

1. Palella FJ Jr, Delaney KM, Moorman AC, Loveless MO, Fuhrer J, Satten GA, et al. Declining morbidity and mortality among patients with advanced human immunodeficiency virus infection. HIV outpatient study investigators. *N Engl J Med.* (1998) 338:853–60. doi: 10.1056/NEJM199803263381301
2. Barre-Sinoussi F, Ross AL, Delfraissy JF. Past, present and future: 30 years of HIV research. *Nat Rev Microbiol.* (2013) 11:877–83. doi: 10.1038/nrmicro3132
3. Maartens G, Celum C, Lewin SR. HIV infection: epidemiology, pathogenesis, treatment, and prevention. *Lancet.* (2014) 384:258–71. doi: 10.1016/S0140-6736(14)60164-1
4. Yazdanpanah Y, Fagard C, Descamps D, Taburet AM, Colin C, Roquebert B, et al. High rate of virologic suppression with raltegravir plus etravirine and darunavir/ritonavir among treatment-experienced patients infected with multidrug-resistant HIV: results of the ANRS 139 TRIO trial. *Clin Infect Dis.* (2009) 49:1441–9. doi: 10.1086/630210
5. Richman DD, Margolis DM, Delaney M, Greene WC, Hazuda D, Pomerantz RJ. The challenge of finding a cure for HIV infection. *Science.* (2009) 323:1304–7. doi: 10.1126/science.1165706
6. Colby DJ, Trautmann L, Pinyakorn S, Leyre L, Pagliuzza A, Kroon E, et al. Rapid HIV RNA rebound after antiretroviral treatment interruption in persons durably suppressed in Fiebig I acute HIV infection. *Nat Med.* (2018) 24:923–6. doi: 10.1038/s41591-018-0026-6
7. Denton PW, Sogaard OS, Tolstrup M. Using animal models to overcome temporal, spatial and combinatorial challenges in HIV persistence research. *J Transl Med.* (2016) 14:44. doi: 10.1186/s12967-016-0807-y
8. Miller CJ, Li Q, Abel K, Kim EY, Ma ZM, Wietgrefe S, et al. Propagation and dissemination of infection after vaginal transmission of simian immunodeficiency virus. *J Virol.* (2005) 79:9217–27. doi: 10.1128/JVI.79.14.9217-9227.2005
9. Barouch DH, Ghneim K, Bosche WJ, Li Y, Berkemeier B, Hull M, et al. Rapid inflammasome activation following mucosal SIV infection of rhesus monkeys. *Cell.* (2016) 165:656–67. doi: 10.1016/j.cell.2016.03.021
10. Hatziioannou T, Evans DT. Animal models for HIV/AIDS research. *Nat Rev Microbiol.* (2012) 10:852–67. doi: 10.1038/nrmicro2911
11. Akkina R, Allam A, Balazs AB, Blankson JN, Burnett JC, Casares S, et al. Improvements and limitations of humanized mouse models for HIV research: NIH/NIAID "Meet the Experts" 2015 workshop summary. *AIDS Res Hum Retroviruses.* (2016) 32:109–19. doi: 10.1089/aid.2015.0258
12. Dash PK, Gendelman HE, Roy U, Balkundi S, Alnouti Y, Mosley RL, et al. Long-acting nanoformulated antiretroviral therapy elicits potent antiretroviral and neuroprotective responses in HIV-1-infected humanized mice. *AIDS.* (2012) 26:2135–44. doi: 10.1097/QAD.0b013e328357f5ad
13. Sillman B, Bade AN, Dash PK, Bhargavan B, Kocher T, Mathews S, et al. Creation of a long-acting nanoformulated dolutegravir. *Nat Commun.* (2018) 9:443. doi: 10.1038/s41467-018-02885-x
14. Zhou T, Su H, Dash P, Lin Z, Dyavar Shetty BL, Kocher T, et al. Creation of a nanoformulated cabotegravir prodrug with improved antiretroviral

profiles. *Biomaterials*. (2018) 151:53–65. doi: 10.1016/j.biomaterials.2017.10.023
15. Victor Garcia J. Humanized mice for HIV and AIDS research. *Curr Opin Virol.* (2016) 19:56–64. doi: 10.1016/j.coviro.2016.06.010
16. Kim J, Peachman KK, Jobe O, Morrison EB, Allam A, Jagodzinski L, et al. Tracking human immunodeficiency virus-1 infection in the humanized DRAG mouse model. *Front Immunol.* (2017) 8:1405. doi: 10.3389/fimmu.2017.01405
17. Gorantla S, Makarov E, Finke-Dwyer J, Gebhart CL, Domm W, Dewhurst S, et al. CD8+ cell depletion accelerates HIV-1 immunopathology in humanized mice. *J Immunol.* (2010) 184:7082–91. doi: 10.4049/jimmunol.1000438
18. Gorantla S, Makarov E, Finke-Dwyer J, Castanedo A, Holguin A, Gebhart CL, et al. Links between progressive HIV-1 infection of humanized mice and viral neuropathogenesis. *Am J Pathol.* (2010) 177:2938–49. doi: 10.2353/ajpath.2010.100536
19. Araínga M, Su H, Poluektova LY, Gorantla S, Gendelman HE. HIV-1 cellular and tissue replication patterns in infected humanized mice. *Sci Rep.* (2016) 6:23513. doi: 10.1038/srep23513
20. Benki S, McClelland RS, Emery S, Baeten JM, Richardson BA, Lavreys L, et al. Quantification of genital human immunodeficiency virus type 1 (HIV-1) DNA in specimens from women with low plasma HIV-1 RNA levels typical of HIV-1 nontransmitters. *J Clin Microbiol.* (2006) 44:4357–62. doi: 10.1128/JCM.01481-06
21. Roy U, McMillan J, Alnouti Y, Gautum N, Smith N, Balkundi S, et al. Pharmacodynamic and antiretroviral activities of combination nanoformulated antiretrovirals in HIV-1-infected human peripheral blood lymphocyte-reconstituted mice. *J Infect Dis.* (2012) 206:1577–88. doi: 10.1093/infdis/jis395
22. Ali N, Flutter B, Sanchez Rodriguez R, Sharif-Paghaleh E, Barber LD, Lombardi G, et al. Xenogeneic graft-versus-host-disease in NOD-scid IL-2Rgammanull mice display a T-effector memory phenotype. *PLoS ONE.* (2012) 7:e44219. doi: 10.1371/journal.pone.0044219
23. Moir S, Chun TW, Fauci AS. Pathogenic mechanisms of HIV disease. *Annu Rev Pathol.* (2011) 6:223–48. doi: 10.1146/annurev-pathol-011110-130254
24. Garcia S, Dadaglio G, Gougeon ML. Limits of the human-PBL-SCID mice model: severe restriction of the V beta T-cell repertoire of engrafted human T cells. *Blood*. (1997) 89:329–36.
25. Strain MC, Little SJ, Daar ES, Havlir DV, Gunthard HF, Lam RY, et al. Effect of treatment, during primary infection, on establishment and clearance of cellular reservoirs of HIV-1. *J Infect Dis.* (2005) 191:1410–8. doi: 10.1086/428777
26. Buzon MJ, Martin-Gayo E, Pereyra F, Ouyang Z, Sun H, Li JZ, et al. Long-term antiretroviral treatment initiated at primary HIV-1 infection affects the size, composition, and decay kinetics of the reservoir of HIV-1-infected CD4 T cells. *J Virol.* (2014) 88:10056–65. doi: 10.1128/JVI.01046-14
27. Hey-Cunningham WJ, Murray JM, Natarajan V, Amin J, Moore CL, Emery S, et al. Early antiretroviral therapy with raltegravir generates sustained reductions in HIV reservoirs but not lower T-cell activation levels. *AIDS*. (2015) 29:911–9. doi: 10.1097/QAD.0000000000000625
28. Luzuriaga K, Gay H, Ziemniak C, Sanborn KB, Somasundaran M, Rainwater-Lovett K, et al. Viremic relapse after HIV-1 remission in a perinatally infected child. *N Engl J Med.* (2015) 372:786–8. doi: 10.1056/NEJMc1413931
29. Hocqueloux L, Prazuck T, Avettand-Fenoel V, Lafeuillade A, Cardon B, Viard JP, et al. Long-term immunovirologic control following antiretroviral therapy interruption in patients treated at the time of primary HIV-1 infection. *AIDS*. (2010) 24:1598–601. doi: 10.1097/QAD.0b013e32833b61ba
30. Gendelman HE, Orenstein JM, Martin MA, Ferrua C, Mitra R, Phipps T, et al. Efficient isolation and propagation of human immunodeficiency virus on recombinant colony-stimulating factor 1-treated monocytes. *J Exp Med.* (1988) 167:1428–41. doi: 10.1084/jem.167.4.1428
31. Gorantla S, Gendelman HE, Poluektova LY. Can humanized mice reflect the complex pathobiology of HIV-associated neurocognitive disorders? *J Neuroimmune Pharmacol.* (2012) 7:352–62. doi: 10.1007/s11481-011-9335-y
32. Mosier DE, Gulizia RJ, Baird SM, Wilson DB, Spector DH, Spector SA. Human immunodeficiency virus infection of human-PBL-SCID mice. *Science*. (1991) 251:791–4. doi: 10.1126/science.1990441
33. Levy JA. Virus-host interactions in HIV pathogenesis: directions for therapy. *Adv Dent Res.* (2011) 23:13–8. doi: 10.1177/0022034511398874
34. Brenchley JM, Schacker TW, Ruff LE, Price DA, Taylor JH, Beilman GJ, et al. CD4+ T cell depletion during all stages of HIV disease occurs predominantly in the gastrointestinal tract. *J Exp Med.* (2004) 200:749–59. doi: 10.1084/jem.20040874
35. Engsig FN, Zangerle R, Katsarou O, Dabis F, Reiss P, Gill J, et al. Long-term mortality in HIV-positive individuals virally suppressed for >3 years with incomplete CD4 recovery. *Clin Infect Dis.* (2014) 58:1312–21. doi: 10.1093/cid/ciu038
36. Cohen MS, Shaw GM, McMichael AJ, Haynes BF. Acute HIV-1 Infection. *N Engl J Med.* (2011) 364:1943–54. doi: 10.1056/NEJMra1011874
37. Valcour V, Chalermchai T, Sailasuta N, Marovich M, Lerdlum S, Suttichom D, et al. Central nervous system viral invasion and inflammation during acute HIV infection. *J Infect Dis.* (2012) 206:275–82. doi: 10.1093/infdis/jis326
38. Nolan DJ, Rose R, Rodriguez PH, Salemi M, Singer EJ, Lamers SL, et al. The spleen is an HIV-1 sanctuary during combined antiretroviral therapy. *AIDS Res Hum Retroviruses*. (2018) 34:123–5. doi: 10.1089/aid.2017.0254
39. Velu V, Mylvaganam G, Ibegbu C, Amara RR. Tfh1 cells in germinal centers during chronic HIV/SIV infection. *Front Immunol.* (2018) 9:1272. doi: 10.3389/fimmu.2018.01272
40. Simonetti FR, Sobolewski MD, Fyne E, Shao W, Spindler J, Hattori J, et al. Clonally expanded CD4+ T cells can produce infectious HIV-1 *in vivo*. *Proc Natl Acad Sci USA*. (2016) 113:1883–8. doi: 10.1073/pnas.1522675113
41. Brehm MA, Shultz LD, Luban J, Greiner DL. Overcoming current limitations in humanized mouse research. *J Infect Dis.* (2013) 208 (Suppl. 2):S125–30. doi: 10.1093/infdis/jit319
42. Mattapallil JJ, Douek DC, Hill B, Nishimura Y, Martin M, Roederer M. Massive infection and loss of memory CD4+ T cells in multiple tissues during acute SIV infection. *Nature*. (2005) 434:1093–7. doi: 10.1038/nature03501
43. Denton PW, Nochi T, Lim A, Krisko JF, Martinez-Torres F, Choudhary SK, et al. IL-2 receptor gamma-chain molecule is critical for intestinal T-cell reconstitution in humanized mice. *Mucosal Immunol.* (2012) 5:555–66. doi: 10.1038/mi.2012.31
44. Joseph SB, Swanstrom R, Kashuba AD, Cohen MS. Bottlenecks in HIV-1 transmission: insights from the study of founder viruses. *Nat Rev Microbiol.* (2015) 13:414–25. doi: 10.1038/nrmicro3471
45. Watanabe S, Ohta S, Yajima M, Terashima K, Ito M, Mugishima H, et al. Humanized NOD/SCID/IL2Rgamma(null) mice transplanted with hematopoietic stem cells under nonmyeloablative conditions show prolonged life spans and allow detailed analysis of human immunodeficiency virus type 1 pathogenesis. *J Virol.* (2007) 81:13259–64. doi: 10.1128/JVI.01353-07
46. Araínga M, Edagwa B, Mosley RL, Poluektova LY, Gorantla S, Gendelman HE. A mature macrophage is a principal HIV-1 cellular reservoir in humanized mice after treatment with long acting antiretroviral therapy. *Retrovirology*. (2017) 14:17. doi: 10.1186/s12977-017-0344-7
47. Koning FA, Otto SA, Hazenberg MD, Dekker L, Prins M, Miedema F, et al. Low-level CD4+ T cell activation is associated with low susceptibility to HIV-1 infection. *J Immunol.* (2005) 175:6117–22. doi: 10.4049/jimmunol.175.9.6117
48. Begaud E, Chartier L, Marechal V, Ipero J, Leal J, Versmisse P, et al. Reduced CD4 T cell activation and *in vitro* susceptibility to HIV-1 infection in exposed uninfected Central Africans. *Retrovirology*. (2006) 3:35. doi: 10.1186/1742-4690-3-35
49. Ward H, Ronn M. Contribution of sexually transmitted infections to the sexual transmission of HIV. *Curr Opin HIV AIDS*. (2010) 5:305–10. doi: 10.1097/COH.0b013e32833a8844
50. Johnson LF, Lewis DA. The effect of genital tract infections on HIV-1 shedding in the genital tract: a systematic review and meta-analysis. *Sex Transm Dis.* (2008) 35:946–59. doi: 10.1097/OLQ.0b013e3181812d15
51. Schacker T, Zeh J, Hu H, Shaughnessy M, Corey L. Changes in plasma human immunodeficiency virus type 1 RNA associated with herpes simplex virus reactivation and suppression. *J Infect Dis.* (2002) 186:1718–25. doi: 10.1086/345771
52. Selhorst P, Masson L, Ismail SD, Samsunder N, Garrett N, Mansoor LE, et al. Cervicovaginal inflammation facilitates acquisition of less infectious HIV variants. *Clin Infect Dis.* (2017) 64:79–82. doi: 10.1093/cid/ciw663

53. Srivastava KK, Fernandez-Larsson R, Zinkus DM, Robinson HL. Human immunodeficiency virus type 1 NL4-3 replication in four T-cell lines: rate and efficiency of entry, a major determinant of permissiveness. *J Virol.* (1991) 65:3900–2.
54. Rose R, Nolan DJ, Maidji E, Stoddart CA, Singer EJ, Lamers SL, et al. Eradication of HIV from tissue reservoirs: challenges for the cure. *AIDS Res Hum Retroviruses*. (2018) 34:3–8. doi: 10.1089/aid.2017.0072
55. Wong JK, Yukl SA. Tissue reservoirs of HIV. *Curr Opin HIV AIDS*. (2016) 11:362–70. doi: 10.1097/COH.0000000000000293

Conflict of Interest Statement: The authors declare that the research was conducted in the absence of any commercial or financial relationships that could be construed as a potential conflict of interest.

Copyright © 2019 Su, Cheng, Sravanam, Mathews, Gorantla, Poluektova, Dash and Gendelman. This is an open-access article distributed under the terms of the Creative Commons Attribution License (CC BY). The use, distribution or reproduction in other forums is permitted, provided the original author(s) and the copyright owner(s) are credited and that the original publication in this journal is cited, in accordance with accepted academic practice. No use, distribution or reproduction is permitted which does not comply with these terms.

frontiers in Microbiology

REVIEW
published: 04 March 2019
doi: 10.3389/fmicb.2019.00401

Non-muscle Myosin II: Role in Microbial Infection and Its Potential as a Therapeutic Target

Lei Tan[1], Xiaomin Yuan[1], Yisong Liu[1], Xiong Cai[2], Shiyin Guo[3] and Aibing Wang[1]**

[1] Hunan Provincial Key Laboratory of Protein Engineering in Animal Vaccines, Research and Development Center for Animal Reverse Vaccinology of Hunan Province, College of Veterinary Medicine, Hunan Agricultural University, Changsha, China, [2] Institute of Innovation and Applied Research in Chinese Medicine, Hunan University of Chinese Medicine, Changsha, China, [3] College of Food Science and Technology, Hunan Agricultural University, Changsha, China*

Currently, the major measures of preventing and controlling microbial infection are vaccinations and drugs. However, the appearance of drug resistance microbial mounts is main obstacle in current anti-microbial therapy. One of the most ubiquitous actin-binding proteins, non-muscle myosin II (NM II) plays a crucial role in a wide range of cellular physiological activities in mammals, including cell adhesion, migration, and division. Nowadays, growing evidence indicates that aberrant expression or activity of NM II can be detected in many diseases caused by microbes, including viruses and bacteria. Furthermore, an important role for NM II in the infection of some microbes is verified. Importantly, modulating the expression of NM II with small hairpin RNA (shRNA) or the activity of it by inhibitors can affect microbial-triggered phenotypes. Therefore, NM II holds the promise to be a potential target for inhibiting the infection of microbes and even treating microbial-triggered discords. In spite of these, a comprehensive view on the functions of NM II in microbial infection and the regulators which have an impact on the roles of NM II in this context, is still lacking. In this review, we summarize our current knowledge on the roles of NM II in microbial-triggered discords and provide broad insights into its regulators. In addition, the existing challenge of investigating the multiple roles of NM II in microbial infection and developing NM II inhibitors for treating these microbial-triggered discords, are also discussed.

Keywords: non-muscle myosin II, co-factors/receptors, mammalian cells, regulatory pathways, regulators, microbial-triggered discords

OPEN ACCESS

Edited by:
Ping An,
Frederick National Laboratory for Cancer Research (NIH), United States

Reviewed by:
Tetsuya S. Tanaka, Elixirgen, LLC, United States
Mei-Ru Chen, National Taiwan University, Taiwan

****Correspondence:***
Shiyin Guo
gsy@hunau.edu.cn
Aibing Wang
bingaiwang@hunau.edu.cn

Specialty section:
This article was submitted to Infectious Diseases, a section of the journal Frontiers in Microbiology

Received: *31 August 2018*
Accepted: *15 February 2019*
Published: *04 March 2019*

Citation:
Tan L, Yuan X, Liu Y, Cai X, Guo S and Wang A (2019) Non-muscle Myosin II: Role in Microbial Infection and Its Potential as a Therapeutic Target. Front. Microbiol. 10:401. doi: 10.3389/fmicb.2019.00401

INTRODUCTION

Diseases caused by microbial infections including viruses and bacteria post a significant risk to public health, even resulting in social panic and huge economic loss duo to the outbreaks, such as Human immunodeficiency virus (HIV) and herpes simplex virus type 1 (HSV-1) (Looker et al., 2017; Bengtson et al., 2018). The most effective methods against microbial infections are vaccines and/or drugs. However, the emergence of drug-resistant strains and viral mutations in some cases are the main issues for antimicrobial means, as these antimicrobial ways mainly target microbial proteins or DNA (De Clercq, 2002). For this reason, novel therapeutic approaches, in particular, new targets should be further explored to develop antimicrobial drugs.

As intracellular parasitic pathogens, viruses and some bacteria utilize host co-factors including receptors to complete a series of life cycles. There are different receptors/co-factors on the host cell surface or inside the cell, which interact with the microbial proteins and participate in microbial entry, proliferation, and release. Therefore, these host proteins can be employed as potential antimicrobial drug targets. For instance, hepatitis B virus (HBV) utilizes heat shock protein 90 (HSP 90) to facilitate the formation of the HBV capsid through the interaction of HSP 90 and HBV core protein dimers, and treating HepG2.2.15 cells with HSP 90 inhibitors clearly decreases HBV replication by interfering with HBV capsid assembly and polymerase activity (Shim et al., 2011).

Non-muscle myosin II (NM II) is a molecular motor that provides force for cell movement via catalyzing hydrolysis of ATP and participates in a wide range of biological processes in many eukaryotic cells, such as cell adhesion, cell migration (Vicente-Manzanares et al., 2009), cell division (Ding and Woollard, 2017), and cell pinocytosis (Ding and Woollard, 2017). NM II forms a hexamer protein complex consisting of three pairs of polypeptides: two heavy chains (NMHC II, ∼200 kDa) that comprise two globular heads and an alpha-helical tail, a pair of regulatory light chains (∼20 kDa) that are involved in the regulation of NM II activity, and a pair of essential light chains (∼17 kDa) which stabilize the heavy chain conformation (Vicente-Manzanares et al., 2009; Zhang and Gunst, 2017). In mammals, the NM II family can be divided into three isoforms (NM IIA, NM IIB, and NM IIC) with their heavy chains encoded by MYH9, MYH10, and MYH14 genes, respectively (Conti and Adelstein, 2008). These three isoforms share high similarity at amino acid level and have distinct dynamic properties, thereby playing overlapping and different roles in the biological processes of eukaryotic cells (Newell-Litwa et al., 2015; Pecci et al., 2018). For instance, the function of NM IIA in visceral endoderm cell-cell adhesion was able to be replaced by NM IIB *in vivo*, while the isoform-specific role of NM IIA in mouse placenta formation could not be substituted (Wang et al., 2010), suggesting the existence of special function of NM II isoforms in certain tissues/cells (Ma et al., 2010; Wang et al., 2010). As an actin-binding protein, NM II is ubiquitously expressed in various mammalian cell types and tissues (Newell-Litwa et al., 2015). However, the contents and distribution of those three isoforms of NM II are different in mammalian tissues/cells (Pecci et al., 2018). Relative high abundance of NM IIA (∼100%) but not NM IIB or NM IIC is detected in mouse spleen, while the relative abundance of NM IIB (∼65%) is higher than those of NM IIA (∼29%) or NM IIC (∼6%) in mouse spinal cord (Golomb et al., 2004). Additionally, the relative abundance of NM IIA is higher in Human Hela and HT29 cell types, but lower in Cos-7 cell type, compared with other two isoforms (Pecci et al., 2018). Notably, aberrant expression/activity of NM II has been detected in many microbial-triggered discords including virus-triggered discords and bacteria-triggered discords. For example, NM IIA is found to interact with Gn proteins of severe fever with thrombocytopenia syndrome virus (SFTSV) and its total expression is also augmented during SFTSV infection, while the application of siRNA specially inhibiting NM IIA expression suppresses the viral infection of cells, suggesting that SFTSV may utilize NM IIA to promote the efficiency of viral infection (Sun et al., 2014).

Considering the involvement of NM II in many physiological processes, a tight association of it with a range of disease pathologies has been established (Roberts and Baines, 2011). In particular, the participation of NM II in microbial-triggered discords has become a new focus in this field, as new findings have been obtained and important progress has recently been made. Additionally, the exploration of NM II as a therapeutic target has achieved fruitful results and novel regulators including inhibitors involved in the regulation of NM II's expression and activity have been identified. Therefore, in this review we intend to provide an updated summary of such new information, with an emphasis on the involvement of NM II and NM II-related pathways in microbial-triggered discords, as well as its novel regulators.

NM II IN MICROBIAL-TRIGGERED DISCORDS

The microbial-triggered discords in which NM II has been identified to participate are summarized in **Table 1**, also shown in **Figure 1** and separately illustrated in the following.

NM II in Virus-Triggered Discords

Herpesvirus

The *Herpesvirus* family, which can affect a variety of organisms including humans, fish, frogs and reptiles, contains over 150 enveloped viruses with double-stranded linear DNA encoding 80 to 100 open reading frames (ORFs) (Boss et al., 2009; Roberts and Baines, 2011). According to the host tissue specificity and replication features, this family can be divided into three subfamilies, namely, α-, β-, and γ-herpesvirina (Roberts and Baines, 2011). Notably, Herpes simplex virus type 1 (HSV-1) and Equid herpesvirus type 1 (EHV-1) of α-herpesvirina, Epstein-Barr virus (EBV) and Kaposi's sarcoma-associated herpesvirus (KSHV) of γ-herpesvirina, have been extensively studied due to their leading infection to humans or animals. The earliest report that NM II is involved in the infection of the *Herpesvirus* family was described by van Leeuwen et al. (2002). Thereafter, accumulating evidence indicates that NM II is implicated in the infection of this virus family and the role/function of NM II during virus infection may be distinct depending on the virus types and infectious processes as illustrated in the following sections.

Epstein-Barr Virus (EBV)

Epstein-Barr virus (EBV) is a nearly ubiquitous pathogen that causes damage to the health of human beings as EBV infects almost 90% of the global population (Hau and Tsao, 2017). EBV infection is associated with approximately 1.5% of all cancers including Hodgkin's lymphoma and Burkitt's lymphoma (Hau and Tsao, 2017; Teow et al., 2017). The implication of NM II in EBV infection was revealed by a recent report. In a series of exploratory experiments, Xiong et al. (2015) first discovered that immunoprecipitation with myc-tagged EBV gH/gL can pull

TABLE 1 | Involvement of non-muscle myosin II (NM II) in microbial-triggered discords.

Pathogen	Alteration of NM II expression or activity	Reference
EBV	Increased NM IIA expression in nasopharyngeal epithelial cells	Xiong et al., 2015
KSHV	Increased activity and expression of NM IIA in HMVEC-d cells; Induced phosphorylation of NM IIA	Valiya Veettil et al., 2010; Bandyopadhyay et al., 2014
HSV-1	Increased both NM IIA and NM IIB cell-surface expression on Vero cells; Induced redistribution of NM IIA from the cytoplasm to the cell surface	Arii et al., 2010, 2015
EHV-1	Increased NMII activity in murine neurons	Cymerys et al., 2016
GIV	Induced variable expression of NM IIA	Yeh et al., 2008
HIV-1	Decreased NM IIA expression in podocyte, murine and human glomerular	Hays et al., 2012
SFTSV	Increased NM IIA expression; Induced redistribution of NM IIA from the cytoplasm to the cell surface	Sun et al., 2014
PRRSV	Increased NM IIA expression; Induced redistribution of NM IIA from the cytoplasm to the cell surface	Gao et al., 2016
RDV	Increased NM II expression	Wei et al., 2008b
LM	Increased activity and expression of NM IIA; Induced tyrosine-phosphorylation of NM IIA	Almeida et al., 2015
NG	Increased NM II activity at pathogen adherent site	Wang et al., 2017

EBV, Epstein Barr virus; KSHV, Kaposi's sarcoma-associated herpesvirus; HSV-1, Herpes simplex virus type 1; EHV-1, Equid herpesvirus type 1; GIV, Grouper iridovirus; HIV-1, Human immunodeficiency virus type 1; SFTSV, Severe fever with thrombocytopenia syndrome virus; PRRSV, Porcine reproductive and respiratory syndrome virus; RDV, Rice dwarf virus; LM, Listeria monocytogenes; NG, Neisseria gonorrhoeae.

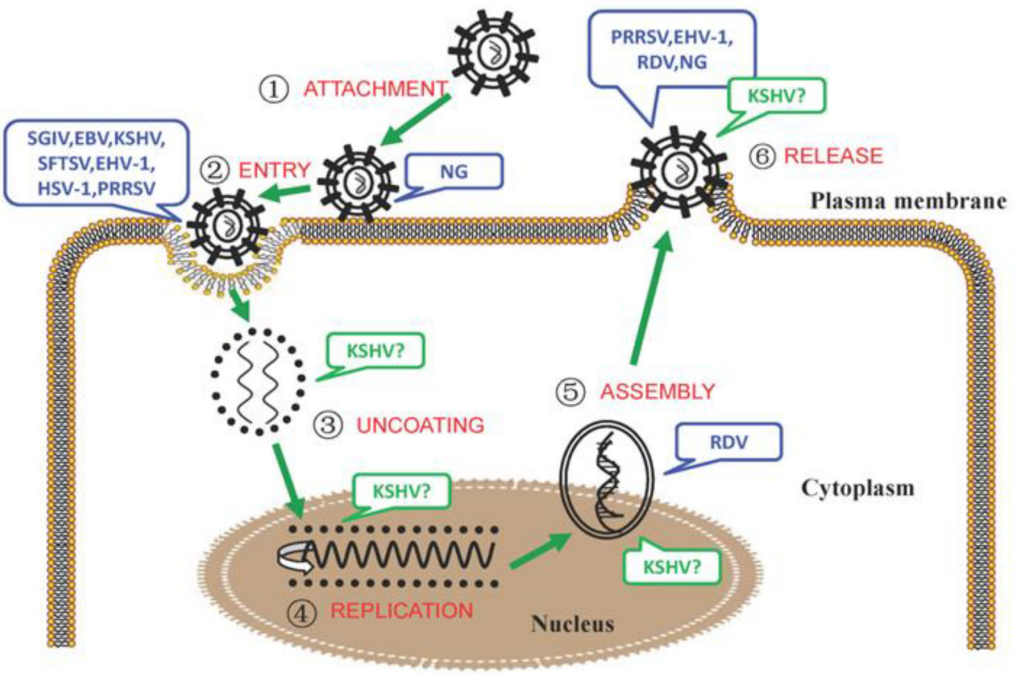

FIGURE 1 | The involvement of NM II in the different processes of microbial infection. ① During the process of intracellular bacterial attachment, the potential roles of NM IIA in NG (*Neisseria gonorrhoeae*) adhesion to the target cells (Wang et al., 2017) were determined; ② In the process of viral entry, the interactions between the glycoprotein H/glycoprotein L (gH/gL) protein of EBV and the C-terminal 1,665–1,960 aa region of NM IIA (Xiong et al., 2015); the adaptor protein (c-Cbl) and NM IIA (KSHV) (Valiya Veettil et al., 2010); the HSV-1 glycoprotein B and NM IIA, NM IIB (Arii et al., 2010, 2015); the glycoprotein Gn of SFTSV and NM IIA (Sun et al., 2014); and the glycoprotein GP5 of PRRSV and the C-terminal domain of NM IIA (Gao et al., 2016) were confirmed. In addition, the potential roles of NM II in EHV-1 (Cymerys et al., 2016), SGIV (Wang et al., 2014) entry were also speculated; ③ During the process of KSHV particle uncoating (Valiya Veettil et al., 2010), the vital roles of NM IIA were conjectured; ④ During the process of viral replication, the potential roles of NM IIA in KSHV infection (Zhu et al., 2005; Lyman and Enquist, 2009) were surmised; ⑤ During the process of viral intracellular capsid assembling and transport, the vital roles of NM IIA in KSHV (Valiya Veettil et al., 2010), RDV (Wei et al., 2008b) infection were suggested; ⑥ During the process of microbial release, the essential roles of NM IIA/NM II in KSHV (Valiya Veettil et al., 2010), EHV-1 (Cymerys et al., 2016), PRRSV (Guo J. et al., 2016), RDV (Wei et al., 2008b), and NG (Wang et al., 2017) intercellular spread were concluded. Note: The infection of microorganisms that NM II or its specific isoform was involved was marked with blue, that NM II or its specific isoform might be involved was marked with green and a "?".

down a 250 kDa protein in EBV infected sphere-like cell (SLCs) lysates and this protein is identified to be non-muscle myosin heavy chain IIA (NMHC IIA), suggesting that EBV gH/gL may interact with NM IIA, as further confirmed in subsequent co-immunoprecipitation and GST pull-down assays (Xiong et al., 2015). Moreover, the interaction of EBV gH/gL with NM IIA is verified to be mediated by the C-terminal 1,665–1,960 amino acids region of NM IIA. Co-localization assay also reveals that EBV infection leads to the redistribution NM IIA to the cell membrane and allows it to more extensively colocalized with the proteins of EBV (Xiong et al., 2015). Additionally, down-regulation of endogenous NM IIA expression by a NM IIA siRNA-mediated knock-down assay and a blocking assay with NMHC IIA antibody lowers the entry efficiency of EBV virions in nasopharyngeal epithelial cells, while over-expression of NM IIA in the cell membrane but not cytoplasm can significantly promote EBV infection efficiency (Xiong et al., 2015). These findings not only demonstrate the important role of NM IIA in mediating the entry of EBV into its target cells, but also imply that any inhibitor interrupting the interaction of NM IIA with the proteins gH/gL, gB, or BMF2 of EBV holds the promise to be an effective agent for preventing EBV entry or infection.

Kaposi's Sarcoma-Associated Herpesvirus (KSHV)

Kaposi's sarcoma-associated herpesvirus (KSHV), etiologically relevant to various tumors including Kaposi's sarcoma (KS), plasmablastic lymphoma, and primary effusion lymphoma (PEL), can infect various target cells both *in vivo* and *in vitro* via diverse patterns of endocytosis. Among these ways, macropinocytosis is regarded as a major route of entry for KSHV and many other viruses (Valiya Veettil et al., 2010). During KSHV entry, the multi-domain adaptor protein of c-Cbl is found to play a major role in membrane blebbing and macropinocytosis (Valiya Veettil et al., 2010). Moreover, immunoprecipitation of c-Cbl with the lysates from KSHV-infected cells followed by mass spectrometry identifies NM IIA as a molecular partner of c-Cbl. The direct interaction of c-Cbl with NM IIA is mediated by the C-terminal region encompassing the proline rich domain (PRD) of c-Cbl. Furthermore, this interaction between c-Cbl and NM IIA is critical for triggering bleb-associated macropinocytosis of KSHV. Either inhibiting NM IIA ATPase activity by its inhibitor blebbistatin or silencing c-Cbl with shRNA, leads to the decreased entry and infection efficiency of KSHV virions (Valiya Veettil et al., 2010). Notably, NM IIA mediated bleb formation in KSHV macropinocytosis is also regulated by other cellular factors, e.g., tyrosine kinase EphrinA2 (EphA2) (Chakraborty et al., 2012), and calcium and integrin binding protein-1 (CIB1). For instance, CIB1, widely expressed in human tissues, is crucial for KSHV entry by promoting the activity of EphA2 to facilitate the interaction of NM IIA with the cytoskeletal cross linker alpha actinin 4, thereby providing the mechanical forces for macropinocytosis (Bandyopadhyay et al., 2014). Additionally, NM IIA is found inside the KSHV virions, suggesting that it may participate in intracellular capsid assemble, transportation and viral egress of KSHV (Zhu et al., 2005; Lyman and Enquist, 2009). However, further investigations are required to substantiate the roles of NM II in these processes.

Herpes Simplex Virus Type 1 (HSV-1)

Herpes simplex virus type 1 (HSV-1) is a world-spread pathogen which infects over a half of adult humans, resulting in diverse ocular, oral, and genital manifestations (Antoine and Shukla, 2014; Lathe and Haas, 2016). Currently, we still have no effective means for treating HSV-1. HSV-1 infection is regarded as a crucial factor for increasing the possibility of being infected with human immunodeficiency virus (HIV), which is characterized by lymphadenectasis and fever with high mortality (Han et al., 2018). An earlier study suggested that NM II may play a role in virus transport and egress during the virus life cycle of HSV-1. This speculation is mainly based on the following observations. NM IIA is firstly found to interact with the HSV-1 major tegument protein VP22 (van Leeuwen et al., 2002). Furthermore, HSV-1 infection leads to the reorganization of NM IIA. Meanwhile, blocking NM II ATPase activity using a myosin-specific inhibitor dramatically reduces the yield of extracellular HSV-1 virus production (van Leeuwen et al., 2002). Subsequent investigations further indicated that members of the NM II family were also involved in other aspects of HSV-1 infection and had overlapping functions during these processes (Arii et al., 2010, 2015). In the course of HSV-1 entering into host cells, both NM IIA and NM IIB are employed as cellular receptors/factors by directly associating with the HSV-1 envelope glycoprotein B (gB) on the cellular surface (Arii et al., 2010, 2015). The HL 60 cell line is relatively insensitive to HSV-1 infection (Pientong et al., 1989). However, over-expression of NM IIA improves the susceptibility of HL60 cells to HSV-1 infection (Arii et al., 2010). On the contrary, antibody blockage and down-regulation of NM IIA in permissive cells inhibit HSV-1 infection. In accordance with the role of NM IIA, knockdown of NM IIB expression in cultured cells that are sensitive to HSV-1 infection significantly suppresses the susceptibility to HSV-1 infection at viral entry and cell-to-cell fusion. On the other hand, up-regulation of NM IIB in target cells dramatically increases their susceptibility to HSV-1 infectivity (Arii et al., 2015). Though more fundamental studies are required, the ubiquitous expression of NM IIA and IIB, together with these important findings above, make them a target for developing medicinally relevant drugs to prevent HSV-1 infection.

Equid Herpesvirus Type 1 (EHV-1)

Equid herpesvirus type 1 (EHV-1) is the main pathogen that affects horses worldwide, causing huge economic loss in the horse industry (Lunn et al., 2009). EHV-1 virions are mainly transmitted from the lymphoid tissue of the upper respiratory tract to the central nervous system, the uterus as well as monocytes which regulate viremia (Shakya et al., 2017), thereby resulting in various clinical symptoms including respiratory disease, abortion, and neonatal death (Lunn et al., 2009; Dunowska, 2014). During EHV-1 infection in cultured cells, the actin cytoskeleton of the infected cells is induced to rearrange its distribution and intimately contact neighboring cells to promote the spread of virions from cell to cell (Dunowska, 2014). A recent study indicated that both application of blebbistatin or 2, 3-butanedione monoxime (BDM) which are well-recognized NM II inhibitors before and after EHV-1 infection are negative factors

for viral entry and egress (Cymerys et al., 2016), respectively. Therefore, it is suggested that EHV-1 utilizes NM II and NM II-associated proteins for viral entry and the egress of progeny virions (Cymerys et al., 2016). However, further studies should be implemented for substantiating what kind of NM II isoforms is essential for EHV-1 infection.

Iridoviridae

The *Iridoviridae* family can be divided into five genera: *Ranavirus, Lymphocystivirus*, *Megalocytivirus*, *Iridovirus,* and *Chloriridovirus* (Murphy et al., 2012). Members of *Iridoviridae,* having a single double-stranded DNA with icosahedral cytoplasm, infect a wide variety of invertebrates and poikilothermic vertebrates, e.g., fish, insects, reptiles, and amphibians. Outbreaks of *Iridoviridae* infection in aquaculture have been reported in recent years and cause severe economic losses to cultured fish worldwide (Jeong et al., 2008; Dong et al., 2017).

Infectious spleen and kidney necrosis virus (ISKNV) of *Iridovirus* genera, Grouper iridovirus (GIV) and Singapore grouper iridovirus (SGIV) of *Ranavirus* genera that mainly infect mandarin and grouper fish, respectively, have initially been studied. The mechanisms of action between the host cells and *Iridoviridae* are intricate. Xu et al. (2011) showed that VP15R protein encoded by the fifteenth ORF of ISKNV is firstly transcribed within 12 h post infection and is verified to be able to bind to the heavy chains of NM II from zebra fish, mice and humans during ISKNV infection. Furthermore, Wang et al. (2014) demonstrated that blocking NM II activity using a NM II kinase inhibitor (ML-7) has a negative impact on SGIV entering into a host cell. Additionally, the transcriptional expression level of NM II A is changeable in GIV-infected grouper kidney (GK-2) cells at different time quantum (Yeh et al., 2008). Though these initial observations suggest a role for NM II in the viral infection of *Iridoviridae*, the exact role/function of NM II requires further investigation too.

Other Viruses

Human immunodeficiency virus type 1 (HIV-1)

Human immunodeficiency virus type 1 (HIV-1) is an enveloped and single-stranded positive sense RNA virus of the *Retrovirus* family, within the order *Lentivirus*. The genome of HIV-1 is approximately 9 kb in length, only encoding a transcription unit and expressing 15 proteins (Stoltzfus, 2009; Hidalgo and Swanson, 2017). HIV-1 infection is a major threat to humans globally, with especially high morbidity and mortality in sub-Saharan Africa. People of African descent infected with HIV-1 is prone to HIV-associated nephropathy (HIVAN) (Husain et al., 2018; Rednor and Ross, 2018). Accumulating evidence indicates that the genetic variants or aberrant expression of MYH9 gene which encodes the heavy chains of NM IIA is closely related with HIVAN (Hays et al., 2012; Colares et al., 2014).

MYH9 (the gene encoding the heavy chains of NM IIA) is found to be abundantly expressed in glomeruli, and specifically podocytes of human tissue. However, glomerular expression of MYH9 was reduced in the kidneys of the transgenic mice that ubiquitously express the HIV provirus genome that lacks gag/pol genes. Furthermore, MYH9 expression was also decreased in the podocytes from these transgenic mice aforementioned or the podocytes transduced with pseudotyped lentivirus containing pNL4-3 Δgag/pol (HIV-1)-EGFP vectors (Hays et al., 2012). Similarly declined expression of MYH9 was also observed in human podocytes transduced with HIV-1. Additionally, the expression of MYH9 was markedly reduced in human glomeruli in the setting of HIVAN (Hays et al., 2012). By using community structure analysis, further evidence showed that NM IIA interacts with protein networks including those of Rho, which mediates podocyte cytoskeletal structure and function, and networks regulated by the HIV-1 gene *nef* (a key mediator of podocytopathy in HIVAN), as well as pathways less well characterized in podocytes. Notably, HIV *nef* regulates signaling cascade including Rho proteins, while Rho pathway stabilizes the formation of actin-myosin filaments. Moreover, the involvement of NM IIA in the Rho cytoskeletal regulating pathway is confirmed (Hays et al., 2012, 2014). Therefore, it is speculated that the reduction of NM IIA expression may be of significance to HIV-1 infection and the pathogenesis of HIVAN (Hays et al., 2012, 2014). Though these observations imply that NM II can be the disturbance target for preventing or treating the infection of HIV, these initial findings warrant further investigation.

Severe fever with thrombocytopenia syndrome virus (SFTSV)

Severe fever with thrombocytopenia syndrome virus (SFTSV) is a novel enveloped, single-stranded negative sense RNA virus of the *Bunyaviridae* family. A case of SFTSV infection was first reported in hilly areas of Henan province of central China in 2009 (Yu et al., 2011). Subsequently, several deaths due to SFTSV infection were confirmed in Japan and South Korea (Kim et al., 2013; Takahashi et al., 2014). Disease manifestations linked to SFTSV include weakness, hemorrhagic fever, thrombocytopenia, encephalitis, and gastrointestinal symptoms, which results in multiple-organ failure with a lethality rate ranging from 12 to 30% in the reported countries (Li et al., 2017).

Sun et al. (2014) showed that the recombinant envelope glycoprotein Gn of SFTSV binds to several kinds of SFTSV susceptible cells such as human umbilical vein endothelial cells and inhibits the infection of this virus to these cells. Importantly, glycoprotein Gn is confirmed to bind to NMHC IIA in immunoprecipitation coupled with the mass spectrometry assay (Sun et al., 2014). Supporting evidence for the involvement of NM IIA in SFTSV infection comes from a series of observations. The expression of NM IIA in susceptible cells incubated with SFTSV displays an initially increased and then decreased alteration when the cells pre-exposed to 4°C for 2 h are then shifted to 37°C for indicated time (i.e., 0–15 min) (Sun et al., 2014). It is suggested that SFTSV may utilize NM IIA for the entrance into the target cells, because 4 and 37°C are permissible temperatures for viral adsorption and penetration of the cell membrane, respectively. Notably, the total protein level of NM IIA is increased during viral infection (Sun et al., 2014). Additionally, application of different NM IIA inhibitors (including siRNA, anti-NM IIA antibody, and ML-7) can effectively suppress SFTSV infection (Sun et al., 2014). On

the contrary, over-expression of NM IIA promotes the efficiency of SFTSV entry into HeLa cells that are less susceptible to this virus (Sun et al., 2014). These findings demonstrate that NMIIA is critical for the entry of SFTSV into target cells. However, it remains unidentified whether NM IIA plays other roles in the virus infection.

Porcine reproductive and respiratory syndrome virus (PRRSV)

Porcine reproductive and respiratory syndrome virus (PRRSV) is an enveloped and single-stranded positive sense RNA virus which belongs to the family *Arteriviridae*, within the order *Nidovirales* (Lunney et al., 2016). PRRSV is considered as one of the most significant pathogens that affects pigs globally, causing porcine reproductive and respiratory syndrome (PRRS) and leading to huge economic losses to the pork industry worldwide (Nieuwenhuis et al., 2012).

Consistent with the role that NM IIA plays as a receptor in HSV-1 infection. NM IIA has been identified to act as a receptor in PRRSV infection as well. Gao et al. (2016) found that the C-terminal domain of NM IIA interacts with glycoprotein GP5 of PRRSV at the early stage of its infection (binding and absorption). During the entry of PRRSV into the target cells, NM IIA is redistributed from the cytoplasm to the plasma membrane and its expression is increased. Suppression of NM IIA expression decreases the yield of PRRSV, while overexpression of NM IIA markedly contributes to viral infection. On the contrary, NM IIB has no these effects (Gao et al., 2016). Further research showed that PRRSV may make use of intercellular nanotubes for the transmission of virions from cell to cell, and the inhibition of NM IIA activity suppresses intercellular nanotube formation as well as the efficiency of intercellular spreading of virions (Guo R. et al., 2016). The latest research of Li et al. (2018) further confirmed that recombinant NM IIA C-terminal domain can block PRRSV infection via interaction with viral glycoprotein GP5. These observations suggest that NM IIA plays multiple roles in the infection of PRRSV at these critical steps such as the entry, cellular transport, even egress of this virus. Therefore, it is believed that NM IIA may directly contribute to the pathogenesis of PRRSV and be utilized as an important target for the development of potential agents against the viral infection.

Rice dwarf virus (RDV)

Rice dwarf virus (RDV), a non-enveloped and double-stranded RNA virus that belongs to *Phytoreovirus*, multiplies in plants as well as invertebrate insect vectors (Wei et al., 2008b). RDV was first discovered in Japan in 1883, and then widely spread in Asian countries including China, Korea, and Nepal, where it causes the loss of rice production. Pns 10 is a non-structural protein responsible for forming tubules which is involved in RDV intercellular spread (Wei et al., 2006). By using a selective myosin motor activity inhibitor (BDM), Wei et al. (2008b) found that the formation of Pns 10 tubules is prevented and the intercellular spread of RDV is inhibited. Similarly, the formation of RDV spherical structures is also inhibited (Wei et al., 2008a). These lines of evidence indicate that the myosin motor (NM II) does mediate RDV infection. However, when NM II executes its fundamental role, i.e., providing force for intracellular transportation, or whether NM II is involved in other processes of viral infection, remains unsolved.

Bacteria-Triggered Discords

Listeria monocytogenes

Listeria monocytogenes (*L. monocytogenes*) is a Gram-positive, non-sporulating and rod-shaped bacterium belonging to the family *Acidobacteriaceae*. It is regarded as a food-borne pathogen with 13 serotypes based on their antigenic diversity. *L. monocytogenes* affects humans globally and causes low morbidity but high mortality (Radoshevich and Cossart, 2017). The clinical symptoms such as gastro-enteritis, bacterial sepsis and meningitis or abortion, vary with the physical conditions and ages of humans, and ingestion of the content of *L. monocytogenes* (Chen et al., 2017; Radoshevich and Cossart, 2017).

Plasma membrane blebs relying on NM II activity are the positive factor for pathogen dissemination (Fackler and Grosse, 2008). Furthermore, NM IIA might have multiple roles in the reaction of intracellular *L. monocytogenes* infection. For instance, Mesquita et al. (2017) found that listeriolysin O (LLO) induces the reorganization of the NM II A network into cortical bundles for the formation of plasma membrane blebs, whereas NM IIA protects plasma membrane integrity against LLO intoxication during *L. monocytogenes* infection (Mesquita et al., 2017). Almeida et al. (2015) also reported that NM IIA is tyrosine-phosphorylated by the Src tyrosine kinase in response to several bacterial pathogens. Importantly, the intracellular level of *L. monocytogenes* was found to positively correlate with the level of NM IIA activity or expression, because the inhibition of NM IIA activity by its inhibitor or the prevention of NM IIA tyrosine-phosphorylation or the depletion of NM IIA expression using siRNA, limited the infection of *L. monocytogenes*. Though in-depth study is required, these facts do confirm the involvement of NM IIA in the infection of these bacterial pathogens (Almeida et al., 2015).

Neisseria gonorrhoeae

Neisseria gonorrhoeae (*N. gonorrhoeae*) is a Gram-negative, non-flagellum and globular bacterium belonging to the family Neisseria bacteria. This pathogen is regarded as a crucial sexual concern because of its worldwide distribution, high susceptibility as well as widespread antimicrobial resistance (Berntsen et al., 2017). As a special human pathogen, *N. gonorrhoeae* infects the mucosal surface of humans via sexual transmission and causes gonorrhea (Wang et al., 2017).

N. gonorrhoeae infection alters actin reorganization, in which NM II plays multiple roles (Wang et al., 2017). As the first line of defense, the epithelial cells protect the host against the invasion of *N. gonorrhoeae*, whereas, *N. gonorrhoeae* infection induces exfoliation of endocervical epithelial cells. Wang et al. (2017) discovered that activated NM II is accumulated and redistributed to the *N. gonorrhoeae* adherent sites during their interaction. Inhibition of Ca^{2+} or myosin light chain kinase (MLCK)-dependent NM II activity decreases the percentage of epithelial exfoliation during *N. gonorrhoeae* infection. Additionally, the

ability of *N. gonorrhoeae* to transmit across target cells, to penetrate into target cells and to induce the disassembly of junctions, is also suppressed (Wang et al., 2017).

NM II INHIBITORS WITH POTENTIAL DRUG APPLICATION

Since most of the microbial infections discussed in this review lead to increased expression and/or activity of NM II, one would imagine that inhibiting its expression and or activity could result in decreased infection by microbials. It becomes clear that there are two ways for NM II inhibitors to affect the functions of NM II. The first one is to interfere with NM IIA expression at the post-transcriptional level, including microRNAs (e.g., let-5p-7f) and siRNA. The other one is to suppress NM II activity via the inhibition of MLCK or the ATPase, which is mediated by a series of inhibitors such as ML-7, ML-9, BDM, and Blebbistatin (see **Table 2**). Despite tremendous progress in identifying and developing NM II inhibitors in recent years, these NM II inhibitors have not been applied to drug development and clinical conditions. The unsolved problems mainly include: (a) the novel NM II inhibitors (microRNA and siRNA) show excellent specificity to the targeted MYH9 mRNA gene and down-regulate NM IIA expression. However, the potential toxicity (Guo J. et al., 2016) and off-target effects (Farooqi et al., 2018) limit their further application; (b) those traditional inhibitors, which are commercial and can be easily obtained, have low specificity, potency, and solubility, as well as (photo) toxicity, and furthermore interfere the activity of all three isoforms of NM II (Roman et al., 2018), restrict their further application.

There are mainly two kinds of kinase phosphorylation that modulates NM II activity, namely MLCK and Rho-associated kinase (ROCK), both MLCK and ROCK act on the myosin light chain molecule at the residues of Thr18 and Ser 19 (Croft et al., 2005). In addition, the regulation of NM II ATPase can also affect its activity (Kim et al., 2008). Traditional NM II inhibitors, including ML-7, ML-9, BDM, and Blebbistatin, usually act via affecting MLCK, ROCK, or ATPase activity. Newly emerging NM II inhibitors (such as microRNA and siRNA) act via modulating the expression of NM II. Application of NM II inhibitors is a good strategy for determining the roles of NM II in cultured cells and tissues under the conditions of microbial infection. More importantly, these NM II inhibitors might be applied as potential drugs/vaccines in treating/preventing these diseases. NM II inhibitors, their mechanisms of action, and chemotherapeutic effects are summarized in **Table 2**.

Novel Inhibitors

MicroRNAs

MicroRNAs (miRNAs) are a family of endogenous, non-coding small RNAs which typically consist of 22 ∼ 24 nucleotides, taking part in regulating gene expression by binding to corresponding mRNA to suppress its formation or translation. Growing evidence indicates the emerging roles for miRNAs in various pathological processes including viral infection and mycoplasm infection (Zhao et al., 2017; Zheng et al., 2018). For example, miRNA let-7f-5p is found to inhibit PRRSV infection via suppression of NM IIA expression which is mediated by directly binding to the 3′ UTR of its target MYH9 mRNA (Li et al., 2016). Therefore, overexpression of let-7f-5p could be a good way to suppresses PRRSV replication in infected cells (Li et al., 2016). However, whether this miRNA can be used as a target for the development of clinical drug/vaccine against PRSSV or the treatment/prevention of other NM II-related microbial infection, and the way to deliver miRNA into target tissues, requires further investigations.

Small Interfering RNA (SiRNA)

Small interfering RNA (siRNA), belonging to the family of RNA interference (RNAi), is a double-stranded RNA which typically consists of 20 ∼ 25 nucleotides. In recent years, siRNA has been widely employed as an effective tool for exploring gene function and drug targets. Based on its unique role in triggering the cleavage of target mRNA (Meng and Lu, 2017), it has been used to inhibit viral infection. For instance, the use of siRNAs targeting NM IIA decreases SFTSV infection efficiency by over 75%, and silencing NM IIB expression via siRNA reduces SFTSV infection efficiency by 11% (Sun et al., 2014). However, application of siRNA targeting NM IIA in RAW264.7 macrophage cells not only suppresses phagosome acidification and recruitment of LAMP-1, but also impairs the ability of host cells to defend against *Escherichia coli* infection (Gomez and Descoteaux, 2018). These facts suggest that the requirement for NM IIA in host defense against infections may depend on the types of microbials. It seems that downregulation of NM IIA alleviates viral infection but promotes the susceptibility to bacteria, respectively (Sun et al., 2014). Whether this is a general rule warrants further investigation.

TABLE 2 | NM II inhibitors with potential drug application.

NM II inhibitors	NM II isoforms	Chemotherapeutic effects	Microbial-triggered discords (references)
MicroRNAs (let-7f-5p)	NM IIA	Directly bind to 3′ UTR of MYH9 gene	PRRSV (Li et al., 2016)
SiRNA	NM IIA NM IIB	Act on the target mRNA	SFTSV (Sun et al., 2014)
ML-7 and ML-9	NM II	Potently inhibits MLCK activity	HSV-1 (Arii et al., 2010)
BDM	NM II	Potently inhibits actin-activated ATPase activity	EHV-1 (Cymerys et al., 2016)
Blebbistatin	NM II	Potently inhibits ATPase activity	EHV-1 (Cymerys et al., 2016), HSV-1 (Antoine and Shukla, 2014), and KSHV (Valiya Veettil et al., 2010)

Traditional Inhibitors

ML-7 and ML-9

Both ML-7 and ML-9 are chemical products of naphthalene sulfonamide, which are effective NM II inhibitors via blocking MLCK (Shi et al., 2007; Arii et al., 2010). Compared with ML-9, ML-7 has been used more widely in experimental studies and clinical applications because of its higher inhibiting effect on smooth muscle MLCK and other MLCK isoforms (Saitoh et al., 1987; Xiong et al., 2017). Arii et al. (2010) found that ML-7 reduces Vero cell susceptibility to HSV-1 infection at the virus entry level by inhibiting NM IIA activity. Moreover, treatment of the murine model with ML-7 before viral inoculation could significantly inhibit HSV-1 infection and improve survival rate. Therefore, both ML-7 and ML-9 are used as novel therapies to block HSV-1 infection by inhibiting MLCK activity (Antoine and Shukla, 2014).

BDM

BDM is an actin-activated myosin ATPase inhibitor, which has been widely applied to cell biological studies (McKillop et al., 1994). As a small molecule, BDM has similar effects to ML-7 in some cases (Forer and Fabian, 2005). For example, both BDM and ML-7 could reduce the efficiency in the protein delivery from Golgi bodies to the endoplasmic reticulum in cells (Durán et al., 2003). When BDM was applied to cultured cells, Cymerys et al. (2016) revealed that progeny virions of EHV-1 could not "escape" from the infected cells, and transmission of virions from cell to cell was inhibited as well. Thus, it is suggested that BDM can be used as a drug for treating NM II-related viral infection.

Blebbistatin

Blebbistatin is a small molecule NM II inhibitor which shows high affinity and selectivity (Kovács et al., 2004). This inhibitor specially binds to the ATPase site of NM II heads and decreases the phosphate release rate, thereby suppressing the activity of NM II (Kovács et al., 2004). In recent years, Blebbistatin has been widely applied in many viral researches including EHV-1 (Cymerys et al., 2016), HSV-1 (Antoine and Shukla, 2014), HIV (Kadiu and Gendelman, 2011), and KSHV (Valiya Veettil et al., 2010). For example, Blebbistatin interferes with the KSHV and HSV-1 internalization process to inhibit the entry of virions (Valiya Veettil et al., 2010; Antoine and Shukla, 2014). Additionally, Blebbistatin could also inhibit EHV-1 intercellular spread (Cymerys et al., 2016).

SUMMARY

Microbial infection is a complex process, which needs to utilize a series of receptors and co-factors on/in the cells for microbial entry, then pathogens multiply inside and release their descendants outside the cell (Tomlin and Piccinini, 2018). In this review, we have comprehensively summarized the essential roles of NM II in diverse microbial-triggered discords, which occur in human beings (Valiya Veettil et al., 2010; Hays et al., 2012; Sun et al., 2014), animals (Cymerys et al., 2016; Gao et al., 2016), and plants (Wei et al., 2008b). Interestingly, most of these reported microbial infections can similarly result in NM II alterations, mainly leading to the up-regulation of NM II expression or activity (see **Table 1**). Developing NM II inhibitors would be a considerable therapy against microbial infection. Therefore, we also in this review discuss the recently reported NM II inhibitors which are applied to the investigation of the effects and the underlying mechanisms of NM II in microbial-triggered discords. These NM II inhibitors have been applied to demonstrating the effect on resisting microbial infections *in vitro*, even *in vivo* (Gao et al., 2016).

Notably, we are still at the beginning of understanding the roles of these important cellular skeleton proteins which are ubiquitously expressed in almost all cell types. Of these skeletal proteins, lines of evidence indicate that NM II acts as a crucial receptor/co-factor for microbial infection, which is mainly confirmed via two methods. The first one is to investigate the expression or activity of the members of the NM II family during microbial infection, the second is to analyze virus infection after the application of NM II inhibitors. However, understanding the precise mechanisms of NM II in microbial infection is ambitious, understanding how altered NM II activity or expression contributes to microbial infection may open a novel approach against these discords if the following questions are well solved: these include what the exact mechanisms of microbial infection leading to the abnormality of NM II activity or expression are; what the exact roles of NM II in the distinct processes of virus infection are; how we can improve the specificity of NM II inhibitors and reduce the side-effects of them and how many virus types there are in which NM II is involved in the infection. In spite of these unsolved problems, NM II does have the potential as a therapeutic target. For example, Blebbistatin (NM II activity inhibitor) was confirmed to inhibit PRRSV infection both *in vitro* (cell model) and *in vivo* (piglet model) without considering its side-effects (Gao et al., 2016). Indeed, due to its properties such as poorly water soluble, cytotoxic, and prone to (photo) degradation, the wide applicability of Blebbistatin is hindered (Rauscher et al., 2018). These facts suggest Blebbistatin is still druggable if enough efforts are taken to improve these adverse features. Meanwhile, *in vitro* studies also demonstrated that downregulated expression of NM II using miRNA or siRNA approach effectively prevents the infection of PRRSV and SFTSV (Sun et al., 2014; Li et al., 2016), whereas *in vivo* evidence conducted in knockdown or knockout animals is still lacking. Therefore, further investigations are required to provide substantial facts.

In summary, NM II, as a molecular motor, plays a major role in cell movement as well as other physiological activities. Confronted with many microbial infections, collective evidence clearly confirms that NM II may act as an important receptor/co-factor and play multiple roles, such as microbial entry, replication and release (Cymerys et al., 2016; Gao et al., 2016). However, our knowledge of the precise mechanisms remains obscure. More detailed understanding of the interaction between NM II and microbial infection should be further explored in this field, which would provide new insights for developing special NM II inhibitors as promising drugs for the control and treatment of

these and other microbial-triggered discords at a clinical level, which differs from the traditional therapeutic strategy.

AUTHOR CONTRIBUTIONS

LT contributed to the development and writing of the paper, reviewing relevant literature, and preparation of tables in the paper. XY and XC contributed to the writing of the paper and provided suggestions on the revision. YL contributed to the drawing of the figure. SG and AW provided substantial, direct, and intellectual contribution to the work. All authors approved the article for publication.

FUNDING

This work was supported by General Program of National Natural Science Foundation of China (Grants Nos. 31571432 and 31802252) and Hunan Provincial Natural Science Foundation of China (Grant No. 2015JC3097). Support was also provided by "Shennong" Scholar funding to AW.

ACKNOWLEDGMENTS

The authors would like to thank Dr. Mary Ann Conti for professional reading on this paper.

REFERENCES

Almeida, M. T., Mesquita, F. S., Cruz, R., Osório, H., Custódio, R., Brito, C., et al. (2015). Src-dependent tyrosine phosphorylation of non-muscle myosin heavy chain-IIA restricts *Listeria monocytogenes* cellular infection. *J. Biol. Chem.* 290, 8383–8395. doi: 10.1074/jbc.M114.591313

Antoine, T. E., and Shukla, D. (2014). Inhibition of myosin light chain kinase can be targeted for the development of new therapies against herpes simplex virus type-1 infection. *Antivir. Ther.* 19, 15–29. doi: 10.3851/imp2661

Arii, J., Goto, H., Suenaga, T., Oyama, M., Kozuka-Hata, H., Imai, T., et al. (2010). Non-muscle myosin IIA is a functional entry receptor for herpes simplex virus-1. *Nature* 467, 859–862. doi: 10.1038/nature09420

Arii, J., Hirohata, Y., Kato, A., and Kawaguchi, Y. (2015). Nonmuscle myosin heavy chain IIb mediates herpes simplex virus 1 entry. *J. Virol.* 89, 1879–1888. doi: 10.1128/jvi.03079-14

Bandyopadhyay, C., Valiya-Veettil, M., Dutta, D., Chakraborty, S., and Chandran, B. (2014). CIB1 synergizes with EphrinA2 to regulate Kaposi's sarcoma-associated herpesvirus macropinocytic entry in human microvascular dermal endothelial cells. *PLoS Pathog.* 10:e1003941. doi: 10.1371/journal.ppat.1003941

Bengtson, A. M., Pence, B. W., Powers, K. A., Weaver, M. A., Mimiaga, M. J., Gaynes, B. N., et al. (2018). Trajectories of depressive symptoms among a population of HIV-infected men and women in routine HIV care in the United States. *AIDS Behav.* 22, 3176–3187. doi: 10.1007/s10461-018-2109-2

Berntsen, S., Karlsen, A. P. H., Pedersen, M. L., and Mulvad, G. (2017). Gonorrhoea in Greenland, incidence and previous preventive measures: a review to improve future strategies. *Int. J. Circumpolar Health.* 76:1350092. doi: 10.1080/22423982.2017.1350092

Boss, I. W., Plaisance, K. B., and Renne, R. (2009). Role of virus-encoded microRNAs in herpesvirus biology. *Trends Microbiol.* 17, 544–553. doi: 10.1016/j.tim.2009.09.002

Chakraborty, S., Veettil, M. V., Bottero, V., and Chandran, B. (2012). Kaposi's sarcoma-associated herpesvirus interacts with EphrinA2 receptor to amplify signaling essential for productive infection. *Proc. Natl. Acad. Sci. U.S.A.* 109, E1163–E1172. doi: 10.1073/pnas.1119592109

Chen, G. Y., Pensinger, D. A., and Sauer, J. D. (2017). Listeria monocytogenes cytosolic metabolism promotes replication, survival and evasion of innate immunity. *Cell. Microbiol.* 19:e12762. doi: 10.1111/cmi.12762

Colares, V. S., Titan, S. M., Pereira Ada, C., Malafronte, P., Cardena, M. M., Santos, S., et al. (2014). MYH9 and APOL1 gene polymorphisms and the risk of CKD in patients with lupus nephritis from an admixture population. *PLoS One* 9:e87716. doi: 10.1371/journal.pone.0087716

Conti, M. A., and Adelstein, R. S. (2008). Nonmuscle myosin II moves in new directions. *J. Cell. Sci.* 121(Pt 1), 11–18. doi: 10.1242/jcs.007112

Croft, D. R., Coleman, M. L., Li, S., Robertson, D., Sullivan, T., Stewart, C. L., et al. (2005). Actin-myosin-based contraction is responsible for apoptotic nuclear disintegration. *J. Cell Biol.* 168, 245–255. doi: 10.1083/jcb.200409049

Cymerys, J., Słońska, A., Skwarska, J., and Bańbura, M. W. (2016). Function of myosin during entry and egress of equid herpesvirus type 1 in primary murine neurons. *Acta Virol.* 60, 410–416. doi: 10.4149/av_2016_04_410

De Clercq, E. (2002). Strategies in the design of antiviral drugs. *Nat. Rev. Drug Discov.* 1, 13–25. doi: 10.1038/nrd703

Ding, S. S., and Woollard, A. (2017). Non-muscle myosin II is required for correct fate specification in the *Caenorhabditis elegans* seam cell divisions. *Sci. Rep.* 7:3524. doi: 10.1038/s41598-017-01675-7

Dong, H. T., Jitrakorn, S., Kayansamruaj, P., Pirarat, N., Rodkhum, C., Rattanarojpong, T., et al. (2017). Infectious spleen and kidney necrosis disease (ISKND) outbreaks in farmed barramundi (*Lates calcarifer*) in Vietnam. *Fish Shellfish Immunol.* 68, 65–73. doi: 10.1016/j.fsi.2017.06.054

Dunowska, M. (2014). A review of equid herpesvirus 1 for the veterinary practitioner. Part A: clinical presentation, diagnosis and treatment. *N. Z. Vet. J.* 62, 171–178. doi: 10.1080/00480169.2014.899945

Durán, J. M., Valderrama, F., Castel, S., Magdalena, J., Tomás, M., Hosoya, H., et al. (2003). Myosin motors and not actin comets are mediators of the actin-based Golgi-to-endoplasmic reticulum protein transport. *Mol. Biol. Cell* 14, 445–459. doi: 10.1091/mbc.E02-04-0214

Fackler, O. T., and Grosse, R. (2008). Cell motility through plasma membrane blebbing. *J. Cell Biol.* 181, 879–884. doi: 10.1083/jcb.200802081

Farooqi, A. A., Khalid, S., and Ahmad, A. (2018). Regulation of cell signaling pathways and miRNAs by resveratrol in different cancers. *Int. J. Mol. Sci.* 19:E652. doi: 10.3390/ijms19030652

Forer, A., and Fabian, L. (2005). Does 2,3-butanedione monoxime inhibit nonmuscle myosin? *Protoplasma* 225, 1–4. doi: 10.1007/s00709-004-0077-z

Gao, J., Xiao, S., Xiao, Y., Wang, X., Zhang, C., Zhao, Q., et al. (2016). MYH9 is an essential factor for porcine reproductive and respiratory syndrome virus infection. *Sci. Rep.* 6:25120. doi: 10.1038/srep25120

Golomb, E., Ma, X., Jana, S. S., Preston, Y. A., Kawamoto, S., Shoham, N. G., et al. (2004). Identification and characterization of nonmuscle myosin II-C, a new member of the myosin II family. *J. Biol. Chem.* 279, 2800–2808. doi: 10.1074/jbc.M309981200

Gomez, C. P., and Descoteaux, A. (2018). Moesin and myosin IIA modulate phagolysosomal biogenesis in macrophages. *Biochem. Biophys. Res. Commun.* 495, 1964–1971. doi: 10.1016/j.bbrc.2017.12.061

Guo, J., Jiang, X., and Gui, S. (2016). RNA interference-based nanosystems for inflammatory bowel disease therapy. *Int. J. Nanomed.* 11, 5287–5310. doi: 10.2147/ijn.s116902

Guo, R., Katz, B. B., Tomich, J. M., Gallagher, T., and Fang, Y. (2016). Porcine reproductive and respiratory syndrome virus utilizes nanotubes for intercellular spread. *J. Virol.* 90, 5163–5175. doi: 10.1128/JVI.00036-16

Han, X. J., Su, D. H., Yi, J. Y., Zou, Y. W., and Shi, Y. L. (2018). A literature review of blood-disseminated P. marneffei infection and a case study of this infection in an HIV-Negative child with comorbid eosinophilia. *Mycopathologia* 184, 129–139. doi: 10.1007/s11046-018-0255-8

Hau, P. M., and Tsao, S. W. (2017). Epstein-barr virus hijacks dna damage response transducers to orchestrate its life cycle. *Viruses* 9:E341. doi: 10.3390/v9110341

Hays, T., D'Agati, V. D., Garellek, J. A., Warren, T., Trubin, M. E., Hyink, D. P., et al. (2012). Glomerular MYH9 expression is reduced by HIV-1. *AIDS* 26, 797–803. doi: 10.1097/QAD.0b013e328351f6cf

Hays, T., Ma'ayan, A., Clark, N. R., Tan, C. M., Teixeira, A., Teixeira, A., et al. (2014). Proteomics analysis of the non-muscle myosin heavy chain IIa-enriched

actin-myosin complex reveals multiple functions within the podocyte. *PLoS One* 9:e100660. doi: 10.1371/journal.pone.0100660

Hidalgo, L., and Swanson, C. M. (2017). Regulation of human immunodeficiency virus type 1 (HIV-1) mRNA translation. *Biochem. Soc. Trans.* 45, 353–364. doi: 10.1042/bst20160357

Husain, N. E., Ahmed, M. H., Almobarak, A. O., Noor, S. K., Elmadhoun, W. M., Awadalla, H., et al. (2018). HIV-associated nephropathy in Africa: pathology, clinical presentation and strategy for prevention. *J. Clin. Med. Res.* 10, 1–8. doi: 10.14740/jocmr3235w

Jeong, J. B., Kim, H. Y., Jun, L. J., Lyu, J. H., Park, N. G., Kim, J. K., et al. (2008). Outbreaks and risks of infectious spleen and kidney necrosis virus disease in freshwater ornamental fishes. *Dis. Aquat. Org.* 78, 209–215. doi: 10.3354/dao01879

Kadiu, I., and Gendelman, H. E. (2011). Human immunodeficiency virus type 1 endocytic trafficking through macrophage bridging conduits facilitates spread of infection. *J. Neuroimmune Pharmacol.* 6, 658–675. doi: 10.1007/s11481-011-9298-z

Kim, K. H., Yi, J., Kim, G., Choi, S. J., Jun, K. I., Kim, N. H., et al. (2013). Severe fever with thrombocytopenia syndrome, South Korea, 2012. *Emerging Infect. Dis.* 19, 1892–1894. doi: 10.3201/eid1911.130792

Kim, K. Y., Kawamoto, S., Bao, J., Sellers, J. R., and Adelstein, R. S. (2008). The B2 alternatively spliced isoform of nonmuscle myosin II-B lacks actin-activated MgATPase activity and in vitro motility. *Biochem. Biophys. Res. Commun.* 369, 124–134. doi: 10.1016/j.bbrc.2007.11.108

Kovács, M., Tóth, J., Hetényi, C., Málnási-Csizmadia, A., and Sellers, J. R. (2004). Mechanism of blebbistatin inhibition of myosin II. *J. Biol. Chem.* 279, 35557–35563. doi: 10.1074/jbc.M405319200

Lathe, R., and Haas, J. G. (2016). Distribution of cellular HSV-1 receptor expression in human brain. *J. Neurovirol.* 23, 376–384. doi: 10.1007/s13365-016-0504-x

Li, L., Xue, B., Sun, W., Gu, G., Hou, G., Zhang, L., et al. (2018). Recombinant MYH9 protein C-terminal domain blocks porcine reproductive and respiratory syndrome virus internalization by direct interaction with viral glycoprotein 5. *Antiviral Res.* 156, 10–20. doi: 10.1016/j.antiviral.2018.06.001

Li, N., Du, T., Yan, Y., Zhang, A., Gao, J., Hou, G., et al. (2016). MicroRNA let-7f-5p inhibits porcine reproductive and respiratory syndrome virus by targeting MYH9. *Sci. Rep.* 6:34332. doi: 10.1038/srep34332

Li, P., Tong, Z. D., Li, K. F., Tang, A., Dai, Y. X., and Yan, J. B. (2017). Seroprevalence of severe fever with thrombocytopenia syndrome virus in China: a systematic review and meta-analysis. *PLoS One* 12:e0175592. doi: 10.1371/journal.pone.0175592

Looker, K. J., Elmes, J. A. R., Gottlieb, S. L., Schiffer, J. T., Vickerman, P., Turner, K. M. E., et al. (2017). Effect of HSV-2 infection on subsequent HIV acquisition: an updated systematic review and meta-analysis. *Lancet Infect Dis.* 17, 1303–1316. doi: 10.1016/s1473-3099(17)30405-x

Lunn, D. P., Davis-Poynter, N., Flaminio, M. J., Horohov, D. W., Osterrieder, K., Pusterla, N., et al. (2009). Equine herpesvirus-1 consensus statement. *J. Vet. Intern. Med.* 23, 450–461. doi: 10.1111/j.1939-1676.2009.0304.x

Lunney, J. K., Fang, Y., Ladinig, A., Chen, N., Li, Y., Rowland, B., et al. (2016). Porcine Reproductive and Respiratory Syndrome Virus (PRRSV): pathogenesis and interaction with the immune system. *Annu. Rev. Anim. Biosci.* 4, 129–154. doi: 10.1146/annurev-animal-022114-111025

Lyman, M. G., and Enquist, L. W. (2009). Herpesvirus interactions with the host cytoskeleton. *J. Virol.* 83, 2058–2066. doi: 10.1128/jvi.01718-08

Ma, X., Jana, S. S., Conti, M. A., Kawamoto, S., Claycomb, W. C., and Adelstein, R. S. (2010). Ablation of nonmuscle myosin II-B and II-C reveals a role for nonmuscle myosin II in cardiac myocyte karyokinesis. *Mol. Biol. Cell* 21, 3952–3962. doi: 10.1091/mbc.E10-04-0293

McKillop, D. F., Fortune, N. S., Ranatunga, K. W., and Geeves, M. A. (1994). The influence of 2,3-butanedione 2-monoxime (BDM) on the interaction between actin and myosin in solution and in skinned muscle fibres. *J. Muscle Res. Cell. Motil.* 15, 309–318. doi: 10.1007/BF00123483

Meng, Z., and Lu, M. (2017). RNA interference-induced innate immunity, off-target effect, or immune adjuvant? *Front. Immunol.* 8:331. doi: 10.3389/fimmu.2017.00331

Mesquita, F. S., Brito, C., Cabanes, D., and Sousa, S. (2017). Control of cytoskeletal dynamics during cellular responses to pore forming toxins. *Commun. Integr. Biol.* 10:e1349582. doi: 10.1080/19420889.2017.1349582

Murphy, F. A., Fauquet, C. M., Bishop, D. H. L., Ghabrial, S. A., Jarvis, A. W., Martelli, G. P., et al. (2012). *Virus Taxonomy: Classification and Nomenclature of Viruses. Sixth Report of the International Committee on Taxonomy of Viruses*. New York, NY: Springer-Verlag.

Newell-Litwa, K. A., Horwitz, R., and Lamers, M. L. (2015). Non-muscle myosin II in disease: mechanisms and therapeutic opportunities. *Dis. Model Mech.* 8, 1495–1515. doi: 10.1242/dmm.022103

Nieuwenhuis, N., Duinhof, T. F., and van Nes, A. (2012). Economic analysis of outbreaks of porcine reproductive and respiratory syndrome virus in nine sow herds. *Vet. Rec.* 170:225. doi: 10.1136/vr.100101

Pecci, A., Ma, X., Savoia, A., and Adelstein, R. S. (2018). MYH9: structure, functions and role of non-muscle myosin IIA in human disease. *Gene* 664, 152–167. doi: 10.1016/j.gene.2018.04.048

Pientong, C., Weisshart, K., Kühn, J. E., Knopf, C. W., and Braun, R. W. (1989). Replication of herpes simplex virus type 1 in differentiated human promyelocytic HL-60 cells. *Virology* 170, 468–476. doi: 10.1016/0042-6822(89)90438-8

Radoshevich, L., and Cossart, P. (2017). Listeria monocytogenes: towards a complete picture of its physiology and pathogenesis. *Nat. Rev. Microbiol.* 16, 32–46. doi: 10.1038/nrmicro.2017.126

Rauscher, A., Gyimesi, M., Kovács, M., and Málnási-Csizmadia, A. (2018). Targeting myosin by blebbistatin derivatives: optimization and pharmacological potential. *Trends Biochem. Sci.* 43, 700–713. doi: 10.1016/j.tibs.2018.06.006

Rednor, S. J., and Ross, M. J. (2018). Molecular mechanisms of injury in HIV-associated nephropathy. *Front. Med.* 7:177. doi: 10.3389/fmed.2018.00177

Roberts, K. L., and Baines, J. D. (2011). Actin in herpesvirus infection. *Viruses* 3, 336–346. doi: 10.3390/v3040336

Roman, B. I., Verhasselt, S., and Stevens, C. V. (2018). The medicinal chemistry and use of myosin II Inhibitor (S)-blebbistatin and its derivatives. *J. Med. Chem.* 61, 9410–9428. doi: 10.1021/acs.jmedchem.8b00503

Saitoh, M., Ishikawa, T., Matsushima, S., Naka, M., and Hidaka, H. (1987). Selective inhibition of catalytic activity of smooth muscle myosin light chain kinase. *J. Biol. Chem.* 262, 7796–7801.

Shakya, A. K., O'Callaghan, D. J., and Kim, S. K. (2017). Comparative genomic sequencing and pathogenic properties of equine herpesvirus 1 KyA and RacL11. *Front. Vet. Sci.* 4:211. doi: 10.3389/fvets.2017.00211

Shi, J., Takahashi, S., Jin, X. H., Li, Y. Q., Ito, Y., Mori, Y., et al. (2007). Myosin light chain kinase-independent inhibition by ML-9 of murine TRPC6 channels expressed in HEK293 cells. *Br. J. Pharmacol.* 152, 122–131. doi: 10.1038/sj.bjp.0707368

Shim, H. Y., Quan, X., Yi, Y. S., and Jung, G. (2011). Heat shock protein 90 facilitates formation of the HBV capsid via interacting with the HBV core protein dimers. *Virology* 410, 161–169. doi: 10.1016/j.virol.2010.11.005

Stoltzfus, C. M. (2009). Chapter 1. Regulation of HIV-1 alternative RNA splicing and its role in virus replication. *Adv. Virus Res.* 74, 1–40. doi: 10.1016/s0065-3527(09)74001-1

Sun, Y., Qi, Y., Liu, C., Gao, W., Chen, P., Fu, L., et al. (2014). Nonmuscle myosin heavy chain IIA is a critical factor contributing to the efficiency of early infection of severe fever with thrombocytopenia syndrome virus. *J. Virol.* 88, 237–248. doi: 10.1128/jvi.02141-13

Takahashi, T., Maeda, K., Suzuki, T., Ishido, A., Shigeoka, T., Tominaga, T., et al. (2014). The first identification and retrospective study of severe fever with thrombocytopenia syndrome in Japan. *J. Infect. Dis.* 209, 816–827. doi: 10.1093/infdis/jit603

Teow, S. Y., Yap, H. Y., and Peh, S. C. (2017). Epstein-barr virus as a promising immunotherapeutic target for nasopharyngeal carcinoma treatment. *J. Pathog.* 2017:7349268. doi: 10.1155/2017/7349268

Tomlin, H., and Piccinini, A. M. (2018). A complex interplay between the extracellular matrix and the innate immune response to microbial pathogens. *Immunology* 155, 186–201. doi: 10.1111/imm.12972

Valiya Veettil, M., Sadagopan, S., Kerur, N., Chakraborty, S., and Chandran, B. (2010). Interaction of c-Cbl with myosin IIA regulates Bleb associated macropinocytosis of Kaposi's sarcoma-associated herpesvirus. *PLoS Pathog.* 6:e1001238. doi: 10.1371/journal.ppat.1001238

van Leeuwen, H., Elliott, G., and O'Hare, P. (2002). Evidence of a role for nonmuscle myosin II in herpes simplex virus type 1 egress. *J. Virol.* 76, 3471–3481. doi: 10.1128/JVI.76.7.3471-3481.2002

Vicente-Manzanares, M., Ma, X., Adelstein, R. S., and Horwitz, A. R. (2009). Non-muscle myosin II takes centre stage in cell adhesion and migration. *Nat. Rev. Mol. Cell Biol.* 10, 778–790. doi: 10.1038/nrm2786

Wang, A., Ma, X., Conti, M. A., Liu, C., Kawamoto, S., and Adelstein, R. S. (2010). Nonmuscle myosin II isoform and domain specificity during early mouse development. *Proc. Natl. Acad. Sci. U.S.A.* 107, 14645–14650. doi: 10.1073/pnas.1004023107

Wang, L. C., Yu, Q., Edwards, V., Lin, B., Qiu, J., Turner, J. R., et al. (2017). *Neisseria gonorrhoeae* infects the human endocervix by activating non-muscle myosin II-mediated epithelial exfoliation. *PLoS Pathog.* 13:e1006269. doi: 10.1371/journal.ppat.1006269

Wang, S., Huang, X., Huang, Y., Hao, X., Xu, H., Cai, M., et al. (2014). A novel marine DNA virus (Singapore grouper iridovirus, SGIV) entry into host cells occurs via clathrin-mediated endocytosis and macropinocytosis in a pH-dependent manner. *J. Virol.* 88, 13047–13063. doi: 10.1128/jvi.01744-14

Wei, T., Hibino, H., and Omura, T. (2008a). Rice dwarf virus is engulfed into and released via vesicular compartments in cultured insect vector cells. *J. Gen. Virol.* 89(Pt 11), 2915–2920. doi: 10.1099/vir.0.2008/002063-0

Wei, T., Shimizu, T., and Omura, T. (2008b). Endomembranes and myosin mediate assembly into tubules of Pns10 of rice dwarf virus and intercellular spreading of the virus in cultured insect vector cells. *Virology* 372, 349–356. doi: 10.1016/j.virol.2007.10.034

Wei, T., Kikuchi, A., Moriyasu, Y., Suzuki, N., Shimizu, T., Hagiwara, K., et al. (2006). The spread of Rice dwarf virus among cells of its insect vector exploits virus-induced tubular structures. *J. Virol.* 80, 8593–8602. doi: 10.1128/jvi.00537-06

Xiong, D., Du, Y., Wang, H. B., Zhao, B., Zhang, H., Li, Y., et al. (2015). Nonmuscle myosin heavy chain IIA mediates Epstein-barr virus infection of nasopharyngeal epithelial cells. *Proc. Natl. Acad. Sci. U.S.A.* 112, 11036–11041. doi: 10.1073/pnas.1513359112

Xiong, Y., Wang, C., Shi, L., Wang, L., Zhou, Z., Chen, D., et al. (2017). Myosin light chain kinase: a potential target for treatment of inflammatory diseases. *Front. Pharmacol.* 8:292. doi: 10.3389/fphar.2017.00292

Xu, X., Lin, T., Huang, L., Weng, S., Wei, W., Li, Z., et al. (2011). VP15R from infectious spleen and kidney necrosis virus is a non-muscle myosin-II-binding protein. *Arch. Virol.* 156, 53–61. doi: 10.1007/s00705-010-0815-9

Yeh, C. H., Chen, Y. S., Wu, M. S., Chen, C. W., Yuan, C. H., Pan, K. W., et al. (2008). Differential display of grouper iridovirus-infected grouper cells by immunostaining. *Biochem. Biophys. Res. Commun.* 372, 674–680. doi: 10.1016/j.bbrc.2008.05.126

Yu, X. J., Liang, M. F., Zhang, S. Y., Liu, Y., Li, J. D., Sun, Y. L., et al. (2011). Fever with thrombocytopenia associated with a novel bunyavirus in China. *N. Engl. J. Med.* 364, 1523–1532. doi: 10.1056/NEJMoa1010095

Zhang, W., and Gunst, S. J. (2017). Nonmuscle (NM) myosin heavy chain phosphorylation regulates the formation of NM myosin filaments, adhesome assembly and smooth muscle contraction. *J. Physiol.* 595, 4279–4300. doi: 10.1113/jp273906

Zhao, Y., Wang, Z., Hou, Y., Zhang, K., and Peng, X. (2017). gga-miR-99a targets SMARCA5 to regulate Mycoplasma gallisepticum (HS strain) infection by depressing cell proliferation in chicken. *Gene* 627, 239–247. doi: 10.1016/j.gene.2017.06.039

Zheng, H., Xu, L., Liu, Y., Li, C., Zhang, L., Wang, T., et al. (2018). MicroRNA-221-5p inhibits porcine epidemic diarrhea virus replication by targeting genomic viral RNA and activating the NF-κB pathway. *Int. J. Mol. Sci.* 19:E3381. doi: 10.3390/ijms19113381

Zhu, F. X., Chong, J. M., Wu, L., and Yuan, Y. (2005). Virion proteins of Kaposi's sarcoma-associated herpesvirus. *J. Virol.* 79, 800–811. doi: 10.1128/jvi.79.2.800-811.2005

Conflict of Interest Statement: The authors declare that the research was conducted in the absence of any commercial or financial relationships that could be construed as a potential conflict of interest.

Copyright © 2019 Tan, Yuan, Liu, Cai, Guo and Wang. This is an open-access article distributed under the terms of the Creative Commons Attribution License (CC BY). The use, distribution or reproduction in other forums is permitted, provided the original author(s) and the copyright owner(s) are credited and that the original publication in this journal is cited, in accordance with accepted academic practice. No use, distribution or reproduction is permitted which does not comply with these terms.

frontiers in Microbiology

ORIGINAL RESEARCH
published: 15 March 2019
doi: 10.3389/fmicb.2019.00475

Clinical Significance of Polymorphisms in Immune Response Genes in Hepatitis C-Related Hepatocellular Carcinoma

Valli De Re[1†], Maria Lina Tornesello[2†], Mariangela De Zorzi[1], Laura Caggiari[1], Francesca Pezzuto[2], Patrizia Leone[3], Vito Racanelli[3], Gianfranco Lauletta[3], Laura Gragnani[4], Angela Buonadonna[1], Emanuela Vaccher[1], Anna Linda Zignego[4], Agostino Steffan[1] and Franco M. Buonaguro[2]*

[1] Centro di Riferimento Oncologico, Cancer Institute, Aviano, Italy, [2] Istituto Nazionale Tumori IRCCS "Fondazione G. Pascale," Naples, Italy, [3] Department of Biomedical Sciences and Human Oncology, Section of Internal Medicine, University of Bari "Aldo Moro", Bari, Italy, [4] Department of Experimental and Clinical Medicine and Department of Oncology, Interdepartmental Hepatology Center MASVE, Azienda Ospedaliero-Universitaria Careggi (AOUC), Florence, Italy

OPEN ACCESS

Edited by:
Cheryl Ann Winkler,
Frederick National Laboratory for Cancer Research (NIH), United States

Reviewed by:
José Ascención Martínez-Álvarez, Universidad de Guanajuato, Mexico
Masaaki Miyazawa, Kindai University, Japan

***Correspondence:**
Valli De Re
vdere@cro.it

[†] These authors have contributed equally to this work

Specialty section:
This article was submitted to Infectious Diseases, a section of the journal Frontiers in Microbiology

Received: 03 July 2018
Accepted: 25 February 2019
Published: 15 March 2019

Citation:
De Re V, Tornesello ML, De Zorzi M, Caggiari L, Pezzuto F, Leone P, Racanelli V, Lauletta G, Gragnani L, Buonadonna A, Vaccher E, Zignego AL, Steffan A and Buonaguro FM (2019) Clinical Significance of Polymorphisms in Immune Response Genes in Hepatitis C-Related Hepatocellular Carcinoma. Front. Microbiol. 10:475. doi: 10.3389/fmicb.2019.00475

Background and Aims: Polymorphisms in the immune response genes can contribute to clearance of hepatitis C virus (HCV) infection but also mediate liver inflammation and cancer pathogenesis. This study aimed to investigate the association of polymorphisms in PD-1 (PDCD1), IFNL3 (IL28B), and TLR2 immune related genes in chronic HCV patients with different hepatic and lymphoproliferative HCV-related diseases.

Methods: Selected PDCD1, IFNL3, and TLR2 genes were tested by molecular approaches in 450 HCV-positive patients with increasing severity of underlying liver diseases [including chronic infection (CHC), cirrhosis and hepatocellular carcinoma (HCC)], in 238 HCV-positive patients with lymphoproliferative diseases [such as cryoglobulinemia and non-Hodgkin lymphoma (NHL)] and in 94 blood donors (BD).

Results: While the rs12979860 IFNL3 T allele was found a good marker associated with HCV-outcome together with the rs111200466 TLR2 del variant, the rs10204525 PD-1.6 A allele was found to have an insignificant role in patients with HCV-related hepatic disorders. Though in Asian patients the combination of IFNL3 and PD-1.6 markers better define the HCV-related outcomes, in our series of Caucasian patients the PD-1.6 A-allele variant was observed very rarely.

Conclusion: Differences in the incidence of HCV-related HCC and clinical response between Asians and Europeans may be partially due to the distribution of PD-1.6 genotype that we found divergent between these two populations. On the other hand, we confirmed in this study that the polymorphic variants within IFNL3 and TLR2 immune response genes are significantly associated with HCV-related disease progression in our cohort of Italian patients.

Keywords: hepatitis virus C, hepatocellular carcinoma, cirrhosis, lymphoproliferative disorders, gene polymorphism, PD-1, IFNL3, TLR2

INTRODUCTION

Hepatocellular carcinoma is the primary malignancy of the liver that often occurs in the setting of underlying chronic liver disease, mostly HBV and/or C virus infection (HBV and HCV, respectively), alcoholic liver disease, and non-alcoholic fatty liver disease. In the last years the incidence rate of HCC has increased in the European and American populations (Ryerson et al., 2016), mostly related to the increase of HCV infection acquired before the availability of the serologic test.

Curative treatment options for HCC are local resection, radioembolization and multikinase inhibitors. Available options in patients with unresectable HCC are liver transplantation, percutaneous ethanol injection, radiofrequency ablation, and transcatheter arterial chemoembolization (Hernaez and El-Serag, 2018).

Unfortunately, most patients have locally advanced or metastatic HCC at diagnosis and are not eligible for either liver resection or transplantation. In these cases, despite the attempt to improve the OS of patients by chemotherapy, radioembolization, and multikinase inhibitor sorafenib, the OS remains poor (Llovet et al., 2008). The role of tumor-infiltrating leukocytes in mediating cancer progression and efficacy of immunotherapy in other malignancies, like melanoma, are now well recognized. Thus, although liver represents an "immune privileged" organ, immunotherapy now quickly evolves as a treatment option for HCC (Prieto et al., 2015). Based on programmed cell death 1 (PD-1) and PD-L ligands checkpoint blockade, the immunotherapy for HCC has shown encouraging results in phase I/II trials of Nivolumab (Checkmate 040 trial) (El-Khoueiry et al., 2017).

The PD-1/PD-L pathway has been demonstrated to be engaged in the inhibition of activated T-cells with PD-1 up-regulated in exhausted CD8 T-cells, a mechanism involved in hepatic viral persistence. The PD-1 expression has been shown to associate with the development of HBV-related liver diseases and the prognosis of HCC patients (Zhang et al., 2010; Li et al., 2013; Li et al., 2016). A recent proteomic study analyzing HCC cancer-immune landscape across tumor, non-tumor, and peripheral blood cells demonstrated the existence of a cancer-immune gradient which become progressively suppressive from the non-tumor to the tumor microenvironment (Chew et al., 2017). Specifically, authors have demonstrated the importance of the immunosuppressive action caused by exhausted tumor-infiltrating memory CD8+ T cells expressing high levels of PD-1, that allows immune evasion by the virus and cancer cells (Blank et al., 2005; Park et al., 2015). The increase number of exhausted PD-1+ T-cells was significantly higher in HBV-related vs. non-viral-associated HCC, and much more increased during the HCC progression stage (stage 1 vs. stage ≥2) (Chew et al., 2017). PD-1 was also found significantly up-regulated in CD8+ cytotoxic T-cells in patients with chronic HCV-infection compared to either HCV-negative subjects or patients with spontaneous HCV resolution (Golden-Mason et al., 2007). *In vitro* blockade of PD-1 has been shown to restore the functional competence of the HCV-specific T-cells (Golden-Mason et al., 2007).

Two SNP on the chromosome 2 within the PDCD1 gene, the rs36084323 G/A (PD-1.1) located -606 base pairs upstream the promoter region at position 242801596 and the rs10204525 G/A (PD-1.6) located at +8669 base pairs in the 3′ UTR at the position 241850169, have been found to be significantly associated with the risk to develop HBV-related cirrhosis and HCC among a Chinese Han population (Zhang et al., 2010; Li et al., 2013; Peng et al., 2015). The mechanisms underlying this association are likely due to the rs36084323 G allele, positioned in a putative binding site for the UCE-2 transcription regulators, causing the increased expression of PD-1 (Sasaki et al., 2014), and the rs10204525 A allele, disrupting the binding sequence for miR-4717 inhibitor within the 3′ UTR of PD-1 mRNA, which drives increased PD-1 expression (Zhang et al., 2015). In fact, the miRNA-4717 was demonstrated to affect the luciferase activity in a dose-dependent manner in cells transfected with a recombinant vector expressing the luciferase reporter gene under the transcription control of the PD-1 promoter containing the rs10204525 G polymorphic variant (Zhang et al., 2015).

Hepatitis C virus leads to chronic hepatitis (CHC) and is a major cause of liver cirrhosis and HCC. HCV is also a lymphotropic virus that triggers B-cells and promotes favorable conditions for B lymphocyte proliferation, including the autoimmune condition MC and B-cell non-Hodgkin lymphoma (B-NHL) (De Re et al., 2007; Sansonno et al., 2007).

By exploring the relationship between innate immunity and HCV-related disorders we found that the IFNL3 C rs12979860 and TLR2 -196-174 ins polymorphisms, both associated with interferon-treatment response and spontaneous HCV-clearance as well as with lower HCV viral load, are associated with a decreased risk of HCV-related diseases and delay the occurrence of cirrhosis and HCC (De Re et al., 2016).

In the present study, we simultaneously analyzed the distribution of polymorphic variants in the PD-1, IFNL3, and TLR2 immune-related genes among Italian patients affected by HCV-related CHC, cirrhosis and HCC (n = 450) and we compared the genotype and allele frequencies with those obtained in patients affected by HCV-related lymphoproliferative diseases, such as MC and NHL, (n = 238) and in healthy BD (n = 94).

PATIENTS AND METHODS

Study Design

A total of 148 HCV-infected patients with CHC without cirrhosis or HCC (48.3% male; median age 57.1 years), 113 patients with HCV-associated cirrhosis (65.4% males; median age 64.5 years), 189 patients with HCV-associated HCC (73.6% male; median age 68.9 years), 238 HCV-infected patients with lymphoproliferative disorders (130 MC, 29.1% male, median age 68.0 and 108 NHL, 47.5% male, median age 66.5 years), and 94 healthy BD (89.6%

Abbreviations: BD, blood donors; 95% CI, 95% confidence interval; CHC, chronic infection; del, deletion; HBV, chronic hepatitis B; HCC, hepatocellular carcinoma; HCV, hepatitis C virus; ins, insertion; INFL, interferon lambda; MAF, minor allele frequency; MC, mixed cryoglobulinemia; NHL, non-Hodgkin lymphoma; OR, odds ratio; OS, overall survival; PCR, polymerase chain reaction; PD-1, programmed cell death protein 1; SNP, single nucleotide polymorphisms; TLR, toll like receptor; UTR, untranslated region.

TABLE 1 | Clinical characteristics and PD-1.6 genotype of 688 HCV-positive patients and 94 HCV-negative BD.

				PD-1.6 A > G (rs10204525)					
	n	**Age**	**Male (%)**		**MAF***	**G/G (%)**	**A/G (%)**	**A/A (%)**	**Viral load#° HCV genotype° (%)**
Control subjects									
BD	94	42.46 ± 10.1	43 (89.6)	94	0.10	76 (80.9)	18 (19.1)	0	– –
HCV infected patients with liver diseases									
CHC	148	57.12 ± 14.1	56 (48.3)	450	0.09	125 (84.5)	20 (13.5)	3 (2.0)	2.32 ± 3.9 51/82 (55.6)
Cirrhosis	113	64.46 ± 11.1	70 (65.4)		0.09	93 (82.3)	19 (16.8)	1 (0.9)	2.71 ± 4.4 15/27 (62.2)
HCC	189	68.86 ± 8.6	103 (73.6)		0.09	154 (81.5)	34 (18.0)	1 (0.5)	1.94 ± 1.9 3/3 (100)
HCV infected patients with lymphoproliferative diseases									
MC	130	68.03 ± 9.9	32 (29.1)	238	0.11	103 (79.2)	26 (20.0)	1 (0.8)	3.32 ± 4.4 40/55 (72.7)
NHL	108	66.53 ± 15.1	47 (47.5)		0.10	87 (80.6)	20 (18.5)	1 (0.9)	3.13 ± 4.2 7/11 (63.6)
Total	782	65.9 ± 13.7	351 (44.9)	782	0.10	638 (81.6)	137 (17.5)	7 (0.9)	2.52 ± 3.9 116/178 (65.2)

*BD, blood donors; CHC, chronic hepatitis C; HCC, hepatocellular carcinoma; MC, mixed cryoglobulinemia; NHL, non-Hodgkin lymphoma; ±, standard deviation; *MAF, minor allele frequency, corresponding to A allele; #viral load, mean in million; °data of viral load and of HCV genotype type 1 were determined in 178 cases.*

male; median age 42.5 years) were included in this study. Some of the individuals recruited for the study are part of a previous study [18]. Cases added as new are: BD n = 94, CHC n = 76, cirrhosis = 13, HCC = 102, MC = 130, NHL = 12. Demographic characteristics of the enrolled patients as well as HCV genotype and viral load were summarized in **Table 1**. Patients with CHC and healthy BD have a lower mean age. Female gender was more frequent among patients with MC.

The diagnosis of chronic HCV infection was based on anti-HCV antibodies, elevated ALT serum levels and HCV RNA positivity for at least 6 months. The diagnosis of HCC was based on the standard criteria listed in the European Association for the Study of the Liver (EASL) that incorporate both invasive and non-invasive measures. Non-invasive criteria include two imaging techniques, both demonstrating a focal lesion >2 cm in diameter with features of arterial hypervascularization. Detection and immunochemical characterization of cryoglobulins were performed according to the consensus protocol proposed by the "Associazione Italiana per la Lotta alle Crioglobulinemie." The diagnosis of NHL in the course of HCV infection has been histopathologically confirmed based on the WHO classification.

The study is in accordance with the principles of the Helsinki Declaration and all subjects provided written informed consent. The study was approved by institutional review boards and independent ethics committees since this was a multicenter study. Particularly, the study of HCC cases was approved by the ethical committee EUDRACT (No. 2010-023602-12), Comitato Etico Indipendente of the Azienda Ospedaliero-Universitaria "Consorziale Policlinico" di Bari, the scientific board and the ethics committee of the Istituto Nazionale Tumori "Fond Pascale"; the institutional review board code SPE 14.084_ AOUC; comitato Etico Area Vasta Centro AOU Careggi, Firenze.

The HCV antibody test was performed by an enzyme immunoassay (III-generation EIA) against HCV-core and HCV-non-structural antigens. The HCV viral load (RNA UI/mL) was assessed by branched DNA technology (Chiron, Emeryville, CA, United States) in serum samples of 201 patients at the time of diagnosis of the HCV-related disorder. HCV genotype was determined by a commercial, certified, diagnostic test (Versant HCV Genotype 2.0, Siemens Healthcare Diagnostics, Deerfield, IL, United States).

Genotyping of PD-1, IFNL3, and TLR2 Polymorphisms

We collected 2 mL of whole blood from each patient and cryopreserved at −20°C until use. Total genomic DNA was extracted from peripheral blood using Qiagen DNAeasy Kit (QIAGEN, Grand Island, NY, United States). We analyzed four polymorphisms within the PD.1, IFNL3, and TLR2 genes, previously described as genetic factors involved in the immune response and hepatic disease progression (Zhang et al., 2010; Park et al., 2015; Li et al., 2016; Asian liver center, 2018; CDC, 2018). They include 3 single-nucleotide changes at positions -606 G/A (rs36084323, PD-1.1) (Xiao et al., 2015) and +8669 G/A (rs10204525, PD-1.6) within the PD-1 gene (Xiao et al., 2015), at position +1825 C/T (rs12979860) in the IFNL3 gene (De Re et al., 2016) and a 22-bp nucleotide del/ins from the position −196 to −174 (rs111200466) in the untranslated 5′-region of TLR2 gene (De Re et al., 2016).

Oligonucleotides used for genotyping were listed in **Supplementary Table S1**. Particularly, PD-1.1 and PD-1.6 were amplified as described by Zhang et al. (2010) by using PCR and products subjected to automated bidirectional direct sequencing analysis (Eurofins Genomics GmbH, Ebersberg, Germany). Briefly, PCR reactions were performed in 50 μL reaction mixture containing 30–300 ng of genomic DNA, 10 pmol of each primer, 1.25 Unit of Hot Master Taq DNA Polymerase (5 Prime GmbH, Hamburg, Germany) and 25 μL of PreMixJ (MasterAmp™ PCR, Epicentre, Madison, WI, United States). DNA was amplified in Sure Cycler 8800 thermal cycler (Agilent Technologies, SantaClara, CA, United States) starting with an initial denaturation at 94°C for 3 min, followed by 30 amplification cycles of denaturation at 94°C for 30 s, annealing at 65°C for 30 s, elongation at 72°C for 1 and 10 min

final elongation at 72°C. PCR amplification generated a fragment of 730 and 490 bp for the PD-1.1 and PD-1.6, respectively.

IFNL3 genotyping was performed using a specific custom TaqMan SNP-genotyping Assay (SNP rs12979860; Applied Biosystem, Foster City, CA, United States) on a 7900HT Fast Real-Time PCR system (Applied Biosystem, Foster City, CA, United States) (De Re et al., 2016). Determination of TLR2 polymorphism was performed by allele-specific PCR method. Fragments of different length (264 and 286 bp), depending on the presence or absence of the del mutation were visualized by electrophoresis on a 3.5% agarose gel stained with ethidium bromide (**Supplementary Figure S1**). Amplicon sequencing was used to validate the genotyping techniques.

Statistical Analysis

Specific tests including Fisher's exact test and one or two-way analysis of variance were used to compare allele and genotype frequency of PD-1, TLR2, and IFNL3 polymorphisms between patient groups with different pathologies and control subjects. Multivariate logistic regression analysis was performed with diagnosis as a dependent variable and independent variables, including age, gender (0 female; 1 male), and each genotype was also considered. *P*-value, OR and 95% CIs were calculated. Genotypes of each polymorphism were assessed according to dominant (0 wild-type homozygote; 1 heterozygote and variant homozygote), recessive (0 wild-type homozygote and heterozygote; 1 variant homozygote) and additive genetic models. Statistical power calculation was performed by using OSSE online tool[1]. Statistical analyses were performed using GraphPad Prism v6 and SNPStats. P value < 0.05 was considered statistically significant.

RESULTS

Genotype Frequencies

The genotype and allele frequencies of PD-1.6 in HCV-related cases and healthy BD are listed in **Table 1**. Male gender was predominant in our cohort of BD (89.6%), due to psychological, cultural, and social reasons. The analysis of PD-1.6 genotype distributions among HCV-related cases, compared to that of BD showed no significant association with the risk of development of liver diseases or lymphoproliferative disorders.

The A-allele MAF PD-1.6 was 0.09 in patients with liver diseases, 0.10 in patients with lymphoproliferative disorders and 0.10 in BD. The frequency of PD-1.6 A/A genotype ranged between 0.5 and 2% in HCV-related cases; 0.8–0.9% in lymphoproliferative disorders and the allele A, and thus the genotype A/A, was not found among BD subjects. Differences in allele frequencies and genotype distribution between HCV-related diseases and BD were not statistically significant. By comparing the distribution of PD-1.6 alleles among all HCV-related liver diseases (CHC, cirrhosis, and HCC) with HCV-related lymphoproliferative disorders (MC, NHL) a significantly higher frequency of A allele was found in the latter group (83/817 and 50/426, respectively, $p = 0.018$). However, no statistically significant difference was observed by comparing the A allele distribution in HCV-related liver diseases or in HCV-related lymphoproliferative disorders with that determined in the BD group. Age and gender of BD did not affect the result of the study: chi-squared test for trend among individuals with <40; <50, and ≥ 50 years old was $p = 0.74$, 0.22, and 0.62 for PD-1, IFNL3, and TLR2, respectively; chi-square test for gender (female vs. male) was $p = 0.67$, 0.83, and 0.92 and for PD-1, IFNL3, and TLR2, respectively. The allele frequency and genotype distribution were also found independent of HCV viral load and HCV genotype (**Table 1**).

The PD-1.1 polymorphism was analyzed in 109 HCC cases and consistently with the allele frequency distribution in the Caucasian population all samples were found G/G homozygous for such polymorphism (data not shown).

The analysis of IFNL3 rs12979860 polymorphism was shown in **Table 2**. There was an increase of T allele frequency, showing an additive genotype trend, in patients with liver diseases, particularly CHC (OR = 1.57; 95% CI, 1.06–2.31), cirrhosis (OR = 2.10; 95% CI, 1.40–3.16), and HCC (OR = 1.79; 95% CI, 1.21–2.64) compared to BD controls. This analysis had 78% power to detect differences in IFNL3 C/T allele distribution.

The frequency of IFNL3 T allele was also higher in patients with hepatic diseases compared to the lymphoproliferative diseases (MAF 0.44 vs. 0.36; OR = 1.77, 95%CI 1.40–2.25, $p < 0.0001$). In particular, patients with more advanced HCV-related liver diseases (i.e., cirrhosis and HCC) the frequency of IFNL3 T/T homozygous genotype was 1.4-fold higher than in MC and NHL, and 3.3 higher than in BD (**Figure 1** and **Table 2**). The IFNL3 T/T genotype was also 2.3-fold higher in MC and NHL patients compared to BD (**Figure 1**).

The distribution of TLR2 ins/del genotypes is shown in **Table 2**. The frequencies of these alleles in the HCV-related groups did not indicate any significant association, with the exception of the −196 to −174 del that was significantly more represented among HCC patients compared to BD controls (del vs. ins OR = 1.97; 95% CI, 1.17–3.31; $p = 0.01$). Moreover, we found a statistically significant difference in the frequency of del allele in HCV-related patients with MC lymphoproliferative disease compared to controls (OR = 1.71; 95% CI 1.00–2.91; $p = 0.05$).

Despite the limited power to detect the effect of TLR2 polymorphism, due to the low MAF, a statistically significant linear trend has been observed for TLR2 del/del genotype (Chi-square = 9.94, $p = 0.0016$) among the HCV-related groups.

Epistatic Interaction Between IFNL3 and TLR2

The above results indicated that only the polymorphic variations in IFNL3 and TLR2 genes were associated with susceptibility to HCV-related diseases in our series (**Tables 1**, **2**). A general linear regression model was used to identify multiloci genotypes associated with different HCV-related diseases. For the analysis, IFNL3-TLR2 genotypes from HCV-related liver and HCV lymphoproliferative diseases were divided into 4 groups, coded

[1]http://osse.bii.a-star.edu.sg/calculation2.php

TABLE 2 | IFNL3 and TLR2 genotypes among 688 HCV-positive cases and 94 HCV-negative BD.

		IFNL3 C > T (rs12979860)					TLR-2 ins/del rs111200466)				
	n	C/C (%)	C/T (%)	T/T (%)	MAF*	OR (95%CI)	Ins/Ins (%)	Ins/Del (%)	Del/Del (%)	MAF*	OR (95%CI)†
Control subjects											
BD	94	42 (44.7)	47 (50.0)	5 (5.3)	0.30	Reference	72 (76.4)	21 (22.3)	1 (1.4)	0.12	Reference
HCV infected patients with liver diseases											
CHC	148	44 (29.7)	88 (59.4)	16 (10.8)	0.41	1.57 (1.1–2.3) $p = 0.02$	101 (68.2)	41 (27.0)	6 (4.7)	0.16	
Cirrhosis	113	26 (23.0)	66 (58.4)	21 (18.6)	0.48	2.10 (1.4–3.2) $p < 0.001$	82 (72.6)	26 (23.0)	5 (4.4)	0.16	
HCC	144	42 (29.2)	78 (54.2)	24 (16.7)	0.43	1.79 (1.2–2.6) $p = 0.003$	97 (67.4)	32 (22.2)	15 (10.4)	0.21	1.97 (1.2–3.3) $p = 0.011$
HCV infected patients with lymphoproliferative diseases											
MC	130	55 (42.3)	59 (45.4)	16 (12.3)	0.35		86 (66.2)	38 (29.2)	6 (4.6)	0.19	1.71 (1.0–2.9) $p = 0.050$
NHL	108	41 (38.0)	54 (50.0)	13 (12.0)	0.37		83 (76.9)	24 (22.2)	1 (0.9)	0.12	
Total	737	250 (33.9)	392 (53.2)	95 (12.9)	0.40		521 (70.7)	182 (24.7)	34 (4.6)	0.16	

*BD, blood donors; CHC, chronic hepatitis C; HCC, hepatocellular carcinoma; MC, mixed cryoglobulinemia; NHL, non-Hodgkin lymphoma; *MAF, minor allele frequency, corresponding to deletion (del) in TLR2 and T-allele in IFNL3; OR, odds ratio; 95% CI, 95% confidence interval; †only significant results have been reported.*

as InsC, InsT DelC, DelT and their frequencies were compared to those obtained in BD and lymphoproliferative vs. liver diseases (**Table 3**). Wild-type TLR2-ins- IFNL3-C was the most frequent group (**Table 3**). Some multilocus genotypes, i.e., ins-T and del-T distinguished patients with liver diseases compared to BD (OR = 1.68; 95% CI 1.06–2.65, $p = 0.028$) and lymphoproliferative vs. HCV-related liver disorders [(OR = 0.72; 95% CI 0.56–0.94), $p = 0.014$ and (OR = 0.43; 95% CI 0.22–0.85), $p = 0.016$, respectively], indicating that these multi loci genes play a significant role in the development of liver diseases among HCV-positive subjects.

Comparison of IFNL3 T-allele distribution between groups of patients affected by different HCV-related liver diseases and healthy BD underlined the role of such polymorphic variant as dominant key factor for the progression of cirrhosis to the most advanced liver diseases in our series (**Table 3**).

PD-1.6 and IFNL3 MAF Frequencies in Different Countries

Surveys of HBV infection and the rate of HCC in different geographic regions showed a great disparity between Asian and other populations. In fact, the incidence of liver cancer is about nine-fold higher in Asians compared to white Americans suggesting that genetic polymorphisms and environmental risk factors may be responsible for such divergences (Asian liver center, 2018; CDC, 2018). Therefore, we compared the frequencies of PD-1.6 and IFNL3 polymorphisms in different countries reported in the NCBI database[2] and the frequencies found in our series (**Table 4**). A significant difference in allele distribution among Asian and Italian population was observed both for the PD-1.6 (MAF 0.66 vs. 0.10) and IFNL3 (0.08 vs. 0.31) polymorphisms as shown in **Table 4**.

[2]http://www.ncbi.nlm.nih.gov/SNP/

DISCUSSION

Previous studies have demonstrated that elevated expression of PD-1 in lymphocytes within the liver, especially exhausted T cells and Tregs, are closely associated with a dysfunction of the immune response in chronic HBV infection and HBV-related HCC (Boni et al., 2007; Fisicaro et al., 2010; Hsu et al., 2010; Wang et al., 2011). Moreover, it has been reported that PD1.1 and PD-1.6 polymorphisms combined with chronic HBV infection contribute to the development of HCC in a Chinese population (Li et al., 2013) and polymorphisms concur in the development of several tumor types and autoimmune disease pathogenesis (Momin et al., 2009; Liu et al., 2011; Tahoori et al., 2011; Li et al., 2013; Tang et al., 2017; Tejeda et al., 2017; Salmaninejad et al., 2018).

Studies focusing on CHC, by Penna et al. (2007) and Radziewicz et al. (2007) have shown that up-regulation of PD-1 affects HCV-specific CD8+ T cell function in the intrahepatic compartment in patient with chronic HCV infection. Blockade of the PD-1/PD-L1 interaction was shown to improve the expansion ability and IFN-γ secretion from HCV-specific CD8+ T cells (Moreno-Cubero and Larrubia, 2016) and control HCV replication in a chimpanzee model of CHC, although the efficacy was noted only in those animals with a critical threshold of pre-existing HCV-specific CD8+ T cells (Fuller et al., 2013). Additional studies showed that PD-1 is also critical in the persistence of chronic viral infections in mice (Barber et al., 2006) and in the progression of acquired immunodeficiency syndrome in humans (Day et al., 2006).

In our series we found a slight but not statistically significant increase of the PD-1.6 A/A genotype in the whole group of patients with HCV-related disorders compared to the control group of BD. However, the frequency of PD-1.6 A/A genotype is

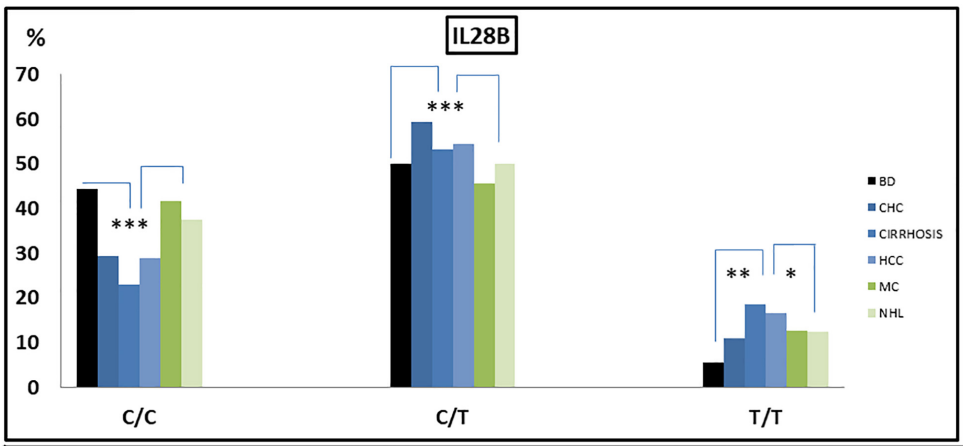

IL28B C/C	CHC(n=148) vs BD (n=94) 44/104 *vs* 42/52 ***P = 0.019***	CHC(n=148) vs MC (n=130) 44/104 *vs* 55/75 ***P = 0.033***	CHC (n=148) vs NHL (n=108) 44/104 *vs* 41/67
	cirrhosis(n=113) vs BD (n=94) 26/87 *vs 42/52* ***P = 0.001***	cirrhosis(n=113) vs MC (n=130) 26/87 *vs 55/75* ***P = 0.002***	cirrhosis(n=113) vs NHL (n=108) 26/87 *vs 41/67* ***P = 0.019***
	HCC(n=144) vs BD (n=94) 42/102 *vs 42/52* ***P = 0.018***	HCC(n=144) vs MC (n=130) 42/102 *vs 55/75* ***P = 0.031***	HCC(n=144) vs NHL (n=108) 42/102 *vs 41/67*
IL28B C/T	CHC(n=148) vs BD (n=94) 88/60 *vs* 47/47	CHC(n=148) vs MC (n=130) 88/60 *vs* 59/71 ***P = 0.022***	CHC (n=148) vs NHL (n=108) 88/60 *vs 54/54*
	cirrhosis(n=113) vs BD (n=94) *66/47 vs* 47/47	cirrhosis(n=113) vs MC (n=130) *66/47 vs* 59/71 ***P = 0.053***	cirrhosis(n=113) vs NHL (n=108) *66/47 vs 54/54*
	HCC(n=144) vs BD (n=94) *78/66 vs* 47/47	HCC(n=144) vs MC (n=130) *78/66 vs* 59/71	HCC(n=144) vs NHL (n=108) *78/66 vs 54/54*
IL28B T/T	CHC(n=148) vs BD (n=94) 16/132 *vs* 5/89	CHC(n=148) vs MC (n=130) 16/132 *vs* 16/114	CHC (n=148) vs NHL (n=108) 16/132 *vs* 13/95
	cirrhosis(n=113) vs BD (n=94) 21/92 *vs 5/89* ***P = 0.005***	cirrhosis(n=113) vs MC (n=130) 21/92 *vs 16/114*	cirrhosis(n=113) vs NHL (n=108) 21/92 *vs 13/95*
	HCC(n=144) vs BD (n=94) 24/120 *vs 5/89* ***P = 0.008***	HCC(n=144) vs MC (n=130) 24/120 *vs 16/114*	HCC(n=144) vs NHL (n=108) 24/120 *vs 13/95*

FIGURE 1 | Frequency of IFNL3 genotype distribution among patients stratified on the basis of their HCV-related disease (n = 643) and blood donors (BD) (n = 94). The frequency of IFNL3 T allele was found increased in HCV-associated liver diseases (CHC, cirrhosis, and HCC) compared to BD and to lymphoproliferative disorders (MC and NHL). BD, blood donors (controls); CHC, chronic hepatitis C; HCC, hepatocellular carcinoma; MC, mixed cryoglobulinemia; NHL, non-Hodgkin lymphoma. *$p < 0.05$; **$p < 0.001$; and ***$p < 0.005$.

very limited, ranging from 0 to 2% (**Table 1**) resulting in a allele-A MAF of 0.10 (**Table 4**), while this unfavorable A/A genotype is the most common genotype (52.6%) in Asian population, with a allele-A MAF of about 0.66 (**Table 4**; Tang et al., 2017; Tejeda et al., 2017).

There are remarkable dissimilarities in the distribution of PD-1.6 polymorphic variants and their association with HCC between the Asian population and our Italian cohort. Since each of these studies comprised almost 1000 cases we are incline to think that differences in the PD-1.6 genotype distribution are consistent and reflect the genetic heterogeneity among various populations. On the contrary to Asian population, in our series we found a very low frequency of PD-1.6 A-allele variant (MAF 0.10, **Table 4**), thus it is hard to think that this mutation has a strong role in HCC in our population. Additionally, it is well known that persistent HBV infection were more likely to be associated with HCC in Asian population, while HCV infection had a higher prevalence among the Caucasian population (Ahmad et al., 2018; Falla et al., 2018). Further studies are needed to determine the distribution of PD-1.6 variants in different geographic regions and to explore their casual role in HCV-related diseases susceptibility worldwide.

Since the PD-1/PD-L1 blockade has proven to be an efficient treatment for HCC (Kudo, 2016), the lack of parallel changes in the frequency of PD-1.6 A allele in HCV-related HCC patients and controls in our series excludes a simple direct effect of PD-1.6 variant in the pathogenesis of HCC. However, we cannot exclude the possibility that other polymorphisms in

TABLE 3 | Comparison of TLR2 and IFNL3 multilocus genotypes frequencies of HCV-related patients with liver (*n* = 405), HCV-related lymphoproliferative diseases (*n* = 238) and blood donors (*n* = 94).

IFNL3	TLR2	BD	CHC	Cirrhosis	HCC	Hepatic diseases	Hepatic vs. BD OR (95%CI), p†	BD	MC	NHL	Lympho-proliferative	Lympho-proliferative vs. hepatic OR (95%CI), p†
C	Ins	0.58	0.47	0.45	0.45	0.45		0.58	0.54	0.53	0.53	
T	Ins	0.29	0.36	0.39	0.35	0.37	1.68 (1.1-2.7) *p = 0.028*	0.29	0.30	0.35	0.32	0.72 (0.6–0.9) *p = 0.014*
C	Del	0.10	0.11	0.10	0.13	0.11		0.10	0.12	0.10	0.11	
T	Del	0.03	0.07	0.07	0.07	0.07		0.03	0.05	0.02	0.04	0.43 (0.2–0.9) *p = 0.016*

BD, blood donors (controls); CHC, chronic hepatitis C; HCC, hepatocellular carcinoma; MC, mixed cryoglobulinemia; NHL, non-Hodgkin lymphoma; †only significant results were reported. OR, odds ratio; 95% CI, 95% confidence interval.

TABLE 4 | Distribution of PD-1.6 allele-A and IFNL3 allele-T frequencies in different populations (available in http://www.ncbi.nlm.nih.gov/SNP/ database) and in our series of HCV-related diseases (*n* = 710).

	MAF	Asian	Nigerian	African	American	European	Italian	HCV*
PD-1.6	A	0.66	0.50	0.39	0.39	0.12	0.10°	0.10
IFNL3	T	0.08	0.50	0.67	0.40	0.31	0.31[&]	0.40

**Data obtained from our series of patients with a chronic HCV infection (n = 710). °data obtained from our series of blood donors (n = 94). [&]mean data from our series of HCV-negative patients (n = 94); n = 134 (Taliani et al., 2013); n = 428 (Falleti et al., 2011).*

PD-1 or in other immune-related genes, such as the rs12979860 polymorphism in IFNL3 gene, could be involved in HCV-related diseases in our Italian population (Ge et al., 2009; Riva et al., 2014; Wack et al., 2015). Alternatively, the discordant correlation between PD-1.6 and HCV-related HCC susceptibility across Asian-European populations could be related to an interaction of the host PD-1.6 gene variant with different environmental factor(s) present in the two populations or HCC development could be related to a different immune check point molecule blockade. Given the important involvement of PD-1 in autoimmunity and chronic viral infections, further researches are deserved to clarify the role of PD-1 polymorphism in these settings.

Genetic polymorphism of IFNL3 was found strongly associated with spontaneous resolution of HCV infection and with response to PEGylated interferon-alpha and ribavirin therapy for chronic HCV (Ge et al., 2009; Tanaka et al., 2009; Xiao et al., 2015; Huang et al., 2017). The IFNL3 and PD-1 markers in conjunction have also been reported to influence the susceptibility and outcomes of HCV infection in the Southeast

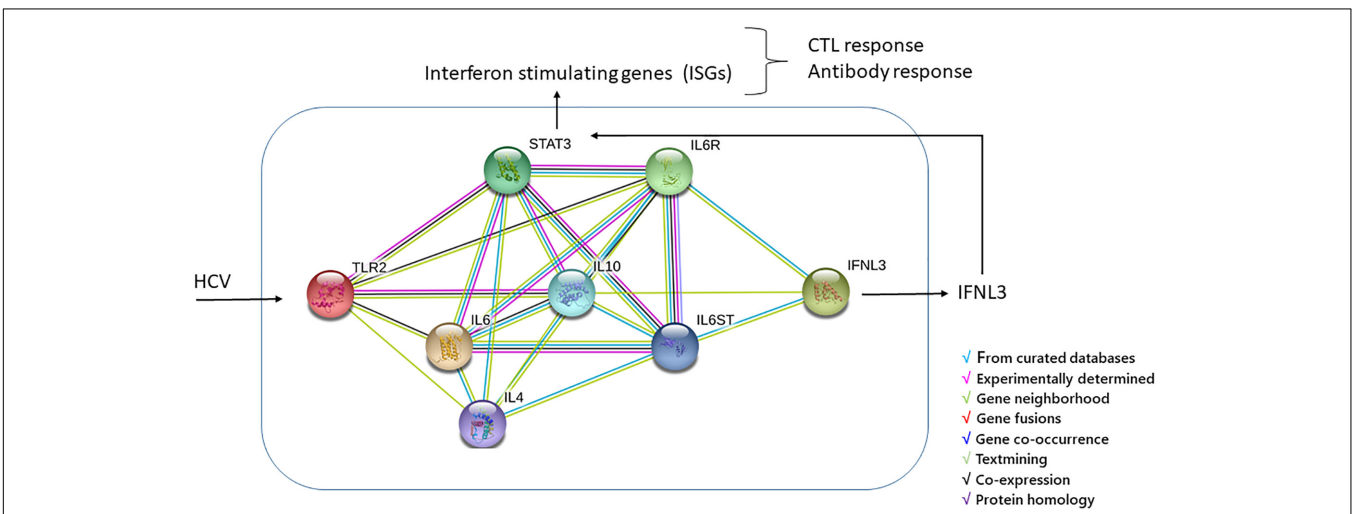

FIGURE 2 | TLR2/IFN-λ3 protein-protein interaction was performed by using String software. The interleukin 6 (IL6) and INF-α, connecting TLR2 and IFN-λ3, can turn on the JAK/STAT pathway, the most important pathway in mediating the inflammatory response to HCV via induction of IFN-stimulated genes (ISGs). The final effect of ISGs results in antigen presentation and a differential expression profile of certain immunomodulatory genes targeting different immune cells and resulting in the polarization of Th1 and Th2 cells, in the modulation of regulatory T-cells and pro-inflammatory cytokines and in the differentiation of dendritic cells (DCs) from monocytes (Egli et al., 2014; Douam et al., 2017; Hemann et al., 2017; Syedbasha and Egli, 2017; Zhou et al., 2018).

China, suggesting their interactions in the disease outcomes (Xiao et al., 2015). In a previous study we found an association between TLR2 ins/del and IFNL3 polymorphisms with HCV-related outcome (De Re et al., 2016). In the present study we demonstrated that the multilocus TLR2-ins/ IFNL3 T genotype was a significant factor for development of HCV-related liver diseases (**Table 3**), and that the impact of rare PD-1.6 variant in Italian population is responsible for the discrepancy between Asian and European results (**Table 4**). In our series the IFNL3 T variant was confirming to be one of the best markers associated with HCV-related pathogenesis, with a marginal role of TLR2 del variant, while in Asian populations the combined IFNL3 and PD-1.6 polymorphisms were found to better define the HCV-related outcomes.

Today, we have no data to demonstrate the effect of an interaction between TLR2 and IFNL3 gene products in HCV-positive patients, nonetheless, a functional links between these genes may be indirectly determined using the STRING[3] software based on genomic associations of genes that are required for a same function. **Figure 2** shows the graphical representation of the model of interaction between TLR2 and IFNL3 leading to effect of IFNL3 gene expression on the janus kinase (JAK)/signal transducer and activator of transcription (STAT) (JAK/STAT) pathway. HCV core and NS3 proteins are known to be able to trigger inflammatory pathways via TLR2, which may act, along with TLR1 and TLR6, as a receptor contributing to the activation of the innate immune system and production of interleukin 6 (IL-6) and Interferon-alpha (IFN-α) (Dolganiuc et al., 2004; Chang et al., 2007). In the past before direct-acting antiviral (DAA) treatment IFN-α therapy was largely demonstrated to reduce the risk of HCC and complications associated with cirrhosis in HCV infected individuals and serum IL-6 elevation has been correlated with liver disease severity, HCV-RNA titer and the activation of the JAK/STAT pathway (Malaguarnera et al., 1997; Sansone and Bromberg, 2012; Egli et al., 2014; Kong et al., 2016; Hemann et al., 2017; Syedbasha and Egli, 2017; Yakut et al., 2018). IFNL3 signal, producing IFN-λ3 molecules, has been demonstrated to inhibit HCV infection and induce anti-viral response also through the JAK-STAT pathway via induction of IFN-stimulated genes (ISGs) (Malaguarnera et al., 1997; Dolganiuc et al., 2004; Yakut et al., 2018). IFNL3 induces a cell type specific immune response due to the cellular expression of IFN-λ3s receptors in fewer cell types (Egli et al., 2014) and activates the JAK-STAT pathway by a feed-forward fashion with substantial differences in terms of the ISGs gene expression induced by IFN-α. Indeed, IFN-λ3 showed many antiviral properties but with an overall smaller response than IFN-α causes (Hemann et al., 2017; Syedbasha and Egli, 2017; Zhou et al., 2018). The IFN-λ3 effect is mainly associated with antigen presentation and a differential expression profile of certain immunomodulatory genes compared to IFN-α and this suggests a specific functional role for IFN-λ3. A critical role of IFN-λ3n in the polarization of Th1 and Th2 cells, in the modulation of regulatory T-cells and pro-inflammatory cytokines and in the differentiation of dendritic cells (DCs) have been well described in several reviews (Egli et al., 2014; Douam et al., 2017; Hemann et al., 2017; Syedbasha and Egli, 2017; Zhou et al., 2018). Of note, during infection with HCV, the expression pattern of many of the ISGs significantly change, most likely due to immunomodulatory effects of HCV proteins and complex inhibitory effects of IFN signaling pathways (Thomas et al., 2012; Egli et al., 2014). In particular, the long-term effects on the Th1/Th2 balance might have implications for the priming of T- and B-cell dependent memory responses, and thus possibly on HCV-related lymphoproliferative malignancy and autoimmune disease prevalence (Egli et al., 2014).

Thus, an indirect interaction between IFNL3 and TLR2 gene products may be suggested from data of literature, but further studies are necessary to confirm the effect of IFNL3 and TLR2 polymorphisms in the prediction of the above reported functional signaling in HCV patients.

This is the first study evaluating the PD1 polymorphisms and the risk of HCV-related disorders in the Italian population. The results should be regarded as descriptive observations and larger studies with more diverse ethnic populations are needed to confirm the association of immune related gene polymorphisms in HCV-related diseases.

In conclusion our study highlighted the importance of geographical difference in the frequencies of PD-1 and IFNL3 genetic polymorphisms in HCV-related diseases particularly in cirrhosis and in HCC susceptibility. Due to the importance of these genes in the immune response to hepatic infection, autoimmune disorders and malignancies as well as their role in the response to new proposed immune check-point treatment for HCC, further studies are needed to better understand the pathogenic role of these genetic variants in HCV-related diseases.

AUTHOR CONTRIBUTIONS

VD and MT wrote the manuscript, provided critical discussion in the manuscript preparation, and revised the manuscript. MD and FP performed the experiments and revised the manuscript. LC, PL, and LG contributed to analyze the data and revise the manuscript. VR, LG, AB, EV, AZ, AS, and FB contributed to collect and analyze the clinical patient's data and revise the manuscript.

FUNDING

MD and LC fellowships were funded by 5X1000_2010_MdS. FP was the recipient of a research fellowship awarded by FIRE/AISF ONLUS (Fondazione Italiana per la Ricerca in Epatologia) http://www.fondazionefegato.it/.

SUPPLEMENTARY MATERIAL

The Supplementary Material for this article can be found online at: https://www.frontiersin.org/articles/10.3389/fmicb.2019.00475/full#supplementary-material

[3] https://string-db.org/cgi/input.pl?sessionId=7AG0SO9%20cCRu4&input%20_page_show_search=on

REFERENCES

Ahmad, A. A., Falla, A. M., Duffell, E., Noori, T., Bechini, A., Reintjes, R., et al. (2018). Estimating the scale of chronic hepatitis B virus infection among migrants in EU/EEA countries. *BMC Infect. Dis.* 18:34. doi: 10.1186/s12879-017-2921-8

Asian liver center (2018). Available at: https//liver.standfort.edu.

Barber, D. L., Wherry, E. J., Masopust, D., Zhu, B., Allison, J. P., Sharpe, A. H., et al. (2006). Restoring function in exhausted CD8 T cells during chronic viral infection. *Nature* 439, 682–687. doi: 10.1038/nature04444

Blank, C., Gajewski, T. F., and Mackensen, A. (2005). Interaction of PD-L1 on tumor cells with PD-1 on tumor-specific T cells as a mechanism of immune evasion: implications for tumor immunotherapy. *Cancer Immunol. Immunother.* 54, 307–314. doi: 10.1007/s00262-004-0593-x

Boni, C., Fisicaro, P., Valdatta, C., Amadei, B., Di, V. P., Giuberti, T., et al. (2007). Characterization of hepatitis B virus (HBV)-specific T-cell dysfunction in chronic HBV infection. *J. Virol.* 81, 4215–4225. doi: 10.1128/JVI.02844-06

CDC (2018). *Draft ACIP Hepatitis Recommandations*. Atlanta, GA: CDC.

Chang, S., Dolganiuc, A., and Szabo, G. (2007). Toll-like receptors 1 and 6 are involved in TLR2-mediated macrophage activation by hepatitis C virus core and NS3 proteins. *J. Leukoc. Biol.* 82, 479–487. doi: 10.1189/jlb.0207128

Chew, V., Lai, L., Pan, L., Lim, C. J., Li, J., Ong, R., et al. (2017). Delineation of an immunosuppressive gradient in hepatocellular carcinoma using high-dimensional proteomic and transcriptomic analyses. *Proc. Natl. Acad. Sci. U.S.A.* 114, E5900–E5909. doi: 10.1073/pnas.1706559114

Day, C. L., Kaufmann, D. E., Kiepiela, P., Brown, J. A., Moodley, E. S., Reddy, S., et al. (2006). PD-1 expression on HIV-specific T cells is associated with T-cell exhaustion and disease progression. *Nature* 443, 350–354. doi: 10.1038/nature05115

De Re, V., Caggiari, L., Simula, M. P., De, V. S., Sansonno, D., and Dolcetti, R. (2007). B-cell lymphomas associated with HCV infection. *Gastroenterology* 132, 1205–1207. doi: 10.1053/j.gastro.2007.02.009

De Re, V., De, Z. M., Caggiari, L., Lauletta, G., Tornesello, M. L., Fognani, E., et al. (2016). HCV-related liver and lymphoproliferative diseases: association with polymorphisms of IL28B and TLR2. *Oncotarget* 7, 37487–37497. doi: 10.18632/oncotarget.9303

Dolganiuc, A., Oak, S., Kodys, K., Golenbock, D. T., Finberg, R. W., Kurt-Jones, E., et al. (2004). core and nonstructural 3 proteins trigger toll-like receptor 2-mediated pathways and inflammatory activation. *Gastroenterology* 127, 1513–1524. doi: 10.1053/j.gastro.2004.08.067

Douam, F., Soto Albrecht, Y. E., Hrebikova, G., Sadimin, E., Davidson, C., Kotenko, S. V., et al. (2017). Type III interferon-mediated signaling is critical for controlling live attenuated yellow fever virus infection in vivo. *mBio* 8:e819–17. doi: 10.1128/mBio.00819-17

Egli, A., Santer, D. M. O., Shea, D., Tyrrell, D. L., and Houghton, M. (2014). The impact of the interferon-lambda family on the innate and adaptive immune response to viral infections. *Emerg. Microbes Infect.* 3:e51. doi: 10.1038/emi.2014.51

El-Khoueiry, A. B., Sangro, B., Yau, T., Crocenzi, T. S., Kudo, M., Hsu, C., et al. (2017). Nivolumab in patients with advanced hepatocellular carcinoma (CheckMate 040): an open-label, non-comparative, phase 1/2 dose escalation and expansion trial. *Lancet* 389, 2492–2502. doi: 10.1016/S0140-6736(17)31046-2

Falla, A. M., Ahmad, A. A., Duffell, E., Noori, T., and Veldhuijzen, I. K. (2018). Estimating the scale of chronic hepatitis C virus infection in the EU/EEA: a focus on migrants from anti-HCV endemic countries. *BMC Infect. Dis.* 18:42. doi: 10.1186/s12879-017-2908-5

Falleti, E., Bitetto, D., Fabris, C., Cussigh, A., Fornasiere, E., Cmet, S., et al. (2011). Role of interleukin 28B rs12979860 C/T polymorphism on the histological outcome of chronic hepatitis C: relationship with gender and viral genotype. *J. Clin. Immunol.* 31, 891–899. doi: 10.1007/s10875-011-9547-1

Fisicaro, P., Valdatta, C., Massari, M., Loggi, E., Biasini, E., Sacchelli, L., et al. (2010). Antiviral intrahepatic T-cell responses can be restored by blocking programmed death-1 pathway in chronic hepatitis B. *Gastroenterology* 138, 682–693. doi: 10.1053/j.gastro.2009.09.052

Fuller, M. J., Callendret, B., Zhu, B., Freeman, G. J., Hasselschwert, D. L., Satterfield, W., et al. (2013). Immunotherapy of chronic hepatitis C virus infection with antibodies against programmed cell death-1 (PD-1). *Proc. Natl. Acad. Sci. U.S.A.* 110, 15001–15006. doi: 10.1073/pnas.1312772110

Ge, D., Fellay, J., Thompson, A. J., Simon, J. S., Shianna, K. V., Urban, T. J., et al. (2009). Genetic variation in IL28B predicts hepatitis C treatment-induced viral clearance. *Nature* 461, 399–401. doi: 10.1038/nature08309

Golden-Mason, L., Palmer, B., Klarquist, J., Mengshol, J. A., Castelblanco, N., and Rosen, H. R. (2007). Upregulation of PD-1 expression on circulating and intrahepatic hepatitis C virus-specific CD8+ T cells associated with reversible immune dysfunction. *J. Virol.* 81, 9249–9258. doi: 10.1128/JVI.00409-07

Hemann, E. A., Gale, M., and Savan, R. (2017). Interferon lambda genetics and biology in regulation of viral control. *Front. Immunol.* 8:1707. doi: 10.3389/fimmu.2017.01707

Hernaez, R., and El-Serag, H. B. (2018). How we approach it: treatment options for hepatocellular carcinoma. *Am. J. Gastroenterol.* 113, 791–794. doi: 10.1038/s41395-018-0008-9

Hsu, P. N., Yang, T. C., Kao, J. T., Cheng, K. S., Lee, Y. J., Wang, Y. M., et al. (2010). Increased PD-1 and decreased CD28 expression in chronic hepatitis B patients with advanced hepatocellular carcinoma. *Liver Int.* 30, 1379–1386. doi: 10.1111/j.1478-3231.2010.02323.x

Huang, H., Duggal, P., Thio, C. L., Latanich, R., Goedert, J. J., Mangia, A., et al. (2017). Fine-mapping of genetic loci driving spontaneous clearance of hepatitis C virus infection. *Sci. Rep.* 20:15843. doi: 10.1038/s41598-017-16011-2

Kong, L., Zhou, Y., Bu, H., Lv, T., Shi, Y., and Yang, J. (2016). Deletion of interleukin-6 in monocytes/macrophages suppresses the initiation of hepatocellular carcinoma in mice. *J. Exp. Clin. Cancer Res.* 35:131. doi: 10.1186/s13046-016-0412-1

Kudo, M. (2016). Immune checkpoint blockade in hepatocellular carcinoma: 2017 update. *Liver Cancer* 6, 1–12. doi: 10.1159/000449342

Li, Z., Li, N., Li, F., Zhou, Z., Sang, J., Chen, Y., et al. (2016). Immune checkpoint proteins PD-1 and TIM-3 are both highly expressed in liver tissues and correlate with their gene polymorphisms in patients with HBV-related hepatocellular carcinoma. *Medicine* 95:e5749. doi: 10.1097/MD.0000000000005749

Li, Z., Li, N., Zhu, Q., Zhang, G., Han, Q., Zhang, P., et al. (2013). Genetic variations of PD1 and TIM3 are differentially and interactively associated with the development of cirrhosis and HCC in patients with chronic HBV infection. *Infect. Genet. Evol.* 14, 240–246. doi: 10.1016/j.meegid.2012.12.008

Liu, X., Hu, L. H., Li, Y. R., Chen, F. H., Ning, Y., and Yao, Q. F. (2011). Programmed cell death 1 gene polymorphisms is associated with ankylosing spondylitis in chinese han population. *Rheumatol. Int.* 31, 209–213. doi: 10.1007/s00296-009-1264-1

Llovet, J. M., Ricci, S., Mazzaferro, V., Hilgard, P., Gane, E., Blanc, J. F., et al. (2008). Sorafenib in advanced hepatocellular carcinoma. *N. Engl. J. Med.* 359, 378–390. doi: 10.1056/NEJMoa0708857

Malaguarnera, M., Di, F. I., Romeo, M. A., Restuccia, S., Laurino, A., and Trovato, B. A. (1997). Elevation of interleukin 6 levels in patients with chronic hepatitis due to hepatitis C virus. *J. Gastroenterol.* 32, 211–215. doi: 10.1007/BF02936370

Momin, S., Flores, S., Angel, B. B., Codner, D. E., Carrasco, P. E., and Perez-Bravo, F. (2009). Interactions between programmed death 1 (PD-1) and cytotoxic T lymphocyte antigen 4 (CTLA-4) gene polymorphisms in type 1 diabetes. *Diabetes Res. Clin. Pract.* 83, 289–294. doi: 10.1016/j.diabres.2008.12.003

Moreno-Cubero, E., and Larrubia, J. R. (2016). Specific CD8(+) T cell response immunotherapy for hepatocellular carcinoma and viral hepatitis. *World J. Gastroenterol.* 22, 6469–6483. doi: 10.3748/wjg.v22.i28.6469

Park, H. J., Park, J. S., Jeong, Y. H., Son, J., Ban, Y. H., Lee, B. H., et al. (2015). PD-1 upregulated on regulatory T cells during chronic virus infection enhances the suppression of CD8+ T cell immune response via the interaction with PD-L1 expressed on CD8+ T cells. *J. Immunol.* 194, 5801–5811. doi: 10.4049/jimmunol.1401936

Peng, H., Li, Q. L., Hou, S. H., Hu, J., Fan, J. H., and Guo, J. J. (2015). Association of genetic polymorphisms in CD8+ T cell inhibitory genes and susceptibility to and progression of chronic HBV infection. *Infect. Genet. Evol.* 36, 467–474. doi: 10.1016/j.meegid.2015.08.018

Penna, A., Pilli, M., Zerbini, A., Orlandini, A., Mezzadri, S., Sacchelli, L., et al. (2007). Dysfunction and functional restoration of HCV-specific CD8 responses in chronic hepatitis C virus infection. *Hepatology* 45, 588–601. doi: 10.1002/hep.21541

Prieto, J., Melero, I., and Sangro, B. (2015). Immunological landscape and immunotherapy of hepatocellular carcinoma. *Nat. Rev. Gastroenterol. Hepatol.* 12, 681–700. doi: 10.1038/nrgastro.2015.173

Radziewicz, H., Ibegbu, C. C., Fernandez, M. L., Workowski, K. A., Obideen, K., Wehbim, M., et al. (2007). Liver-infiltrating lymphocytes in chronic human hepatitis C virus infection display an exhausted phenotype with high levels of PD-1 and low levels of CD127 expression. *J. Virol.* 81, 2545–2553. doi: 10.1128/JVI.02021-06

Riva, E., Scagnolari, C., Turriziani, O., and Antonelli, G. (2014). Hepatitis C virus and interferon type III (interferon-lambda3/interleukin-28B and interferon-lambda4): genetic basis of susceptibility to infection and response to antiviral treatment. *Clin. Microbiol. Infect.* 20, 1237–1245. doi: 10.1111/1469-0691.12797

Ryerson, A. B., Eheman, C. R., Altekruse, S. F., Ward, J. W., Jemal, A., Sherman, R. L., et al. (2016). Annual report to the nation on the status of cancer, 1975-2012, featuring the increasing incidence of liver cancer. *Cancer* 122, 1312–1337. doi: 10.1002/cncr.29936

Salmaninejad, A., Khoramshahi, V., Azani, A., Soltaninejad, E., Aslani, S., Zamani, M. R., et al. (2018). PD-1 and cancer: molecular mechanisms and polymorphisms. *Immunogenetics* 70, 73–86. doi: 10.1007/s00251-017-1015-5

Sansone, P., and Bromberg, J. (2012). Targeting the interleukin-6/Jak/stat pathway in human malignancies. *J. Clin. Oncol.* 20, 1005–1014. doi: 10.1200/JCO.2010.31.8907

Sansonno, D., Carbone, A., De Re, V., and Dammacco, F. (2007). Hepatitis C virus infection, cryoglobulinaemia, and beyond. *Rheumatology* 46, 572–578. doi: 10.1093/rheumatology/kel425

Sasaki, H., Tatemaysu, T., Okuda, K., Moriyama, S., Yano, M., and Fujii, Y. (2014). PD-1 gene promoter polymorphisms correlate with a poor prognosis in non-small cell lung cancer. *Mol. Clin. Oncol.* 2, 1035–1042. doi: 10.3892/mco.2014.358

Syedbasha, M., and Egli, A. (2017). Interferon lambda: modulating immunity in infectious diseases. *Front. Immunol.* 8:119. doi: 10.3389/fimmu.2017.00119

Tahoori, M. T., Pourfathollah, A. A., Akhlaghi, M., Daneshmandi, S., Nicknam, M. H., and Soleimanifar, N. (2011). Association of programmed cell death-1 (PDCD-1) gene polymorphisms with rheumatoid arthritis in Iranian patients. *Clin. Exp. Rheumatol.* 29, 763–767.

Taliani, G., Spaziante, M., Biliotti, E., Borro, M., Palazzo, D., Grieco, S., et al. (2013). IL28B gene polymorphisms and US liver fatty changes in patients who spontaneously cleared hepatitis C virus infection. *PLoS One* 8:e67301. doi: 10.1371/journal.pone.0067301

Tanaka, Y., Nishida, N., Sugiyama, M., Kurosaki, M., Matsuura, K., Sakamoto, N., et al. (2009). Genome-wide association of IL28B with response to pegylated interferon-alpha and ribavirin therapy for chronic hepatitis C. *Nat. Genet.* 41, 1105–1109. doi: 10.1038/ng.449

Tang, W., Chen, S., Chen, Y., Lin, J., Lin, J., Wang, Y., et al. (2017). Programmed death-1 polymorphisms is associated with risk of esophagogastric junction adenocarcinoma in the chinese han population: a case-control study involving 2,740 subjects. *Oncotarget* 8, 39198–39208. doi: 10.18632/oncotarget.17338

Tejeda, C., Broadaway, A. K., Ombrello, M. J., Brown, M. R., Ponder, L. A., Pichavant, M. R., et al. (2017). Case-control association study of autoimmunity associated variants in PDCD1 and juvenile idiopathic arthritis. *Curr. Rheumatol. Rev.* 13, 219–223. doi: 10.2174/1573397113666170104123113

Thomas, E., Gonzalez, V. D., Li, Q., Modi, A. A., Chen, W., Noureddin, M., et al. (2012). HCV infection induces a unique hepatic innate immune response associated with robust production of type III interferons. *Gastroenterology* 142, 978–988. doi: 10.1053/j.gastro.2011.12.055

Wack, A., Terczynska-Dyla, E., and Hartmann, R. (2015). Guarding the frontiers: the biology of type III interferons. *Nat. Immunol.* 16, 802–809. doi: 10.1038/ni.3212

Wang, B. J., Bao, J. J., Wang, J. Z., Wang, Y., Jiang, M., Xing, M. Y., et al. (2011). Immunostaining of PD-1/PD-Ls in liver tissues of patients with hepatitis and hepatocellular carcinoma. *World J. Gastroenterol.* 17, 3322–3329. doi: 10.3748/wjg.v17.i28.3322

Xiao, W., Zhang, Q., Deng, X. Z., Jiang, L. F., Zhu, D. Y., Pei, J. P., et al. (2015). Genetic variations of IL-28B and PD-1 are in association with the susceptibility and outcomes of HCV infection in southeast china. *Infect. Genet. Evol.* 32, 89–96. doi: 10.1016/j.meegid.2015.02.022

Yakut, M., Ozkan, H., Karakaya, F., and Erdal, H. (2018). Diagnostic and prognostic role of serum interleukin-6 in malignant transformation of liver cirrhosis. *Eur. J. Hepatogastroenterol.* 8, 23–30. doi: 10.5005/jp-journals-10018-1253

Zhang, G., Li, N., Li, Z., Zhu, Q., Li, F., Yang, C., et al. (2015). microRNA-4717 differentially interacts with its polymorphic target in the PD1 3' untranslated region: a mechanism for regulating PD-1 expression and function in HBV-associated liver diseases. *Oncotarget* 6, 18933–18944. doi: 10.18632/oncotarget.3662

Zhang, G., Liu, Z., Duan, S., Han, Q., Li, Z., Lv, Y., et al. (2010). Association of polymorphisms of programmed cell death-1 gene with chronic hepatitis B virus infection. *Hum. Immunol.* 71, 1209–1213. doi: 10.1016/j.humimm.2010.08.014

Zhou, J., Wang, Y., Chang, Q., Ma, P., Hu, Y., and Cao, X. (2018). Type III interferons in viral infection and antiviral immunity. *Cell Physiol. Biochem.* 51, 173–185. doi: 10.1159/000495172

Conflict of Interest Statement: The authors declare that the research was conducted in the absence of any commercial or financial relationships that could be construed as a potential conflict of interest.

Copyright © 2019 De Re, Tornesello, De Zorzi, Caggiari, Pezzuto, Leone, Racanelli, Lauletta, Gragnani, Buonadonna, Vaccher, Zignego, Steffan and Buonaguro. This is an open-access article distributed under the terms of the Creative Commons Attribution License (CC BY). The use, distribution or reproduction in other forums is permitted, provided the original author(s) and the copyright owner(s) are credited and that the original publication in this journal is cited, in accordance with accepted academic practice. No use, distribution or reproduction is permitted which does not comply with these terms.

frontiers in Microbiology

ORIGINAL RESEARCH
published: 02 April 2019
doi: 10.3389/fmicb.2019.00636

Elucidating the Host Interactome of EV-A71 2C Reveals Viral Dependency Factors

Ye Li[1†], Xia Jian[1†], Peiqi Yin[1], Guofeng Zhu[2] and Leiliang Zhang[3]*

[1] NHC Key Laboratory of Systems Biology of Pathogens, Institute of Pathogen Biology, Peking Union Medical College, Chinese Academy of Medical Sciences, Beijing, China, [2] National Laboratory of Biomacromolecules, CAS Center for Excellence in Biomacromolecules, and Key Laboratory of RNA Biology, Institute of Biophysics, Chinese Academy of Sciences, Beijing, China, [3] Institute of Basic Medicine, Shandong Academy of Medical Sciences, Jinan, China

Viral protein 2C plays a critical role in EV-A71 replication. The discovery of 2C binding proteins will likely provide potential targets to treat EV-A71 infection. Here, we provide a global proteomic analysis of the human proteins that interact with the EV-A71 2C protein. TRIM4, exportin2, and ARFGAP1 were validated as 2C binding partners. Further functional studies revealed that TRIM4, exportin2, and ARFGAP1 were novel host dependency factors for EV-A71. Moreover, enteroviruses' 2C family proteins interacted with exportin2 and ARFGAP1. In conclusion, our study provides a cellular interactome of the EV-A71 2C and identifies the proviral roles of TRIM4, exportin2, and ARFGAP1 in EV-A71 infection.

Keywords: EV-A71, 2C, TRIM4, exportin2, ARFGAP1

OPEN ACCESS

Edited by:
Ju-Tao Guo,
Baruch S. Blumberg Institute, United States

Reviewed by:
Ping Zhao,
Second Military Medical University, China
Ke Lan,
State Key Laboratory of Virology, Wuhan University, China

****Correspondence:***
Leiliang Zhang
armzhang@hotmail.com

†Co-first authors

Specialty section:
This article was submitted to Virology, a section of the journal Frontiers in Microbiology

Received: *13 July 2018*
Accepted: *13 March 2019*
Published: *02 April 2019*

Citation:
Li Y, Jian X, Yin P, Zhu G and Zhang L (2019) Elucidating the Host Interactome of EV-A71 2C Reveals Viral Dependency Factors. Front. Microbiol. 10:636. doi: 10.3389/fmicb.2019.00636

INTRODUCTION

Enterovirus A71 (EV-A71) is one of the major pathogens that leads to hand, foot and mouth disease (HFMD) in young children and infants, and has become a serious threat to global public health (Baggen et al., 2018). EV-A71 outbreaks have been reported particularly in the Asia-Pacific region over the past 15 years. However, current anti-EV-A71 therapy is limited. Development of effective anti-EV-A71 drugs have been hampered by the lack of a detailed understanding of the virus-host interactions that could represent amenable targets for antiviral therapy.

Enterovirus A71 with a positive-stranded RNA genome belongs to the human enterovirus species A of the genus enterovirus within the family *Picornaviridae* (Baggen et al., 2018). The viral genome encodes a single polyprotein precursor which could be proteolytically cleaved to four structural and seven non-structural proteins. The non-structural protein 2C of EV-A71 with 329 amino acids directs replication complexes to cell membranes and contains NTPase and helicase activities (Yuan et al., 2018). Several host factors associated with 2C have been identified. For instance, EV-A71 2C recruited reticulon3 to the viral replication complex (Tang et al., 2007). Coatomer is required for EV-A71 replication and associates with 2C (Wang et al., 2012). 2C binds IKKβ and protein phosphatase 1 to suppress IKKβ phosphorylation (Zheng et al., 2011; Li et al., 2016). By interacting with RelA, 2C inhibited the NF-kB pathway (Du et al., 2015).

Although 2C plays central roles in EV-A71 replication and counteracting the antiviral host defense, there is limited information on how the interaction of 2C with host proteins may contribute to EV-A71 infection. To fill this knowledge gap and advance our understanding of

2C biology, we applied GST pulldown or GFP-Trap immunoprecipitation methods coupled with mass spectrometry analysis to identify the potential binding partners for 2C. Tripartite Motif Protein 4 (TRIM4), exportin2 and ADP Ribosylation Factor GTPase Activating Protein 1 (ARFGAP1) were validated as 2C interacting proteins. Moreover, we demonstrated that TRIM4, exportin2, and ARFGAP1 were required for EV-A71 replication. Our studies will provide the new strategies for the development of host-based antiviral therapy.

MATERIALS AND METHODS

Cells and Reagents

RD and 293T cells were cultured in Dulbecco's Modified Eagle's Medium (DMEM, Thermo scientific, Waltham, MA, United States) supplemented with 10% fetal bovine serum (FBS), gentamicin, and glutamine. EV-A71 was cultured in RD cells. The EV-A71 virus used in our study is from the Fuyang strain. QS11 was purchased from Sigma-Aldrich (Piscataway, NJ, United States).

Antibodies

Mouse antibodies used in this study are listed: anti-actin (Sigma-Aldrich, Piscataway, NJ, United States, catalog no. A2228), anti-dsRNA J2 (English and Scientific Consulting, Hungary), anti-exportin2 (Santa Cruz Biotechnology, Santa Cruz, CA, United States, catalog no. sc-271537), anti-FLAG (Sigma-Aldrich, Piscataway, NJ, United States, catalog no. A2220), anti-GFP (Xuheyuan, Beijing, China, catalog no. XHY038L), anti-Myc (Cell signaling technology, Danvers, MA, United States, catalog no. 2276), anti-HA (Cell signaling technology, Danvers, MA, United States, catalog no. 3724). Rabbit antibodies used in this study are listed: anti-Myc (Cell signaling technology, Danvers, MA, United States, catalog no. 2278) anti-GFP (Xuheyuan, Beijing, China, catalog no. XHY026L), anti-ARFGAP1 (BETHYL, Montgomery, TX, United States, catalog no. A302-029A), anti-TRIM4 (CUSABIO, Wuhan, China, catalog no. CSB-PA866336LA01HU), anti-exportin2 (Abcam, Cambridge, MA, United States, catalog no. ab151546), anti-2C (generated against a peptide from EV-A71 2C [CRDRKSKVRYSVDTVVSELIREYNNRS] conjugated to keyhole limpet hemocyanin [KLH]). Secondary antibodies are HRP-conjugated ECL goat anti-rabbit IgG (Sigma-Aldrich, St. Louis, MO, United States, catalog No. A6154), HRP-conjugated ECL goat anti-mouse IgG (Jackson ImmunoResearch, West Grove, PA, United States, catalog No. A4416), donkey anti-mouse-Alexa Fluor 555, and donkey anti-rabbit-Alexa Fluor 488 (Invitrogen, Carlsbad, CA, United States).

Plasmids

Constructs encoding for 2C, 2C(126-263), 2C(264-329), ARFGAP1(1-415), ARFGAP1(1-136), and ARFGAP1(137-415) were appended to the carboxyl terminus of glutathione-s-transferase (GST) and were generated using pGEX4T-1 expression plasmids (Amersham Biosciences, Piscataway, NJ, United States). Plasmids expressing TRIM4-Flag and HA-TRIM4 are from Sino Biological (Beijing, China). Plasmid transfected into the cells was performed using FuGENE HD (Promega, Madison, WI, United States) according to the manufacturer instructions.

Immunofluorescence Microscopy

All procedures were performed at room temperature. Cells in glass coverslips were fixed with 4% formaldehyde in PBS buffer for 5 min. Fixed cells were incubated with blocking solution (PBS containing 10% normal donkey serum) for 5 min and were then incubated with primary antibodies diluted in a permeabilized buffer (0.3% Triton X-100 in PBS containing 10% normal donkey serum) for 1 h. The coverslips were washed three times with blocking solution, followed by incubation with Fluor 488 or Alexa Fluor 555 conjugated secondary antibodies for 1 h. After washing with blocking solution three times, the coverslips were mounted with mounting medium. The cells were imaged with a Leica TCS SP5 microscope (Germany) using a 40× oil immersion lens.

Immuno-Precipitation Assays

Briefly, cells were lysed in lysis buffer 1 (1% Triton X-100, 50 mM Tris pH 7.4, 150 mM NaCl, protease inhibitor cocktail) or lysis buffer 2 (1% Triton X-100, 50 mM Tris pH 7.4, 90 mM KCl, 2.5 mM $MgCl_2$, protease inhibitor cocktail) and incubated with protein A/G beads for 30 min at 4°C to reduce non-specific binding affinity. Cell lysates were then incubated with protein A/G beads pre-bound with 1 μg antibody for 1 h at 4°C. Samples were washed three times with washing buffer (50 mM Tris pH 7.4, 150 mM NaCl, 0.1% Triton X-100), and analyzed by Western blotting.

GFP-Trap Assays

Cells were lysed with lysis buffer (50 mM Tris pH = 7.5, 150 mM NaCl, 0.5 mM EDTA, 0.5% NP-40, protease inhibitor cocktail) and cell lysates were incubated with GFP-Trap_A beads (ChromoTek, Planegg-Martinsried, Germany) for 1 h at 4°C. The beads were washed three times with wash buffer (50 mM Tris pH = 7.5, 150 mM NaCl, 0.5 mM EDTA) and analyzed by Western blotting.

GST Pulldown Assay

The expression of the GST fusion protein was induced by 0.5 mM IPTG in *E. coli Rosetta* (DE3) at 37°C for 5 h. Bacteria were lysed with lysis buffer (50 mM Tris pH 6.8, 1 mM EDTA, 100 mM NaCl) and GST fusion proteins were purified using the glutathione-sepharose beads. For the pull-down assay, cell lysates in GST pull-down buffer 1 (1% Triton X-100, 50 mM Tris pH 7.4, 150 mM NaCl, protease inhibitor cocktail) or lysis buffer 2 (1% Triton X-100, 50 mM Tris pH 7.4, 90 mM KCl, 2.5 mM $MgCl_2$, protease inhibitor cocktail) were incubated with GST fusion proteins for 1 h at 4°C. Glutathione beads were then pelleted and washed three times with PBS buffer. Samples were analyzed by Western blotting.

Mass Spectrometry

For mass spectrometry identification, protein complexes pulled down from RD cells were sent to Beijing Protein Innovation. The LC-MS/MS system was composed of a Q Exactive (Thermo scientific, Waltham, MA, United States) mass spectrometer system connected to a Dionex UltiMate 3000. The columns consisted of Thermo 3 μm C18 Acclaim PepMap100 column and Agela Technologies 5 μm C18 Venusil × BPC column. The extract was injected, and the peptides eluted from the column by a 0.1% FA H_2O /0.1% FA acetonitrile gradient. The nanospray ion source was operated at 1.8 kV.

The data was analyzed using Mascot Software v2.3.0 (Matrix Sciences, London, United Kingdom). The peptide masses were compared with the theoretical peptide masses of all proteins from humans using the SWISS-PROT databases with MASCOT search engine software (Matrix Science).

Knockdown by siRNA

The siRNAs were transfected into cells using Lipofectamine™ RNAiMAX Transfection Reagent (Invitrogen, Carlsbad, CA, United States). The siRNAs used for TRIM4, exportin2, ARFGAP1 knockdown were from GenePharma (Shanghai, China) and were as follows: GAAGUUGAGAGUAGAGAUATT (TRIM4 #1), GAGAUUGAACAAAGAAGAATT (TRIM4 #2), GAAGACAGUGUGCCAGAUATT (TRIM4 #3), GCATGGAA TTACAAAGCAAA (exportin2 #1), GACGGUAUCAAAUAU AUUATT (exportin2 #2), GGAACUCAGCGAUGCAAAUTT (exportin2 #3), ACAUUGAGCUUGAGAAGAU (ARFGAP1 #1), and ACAGGAGAAGUACAACAGCAGA (ARFGAP1 #2).

Quantitative PCR (qPCR)

Total cellular and viral RNA was isolated using RNeasy Mini columns (QIAGEN) and reverse transcribed by random priming with the High Capacity cDNA Reverse Transcription Kit (Applied Biosystems; Foster City, CA, United States), then quantitated by qPCR using the DyNAmo HS SYBR Green qPCR Kit (Finnzyme; Espoo, Finland). Sequences of primers used in qPCR were as follows: The forward and reverse primers for EV-A71 were 5′- GCAGCCCAAAAGAACTTCAC-3′ and 5′-ATTTCAGCAGCTTGGAGTGC-3′; the forward and reverse primers for GAPDH were 5′-ACCTTCCCCATGGTGTCTG A-3′ and 5′-GCTCCTCCTGTTCGACAGTCA-3′; the forward and reverse primers for exportin2 were 5′- CGCACCGTTT GTTGAGATTC-3′ and 5′-TGATGAGAGTAGGGATGTAGG G-3′; the forward and reverse primers for TRIM4 were 5′-ATGCTAAAGCGATTCCAAGTG-3′ and 5′-CAAGAAC TGGCTGATGCTGTAT-3′; the forward and reverse primers for ARFGAP1 were 5′- GCGCATCCTCATTGCAG-3′ and 5′-CTTCCTGGTTCTTGGGCTG-3′.

Virus Entry Assay

The EV-A71 virus entry was measured as previously described (Xu et al., 2016). Briefly, RD cells were washed with cold PBS, followed by incubation with viruses on ice. Cells were then incubated with viruses for 30 min on ice. The cells were washed with cold PBS and then incubated at 37°C for 1 h to allow virus entry before being treated with trypsin to remove any viruses that bound to the cell surface. Total RNA was isolated, and the levels of viral RNA were determined by qPCR.

Plaque Assay

Virus titers were measured through a plaque assay. RD cells were seeded into 6-well plates. The EV-A71 virus was diluted with 10-fold serial dilutions and then incubated with RD cells for 2 h at 37°C. The cells were overlaid with DMEM (10% FBS) containing 1% agarose. Three days later, the cells were stained with Crystal violet and the viral plaques were counted.

Cell Viability Assay

Cell viability was assessed using the Cell Titer-Glo Luminescent Cell Viability Assay Kit (Promega, Madison, WI, United States) according to the manufacturer's protocol.

Statistics

Statistically significant differences were assessed using the paired Student's *t*-test from GraphPad Prism 5 (GraphPad Software Inc., La Jolla, CA, United States). Data represent the averages from at least three independent experiments ± (standard deviation) SD, unless stated otherwise. ns, no significance; $^{*}P < 0.05$; $^{**}P < 0.001$; $^{***}P < 0.0001$.

RESULTS

Identification of 2C Interacting Proteins

To elucidate the interactome of EV-A71 2C, we performed GST pull-down coupled with mass spectrometry. Constructs encoding for GST-2C, GST-2C(1-125), GST-2C(126-263), or GST-2C(264-329) were appended to the carboxyl terminus of GST and were generated using pGEX4T-1 expression plasmids. GST-2C(1-125) was not soluble in the bacteria and thus was removed from the study. The GST fusion protein or GST was accumulated onto glutathione beads and incubated with cell lysates for pull-down assay. We also applied the GFP-Trap to precipitate GFP-2C or GFP associated proteins. For mass spectrometry identification, the protein complexes pulled down were sent to Beijing Protein Innovation. To analyze the mass spectrometry results, we excluded the proteins that showed up in the control GST or the control GFP-Trap condition. We identified 74 hits for GST-2C (**Supplementary Table 1**), 39 hits for GST-2C(126-263) (**Supplementary Table 2**), 24 hits for GST-2C(264-329) (**Supplementary Table 3**), and 504 hits for GFP-2C (**Supplementary Table 4**). The top ten biological processes in the Gene Ontology (GO)-term analysis of GST-2C binding partners is shown in **Figure 1A**. The top ten biological processes in the GO-term analysis of GFP-2C binding partners are shown in **Figure 1B**. There are 27 overlapped hits for GST-2C and GFP-2C (**Figure 1C**), 15 overlapped binding proteins for GST-2C and GST-2C(126-263) (**Figure 1D**), and eight overlapped binding proteins for GST-2C and GST-2C(264-329) (**Figure 1E**). In the overlapped binding proteins, most were transcription factors, protein chaperons, ribosomal proteins, or histones, which were sticky. Thus, we picked up TRIM4 and exportin2 to investigate

A

Biological Process (GO)			
pathway ID	*pathway description*	*count in gene set*	*false discovery rate*
GO:0006886	intracellular protein transport	16	1.38e-05
GO:0032482	Rab protein signal transduction	7	3.44e-05
GO:0006414	translational elongation	9	7.37e-05
GO:0034613	cellular protein localization	17	0.000208
GO:0046907	intracellular transport	18	0.00021
GO:0015031	protein transport	17	0.000414
GO:1902580	single-organism cellular localization	14	0.000643
GO:0051649	establishment of localization in cell	19	0.0019
GO:0019058	viral life cycle	8	0.00212
GO:0000184	nuclear-transcribed mRNA catabolic process, nonsense-mediated decay	6	0.00213

B

Biological Process (GO)			
pathway ID	*pathway description*	*count in gene set*	*false discovery rate*
GO:0006613	cotranslational protein targeting to membrane	57	3.36e-65
GO:0006614	SRP-dependent cotranslational protein targeting to membrane	56	1.3e-64
GO:0072599	establishment of protein localization to endoplasmic reticulum	57	1.78e-64
GO:0045047	protein targeting to ER	56	5.4e-64
GO:0070972	protein localization to endoplasmic reticulum	58	2.12e-61
GO:0006612	protein targeting to membrane	59	1.52e-56
GO:0072594	establishment of protein localization to organelle	73	4.78e-53
GO:0000184	nuclear-transcribed mRNA catabolic process, nonsense-mediated decay	50	2.48e-52
GO:0090150	establishment of protein localization to membrane	64	3.4e-52
GO:0006886	intracellular protein transport	94	1e-51

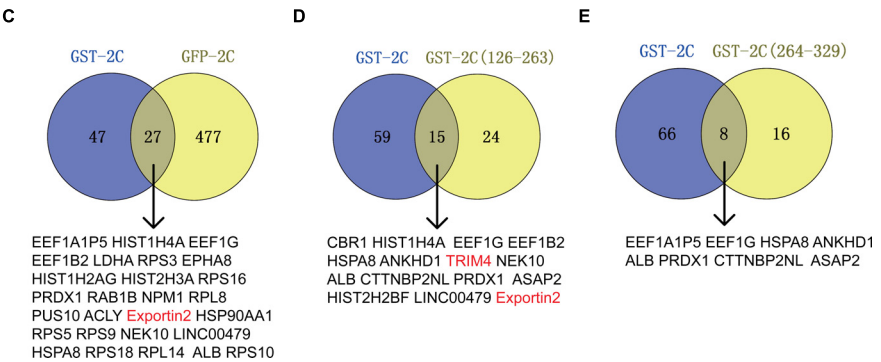

FIGURE 1 | Host interactome analysis of the EV-A71 2C protein. **(A)** Gene Ontology (GO)-term analysis of potential binding partners for GST-2C. **(B)** GO-term analysis of potential binding partners for GFP-2C. **(C)** Venn diagram showing the overlap of potential binding partners for GST-2C and GFP-2C. **(D)** Venn diagram showing the overlap of potential binding partners for GST-2C and GST-2C(126-263). **(E)** Venn diagram showing the overlap of potential binding partners for GST-2C and GST-2C(264-329).

their role in the viral life cycle. Key components of COPI including coatomer and ARF1 have been identified as host factors for EV-A71 (Wang et al., 2014), thus we also chose another COPI component ARFGAP1, from the hit for GFP-2C, for further study.

Confirmation of the Interaction Between TRIM4 and 2C

To validate the interaction between TRIM4 and 2C, 293T cells were transiently transfected with constructs expressing Flag-tagged TRIM4 or HA-tagged TRIM4. Cell lysates were incubated with Glutathione-Sepharose beads containing GST or GST-2C. We found that GST-2C but not GST was able to pull down TRIM4 (**Figures 2A,B**).

To further confirm the interaction between TRIM4 and 2C, 293T cells were transiently transfected with constructs expressing Flag-tagged TRIM4 and Myc-tagged 2C. As shown in **Figure 2C**, mouse Myc antibody but not control mouse IgG was able to precipitate TRIM4. To validate the interaction between TRIM4 and 2C during virus infection, lysates from RD cells infected with EV-A71 were incubated with rabbit TRIM4 antibody or control rabbit IgG. As shown in **Figure 2D**, TRIM4 associated with 2C during EV-A71 infection.

The specific interaction of EV-A71 2C with TRIM4 prompted us to examine whether these proteins colocalized by immunofluorescence microscopy. First, 293T cells transfected constructs expressing GFP-2C and TRIM4-Flag were subjected to immunofluorescence staining, using rabbit anti-Flag antibody. As shown in **Figure 2E**, TRIM4 colocalized with the EV-A71 2C protein. Next, 293T cells transfected constructs expressing GFP-2C were subjected to immunofluorescence staining, using rabbit anti-TRIM4 antibody. Endogenous TRIM4 were also colocalized with GFP-2C (**Figure 2F**).

The Roles of TRIM4 in EV-A71 Replication

To access the role of TRIM4 in the EV-A71 life cycle, we applied a siRNA strategy to silence TRIM4. The EV-A71 2C and VP1 proteins were reduced when TRIM4 was knocked down by two siRNA 3 days before EV-A71 infection

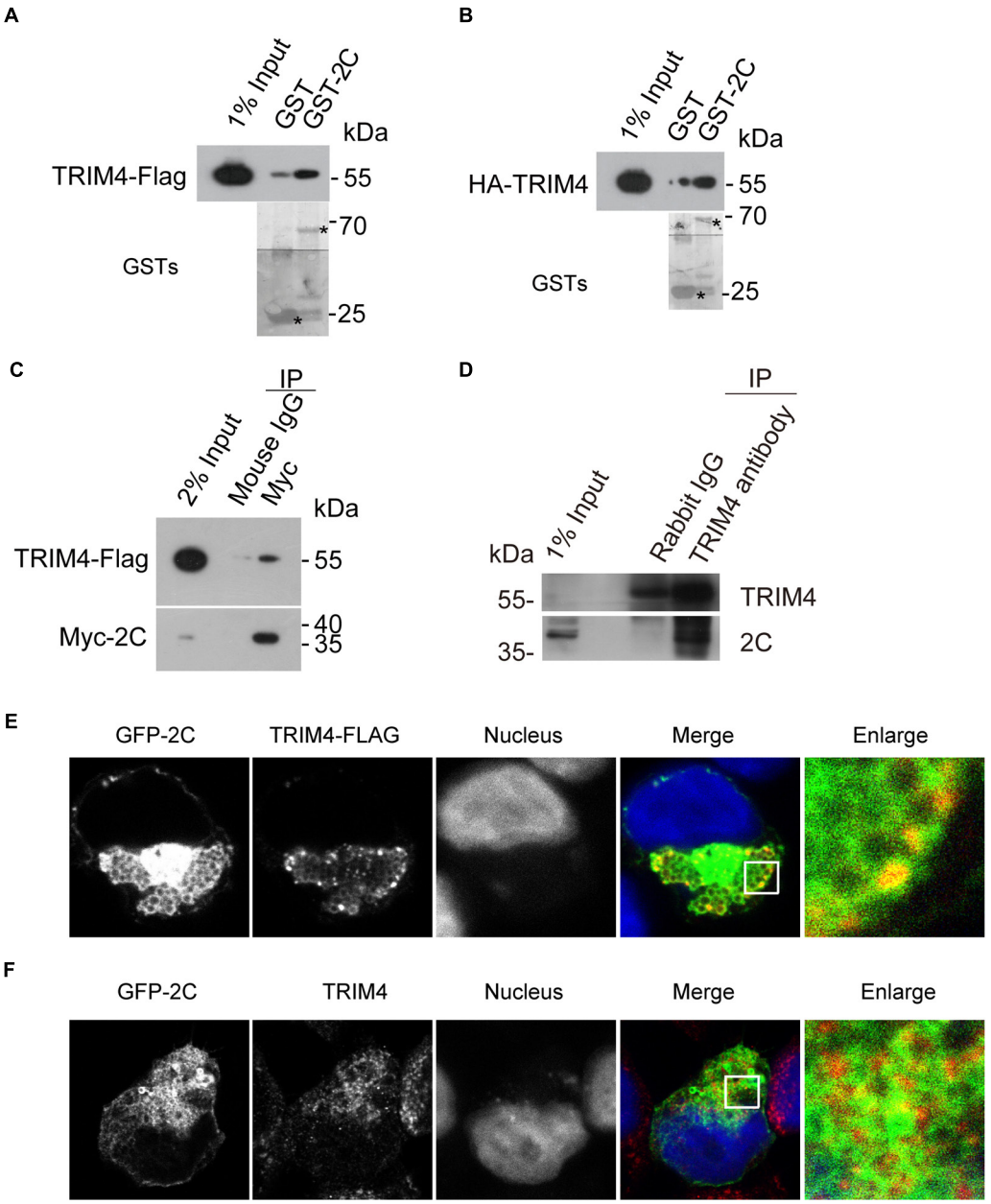

FIGURE 2 | Validation of the interaction between TRIM4 and 2C. **(A)** Validation of the interaction between the GST-2C and TRIM4-Flag. Cell lysates from 293T cells transfected with the plasmid expressing TRIM4-Flag were pulled down by GST–2C or GST followed by Western blotting. * indicated GST or GST fustion proteins. **(B)** Validation of the interaction between the GST-2C and HA-TRIM4. Cell lysates from 293T cells transfected with the plasmid expressing HA-TRIM4 were pulled down by GST–2C or GST followed by Western blotting. * indicated GST or GST fustion proteins. **(C)** Immunoblots showing the association of 2C with TRIM4 in transfected 293T cells by a co-immunoprecipitation assay. 293T cells were transfected with TRIM4-Flag and Myc-2C for 48 h. Cell lysates were incubated with mouse anti-Flag antibody or mouse IgG, and co-immunoprecipitated proteins were subjected to Western blotting for analysis. **(D)** Validation of the interaction between the 2C and TRIM4 during EV-A71 replication. Cell lysates from RD cells infected with EV-A71 were immunoprecipitated by rabbit TRIM4 antibody or control rabbit IgG followed by Western blotting. **(E)** Colocalization of GFP-2C with TRIM4-Flag in 293T cells. 293T cells transfected with GFP-2C and TRIM4-Flag were fixed by PFA and immunofluorescently labeled for Flag. DAPI staining indicates the nucleus (blue). **(F)** Colocalization of GFP-2C with TRIM4 in 293T cells. 293T cells transfected with GFP-2C were fixed by PFA and immunofluorescently labeled for TRIM4. DAPI staining indicates the nucleus (blue).

(**Figure 3A**). TRIM4 depletion also reduced EV-A71 viral RNA replication assessed by QPCR (**Figure 3B**). However, silencing TRIM4 did not change virus entry (**Figure 3C**). Furthermore, the EV-A71 virus titer was reduced by siRNA against TRIM4 (**Figure 3D**). Altogether, TRIM4 is required for EV-A71 replication.

Next, we examined the localization of TRIM4 in EV-A71 infected cells. As shown in **Figure 3E**, TRIM4 colocalized with

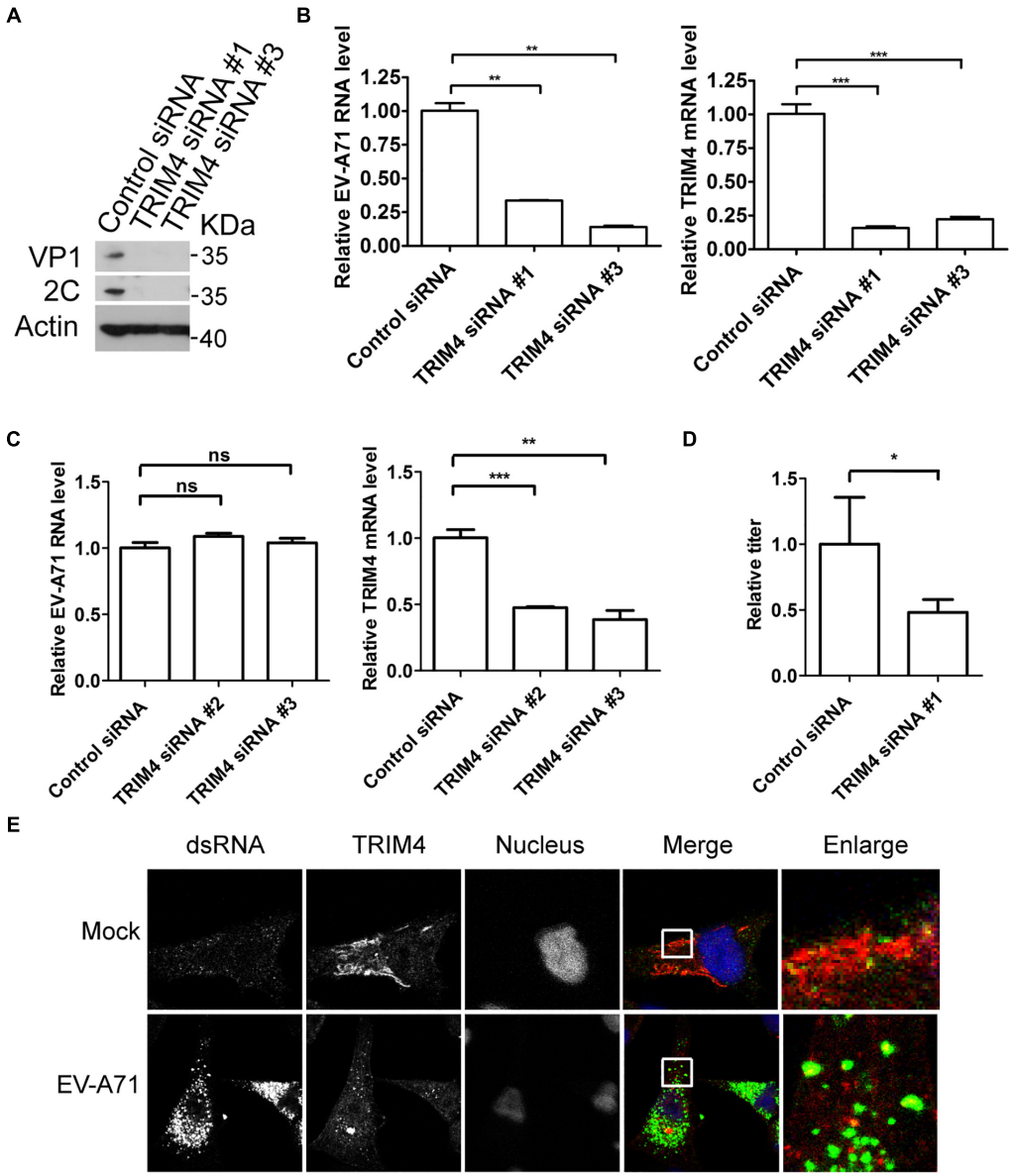

FIGURE 3 | TRIM4 is required for EV-A71 replication. **(A)** RD cells were treated with siRNA targeting TRIM4 or control siRNA for 72 h and infected with EV-A71 (MOI = 1) for another 8 h. The cell lysates were analyzed by immunoblotting with the indicated antibodies. **(B)** RD cells were treated with siRNAs targeting TRIM4 or control siRNA for 72 h and then infected with EV-A71 (MOI = 1) for 6 h. Relative levels of EV-A71 RNA and TRIM4 mRNA were quantified by qPCR and normalized to GAPDH mRNA. Data represent the averages from at least three independent experiments ± SD. **, $P < 0.001$; ***, $P < 0.0001$. **(C)** RD cells were treated with siRNA targeting TRIM4 or control siRNA for 72 h. Cells were then incubated with viruses for 30 min on ice. The cells were washed with cold PBS and then incubated at 37°C for 1 h to allow virus entry before treated with trypsin to remove any viruses that bound to cell surface. ns, no significance; **, $P < 0.001$; ***, $P < 0.0001$. **(D)** RD cells were treated with siRNA targeting TRIM4 or control siRNA for 72 h and infected with EV-A71 (MOI = 1) for another 20 h. Virus from the supernatant was tittered. *, $P < 0.05$. **(E)** RD cells were infected with EV-A71 (MOI = 1) or mock infected for 8 h and then stained with antibodies against dsRNA and TRIM4. DAPI staining indicates the nucleus (blue).

viral dsRNA, indicating that TRIM4 might be involved in viral replication.

Confirmation of the Interaction Between Exportin2 and 2C

To validate the interaction between exportin2 and 2C, lysates from 293T cells were incubated with GST and GST-2C. GST-2C but not GST was able to pull down exportin2 (**Figure 4A**). To map the region in 2C for the association with exportin2, 293T cell lysates were incubated with GST, GST-2C(126-263), and GST-2C(264-329). As shown in **Figure 4B**, GST-2C(126-263) but not GST-2C(264-329) was able to interact with exportin2.

Next, we accessed whether 2C-exportin2 interaction is conserved in enteroviruses. Constructs encoding the GFP tagged

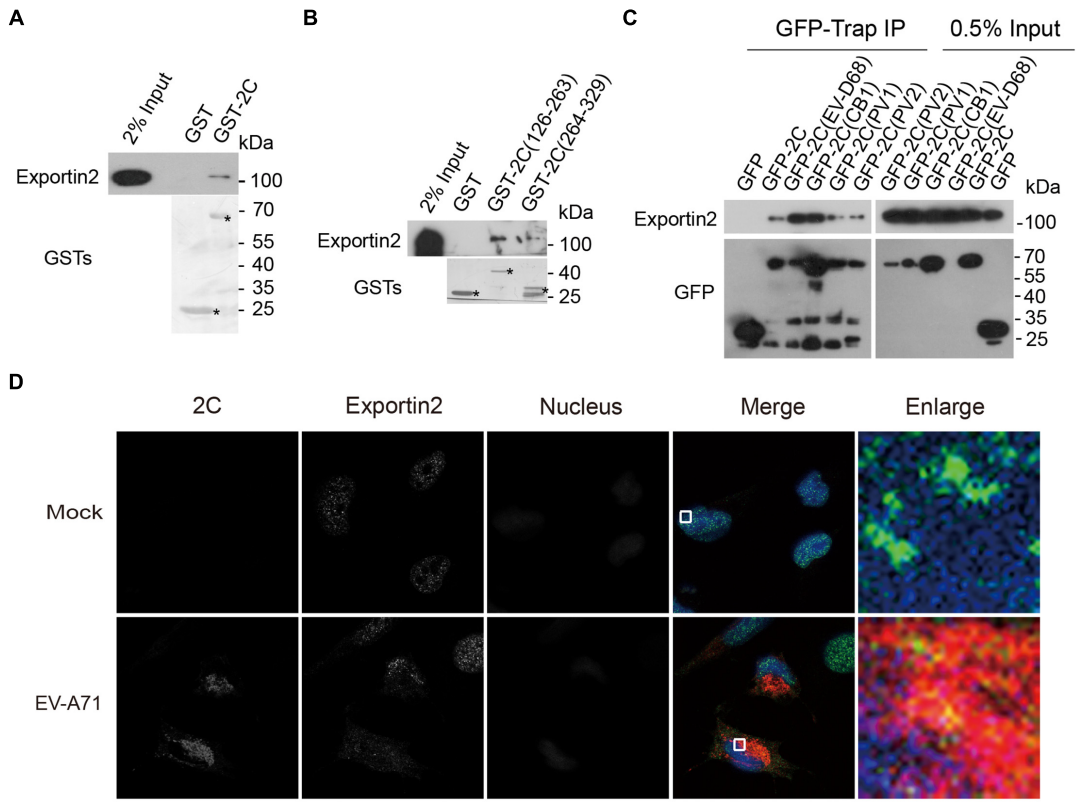

FIGURE 4 | Validation of the interaction between exportin2 and 2C. **(A)** Validation of the interaction between the GST-2C and exportin2. Cell lysates from 293T cells were pulled down by GST-2C or GST followed by Western blotting. * indicated GST or GST fustion proteins. **(B)** Identification of the interaction between the GST-2C(126-263) and exportin2. Cell lysates from 293T cells were pulled down by GST-2C(126-263), GST-2C(264-329), or GST followed by Western blotting. * indicated GST or GST fustion proteins. **(C)** 293T cells were transfected with constructs encoding GFP tagged 2C proteins from PV1, PV2, CB1, EV-D68, or EV-A71 and then immunoprecipitated with GFP-Trap. Samples were analyzed with Western blotting. **(D)** Colocalization of 2C with exportin2 in RD cells. RD cells were infected with EV-A71 (MOI = 1) or mock infected for 8 h and then stained with antibodies against 2C and exportin2. DAPI staining indicates the nucleus (blue).

2C proteins from poliovirus type I (PV1), poliovirus type II (PV2), coxsackievirus B1 (CB1), enterovirus D68 (EV-D68), and EV-A71 were transfected into 293T cells. We performed the GFP-Trap experiment to investigate whether enteroviruses' 2C proteins could bind exportin2. All enteroviruses' 2C proteins we tested were able to interact with exportin2 (**Figure 4C**), suggesting that those interactions are conserved across enteroviruses. Next, we examined whether 2C and exportin2 colocalized by immunofluorescence microscopy. RD cells infected with EV-A71 (MOI = 1) or mock infected for 8 h were subjected to immunofluorescence staining using rabbit anti-2C antibody and mouse anti-exportin2 antibody. As shown in **Figure 4D**, endogenous exportin2 colocalized with 2C in EV-A71-infected cells, indicating that exportin2 could associate with 2C in the same intracellular area.

The Roles of Exportin2 in EV-A71 Replication

To access the potential role of exportin2 in the EV-A71 life cycle, we applied the siRNA strategy to silencing exportin2. The EV-A71 VP1 protein was decreased when exportin2 was knocked down by three siRNA 3 days before EV-A71 infection (**Figure 5A**). Exportin2 depletion also reduced EV-A71 viral RNA replication assessed by QPCR (**Figure 5B**). Interestingly, silencing exportin2 increased virus entry (**Figure 5C**). Moreover, the EV-A71 virus titer was reduced by siRNA against exportin2 (**Figure 5D**). Altogether, exportin2 is a host dependency factor for EV-A71.

Next, we examined the localization of exportin2 in EV-A71 infected cells. As shown in **Figure 5E**, exportin2 partially colocalized with viral dsRNA, indicating that exportin2 might be involved in viral replication.

Validation of the Interaction Between ARFGAP1 and 2C

To validate the interaction between ARFGAP1 and 2C, lysates from 293T cells were incubated with GST and GST-2C. GST-2C but not GST was able to pull down ARFGAP1 (**Figure 6A**). To identify the critical region of ARFGAP1 for association with 2C, lysates from 293T cells transfected with constructs expressing GFP-2C were incubated with GST, GST-ARFGAP1(1-136), or GST-ARFGAP1(137-415). GST-ARFGAP1(1-136) but not GST-ARFGAP1(137-415) was able to pull down ARFGAP1 (**Figure 6B**). To identify the critical region of 2C for association

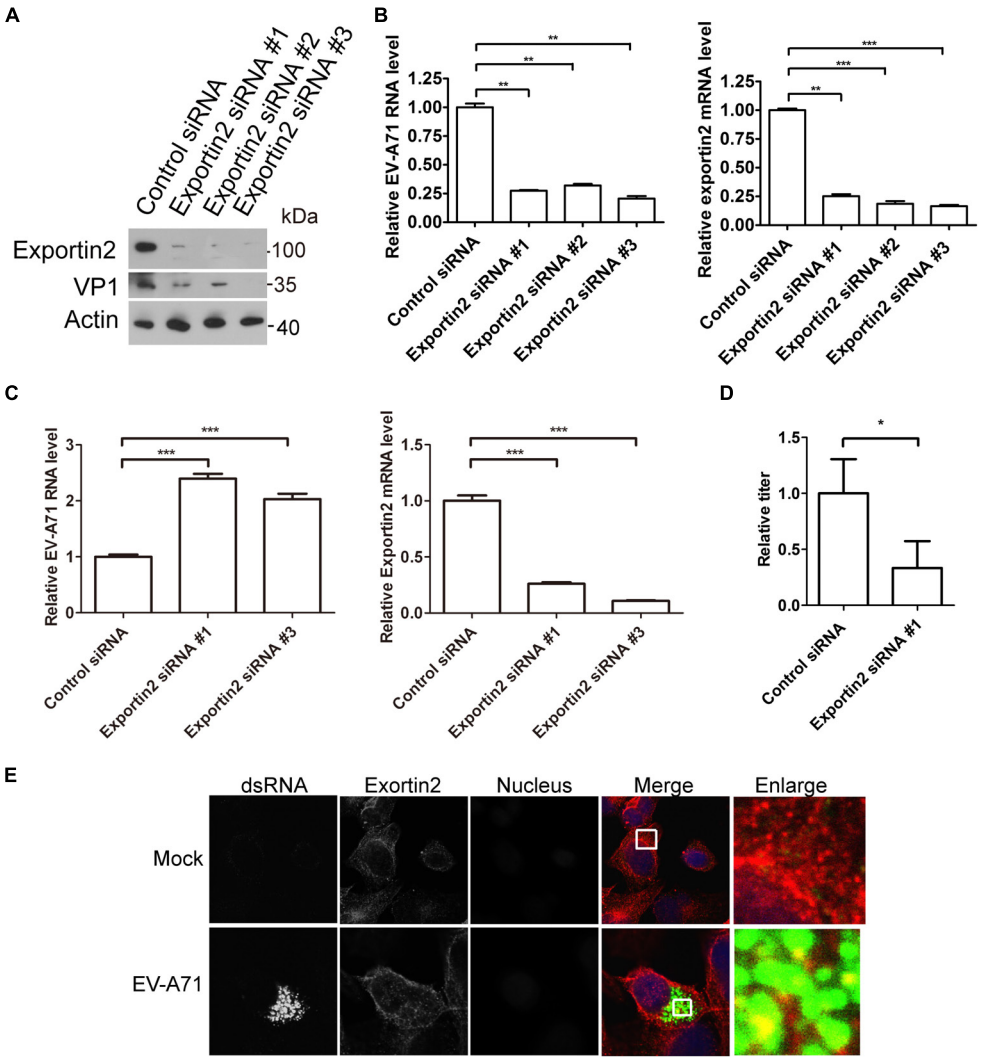

FIGURE 5 | Exportin2 is required for EV-A71 replication. **(A)** RD cells were treated with siRNA targeting exportin2 or control siRNA for 72 h and infected with EV-A71 (MOI = 1) for another 8 h. The cell lysates were analyzed by immunoblotting with the indicated antibodies. **(B)** RD cells were treated with siRNAs targeting exportin2 or control siRNA for 72 h and then infected with EV-A71 (MOI = 1) for 6 h. Relative levels of EV-A71 RNA and exportin2 mRNA were quantified by qPCR and normalized to GAPDH mRNA. Data represent the averages from at least three independent experiments ± SD. **, $P < 0.001$; ***, $P < 0.0001$. **(C)** RD cells were treated with siRNA targeting exportin2 or control siRNA for 72 h. Cells were then incubated with viruses for 30 min on ice. The cells were washed with cold PBS and then incubated at 37°C for 1 h to allow virus entry before treated with trypsin to remove any viruses that bound to cell surface. ***, $P < 0.0001$. **(D)** RD cells were treated with siRNA targeting exportin2 or control siRNA for 72 h and infected with EV-A71 (MOI = 1) for another 20 h. Virus from the supernatant was tittered. *, $P < 0.05$. **(E)** RD cells were infected with EV-A71 (MOI = 1) or mock infected for 8 h and then stained with antibodies against dsRNA and exportin2. DAPI staining indicates the nucleus (blue).

with ARFGAP1, 293T cells were transiently transfected with constructs expressing GFP-tagged 2C(1-125), 2C(126-263), or 2C(264-329). Lysates were incubated with GST, GST-ARFGAP1(1-136). 2C(264-329) but not 2C(1-125) nor 2C(126-263) was able to pull down ARFGAP1(1-136) (**Figure 6C**). To further confirm the interaction between ARFGAP1 and 2C(264-329), lysates from RD cells were incubated with GST, GST-2C(126-263), or GST-2C(264-329). GST-2C(264-329) but not GST-2C(126-263) was able to pull down ARFGAP1 (**Figure 6D**).

Next, we investigated whether 2C-ARFGAP1 interaction is conserved in enteroviruses. Constructs encoding GFP tagged 2C proteins from PV1, PV2, CB1, EV-D68, and EV-A71 were transfected into 293T cells. We performed the GST pull-down experiment to investigate whether enteroviruses' 2C proteins were able to bind ARFGAP1. All enteroviruses' 2C proteins in our study associated with ARFGAP1 (**Figures 6E–H**), indicating that 2C-ARFGAP1 interaction is conserved across enteroviruses.

To confirm the interaction between ARFGAP1 and 2C during viral replication, lysates from RD cells infected with EV-A71 were immunoprecipitated by rabbit ARFGAP antibody or control rabbit IgG. As shown in **Figure 6I**, 2C associated with ARFGAP1 during EV-A71 infection.

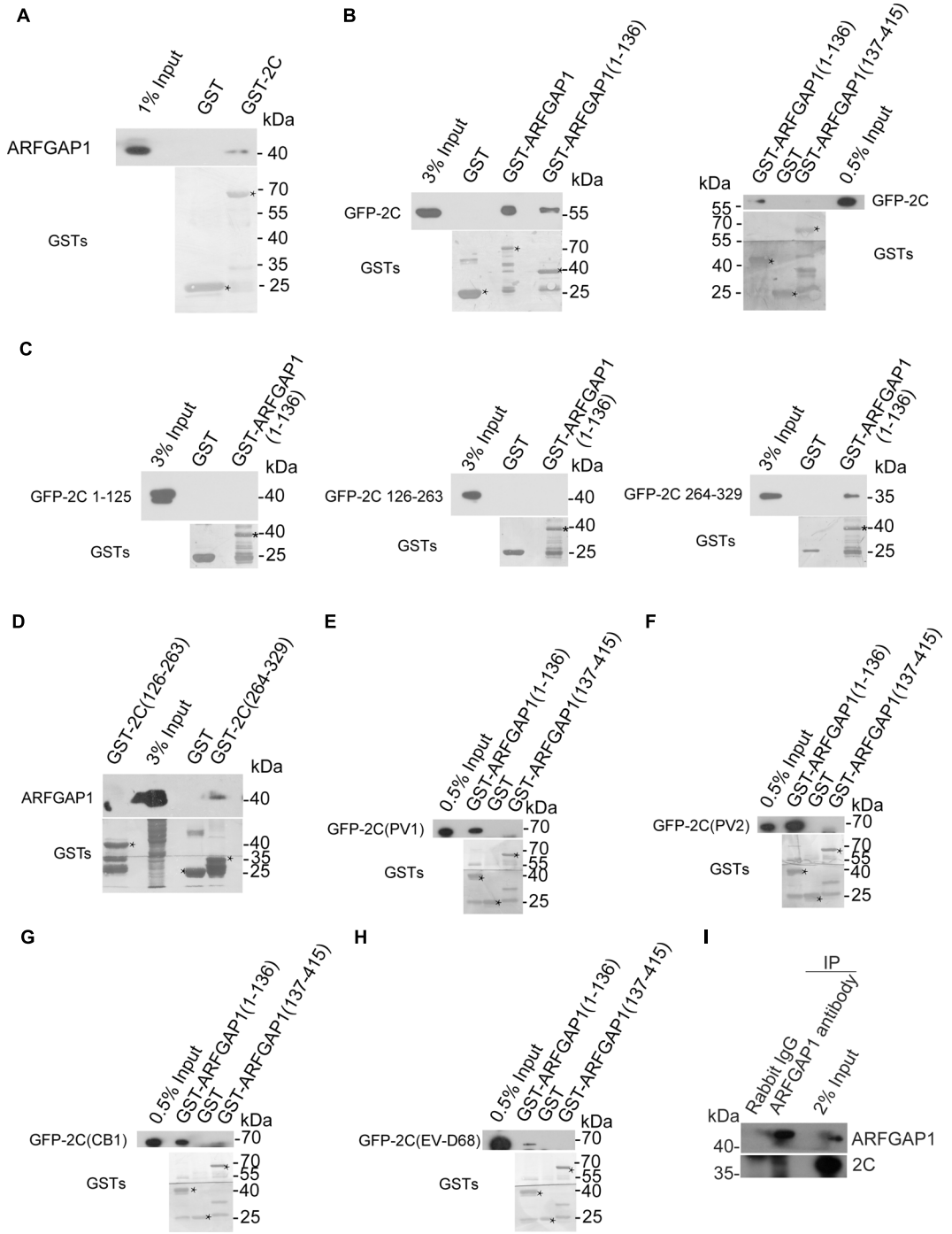

FIGURE 6 | Validation of the interaction between ARFGAP1 and 2C. **(A)** Validation of the interaction between the GST-2C and ARFGAP1. Cell lysates from 293T cells were pulled down by GST–2C or GST followed by Western blotting. * indicated GST or GST fustion proteins. **(B)** Identification of the interaction between the GFP-2C and GST-ARFGAP1(1-136). Cell lysates from 293T cells transfected with GFP-2C were pulled down by GST-ARFGAP1(1-136), GST-ARFGAP1(137-415), or GST followed by Western blotting. * indicated GST or GST fustion proteins. **(C)** Identification of the interaction between the GST-2C(264-329) and GST-ARFGAP1(1-136). Cell lysates from 293T cells transfected with GFP-2C(1-125), GFP-2C(126-263), or GFP-2C(264-329) were pulled down by GST-ARFGAP1(1-136) or GST followed by Western blotting. * indicated GST or GST fustion proteins. **(D)** Confirmation of the interaction between the GST-2C(264-329) and ARFGAP1(1-136). Cell lysates from 293T cells were pulled down by GST-2C(126-263), GST-2C(264-329), or GST followed by Western blotting. **(E–H)** Constructs encoding GFP tagged 2C proteins from PV1 **(E)**, PV2 **(F)**, CB1 **(G)**, and EV-D68 **(H)** were transfected into 293T cells. Cell lysates were pulled down by GST-ARFGAP1(1-136), GST-ARFGAP1(137-415), or GST followed by Western blotting. * indicated GST or GST fustion proteins. **(I)** Validation of the interaction between the 2C and ARFGAP1 during EV-A71 replication. Cell lysates from RD cells infected with EV-A71 were immunoprecipitated by rabbit ARFGAP1 antibody or control rabbit IgG followed by Western blotting.

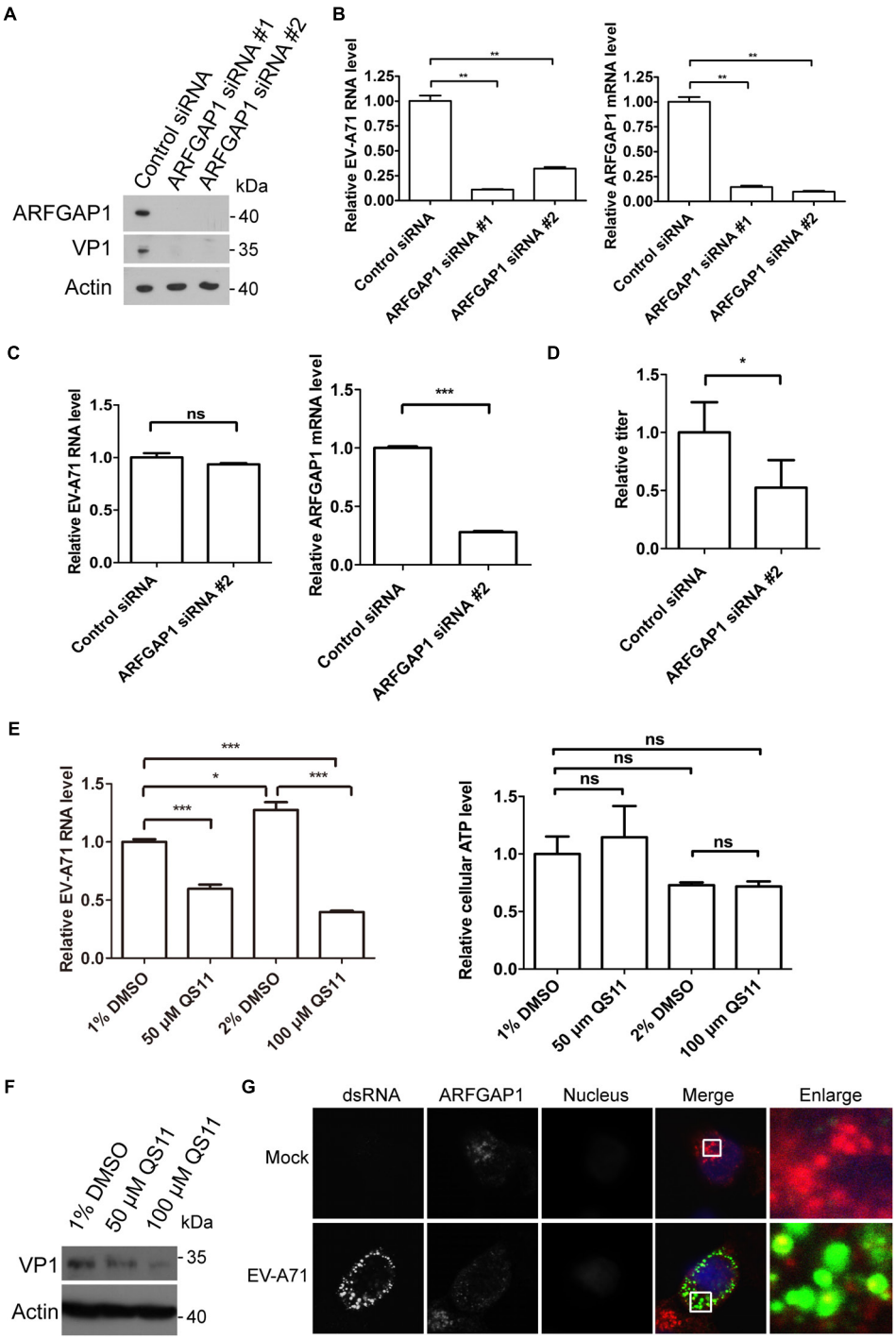

FIGURE 7 | ARFGAP1 is required for EV-A71 replication. **(A)** RD cells were treated with siRNA targeting ARFGAP1 or control siRNA for 72 h and infected with EV-A71 (MOI = 1) for another 8 h. The cell lysates were analyzed by immunoblotting with the indicated antibodies. **(B)** RD cells were treated with siRNAs targeting ARFGAP1 or control siRNA for 72 h and then infected with EV-A71 (MOI = 1) for 6 h. Relative levels of EV-A71 RNA and ARFGAP1 mRNA were quantified by qPCR and normalized to GAPDH mRNA. Data represent the averages from at least three independent experiments ± SD. **, $P < 0.001$. **(C)** RD cells were treated with siRNA targeting ARFGAP1 or control siRNA for 72 h. Cells were then incubated with viruses for 30 min on ice. The cells were washed with cold PBS and then incubated at 37°C for 1 h to allow virus entry before treated with trypsin to remove any viruses that bound to cell surface. ns, no significance; ***, $P < 0.0001$. **(D)** RD cells were treated with siRNA targeting ARFGAP1 or control siRNA for 72 h and infected with EV-A71 (MOI = 1) for another 20 h. Virus from the supernatant was tittered. *, $P < 0.05$. **(E)** RD cells were infected with EV-A71 (MOI = 1) for 1 h and then treated with QS11 or DMSO for 5 h. Total RNA was isolated, and the levels of viral RNA were determined by qPCR. The cell viability was measured by cellular ATP level. ns, no significance; *, $P < 0.01$; ***, $P < 0.0001$. **(F)** RD cells were infected with EV-A71 (MOI = 1) for 1 h and then treated with QS11 or DMSO for 7 h. The cell lysates were analyzed by immunoblotting with the indicated antibodies. **(G)** RD cells were infected with EV-A71 (MOI = 1) or mock infected for 8 h and then stained with mouse dsRNA antibody and rabbit ARFGAP1 antibody. DAPI staining indicates the nucleus (blue).

The Roles of ARFGAP1 in EV-A71 Replication

To access the role of ARFGAP1 in the EV-A71 life cycle, we applied the siRNA strategy to silencing ARFGAP1 and used QS11 (an inhibitor of ARFGAP1) to disrupt COPI. The EV-A71 VP1 protein was decreased when ARFGAP1 was knocked down by two siRNA 3 days before EV-A71 infection (**Figure 7A**). ARFGAP1 depletion also reduced EV-A71 viral RNA replication assessed by QPCR (**Figure 7B**). However, silencing ARFGAP1 did not change the virus entry (**Figure 7C**). Furthermore, the EV-A71 virus titer was reduced by siRNA against ARFGAP1 (**Figure 7D**). Consistent with the proviral role of COPI in EV-A71 replication (Wang et al., 2012), we found that QS11 reduced EV-A71 replication while the cell viability was not changed by QS11 (**Figures 7E,F**). Altogether, ARFGAP1 promoted EV-A71 replication.

Next, we examined the localization of ARFGAP1 in EV-A71 infected RD cells. As shown in **Figure 7G**, ARFGAP1 partially colocalized with viral dsRNA, further indicating that ARFGAP1 might promote viral replication.

DISCUSSION

EV-A71 replication relies on many host factors (Shih et al., 2011). Identifying novel viral host factors will help us better understand EV-A71 biology. In the present study, we applied GST pull-down or GFP-Trap immunoprecipitation coupled with mass spectrometry to identify the cellular interactome of EV-A71. Similar strategies have been applied to identify the host interactomes for other viruses (Gao et al., 2017; Hafirassou et al., 2017; Li et al., 2017; Coyaud et al., 2018; Wang et al., 2018). We demonstrated that the EV-A71 2C protein interacted with TRIM4, exportin2, and ARFGAP1. TRIM4, exportin2, and ARFGAP1 are required for EV-A71 replication. Moreover, exportin2 and ARFGAP1 also interact with 2C proteins encoded by other enteroviruses. Further characterization of the other hits identified in this study may be beneficial for a better understanding of the biology of EV-A71 and 2C.

We have previously performed yeast 2 hybrid unbiased screenings to identify 2C binding partners, and several important regulators including p65 have been identified (Du et al., 2015). Others have identified more 2C-associated host proteins including reticulon3, coatomer, IKKβ and protein phosphatase 1 (Tang et al., 2007; Zheng et al., 2011; Wang et al., 2012; Li et al., 2016). Three 2C-associated host proteins (hnRNPK, COPB2, and PKM) were on the list of our MS SPEC results, indicating the validity of our screen. Some of the previously identified factors (reticulon3, p65, protein phosphatase 1) were not on our screening list and we identified several novel 2C associate factors, including TRIM4, exportin2, and ARFGAP1. The differences can be explained by the specific features of the individual screening methods. The design of this study is the use of the GST fusion protein or GFP-2C coupled with MS SPEC. This may help identify transcription related factors, which are normally excluded in the Y2H screen.

In this study, we found that TRIM4 is required for EV-A71 replication. As a member of the TRIM family, TRIM4 contains 500 amino acids, including three zinc-binding domains, one RING-finger domain, one type 1 B-box, one type 2 B-box and one coiled-coil domain. TRIM4 is localized in the cytoplasmic body and is widely expressed in many tissues and cells, but its function is poorly understood (Tomar et al., 2015). Recently, studies have shown that TRIM4 can regulate the K63 ubiquitination of the Retinoic Acid-Inducible Gene 1 Protein (RIG-I) and the assembly of mitochondrial antiviral signal complexes (Yan et al., 2014). Other studies have shown that TRIM4 plays a role in the regulation of oxidative stress induced cell death by interacting with peroxiredoxin 1 (PRX1) (Tomar et al., 2015). Upon EV-A71 infection, TRIM4 localized with viral dsRNA. TRIM4 might be involved in EV-A71 replication organelle formation by association with 2C. The other possibility is that TRIM4 regulates mitochondrial ROS generation (Tomar et al., 2015), which is critical for EV71 infection. Future studies need to be done to dissect the detailed mechanism of how TRIM4 promotes EV-A71 replication.

Some proteins with nuclear localization sequences need cofactors to transport to the nucleus, and importin α/β heterodimers play an important role in this process (Goldfarb et al., 2004; Kimura and Imamoto, 2014). Importin α binds to nuclear localization sequences, while importin β regulates transport through nuclear pore complexes. When proteins are transported to the nucleus, they are widely distributed in the nucleus, whereas RanGTP binds to importin β and replaces importin α. Importin α must return to the cytoplasm, and the protein that binds to it remains in the nucleus to complete the transport process. The transport of importin α from nucleus to cytoplasm is regulated by exportin2, also named the chromosome segregation 1-like protein (CSE1L) and the cellular apoptosis susceptibility protein (CAS) (Behrens et al., 2003). Only in the presence of RanGTP can exportin2 bind tightly with importin α to form an importin α/exportin2/RanGTP complex (Tanaka et al., 2007; Jiang, 2016). Importin α is released in the cytoplasm and interacts with RanBP1 and RanGAP1. The identification of exportin2 as a positive regulator for EV-A71 replication is interesting. Exportin2 is a multi-functional protein that plays a role in apoptosis, chromosome assembly during mitosis, cellular proliferation, microvesicles formation, and nucleocytoplasmic transport (Bera et al., 2001; Tanaka et al., 2007; Jiang, 2016). Exportin2 shuttles the importins from the nucleus to the cytoplasm, where importins deliver transcription factors to the nucleus (Stewart, 2007). We speculated that exportin2 possibly functions by facilitating the nuclear import of certain transcription factors transcribing the proviral host factors for EV-A71.

In eukaryotic cells, the transport of intracellular cargo is mainly accomplished by coated vesicles, such as COPI, COPII and the clathrin vesicle. COPI coat, which mediates vesicle transport from Golgi to endoplasmic reticulum (ER), is composed of coatomer, its accessory proteins and cargoes (Hsu and Yang, 2009). The accessory proteins in COPI are

ADP Ribosylation Factor 1 (ARF1), Golgi Brefeldin A Resistant Guanine Nucleotide Exchange Factor 1 (GBFl), ARFGAP1 (Hsu and Yang, 2009; Hsu, 2011). There are two forms of ARF1: GTP-ARF1 and GDP-ARF1. ARF1 is activated from GBF1 to GTP-ARF1, while ARFGAP1 can turn ARF1 into GDP form (Hsu and Yang, 2009). In addition, studies have shown that ARFGAP1 is a component of the COPI vesicle and also plays a cargo sorting role in COPI vesicle formation (Yang et al., 2002; Lee et al., 2005). Identifying the proviral role of ARFGAP1 further reinforces the critical role of COPI in EV-A71 replication. Previous studies suggests that key components of COPI, including coatomer and ARF1, are host factors of EV-A71 (Wang et al., 2012, 2014). Previously, ARFGAP1 was also participated in the replication of hepatitis C virus replication (Li et al., 2014). We speculated that EV-A71 2C recruited ARFGAP1 to the viral replication area through protein-protein interaction. ARFGAP1 together with other COPI components promoted EV-A71 replication.

CONCLUSION

In summary, we elucidated the host interactome of EV-A71 2C. Functional characterization of selected interaction partners *in vitro* revealed three host dependency factors including TRIM4, exportin2, and ARFGAP1 for EV-A71 replication. Our proteomic results provide a data-rich resource for the study of EV-71 in general. The host dependency factors we identified may contribute to the development of novel antiviral therapeutic avenues.

AUTHOR CONTRIBUTIONS

YL and XJ performed the majority of the experiments with help from PY. GZ offered technical assistance. YL and LZ analyzed the data. LZ conceived the research and wrote the manuscript.

FUNDING

This work was supported by grants from National Natural Science Foundation of China (81871663 and 81672035), National Key Plan for Research and Development of China (2016YFD0500300), and The Innovation Project of Shandong Academy of Medical Sciences.

SUPPLEMENTARY MATERIAL

The Supplementary Material for this article can be found online at: https://www.frontiersin.org/articles/10.3389/fmicb.2019.00636/full#supplementary-material

REFERENCES

Baggen, J., Thibaut, H. J., Strating, J., and van Kuppeveld, F. J. M. (2018). The life cycle of non-polio enteroviruses and how to target it. *Nat. Rev. Microbiol.* 16, 368–381. doi: 10.1038/s41579-018-0005-4

Behrens, P., Brinkmann, U., and Wellmann, A. (2003). CSE1L/CAS: its role in proliferation and apoptosis. *Apoptosis* 8, 39–44. doi: 10.1023/A:1021644918117

Bera, T. K., Bera, J., Brinkmann, U., Tessarollo, L., and Pastan, I. (2001). Cse1l is essential for early embryonic growth and development. *Mol. Cell Biol.* 21, 7020–7024. doi: 10.1128/MCB.21.20.7020-7024.2001

Coyaud, E., Ranadheera, C., Cheng, D. T., Goncalves, J., Dyakov, B., Laurent, E., et al. (2018). Global interactomics uncovers extensive organellar targeting by Zika virus. *Mol. Cell Proteomics* 17, 2242–2255. doi: 10.1074/mcp.TIR118.000800

Du, H., Yin, P., Yang, X., Zhang, L., Jin, Q., and Zhu, G. (2015). Enterovirus 71 2C protein inhibits NF-kappaB activation by binding to RelA(p65). *Sci. Rep.* 5:14302. doi: 10.1038/srep14302

Gao, Z., Hu, J., Liang, Y., Yang, Q., Yan, K., Liu, D., et al. (2017). Generation and comprehensive analysis of host cell interactome of the PA protein of the highly pathogenic H5N1 avian influenza virus in mammalian cells. *Front. Microbiol.* 8:739. doi: 10.3389/fmicb.2017.00739

Goldfarb, D. S., Corbett, A. H., Mason, D. A., Harreman, M. T., and Adam, S. A. (2004). Importin alpha: a multipurpose nuclear-transport receptor. *Trends Cell Biol.* 14, 505–514. doi: 10.1016/j.tcb.2004.07.016

Hafirassou, M. L., Meertens, L., Umana-Diaz, C., Labeau, A., Dejarnac, O., Bonnet-Madin, L., et al. (2017). A global interactome map of the dengue virus NS1 identifies virus restriction and dependency host factors. *Cell Rep.* 21, 3900–3913. doi: 10.1016/j.celrep.2017.11.094

Hsu, V. W. (2011). Role of ArfGAP1 in COPI vesicle biogenesis. *Cell Logist.* 1, 55–56. doi: 10.4161/cl.1.2.15175

Hsu, V. W., and Yang, J. S. (2009). Mechanisms of COPI vesicle formation. *FEBS Lett.* 583, 3758–3763. doi: 10.1016/j.febslet.2009.10.056

Jiang, M. C. (2016). CAS (CSE1L) signaling pathway in tumor progression and its potential as a biomarker and target for targeted therapy. *Tumour Biol.* 37, 13077–13090. doi: 10.1007/s13277-016-5301-x

Kimura, M., and Imamoto, N. (2014). Biological significance of the importin-beta family-dependent nucleocytoplasmic transport pathways. *Traffic* 15, 727–748. doi: 10.1111/tra.12174

Lee, S. Y., Yang, J. S., Hong, W., Premont, R. T., and Hsu, V. W. (2005). ARFGAP1 plays a central role in coupling COPI cargo sorting with vesicle formation. *J. Cell Biol.* 168, 281–290. doi: 10.1083/jcb.200404008

Li, H., Yang, X., Yang, G., Hong, Z., Zhou, L., Yin, P., et al. (2014). Hepatitis C virus NS5A hijacks ARFGAP1 to maintain a phosphatidylinositol 4-phosphate-enriched microenvironment. *J. Virol.* 88, 5956–5966. doi: 10.1128/JVI.03738-13

Li, Q., Zheng, Z., Liu, Y., Zhang, Z., Liu, Q., Meng, J., et al. (2016). 2C proteins of enteroviruses suppress IKKbeta phosphorylation by recruiting protein phosphatase 1. *J. Virol.* 90, 5141–5151. doi: 10.1128/JVI.03021-15

Li, Y., Zhang, L., and Ke, Y. (2017). Cellular interactome analysis of vaccinia virus K7 protein identifies three transport machineries as binding partners for K7. *Virus Genes* 53, 814–822. doi: 10.1007/s11262-017-1504-5

Shih, S. R., Stollar, V., and Li, M. L. (2011). Host factors in enterovirus 71 replication. *J. Virol.* 85, 9658–9666. doi: 10.1128/JVI.05063-11

Stewart, M. (2007). Molecular mechanism of the nuclear protein import cycle. *Nat. Rev. Mol. Cell Biol.* 8, 195–208. doi: 10.1038/nrm2114

Tanaka, T., Ohkubo, S., Tatsuno, I., and Prives, C. (2007). hCAS/CSE1L associates with chromatin and regulates expression of select p53 target genes. *Cell* 130, 638–650. doi: 10.1016/j.cell.2007.08.001

Tang, W. F., Yang, S. Y., Wu, B. W., Jheng, J. R., Chen, Y. L., Shih, C. H., et al. (2007). Reticulon 3 binds the 2C protein of enterovirus 71 and is required for viral replication. *J. Biol Chem.* 282, 5888–5898. doi: 10.1074/jbc.M611145200

Tomar, D., Prajapati, P., Lavie, J., Singh, K., Lakshmi, S., Bhatelia, K., et al. (2015). TRIM4; a novel mitochondrial interacting RING E3 ligase, sensitizes the cells to hydrogen peroxide (H2O2) induced cell death. *Free Radic Biol. Med.* 89, 1036–1048. doi: 10.1016/j.freeradbiomed.2015.10.425

Wang, J., Du, J., and Jin, Q. (2014). Class I ADP-ribosylation factors are involved in enterovirus 71 replication. *PLoS One* 9:e99768. doi: 10.1371/journal.pone.0099768

Wang, J., Wu, Z., and Jin, Q. (2012). COPI is required for enterovirus 71 replication. *PLoS One* 7:e38035. doi: 10.1371/journal.pone.0038035

Wang, Q., Li, Q., Liu, T., Chang, G., Sun, Z., Gao, Z., et al. (2018). Host interaction analysis of PA-N155 and PA-N182 in chicken cells reveals an essential role of UBA52 for replication of H5N1 avian influenza virus. *Front. Microbiol.* 9:936. doi: 10.3389/fmicb.2018.00936

Xu, F., Zhao, X., Hu, S., Li, J., Yin, L., Mei, S., et al. (2016). Amphotericin B inhibits enterovirus 71 replication by impeding viral entry. *Sci. Rep.* 6:33150. doi: 10.1038/srep33150

Yan, J., Li, Q., Mao, A. P., Hu, M. M., and Shu, H. B. (2014). TRIM4 modulates type I interferon induction and cellular antiviral response by targeting RIG-I for K63-linked ubiquitination. *J. Mol. Cell Biol.* 6, 154–163. doi: 10.1093/jmcb/mju005

Yang, J. S., Lee, S. Y., Gao, M., Bourgoin, S., Randazzo, P. A., Premont, R. T., et al. (2002). ARFGAP1 promotes the formation of COPI vesicles, suggesting function as a component of the coat. *J. Cell Biol.* 159, 69–78. doi: 10.1083/jcb.200206015

Yuan, J., Shen, L., Wu, J., Zou, X., Gu, J., Chen, J., et al. (2018). Enterovirus A71 proteins: structure and function. *Front. Microbiol.* 9:286. doi: 10.3389/fmicb.2018.00286

Zheng, Z., Li, H., Zhang, Z., Meng, J., Mao, D., Bai, B., et al. (2011). Enterovirus 71 2C protein inhibits TNF-alpha-mediated activation of NF-kappaB by suppressing IkappaB kinase beta phosphorylation. *J. Immunol.* 187, 2202–2212. doi: 10.4049/jimmunol.1100285

Conflict of Interest Statement: The authors declare that the research was conducted in the absence of any commercial or financial relationships that could be construed as a potential conflict of interest.

Copyright © 2019 Li, Jian, Yin, Zhu and Zhang. This is an open-access article distributed under the terms of the Creative Commons Attribution License (CC BY). The use, distribution or reproduction in other forums is permitted, provided the original author(s) and the copyright owner(s) are credited and that the original publication in this journal is cited, in accordance with accepted academic practice. No use, distribution or reproduction is permitted which does not comply with these terms.

frontiers in Genetics

REVIEW
published: 23 July 2019
doi: 10.3389/fgene.2019.00616

Host Genetics of Cytomegalovirus Pathogenesis

Efe Sezgin[1], Ping An[2] and Cheryl A. Winkler[2]*

[1] Laboratory of Nutrigenomics and Epidemiology, Izmir Institute of Technology, Urla, Turkey, [2] Basic Research Laboratory, Center for Cancer Research, National Cancer Institute, Leidos Biomedical Research, Inc., Frederick National Laboratory for Cancer Research, Frederick, MD, United States

Human cytomegalovirus (HCMV) is a ubiquitous herpes virus (human herpes virus 5) with the highest morbidity and mortality rates compared to other herpes viruses. Risk groups include very young, elderly, transplant recipient, and immunocompromised individuals. HCMV may cause retinitis, encephalitis, hepatitis, esophagitis, colitis, pneumonia, neonatal infection sequelae, inflammatory, and age-related diseases. With an arsenal of genes in its large genome dedicated to host immune evasion, HCMV can block intrinsic cellular defenses and interfere with cellular immune responses. HCMV also encodes chemokines, chemokine receptors, and cytokines. Therefore, genes involved in human viral defense mechanisms and those encoding proteins targeted by the CMV proteins are candidates for host control of CMV infection and reactivation. Although still few in number, host genetic studies are producing valuable insights into biological processes involved in HCMV pathogenesis and HCMV-related diseases. For example, genetic variants in the immunoglobulin GM light chain can influence the antibody responsiveness to CMV glycoprotein B and modify risk of HCMV-related diseases. Moreover, CMV infection following organ transplantation has been associated with variants in genes encoding toll-like receptors (TLRs), programmed death-1 (*PD-1*), and interleukin-12p40 (*IL-12B*). A KIR haplotype (2DS4+) is proposed to be protective for CMV activation among hematopoietic stem cell transplant patients. Polymorphisms in the interferon lambda 3/4 (*IFNL3/4*) region are shown to influence susceptibility to CMV replication among solid organ transplant patients. Interestingly, the *IFNL3/4* region is also associated with AIDS-related CMV retinitis susceptibility in HIV-infected patients. Likewise, interleukin-10 receptor 1 (*IL-10R1*) variants are shown to influence CMV retinitis development in patients with AIDS. Results from genome-wide association studies suggest a possible role for microtubule network and retinol metabolism in anti-CMV antibody response. Nevertheless, further genetic epidemiological studies with large cohorts, functional studies on the numerous HCMV genes, and immune response to chronic and latent states of infection that contribute to HCMV persistence are clearly necessary to elucidate the genetic mechanisms of CMV infection, reactivation, and pathogenesis.

Keywords: cytomegalovirus, host genetics, viral pathogenesis, immune response, genetic epidemiology

OPEN ACCESS

Edited by:
Dana C. Crawford, Case Western Reserve University, United States

Reviewed by:
Rui Medeiros, Portuguese Oncology Institute, Portugal
Michael G. Brown, University of Virginia, United States
David Navarro, Clinical University Hospital Valencia, Spain

****Correspondence:***
Efe Sezgin
efesezgin@iyte.edu.tr

Specialty section:
This article was submitted to Applied Genetic Epidemiology, a section of the journal Frontiers in Genetics

Received: *28 September 2018*
Accepted: *13 June 2019*
Published: *23 July 2019*

Citation:
Sezgin E, An P and Winkler CA (2019) Host Genetics of Cytomegalovirus Pathogenesis. Front. Genet. 10:616. doi: 10.3389/fgene.2019.00616

INTRODUCTION

Human cytomegalovirus (HCMV), also called human herpes virus 5 (HHV5), is a beta herpesvirus that belongs to the Herpesviridae family (Davison, 2007; Davison and Bhella, 2007; Liu and Zhou, 2007). HCMV exhibits broad cellular tropism, capable of infecting most cell types and organs. As an opportunistic pathogen, HCMV is ubiquitous with a global infection distribution and causes more morbidity and mortality compared to any other herpes virus (Wills et al., 2007). Major HCMV transmission routes include saliva, sexual contact, placental transfer, breast feeding, blood transfusion, solid organ transplantation, and hematopoietic stem cell transplantation (HSCT; Pass, 1985; Ho, 1990). The incidence of infection and prevalence increases progressively with age, reaching over 70% prevalence by age 70 in developed countries. The seroprevalence rates can be more than 90% among lower socioeconomic groups, men who have sex with men, and in developing countries (Pass, 1985; Ho, 1990; Stagno and Cloud, 1990; Razonable, 2005; Cannon, 2009; Beam and Razonable, 2012).

HCMV, with a double-stranded linear DNA genome ranging between 196 and 241 kbp (thousand base pairs), has the largest genome among the betaherpesviruses. The genome can encode over 160 gene products, a number much higher than other betaherpesviruses (Murphy et al., 2003a; Murphy et al., 2003b; Dolan et al., 2004). Only a subset of the 160 genes have roles in herpesvirus core function such as DNA replication, DNA encapsulation, and virion maturation, whereas the majority are involved in viral persistence, latency, diverse cellular tropism, and host immune response modulation, indicating complex interactions throughout HCMV co-evolution with its human host (Stern-Ginossar et al., 2012). For example, HCMV encodes homologs of cellular chemokines, chemokine receptors, and cytokines, which might contribute to immune evasion of infected host cells (McSharry et al., 2012).

The recognition of CMV as a medically important virus goes back to early 1930s when cytomegalic inclusion disease, a severe form of congenital CMV disease with an owl's eye appearance of inclusion bodies in cells from multiple organs of the infants, was observed. By 1970s, the pathogenic organ disease and HCMV link was well established, and HCMV-like viruses were isolated from other mammals. Due to the high social and medical cost of congenital CMV disease (i.e., sensorineural hearing loss and other severe neurological injury), vaccine development is a high public health priority (Plotkin, 2004; Arvin et al., 2004). HCMV continued to draw increasing medical attention as an opportunistic infection in immunocompromised individuals receiving organ transplants and the elderly. Moreover, persistent HCMV infection has been demonstrated to accelerate immunosenescence also known as human immune aging (Koch et al., 2006; Koch et al., 2007; Pawelec et al., 2009; Wistuba-Hamprecht et al., 2013; Pawelec, 2014). The onset of the HIV epidemic and the concomitant increase in AIDS-related CMV infections led to the development of several antiviral drugs (Plotkin, 2004; Griffiths and Boeckh, 2007; Kotton, 2013; Shin et al., 2014; Vora et al., 2018). However, currently there is no protective vaccination, and viral resistance against available antiviral drugs necessitates continuing research and investment in better understanding of CMV pathogenesis (Plotkin, 2002; Schleiss et al., 2006; Heineman, 2007; Griffiths and Boeckh, 2007; Plotkin and Boppana, 2018).

Most reviews in CMV literature focus on the viral and immune response aspects of the pathogenesis. However, host genetics of viral infection and pathogenesis can identify biological pathways that may lead to novel therapeutics. This review takes a different approach and aims to cover the current cumulative state of the knowledge in the host genetics of CMV pathogenesis in different risk groups. Different phenotypic outcomes of HCMV susceptibility are presented in the following sections. The details of genetic associations such as cohorts, odds ratios, P-values, and sample size are presented in **Table 1**. A summary figure of interactions between host genes and HCMV in different phenotypic outcomes based on literature reports is presented in **Figure 1**.

HOST GENETICS OF HUMORAL IMMUNITY TO HCMV

HCMV immune human sera contain neutralizing antibodies against principal CMV envelope proteins (such as gB), tegument phosphoprotein pp150 (UL32), and nonstructural DNA binding phosphoprotein pp52 (UL44) (Landini, 1993). Humoral immunity to CMV can be protective against blood-borne spread of virus, transplacental transmission, and CMV acquisition and disease (Jonjic et al., 1994; Plotkin et al., 1994; Schoppel et al., 1998; Fields et al., 2001; Schleiss et al., 2004). There is differential response to CMV exposure, and not everyone exposed to HCMV develops a CMV-related disease, suggesting a possible role for host genetic variation in antibody response to HCMV.

Immunoglobulins, also known as antibodies, constitute a critical part of the humoral immune response by specifically recognizing and binding to particular antigens. Immunoglobulin G is the most common type of antibody in circulation. Variation in genes that code for immunoglobulin (Ig) GM (gamma marker) creates several alleles (also referred as allotypes), (i.e., GM 3 and GM 17) with different binding affinities to antigens such as HCMV glycoprotein B (gB). The effect of genetic variation in humoral immunity on susceptibility to HCMV disease has been suggested by the studies that focus on association between immunoglobulin (Ig) GM allotype variation and HCMV antibody response. Pandey et al. reported a significant effect of immunoglobulin GM genotypes on antibody responsiveness to HCMV glycoprotein B (gB) (Pandey, 2014a). The study showed significant differences in antibody response to HCMV between GM 3 and GM 17 alleles. HCMV codes for a Fc gamma receptor (FcgR)-like protein (coded by the HCMV *RL13* gene) that can bind to the anti-HCMV IgG antibody, thus reducing the number of free anti-HCMV antibodies in circulation, and giving survival advantage to the virus. The GM 3 allele has higher affinity to HCMV FcgR-like protein (through bipolar bridging) compared to the GM 17 allele, leaving lower concentration of free anti-HCMV gB antibodies circulating in the system. They also drew attention to B-cell-mediated antigen

TABLE 1 | Loci reported to be involved in HCMV and related disease susceptibility.

Phenotype	Gene	Variant/genotype	Location	Sample size	Model	Effect	P-value	Population	Study group	Ref.
Humoral immunity										
	IGHG1	GM 3	Exon	131	Recessive	Reduced anti-HCMV Glycoprotein B Immunoglobulin G (IgG) Antibody level	0.01	USA/Europeans	Upper Midwest Health Study	(Pandey et al., 2014c)
	IGHG1	GM 5	Exon	131	Recessive	Reduced anti-HCMV Glycoprotein B Immunoglobulin G (IgG) Antibody level	0.01	USA/Europeans	Upper Midwest Health Study	(Pandey et al., 2014c)
	AGBL1	rs2011905 -C Allele	Intron	2442	Allelic	Increased anti-CMV IgG titer	1.9×10^{-6}	CVD-Finns	24–39 year old participants (GWAS)	(Kuparinen et al., 2012)
	CD53	rs2885805 -A allele	Intron	2442	Allelic	Decreased anti-CMV IgG titer	4.6×10^{-6}	CVD-Finns	24–39 year old participants (GWAS)	(Kuparinen et al., 2012)
	EFCAB4B	rs4766152 -G allele	Intron	2442	Allelic	Decreased anti-CMV IgG titer	5.1×10^{-6}	CVD-Finns	24–39 year old participants (GWAS)	(Kuparinen et al., 2012)
	FREM2	rs9594293 -A allele	Intron	2442	Allelic	Decreased anti-CMV IgG titer	6.8×10^{-6}	CVD-Finns	24–39 year old participants (GWAS)	(Kuparinen et al., 2012)
	MCPH1	rs1707715 - G allele	Intron	2442	Allelic	Increased anti-CMV IgG titer	7.8×10^{-6}	CVD-Finns	24–39 year old participants (GWAS)	(Kuparinen et al., 2012)
	TTC7B	rs1779382 - A allele	Intron	2442	Allelic	Increased anti-CMV IgG titer	9.1×10^{-6}	CVD-Finns	24–39 year old participants (GWAS)	(Kuparinen et al., 2012)
	LOC728667 or LINC00596	rs1288981 - T allele	Between genes	1300	Allelic	Decreased IgG antibody response against HCMV	8.2×10^{-7}	Mexican Americans in the San Antonio Family Study	16–94 year old participants (GWAS)	(Rubicz et al., 2015)
Cancer susceptibility										
	IGHG1	GM 3	–	253 (120 case, 133 control)	Recessive	Increased risk of Glioma	0.04	Portugal/European	Patients with glioma	(Pandey et al., 2014b)
	IGHG1	GM 3/ GM 17	–	253 (120 case, 133 control)	Genotype	Increased risk of Glioma	0.02	Portugal/European	Patients with glioma	(Pandey et al., 2014b)
	IGHG1	GM 3	–	258 case–control pair	Additive	Increased breast cancer risk	0.01	Brazil/Europeans	Patients with invasive breast cancer	(Pandey et al., 2012)
	IGHG1	GM 3	–	251	Additive and Recessive	Reduced anti-HCMV Glycoprotein B Immunoglobulin G (IgG) Antibody level	0.01–0.03	Brazil/Europeans	Breast cancer free controls	(Pandey et al., 2016)
HCMV disease in transplantation										
Solid organ transplantation										
	TLR2	R753Q (rs5743708, 2258 G > A)	Exon	737 (92 cases, 645 controls)	Recessive	Increased risk of CMV disease after liver transplantation	0.003	USA/Europeans	Patients who received liver transplantation at the Mayo Clinic in Rochester, Minnesota	(Kang et al., 2012)
	TLR2	R753Q (rs5743708, 2258 G > A)	Exon	92	Recessive	Increased HCMV viral load and risk of CMV disease after liver transplantation	0.003–0.04	USA/Europeans	Patients who received liver transplantation at the Mayo Clinic in Rochester, Minnesota	(Kijpittayarit et al., 2007)
	TLR4	D299G (rs4986790) or T399I (rs498679)	Exon	245	Presence of any of the variants	Increased risk of primary HCMV infection and disease	0.02	Spain	Patients who received kidney or kidney-pancreas transplantation	(Cervera et al., 2007)
	TLR9	rs5743836 – TT genotype	Upstream	315	Recessive	Lower incidence of HCMV infection	0.035	Spain	Patients received kidney transplantation in the OPERA study	(Fernandez-Ruiz et al., 2015)

(Continued)

TABLE 1 | Continued

Phenotype	Gene	Variant/genotype	Location	Sample size	Model	Effect	P-value	Population	Study group	Ref.
	DC-SIGN	rs735240 – GG genotype	Upstream	315	Recessive	Higher incidence of HCMV infection	0.008	Spain	Patients received kidney transplantation in the OPERA study	(Fernandez-Ruiz et al., 2015)
	MBL2	Biochemical deficiency/ Null	–	16	Recessive	Increased risk of HCMV infection	0.005	Univ. Hospital, Lausanne, CH	Patients who received kidney transplantation	(Manuel et al., 2007)
	PDCD1/ PD-1	rs11568821 - G allele	Intron	469	Recessive	Increased risk of HCMV infection	0.01	Univ. Hospital, Tours, France	Patients who received kidney transplantation	(Hoffmann et al., 2010)
	PDCD1/ PD-1	rs11568821 -A allele	Intron	1119	Dominant	Improved kidney graft survival recipients receiving grafts from CMV-positive donors	0.002	Univ. Hospital, Tours, France	Patients who received kidney transplantation	(Forconi et al., 2017)
	PDCD1/ PD-1	rs11568821 -A allele	Intron	181	Dominant	Improved lung graft survival recipients receiving grafts from CMV-positive donors	0.006	University Hospital of Tours, France	Patients who received lung transplantation	(Forconi et al., 2017)
	IFNG	+874T/A (rs2430561) -TT genotype	Intron	170	Genotypic	High level of viremia and HCMV disease	0.001	USA/Europeans	Patients who received lung transplantation	(Mitsani et al., 2011)
	IFNG	+874T/A (rs2430561) -AA genotype		247	Genotypic	Increased risk of HCMV infection and disease	0.01	USA/Hispanics	Patients who received kidney transplantation	(Vu et al., 2014)
	IFNL3/ IFNL4	rs8099917 -G allele	5' Upstream region	38 (17 with CMV replication, 21 no CMV replication)	Dominant	Reduced HCMV replication	0.04	University of Alberta, Canada	Patients who received solid organ transplantation	(Egli et al., 2014)
	IFNL3/ IFNL4	rs368234815 -G allele	CpG region, 5' Upstream	840	Recessive	Increased risk of HCMV replication and disease	0.05	Europeans/Swiss Transplant Cohort Study	Patients who received solid organ transplantation	(Manuel et al., 2015)
	IFNL3/ IFNL4/IL28B	rs12979860 – T allele	Intro	315	Allelic	Lower incidence of HCMV infection	0.03	Spain	Patients received kidney transplantation in the OPERA study	(Fernandez-Ruiz et al., 2015)
	IL-10	-1082A/G -AA genotype	5' Upstream	408	Genotypic	Reduced incidence of HCMV infection	0.03	Finland	Patients who received kidney transplantation	(Alakulppi et al., 2006)
	IL-12B	rs3212227 -C allele (IL-12p40)	3′-untransla-ted region	469	Allelic	Increased risk of HCMV infection	0.04	University Hospital of Tours, France	Patients who received kidney transplantation	(Hoffmann et al., 2008)
	MICA	rs2596538	5' Upstream region	181	Allelic	Protective against HCMV infection and disease	0.001	University Hospital Essen, Germany	Patients who received kidney transplantation	(Rohn et al., 2018)
Hematopoietic transplantation										
	IFNL3/ IFNL4	rs12979860 -T allele	Intron	151	Genotypic	Protective against HCMV infection	0.04	University Clinic Hospital of Valencia, Spain	Patients who received allogeneic stem cell transplantation	(Bravo et al., 2014)
	IFNL3/ IFNL4	rs12979860 -T allele	Intron	142	Recessive	Protective against HCMV infection	0.05	University Clinic Hospital of Valencia, Spain	Patients who received allogeneic stem cell transplantation	(Corrales et al., 2017)
	IFNL3/ IFNL4	rs12979860 -T allele; rs368234815-ΔG allele	Intron; Exon	99	Compound Genotypic	Increased risk of HCMV activation	< 0.05	Italian cohorts	Patients who received allogeneic stem cell transplantation	(Annibali et al., 2018)
	IL-10	rs1800893 -G allele	5' Upstream	154 (83 HCMV activation, 71 control)	Additive	Increased risk of HCMV disease	0.009	Multinational/ Europeans	Patients who received allogeneic stem cell transplantation	(Loeffler et al., 2006)
	IL-10	rs1800896 -G allele	5' Upstream	154 (83 HCMV activation, 71 control)	Additive	Increased risk of HCMV disease	0.001	Multinational/ Europeans	Patients who received allogeneic stem cell transplantation	(Loeffler et al., 2006)
	IL-10	rs1878672 -G allele	Intron	154 (83 HCMV activation, 71 control)	Additive	Increased risk of HCMV disease	0.003	Multinational/ Europeans	Patients who received allogeneic stem cell transplantation	(Loeffler et al., 2006)

(Continued)

TABLE 1 | Continued

Phenotype	Gene	Variant/genotype	Location	Sample size	Model	Effect	P-value	Population	Study group	Ref.
	IL-10	rs3024492 -T allele	Intron	154 (83 HCMV activation, 71 control)	Additive	Increased risk of HCMV disease	0.04	Multinational/ Europeans	Patients who received allogeneic stem cell transplantation	(Loeffler et al., 2006)
	IL-7	rs6897932 -T allele	Exon	460	Genotypic	Increased risk of HCMV infection	0.007	Copenhagen University, Denmark	Patients who received allogeneic stem cell transplantation	(Kielsen et al., 2018)
	CCL2 (MCP1)	rs1024611 -T allele	5' Upstream	154 (83 HCMV activation, 71 control)	Additive	Increased risk of HCMV reactivation	0.03	Multinational/ Europeans	Patients who received allogeneic stem cell transplantation	(Loeffler et al., 2006)
	CCL2 (MCP1)	rs13900 -T allele	Exon	154 (83 HCMV activation, 71 control)	Additive	Increased risk of HCMV reactivation	0.02	Multinational/ Europeans	Patients who received allogeneic stem cell transplantation	(Loeffler et al., 2006)
	CCR5	rs17141079 -T allele	Intron	154 (83 HCMV activation, 71 control)	Additive	Increased risk of HCMV disease	0.02	Multinational/ Europeans	Patients who received allogeneic stem cell transplantation	(Loeffler et al., 2006)
	CCR5	rs1800023 -G allele	5' Upstream	154 (83 HCMV activation, 71 control)	Additive	Increased risk of HCMV disease	0.01	Multinational/ Europeans	Patients who received allogeneic stem cell transplantation	(Loeffler et al., 2006)
	CCR5	rs1800023 -A allele	5' Upstream	102	Additive, Recessive	Increased CMV DNAemia and DNA peak	0.02, 0.05	Spanish cohort	Patients who received allogeneic stem cell transplantation	(Corrales et al., 2015)
	CCR5	rs2734648 -T allele	5' Upstream	154 (83 HCMV activation, 71 control)	Additive	Increased risk of HCMV disease	0.01	Multinational/ Europeans	Patients who received allogeneic stem cell transplantation	(Loeffler et al., 2006)
	CD209 (DC-SIGN)	rs2287886 -T allele	5' Upstream	194 (70 HCMV reactivation, 59 HCMV disease, 65 control)	Allelic	Increased risk of development of HCMV reactivation and disease	0.003	Germany/ Europeans	Patients who received allogeneic stem cell transplantation	(Mezger et al., 2008)
	CD209 (DC-SIGN)	rs735240 -A allele	5' Upstream	194 (70 HCMV reactivation, 59 HCMV disease, 65 control)	Allelic	Increased risk of development of HCMV reactivation and disease	0.01	Germany/ Europeans	Patients who received allogeneic stem cell transplantation	(Mezger et al., 2008)
	SDC2	rs1042381 -T allele	Exon	194 (70 HCMV reactivation, 59 HCMV disease, 65 control)	Allelic	Increased risk of development of HCMV reactivation and disease	0.04	Germany/ Europeans	Patients who received allogeneic stem cell transplantation	(Mezger et al., 2008)
	KIR2DS4	KIR1D+ (deletion) haplotype	–	165	Recessive	Increased risk of HCMV reactivation	0.002	Chinese cohort	Patients with hematopoietic stem cell transplantation	(Wu et al., 2016)
	STAT4	Rs7574865 -T allele	Intron	161	Recessive	Increased risk of HCMV infection	0.01	Seoul National University, Korea	Patients with hematopoietic stem cell transplantation	(Wun et al., 2017)
	FOXP3	Rs3761548 -C allele	Intron	171	Recessive	Increased risk of HCMV infection	0.01	Seoul National University, Korea	Patients with hematopoietic stem cell transplantation	(Piao et al., 2016)
HCMV disease in HIV infection										
	IL-10	rs3024496 -C Allele	3' UTR	534 (110 cases, 424 controls)	Dominant	Susceptible to CMV-Retinitis	0.05	USA/African Americans	Patients with AIDS	(Sezgin et al., 2010)
	IL-10	rs3024500 -C Allele	3' UTR	534 (110 cases, 424 controls)	Dominant	Susceptible to CMV-Retinitis	0.02	USA/African Americans	Patients with AIDS	(Sezgin et al., 2010)
	IL-10R1 (IL10RA)	rs2228055 -G allele	Exon	750 (200 cases, 550 controls)	Haplotypic	Susceptible to CMV-Retinitis	0.04	USA/Europeans	Patients with AIDS	(Sezgin et al., 2010)
	IL-10R1 (IL10RA)	rs2229114 -T allele	Exon	750 (200 cases, 550 controls)	Allelic	Protective against CMV-Retinitis	0.03	USA/Europeans	Patients with AIDS	(Sezgin et al., 2010)

(Continued)

TABLE 1 | Continued

Phenotype	Gene	Variant/genotype	Location	Sample size	Model	Effect	P-value	Population	Study group	Ref.
	CCR5	rs1799988	5' UTR, CCR5 P1 Promoter Haplotype	117	Haplotypic	Increased risk of CMV-Retinitis progression	0.007	USA/African Americans	Patients with AIDS	(Sezgin et al., 2011)
	CCR5	rs1799988	5' UTR, CCR5 P1 Promoter Haplotype	203	Haplotypic	Increased risk of mortality in patients with CMV-Retinitis	0.05	USA/African Americans	Patients with AIDS	(Sezgin et al., 2011)
	CXCL12 (SDF1)	rs1801157 -A allele	3′-untranslat-ed region	117	Dominant	Increased risk of CMV-Retinitis progression	0.008	USA/African Americans	Patients with AIDS	(Sezgin et al., 2011)
	TNF	4-1-G-2-2-1	5' Upstream	222 (52 CMV-retinitis, 170 control)	Haplotypic	Susceptible to CMV-Retinitis	0.03	Brazilian cohort (mixed race)	Patients with AIDS	(Deghaide et al., 2009)
	TNF	TNFc1	5' Upstream	222 (52 CMV-retinitis, 170 control)	Allelic	Protective against CMV-Retinitis	0.04	Brazilian cohort (mixed race)	Patients with AIDS	(Deghaide et al., 2009)
	IFNL3/ IFNL4	rs368234815 -G allele	CpG region, 5' Upstream	1134	Recessive	Increased risk of CMV-retinitis	0.007	Europeans/Swiss HIV Cohort Study	Patients with HIV infection	(Bibert et al., 2014)
HCMV disease in vertical transmission										
	TLR2	rs1898830 -AG genotype	Intron	170 (87 case, 83 control)	Genotypic	decreased risk of congenital HCMV infection	0.03	Japanese cohort	Children with congenital HCMV infection	(Taniguchi et al., 2013)
	TLR2	rs1898830 -GG genotype	Intron	83 (33 case, 50 control)	Recessive	Protection against HCMV transmission	0.008	Israeli cohort	Pregnant women with HCMV infection	(Eldar-Yedidia et al., 2017)
	TLR2	rs3804100 (1350 T > C) -CC genotype	Exon	170 (87 case, 83 control)	Genotypic	Increased risk of congenital HCMV infection	0.01	Japanese cohort	Children with congenital HCMV infection	(Taniguchi et al., 2013)
	TLR2	Arg677Trp (rs121917864, 2029 C > T)	Exon	229 (151 case, 78 control)	Allelic	Reduced risk of infection only in adults	< 0.001	Polish cohort	HCMV-infected children and adults	(Jablonska et al., 2014)
	TLR4	D299G (rs4986790)	Exon	229 (151 case, 78 control)	Allelic	Reduced risk of infection only in adults	0.02	Polish cohort	HCMV-infected children and adults	(Jablonska et al., 2014)
	TLR2	R753Q (rs5743708, 2258 G > A)	Exon	51 (20 case, 30 control)	Genotypic	increased risk of congenital HCMV infection	0.02	Polish cohort	HCMV-infected fetuses and neonates	(Wujcicka et al., 2017a)
	TLR9	rs352140 (2848 G > A) - A allele	Exon (synonymous change)	131 (66 case, 65 control)	Dominant	Reduced risk of HCMV infection in pregnant women	0.03	Polish cohort	HCMV-infected pregnant women	(Wujcicka et al., 2017b)
	TLR9	rs352140 (2848 G > A) -TC genotype	Exon (synonymous change)	142 (72 case, 70 control)	Genotypic	Increased risk of HCMV infection in infants	0.02	Polish cohort	Congenitally HCMV-infected infants	(Paradowska et al., 2016)
	TLR9	Rs187084 (-1486 T > C) -C allele	Upstream	142 (72 case, 70 control)	Dominant	Increased risk of HCMV infection in infants	0.02	Polish cohort	Congenitally HCMV-infected infants	(Paradowska et al., 2016)
	IL1A	-889 C > T	5' Upstream	51 (20 case, 31 control)	Allelic	increased risk of congenital HCMV infection and onset of related symptoms	< 0.0001	Polish Mother's Memorial Hospital, Poland	Fetuses and Neonates with HCMV infection	(Wujcicka et al., 2017c)
	IL1A	-889 C > T	5' Upstream	129 (65 case, 64 control)	Recessive	Decreased risk of HCMV infection	0.05	Polish Mother's Memorial Hospital, Poland	Pregnant women	(Wujcicka et al., 2017d)
	IL1B	rs1143634 (+3954 C > T) -T allele	Exon	51 (20 case, 31 control)	Allelic	increased risk of congenital HCMV infection and onset of related symptoms	< 0.0001	Polish Mother's Memorial Hospital, Poland	Fetuses and Neonates with HCMV infection	(Wujcicka et al., 2017c)
	IL1B	rs16944 -T allele	5' Upstream	470 (72 case, 398 control)	Genotypic	increased risk of intrauterine HCMV infection	0.03	Infants enrolled at the Children's Memorial Health Institute in Warsaw, Poland	Infants with HCMV infection	(Kasztelewicz et al., 2017)

(Continued)

TABLE 1 | Continued

Phenotype	Gene	Variant/genotype	Location	Sample size	Model	Effect	P-value	Population	Study group	Ref.
	IL6	-174 G > C	5' Upstream	129 (65 case, 64 control)	Recessive	Decreased risk of HCMV infection in their offspring	0.02	Polish Mother's Memorial Hospital, Poland	Pregnant women	(Wujcicka et al., 2017d)
	CCL2 (MCP1)	rs13900 -T allele	Exon	470 (72 case, 398 control)	Genotypic	increased risk of hearing loss at birth	0.03	Infants enrolled at the Children's Memorial Health Institute in Warsaw, Poland	Infants with HCMV infection	(Kasztelewicz et al., 2017)
	TNF	rs1799964 -T allele	5' Upstream	470 (72 case, 398 control)	Genotypic	increased risk of intrauterine HCMV infection	0.03	Infants enrolled at the Children's Memorial Health Institute in Warsaw, Poland	Infants with HCMV infection	(Kasztelewicz et al., 2017)

All values and information are based on the cited paper. Whenever case–control status or disease-specific divisions of patients were available, they are reported under the sample size column.
IGHG1: Immunoglobulin GM γ chain marker.
CVD-Finns: Cardiovascular risks in young Finns study.

processing/presentation pathway as an alternative mechanism underlying GM allotypes' differential responsiveness to HCMV gB. One of the strategies that HCMV has evolved for evading host immunosurveillance involves generating proteins with similar functional properties to the Fcγ receptor for IgG (FcγR). FcγR interferes with the anti-HCMV IgG antibody's binding to the virus, thus giving survival advantage to HCMV against antibody-dependent cellular cytotoxicity, antibody-dependent cellular phagocytosis, and antibody-dependent complement-dependent cytotoxicity (Atalay et al., 2002; Namboodiri and Pandey, 2011).

A major issue in genetic epidemiology studies of antibody variation is that most of the genetic variation is ethnic and population specific. For example, GM 3 is rare among people of African descent. Moreover, the genetic background influencing overall immune response will be different between races and populations. Therefore replication and translation of results from one study to another is not always possible. Ethnic and population-specific genetic variation can also lead to hidden population stratification even in the same country, which is major factor confounding the genetic association results. Given the complex genetic nature of humoral immune response to HCMV, much larger studies with more balanced case and control groups are needed to test the GM associations with HCMV response.

HOST GENETICS OF HCMV IN CANCERS

HCMV is not considered an oncogenic virus; however, HCMV viral DNA, RNA, and protein have been frequently found in neoplastic tissues including gliomas, breast cancer, and neuroblastoma (Cobbs et al., 2002; Harkins et al., 2010; Cobbs, 2011; Taher et al., 2013; Wolmer-Solberg et al., 2013). Moreover, HCMV infection leads to changes in cell physiology, tumor microenvironment, inhibition of apoptosis, and evasion from immune detection that are characteristics of cancer development (Hanahan and Weinberg, 2011). Not all HCMV-infected individuals develop cancers, suggesting that host genetics of HCMV response may influence HCMV-mediated cancer risk. Indeed, studies with glioma patient cohorts showed a modulating effect of GM alleles on the risk of gliomas, where the IgGM 3 homozygotes were over twice, and the GM 3/17 heterozygotes were over three times as likely to develop glioma (Pandey, 2014a; Pandey et al., 2014b). The magnitude of antibody responsiveness to HCMV glycoprotein B (gB) has also been implicated in breast cancer susceptibility. The GM 3 allele of IgG1 was reported to be significantly associated with increased susceptibility to breast cancer in Caucasian subjects from Brazil; however, the association was not significant in other population groups (Pandey et al., 2012). In a follow-up study, breast cancer-free individuals had significantly higher levels of anti-gB IgG antibodies than patients with breast cancer; however, there was interindividual and interethnic variability in the magnitude of antibody response, and interactions with other genes of the immune system were apparent (Pandey et al., 2016). Functional studies indicate that the binding of HCMV FcgR-like protein to

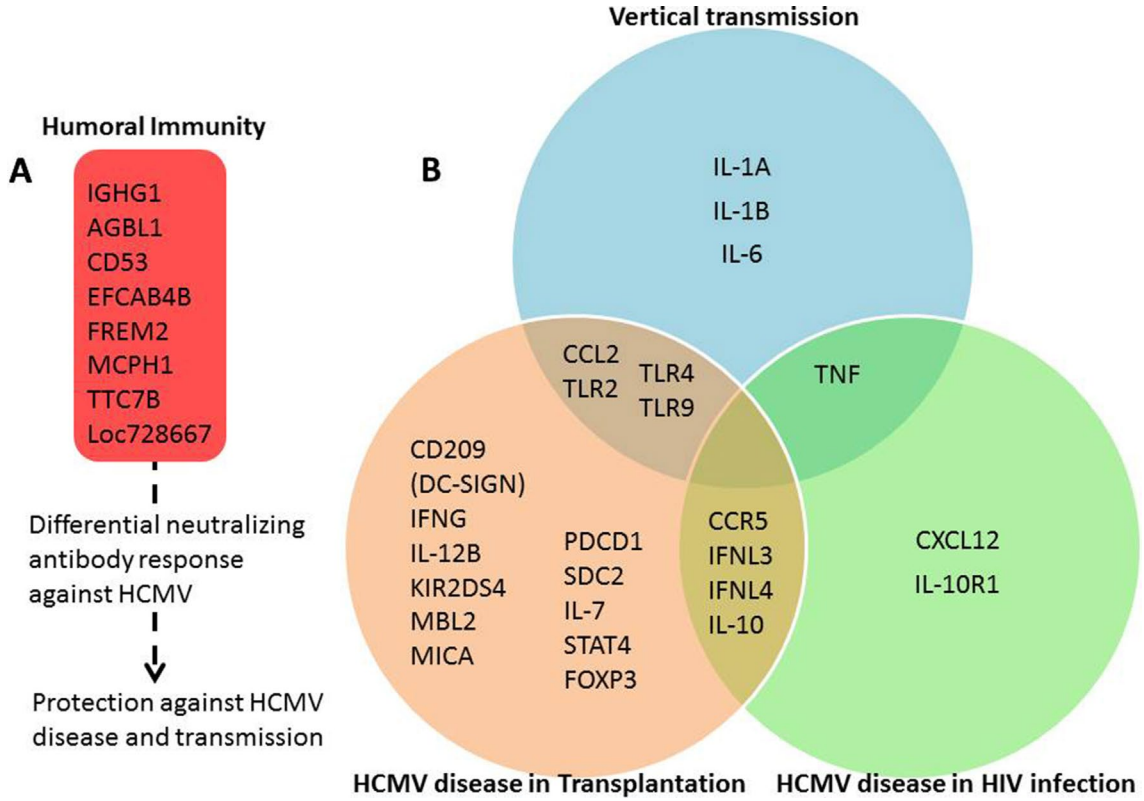

FIGURE 1 | Human genes involved in response to HCMV and related diseases. Summary figure representing the interaction between host genes and HCMV in different phenotypic outcomes based on literature reports as listed and cited in **Table 1**. **(A)** Genes modulating humoral immunity response against HCMV. **(B)** Innate and adaptive immune response modulating genes unique to and shared between susceptibility to HCMV disease in transplantation, HIV infection, and vertical transmission categories. The grouping of genes among the phenotypic outcomes is deduced based on association results and related literature detailed in **Table 1**. "Vertical transmission" category is based on studies of transmission of HMCV from mother to fetus or newborn. "HCMV disease in transplantation" category includes results from solid organ and stem cell transplantation studies. "HCMV disease in HIV infection" category includes results from HIV-infected patients.

GM 17 allele expressing IgG antibodies was significantly higher than GM 3 expressing antibodies, providing possible mechanistic insights for increased breast cancer risk in some HCMV-infected patients (Pandey et al., 2017).

Significant association of rare GM genotypes with neuroblastoma, a rare extracranial solid tumor, has been reported (Morell et al., 1977), but the mechanism underlying this association is still not clear. These uncommon GM genotypes include the GM 3, the allele with high affinity to HCMV TRL11/IRL11-encoded FcγR. Reports documenting early and late HCMV protein expression in primary neuroblastomas and neuroblastoma xenografts suggest either infection and transformation of neuroblastoma progenitor cells or direct infection of neuroblastoma cells and disturbance of intracellular pathways leading to neoplasms (Wolmer-Solberg et al., 2013). The mechanisms underlying the increased HCMV associated cancer risk with the GM 3 allele may also be involved in neuroblastoma cases as well.

Independent cohort and functional studies make a case for significant influence of host genetic variation in humoral immunity on response to HCMV disease (**Table 1**, **Figure 1**). However, increased cancer risk associated with increased HCMV susceptibility is still a hypothesis to be tested. Clearly, larger multi-ethnic, multi-cohort host genetic, and comprehensive functional studies are needed to uncover the host genetics of humoral immunity to HCMV and HCMV associated cancers.

HOST GENETICS OF HCMV DISEASE IN TRANSPLANT PATIENTS

HCMV is a common opportunistic infection among immunocompromised individuals. Individuals are maximally immunocompromised due to use of immunosuppressants during solid organ or HSCT procedures and thus are prone to HCMV reactivation (of the latent virus), primary infection, and reinfection. HCMV infections can cause severe morbidity and transplant failure, which frequently results in extended hospital stay and substantially higher cost of care (Falagas et al., 1997; Kim et al., 2000; Ljungman et al., 2002; Ramanan and Razonable, 2013). Transplantations from a seropositive individual to a seronegative individual (R-/D+) pose the greatest risk for HCMV-associated disease in the transplant recipient patients (Cope et al., 1997; Lowance et al., 1999). Therefore, determining

the serologic status of the recipient and donor is important in assessing the risk of HCMV-associated disease. However, it can be hard to find serostatus matched donor and recipients, and even serostatus matching does not completely eliminate HCMV-associated morbidity.

Coordinated innate and adaptive immune response is crucial for control of HCMV infection in immunocompromised transplant recipients. Whereas innate interferon (IFN) and natural killer (NK) cell responses are important in immediate control of CMV infection, adaptive T cell immune responses are important in both active infection and reactivation control phases (Crough and Khanna, 2009; Zelini et al., 2010; Reddehase, 2013; Muntasell et al., 2013). To reduce the number of HCMV-associated adverse outcomes and better identify transplant patients for HCMV prophylaxis, several candidate innate and adaptive immune-related gene studies have been conducted (**Table 1**).

Solid Transplantation Studies

A family of transmembrane proteins, the Toll-like receptors (TLRs), are part of the innate immune system and play crucial roles in the activation of the immune system by regulating the production of antiviral peptides and inflammatory cytokines against viral replication. The detection of CMV envelope glycoproteins B (gB) and H (gH) by TLR2 leads to nuclear factor-kB (NF-kB) activation and cytokine secretion against CMV (Boehme et al., 2006). Clinical studies showed that polymorphisms in TLR-2 (Kijpittayarit et al., 2007; Kang et al., 2012), TLR-4, TLR-9 (Fernandez-Ruiz et al., 2015), and mannose binding lectin (Cervera et al., 2007; Manuel et al., 2007) can be associated with increased risk of HCMV infection and disease after transplantation.

Genetic variants of MICA (major histocompatibility complex class I chain-related protein A) and its activating receptor NKG2D (natural killer group 2 member D) receptor may be associated with HCMV disease risk among kidney transplant patients. A candidate gene association study identified a regulatory MICA variant (rs2596538) in the kidney donors that can be a protective prognostic determinant for CMV disease. This functional variant was able to predict the development of CMV infection and disease during the first year after kidney transplantation (**Table 1**: Rohn et al., 2018). Membrane-associated molecule PD-1 (programmed death-1) regulates immune responses by inhibiting T cell receptor signaling, cytokine production in effector T cells, and expression on regulatory T cells (Sharpe et al., 2007; Franceschini et al., 2009). PD-1's expression also correlates with CMV viremia in transplant patients (Sester et al., 2008). An upstream regulatory region variant (rs11568821) that impairs the function of PD-1 (also called PD-1.3) has been investigated in HCMV infection in kidney and lung graft recipients. The PD-1.3 variant has been shown to be associated with higher risk of HCMV infection (Hoffmann et al., 2010) and lung allograft survival in recipients from HCMV-positive donors (Forconi et al., 2017). Dendritic cell-specific ICAM 3-grabbing nonintegrin (DC-SIGN) variants were also reported to be associated with higher incidence of HCMV infection in kidney transplant patients (Fernandez-Ruiz et al., 2015).

Cytokines, signaling molecules of the immune system, regulate pro-inflammatory and anti-inflammatory responses, and play important roles in antiviral response. Cytokines also play a role in HCMV infection, reactivation, and disease (Asanuma et al., 1995; Zeevi et al., 1999; Faist et al., 2010; van de Berg et al., 2010; Biron and Tarrio, 2015; Nabekura and Lanier, 2016). Studies of functional gene polymorphisms in pro-inflammatory and anti-inflammatory cytokines with HCMV disease identified IFNG (interferon-gamma) +874 A/T polymorphism as a risk factor for HCMV disease in kidney and lung transplant patients, where the +874 A allele, a low IFNG producer (reduced gene expression), is associated with increased risk for HCMV infection and disease after organ transplantation (Mitsani et al., 2011; Vu et al., 2014). In a Finnish renal transplant cohort, the donor interleukin-10 (IL-10) gene polymorphism –1082AA was observed to influence HCMV infection risk. Recipient IL-10, IL-6, and IFNG polymorphisms also show significant associations with HCMV reactivation and disease risk (Alakulppi et al., 2006). A possible association between IL-12p40 gene polymorphisms in the recipient and high risk of HCMV infection was also reported after kidney transplantation (Hoffmann et al., 2008).

Type III interferon, also called interferon lambda (INFL3 or formerly IL-28B), has gained much attention as an important viral response element in recent years (Kotenko, 2011; Hayes et al., 2012). In a cohort of solid organ transplant patients from Alberta, a functional single nucleotide polymorphism (SNP) (rs8099917) associated with lower INFL3 (IL-28B) expression during CMV infection, but higher IFN-stimulated gene expression showed a protective effect against CMV replication (Egli et al., 2014). A follow-up Swiss Transplant Cohort study compared the cumulative incidence of CMV replication between patients with different TT/-G (rs368234815) genotype in the CpG region upstream of IFNL3. Patients with the –G/–G genotype had higher cumulative incidence of CMV replication. The study suggest that IFNL3 TT/-G (rs368234815) variant can be a CMV replication controller, particularly in patients not receiving antiviral prophylaxis (Manuel et al., 2015). Fernandez-Ruiz et al. (2015) also reported a lower incidence of HCMV infections among kidney transplant patients with IL28B (IFNL3) rs12979860-T allele.

Hematopoietic Transplantation Studies

Although still few in number, host genetics of HCMV susceptibility among HSCT cases have also been investigated (**Table 1**). Similar to solid organ transplant studies, several candidate innate and adaptive immunity genes have been examined. Results from solid organ transplantation studies stimulated cytokine and interferon research in HCMV disease in stem cell transplant settings. In a comprehensive immunogenetic study, allogeneic stem cell transplant patients with HCMV reactivation (DNAemia), patients with HCMV disease, and patients without HCMV reactivation were examined (Loeffler et al., 2006). Polymorphisms in the CCR5, IL-10, and MCP1 were observed to contribute to HCMV reactivation and disease after allogeneic stem cell transplantation (Loeffler et al., 2006; Corrales et al., 2015). In a follow-up study, this research

group extended their investigation and observed a significant association between promoter region variants, which influenced the expression levels of DC-SIGN on dendritic cells, and increased risk of development of HCMV reactivation and disease (Mezger et al., 2008). Protective effects of the INFL3 rs12979860 C/T polymorphism against CMV infection (Bravo et al., 2014; Corrales et al., 2017) and INFL3 rs12979860 IFNL4 rs368234815 compound genotype against HCMV reactivation (Annibali et al., 2018) in the allogeneic stem cell transplant setting were also reported. Killer immunoglobulin-like receptors (KIR) are cell surface receptors found on NK and certain T cells. The activating and inhibitory signals are transmitted to NK cells through KIR proteins, by which NK cells respond quickly to infections. In a Chinese cohort HLA-matched HSCT patients, patients receiving HSCT from donors with heterozygote 2DS4+/1D+ KIR haplotype showed at least 20% less CMV reactivation compared to donors with other haplotypes (Wu et al., 2016). This observation suggests that donor KIR haplotype should be evaluated for HLA-matched HSCT cases. More recently functional genetic variants in *FOXP3* (Piao et al., 2016), *STAT4* (Wun et al., 2017), and *IL-7*(Kielsen et al., 2018) are reported to influence HCMV infection after HSCT in independent cohort studies.

Host genetics of HCMV disease in transplant patients provide hints towards promising genetic markers to predict CMV viremia (**Table 1**, **Figure 1**). However, these studies are complicated due to several factors, including donor and recipient serostatus, type and dose of immunosuppressive drugs used, and ethnicity of the patient cohort. These factors also lead to significant heterogeneity among the studies confounding the efficacy of a meta-analysis of the individual studies to reach a consensus on securely identified markers and causal variants. The transplant community is still far from developing well accepted genetic markers for personalized CMV approaches (such as decisions on prophylactic and preemptive therapies) to be used in the clinic.

HOST GENETICS OF HCMV DISEASE IN HIV-INFECTED PATIENTS

Patients with HIV infection are another group of immunocompromised individuals that are at high risk for CMV disease. Before the use of ART (antiretroviral therapy), up to 40% of adults with AIDS developed CMV disease (Gallant et al., 1992). Although the incidence of CMV infection has declined dramatically, new cases continue to occur (Sezgin et al., 2018). Among HIV-infected patients the risk of CMV disease is linked to CD4+ T-cell counts. The most common CMV disease among patients with uncontrolled HIV infection is CMV-Retinitis that may develop when CD4+ T-cell counts drop below 50–100 CD4+ cells/μl (Jabs, 1995; Dunn and Jabs, 1995; Heiden et al., 2007). While some patients with low CD4+ T-cell counts remain asymptomatic, others can progress to CMV disease rather quickly. Host genetic variants in genes involved in regulation of innate and adaptive immune responses may have a role in this differential susceptibility to CMV among HIV-infected patients as they have in other immunocompromised groups such as transplant patients.

A comprehensive candidate gene study on host genetics of CMV-Retinitis among HIV-infected patients was conducted in Longitudinal Studies of Ocular Complications of AIDS (LSOCA) cohort (**Table 1**). The study showed that human interleukin-10 receptor (IL-10R1) variants that potentially interfere with IL-10 binding and signal transduction can influence CMV-Retinitis occurrence in European Americans (Sezgin et al., 2010). The same study also suggested a possible role of IL-10 variants on CMV-Retinitis risk among African Americans (Sezgin et al., 2010). In a follow-up study of the same cohort, cytokine and cytokine receptor [*CCR5* and stromal derived factor (*SDF-1*)] genetic variants have been observed to influence retinitis progression (Sezgin et al., 2011). In a different cohort study, *TNF* polymorphisms were also linked to susceptibility to CMV retinitis in white patients, though with rather small sample size (Deghaide et al., 2009). In a large Swiss HIV Cohort Study, the effect of *IFNL3* TT/-G substitution, the variant that increased susceptibility to CMV replication in transplant patients (Manuel et al., 2015), was also shown to be associated with higher risk of CMV retinitis (Bibert et al., 2014).

Although subject to complex confounding factors and high false discovery rates, host candidate gene studies of immunocompromised groups cumulatively indicate possible effects of innate and adaptive immune gene variants on CMV disease (**Table 1**, **Figure 1**). More studies should be designed to replicate and validate these results.

HOST GENETICS OF VERTICAL HCMV TRANSMISSION

Vertical transmission of HCMV from mother to fetus or newborn is common and plays an important role in maintaining infection in the population (Stagno et al., 1982a; Whitley, 2004). Prenatal infection rates are highest in low income countries or low socioeconomic populations, where risk of maternal seropositivity is also high (Stagno et al., 1982b; Stagno et al., 1982c). Recurrent and primary HCMV infection during pregnancy can cause congenital infection of the newborn and may lead to severe clinical complications such as hearing defects, birth defects, and irreversible neurodevelopmental sequelae (Boppana et al., 1992; Boppana et al., 1999; Gaytant et al., 2002).

Host candidate genetic studies of congenital HCMV infection mainly have focused on innate immune system, such as TLRs and Mannan-binding lectins, and cytokine genes (**Table 1**, **Figure 1**). In children with congenital HCMV disease, the TLR2 1350 T > C variant (rs3804100) was reported to be associated with the infection, although no relationship was established with the course of infection (HCMV disease) (Taniguchi et al., 2013). Eldar-Yedidia et al. (2017) reported a protective effect of TLR2 rs1898830 –GG genotype against HCMV transmission to fetus. A follow-up study investigating the influence of Arg677Trp (rs121917864, 2029 C > T) and Arg753Gln (rs5743708) variants in the TLR2, and Asp299Gly variant in the TLR4 on the risk of CMV infection in infants and adults found that heterozygosity for the TLR2 Arg677Trp was significantly associated with a lower risk of CMV infection in adults but not in infants. The same study

also reported TLR4 Asp299Gly association with lower viremia in the adults (Jablonska et al., 2014). In a study of HCMV-infected fetuses and neonates, and controls, Wujcicka et al. (2017a) reported TLR2 2258 G > A SNP (rs5743708) to be associated with increased risk of congenital HCMV infection, but no effect of TLR2 1350 T > C and 2029 C > T variants on HCMV risk was observed. The same group in an independent study evaluated the role of TLR2, TLR4, and TLR9 variants in HCMV infection among pregnant women. Only the TLR9 2848 G > A (rs352140) variant was reported to be associated with HCMV infection risk in pregnant women (Wujcicka et al., 2017b). Increased HCMV infection risk in infants with TLR9 -1486 T > C and TLR9 2848 C > T variants is also reported (Paradowska et al., 2016).

Another important player in the innate immune system is the Mannan-binding lectin (MBL), a pattern recognition molecule and a first line defense antimicrobial factor (Kilpatrick, 2002). Mutations in the promoter region and first exon of *MBL2* were reported to be associated with lower serum MBL concentrations (Madsen et al., 1995). In a Polish study, MBL2 functional gene polymorphisms that influence serum MBL concentrations were examined in prenatal and perinatal CMV infections (Szala et al., 2011). However, no significant influence on susceptibility to prenatal or perinatal HCMV infections was observed (Szala et al., 2011).

HCMV infection during pregnancy can affect the cytokine profile within a HCMV-infected placenta and shift the cytokine expression toward a proinflammatory state with implications for adverse pregnancy outcomes (Hamilton et al., 2012; Scott et al., 2012). As host genetic variants in cytokine-related genes were shown to influence susceptibility to HCMV infection and disease in transplant patients and patients with AIDS, several congenital infection studies also investigated the association of cytokine and cytokine receptor variants on HCMV susceptibility. Kasztelewicz et al. (2017) compared the allelic distribution of 11 candidate SNPs in eight genes (TNF rs1799964 and rs1800629, TNFRSF1A rs4149570, IL-1B rs16944 and rs1143634, IL-10 rs1800896, IL-10RA rs4252279, IL-12B rs3212227, CCL2 rs1024611 and rs13900, CCR5 rs333) between a group of infants (n = 72) with confirmed intrauterine CMV infection and 398 uninfected controls. IL-1B (rs16944) and TNF (rs1799964) variants were significantly associated with intrauterine HCMV infection. Moreover, they identified CCL2 (rs13900) as a genetic risk factor for hearing loss at birth and at 6 months of age (Kasztelewicz et al., 2017). Wujcicka et al. examined the effects of fetal and maternal IL-1A, IL-1B, IL-6, IL-12B, and TNFA gene variants on HCMV infection and disease in neonates and fetuses in two independent Polish cohort studies. In one study, they reported that IL-1A and IL-1B variants increased the risk of congenital HCMV infection in neonates and fetuses, as well as the onset of disease-related symptoms (Wujcicka et al., 2017c). The other study of pregnant women also reported possible effects of IL-1A, IL-1B, and IL-6 on the occurrence and development of HCMV infection in the neonate (Wujcicka et al., 2017d).

Deciphering the contribution of hot genetics to HCMV vertical transmission and related disease outcomes may be the hardest of all HCMV-related disease studies. Firstly, the susceptibility of the pregnant mother to HCMV needs to be considered, where the immune response will be modified due to pregnancy further complicating the interaction between the host and HCMV. Secondly, if the mother cannot clear the infection, and HCMV finds its way to fetus, then the immune response by the infant, which is rather immature and still developing, will be involved with a genetic make-up different than that of the mother. Aforementioned reports should be considered as early attempts of a rather challenging research agenda. High-throughput genetic and immune profiling methods with much larger cohorts are necessary to understand the genetic and non-genetic factors involved in HCMV vertical transmission.

GWAS OF HCMV INFECTION

Genome-wide association studies (GWASs) have made significant contributions for discovering genetic factors underlying complex phenotypes and diseases. Unlike traditional hypothesis-driven candidate gene studies, where only a few candidate genes are targeted, in GWAS all human genes become potential candidates for the phenotype of interest. Therefore, GWAS approach can discover genes and their variants that may look irrelevant to the phenotype of interest, which in return can lead to discovery of novel biological pathways involved in development of this phenotype.

The first GWAS was conducted to identify genetic polymorphisms associated with the susceptibility to HCMV and strength of anti-HCMV immunoglobulin G (IgG) response to CMV infection (Kuparinen et al., 2012). The study included 1486 anti-CMV IgG seropositive and 648 seronegative individuals genotyped on an Illumina BeadChip containing 670,000 probes. Although no strong genetic components were observed, the study identified 10 new candidate loci that showed suggestive association with anti-CMV IgG titer (**Table 1**). Annotated genes among these loci suggested a possible role for microtubule network in anti-CMV antibody response (Kuparinen et al., 2012). Another GWAS, aiming to localize the loci influencing serological phenotypes to common viral infections, found suggestive evidence of association for modifying IgG antibody response to HCMV (anti-CMV) on chromosome 14 (Rubicz et al., 2015). A retinol metabolism gene, *DHRS4*, near the associated SNP, was proposed to be a candidate for further evaluation. These two studies show that GWAS approach can be productive in HCMV field; however, one also needs to consider the fact that there was no overlap of identified genes between the two GWASs, although the phenotypes were similar. Curiously, none of the candidate innate and adaptive immune genes examined so far were top hits in these GWASs.

Challenge and Future Directions

Clinical management of CMV infection is particularly challenging due to the arsenal of host immune evasion strategies encoded by its large genome and its complex interactions with its human host. As we show in this review, with a few exceptions, most of the genetic loci identified to date have not been replicated or validated in sufficiently powered cohort studies, suggesting that only a small fraction of variance in

host response is likely due to genetic variation. To address the role of host genetic variation in immune response to HCMV and CMV disease, large prospective studies and genome-wide approaches are required to securely identify causal variants involved in immune response and pathophysiological mechanisms leading to CMV disease.

AUTHOR CONTRIBUTIONS

ES designed the study, conducted literature research, and wrote and edited the manuscript. PA and CW wrote and edited the manuscript.

FUNDING

This project has been funded in whole or in part with federal funds from the National Cancer Institute, National Institutes of Health, under contract HHSN26120080001E. This research was supported in part by the Intramural Research Program of the NIH, National Cancer Institute, Center for Cancer Research. The content of this publication does not necessarily reflect the views or policies of the Department of Health and Human Services, nor does mention of trade names, commercial products, or organizations imply endorsement by the U.S. Government.

The funders had no role in study design, data collection and analysis, decision to publish, or preparation of the manuscript.

REFERENCES

Alakulppi, N. S., Kyllonen, L. E., Salo, H. M., Partanen, J., Salmela, K. T., and Laine, J. T. (2006). The impact of donor cytokine gene polymorphisms on the incidence of cytomegalovirus infection after kidney transplantation. *Transpl. Immunol.* 16 (3–4), 258–262. doi: 10.1016/j.trim.2006.09.007

Annibali, O., Piccioni, L., Tomarchio, V., Circhetta, E., Sarlo, C., Franceschini, L., et al. (2018). Impact of IFN lambda 3/4 single nucleotide polymorphisms on the cytomegalovirus reactivation in autologous stem cell transplant patients. *PLoS One* 13 (7), e0200221. doi: 10.1371/journal.pone.0200221

Arvin, A. M., Fast, P., Myers, M., Plotkin, S., Rabinovich, R., and National Vaccine Advisory Committee (2004). Vaccine development to prevent cytomegalovirus disease: report from the National Vaccine Advisory Committee. *Clin. Infect. Dis.* 39 (2), 233–239. doi: 10.1086/421999

Asanuma, H., Numazaki, K., Nagata, N., and Chiba, S. (1995). Cytokine response and polymerase chain reaction study of peripheral blood mononuclear cells in infants with human cytomegalovirus infection. *FEMS Immunol. Med. Microbiol.* 12 (2), 153–158. doi: 10.1111/j.1574-695X.1995.tb00187.x

Atalay, R., Zimmermann, A., Wagner, M., Borst, E., Benz, C., Messerle, M., et al. (2002). Identification and expression of human cytomegalovirus transcription units coding for two distinct Fcgamma receptor homologs. *J. Virol.* 76 (17), 8596–8608. doi: 10.1128/JVI.76.17.8596-8608.2002

Beam, E., and Razonable, R. R. (2012). Cytomegalovirus in solid organ transplantation: epidemiology, prevention, and treatment. *Curr. Infect. Dis. Rep.* 14 (6), 633–641. doi: 10.1007/s11908-012-0292-2

Bibert, S., Wojtowicz, A., Taffe, P., Manuel, O., Bernasconi, E., Furrer, H., et al. (2014). The IFNL3/4 DeltaG variant increases susceptibility to cytomegalovirus retinitis among HIV-infected patients. *AIDS* 28 (13), 1885–1889. doi: 10.1097/QAD.0000000000000379

Biron, C. A., and Tarrio, M. L. (2015). Immunoregulatory cytokine networks: 60 years of learning from murine cytomegalovirus. *Med. Microbiol. Immunol.* 204 (3), 345–354. doi: 10.1007/s00430-015-0412-3

Boehme, K. W., Guerrero, M., and Compton, T. (2006). Human cytomegalovirus envelope glycoproteins B and H are necessary for TLR2 activation in permissive cells. *J. Immunol.* 177 (10), 7094–7102. doi: 10.4049/jimmunol.177.10.7094

Boppana, S. B., Fowler, K. B., Britt, W. J., Stagno, S., and Pass, R. F. (1999). Symptomatic congenital cytomegalovirus infection in infants born to mothers with preexisting immunity to cytomegalovirus. *Pediatrics* 104 (1 Pt 1), 55–60. doi: 10.1542/peds.104.1.55

Boppana, S. B., Pass, R. F., Britt, W. J., Stagno, S., and Alford, C. A. (1992). Symptomatic congenital cytomegalovirus infection: neonatal morbidity and mortality. *Pediatr. Infect. Dis. J.* 11 (2), 93–99. doi: 10.1097/00006454-199202000-00007

Bravo, D., Solano, C., Gimenez, E., Remigia, M. J., Corrales, I., Amat, P., et al. (2014). Effect of the IL28B Rs12979860 C/T polymorphism on the incidence and features of active cytomegalovirus infection in allogeneic stem cell transplant patients. *J. Med. Virol.* 86 (5), 838–844. doi: 10.1002/jmv.23865

Cannon, M. J. (2009). Congenital cytomegalovirus (CMV) epidemiology and awareness. *J. Clin. Virol.* 46 Suppl 4, S6–S10. doi: 10.1016/j.jcv.2009.09.002

Cervera, C., Lozano, F., Saval, N., Gimferrer, I., Ibanez, A., Suarez, B., et al. (2007). The influence of innate immunity gene receptors polymorphisms in renal transplant infections. *Transplantation* 83 (11), 1493–1500. doi: 10.1097/01.tp.0000264999.71318.2b

Cobbs, C. S. (2011). Evolving evidence implicates cytomegalovirus as a promoter of malignant glioma pathogenesis. *Herpesviridae* 2 (1), 10. doi: 10.1186/2042-4280-2-10

Cobbs, C. S., Harkins, L., Samanta, M., Gillespie, G. Y., Bharara, S., King, P. H., et al. (2002). Human cytomegalovirus infection and expression in human malignant glioma. *Cancer Res.* 62 (12), 3347–3350.

Cope, A. V., Sabin, C., Burroughs, A., Rolles, K., Griffiths, P. D., and Emery, V. C. (1997). Interrelationships among quantity of human cytomegalovirus (HCMV) DNA in blood, donor-recipient serostatus, and administration of methylprednisolone as risk factors for HCMV disease following liver transplantation. *J. Infect. Dis.* 176 (6), 1484–1490. doi: 10.1086/514145

Corrales, I., Gimenez, E., Solano, C., Amat, P., de la Camara, R., Nieto, J., et al. (2015). Incidence and dynamics of active cytomegalovirus infection in allogeneic stem cell transplant patients according to single nucleotide polymorphisms in donor and recipient CCR5, MCP-1, IL-10, and TLR9 genes. *J. Med. Virol.* 87 (2), 248–255. doi: 10.1002/jmv.24050

Corrales, I., Solano, C., Amat, P., Gimenez, E., de la Camara, R., Nieto, J., et al. (2017). IL28B genetic variation and cytomegalovirus-specific T-cell immunity in allogeneic stem cell transplant recipients. *J. Med. Virol.* 89 (4), 685–695. doi: 10.1002/jmv.24676

Crough, T., and Khanna, R. (2009). Immunobiology of human cytomegalovirus: from bench to bedside. *Clin. Microbiol. Rev.* 22 (1), 76–98. doi: 10.1128/CMR.00034-08

Davison, A. J. (2007). "Overview of classification," in *Human Herpesviruses: Biology, Therapy, and Immunoprophylaxis*. Eds. A. Arvin, G. Campadelli-Fiume, E. Mocarski, et al. (Cambridge: Cambridge University Press).

Davison, A. J., and Bhella, D. (2007). "Comparative genome and virion structure," in *Human Herpesviruses: Biology, Therapy, and Immunoprophylaxis*. Eds. A. Arvin, G. Campadelli-Fiume, E. Mocarski, et al. (Cambridge: Cambridge University Press).

Deghaide, N. H., Rodrigues Mde, L., Castelli, E. C., Mendes-Junior, C. T., Figueiredo, J. F., and Donadi, E. A. (2009). Tumor necrosis factor region polymorphisms are associated with AIDS and with cytomegalovirus retinitis. *AIDS* 23 (13), 1641–1647. doi: 10.1097/QAD.0b013e32832e5591

Dolan, A., Cunningham, C., Hector, R. D., Hassan-Walker, A. F., Lee, L., Addison, C., et al. (2004). Genetic content of wild-type human cytomegalovirus. *J. Gen. Virol.* 85 (Pt 5), 1301–1312. doi: 10.1099/vir.0.79888-0

Dunn, J. P., and Jabs, D. A. (1995). Cytomegalovirus retinitis in AIDS: natural history, diagnosis, and treatment. *AIDS Clin. Rev.*, 99–129.

Egli, A., Levin, A., Santer, D. M., Joyce, M., O'Shea, D., Thomas, B. S., et al. (2014). Immunomodulatory Function of Interleukin 28B during primary infection with cytomegalovirus. *J. Infect. Dis.* 210 (5), 717–727. doi: 10.1093/infdis/jiu144

Eldar-Yedidia, Y., Hillel, M., Cohen, A., Bar-Meir, M., Freier-Dror, Y., and Schlesinger, Y. (2017). Association of toll-like receptors polymorphism and intrauterine transmission of cytomegalovirus. *PLoS One* 12 (12), e0189921. doi: 10.1371/journal.pone.0189921

Faist, B., Fleischer, B., and Jacobsen, M. (2010). Cytomegalovirus infection- and age-dependent changes in human CD8+ T-cell cytokine expression patterns. *lin. Vaccine Immunol.* 17 (6), 986–992. doi: 10.1128/CVI.00455-09

Falagas, M. E., Arbo, M., Ruthazer, R., Griffith, J. L., Werner, B. G., Rohrer, R., et al. (1997). Cytomegalovirus disease is associated with increased cost and hospital length of stay among orthotopic liver transplant recipients. *Transplantation* 63 (11), 1595–1601. doi: 10.1097/00007890-199706150-00010

Fernandez-Ruiz, M., Corrales, I., Arias, M., Campistol, J. M., Gimenez, E., Crespo, J., et al. (2015). Association between individual and combined SNPs in genes related to innate immunity and incidence of CMV infection in seropositive kidney transplant recipients. *Am. J. Transplant.* 15 (5), 1323–1335. doi: 10.1111/ajt.13107

Fields, B. N., Knipe, D. M., Howley, P. M., and Griffin, D. E. (2001). *Fields virology*. Philadelphia: Lippincott Williams & Wilkins.

Forconi, C., Gatault, P., Miquelestorena-Standley, E., Noble, J., Al-Hajj, S., Guillemain, R., et al. (2017). Polymorphism in programmed cell death 1 gene is strongly associated with lung and kidney allograft survival in recipients from CMV-positive donors. *J. Heart Lung Transplant.* 36 (3), 315–324. doi: 10.1016/j.healun.2016.08.014

Franceschini, D., Paroli, M., Francavilla, V., Videtta, M., Morrone, S., Labbadia, G., et al. (2009). PD-L1 negatively regulates CD4+CD25+Foxp3+ Tregs by limiting STAT-5 phosphorylation in patients chronically infected with HCV. *J. Clin. Invest.* 119 (3), 551–564. doi: 10.1172/JCI36604

Gallant, J. E., Moore, R. D., Richman, D. D., Keruly, J., and Chaisson, R. E. (1992). Incidence and natural history of cytomegalovirus disease in patients with advanced human immunodeficiency virus disease treated with zidovudine. The Zidovudine Epidemiology Study Group. *J. Infect. Dis.* 166 (6), 1223–1227. doi: 10.1093/infdis/166.6.1223

Gaytant, M. A., Steegers, E. A., Semmekrot, B. A., Merkus, H. M., and Galama, J. M. (2002). Congenital cytomegalovirus infection: review of the epidemiology and outcome. *Obstet. Gynecol. Surv.* 57 (4), 245–256. doi: 10.1097/00006254-200204000-00024

Griffiths, P. D., and Boeckh, M. (2007). "Antiviral therapy for human cytomegalovirus," in *Human Herpesviruses: Biology, Therapy, and Immunoprophylaxis*. Eds. A. Arvin, G. Campadelli-Fiume, E. Mocarski, et al. (Cambridge: Cambridge University Press).

Hamilton, S. T., Scott, G., Naing, Z., Iwasenko, J., Hall, B., Graf, N., et al. (2012). Human cytomegalovirus-induces cytokine changes in the placenta with implications for adverse pregnancy outcomes. *PLoS One* 7 (12), e52899. doi: 10.1371/journal.pone.0052899

Hanahan, D., and Weinberg, R. A. (2011). Hallmarks of cancer: the next generation. *Cell* 144 (5), 646–674. doi: 10.1016/j.cell.2011.02.013

Harkins, L. E., Matlaf, L. A., Soroceanu, L., Klemm, K., Britt, W. J., Wang, W., et al. (2010). Detection of human cytomegalovirus in normal and neoplastic breast epithelium. *Herpesviridae* 1 (1), 8. doi: 10.1186/2042-4280-1-8

Hayes, C. N., Imamura, M., Aikata, H., and Chayama, K. (2012). Genetics of IL28B and HCV–response to infection and treatment. *Nat. Rev. Gastroenterol. Hepatol.* 9 (7), 406–417. doi: 10.1038/nrgastro.2012.101

Heiden, D., Ford, N., Wilson, D., Rodriguez, W. R., Margolis, T., Janssens, B., et al. (2007). Cytomegalovirus retinitis: the neglected disease of the AIDS pandemic. *PLoS Med.* 4 (12), e334. doi: 10.1371/journal.pmed.0040334

Heineman, T. C. (2007). "Human cytomegalovirus vaccines," in *Human Herpesviruses: Biology, Therapy, and Immunoprophylaxis*. Eds. A. Arvin, G. Campadelli-Fiume, E. Mocarski, et al. (Cambridge: Cambridge University Press).

Ho, M. (1990). Epidemiology of cytomegalovirus infections. *Rev. Infect. Dis.* 12 Suppl 7, S701–S710. doi: 10.1093/clinids/12.Supplement_7.S701

Hoffmann, T. W., Halimi, J. M., Buchler, M., Velge-Roussel, F., Goudeau, A., Al Najjar, A., et al. (2008). Association between a polymorphism in the IL-12p40 gene and cytomegalovirus reactivation after kidney transplantation. *Transplantation* 85 (10), 1406–1411. doi: 10.1097/TP.0b013e31816c7dc7

Hoffmann, T. W., Halimi, J. M., Buchler, M., Velge-Roussel, F., Goudeau, A., Al-Najjar, A., et al. (2010). Association between a polymorphism in the human programmed death-1 (PD-1) gene and cytomegalovirus infection after kidney transplantation. *J. Med. Genet.* 47 (1), 54–58. doi: 10.1136/jmg.2009.068841

Jablonska, A., Paradowska, E., Studzinska, M., Suski, P., Nowakowska, D., Wisniewska-Ligier, M., et al. (2014). Relationship between toll-like receptor 2 Arg677Trp and Arg753Gln and toll-like receptor 4 Asp299Gly polymorphisms and cytomegalovirus infection. *Int. J. Infect. Dis.* 25, 11–15. doi: 10.1016/j.ijid.2014.04.001

Jabs, D. A. (1995). Ocular manifestations of HIV infection. *Trans. Am. Ophthalmol. Soc.* 93, 623–683.

Jonjic, S., Pavic, I., Polic, B., Crnkovic, I., Lucin, P., and Koszinowski, U. H. (1994). Antibodies are not essential for the resolution of primary cytomegalovirus infection but limit dissemination of recurrent virus. *J. Exp. Med.* 179 (5), 1713–1717. doi: 10.1084/jem.179.5.1713

Kang, S. H., Abdel-Massih, R. C., Brown, R. A., Dierkhising, R. A., Kremers, W. K., and Razonable, R. R. (2012). Homozygosity for the toll-like receptor 2 R753Q single-nucleotide polymorphism is a risk factor for cytomegalovirus disease after liver transplantation. *J. Infect. Dis.* 205 (4), 639–646. doi: 10.1093/infdis/jir819

Kasztelewicz, B., Czech-Kowalska, J., Lipka, B., Milewska-Bobula, B., Borszewska-Kornacka, M. K., Romanska, J., et al. (2017). Cytokine gene polymorphism associations with congenital cytomegalovirus infection and sensorineural hearing loss. *Eur. J. Clin. Microbiol. Infect. Dis.* 36 (10), 1811–1818. doi: 10.1007/s10096-017-2996-6

Kielsen, K., Enevold, C., Heilmann, C., Sengelov, H., Pedersen, A. E., Ryder, L. P., et al. (2018). Donor genotype in the interleukin-7 receptor alpha-chain predicts risk of graft-versus-host disease and cytomegalovirus infection after allogeneic hematopoietic stem cell transplantation. *Front. Immunol.* 9, 109. doi: 10.3389/fimmu.2018.00109

Kijpittayarit, S., Eid, A. J., Brown, R. A., Paya, C. V., and Razonable, R. R. (2007). Relationship between Toll-like receptor 2 polymorphism and cytomegalovirus disease after liver transplantation. *Clin. Infect. Dis.* 44 (10), 1315–1320. doi: 10.1086/514339

Kilpatrick, D. C. (2002). Mannan-binding lectin: clinical significance and applications. *Biochim. Biophys. Acta* 1572 (2-3), 401–413. doi: 10.1016/S0304-4165(02)00321-5

Kim, W. R., Badley, A. D., Wiesner, R. H., Porayko, M. K., Seaberg, E. C., Keating, M. R., et al. (2000). The economic impact of cytomegalovirus infection after liver transplantation. *Transplantation* 69 (3), 357–361. doi: 10.1097/00007890-200002150-00008

Koch, S., Larbi, A., Ozcelik, D., Solana, R., Gouttefangeas, C., Attig, S., et al. (2007). Cytomegalovirus infection: a driving force in human T cell immunosenescence. *Ann. N. Y. Acad. Sci.* 1114, 23–35. doi: 10.1196/annals.1396.043

Koch, S., Solana, R., Dela Rosa, O., and Pawelec, G. (2006). Human cytomegalovirus infection and T cell immunosenescence: a mini review. *Mech. Ageing Dev.* 127 (6), 538–543. doi: 10.1016/j.mad.2006.01.011

Kotenko, S. V. (2011). IFN-lambdas. *Curr. Opin. Immunol.* 23 (5), 583–590. doi: 10.1016/j.coi.2011.07.007

Kotton, C. N. (2013). CMV: prevention, diagnosis and therapy. *Am. J. Transplant.* 13 Suppl 3, 24–40. doi: 10.1111/ajt.12006

Kuparinen, T., Seppala, I., Jylhava, J., Marttila, S., Aittoniemi, J., Kettunen, J., et al. (2012). Genome-wide association study does not reveal major genetic determinants for anti-cytomegalovirus antibody response. *Genes Immun.* 13 (2), 184–190. doi: 10.1038/gene.2011.71

Landini, M. P. (1993). New approaches and perspectives in cytomegalovirus diagnosis. *Prog. Med. Virol.* 40, 157–177.

Liu, F., and Zhou, Z. H. (2007). "Comparative virion structures of human herpesviruses," in *Human Herpesviruses: Biology, Therapy, and Immunoprophylaxis*. Eds. A. Arvin, G. Campadelli-Fiume, E. Mocarski, et al. (Cambridge: Cambridge University Press).

Ljungman, P., Griffiths, P., and Paya, C. (2002). Definitions of cytomegalovirus infection and disease in transplant recipients. *Clin. Infect. Dis.* 34 (8), 1094–1097. doi: 10.1086/339329

Loeffler, J., Steffens, M., Arlt, E. M., Toliat, M. R., Mezger, M., Suk, A., et al. (2006). Polymorphisms in the genes encoding chemokine receptor 5, interleukin-10, and monocyte chemoattractant protein 1 contribute to cytomegalovirus reactivation and disease after allogeneic stem cell transplantation. *J. Clin. Microbiol.* 44 (5), 1847–1850. doi: 10.1128/JCM.44.5.1847-1850.2006

Lowance, D., Neumayer, H. H., Legendre, C. M., Squifflet, J. P., Kovarik, J., Brennan, P. J., et al. (1999). Valacyclovir for the prevention of cytomegalovirus disease after renal transplantation. International Valacyclovir Cytomegalovirus Prophylaxis Transplantation Study Group. *N. Engl. J. Med.* 340 (19), 1462–1470. doi: 10.1056/NEJM199905133401903

Madsen, H. O., Garred, P., Thiel, S., Kurtzhals, J. A., Lamm, L. U., Ryder, L. P., et al. (1995). Interplay between promoter and structural gene variants control basal serum level of mannan-binding protein. *J. Immunol.* 155 (6), 3013–3020.

Manuel, O., Pascual, M., Trendelenburg, M., and Meylan, P. R. (2007). Association between mannose-binding lectin deficiency and cytomegalovirus infection

after kidney transplantation. *Transplantation* 83 (3), 359–362. doi: 10.1097/01.tp.0000251721.90688.c2

Manuel, O., Wojtowicz, A., Bibert, S., Mueller, N. J., van Delden, C., Hirsch, H. H., et al. (2015). Influence of IFNL3/4 polymorphisms on the incidence of cytomegalovirus infection after solid-organ transplantation. *J. Infect. Dis.* 211 (6), 906–914. doi: 10.1093/infdis/jiu557

McSharry, B. P., Avdic, S., and Slobedman, B. (2012). Human cytomegalovirus encoded homologs of cytokines, chemokines and their receptors: roles in immunomodulation. *Viruses* 4 (11), 2448–2470. doi: 10.3390/v4112448

Mezger, M., Steffens, M., Semmler, C., Arlt, E. M., Zimmer, M., Kristjanson, G. I., et al. (2008). Investigation of promoter variations in dendritic cell-specific ICAM3-grabbing non-integrin (DC-SIGN) (CD209) and their relevance for human cytomegalovirus reactivation and disease after allogeneic stem-cell transplantation. *Clin. Microbiol. Infect.* 14 (3), 228–234. doi: 10.1111/j.1469-0691.2007.01902.x

Mitsani, D., Nguyen, M. H., Girnita, D. M., Spichty, K., Kwak, E. J., Silveira, F. P., et al. (2011). A polymorphism linked to elevated levels of interferon-gamma is associated with an increased risk of cytomegalovirus disease among Caucasian lung transplant recipients at a single center. *J. Heart Lung Transplant.* 30 (5), 523–529. doi: 10.1016/j.healun.2010.11.008

Morell, A., Scherz, R., Kaser, H., and Skvaril, F. (1977). Evidence for an association between uncommon Gm phenotypes and neuroblastoma. *Lancet* 1 (8001), 23–24. doi: 10.1016/S0140-6736(77)91657-9

Muntasell, A., Vilches, C., Angulo, A., and Lopez-Botet, M. (2013). Adaptive reconfiguration of the human NK-cell compartment in response to cytomegalovirus: a different perspective of the host-pathogen interaction. *Eur. J. Immunol.* 43 (5), 1133–1141. doi: 10.1002/eji.201243117

Murphy, E., Rigoutsos, I., Shibuya, T., and Shenk, T. E. (2003a). Reevaluation of human cytomegalovirus coding potential. *Proc. Natl. Acad. Sci. U.S.A.* 100 (23), 13585–13590. doi: 10.1073/pnas.1735466100

Murphy, E., Yu, D., Grimwood, J., Schmutz, J., Dickson, M., Jarvis, M. A., et al. (2003b). Coding potential of laboratory and clinical strains of human cytomegalovirus. *Proc. Natl. Acad. Sci. U.S.A.* 100 (25), 14976–14981. doi: 10.1073/pnas.2136652100

Nabekura, T., and Lanier, L. L. (2016). Tracking the fate of antigen-specific versus cytokine-activated natural killer cells after cytomegalovirus infection. *J. Exp. Med.* 213 (12), 2745–2758. doi: 10.1084/jem.20160726

Namboodiri, A. M., and Pandey, J. P. (2011). The human cytomegalovirus TRL11/IRL11-encoded FcgammaR binds differentially to allelic variants of immunoglobulin G1. *Arch. Virol.* 156 (5), 907–910. doi: 10.1007/s00705-011-0937-8

Pandey, J. P., Kistner-Griffin, E., Iwasaki, M., Bu, S., Deepe, R., Black, L., et al. (2012). Genetic markers of immunoglobulin G and susceptibility to breast cancer. *Hum. Immunol.* 73 (11), 1155–1158. doi: 10.1016/j.humimm.2012.07.340

Pandey, J. P. (2014a). Immunoglobulin GM genes, cytomegalovirus immunoevasion, and the risk of glioma, neuroblastoma, and breast cancer. *Front. Oncol.* 4, 236. doi: 10.3389/fonc.2014.00236

Pandey, J. P., Kaur, N., Costa, S., Amorim, J., Nabico, R., Linhares, P., et al. (2014b). Immunoglobulin genes implicated in glioma risk. *Oncoimmunology* 3, e28609. doi: 10.4161/onci.28609

Pandey, J. P., Kistner-Griffin, E., Radwan, F. F., Kaur, N., Namboodiri, A. M., Black, L., et al. (2014c). Immunoglobulin genes influence the magnitude of humoral immunity to cytomegalovirus glycoprotein B. *J. Infect. Dis.* 210 (11), 1823–1826. doi: 10.1093/infdis/jiu367

Pandey, J. P., Gao, G., Namboodiri, A. M., Iwasaki, M., Kasuga, Y., Hamada, G. S., et al. (2016). Humoral immunity to cytomegalovirus glycoprotein B in patients with breast cancer and matched controls: contribution of immunoglobulin gamma, kappa, and Fcgamma receptor genes. *J. Infect. Dis.* 213 (4), 611–617. doi: 10.1093/infdis/jiv472

Pandey, J. P., Namboodiri, A. M., Mohan, S., Nietert, P. J., and Peterson, L. (2017). Genetic markers of immunoglobulin G and immunity to cytomegalovirus in patients with breast cancer. *Cell Immunol.* 312, 67–70. doi: 10.1016/j.cellimm.2016.11.003

Paradowska, E., Jablonska, A., Studzinska, M., Skowronska, K., Suski, P., Wisniewska-Ligier, M., et al. (2016). TLR9 -1486T/C and 2848C/T SNPs are associated with human cytomegalovirus infection in infants. *PLoS One* 11 (4), e0154100. doi: 10.1371/journal.pone.0154100

Pass, R. F. (1985). Epidemiology and transmission of cytomegalovirus. *J. Infect. Dis.* 152 (2), 243–248. doi: 10.1093/infdis/152.2.243

Pawelec, G. (2014). Immunosenenescence: role of cytomegalovirus. *Exp. Gerontol.* 54, 1–5. doi: 10.1016/j.exger.2013.11.010

Pawelec, G., Derhovanessian, E., Larbi, A., Strindhall, J., and Wikby, A. (2009). Cytomegalovirus and human immunosenescence. *Rev. Med. Virol.* 19 (1), 47–56. doi: 10.1002/rmv.598

Piao, Z., Kim, H. J., Choi, J. Y., Hong, C. R., Lee, J. W., Kang, H. J., et al. (2016). Effect of FOXP3 polymorphism on the clinical outcomes after allogeneic hematopoietic stem cell transplantation in pediatric acute leukemia patients. *Int. Immunopharmacol.* 31, 132–139. doi: 10.1016/j.intimp.2015.12.022

Plotkin, S. A. (2002). Is there a formula for an effective CMV vaccine? *J. Clin. Virol.* 25 Suppl 2, S13–S21. doi: 10.1016/S1386-6532(02)00093-8

Plotkin, S. A. (2004). Congenital cytomegalovirus infection and its prevention. *Clin. Infect. Dis.* 38 (7), 1038–1039. doi: 10.1086/382542

Plotkin, S. A., and Boppana, S. B. (2018). Vaccination against the human cytomegalovirus. *Vaccine*. doi: 10.1016/j.vaccine.2018.02.089

Plotkin, S. A., Higgins, R., Kurtz, J. B., Morris, P. J., Campbell, D. A., Jr., Shope, T. C., et al. (1994). Multicenter trial of Towne strain attenuated virus vaccine in seronegative renal transplant recipients. *Transplantation* 58 (11), 1176–1178. doi: 10.1097/00007890-199412270-00006

Ramanan, P., and Razonable, R. R. (2013). Cytomegalovirus infections in solid organ transplantation: a review. *Infect. Chemother.* 45 (3), 260–271. doi: 10.3947/ic.2013.45.3.260

Razonable, R. R. (2005). Epidemiology of cytomegalovirus disease in solid organ and hematopoietic stem cell transplant recipients. *Am. J. Health Syst. Pharm.* 62 (8 Suppl 1), S7–S13. doi: 10.1093/ajhp/62.suppl_1.S7

Reddehase, M. J. (2013). *Cytomegaloviruses: from molecular pathogenesis to intervention*. Norfolk: Caister academic Press.

Rohn, H., Tomoya Michita, R., Schwich, E., Dolff, S., Gackler, A., Trilling, M., et al. (2018). The donor major histocompatibility complex class I chain-related molecule A allele rs2596538 G predicts cytomegalovirus viremia in kidney transplant recipients. *Front. Immunol.* 9, 917. doi: 10.3389/fimmu.2018.00917

Rubicz, R., Yolken, R., Drigalenko, E., Carless, M. A., Dyer, T. D., Kent, J., Jr., et al. (2015). Genome-wide genetic investigation of serological measures of common infections. *Eur. J. Hum. Genet.* 23 (11), 1544–1548. doi: 10.1038/ejhg.2015.24

Schleiss, M. R., Bourne, N., Stroup, G., Bravo, F. J., Jensen, N. J., and Bernstein, D. I. (2004). Protection against congenital cytomegalovirus infection and disease in guinea pigs, conferred by a purified recombinant glycoprotein B vaccine. *J. Infect. Dis.* 189 (8), 1374–1381. doi: 10.1086/382751

Schleiss, M. R., Stroup, G., Pogorzelski, K., and McGregor, A. (2006). Protection against congenital cytomegalovirus (CMV) disease, conferred by a replication-disabled, bacterial artificial chromosome (BAC)-based DNA vaccine. *Vaccine* 24 (37-39), 6175–6186. doi: 10.1016/j.vaccine.2006.06.077

Schoppel, K., Schmidt, C., Einsele, H., Hebart, H., and Mach, M. (1998). Kinetics of the antibody response against human cytomegalovirus-specific proteins in allogeneic bone marrow transplant recipients. *J. Infect. Dis.* 178 (5), 1233–1243. doi: 10.1086/314428

Scott, G. M., Chow, S. S., Craig, M. E., Pang, C. N., Hall, B., Wilkins, M. R., et al. (2012). Cytomegalovirus infection during pregnancy with maternofetal transmission induces a proinflammatory cytokine bias in placenta and amniotic fluid. *J. Infect. Dis.* 205 (8), 1305–1310. doi: 10.1093/infdis/jis186

Sester, U., Presser, D., Dirks, J., Gartner, B. C., Kohler, H., and Sester, M. (2008). PD-1 expression and IL-2 loss of cytomegalovirus- specific T cells correlates with viremia and reversible functional anergy. *Am. J. Transplant.* 8 (7), 1486–1497. doi: 10.1111/j.1600-6143.2008.02279.x

Sezgin, E., Van Natta, M. L., Thorne, J. E., Puhan, M. A., Jabs, D. A., and Longitudinal Studies of the Ocular Complications od AIDS (SOCA) Research Group. (2018). Secular trends in opportunistic infections, cancers and mortality in patients with AIDS during the era of modern combination antiretroviral therapy. *HIV Med*. 19 (6), 411–419. doi: 10.1111/hiv.12609

Sezgin, E., Jabs, D. A., Hendrickson, S. L., Van Natta, M., Zdanov, A., Lewis, R. A., et al. (2010). Effect of host genetics on the development of cytomegalovirus retinitis in patients with AIDS. *J. Infect. Dis.* 202 (4), 606–613. doi: 10.1086/654814

Sezgin, E., van Natta, M. L., Ahuja, A., Lyon, A., Srivastava, S., Troyer, J. L., et al. (2011). Association of host genetic risk factors with the course of cytomegalovirus retinitis in patients infected with human immunodeficiency

virus. *Am. J. Ophthalmol.* 151 (6), 999–1006 e1004. doi: 10.1016/j.ajo.2010.11.029

Sharpe, A. H., Wherry, E. J., Ahmed, R., and Freeman, G. J. (2007). The function of programmed cell death 1 and its ligands in regulating autoimmunity and infection. *Nat. Immunol.* 8 (3), 239–245. doi: 10.1038/ni1443

Shin, L. Y., Sheth, P. M., Persad, D., Kovacs, C., Kain, T., Diong, C., et al. (2014). Impact of CMV therapy with valganciclovir on immune activation and the HIV viral load in semen and blood: an observational clinical study. *J. Acquir. Immune Defic. Syndr.* 65 (3), 251–258. doi: 10.1097/01.qai.0000435256.34306.c1

Stagno, S., and Cloud, G. A. (1990). Changes in the epidemiology of cytomegalovirus. *Adv. Exp. Med. Biol.* 278, 93–104. doi: 10.1007/978-1-4684-5853-4_10

Stagno, S., Dworsky, M. E., Torres, J., Mesa, T., and Hirsh, T. (1982a). Prevalence and importance of congenital cytomegalovirus infection in three different populations. *J. Pediatr.* 101 (6), 897–900. doi: 10.1016/S0022-3476(82)80006-1

Stagno, S., Pass, R. F., Dworsky, M. E., and Alford, C. A., Jr. (1982b). Maternal cytomegalovirus infection and perinatal transmission. *Clin. Obstet. Gynecol.* 25 (3), 563–576. doi: 10.1097/00003081-198209000-00014

Stagno, S., Pass, R. F., Dworsky, M. E., Henderson, R. E., Moore, E. G., Walton, P. D., et al. (1982c). Congenital cytomegalovirus infection: the relative importance of primary and recurrent maternal infection. *N. Engl. J. Med.* 306 (16), 945–949. doi: 10.1056/NEJM198204223061601

Stern-Ginossar, N., Weisburd, B., Michalski, A., Le, V. T., Hein, M. Y., Huang, S. X., et al. (2012). Decoding human cytomegalovirus. *Science* 338 (6110), 1088–1093. doi: 10.1126/science.1227919

Szala, A., Paradowska, E., Nowakowska, D., Swierzko, A. S., Dzierzanowska-Fangrat, K., Sokolowska, A., et al. (2011). Mannan-binding lectin-2 (MBL2) gene polymorphisms in prenatal and perinatal cytomegalovirus infections. *Mol. Immunol.* 48 (15-16), 2203–2206. doi: 10.1016/j.molimm.2011.06.220

Taher, C., de Boniface, J., Mohammad, A. A., Religa, P., Hartman, J., Yaiw, K. C., et al. (2013). High prevalence of human cytomegalovirus proteins and nucleic acids in primary breast cancer and metastatic sentinel lymph nodes. *PLoS One* 8 (2), e56795. doi: 10.1371/journal.pone.0056795

Taniguchi, R., Koyano, S., Suzutani, T., Goishi, K., Ito, Y., Morioka, I., et al. (2013). Polymorphisms in TLR-2 are associated with congenital cytomegalovirus (CMV) infection but not with congenital CMV disease. *Int. J. Infect. Dis.* 17 (12), e1092–e1097. doi: 10.1016/j.ijid.2013.06.004

van de Berg, P. J., Heutinck, K. M., Raabe, R., Minnee, R. C., Young, S. L., van Donselaar-van der Pant, K. A., et al. (2010). Human cytomegalovirus induces systemic immune activation characterized by a type 1 cytokine signature. *J. Infect. Dis.* 202 (5), 690–699. doi: 10.1086/655472

Vora, S. B., Brothers, A. W., Waghmare, A., and Englund, J. A. (2018). Antiviral combination therapy for cytomegalovirus infection in high-risk infants. *Antivir. Ther. (Lond.).* 23 (6), 505–511. doi: 10.3851/IMP3238

Vu, D., Shah, T., Ansari, J., Sakharkar, P., Yasir, Q., Naraghi, R., et al. (2014). Interferon-gamma gene polymorphism +874 A/T is associated with an increased risk of cytomegalovirus infection among Hispanic renal transplant recipients. *Transpl. Infect. Dis.* 16 (5), 724–732. doi: 10.1111/tid.12285

Whitley, R. J. (2004). Congenital cytomegalovirus infection: epidemiology and treatment. *Adv. Exp. Med. Biol.* 549, 155–160. doi: 10.1007/978-1-4419-8993-2_21

Wills, M. R., Carmichael, A. J., Sinclair, J., and Sissons, J. P. (2007). "Immunobiology and host response," in *Human Herpesviruses: Biology, Therapy, and Immunoprophylaxis*. Eds. A. Arvin, G. Campadelli-Fiume, E. Mocarski, et al. (Cambridge: Cambridge University Press).

Wistuba-Hamprecht, K., Frasca, D., Blomberg, B., Pawelec, G., and Derhovanessian, E. (2013). Age-associated alterations in gammadelta T-cells are present predominantly in individuals infected with Cytomegalovirus. *Immun. Ageing* 10 (1), 26. doi: 10.1186/1742-4933-10-26

Wolmer-Solberg, N., Baryawno, N., Rahbar, A., Fuchs, D., Odeberg, J., Taher, C., et al. (2013). Frequent detection of human cytomegalovirus in neuroblastoma: a novel therapeutic target? *Int. J. Cancer* 133 (10), 2351–2361. doi: 10.1002/ijc.28265

Wu, X., Yao, Y., Bao, X., Zhou, H., Tang, X., Han, Y., et al. (2016). KIR2DS4 and its variant KIR1D are associated with acute graft-versus-host disease, cytomegalovirus, and overall survival after sibling-related HLA-matched transplantation in patients with donors with KIR gene haplotype A. *Biol. Blood Marrow Transplant.* 22 (2), 220–225. doi: 10.1016/j.bbmt.2015.10.004

Wun, C. M., Piao, Z., Hong, K. T., Choi, J. Y., Hong, C. R., Park, J. D., et al. (2017). Effect of donor STAT4 polymorphism rs7574865 on clinical outcomes of pediatric acute leukemia patients after hematopoietic stem cell transplant. *Int. Immunopharmacol.* 43, 62–69. doi: 10.1016/j.intimp.2016.12.007

Wujcicka, W., Paradowska, E., Studzinska, M., Wilczynski, J., and Nowakowska, D. (2017a). TLR2 2258 G > A single nucleotide polymorphism and the risk of congenital infection with human cytomegalovirus. *Virol. J.* 14 (1), 12. doi: 10.1186/s12985-016-0679-z

Wujcicka, W., Paradowska, E., Studzinska, M., Wilczynski, J., and Nowakowska, D. (2017b). Toll-like receptors genes polymorphisms and the occurrence of HCMV infection among pregnant women. *Virol. J.* 14 (1), 64. doi: 10.1186/s12985-017-0730-8

Wujcicka, W., Wilczynski, J., Paradowska, E., Studzinska, M., and Nowakowska, D. (2017c). The role of single nucleotide polymorphisms, contained in proinflammatory cytokine genes, in the development of congenital infection with human cytomegalovirus in fetuses and neonates. *Microb. Pathog.* 105, 106–116. doi: 10.1016/j.micpath.2017.02.017

Wujcicka, W. I., Wilczynski, J. S., and Nowakowska, D. E. (2017d). Association of SNPs from IL1A, IL1B, and IL6 genes with human cytomegalovirus infection among pregnant women. *Viral Immunol.* 30 (4), 288–297. doi: 10.1089/vim.2016.0129

Zeevi, A., Spichty, K., Banas, R., Cai, J., Donnenberg, V. S., Donnenberg, A. D., et al. (1999). Clinical significance of cytomegalovirus-specific T helper responses and cytokine production in lung transplant recipients. *Intervirology* 42 (5–6), 291–300. doi: 10.1159/000053963

Zelini, P., Lilleri, D., Comolli, G., Rognoni, V., Chiesa, A., Fornara, C., et al. (2010). Human cytomegalovirus-specific CD4(+) and CD8(+) T-cell response determination: comparison of short-term (24h) assays vs long-term (7-day) infected dendritic cell assay in the immunocompetent and the immunocompromised host. *Clin. Immunol.* 136 (2), 269–281. doi: 10.1016/j.clim.2010.04.008

Conflict of Interest Statement: PA and CW are employees of Leidos Biomedical Research, Inc., and declare no competing interest.

The remaining authors declares that the research was conducted in the absence of any commercial or financial relationships that could be construed as a potential conflict of interest.

Copyright © 2019 Sezgin, An and Winkler. This is an open-access article distributed under the terms of the Creative Commons Attribution License (CC BY). The use, distribution or reproduction in other forums is permitted, provided the original author(s) and the copyright owner(s) are credited and that the original publication in this journal is cited, in accordance with accepted academic practice. No use, distribution or reproduction is permitted which does not comply with these terms.

frontiers in Genetics

REVIEW
published: 13 August 2019
doi: 10.3389/fgene.2019.00696

Host Genetic Determinants of Hepatitis B Virus Infection

*Zhenhua Zhang[1,2], Changtai Wang[3], Zhongping Liu[1], Guizhou Zou[1], Jun Li[2] and Mengji Lu[4]**

[1] Department of Infectious Diseases, the Second Affiliated Hospital of Anhui Medical University, Hefei, China, [2] College of Pharmacy, Anhui Medical University, Hefei, China, [3] Department of Infectious Diseases, the Affiliated Anqing Hospital of Anhui Medical University, Anqing, China, [4] Institute of Virology, University Hospital of Duisburg-Essen, Essen, Germany

Chronic hepatitis B virus (HBV) infection is still a major health problem worldwide. Recently, a great number of genetic studies based on single nucleotide polymorphisms (SNPs) and genome-wide association studies have been performed to search for host determinants of the development of chronic HBV infection, clinical outcomes, therapeutic efficacy, and responses to hepatitis B vaccines, with a focus on human leukocyte antigens (HLA), cytokine genes, and toll-like receptors. In addition to SNPs, gene insertions/deletions and copy number variants are associated with infection. However, conflicting results have been obtained. In the present review, we summarize the current state of research on host genetic factors and chronic HBV infection, its clinical type, therapies, and hepatitis B vaccine responses and classify published results according to their reliability. The potential roles of host genetic determinants of chronic HBV infection identified in these studies and their clinical significance are discussed. In particular, HLAs were relevant for HBV infection and pathogenesis. Finally, we highlight the need for additional studies with large sample sizes, well-matched study designs, appropriate statistical methods, and validation in multiple populations to improve the treatment of HBV infection.

Keywords: hepatitis B virus, genetic determinants, human leukocyte antigen, susceptibility gene, single nucleotide polymorphism, genome-wide association study

OPEN ACCESS

Edited by:
Cheryl Ann Winkler, Frederick National Laboratory for Cancer Research (NIH), United States

Reviewed by:
Michael Scheurer, Baylor College of Medicine, United States
Guangwen Cao, Second Military Medical University, China

***Correspondence:**
Mengji Lu
mengji.lu@uni-due.de

Specialty section:
This article was submitted to Applied Genetic Epidemiology, a section of the journal Frontiers in Genetics

Received: *07 November 2018*
Accepted: *03 July 2019*
Published: *13 August 2019*

Citation:
Zhang Z, Wang C, Liu Z, Zou G, Li J and Lu M (2019) Host Genetic Determinants of Hepatitis B Virus Infection. Front. Genet. 10:696. doi: 10.3389/fgene.2019.00696

INTRODUCTION

With 292 million people infected and a global prevalence of 3.9%, hepatitis B virus (HBV) infection is still a major global public health problem (Polaris Observatory Collaborators, 2018). The outcomes of HBV infection are highly diverse, including acute hepatitis, self-limiting recovery, chronic hepatitis, cirrhosis, liver cancer, and liver failure (**Figure 1**) (European Association For The Study Of The Liver, 2017). In the natural history of HBV infection, there is substantial variation in the course of disease development and clinical outcomes depending on the transmission pattern, timing of infection, sex, immune status, host genetic factors, and underlying diseases in infected individuals. The disease outcome is related to viral, environmental, and host factors (Ganem and Prince, 2004; Rehermann and Bertoletti, 2015). With respect to host factors, in addition to age, gender, alcohol, obesity, diabetes, and renal failure, host gene variants may also affect the clinical course of HBV infection (Laskus et al., 1992; He et al., 2006; Thursz et al., 2011; Yano et al., 2013; Matsuura et al., 2016). Since the implementation of the Human Genome Project, great progress has been made in genetic and disease-related research, providing a basis for advances in precision medicine. Host genetic polymorphisms mainly include single nucleotide polymorphisms (SNPs),

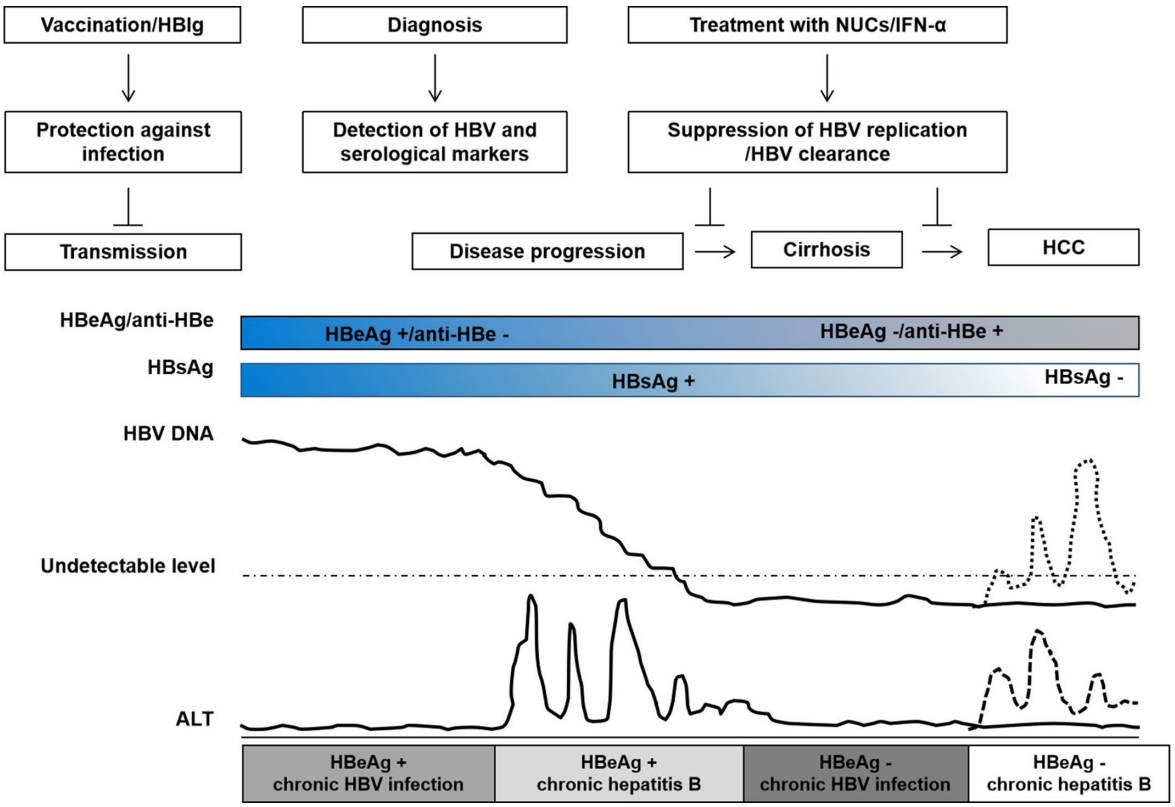

FIGURE 1 | Natural history of chronic hepatitis B virus (HBV) infection, interventions, and clinical outcomes. The natural history of HBV infection is typically classified into four clinical states: HBeAg+ chronic HBV infection, HBeAg+ chronic hepatitis, HBeAg– chronic HBV infection, and HBeAg– chronic hepatitis according to the guideline of European Association for the Study of the Liver (EASL). Patients with chronic HBV infection do not necessarily experience all states. HBV vaccine and/or HBIg injection may prevent HBV transmission; during HBeAg+ chronic hepatitis, treatment with nucleos(t)ide analogs (NUCs) or interferon-alpha (IFN-α) may suppress HBV replication, slow disease progression, and reduce the risk of cirrhosis and hepatocellular carcinoma; HBV reactivation may occur during HBeAg– chronic HBV infection in patients with HBsAg and/or anti-HBc positive after chemotherapy or immunosuppression. The course of HBV infection and disease progression are variable, indicating that host genetic determinants play an important role in HBV infection.

insertions/deletions, and copy number variations (CNVs). Owing to technological limitations, current research mainly focuses on the relationships between SNPs and susceptibility to diseases.

Two approaches are frequently used to screen susceptibility genes for HBV-related diseases and outcomes. First, genome-wide association study (GWAS) have become a common tool for genetic association research focused on complex diseases (Hardy and Singleton, 2009), including HBV infection. In the first stage of GWAS, patient samples are typically used to screen a large number of candidate SNP loci using TaqMan probes, SNPstream genotyping technology, SNaPshot genotyping, SNP chips, and other methods, with several rounds of validation to finally identify SNPs. Second, the traditional approach is the selection of candidate genes predicted to play a role in HBV-related diseases or treatment responses based on theory and previous analyses, followed by verification by comparisons of SNP genotype frequencies in patient and control groups.

Many clinical relevant aspects of HBV prevention, infection, and treatment are potentially related to host genetics (Kamatani et al., 2009; Mbarek et al., 2011; Brouwer et al., 2014; Chang et al., 2014; Hosaka et al., 2015; Jiang et al., 2015; Jiang et al., 2016a; Brouwer et al., 2019). Hepatitis B vaccines are widely used and effective for the prevention of new HBV infections. However, the overall success rate of hepatitis B vaccination is about 90% (Bruce et al., 2016; Hu et al., 2018). The outcome of HBV infection can vary dramatically, depending on both host and viral factors. A major part of patients do not experience clinically relevant symptoms during the acute infection phase while others have acute illness with symptoms that last several weeks. Without any intervention, about 95% of intrauterine or perinatal HBV infections but only about 5% in adults develop into chronic infections (Stevens et al., 1975; Wright and Lau, 1993; Petrova and Kamburov, 2010). HBV persistence is a major risk for developing chronic hepatitis B, cirrhosis, hepatocellular carcinoma, or acute liver failure (Wright and Lau, 1993; Zhang et al., 2013a). A small number of patients develop occult HBV infection (OBI) without detectable serum HBsAg but HBV DNA in the serum or liver (Torbenson and Thomas, 2002; Raimondo et al., 2008; Raimondo et al., 2019; Seed et al., 2019). Interferon-alpha (IFN-α) and nucleos(t)ide analogs (NUCs) have been approved and are widely used for the treatment of chronic hepatitis B (European Association

For The Study Of The Liver, 2017). Regimens such as antiviral treatment with tenofovir and entecavir provide results in viral suppression in around 95% of patients, have limited associated resistance, and prevent liver disease progression, cirrhosis, and HCC. However, these treatments do not regularly achieve clinical cure or HBsAg clearance and the incidence of cirrhosis or HCC is still significantly higher in treated patients than those without HBV infection (**Figure 1**). Many studies have shown that host genetic polymorphisms may influence HBV infection, including hepatitis B vaccine responses, chronic HBV infection (CHI), intrauterine transmission (IT), OBI, liver cirrhosis (LC), hepatocellular carcinoma (HCC), liver transplantation (LT), and the antiviral efficacy of IFNs and NUCs (Kamatani et al., 2009; Davila et al., 2010; Li et al., 2012b; Chang et al., 2014). These studies have demonstrated that host genetics play an important role in HBV infection and pathogenesis (**Figure 2**). Yet, many contradictory or ambiguous findings have been reported.

In this review, we summarize the current state of research on the role of host genetic determinants of CHI, its clinical type, therapeutic responses, and responses to hepatitis B vaccines (**Tables S2–7**). More than 500 publications varying in quality have focused on this topic. Thus, we assessed the reliability of these studies according to the sample size, type of technology, and analysis methods. Note that for great many genes related to HBI or vaccine efficacy, only a single study was available. For intrauterine infections, OBI, drug efficacy, and other factors, all published papers were included owing to the small sample size. We also considered whether there are valid contradictions among studies. We classified studies into three categories: very relevant (I), possibly relevant (II), and unable to confirm (III) (**Table 1**; **Table S1**), as a guide for readers. The topic of host genetics and end-stage liver diseases, including HCC, is reviewed by An et al. (An et al., 2018) in this special issue and therefore is not included in our review.

CHRONIC HBV INFECTION

Early epidemiological data showed that chronic HBV infection is very frequently established in infants born to HBV carrier mothers or in young children (Stevens et al., 1975; Li et al., 2015) and shows a strong gender disparity with significantly higher susceptibility of male patients (Lee et al., 1999; Su et al., 2007; Liaw et al., 2009; Wang et al., 2015). Adequate

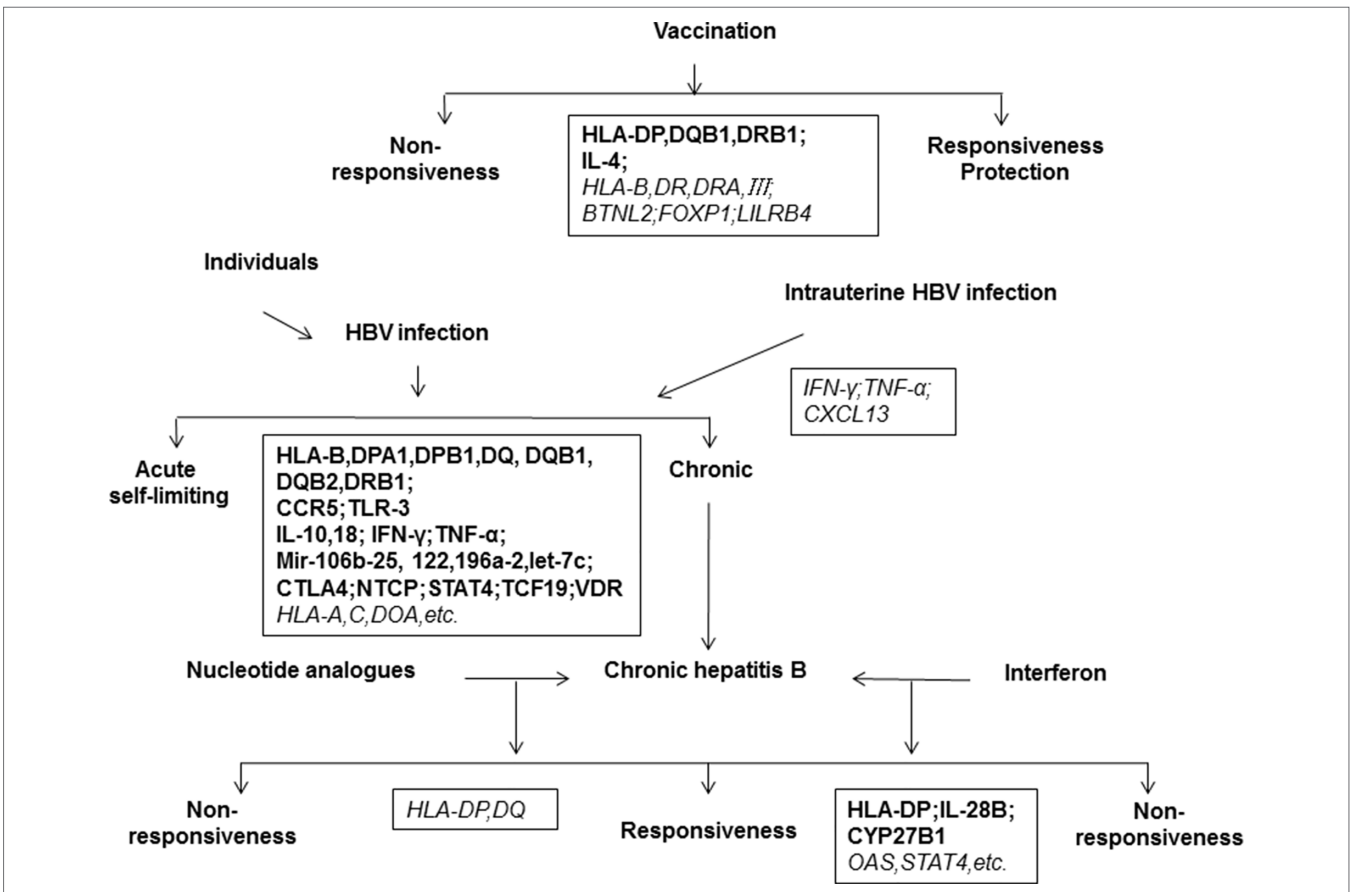

FIGURE 2 | Host genetic determinants of HBV infection. The outcomes of HBV infection are highly diverse, including acute hepatitis, self-limiting recovery, chronic hepatitis, cirrhosis, liver cancer, and liver failure. The disease outcome is related to viral, environmental, and host factors. This map shows important host genes that may be associated with clinical outcomes of HBV infection or Hepatitis B vaccination. Black boxes show the relevant genes identified, in which the bold letter indicates a high degree of correlation and the italic indicates a possible correlation to clinical features of HBV infection.

TABLE 1 | Classification of host genetic determinants associated with hepatitis B virus (HBV)-related liver diseases and responses to HBV vaccines.

Category	Relevance	Description
I	High	▲ Meta-analysis suggests that one or more SNP loci are associated with HBV-related diseases. ▲ More than three studies suggest that the same SNP locus is associated with HBV-related diseases.
II	Likely	▲ GWAS suggests that one or more SNP loci are associated with HBV-related diseases. ▲ At least two studies suggest that the same SNP locus is associated with HBV-related diseases. ▲ A single sample with a total sample size of more than 1,000 indicates that SNP loci are associated with disease.
III	Not fully confirmed	▲ A single study with a total sample size of less than 1,000 indicates that SNP loci are associated with HBV-related diseases. ▲ Meta-analysis suggest that there was no correlation, but some studies suggested a correlation with HBV-related diseases. ▲ The majority of studies suggest no correlation with HBV-related diseases. ▲ Single studies with a total sample size of more than 1,000 indicated no correlation with HBV-related diseases. ▲ The total sample size was less than 500 cases. ▲ For the same SNP loci, there are contradictions between different MA or GWAS. ▲ The sample size is greater than 1,000, and the results (the same SNP locus) of studies contradict each other. ▲ Less than two studies failed to show a correlation. ▲ A total sample size of 500–1,000 study subjects, and no correlation is found.

1. The total sample size refers to the sample size of a single study, including the experimental and control group.
2. The study groups of intrauterine infection, OBI, IFN-α, and NUCs were changed to 200 and 500 (500 and 1,000 for CHI and HBV vaccine groups, respectively), and the other assessment criteria remain the same.

host immune responses to HBV are essential for sustained viral control (Bertoletti and Gehring, 2006). HBV control is associated with vigorous, multi-specific T cell responses in the host. In chimpanzees, T cell depletion prevents HBV clearance (Thimme et al., 2003; Asabe et al., 2009; Hoogeveen et al., 2018), demonstrating the essential role of cellular immunity in HBV control. Chronic HBV infection is associated with impaired immune responses (Guidotti et al., 2015; Lebosse et al., 2017). Thus, great efforts have been made to identify associations between host immunogenetics and chronic HBV infection. A number of host genetic variants, such as mutations in human leukocyte antigens (HLAs), cytokine and chemokine genes, toll-like receptor (TLRs), microRNAs, vitamin D–related genes, and HBV receptor sodium taurocholate cotransporting polypeptide (NTCP), have been found to influence the outcome of HBV infection (**Table 2**; **Tables S1**, **S2**). The SNPs loci of genes very relevant or possibly relevant with chronic HBV infection are listed in **Table 2**. Other SNPs loci of genes that are still unable to confirm are listed in **Tables S1** and **S2**.

HLA is the human major histocompatibility complex (MHC) and a central element of antiviral immune defense (Shiina et al., 2009). HLA genes are classified as class I (HLA-A, B, C, E, F, and G) and II (HLA-DP, DQ, DR, DM, and DO) (Koller et al., 1989; van Lith et al., 2010). When a pathogen enters the body, it is engulfed by antigen-presenting cells (APCs) and the pathogen proteins are digested into small pieces and loaded onto HLA antigens. They are then displayed by APCs to T cells, which produce a variety of effector molecules to eliminate the pathogen. Therefore, HLAs can affect the outcome of infectious diseases (Singh et al., 2007; Goulder and Walker, 2012; Wang et al., 2016). Genetic polymorphisms, especially in HLA class II genes, are significantly associated with HBV infection and pathogenesis according to many studies (Kamatani et al., 2009; Zhang et al., 2014b; He et al., 2015; Wasityastuti et al., 2016; Trinks et al., 2017). Kamatani et al. (Kamatani et al., 2009) performed a GWAS of chronic HBV infection using 786 cases and 2,201 HBsAg seronegative controls in the Japanese population, followed by a replication study of three additional Japanese and Thai cohorts consisting of 1,300 cases and 2,100 controls. HLA-DPA1 rs3077 and HLA-DPB1 rs9277535 were significantly associated with chronic HBV infection in the Asian population (combined OR [95% CI] = 0.56 [0.51–0.61], $P = 2.31 \times 10^{-38}$; OR [95% CI] = 0.57 [0.52–0.62], $P = 6.34 \times 10^{-39}$, respectively). They also identified four associated haplotypes: HLA-DPA1*0202-DPB1*0501 and HLA-DPA1*0202-DPB1*0301 were associated with susceptibility to chronic hepatitis B and HLA-DPA1*0103-DPB1*0402 and HLA-DPA1*0103-DPB1*0401 showed a protective effect. Several GWAS of Asian populations have also shown that SNPs in HLA regions, such as HLA-DP (rs9277535, rs3077, rs9366816, and rs9277542), HLA-DQ (rs2856718, rs7453920, rs9276370, rs7756516, and rs7453920), HLA-DPB1 (positions 84–87), HLA-C (Leu-15, rs3130542, and rs2853953), HLA-DRB1*13, HLA-J (rs400488), and HLA-DOA (rs378352), are associated with chronic HBV infection (Mbarek et al., 2011; Nishida et al., 2012; Hu et al., 2013; Kim et al., 2013; Chang et al., 2014; Jiang et al., 2015; Zhu et al., 2016b). Many studies have provided evidence based on case–control samples and conventional PCR-based detection methods that HLA molecules may be crucial determinants of the outcomes of HBV infection in Asian, European, African-American, Saudi Arabian, and Caucasian populations (Thomas et al., 2012; Al-Qahtani et al., 2014; Trinks et al., 2017). However, some studies have reported contradictory results. A study of the Chinese Zhuang population found no association between HLA-DPA1 rs3077 and chronic HBV infection (Wang et al., 2011). Akgöllü et al. (Akgöllü et al., 2017) suggested that HLA-DP rs3077 is not associated with HBV infection in the Turkish population. Vermehren et al. (Vermehren et al., 2012) failed to confirm an association of HLA-DPB1 rs9277535 with hepatitis B in Caucasians. A comprehensive meta-analysis suggested that HLA-DP/DQ (rs3077, rs9277535, rs9275572, rs9275319, rs2856718, and rs7453920) is associated with susceptibility to HBV or the clearance of HBV infection (Zhang et al., 2013e; Yu et al., 2015; Xu et al., 2017b; Xu et al., 2018). A meta-analysis by Huang et al. (Huang et al., 2016) suggested that HLA-DQB1*0201, DQB1*0301, and DQB1*0502 are associated with an increased risk of CHB (chronic hepatitis B), while HLA-DQB1*0303 and DQB1*0604 are associated with a decreased risk of CHB.

TABLE 2 | Host genetic factors associated with chronic HBV infection.

Category	Gene ontology	Gene	Genetic determinants (SNP/Hap/CNVs)	Main reference
I	HLA	HLA-B	*07, *58	Seshasubramanian et al., 2018
		HLA-DPA1	rs3077	Kamatani et al., 2009; Mbarek et al., 2011; Yan et al., 2012b; Jiang et al., 2015
		HLA-DPB1	rs2281388, rs9277535, rs9277542	Kamatani et al., 2009; Mbarek et al., 2011; Nishida et al., 2012; Yan et al., 2012b; Zhang et al., 2013b; Jiang et al., 2015; Trinks et al., 2017
		HLA-DQ	rs9275319, rs9275572	Al-Qahtani et al., 2014; Zhang et al., 2014b; Kim et al., 2015; Xu et al., 2018
		HLA-DQB1	*0201, *0301, *0303, *0502, *0604, rs2856718	Mbarek et al., 2011; Jiang et al., 2015; Huang et al., 2016; Xu et al., 2017b; Xu et al., 2018
		HLA-DQB2	rs7453920	Hu et al., 2013; Jiang et al., 2015; Xu et al., 2017b; Xu et al., 2018
		HLA-DRB1	*13	Zhu et al., 2016b
	Cytokines	IL-10	−592	Cheong et al., 2006; Chen et al., 2010
		IL-18	−137	Karra et al., 2015
		IFN-γ	+874	Sun et al., 2015
		TNF-α	−238, −308, −857, −863	Kim et al., 2003; Cheong et al., 2006; Shi et al., 2012; Zheng et al., 2012
	Chemokines	CCR5	Δ32	Suneetha et al., 2006
	TLRs	TLR-3	rs3775291	Geng et al., 2016
	MicroRNAs	MiR-106b-25	rs999885	Liu et al., 2012b; Zhou et al., 2015
		miR-122	rs3783553	Zhou et al., 2015
		miR-196a-2	rs11614913	Zhou et al., 2015; Al-Qahtani et al., 2017
		miR-let-7c	rs6147150	Zhou et al., 2015
	Others	CTLA-4	rs231775, rs5742909	Schott et al., 2007; Huang et al., 2013; Xu et al., 2013
		NTCP	rs2296651	Hu et al., 2016; Wang et al., 2017a; Nfor et al., 2018
		STAT4	rs7574865	Kim et al., 2015; Jiang et al., 2016b
		TCF19	rs1419881	Kim et al., 2013; Jiang et al., 2015
		VDR	FokI	He et al., 2018
II	HLA	HLA-A	*33:03:01	Miao et al., 2013
		HLA-B	*13:01:01	Miao et al., 2013
		HLA-C	Leu-15, rs2853953, rs3130542	Hu et al., 2013; Jiang et al., 2015; Zhu et al., 2016b
		HLA-DOA	rs378352	Jiang et al., 2015
		HLA-DP	rs9366816	Chang et al., 2014
		HLA-DPA1	rs2301220, rs2395309, rs9277341	Guo et al., 2011; Li et al., 2011a
		HLA-DPB1	rs9277534, *0201, *0401, *0901, positions 84–87, *0402, *0501, *0201-*0401, *0201-*0402, *0201-*0501, *0401-*0402, *0401-*0501, *0402-*0402, *0402-*0501, *0501-*0501, *0501-*0901, *0501*others, rs9277378, rs10484569, rs3117222, rs9380343, rs3135021, G-A-G-A-T-T[1], G-G-G-G-T-C[2]	Guo et al., 2011; Thomas et al., 2012; Wong et al., 2013; Zhang et al., 2013e; Hu et al., 2014; Nishida et al., 2014; Nishida et al., 2015; Zhu et al., 2016b
		HLA-DQ	A1*0101-B1*0501, A1*0102-B1*0303, A1*0102-B1*0604, A1*0301-B1*0601, A1*0102-B1*0602, A1*0301-B1*0302, A1*0301-B1*0303, A1*0301-B1*0401, A1*0501-B1*0301	Mbarek et al., 2011
		HLA-DQA2	rs9276370	Chang et al., 2014
		HLA-DQB2	rs7756516	Chang et al., 2014
		HLA-DPA1/ DPB1	A-A[3], A-A[4], T-A-T[5],C-A-T[6],A1*0103-B1*0401, A1*0103-B1*0402, A1*0202-B1*0301, A1*0202-B1*0501, A-A-C-T[7], A-A-C-C//A-G-T-G-C-C[8], A-A-C-T//A-G-T-G-C-C[9], G-G-T-C//A-G-T-G-C-C[10]	Kamatani et al., 2009; Guo et al., 2011; Li et al., 2011a; Wang et al., 2011; Wong et al., 2013
		HLA-DP/DQ	T-T-G-A-T[11], T-T-G-G-T[12], carrying 4–6 variant alleles, G-A[13], A-G[14], A-A[15]	Hu et al., 2012; Chang et al., 2014; Al-Qahtani et al., 2014
		HLA-J	rs400488	Zhu et al., 2016b
	Cytokines	IL-10RB	rs2834167	Romporn et al., 2013; Ma et al., 2014
		IL-12B	rs3212227	He et al., 2015
		IL-16	rs11556218	Li et al., 2011b
		IL-21	rs2221903	Li et al., 2013a
		IFN-α2	p.Ala120Thr	Zhao et al., 2012
		IFN-αR2	rs1051393, rs12233338	Ma et al., 2018a
		IFNLR1	rs4649203, rs7525481	Ma et al., 2018a
		IFN-γR1	rs3799488	He et al., 2015
		IFN-γR2	rs1059293	He et al., 2015
		TNF-α	T-C-C-G-G-G[16], C-A-C-G-G-G[17]	Kim et al., 2003
		TGF-α	+106151, +103461, A-T-G-T-T-T-T-C-T[18]	Kim et al., 2009

(Continued)

TABLE 2 | Contiued

Category	Gene ontology	Gene	Genetic determinants (SNP/Hap/CNVs)	Main reference
	TLRs	TLR-3	rs1879026	Al-Qahtani et al., 2012a
		TLR-9	rs352140	He et al., 2015
	MicroRNAs	miR-30a	rs1358379	Al-Qahtani et al., 2017
		miR-101-2	rs12375841, T-C[19]	Bae et al., 2012
		miR-122	rs4309483	Liu et al., 2014b
		miR-219-1	rs107822, rs213210, rs421446, C-A-C[20], T-G-T[21]	Cheong et al., 2013
		miR-323b	rs56103835	Yu et al., 2014
		miR-423	rs6505162	Al-Qahtani et al., 2017
		miR-492	rs2289030	Al-Qahtani et al., 2017
	Others	C2	p.Glu318Asp, rs7746553, rs9267673, rs9267665, rs9267677, rs9279450, rs10947223	Zhao et al., 2012; Namgoong et al., 2018
		CD40	rs1883832	Jiang et al., 2015
		CFB	rs12614	Jiang et al., 2015
		CTLA-4	rs3087243, C-A-C-C-G[22], T/C-A-C-C-G[23], T-A-C-C-A[24]	Thio et al., 2004; Chen et al., 2010
		EHMT2	rs7887, rs652888, rs35875104, rs41267090	Jiang et al., 2015; Shin et al., 2017
		ESR1	+29	Deng et al., 2004
		IFN4/HLA-DQ	rs12971396-rs9275319, rs12971396-rs12979860-rs9275319	Fan et al., 2016a
		INST10	rs7000921	Li et al., 2016
		KIF1B	A-T-A[25]	Al-Qahtani et al., 2012b
		MCP1	–2518, –2518/–2076(–/ht2), –2518/–2076(ht2/ht2)	Park et al., 2006; Chen et al., 2010
		MIF	rs755622	Moudi et al., 2016
		MxA	–123	Cao et al., 2009; Rebbani et al., 2017
		MX1	rs467960	He et al., 2015
		NF-κB	rs2233406, rs3138053	Zhang et al., 2014a
		NLRX1	p.Arg707Cys	Zhao et al., 2012
		NOTCH4	rs422951	Jiang et al., 2015
		NTCP	rs943277, rs4646285	Wang et al., 2017a; Wu et al., 2018a
		OCT4	rs13409, rs885952, rs879882, rs1265163, rs2394882, rs3094193, rs3130501, rs3130503, rs3130931, rs3132526, rs3757349, rs9263800, rs117265349	Shin et al., 2017
		PAPL	rs423058	Ma et al., 2014
		SOCS3	rs111033850, rs12953258, C-C[26]	Hoan et al., 2017
		SPP1	–1800, T-T-C-T-A[27]	Shin et al., 2007
		STAT4	rs8179673, rs10168266, rs11889341, C-T-C-T-T[28]	Jiang et al., 2016b, Lu et al., 2015b
		TMEM2	p.Ser1254Asn	Zhao et al., 2012
		TMEM2/IFNA2/NLRX1/C2	p.Ser1254-Asn/p.Ala120Thr/p.Arg707Cys/p.Glu318Asp	Zhao et al., 2012
		UBE2L3	rs2266959, rs4821116	Liu et al., 2018d, Hu et al., 2013
		VARS2	rs1043483, rs1264295, rs2249464, rs2517459, rs2532932, rs9394021,	Cheong et al., 2015
		ZNRD1	rs3757328, G-G-A[29]	Wen et al., 2015

Haplotypes

[1]G-A-G-A-T-T, rs9277535-rs10484569-rs3128917-rs2281388-rs3117222-rs9380343; [2]G-G-G-G-T-C, rs9277535-rs10484569-rs3128917-rs2281388-rs3117222-rs9380343; [3]A-A, rs3077-rs9277535; [4]A-A, rs2395309-rs9277535; [5]T-A-T, rs3077-rs9277378-rs3128917; [6]C-A-T, rs3077-rs9277378-rs3128917; [7]A-A-C-T, rs2395309-rs3077-rs2301220-rs9277341; [8]A-A-C-C//A-G-T-G-C-C, rs2395309-rs3077-rs2301220-rs9277341//rs9277535-rs10484569-rs3128917 -rs2281388-rs3117222-rs9380343; [9]A-A-C-T//A-G-T-G-C-C, rs2395309-rs3077-rs2301220-rs9277341//rs9277535-rs10484569-rs3128917 -rs2281388-rs3117222-rs9380343; [10]G-G-T-C//A-G-T-G-C-C, rs2395309-rs3077-rs2301220-rs9277341//rs9277535-rs10484569-rs3128917 -rs2281388-rs3117222-rs9380343; [11]T-T-G-A-T, rs9276370-rs7756516-rs7453920-rs9277535-rs9366816; [12]T-T-G-G-T, rs9276370-rs7756516-rs7453920-rs9277535-rs9366816; [13]G-A, rs2856718- rs9275572; [14]A-G, rs2856718- rs9275572; [15]A-A, rs2856718-rs9275572; [16]T-C-C-G-G-G, -1031/-863/-857/-308/-238/-163; [17]C-A-C-G-G-G, -1031/-863/-857/-308/-238/-163; [18]A-T-G-T-T-T-T-C-T, +88344/+102906/+103432/+103437/+103461/+104261/+104802/+106151/+106318; [19]T-C, rs12375841-rs17803780; [20]C-A-C, rs421446-rs107822-rs213210; [21]T-G-T, rs421446-rs107822-rs213210; [22]C-A-C-C-G, -1722/-1661/-658/-319/+49; [23]T/C-A-C-C-G, -1722/-1661/-658/-319/+49; [24]T-A-C-C-A, -1722/-1661/-658/-319/+49; [25]A-T-A, rs17401966-rs12734551-rs3748578; [26]C-C, rs111033850-rs12953258; [27]T-T-C-T-A, -1800/-1627/+4645/+5806/+6139; [28]C-T-C-T-T, rs8179673-rs7574865-rs4274624-rs11889341-rs10168266; [29]G-G-A, rs3757328-rs6940552-rs9261204.

Another meta-analysis indicated that HLA B*07 and B*58 protect against chronic HBV infection (Seshasubramanian et al., 2018). Recent studies have shown that non-classical HLA-class I molecules, including HLA-E may also be related to hepatitis B virus infection (Zidi et al., 2016). Available data are consistent with the fact that cellular immunity is a major determinant for HBV control. However, it is not clear how the identified genetic variation influences immune functions in the host and specific immune responses to HBV. These critical questions need to be answered in future studies.

Cytokines are key antiviral and immunomodulatory molecules produced by immune cells and certain non-immune

cells; they are involved in host defense against HBV infection and pathogenesis (Koziel, 1999; Shin et al., 2016). The antiviral and immunomodulatory functions of a number of cytokines, like type I and II IFNs, TNF-α, IL-10, and IL-21, play essential roles in the direct suppression of HBV replication in hepatocytes (Phillips et al., 2010), mediating the antiviral functions of T cells (Freeman et al., 2012), and the modulation of adaptive immune responses to HBV (Lin and Young, 2014; Gehring and Protzer, 2019). IFN-γ and TNF-α are major antiviral mediators of specific CD8+T cells and are required for HBV control in primary HBV infections (Phillips et al., 2010; Bertoletti and Ferrari, 2013). IL-10 may contribute to negative regulation of host immune responses and thereby plays a role in viral persistence (Saraiva and O'Garra, 2010). IL-18 is a cytokine that belongs to the IL-1 superfamily and is produced by macrophages and other cells (Mavragani and Moutsopoulos, 2014). Recently, IL-21 has drawn attention in the field of HBV research owing to its potential association with viral control *via* follicular helper T cell functions (Johnson and Jameson, 2009). A series of studies have identified associations between genes encoding cytokines (including IL-1, IL-4, IL-6, IL-10/IL-10RB, IL-12/IL-12B, IL-18, IL-27, IL-28B, IFN-γ, TNF-α, and TGF-β) and chronic HBV infection (Cheong et al., 2006; Du et al., 2006; Liu et al., 2006; Chen et al., 2010; Fletcher et al., 2011; Ma et al., 2014; Saxena et al., 2014; Talaat et al., 2014; He et al., 2015; Karataylı et al., 2015; Karra et al., 2015; Eskandari et al., 2017b). Clinical researches have revealed correlations between IL-18 -607C/A and -137G/C (rs1946519 and rs187238) polymorphisms and the risk of HBV infection (Karra et al., 2015). The study of a Indian population by Karra et al. involving 271 patients with hepatitis B–related liver diseases, including 109 with spontaneous recovery, 162 patients with persistent HBV infection, and 280 healthy volunteers, indicated that the −607A allele in the promoter region of the IL-18 gene may protect against HBV infection (healthy controls *vs*. cases, OR [95% CI] = 0.711 [0.559–0.904], $P = 0.005$). The AA genotype was associated with spontaneous clearance (spontaneous recovery *vs*. persistent HBV infection, OR [95% CI] = 2.765 [1.582–4.832], $P = 0.0002$), while the CC genotype was associated with HBV infection (persistent HBV infection *vs*. spontaneous recovery, OR [95% CI] = 0.318 [0.151–0.67], $P = 0.001$). Moreover, the -137C allele (cases *vs*. healthy controls, OR [95% CI] = 1.355 [1.037–1.771], $P = 0.025$) and the GC genotype (cases *vs*. healthy controls, OR [95% CI] = 1.558 [1.11–2.185], $P = 0.01$) were associated with persistent HBV infections. SNPs (−1,082, −592) within the IL-10 gene have been reported to be associated with susceptibility or the clearance of HBV infection (Cheong et al., 2006; Talaat et al., 2014). Further studies are needed to determine the functions of these cytokines in HBV infection and thereby to explain these conflicting results.

IL-28B SNPs are major determinants of HCV clearance and the efficacy of IFN therapy (Ge et al., 2009; Prokunina-Olsson et al., 2013). This locus encodes a cytokine that is distantly related to type I interferons and the IL-10 family and is induced by viral infection (Sheppard et al., 2003). A systematic review by Lee et al. (Lee et al., 2014) including 4,028 patients with chronic hepatitis B and 2,327 spontaneously recovered controls from 11 case–control studies indicated that there is no significant association between IL28B SNPs (rs12979860, rs12980275, and rs8099917) and spontaneous HBV clearance. These findings are not surprising, as the mechanisms underlying HBV control may differ substantially from those underlying HCV infection.

Interferon gamma (IFN-γ) is a type II interferon and is critical for innate and adaptive immunity against viral, bacterial, and protozoal infections (Schoenborn and Wilson, 2007). Cellular responses to IFN-γ are activated by its interaction with a heterodimeric receptor consisting of IFN-γ receptor 1 (IFN-γR1) and IFN-γ receptor 2 (IFN-γR2) (Robek et al., 2004). Previous studies have reported that several polymorphisms in IFN-γ, IFN-γR1, and IFN-γR2 are associated with the natural history of HBV infection (Liu et al., 2006; Khanizadeh et al., 2012). In a study by Liu et al. (Liu et al., 2006) including 181 patients with HBV infection and 272 gender, age-matched healthy controls, the A allele frequency of IFN-γ +874 (OR [95% CI] = 2.25 [1.69–2.99], $P < 0.0001$), and the AG haplotype (+874A and +2109G) ($P < 0.0001$) were found to significantly influence susceptibility to HBV infection in the Chinese population. A meta-analysis by Sun et al. (Sun et al., 2015) suggested that the IFN-γ +874T/A polymorphism contributes to an increased risk of HBV-related diseases, especially in Asians.

Chemokines are a family of small cytokines found in all vertebrates, some viruses, and some bacteria; they guide cells of the innate and adaptive immune systems. Some chemokines are involved in the control of immune cells during immune surveillance, directing lymphocytes to lymph nodes, to screen for pathogen invasion *via* interactions with APCs residing in these tissues (Kehrl, 2006; Mélik-Parsadaniantz and Rostène, 2008).

To date, studies of cytokine and chemokine genes have evaluated limited numbers of SNPs with small sample sizes, and rather inconsistent results have been obtained. Therefore, future large-scale and multi-center studies are needed to establish the relationship between the genetic control of cytokine- and chemokine-related functions and chronic HBV infection, given the importance of cytokines in anti-HBV immune responses.

TLRs play key roles as pattern recognition receptors; they activate the innate immune system (Chang, 2010; Kondo et al., 2011) and are required for efficient host defense against viral infection. Deficiencies in TLR or TLR-related signaling greatly reduce host-specific T cell responses to HBV and may contribute to HBV persistence (Ma et al., 2017). Thus, genetic variation in TLRs is expected to impact the susceptibility to chronic HBV infection (Al-Qahtani et al., 2012a; He et al., 2015; Huang et al., 2015; Zhu et al., 2017). Multiple SNPs in TLR genes (TLR3 rs1879026, rs3775290, and rs3775291, TLR7 rs179010, and TLR9 rs352140) have been examined for their association with the risk of HBV infection (He et al., 2015; Huang et al., 2015; Zhu et al., 2017). SNPs in TLR3 may be associated with an increased risk of chronic HBV infection. Al-Qahtani et al. (Al-Qahtani et al., 2012a) investigated SNPs in the TLR3 gene in Saudi Arabian patients chronically infected with HBV, including 707 patients and 600 uninfected controls. Only TLR3 rs1879026 (OR [95% CI] = 0.809 [0.655–0.999], $P = 0.0480$) and the GCGA haplotype (rs1879026, rs5743313, rs5743314, and rs5743315) ($P = 0.0339$) potentially contribute to the risk of HBV infection. Huang et al. (Huang et al., 2015) indicated that the TT genotype of TLR3

rs3775290 is closely correlated with a decreased risk of CHB. A meta-analysis by Geng et al. (Geng et al., 2016) demonstrated a significant effect of TLR3 rs3775291 and HBV-related diseases.

MicroRNAs (miRNAs) are a group of endogenous, highly conserved, small noncoding RNAs that modulate various cellular processes and play key roles in host–virus interactions and the pathogenesis of viral diseases (Qureshi et al., 2014). HBV replication is also regulated by miRNAs *via* their cellular targets (Zhang et al., 2011a; Zhang et al., 2013d; Lin et al., 2017). Hundreds of SNPs in miRNAs have been reported. Recent studies have shown that some miRNAs may play a role in anti-HBV defense (Su et al., 2011). In addition, miRNA polymorphisms are related to hepatitis B infection (Bae et al., 2012; Cheong et al., 2013; Al-Qahtani et al., 2017). A study of a Saudi Arabian population including 1,352 HBV-infected patients and 600 uninfected healthy individuals found that SNPs in different microRNA genes, including miR-149 (rs2292832), miR-146a (rs2910164), miR-196a-2 (rs11614913), and miR-30a (rs1358379), were associated with hepatitis B infection, while other SNPs in microRNA genes, including miR-423 (rs6505162), miR-492 (rs2289030), miR-146a (rs2910164), miR-196a-2 (rs11614913), and miR-30a (rs1358379) were associated with HBV clearance (Al-Qahtani et al., 2017). A meta-analysis (Zhou et al., 2015) has shown that the carriers of miR-196a-2*T (rs11614913), miR-122*del (rs3783553), miR-106b-25*A (rs999885), and miR-let-7c*del (rs6147150) alleles in the Asian population have an increased risk of chronic HBV infection.

Cytotoxic T-lymphocyte-associated protein 4 (CTLA4) is expressed by T lymphocytes and plays a key role as a negative regulator of T-cell responses (Buchbinder and Hodi, 2015). Several studies have evaluated the association between CTLA4 polymorphisms and chronic HBV infection. In particular, the + 49A/G polymorphism (rs231775) of CTLA4 may influence susceptibility to HBV infection in the Chinese population (Chen et al., 2010). Mohammad et al. (Mohammad et al., 2006) found that CTLA-4 -318 polymorphisms (rs5742909), but not +49 and −1,172 polymorphisms (rs733618) are significantly associated with susceptibility to chronic HBV infection in the Iranian population (OR = 0.49, 95% = 0.206–1.162, $P = 0.012$). Another study also showed that the CTLA4 −318C > T, but not +49G > A, is associated with chronic HBV infection (Schott et al., 2007). A meta-analysis (Xu et al., 2013) suggested that the A allele of the CTLA4 +49 polymorphism is significantly associated with an increased risk of persistent HBV infection, whereas the G allele may influence viral clearance. Another meta-analysis also suggested that the CTLA-4 +49A/G polymorphism is significantly correlated with persistent HBV infection in the Asian population (Huang et al., 2013).

NTCP encoded by the solute carrier family 10 member 1 (SLC10A1) gene is mainly expressed in hepatocytes and a functional receptor for HBV and hepatitis D virus (Hagenbuch and Meier, 1994; Yan et al., 2012a). NTCP rs2296651 (S267F) has been found to be related to HBV susceptibility in the Asian population (Hu et al., 2016; Yang et al., 2016a; Nfor et al., 2018; Wu et al., 2018a). In a larger cohort of Taiwanese patients, including 3,801 with chronic HBV infection and 3,801 matched HBsAg seronegative controls, the AA genotype of the S267F variant (rs2296651) was associated with resistance to chronic HBV infection (OR = 0.13, 95% CI = 0.05–0.34, $P < 0.001$), but there were no significant associations with serological outcomes, including HBV DNA detectability and HBeAg and HBsAg seroclearance (Hu et al., 2016). However, the S267F variant is absent in the Moroccan population (Ezzikouri et al., 2017). A large cohort study did not confirm the association between the common and rare alleles or CNVs in the SLC10A1 gene with the risk of persistent HBV infection in a population from Southern China (Zhang et al., 2017). A meta-analysis including 14,591 chronically HBV-infected patients and 12,396 healthy controls suggested that the A allele and GA genotypes of rs2296651 are inversely correlated with chronic HBV infection. They also reported that NTCP rs4646287, rs7154439, and rs4646296 show no significant correlation with HBV infection (Wang et al., 2017a).

The signal transducer and activator of transcription (STAT) protein family mediates many aspects of cellular immunity, proliferation, apoptosis, and differentiation (Miklossy et al., 2013). STAT proteins are involved in the development and function of the immune system and play a role in maintaining immune tolerance (Singh et al., 2009). In HBV infection, polymorphisms in STAT4 are related to the clinical outcome of HBV infection (Lu et al., 2015b; Jiang et al., 2016b). A case–control study including 1,610 Chinese patients with chronic HBV infection and 1,423 uninfected control subjects showed that the STAT4 SNPs rs7574865, rs10168266, rs11889341, and rs8179673 are significantly associated with the risk of HBV infection and inversely related to HBV clearance. They also found that the CTCTT haplotype, formed by the SNPs rs8179673, rs7574865, rs4274624, rs11889341, and rs10168266, is related to HBV infection susceptibility and clearance in the Chinese Han population. A meta-analysis including 8,944 chronically HBV-infected patients, 8,451 healthy individuals, and 2,081 subjects with HBV clearance demonstrated that STAT4 rs7574865 is significantly associated with HBV infection (OR [95% CI] = 1.14 [1.07–1.21]; $P = 3.8 \times 10^{-5}$) and clearance (OR [95% CI] = 1.20 [1.07–1.35], $P = 0.002$) (Jiang et al., 2016b). Lu et al. (Lu et al., 2015b) showed that STAT4 minor alleles (rs7574865, rs7582694, rs11889341, and rs8179673) are associated with spontaneous HBV clearance. Another meta-analysis by Liao et al. (Liao et al., 2014) did not confirm the correlation between STAT4 rs7574865 and HBV susceptibility or clearance. Thus, the association of STAT4 polymorphisms with HBV infection requires further verification.

Signal transducer and activator of transcription 3 (STAT3) and nuclear factor-kappaB (NF-κB) pathways may play a significant role in chronic HBV infection. A Chinese Han population study showed that STAT3 rs1053004 and rs1053005 polymorphisms and haplotypes formed by rs1053004 and rs1053005 might contribute to the susceptibility to chronic HBV infection (Li et al., 2018). Another Chinese study also found that the SNPs rs2233406 (CT versus CC) and rs3138053 (AG or AG+GG versus AA) in the promoter region of NFKBIA were significantly associated with decreased risk of HBV persistence, especially in genotype B HBV-infected subjects (Zhang et al., 2014a). Unfortunately, related research is still not sufficient and mainly

focused on HCC. Their role of HBV infection needs to be better defined by future research.

Using a GWAS approach, several loci that are strongly associated with HBV clearance or susceptibility to chronic HBV infection have been identified, including TCF19 (Kim et al., 2013; Jiang et al., 2015), UBE2L3 (Hu et al., 2013; Jiang et al., 2015), CFB (Jiang et al., 2015), NOTCH4 (Jiang et al., 2015), CD40 (Jiang et al., 2015), EHMT2 (Kim et al., 2013; Jiang et al., 2015; Shin et al., 2019), and INTS10 (Li et al., 2016).

Vitamin D has the ability to activate the innate immune system and dampen the adaptive immune system (Hewison, 2011). A vitamin D deficiency is associated with an increased risk or severity of viral infections (Beard et al., 2011). Vitamin D has both anti-inflammatory and anti-microbial effects and may play an active role in HBV infection (Bellamy et al., 1999; Beard et al., 2011; Gao et al., 2017). Vitamin D–related genes include 1-α-hydroxylase (CYP27B1), cytochrome P450 family 2 subfamily R polypeptide 1 (CYP2R1), vitamin D–binding protein (GC), VDR, 7-dehydrocholesterol reductase (DHCR7), sterol 27-hydroxylase (CYP27A1), and cytochrome P450 family 24 subfamily A member 1 (CYP24A1). Vitamin D–related genes have recently been found to play an important role in HBV susceptibility (Chatzidaki et al., 2012; Gao et al., 2017). The majority of these studies have focused on four SNPs in VDR: ApaI (rs7975232), TaqI (rs731236), FokI (rs10735810), and BsmI (rs1544410). Chatzidaki et al. (Chatzidaki et al., 2012) found that the joint haplotype of the VDR ApaI α allele and TaqI T allele is related to the outcome of HBV infection in children in the context of mother-to-child transmission (RR [95% CI] = 1.74 [0.97–3.13], P = 0.049). A meta-analysis (He et al., 2018) has reported that the genotypes FF, Ff, and allele F of FokI in VDR increase the risk of HBV infection. However, no associations were found between VDR ApaI and BsmI polymorphisms and HBV infection.

There is a marked difference in HBV infection rates between populations in East/Southeast Asia and Western world. For instance, the prevalence of HBsAg was as high as 10% in the Chinese population prior to the initiation of the HBV vaccination program but less than 1% in the Caucasian population (Fattovich et al., 2008; Yin et al., 2010). The reason for this difference is not completely clear. The role of host genetic determinants is also not well-established. Li et al. (Li et al., 2015) summarized multiple studies and found that some genetic loci with rare alleles include rs3138053 (NFKBIA), rs2856718, rs7453920, and rs9275319 (HLA-DQ), and rs9277378, rs2395309, rs2301220, and rs9277341 (HLA-DP) are significantly associated with decreased risks of development of chronic HBV infection. These loci are different between the Chinese Han and European populations, indicating that the Chinese Han patients may be inherently more prone to develop chronic infection once exposed to HBV, whereas Europeans tend to recover from HBV infection spontaneously (Li et al., 2015). A study including Chinese Han and Uyghur populations reported that there are some differences in HLA-DP/DQ polymorphisms that affect susceptibility and resistance to HBV infection (Xiang et al., 2016). A meta-analysis by Geng et al. (2016) demonstrated that TNF-α-238 increases the risk in the European population but not in an Asian population in all genetic models. Therefore, the genetic determinants may contribute the different rates of chronic HBV infection in Asian and European populations. However, future global multicenter research is needed to precisely define such host genetic determinants.

HBV infection often occurs in families. If a mother is chronically HBV infected, infants have an extremely high chance of establishing a chronic HBV infection in the absence of medical interventions (Stevens et al., 1975; Chen et al., 2018; Dionne-Odom et al., 2018). HBV exposure during infancy or early childhood is more prone to the development of chronic infection and HBV infection-related diseases (Lai and Yuen, 2007). Studies have shown that spontaneous HBsAg clearance is most likely to occur in patients born to mothers of non-HBsAg carriers (Chiu et al., 2014). Globally, a total of 42.1% of infants naturally born to HBsAg carrier mothers but only 2.9% of infants with HBV passive–active immunoprophylaxis acquired HBV infection perinatally (Li et al., 2015). The rate of vertical HBV infection had stayed constant (approximately 0.3%) until immunoprophylaxis of mother-to-infant transmission was implemented in 1986 in Japan. In contrast, horizontal HBV transmission decreased from 1.43 to 0.10% in men and from 0.95 to 0.03% in women over years. The decrease of horizontal transmission of HBV may be due to many factors, including improved socioeconomic environments, advanced medical maneuvers and equipment, and careful vaccination procedures (Sato et al., 2014). However, the current studies on host genetic and chronic HBV infection did not separate vertical from horizontal transmission, nor did they stratify the age at the time of infection. The role of environmental exposure including early exposure of HBV in the childhood when immune function is immature, and their interaction with the genetic predisposition is still not clarified.

In studies of associations between host genetic determinants and chronic HBV infection to date, reported OR values for significant associations typically range from 1 to 2. Thus, these determinants have much less influence than the HBV infection status of the mother or the age of the HBV infection. Nevertheless, some genetic variants, like mutations in NTCP, may play a decisive role in HBV infection. NTCP variation could prevent the binding of the HBV virion to receptors on hepatocytes and therefore limit viral infection (Yan et al., 2012a). Such findings may provide mechanistic insights into the viral life cycle and new targets for drug development. Many genetic determinants (HLA, TLR, IL) may modulate host innate and adaptive immunity and significantly influence the course and outcome HBV infection (Kamatani et al., 2009; Mbarek et al., 2011; Kim et al., 2013; Jiang et al., 2015; Geng et al., 2016) (**Table 2**; **Table S2**). It will be useful to identify the functional relevance of these genetic polymorphisms in cellular signaling and other processes, with the goal of identifying new targets. Many factors contribute to the development of chronic HBV infection, such as the mode of transmission (vertical or horizontal transmission), age at the time of infection, the presence of underlying diseases involving other organs, and the use of immune inhibitors (Pawlowska et al., 2016; Chien et al., 2019). The majority of studies do not including subgroup analyses of these factors, which may have a significant impact on the reliability of the results. Furthermore, there are substantial variations among studies from different countries

and regions due to differences in the study populations, genetic background, and polymorphisms. Therefore, it may be necessary to conduct stratified analyses of HBV infection time, ethnicity, host immune status, and mode of transmission to further determine the impact of HLA-DP, DQ, and DR on chronic hepatitis B or clearance. Nevertheless, the available information suggests that genetic variation in host immune-related genes has substantial contribution to the outcome of HBV infection. Future research is necessary to uncover the mechanisms underlying these associations.

INTRAUTERINE TRANSMISSION

Mother-to-child transmission is the major route of HBV infection in developing countries (Stevens et al., 1975; Shao et al., 2007; Li et al., 2015). Intrauterine transmission is the main explanation for mother-to-child transmission, since the implementation of effective measures against HBV infection, such as antiviral treatment, vaccination, and the application of hepatitis B immunoglobulins (Gu et al., 2004; Brown et al., 2016; Ren et al., 2016). Therefore, blocking intrauterine HBV transmission is an important part of the eradication of HBV infection in the general population (Peng et al., 2019). Unfortunately, the incidence of intrauterine HBV infection remains high (Han et al., 2011). The exact mechanism underlying intrauterine infection with HBV has not been fully elucidated (Xu et al., 2008). Previous studies have shown that genetic factors could play an important role in determining the outcome of HBV intrauterine infection (Yu et al., 2006; Xu et al., 2008; Gao et al., 2015b; Liu et al., 2018d). Based on twin and family study, host genetic factors are critical for the development of chronic HBV infection (Lin et al., 1989). Up to date, SNPs in the host genes IFN-γ, TNF-α, CXCL13, PDCD1, TLR3, and TLR9 were found to be relevant for intrauterine transmission (Yu et al., 2006; Gao et al., 2015b; Wan et al., 2016; Liu et al., 2018c; Gao et al., 2015b) (**Table S3**).

A number of host genes may play important roles in HBV intrauterine infection (**Table 3**, **Tables S1**, **S3**). Yu et al. (Yu et al., 2006) showed that a SNP (+874) in IFN-γ is associated with HBV intrauterine infection (both $P < 0.05$). Wan et al. (Wan et al., 2016) investigated associations between candidate genes (SLC10A1, HLA-DP, HLA-C, CXCR5, CXCL13, TLR-3, TLR-4, TLR-9, and UBE2L3) and HBV intrauterine infection in a sample of 44 neonates with HBV intrauterine infection and 662 neonatal controls. They demonstrated that only the rs355687 CT genotype of CXCL13 was associated with susceptibility to

TABLE 3 | Host genetic factors associated with intrauterine hepatitis B infection or response to interferon-alpha (IFN-α) or nucleos(t)ide analog (NUC).

Category	Gene ontology	Gene	Genetic determinants (SNP/Hap/CNVs)	Main reference
Host genetic factors associated with susceptibility to intrauterine hepatitis B infection				
II	Cytokines	IFN-γ	+874	Yu et al., 2006
	Chemokines	CXCL13	rs355687	Wan et al., 2016
Host genetic factors associated response to IFN-α treatment				
I	HLA	HLA-DP	rs3077	Tseng et al., 2011; Tangkijvanich et al., 2016
	Chemokines	IL-28B	rs8099917, rs12979860, rs12980275	Sonneveld et al., 2012; Guo et al., 2013; Boglione et al., 2014; Wu et al., 2015a; Cusato et al., 2017
	Others	CYP27B1	rs4646536	Boglione et al., 2015; Cusato et al., 2017; Limothai et al., 2017
II	HLA	HLA-DP	rs9277535	Brouwer et al., 2014; Cheng et al., 2014
		HLA-DQA1-DQB1-DRB1	*0302-*0303-*09	Zhu et al., 2011
		HLA-DQB1	*0303	Zhu et al., 2011
		HLA-DRB1	*08	Zhu et al., 2011
		HLA-A, B, C	*1101-*4601-*0102	Zhu et al., 2011
	Cytokines	IL-28B	A-C[1]	Wu et al., 2015a
	Others	CYP24A1	rs2248359	Cusato et al., 2017
		CYP27B1	rs10877012	Cusato et al., 2017
		G3BP2	rs3821977	Brouwer et al., 2019
		OAS	G-T-G-A[2], C-C-T-A[3], C-C-C-A[4], A-C-T-A[5]	Wu et al., 2009; Ren et al., 2011
		OAS3	rs2072136	Ren et al., 2011
		PRELID2	rs371991	Brouwer et al., 2019
		STAT4	rs7574865	Jiang et al., 2016a
		TRAPPC9	rs78900671	Brouwer et al., 2019
		VDBP	rs7041	Cusato et al., 2017
		VDR	rs1544410, rs731236, rs11568820, rs10735810	Cusato et al., 2017
Host genetic factors associated response to NUC treatment				
II	HLA	HLA-DP	rs3077	Hosaka et al., 2015; Su et al., 2018
		HLADQ	rs9275572, rs9276370	Chang et al., 2014; Zhang et al., 2014b

Haplotypes

[1]A-C, rs12980275-rs12979860; [2]G-T-G-A, rs3177979-rs1293747-rs4767043-rs10849829; [3]C-C-T-A, rs2285934-rs2072138-rs2072136-rs10849829; [4]C-C-C-A, rs2285934-rs2072138-rs2072136-rs10849829; [5]A-C-T-A, rs2285934-rs2072138-rs2072136-rs10849829.

HBV intrauterine infection (OR [95% CI] = 0.25 [0.08–0.82], $P = 0.022$).

A case–control study of the Chinese population including 69 HBsAg-positive mother–newborn pairs with intrauterine infection and 138 mother–newborn pairs without intrauterine infection assessed the involvement of the LTβR/APOBEC3B signaling pathway and PD-1/PD-L1 signaling pathway genes, including LTA, LTBR, TNFSF14, PDCD1, APOBEC3B, CD274, CD40, and CD40LG, in HBV intrauterine transmission. They found that the maternal rs2227981 TT genotype of the PDCD1 gene is associated with a decreased risk of intrauterine HBV infection (OR 0.11, 95% CI = 0.01–0.95, $P = 0.045$). There was no significant correlation between the remaining genes and the risk of intrauterine HBV infection (Liu et al., 2018c). Only a few studies have evaluated genetic susceptibility to intrauterine transmission. It is often difficult to distinguish whether a child acquired an HBV infection by the intrauterine or intra-natal route. HBV infection by intrauterine transmission is mainly identified by a blood test at birth. However, this approach may result in false positives due to maternal blood contamination during birth, especially when sensitive PCR methods for HBV DNA detection are used. Moreover, the sample sizes of existing studies are not large enough; thus, the reliability of studies could be questioned. Further research is needed to improve the diagnostic accuracy of intrauterine HBV infection and explore the relationship between HBV intrauterine infection and susceptibility genes as well as other risk factors associated with HBV intrauterine infection.

There is no effective intervention available to prevent intrauterine HBV infection. Neither antiviral treatment during the late phase of pregnancy nor perinatal vaccination/hyperimmunoglobulin application changed the rate of intrauterine HBV infection (Pan et al., 2012a; Brown et al., 2016). Therefore, the identification of relevant genetic determinants could be very helpful.

OCCULT HBV INFECTION

OBI is defined by serum HBV DNA positivity but negative serum HBsAg detection (Torbenson and Thomas, 2002; Raimondo et al., 2008; Raimondo et al., 2019; Seed et al., 2019). If blood from patients with OBI is transfused to other persons, post-transfusion hepatitis may occur (Seo et al., 2011). OBI may also be associated with hepatitis B vaccination failure, vertical HBV transmission, organ transplant failure, cirrhosis, and liver cancer (Raimondo et al., 2013).

The mechanisms underlying OBI have yet to be elucidated and may be related to HBV mutations in the pre-S/S genomic region or antigen–antibody cycle immune complex formation (Zhang et al., 2011b; Samal et al., 2012). Some investigators have suggested that host genetic factors, especially immune-related factors including HLAs, IL10, CXCL12, and VDR, may play a role in the occurrence of OBI (Arababadi et al., 2010; Hassanshahi et al., 2010; Mardian et al., 2017; Wang et al., 2017b) (**Tables S1**, **S4**). Wang et al. (Wang et al., 2017b) performed a case–control study with 107 patients with OBI and 280 healthy individuals to assess associations of SNPs in HLA loci, including HLA-A, -B, -C, -DRB1, and -DQB1, in Chinese patients. They found that HLA-B*44:03 (OR = 2.146, 95% CI = 1.070–4.306, $P = 0.028$), C*07:01 (OR = 4.693, 95% CI = 1.822–12.086, $P = 0.000$), DQB1*02:02 (OR = 1.919, 95% CI = 1.188–3.101, $P = 0.007$), and DRB1*07:01 (OR = 2.012, 95% CI = 1.303–3.107, $P = 0.001$) were strongly associated with susceptibility to OBI, while DRB1*08:03 (OR = 0.395, 95% CI = 0.152–1.027, $P = 0.049$), DRB1*15:01 (OR = 0.495, 95% CI = 0.261–0.940, $P = 0.029$), and DQB1*06:02 (OR = 0.500, 95% CI = 0.249–1.005, $P = 0.048$) alleles were more prevalent in the healthy control group. Mardian et al. (Mardian et al., 2017) found a significant association between the minor allele "T" of HLA-DP (rs3077) and the TGA haplotype (rs3077–rs3135021–rs9277535) and OBI in Indonesian blood donors. Therefore, HLA polymorphisms are an important factor in OBI infection and additional studies are needed to validate these findings. Iranian researchers have shown that the genotypes and alleles of IL-10 (-592) (Ahmadabadi et al., 2012), the +801 region of CXCL12 (Hassanshahi et al., 2010), and the T/T allele of exon 9 of VDR (Arababadi et al., 2010) may be associated with OBI.

Owing to the low frequency of OBI, the accumulation of cases is difficult and time-consuming. Thus, the number of cases included in studies is always small (generally less than 100 cases). In addition, the occurrence of OBI is also related to HBV mutations (Samal et al., 2012). OBI diagnostic criteria are not uniform among studies. Both viral and host factors need to be considered in future analyses. Patients with OBI are positive for HBV DNA but negative for HBsAg. Thus, there could be specific mechanisms for the control of HBsAg production without affecting HBV DNA synthesis. Recently, Lin et al. found that autophagy and related genes (e.g., Rab7) may determine HBsAg production (Lin et al., 2017; Lin et al., 2019), but further studies are needed to evaluate this.

ANTIVIRAL EFFICACY OF INTERFERON-α OR NUCLEOS(T)IDE ANALOGUES

IFN-α and NUCs have been approved and are widely used for the treatment of chronic hepatitis B and slow down liver disease progression, cirrhosis, and HCC (Lee and Keeffe, 2011; European Association For The Study Of The Liver, 2017). However, NUCs and IFN-α alone or combined treatment are rare to achieve functional cure (Reijnders et al., 2010; Zoulim and Locarnini, 2012; Terrault et al., 2016; Revill et al., 2019). Extensive studies have identified host genetic genes, alanine aminotransferase (ALT) levels, HBV genotype, and HBV DNA, anti-HBc, and HBsAg levels as important predictors of treatment efficacy (Brouwer et al., 2014; Fan et al., 2016b; Zhu et al., 2016a). Accumulating evidence suggests that host genetics play an important role in the patient response to IFN-α or NUCs (**Table 3**; **Tables S1**, **S5**, **S6**).

IFN-α is a cytokine with a broad-spectrum effect against viruses and tumors. It is able to inhibit cell growth and exerts immunomodulatory effects. IFN-α exerts antiviral activity mainly *via* the Janus-activated kinase-signal transducer and

activator of transcription (JAK-STAT) signaling pathway and interferon-stimulating genes (ISGs) (Levy and Darnell, 2002). IFN-α binds to type I IFN receptor (IFN-αR1) on the surface of target cells and induces the synthesis of antiviral proteins, such as MxA, 2',5'-oligoadenylate synthetase (OAS), protein kinase (PKR), and adenosine deaminases acting on RNA (ADAR) (Samuel, 2001). In addition, IFN-α upregulates HLAs and thereby modulates adaptive immunity. Thus, host genetic polymorphisms, particularly those associated with IFN signaling pathways, may potentially alter the responsiveness to IFN-α therapy. Many studies have evaluated the relationship between the outcome of IFN-α treatment for CHB and host genetics and identified the potential relevance of HLAs, STAT4, vitamin D–related genes, and some ISGs (Tseng et al., 2011; Brouwer et al., 2014; Wu et al., 2014; Jiang et al., 2016a; Thanapirom et al., 2017; Brouwer et al., 2019) (**Table S5**).

The first GWAS published to date did not find any candidate gene associated with the efficacy of IFN-α treatment. This may be explained by an insufficient sample size, with only 43 patients (Chang et al., 2014). Recently, Brouwer et al. (Brouwer et al., 2019) published a GWAS on the efficacy prediction of PEG-IFN in the treatment of CHB, including 1,058 patients from 21 centers from Europe, Asia, and North America. A SNP rs78900671 GC allele (TRAPPC9, COL22A1) had been identified to have the strongest association with response to PEG-IFN treatment ($P = 6.43\times10^{-7}$). Another SNP PRELID2 rs371991 ($P = 3.44\times10^{-6}$) was associated with the primary response to PEG-IFN treatment in HBeAg-positive patients while G3BP2 rs3821977 ($P = 2.46\times10^{-6}$) was associated with response in HBeAg-negative patients. Yet the correlation between these SNP loci and the efficacy of interferon treatment needs confirmation by future studies.

HLA molecules play an important role in the recognition of viral proteins and regulation of adaptive immunity. Adaptive immunity is upregulated by IFN-α treatment and essential for sustained responses and HBV control (Bengsch and Thimme, 2018; Ma et al., 2018b). Thus, HLAs may be an important genetic marker for the prediction of IFN-α efficacy. Many studies have analyzed the relationship between HLA genes and the IFN-α response (Tseng et al., 2011; Zhu et al., 2011; Brouwer et al., 2014; Tangkijvanich et al., 2016). A study of a Taiwan population by Tseng et al. (Tseng et al., 2011) including 115 HBeAg-positive patients with CHB who received peginterferon (PEG-IFN) therapy showed that the HLA-DPA1 rs3077 GG genotype (OR [95% CI] = 3.49 [1.12–10.84], $P = 0.031$) is associated with HBeAg seroconversion at 6 months of therapy. Brouwer et al. (Brouwer et al., 2014) evaluated 262 Caucasian patients with chronic HBV infection who were treated with PEG-IFN for 1 year and found that the HLA-DPB1 (rs9277535) G-allele and haplotype block GG combining HLA-DPB1 (rs9277535) and HLA-DPA1 (rs3077) are strongly associated with virological (HBV DNA <2,000 IU/ml at 6 months post-treatment) and serological responses (HBeAg seroconversion combined with HBV DNA <2,000 IU/ml at 6 months post-treatment) to PEG-IFN therapy. Zhu et al. (Zhu et al., 2011) reported that the HLA-DQB1*0303 or DRB1*08 alleles and the *1101-*4601-*0102 (HLA-A, B, C) or *0302-*0303-*09 (HLA-DQA1, DQB1, DRB1) haplotypes are associated with the efficacy of IFN therapy in the Chinese population. However, some studies have failed to observe a relationship between HLA variants and the response to IFN-α- or PEG IFN-based treatment (Limothai et al., 2016).

IFN-λ3 is encoded by the IL-28B gene, which regulates the immune system by activating the JAK-STAT signaling pathway, thereby exerting an antiviral effect (Liu et al., 2012a). Recent GWAS has revealed that IL28B is associated with the efficacy of anti-HCV treatment (Ge et al., 2009). In a large international collaborative study of 205 HBeAg-positive patients with CHB who received PEG-IFN-α-2a or PEG-IFN-α-2b, IL28B rs12979860 and rs12980275 were independent predictors of HBeAg seroconversion in response to PEG-IFN (Sonneveld et al., 2012). Boglione et al. (Boglione et al., 2014) examined the effect of the IL28B gene polymorphisms rs12979860, rs8099917, and rs12980275 on the response to PEG-IFN in 190 chronically HBV-infected, HBeAg-negative patients and showed that rs12979860 CC, rs8099917 TT, and rs12980275 AA are significantly associated with HBV-DNA < 2,000 IU/ml post-treatment, while rs12979860 CC and rs12980275 AA are significantly associated with qHBsAg > 1 log during therapy. Many other research teams worldwide have indicated that IL-28B is involved in the efficacy of IFN-α therapy (Lampertico et al., 2013; Wu et al., 2015a; Cusato et al., 2017). However, variable and inconclusive results have been obtained (Cheng et al., 2014; Tangkijvanich et al., 2016). A study in Taiwan showed that IL28B rs12979860 is not associated with the virological response to PEG-IFN alpha-2b with or without entecavir in patients with HBeAg-negative CHB (Tangkijvanich et al., 2016). A Chinese study also suggested that IL28B (rs12979860 and rs8099917) has no significant association with the response to IFN-α or PEG IFN (Cheng et al., 2014). To determine whether IL28B polymorphisms play a role in the response to interferons, further large-scale cohort studies of homogenous patient populations are necessary.

Vitamin D has important immunomodulatory effects on innate and adaptive immune responses (Hewison, 2011). Vitamin D enhances the IFN-α-mediated activation of the JAK-STAT pathway, increases the expression levels of antiviral proteins, and improves the overall antiviral ability (Lange et al., 2014). Vitamin D–related genes, including VDR (Cusato et al., 2017), CYP27B1 (Cusato et al., 2017), CYP24A1 (Cusato et al., 2017), CYP2R1 (Thanapirom et al., 2017), DHCR7 (Thanapirom et al., 2017), and DBP/GC (Cusato et al., 2017; Thanapirom et al., 2017), have been evaluated for potential associations with the outcome of IFN-α therapy in patients with CHB. Several studies in China, Thailand, and Italy have shown that polymorphisms in the rs4646536 and rs10877012 loci of CYP27B1 may be related to the efficacy of IFN-α in patients with CHB; OR values reported in studies of Italy (Cusato et al., 2017), Thailand (Limothai et al., 2017), and Italy (Boglione et al., 2015) were 2.87, 3.13, and 3.13 for the rs4646536 locus (all $P < 0.01$); and the OR values for studies of Italy (Cusato et al., 2017) was 3.13 for the rs10877012 locus (both $P < 0.001$). Therefore, the TT (rs4646536) and GG (rs10877012) genotypes may be predictors of sustained HBeAg seroconversion in HBeAg-positive patients treated with IFN-α. Cusato et al. (Cusato et al., 2017) evaluated SNPs in vitamin D pathway genes in HBeAg-negative patients with CHB treated with PEG-IFN-α, suggesting that VDR (rs7975232 [ApaI],

rs11568820 [Cdx2], rs10735810 [FokI]), CYP27B1 (rs4646536 [+2838], rs10877012 [−1260]), VDBP (rs7041), and CYP24A1 (rs2248359) are correlated with the clinical outcomes of PEG-IFN-α treatment. Thanapirom et al. (Thanapirom et al., 2017) showed that the CYP2R1 (rs12794714) TT genotype is a predictor of sustained HBeAg seroconversion in HBeAg-positive patients treated with Peg-IFN-α (OR [95% CI] = 4.53 [1.51–13.61], $P = 0.01$), whereas SNPs in DHCR7 (rs12785878), CYP27B1 (rs10877012), CYP2R1 (rs2060793), GC (rs4588, rs7041, rs222020, and rs2282679), and VDR (FokI, BsmI, Tru9I, ApaI, TaqI) are not related to HBeAg seroconversion. Several studies have investigated the role of other SNPs in vitamin D pathway genes in predicting the outcome of IFN-α therapy, but their predictive value remains controversial (Thanapirom et al., 2017). Differences among studies could be explained by several factors, such as differences in study design, sample size, ethnicity, and genotyping methods.

SNPs in JAK-STAT pathway genes and ISGs may contribute to the antiviral effects of IFN-based therapy (Kong et al., 2007; Ren et al., 2011; Wu et al., 2014; Jiang et al., 2016a). OAS3, MxA-88, and STAT4 genes in the IFN signaling pathway may have predictive value for the efficacy of interferons, but further studies are needed to verify this.

NUCs (e.g., lamivudine [LAM], adefovir [ADV], telbivudine [LdT], entecavir [ETV], and tenofovir [TDF]) inhibit HBV replication mainly by inhibiting HBV DNA polymerase. They bind competitively to HBV DNA polymerase and are incorporated into the DNA chain, resulting in the termination of DNA synthesis and inhibition of HBV replication (Lok et al., 2007; European Association For The Study Of The Liver, 2017). As the direct effect of NUCs on HBV does not require host functions and may not be directly related to host genetics, few studies have evaluated the correlation between host gene SNPs and drug efficacy, and these have generally yielded negative results (**Table 3**; **Tables S1**, **S6**).

There were significant differences in the patterns of HBsAg decline, and seroclearance during LAM therapy in Japanese patients with HBeAg-positive CHB was associated with HLA-DPA1 (rs3077), HLA-DPB1 (rs9277535), and A alleles at rs3077 and rs9277535 (Hosaka et al., 2015). A GWAS (Chang et al., 2014) with small sample sizes (LAM group, $n = 119$; ETV group, $n = 64$) of male Taiwanese individuals revealed that the TT genotype of rs9276370 (HLA-DQA2) is highly associated with a non-sustained response in the LAM group (OR [95% CI] = 5.41 [1.73–16.95], $P = 0.0037$), but not in the ETV group (OR [95% CI] = 0.68 [0.16–2.86], $P = 0.5954$). Zhang et al. (Zhang et al., 2014b) reported that the HLA-DQ (rs9275572) A allele is associated with viral and biochemical responses to LAM treatment in Chinese patients.

Using a small sample size ($n = 76$), our team evaluated the virological responses associated with the ESR1 PvuII T/C genotype in nucleoside-naive patients with chronic hepatitis B treated with ETV after 48 and 96 weeks of treatment; we did not detect associations between XbaI polymorphisms and virological response (Zhang et al., 2013c). Another study also found that CTLA4 (rs231775) and HLA-DPA1 (rs3077) are associated with predictors of relapse and outcomes after discontinuing TDF and ETV therapy in Taiwan patients with CHB (Su et al., 2018). However, the sample sizes of these studies are insufficient.

The main issues with studies of the efficacy of IFN/NUCs are as follows. 1) ALT, HBsAg, HBeAg, anti-HBc, HBV DNA, and HBV genotype may affect the efficacy of IFN/NUCs, and it is difficult to control for these confounding factors. 2) Some studies do not distinguish between HBeAg-positive or -negative patients, resulting in the inconsistent use of drugs as well as differences in treatment duration. 3) The criteria for determining efficacy and time points for evaluations are often inconsistent. 4) Many studies include small sample sizes and a lack of secondary verification. 5) Different and even contradictory results have been reported. Despite studies showing that several SNP sites in IL28B are closely related to the efficacy of IFN-α for the treatment of HCV infection, it is difficult to confirm that any host genetic determinant is significantly related to the efficacy of IFN-α or NUCs in chronic HBV infection without resolving these issues. It is necessary to clarify whether host genetic factors determine the efficacy of antiviral therapies. Currently, available antiviral treatments based on IFN-α/NUCs are not effective to clear HBV covalently closed circular DNA (cccDNA). Information about the involvement of host factors in antiviral activity may be helpful to optimize treatment approaches.

Attempts to improve the response by administering two different NUCs or a combination of NUCs and IFN-α failed to increase the rate of "functional cure." New drug candidates targeting different steps of HBV life cycle including entry, cccDNA formation, viral transcription, capsid assembly, and secretion of viral envelope proteins were developed and partly tested in clinical trials (Qazi et al., 2018; Tu and Urban, 2018; Yang and Lu, 2018; Yang et al., 2019). Immunotherapeutic approaches to enhance antiviral immunity using IL-15, TLR agonists, retinoic acid inducible gene I (RIG-I) agonist, stimulator of IFN genes (STING) agonist or based on engineered T cells are also under investigation (Ma et al., 2015; Zhang and Lu, 2015; Guo et al., 2017; Koh et al., 2018). A new drug targeting cIAPs has being now tested in a clinical trial phase I (Liu et al., 2018a). Checkpoint inhibitors like anti-PD1 are able to stimulate host adaptive immunity and considered as potential drug candidates to treat chronic HBV infection (Liu et al., 2014a; Liu et al., 2018b). Such innovative drugs, Along with current available therapies, will offer the prospect of a markedly improved response to treatments and an increased rate of functional cure (Ko et al., 2015; Blank et al., 2016; Di Scala et al., 2016; Zhu et al., 2019). Those new drug candidates, especially for immunotherapies, may exert the antiviral actions in dependence on host genetic background. Some genetic determinants found in the previous studies like SNPs in HLA loci may reappear again in such studies. Their efficacy in anti-HBV treatment related to human genetics remains to be a topic for future studies.

RESPONSE TO HEPATITIS B VACCINATION

Hepatitis B vaccines are widely used for the prevention of new HBV infections and are the most effective way to prevent

HBV transmission (Kew, 1995; Ni et al., 2012; Bruce et al., 2016). The overall success rate of vaccination is about 90%. Several factors, such as age, gender, body mass index (BMI), immunosuppression, vaccine escape mutations, and premature birth, are associated with a failure to respond to hepatitis B vaccination (Zuckerman, 2006; Kang et al., 2014; Yang et al., 2016b). A twin study indicated that the immune response to hepatitis B vaccination has a high heritability (77%) (Newport et al., 2004). Yan et al. investigate the overall contribution of genetic and environmental effects on poor response to HBV vaccination in Chinese infants. They found that the HBV vaccine response in infants is dominantly determined by genetic effect by 91%, compared with perinatal environmental factors (Yan et al., 2013). Genetic factors may have important roles in the immune response to hepatitis B vaccination, and many studies have focused on the identification of these genes including HLAs and IL4 (Png et al., 2011; Cui et al., 2013; Li et al., 2013b; Nishida et al., 2018) (**Table 4**; **Tables S1**, **S7**).

A recent GWAS has shown that genetic variants in HLA loci are strongly associated with chronic HBV infection. Difference in host immune responses to HBV antigens are largely explained by HLA alleles (Ovsyannikova et al., 2004). Associations of SNPs in HLA regions, including -A, -B, -DR, and -DQ loci, with the response to hepatitis B vaccines have been identified (Davila et al., 2010; Png et al., 2011; Yoon et al., 2014; Roh et al., 2016). A GWAS of an Indonesian population including 3,614 hepatitis B vaccine recipients suggested that HLA loci, including HLA-DR (rs3135363) ($P = 6.53 \times 10^{-22}$; OR = 1.53, 95% CI = 1.35–1.74), HLA-DP (rs9277535) ($P = 2.91 \times 10^{-12}$; OR = 0.72, 95% CI = 0.63–0.81), and HLA class III (rs9267665) ($P = 1.24 \times 10^{-17}$; OR = 2.05, CI = 1.64–2.57), are strongly associated with the response to hepatitis B vaccination (Png et al., 2011). Other GWAS have found that HLA-DRB1 (rs477515, rs28366298, and rs13204672), HLA-DP (rs7770370), and multiple HLA-DRB1-DQB1 haplotypes are associated with the response to hepatitis B vaccines (Davila et al., 2010; Wu et al., 2015b). Although similar results have been obtained in several additional studies (Yoon et al., 2014; Roh et al., 2016; Sakai et al., 2017), other studies do not support these associations, likely owing to the sample sizes, statistical methods, or the use of different vaccines (Okada et al., 2017; Xu et al., 2017a). A meta-analysis (Li et al., 2013b) has shown that HLA class II genotypes (HLA-DRB1*01, DRB1*1301, DRB1*15, HLA-DQB1*05, DQB1*0501, DQB1*06, DQB1*0602) are associated with the antibody response to the hepatitis B vaccine, while the opposite results were found for DRB1*03 (DRB1*0301), DRB1*04, DRB1*07, DRB1*1302, and DQB1*02. Taken together, HLA is an important marker for the response to the hepatitis B vaccine; multicenter studies are needed for verification and to determine the mechanism underlying this association.

Cytokines play key roles in regulating immune responses and may modulate responses to HBV vaccines (Harber et al., 2000; Howe et al., 2005). Among these cytokine genes, IL-4 induces the differentiation of naive helper T cells to Th2 cells

TABLE 4 | Host genetic factors associated with response to hepatitis B vaccine.

Category	Gene ontology	Gene	Genetic determinants (SNP/Hap/CNVs)	Main reference
I	HLA	HLA-DP	rs9277535	Png et al., 2011; Wu et al., 2015b
		HLA-DQB1	*02, *05, *0501, *06, *0602	Li et al., 2013b; Nishida et al., 2018
		HLA-DRB1	*01, *03, *0301, *04, *07, *1301, *1302,*15	Li et al., 2013b; Yoon et al., 2014; Nishida et al., 2018
	Cytokines	IL-4	rs2070874, rs2227284, rs2243250	Wang et al., 2012; Cui et al., 2013
II	HLA	HLA-B	*62	Yoon et al., 2014; Roh et al., 2016
		HLA-DP	rs2116260, rs3128961, rs35953215, rs3830066, rs4282438, rs5025825, rs6457709, rs7770370, rs9277542, *04:02, *05:01, *09:01, *02:02, *03:01:01, *04:01:01, A-G-A-G-G[1], A-G[2], A-G-A-G-G-A-G[3]	Wu et al., 2015b; Sakai et al., 2017; Nishida et al., 2018
		HLA-DQB1	*0401	Xu et al., 2017a; Nishida et al., 2018
		HLA-DR	rs3135363	Png et al., 2011
		HLA-DRA	rs7192, rs2395177, rs5000563	Davila et al., 2010
		HLA-DRB1	*01:01, *04:05, *08, *08:03, *15:01, rs477515, rs13204672, rs28366298	Sakai et al., 2017; Nishida et al., 2018
		HLA-DRB1-DQB1	*01:01-*05:01,*04:05-*04:01,*08:03-*06:01,*14:06-*03:01, *15:01-*06:02	Nishida et al., 2018
		HLA-III	rs9267665	Png et al., 2011
	Others	BTNL2	rs2076530, rs3763311, rs3763313, rs3763316, rs3806156, rs3817963, rs4248166, rs9268494, rs9268501, A-A[4], C-G[5], G-T-A-T-C-A-G[6], G-T-A-T-C[7], G-C-A-T-C[8]	Davila et al., 2010; Pan et al., 2014; Yang et al., 2014; Nishida et al., 2018
		FOXP1	rs6789153	Davila et al., 2010
		LILRB4	rs1654668	Davila et al., 2010

Haplotypes

[1]A-G-A-G-G, rs5025825-rs6457709-rs35953215-rs3830066-rs7770370; [2]A-G, rs3128961-rs9277535; [3]A-G-A-G-G-A-G, rs5025825-rs6457709-rs35953215-rs3830066-rs7770370-rs3128961-rs9277535; [4]A-A, rs3806156-rs2076530; [5]C-G, rs3806156-rs2076530; [6]G-T-A-T-C-A-G, rs9268501-rs3763316- rs3763313-rs3763311- rs9268494-rs3806156-rs2076530; [7]G-T-A-T-C, rs9268501-rs3763316- rs3763313-rs3763311-rs9268494; [8]G-C-A-T-C, rs9268501-rs3763316- rs3763313-rs3763311-rs9268494.

and is a key regulator of humoral immune responses. Genetic polymorphisms in IL-4 have been reported to be associated with the response to the hepatitis B vaccine in many studies (Chen et al., 2011; Wang et al., 2012), such as IL-4 (rs2070874, rs2243250, rs2227282, rs2243248, rs2227284) (Chen et al., 2011; Wang et al., 2012), IL-4RA (rs1805015) (Chen et al., 2011), IL-12B (rs17860508) (Pan et al., 2012b), and IL-13 (rs1295686) (Chen et al., 2011) that are associated with responses to the hepatitis B vaccine. In a meta-analysis of eight published studies, Cui et al. (Cui et al., 2013) evaluated associations of IL4 genetic polymorphisms, including rs2243250 (C > T), rs2070874 (C > T), rs2227284 (A > C), rs2227282 (C > G), and rs2243248 (G > T), with the response to the hepatitis B vaccine. The analysis suggested that the T allele of rs2243250, the T allele of rs2070874, and the C allele of rs2227284 in IL4 may be useful biomarkers for predicting favorable responses to the hepatitis B vaccine, especially in the Asian population. Relatively few studies have examined other cytokine genes.

Other studies have suggested that polymorphisms in other host genes (BTNL2, FOXP1, LILRB4, TLR2, VDR, etc.) may be related to responses to hepatitis B vaccination (Davila et al., 2010; Chen et al., 2011; Grzegorzewska et al., 2014), but further validation of these results is required.

The overall success rate of vaccination is about 90% (Zuckerman, 2006), and the factors that affect the success of vaccination mainly include 1) the type of vaccine; 2) the dose, mode, and frequency of inoculation; 3) the vaccination schedule; 4) ethnic differences; 5) the age at vaccination; 6) the presence of severe heart, liver, and kidney disease; 7) OBI status; and 8) assessment criteria for successful vaccination. When analyzing the effect of SNPs on the success of vaccination, it is important to match patients with respect to the main factors or perform appropriate statistical analyses to account for these factors. However, at present, correlation analyses are relatively simple. In addition, most subjects are under 20 years of age, and age is related to the rate of antibody production in response to the hepatitis B vaccine. These factors can lead to differences and contradictory results among studies. Further in-depth analyses of host genes may be helpful for understanding the mechanisms underlying the response to hepatitis B vaccination and for exploring new approaches for the development of more effective hepatitis B vaccines. Furthermore, studies should evaluate whether so-called non-responders, who do not produce anti-HBs antibodies after vaccination, may develop chronic HBV infection. It would be useful to determine the genetic factors leading to non-responsiveness to HBV vaccines.

CONCLUSION

A large number of studies have reported host genetic factors that are associated with chronic HBV infection, clinical type, therapeutic responses, or responses to hepatitis B vaccines (**Figure 2**). Host innate and adaptive immunity represent the major determinants of the outcome of HBV infection. The genetic diversity of many genes related to innate and adaptive immunity have been found to be relevant for hepatitis B vaccination, HBV infection, and antiviral therapy (**Figure 3**).

HBV vaccines induce specific B cell responses, leading to the production of protective antibodies. The genetic polymorphism in many genes like HLAs and IL-4 has an impact on antigen presentation or cytokine production and thereby on antibody production, resulting in different degrees of responsiveness to vaccination (Png et al., 2011; Wang et al., 2012; Cui et al., 2013; Li et al., 2013b; Akcay et al., 2018; Nishida et al., 2018). The polymorphism in NTCP may determine the process of HBV entry (Yan et al., 2012a; Hu et al., 2016; Yang et al., 2016a; Nfor et al., 2018; Wu et al., 2018a). Many host factors may influence the innate and adaptive immunity including activation and phagocytosis of macrophages, antigen presentation by APCs, and priming and functionality of HBV-specific T cells, influencing HBV clearance and persistence (Bertoletti and Ferrari, 2016; Akcay et al., 2018; Lang et al., 2019; Rehermann and Thimme, 2019). It is well recognized that the recognition and presentation of HBV antigens by DCs to specific T cells initiate specific T cell antibody responses (Schurich et al., 2011; Das et al., 2012; Guidotti et al., 2015; Gehring and Protzer, 2019; Rehermann and Thimme, 2019; Zhu et al., 2019). IFNs and proinflammatory cytokines also contribute to HBV pathogenesis and control (Maini and Gehring, 2016; Hong and Bertoletti, 2017; Lang et al., 2019; Zhu et al., 2019). The genetic polymorphisms in relevant human genes could directly or indirectly determine these immune functions (**Figure 3**). Owing to the complexity of the genetic basis for infection characteristics, it is unlikely that clinical parameters can be attributed to variation in a single genetic factor. Furthermore, contradictory results are not unexpected. As age and mother-to-child transmission of HBV infection have great impacts (Li et al., 2015), host genetic factors are usually not the only determinants for chronic HBV infection, HBV intrauterine infection, its clinical outcome, or antiviral therapies.

Owing to the complexity of the pathogenesis of HBV, future studies should apply strict criteria for patient selection and for the selection of matched controls according to various factors, like age, route of transmission, time of infection, race, and host immune status, to identify relevant host factors. It is also necessary to standardize the diagnosis of HBV-related diseases. Results should be verified using different ethnic groups and confirmed by future controlled studies with large sample sizes as well as meta-analyses. Importantly, understanding the biological functions of candidate genetic markers is essential to gain mechanistic insight into HBV-related diseases.

At the moment, genetic markers associated with host responses to HBV infection/vaccines and HBV-related diseases could be classified into three categories according to the quality of studies. Some markers, like human HLAs, are clearly important determinants of HBV pathogenesis and the response to HBV vaccines. However, the precise functions of these loci in HBV infection are unclear. For example, the immunological effects of genetic variation in HLAs are not obvious, though these mutations are likely to contribute to HBV-specific immunity.

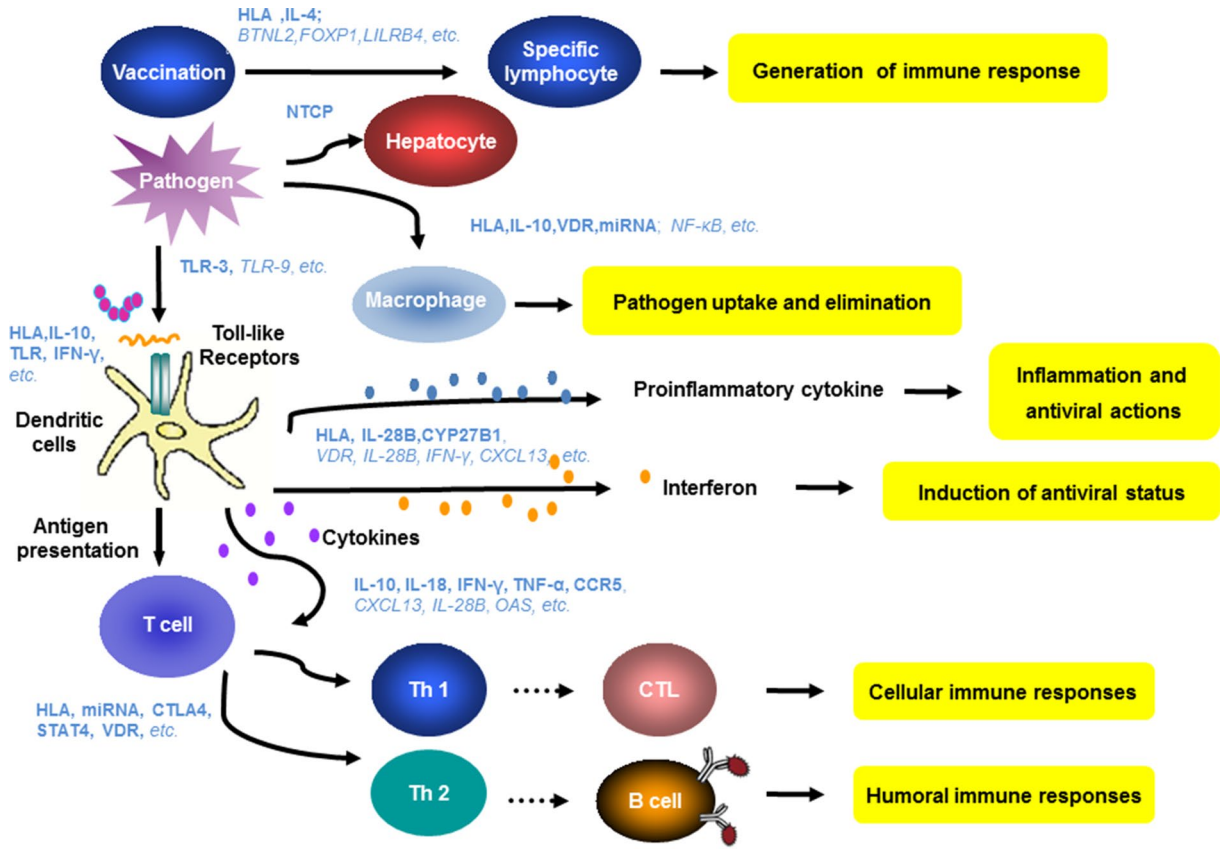

FIGURE 3 | Host genes and immune mechanisms involved in HBV infection. Host innate and adaptive immunity represent the major determinants of the outcome of HBV infection. The genetic diversity of many genes related to innate and adaptive immunity have been found to be relevant for hepatitis B vaccination, HBV infection, and antiviral therapy. Blue letters show the relevant genes identified in the previous studies. The bold and italic letters indicate a high degree or potential correlation of the indicated host factors to clinical features of HBV infection.

Future research should consider interactions between genetic factors and other factors, including viral genotypes/subtypes, population characteristics, other genes, and environmental factors (**Table 1**; **Table S1**). Additional candidate genes that may play a role in the pathogenesis of HBV require confirmation by large-scale, multi-center validation studies. In these future studies, it will be important to stratify populations, match samples, and choose appropriate control groups to improve the reliability of results (**Table 1**; **Table S1**). Additional candidate genes with unconfirmed relevance owing to small samples sizes and studies with different designs should be evaluated by future controlled studies with suitable study subjects and meta-analyses (**Table 1**; **Table S1**).

Recently, our understanding in HBV infection and pathogenesis is fast growing. The knowledge about the molecular and physiological mechanisms of HBV pathogenesis will help us to improve future study design and develop better criteria for patient recruitment. New diagnostic methods like quantitative HBsAg and anti-HBc assays may provide more information to select suitable patient cohorts. The development of genomic and proteomic analysis tools will also enable us to define novel parameters—for example, at the level of single cells or protein chemistry, thereby opening new ways to define genetic determinants for HBV pathogenesis.

AUTHOR CONTRIBUTIONS

ZZ and CW reviewed the literature. ZZ, CW, ZL, and GZ wrote the manuscript. JL and ML participated in the coordination of the study and manuscript modification. ML conceived the project. All authors contributed, read, and approved the manuscript.

FUNDING

This work was supported by the Natural Science Foundation of Anhui Province (Grant no. 1608085MH162).

SUPPLEMENTARY MATERIAL

The Supplementary Material for this article can be found online at: https://www.frontiersin.org/articles/10.3389/fgene.2019.00696/full#supplementary-material

REFERENCES

Ahmadabadi, B. N., Hassanshahi, G., Arababadi, M. K., Leanza, C., and Kennedy, D. (2012). The IL-10 promoter polymorphism at position -592 is correlated with susceptibility to occult HBV infection. *Inflammation* 35, 818–821. doi: 10.1007/s10753-011-9381-x

Akgöllü, E., Bilgin, R., Akkız, H., Ülger, Y., Kaya, B. Y., Karaoğullarından, Ü., et al. (2017). Association between chronic hepatitis B virus infection and HLA-DP gene polymorphisms in the Turkish population. *Virus Res.* 232, 6–12. doi: 10.1016/j.virusres.2017.01.017

Al-Qahtani, A., Al-Ahdal, M., Abdo, A., Sanai, F., Al-Anazi, M., Khalaf, N., et al. (2012a). Toll-like receptor 3 polymorphism and its association with hepatitis B virus infection in Saudi Arabian patients. *J. Med. Virol.* 84, 1353–1359. doi: 10.1002/jmv.23271

Al-Qahtani, A., Al-Anazi, M., Viswan, N. A., Khalaf, N., Abdo, A. A., Sanai, F. M., et al. (2012b). Role of single nucleotide polymorphisms of KIF1B gene in HBV-associated viral hepatitis. *PLoS One* 7, e45128. doi: 10.1371/journal.pone.0045128

Al-Qahtani, A. A., Al-Anazi, M. R., Abdo, A. A., Sanai, F. M., Al-Hamoudi, W., Alswat, K. A., et al. (2014). Association between HLA variations and chronic hepatitis B virus infection in Saudi Arabian patients. *PLoS One* 9, e80445. doi: 10.1371/journal.pone.0080445

Al-Qahtani, A. A., Al-Anazi, M. R., Nazir, N., Wani, K., Abdo, A. A., Sanai, F. M., et al. (2017). Association of single nucleotide polymorphisms in microRNAs with susceptibility to hepatitis B virus infection and HBV-related liver complications: a study in a Saudi Arabian population. *J. Viral Hepat.* 24, 1132–1142. doi: 10.1111/jvh.12749

Akcay, I. M., Katrinli, S., Ozdil, K., Doganay, G. D., and Doganay, L. (2018). Host genetic factors affecting hepatitis B infection outcomes: insights from genome-wide association studies. *World J. Gastroenterol.* 24, 3347–3360. doi: 10.3748/wjg.v24.i30.3347

An, P., Xu, J., Yu, Y., and Winkler, C. A. (2018). Host and viral genetic variation in HBV-related hepatocellular carcinoma. *Front. Genet.* 9, 261. doi: 10.3389/fgene.2018.00261

Arababadi, M. K., Pourfathollah, A. A., Jafarzadeh, A., Hassanshahi, G., and Rezvani, M. E. (2010). Association of exon 9 but not intron 8 VDR polymorphisms with occult HBV infection in south-eastern Iranian patients. *J. Gastroenterol. Hepatol.* 25, 90–93. doi: 10.1111/j.1440-1746.2009.05950.x

Asabe, S., Wieland, S. F., Chattopadhyay, P. K., Roederer, M., Engle, R. E., Purcell, R. H., et al. (2009). The size of the viral inoculum contributes to the outcome of hepatitis B virus infection. *J. Virol.* 83, 9652–9662. doi: 10.1128/JVI.00867-09

Bae, J. S., Kim, J., Pasaje, C. F. A., Cheong, H. S., Lee, T. H., Koh, I. S., et al. (2012). Association study of genetic variations in microRNAs with the risk of hepatitis B-related liver diseases. *Dig. Liver Dis.* 44, 849–854. doi: 10.1016/j.dld.2012.04.021

Beard, J. A., Bearden, A., and Striker, R. (2011). Vitamin D and the anti-viral state. *J. Clin. Virol.* 50, 194–200. doi: 10.1016/j.jcv.2010.12.006

Bellamy, R., Ruwende, C., Corrah, T., K., P. W. J. M., Thursz, M., Whittle, H. C., et al. (1999). Tuberculosis and chronic hepatitis B virus infection in Africans and variation in the vitamin D receptor gene. *J. Infect. Dis.* 179, 721–724. doi: 10.1086/314614

Bengsch, B., and Thimme, R. (2018). For whom the interferons toll – TLR7 mediated boosting of innate and adaptive immunity against chronic HBV infection. *J. Hepatol.* 68, 883–886. doi: 10.1016/j.jhep.2018.01.025

Bertoletti, A., and Ferrari, C. (2013). Innate and adaptive immune responses in chronic hepatitis B virus infections: towards restoration of immune control of viral infection. *Postgrad. Med. J.* 89, 294–304. doi: 10.1136/postgradmedj-2011-301073rep

Bertoletti, A., and Ferrari, C. (2016). Adaptive immunity in HBV infection. *J. Hepatol.* 64, S71–S83. doi: 10.1016/j.jhep.2016.01.026

Bertoletti, A., and Gehring, A. J. (2006). The immune response during hepatitis B virus infection. *J. Gen. Virol.* 87, 1439–1449. doi: 10.1099/vir.0.81920-0

Blank, A., Markert, C., Hohmann, N., Carls, A., Mikus, G., Lehr, T., et al. (2016). First-in-human application of the novel hepatitis B and hepatitis D virus entry inhibitor myrcludex B. *J. Hepatol.* 65, 483–489. doi: 10.1016/j.jhep.2016.04.013

Boglione, L., Cusato, J., Allegra, S., Esposito, I., Patti, F., Cariti, G., et al. (2014). Role of IL28-B polymorphisms in the treatment of chronic hepatitis B HBeAg-negative patients with peginterferon. *Antiviral Res.* 102, 35–43. doi: 10.1016/j.antiviral.2013.11.014

Boglione, L., Cusato, J., De Nicolò, A., Cariti, G., Di Perri, G., and D'Avolio, A. (2015). Role of CYP27B1+2838 promoter polymorphism in the treatment of chronic hepatitis B HBeAg negative with PEG-interferon. *J. Viral Hepat.* 22, 318–327. doi: 10.1111/jvh.12288

Brouwer, W. P., Chan, H. L., Lampertico, P., Hou, J., Tangkijvanich, P., Reesink, H. W., et al. (2019). Genome wide association study identifies genetic variants associated with early and sustained response to (Peg)interferon in chronic hepatitis B patients: the GIANT-B study. *Clin. Infect. Dis.* doi: 10.1093/cid/ciz084

Brouwer, W. P., Sonneveld, M. J., Tabak, F., Simon, K., Cakaloglu, Y., Akarca, U. S., et al. (2014). Polymorphisms of HLA-DP are associated with response to peginterferon in Caucasian patients with chronic hepatitis B. *Aliment Pharmacol. Ther.* 40, 811–818. doi: 10.1111/apt.12910

Brown, R. S., McMahon, B. J., Lok, A. S., Wong, J. B., Ahmed, A. T., Mouchli, M. A., et al. (2016). Antiviral therapy in chronic hepatitis B viral infection during pregnancy: a systematic review and meta-analysis. *Hepatology* 63, 319–333. doi: 10.1002/hep.28302

Bruce, M. G., Bruden, D., Hurlburt, D., Zanis, C., Thompson, G., Rea, L., et al. (2016). Antibody levels and protection after hepatitis B vaccine: results of a 30-year follow-up study and response to a booster dose. *J. Infect. Dis.* 214, 16–22. doi: 10.1093/infdis/jiv748

Buchbinder, E., and Hodi, F. S. (2015). Cytotoxic T lymphocyte antigen-4 and immune checkpoint blockade. *J. Clin. Invest.* 125, 3377–3383. doi: 10.1172/JCI80012

Cao, B., Liu, X., Hou, F., Li, W., Han, Z., Zhang, Q., et al. (2009). The haplotype of the MxA gene promoter is associated with hepatitis B virus infection in a Chinese population. *Liver Int.* 29, 1383–1388. doi: 10.1111/j.1478-3231.2009.02053.x

Chang, Z. L. (2010). Important aspects of Toll-like receptors, ligands and their signaling pathways. *Inflamm. Res.* 59, 791–808. doi: 10.1007/s00011-010-0208-2

Chang, S. W., Fann, C. S., Su, W. H., Wang, Y. C., Weng, C. C., Yu, C. J., et al. (2014). A genome-wide association study on chronic HBV infection and its clinical progression in male Han-Taiwanese. *PLoS One* 9, e99724. doi: 10.1371/journal.pone.0099724

Chatzidaki, V., Choumerianou, D., Dimitriou, H., Kouroumalis, E., and Galanakis, E. (2012). Genetic variants associated with susceptibility to mother-to-child transmission of hepatitis B virus. *Eur. J. Gastroenterol. Hepatol.* 24, 1185–1190. doi: 10.1097/MEG.0b013e328356440f

Chen, D., Zeng, Y., Zhou, J., Yang, L., Jiang, S., Huang, J., et al. (2010). Association of candidate susceptible loci with chronic infection with hepatitis B virus in a Chinese population. *J. Med. Virol.* 82, 371–378. doi: 10.1002/jmv.21716

Chen, H. L., Zha, M. L., Cai, J. Y., and Qin, G. (2018). Maternal viral load and hepatitis B virus mother-to-child transmission risk: a systematic review and meta-analysis. *Hepatol. Res.* 48, 788–801. doi: 10.1111/hepr.13072

Chen, J., Liang, Z., Lu, F., Fang, X., Liu, S., Zeng, Y., et al. (2011). Toll-like receptors and cytokines/cytokine receptors polymorphisms associate with non-response to hepatitis B vaccine. *Vaccine* 29, 706–711. doi: 10.1016/j.vaccine.2010.11.023

Cheng, L., Sun, X., Tan, S., Tan, W., Dan, Y., Zhou, Y., et al. (2014). Effect of HLA-DP and IL28B gene polymorphisms on response to interferon treatment in hepatitis B e-antigen seropositive chronic hepatitis B patients. *Hepatol. Res.* 44, 1000–1007. doi: 10.1111/hepr.12284

Cheong, H. S., Lee, J. H., Yu, S. J., Yoon, J. H., Lee, H. S., Cheong, J. Y., et al. (2015). Association of VARS2-SFTA2 polymorphisms with the risk of chronic hepatitis B in a Korean population. *Liver Int.* 35, 1934–1940. doi: 10.1111/liv.12740

Cheong, J. Y., Cho, S. W., Hwang, I. L., Yoon, S. K., Lee, J. H., Park, C. S., et al. (2006). Association between chronic hepatitis B virus infection and interleukin-10, tumor necrosis factor-alpha gene promoter polymorphisms. *J. Gastroenterol. Hepatol.* 21, 1163–1169. doi: 10.1111/j.1440-1746.2006.04304.x

Cheong, J. Y., Shin, H. D., Kim, Y. J., and Cho, S. W. (2013). Association of polymorphism in MicroRNA 219-1 with clearance of hepatitis B virus infection. *J. Med. Virol.* 85, 808–814. doi: 10.1002/jmv.23551

Chien, R., Kao, J., Peng, C., Chen, C., Liu, C., Huang, Y., et al. (2019). Taiwan consensus statement on the management of chronic hepatitis B. *J. Formos. Med. Assoc.* 118, 7–38. doi: 10.1016/j.jfma.2018.11.008

Chiu, Y. C., Liao, S. F., Wu, J. F., Lin, C. Y., Lee, W. C., Chen, H. L., et al. (2014). Factors affecting the natural decay of hepatitis B surface antigen in children with chronic hepatitis B virus infection during long-term follow-up. *J. Pediatr.* 165, 767–772. doi: 10.1016/j.jpeds.2014.06.059

Cui, W., Sun, C., Deng, B., and Liu, P. (2013). Association of polymorphisms in the interleukin-4 gene with response to hepatitis B vaccine and susceptibility

to hepatitis B virus infection: a meta-analysis. *Gene* 525, 35–40. doi: 10.1016/j.gene.2013.04.065

Cusato, J., Boglione, L., De Nicolò, A., Imbornone, R., Cardellino, C. S., Ghisetti, V., et al. (2017). Association of vitamin D pathway SNPs and clinical response to interferon in a cohort of HBeAg-negative patients. *Pharmacogenomics* 18, 651–661. doi: 10.2217/pgs-2016-0041

Das, A., Ellis, G., Pallant, C., Lopes, A. R., Khanna, P., Peppa, D., et al. (2012). IL-10-producing regulatory B cells in the pathogenesis of chronic hepatitis B virus infection. *J. Immunol.* 189, 3925–3935. doi: 10.4049/jimmunol.1103139

Davila, S., Froeling, F. E. M., Tan, A., Bonnard, C., Boland, G. J., Snippe, H., et al. (2010). New genetic associations detected in a host response study to hepatitis B vaccine. *Genes Immun.* 11, 232–238. doi: 10.1038/gene.2010.1

Deng, G., Zhou, G., Zhai, Y., Li, S., Li, X., Li, Y., et al. (2004). Association of estrogen receptor alpha polymorphisms with susceptibility to chronic hepatitis B virus infection. *Hepatology* 40, 318–326. doi: 10.1002/hep.20318

Di Scala, M., Otano, I., Gil-Fariña, I., Vanrell, L., Hommel, M., Olagüe, C., et al. (2016). Complementary Effects of Interleukin-15 and alpha interferon induce immunity in hepatitis B virus transgenic mice. *J. Virol.* 90, 8563–8574. doi: 10.1128/JVI.01030-16

Dionne-Odom, J., Njei, B., and Tita, A. T. N. (2018). Elimination of vertical transmission of hepatitis B in Africa: a review of available tools and new opportunities. *Clin. Ther.* 40, 1255–1267. doi: 10.1016/j.clinthera.2018.05.016

Du, T., Guo, X. H., Zhu, X. L., Li, J. H., Lu, L. P., Gao, J. R., et al. (2006). Association of TNF-alpha promoter polymorphisms with the outcomes of hepatitis B virus infection in Chinese Han population. *J Viral Hepat.* 13, 618-624. doi: 10.1111/j.1365-2893.2006.00731.x

Eskandari, E., Metanat, M., Pahlevani, E., and Nakhzari-Khodakheir, T. (2017b). Association between TGFβ1 polymorphisms and chronic hepatitis B infection in an Iranian population. *Rev. Soc. Bras. Med. Trop.* 50, 301–308. doi: 10.1590/0037-8682-0266-2016

European Association For The Study Of The Liver (2017). EASL 2017 Clinical Practice Guidelines on the management of hepatitis B virus infection. *J. Hepatol.* 67, 370–398. doi: 10.1016/j.jhep.2017.03.021

Ezzikouri, S., Chihab, H., Elhabazi, A., Wakrim, L., and Benjelloun, S. (2017). Lack of Ser267Phe variant of sodium taurocholate cotransporting polypeptide among Moroccans regardless of hepatitis B virus infection status. *BMC Infect. Dis.* 17, 99. doi: 10.1186/s12879-017-2214-2

Fan, J. H., Hou, S. H., Qing-Ling, L., Hu, J., Peng, H., and Guo, J. J. (2016a). Association of HLA-DQ and IFNL4 polymorphisms with susceptibility to hepatitis B virus infection and clearance. *Ann. Hepatol.* 15, 532–539. doi: 10.5604/16652681.1202946

Fan, R., Sun, J., Yuan, Q., Xie, Q., Bai, X., Ning, Q., et al. (2016b). Baseline quantitative hepatitis B core antibody titre alone strongly predicts HBeAg seroconversion across chronic hepatitis B patients treated with peginterferon or nucleos(t)ide analogues. *Gut* 65, 313–320. doi: 10.1136/gutjnl-2014-308546

Fattovich, G., Bortolotti, F., and Donato, F. (2008). Natural history of chronic hepatitis B: special emphasis on disease progression and prognostic factors. *J. Hepatol.* 48, 335–352. doi: 10.1016/j.jhep.2007.11.011

Fletcher, G. J., Samuel, P., Christdas, J., Gnanamony, M., Ismail, A. M., Anantharam, R., et al. (2011). Association of HLA and TNF polymorphisms with the outcome of HBV infection in the South Indian population. *Genes Immun.* 12, 552–558. doi: 10.1038/gene.2011.32

Freeman, B. E., Hammarlund, E., Raue, H. P., and Slifka, M. K. (2012). Regulation of innate CD8+ T-cell activation mediated by cytokines. *Proc. Natl. Acad. Sci. U.S.A.* 109, 9971–9976. doi: 10.1073/pnas.1203543109

Ganem, D., and Prince, A. M. (2004). Hepatitis B virus infection–natural history and clinical consequences. *N. Engl. J. Med.* 350, 1118–1129. doi: 10.1056/NEJMra031087

Gao, W., Wang, R., Wang, X., Wu, H., Wang, Y., Lu, X., et al. (2017). Vitamin D serum levels and receptor genetic polymorphisms are associated with hepatitis B virus and HIV infections and IFN-λ levels. *Biomark. Med.* 11, 733–740. doi: 10.2217/bmm-2017-0022

Gao, Y., Guo, J., Zhang, F., Guo, Z., Zhang, L. R., Wang, T., et al. (2015b). Evaluation of neonatal Toll-like receptors 3 (c.1377C/T) and 9 (G2848A) gene polymorphisms in HBV intrauterine transmission susceptibility. *Epidemiol. Infect.* 143, 1868–1875. doi: 10.1017/S0950268814002921

Ge, D., Fellay, J., Thompson, A. J., Simon, J. S., Shianna, K. V., Urban, T. J., et al. (2009). Genetic variation in IL28B predicts hepatitis C treatment-induced viral clearance. *Nature* 461, 399–401. doi: 10.1038/nature08309

Gehring, A. J., and Protzer, U. (2019). Targeting innate and adaptive immune responses to cure chronic HBV infection. *Gastroenterology* 156, 325–337. doi: 10.1053/j.gastro.2018.10.032

Geng, P., Song, L., An, H., Huang, J., Li, S., and Zeng, X. (2016). Toll-like receptor 3 is associated with the risk of HCV infection and HBV-related diseases. *Medicine (Baltimore)* 95, e2302. doi: 10.1097/MD.0000000000002302

Goulder, P. J., and Walker, B. D. (2012). HIV and HLA class I: an evolving relationship. *Immunity* 37, 426–440. doi: 10.1016/j.immuni.2012.09.005

Grzegorzewska, A. E., Jod Owska, E. B., Mostowska, A., Sowi Ska, A., and Jagodzi Ski, P. P. (2014). Single nucleotide polymorphisms of vitamin D binding protein, vitamin D receptor and retinoid X receptor alpha genes and response to hepatitis B vaccination in renal replacement therapy patients. *Expert Rev. Vaccines* 13, 1395–1403. doi: 10.1586/14760584.2014.962521

Gu, S. Q., Zhu, Q. R., Yu, H., Fei, L. E., Dong, Z. Q., and Pu, D. P. (2004). Relationship between genetic polymorphism of tumor necrosis factor-alpha and susceptibility to intrauterine HBV infection. *Zhonghua Gan Zang Bing Za Zhi* 12, 538–539.

Guidotti, L. G., Isogawa, M., and Chisari, F. V. (2015). Host–virus interactions in hepatitis B virus infection. *Curr. Opin. Immunol.* 36, 61–66. doi: 10.1016/j.coi.2015.06.016

Guo, F., Tang, L., Shu, S., Sehgal, M., Sheraz, M., Liu, B., et al. (2017). Activation of stimulator of interferon genes in hepatocytes suppresses the replication of hepatitis B virus. *Antimicrob. Agents Chemother.* 61, e00771-17. doi: 10.1128/AAC.00771-17

Guo, X., Yang, G., Yuan, J., Ruan, P., Zhang, M., Chen, X., et al. (2013). Genetic variation in interleukin 28B and response to antiviral therapy in patients with dual chronic infection with hepatitis B and C viruses. *PLoS One* 8, e77911. doi: 10.1371/journal.pone.0077911

Guo, X., Zhang, Y., Li, J., Ma, J., Wei, Z., Tan, W., et al. (2011). Strong influence of human leukocyte antigen (HLA)-DP gene variants on development of persistent chronic hepatitis B virus carriers in the Han Chinese population. *Hepatology* 53, 422–428. doi: 10.1002/hep.24048

Hagenbuch, B., and Meier, P. J. (1994). Molecular cloning, chromosomal localization, and functional characterization of a human liver Na+/bile acid cotransporter. *J. Clin. Invest.* 93, 1326–1331. doi: 10.1172/JCI117091

Han, G., Cao, M., Zhao, W., Jiang, H., Wang, C., Bai, S., et al. (2011). A prospective and open-label study for the efficacy and safety of telbivudine in pregnancy for the prevention of perinatal transmission of hepatitis B virus infection. *J. Hepatol.* 55, 1215–1221. doi: 10.1016/j.jhep.2011.02.032

Harber, M., Sundstedt, A., and Wraith, D. (2000). The role of cytokines in immunological tolerance: potential for therapy. *Expert Rev. Mol. Med.* 2, 1–20. doi: 10.1017/S1462399400002143

Hardy, J., and Singleton, A. (2009). Genomewide association studies and human disease. *N. Engl. J. Med.* 360, 1759–1768. doi: 10.1056/NEJMra0808700

Hassanshahi, G., Arababadi, M. K., Khoramdelazad, H., Yaghini, N., and Zarandi, E. R. (2010). Assessment of CXCL12 (SDF-1α) polymorphisms and its serum level in posttransfusion occult HBV-infected patients in Southeastern Iran. *Arch. Med. Res.* 41, 338–342. doi: 10.1016/j.arcmed.2010.07.001

He, D., Tao, S., Guo, S., Li, M., Wu, J., Huang, H., et al. (2015). Interaction of TLR-IFN and HLA polymorphisms on susceptibility of chronic HBV infection in Southwest Han Chinese. *Liver Int.* 35, 1941–1949. doi: 10.1111/liv.12756

He, Q., Huang, Y., Zhang, L., Yan, Y., Liu, J., Song, X., et al. (2018). Association between vitamin D receptor polymorphisms and hepatitis B virus infection susceptibility: a meta-analysis study. *Gene* 645, 105–112. doi: 10.1016/j.gene.2017.12.027

He, Y. L., Zhao, Y. R., Zhang, S. L., and Lin, S. M. (2006). Host susceptibility to persistent hepatitis B virus infection. *World J. Gastroenterol.* 12, 4788–4793. doi: 10.3748/wjg.v12.i30.4788

Hewison, M. (2011). Vitamin D and innate and adaptive immunity. *Vitam. Horm.* 86, 23–62. doi: 10.1016/B978-0-12-386960-9.00002-2

Hoan, N. X., Van Tong, H., Giang, D. P., Cuong, B. K., Toan, N. L., Wedemeyer, H., et al. (2017). SOCS3 genetic variants and promoter hypermethylation in patients with chronic hepatitis B. *Oncotarget* 8, 17127–17139. doi: 10.18632/oncotarget.15083

Hong, M., and Bertoletti, A. (2017). Tolerance and immunity to pathogens in early life: insights from HBV infection. *Semin. Immunopathol.* 39, 643–652. doi: 10.1007/s00281-017-0641-1

Hong, M., Sandalova, E., Low, D., Gehring, A. J., Fieni, S., Amadei, B., et al. (2015). Trained immunity in newborn infants of HBV-infected mothers. *Nat. Commun.* 6, 6588. doi: 10.1038/ncomms7588

Hoogeveen, R. C., Robidoux, M. P., Schwarz, T., Heydmann, L., Cheney, J. A., Kvistad, D., et al. (2018). Phenotype and function of HBV-specific T cells is determined by the targeted epitope in addition to the stage of infection. *Gut*. 68, 893-904. doi: 10.1136/gutjnl-2018-316644

Hosaka, T., Suzuki, F., Kobayashi, M., Fukushima, T., Kawamura, Y., Sezaki, H., et al. (2015). HLA-DP genes polymorphisms associate with hepatitis B surface antigen kinetics and seroclearance during nucleot(s)ide analogue therapy. *Liver Int.* 35, 1290–1302. doi: 10.1111/liv.12652

Howe, R. C., Dhiman, N., Ovsyannikova, I. G., and Poland, G. A. (2005). Induction of CD4 T cell proliferation and *in vitro* Th1-like cytokine responses to measles virus. *Clin. Exp. Immunol.* 140, 333–342. doi: 10.1111/j.1365-2249.2005.02766.x

Hu, L., Zhai, X., Liu, J., Chu, M., Pan, S., Jiang, J., et al. (2012). Genetic variants in human leukocyte antigen/DP-DQ influence both hepatitis B virus clearance and hepatocellular carcinoma development. *Hepatology*. 55, 1426-1431. doi: 10.1002/hep.24799

Hu, H., Liu, J., Lin, Y., Luo, W., Chu, Y., Chang, C., et al. (2016). The rs2296651 (S267F) variant on NTCP (SLC10A1) is inversely associated with chronic hepatitis B and progression to cirrhosis and hepatocellular carcinoma in patients with chronic hepatitis B. *Gut* 65, 1514–1521. doi: 10.1136/gutjnl-2015-310686

Hu, Y., Chen, Y., Wang, Y., and Liang, H. (2018). Hepatitis B vaccination among 1999–2017 birth cohorts in Zhejiang Province: the determinants associated with infant coverage. *Int. J. Environ. Res. Public Health* 15, E2915. doi: 10.3390/ijerph15122915

Hu, Z., Liu, Y., Zhai, X., Dai, J., Jin, G., Wang, L., et al. (2013). New loci associated with chronic hepatitis B virus infection in Han Chinese. *Nat. Genet.* 45, 1499–1503. doi: 10.1038/ng.2809

Hu, Z., Yang, J., Xiong, G., Shi, H., Yuan, Y., Fan, L., et al. (2014). HLA-DPB1 variant effect on hepatitis B virus clearance and liver cirrhosis development among Southwest Chinese population. *Hepat. Mon.* 14, e19747. doi: 10.5812/hepatmon.19747

Huang, J. M., Xiong, L. S., Wang, J., Liu, Y. F., Zhu, Q. R., Lei, J., et al. (2016). Association between the HLA-DQB1 polymorphisms and the susceptibility of chronic hepatitis B: a comprehensive meta-analysis. *Biomed. Rep.* 4, 557–566. doi: 10.3892/br.2016.632

Huang, R., Hao, Y., Fan, Y., Yang, C., Wu, K., Cao, S., et al. (2013). Association between cytotoxic T-lymphocyte-associated antigen 4 + 49A/G polymorphism and persistent hepatitis B virus infection in the Asian population: evidence from the current studies. *Genet. Test. Mol. Biomarkers* 17, 601–606. doi: 10.1089/gtmb.2013.0069

Huang, X., Li, H., Wang, J., Huang, C., Lu, Y., Qin, X., et al. (2015). Genetic polymorphisms in Toll-like receptor 3 gene are associated with the risk of hepatitis B virus-related liver diseases in a Chinese population. *Gene* 569, 218–224. doi: 10.1016/j.gene.2015.05.054

Jiang, D., Wu, X., Qian, J., Ma, X., Yang, J., Li, Z., et al. (2016a). Genetic variation in STAT4 predicts response to interferon-α therapy for hepatitis B e antigen-positive chronic hepatitis B. *Hepatology* 63, 1102–1111. doi: 10.1002/hep.28423

Jiang, D. K., Ma, X. P., Yu, H., Cao, G., Ding, D. L., Chen, H., et al. (2015). Genetic variants in five novel loci including CFB and CD40 predispose to chronic hepatitis B. *Hepatology* 62, 118–128. doi: 10.1002/hep.27794

Jiang, X., Su, K., Tao, J., Fan, R., Xu, Y., Han, H., et al. (2016b). Association of STAT4 polymorphisms with hepatitis B virus infection and clearance in Chinese Han population. *Amino Acids* 48, 2589–2598. doi: 10.1007/s00726-016-2283-3

Johnson, L. D., and Jameson, S. C. (2009). A chronic need for IL-21. *Science* 324, 1525–1526. doi: 10.1126/science.1176487

Kamatani, Y., Wattanapokayakit, S., Ochi, H., Kawaguchi, T., Takahashi, A., Hosono, N., et al. (2009). A genome-wide association study identifies variants in the HLA-DP locus associated with chronic hepatitis B in Asians. *Nat. Genet.* 41, 591–595. doi: 10.1038/ng.348

Kang, W., Ding, Z., Shen, L., Zhao, Z., Huang, G., Zhang, J., et al. (2014). Risk factors associated with immunoprophylaxis failure against mother to child transmission of hepatitis B virus and hepatitis B vaccination status in Yunnan province, China. *Vaccine* 32, 3362–3366. doi: 10.1016/j.vaccine.2014.04.045

Karataylı, S. C., Bozdayı, M., Karataylı, E., Öztürk, T., Husseini, A. A., Albayrak, R., et al. (2015). Interleukin-28 gene polymorphisms may contribute to HBsAg persistence and the development of HBeAg-negative chronic hepatitis B. *Liver Int.* 35, 846–853. doi: 10.1111/liv.12595

Karra, V. K., Gumma, P. K., Chowdhury, S. J., Ruttala, R., Polipalli, S. K., Chakravarti, A., et al. (2015). IL-18 polymorphisms in hepatitis B virus related liver disease. *Cytokine* 73, 277–282. doi: 10.1016/j.cyto.2015.02.015

Kehrl, J. H. (2006). Chemoattractant receptor signaling and the control of lymphocyte migration. *Immunol. Res.* 34, 211–227. doi: 10.1385/IR:34:3:211

Kew, M. C. (1995). Protective efficacy of hepatitis B vaccination. *Lancet* 345, 1065–1066. doi: 10.1016/S0140-6736(95)90813-7

Khanizadeh, S., Ravanshad, M., Mohebbi, S. R., Naghoosi, H., Tahaei, M. E., Mousavi Nasab, S. D., et al. (2012). Polymorphisms within the promoter region of the gamma interferon (IFN-γ) receptor1 gene are associated with the susceptibility to chronic HBV infection in an Iranian population. *Hepat. Mon.* 12, e7283. doi: 10.5812/hepatmon.7283

Kim, L. H., Cheong, H. S., Namgoong, S., Kim, J. O., Kim, J., Park, B. L., et al. (2015). Replication of genome wide association studies on hepatocellular carcinoma susceptibility loci of STAT4 and HLA-DQ in a Korean population. *Infect. Genet. Evol.* 33, 72–76. doi: 10.1016/j.meegid.2015.04.013

Kim, Y. J., Kim, H. Y., Kim, J. S., Lee, J. H., Yoon, J. H., Kim, C. Y., et al. (2009). Putative association of transforming growth factor-α polymorphisms with clearance of hepatitis B virus and occurrence of hepatocellular carcinoma in patients with chronic hepatitis B virus infection. *J. Viral Hepat.* 17, 518–526. doi: 10.1111/j.1365-2893.2009.01205.x

Kim, Y. J., Kim, H. Y., Lee, J., Yu, S. J., Yoon, J., Lee, H., et al. (2013). A genome-wide association study identified new variants associated with the risk of chronic hepatitis B. *Hum. Mol. Genet.* 22, 4233–4238. doi: 10.1093/hmg/ddt266

Kim, Y. J., Lee, H. S., Yoon, J. H., Kim, C. Y., Park, M. H., Kim, L. H., et al. (2003). Association of TNF-alpha promoter polymorphisms with the clearance of hepatitis B virus infection. *Hum. Mol. Genet.* 12, 2541–2546. doi: 10.1093/hmg/ddg262

Ko, C., Park, W. J., Park, S., Kim, S., Windisch, M. P., and Ryu, W. S. (2015). The FDA-approved drug irbesartan inhibits HBV-infection in HepG2 cells stably expressing sodium taurocholate co-transporting polypeptide. *Antivir. Ther.* 20, 835–842. doi: 10.3851/IMP2965

Koh, S., Kah, J., Tham, C. Y. L., Yang, N., Ceccarello, E., Chia, A., et al. (2018). Nonlytic lymphocytes engineered to express virus-specific T-cell receptors limit HBV infection by activating APOBEC3. *Gastroenterology* 155, 180–193. doi: 10.1053/j.gastro.2018.03.027

Koller, B. H., Geraghty, D. E., DeMars, R., Duvick, L., Rich, S. S., and Orr, H. T. (1989). Chromosomal organization of the human major histocompatibility complex class I gene family. *J. Exp. Med.* 169, 469–480. doi: 10.1084/jem.169.2.469

Kondo, Y., Ueno, Y., and Shimosegawa, T. (2011). Toll-like receptors signaling contributes to immunopathogenesis of HBV infection. *Gastroenterol. Res. Pract.* 2011, 810939. doi: 10.1155/2011/810939

Kong, X., Zhang, X., Gong, Q., Gao, J., Zhang, S., Wang, L., et al. (2007). MxA induction may predict sustained virologic responses of chronic hepatitis B patients with IFN-alpha treatment. *J. Interferon Cytokine Res.* 27, 809–818. doi: 10.1089/jir.2006.0163

Koziel, M. J. (1999). Cytokines in viral hepatitis. *Semin. Liver Dis.* 19, 157–169. doi: 10.1055/s-2007-1007107

Lai, C. L., and Yuen, M. F. (2007). The natural history of chronic hepatitis B. *J. Viral Hepat.* 14Suppl 1, 6–10. doi: 10.1111/j.1365-2893.2007.00909.x

Lampertico, P., Viganò, M., Cheroni, C., Facchetti, F., Invernizzi, F., Valveri, V., et al. (2013). IL28B polymorphisms predict interferon-related hepatitis B surface antigen seroclearance in genotype D hepatitis B e antigen–negative patients with chronic hepatitis B. *Hepatology* 57, 890–896. doi: 10.1002/hep.25749

Lang, J., Neumann-Haefelin, C., and Thimme, R. (2019). Immunological cure of HBV infection. *Hepatol. Int.* 13, 113–124. doi: 10.1007/s12072-018-9912-8

Lange, C. M., Gouttenoire, J., Duong, F. H. T., Morikawa, K., Heim, M. H., and Moradpour, D. (2014). Vitamin D receptor and Jak-STAT signaling crosstalk results in calcitriol-mediated increase of hepatocellular response to IFN-α. *J. Immunol.* 192, 6037–6044. doi: 10.4049/jimmunol.1302296

Laskus, T., Radkowski, M., Lupa, E., Horban, A., Cianciara, J., and Slusarczyk, J. (1992). Prevalence of markers of hepatitis viruses in out-patient alcoholics. *J. Hepatol.* 15, 174–178. doi: 10.1016/0168-8278(92)90032-K

Lebosse, F., Testoni, B., Fresquet, J., Facchetti, F., Galmozzi, E., Fournier, M., et al. (2017). Intrahepatic innate immune response pathways are downregulated in untreated chronic hepatitis B. *J. Hepatol.* 66, 897–909. doi: 10.1016/j.jhep.2016.12.024

Lee, M., and Keeffe, E. B. (2011). Hepatitis B: modern end points of treatment and the specter of viral resistance. *Gastroenterol. Clin. North Am.* 40, 495–505. doi: 10.1016/j.gtc.2011.06.004

Lee, C. M., Lu, S. N., Changchien, C. S., Yeh, C. T., Hsu, T. T., Tang, J. H., et al. (1999). Age, gender, and local geographic variations of viral etiology of

hepatocellular carcinoma in a hyperendemic area for hepatitis B virus infection. *Cancer* 86, 1143–1150. doi: 10.1002/(SICI)1097-0142(19991001)86:7<1143::AID-CNCR7>3.0.CO;2-Z

Lee, D. H., Lee, J. H., Kim, Y. J., Park, N. H., Cho, Y., Lee, Y. B., et al. (2014). Relationship between polymorphisms near the IL28B gene and spontaneous HBsAg seroclearance: a systematic review and meta-analysis. *J. Viral Hepat.* 21, 163–170. doi: 10.1111/jvh.12193

Levy, D. E., and Darnell, J. E. (2002). Stats: transcriptional control and biological impact. *Nat. Rev. Mol. Cell Biol.* 3, 651–662. doi: 10.1038/nrm909

Li, J., Yang, D., He, Y., Wang, M., Wen, Z., Liu, L., et al. (2011a). Associations of HLA-DP variants with hepatitis B virus infection in southern and northern Han Chinese populations: a multicenter case-control study. *PLoS One* 6, e24221. doi: 10.1371/journal.pone.0024221

Li, M., Li, F., Li, N., Sang, J., Fan, X., Deng, H., et al. (2018). Association of polymorphism rs1053005 in STAT3 with chronic hepatitis B virus infection in Han Chinese population. *BMC Med. Genet.* 19, 52. doi: 10.1186/s12881-018-0569-x

Li, N., Zhu, Q., Li, Z., Han, Q., Chen, J., Lv, Y., et al. (2013a). IL21 and IL21R polymorphisms and their interactive effects on serum IL-21 and IgE levels in patients with chronic hepatitis B virus infection. *Hum. Immunol.* 74, 567–573. doi: 10.1016/j.humimm.2013.01.005

Li, S., Deng, Y., Chen, Z. P., Huang, S., Liao, X. C., Lin, L. W., et al. (2011b). Genetic polymorphism of interleukin-16 influences susceptibility to HBV-related hepatocellular carcinoma in a Chinese population. *Infect. Genet. Evol.* 11, 2083–2088. doi: 10.1016/j.meegid.2011.09.025

Li, S., Qian, J., Yang, Y., Zhao, W., Dai, J., Bei, J. X., et al. (2012b). GWAS identifies novel susceptibility loci on 6p21.32 and 21q21.3 for hepatocellular carcinoma in chronic hepatitis B virus carriers. *PLoS Genet.* 8, e1002791. doi: 10.1371/journal.pgen.1002791

Li, Y., Si, L., Zhai, Y., Hu, Y., Hu, Z., Bei, J., et al. (2016). Genome-wide association study identifies 8p21.3 associated with persistent hepatitis B virus infection among Chinese. *Nat. Commun.* 7, 11664. doi: 10.1038/ncomms11664

Li, Z., Hou, X., and Cao, G. (2015). Is mother-to-infant transmission the most important factor for persistent HBV infection? *Emerg. Microbes Infect.* 4, e30. doi: 10.1038/emi.2015.30

Li, Z., Nie, J., Li, J., and Zhuang, H. (2013b). The effect of HLA on immunological response to hepatitis B vaccine in healthy people: a meta-analysis. *Vaccine* 31, 4355–4361. doi: 10.1016/j.vaccine.2013.06.108

Liao, Y., Cai, B., Li, Y., Chen, J., Tao, C., Huang, H., et al. (2014). Association of HLA-DP/DQ and STAT4 polymorphisms with HBV infection outcomes and a mini meta-analysis. *PLoS One* 9, e111677. doi: 10.1371/journal.pone.0111677

Liaw, Y. F., Jen, C. L., You, S. L., Chen, T. H., Lu, S. N., Yeh, S. H., et al. (2009). Hepatitis B virus DNA levels and outcomes in chronic hepatitis B. *Hepatology* 49, S72–S84. doi: 10.1002/hep.22884

Limothai, U., Chuaypen, N., Khlaiphuengsin, A., Chittmittraprap, S., Poovorawan, Y., and Tangkijvanich, P. (2017). Association of vitamin-D-related genetic variations and treatment response to pegylated interferon in patients with chronic hepatitis B. *Antivir. Ther.* 22, 681–688. doi: 10.3851/IMP3154

Limothai, U., Chuaypen, N., Khlaiphuengsin, A., Posuwan, N., Wasitthankasem, R., Poovorawan, Y., et al. (2016). Association of interferon-gamma inducible protein 10 polymorphism with treatment response to pegylated interferon in HBeAg-positive chronic hepatitis B. *Antivir. Ther.* 21, 97–106. doi: 10.3851/IMP2992

Lin, F. C., and Young, H. A. (2014). Interferons: success in anti-viral immunotherapy. *Cytokine Growth Factor Rev.* 25, 369–376. doi: 10.1016/j.cytogfr.2014.07.015

Lin, T. M., Chen, C. J., Wu, M. M., Yang, C. S., Chen, J. S., Lin, C. C., et al. (1989). Hepatitis B virus markers in Chinese twins. *Anticancer Res.* 9, 737–741.

Lin, Y., Deng, W., Pang, J., Kemper, T., Hu, J., Yin, J., et al. (2017). The microRNA-99 family modulates hepatitis B virus replication by promoting IGF-1R/PI3K/Akt/mTOR/ULK1 signaling-induced autophagy. *Cell. Microbiol.* 19, e12709. doi: 10.1111/cmi.12709

Lin, Y., Wu, C., Wang, X., Kemper, T., Squire, A., Gunzer, M., et al. (2019). Hepatitis B virus is degraded by autophagosome-lysosome fusion mediated by Rab7 and related components. *Protein Cell* 10, 60–66. doi: 10.1007/s13238-018-0555-2

Liu, H., Hou, J., and Zhang, X. (2018a). Targeting cIAPs, a new option for functional cure of chronic hepatitis B infection? *Virol. Sin.* 33, 459–461. doi: 10.1007/s12250-018-0062-x

Liu, J., Zhang, E., Ma, Z., Wu, W., Kosinska, A., Zhang, X., et al. (2014a). Enhancing virus-specific immunity *in vivo* by combining therapeutic vaccination and PD-L1 blockade in chronic hepadnaviral infection. *PLoS Pathog.* 10, e1003856. doi: 10.1371/journal.ppat.1003856

Liu, J., Pan, W., and Yang, D. (2018b). The era of immune checkpoint therapy: from cancer to viral infection-a mini comment on the 2018 medicine nobel prize. *Virol. Sin.* 33, 467–471. doi: 10.1007/s12250-018-0077-3

Liu, M., Cao, B., Zhang, H., Dai, Y., Liu, X., and Xu, C. (2006). Association of interferon-gamma gene haplotype in the Chinese population with hepatitis B virus infection. *Immunogenetics* 58, 859–864. doi: 10.1007/s00251-006-0161-y

Liu, M. Q., Zhou, D. J., Wang, X., Zhou, W., Ye, L., Li, J. L., et al. (2012a). IFN-lambda3 inhibits HIV infection of macrophages through the JAK-STAT pathway. *PLoS One* 7, e35902. doi: 10.1371/journal.pone.0035902

Liu, T., Wan, Z., Peng, S., Wang, Y., Chen, H., Li, X., et al. (2018c). Genetic variations in LTA gene and PDCD1 gene and intrauterine infection of hepatitis B virus: a case–control study in China. *Amino Acids* 50, 877–883. doi: 10.1007/s00726-018-2568-9

Liu, Y., Song, C., Ni, H., Jiao, W., Gan, W., Dong, X., et al. (2018d). UBE2L3, a susceptibility gene that plays oncogenic role in hepatitis B-related hepatocellular carcinoma. *J. Viral Hepat.* 25, 1363–1371. doi: 10.1111/jvh.12963

Liu, Y., Xie, K., Wen, J., Deng, M., Li, J., and Hu, Z. (2014b). A genetic variant in microRNA-122 regulatory region confers risk for chronic hepatitis B virus infection and hepatocellular carcinoma in Han Chinese. *J. Med. Virol.* 86, 1669–1674. doi: 10.1002/jmv.23996

Liu, Y., Zhang, Y., Wen, J., Liu, L., Zhai, X., Liu, J., et al. (2012b). A genetic variant in the promoter region of miR-106b-25 cluster and risk of HBV infection and hepatocellular carcinoma. *PLoS One* 7, e32230. doi: 10.1371/journal.pone.0032230

Lok, A. S., Zoulim, F., Locarnini, S., Bartholomeusz, A., Ghany, M. G., Pawlotsky, J., et al. (2007). Antiviral drug-resistant HBV: standardization of nomenclature and assays and recommendations for management. *Hepatology* 46, 254–265. doi: 10.1002/hep.21698

Lu, Y., Zhu, Y., Peng, J., Wang, X., Wang, F., and Sun, Z. (2015b). STAT4 genetic polymorphisms association with spontaneous clearance of hepatitis B virus infection. *Immunol. Res.* 62, 146–152. doi: 10.1007/s12026-015-8645-1

Ma, N., Zhang, X., Yang, L., Zhou, J., Liu, W., Gao, X., et al. (2018a). Role of Functional IFNL4, IFNLR1, IFNA, IFNAR2 polymorphisms in Hepatitis B virus-related liver disease in Han Chinese population. *J. Viral Hepat.* 25, 306–313. doi: 10.1111/jvh.12817

Ma, N., Zhang, X., Yu, F., Gao, P., Fan, Q., Liu, L., et al. (2014). Role of IFN-ks, IFN-ks related genes and the DEPDC5 gene in hepatitis B virus-related liver disease. *J. Viral Hepat.* 21, e29–e38. doi: 10.1111/jvh.12235

Ma, Z., Cao, Q., Xiong, Y., Zhang, E., and Lu, M. (2018b). Interaction between hepatitis B virus and toll-like receptors: current status and potential therapeutic use for chronic hepatitis B. *Vaccines (Basel)* 6, 6. doi: 10.3390/vaccines6010006

Ma, Z., Liu, J., Wu, W., Zhang, E., Zhang, X., Li, Q., et al. (2017). The IL-1R/TLR signaling pathway is essential for efficient CD8+ T-cell responses against hepatitis B virus in the hydrodynamic injection mouse model. *Cell. Mol. Immunol.* 14, 997–1008. doi: 10.1038/cmi.2017.43

Ma, Z., Zhang, E., Yang, D., and Lu, M. (2015). Contribution of Toll-like receptors to the control of hepatitis B virus infection by initiating antiviral innate responses and promoting specific adaptive immune responses. *Cell. Mol. Immunol.* 12, 273–282. doi: 10.1038/cmi.2014.112

Maini, M. K., and Gehring, A. J. (2016). The role of innate immunity in the immunopathology and treatment of HBV infection. *J. Hepatol.* 64, S60–S70. doi: 10.1016/j.jhep.2016.01.028

Mardian, Y., Yano, Y., Wasityastuti, W., Ratnasari, N., Liang, Y., Putri, W. A., et al. (2017). Genetic polymorphisms of HLA-DP and isolated anti-HBc are important subsets of occult hepatitis B infection in Indonesian blood donors: a case-control study. *Virol. J.* 14, 201. doi: 10.1186/s12985-017-0865-7

Matsuura, K., Isogawa, M., and Tanaka, Y. (2016). Host genetic variants influencing the clinical course of Hepatitis B virus infection. *J. Med. Virol.* 88, 371–379. doi: 10.1002/jmv.24350

Mavragani, C. P., and Moutsopoulos, H. M. (2014). Sjögren's syndrome. *Annu. Rev. Pathol.* 9, 273–285. doi: 10.1146/annurev-pathol-012513-104728

Mbarek, H., Ochi, H., Urabe, Y., Kumar, V., Kubo, M., Hosono, N., et al. (2011). A genome-wide association study of chronic hepatitis B identified novel risk locus in a Japanese population. *Hum. Mol. Genet.* 20, 3884–3892. doi: 10.1093/hmg/ddr301

Mélik-Parsadaniantz, S., and Rostène, W. (2008). Chemokines and neuromodulation. *J. Neuroimmunol.* 198, 62–68. doi: 10.1016/j.jneuroim.2008.04.022

Miao, F., Sun, H., Pan, N., Xu, J., Qiu, J., Shen, Y., et al. (2013). Association of human leukocyte antigen class I polymorphism with spontaneous clearance of hepatitis B surface antigen in Qidong Han population. *Clin. Dev. Immunol.* 2013, 145725. doi: 10.1155/2013/145725

Miklossy, G., Hilliard, T. S., and Turkson, J. (2013). Therapeutic modulators of STAT signalling for human diseases. *Nat. Rev. Drug Discov.* 12, 611–629. doi: 10.1038/nrd4088

Mohammad, A. A., Hajilooi, M., Ranjbar, M., Fallahian, F., and Mousavi, S. (2006). Cytotoxic T-lymphocyte antigen 4 gene polymorphisms and susceptibility to chronic hepatitis B. *World J. Gastroenterol.* 12, 630–635. doi: 10.3748/wjg.v12.i4.630

Moudi, B., Heidari, Z., Mahmoudzadeh-Sagheb, H., and Hashemi, M. (2016). Gene polymorphisms of macrophage migration inhibitory factor affect susceptibility to chronic hepatitis B virus infection in an Iranian cohort. *Microbiol. Immunol.* 60, 390–396. doi: 10.1111/1348-0421.12382

Namgoong, S., Shin, J., Cheong, H. S., Kim, L. H., Kim, J. O., Seo, J. Y., et al. (2018). Genetic association of complement component 2 variants with chronic hepatitis B in a Korean population. *Liver Int.* 38, 1576–1582. doi: 10.1111/liv.13675

Newport, M. J., Goetghebuer, T., Weiss, H. A., Whittle, H., Siegrist, C., Marchant, A., et al. (2004). Genetic regulation of immune responses to vaccines in early life. *Genes Immun.* 5, 122–129. doi: 10.1038/sj.gene.6364051

Nfor, O. N., Wu, M. F., Debnath, T., Lee, C. T., Lee, W., Liu, W. H., et al. (2018). Hepatitis B virus infection in Taiwan: the role of NTCP rs2296651 variant in relation to sex. *J. Viral Hepat.* 25, 1116–1120. doi: 10.1111/jvh.12912

Ni, Y. H., Chang, M. H., Wu, J. F., Hsu, H. Y., Chen, H. L., and Chen, D. S. (2012). Minimization of hepatitis B infection by a 25-year universal vaccination program. *J. Hepatol.* 57, 730–735. doi: 10.1016/j.jhep.2012.05.021

Nishida, N., Ohashi, J., Sugiyama, M., Tsuchiura, T., Yamamoto, K., Hino, K., et al. (2015). Effects of HLA-DPB1 genotypes on chronic hepatitis B infection in Japanese individuals. *Tissue Antigens* 86, 406–412. doi: 10.1111/tan.12684

Nishida, N., Sawai, H., Kashiwase, K., Minami, M., Sugiyama, M., Seto, W., et al. (2014). New susceptibility and resistance HLA-DP alleles to HBV-related diseases identified by a trans-ethnic association study in Asia. *PLoS One* 9, e86449. doi: 10.1371/journal.pone.0086449

Nishida, N., Sawai, H., Matsuura, K., Sugiyama, M., Ahn, S. H., Park, J. Y., et al. (2012). Genome-wide association study confirming association of HLA-DP with protection against chronic hepatitis B and viral clearance in Japanese and Korean. *PLoS One* 7, e39175. doi: 10.1371/journal.pone.0039175

Nishida, N., Sugiyama, M., Sawai, H., Nishina, S., Sakai, A., Ohashi, J., et al. (2018). Key HLA-DRB1-DQB1 haplotypes and role of the BTNL2 gene for response to a hepatitis B vaccine. *Hepatology* 68, 848–858. doi: 10.1002/hep.29876

Okada, Y., Uno, N., Sato, S., Mori, S., Sasaki, D., Kaku, N., et al. (2017). Strong influence of human leukocyte antigen-DP variants on response to hepatitis B vaccine in a Japanese population. *Vaccine* 35, 5662–5665. doi: 10.1016/j.vaccine.2017.08.045

Ovsyannikova, I. G., Jacobson, R. M., Vierkant, R. A., Shane Pankratz, V., Jacobsen, S. J., and Poland, G. A. (2004). Associations between human leukocyte antigen (HLA) alleles and very high levels of measles antibody following vaccination. *Vaccine* 22, 1914–1920. doi: 10.1016/j.vaccine.2003.11.016

Pan, C. Q., Duan, Z. P., Bhamidimarri, K. R., Zou, H. B., Liang, X. F., Li, J., et al. (2012a). An algorithm for risk assessment and intervention of mother to child transmission of hepatitis B virus. *Clin. Gastroenterol. Hepatol.* 10, 452–459. doi: 10.1016/j.cgh.2011.10.041

Pan, L., Zhang, L., Zhang, W., Wu, X., Li, Y., Yan, B., et al. (2014). A genome-wide association study identifies polymorphisms in the HLA-DR region associated with non-response to hepatitis B vaccination in Chinese Han populations. *Hum. Mol. Genet.* 23, 2210–2219. doi: 10.1093/hmg/ddt586

Pan, L., Zhang, W., Liang, Z., Wu, X., Zhu, X., Li, J., et al. (2012b). Association between polymorphisms of the cytokine and cytokine receptor genes and immune response to hepatitis B vaccination in a Chinese Han population. *J. Med. Virol.* 84, 26–33. doi: 10.1002/jmv.22251

Park, B. L., Kim, Y. J., Cheong, H. S., Kim, L. H., Choi, Y. H., Lee, H. S., et al. (2006). Association of common promoter polymorphisms of MCP1 with hepatitis B virus clearance. *Exp. Mol. Med.* 38, 694–702. doi: 10.1038/emm.2006.82

Pawlowska, M., Pniewska, A., Pilarczyk, M., Kozielewicz, D., and Domagalski, K. (2016). Prophylaxis of vertical HBV infection. *Expert Opin. Drug Saf.* 15, 1361–1368. doi: 10.1080/14740338.2016.1211106

Peng, S., Wan, Z., Liu, T., Zhu, H., and Du, Y. (2019). Incidence and risk factors of intrauterine transmission among pregnant women with chronic hepatitis B virus infection. *J. Clin. Gastroenterol.* 53, 51–57. doi: 10.1097/MCG.0000000000001001

Petrova, M., and Kamburov, V. (2010). Breastfeeding and chronic HBV infection: clinical and social implications. *World J. Gastroenterol.* 16, 5042–5046. doi: 10.3748/wjg.v16.i40.5042

Phillips, S., Chokshi, S., Riva, A., Evans, A., Williams, R., and Naoumov, N. V. (2010). CD8+ T cell control of hepatitis B virus replication: direct comparison between cytolytic and noncytolytic functions. *J. Immunol.* 184, 287–295. doi: 10.4049/jimmunol.0902761

Png, E., Thalamuthu, A., Ong, R. T. H., Snippe, H., Boland, G. J., and Seielstad, M. (2011). A genome-wide association study of hepatitis B vaccine response in an Indonesian population reveals multiple independent risk variants in the HLA region. *Hum. Mol. Genet.* 20, 3893–3898. doi: 10.1093/hmg/ddr302

Polaris Observatory Collaborators (2018). Global prevalence, treatment, and prevention of hepatitis B virus infection in 2016: a modelling study. *Lancet Gastroenterol. Hepatol.* 3, 383–403. doi: 10.1016/S2468-1253(18)30056-6

Prokunina-Olsson, L., Muchmore, B., Tang, W., Pfeiffer, R. M., Park, H., Dickensheets, H., et al. (2013). A variant upstream of IFNL3 (IL28B) creating a new interferon gene IFNL4 is associated with impaired clearance of hepatitis C virus. *Nat. Genet.* 45, 164–171. doi: 10.1038/ng.2521

Qazi, S., Schlicksup, C. J., Rittichier, J., VanNieuwenhze, M. S., and Zlotnick, A. (2018). An assembly-activating site in the hepatitis B virus capsid protein can also trigger disassembly. *ACS Chem. Biol.* 13, 2114–2120. doi: 10.1021/acschembio.8b00283

Qureshi, A., Thakur, N., Monga, I., Thakur, A., and Kumar, M. (2014). VIRmiRNA: a comprehensive resource for experimentally validated viral miRNAs and their targets. *Database (Oxford)* 2014, 1–10. doi: 10.1093/database/bau103

Raimondo, G., Allain, J. P., Brunetto, M. R., Buendia, M. A., Chen, D. S., Colombo, M., et al. (2008). Statements from the Taormina expert meeting on occult hepatitis B virus infection. *J. Hepatol.* 49, 652–657. doi: 10.1016/j.jhep.2008.07.014

Raimondo, G., Caccamo, G., Filomia, R., and Pollicino, T. (2013). Occult HBV infection. *Semin. Immunopathol.* 35, 39–52. doi: 10.1007/s00281-012-0327-7

Raimondo, G., Locarnini, S., Pollicino, T., Levrero, M., Zoulim, F., Lok, A. S., et al. (2019). Update of the statements on biology and clinical impact of occult hepatitis b virus infection. *J. Hepatol.* doi: 10.1016/j.jhep.2019.03.034

Rebbani, K., Ababou, M., Nadifi, S., Kandil, M., Marchio, A., Pineau, P., et al. (2017). Myxovirus resistance 1 gene polymorphisms and outcomes of viral hepatitis B and C infections in Moroccan patients. *J. Med. Virol.* 89, 647–652. doi: 10.1002/jmv.24642

Rehermann, B., and Bertoletti, A. (2015). Immunological aspects of antiviral therapy of chronic hepatitis B virus and hepatitis C virus infections. *Hepatology* 61, 712–721. doi: 10.1002/hep.27323

Rehermann, B., and Thimme, R. (2019). Insights from antiviral therapy into immune responses to hepatitis B and C virus infection. *Gastroenterology* 156, 369–383. doi: 10.1053/j.gastro.2018.08.061

Reijnders, J. G., Perquin, M. J., Zhang, N., Hansen, B. E., and Janssen, H. L. (2010). Nucleos(t)ide analogues only induce temporary hepatitis B e antigen seroconversion in most patients with chronic hepatitis B. *Gastroenterology* 139, 491–498. doi: 10.1053/j.gastro.2010.03.059

Ren, S., Yu, H., Zhang, H., Liu, Y., Huang, Y., Ma, L., et al. (2011). Polymorphisms of interferon-inducible genes OAS associated with interferon-α treatment response in chronic HBV infection. *Antiviral Res.* 89, 232–237. doi: 10.1016/j.antiviral.2011.01.006

Ren, Y., Guo, Y., Feng, L., Li, T., and Du, Y. (2016). Controversy and strategies exploration in blocking mother-to-child transmission of hepatitis B. *Int. Rev. Immunol.* 35, 249–259. doi: 10.3109/08830185.2015.1096934

Revill, P. A., Chisari, F. V., Block, J. M., Dandri, M., Gehring, A. J., Guo, H., et al. (2019). A global scientific strategy to cure hepatitis B. *Lancet Gastroenterol. Hepatol.* doi: 10.1016/S2468-1253(19)30119-0

Robek, M. D., Boyd, B. S., Wieland, S. F., and Chisari, F. V. (2004). Signal transduction pathways that inhibit hepatitis B virus replication. *Proc. Natl. Acad. Sci. U.S.A.* 101, 1743–1747. doi: 10.1073/pnas.0308340100

Roh, E. Y., Yoon, J. H., In, J. W., Lee, N., Shin, S., and Song, E. Y. (2016). Association of HLA-DP variants with the responsiveness to Hepatitis B virus vaccination in Korean Infants. *Vaccine* 34, 2602–2607. doi: 10.1016/j.vaccine.2016.03.090

Romporn, S., Hirankarn, N., Tangkijvanich, P., and Kimkong, I. (2013). Association of IFNAR2 and IL10RB genes in chronic hepatitis B virus infection. *Tissue Antigens* 82, 21–25. doi: 10.1111/tan.12133

Sakai, A., Noguchi, E., Fukushima, T., Tagawa, M., Iwabuchi, A., Kita, M., et al. (2017). Identification of amino acids in antigen-binding site of class II HLA proteins independently associated with hepatitis B vaccine response. *Vaccine* 35, 703–710. doi: 10.1016/j.vaccine.2016.08.068

Samal, J., Kandpal, M., and Vivekanandan, P. (2012). Molecular mechanisms underlying occult hepatitis B virus infection. *Clin. Microbiol. Rev.* 25, 142–163. doi: 10.1128/CMR.00018-11

Samuel, C. E. (2001). Antiviral actions of interferons. *Clin. Microbiol. Rev.* 14, 778–809. doi: 10.1128/CMR.14.4.778-809.2001

Saraiva, M., and O'Garra, A. (2010). The regulation of IL-10 production by immune cells. *Nat. Rev. Immunol.* 10, 170–181. doi: 10.1038/nri2711

Sato, T., Do, S. H., Asao, T., Akita, T., Katayama, K., Tatara, K., et al. (2014). Estimating numbers of persons with persistent hepatitis B virus infection transmitted vertically and horizontally in the birth cohort during 1950-1985 in Japan. *Hepatol. Res.* 44, E181–E188. doi: 10.1111/hepr.12288

Saxena, R., Chawla, Y. K., Verma, I., and Kaur, J. (2014). Effect of IL-12B, IL-2, TGF-β1, and IL-4 polymorphism and expression on hepatitis B progression. *J. Interferon Cytokine Res.* 34, 117–128. doi: 10.1089/jir.2013.0043

Schoenborn, J. R., and Wilson, C. B. (2007). Regulation of interferon-gamma during innate and adaptive immune responses. *Adv. Immunol.* 96, 41–101. doi: 10.1016/S0065-2776(07)96002-2

Schott, E., Witt, H., Pascu, M., van Boemmel, F., Weich, V., Bergk, A., et al. (2007). Association of CTLA4 single nucleotide polymorphisms with viral but not autoimmune liver disease. *Eur. J. Gastroenterol. Hepatol.* 19, 947–951. doi: 10.1097/MEG.0b013e3282efa240

Schurich, A., Khanna, P., Lopes, A. R., Han, K. J., Peppa, D., Micco, L., et al. (2011). Role of the coinhibitory receptor cytotoxic T lymphocyte antigen-4 on apoptosis-Prone CD8 T cells in persistent hepatitis B virus infection. *Hepatology* 53, 1494–1503. doi: 10.1002/hep.24249

Seed, C. R., Allain, J. P., Lozano, M., Laperche, S., Gallian, P., Gross, S., et al. (2019). International forum on occult hepatitis B infection and transfusion safety. *Vox Sang.* 114, 397–406. doi: 10.1111/vox.12744

Seo, D. H., Whang, D. H., Song, E. Y., Kim, H. S., and Park, Q. (2011). Prevalence of antibodies to hepatitis B core antigen and occult hepatitis B virus infections in Korean blood donors. *Transfusion* 51, 1840–1846. doi: 10.1111/j.1537-2995.2010.03056.x

Seshasubramanian, V., Soundararajan, G., and Ramasamy, P. (2018). Human leukocyte antigen A, B and hepatitis B infection outcome: a meta-analysis. *Infect. Genet. Evol.* 66, 392–398. doi: 10.1016/j.meegid.2017.07.027

Shao, Z., Xu, D., Xu, J., Li, J., Yan, Y., Men, K., et al. (2007). Maternal hepatitis B virus (HBV) DNA positivity and sexual intercourse are associated with HBV intrauterine transmission in China: a prospective case-control study. *J. Gastroenterol. Hepatol.* 22, 165–170. doi: 10.1111/j.1440-1746.2006.04462.x

Sheppard, P., Kindsvogel, W., Xu, W., Henderson, K., Schlutsmeyer, S., Whitmore, T. E., et al. (2003). IL-28, IL-29 and their class II cytokine receptor IL-28R. *Nat. Immunol.* 4, 63–68. doi: 10.1038/ni873

Shi, K. Q., Cai, X. H., Xiao, D. D., Wu, S. J., Peng, M. M., Lin, X. F., et al. (2012). Tumour necrosis factor-α-857T allele reduces the risk of hepatitis B virus infection in an Asian population. *J. Viral Hepat.* 19, e66–e72. doi: 10.1111/j.1365-2893.2011.01540.x

Shiina, T., Hosomichi, K., Inoko, H., and Kulski, J. K. (2009). The HLA genomic loci map: expression, interaction, diversity and disease. *J. Hum. Genet.* 54, 15–39. doi: 10.1038/jhg.2008.5

Shin, E. C., Sung, P. S., and Park, S. H. (2016). Immune responses and immunopathology in acute and chronic viral hepatitis. *Nat. Rev. Immunol.* 16, 509–523. doi: 10.1038/nri.2016.69

Shin, H. D., Park, B. L., Cheong, H. S., Yoon, J. H., Kim, Y. J., and Lee, H. S. (2007). SPP1 polymorphisms associated with HBV clearance and HCC occurrence. *Int. J. Epidemiol.* 36, 1001–1008. doi: 10.1093/ije/dym093

Shin, J., Cheong, H. S., Kim, J. Y., Lee, J., Yu, S. J., Yoon, J., et al. (2019). Identification of additional EHMT2 variant associated with the risk of chronic hepatitis B by GWAS follow-up study. *Genes Immun.* 20, 1–9. doi: 10.1038/s41435-017-0004-x

Shin, J. G., Cheong, H. S., Lee, K., Ju, B. G., Lee, J. H., Yu, S. J., et al. (2017). Identification of novel OCT4 genetic variant associated with the risk of chronic hepatitis B in a Korean population. *Liver Int.* 37, 354–361. doi: 10.1111/liv.13245

Singh, R., Kaul, R., Kaul, A., and Khan, K. (2007). A comparative review of HLA associations with hepatitis B and C viral infections across global populations. *World J. Gastroenterol.* 13, 1770–1787. doi: 10.3748/wjg.v13.i12.1770

Singh, R. K., Dai, Y., Staudinger, J. L., and Muma, N. A. (2009). Activation of the JAK-STAT pathway is necessary for desensitization of 5-HT2A receptor-stimulated phospholipase C signalling by olanzapine, clozapine and MDL 100907. *Int. J. Neuropsychopharmacol.* 12, 651–665. doi: 10.1017/S1461145708009590

Sonneveld, M. J., Wong, V. W. S., Woltman, A. M., Wong, G. L. H., Cakaloglu, Y., Zeuzem, S., et al. (2012). Polymorphisms near IL28B and serologic response to peginterferon in HBeAg-positive patients with chronic hepatitis B. *Gastroenterology* 142, 513–520.e1. doi: 10.1053/j.gastro.2011.11.025

Stevens, C. E., Beasley, R. P., Tsui, J., and Lee, W. C. (1975). Vertical transmission of hepatitis B antigen in Taiwan. *N. Engl. J. Med.* 292, 771–774. doi: 10.1056/NEJM197504102921503

Su, C., Hou, Z., Zhang, C., Tian, Z., and Zhang, J. (2011). Ectopic expression of microRNA-155 enhances innate antiviral immunity against HBV infection in human hepatoma cells. *Virol. J.* 8, 354. doi: 10.1186/1743-422X-8-354

Su, F. H., Chen, J. D., Cheng, S. H., Lin, C. H., Liu, Y. H., and Chu, F. Y. (2007). Seroprevalence of hepatitis-B infection amongst Taiwanese university students 18 years following the commencement of a national hepatitis-B vaccination program. *J. Med. Virol.* 79, 138–143. doi: 10.1002/jmv.20771

Su, T., Yang, H., Tseng, T., Liou, J., Liu, C., Chen, C., et al. (2018). Distinct relapse rates and risk predictors after discontinuing tenofovir and entecavir therapy. *J. Infect. Dis.* 217, 1193–1201. doi: 10.1093/infdis/jix690

Sun, Y., Lu, Y., Li, T., Xie, L., Deng, Y., Li, S., et al. (2015). Interferon gamma +874T/A polymorphism increases the risk of hepatitis virus-related diseases: evidence from a meta-analysis. *PLOS ONE* 10, e0121168. doi: 10.1371/journal.pone.0121168

Suneetha, P. V., Sarin, S. K., Goyal, A., Kumar, G. T., Shukla, D. K., and Hissar, S. (2006). Association between vitamin D receptor, CCR5, TNF-α and TNF-β gene polymorphisms and HBV infection and severity of liver disease. *J. Hepatol.* 44, 856–863. doi: 10.1016/j.jhep.2006.01.028

Talaat, R. M., Dondeti, M. F., El-Shenawy, S. Z., and Khamiss, O. A. (2014). Association between IL-10 gene promoter polymorphism and hepatitis B viral infection in an Egyptian population. *Biochem. Genet.* 52, 387–402. doi: 10.1007/s10528-014-9655-8

Tangkijvanich, P., Chittmittraprap, S., Poovorawan, K., Limothai, U., Khlaiphuengsin, A., Chuaypen, N., et al. (2016). A randomized clinical trial of peginterferon alpha-2b with or without entecavir in patients with HBeAg-negative chronic hepatitis B: role of host and viral factors associated with treatment response. *J. Viral Hepat.* 23, 427–438. doi: 10.1111/jvh.12467

Terrault, N. A., Bzowej, N. H., Chang, K. M., Hwang, J. P., Jonas, M. M., Murad, M. H., et al. (2016). AASLD guidelines for treatment of chronic hepatitis B. *Hepatology* 63, 261–283. doi: 10.1002/hep.28156

Thanapirom, K., Suksawatamnuay, S., Sukeepaisarnjareon, W., Tanwandee, T., Charatcharoenwitthaya, P., Thongsawat, S., et al. (2017). Genetic variation in the vitamin D pathway CYP2R1 gene predicts sustained HBeAg seroconversion in chronic hepatitis B patients treated with pegylated interferon: a multicenter study. *PLoS One* 12, e0173263. doi: 10.1371/journal.pone.0173263

Thimme, R., Wieland, S., Steiger, C., Ghrayeb, J., Reimann, K. A., Purcell, R. H., et al. (2003). CD8+ T cells mediate viral clearance and disease pathogenesis during acute hepatitis B virus infection. *J. Virol.* 77, 68–76. doi: 10.1128/JVI.77.1.68-76.2003

Thio, C. L., Mosbruger, T. L., Kaslow, R. A., Karp, C. L., Strathdee, S. A., Vlahov, D., et al. (2004). Cytotoxic T-lymphocyte antigen 4 gene and recovery from hepatitis B virus infection. *J. Virol.* 78, 11258–11262. doi: 10.1128/JVI.78.20.11258-11262.2004

Thomas, R., Thio, C. L., Apps, R., Qi, Y., Gao, X., Marti, D., et al. (2012). A novel variant marking HLA-DP expression levels predicts recovery from hepatitis B virus infection. *J. Virol.* 86, 6979–6985. doi: 10.1128/JVI.00406-12

Thursz, M., Yee, L., and Khakoo, S. (2011). Understanding the host genetics of chronic hepatitis B and C. *Semin. Liver Dis.* 31, 115–127. doi: 10.1055/s-0031-1276642

Torbenson, M., and Thomas, D. L. (2002). Occult hepatitis B. *Lancet Infect. Dis.* 2, 479–486. doi: 10.1016/S1473-3099(02)00345-6

Trinks, J., Nishida, N., Hulaniuk, M. L., Caputo, M., Tsuchiura, T., Marciano, S., et al. (2017). Role of HLA-DP and HLA-DQ on the clearance of hepatitis B

virus and the risk of chronic infection in a multiethnic population. *Liver Int.* 37, 1476–1487. doi: 10.1111/liv.13405

Tseng, T., Yu, M., Liu, C., Lin, C., Huang, Y., Hsu, C., et al. (2011). Effect of host and viral factors on hepatitis B e antigen-positive chronic hepatitis B patients receiving pegylated interferon-α-2a therapy. *Antivir. Ther.* 16, 629–637. doi: 10.3851/IMP1841

Tu, T., and Urban, S. (2018). Virus entry and its inhibition to prevent and treat hepatitis B and hepatitis D virus infections. *Curr. Opin. Virol.* 30, 68–79. doi: 10.1016/j.coviro.2018.04.004

van Lith, M., McEwen-Smith, R. M., and Benham, A. M. (2010). HLA-DP, HLA-DQ, and HLA-DR have different requirements for invariant chain and HLA-DM. *J. Biol. Chem.* 285, 40800–40808. doi: 10.1074/jbc.M110.148155

Vermehren, J., Lotsch, J., Susser, S., Wicker, S., Berger, A., Zeuzem, S., et al. (2012). A common HLA-DPA1 variant is associated with hepatitis B virus infection but fails to distinguish active from inactive Caucasian carriers. *PLoS One* 7, e32605. doi: 10.1371/journal.pone.0032605

Wan, Z., Lin, X., Li, T., Zhou, A., Yang, M., Hu, D., et al. (2016). Genetic variant in CXCL13 gene is associated with susceptibility to intrauterine infection of hepatitis B virus. *Sci. Rep.* 6, 26465. doi: 10.1038/srep26465

Wang, L., Wu, X., Zhang, W., Zhu, D., Wang, Y., Li, Y., et al. (2011). Evaluation of genetic susceptibility loci for chronic hepatitis B in Chinese: two independent case-control studies. *PLoS One* 6, e17608. doi: 10.1371/journal.pone.0017608

Wang, L., Zou, Z., and Wang, K. (2016). Clinical relevance of HLA gene variants in HBV infection. *J. Immunol. Res.* 2016, 9069375. doi: 10.1155/2016/9069375

Wang, P., Mo, R., Lai, R., Xu, Y., Lu, J., Zhao, G., et al. (2017a). Genetic variations of NTCP are associated with susceptibility to HBV infection and related hepatocellular carcinoma. *Oncotarget* 8, 105407–105424. doi: 10.18632/oncotarget.22211

Wang, S. H., Chen, P. J., and Yeh, S. H. (2015). Gender disparity in chronic hepatitis B: mechanisms of sex hormones. *J. Gastroenterol. Hepatol.* 30, 1237–1245. doi: 10.1111/jgh.12934

Wang, T., Shen, C., Chen, L., Liu, S., and Ji, Y. (2017b). Association of human leukocyte antigen polymorphisms with occult hepatitis B virus infection in a Shaanxi Han population. *J. Gene Med.* 19, e2987. doi: 10.1002/jgm.2987

Wang, Y., Xu, P., Zhu, D., Zhang, S., Bi, Y., Hu, Y., et al. (2012). Association of polymorphisms of cytokine and TLR-2 genes with long-term immunity to hepatitis B in children vaccinated early in life. *Vaccine* 30, 5708–5713. doi: 10.1016/j.vaccine.2012.07.010

Wasityastuti, W., Yano, Y., Ratnasari, N., Triyono, T., Triwikatmani, C., Indrarti, F., et al. (2016). Protective effects of HLA-DPA1/DPB1 variants against hepatitis B virus infection in an Indonesian population. *Infect. Genet. Evol.* 41, 177–184. doi: 10.1016/j.meegid.2016.03.034

Wen, J., Liu, Y., Liu, J., Liu, L., Song, C., Han, J., et al. (2015). Expression quantitative trait loci in long non-coding RNA ZNRD1-AS1 influence both HBV infection and hepatocellular carcinoma development. *Mol. Carcinog.* 54, 1275–1282. doi: 10.1002/mc.22200

Wong, D. K., Watanabe, T., Tanaka, Y., Seto, W. K., Lee, C. K., Fung, J., et al. (2013). Role of HLA-DP polymorphisms on chronicity and disease activity of hepatitis B infection in Southern Chinese. *PLoS One* 8, e66920. doi: 10.1371/journal.pone.0066920

Wright, T. L., and Lau, J. Y. (1993). Clinical aspects of hepatitis B virus infection. *Lancet* 342, 1340–1344. doi: 10.1016/0140-6736(93)92250-W

Wu, H., Zhao, G., Qian, F., Liu, K., Xie, J., Zhou, H., et al. (2015a). Association of IL28B polymorphisms with peginterferon treatment response in Chinese Han patients with HBeAg-positive chronic hepatitis B. *Liver Int.* 35, 473–481. doi: 10.1111/liv.12491

Wu, T., Chen, C., Lai, S., Lin, H. H., Chu, C., and Wang, L. (2015b). SNP rs7770370 in HLA-DPB1 loci as a major genetic determinant of response to booster hepatitis B vaccination: results of a genome-wide association study. *J. Gastroenterol. Hepatol.* 30, 891–899. doi: 10.1111/jgh.12845

Wu, W., Zeng, Y., Lin, J., Wu, Y., Chen, T., Xun, Z., et al. (2018a). Genetic variants in NTCP exon gene are associated with HBV infection status in a Chinese Han population. *Hepatol. Res.* 48, 364–372. doi: 10.1111/hepr.13007

Wu, X., Shi, W., Wu, J., Zhu, X., Chen, K., Zheng, S., et al. (2014). A functional polymorphism in ADAR1 gene affects HBsAg seroclearance both spontaneously and interferon induced. *Liver Int.* 34, 1560–1565. doi: 10.1111/liv.12444

Wu, X., Zhu, X., Zhu, S., Li, J., Ma, J., Li, Z., et al. (2009). A pharmacogenetic study of polymorphisms in interferon pathway genes and response to interferon-alpha treatment in chronic hepatitis B patients. *Antiviral Res.* 83, 252–256. doi: 10.1016/j.antiviral.2009.06.003

Xiang, X., Guo, Y., Yang, L., Ge, Q., Mijit, S., and Xu, F. (2016). Association of human leukocyte antigen DP/DQ gene polymorphisms with chronic hepatitis B in Chinese Han and Uygur populations. *Infect. Genet. Evol.* 43, 407–411. doi: 10.1016/j.meegid.2016.06.022

Xu, B., Zhu, D., Bi, Y., Wang, Y., Hu, Y., and Zhou, Y. (2017a). Minimal association of alleles of human leukocyte antigen class II gene and long-term antibody response to hepatitis B vaccine vaccinated during infancy. *Vaccine* 35, 2457–2462. doi: 10.1016/j.vaccine.2017.03.021

Xu, H., Zhao, M., He, J., and Chen, Z. (2013). Association between cytotoxic T-lymphocyte associated protein 4 gene +49 A/G polymorphism and chronic infection with hepatitis B virus: a meta-analysis. *J. Int. Med. Res.* 41, 559–567. doi: 10.1177/0300060513483387

Xu, T., Sun, M., and Wang, H. (2017b). Relationship between HLA-DQ gene polymorphism and hepatitis B virus infection. *Biomed. Res. Int.* 2017, 9679843. doi: 10.1155/2017/9679843

Xu, T., Zhu, A., Sun, M., Lv, J., Qian, Z., Wang, X., et al. (2018). Quantitative assessment of HLA-DQ gene polymorphisms with the development of hepatitis B virus infection, clearance, liver cirrhosis, and hepatocellular carcinoma. *Oncotarget* 9, 96–109. doi: 10.18632/oncotarget.22941

Xu, Y. Y., Yu, J. Y., Zhong, Y. W., Song, H. B., Liu, H. H., Jia, L. L., et al. (2008). Association between the frequency of class II HLA antigens and the susceptibility to intrauterine infection of hepatitis B virus. *Int J Biol Sci* 4, 111–115. doi: 10.7150/ijbs.4.111

Yan, H., Zhong, G., Xu, G., He, W., Jing, Z., Gao, Z., et al. (2012a). Sodium taurocholate cotransporting polypeptide is a functional receptor for human hepatitis B and D virus. *Elife* 1, e00049. doi: 10.7554/eLife.00049

Yan, K., Cai, W., Cao, F., Sun, H., Chen, S., Xu, R., et al. (2013). Genetic effects have a dominant role on poor responses to infant vaccination to hepatitis B virus. *J. Hum. Genet.* 58, 293–297. doi: 10.1038/jhg.2013.18

Yan, Z., Tan, S., Dan, Y., Sun, X., Deng, G., and Wang, Y. (2012b). Relationship between HLA-DP gene polymorphisms and clearance of chronic hepatitis B virus infections: case–control study and meta-analysis. *Infect. Genet. Evol.* 12, 1222–1228. doi: 10.1016/j.meegid.2012.03.026

Yang, C., Pan, L., Zhang, L., Wu, X., Zhu, X., Yan, B., et al. (2014). BTNL2 associated with the immune response to hepatitis B vaccination in a Chinese Han population. *J. Med. Virol.* 86, 1105–1112. doi: 10.1002/jmv.23934

Yang, J., Yang, Y., Xia, M., Wang, L., Zhou, W., Yang, Y., et al. (2016a). A genetic variant of the NTCP gene is associated with HBV infection status in a Chinese population. *BMC Cancer* 16, 211. doi: 10.1186/s12885-016-2257-6

Yang, L., and Lu, M. (2018). Small molecule inhibitors of hepatitis B virus nucleocapsid assembly: a new approach to treat chronic HBV infection. *Curr. Med. Chem.* 25, 802–813. doi: 10.2174/0929867324666170704121800

Yang, L., Liu, F., Tong, X., Hoffmann, D., Zuo, J., and Lu, M. (2019). Treatment of chronic hepatitis B virus infection using small molecule modulators of nucleocapsid assembly: recent advances and perspectives. *ACS Infect. Dis.* 5, 713–724. doi: 10.1021/acsinfecdis.8b00337

Yang, S., Tian, G., Cui, Y., Ding, C., Deng, M., Yu, C., et al. (2016b). Factors influencing immunologic response to hepatitis B vaccine in adults. *Sci. Rep.* 6, 27251. doi: 10.1038/srep27251

Yano, Y., Seo, Y., Azuma, T., and Hayashi, Y. (2013). Hepatitis B virus and host factors. *Hepatobiliary Surg. Nutr.* 2, 121–123. doi: 10.3978/j.issn.2304-3881.2012.10.10

Yin, J., Zhang, H., He, Y., Xie, J., Liu, S., Chang, W., et al. (2010). Distribution and hepatocellular carcinoma-related viral properties of hepatitis B virus genotypes in Mainland China: a community-based study. *Cancer Epidemiol. Biomarkers Prev.* 19, 777–786. doi: 10.1158/1055-9965.EPI-09-1001

Yoon, J. H., Shin, S., In, J. W., Chang, J. Y., Song, E. Y., and Roh, E. Y. (2014). Association of HLA alleles with the responsiveness to hepatitis B virus vaccination in Korean infants. *Vaccine* 32, 5638–5644. doi: 10.1016/j.vaccine.2014.08.007

Yu, H., Zhu, Q. R., Gu, S. Q., and Fei, L. E. (2006). Relationship between IFN-gamma gene polymorphism and susceptibility to intrauterine HBV infection. *World J. Gastroenterol.* 12, 2928–2931. doi: 10.3748/wjg.v12.i18.2928

Yu, L., Cheng, Y., Cheng, M., Yao, Y., Zhang, Q., Zhao, X., et al. (2015). Quantitative assessment of common genetic variations in HLA-DP with hepatitis B virus infection, clearance and hepatocellular carcinoma development. *Sci. Rep.* 5, 14933. doi: 10.1038/srep14933

Yu, S. J., Kim, J. W., Lee, J. H., Yoon, J. H., Lee, H. S., Cheong, J. Y., et al. (2014). Association of a microRNA-323b polymorphism with the persistence of hepatitis B virus infection by the enhancement of viral replication. *J. Viral Hepat.* 21, 853–859. doi: 10.1111/jvh.12215

Zhang, E., and Lu, M. (2015). Toll-like receptor (TLR)-mediated innate immune responses in the control of hepatitis B virus (HBV) infection. *Med. Microbiol. Immunol.* 204, 11–20. doi: 10.1007/s00430-014-0370-1

Zhang, C., Zhong, Y., and Guo, L. (2013a). Strategies to prevent hepatitis B virus infection in China: immunization, screening, and standard medical practices. *Biosci. Trends* 7, 7–12. doi: 10.5582/bst.2013.v7.1.7

Zhang, Q., Ji, X. W., Hou, X. M., Lu, F. M., Du, Y., Yin, J. H., et al. (2014a). Effect of functional nuclear factor-kappaB genetic polymorphisms on hepatitis B virus persistence and their interactions with viral mutations on the risk of hepatocellular carcinoma. *Ann. Oncol.* 25, 2413–2419. doi: 10.1093/annonc/mdu451

Zhang, Q., Yin, J., Zhang, Y., Deng, Y., Ji, X., Du, Y., et al. (2013b). HLA-DP polymorphisms affect the outcomes of chronic hepatitis B virus infections, possibly through interacting with viral mutations. *J. Virol.* 87, 12176–12186. doi: 10.1128/JVI.02073-13

Zhang, T. T., Ye, J., Xia, S. L., Zhang, Y. F., Su, Q., Zhang, Z. H., et al. (2013c). Polymorphism of estrogen receptor alpha (ESR1) is associated with virological response to entecavir (ETV) in nucleoside-naïve adult patients with chronic hepatitis B. *Infection* 41, 371–378. doi: 10.1007/s15010-012-0320-z

Zhang, X., Hou, J., and Lu, M. (2013d). Regulation of hepatitis B virus replication by epigenetic mechanisms and microRNAs. *Front. Genet.* 4, 202. doi: 10.3389/fgene.2013.00202

Zhang, X., Jia, J., Dong, J., Yu, F., Ma, N., Li, M., et al. (2014b). HLA-DQ polymorphisms with HBV infection: different outcomes upon infection and prognosis to lamivudine therapy. *J. Viral Hepat.* 21, 491–498. doi: 10.1111/jvh.12159

Zhang, X., Ni, X., Jia, J., Dong, J., Yu, F., Ma, N., et al. (2013e). Association of the rs3077 and rs9277535 polymorphisms in HLA-DP with hepatitis B virus infection and spontaneous clearance: a meta-analysis. *Scand. J. Gastroenterol.* 48, 736–744. doi: 10.3109/00365521.2013.787643

Zhang, X., Zhang, E., Ma, Z., Pei, R., Jiang, M., Schlaak, J. F., et al. (2011a). Modulation of hepatitis B virus replication and hepatocyte differentiation by MicroRNA-1. *Hepatology* 53, 1476–1485. doi: 10.1002/hep.24195

Zhang, Y., Li, Y., Wu, M., Cao, P., Liu, X., Ren, Q., et al. (2017). Comprehensive assessment showed no associations of variants at the SLC10A1 locus with susceptibility to persistent HBV infection among Southern Chinese. *Sci. Rep.* 7, 46490. doi: 10.1038/srep46490

Zhang, Z. H., Li, L., Zhao, X. P., Glebe, D., Bremer, C. M., Zhang, Z. M., et al. (2011b). Elimination of hepatitis B virus surface antigen and appearance of neutralizing antibodies in chronically infected patients without viral clearance. *J. Viral Hepat.* 18, 424–433. doi: 10.1111/j.1365-2893.2010.01322.x

Zhao, Q., Peng, L., Huang, W., Li, Q., Pei, Y., Yuan, P., et al. (2012). Rare inborn errors associated with chronic hepatitis B virus infection. *Hepatology* 56, 1661–1670. doi: 10.1002/hep.25850

Zheng, M. H., Xiao, D. D., Lin, X. F., Wu, S. J., Peng, M. M., Yu, X. Y., et al. (2012). The tumour necrosis factor-α-238A allele increases the risk of chronic HBV infection in European populations. *J. Viral Hepat.* 19, e11–e17. doi: 10.1111/j.1365-2893.2011.01491.x

Zhou, G. Q., Meng, H., Wang, J. R., Sun, F. X., Wang, X. J., Wang, R. B., et al. (2015). Functional polymorphisms in microRNA gene and hepatitis B risk among Asian population: a meta-analysis. *Genet. Mol. Res.* 14, 4767–4777. doi: 10.4238/2015.May.11.9

Zhu, H., Wang, C., Zhang, Y., Wei, S., Li, X., and Zhang, Z. (2016a). Prediction model for sustained hepatitis B e antigen seroconversion to peginterferon alfa-2a in chronic hepatitis B. *J. Gastroenterol. Hepatol.* 31, 1963–1970. doi: 10.1111/jgh.13414

Zhu, J., Zhang, T., Cao, L., Li, A., Zheng, K., Zhang, N., et al. (2017). Toll like receptor7 polymorphisms in relation to disease susceptibility and progression in Chinese patients with chronic HBV infection. *Sci. Rep.* 7, 12417. doi: 10.1038/s41598-017-12698-5

Zhu, M., Dai, J., Wang, C., Wang, Y., Qin, N., Ma, H., et al. (2016b). Fine mapping the MHC region identified four independent variants modifying susceptibility to chronic hepatitis B in Han Chinese. *Hum. Mol. Genet.* 25, 1225–1232. doi: 10.1093/hmg/ddw003

Zhu, W., Liu, H., and Zhang, X. (2019). Toward curative immunomodulation strategies for chronic hepatitis B virus infection. *ACS Infect. Dis.* 5, 703–712. doi: 10.1021/acsinfecdis.8b00297

Zhu, X., Du, T., Wu, X., Guo, X., Niu, N., Pan, L., et al. (2011). Human leukocyte antigen class I and class II genes polymorphisms might be associated with interferon α therapy efficiency of chronic hepatitis B. *Antiviral Res.* 89, 189–192. doi: 10.1016/j.antiviral.2011.01.001

Zidi, I., Laaribi, A. B., Bortolotti, D., Belhadj, M., Mehri, A., Yahia, H. B., et al. (2016). HLA-E polymorphism and soluble HLA-E plasma levels in chronic hepatitis B patients. *HLA* 87, 153–159. doi: 10.1111/tan.12767

Zoulim, F., and Locarnini, S. (2012). Management of treatment failure in chronic hepatitis B. *J. Hepatol.* 56 Suppl 1, S112–S122. doi: 10.1016/S0168-8278(12)60012-9

Zuckerman, J. N. (2006). Protective efficacy, immunotherapeutic potential, and safety of hepatitis B vaccines. *J. Med. Virol.* 78, 169–177. doi: 10.1002/jmv.20524

Conflict of Interest Statement: The authors declare that the research was conducted in the absence of any commercial or financial relationships that could be construed as a potential conflict of interest.

Copyright © 2019 Zhang, Wang, Liu, Zou, Li and Lu. This is an open-access article distributed under the terms of the Creative Commons Attribution License (CC BY). The use, distribution or reproduction in other forums is permitted, provided the original author(s) and the copyright owner(s) are credited and that the original publication in this journal is cited, in accordance with accepted academic practice. No use, distribution or reproduction is permitted which does not comply with these terms.

frontiers in Genetics

REVIEW
published: 13 September 2019
doi: 10.3389/fgene.2019.00799

Large-Scale "OMICS" Studies to Explore the Physiopatholgy of HIV-1 Infection

Sigrid Le Clerc[1], Sophie Limou[2,3,4] and Jean-François Zagury[1]**

[1] Laboratoire GBCM, EA7528, Conservatoire National des Arts et Métiers, HESAM Université, Paris, France, [2] Centre de Recherche en Transplantation et Immunologie UMR1064, INSERM, Université de Nantes, Nantes, France, [3] Institut de Transplantation en Urologie et Néphrologie (ITUN), CHU de Nantes, Nantes, France, [4] Computer Sciences and Mathematics Department, Ecole Centrale de Nantes, Nantes, France

In this review, we present the main large-scale experimental studies that have been performed in the HIV/AIDS field. These "omics" studies are based on several technologies including genotyping, RNA interference, and transcriptome or epigenome analysis. Due to the direct connection with disease evolution, there has been a large focus on genotyping cohorts of well-characterized patients through genome-wide association studies (GWASs), but there have also been several *in vitro* studies such as small interfering RNA (siRNA) interference or transcriptome analyses of HIV-1–infected cells. After describing the major results obtained with these omics technologies—including some with a high relevance for HIV-1 treatment—we discuss the next steps that the community needs to embrace in order to derive new actionable therapeutic or diagnostic targets. Only integrative approaches that combine all big data results and consider their complex interactions will allow us to capture the global picture of HIV molecular pathogenesis. This novel challenge will require large collaborative efforts and represents a huge open field for innovative bioinformatics approaches.

Keywords: HIV, genome-wide association study, genomics, omics, big data

OPEN ACCESS

Edited by:
Dana C. Crawford, Case Western Reserve University, United States

Reviewed by:
Paul J. McLaren, Public Health Agency of Canada (PHAC), Canada
Eric O. Johnson, RTI International, United States

****Correspondence:***
Sophie Limou
sophie.limou@univ-nantes.fr
Jean-François Zagury
zagury@cnam.fr

Specialty section:
This article was submitted to Applied Genetic Epidemiology, a section of the journal Frontiers in Genetics

Received: *30 January 2019*
Accepted: *30 July 2019*
Published: *13 September 2019*

Citation:
Le Clerc S, Limou S and Zagury J-F (2019) Large-Scale "OMICS" Studies to Explore the Physiopatholgy of HIV-1 Infection. Front. Genet. 10:799. doi: 10.3389/fgene.2019.00799

INTRODUCTION

HIV remains a major global public health issue, having claimed more than 35 million lives so far. In 2017, 940,000 people died from HIV-related causes globally (Global AIDS Update, 2016). The active anti-retroviral therapies are efficient and have saved many lives but still present multiple caveats: need for high compliance, permanent treatment, and unwanted side effects and complications (Li et al., 2017). Developing alternative and simple solutions such as immunoprophylactic or immunotherapeutic options remains a public health priority. In line with this, a better understanding of the molecular etiology of disease progression is essential.

Due to the impact of the disease in the Western world, HIV research has been the subject of intense efforts for the past 35 years and has helped in promoting several new research technologies, in particular with high-throughput studies from the "omics" era.

In this review, we will present large-scale studies based on various technologies that have been undertaken to tackle HIV molecular etiology and their main results. These large-scale studies encompass mainly genomics with genome-wide association studies (GWASs) based on genotyping chips and with exome sequencing, transcriptomic studies from SIV and HIV patient

cells, and small interfering RNA (siRNA) studies in sensitive cell lines. We will also briefly describe the results obtained from proteomics and epigenomics screenings.

A SHORT RECALL ON HIV-1 INFECTION AND MARKERS

There are three successive stages in HIV infection: the acute primary infection, the asymptomatic stage and symptomatic HIV infection, and acquired immunodeficiency syndrome (AIDS). Depending on the individual, AIDS, the most advanced stage of the infection course, can occur within a few months to several years after HIV infection, with an average of around 8 years in the Western world. This stage has been defined by the Center for Disease Control (CDC) either as a drop of CD4 T-cell count below 200/mm^3 or as the appearance of opportunistic infections or some cancers (Center for Disease Control and Prevention, 1992). Quite early, AIDS cohorts were enrolled and prospectively followed, and it became apparent that this infection was exhibiting a considerable phenotypic heterogeneity at different levels: virus acquisition, disease progression, viral load control, and response to treatment (Langlade-Demoyen et al., 1994; Ludlam et al., 1985; Fowke et al., 1996; Pantaleo and Fauci, 1996; Hetherington et al., 2002; Mallal et al., 2002; Saksena et al., 2007). For instance, some individuals, called long-term non-progressors, are infected but never progress to AIDS; the elite controllers have never exhibited any detectable viral load; and the rapid progressors reach the AIDS stage within a few months following their infection. This phenotypic variability may be attributed to a complex interplay between viral, environmental, and host genetic factors that could be investigated through several types of large-scale studies or omics.

If the CD4 cell count was the major marker to follow HIV-1 infection and immune deficiency in patients in the early 1980s, the progress of molecular biology techniques has made it possible to measure precisely HIV-1 viral load in the blood (i.e., the number of viral particles present in each ml of serum) by the late 1990s. Together with the CD4 cell count, this marker has become very useful to evaluate the status of an infected patient, either a low viral load suggesting a good control of HIV-1 infection or a high viral load suggesting a progressive infection at an early stage of infection or an uncontrolled infection at a late disease stage (AIDS). Most cohorts focus on viral load outcomes (e.g., viral control, viral load at set point), but (slow and rapid) progression phenotypes have also been defined based on the CD4 counts (e.g., the GRIV cohort).

GENETIC ASSOCIATION STUDIES

Host genes associated with various phenotypes have been extensively explored since the mid-1990s. The concept is as follows: if a particular phenotype (for instance, elite control) is statistically associated with the presence or absence of a genetic variant, the corresponding gene or its product may be involved in the molecular mechanisms of viral infection/dissemination. Genetic association studies can thus provide new clues on the molecular mechanisms of infection and disease progression and, in the long run, identify new targets for the development of new therapeutic or diagnostic strategies. Initial studies have focused on candidate genes such as *HLA* (Kaslow et al., 1996; Carrington et al., 1999; Hendel et al., 1999), and a large number of host genetic associations with HIV outcomes have been identified. The main confirmed association was a 32-base-pair deletion in the *CCR5* gene (*CCR5-Δ32*) (Dean et al., 1996; Liu et al., 1996; Samson et al., 1996; Rappaport et al., 1997), but other variants closely located in the *CCR5* promoter (Martin et al., 1998; McDermott et al., 1998) or in the nearby *CCR2* gene (Smith et al., 1997) were also influential. This deletion led to the expression of a truncated and non-functional cell surface CCR5 protein that happened to be the major HIV-1 entry co-receptor (Alkhatib et al., 1996; Deng et al., 1996; Liu et al., 1996). Other candidate gene studies pointed to immunity-related genes (e.g., *KIR*, *IL10*, *IFNγ*) and genes encoding HIV restriction factors (e.g., *CCL5*, *APOBEC3G*, *CUL5*) but were only partially replicated according to the phenotype and cohort tested. The functional interpretation for most of these variants is yet to be discovered, but the detailed account of each candidate gene is beyond the scope of this article and has been covered by previous enlightening reviews (Fellay, 2009; An and Winkler, 2010). Overall, most of the candidate gene associations displayed small to modest effect sizes and, combined all together, account for a small fraction of the phenotype variability (O'Brien and Nelson, 2004).

GENOME-WIDE ASSOCIATION STUDIES

It was only in 2007 that the first large-scale genetic association studies or GWASs have been published with the seminal publication by Fellay et al. that focused mainly on viral load at set point as the main phenotype of interest (Fellay et al., 2007). These large-scale genomic studies have relied on genotyping chips targeting simultaneously hundreds of thousands to millions of specific genetic markers called single nucleotide polymorphisms (SNPs), the most frequent polymorphisms in the human genome, that can be rapidly and easily genotyped. In contrast to the candidate gene strategy, this approach measures and analyzes gene variants across the whole human genome in an effort to identify common genetic risk factors in the population without any biological hypothesis *a priori*. Since the 2007 publication, GWASs have taken the place of candidate gene studies in AIDS. More than 20 GWASs focusing on various phenotypes and cohorts have been published, and **Table 1** summarizes these studies with their main characteristics (see also (Limou and Zagury, 2013)): date of the publication, origin of the cohort, size of the cohort, phenotype(s) of interest, genotyping chip type, associated SNP(s), best P-value, possible causing gene(s) involved, and publication reference number.

TABLE 1 | GWASs published in the AIDS field since 2007. 5×10^{-8} is the standard threshold for considering an association as significant in a GWAS, and the significant ones in the table are in bold.

Publication year	Discovery sample origin	Discovery sample size	Reported trait	Microarray type	Main SNPs	P-value	Gene(s)	Reference
2007	European	486	HIV-1 viral set point	Illumina HumanHap550	rs239502, rs9264942	**9.36×10^{-12}, 3.77×10^{-9}**	*HLA-B*5701*	(Fellay et al., 2007)
2009	European	2362	HIV-1 control (elite and viremic)	Illumina HumanHap550, Illumina Human1M	rs239502, rs9264942	**5×10^{-35}, 6×10^{-32}**	*HCP5/HLA-B*5701, HLA-C*	(Fellay et al., 2009)
2009	European	1071	AIDS progression	Illumina HumanHap550, Illumina Human1M	rs9264942, rs2395029	**6×10^{-12}, 1×10^{-11}**	*HLA-C, HCP5/ HLA-B*5701*	(Fellay et al., 2009)
2009	European	85 rapid progressors HIV(+), 1,352 CTR HIV(–)	AIDS progression	Illumina HumanHap300	rs4118325	6×10^{-7}	*PRMT6*	(Le Clerc et al., 2009)
2009	European	275 non-progressors HIV(+), 1,352 CTR HIV(–)	AIDS progression	Illumina HumanHap300	rs2395029	**6.79×10^{-10}, 6.79×10^{-8}**	*HCP5/ HLA-B*5701*	(Limou et al., 2009)
2010	European	156	HIV-1 progression	Affymetrix Human Mapping 500K	rs17762192	6.23×10^{-7}	*PROX1-AS1*	(Herbeck et al., 2010)
2010	African American or Afro-Caribbean	515	HIV-1 viral set point	Illumina HumanHap1M, HumanHap1M-Duo, HumanHap550K	rs454422	1.46×10^{-6}	*MCM8*	(Pelak et al., 2010)
2010	European	1712	HIV-1 control	Illumina HumanHap650Y	rs9264942, rs4418214	**6.3×10^{-16}**	*HLA-C, MICA*	(International H.I.V. Controllers Study et al., 2010)
2010	African American or Afro-Caribbean	677	HIV-1 control	Illumina HumanHap650Y	rs2523608	**3.7×10^{-15}**	-	(International H.I.V. Controllers Study et al., 2010)
2010	Sub-Saharan African	848 high-risk HIV(–), 531 HIV(+)	HIV-1 susceptibility	Illumina Human1M or 1M-Duo	rs842304	3.97×10^{-6}	-	(Petrovski et al., 2011)
2010	Sub-Saharan African	100 HIV(+) infants, 126 HIV(–)	HIV susceptibility (mother-to-child transmission)	Illumina HumanHap650Y	rs12306	3.92×10^{-5}	*WSB1*	(Joubert et al., 2010)
2011	European	191	HIV-1 replication *in vitro*	Illumina Human610-Quad	rs12483205	2.16×10^{-5}	*DYRK1A*	(Bol et al., 2011)
2011	Sub-Saharan African, African unspecified	302 high-risk HIV(–), 496 HIV(+)	HIV-1 susceptibility	Illumina HumanHap1M-Duo	rs3745760	7.83×10^{-7}	*GLTSCR1*	(Lingappa et al., 2011)
2011	Sub-Saharan African, African unspecified	403	HIV-1 viral set point	Illumina HumanHap1M-Duo	rs13111989	2.15×10^{-7}	*VEGFC*	(Lingappa et al., 2011)
2011	European	755	AIDS progression	Affymetrix Human Array 6.0	rs11884476	**3.37×10^{-9}**	*PARD3B*	(Troyer et al., 2011)
2011	European	404	HIV-1 progression	Illumina HumanHap300	rs1523635	3.5×10^{-6}	*AGR3*	(van Manen et al., 2011)
2013	European	430 high-risk HIV(–) and 765 HIV(+)	HIV-1 susceptibility	Illumina Human1M or 1M-Duo	-	-	-	(Lane et al., 2013)
2013	European	6,334 HIV-1(+), 7,247 HIV-1(–)	HIV-1 susceptibility	Meta-analysis/ imputation	-	-	-	(McLaren et al., 2013)
2015	African American or Afro-Caribbean and European	628 high-risk HIV(–) vs. 1,376 HIV(+), 327 high-risk HIV(–) vs. 805 HIV(+)	HIV-1 susceptibility	Illumina HumanOmni1-Quad	rs4878712	4.38×10^{-8}, 7.78×10^{-4}	*CD33, FRMPD1*	(Johnson et al., 2015)
2015	European	6,315	HIV-1 viral set point	Meta-analysis/ imputation	rs59440261, rs1015164	**2×10^{-83}, 1.5×10^{-19}**	*HLA-B*5701, CCRL2*	(McLaren et al., 2015)
2015	East Asian	538	HIV-1 viral set point	Illumina Human660W-Quad	rs2442719	8×10^{-7}	*HLA-B*	(Wei et al., 2015)
2017	Sub-Saharan Africans	556	AIDS progression	Illumina HumanOmni2.5M	rs2535307	3.72×10^{-7}	*HCG22*	(Xie et al., 2017)

CTR, controls

The following major conclusions can be underlined from these GWA studies:

1. One signal was repeatedly replicated in several cohorts (of European descent) both for the viral load phenotype and also for the non-progression phenotype: rs2395029, an SNP in the *HCP5* gene within the *MHC* region, which was described in nearly full linkage disequilibrium (LD) with the *HLA*-B*5701 allele (Fellay et al., 2007; Dalmasso et al., 2008; Limou et al., 2009; McLaren et al., 2013; McLaren et al., 2017). This *HLA* allele could be critical for the destruction of infected cells *via* a yet-unidentified CD8 T-cell epitope, but we cannot exclude a role for other polymorphisms in the *HLA* region and possibly outside of the class I *HLA* genes, with relevant genes highlighted through LD such as *MICB* and *TNF* (Kulkarni et al., 2011). Similarly, in African Americans, the *HLA*-B*5703 allele was demonstrated to be important for viral control (Pelak et al., 2010; McLaren et al., 2012; McLaren et al., 2017). Beyond B*57 alleles, *HLA* seems to play a major role in viral control, as another SNP located 35 kb upstream of *HLA-C* was also identified in Europeans (Limou et al., 2009; McLaren et al., 2017). This −35 kb SNP was correlated with higher HLA-C cell surface expression (Thomas et al., 2009), which can be regulated through microRNA (miRNA) binding (Kulkarni et al., 2011) and through the binding of the Oct1 transcription factor (Vince et al., 2016).
2. In 2011, the HIV/AIDS research community conducted a massive effort to bring together their genomic data in order to gain statistical power of detection. This collaborative effort, named the International Consortium for the Genetics of HIV-1 (ICGH), gathered up to 6,300 HIV-infected individuals and 7,200 HIV-uninfected controls who were genotyped on various Illumina or Affymetrix platforms. A first publication emerged from this consortium in 2013; it focused on HIV-1 acquisition and confirmed the major role of *CCR5*-Delta32 in resistance to infection but did not identify any additional common genetic variant (McLaren et al., 2013). A second study was published 2 years later on viral control and disease progression and confirmed the complementary roles of *CCR5* locus variants and of *HLA* genetic variants coding for amino acids in the peptide binding grooves of HLA-A and HLA-B (McLaren et al., 2015). In spite of the large sample size, no other locus reached genome-wide significance. These reports conclude that future genetic studies should target other classes of genetic variants (e.g., low or rare frequency), non-European populations, and well-defined homogeneous phenotypes (McLaren et al., 2015).
3. In addition, the numerous GWASs have identified novel candidate genes, which all deserve further exploration, notably the ones that reached genome-wide significance (see **Table 1**). In particular, a genetic variant within the *CXCR6* gene was associated with long-term non-progression in four independent cohorts (Limou et al., 2010). This signal was only identified in individuals without sustained viral control, which explains why it was not highlighted in the consortium that mainly focused on viral control. Finally, the absence of replication for many other signals presented in **Table 1** does not discount their scientific interest but complicates their biological interpretation.

NEXT-GENERATION SEQUENCING STUDIES

GWASs rely on common SNPs (typically >1% in the population) and hardly take into account the possible effect of rare variants or other classes of genetic polymorphisms such as indels or copy number variants that can also significantly impact disease outcome. To investigate the impact of such variants, we first focused on low-frequency SNPs (<5%) in our progression GWASs and identified the gene *RICH2* associated with non-progression, which interacts with BST-2, a major known HIV restriction factor (Le Clerc et al., 2011). Later, several studies based on next-generation sequencing (NGS) have emerged. Due to the high cost of such studies and to maximize statistical power of detection, these screenings have targeted coding variants (exome) and patients with very specific and extreme disease outcome. To our knowledge, only one publication has emerged from these studies (McLaren et al., 2017), which focused on 1,327 subjects, many of whom were elite and viral controllers. In spite of the significant number of patients studied, only variants in the *HLA* region came out, and this study suggested that exonic variants with large effect sizes are unlikely to have a major contribution to host control of HIV infection (McLaren et al., 2017).

FUNCTIONAL GENOMIC SCREENINGS

Systematic inactivation of gene expression through siRNA and small hairpin RNA (shRNA) offers a unique chance to identify host genes required for HIV replication. In large-scale studies, authors used siRNAs (Brass et al., 2008; Konig et al., 2008; Zhou et al., 2008) or shRNAs (Yeung et al., 2009) to silence *in vitro* most known genes one by one in HIV permissive cell lines. These screenings identified 273 (Brass et al., 2008), 213 (Konig et al., 2008), 311 (Zhou et al., 2008), and 252 (Yeung et al., 2009) HIV host dependency factors, respectively, for a total of 842 putative candidates. However, the overlap between the different studies was very low, suggesting low reproducibility and/or high false positive, which might not be surprising considering the different experimental models (cell lines, HIV strains, and measurement modes of HIV replication). Overall, these studies still provide an interesting list of candidate cellular factors and pathways potentially implicated in HIV-1 replication that could be considered as relevant targets for drug development.

The development of the CRISPR–Cas9 technology to screen each gene with a library of single-guided RNA offers a greater sensitivity and specificity than interference based-RNA (Wang et al., 2014). A recent report used this technology to screen a CD4 T-cell line and identified five host factors required for HIV replication, including CD4, C-C motif chemokine

receptor 5 (CCR5), and activated leukocyte cell adhesion molecule (ALCAM (Park et al., 2017). These factors were further validated in primary human CD4 T-cells and therefore represent major candidates for a therapeutic intervention.

TRANSCRIPTOMIC STUDIES

The first descriptions of transcriptome analysis by DNA microarrays were in cancer in 2002 (Pomeroy et al., 2002; van 't Veer et al., 2002). In AIDS, the first large-scale transcriptomic study (4,600 transcripts) was published in 2003 (van 't Wout et al., 2003). This study analyzed gene expression in HIV-infected CD4 T-cell lines at different time points and revealed the inhibition of genes involved in cell division, transcription, translation, splicing, and also cholesterol biosynthesis (van 't Wout et al., 2003). An exon transcriptome microarray analysis of purified HIV-infected cells revealed host cell factors required for viral replication and alternative splicing events (Imbeault et al., 2012). A bioinformatic analysis of HIV-resistant activated CD4 T-cells (due to CD3/CD28 antibodies' co-stimulation) highlighted a few dozen genes critical for resistance or permissivity (Xu et al., 2013).

Several microarray studies focused on non-human primate models, such as cynomolgus monkeys (Bosinger et al., 2004) and African green monkeys (non-pathogenic model) vs. rhesus macaques (pathogenic model) (Jacquelin et al., 2009). These reports mainly identified a major role for IFN-stimulated genes, as well as a differential expression of some innate genes (such as LPS receptors CD14 and TLR4) and some apoptosis-related genes (Bosinger et al., 2004).

Finally, numerous transcriptome studies explored differential gene expression in HIV-infected individuals. A first report in 2005 claimed to have found (Ockenhouse et al., 2005) a 10-gene signature for HIV-1 serostatus and a 6-gene signature for subjects experiencing a CD4+ T-cell decrease (Ockenhouse et al., 2005). The genes identified were primarily linked with immune response and apoptosis, mitochondrial function, and RNA binding (downregulated in subjects with better prognosis) (Ockenhouse et al., 2005). A study focusing on HIV-1–resistant individuals (Huang et al., 2011) found a set of 185 HIV-1 resistance genes, suggesting a major role for *nef* in disease pathogenesis, and among them pointed out 29 potential targets for AIDS prevention or therapy (Huang et al., 2011). By comparing the complementary DNA (cDNA) profiles of CD3+ T-cells in long-term non-progressors vs. medium progressors (Salgado et al., 2011), 325 genes appeared over-expressed in regular progressors (from DNA replication, cell cycle, and DNA damage pathways), vs. 136 over-expressed genes in long-term non-progressors (from cytokine–cytokine receptor interaction and negative control of apoptosis pathways) (Salgado et al., 2011). The transcriptome comparison of CD4+ T-cells and CD8+ T-cells from rapid progressors, viremic non-progressors, and elite controllers showed a lower expression of IFN-stimulated genes and an upregulation of *CASP1*, *CD38*, *LAG3*, *TNFSF13B*, *SOCS1*, and *EEF1D* genes in viremic non-progressors (Rotger et al., 2011). Finally, a transcriptomic screening also targeted miRNA expression profiles in peripheral blood mononuclear cell (PBMC) from rapid and chronic progressors and identified five downregulated miRNAs in rapid progressors that all converged to the apoptosis pathway (Zhang et al., 2013).

PROTEOMIC AND EPIGENOMIC STUDIES

Some proteomic studies have also been performed, but they were not very reproducible, as indicated in a recent review by Donnelly and Ciborowski (2016). To our knowledge, few epigenomic studies have been published to date in HIV/AIDS. One Korean group performed two chromatin immunoprecipitation sequencing (ChIP-seq) analyses in HIV latently infected CD4 T-cell lines to investigate the impact of H3K4me3 and H3K9ac histone modifications on latency. They revealed several potential candidate genes, including *NFIX*, tumor necrosis factor (TNF) receptor association factor 4 (*TRAF4*), and cell cycle regulating genes such as *CDKN1A* (p21) and *CCND2* (Park et al., 2014; Kim et al., 2017). Finally, the blood DNA methylation signatures of HIV-infected and uninfected subjects were compared through an epigenome-wide association study (EWAS), which highlighted a down-methylation of *NLC5* promoter in HIV-infected subjects (Zhang et al., 2016). This host gene encodes a key regulator of class I *HLA* gene expression and confirms the major role of the *MHC* locus in HIV viral control. Interestingly, *NLC5* promoter and additional *MHC* clusters also appeared differentially methylated in HIV–Hepatitis C virus (HCV) co-infected subjects (Zhang et al., 2017), emphasizing the importance of inflammation-related genes in the course of HIV infection. Overall, these studies are promising and underline the need for additional large-scale epigenetic studies in order to better capture the breadth of host–HIV complex interactions.

CONCLUSION AND FUTURE DIRECTIONS

In this review, we have presented numerous large-scale genomic and transcriptomic analyses that have taken place in the AIDS field, which are the consequences of the progress in molecular biology and biochemistry technologies. One can see that a huge research effort has been dedicated to genetic association studies, and this is logical since this experimental approach deals with real *in vivo* data, i.e., cohorts of patients and HIV-1 infection *in vivo*. Nevertheless, it was slightly surprising to observe that the main signals found by GWAS, in the *HLA* and *CCR5* loci, had already been identified by previous candidate gene approaches. This apparent limitation could be explained by the yet-unidentified role of other polymorphisms such as copy number variations (CNVs) or interacting gene variants. It could also be explained by the statistical constraints (such as stringent multiple testing corrections) that limit the use of genetic association data (numerous false negatives) and the overall low number of samples at stake (a few thousands) compared to other human diseases such as diabetes or obesity (hundreds of thousands) (Shungin et al., 2015; Fuchsberger et al., 2016). In light of the available biological

information provided by the other large-scale studies such as transcriptomic or functional genomic studies presented in this review, it appears important to reanalyze the genomic data by integrating biological information in order to enhance the genetic association results. For instance, our group has successfully implemented such approaches by pre-selecting relevant SNPs defined either by their low frequency (Le Clerc et al., 2011) or by their functional impact as potential expression quantitative trait loci (eQTLs) (Spadoni et al., 2015). More generally, there are several methods for data integration, the first one being to cross-check the results obtained by one method through another, for instance, using GWAS to identify SNPs with low P-values, even non-significant, and then using transcriptomics to pick genes that are differentially expressed in a relevant cell type or tissue. By combining two (or more) methods, researchers can zoom in on specific genes of high interest. This has been implemented with the development of PrediScan (Gamazon et al., 2015). Another example of cross-checking is the results obtained by metabolome analysis and GWAS in which the researchers have found that metabolites present at high levels in the blood of some subjects are highly correlated with specific variants present in the genes of enzymes involved in their metabolism (Illig et al., 2010). Other methods of data integration rely on rescuing genes by correlating signals not only at the gene level but also at the pathway level: for instance, one can suspect that if a gene X in a biological pathway is important for a clinical phenotype, the genes present upstream in the biological pathway may impact this gene X expression and, as a consequence, also become targets of interest. One will thus have to look for cross-checks at the level of pathways (Chen et al., 2011). Importantly, it is essential for data integration to perform all these cross-checks in a smart and automated manner. Finally, more sophisticated statistical approaches have recently emerged outside of the HIV field, such as the Bayesian method for data integration (Kichaev et al., 2014; Pickrell, 2014; Finucane et al., 2015; Yang et al., 2017; International Multiple Sclerosis Genetics Consortium, 2019). These new methods are yet to be implemented in the relatively small HIV/AIDS cohorts but might reveal novel underlying physiopathological mechanisms.

With the massive research effort to fight AIDS, this has been a true field of experimentation and development for novel technologies. A first challenge is now the cross-usage of all this information gathered from so many large-scale studies, to transform this "gold mine" into diagnostic or therapy strategies to fight AIDS, and the same integration of omics big data should of course take place also for other human diseases. This systems biology challenge has not yet been met. A second challenge is to pursue the exploration of alternative technologies such as epigenomics or proteomics to derive more understanding of HIV-1 molecular pathogenesis. We hope that the AIDS field will remain a "cultural" leader for research progress in order to fully understand the molecular mechanisms at stake in HIV-1 infection and AIDS and allow the rationale development of diagnostic and therapeutic strategies to finally tackle the HIV-1 virus.

AUTHOR CONTRIBUTIONS

SLC, SL, and J-FZ conceived this review, performed the bibliography search, and wrote it in a collective manner.

FUNDING

The authors have had their work funded from several sources. This review was directly funded by their employer: Conservatoire National des Arts et Métiers et Ecole Centrale de Nantes.

REFERENCES

Alkhatib, G., Combadiere, C., Broder, C. C., Feng, Y., Kennedy, P. E., Murphy, P. M., et al. (1996). CC CKR5: a RANTES, MIP-1alpha, MIP-1beta receptor as a fusion cofactor for macrophage-tropic HIV-1. *Science* 272 (5270), 1955–1958. doi: 10.1126/science.272.5270.1955

An, P., and Winkler, C. A. (2010). Host genes associated with HIV/AIDS: advances in gene discovery. *Trends Genet.* 26 (3), 119–131. doi: 10.1016/j.tig.2010.01.002

Bol, S. M., Moerland, P. D., Limou, S., van Remmerden, Y., Coulonges, C., van Manen, D., et al. (2011). Genome-wide association study identifies single nucleotide polymorphism in DYRK1A associated with replication of HIV-1 in monocyte-derived macrophages. *PLoS One* 6 (2), e17190. doi: 10.1371/journal.pone.0017190

Bosinger, S. E., Hosiawa, K. A., Cameron, M. J., Persad, D., Ran, L., Xu, L., et al. (2004). Gene expression profiling of host response in models of acute HIV infection. *J. Immunol.* 173 (11), 6858–6863. doi: 10.4049/jimmunol.173.11.6858

Brass, A. L., Dykxhoorn, D. M., Benita, Y., Yan, N., Engelman, A., Xavier, R. J., et al. (2008). Identification of host proteins required for HIV infection through a functional genomic screen. *Science* 319 (5865), 921–926. doi: 10.1126/science.1152725

Carrington, M., Nelson, G. W., Martin, M. P., Kissner, T., Vlahov, D., Goedert, J. J., et al. (1999). HLA and HIV-1: heterozygote advantage and B*35–Cw*04 disadvantage. *Science* 283 (5408), 1748–1752. doi: 10.1126/science.283.5408.1748

Center for Disease Control and Prevention (1992). 1993 revised classification system for HIV infection and expanded surveillance case definition for AIDS among adolescents and adults. *MMWR Recomm. Rep.* 41 (RR-17), 1–19.

Chen, M., Cho, J., and Zhao, H. (2011). Incorporating biological pathways *via* a Markov random field model in genome-wide association studies. *PLoS Genet.* 7 (4), e1001353. doi: 10.1371/journal.pgen.1001353

Dalmasso, C., Carpentier, W., Meyer, L., Rouzioux, C., Goujard, C., Chaix, M. L., et al. (2008). Distinct genetic loci control plasma HIV-RNA and cellular HIV-DNA levels in HIV-1 infection: the ANRS genome wide association 01 study. *PLoS One* 3 (12), e3907. doi: 10.1371/journal.pone.0003907

Dean, M., Carrington, M., Winkler, C., Huttley, G. A., Smith, M. W., Allikmets, R., et al. (1996). Genetic restriction of HIV-1 infection and progression to AIDS by a deletion allele of the CKR5 structural gene. hemophilia growth and development study, multicenter AIDS cohort study, multicenter hemophilia cohort study, san francisco city cohort, ALIVE study. *Science* 273 (5283), 1856 1862. doi: 10.1126/science.273.5283.1856

Deng, H., Liu, R., Ellmeier, W., Choe, S., Unutmaz, D., Burkhart, M., et al. (1996). Identification of a major co-receptor for primary isolates of HIV-1. *Nature* 381 (6584), 661–666. doi: 10.1038/381661a0

Donnelly, M. R., and Ciborowski, P. (2016). Proteomics, biomarkers, and HIV 1: a current perspective. *Proteomics Clin. Appl.* 10 (2), 110–125. doi: 10.1002/prca.201500002

Fellay, J. (2009). Host genetics influences on HIV type-1 disease. *Antivir. Ther.* 14 (6), 731–738. doi: 10.3851/IMP1253

Fellay, J., Ge, D., Shianna, K. V., Colombo, S., Ledergerber, B., Cirulli, E. T., et al. (2009). Common genetic variation and the control of HIV-1 in humans. *PLoS Genet.* 5 (12), e1000791. doi: 10.1371/journal.pgen.1000791

Fellay, J., Shianna, K. V., Ge, D., Colombo, S., Ledergerber, B., Weale, M., et al. (2007). A whole-genome association study of major determinants for host control of HIV-1. *Science* 317 (5840), 944–947. doi: 10.1126/science.1143767

Finucane, H. K., Bulik-Sullivan, B., Gusev, A., Trynka, G., Reshef, Y., Loh, P. R., et al. (2015). Partitioning heritability by functional annotation using genome-wide association summary statistics. *Nat. Genet.* 47 (11), 1228–1235. doi: 10.1038/ng.3404

Fowke, K. R., Nagelkerke, N. J., Kimani, J., Simonsen, J. N., Anzala, A. O., Bwayo, J. J., et al. (1996). Resistance to HIV-1 infection among persistently seronegative prostitutes in Nairobi, Kenya. *Lancet* 348 (9038), 1347–1351. doi: 10.1016/S0140-6736(95)12269-2

Fuchsberger, C., Flannick, J., Teslovich, T. M., Mahajan, A., Agarwala, V., Gaulton, K. J., et al. (2016). The genetic architecture of type 2 diabetes. *Nature* 536 (7614), 41–47. doi: 10.1038/nature18642

Gamazon, E. R., Wheeler, H. E., Shah, K. P., Mozaffari, S. V., Aquino-Michaels, K., Carroll, R. J., et al. (2015). A gene-based association method for mapping traits using reference transcriptome data. *Nat. Genet.* 47 (9), 1091–1098. doi: 10.1038/ng.3367

Global AIDS Updated. (2016). UNAIDS. http://www.unaids.org/en/resources/documents/2016/Global-AIDS-update-2016.

Hendel, H., Caillat-Zucman, S., Lebuanec, H., Carrington, M., O'Brien, S., Andrieu, J. M., et al. (1999). New class I and II HLA alleles strongly associated with opposite patterns of progression to AIDS. *J. Immunol.* 162 (11), 6942–6946.

Herbeck, J. T., Gottlieb, G. S., Winkler, C. A., Nelson, G. W., An, P., Maust, B. S., et al. (2010). Multistage genomewide association study identifies a locus at 1q41 associated with rate of HIV-1 disease progression to clinical AIDS. *J. Infect. Dis.* 201 (4), 618–626. doi: 10.1086/649842

Hetherington, S., Hughes, A. R., Mosteller, M., Shortino, D., Baker, K. L., Spreen, W., et al. (2002). Genetic variations in HLA-B region and hypersensitivity reactions to abacavir. *Lancet* 359 (9312), 1121–1122. doi: 10.1016/S0140-6736(02)08158-8

Huang, T., Xu, Z., Chen, L., Cai, Y. D., and Kong, X. (2011). Computational analysis of HIV-1 resistance based on gene expression profiles and the virus–host interaction network. *PLoS One* 6 (3), e17291. doi: 10.1371/journal.pone.0017291

Illig, T., Gieger, C., Zhai, G., Romisch-Margl, W., Wang-Sattler, R., Prehn, C., et al. (2010). A genome-wide perspective of genetic variation in human metabolism. *Nat. Genet.* 42 (2), 137–141. doi: 10.1038/ng.507

Imbeault, M., Giguere, K., Ouellet, M., and Tremblay, M. J. (2012). Exon level transcriptomic profiling of HIV-1–infected CD4(+) T cells reveals virus-induced genes and host environment favorable for viral replication. *PLoS Pathog.* 8 (8), e1002861. doi: 10.1371/journal.ppat.1002861

International H.I.V. Controllers Study, Pereyra, F., Jia, X., McLaren, P. J., Telenti, A., de Bakker, P. I., et al. (2010). The major genetic determinants of HIV-1 control affect HLA class I peptide presentation. *Science* 330 (6010), 1551–1557. doi: 10.1126/science.1195271

International Multiple Sclerosis Genetics Consortium (2019). A systems biology approach uncovers cell-specific gene regulatory effects of genetic associations in multiple sclerosis. *Nat. Commun.* 10 (1), 2236. doi: 10.1038/s41467-019-09773-y

Jacquelin, B., Mayau, V., Targat, B., Liovat, A. S., Kunkel, D., Petitjean, G., et al. (2009). Nonpathogenic SIV infection of African green monkeys induces a strong but rapidly controlled type I IFN response. *J. Clin. Invest.* 119 (12), 3544–3555. doi: 10.1172/JCI40093

Johnson, E. O., Hancock, D. B., Gaddis, N. C., Levy, J. L., Page, G., Novak, S. P., et al. (2015). Novel genetic locus implicated for HIV-1 acquisition with putative regulatory links to HIV replication and infectivity: a genome-wide association study. *PLoS One* 10 (3), e0118149. doi: 10.1371/journal.pone.0118149

Joubert, B. R., Lange, E. M., Franceschini, N., Mwapasa, V., North, K. E., Meshnick, S. R., et al. (2010). A whole genome association study of mother-to-child transmission of HIV in Malawi. *Genome Med.* 2 (3), 17. doi: 10.1186/gm138

Kaslow, R. A., Carrington, M., Apple, R., Park, L., Munoz, A., Saah, A. J., et al. (1996). Influence of combinations of human major histocompatibility complex genes on the course of HIV-1 infection. *Nat. Med.* 2 (4), 405–411. doi: 10.1038/nm0496-405

Kichaev, G., Yang, W. Y., Lindstrom, S., Hormozdiari, F., Eskin, E., Price, A. L., et al. (2014). Integrating functional data to prioritize causal variants in statistical fine-mapping studies. *PLoS Genet.* 10 (10), e1004722. doi: 10.1371/journal.pgen.1004722

Kim, K. C., Lee, S., Son, J., Shin, Y., Yoon, C. H., Kang, C., et al. (2017). Identification of novel genes associated with HIV-1 latency by analysis of histone modifications. *Hum. Genomics* 11 (1), 9. doi: 10.1186/s40246-017-0105-7

Konig, R., Zhou, Y., Elleder, D., Diamond, T. L., Bonamy, G. M., Irelan, J. T., et al. (2008). Global analysis of host–pathogen interactions that regulate early-stage HIV-1 replication. *Cell* 135 (1), 49–60. doi: 10.1016/j.cell.2008.07.032

Kulkarni, S., Savan, R., Qi, Y., Gao, X., Yuki, Y., Bass, S. E., et al. (2011). Differential microRNA regulation of HLA-C expression and its association with HIV control. *Nature* 472 (7344), 495–498. doi: 10.1038/nature09914

Lane, J., McLaren, P. J., Dorrell, L., Shianna, K. V., Stemke, A., Pelak, K., et al. (2013). A genome-wide association study of resistance to HIV infection in highly exposed uninfected individuals with hemophilia A. *Hum. Mol. Genet.* 22 (9), 1903–1910. doi: 10.1093/hmg/ddt033

Langlade-Demoyen, P., Ngo-Giang-Huong, N., Ferchal, F., and Oksenhendler, E. (1994). Human immunodeficiency virus (HIV) nef-specific cytotoxic T lymphocytes in noninfected heterosexual contact of HIV-infected patients. *J. Clin. Invest.* 93 (3), 1293–1297. doi: 10.1172/JCI117085

Le Clerc, S., Coulonges, C., Delaneau, O., Van Manen, D., Herbeck, J. T., Limou, S., et al. (2011). Screening low-frequency SNPS from genome-wide association study reveals a new risk allele for progression to AIDS. *J. Acquir. Immune. Defic. Syndr.* 56 (3), 279–284. doi: 10.1097/QAI.0b013e318204982b

Le Clerc, S., Limou, S., Coulonges, C., Carpentier, W., Dina, C., Taing, L., et al. (2009). Genomewide association study of a rapid progression cohort identifies new susceptibility alleles for AIDS (ANRS Genomewide Association Study 03). *J. Infect. Dis.* 200 (8), 1194–1201. doi: 10.1086/605892

Li, H., Marley, G., Ma, W., Wei, C., Lackey, M., Ma, Q., et al. (2017). The role of ARV associated adverse drug reactions in influencing adherence among HIV-infected individuals: a systematic review and qualitative meta-synthesis. *AIDS Behav.* 21 (2), 341–351. doi: 10.1007/s10461-016-1545-0

Limou, S., Coulonges, C., Herbeck, J. T., van Manen, D., An, P., Le Clerc, S., et al. (2010). Multiple-cohort genetic association study reveals CXCR6 as a new chemokine receptor involved in long-term nonprogression to AIDS. *J. Infect Dis.* 202 (6), 908–915. doi: 10.1086/655782

Limou, S., Le Clerc, S., Coulonges, C., Carpentier, W., Dina, C., Delaneau, O., et al. (2009). Genomewide association study of an AIDS-nonprogression cohort emphasizes the role played by HLA genes (ANRS Genomewide Association Study 02). *J. Infect. Dis.* 199 (3), 419–426. doi: 10.1086/596067

Limou, S., and Zagury, J. F. (2013). Immunogenetics: genome-wide association of non-progressive HIV and viral load control: HLA genes and beyond. *Front. Immunol.* 4, 118. doi: 10.3389/fimmu.2013.00118

Lingappa, J. R., Petrovski, S., Kahle, E., Fellay, J., Shianna, K., McElrath, M. J., et al. (2011). Genomewide association study for determinants of HIV-1 acquisition and viral set point in HIV-1 serodiscordant couples with quantified virus exposure. *PLoS One* 6 (12), e28632. doi: 10.1371/journal.pone.0028632

Liu, R., Paxton, W. A., Choe, S., Ceradini, D., Martin, S. R., Horuk, R., et al. (1996). Homozygous defect in HIV-1 coreceptor accounts for resistance of some multiply-exposed individuals to HIV-1 infection. *Cell* 86 (3), 367–377. doi: 10.1016/S0092-8674(00)80110-5

Ludlam, C. A., Tucker, J., Steel, C. M., Tedder, R. S., Cheingsong-Popov, R., Weiss, R. A., et al. (1985). Human T-lymphotropic virus type III (HTLV-III) infection in seronegative haemophiliacs after transfusion of factor VIII. *Lancet* 2 (8449), 233–236. doi: 10.1016/S0140-6736(85)90288-0

Mallal, S., Nolan, D., Witt, C., Masel, G., Martin, A. M., Moore, C., et al. (2002). Association between presence of HLA-B*5701, HLA-DR7, and HLA-DQ3

and hypersensitivity to HIV-1 reverse-transcriptase inhibitor abacavir. *Lancet* 359 (9308), 727–732. doi: 10.1016/S0140-6736(02)07873-X

Martin, M. P., Dean, M., Smith, M. W., Winkler, C., Gerrard, B., Michael, N. L., et al. (1998). Genetic acceleration of AIDS progression by a promoter variant of CCR5. *Science* 282 (5395), 1907–1911. doi: 10.1126/science.282.5395.1907

McDermott, D. H., Zimmerman, P. A., Guignard, F., Kleeberger, C. A., Leitman, S. F., and Murphy, P. M. (1998). CCR5 promoter polymorphism and HIV-1 disease progression. Multicenter AIDS Cohort Study (MACS). *Lancet* 352 (9131), 866–870. doi: 10.1016/S0140-6736(98)04158-0

McLaren, P. J., Coulonges, C., Bartha, I., Lenz, T. L., Deutsch, A. J., Bashirova, A., et al. (2015). Polymorphisms of large effect explain the majority of the host genetic contribution to variation of HIV-1 virus load. *Proc. Natl. Acad. Sci. U. S. A.* 112 (47), 14658–14663. doi: 10.1073/pnas.1514867112

McLaren, P. J., Coulonges, C., Ripke, S., van den Berg, L., Buchbinder, S., Carrington, M., et al. (2013). Association study of common genetic variants and HIV-1 acquisition in 6,300 infected cases and 7,200 controls. *PLoS Pathog.* 9 (7), e1003515. doi: 10.1371/journal.ppat.1003515

McLaren, P. J., Pulit, S. L., Gurdasani, D., Bartha, I., Shea, P. R., Pomilla, C., et al. (2017). Evaluating the impact of functional genetic variation on HIV-1 control. *J. Infect. Dis.* 216 (9), 1063–1069. doi: 10.1093/infdis/jix470

McLaren, P. J., Ripke, S., Pelak, K., Weintrob, A. C., Patsopoulos, N. A., Jia, X., et al. (2012). Fine-mapping classical HLA variation associated with durable host control of HIV-1 infection in African Americans. *Hum. Mol. Genet.* 21 (19), 4334–4347. doi: 10.1093/hmg/dds226

O'Brien, S. J., and Nelson, G. W. (2004). Human genes that limit AIDS. *Nat. Genet.* 36 (6), 565–574. doi: 10.1038/ng1369

Ockenhouse, C. F., Bernstein, W. B., Wang, Z., and Vahey, M. T. (2005). Functional genomic relationships in HIV-1 disease revealed by gene-expression profiling of primary human peripheral blood mononuclear cells. *J. Infect. Dis.* 191 (12), 2064–2074. doi: 10.1086/430321

Pantaleo, G., and Fauci, A. S. (1996). Immunopathogenesis of HIV infection. *Annu. Rev. Microbiol.* 50, 825–854. doi: 10.1146/annurev.micro.50.1.825

Park, J., Lim, C. H., Ham, S., Kim, S. S., Choi, B. S., and Roh, T. Y. (2014). Genome-wide analysis of histone modifications in latently HIV-1 infected T cells. *AIDS* 28 (12), 1719–1728. doi: 10.1097/QAD.0000000000000309

Park, R. J., Wang, T., Koundakjian, D., Hultquist, J. F., Lamothe-Molina, P., Monel, B., et al. (2017). A genome-wide CRISPR screen identifies a restricted set of HIV host dependency factors. *Nat. Genet.* 49 (2), 193–203. doi: 10.1038/ng.3741

Pelak, K., Goldstein, D. B., Walley, N. M., Fellay, J., Ge, D., Shianna, K. V., et al. (2010). Host determinants of HIV-1 control in African Americans. *J. Infect. Dis.* 201 (8), 1141–1149. doi: 10.1086/651382

Petrovski, S., Fellay, J., Shianna, K. V., Carpenetti, N., Kumwenda, J., Kamanga, G., et al. (2011). Common human genetic variants and HIV-1 susceptibility: a genome-wide survey in a homogeneous African population. *AIDS* 25 (4), 513–518. doi: 10.1097/QAD.0b013e328343817b

Pickrell, J. K. (2014). Joint analysis of functional genomic data and genome-wide association studies of 18 human traits. *Am. J. Hum. Genet.* 94 (4), 559–573. doi: 10.1016/j.ajhg.2014.03.004

Pomeroy, S. L., Tamayo, P., Gaasenbeek, M., Sturla, L. M., Angelo, M., McLaughlin, M. E., et al. (2002). Prediction of central nervous system embryonal tumour outcome based on gene expression. *Nature* 415 (6870), 436–442. doi: 10.1038/415436a

Rappaport, J., Cho, Y. Y., Hendel, H., Schwartz, E. J., Schachter, F., and Zagury, J. F. (1997). 32 bp CCR-5 gene deletion and resistance to fast progression in HIV-1 infected heterozygotes. *Lancet* 349 (9056), 922–923. doi: 10.1016/S0140-6736(05)62697-9

Rotger, M., Dalmau, J., Rauch, A., McLaren, P., Bosinger, S. E., Martinez, R., et al. (2011). Comparative transcriptomics of extreme phenotypes of human HIV-1 infection and SIV infection in sooty mangabey and rhesus macaque. *J. Clin. Invest.* 121 (6), 2391–2400. doi: 10.1172/JCI45235

Saksena, N. K., Rodes, B., Wang, B., and Soriano, V. (2007). Elite HIV controllers: myth or reality? *AIDS Rev.* 9 (4), 195–207.

Salgado, M., Lopez-Romero, P., Callejas, S., Lopez, M., Labarga, P., Dopazo, A., et al. (2011). Characterization of host genetic expression patterns in HIV-infected individuals with divergent disease progression. *Virology* 411 (1), 103–112. doi: 10.1016/j.virol.2010.12.037

Samson, M., Libert, F., Doranz, B. J., Rucker, J., Liesnard, C., Farber, C. M., et al. (1996). Resistance to HIV-1 infection in Caucasian individuals bearing mutant alleles of the CCR-5 chemokine receptor gene. *Nature* 382 (6593), 722–725. doi: 10.1038/382722a0

Shungin, D., Winkler, T. W., Croteau-Chonka, D. C., Ferreira, T., Locke, A. E., Magi, R., et al. (2015). New genetic loci link adipose and insulin biology to body fat distribution. *Nature* 518 (7538), 187–196. doi: 10.1038/nature14132

Smith, M. W., Dean, M., Carrington, M., Winkler, C., Huttley, G. A., Lomb, D. A., et al. (1997). Contrasting genetic influence of CCR2 and CCR5 variants on HIV-1 infection and disease progression. Hemophilia Growth and Development Study (HGDS), Multicenter AIDS Cohort Study (MACS), Multicenter Hemophilia Cohort Study (MHCS), San Francisco City Cohort (SFCC), ALIVE Study. *Science* 277 (5328), 959–965. doi: 10.1126/science.277.5328.959

Spadoni, J. L., Rucart, P., Le Clerc, S., van Manen, D., Coulonges, C., Ulveling, D., et al. (2015). Identification of genes whose expression profile is associated with non-progression towards AIDS using eQTLs. *PLoS One* 10 (9), e0136989. doi: 10.1371/journal.pone.0136989

Thomas, R., Apps, R., Qi, Y., Gao, X., Male, V., O'HUigin, C., et al. (2009). HLA-C cell surface expression and control of HIV/AIDS correlate with a variant upstream of HLA-C. *Nat. Genet.* 41 (12), 1290–1294. doi: 10.1038/ng.486

Troyer, J. L., Nelson, G. W., Lautenberger, J. A., Chinn, L., McIntosh, C., Johnson, R. C., et al. (2011). Genome-wide association study implicates PARD3B-based AIDS restriction. *J. Infect. Dis.* 203 (10), 1491–1502. doi: 10.1093/infdis/jir046

van 't Veer, L. J., Dai, H., van de Vijver, M. J., He, Y. D., Hart, A. A., Mao, M., et al. (2002). Gene expression profiling predicts clinical outcome of breast cancer. *Nature* 415 (6871), 530–536. doi: 10.1038/415530a

van 't Wout, A. B., Lehrman, G. K., Mikheeva, S. A., O'Keeffe, G. C., Katze, M. G., Bumgarner, R. E., et al. (2003). Cellular gene expression upon human immunodeficiency virus type 1 infection of CD4(+)-T-cell lines. *J. Virol.* 77 (2), 1392–1402. doi: 10.1128/JVI.77.2.1392-1402.2003

van Manen, D., Delaneau, O., Kootstra, N. A., Boeser-Nunnink, B. D., Limou, S., Bol, S. M., et al. (2011). Genome-wide association scan in HIV-1–infected individuals identifying variants influencing disease course. *PLoS One* 6 (7), e22208. doi: 10.1371/journal.pone.0022208

Vince, N., Li, H., Ramsuran, V., Naranbhai, V., Duh, F. M., Fairfax, B. P., et al. (2016). HLA-C level is regulated by a polymorphic Oct1 binding site in the HLA-C promoter region. *Am. J. Hum. Genet.* 99 (6), 1353–1358. doi: 10.1016/j.ajhg.2016.09.023

Wang, T., Wei, J. J., Sabatini, D. M., and Lander, E. S. (2014). Genetic screens in human cells using the CRISPR–Cas9 system. *Science* 343 (6166), 80–84. doi: 10.1126/science.1246981

Wei, Z., Liu, Y., Xu, H., Tang, K., Wu, H., Lu, L., et al. (2015). Genome-wide association studies of HIV-1 host control in ethnically diverse Chinese populations. *Sci. Rep.* 5, 10879. doi: 10.1038/srep10879

Xie, W., Agniel, D., Shevchenko, A., Malov, S. V., Svitin, A., Cherkasov, N., et al. (2017). Genome-wide analyses reveal gene influence on HIV disease progression and HIV-1C acquisition in Southern Africa. *AIDS Res. Hum. Retroviruses* 33 (6), 597–609. doi: 10.1089/aid.2016.0017

Xu, W. W., Han, M. J., Chen, D., Chen, L., Guo, Y., Willden, A., et al. (2013). Genome-wide search for the genes accountable for the induced resistance to HIV-1 infection in activated CD4+ T cells: apparent transcriptional signatures, co-expression networks and possible cellular processes. *BMC Med. Genomics* 6, 15. doi: 10.1186/1755-8794-6-15

Yang, J., Fritsche, L. G., Zhou, X., Abecasis, G., and International Age-Related Macular Degeneration Genomics Consortium (2017). A scalable Bayesian method for integrating functional information in genome-wide association studies. *Am. J. Hum. Genet.* 101 (3), 404–416. doi: 10.1016/j.ajhg.2017.08.002

Yeung, M. L., Houzet, L., Yedavalli, V. S., and Jeang, K. T. (2009). A genome-wide short hairpin RNA screening of Jurkat T-cells for human proteins contributing to productive HIV-1 replication. *J. Biol. Chem.* 284 (29), 19463–19473. doi: 10.1074/jbc.M109.010033

Zhang, X., Hu, Y., Justice, A. C., Li, B., Wang, Z., Zhao, H., et al. (2017). DNA methylation signatures of illicit drug injection and hepatitis C are associated with HIV frailty. *Nat. Commun.* 8 (1), 2243. doi: 10.1038/s41467-017-02326-1

Zhang, X., Justice, A. C., Hu, Y., Wang, Z., Zhao, H., Wang, G., et al. (2016). Epigenome-wide differential DNA methylation between HIV-infected and uninfected individuals. *Epigenetics* 11 (10), 750–760. doi: 10.1080/15592294.2016.1221569

Zhang, Z. N., Xu, J. J., Fu, Y. J., Liu, J., Jiang, Y. J., Cui, H. L., et al. (2013). Transcriptomic analysis of peripheral blood mononuclear cells in rapid progressors in early HIV infection identifies a signature closely correlated with disease progression. *Clin. Chem.* 59 (8), 1175–1186. doi: 10.1373/clinchem.2012.197335

Zhou, H., Xu, M., Huang, Q., Gates, A. T., Zhang, X. D., Castle, J. C., et al. (2008). Genome-scale RNAi screen for host factors required for HIV replication. *Cell Host Microbe* 4 (5), 495–504. doi: 10.1016/j.chom.2008.10.004

Conflict of Interest Statement: The authors declare that the research was conducted in the absence of any commercial or financial relationships that could be construed as a potential conflict of interest.

Copyright © 2019 Le Clerc, Limou and Zagury. This is an open-access article distributed under the terms of the Creative Commons Attribution License (CC BY). The use, distribution or reproduction in other forums is permitted, provided the original author(s) and the copyright owner(s) are credited and that the original publication in this journal is cited, in accordance with accepted academic practice. No use, distribution or reproduction is permitted which does not comply with these terms.

Advantages of publishing in Frontiers

OPEN ACCESS
Articles are free to read for greatest visibility and readership

FAST PUBLICATION
Around 90 days from submission to decision

HIGH QUALITY PEER-REVIEW
Rigorous, collaborative, and constructive peer-review

TRANSPARENT PEER-REVIEW
Editors and reviewers acknowledged by name on published articles

Frontiers
Avenue du Tribunal-Fédéral 34
1005 Lausanne | Switzerland

Visit us: www.frontiersin.org
Contact us: info@frontiersin.org | +41 21 510 17 00

REPRODUCIBILITY OF RESEARCH
Support open data and methods to enhance research reproducibility

DIGITAL PUBLISHING
Articles designed for optimal readership across devices

FOLLOW US
@frontiersin

IMPACT METRICS
Advanced article metrics track visibility across digital media

EXTENSIVE PROMOTION
Marketing and promotion of impactful research

LOOP RESEARCH NETWORK
Our network increases your article's readership